FEB - FRESENIUS ENVIRONMENTAL BULLETIN
Founded jointly by F. Korte and F. Coulston
Production by PSP - Vimy Str. 1e, 85354 Freising, Germany in
cooperation with PRT-Parlar Research & Technology
Vimy Str 1e, 85354 Freising

Printed in Germany-ISSN 1018-4619

Fresenius Environmental Bulletin is abstracted/indexed in:
Biology & Environmental Sciences, BIOSIS, CAB International, Cambridge Scientific abstracts, Chemical Abstracts, Current Awareness, Current Contents/Agriculture, CSA Civil Engineering Abstracts, CSA Mechanical & Transportation Engineering, IBIDS database, Information Ventures, NISC, Research Alert, Science Citation Index (SCI), Scisearch, Selected Water Resources Abstracts

CONTENTS

ORIGINAL PAPERS

© by PSP Volume 25 – No. 7/2016, pages 2261-2268 Fresenius Environmental Bulletin

ANALYSIS OF ENVIRONMENTAL EFFECTS ON A SHIP POWER PLANT INTEGRATED WITH WASTE HEAT RECOVERY SYSTEM

Cengiz Deniz, Yalcin Durmusoglu[1]

[1]Istanbul Technical University, Maritime Faculty, Department of Marine Engineering, 34940 Tuzla-Istanbul, Turkey.

ABSTRACT

Waste heat recovery has attracted attention throughout the world because of the greenhouse effect by fossil fuels, their depletion, and safety of energy demand. It is also considered as a free source of energy requirements. For this purpose, various methods have been developed and implemented in order to recover energy from waste heat in industrial power plants in recent years. Marine power plants use fossil fuels to meet a major amount of their energy requirements. Therefore, this leads to not only increase energy production costs and environmental pollution but also decrease ship energy efficiency. Therefore, environmental friendly methods need to be preferred by increasing the ship energy efficiency and decreasing energy production costs. In this study, waste heat recovery methods have been investigated and their effects on ship energy efficiency and environmental pollution have been analyzed. A novel concept has been definite which is called specific emissions ratio (SER) for a waste heat recovery system. SER can be indicated a decreasing of emissions rate of a waste heat recovery plants. It is shown in the results that the value of SER for CO_2 gas component is 3.51 t(kW year)$^{-1}$ in the application without waste heat recovery whereas the same value goes down to 3.29 t(kW year)$^{-1}$ with the application of waste heat recovery. This system leads to the saving of 0.22 tons of fuel per unit kW power.

KEYWORDS:
Air pollution, Environment effect, Marine power plant, Ship energy efficiency, Waste heat recovery.

INTRODUCTION

Today, almost 90% of the world goods are carried by maritime transport account for over 90% of European Union external trade and 43% of its internal trade due to the marine transportation sector is one of the major causes of air pollution [1]. Emissions from ships affect global air quality, people's health, the marine ecology, and global warming. Carbon dioxides (CO_2), carbon monoxide (CO), particulate matter (PM), nitrogen oxides (NO_x), and sulfur oxides (SO_x) are the most significant pollutants emitted from marine diesel engines. Ships emit a range of gases from their operations at sea and in port areas. The emissions produced by navigation result from the combustion of fuel in internal combustion engines.

Annex VI of the MARPOL convention, adopted by International Maritime Organization (IMO) in 1997, sets limits on NO_x and SO_x emissions from ship exhaust gases for the prevention of air pollution from ships. The IMO has also specified Energy Efficiency Design Index (EEDI) and Ship Energy Efficiency Management Plan (SEEMP) that will reduce greenhouse gas emission. In the sixty second and sixty third meetings held by Marine Environment Protection Committee (MEPC), IMO started Energy Efficiency Design Index (EEDI) application in order to reach greenhouse gas emission targets identified by MARPOL Regulation Annex VI for ships navigating on international waters [2]. EEDI, is an index which is calculated for every ship and indication of the energy efficiency of the ship in question. This index has to be below the limits required by IMO. EEDI is the amount of CO2 emitted per mile and per load to the atmosphere by the ships (g CO2/ dwt. nm). With the implementation of EEDI, ship operators should take a series of technical measures in order to reduce their CO_2 emissions. The proposed or feasible technical measures on CO_2 reduction mainly is aimed to improving energy efficiency of ships. Ship energy efficiency can be improved by utilizing waste heat recovery (WHR) systems.

Waste heat recovery means providing more energy production by the regular fuel consumption [3]. In other words, it leads to energy production efficiency. WHR systems are also environmental friendly implementations. While there is an increase in energy recovery, additional fuel consumption is not required. In this way, more fuel is saved. There will be a decrease in harmful exhaust gas emissions to the atmosphere by saving

the fuel. In short, WHR systems will form more environmental friendly effects by decreasing the amount of exhaust gas emissions produced per power in industrial power plants. Ships are floating energy power plants. They produce energy by their power and propulsion systems while providing safe and economical transportation services from one port to another in their economic life. Moreover, ships require electricity for maneuvering, hotels and operation of all electrical and electronic equipment. All energy requirements of the ships are met by main diesel engines and generators that use fossil fuels. There is much auxiliary machinery powered by electrical energy. In view of all these facts, costs of the energy production on ships reach high levels annually. For this reason, energy saving and energy efficiency on ships cannot be ignored. In addition, implementations have been developed in order to limit the exhaust gas emissions from ships due to international regulations [4] and sanctions are being enforced. (Although afore mentioned regulations cover all environment and air pollution created by ships, only the air pollution is considered because of the scope of this study) [5,6].

Taking the given facts in consideration, the importance of WHR systems on ships cannot be overestimated. In this study, is introduced a container ship power plant equipped a WHR system which is produced an electricity power by steam turbine (turbo generator) and the effects of the systems on ship energy efficiency and air pollution is also investigated. For this purpose, technical data regarding the sample ship have been gathered and calculations thermodynamic performance is made. In addition, distributions of the WHR, fuel, exhaust gas and pollutant components has been investigated and identified by using a preferable model in the literature. Also it is defined a novel concept called specific emissions ratio (SER) for the performance of emitted to the atmosphere from the WHR system.

MATERIALS AND METHODS

Main propulsion systems of a ship mainly include power machinery that work according to theoretical diesel cycle. On the other hand energy production in WHR system is theoretically based on Rankine cycle. In short, main propulsion systems are operated by ship diesel engines whereas power is produced by steam turbines in WHR systems. Figure 1 shows the WHR system which is produced electricity power by steam turbine of the ship. The exhaust gas boiler is the main part of the WHR system. The boiler consists of the economizer, the evaporator, and the super heater. WHR system extracts heat energy from the exhaust gas by heating, evaporating and superheating water in heat exchangers in the stack. The feed water is pumped by the feed water pump into the water/steam drum. The heating medium is the saturated water contained in the drum, which is pumped by the economizer circulating water pump. The saturated steam is advanced into the super heater section of the boiler. The superheated steam enters into the steam turbine stages of turbo generator, where it expands producing mechanical power and driving the electric generator. The condensate steam is then pumped into the feed water tank (hot well). A schematic diagram of WHR system and its components analyzed in this study is illustrated in Figure 2. The system is composed of a main diesel.

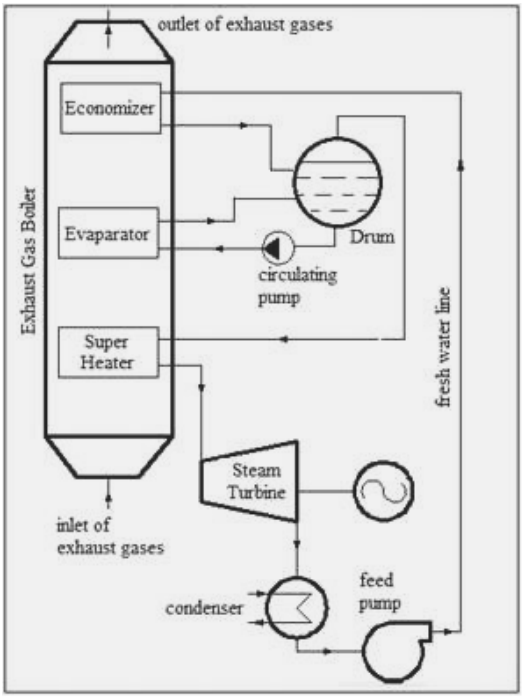

FIGURE 1
Detail drawing of a WHR system equipped with steam turbine on exhaust gas boiler

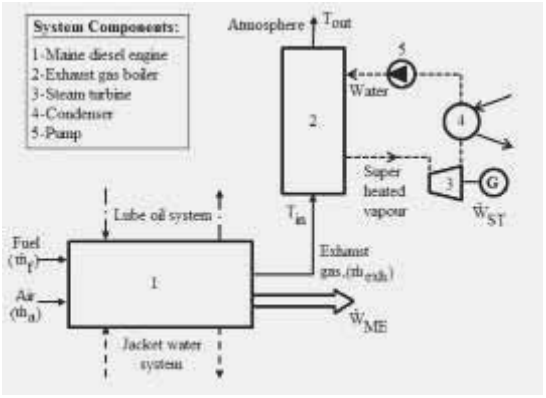

FIGURE 2
A schematic diagram of waste heat recovery system and its components analyzed in this study

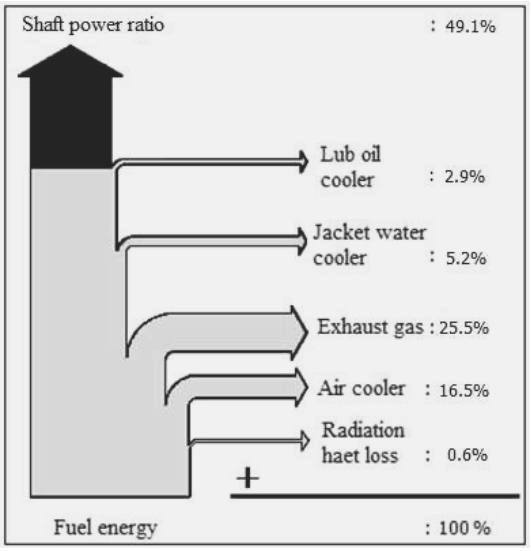

FIGURE 3
Net and wasted energy rates of a main engine system without a WHR application (MAN B&W, 2012).

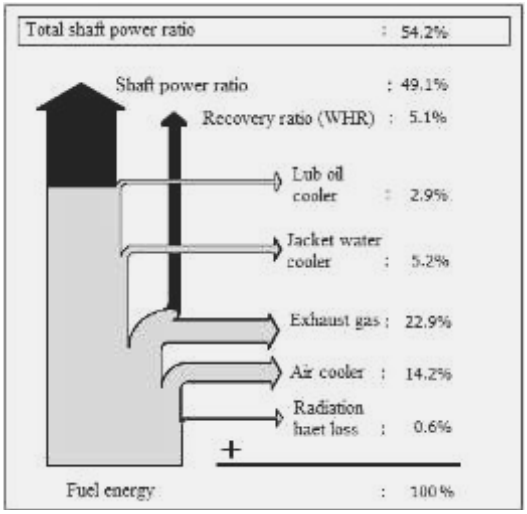

FIGURE 4
Net and wasted energy rates of a main engine system with a WHR application (MAN B&W, 2012).

engine, an exhaust gas boiler, a steam turbine, a condenser and a pump

Sankey diagrams are a specific type of energy flow diagram, in which the width of the arrows is shown proportionally to the flow quantity. Also, it can be utilized an energy efficiency analysis in a processes. Sankey diagrams are shown in Figure 3 and Figure 4 supplied by a marine engine system without WHR and with WHR applications, respectively. There are 4.9% much more energy can be recovered by main engine machinery on a marine power plant. The main engine of a ship without a WHR system produces 49.1% net power while the rest of the power (50.7%) is used in the following ways: 2.9% goes to lubrication system, 5.2% goes to jacket cooling water, 25.5% goes to exhaust gas, 16.5% air cooler and 0.6% goes to radiation transfer (Figure 3) [7]. As it can be seen, power produced by burning fossil fuels is much lower than wasted power. In other words, most a lot of the Money spent for energy is wasted. The application of WHR system on the same engine and the ship is shown in Figure 4. As can be seen in the figure, the net power has been increased to 54.2%. It can be understood that this increase is achieved by recovering energy from exhaust gases. As a result, energy wasted through exhaust gases is decreased to 22.9% [8].

Theoretical calculation and analysis of the conversion will be based on diesel and Rankine cycle principles. Furthermore, fuel savings provided by WHR power production and decreases in exhaust gases are also included in the analysis. Also the ISO Standard Conditions are assumed for the calculation methods. An algorithm, given in Figure 5, is prepared in order to simplification understand the calculation methodology and the detailed calculation formulas are given in the follow.

TABLE 1
Specifications of the container ship

Length	295	m
T.E.U.	4,200	-
Breadth	32	m
Draught	12.6	m
Tonnage	55,000	DWT
Service speed	25	knots

TABLE 2
Machinery specifications of the container ship

Type	Sulzer	12RTA 84(C)
Bore	84	cm
Stroke	240	cm
Cylinder number	12	-
Speed (Slow speed)	102	rpm (Full load)
Power	48.6	MW (Full load)
sfoc	168	g/kW.h (Full load)
Fuel consumption	196	ton.day^{-1}
Cruising day	275	day.year^{-1}

For a case study, a container ship which installed on a waste heat recovery system is considered for calculation and real data are used from the ship which properties are shown in Table 1 and Table 2. Net power produced by ship WHR system can be found in the following equation:

$$\dot{W}_{NET} = \dot{W}_{ME} + \dot{W}_{ST} \qquad (1)$$

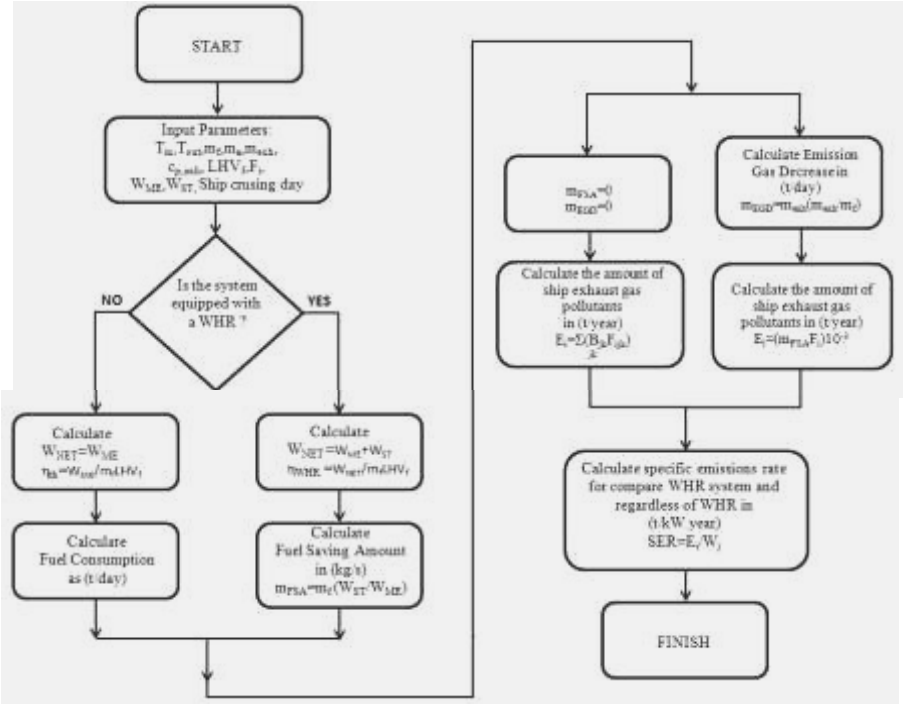

FIGURE 5
The algorithm of calculation methodology for this study

Where $\dot{W}_{ME}$ and $\dot{W}_{ST}$ indicate net power produced by main engine in WHR system and steam turbine power by the use of waste heat respectively in terms of kW. The efficiency of the WHR system can be found in the following equation,

$$\eta_{WHR} = \frac{\dot{W}_{NET}}{\dot{m}_f LHV_f} \qquad (2)$$

Where $\dot{m}_f$ and LHV_f indicate the amount of fuel consumption (kg/s) and low heating value of the fuel (kJ/kg) respectively. The purpose of WHR applications is to produce more power by consuming the same amount of fuel. In other words, power production per fuel consumption can be increased by the use of Waste Heat Recovery (kWh/g-fuel). In this way, fuel savings, and decrease in emissions can be achieved. Fuel saving amount ($\dot{m}_{FSA}$) provided by WHR system can be calculated in kg/s as follows,

$$\dot{m}_{FSA} = \dot{m}_f \left(\frac{\dot{W}_{ST}}{\dot{W}_{ME}} \right) \qquad (3)$$

The steam turbine is utilized the waste heat supplied by main engine exhaust gas for producing energy. In the other words there is no supplemental fuel consumption while the steam turbine producing more energy.

Fuel saving will also lead to decreased exhaust gas emission in proportion to the saved amount. $\dot{m}_{EGD}$ "Mass of Exhaust Gas Decrease", is explained by the correlation between the amount of fuel consumed by ship main engine and resulting exhaust gas flow. Decrease in the exhaust gas is explained as follows,

$$\dot{m}_{EGD} = \dot{m}_{FSA} \left(\frac{\dot{m}_{exh}}{\dot{m}_f} \right) \qquad (4)$$

where $\dot{m}_{EGD}$ is expressed in unit of kg/s. In addition, $\dot{m}_{exh}$ is the exhaust gas amount emitted to the environment by the ship main engine with regard to the fuel that is consumed. Relation between exhaust flow, fuel flow and air flow can be expressed as follows,

$$\dot{m}_f + \dot{m}_a = \dot{m}_{exh} \qquad (5)$$

When both sides of equation (5) is divided by the fuel flow, the following equation is found,

$$1 + \frac{\dot{m}_a}{\dot{m}_f} = \frac{\dot{m}_{exh}}{\dot{m}_f} \qquad (6)$$

when we consider coefficient air flow as $\lambda = \frac{\dot{m}_a}{\dot{m}_f}$, equation (6) can be expressed,

TABLE 3
Emission factors (F) on cruising mode for a ship [9,10]

Types of Main Engine	Emission Factors in kg/ton-*fuel*					
	CO_2	**CO**	**NO_x**	**SO_2**	**VOC**	**PM**
High speed diesel engine	3170	7.4	57	54	2.4	1.2
Medium speed diesel engine	3170	7.4	57	54	2.4	1.2
Slow speed diesel engine	3170	7.4	87	54	2.4	7.6

$$\frac{\dot{m}_{exh}}{\dot{m}_f} = (1+\lambda) \qquad (7)$$

Where λ is air-fuel ratio. In view of equation (6) and (7), equation (4) can be expressed in a simple way,

$$\dot{m}_{EGD} = \dot{m}_{FSA}(1+\lambda). \qquad (8)$$

$\dot{m}_{EGD}$ expression indicates the decrease in exhaust gas amount caused by the fuel saving in a WHR system. However exhaust gas components that are emitted to the atmosphere are also calculated in this expression. Literature survey shows that CO_2, CO, NO_x, SO_2, PM, VOC are the main pollutants in the models and calculations of air pollution caused by ships. Trozzi ve Vaccaro (1998) model that can be used to calculate the amount of ship exhaust gas pollutants is shown below [9].

$$E_i = \sum_{jk}\left(B_{jk} \cdot F_{ijk}\right). \qquad (9)$$

In this expression *i* shows the type of exhaust gas pollutants (CO_2, CO, NO_x, SO_2, PM, VOC…); *j* shows the types of fuels that is used (MDO, FO,…); *k* shows the type of ship main engine (MDE, ST, GT,…); and E_i, shows the total amount of exhaust gas produced by the ships. The total amount of exhaust gas is usually calculated in terms of (kg/s) or (ton/year). B_{jk} in equation 4 shows fuel consumption of a ship with a *k* type machinery that uses a *j* type fuel. In addition, F_{ijk} is the coefficient of the exhaust gas emission factor belonging to *i* exhaust gas pollutant that is emitted to the atmosphere by a *k* type machinery in (kg-*i*/ton-*fuel*). The values for emission factors which are also referenced by Vaccaro and Trozzi are given in Table 3. Since WHR systems are considered to save money under full load conditions. Table 3 is only arranged according to ship full ahead cruising mode [10-14]. Taking into consideration the notations used in this study, equation (9) can be expressed as follow in (kg/s),

$$E_i = \left(\dot{m}_{FSA} \cdot F_i\right) \cdot 10^{-3} \qquad (10)$$

where F_i is emission factor (kg_i /ton_{fuel}) and shown in Table 3. Decreases in exhaust gas pollutant provided by ship WHR systems have been calculated by using the data in equation (10) and Table 3. The evidence in the calculations is obtained by using data from the container ship and the WHR system. All the specifications and data regarding the container ship are shown between Tables 1, Table 2 and Table 4.

TABLE 1
Data of the exhaust boiler of the container ship

Mass rate of exhaust gas	$(\dot{m}_{exh})$	66.67	kg/s
Böiler inlet temperature	(T_{in})	650	K
Boiler outlet temperature	(T_{out})	436	K
Stream turbine power	$(\dot{W}_{ST})$	1600	kW

A new approach is used in this study which is the novel concept for analysis of a power plant equipped with waste heat recovery system. It is well indicate values for comparison the plant with WHR and regardless of WHR. The method is called specific emissions rate (SER). It is defined as amounts of yearly emissions per a unit power produced by power plant in (t/kW.year) and given in follow,

$$SER = \frac{E_i}{\dot{W}_j} \qquad (11)$$

where E_i explained above. $\dot{W}$ is the total power values produced by heat engines in a power plant. (j=marine diesel engine, steam turbine, gas turbine etc.).

RESULTS AND DISCUSSION

In this study is discussed the environmental effects of ship power plant equipped a WHR. For this purpose, technical data regarding the sample ship have been gathered and calculations thermodynamic performance is made. The parameters are real data and taken from the container ship. In addition, distributions of WHR, fuel, exhaust gas and pollutant components has been investigated and identified by using a preferable model in the literature. Also it is defined a novel concept called specific emissions ratio (SER) for the performance of emitted to the atmosphere from a waste heat recovery systems.

TABLE 2
The results of comparative performance analysis

Application Type	$\dot{W}_{NET}$ (kW)	η_{WHR} (%)	$\dot{m}_{FSA}$ (t/day)	$\dot{m}_{EGD}$ (t/day)
With Waste Heat Recovery	50200	51.80	6.451	190
Without Waste Heat Recovery	48600	48.51	-	-

TABLE 3
Gain the exhaust gas emissions with WHR application in the container ship plant

Type of Plant	Amount of Emissions in t(year)$^{-1}$					
	CO_2	CO	NO_x	SO_2	VOC	PM
Without Waste Heat Recovery	170824	399	4688	2910	129	410
With Waste Heat Recovery	165200	386	4534	2814	125	396
Gain	5624	13	154	96	4	13

TABLE 4
Comparison of annually specific emissions ratio for the container ship power plant

Type of Plant	Specific Emissions Rate (SER) in t(kW.year)$^{-1}$					
	CO_2	CO	NO_x	SO_2	VOC	PM
Without Waste Heat Recovery	3.51	0.01	0.10	0.06	0.003	0.01
With Waste Heat Recovery	3.29	0.01	0.09	0.06	0.002	0.01

Table 5 shows that an increase of 1600 kW can be achieved in gross power by using the WHR application. With this power increase, 6.45 tons fuel has been saved per day. This energy saving is achieved by WHR without consuming any fuel. As a result, the net efficiency of the system has risen to 51.8%. With the power increase without fuel consumption environment is also protected. The atmosphere is prevented 190 ton of exhaust gas emissions per day thanks to WHR applications by the container ship main engine. In other words, if the ship main engine produces 50200 kW power, this machine would burn excessive 6.45 ton of fuel per day. As a result, an excessive 190 ton of exhaust gas would be not emitted to the atmosphere.

The benefits from the reduction in total exhaust gas components are shown in Table 6.

As it can be seen in Table 6 there is a decrease in the exhaust gas components emitted to the atmosphere approximately 5905 ton per year in total by WHR systems. Table 7 shows the amount of exhaust gas component per unit power produced by the WHR system. Accordingly the decrease in exhaust gas components per unit power produced by the WHR system is clearly shown. For instance, the value of SER for CO_2 gas component is 3.51 t(kW year)$^{-1}$ in the application without WHR whereas the same value goes down to 3.29 t(kW year)$^{-1}$ with the application of the WHR. This system leads to the saving of 0.22 ton of fuel per unit kW power. As a consequently, a SER parameter is an important indications in order to environmental effects analysis for ship power plants and also thermal plants, nuclear plants, etc.

Also a Sankey diagram for energy balance is drawn and given in Figure 6 to the container ship. Regarding to the case study, the amount of fuel saving and due to the amount of emissions decreased are calculated in the container ship. It is clearly understand from the Figure 6, there is a heat recovery from the exhaust gas approximately 3.3% and produced 1600 kW electricity energy by steam turbine. Therefore, the container ship plant has got a 51.8% total shaft power.

The SER parameter is increase on a power plant; it is mean that environmental effects can be glowingly improved. SER is implied in this study to the container waste heat recovery system and the results are shown in Table 7.

As a consequently the traditional WHR systems are a good solution for recovery of energy with consuming same fuel and due to increased the energy efficiency for power plants. Also a cost of energy saving and an environment effects are decreased when increased of an energy efficiency for a system. But there is a still some heat energy recovery potential from the exhaust gases. This energy cannot be recovery by WHR systems. Some novel technological applications have been developed and installed in shore power plants to recovery this low grade energy. That is we can improve the system and due to increase the energy efficiency much more on ship power plants.

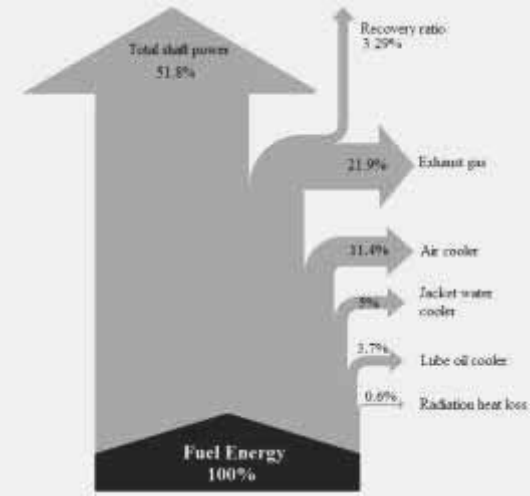

FIGURE 6
The sankey diagram of case study

CONCLUSION

In this study, the environmental effects of WHR implemented in a sample container ship with diesel engine have been studied. In conclusion, WHR applications enable the production of more power with the same fuel amount. These systems do not consume excessive fuel and more power is produced for the power plant. Despite the common belief, not only saving in the fuel amount and the cost is achieved, but also environment is protected. In this vein, if these types of systems are improved and ship applications are developed, significant steps will be taken.

In view of EEDI that has gone into effect for ships in recent years, WHR applications are of utmost importance. Not only waste heat from exhaust gas boiler, but also other types of waste energy can be identified on ships that is a purpose for the future study. Consequently, benefits can be derived from these types of energy. Thanks to recent research, the application of organic Rankine cycle (ORC) method on ships is possible. ORC has been commonly used in industrial areas. By the use of ORC energy savings can be achieved from waste heat at very low temperatures. Apart from this, absorption cooling systems used in waste heat process can be given as another example.

In brief, ship owners need to examine the current onboard operation conditions and analyze the efficiency of their ships. Then, they need to be able to recover energy from waste heat by using WHR systems. Thus, small investments could lead to substantial profits.

NOMENCLATURE

Abbreviations
MARPOL: International convention for the prevention of pollution from ships
IMO: International maritime organization
EEDI: Energy efficiency design index
SEEMP: Ship energy efficiency management plan
MEPC: Marine environment protection committee
WHR: Waste heat recovery
ISO**:** International organization for standardization
LHV: Low heat value
FSA: Fuel saving amount
EGD: Exhaust gas decrease
ST: Steam turbine
ME: Ship main engine
W: Power production
Q: Heat production
CO_2: Carbon dioxide
CO: Carbon monoxide
NO_x: Nitrogen oxide
SO_2: Sulfur dioxide
PM: Particular matter
VOC: Volatile organic compound
E: Exhaust gas pollutants
B: Fuel consumption of a ship
F: Emission factors
MDE: Marine diesel engine
GT: Gas turbine
MDO: Marine diesel oil
FO: Fuel oil
ORC: Organic Rankine cycle
Greek Symbols
η: Efficiency
λ: Air-Fuel ratio
Subscriptions
i: Types of pollutants
j: Types of fuels
k: Types of ship main engines
m: Mass flow rate
f: Fuel
a: Air
exh: Exhaust gas

REFERENCES

[1] UNCTAD, (2007). Review of Maritime Transport. Report by the UNCTAD secretariat, United Nations, New York and Geneva, 2007.
[2] IMO Marine Environment Protection Committee (MEPC, 2013), 65th session. Energy-efficiency regulations, London.
[3] Reports of the Energy Efficiency Association (EES) (2010). The Energy Efficiency Strategy Documentation between 2010-2023. Istanbul, Turkey.

[4] International Convention for the Prevention of Pollution from Ships (MARPOL), Annex VI, 2005.
[5] Tien, W.K., Yeh, R.H. and Hong, J.M. (2007). Theoretical analysis of cogeneraiton system for ships. Energy Conversion and Management, 48, 1965-1974.
[6] Deniz, C. and Durmusoglu, Y. (2008). Estimating shipping emissions in the region of the Sea of Marmara, Turkey. Science of the Total Environment, 390(1), 255-261.
[7] MAN Diesel & Turbo SE. (2011) TCS-PTG Savings with extra power. Augsburg, Germany.
[8] MAN Diesel & Turbo SE. (2012). Waste Heat Recovery System (WHRS) for reduction of fuel consumption, emissions and EEDI. Germany.
[9] Trozzi C. and Vaccaro R. (1998). Methodologıes for Estimating Future Air Pollutant Emissions from Ships. Techne report, MEET RF98b.
[10] EMEP, MSC-W Note 1/99. (1999). EMEP emission data, Status Report.
[11] Endresen, Ø., E. Sørgard, J. K. Sundet, S. B. Dalsøren, I. S. A. Isaksen, T. F. Berglen, and G. Gravir. (2003). Emission from international sea transportation and environmental impact. J. Geophy. Res., 108 (17), 1401-1422.
[12] Cooper, D et al., (2004). Methodology for calculating emissions from ships 1. Update of emission factors. SMED Project report (www.smed.se).
[13] Corbett J, Fischbeck P., (1997). Emissions from ships. Science 278(5339), 823-824.
[14] EPA420-R-00-002, Analysis of Commercial Marine Vessels Emissions and Fuel Consumption Data, 2000.

Received: **25.02.2015**
Accepted: **19.03.2016**

CORRESPONDING AUTHOR

Yalcin Durmusoglu,
Department of Marine Engineering, ITU Maritime Faculty, Tuzla, Istanbul, Turkey.

E-mail: ydurmusoglu@itu.edu.tr

© by PSP Volume 25 – No. 4/2016, pages 2269-2277 Fresenius Environmental Bulletin

ASSESSMENT OF NUTRIENTS AND ORGANIC MATTER IN SEDIMENTS OF DONGPING LAKE, CHINA

Yanhao Zhang[1,2], Lilong Huang[1], Zhibin Zhang[1,3]*, Yufeng Lv[1], Cuizhen Sun[1], Weimin Wu[3], Taha Marhaba[4]

[1]College of Municipal and Environmental Engineering, Shandong Jianzhu University, Jinan 250101, China
[2]Co-Innovation Center of Green Building, Jinan 250101, China
[3]Center for Sustainable Development & Global Competitiveness, Stanford University, Stanford, CA 94305, USA
[4]John A. Reif, Jr. Department of Civil and Environmental Engineering, New Jersey Institute of Technology, Newark, New Jersey 07102, USA

ABSTRACT

Dongping Lake is the second largest freshwater lake in Shandong Province, China. Currently, it is an important reservoir for regulating water for the Eastern Route of South-to-North Water Diversion Project, and the water quality assurance of it is of great importance. The total nitrogen, total phosphorus and organic matters in both surface water and sediment in Dongping Lake were determined to assess the level of contamination. The concentrations of TN, TP and COD_{Cr} in the surface water were 0.38±0.06~1.17±0.16, <0.020 ± 0.003 mg/L,14.0±2.1~20.0±3.2 mg/L respectively, lower than Grade III of the "China surface water quality standard (GB3838-2002)". The contents of TN and TP in sediment in the estuary of Dawen River were higher because of the wastewater drainage from Dawen Rive, while the OM concentration were higher in southwest of Dongping Lake, probably due to the precipitation of dead hydrophytes in the aquaculture area. The result of assessment using enrichment factor method showed that the sediment situated around of Lashan wharf and estuary of Dawen River were moderately severe enrichment of phosphorus, and the sediment at estuary of Dawen River were moderately enrichment of nitrogen, and sediment in all region of Dongping Lake were minor enrichment of organic matters. The result of Geoaccumulation index indicated that sediments in Dongping Lake were uncontaminated to be moderately contaminated.

KEYWORDS:
South-to-North Water Diversion Project, Sediments, Nutrients, Distribution characteristic, Assessment

INTRODUCTION

The contents of nitrogen and phosphorus are known to play a key role in determining the ecological status of aquatic systems [1-5]. Nitrogen and phosphorus in excess may lead to diverse blooms, loss of oxygen, taste and odour problems, fish deaths and loss of biodiversity [6, 7]. Nitrogen and phosphorus enrichment seriously degrades aquatic ecosytems, impairing the use of water for dringking, industry, agriculture, recreation and other purposes [8]. Several studies in the past have associated oligotrophy with the absence of measurable concentrations of nutrient and have defined eutrophication as a qualitative parameter referring simply to nutrient or organic matter enrichment from external sources and resulting in high biological productivity [9-11]. However, for the freshwater bodies, contaminated sediments are regarded as the most important sources of nutrients leading subsequently to eutrophication [12, 13]. Nutrient release processes have a significant impact on the water quality and may result in continuous eutrophication of lakes and rivers, even when external nutrient sources are under control [14-16]. Phosphorus is a major nutrient controlling eutrophication in many aquatic systems [7, 17]. Along with the rapid economic growth, tourism and industrialization, the sediment P separation can enhance the understanding of P cycling in the aquatic ecosystem [18]. It is believed that controlling P is the best approach for reducing eutrophication [19].

Dongping Lake is a adjusting and important freshwater lake on the Eastern Route of the South-to-North Water Diversion (SNWD) project, and the location of the lake is very important for the project [20]. According to the "Water Pollution Prevention Planning of SNWD Project for Shandong (China) Section", its water quality should meet the Grade III of the "China surface water quality standard (GB3838–2002)". So the water quality is the most important element in the success of the Eastern Route of the SNWD [21]. Dawen River is the main river flowing to Dongping Lake. Domestic sewage and industrial waste water without treatment from cities (Laiwu, Xintai, Feicheng, Ningyang and Dongping) has discharged into Dawen River last century 90s. Therefore, investigation of the nutrients and organic matter distribution

characteristics of the water and surface sediments in Dongping Lake is clearly essential. There was some previous research on phosphorus distribution in sediment of Dongping Lake [22-24], while, there is still a lack of investigation of nitrogen and organic matters pollution for the water and sediments in Dongping Lake.

Therefore, this paper will systematically investigate the distributions of total nitrogen (TN), total phosphorus (TP) and organic matter in the water and sediment and assess of sediment contamination in Dongping Lake. This work lays groundwork towards a comprehensive understanding of the current nutrient levels of Dongping Lake and provides essential knowledge for establishing appropriate water quality management policies and remediation strategies.

MATERIALS AND METHODS

Study area. As shown in Fig.1 (left), the water of Yangtze River water will be transported more than 1100 km from Yangzhou to Tianjin and Beijing in the SNWD project. Dongping Lake in the red circle, an important reservoir (35°30' ～ 36°20'N, 116°00' ～ 116°30'E), serves serve a pivotal role in the Eastern Route of SNWD of China and water transmission from the west to the east of Shandong Province. Additionally, the lake plays a major role in regulating the Yellow River and Dawen River floods. Dongping Lake is the second largest fresh-water lake in Shandong Province, China, and also the only large natural inland lake still existing after thousands of years' geological and morphological changes in the lower reaches of the Yellow River [21]. The current size of the lake, including the old and the new lake, is about 627 km^2. The multi-annual mean water depth of the lake is 2-4 m, with a perennial area of 124 km^2. The recharge coefficient of the lake is 61.2, and the total storage volume is 4.0 billion m^3. Depth varies slightly annually and seasonally. Recharge to Dongping Lake relies mainly on surface runoff via the Dawen River. The water in the lake flows north through the Xiaoqing River and enters the Yellow River. Dongping Lake is being utilized for flood control, irrigation, water supply, aquatic breeding and tourism [21].

Sampling sites. As shown in Fig.1, Dawen River, a main tributary, originates in north of Xuangu Mountain, and collects water from branches of the Tai-Yimeng mountain range. Affected by the terrain, Dawen River winds its way from west to east, and then flows into Dongping Lake. Then, the water run through the lake from south to north, out of the lake in the north, and flew into the Yellow River. Driven by the natural hydraulic flow, nutrients are transported from the upstream lake to the downstream lake as indicated by the arrow in Fig. 1. In this study, surface

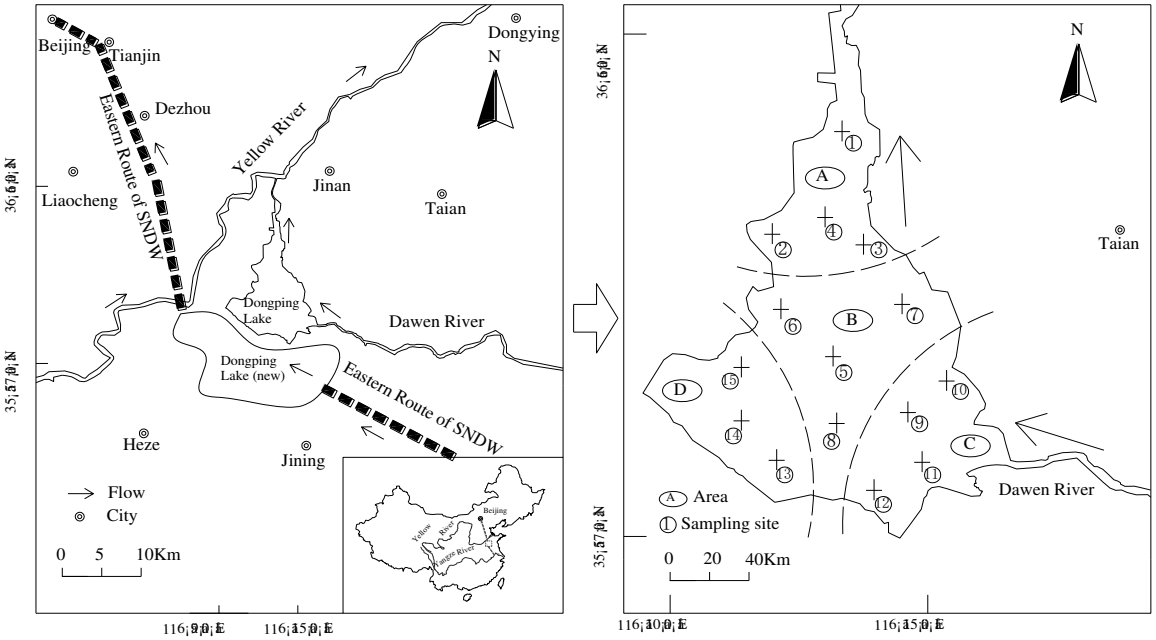

FIGURE 1
Geographic map of Dongping Lake and sampling sites (Right: A-downstream lake, B-Center of the lake, C-Estuary of Dawen River, D-Southwest of the lake (aquaculture area).

TABLE 1
Water quality and its characteristics of the sampling fields

Site fields	Salinity（mg/L）	DO	pH	Transparency（cm）	Water depth（m）	Other details
C-Estuary of Dawen River	524±22	6.91±0.34	7.0±0.3	30±15	1.2±0.6	lots of wharf
D-Southwest of the lake	451±20	9.25±0.61	6.5±0.3	35±10	2.8±0.4	aquaculture region
B-Center of the lake	470±16	7.01±0.30	6.5±0.2	31±10	2.3±0.5	
A-Downstream of the lake	426±12	8.74±0.26	7.0±0.4	65±10	3.0±0.6	effluent water flowing to Yellow River

sediment samples (0-20 cm below the water–surface interface) and the surface water (0-20 cm below the water surface) were collected respectively at 15 sites across the lake to study the spatial distribution of nutrient contents within the lake. The samples were mainly located at the downstream of the lake (A area), the center of the lake (B erea), the estuary of Dawen River (C area), and the southwest of the lake (D area), respectively (Fig.1 right).

The salinity, DO, pH, and transparency for the water were shown in Table 1. The salinity, DO and pH of water in Dongping Lake were 426±12~524 ±22mg/L, 6.91±0.34~9.25±0.61 mg/L and 6.5± 0.2~7.0±0.3, respectively.

Sampling collection and analysis. Surface layer sediment (0-20 cm) samples were collected with a home-made core Plexiglas sampler from the aforementioned sampling sites in April, 2012. The samples collected from each site consisted of 3 parallel samples. Following collection, the samples were sealed in plastic bags and stored in a refrigerator at 4ºC without exposure to light. Sediment samples were air dried for 30 day at room temperature with exposure to the day light. Then, the large solid components (stones and plant) were removed by a 0.15-mm sieve. The sieved samples were stored in air-sealed plastic bags before further analysis. At the same time, the surface water samples were collected, and stored in 500 ml polyethylene bottles at a cooler at 4ºC. All of the samples were sent to Environmental Laboratory, Shandong Jianzhu University for further analyses.

TN, TP. and COD_{Cr} in the water were determined according to "Methods for examination of water and wastewater" [25].

Sediment samples were air dried at room temperature in daylight. Then, the large solid debris (such as stones and plant) in the dried samples was removed by a 100 mesh sieve. The sieved samples were stored in air-sealed plastic bags before further analysis.

To measure TP in the sediment samples, 0.25 g sediment samples were digested in Teflon vessels with 12 mL HNO_3 (65%): HCl (37%) = (3:1) mixture in a microwave oven (MARS X-press, CEM) [26, 27]. Then, TP in acid digested extract was determined by the ascorbic acid method using a Shimazu spectrophotometer (UV3600) [28]. TN was determined using an elemental analyzer (CE440, Exeter Analytical, Inc., North Chelmsford, MA, USA). To measure OM, the sediment samples were first dried at 60ºC for 24 h to remove moisture [29]. Then, the samples were weighed and heated in a muffle furnace at 550ºC for 2 h to further remove OM. Finally, the sediment samples were re-weighed to calculate OM percentage, which was the difference between the ash weight and dry weight divided by the dry weight. All samples were analyzed in triplicate, and the results were expressed as mean and standard deviation.

All samples were analyzed in triplicate, and the results were expressed as mean and standard deviation. SURFER software (Golden Software Inc.) is used to analyze the spatial distribution of sedimentary TN, TP and OM in Dongping Lake.

Assessment of sediment contamination. Enrichment factor (EF) and Geoaccumulation index (I_{geo}) were mainly used to assess the degree of heavy metal contamination in sediments. In this study, we evaluated the TN, TP and OM in sediments of Dongping Lake using modified EF and I_{geo}.

EF. EF is defined using the relationship below (Eq. (1)) [30]:

$$EF_i = C_i / C_{BV} \quad (1)$$

EF_i is the enrichment factor of the nutrient i. C_i is the concentration of the nutrient i in sediment samples and C_{BV} is the environmental background value. In this paper, C_{BV} value was obtained from annual monitoring for Dongping Lake sediment [31]. Depending on the calculated values of EF, the sediment contamination can be classified as no enrichment when EF<1, minor enrichment when EF

is 1~3, moderate enrichment when EF is 3~5, moderately severe enrichment when EF is 5~10, severe enrichment when EF is 10~25, very severe enrichment when EF is 25−50, and extremely severe enrichment when EF is >50 [30].

I_{geo}. I_{geo} is calculated by the following equation (Eq. (2)) [6]:

$$I_{geo} = Log_2(C_n)/[1.5(B_n)] \quad (2)$$

C_n is the concentration of the nutrients in sediment samples and B_n is the background concentration of the nutrient. Factor 1.5 is the background matrix correction factor due to lithospheric effects. The I_{geo} consists of seven classes [32]. $I_{geo} \leq 0$ is practically uncontaminated; $0<I_{geo}\leq 1$ is uncontaminated to moderately contaminated; $1<I_{geo}\leq 2$ is moderately contaminated; $2<I_{geo}\leq 3$ is moderately to heavily contaminated; $3<I_{geo}\leq 4$ is heavily contaminated; $4<I_{geo}\leq 5$ is heavily to extremely contaminated; $5<I_{geo}$ is extremely contaminated [33].

RESULTS

Nutrient and COD concentrations in surface water. Mean concentrations of nutrients and COD_{Cr} in surface water samples at each sites in this study, and maximum concentrations reported from previous studies were shown in Table 2.

As shown in Table 2, TN concentrations in the surface water ranged from 0.38±0.06~1.17±0.16 mg/L, and COD_{Cr} concentrations ranged from 14.0±2.1~20.0±3.2 mg/L, TP concentrations varied from 0.00±0.00~0.020±0.003 mg/L. The higher TN and COD_{Cr} concentrations were recorded at sites 5, 6 and 8 situated the estuary of Dawen River. TP concentrations at each site were all low. The highest TN concentration was more than two times higher than the lowest TN concentration, while the highest COD_{Cr} concentration was only a little higher than the lowest COD_{Cr} concentration. Except the TN concentrations in sites 5, 6, 8 exceeded the standard values of Grade III in the "China surface water quality standard (GB3838-2002)", all the concentrations of TN, TP, COD_{Cr} can meet the Grade III standard values in China. Compared with the maximum concentrations reported by previous studies conducted in the same area [34, 35], the water qualities of TN and TP were improved greatly in recent.

TN, TP and organic matter concentrations in surface sediments. As shown in Fig.2a and Fig.2b, the distribution pattern of TN was in the range of 426.0±52.3~839.0±123.0 mg/kg, with an average of 647.0±87.6 mg/kg. TP contents in sediments were in the range of 167.0±23.4~488.0±63.2 mg/kg, with an average of 336.0±43.2 mg/kg. Concentrations of TP in sediment of Nansi Lake were 759.0~896.0 mg/L, and mean of 816.0 mg/L [28], was obviously higher than those of Dongping Lake. Sites of higher TN and TP concentrations were found in the southeast of Dongping Lake, which are the estuary of Dawen River.

TABLE 2
Mean concentrations of nutrients and COD in surface water samples at typical sites in this study, and concentrations reported for previous studies

Sites	Mean concentrations of nutrients and COD_{Cr} (mg/L)			
	TN	TP	COD_{Cr}	References
1	0.38±0.06~	0.00±0.000	14±2.1	This study
2	0.82±0.11	0.01±0.002	16±2.4	
3	0.99±0.14	0.02±0.003	15±1.7	
4	0.51±0.12	0.01±0.002	11±1.2	
5	0.62±0.06	0.01±0.002	14±1.8	
6	0.70±0.03	0.01±0.002	15±2.1	
7	0.68±0.05	0.01±0.001	13±1.2	
8	0.63±0.06	0.01±0.002	13±1.5	
9	1.12±0.18	0.01±0.002	17±2.1	
10	1.17±0.16	0.01±0.002	15±2.8	
11	1.36±0.23	0.01±0.001	20±3.2	
12	0.43±0.06	0.02±0.003	16±2.6	
13	1.02±0.15	0.01±0.001	16±1.8	
14	1.02±0.15	0.01±0.001	17±2.2	
15	1.06±0.15	0.01±0.001	15±2.1	
	4.75±0.76	0.10±0.002	--	[34]
	1.34-14.60	0.081-0.182	44-65.6	[35]

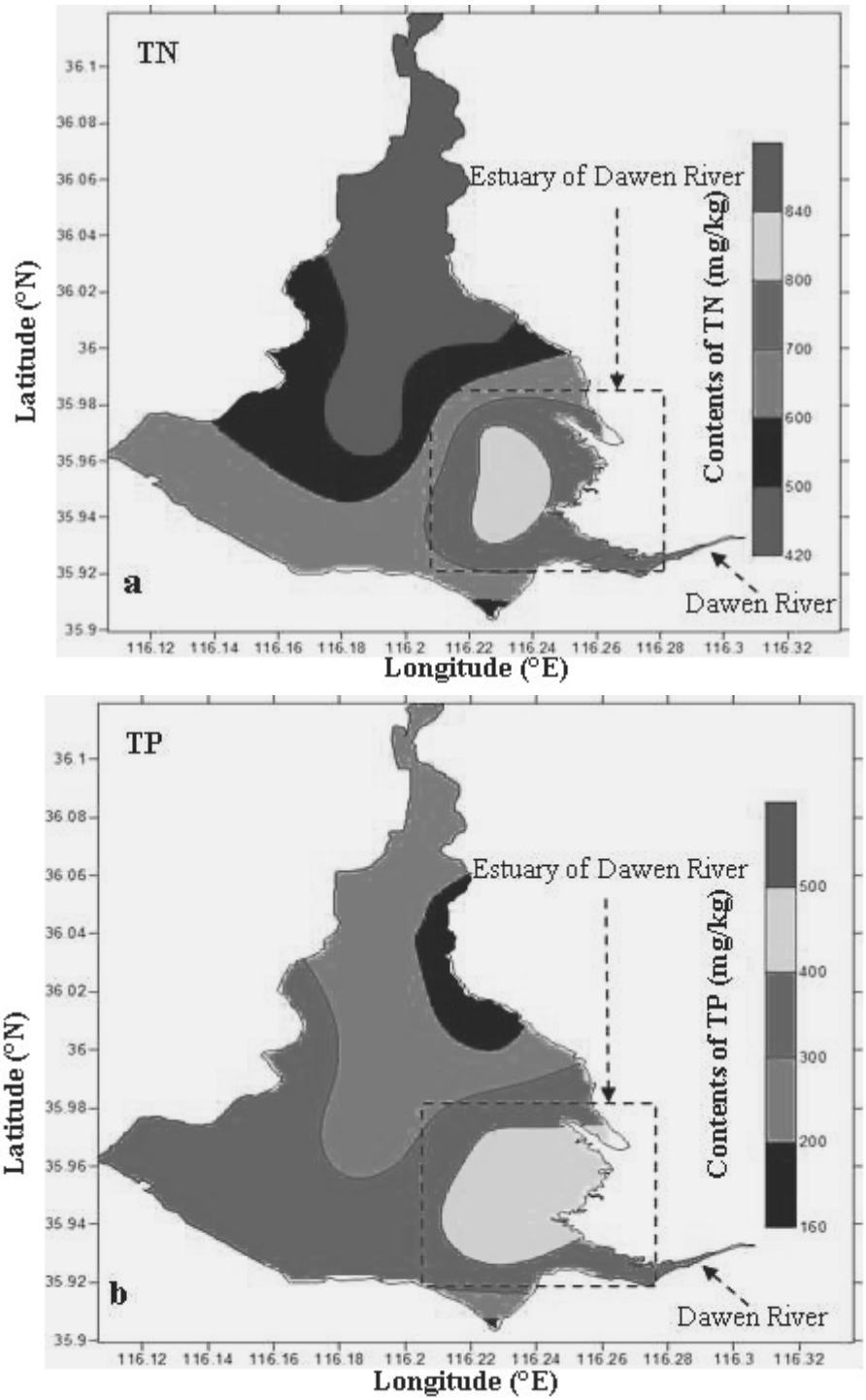

FIGURE 2
Distribution of TN and TP contents in surface sediments of Dongping Lake (a. TN; b, TP)

The distribution of OM in surface sediments of Dongping Lake was shown in Fig.3. OM contents in sediments were in the range of 48981.0±6435.2~124924.0±18943.6 mg/kg, with an average of 87658.0±12653.1 mg/kg. Concentrations of OM in sediment of Nansi Lake were mean of 118300.2 mg/kg [28]. Thus, the OM concentrations in sediment of most Dongping Lake were lower than in Nansi Lake. Sites of higher concentrations were at southwest of Dongping Lake.

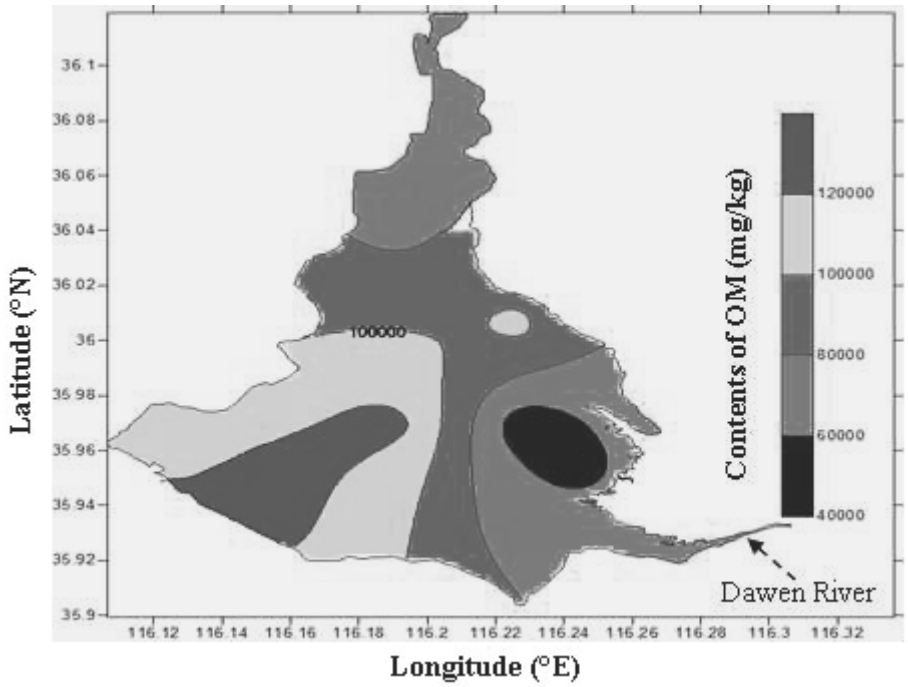

FIGURE 3
Distribution of OM contents in surface sediments of Dongping Lake

DISCUSSION AND CONCLUSIONS

Distribution characteristics of TN, TP and OM in sediments. Nutrients of Dongping Lake mainly come from industrial wastewater, domestic sewage and surface runoff of Dawen River basin and valleys of Dongping Lake and so on [22, 36]. According to an estimation, the most important sources of nutrients is Dawen River and input of the river accounts for about 82.61% of the total phosphorus input, were higher than valleys of Dongping Lake (14.47%) [22]. According to statistics, industrial and urban household wastewater discharge was about 1.64×10^4 t/a, COD_{Cr} was 6.42×10^4 t/a, and most of the discharging wastewater was worse than Grade V during 1995~2004. Some studies also showed that phosphorus in industrial wastewater and domestic sewage discharge of Dawen River have increased these years, and the input of TN and TP from Dawen River were 4218 t/a and 161 t/a, respectively. However, the TN and TP in the Lake from the aquaculture and others only accounted for 17.6% and 17.4%, respectively [36]. So, the sites of higher TN and COD_{Cr} concentrations in water, higher TN and TP concentrations in sediment were mainly located at the estuary of Dawen River, mostly due to the wastewater from the upstream of Dawen River.

The concentrations of OM in sediment at southwest of Dongping Lake were higher than other regions, probably due to that there were the precipitation of lots of dead hydrophytes at the southwest regions when sediment samples were collected.

Assessment of TN, TP and OM for sediments. EFs of TN, TP and OM for sediments. As shown in table 3, the results suggested that the pollution extent of the sediment decreased from the upstream to the downstream in the lake. The phosphorus were moderately severe enrichment (5<EF<10) in the sediments at sites around the estuary of Dawen River. The nitrogen were moderately enrichment (3<EF<5) in the sediments of sites around of estuary of Dawen River. The organic matters were minor enrichment (1<EF<3) in the sediments of all lake.

I_{goe}s of TN, TP and OM for sediments. As shown in table 4, the I_{goe}s ($0<I_{goe}s<1$) showed that the sediments of all sites were uncontaminated to moderately contaminated by nitrogen, phosphorus and organic matters. The I_{goe}s of TN and TP in sediments around the southeast of Dongping Lake were greater than those in other sites, while the I_{goe}s of OM in sediments around the southwest of the Lake were greater. The sites with

TABLE 3
***EF*s of TN, TP and OM for sediments of all sites in Dongping Lake**

Sites	*EF*		
	TP	TN	OM
1	3.64	1.80	1.52
2	6.98	2.25	1.96
3	2.86	1.85	2.11
4	2.78	2.10	1.86
5	4.14	1.65	2.55
6	3.54	1.76	1.85
7	3.78	1.82	2.02
8	3.50	1.96	2.65
9	7.16	2.77	1.34
10	7.25	3.25	1.00
11	8.34	3.25	1.39
12	1.95	1.90	1.68
13	5.60	2.15	1.80
14	3.98	2.25	2.10
15	5.92	2.66	2.54

higher contents of TN and TP in sediments were probably caused by the reason that the southeast of Dongping Lake was the estuary of Dawen River, which has been brought lots of nitrogen and phosphorus to the lake since 1980s [31]. The higher OM in sediments probably was due to cage culture in the southwest region of the lake, which resulted in the precipitation of lots of aquatic plants in the winter.

The distribution and pollution level of nutrients in the surface water and sediment in Dongping Lake were investigated. The result showed that all the concentrations of TN, TP, COD_{Cr} in the lake water could meet the Grade III standard values of the "China surface water quality standard (GB3838-2002)" except of TN contents a little bit higher over the standard value in the estuary of Dawen River. And the higher concentrations of TN and TP in the sediment were also recorded at the estuary of Dawen River. The higher OM concentrations were found at southwest

TABLE 4
***I_{goe}*s of TN, TP and OM for sediments of all sites in Dongping Lake**

Sites	I_{goe}		
	TP	TN	OM
1	0.045	0.014	0.00021
2	0.051	0.014	0.00022
3	0.043	0.014	0.00022
4	0.048	0.014	0.00021
5	0.046	0.014	0.00023
6	0.051	0.014	0.00022
7	0.047	0.014	0.00022
8	0.042	0.014	0.00021
9	0.051	0.015	0.00022
10	0.051	0.015	0.00021
11	0.052	0.015	0.00022
12	0.040	0.014	0.00022
13	0.045	0.015	0.00022
14	0.046	0.015	0.00023
15	0.049	0.015	0.00023

of Dongping Lake, probably due to the dead plants resulted from the aquaculture.

The EFs showed that phosphorus in sediment situated at the estuary of the Dawen River, which were moderately severe enrichment. While the nitrogen in sediment at the estuary of Dawen River were moderately enrichment and the organic matters in sediment of Dongping Lake were minor enrichment. From the analysis of the I_{geo}s indexes, the sediments in Dongping Lake were in pollution grade of "uncontaminated to moderately contaminated" with nitrogen, phosphorus and organic matters.

ACKNOWLEDGEMENTS

This study was funded by the Department of Environmental Protection of Shandong Province (No.SDHBPJ-ZB-09) and Natural Science Foundation of Shandong Province for providing the financial support (No. BS2013HZ028). Special thanks to Mr. Zhang for assistance with the proofreading of this manuscript.

REFERENCES

[1] Jarvie, H. P., Whitton, B. A., and Neal, C. (1998) Nitrogen and phosphorus in east coast British rivers: Speciation, sources and biological significance, Science of the Total Environment 210, 79-109.

[2] Shimada. (2014) Effects of Water Table Control by Farm-oriented Enhancing Aquatic System on Photosynthesis, Nodule Nitrogen Fixation, and Yield of Soybeans (vol 15, pg 132, 2012), Plant Production Science 17, Viii-Viii.

[3] Smith, I., and Schallenberg, M. (2013) Occurrence of the agricultural nitrification inhibitor, dicyandiamide, in surface waters and its effects on nitrogen dynamics in an experimental aquatic system, Agriculture Ecosystems & Environment 164, 23-31.

[4] Ni, Z. K., and Wang, S. R. (2015) Historical accumulation and environmental risk of nitrogen and phosphorus in sediments of Erhai Lake, Southwest China, Ecological Engineering 79, 42-53.

[5] Wang, L. Q., and Liang, T. (2015) Distribution Characteristics of Phosphorus in the Sediments and Overlying Water of Poyang Lake, PLoS One 10.

[6] Varol, M., and Sen, B. (2012) Assessment of nutrient and heavy metal contamination in surface water and sediments of the upper Tigris River, Turkey, CATENA 92, 1-10.

[7] Dunne, E. J., Coveney, M. F., Hoge, V. R., Conrow, R., Naleway, R., Lowe, E. F., Battoe, L. E., and Wang, Y. P. (2015) Phosphorus removal performance of a large-scale constructed treatment wetland receiving eutrophic lake water, Ecological Engineering 79, 132-142.

[8] Carpenter, S. R., Caraco, N. F., Correll, D. L., Howarth, R. W., Sharpley, A. N., and Smith, V. H. (1998) Nonpoint pollution of surface waters with phosphorus and nitrogen, Ecological Applications 8, 559-568.

[9] McCarthy, J. J., and Goldman, J. C. (1979) Nitrogenous nutrition of marine phytoplankton in nutrient-depleted waters, Science 203, 670-672.

[10] Ignatiades, L., Karydis, M., and Vounatsou, P. (1992) A possible method for evaluating oligotrophy and eutrophication based on nutrient concentration scales, Marine Pollution Bulletin 24 238-243.

[11] Kucuksezgin, F., Balci, A., Kontas, A., and Altay, O. (1995) Distribution of Nutrients and Chlorophyll-a in the Aegean Sea, Oceanologica Acta 18, 343-352.

[12] Li, D. P., Huang, Y., and Li, W. (2007) Study on remediation of city river water body by technology of aerating sediments, China Water And Wastewater (in Chinese with English Abstract) 23, 22-26.

[13] Wu, Y., Hu, J., Jin, X., Ke, P., Chen, X., and Liu, J. (2005) Chemical characteristics of nitrogen and phosphorus in the sediments of the typical bays in Dianchi Lake and calculation of their dredging layers, Journal of Environmental Science (in Chinese with English Abstract) 26, 77-80.

[14] Abrams, M. M., and Jarrell, W. M. (1995) Soil-Phosphorus as a Potential Nonpoint-Source for Elevated Stream Phosphorus Levels, Journal of Environmental Quality 24, 132-138.

[15] Tian, J. R., and Zhou, P. J. (2007) Phosphorus fractions of floodplain sediments and phosphorus exchange on the sediment-water interface in the lower reaches of the Han River in China, Ecological Engineering 30, 264-270.

[16] Xie, L. Q., Xie, P., and Tang, H. J. (2003) Enhancement of dissolved phosphorus release from sediment to lake water by Microcystis blooms - an enclosure experiment in a hyper-eutrophic, subtropical Chinese lake, Environmental Pollution 122, 391-399.

[17] Worsfold, P. J., Gimbert, L. J., Mankasingh, U., Omaka, O. N., Hanrahan, G., Gardolinski, P. C. F. C., Haygarth, P. M., Turner, B. L., Keith-Roach, M. J., and McKelvie, I. D. (2005) Sampling, sample treatment and quality assurance issues for the determination of phosphorus species in natural waters and soils, Talanta 66, 273-293.

[18] Gunduz, B., Aydin, F., Aydin, I., and Hamamci, C. (2011) Study of phosphorus distribution in coastal surface sediment by sequential extraction procedure (NE Mediterranean Sea, Antalya-Turkey), Microchemical Journal 98, 72-76.
[19] Liu, S. M., Zhang, J., and Li, D. J. (2004) Phosphorus cycling in sediments of the Bohai and Yellow Seas, Estuarine Coastal and Shelf Science 59, 209-218.
[20] Feng, S., Li, L. X., Duan, Z. G., and Zhang, J. L. (2007) Assessing the impacts of South-to-North Water Transfer Project with decision support systems, Decision Support Systems 42, 1989-2003.
[21] Tian, C., Lu, X. T., Pei, H. Y., Hu, W. R., and Xie, J. (2013) Seasonal dynamics of phytoplankton and its relationship with the environmental factors in Dongping Lake, China, Environmental Monitoring and Assessment 185, 2627-2645.
[22] Chen, S. Y., Chen, Y. Y., Liu, J. Z., Zhang, J., and Wu, A. Q. (2011) Vertical Variation of Phosphorus Forms in Core Sediments from Dongping Lake, China, 2011 3rd International Conference on Environmental Science and Information Application Technology Esiat 2011, Vol 10, Pt B 10, 1797-1801.
[23] Chen, Y. Y., Chen, S. Y., Liu, J. Z., Yao, M., Sun, W. B., and Zhang, Q. (2013) Environmental evolution and hydrodynamic process of Dongping Lake in Shandong Province, China, over the past 150 years, Environmental Earth Sciences 68, 69-75.
[24] Chen, Y. Y., Chen, S. Y., Ma, C. M., Yu, S. Y., Yang, L. W., Zhang, Z. K., and Yao, M. (2014) Palynological evidence of natural and anthropogenic impacts on aquatic environmental changes over the last 150 years in Dongping Lake, North China, Quaternary International 349, 2-9.
[25] Rand M., Greenberg A. E., and J., T. M. (1976) Standard methods for the examination of water and wastewater, Prepared and published jointly by American Public Health Association, American Water Works Association, and Water Pollution Control Federation.
[26] Loring, D., and Rantala, R. (1992) Manual for the geochemical analyses of marine sediments and suspended particulate matter, Earth-Science Reviews 32, 235-283.
[27] Soto-Jimenez, M. F., Paez-Osuna, F., and Bojorquez-Leyva, H. (2003) Nutrient cycling at the sediment-water interface and in sediments at Chiricahueto marsh: a subtropical ecosystem associated with agricultural land uses, Water Research 37, 719-728.
[28] Zhang, Z. B., Tan, X. B., Wei, L. L., Yu, S. M., and Wu, D. J. (2012) Comparison between the lower Nansi Lake and its inflow rivers in sedimentary phosphorus fractions and phosphorus adsorption characteristics, Environmental Earth Sciences 66, 1569-1576.
[29] Orr, T. B., Meister, S. M., and Halbrook, R. S. (2004) Density and sediment organic matter content as potential confounding factors in sediment toxicity tests with Hyalella azteca, Bulletin of Environmental Contamination and Toxicology 73, 371-378.
[30] Sakan, S. M., Dordevic, D. S., Manojlovic, D. D., and Predrag, P. S. (2009) Assessment of heavy metal pollutants accumulation in the Tisza river sediments, Journal of Environmental Management 90, 3382-3390.
[31] Compiling Team for Annals of Dongping County Shandong Province. (2006) Annals of Dongping County (1986-2003), Zhonghua Book Company, Beijing.
[32] Müller, G. (1981) Schwermetallbelstung der sedimente des Neckars und seiner Neben flusse: eine Bestandsaufnahme, Chemiker-Zeitung 105, 157-164.
[33] Bhuiyan, M. A. H., Parvez, L., Islam, M. A., Dampare, S. B., and Suzuki, S. (2010) Heavy metal pollution of coal mine-affected agricultural soils in the northern part of Bangladesh, Journal of Hazardous Materials 173, 384-392.
[34] He, D. J., Xing, Y. H., Jiang, R. X., and Cheng, L. (2010) Distribution of Nitrogen and Phosphorus in Water and Eutrophication Assessment of Dongping Lake Environmental Science & Technology (in Chinese with English Abstract) 8, 10-13.
[35] Jiang, D., Liu, C., Liu, G., Wang, W., and Liu, J. (2002) Analysis of water environment in Dongping Lake and its vicinity, Trans Oceanol Limnol 4, 12-15.
[36] Pang, Q., Ge, H., Ji, L., and Wang, W. (2008) Study on main factors affecting water quality of Dongping Lake (in Chinese with English Abstract), Yellow River 30, 50-55.

Received: **19.06.2015**
Accepted: **18.04.2016**

CORRESPONDING AUTHOR

Zhibin Zhang
College of Municipal and Environmental Engineering,
Shandong Jianzhu University,
Jinan 250101, China

e-mail: sdzyh66@126.com

© by PSP Volume 25 – No. 7/2016, pages 2278-2283 Fresenius Environmental Bulletin

DYNAMICS AND ENERGY TRANSFER OF AMMONIA STRIPPING BY GRANULAR ACTIVATED CARBON UNDER MICROWAVE RADIATION

Li Peng *, Linlong Hu

Sichuan College of Architecture Technology ,Deyang, , China (618000)

ABSTRACT

Removal of ammonia in a batch reactor using granular activated carbon (GAC) and microwave (MW) radiation proceeded via stripping as the principal mechanism. The removal rates were below the theoretical values of $NH_3 \cdot H_2O$ across the pH range studied. Higher removal rates were achieved at higher GAC dosages. Conversely, the initial concentration of ammonia nitrogen (500–5000 mg/L) minimally influenced the removal rate. Dynamics studies showed that the process followed first-order kinetics in two sections of the mass transfer process, with coefficients K_1 (0–1 min) and K_2 (1–6 min) that were higher than that associated with conventional stripping. Furthermore, K_1 was larger than K_2 owing to rapid solution temperature increases during the first 1 min of MW irradiation. Under MW irradiation, the porous surface of GAC in solution generated numerous small steam bubbles continuously that assisted the removal of ammonia in solution. Furthermore, owing to the porous structure of GAC and steam bubble production, GAC offered a more efficient path of energy transfer from MW to liquid that enhanced the heat transfer efficiency from MW power to heat. Hence, the combined use of MW irradiation and GAC is less energy intensive than the use of MW irradiation solely.

KEYWORDS:
ammonia nitrogen, dynamic, energy transfer, granular activated carbon, microwave

INTRODUCTION

Ammonia nitrogen in high concentrations is commonly present in landfill leachate and wastewater from the coke, tannery, and textile industries, as well as in plant fertilizers [1]. The resulting low C/N ratio leads to the suppression of microorganism activity in biological treatment systems[2、3].

Stripping is universally applied in the pretreatment of ammonia-rich wastewater owing to its efficiency and stability. However, stripping is an energy-intensive and expensive process because it requires heating and aeration. In contrast, the use of microwave (MW) irradiation towards the removal of ammonia in solution has led to sound results [4、5]. The removal of ammonia in solution using MW irradiation is known to operate via a primary air-stripping mechanism [6]. Carbon is known to generate high temperature increases in surrounding media when exposed to MW radiation [4]. Moreover, it was demonstrated in a patent [5]that the combined use of MW irradiation and activated carbon powder results in a rapid response and high efficiency[6] when compared with other stripping methods. For ease of separation following treatment, granular activated carbon (GAC) was used as a fixed bed [7] and continuous flow through the system was obtained. The results showed that the system was effective and achieved consistently high ammonia removal efficiencies of 94% without additional aeration.

In this study, the effect of pH, irradiation time, and concentration and amount of GAC was investigated in batch reactor mode. Subsequently, dynamics studies on the removal of ammonia by MW and GAC combined technology (MW-GAC) were conducted. The high ammonia removal efficiencies using MW-GAC were ascribed to the production of steam bubbles and efficient energy transfer paths generated during the process.

MATERIALS AND METHODS

GAC obtained from walnut shells[8]was washed and oven dried at 378 K prior to use. The removal rates of ammonia in solution using GAC

and MW irradiation were studied. Studies investigating the effects of various parameters (e.g., pH, irradiation time, and dosage of GAC) on the removal rates of ammonia in solution as well as the dynamics of the process were conducted using the set up shown in Fig. 1.

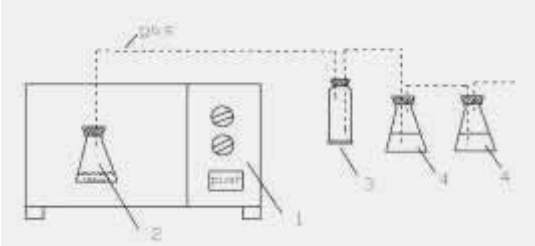

FIGURE 1
Schematic of the MW-GAC system.
1: microwave oven; 2: reaction flask; 3: breath bottle; and 4: off-gas treatment system.

A microwave oven with a microwave chemistry reactor (MCL-2, 500 W, 2450 MHz) was used as the MW source. In a typical experiment, a solution (100 mL) containing a known amount of GAC was introduced onto the reactor for a predetermined amount of time. The off-gas diffused through two conical flasks containing 100 mL 0.5 M H_2SO_4 to collect ammonia in the gas phase. The breath bottle was used to prevent back-flow of the liquid to the reactor when the MW irradiation was turned off. The temperature of the solution in the flask in the presence and absence of GAC following MW irradiation was measured.

RESULTS AND DISCUSSION

Effect of pH. Because the ammonia nitrogen removal efficiency is highly sensitive to pH changes, the effect of pH was first examined. The ammonia nitrogen removal rates using MW irradiation solely and the MW-GAC system were measured as a function of pH as shown in Fig. 2. For comparison purposes, the theoretical values are also presented [9].

As observed from Fig. 2, with increasing pH values, the removal rate increased significantly. The equilibrium between soluble ammonium ions NH^{4+} and dissolved molecular ammonia NH_3 in wastewater is determined mostly by pH[9]. The equilibrium reaction is shown in Equation 1 and the associated NH_3 distribution coefficient, α_{NH3}, can be calculated using Equation 2 as follows:

$$NH_3 + H_2O \leftrightarrow NH_4^+ + OH^- \qquad (1)$$

$$\alpha_{NH_3} = \frac{[NH_3]}{[NH_3]+[NH_4^+]} \qquad (2)$$

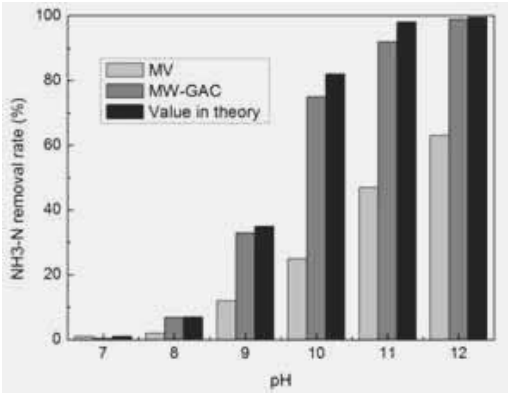

FIGURE 2
Removal rates of NH_3-N by MW and MW-GAC as a function of pH, theoretical values are also presented.

High pH values favor ammonia volatilization by shifting the position of the equilibrium of the reaction shown in Equation 1 to left. At pH 11, 98.2% of ammonia nitrogen in the form of NH_3 is expected in theory. As observed, this value was consistent with the ammonia removal rate of 94% achieved by the MW-GAC system, which was considerably higher than that achieved using the MW system (i.e., 50%). The same trend was obtained at the other studied pH conditions. According to literature studies [10], the MW system can achieve higher removal rates of 90% in the presence of aeration and under adequate reaction times. Thus, these findings indicate that the principal mode of ammonia removal using either the MW-GAC or MW system is via stripping. However, the removal efficiency achieved by the MW-GAC system is considerably higher than that achieved by the MW system.

A solution pH of 11 was selected in the subsequent studies. Moreover, pH 11 is typically used in the industry and research studies. Additionally, pH 11 is commonly selected because it is the optimal pH in terms of both performance efficiency and economical considerations.

Effect of GAC amount. GAC is an important component of the MW-GAC system. The amount of GAC in solution influences temperature increases and steam generation. Variations in the NH_3-N removal rate and reaction temperature as a function

of irradiation time and amount of GAC are showed in Fig. 3.

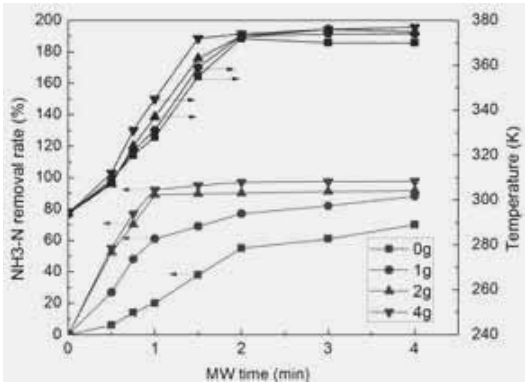

FIGURE 3
Variations in the NH_3-N removal rate and reaction temperature as a function of irradiation time and amount of GAC.

It is widely known that high aqueous solution temperatures result in low solubility of NH_3-N. Although carbon can absorb microwave irradiation and subsequently increase the solution temperature rapidly, a delay is observed at the early stages of the process because of initial heat removal by water. Consequently, a temperature difference as a function of GAC dosage was not obvious in the first 0.5 min of the reaction. In contrast, very minor temperature variations were observed as the dosage of GAC varies within a reaction time period of 0.5–1.5 min. Conversely, distinct ammonia nitrogen removal rate variations were noted at the early stages of the reaction. These findings indicate a discrepancy between the temperature difference and removal rates achieved.

This discrepancy was attributed to the means of heat transfer to the liquid i.e., via steam bubbles, which facilitated the removal/stripping of molecular ammonia. The higher the content of GAC in the system, the higher the content of generated steam bubbles, and consequently the higher the removal rates of ammonia nitrogen. Fast removal of ammonia at the early stages of the process was attributed to the combined temperature rise of water and steam bubble production in the presence of GAC.

Based on the conditions used herein (i.e., 100 mL solution), a GAC dosage of 2 g was chosen as the most economical amount to achieve high nitrogen removal rates. Higher dosages of GAC would instigate further steam production and liquid evaporation, leading to lower concentrations of condensate.

Effect of initial concentration. Here, the removal rates of ammonia using the MW-GAC system at different initial ammonia concentrations were investigated, and the results are shown in Fig. 4.

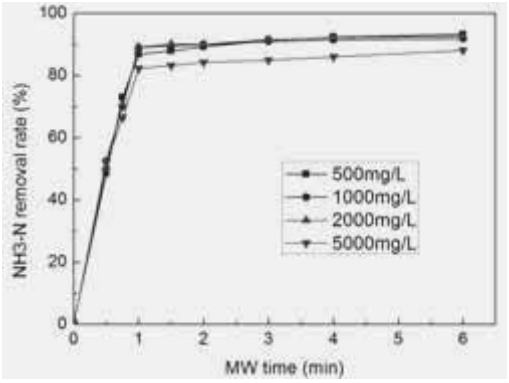

FIGURE 4
Removal rates of NH_3-N as a function of irradiation time and initial ammonia concentration.

As observed from Fig. 4, significant ammonia removal rates using the MW-GAC system were achieved even at a high initial ammonia concentration of 5000 mg/L. At high solution concentrations, with the escape of molecular NH_3, pH decreases, which limits the maximum removal rate. Concurrently, high concentrations of $NH_3 \cdot H_2O$ facilitate contact between steam and air that consequently leads to slight increases in the removal rate[11]. However, in the current MW-GAC system, no contact issues are expected owing to the onset of strong turbulence upon mixing of the GAC and MW components. As a result, increasing the initial concentration to 10-fold led to a slight decrease (of ~6%) in the removal efficiency.

The experimental results suggest that unlike the effect of pH, irradiation time, and amount of GAC, the effect of initial ammonia concentration was relatively small.

Dynamics of ammonia removal by MW-GAC. Ammonia removal by MW-GAC can be described as a mass transfer process, involving water evaporation [12] and an air-stripping mechanism[13]. At a given GAC dosage and pH, the concentration of NH_3 at different reaction times can be expressed as follows:

$$\ln(\frac{C_1}{C_2}) = -KF(t_1 - t_2) \quad (3)$$

where C_1 and C_2 denote the concentration of NH_3 at time t_1 and t_2, respectively; t_2 is no greater than the value required for obtaining C_2 that is equivalent to the theoretical value at a given pH.

Assuming that the reaction follows first-order kinetics, i.e., NH_3 converts into the gas phase from liquid under the action of MW-GAC, K is a constant, as deduced by the slopes of the curves shown in Fig. 5.

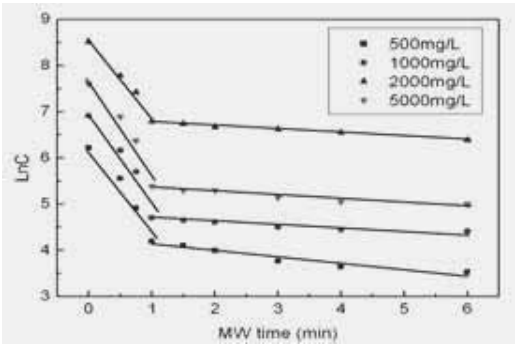

FIGURE 5
Relationship between ln C and t at different initial concentrations.

Analysis of the kinetics data reveals that the mass transfer coefficient K values obtained at varying initial concentrations were relatively stable and comparable in the range of 0–1 min (K_1). The mass transfer coefficient K values obtained in the range of 1–6 min (K_2) were smaller when compared with K_1. The results are summarized in Table 1.

The discrepancy between K_1 and K_2 was influenced by the temperature of the liquid. At the early stages of the reaction (i.e., 0–1 min), the rise in the temperature of water and stripping of small bubbles occurred simultaneously. As a result, the solubility of NH_3-N decreased with increases in the temperature, consequently leading to K_1 values that were higher than K_2 values. K_2 mainly reflects the bubbling process as the temperature of water was as high as 363 K at 1 min of reaction.

K values were associated with other stripping processes (e.g., air-stripping, steam-stripping, and stripping tower) at a pH 11 range between 0.0016 and 0.0033 min^{-1} [13、14], which are considerably lower than K_1 and K_2 obtained here using the current MW-GAC system. K values in the literatures were measured within a certain temperature range(like 20-80℃), with air or steam stripping as the main mode of removal mechanism. Hence, they were comparable to K_2 obtained herein instead of K_1, which reflects the temperature and bubbling.

Energy transfer path. Bubble evolution from the porous surface of GAC is schematically shown in Fig. 6.

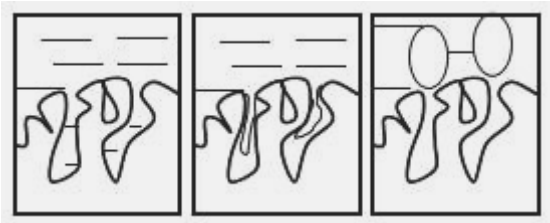

FIGURE 6
Schematic of bubble generation on the porous surface of GAC.

The cyclic process involves three steps: (1) upon prompt heating of GAC by MW, the liquid nearby evaporates, leading to the formation of small steam bubbles; (2) the bubbles grow and finally escape the pores; (3) as a result, a vacuum is created in the pores that forces the liquid into the pores. Bubbling in the MW-GAC system can assist

TABLE 1
Mass transfer coefficient K and corresponding coefficient of determination (R^2)

Initial concentration (mg/L)	K_1 (min^{-1}) (R^2) (0–1 min)	K_2 (min^{-1}) (R^2) (1–6 min)
500	1.988 (0.961)	0.137 (0.922)
1000	2.094 (0.936)	0.060 (0.896)
2000	1.672 (0.983)	0.077 (0.982)
5000	2.111 (0.935)	0.079 (0.909)

with removing ammonia nitrogen in solution as well as enhancing the efficiency of energy transfer by increasing the contact interface between steam and liquid.

Though the test results indicate that the MW-GAC system is effective for removing ammonia, analysis of the associated energy consumption is necessary to determine the practical application of this technology. The energy transfer paths and efficiency of the MW-GAC and MW systems were compared (the MW system is more energy efficient than the traditional steam-stripping method, as reported [9]). The energy transfer paths and efficiency of the MW-GAC and MW systems are shown in Fig. 7.

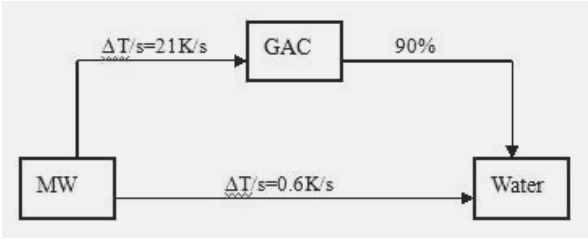

FIGURE 7
Energy transfer paths and efficiency of the MW-GAC and MW systems.

As observed from Fig. 7, GAC can absorb MW and subsequently induce a temperature rise per unit of time that was higher (i.e., 21 K/s) than that generated by water (i.e., 0.6 K/s) under exposure of MW irradiation only [15] at the same given weight; this corresponds to a 35-fold increase. Compared with the MW system, the MW-GAC system involves an additional heat transfer step from GAC to water; however, only 10% of heat loss was noted during the heat-transfer process. The coefficient of boiling heat transfer from a porous surface was 2-to10-fold higher than that of conventional heat transfer, resulting in high heat transfer efficiencies of up to 90% [16]. Thus, it can be deduced that the MW-GAC system was less energy intensive than the MW system towards the removal of ammonia.

In the batch system, a small amount of GAC or a short reaction time was used to prevent complete evaporation of water to maximize the energy-saving effect. As observed from Fig.2, in general, the temperature of the liquid in the combined presence of MW irradiation and GAC was slightly higher than that observed in the presence of MW only. However, a slight delay in the temperature rise was observed in the MW-GAC system because GAC required some time to heat up. This finding is consistent with the energy-transfer paths and efficiency obtained for the GAC-MW and MW systems.

CONCLUSION

Ammonia nitrogen removal by MW-GAC was deduced to proceed via a stripping mechanism because the removal rates remained below the theoretical values under the range of pH studied. Higher dosages of GAC led to higher ammonia nitrogen removal rates. In contrast, the initial concentration of ammonia nitrogen had minimal influence on the ammonia nitrogen removal rate. Additionally, the dynamics of ammonia removal process using the MW-GAC system was examined. The process followed a first-order kinetics, with two associated mass transfer coefficients of K_1 (0–1 min) and K_2 (1–6 min). The mass transfer coefficients obtained here were considerably higher than that of conventional stripping. Furthermore, K_1 was significantly higher than K_2 owing to the rapid solution temperature rise within the first 1 min of reaction that helped decrease the solubility of ammonia in solution.

Additionally, bubbling in the MW-GAC system contributed to the removal of ammonia in solution and heating of water by a boiling heat-transfer process on the porous surface of GAC. The presence of GAC in the MW system generated an additional path for energy transfer between MW and liquid. Accordingly, the current system is less energy intensive than the MW system towards ammonia stripping owing to the strong MW absorption ability of GAC and efficient boiling heat transfer.

REFERENCES

[1] Jung, J. Y., Chung, Y. C., Shin,H. S., Son,D. H., Enhanced Ammonia Nitrogen Removal Using Consistent Biological Regeneration and Ammonium Exchange of Zeolite in Modified SBR Process, Water Res. 2004, 38, 347–354

[2] Mecler, H.,Nutt,S., Marvan, I., P. Sutton.,Combined Treatment of Coke Plant Wastewater and Blast Furnace Blow Down Water in a Coupled Biological Fluidized Bed System, J. Water Pollut. Control Fed 1984, 56, 192–198.

[3] Y. Qian, Y. Wen, H. Zhang, Efficiency of Pretreatment Methods in the Activated Sludge Removal of Refractory Compounds in Coke-plant Wastewater, Water Res.1994, 28, 701–710.
[4] Ania,C. O., Menendez,J. A., Parra,J. B., Pis, J. J., Microwave Induced Regeneration of Activated Carbons Polluted with Pheno1. Carbon 2004,42, 1383—1387.
[5] Yao,Y., Zhou,J., Gao, L., Method for Treating Ammonia Nitrogen Waste-water. Chinese patent 2013,102001721.
[6] Lin, L., Yuan ,S. H., Chen, J., Xu, Z. Q., Lu, X. H., Removal of ammonia nitrogen in wastewater by microwave radiation. J. Hazard. Mater 2009, 161, 1063– 1068.
[7] Peng, L., Chen,,Y., Jiang, W. J., Removal of Ammonia Nitrogen by Granular Activated Carbon and Microwave Radiation (GAC-MW) , Fresenius Environ. Bull 2013, 22(10a), 3053-3058.
[8] Chen, J., Chen, Y., Jiang, X., Peng, J. F., Jiang,W.J., Characterization of Pyrolusite-modified Activated Carbon Prepared from Walnut Shell and the Application of Flue Gas Desulfurization. Fresenius Environ. Bull 2012, 21, 2901-2907
[9] Lin, L. Chan, G.Y.S., Jiang, B.L., Lan, C. Y., Use of Ammonia Nitrogen Tolerant Microalgae in Landfill Leachate Treatment. Waste Manage. (Oxford) 2007, 27, 1376–1382.
[10] Lin, L. , Chen,J. , Xu, Z. Q., Yuan,S. H. , Cao,M. H. , Liu,H. C., Lu,X. H., Removal of ammonia nitrogen in wastewater by microwave radiation: A pilot-scale study. J. Hazard. Mater 2009, 168, 862-867
[11] Huang,H. M., Xiao,X. M., Yan,B., Experimental Research on Treatment of Ammonia Nitrogen Wastewater by Ammonia Stripping in a Rare Earths Separation Factory, Chin. J. Environ. Eng. 2008, 2(8), 1062-1065
[12] Tahmasebi,A., Yu,J. L., Han, Y. N., Zhao, H., Sankar, B. C., A kinetic Study of Microwave and Fluidized-bed Drying of a Chinese Lignite, Chem. Eng. Res. Des.2014, 91(1), 54-56
[13] Shen,Y. L., Wang,B. Z., Dynamics and mechanism of ammonia removal by stripping. Pollut. Control Technol. 1999, 12(2), 67-71
[14] Smith, P. G., Arab, F. K., The Role of Air Bubbles in the Desorption of Ammonia from Landfill Leachates in High pH Aerated Lagoon. Water Air Soil Poll. 1988, 38(3-4), 333-343
[15] Jin, Q. H., Dai,S.S., Huang, K. M., Microwave Chemistry, Science Press, Beijing 1999, p. 13-16.
[16] Chen, Z. X., Study on Dynamics of Enhanced Boiling Heat Transfer of the Powder Porous surface, Chemical Engineering (China) 1996,24 (4), 47-53

Received: **09.07.2015**
Accepted: **07.12.2015**

CORRESPONDING AUTHOR

Li Peng
College of Architectural Technology, Deyang 618000, China

Email: pengli_120@163.com;

by PSP Volume 25 – No 7/2016, pages 2284-2291 Fresenius Environmental Bulletin

POLLUTION SOURCES OF GROUNDWATER QUALITY IN THE BASEMENT ROCKS IN OYO STATE, NIGERIA, USING MULTIVARIATE STATISTICS

[1]Awomeso J Awonusi, *[2]Taiwo A Matthew, [1]Alade-Dauda Omolara F, [2]Ojekunle Z Oluseyi , [2]Oyebanji F Funmilola, [1]Ayantobo O Olusola, [3]Taiwo O Tunrayo

[1]Department of Water Resources Management and Agrometeorology,
[2]Department of Environmental Management and Toxicology,
[3]Department of Pure & Applied Zoology,
Federal University of Agriculture, PMB 2240, Abeokuta, Ogun State, NIGERIA.

ABSTRACT

The study was carried out to identify the likely sources of groundwater pollution in the basement rocks of eight (8) Local Government Areas in Oyo State, Southwestern, Nigeria. Groundwater data between 2008 and 2009 were collected from the Water and Sanitation Department of Oyo State Water Corporation. The multivariate statistical technique of Principal Component Analysis (PCA) was applied to the collected groundwater information using SPSS statistical package version 16.0. The results of chemical parameters of groundwater showed high concentrations of calcium, nitrate and bicarbonate ions. Fe was also observed at high concentration in the groundwater samples. The multivariate analysis of PCA applied for source identification of potential groundwater pollution revealed sources including anthropogenic, geological (bedrock weathering), nutrients and thermal/industrial. The Piper diagram showed an abundance of calcium in the cationic region and bicarbonate in the anionic region. The results of groundwater analysis indicated that treatments may be required for the analysed groundwater to be suitable for drinking.

KEYWORDS:
groundwater quality, source identification, piper diagram, sodium adsorption ratios

INTRODUCTION

Groundwater is widely accepted as the pure form of water in relation to surface water due to its purification in the soil column through anaerobic decomposition, filtration and ion exchange [1]. It is therefore being excessively consumed in most rural and semi-urban areas of the world (www.waset.com). In areas where other sources of water supply are inadequate or lacking; groundwater has been utilized for agricultural purposes and other human activities. In Southwestern Nigeria, groundwater is exploited through sinking of boreholes and hand-dug wells [2-4]. However, the cost of construction of boreholes in Nigeria is very high; this therefore makes its availability to those who are financial capable [5]. The greater numbers of poor masses rely on shallow hand-dug wells for daily supply of domestic and drinking water. Shallow hand-dug wells are often contaminated or poorly managed in a non-hygienic way [3, 6]. This may increase the outbreak of water-borne diseases [6-7].

The necessity of assessing the quality of groundwater resources in Nigeria is therefore essential. The physical and chemical properties of groundwater are highly dependent on the basement rocks, which act as an aquifer for underground water [8]. The chemical characteristics of groundwater also depend on water chemistry in the recharge area and the different geochemical processes that are occurring in the subsurface [9-10]. Geochemical processes influence the seasonal and spatial variations, and the chemistry of subsurface water [11]. Substantial number of published studies have examined and discussed the conditions of groundwater in Southwestern Nigeria. Some of these studies were carried out in major cities including Abeokuta, Ifo, Agbabu, Sango, Agbara, Ibadan and Lagos [3-4, 6, 12-15]. In these studies, only few authors have applied multivariate statistics to identify sources of pollutants to groundwater [4, 12]. The main objective of this study is application of multivariate statistical method for identification of pollution sources to groundwater resource in Oyo State.

MATERIALS AND METHODS

Geological description of the study areas. Oyo State lies mostly on lowland punctuated by rocky outcrops and hills. Most of the outcrops are

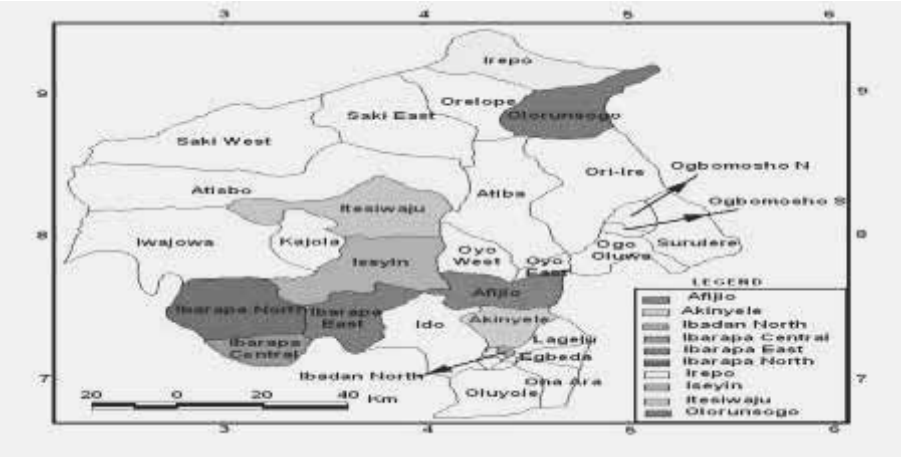

FIGURE 1
Map of Oyo State showing the study Local Government Areas

mainly schist and quartzite inselbergs [16]. The State is mostly covered by the Pre-Cambrian igneous and metamorphic rocks, which extend to Ilorin, Kabba and Ondo [16]. The older granites have resulted in smooth domed inselbergs, particularly in areas around Iseyin, Igbeti and the greater parts of Oyo North [16].

Data collection. Data on physical and chemical parameters of groundwater from the study areas were obtained from the Water and Sanitation Department of Oyo State Water Corporation, Southwest Region, Nigeria. Parameters of interest were pH, temperature, electrical conductivity (EC), Na^+, K^+, Ca^{2+}, Mg^{2+}, SO_4^{2-}, NO_3^-, PO_4^{3-}, Cl^-, HCO_3^-, Fe and Mn. The datasets covered the groundwater information from 100 boreholes located in Ibadan North, Ibadan Northwest, Ibadan Southeast, Akinyele, Iseyin, Ibarapa North, Ibarapa Central and Ibarapa East Local Government Areas (LGAs), which lies within the crystalline basement rock area of Oyo state.

Data Analysis. Groundwater data were evaluated for descriptive statistics and Pearson's correlation coefficient using SPSS for Windows version 16.0. Multivariate analysis of PCA was also carried out with SPSS. Piper plot was developed from the data using Aquachem 4.0 software package.

RESULTS AND DISCUSSION

Figure 2 shows the box plots of groundwater quality parameters in the study areas. As stated earlier, groundwater data collected from eight (8) Local Government Areas (LGAs) were analyzed and merged into six LGAs. Data collected from the LGAs in Ibadan were merged together. The results presented in the box plots revealed lowest median concentrations of most parameters in Iseyin (except electrical conductivity and Na^+). Elevated median concentrations of Fe and SO_4^{2-} were observed at Akinyele LGA. Almost all the water parameter data of the study areas appeared to have their ranges within the World Health Organization (WHO) permissible limits in drinking water. However, the range concentrations of Fe and NO_3^- were greater than the WHO limits of 0.3 and 10 mg/L, respectively. There is a less concern about Fe concentration in water since its guideline was not health-based [17]. But the detrimental health effects of NO_3^- have been severally discussed in published studies [3-4, 6, 18]. High nitrate concentration in groundwater samples in these study areas therefore calls for serious health concerns, especially in children. Nitrate pollution is a serious water quality issue in the Southwestern Nigeria [4]. Urgent actions needed to be taken by the Health Authorities in these Local Government Areas. One of the major sources of nitrate in groundwater aquifers in the Southwestern Nigeria may be related to leachates of numerous septic tanks constructed all over their cities and towns [14].

Table 2 shows the summary of the physical and chemical parameters in all the study areas. The average concentrations of Fe, Mg^{2+} and NO_3^- were higher than the WHO permissible limits in drinking water. Data of other parameters lied within the WHO standards. The mean fluoride concentration (0.66±0.73 mg/L) of the groundwater was found in the normal range that would not initiate health problems. Fluoride concentration below 0.5 mg/L has the tendency of destroying bone and teeth structures [19-21]. On the other hand, elevated fluoride greater than 1.5 mg/L may result into

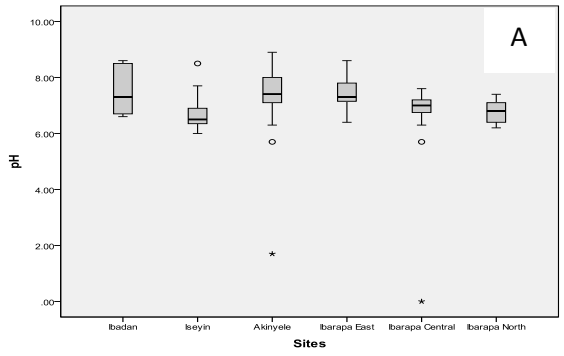
A
pH
10.00
8.00
6.00
4.00
2.00
.00
Ibadan
Iseyin
Akinyele
Ibarapa East
Ibarapa Central
Ibarapa North
Sites

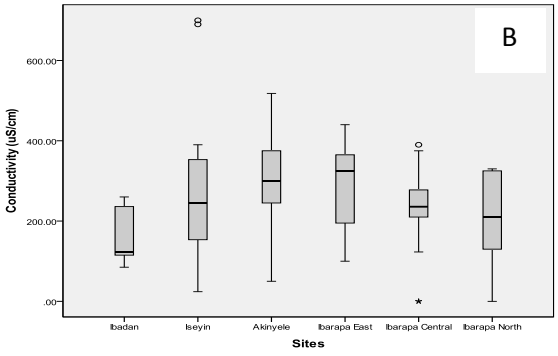
B
Conductivity (uS/cm)
600.00
400.00
200.00
.00
Ibadan
Iseyin
Akinyele
Ibarapa East
Ibarapa Central
Ibarapa North
Sites

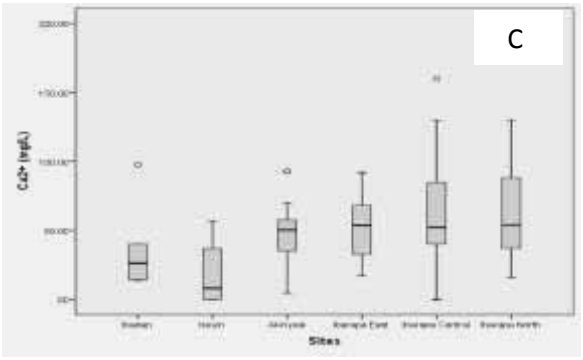
C
Ca2+ (mg/L)
Sites

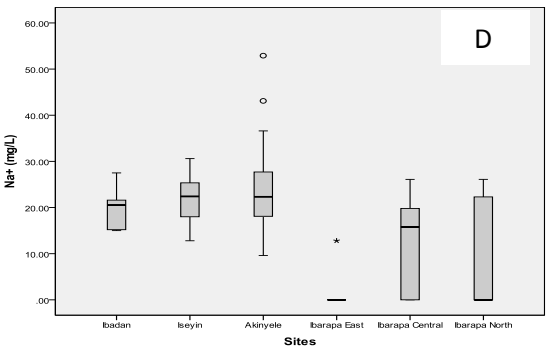
D
Na+ (mg/L)
60.00
50.00
40.00
30.00
20.00
10.00
.00
Ibadan
Iseyin
Akinyele
Ibarapa East
Ibarapa Central
Ibarapa North
Sites

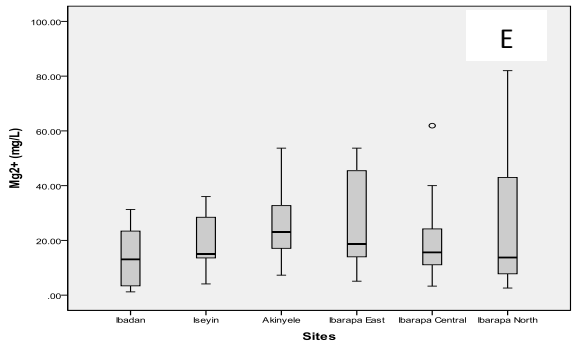
E
Mg2+ (mg/L)
100.00
80.00
60.00
40.00
20.00
.00
Ibadan
Iseyin
Akinyele
Ibarapa East
Ibarapa Central
Ibarapa North
Sites

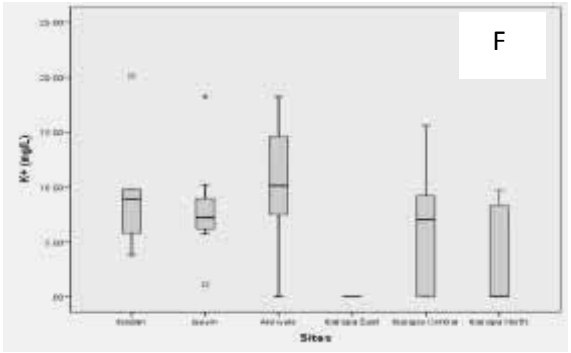
F
K+ (mg/L)
Sites

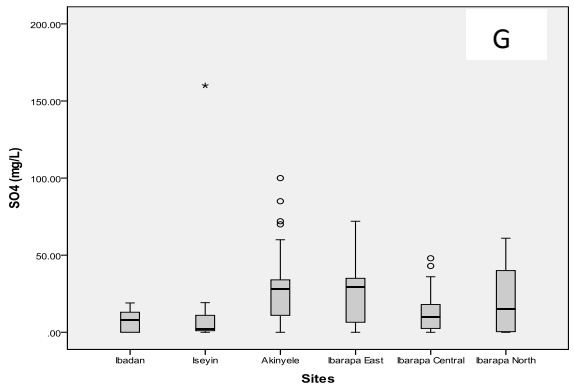
G
SO4 (mg/L)
200.00
150.00
100.00
50.00
.00
Ibadan
Iseyin
Akinyele
Ibarapa East
Ibarapa Central
Ibarapa North
Sites

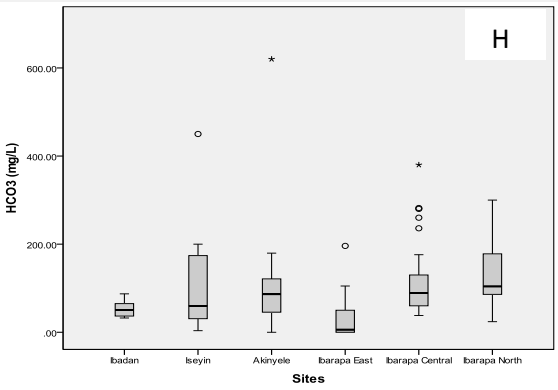
H
HCO3 (mg/L)
600.00
400.00
200.00
.00
Ibadan
Iseyin
Akinyele
Ibarapa East
Ibarapa Central
Ibarapa North
Sites

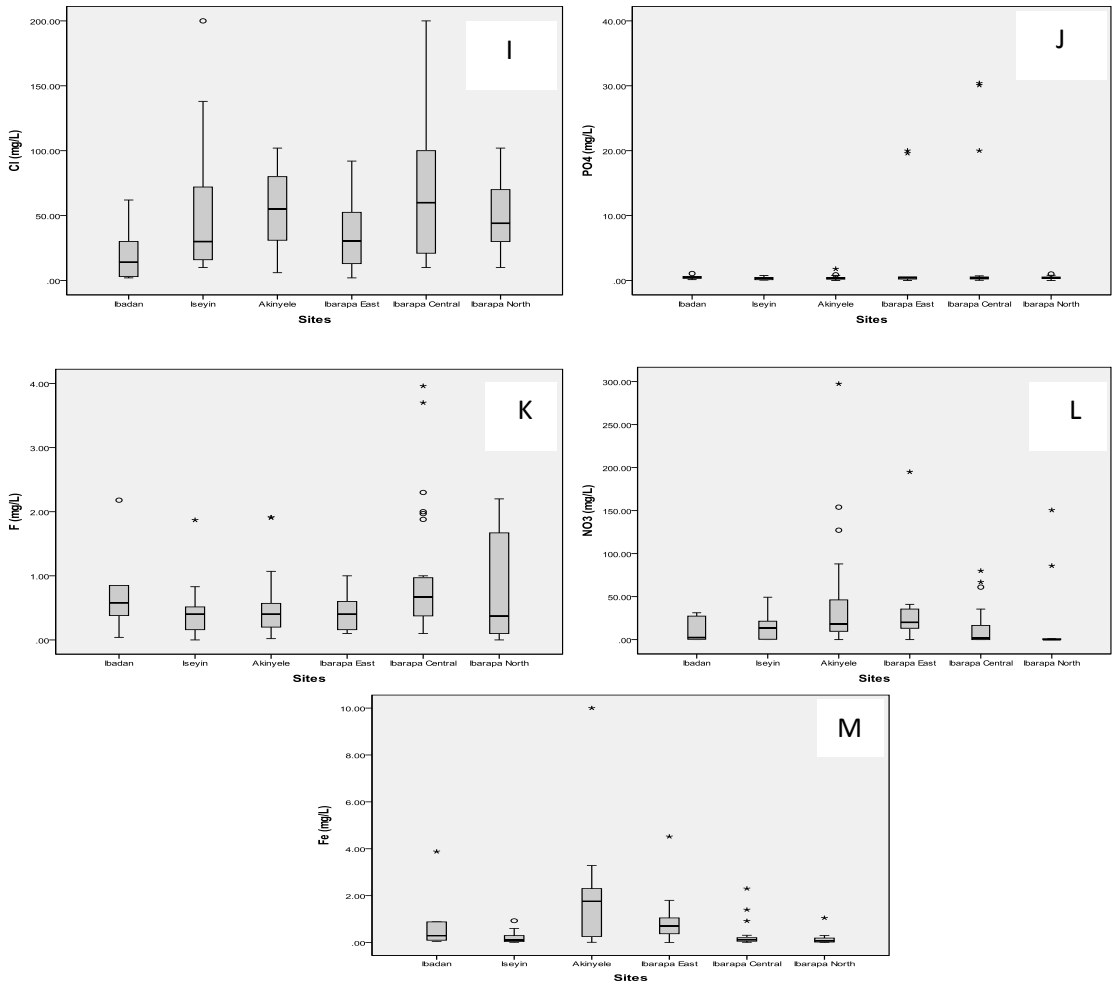

FIGURE 2
Box plots of groundwater parameters observed in the basement rocks of Oyo State. The horizontal line in the middle of the box represents the median while the lower and upper lines of the box are 25th and 75th percentiles, respectively. The whiskers on top and below the box represent the maximum minimum values, respectively. The circles and asterisks represent the outlier values

TABLE 2
The pooled mean concentrations of groundwater quality of Oyo basement rocks

Parameter	Mean	Range	WHO (2013)
pH	7.07±1.15	0.0-8.90	6.5-8.5
EC (µS/cm)	263.10±127.96	0.0-700	1000
Ca^{2+} (mg/L)	50.41±31.21	0.0-160	75
Mg^{2+} (mg/L)	23.03±1.59	1.20-82	0.20
Na^{+} (mg/L)	16.02±11.85	0.0-52.90	200
K^{+} (mg/L)	6.88±5.62	0.0-20.10	NA
SO_4^{2-}(mg/L)	21.53±24.56	0.0-160	100
HCO_3^{-} (mg/L)	101.39±98.16	0.0-620	NA
Cl^{-} (mg/L)	54.89±41.96	2.00-200	250
PO_4^{3-} (mg/L)	1.56±5.31	0.0-30.40	NA
F^{-} (mg/L)	0.66±0.73	0.0-3.69	1.5
NO_3^{-} (mg/L)	26.47±44.93	0.0-297.40	10
Fe (mg/L)	0.89±1.37	0.0-10	0.3

NA- Not Available

dental and skeletal fluorosis, and bone deformation in children and adults [22].

Table 3 presents the results of PCA conducted on the pooled groundwater data from the study areas. The percentage of variability of dataset

TABLE 3
Rotated Principal Component Analysis of the Basement Groundwater Samples

	Component							
	1	2	3	4	5	6	7	Communalities
Depth	.041	-.232	.351	-.301	.008	.104	-.637	**.686**
Temperature	.041	.002	.174	-.235	.126	.029	**.761**	**.683**
pH	.022	.071	.036	-.009	**.797**	.053	.055	**.648**
TDS	**.879**	-.031	-.016	.063	.081	-.087	-.094	**.800**
Conductivity	**.902**	.163	.015	-.068	.046	.032	.102	**.859**
Ca^{2+}	-.036	-.205	.358	**.790**	-.108	.111	.003	**.820**
Mg^{2+}	.178	-.077	-.330	**.742**	.153	-.089	-.112	**.741**
Na^{+}	.142	**.847**	-.039	-.168	.013	.022	.071	**.773**
K^{+}	-.050	**.853**	.092	-.050	.064	.098	.081	**.761**
SO_4^{2-}	.463	.018	.026	.285	.474	.069	.144	**.547**
HCO_3^{-}	.272	.020	**.604**	-.013	.196	.201	.030	**.519**
Cl^{-}	**.520**	.030	.349	.229	-.384	.046	-.082	**.603**
PO_4^{3-}	-.113	-.472	-.011	.061	-.341	**.595**	.243	**.769**
F^{-}	-.002	.169	**.730**	.106	-.131	-.237	.022	**.647**
NO_3	.214	.373	**-.524**	.196	-.049	.141	.052	**.523**
Fe	.020	.287	-.102	-.004	.203	**.790**	-.126	**.774**
% Variance	14.2	12.8	10.7	9.7	8.0	7.2	7.1	(70%)

varied from 7.1 to 14.2%; while 70% of the total dataset was explained by the seven factors identified. Factor 1, with the higher percentage of variance of 14.2% was highly significant for TDS, conductivity and chloride (Cl^-). High concentration of chloride in water may be traced to runoff of contaminants from domestic wastes, landfill leachates, percolation of sewage from septic tanks, industrial effluents and animal feeds [4, 23]. Edet and Worden [24] have attributed elevated concentration of EC, TDS and Cl^- in surface water sampled in Calabar to tidal flushing. The influence by tidal flushing may not be feasible in respect to the mobilization of these substances into the groundwater sampled in this study. This factor may be best designated anthropogenic source. Factor 2 has high significant loadings for Na^+ and K^+, this source is probably a marine source [4]. As explained in component 1, intrusion of saline water into the sampled groundwater aquifer in these areas is out of context. Na^+ and K^+ occurrence may also be linked to soil components [25]. This source might suggest a bedrock weathering [4]. Factor 3 is characterized by high loadings for HCO_3^-, F^- and NO_3^-. This factor may be described as a nutrient source from infiltration of sewage from septic tanks and agricultural runoff into the groundwater resource. Intensive agricultural practices including heavy use of N-fertilizer may lead to enrichment of groundwater with NO_3^- [26].

Fluoride pollution in groundwater may similarly occur as a result of sewage infiltration [27]. The main factors controlling the concentration of fluoride are climate and accessory minerals in the rock mineral assemblage through which the groundwater is circulating [28]. Factor 4 has high positive loadings for calcium (Ca^{2+}) and magnesium (Mg^{2+}) indicating a hardness source from the underlying bedrock (4). Factor 5 is positively significant for pH only, which might suggest the bedrock weathering source. pH is an important factor that regulates the geochemical equilibrium or solubility of substances in groundwater [29, 30]. Factor 6 has high significant values of PO_4^{3-} and Fe indicating a nutrient source. Phosphate is majorly emanated from nutrient sources, while Fe in the groundwater may originate from natural (bedrock weathering) and/or anthropogenic sources (e.g. from faecal contamination, industrial and vehicular emissions) [4]. Feacal pollution is a major contaminant in both surface and groundwater resources in Nigeria [31, 32]. Factor 7 has a high loading for temperature, which could be as a result of thermal pollution source or industrial discharges [4]. This source is anti-correlated with the depth of the sampled groundwater resources. This indicates that, as the depth increases, temperature decreases. The shallow nature of the wells might also expose the groundwater to thermal pollution.

Figure 4 shows the Piper diagram of groundwater samples in the study area. In the cation trilinear region, it was observed that 70% of the points (Akinyele, Ibarapa Central, Ibarapa North, Ibadan Northwest, Ibadan North, Iseyin, Ibadan southeast and Ibarapa East) lied within the Ca^{2+} axis. This showed the significance and abundance of calcium ion in water samples collected from the different sampling sites with respect to geological formations within the region while 20% of the

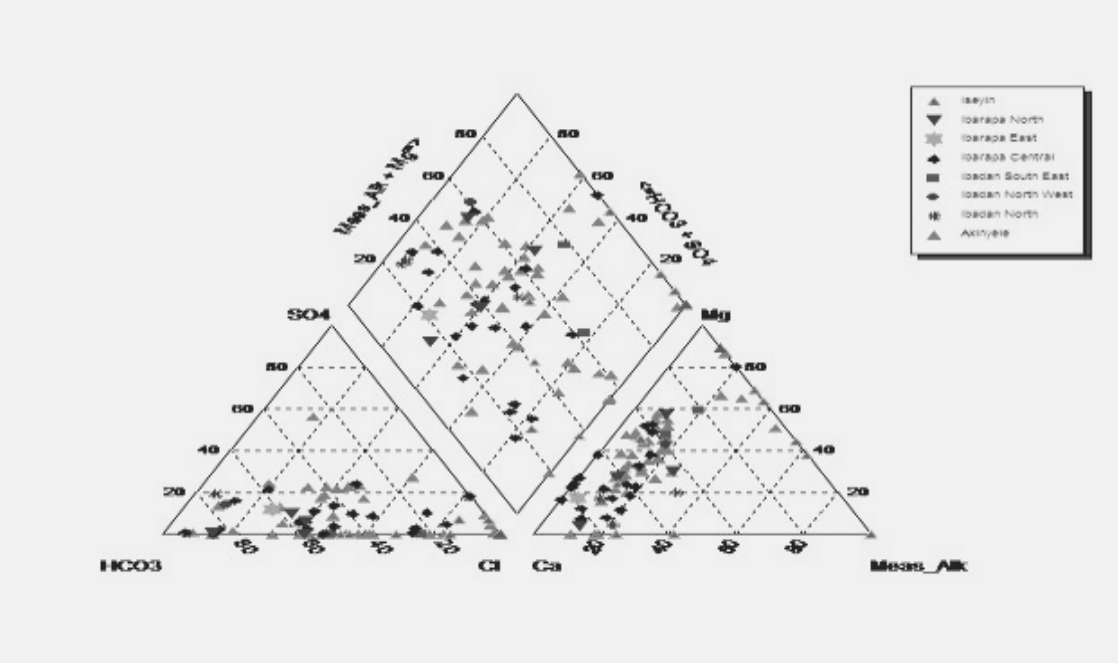

FIGURE 4
The Piper diagram of the sampled groundwater ionic species. The water facies is divided into four equal parts in both the cations (HCO_3^-, Cl^-, SO_4^{2-}) and anions (Na^+, K^+, Ca^{2+}, Mg^{2+}) region

points lied in the non-dominant axis and 10% lay in the measure alkaline ($Na^+ + K^+$) and magnesium axis. In anionic region, 40% of points (Akinyele, Ibarapa North, Ibarapa Central, Ibarapa East, Ibadan North) lied within the HCO_3^- axis showing the abundance of bicarbonate ion in the water collected in that region while 40% of points (Akinyele, Ibarapa Central, Iseyin and Ibadan Southeast) lied within the Cl^- axis, which showed the abundance of chloride ion. The type of water constituents predominant in this study area is the Cl-HCO_3 and Ca-Mg water type which implies that the groundwater quality variations are mainly related to the presence and dissolution of some carbonate, dolomitic and evaporite minerals in relatively less saline water type [33, 34]; natural processes and water-rock interaction in mixed water type; and water-rock interaction in blended water type.

CONCLUSION

This study was able to assess one-hundred (100) samples of groundwater collected from eight Local Government Areas in Oyo basement rocks. The data showed elevated concentrations of Fe and NO_3^- greater than the WHO permissible limits. The multivariate statistics applied to identify the sources of pollutants in the groundwater revealed sources including anthropogenic, geological (bedrock weathering), nutrients and thermal/industrial. The aquifers in the locations are enriched in Na-ion and have a high strength of cation exchange in the hydrochemistry. The analyzed groundwater in the basement rock of Oyo had reported high nitrate and Fe concentrations and therefore must be treated before drinking and domestic use.

ACKNOWLEDGMENT

The authors are grateful to Water and Sanitation Department of Oyo State Water Corporation for providing us with the groundwater data used in this study.

REFERENCES

[1] Kannan, N. and Joseph, S. (2010) Quality of groundwater in the shallow aquifers of a paddy dominated agricultural river basin, Kerala, India. Intl. J. Civil Environ. Eng., 2, 160-178.

[2] Gbadebo, A.M., Oyedepo, J.A. and Taiwo, A.M. (2010) Variability of nitrate in groundwater in some parts of Southwestern Nigeria. Pacific J. Sci. Technol., 11(2), 572-584.

[3] Orebiyi, E.O., Awomeso, J.A., Martins, O., Idowu, A.O., Oguntoke, O. and Taiwo, A.M. (2010) Assessment of pollution hazards of shallow well water in Abeokuta and environs. Am. J. Environ. Sci., 6, 50–56. DOI: 10.3844/ajessp.2011.525.530.

[4] Taiwo, A.M. (2012) Source identification and apportionment of pollution sources to

groundwater quality in major cities in Southwest, Nigeria. Geofizika, 29, 157-174.
[5] Ojo, O.I. (2002) Construction and maintenance of borehole in Anambra State (PTf sponsored project experience), M.Sc. Seminar Report, University of Ibadan, Department of Agricultural Environmental Engineering, Nigeria.
[6] Taiwo, A.M., Adeogun, A.O., Olatunde, K.A. and Adegbite, K.I. (2011) Analysis of groundwater quality of hand-dug wells in peri-urban area of Obantoko, Abeokuta, Nigeria for selected physico-chemical parameters. Pacific J. Sci. Technol., 12(1), 527-534.
[7] Lefort, R. (2006) Down to the last drop. UNESCO Sources. 84, 7.
[8] Olajuyigbe, A.E., Prossy, A., Abdul-Azeez, A.S. and Eunice, S. (2013) Spatial analysis of factors responsible for incidence of water borne diseases in Ile-Ife, Nigeria. J. Sustain. Soc., 1(4), 96-113.
[9] Kumar, M., Ramanathan, A.L., Rao, M.S. and Kumar, B. (2006) Identification and evaluation of hydrogeochemical processes in the groundwater environment of Delhi, India. Environ. Geol., 50(7), 1025-1039.
[10] Singh, C.K. and Mukherjee, S. (2010) Geochemical assessment of groundwater quality integrating multivariate statistical analysis with GIS in Shiwaliks of Punjab, India. In: Geochim et Cosmochim Acta., 74(12), A967-A967.
[11] Matthess, G. (1982) The properties of groundwater. Wiley, New York, pp. 498.
[12] Ogunribido, T.H.T. and Kehinde-Philips, O.O. (2011) Multivariate statistical analysis for the assessment of hydrogeochemistry of groundwater in Agbabu Area, S.W. Nigeri a. Proceedings of the Environmental Management Conference, Federal University of Agriculture, Abeokuta, Nigeria. Federal University of Agriculture, Abeokuta.
[13] Ayedun, H., Oyede, R. T., Osinfade, B. G., Oguntade, B. K., Umar, B. F. and Abiaziem, C. V., Groundwater quality around new cement factory, Ibese, Ogun State, Southwest Nigeria, Afric. J. Pure Appl. Chem., 6(13), 219-223, (2011).
[14] Gbadebo, A.M. and Taiwo, A.M., Geochemical characterization of phraetic aquifers in area of Sango, Southwestern, Nigeria. World Appl. Sci. J., 12, 815–821, (2011).
[15] Nkolika, I.C. and Onianwa, P.C. (2011). Preliminary study of the impact of poor waste management on the physicochemical properties of ground water in some areas of Ibadan. Research Journal of Environmental Science 5, 194-199.
[16] FRN (2012)Youth Employment and Social Support Operation (YESSO). Federal Republic of Nigeria. Final Report E4094. www-wds.worldbank.org/external/. Accessed:17/07/14.
[17] WHO (2008) Guidelines for drinking water quality. 3rd Ed. Health criteria and supporting information, Geneva.
[18] Li, Y. H., Li, H. B., Xu, X. Y., Zhou, Y. C., & Gong, X. (2015). Microbial distributions for nitrogen removal in a subsurface wastewater infiltration system. Fres. Environ. Bullet., 24 (5), 1747-1751.
[19] Ward, M.H., deKok, T. M., Levallois, P., Brender, J., Gulis, G. and Nolan, B. T. (2005) Workgroup report: drinking water nitrate and health-recent findings and research needs. Environ. Health Perspect., 113, 1607-1614.
[20] Edmunds, W.M. and Smedley, P.L.(1996) Groundwater geochemistry and health: An overview. In: Environmental geochemistry and health (Eds Appleton, J.D., Fuge, R.and Mccall, G.J.H.). Geological Society, London. Special Publication 113, 91-105.
[21] Edmunds, W.M. and Smedley, P.L. (2003) Fluoride in natural waters occurrence, controls and health aspects. In: Medical geology. New York (Ed. Selenus, O.), Academic Press.
[22] Susheela, A.K., Kumar, A., Betnagar, M. and Bahadur, M. (1993) Prevalence of endemic fluorosis with gastro-intestinal manifestations in people living in some north-Indian villages. Fluoride, 26, 97-104.
[23] Jha, A. N. and Verma, P. K. (2000) Physico-chemical properties of drinking water in town area of Godda district under Santal Pargana (Bihar), India. Poll. Res., 19(2), 75–85.
[24] Edet, A., and Worden, R. H. (2009) Monitoring of the physical parameters and evaluation of the chemical composition of river and groundwater in Calabar (Southeastern Nigeria). Environ. Monit. Assess., 157(1-4), 243-258.
[25] Guo, H. and Wang, Y. (2004) Hydrogeochemical processes in shallow quaternary aquifer from the northern part of Datong Basin. Chine. Appl. Geochem., 19, 19-27.
[26] Suthar, S., Preeti, B., Sushma, S., Pravin, K.M., Arvind, K.N., Nagraj, S.P. (2009) Nitrate contamination in groundwater of some rural areas of Rajasthan, India. J. Hazard. Mater., 171(1), 189-199.
[27] Ohio EPA (2012) Fluoride in Ohio's groundwater. Division of drinking and ground waters Technical Series on groundwater quality. ehttp://www.epa.ohio.gov/Portals/28/documents/ gwqcp/fluoride_ts.pdf. Accessed: 14/07/14.

[28] Handa, B. K. (1975) Geochemistry and genesis of fluoride containing ground water in India. Groundwater, 13(3), 275–281.
[29] Shyamala, R., Shanthi, M. and Lalitha, P. (2008) Physicochemical analysis of borewell water samples of Telungupalayam area in Coimbatore District, Tamilnadu, India. E-Journal Chem., 5(4), 924-929.
[30] Yadav, K.K., Gupta, N., Kumar, V., Arya, S. and Singh, D. (2013) Physico-chemical analysis of selected ground water samples of Agra city, India. Rec. Res. Sci. Technol., 4(11).
[31] Adetunji, V. O. and Odetokun, I. A. (2011) Groundwater contamination in Agbowo community, Ibadan Nigeria: impact of septic tanks distances to well. Malayas J. Microbiol., 7(3), 159-166.
[32] Galadima, A., Garba, Z. N., Leke, L., Almustapha, M. N. and Adam, I. K. (2011) Domestic water pollution among local communities in Nigeria-causes and consequences. Euro. J. Sci. Res., 52(4), 592-603.
[33] Belkhiri, L., Mouni, L. and Tiri, A. (2012) Water–rock interaction and geochemistry of groundwater from the Ain Azel aquifer, Algeria. Environ. Geochem. Health, 34(1), 1-13.
[34] Margiotta, S., Mongelli, G., Paternoster, M., Sinisi, R., and Summa, V. (2014). seasonal Groundwater monitoring for trace-element distribution and Cr (vi) pollution in an area affected by negligible anthropogenic effects. Fresen. Environ. Bull.., 23 (12 C), 3482-3494.

Received: **29.07.2015**
Accepted: **12.12.2015**

CORRESPONDING AUTHOR

Adewale Matthew Taiwo
Department of Environmental Management and Toxicology Federal University of Agriculture,
PMB 2240, Abeokuta, Ogun State, NIGERIA

e-mail: taiwoademat@gmail.com

© by PSP Volume 25 – No.7/ 2016, pages 2292-2297 Fresenius Environmental Bulletin

RESEARCH ADVANCES IN ORGANOPHOSPHORUS PESTICIDE DEGRADATION: A REVIEW

Xiyan Ji, Qiang Wang, Wudi Zhang, Fang Yin

Yunnan Normal University, Kunming 650500, P. R. China

ABSTRACT

The technologies related to the microbial biodegradation of organophosphorus pesticide biodegradation are currently being heavily researched. This article reviews various types of microbial degradation of organophosphorus pesticide, degradation mechanism and degradation genes and discusses the recent development trend of microbial degradation of organophosphorus pesticide. This paper also introduces the current research status of biodegradation technologies around the world including China. This paper primarily presents the research results of organophosphorus pesticide biodegradation. Lastly, the authors exhibited some suggestions for further researches.

KEYWORDS:
organophosphorus pesticide (OPs); biodegradation; microbial degradation; microbial species; degrading mechanism; degradation genes

INTRODUCTION

Pesticide is termed as chemical that kills or slows down the growth of undesirable organisms. Today, organophosphorus pesticide (OPs) is the most commonly used category of pesticide used in agriculture and horticulture practices, with as many as 150 kinds of organophosphorus commodity pesticides available in the world [1]. In China, about 30 pesticides including insecticide, herbicide and bactericide have been commonly used.

Pesticides are biologically active compounds designed to interfere with metabolic processes and environmental safety. And many researchers pay attention to the field of OPs degradation. Fodale's result shows that 47 strains were isolated from Sicilian soils under different management systems [2].Wang's result suggests that MTM (mesoporous TiO2 membrane) TiO2 membrane has good potential for treatment of aqueous organophosphorus pesticides [3]. Kotonia used gas chromatography-mass spectrometry (GC-MS) to determinate 14 insecticides and metabolites in grapes and peaches [4].

Generally, OPs contain two primary varieties, phosphate, and O-ethyl-S-propyl phosphorothiolatex, as seen in Fig1. Among the OPs that most widely produced and used in China, R1 or R2 represents methoxyl (CH3O) or ethoxy (C2H5O). X is for oxygen atom (O) or sulphur atom (S). Z is for alkoxy, phenoxyl or other complicated substituent group. It can form a variety of compounds depending on which different substituent group is present. According to their structures, organophosphorus pesticides can be divided into phosphate, phosphonic acid ester, and phosphorous amides with corresponding glucosinolates derivatives.

Among the toxic pesticides, organophosphorus pesticide is the most common. Organophosphorus pesticide toxicity studies had shown that organophosphorus pesticides have alkylation function which can poison animals and human body. They can be absorbed by inhalation, ingestion, and skin penetration. Thousands of humans including children are affected by OPs toxicity across the world annually. For instance, children exposed to OPs are more likely to suffer from attention deficit hyperactivity disorder (ADHD) (Samuels and Obare, 2011). Importantly, frequent use of OPs in agricultural practices and their presence as residues in fruits, vegetables, livestock, poultry products and municipal aquifers are considered vectors for the exposure. As such, OPs degradation has been a major concern in environmental chemistry and is currently being studied worldwide. This has lead to major advancements in OPs degradation technologies. The definition of OPs degradation is that OPs chemical structure changes under some factors correlated with environment, where the OPs molecules are degrade into smaller molecules such as CO2, PO43- and H2O. The degradation phenomenon is divided into 3 steps [5]: ①Initial degradation: OPs parent structure breaks down, leading the change in characteristics; ②Secondary degradation: The products of

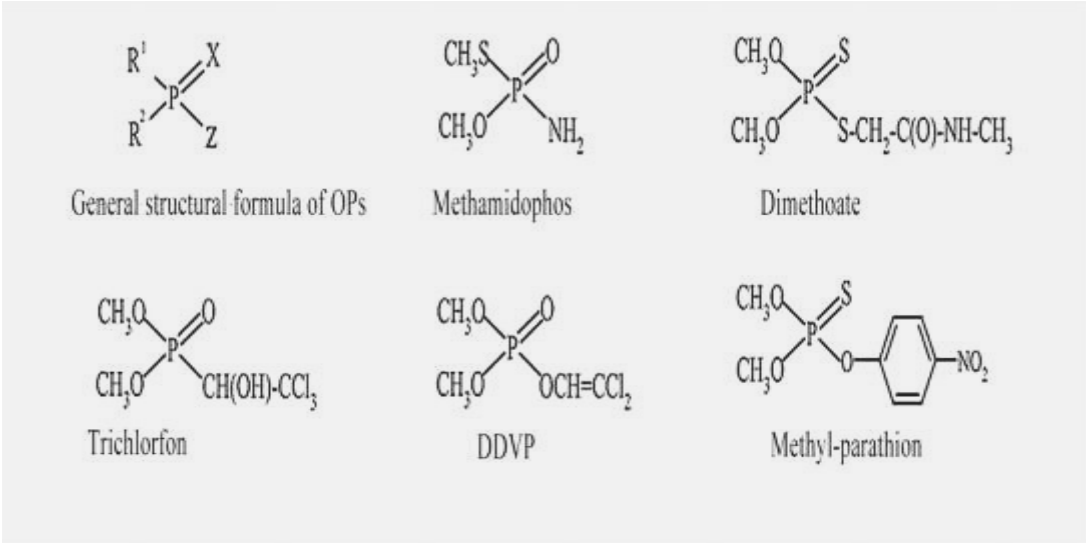

R1 and R2 represent methoxyl (CH3O) and ethoxy (C2H5O), respectively.
X is for oxygen atom (O) or sulphur atom (S).
Z is for alkoxy, phenoxyl or other complicated substituent group.

FIGURE 1
Organophosphorus pesticide general structure formula and several typical organophosphorus pesticide chemical structures.

degradation don't pollute the environment; ③ Final degradation: The substrate (organophosphorus pesticide) fully transformed into inorganic substances such as CO_2, PO_4^{3-} and H_2O. Although, there are a lot of studies on organophosphorus pesticide degradation very few reports touch on microbial degradation. We seek to fill this void and will primarily discuss biodegradation methods and microbial degradation.

Biodegradation Method. Although traditional physical and chemical degradation treatments are effective against OPs, has good effect, the cost is too high and easy to cause secondary pollution, so it only can be used as an assessment method. In contrast, bioremediation technology has been developed to remove and control the organic matter pollution, and has recently become the most popular method. The basic purpose of this technology is to use a variety of methods to strengthen the microbial community and accelerate the degradation of organic pollutants in the environment [5]. Moreover, microbiological degradation is considered as an effective and environment friendly method to eliminate OPs pollution. Since the 1940's research has confirmed the microbial degradation of pesticide played an important role, and has attempted to isolate of pesticide degrading bacteria and the degradation pathway [6,7].

High Efficient Bacteria Separation. Long-term mass production and extensive use of organophosphorus pesticide in China has lead to serious water and soil pollution as well as, lead to excessive pesticide residues on agricultural products, sparking food safety problems. Excessive OPs residue has become a major inhibitor to the expansion of China's agricultural product exports. Therefore, it is necessary to establish an effective method to control environmental pollution and remove agricultural farming pesticides residues. With the strong metabolic diversity, microorganisms have many advantages in the degradation process of pesticides [8]. At present, the separated microorganisms include bacteria, fungi and actinomycete. Bacteria played an important role in the degradation process because of its various biochemical adaptability and good ability of inducing mutants.

In recent years, the in-depth study on biodegradation pathway has provided the possibility for bioremediation. Any microorganisms have been isolated and identified, including *Agrobacterium Escherichia coli*, *Flavobacterium* sp., *Bacillus stearothemophilus*, *Pseudomonas*, strain B-1, strain SC, F. sp. Strain ATCC27551, *Alteromonas species*, *Arthrobacter*, *Nocardia*sp., *Corynebacterium glutamicum*, *Burkholderia* sp. Strain NF100, *Bacillus cereus* J5, WBC-3, cyanobacterium Anabaena sp. Strain PCC7120, *Ochrobacterum* sp. B2.

Some studies have reported the effects of microorganism on biodegradation of pesticides. For instance, Zhang et al. [8] investigated degradation of methyl parathion in soil and Chinese chive by strain DLL-1at concentrations of 7.5, 15, 22.5, 75 kg(a.i.)ihm^{-2}. From their result, usage of methyl

parathion at 7.5, 15 and 22.5 kg(a.i.)ihm^{-2} resulted in the average amount of residue of 0.663, 1.270 and 1.901mgnt -1, respectively in Chinese chive. The natural degradation rate was 98.94% , 96.44%, and 96.04% corresponding to the 3 levels of usage. At the concentration of 75 kg·hm^{-2} of degradation bacterium, the amount of pesticide residue in Chinese chive and its soil were 0.269 and 0.099 mg·kg^{-1} respectively which were decreased by 78.82% and 98.68% compared with the control. Thus, the amount of pesticide residue could be significantly decreased through the application of high effective degrading microbial agents. However, usage of degradation bacterium more than 75kg·hm^{-2} did not increase the degradation rate further. In bacterial isolation study, Jia et al. [9] have found that a strain P_{m-6} of methamidophos-degrading bacterium was successfully isolated from the pesticides-containing soil in a pesticide factory. The strain was identified as Acinetobacter sp. This bacterium was stable when store for 30 days at 4℃ with slight change in capability. Likewise, Meiqin Yi [10] isolated three strains of Fungi (Hw 23, Hw 26 and Hw 27) using liquid enrichment culture from active sludge at Huayang Pesticide Factory for degradation of methyl parathion. They were able to use methyl parathion as the carbon and energy for growth. Daiet al [11] and Qiu et al [12] argued convincingly that a triazophos degrading bacterium designated as mp-4 wereisolated from soils that have long been subjected to organophosphate pollution. Strain mp-4 was identified as *Ochrobactrum.*sp based on its biochemical-physiological characteristic and the 16 SrDNA homologue sequence analysis. Strain mp-4 can grow with triazophos as its sole carbon source and degrade it at a rate of 98.3%. The optimal growth temperature and pH for mp-4 are 30℃ and 6.6, respectively. At the temperature of 27-32℃ and pH of 7.5-8.8, Mp-4 can degrade triazophos well. Thus, many research showed principal mechanism for microorganism adaption to organophosphorus pesticides contained environment and efficiency of microorganism for pesticides degradation or removal. Different studies showed that some organophosphorus pesticide can have a variety of degrading bacteria present at the same time, while one kind of bacteria can degrade kinds of OPs. This reflects the diversity of microorganisms and microbial functional diversity.

With the continuous development of biotechnology, people have made a lot of beneficial explorations on OPs degradation finding that mesophilic microorganisms exert a great pole course in the OPs degradation in the natural environment. The use bioremediation technology is effective, economical and environmental friendly technology to accelerate the degradation of OPs [13, 14]. However, most of the studies on OPs degradation recommend moderated temperature and high concentration conditions, so mostly the microorganisms are usually isolated on room temperature. In high altitude area or cold region, the temperature is mostly below the normal temperature and degradation efficiency will be affected, while also requiring a low concentration in the water [15]. All of these disadvantages constitute a barrier to microbial growth. As a consequence, He Li [16, 17] found that the bacterial strain, which was isolated from the polluted soil in north-east china, was capable of degrading various organophosphorus pesticides effectively. Strain SA-8 was initially identified as *Plwsimona*s sp. according to its biochemical characters. The optimal temperature and pH value for strain SA-8 growth were 20℃ and 7.0 respectively. The biodegradation rate of methyl-parathion can reach 93% after 24h cultivation in suitable conditions. When the temperature is 10℃, its degradation rate is 66.2%, but only 27.3% degradation rate at 35 ℃. The experiment demonstrated that strain SA-8 is a good psychrotroph.

Microbial Degrading Mechanism of OPs. Organophosphorus pesticides usually contain P-O and S- P bonds. In addition, some OPs (e.g. methamidophos) also contain P-N bond. The degradation of OPs by bacteria is generally carried out through the hydrolases and transfer enzymes function, acting on P-O-alkyl, P-O-aryl, O=P-NH_2, =C-NH_2. The study on the OPs degradation pathway found that microorganisms can break the P-O bond or P-S bond and some depurated organophosphorus pesticide hydrolase (OPH) have significantly difference in substrate specificity, sensitivity to the chemicals and molecular weight. Initial metabolism of OPs is hydrolytic reaction, and its initial products are O, O-dimethyl dithiophosphoric acid and p-nitrophenol [18,19].

M. B. Angelica also confirmed that the P-S bonds of organophosphorus pesticides can be cut off by chlorinated pesticides. Some researchers for instance, Donna & Ulrica [20] and, Thomas and Macaskie [21] studies showed that there is a certain correlation between the microbial phosphate solubilizing capacity and the pH of culture medium, however they also found that decrease in pH value is not the necessary conditions of the phosphate solubilizing. Further research on this area could be interesting and important.

According to Liu et al. [22] and, Liang et al. [23] degradation process caused by intracellular enzyme can be divided into 3 steps: firstly, as is a kind of dynamic balance, i.e. OPs compounds absorb on cell membrane; secondly, OPs compounds that absorb on cell membrane go into cell under the constant biomass condition and the penetration rate determines the amount of compounds inside cell; thirdly, as a enzymatic reaction in the cell which is a quick process and

also not a limiting step. *Pseudomonas stutzeri* JHY01 was capable of degrading Chlorpyrifos, a typical organophosphorus pesticide [24, 25]. The ultrasonic cell-break method was used to extract the degrading enzyme. Lan et al [24] or Jeon et al [25] conducted a study on the chlorpyrifos degradation through extracellular enzyme, intracellular enzyme and cell fragment. Their experimental results showed the degradation rates of chlorpyrifos by extracellular enzyme, intracellular enzyme and cell fragment were 8.41%, 79.85% and 77.14%, respectively, indicating that Chlorpyrifos-degrading enzymes were typical intracellular enzymes. Later, orthogonal experiments were designed by them to optimize the extraction conditions of the degrading enzymes. The degrading activity of the crude enzymes was maximal (with the degradation rate 84.47%) at the following ultrasonic conditions: the ratio of cells biomass to extraction buffer volume 1:4 (g/ml), ultrasonic treatment for 4 seconds, totally 30 times at interval of 4 seconds (UAS, Sonics-VCX500, 500W, 25KHz). According to Wang et al [26], an organophosphorus hydrolase from strain *Aspergillus niger* J6 was isolated and purified by means of cell disruption, ammonium sulfate precipitation and *Sephadex* G-75 chromatography. In addition, enzymatic properties were also studied. The results showed that the degradation enzyme was located on the cell membrane, with its molecular weight being 66 000 by SDS-PAGE. The optimal reactive temperature and pH of the degradation enzyme was 70 ℃ and pH 7.0 respectively. Some metal ions (Fe^{3+},Cu^{2+},Li^{+},Zn^{2+},Mg^{2+}) and chemical reagents (NaN_3, EDTA, SDS and PSMF) showed synergistic effect on the degradation enzyme activity, while Mn^{2+} displayed slight inhibition, and Ca^{2+} had strong inhibition [26].

Organophosphorus Pesticides Degradation Microorganisms. In recent years, many researchers had screened various kinds of bacteria (fungi, actinomycetes, algae and other microbial strains) which have the ability to degrade the organic phosphorus pesticide through the enrichment, isolation and screening technology from the natural soil. These microorganisms can be classified into Shah Ray Ties, *Pseudomonas*, *Burkholderia* spp., *Roseomonas*, *Ochrobactrum*, *Klebsiella*, Bacillus E6, Plesiomonas sp. M6, fecal production alkali bacillus, sp. Diaphorobacter, Klebsiella sp., and Holder Burke (sp. Burkholderia). Table 1 summarizes the microorganism and types of organic phosphorus which can degrade by corresponding bacteria.

Xu Gangming [27,28] reported that strains from three pesticide factory sewage treatment pool of activated sludge, which degraded Chlorpyrifos effectively. These strains are bacterial and accessory bacteria (Paracoccus sp. DM/TRP), serratia sp. TCR, and Trichosporon sp.TCF. Based on the expressed mpd gene sequence and opd gene, he designed several pair gene primers. Gene amplification in different conditions was made using general PCR and Touch-Down PCR (TD-PCR) by taking total bacterial NDA as a template. These strains can be completely mineralized and degrade chlorpyrifos, the same with intermediate product trichloropyrindinol.

DISCUSSION AND CONCLUSIONS

Substantial progress has been accomplished in the development of technologies for OP pesticides degradation in recent years. However, at present, the separation of strains and microbial degradation are limited to the lab-scale, and still remains to be applied in the field practice. This could be mainly due to need for degradation conditions for the effective use of microbial degradation of organophosphorus pesticides that are hard to achieve outside of the lab. Temperature, pH, concentration of organophosphorus pesticide and microbial essential nutrients will change a relatively large range, under natural conditions. It can't ensure the effect of the microbial breeding, even may inhibit its growth. Therefore, further future study of microbial degradation of organophosphorus pesticide should emphatically focus on the following several aspects: ①Explore the degradation strains with growing conditions which are similar to the natural environment; cultivation, development and utilization of high efficient bacteria for organophosphorus pesticide, establish high efficient degradation bacterium seed (gene) bank. ②Extract the related genes and remove into a common species, such as e-coli, etc. for degradation enzyme gene cloning and expression, constructing engineering bacteria, improve the ability of degradation, prepare degradation enzyme, on the basis of identification of degradation enzyme gene. ③Field practice of

TABLE 1
Organophosphorus pesticide degrading microorganism.

OPs.	Microorganism
Isocarbophos	Bacillus latersprorus, Serratia, Pseudomonas
Triazophos	Roseomonas, Ochrobactrumanthropi, Alcaligenesfaecalis, Klebsiellaaerogenes
Chlorpyrifos	Pseudomonas, Diaphorobacter sp.
Parathion-methyl	Pseudomonas, Diaphorobacter sp.
Fenitrothion	Burkholderia cenocepacia, Diaphorobacter sp.

biological pesticide which can help to reduce the use of heavy toxicity pesticides; ④Promotion of more applied research on the microbial method that dealing with degradation of contaminants practically in real field to the practice.

ACKNOWLEDGEMENTS

This work was supported by Research Fund for the Doctoral Program of Higher Education (20135303110001), National Natural Science Foundation of China (51366015), Applied Basic Research Programs of Yunnan Province (2014FA030), and Science and Technology Innovation Platform Construction Plan of Yunnan Province (2013DH041).

REFERENCES

[1] S. G. Dai, Environmental Chemistry [M], Beijing, Higher Education Press (1997).

[2] R.Fodale, C.De Pasquale, L.Lo Piccolo, et al, (2007) Isolation of organophosphorus-degrading bacteria from agricultural mediterranean soils, *Fresenius Environmental Bulletin,*19 (10B), 2396-2403.

[3] P.Wang, D.S.Bi, Y.Chen, (2015) Ultraviolet irradiation of a mesoporous TiO_2 membrane for removing organophosphorus pesticides from water, *Fresenius Environmental Bulletin,*24 (5A), 1779-1785.

[4] C.A. Kotonia, K.S.Liapis, V.N.Ziogas, Determination of residues of 14 insecticides and metabolites in grapes and peaches by gas chromatography - mass spectrometry, *Fresenius Environmental Bulletin,* 16 (3), 223-226.

[5] Z. G. Jin, T. Zhang, H. L. Zhu, Pollutant Biodegradation [M], Shanghai, East China University of Science and Technology Press (1997).

[6] D. S. Tara, H. Irene, J. L. Michael, (2000) Enrichment of an endosulfan-degrading mixed bacterial culture, *Applied and Environ Microbiol*,66 (7), 2822–2828.

[7] Z. Liu, S. P. Li, (2003) Mutation breeding of methyl parathion degrading strain DLL-1 (Pseudomonas sp.), *ActaPedologicaSinica*, 40 (2), 293-298.

[8] R. F. Zhang, J. D. Jiang, Z. L. Cui. (2004) Degradation of methyl parathion in soil and Chinese chive by strain DLL-1, *Chinese journal of applied ecology*, 15 (2), 295-298.

[9] R. Jia, Z. R. Hong, Q. Li, Y. Wang, (1997) Isolation of methamidophos-degrading bacterium and studies on its properties, *Journal of Anhui University Natural Science Edition*, 21 (1), 98-101.

[10] M. Q. Yi, K. Y. Wang, X. Y. Jiang, Y. J. Wang, (2000) Studies on the isolation and characterization of fungi for degradation of methyl parathion, *Chinese Journal of Pesticide Science*, 2 (4),40-43.

[11] Q. H. Dai, R. F. Zhang, J. D. Jiang, L. F. Gu, S. P. Liu, (2005) Isolation, identification and characterization of triazophosdegrading bacterium mp4, *ActaPedologicaSinica*, 42 (1), 111-115.

[12] S. L Qiu, Z. L. Cui, B. Fan, Q. H. Dai, S. P. Li, (2004) Construction of GFP-Labelled pseudomonas putida DLL-1, a methylparathion-degrading bacterium, *Chinese Journal of Applied and Environmental Biology*, 10 (6), 778-781.

[13] A. Bonnechere, V Hanot, C Bragard, et al. (2013) Effect of household and industrial processing on the levels of pesticide residues and degradation products in melons, *Food Additives and Contaminants Part A, Chemistry, Analysis, Control, Exposure and Risk Assessment*, 29 (7), 1058-1066.

[14] D. Sun, J. Qiu, Y. Wu. (2012) Enantioselective degradation of indoxacarb in cabbage and soil under field conditions, *Chirality*, 24, 628-633.

[15] F. Dong, B. Chankvetadze (2013). Chiral triazole fungicide difenoconazole: absolute stereochemistry, stereoselective bioactivity, aquatic toxicity, and environmental behavior in vegetables and soil, Environment Science and Technology, 47, 3386-3394.

[16] H. Li, W.Q. Liang, X. Y. Wu, Y. H. Liu, (2010) Research on biodegradation of organophosphorus insecticide by a novel psychrotrophic Bacterium SA-8, *ActaScientiarum Nature AliumUniversitatisSunyatseni*, 43 (3), 131-132.

[17] S. Dayananda, K. Syed, M. Mike (2003). Transposon-like organization of the plasmid-borne organophosphate degradation gen cluster found in Flavobacterium sp., *Appl Environ Microbiol*, , 69, 2533-2539.

[18] F. Oppong, G. Sagar, (1992) Degradation of triasulfuron in soil under laboratory conditions, *Weed Research*, 32, 167-173.

[19] N. Sethunathan, T. Yoshida. (1973) A flavobacterium sp. that de-grades diazinon and parathion. Can J Microbial, 19, 873 -875.

[20] C. Donna, S. Ulrica, (2001) Cocomposting of cattle manure and hydrocarbon contaminated flare pit soil, *Compost Science and Utilization*, 9(4), 322-335.

[21] R. A. Thomas,L. E. Macaskie. (1998) The effect of growth conditions on thebiodegradation of acid mine drainage waters by a naturally-occurringmixed microbial culture. *Appl. Microbial.Biotechnology*, 49, 202-209.

[22] Y.H. Liu, Y. C. Chung, Y. Xiong. (2001)

Purification and characterization of a dimethoatedegrading enzyme of Aspergillus niger ZHY256, isolated from sewage, Appl. Environ Microbial,67, 3746- 3749.

[23] W.Q.Liang, Wang Z. Y., Li H. (2005) Purification and char-acterizationof a novel pyrethroid hydrolase from aspergil-lusniger ZD11,*Journal of Agricultural and Food*, *Chemistry*,53, 7415- 7420.

[24] Y. H. Lan, M. Xie, F. L. Chen, F. H. Wang, S. Y. Zhou. (2008) Localization and extraction conditions of chlorpyrifos-degrading enzyme from Pseudomonas stutzeri, *Chinese Journal of Biological Control*,24 (4), 349-353.

[25] Y. H. Jeon, S. P. Chang, I. G. Hwang. (2003) Involvement of growth-promoting rhizobacteriumPaenibacilluspolymyxa in root rot of stored Korean Ginseng,Journal of Microbiology and Biotechnology, 13 (6), 881-891.

[26] J. W. Wang, J. Zhen, B. E. Xie, Y. Y. Liu, G. J. Li.(2012) Purification of a organophosphorus pesticide- degrading enzyme from As-pergillusniger J6 and its properties, *Jiangsu J. of Agr . Sci.*, 28(3), 549-554.

[27] G.M. Xu. (2007) Isolation and Characterization of Organophosphorus Degrading Microbes and Their Mineralizing Mechanism [D], Shandong Agricultural University.

[28] Tova A. Samuels and Sherine O. Obare (2011). Advances in Analytical Methods for Organophosphorus Pesticide Detection, Pesticides in the Modern World - Trends in Pesticides Analysis, Dr. Margarita Stoytcheva (Ed.),ISBN:978-953-307-437-5, InTech, Availablefrom: http://www.intechopen.com/books/pesticides-in-themodern-world-trends-in-pesticides-analysis/advances-in-analytical-methods-for-organophosphorus-pesticidedetection.

Received: **11.08.2015**
Accepted: **10.12.2015**

CORRESPONDING AUTHOR

Wudi Zhang
Energy and Environmental Science School, Yunnan Normal University No.768, Jingming St. Kunming City, Yunnan Prov., China, 650500

Email: wootichang@163.com

© by PSP Volume 25 – No. 7/2016, pages 2298-2304 Fresenius Environmental Bulletin

THE EFFECT OF DIFFERENT SALINITIES ON DENSITY OF *NANNOCHLOROPSIS OCULATA* UNDER LABORATORY CONDITIONS

Esmaeil Kouhgardi [1]*, Leila Khalifeh[2], Tirdad Maqsoudloo[3]

[1, 2, 3] Natural Resources Department, Bushehr branch, Islamic Azad University, Bushehr, Iran

ABSTRACT

Nannochloropsis microalgae are one of the sea unicellular algae that belong to the division of green algae and the subdivision of Estigomatophyceae. This research has been conducted to study the growth of *N.oculata* algae in Conway medium under different five salinities (15, 20, 25, 30 and 35 part per thousand) with three repetitions in a laboratory environment. During 14 days of *N.oculata* culture in Conway medium and different salinities, the growth of the species has been studied through numerating method by Hemocytometer slide. According to the results, it was revealed that there is no significant statistical difference among treatments with salinities of 15 and 35 ppt. However, there is a significant statistical different among other treatments ($P<0.05$). The utmost growth was observed in Conway medium with a degree of salinity given as 25 ppt and for 44 * 10^6 cells per milliliter. Thus, it will be concluded that degree of salinity may independently affect cellular density. In fact, range of salinity that is usable for culture of this species is introduced a salinity of 20-35 and desirable salinity is introduced as 25 ppt. Besides other effective elements involved in culture of *N.oculata*, the said salinity may play a great role affecting increase of biomass of this species in mediums.

KEYWORDS:
Microalgae, Nannochloropsis, Medium, Growth, Salinity

INTRODUCTION

Nannochloropsis alga is one of the sea unicellular algae that belong to the division of green algae and subdivision of Estigomatophyceae. In the past, because of its round appearance that makes it similar to Chlorellaalgae, it is called sea Chlorella. The basic structure of the alga was identified in 1986. Since then, it has been called "Nannochloropsis" [6].

Different identified species of the alga are mainly of sea type. However, there are some species living in drinkable water and brackish water.

Since Nannochloropsis has high quantity of protein and unsaturated fatty acids, it is of great importance in aquatic farming. Thanks to its high level of nutritious such as high Ecoza-Pentanoic Acid (EPA) and the effective role of this species as an option replacing poly-unsaturated fatty acids (PUFA), its importance in feeding the of sea fish larva becomes evident, also all microalga extracts showed antifungal effects on marine species [10].

In farming the algae, further to physical elements (light, temperature, blowing and the ones), they need a medium for fulfillment of their vital activities. The medium or food includes such elements as macro-elements and micro-elements. These elements are designed for growth mechanism of algae in form of medium formulas. Thus, adding feed solutions and ready-made or chemical fertilizers, the said materials are prepared for the algae so that they will have growth and increase of cellular density in specific mediums [9]. The aforesaid materials are really necessary for growth of algae. They usually play a prominent role in structure of algae. For example, DNA and RNA structures are useful for skeleton development, energy supply in form of ATP in structure of proteins and amino acids in cellular wall and other advantages of algae [11]. Natural carotenoid of *Nannochloropsis sp.* has successfully promoted comparable pigmentation in *P.semisulcatus* that is a highly significant development for commercial aquaculture [4].

MATERIALS AND METHODS

The required materials are 15 water bottles of 2 liters each with the required salinities (15, 20, 25, 30 and 35 part per thousand (ppt)) and five treatments with three repetitions. Each bottle was filled using 1500 milliliters of water of the desirable salinity. Conway medium of 1.5 milliliters was inserted to the medium after it reached the temperature the same as that of the environment. Then, stock of Nannochloropsis of 1.5 milliliters was added to the bottle carefully after being

homogenized. Blowing was conducted by using an air pump. Lighting of the environment was provided by using two florescent lamps that were connected in parallel form in front of the mediums. Culture of the alga was carried out in the light intensity of 5000 Lux. The temperature was kept unchanged at about 25 degrees centigrade. One milliliter of the water of the medium was put on Hemocytometer slide every day. The cells were counted under microscope and increasing and decreasing trend of its growth was studied. The Hemocysto meter slide has nine cells (4 cells with 16 divisions and five cells with double divisions). In order to numerate the cells at high density, the following method is used:

The cells available in the middle square have double divisions and used for numerating the microalgae. In this research, due to high density of cells, small squares have been used. Thus, the cells available in the smaller square (4 cells in one angle and one cell in the center) were numerated. Contrary to other side squares, this middle square enjoys 16 cells. Then, cellular density is calculated by using the following formula:

Number of cells per 5 m^2 *5= total number of cells in 25 m^2

Total number of cells in 25 m^2*10^4 = total number of cells in one milliliter of medium [5].

25= number of cells in the middle of numerating slide and

5= number of the cells of slid numerated

RESULTS

The results obtained from daily culture of *N.oculata* by using Hemocyto meter slide and optic microscope within 14 days of culture period in Conway medium and five degrees of salinities (15, 20, 25, 30, and 35 ppt) and by unit number of cell in milliliter are given as follows (Table 1):

TABLE 1
Average density of *N.oculata* affected by different treatments of salinity during culture period.

Treatment / Day of Culture	15 ppt	20 ppt	25 ppt	30 ppt	35 ppt
1	4200000	5400000	5583333	4283333	4250000
2	5266667	6733333	7683333	5300000	5883333
3	7116667	8866667	9383333	7583333	7483333
4	9050000	7800000	12158333	9750000	9300000
5	10983333	13333333	14933333	11916667	11116667
6	14350000	17916667	20200000	17116667	15616667
7	14766667	22050000	22250000	19937506	18183333
8	20783333	23100000	24566667	25966667	22966667
9	22733333	32000000	33750000	29200000	24850000
10	24450000	32900000	37633333	27450000	24833333
11	18241667	35875000	39841667	27858333	21666667
12	12033333	38850000	42050000	28266667	17400000
13	11933333	19350000	26150000	19600000	14066667
14	11700000	22383333	21216667	19416667	12250000

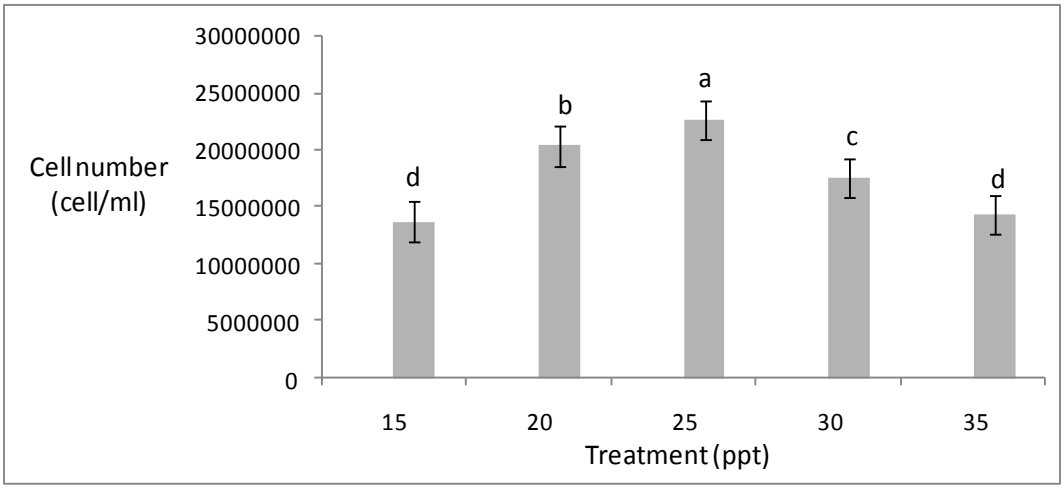

FIGURE 1
Comparing the treatments with respect to cellular numeration (a, b, c, and d reveals a significant difference at level of 0.05).

Comparing the treatments with respect to numerating the number of cells of species subject of study per each milliliter of medium, no significant different has been found between treatments of salinity of 15 and 35 ppt. However, there is a significant statistical different among other treatments ($p<0.05$). This has been shown in figure 1.

Comparing different treatments, the results reveal that the salinity of 25 ppt and for $44*10^6$ cells per milliliter obtained the first rating and the salinity of 20 by $39.9*10^6$ obtained the second rating; the salinity of 30 by $30*10^6$ and the salinity of 35 by $25*10^6$ obtained the third and fourth ratings and the salinity of 15 by $24.9*10^6$ cells per milliliters respectively.

Cellular numeration affected by salinity of 15 ppt. The results obtained from cellular numeration affected by the salinity of 15 units per thousand on average from three repetitions that have been test given and shown in figure 2. From the first through the tenth day, a noticeable increase was observed in growth of the respective treatment (phase of increase). Then, on the 11^{th} and 12^{th} days, the growth has shown a noticeable decrease (phase of decrease) and on the 13^{th} and 14^{th} day, the growth has reached a stable rate (phase of stability).

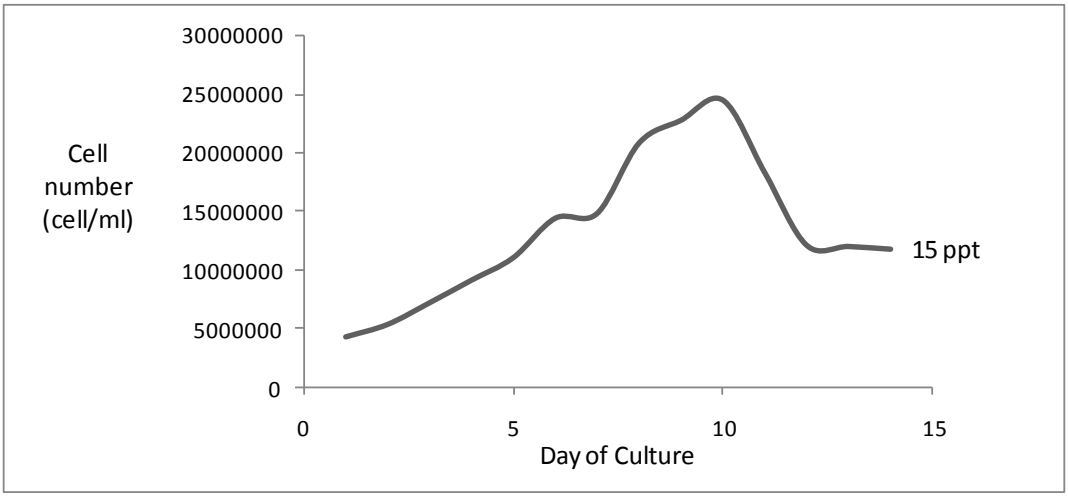

FIGURE 2
Growth of Nannochloropsis in Conway medium affected by salinity of 15 ppt.

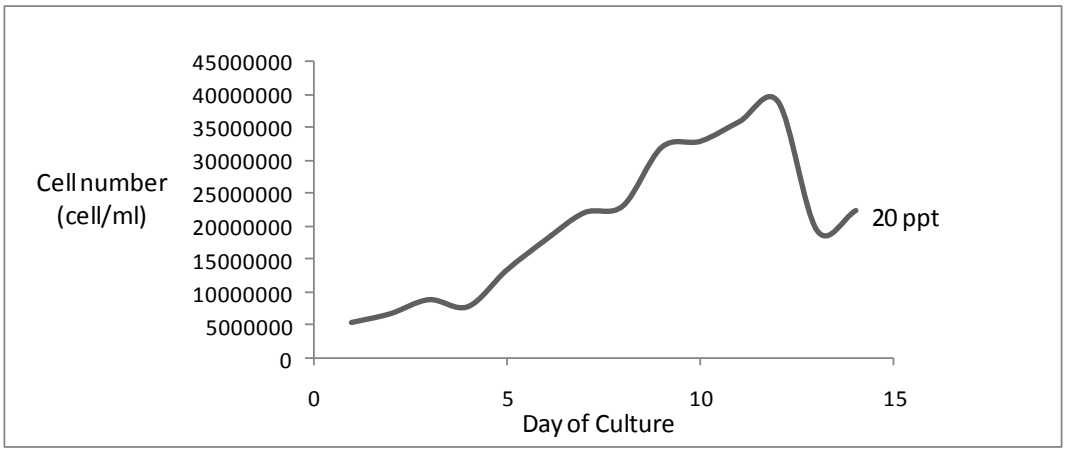

FIGURE3
Growth of Nannochloropsis in Conway medium affected by salinity of 20 ppt.

Cellular numerating affected by the salinity of 20 ppt. The results obtained from cellular numeration affected by the salinity of 20 units per thousand on average from three repetitions that were testes, have been given and shown in figure 3.

From the 1st through the 11th day, a noticeable increase in growth was observed (phase of increase and decrease of growth was intangible). On the 12th day, a noticeable decrease in growth (phase of decrease) was observe. Then, on the 14th day, a slight increase was observed in growth of the said alga once again.

Cellular numeration affected by salinity of 25 ppt. The results obtained from cellular numeration affected by the salinity of 25 units per thousand on average from three repetitions that were tested, have been given and shown in figure 4. From the first to the twelfth days, a noticeable increase (phase of increase) and on the 13th and 14th days, a quick decrease in growth were observed respectively (phase of decrease).

Cellular numeration affected by the salinity of 30 ppt. The results obtained from cellular numeration affected by the salinity of 30 units per thousand on average from three repetitions that were tested have been given and shown in figure 5. In this treatment, from the first through the ninth day, an increase in growth (phase of increase) and from the 9th to the 11th days, a slight decrease in number of cells and on the 12th day, a slight increase in growth and in the 13th day, quick

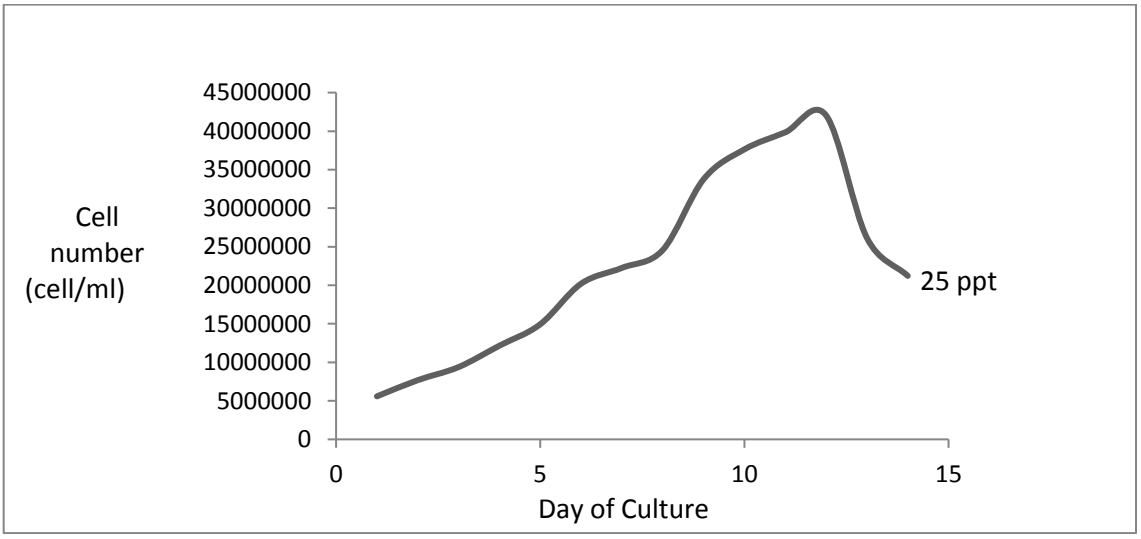

FIGURE 4
Growth of Nannochloropsis in Conway medium affected by salinity of 25 ppt.

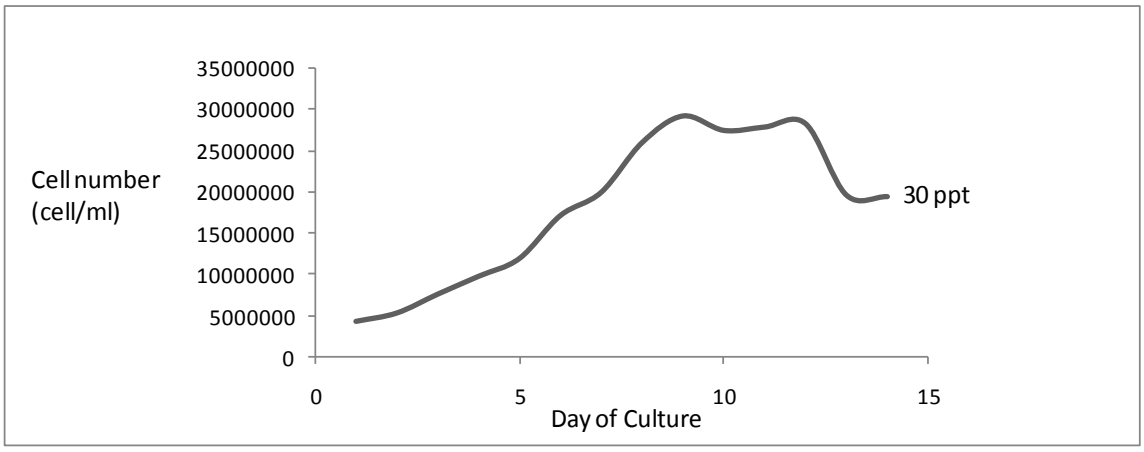

FIGURE 5
Growth of Nannochloropsis in Conway medium affected by salinity of 30 ppt.

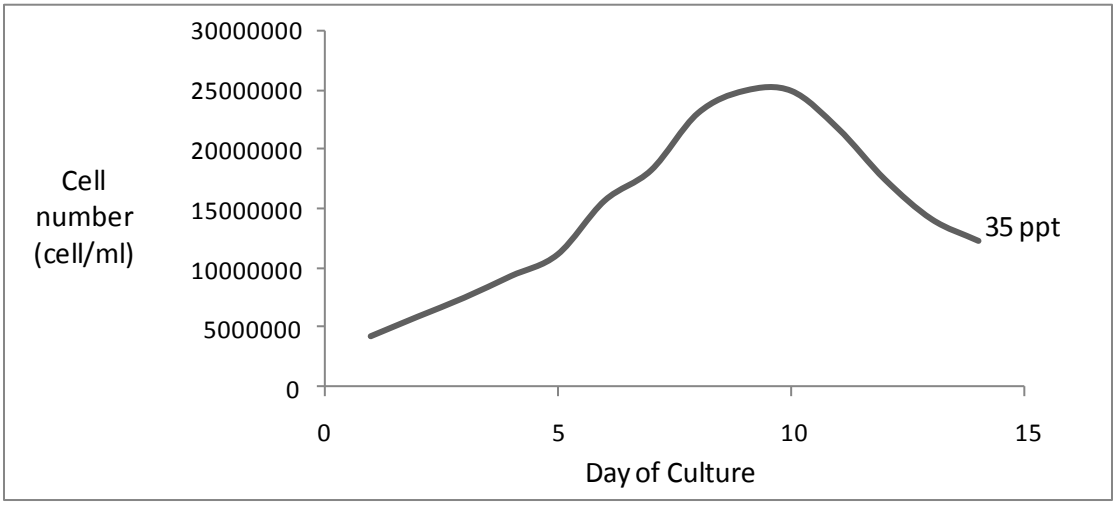

FIGURE 6
Growth of Nannochloropsis in Conway medium affected by the salinity of 35 ppt.

decrease in growth (phase of decrease) have been observed respectively. Then, on the 14th day, slight increase in growth was observed in number of cells accordingly.

Cellular numeration affected by the salinity of 35 ppt. The results obtained from the cellular numeration affected by the salinity of 35 units per thousand on average from three repetitions that were tested, have been given and shown in figure 6. In this treatment, from the 1st through the 10th days, the growth has increased (phase of increase) and from the 11th and 14th days, the growth has decreased (phase of decrease) respectively.

DISCUSSION AND CONCLUSIONS

Considering the goals of research based on study and growth in Conway medium with five degrees of salinities of 15, 20, 25, 30 and 35 ppt in term of determination of the best and the most suitable degree of salinity, the results of this research and those obtained from other researches will be discussed.

Study of the purification of *N.oculata* unicellular alga by using different concentration of salinity (25, 35, 45 ppt) in Walne's medium and found that there was a significant difference in salinity difference for growth of the species so that the utmost growth of *N.oculata* was in the salinity of 25 ppt. Although another medium was used in this research, the results of difference in salinities chosen in this research showed significant results. Consequently, the best degree of salinity for the growth of the aforesaid species was the salinity of 25 ppt. The results obtained exactly conform to the aforesaid research [3].

In a research the growth of *N.oculata* microalgae in Conway medium and at three degrees of salinity (20, 25 and 30 units per thousand) was

studied. According to the results obtained from the said study, the utmost growth was observed in the salinity of 25 units per thousand. In this research, from all degrees of salinities chosen, the utmost growth was observed at degree of salinity of 25 units per thousand [9].

Investigation of the growth and approximate compound of *N.oculata* in the Conway medium with a degree of salinity of 30 units per thousand and pH of 8 in exterior conditions in shadow at 24-36 degrees centigrade and light intensity of 140 Micromoles per m^2/second and under laboratory conditions at 20 degrees centigrade and light intensity of 150 Micromoles per m2/second. The results of the said research revealed that more quick growth occurred in the exterior medium by $11*10^6$ cells per milliliters. Concerning the fact that this research was conducted under laboratory conditions at 25 degrees centigrade, the growth of the species in Conway medium with a salinity of 30 ppt reached $30*10^6$ cells per milliliter. Eventually, the most desirable yield was observed compared to the aforesaid research [1].

Considering the research conducted on *N.oculata* during the 10-day period in Conway medium at 25 degrees centigrade, with a salinity of 30 units per thousand at light intensity of 5000 Lux within a 12-day period of darkness and 12 hours of lightness and according to the results obtained from this research, number of cells obtained from numerating using a slide on the 10^{th} day reached to $15*10^6$ cells per milliliter. Also, in this research, in equal medium and degree of salinity during the same number of days as mentioned above, number of cells obtained from numeration has reached to $27*10^6$ cells per milliliter. Concerning the fact that this research was conducted at light intensity of 5000 Lux within a lightness period of 18 hours and 6 hours of darkness, a noticeable increase was observed in growth of the aforesaid microalgae. The case of superiority of this research is long period of lightness [2].

Results of study the effect of salinities of 15, 25, 35, 45 and 55 units per thousand on the growth, biochemical compound and fat products of Nannochloropsis in a 19-day study under controlled culture revealed that the dry biomass of *N.oculata* at salinity of 25 units per thousand showed the highest cellular density from among other treatments within the first ten days of culture. In this research, from among all degrees of salinities chosen, the utmost growth was observed at degree of salinity given as 25 units per thousand [8].

There is a research and studied the effect of salinity on growth and fat for producing biological fuel in Nannochloropsis microalgae [7]. Culture of the said alga was conducted in brackish waters to very salty ones. The utmost growth of alga and biomass was observed within the range of salinity of 22 through 34 units per thousand. Since in this research, the desirable salinity for maximum cellular density and growth of alga was determined as 25 units per thousand. Thus, the results obtained from this research are confirmed accordingly.

Concerning the fact that in this research, Conway medium in different salinities were used, the results revealed that the treatment of salinity of 25 units per thousand has obtained the first rating in term of growth [7]. Thus, one may come up with this conclusion that degree of salinity may independently affect the cellular growth. In fact, range of salinity used for culture of this species has been introduced as 20-30 units per thousand and the desirable salinity as 25 units per thousand accordingly. Besides other factors involved in culture of this species, the said salinity shall play an effective role in increase of biomass of the said species in mediums accordingly.

ACKNOWLEDGEMENTS

Thanks to the Islamic Azad University of Bushehr and all person that cooperate with us to plan and project the study.

REFERENCES

[1] Banerjee, S., Hew, W.E., Khatoon, K. and Shariff, M. (2011) Growth and proximate composition of tropical marine *Chaetoceros calcitrans* and *Nannochloropsis oculata* cultured out door and under laboratory conditions. African Journal of Biotechnology 10(8), 1375-1383. DOI: 10.5897/AJB10.1748.

[2] Devi, Sh., Santhanam, P., Rekha, V., Ananth, S., Balaji Prasath, B., Nandakumar, R., Jeyanthi, S. and Dinesh Kumar, S. (2012) Culture and biofuel producing efficacy of marine microalgae *Dunaliella salina* and *Nannochloropsis sp*. Journal of Algal Biomass Utilization 3(4), 38–44.

[3] Ghezelbash, F., Farbodnia, T. and Agh, N. (2009) Purification of Unicellular algae *Nannochloropsis sp.* and *Isochrysis sp.* by using different light intensity and salt concentrations. Iranian Journal of Biology 22(1), 95-102.

[4] Gocer, M., Yanar, Y. and Yanar, M. (2006) Effects of carotenoids from *Duneliella salina* and *Nannochloropsis sp.* on pigmentation, proximate composition, meat yield and growth of *Penaeus semisulcatus*. Advances in Food Sciences 28 (2), 89-93.

[5] Haran, M.P. (1992) Manual on shrimp hatchery operation and management (Penaeusmonodon). TASPARC, p. 114.

[6] Maruyama, I., Nakamura T., Matsubayashi T., Ando Y. and Maeda, T. (1986) Identification

of the alga known as “marine Chlorella” as a member of the Eustigmatophyceae. Japanese Journal of Phycology 34, 319-325.

[7] Meridith, L., Wiebke, J., Alina, A. and Omar Holguin, F. (2013) Effects of salinity on growth and lipid accumulation of biofuel microalga *Nannochloropsis salina* and invading organisms. Biomass and Bioenergy 54, 83-88. DOI: 10.1016/j.biombioe.2013.03.026

[8] Na, G., Qiang, L., Gang, L., Yehui, T., Liangmin, H. and Junda, L. (2012) Effect of salinity on growth, biochemical composition and lipid productivity of *Nannochloropsis oculata* cs179. Engineering in life sciences 12(6), 631- 637.DOI: 10.1002/elsc.201100204

[9] Naghibi, M., Ghaeni, M. and Masoumizadeh, Z. (2013) Investigation of cell density and chlorophyll of *Nannochloropsis oculata* in Conway medium in different salinities. Proceeding of fisheries and aquatics conference, Bandarabbas, p 53-59.

[10] Ozturk, S., Aslim, B. and Beyatli, Y. (2006) Biological screening of microalgae isolated from different freshwaters of Turkey: antimicrobial activity, viability and brine shrimp lethality. Fresenius Environmental Bulletin 15 (10), 1232-1237.

[11] Salavatian, M., Azari Takami, Gh., Keyvan, A., Vahabzadeh. H. and Rajabinezhad, R. (2006) Evaluation of growth and biomass of *Nannochloropsis oculata*. Iranian Journal of Marine Sciences 5 (1, 2), 43-53.

Received: **22.06.2015**
Accepted: **20.12.2015**

CORRESPONDING AUTHOR

Esmaeil Kouhgardi
Natural Resources Department,
Bushehr branch,
Islamic Azad University,
Bushehr, Iran

e-mail: Kouhgardi@iaubushehr.ac.ir

© by PSP Volume 25 – No. 7/2016, pages 2305-2318 Fresenius Environmental Bulletin

CALCULATION AND TEMPORAL VARIABILITY OF VENTILATION COEFFICIENT DEPENDING ON LOCATION AND CHARACTERISTICS OF HOUSES IN BALIKESIR CITY CENTER

Nadir Ilten[1,] *, Lokman Hakan Tecer[2], Ayse Tülay Selici[3]

[1]Department of Mechanical Engineering, Balıkesir University, Balıkesir, Turkey
[2]Department of Environmental Engineering, Namık Kemal University,Çorlu/Tekirdağ,Turkey
[3]Balıkesir Municipality, Balıkesir, Turkey

ABSTRACT

In recent years, there has been much research on indoor air quality, owing to a growing interest in improvement of air quality in residential buildings. People spend most of their time indoors, where air quality is affected by many factors such as location and structure of housing, ventilation systems, and comfort parameters. CO_2 and other indoor gas concentrations are important indicators of indoor air quality. The aim of this study is to determine the effects of various factors such as location and characteristics of housing and smoking status on carbon dioxide (CO_2) concentrations and air exchange rates in 29 representative buildings in Balıkesir, Turkey. CO_2 concentrations were measured using a non-dispersive infrared method, air changes per hour (ACH) were estimated using a CO_2 balance method, and other parameters were recorded. Mean CO_2 concentrations were 667 and 1011 ppm in summer and winter, respectively. Estimated mean air exchange rates were 1.04 and 0.70 ACH in summer and winter, respectively. The analysis showed that CO_2 concentrations and ACH were affected by the area of houses, season, ventilation systems and ventilation duration. CO_2 concentrations in winter were higher in all buildings relative to summer in the residential area. Air exchange rates were primarily affected by duration of ventilation, house area, distances to main roads, and smoking status.

KEYWORDS:
air change rate, carbon dioxide, indoor air quality, residential building, Balıkesir, Turkey

INTRODUCTION

People spend about 90% of their time indoors and it is known that air quality of the indoor environment is affected by outdoor air pollution [1]. Ventilation systems and the location of houses affect indoor air pollutant levels [2].

Industrial operations and heavy motor vehicle traffic negatively affect outdoor air quality, thereby readily affecting indoor air media. Ventilation type, ventilation rate and pollutant composition in the indoor environment are parameters used to determine the contribution of outdoor pollutants to indoor pollution [3]. These factors are used to determine conditions called closed building syndrome, sick building syndrome and building-related illness. These conditions might lead to health problems [4].

Indoor pollutant sources and concentrations, building materials, human activities and ventilation systems represent a combination of various complex conditions that determine indoor air quality [5]. Indoor air pollutants were measured very high in different indoor areas of massive public congregations such as bars, schools, exhibition centers and churches [6]. Air transport from leakage, ventilation, and change of location mechanisms between indoors and outdoors affect indoor pollution emission [7, 8, 9, 10]. Under normal conditions, CO_2 makes up about 0.03% of air in the atmosphere. CO_2 concentration varies between 330 and 500 ppm, depending on environmental factors [11].

A human body performing normal daily activities produces 20 liters (L; 0.02 m^3) of CO_2 per hour [4].

Levels of CO_2 emissions that depend on human activity (mobility) are listed in Table 1 [12].

Amounts of breathing, oxygen consumption and CO_2 production based on mobility are shown in Figure 1 [13].

TABLE 1
CO_2 levels emitted depending on human activities.

Position	Activity Degree	CO_2Emission Amount (liter/hour)
Sitting	I	15
Light activity	II	23
Medium activity or slow walking	III	30
Heavy activity or fast walking	IV	30

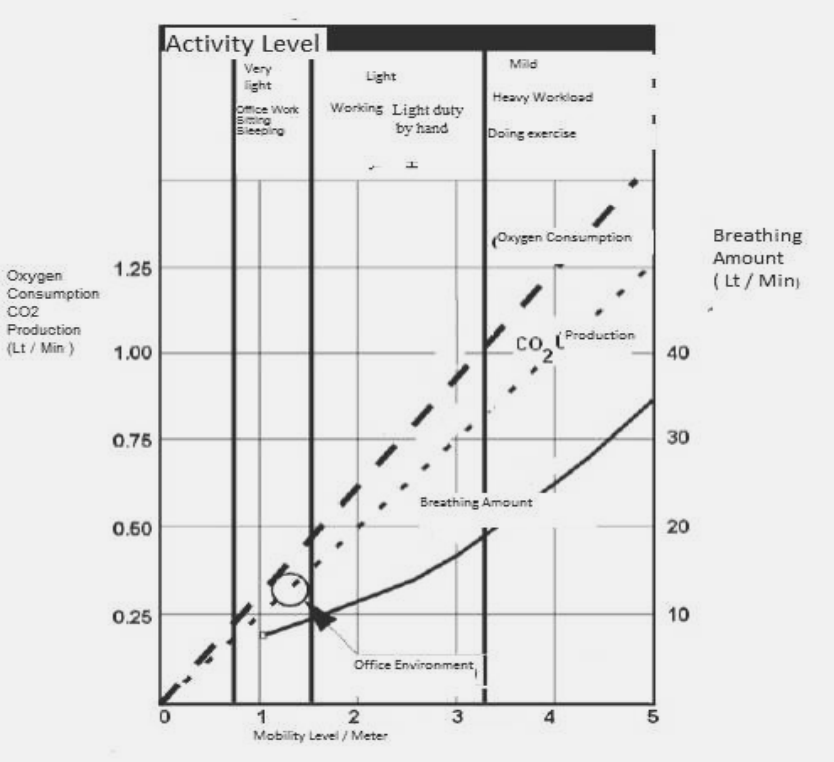

FIGURE 1
Oxygen Consumption and CO_2 Production Depending on Physical Activities [13].

Air change rate (ACR) is accepted as a personal air pollution exposure for indoor environments [14]. In addition, pollutants originating outdoors that enter houses via filtration, open doors and windows, natural ventilation and mechanical ventilation characterize indoor pollution [15]. ACR is also used to evaluate energy consumption of mechanical heating and ventilation equipment [16].

There are many studies that analyze ACR and change of indoor CO_2 concentration [13, 17].

In this study, indoor ACR and air quality were calculated in 29 houses in the city center of Balıkesir, Turkey.

MATERIALS AND METHODS

The city of Balıkesir extends to within the Marmara and Aegean regions, with most of its area in the former. The total area of Balıkesir is 14,456 km^2, about 1.9 % that of Turkey. The central district population of Balıkesir is 259,157 according to a 2009 census [18].

Balıkesir in winter is under the influence of very cold air masses from the north and relatively warm masses from the Mediterranean Sea. A high pressure system in winter reduces the probability of rain and causes strong air pollution [19].

Annual average temperature in Balıkesir is 14.5°C. Average temperature in winter (October–March) is 8.97°C. Wind speeds decrease in winter and spring and increase in summer and fall. Fog occurs province-wide during winter in Balıkesir, generating 95% to 100% humidity. High fossil fuel

consumption because of cold temperatures combined with fog in winter causes air pollution [20].

The main reason for the winter air pollution in Balıkesir is the consumption of fossil fuels for energy and heating. Industrial activity and traffic also affects the air quality. The population, topography and winter meteorological conditions increase pollution. The bowl-shaped topography of the city center and weakening winds in winter, as well as the high pressure and decreasing air temperature are all factors that increase air pollution [21].

According to a study in Balıkesir between 1999 and 2005 during winter, statistical relationships between meteorological factors (temperature, wind speed, humidity and pressure) and air pollution were investigated. A high level of air pollution was identified under light wind speeds, low temperature, high pressure and high humidity in winter [22].

In the city center of Balıkesir, 33.5% of houses are heated with stoves, 24.5% with central heating systems, and 42% with combi boilers. General domestic coal is used for heating with stoves. High heat-value coal imported from other countries or natural gas is used for central heating and natural gas for combi boilers. For heating houses, it has been found that natural gas usage accounts for 43% of fuel, domestic coal 30%, and imported coal 22% [23].

Data Collection. In this study, CO_2 level and comfort parameters such as temperature and humidity were measured continually for 24 hours over 5 days, in 29 houses in the Balıkesir city center. Measurements of indoor and outdoor air quality levels were taken simultaneously. The studies were performed by two measurement companies in summer (July–September 2009) and winter (January–March 2010).

Sampling points chosen according to three different socio-demographic characteristics to be able to distinguish and compare the source of pollutants is shown in Figure 2. According to the evaluations, 1st region poor, 2nd middle and 3rd have been identified as high socio-economic groups. These are as follows. According to socioeconomic status, in the first region, there are 11 districts with total population 62,661. In the second region, representing low economic status, there are 24 districts with a total of 120,239 people. In the third region of high economic status, there are five districts and a total of 58,501 people.

The distribution of buildings in these regions is as follows. Measurements were performed in eight buildings in the first region, 15 in the second and seven in the third. We considered the location of the micro-environment in the regions (distance from the street and traffic), smoking in houses and offices, fuel type (natural gas, fuel oil, coal) for heating, equipment for heating, and systems used in the kitchen (LPG, natural gas, electricity).

Indoor CO_2 measurement devices are located in the kitchen of the house and approximately 1.5-2 m in height. They are installed away from the balcony doors and windows and also 1 m away in distance from the furnace type incineration system. Information given to the family members about the activities that may directly affect measures and it is requested to comply specified measurement procedure. Daily life was continued where the measurement were obtained and continuous measurements were taken.

Telair 7001 CO_2 / Temperature Monitor, which uses "NDIR-Automatic Measurement Method with Infrared Rays, is used to determine indoor CO_2 concentration, temperature and humidity values to. The device consists of display unit and a data storage unit (data logger) (Figure 3).

The measurement accuracy of the device is 1 ppm for CO_2 concentration, of 0.01 °C for temperature, and 0.01% for relative humidity (Telaire 7001). Device is adjusted before the measurements were made. In the adjustments; start and end time of the measurement and measurement point information are entered to the data storage unit via a computer. After the measurements completed, data in the data storage unit is transferred to the computer using the software called HOBO ware (version 2.1.1_18). Then these data were converted to Excel format for later use in analysis. The measurement range is in the 0-10,000 ppm and measurement accuracy is ± 1 ppm.

An ASTM E741 test method was used for ACR calculation. In this method, the ventilation coefficient can be identified under certain conditions, from tracking CO_2 gas concentration in the indoor environment.

FIGURE 2
Indoor Air Quality Sampling Points.

(a) **(b)**

FIGURE 3
CO_2/Temperature Monitor (a) and Data Logger (b).

The outdoor air flow equation of the method is [24]:

$Q_p = 10^6 x G_p / (C_{in,eq} - C_{out})$, where **(1)**

Q_p = outdoor airflow rate per person into the zone, L/s per person,

G_p = CO_2 production rate in indoor environment per person (L/s),
$C_{in,eq}$ = steady-state CO_2 concentration in indoor environment (ppm),
C_{out} = outdoor environment CO_2 concentration (ppm).
ACR of the room can be calculated per hour [25].

$ACR = Q_p / V_{room}$, where **(2)**

V_{room} is volume (m^3) of the room.

Analyses of ventilation and indoor air quality were dependent on indoor and outdoor CO_2 amount measured inside and outside of buildings in Balıkesir.

RESULTS AND DISCUSSION

In 29 houses in Balıkesir city center, averages and standard deviations (SD) of CO_2 levels in summer and winter were 667 ppm (127 ppm) and 1011 ppm (398 ppm), respectively. Outdoor CO_2 measurements were 405 ppm (99 ppm) in summer and 443 ppm (120 ppm) in winter.

We found average and SD of ACR in winter and summer of 1.04 h^{-1}(0.64) and 0.70 h^{-1}(0.67) respectively. Average air leakage rates (and SD) were 78.34 L/sec (45.15) in summer and 48.80 L/sec (40.69) in winter. Descriptive statistics of measured parameters are given in Table 2.

TABLE 2
Statistical data of pollution, ventilation and physical features in the houses.

		N	Minimum	Maximum	Mean	Std. Deviation
CO_2(Indoor environment-Summer)	ppm	29	419	874	627	127
CO_2(Indoor environment-Winter)	ppm	29	538	2062	1011	398
Houses – Square	m^2	29	50	175	107,10	27,15
Q_P(summer)	lt/sec	29	21	220	78,34	45,15
ACR (summer)	h^{-1}	29	0,23	2,98	1,05	0,64
Q_P(winter)	lt/sec	29	7,57	145,78	48,80	40,69
ACR (winter)	h^{-1}	29	0,09	2,18	0,70	0,67

In this study, outdoor air leakage was detected above the 50 L/s limit [14] in most houses during summer, but below this limit in winter (Figure 4).

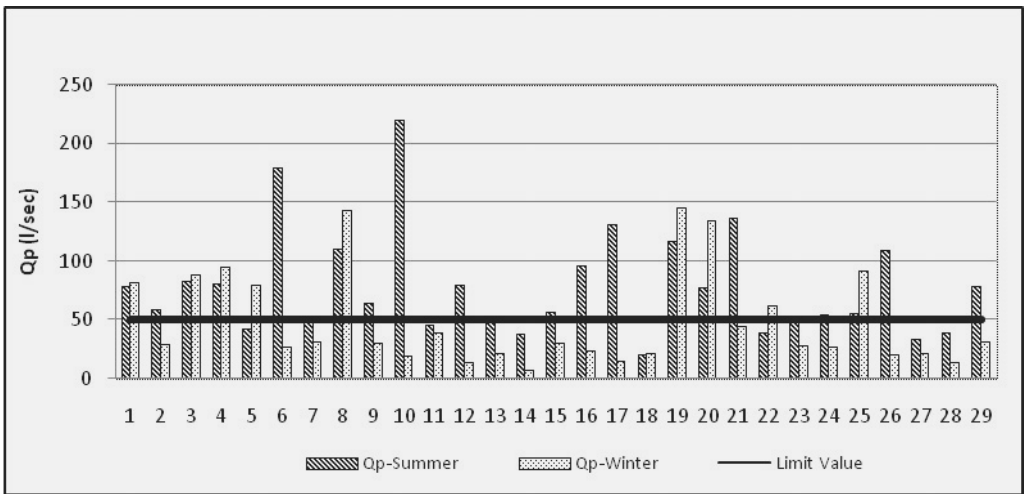

FIGURE 4
Air Leakage Rates Measured in Houses [27].

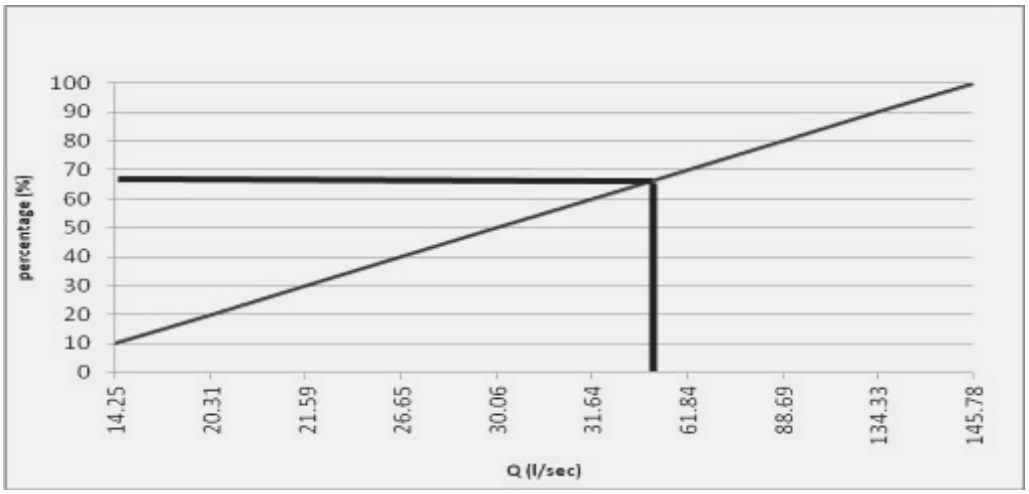

(a)

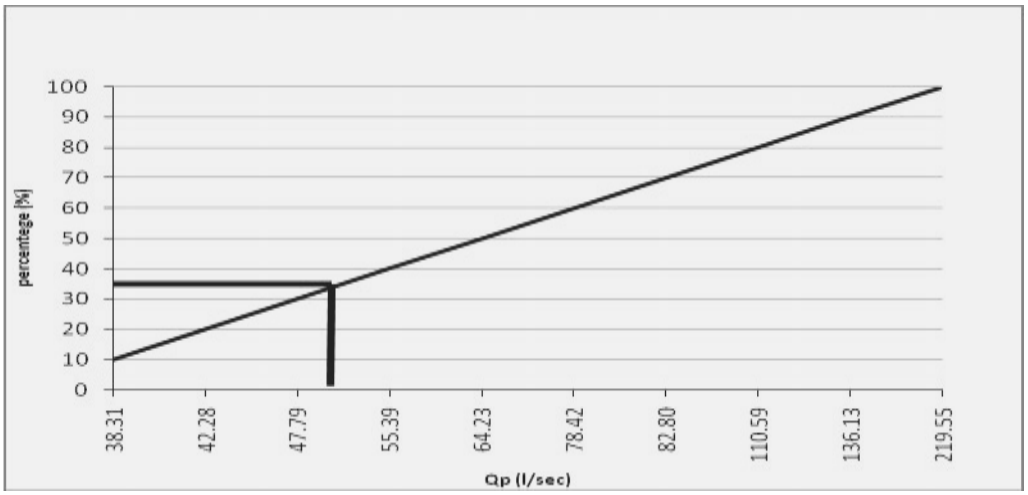

(b)

FIGURE 5
Outdoor Air Leakage in the Summer (a) and Winter (b) Season [27].

Cumulative percentage changes of Qp are given in Figure 5**.**

Figure 6 shows that the amount of air coming from outdoors into the indoor environment was less than the limit value in 33% of houses during summer and in 66% during winter**.** Open doors and windows in summer increased air leakage into the indoor environment.

Average ACR (h^{-1}) of the dwellings in winter and summer is summarized in Figure 6. Minimum ACR in most houses was greater than 0.35 h^{-1} in summer. However, in winter, lower ACR values were found. A study in Denmark indicated that ventilation rates in 57% of houses where children aged 3–5 years were living was below 0.5 h^{-1} [26].

According to an ACR cumulative percentage graphic (Figure 7), ACR in almost all the houses exceeded the limit value in summer. In winter, the value in 47% of the houses was below the limit [27].

Qp in all regions of the city was found to exceed the limit value (50 L/s) in summer. In the second and third regions, Qp was below this limit in winter (Figure 8).

The distribution of the outdoor air leakage values by region in summer time were 85.09 L / s (± 44.02) in first region, 83.83 L / s (± 52.79) in 2nd region, and 59.65 L / s (± 25.97) in 3rd region, while in the winter, 71.81 L / s (± 40.58) in region 1, 43.45 L / s (± 43.26) in 2, and Region, 33.20 L / s (± 26.34) in 3rd region. Differences in Qp among the three regions are mainly due to different proximities to the city center and temporal variability.

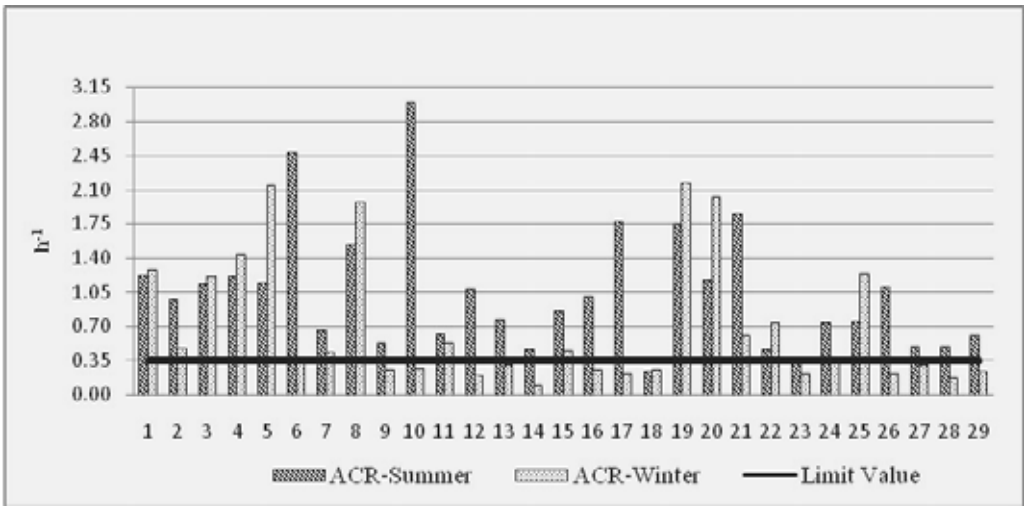

FIGURE 6
Air Change Rate During Winter and Summers (h^{-1}) [27].

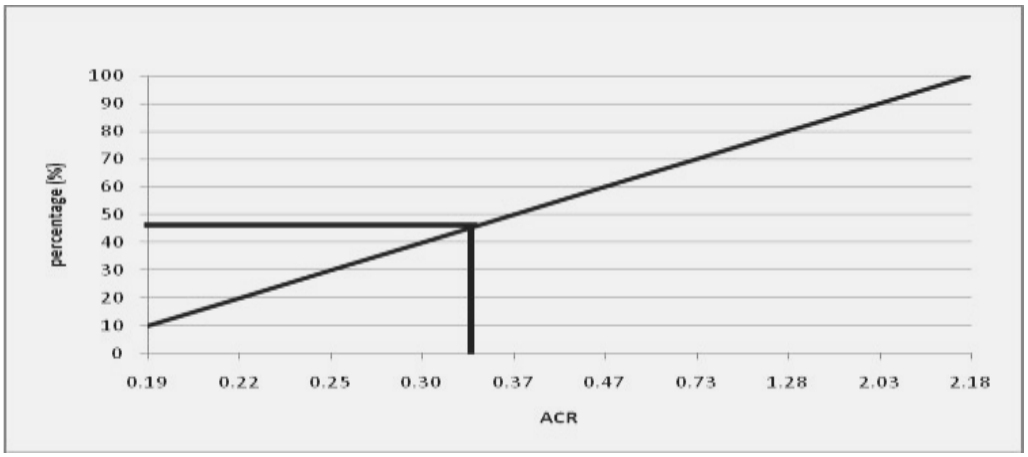

(a)

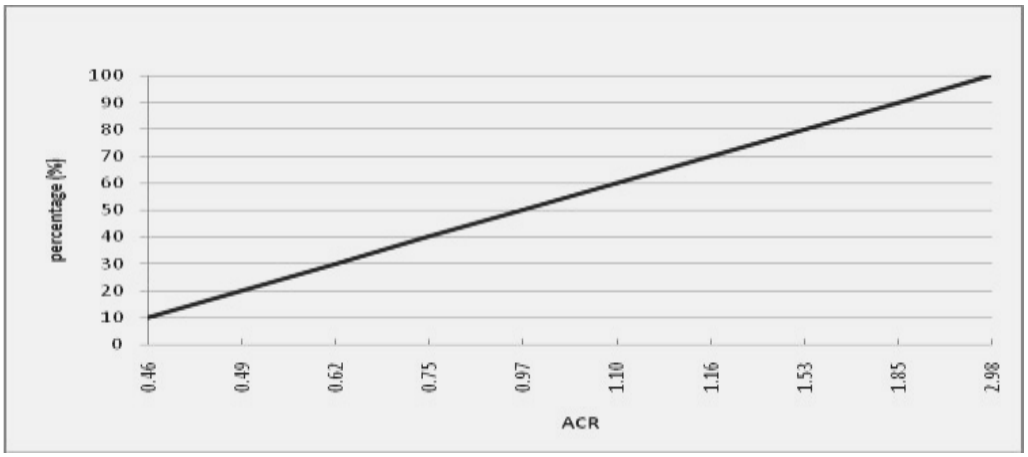

(b)

FIGURE 7
Seasonal Cumulative Distributions of Air Change Rate in the Houses in the Summer (a) and Winter (b) Seasons (%) [27].

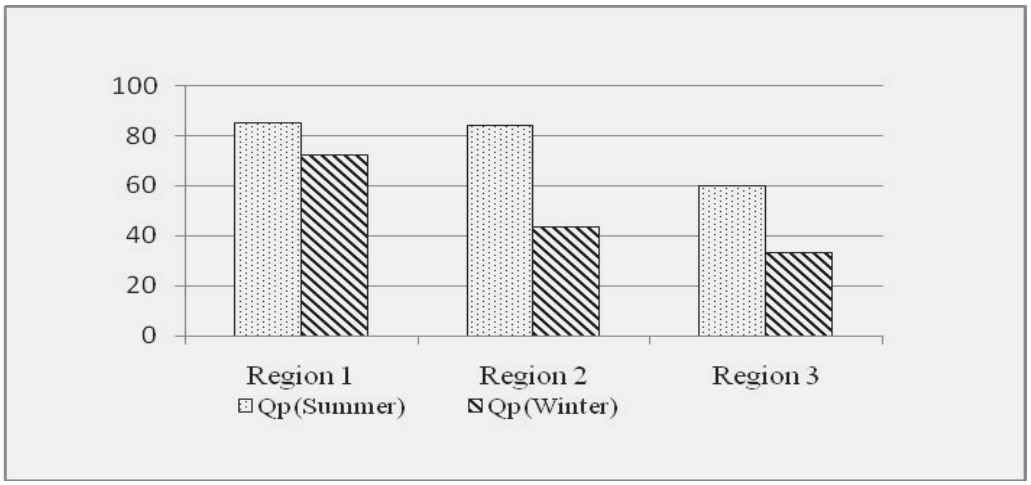

FIGURE 8
Outdoor Air Leakage Values Depending on the Different Socia Economic Region Summer and Winter Season (lt/sec).

Indoor CO_2 rates were less than the limit of 1000 ppm in the houses during summer, but above this limit during winter (Figures 9, 10 and 11). Figure 11 shows that in winter, 43% of houses exceeded the 1000 ppm limit**.**

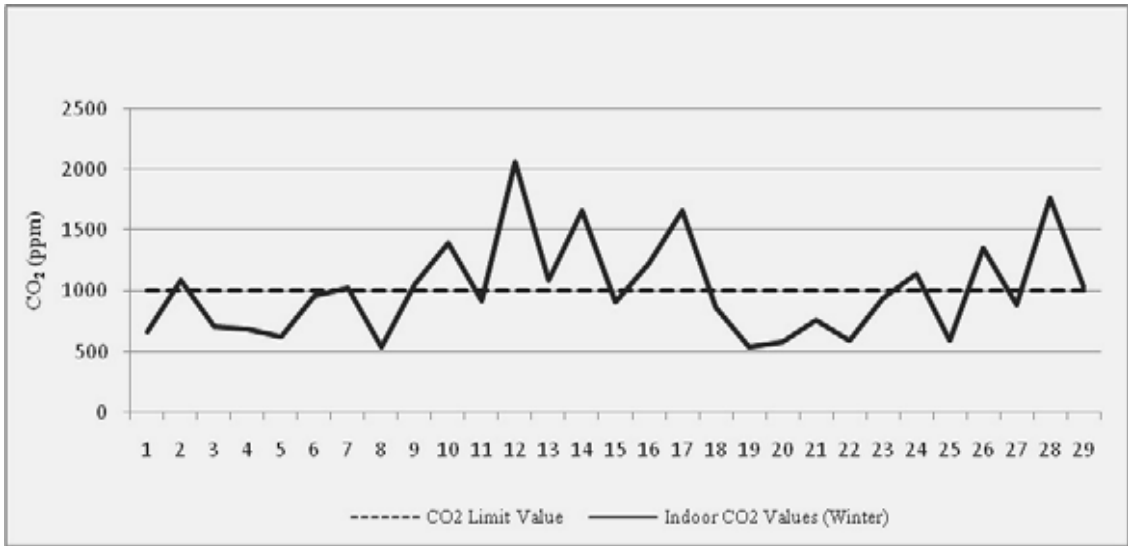

FIGURE 9
Indoor CO_2 Levels in the Winter Season [27].

We analyzed parameters that affect pollution and ACR such as cigarette consumption, ventilation period, area of the houses, distances to main roads, and indoor environment, in 29 houses.

In houses where people smoked, average Q_p was 45.91 L/s (± 37.24) in winter. In non-smoking houses, this was 52.36 L/s (± 45.83). In houses with smokers, ventilation was low, below the standard rate.

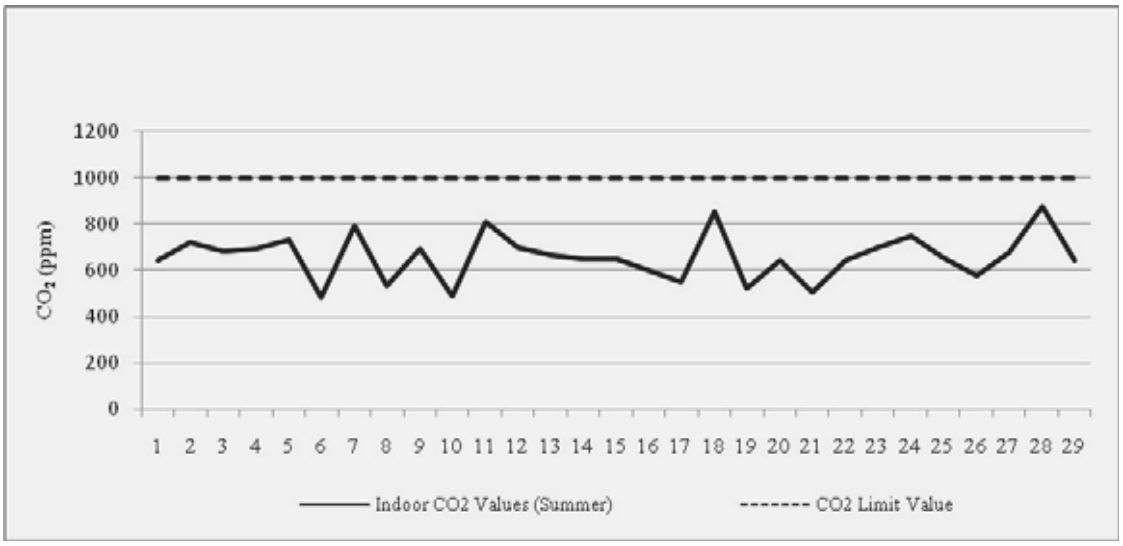

FIGURE 10
Indoor CO_2 levels in the Summer Season [27].

It was also found that Q_p was 84.65 L/s (±51.98) (smoking houses) and 70.59 L/s (±31.90) (non-smoking houses) in summer, which are above the limit value. In winter, ACR was 0.69 h^{-1}(±0.68) (smoking houses) and 0.72 h^{-1}(±0.68) (non-smoking houses), whereas in summer, this rate was 1.15 h^{-1}(±0.76) (smoking houses) and 0.93 h^{-1}(±0.45) (non-smoking houses). ACR in winter was less than in summer.

Statistical data for comfort parameters such as temperature, relative humidity and ACR measured in indoor environments are found in Table 3. Relative humidity measured in summer was below the limit of 60% and, in winter, it exceeded this value in some houses.

Table 4 lists ACR measured in the houses according to cigarette consumption, ventilation duration, house area, indoor comfort parameters, and distances to main roads. This table reveals that human activities and physical conditions in naturally ventilated indoor environments affect ACR and that the standard ACR of 0.35 is not usually met in winter.

TABLE 3
Statistical data of comfort parameters.

	N	Minimum	Maximum	Mean	Std. Deviation
R. Humidity-Summer	29	33,12	53,63	44,36	4,82
Temperature -Summer	29	25,07	30,81	27,67	1,49
R. Humidity-Winter	29	31,11	73,04	53,39	12,09
Temperature -Winter	29	4,62	25,41	17,29	5,67
ACR-Summer	29	0,23	2,98	1,05	0,64
ACR-Winter	29	0,09	2,18	0,70	0,67

Change of ACR in comfort parameters was also determined in summer and winter according to average humidity and temperature. ACR (and SD) corresponding to above and below average humidity values measured in summer were 1.09 h^{-1}(±0.56) and 1.01 h^{-1}(±0.71), respectively. Corresponding values in winter were 1.02 h^{-1}(±0.82) and 0.51 h^{-1}(±0.48). ACR (and SD) corresponding to above and below average temperature values measured in summer were 0.84 h^{-1}(±0.48) and 1.19 h^{-1}(±0.71), respectively. Analogous values in winter were 0.35 h^{-1}(±0.27) and 1.20 h^{-1}(±0.75).

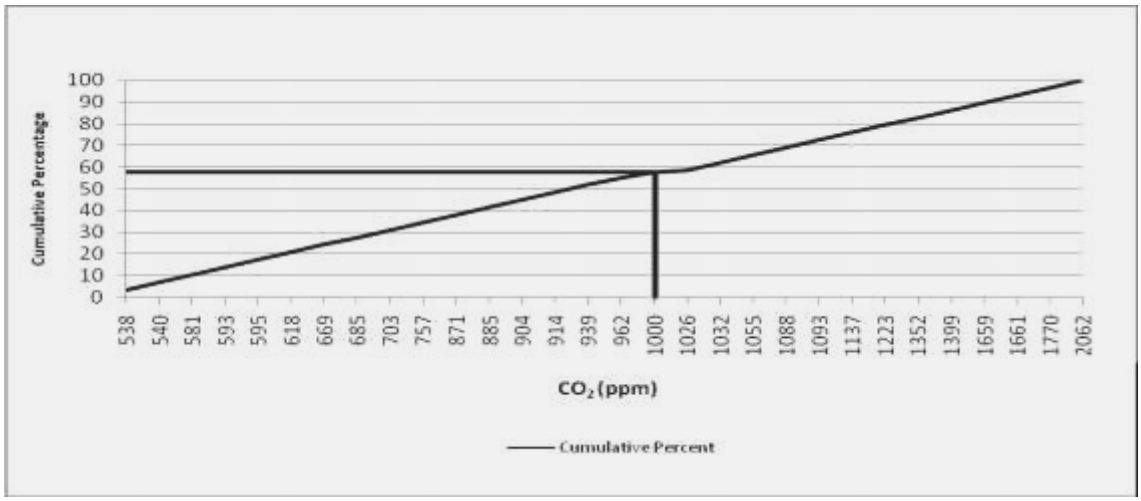

(a)

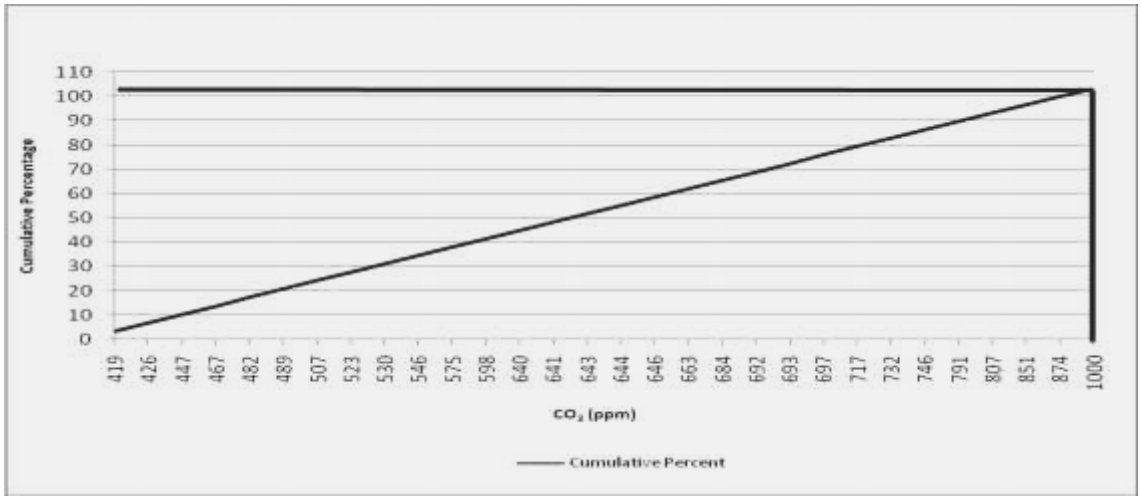

(b)

FIGURE 11
Seasonal Cumulative Distributions of CO_2 Concentration in the Houses in the Summer (a) and Winter (b) Seasons (%) [27].

TABLE 4
Air Change Rate in the Houses.

		Summer (h^{-1})	Winter (h^{-1})
General Average		1,04 (± 0,64)	0.70 (± 0,67)
Cigarette Consumption	Yes	1,15 (± 0,76)	0,69 (± 0,68)
	No	0,93 (± 0,45)	0,72 (± 0,68)
Square Meter (m^2)	>107	0,58 (± 0,29)	0,27 (± 0.18)
	<107	1,26 (± 0,64)	0,90 (± 0,72)
Distance to Main Road	Far	1,12 (± 0,62)	0,85 (± 0,71)
	Close	0,94 (± 0,68)	0,47 (± 0,54)
Ventilation Duration (hour)	<2	1,18 (± 0,89)	0,48 (± 0,42)
	>2	0,98 (± 0,47)	0,82 (± 0,75)

Relative to area of the houses above and below 107 m^2, ACR (and SD) was respectively 0.58 h^{-1}(±0.29) and 1.26 h^{-1}(±0.64) in summer, and 0.27 h^{-1}(±0.18) and 0.90 h^{-1}(±0.72) in winter. There was a relationship between house area and ACR. It was less and below the limit value in houses with large area in winter. In summer, there was low ACR in such houses compared with those with small area (Figure 12).

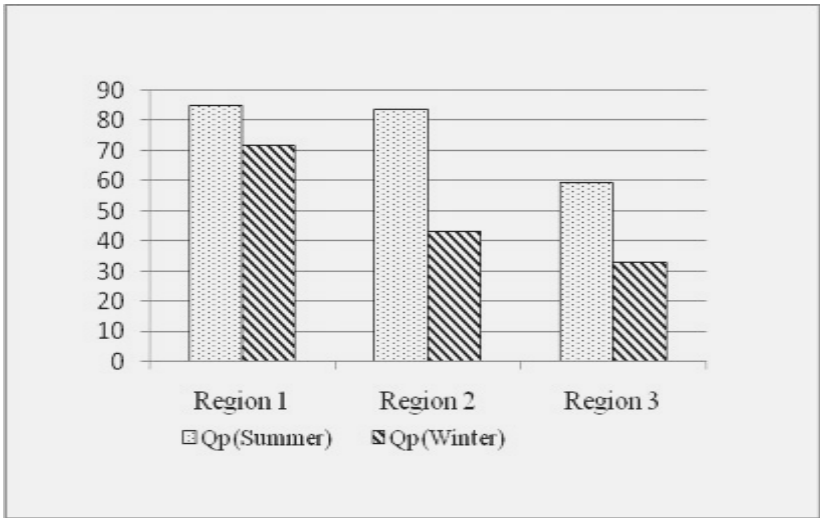

FIGURE 12
Air Change Rate Depending on the Areas of the Houses.

Upon evaluating distance and proximity of ACR to main roads, values in summer were 1.12 h^{-1}(±0.62) and 0.94 h^{-1}(±0.68), respectively, and 0.85 h^{-1}(±0.71) and 0.47 h^{-1}(±0.54) in winter. ACR was lower in houses close to main roads in both seasons.

Data related to ventilation duration in the houses were from surveys, which were found to be around 2 hours. According to the relationship between ventilation duration and ACR in the 29 houses for duration less or greater than 2 hours, the respective rates were 1.18 h^{-1}(±0.89) and 0.98 h^{-1}(±0.47) in summer, and 0.48 h^{-1}(±0.42) and 0.82 h^{-1}(±0.75) in winter. ACR was usually higher because of open windows in summer and lower in winter since houses are less ventilated.

Table 5 shows the comparison of the results of other studies and current study results. The results found by this study are comparable with other studies results. For example, indoor CO_2 concentration was reported at 1603 ppm in winter and 405 ppm in summer at 64 schools. It was also reported that in winter, CO_2 concentration increased because of insufficient ventilation, which is important in determining indoor environment quality [28]. In South Korea in 10 houses, it was found that CO_2 concentrations gradually increased after cooking was begun, but decreased whenever residents used natural or mechanical ventilation [29].

According to another study determining ACR carried out [30], winter ACRs were 2.2–3.3 h^{-1} and 5.3–19.7 h^{-1} in summer. In Northern Europe, It was reported that the median ACR was 0.42 h^{-1} (average 0.55 h^{-1}) in winter according to data collected from 2844 houses [31]. In Sweden, 60% of 390 multifamily houses and 80% of single-family houses did not meet the 0.5 h^{-1} ACR specified in the building code [32].

CONCLUSION

It is determined that carbon dioxide concentrations in 29 houses along with ACR and outdoor air leakage in summer and winter. ACR was higher in summer than in winter. The reason for this is typically open doors and windows, which enhances air circulation.

There is a similar relationship between outdoor air leakage and ACR, with the latter higher in summer than in winter. It was found that this leakage was above the standard of 50 L/s in 77% of houses in summer, and 34% in winter. Insufficient ventilation in the houses during winters might be the reason for this difference.

TABLE 5
Comparison of CO2 concentrations and ACR values.

Parameters	Unit	N	Mean	explain	Ref
CO_2	ppm	29 house	627	summer	this study
			1011	winter	
			<1000	with a mechanical ventilation system	Griffiths and Eftechari, 2008
			1400	windows are closed	
		64 school	405	summer	Fromme et al., 2007
			1603	winter	
ACR	h^{-1}	29 house	1,05	summer	this study
			0,7	winter	
			5,3-19,7	summer	Loupa et al., 2006
			2,2-3,3	winter	
			0,55	winter	Andersan et al., 1997
			1,6	summer	Fromme et al., 2007
			0,61	winter	

Most of the houses met the 0.35 h^{-1} limit for ACR in summer, but only 53% did so in winter.

Indoor CO_2 pollution levels in the houses were measured in winter and summer. CO_2 concentration was found to exceed the 1000 ppm limit in winter, but was less than this value in summer. In winter, 57% of houses exceeded the limit, but none during summer. It is believed that factors such as outdoor air pollution and leakage into the indoor environment, insufficient ventilation, cigarette consumption, and cooking are important in winter.

There was low ACR in houses with smokers relative to houses without them. It is thought that increasing CO_2 from cigarette consumption impacts the ACR.

Higher ACR was found indoors with higher humidity in both summer and winter. ACR was lower in indoor environments with higher temperatures. ACR was higher in houses with smaller areas.

There were smaller ACR values in houses close to main roads. It is believed that in such houses, pollution from traffic affects their indoor environment.

It appeared that ventilation duration influenced ACR more strongly in winter. It is thought that ACR is lower in houses with short ventilation duration in winter, and that indoor pollution reduces ACR owing to insufficient ventilation.

ACKNOWLEDGEMENT

This study was financially supported by the Scientific and Technological Research Council of Turkey (Project No. 108Y166).

REFERENCES

[1] USEPA (1991) Indoor air quality: Sick building syndrome (EPA/402-F-94-004), Indoor Air Group, Resarch Triangle Park, North Cardina.

[2] World Health Organization (WHO) (2003-2004) Health risk assesment of indoor air quality (Mog/HSE/4.3/001,AC.01.03.01.Aw), Ulan boatar Mongalia.

[3] Jones, A.P. (1999) Indoor air quality and health. Atmospheric Environment, 33, 4535–4564.

[4] Schramek, E. (1999) Recknagel-Sprenger Schramek- Heating and Air Conditioning Technology Handbook, TTMD, Ankara, Turkey.

[5] Li, Y., Chen, Z. (2003). A balance-point method for assessing the effect of natural ventilation on indoor particle concentrations. Atmospheric Environment, 37, 4277-4285.

[6] G. Gaidajis, and K. Angelakoglou (2012) Indoor air quality in terms of mass concentrations of particulate matter in areas of massive public

congregation. Fresen. Environ. Bull., Issue 1/8/2012.
[7] Thatcher, T.L. and Laytol, D.W. (1995) Deposition, re-suspension and penetration of particles within a residence. Atmospheric Environment, 29, 1487–1497.
[8] Moriske, H.J., Drews, M., Ebert, G., Menk, G., Scheller, C., Schondube, M. and Konieczny, L. (1996) Indoor air pollution by different heating systems: coal burning, open fire place and central heating. Toxicology Letters, 88, 349-354.
[9] Quackenboss, J.J., Lebowitz, M.D. and Crutchfield, C.D. (1989) Indoor-outdoor relationships for particulate matter: exposure classifications and health effects. Environment International, 15, 353-360.
[10] Polodori A., Fine PM., White V. and Kuran PS. (2013) Pilot study of high performance air filtration for classroom applications. Indoor Air, 23, 185-195.
[11] ASHRAE, (2003) ASHRAE Handbook CD, 2001 Fundamentals, Chapter 9: Indoor Environmental Health. Atlanta, USA.
[12] Doğan, H. (2002) Applied Ventilation and Air Conditioning Technology, Seçkin Publishing, Ankara, Turkey.
[13] Schell, M. B., Turner, S. C. and Omar, S. (1998) Application of CO2-Based Demand-Controlled Ventilation Using ASHRAE Standard 62: Optimizing Energy Use and Ventilation, ASHRAE Transactions, 104(2), 1213-1225.
[14] Pandian, M.D., Ott, W.R. and Behar J.V. (1993) Residential air change rates for use in indoor air and exposure modeling studies. Journal of Exposure Analysis and Environmental Epidemiology, 3, 407-416.
[15] Chao, C.Y.H. and Tung, T.C. (2001) An emperial model for outdoor contaminant transmission into residential buildings and experimental verification. Atmospheric Environment, 35, 1585-1596.
[16] ASHRAE, (2010) Standard 62.2-2010 - Ventilation and Acceptable Indoor Air Quality in Low- Rise Residential Buildings.
[17] Griffiths M. and Eftekhari M. (2008) Control of CO_2 in a naturally ventilated classroom. Energy and Building, 40, 556-560.
[18] TSA, (2013) Turkey Statistical Agency, www.tuik.gov.tr.
[19] BG, (2013) Balıkesir Government, www.balikesir.gov.tr.
[20] BMO, (2013) Balıkesir Meteorology Office, Daily Climatological Data, Balıkesir, Turkey.
[21] BGOPHD, (2013). Balıkesir Governor's Office Public Health Directorate, www.balikesir.saglik.gov.tr.
[22] İlten N. and Selici A.T. (2008) Investigating the impact of some meteorological parameters on air pollution in Balıkesir, Turkey. *Environmental Monitoring and Assesment*, 140, 347-277.
[23] İlten, N., Tecer, L.H. and Selici A.T. (2011) Calculation of Pollutant Emissions are Related to Energy Consumption in Residential, 18. National Thermal Science and Technology Congress. 165-170.
[24] Persily, A.K. (1997). Evaluating Building IAQ and Ventilation with Indoor Carbon Dioxide.http://fire.nist.gov/bfrlpubs/build97/PDF/b97044.pdf.
[25] Bas, E. (2004) Indoor Air Quality-A Guide for Facility Managers, The Fairmont Pres, Lilburn,Georgia.
[26] Bekö, G., Lund, T., Nors, F., Toftum, J. and Clausen, G. (2010) Ventilation rates in the bedrooms of 500 Danish children. Building and Environment, 45, 2289-2295.
[27] Selici, A. T. (2014) Investigation of indoor air quality based on sources of pollutant and comfort parameters and energy consumption, Phd Thesis, Balıkesir Üniversity Institue of Science, 80-82-83, Balıkesir.
[28] Fromme, H., Twardella, D., Dietrich, S., Heitmann, D., Schierl R., Liebl, B. And Rüden, H. (2007) Particulate matter in the indoor air of classrooms-exploratory results from Munich and surrounding area, Atmospheric Environment, 41, 854-866.
[29] Lee, H. Lee, Y.J., Park, Y.S., Kim, W.Y., Lee, Y. (2012) The Improvement of ventilation behaviours in kitchen of residential buildings. Indoor and Built Environment, 21(1), 48-61.
[30] Loupa, G., Charpantidou, E., Kioutsioukis, S. and Rapsomanikis, S. (2006) Indoor microclimate, ozone and nitrogen oxides in two medieval churches in Cyprus, Atmospheric Environment, 40, 7457-7466.
[31] Andersen, C.E., Bergsoe, N.C., Majborn, B. and Ulbak K. (1997) Radon and natural ventilation in newer Danish single-family houses. Indoor Air Qual Clim, 7(4):278-86.
[32] Bornehag, C.G., Sundell, J., Hagerhed-Engman, L. and Sigsgaard, T. (2005) Association between ventilation rates in 390 Swedish homes and allergic symptoms in children. Indoor Air, 15(4), 275-280.

Received: 14.08.2015
Accepted: 11.12.2015

CORRESPONDING AUTHOR

Nadir Ilten
Balikesir University
Faculty of Engineering
Department of Mechanical Engineering
10145 Balikesir – TURKEY

e-mail: nilten@balikesir.edu.tr

© by PSP Volume 25 – No. 7/2016, pages 2319-2330 Fresenius Environmental Bulletin

THE PROTECTION OF *GLYCYRRHIZA POLYSACCHARIDE* ON 2,3,7,8–TETRACHLORODIBENZO-*P*-DIOXIN INDUCED JIAN CARP（*CYPRINUS CARPIO VAR.JIAN*）LIVER INJURY USING PRECISION-CUT LIVER SLICES

Jin-Liang Du[1,2], Li-Ping Cao[1,2], Rui Jia[3], Guo-Jun Yin[1,2,3*]

1.Key Laboratory of Freshwater Fisheries and Germplasm Resources Utilization, Ministry of Agriculture, Freshwater Fisheries Research Center, Chinese Academy of Fishery Sciences，Wuxi 214081, China;
2.International Joint Research Laboratory for Fish Immunopharmacology, Freshwater Fisheries Research Center, Chinese Academy of Fishery Sciences, Wuxi 214081, China;
3.Wuxi Fisheries College, Nanjing Agricultural University, Wuxi 214081, China

ABSTRACT

Exposure to 2,3,7,8-tetrachlorodibenzo-*p*-dioxin (TCDD) represents a potential health risk and hepatotoxicity. The aim of this study was to evaluate the protective effects of *Glycyrrhiza polysaccharide* (GPS) against2,3,7,8–tetrachloro-dibenzo-*p*-dioxin (TCDD)-induced hepatotoxicity in Jian carp using Precision-Cut Liver Slices (PCLS). In this study, PCLS were divided into six groups, five treatment groups (pre-treatment group, post-treatment group, pre and post-treatment group, TCDD group, GPS control group), and one blank control group, GPS (0.2, 0.4 and 0.8 mg mL^{-1}) was added to the PCLS before (pretreatment), after (post-treatment) and both before and after (pre- and post-treatment) the incubation of the PCLS with TCDD at 0.3 μg L^{-1} in the culture medium. The results showed, after PCLS treated with GPS, it was indicated that pre- and post-treatment group had the best effect on relieving TCDD damage, it could significantly inhibited the elevation of glutamate pyruvate transaminase (GPT), glutamate oxalate transaminase (GOT), lactate dehydrogenase (LDH), malondialdehyde (MDA), tumor necrosis factor-α (TNF-α), interleukin-1β (IL-1β) and immunoglobulin M(IgM), and significantly increased the level of superoxide dismutase (SOD) and glutathione S-transferase (GST). GPS can also reduce the expression of AhR2, ARNT2, CYP1A mRNA in different degrees. The present findings might provide new insight into the development of therapeutic and preventive approaches of TCDD toxicity.

KEYWORDS:
2,3,7,8-tetrachlorodibenzo-*p*-dioxin, Precision-Cut Liver Slices, *Glycyrrhiza polysaccharide*, Aryl hydrocarbon (AhR2), Aryl hydrocarbon receptor nuclear translocator (ARNT2), Cytochrome P4501A (CYP1A)

INTRODUCTION

In recent years, the toxicity mechanism of dioxins has become a hot research topic. Dioxins are organic pollutants which can exist in soil, air and water, and originate mainly from industrial garbage and waste incineration[1]. It usually enriches in adipose tissue, and can be gradually amplified by the food chains. It seriously interferes with the normal function of the endocrine system of the organism and displays a wide spectrum of toxic effects, including dermal toxicity, reproductive toxicity, immunotoxicity, and hepatotoxicity [2, 3]. Previous experiments have shown that many chemicals, such as microcystin, dioxin, and lipopolysaccharide (LPS) can cause liver damage[4]. The current research on TCDD mainly relates to the environment and mammals. In humans, short-term exposure to high levels of TCDD often presents as liver damage and chloracne, while low-dose long-term exposure has been linked to immune deficiency, diabetes, and various cancer type[5-8]. Only less reports about the fish, such as the report about the effects of 2,3,7,8–tetrachlorodi benzo-*p*-dioxin on the growth of fish[9].

Typically, TCDD is biotransformation in the liver, so liver is the main storage site and target organ. The liver has long been thought to play the

major role in drug metabolism, first pass metabolism was almost exclusively attributed to the liver, the metabolic capacity of the intestine has been increasingly recognized. Nowadays, PCLS is widely used in pharmaceutical drug discovery and development as an approach for toxicological screening of new drugs[10-12], although the procedure of PCLS was easy adapted to many species, this technology has rarely been used in fish, especially the Jian Carp.

At present, for TCDD therapy, some researchers found that astaxanthin prevented the suppression of antioxidant enzymes in the livers of animals exposed to TCDD [13]. Some researchers also studied L-glutamine (Gln) in alleviating the toxicity of TCDD in liver of rats[14]. There are no reports about used Chinese herbal medicine to treat and prevent TCDD toxicity. Chinese medicinal herbs have been widely used in animal disease, *Glycyrrhiza* was one of the common traditional Chinese herbal medicine, *Glycyrrhiza polysaccharide* (GPS) was the active polysaccharides extracted from *Glycyrrhiza*, GPS mainly consists of rhamnose, glucose, arabinose, galactose, which could adjust the immunity, anti-tumor, anti -virus, antioxidant and so on. In the latest research, GPS has good scavenging effect on DPPH, OH^-, O_2^-.[15]. GPS, one of the major active components, can bolster the body's ability to fight disease by activating proteins in the immune system[16]. Although numerous studies have reported its beneficial effects in mammals, there is a lack of reports on its function in aquatic animals.

In this study, a liver damage model of *Cyprinus carpio var. Jian* (Jian carp) was established by TCDD induction, and the effects of GPS on changes in the liver indices, liver-associated enzymes, and the expression of AhR2, ARNT2, CYP1A mRNA in the liver were investigated.

MATERIALS AND METHODS

Chemicals. L-15 medium, dimethyl sulfoxide (DMSO), 2,2-diphenyl-1-picrylhydrazyl (DPPH), EDTA, Dulbecco's phosphate-buffered saline (D-PBS), gentamicin sulfate, insulin, streptomycin/penicillin and heparin were purchased from Sigma Company (Sigma-Aldrich Co. LLC., santa clara, CA, USA). Fetal bovine serum (FBS) and cell culture plates were ordered from Gibco Company (Gibco Company, Carlsbad, CA, USA). TNF-α, IL-1β, IgM were purchased from Shanghai Zhaorui bio-tech Co., Ltd (Shanghai Zhaorui bio-tech Co., Ltd, Shanghai, CN). TCDD was the product of Toronto Research Chemicals (Toronto Research Chemicals, Toronto, Ontario, CAN) (CAS1746-01-6, purity 98 %). *Glycyrrhiza polysaccharide* (GPS) was purchased from Nantong universal plant extract co., Ltd (Nantong universal plant extract co., Ltd., Nantong, CN). All other reagents used in the experiment were of analytical grade.

Fish. Jian carp were obtained from the Freshwater Fish Research Center of Chinese Academy of Fishery Sciences, Wuxi, China. Fish were reared at 26 ℃ in a recirculation system and fed adlibitum twice a day with diets containing 40 % crude protein, 10 % crude lipid, 10 % ash and an energy content of 21 kJ g^{-1}DM.

Preparation and culture of slices. In sterile conditions, the livers were immediately excised and placed in cold L-15 medium containing with 25 mM D-glucose, 50 μg ml^{-1} gentamicin, and 2.5 mg mL^{-1} fungizone previously gassed with 95% O_2, 5% CO_2 by basic method, the liver was cut into pieces of 5 mm × 5 mm × 5 mm and embedded in a low melting point agarose. The slices were prepared using a ZQP-86 tissue slicer (Zhejiang Jinhua Kedi Instrumental Equipment Co., Ltd., Jinhua, CN) and cultured in 24-well plate in oxygenated L-15 at 27 ℃.

(1)Thickness

The slices are fixed to 200, 300, 400 and 500 μm, respectively. Different thickness of slices were cultured in 24-well plate for 0, 8, 16, 24 and 48 hours at 27 ℃. Then the biochemical indices were measured.

(2)PH

The slices of 300 μm thickness were incubated in L-15 medium with different pH (6.8, 7.0 and 7.2) for 0, 8, 16, 24 and 48 hours at 27 ℃. Then the biochemical indices were measured.

(3)Viability assay

PCLS viability was estimated by adenosine triphosphate (ATP) content. The viability of the tissue slices were measured via ATP determination using the ATP Determination Kit (Nanjing Jiancheng Bioengineering Institute, Nanjing, CN). The results are expressed as μmol ATP g $protein^{-1}$.

DPPH assay. To determine the radical scavenging activity of GPS, DPPH assay was conducted according to the methods described previously. Different methanolic dilutions of extract were prepared (0.05-0.35 mg mL^{-1}). Briefly, 2.0 mL GPS extract was added to 2 mL DPPH solution (90 μM in methanol) as the free radical source. The mixtures were shaken vigorously and allowed to stand at room temperature for 30 min. The decrease of solution absorbance due to proton donating activity of components of each extract was determined at 519 nm. Lower absorbance of the reaction mixture indicates higher free radical scavenging activity. The DPPH with corresponding solvents (without plant material) serves as control. The DPPH radical scavenging activity was calculated using the following formula: DPPH radical scavenging activity (%) = [(A0 – A1 /A0) ×100], where A0 is the absorbance of the control, and A1 is the absorbance of extract or standard sample.

Treatments of Precision-Cut Liver Slices with GPS. The hepatoprotective effect of GPS was investigated using an *in vitro* model of TCDD-induced PCLS injury. Six groups were set up as follows:

(1)Control: slices were cultured in L-15 for 3 h.

(2)GPS control: slices were cultured with GPS at 0.8 mg mL^{-1} in L-15 for 3 h.

(3)TCDD control: slices were cultured with 0.3 μg L^{-1} in L-15 for 3 h.

(4)Pre-treatment group: The PCLS were firstly incubated with 0.2, 0.4, 0.8 mg mL^{-1} of GPS for 3 h, then washed and incubated with TCDD at the concentration of 0.3 μg L^{-1} for another 3 h.

(5)Post treatment group: The PCLS were incubated with TCDD at the concentration of 0.3 μg L^{-1} for 3 h, then washed and incubated with GPS at the concentrations of 0.2, 0.4, 0.8 mg mL^{-1} for another 3 h.

(6)Pre and post treatment group: The PCLS were first incubated with 0.2, 0.4, 0.8 mg mL^{-1} of GPS for 3 h, and then, TCDD was added at a final concentration of 0.3 μg L^{-1}; with 3 h incubation of TCDD, the PCLS were further treated with GPS at the concentrations of 0.2, 0.4, 0.8 mg mL^{-1} for another 3 h.

For each set of conditions, six experiments were performed. At the end of experiment, the supernatants and slices from each individual well were collected and stored at - 20 ℃.

Biochemical index assays. GPT, GOT, TNF-α, IL-1β, IgM in the culture supernatants and LDH, ATP, MDA, SOD, GST, in the liver slice homogenates were measured using kits from Nanjing Jiancheng Bioengineering Institute (Nanjing Jiancheng Bioengineering Institute, Nanjing, CN). Protein content in the liver slice homogenate was determined using BCA test kit. GPT, GOT were expressed as U L^{-1}, SOD, GSH-ST were expressed as U mg^{-1} protein, TNF-α, IL-1β were expressed as ng L^{-1}, IgM was expressed as ng mL^{-1}, LDH was expressed as U g^{-1} protein, ATP were expressed as μmol g^{-1} protein, and MDA was expressed as nmol mg^{-1} protein.

Western blotting assay. The levels of CYP1A protein were determined by immunoblotting. Protein samples were boiled for 5 min in loading buffer (Beyotime Institute of Biotechnology, Haimen, CN), loaded onto a 12 % SDS polyacrylamide gel, separated electrophoretically, and transferred to a cellulose acetate membrane. The cellulose acetate membrane was blocked with sealing fluid and the proteins were probed with a mouse anti-fish CYP1A monoclonal antibody (Biosense, Thane West, India; 1:3000 dilution). The β-actin protein was used as the internal control. Alkaline phosphatase-labeled anti-mouse IgG antibody (Beyotime, Haimen, China; 1:3000 dilution) was used as the secondary antibody in the staining reaction. The amount of immunoreactive product in each lane was determined using Quantity One software (BioRad Laboratories, Hercules, CA, USA).

Gene expression analysis of CYP1A, AhR2,ARNT2. Total RNA was extracted from fish liver using a fast pure RNA kit (TaKaRa Biotechnology Co., Ltd., Dalian, CN), according to the manufacturer's instructions. The RNA quality was detected by gel electrophoresis, the RNA concentration was determined by GeneQuant 1300 (GE Healthcare Biosciences, Piscataway, NJ, USA), and normalized to a common concentration with DEPC treated water (Invitrogen, Carlsbad, CA, USA) before proceeding to cDNA synthesis. The procedure for reverse transcription was carried out according to the manufacturer's instructions (Invitrogen, Carlsbad, CA, USA), and the products (cDNA) were then stored at -20 ℃ for qRT-PCR.

Real-time quantitative PCR (qRT-PCR) was performed to detect the gene expression of AhR,

ARNT, and CYP1A in fish liver using SYBR Premix Ex Taq (TaKaRa Biotechnology Co., Ltd., Dalian, CN), and the reaction was performed on an ABI PRISM 7500 Detection System (Applied Bio systems, Foster city, CA, USA). The program was set to run for one cycle at 95 ℃ for 30 s, 33 cycles at 95 ℃ for 5 s and at 60 ℃ for 34 s. The primers used in this study are listed in Table l. The specificity of PCR amplification was confirmed by agarose gel electrophoresis and melting curve analysis. The gene expression results were analyzed using the $2^{-\Delta\Delta Ct}$ method.

TABLE l
Sequence of primers used for quantitative real-time PCR.

Gene	PCR sequence
AhR2	F: ATTCCCTTCCTCAAAAACCGT
	R: AGTCCAGGATTGGCAGCGT
ARNT2	F: TGGATATGAACGGACTCTCTGTG
	R: CCTGTTGGAAGCTCTCTCGC
CYP1A	F: TGACAAGGACAACATCCGAGAC
	R: TAGACGACAGCCCAAGACAGAG
β-actin	F:GTCAAGTCCGTTGAGATGCACC
	R:GGATGATGACCTGAGCATTGAAGC

Statistical analysis. The data were analyzed with one-way ANOVA using the SPSS 17.0 software and expressed as means ± standard deviation of the means. * $P < 0.05$ and ** $P < 0.01$ were taken as statistically significance.

RESULTS

Effects of different cultured conditions on the biochemical indices. The level of ATP in liver slices of different thickness at various time points are presented in Figure 1a. The results showed that there was no detectable depletion of ATP in slices at 300 μm and 500 μm for 16 hours culture, indicating that the slices at 300 μm and 500 μm can keep normal energy metabolism with no significant change for up to 16 hours.

As shown in Figure 1(b, c, d), there were no significant increase in both GOT and GPT leakage from the liver slices at 300 μm and 400 μm after cultured 16 hours, and LDH leakage from slices at 300 μm showed significant increase after cultured for 24 hours, indicating that the slices at 300 μm can remain stable for more than 16 hours

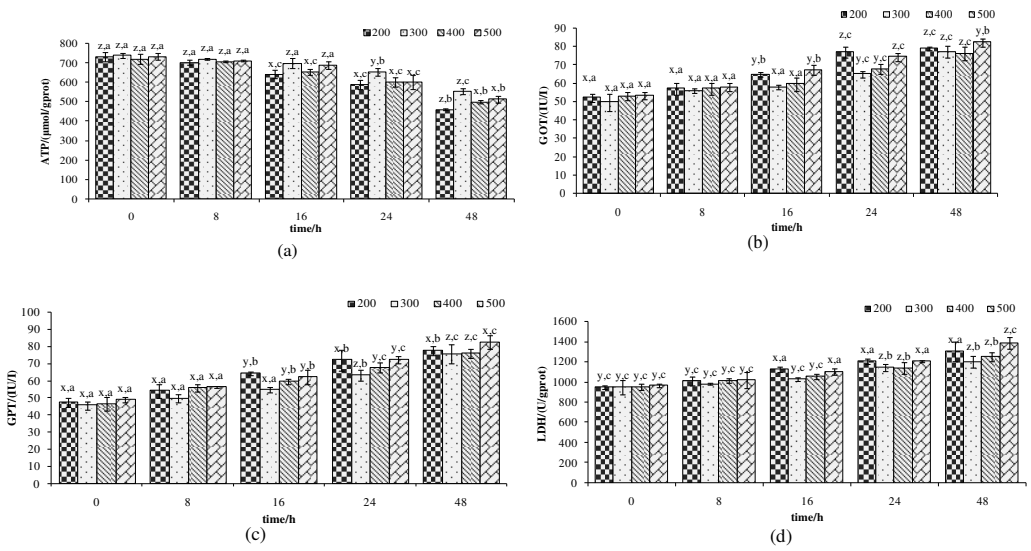

FIGURE 1
The effects of different slices thickness on the level of ATP (a), GOT (b), GPT (c) and LDH (d) at different times. Values are expressed as mean±SD (n=3). $^{x, y, z}$ significant differences ($P < 0.05$) between different thicknesses at various time point; $^{a, b, c}$ significant differences ($P < 0.05$) between different cultured times at each thickness.

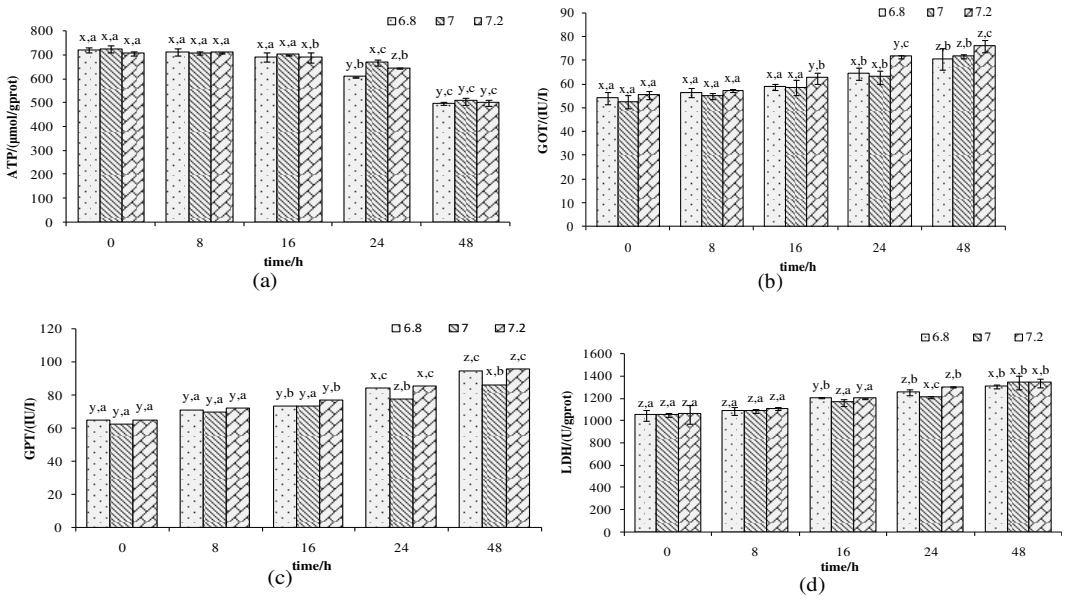

FIGURE 2
The effects of different cultured pH on the level of ATP (a), GOT (b), GPT (c) and LDH (d) after cultured for different time. Values are expressed as mean±SD (n=3). x, y, z significant differences (*P < 0.05*) between different thicknesses at each cultured time;a, b, c significant differences (*P< 0.05*) between different cultured time at each thickness.

The level of ATP in liver slices at 300 μm for different time is presented in Figure 2a. There was a remarked depletion of ATP in slices at pH 7.2 after cultured for 16 hours, however, no detectable depletion of ATP in slices at pH 6.8, 7.0 after cultured for 16 hours was observed, demonstrating that the slices can keep stable energy metabolism for up to 16 hours.

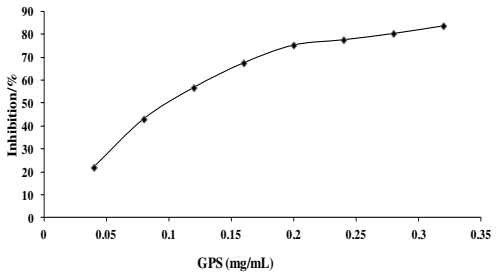

FIGURE 3
Radical scavenging activity of GPS: the inhibition of DPPH changed as the concentration of GPS varied.

The leakages of GOT, GPT and LDH in liver slices at each cultured time are presented in Figure 2 (b, c, d). There were no significant increase in GOT leakage from the liver slices at pH 6.8 and 7.0 after cultured 16 hours, but LDH and GPT leakage from slices at pH 6.8 showed significant increase after cultured for 16 hours, indicating that the slices at pH 7 can remain stable for more than 16 hours.

Radical scavenging activity of GPS. In order to verify the antioxidant power of GPS and its free radical scavenging potency, the DPPH assay was performed. The results showed that GPS even at lower concentration exerted a potent radical scavenging activity (Figure 3).

Effects of GPS on GOT, GPT and LDH activities. As shown in Figure 4, cultured PCLS treated with TCDD, the activities of GOT, GPT, LDH in PCLS culture medium increased significantly (*P<0.01*). When PCLS were treated with GPS at 3 different concentrations, pre-treatment, post-treatment and pre- and post-treatment of the PCLS significantly reduced the increasing activities of GPT, GOT and LDH induced by TCDD.

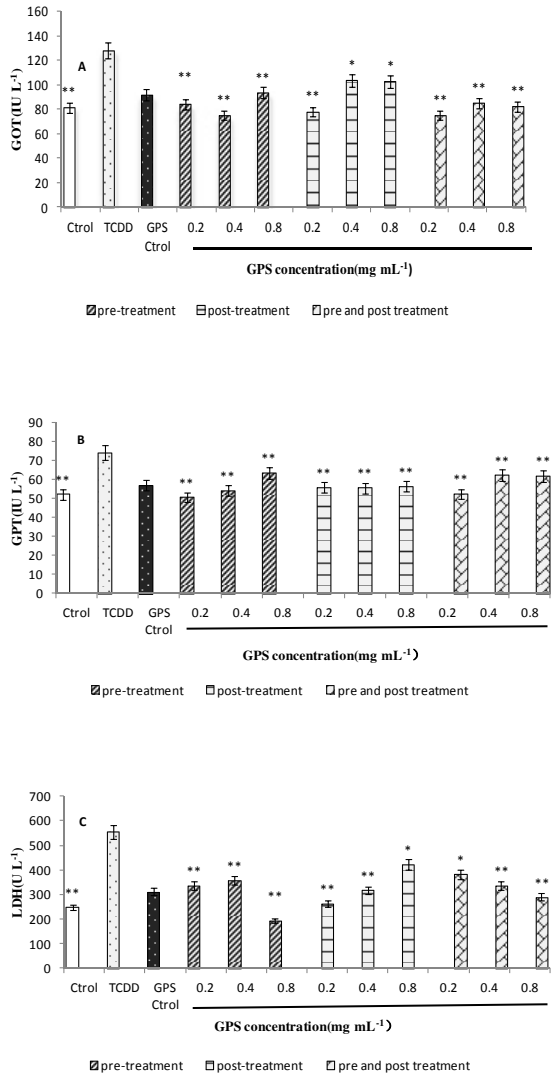

FIGURE 4
Effects of GPS on the activity of GOT(A), GPT(B), LDH(C) in TCDD-treated PCLS culture medium
Ctrol: slices cultured in L- 15; GPS Ctrol: slices cultured in L- 15 with GPS at 0.8 mg mL^{-1}; TCDD: slices cultured in L- 15 with TCDD at 0.3 μg L^{-1}. Values are expressed as mean ± SD (n=6). * *P <0.05*; ***P<0.01*, compared with TCDD group.

Effects of GPS on hepatic antioxidant enzyme activities. As shown in Figure 5, compared with the control group, the SOD activity and amount of GST reduced significantly when PCLS were treated with TCDD alone (*P<0.01*). Pre-treatment with GPS at 0.2, 0.8 mg mL^{-1} significantly increased SOD activity, post-treatment with GPS at 0.4, 0.8 mg mL^{-1} significantly increased SOD activity and amount of GST, pre- and post-treatment with GPS at 0.4 mg mL^{-1} significantly increased SOD activity and amount of GST.

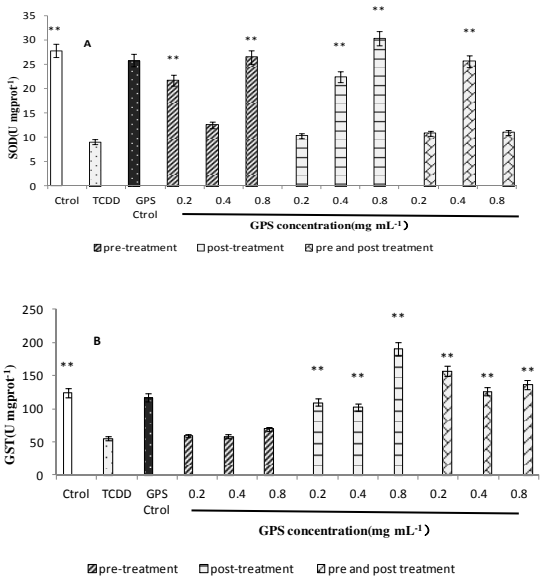

FIGURE 5
Effects of GPS on the contents of SOD(A), GST(B) in TCDD-induced liver injury.
Ctrol: slices cultured in L- 15; GPS Ctrol: slices cultured in L- 15 with GPS at 0.8 mg mL^{-1}; TCDD: slices cultured in L- 15 with TCDD at 0.3 μg L^{-1}. Values are expressed as mean ± SD (n=6). * *P <0.05*; ***P<0.01*, compared with TCDD group.

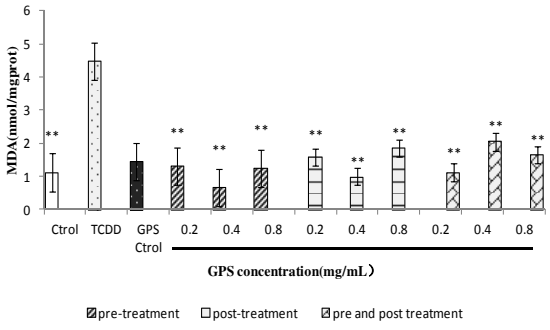

FIGURE 6
Effects of GPS on slices lipid peroxidation in TCDD-induced liver injury.
Ctrol: slices cultured in L- 15; GPS Ctrol: slices cultured in L- 15 with GPS at 0.8 mg mL^{-1}; TCDD: slices cultured in L- 15 with TCDD at 0.3 μg L^{-1}. Values are expressed as mean ± SD (n=6). * *P <0.05*; ***P<0.01*, compared with TCDD group.

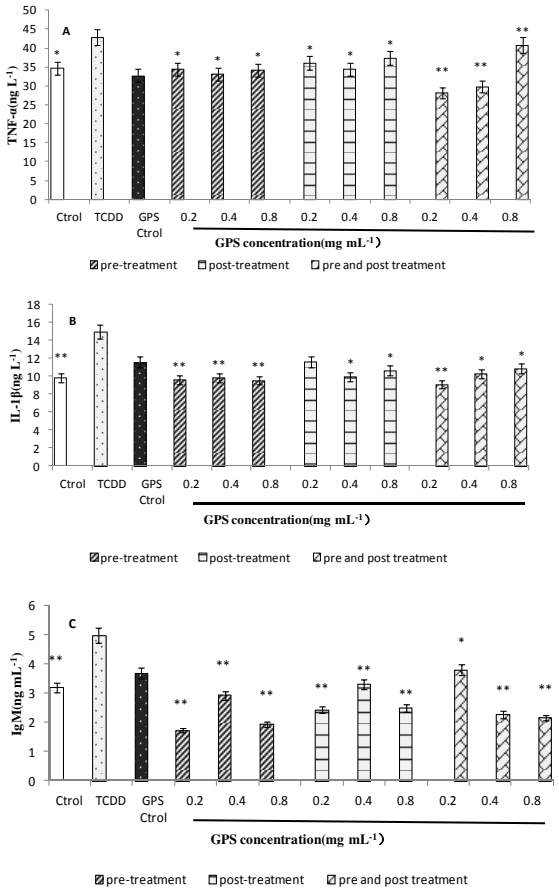

FIGURE 7
Effects of GPS on the contents of TNF-α(A), IL-1β(B), IgM(C) in TCDD-treated PCLS culture medium. Ctrol: slices cultured in L- 15; GPS Ctrol: slices cultured in L- 15 with GPS at 0.8 mg mL^{-1}; TCDD: slices cultured in L- 15 with TCDD at 0.3 μg L^{-1}. Values are expressed as mean ± SD (n=6). * *P <0.05*; ***P<0.01*, compared with TCDD group

Effects of GPS on lipid peroxidation . As shown in Figure 6, cultured PCLS treated with TCDD alone showed a threefold increase in the amount of MDA released into the medium (*P<0.01*). The inhibited MDA formation was significantly inhibited in pre-treatment, post-treatment and pre- and post-treatment.

Effects of GPS on TNF-α, IL-1β, IgM amounts. As shown in Figure 7, cultured PCLS treated with TCDD, the amounts of TNF-α, IL-1β, IgM in PCLS had an increased trend (*P<0.01* or *P<0.05*). In 3 treatment groups, GPS at the concentration of 0.2, 0.4 and 0. 8 mg mL^{-1} could obviously decrease the amounts of TNF-α, IL-1β, IgM to different degrees (*P<0.01* or *P<0.05*).

Effects of GPS on CYP1A protein expression. As shown in Figure 8, the expression of CYP1A was low in control group and GPS control group, after treated with TCDD, the expression of CYP1A in PCLS increased; when precision cut liver slices were treated with 3 different concentrations of GPS, in pre-treatment group, with the concentration increased, the protein expression of CYP1A decreased , these results showed that GPS had some effect on anti liver damage which induced by TCDD. In post-treatment, GPS at the concentration of 0.2, 0.8 mg mL^{-1} could decrease the protein expression of CYP1A; and in pre- and post-treatment, GPS at the concentration of 0.2, 0.4 and 0.8 mg mL^{-1} could decrease the protein expression of CYP1A.

Effects of GPS on CYP1A , AhR2 and ARNT2 gene expression. As shown in Figure 9, AhR2, ARNT2, CYP1A mRNA expression increased significantly in TCDD treatment group compared to the normal control. When PCLS were treated with 3 different concentrations of GPS, in pre-treatment group, GPS at the concentration of**.** 0.8 mg mL^{-1} had the best effect on decreasing the expression of CYP1A mRNA; in post-treatment group, GPS at the concentration of 0.4, 0.8 mg mL^{-1} had the best effect on decreasing the expressions of AhR2, ARNT2,

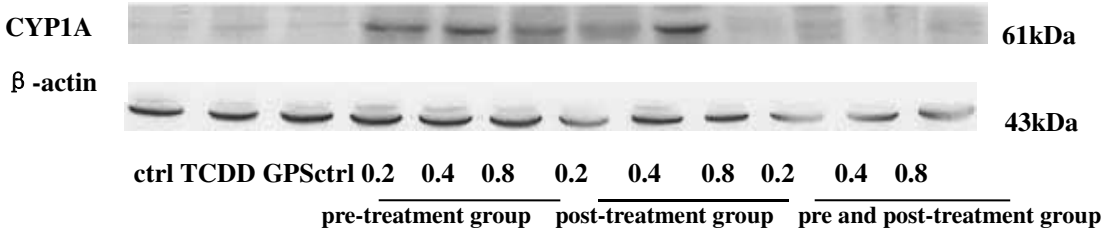

FIGURE 8
Effects of GPS on the protein expression of CYP1A by western blotting.

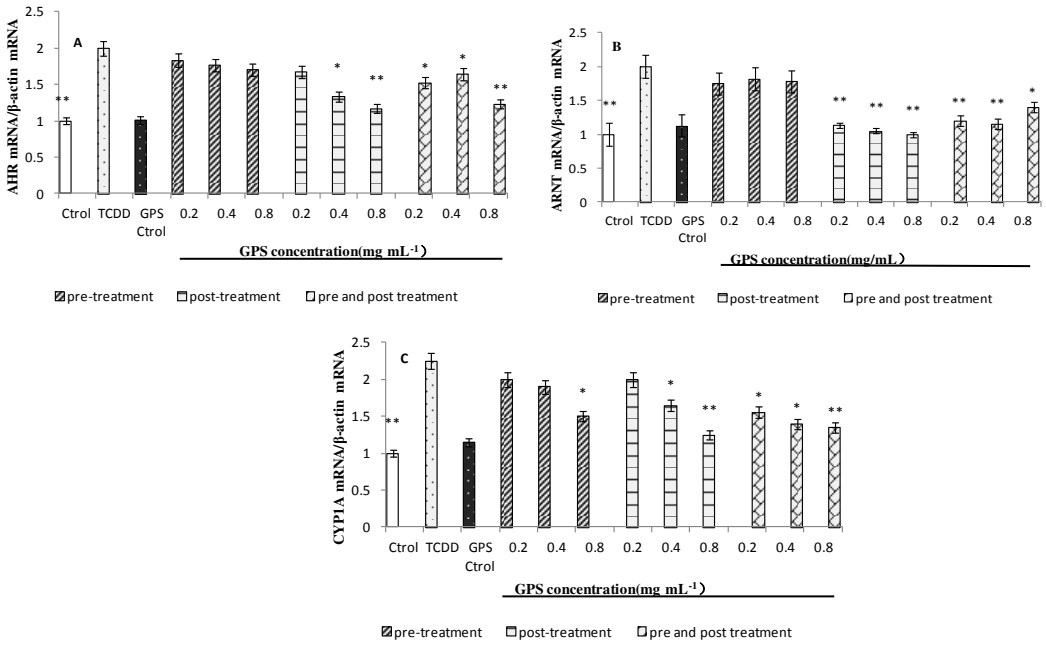

FIGURE 9

Effects of GPS on AHR2(A), ARNT2(B), CYP1A(C) mRNA expression levels of PCLS injury induced by TCDD. Ctrol: slices cultured in L- 15; GPS Ctrol: slices cultured in L- 15 with GPS at 0.8 mg mL^{-1}; TCDD: slices cultured in L- 15 with TCDD at 0.3 μg L^{-1}. Values are expressed as mean ± SD (n=6). * *P <0.05*; ***P<0.01*, compared with TCDD group.

CYP1A mRNA; in pre- and post-treatment group, GPS at all the three concentrations significantly decreased the expression of AhR2, ARNT2, CYP1A mRNA to different degrees.

DISCUSSION

In the past decades, the development of *in vitro* models to study the toxicity of manmade chemicals in fish species often used hepatocytes and hepatoma cell lines [17]. But these methods have limited ability to research the *in vivo* toxicity, they couldn't accurately reflect the effects of drugs or poison on fish liver . In this study, PCLS were used to screen drugs for relieving TCDD induced liver injury in Jian carp for the first time. PCLS have been confirmed by microarrays that PCLS more closely predicted *in vivo* toxicity than isolated hepatocytes or established cell lines[18]. The best preparation and cultivation condition of liver slices is the key to the success of this experiment, so we set different thickness and medium pH to evaluate the slices viability and measured different biochemical indices to analyze the optimal slice thickness and medium pH. The results showed that the slices at 300 μm in the pH 7 medium kept good bioactivity for more than 16 hours.

About the toxicity mechanism of TCDD, the study mainly focus on oxidative stress. Oxidative stress is an important mechanism of chemical toxicity including TCDD, CCl_4, ethanol. Normally, the antioxidant system made production and elimination of activated oxygen in a balanceable and dynamic state, it could prevent excessive ROS caused oxidative stress, kept the body balance, and maintained the normal structure and function of cells. when the body metabolism imbalance, it will cause oxidative damage to the body.

GOT, GPT, LDH are the most sensitive indicator of liver diseases, their values also reflect the degree of injury[19]. In this experiment, GOT, GPT, LDH activities in model group were significantly higher than those in control group, after treated with 3 different concentrations of GPS, GPS at all the three concentrations significantly reduced the activities of GOT, GPT, LDH (*P<0.01*). Our results were consistent with the report from Cao [20] that GPS could markedly inhibit the levels of GOT, GPT and LDH induced by t-BHP.

Lipid peroxidation was an important parameter of oxidative stress, and it usually was

reflected by levels of MDA [21]. MDA usually combined with SOD or GST to reflect the degree of injury of oxygen free radical on the cells. The antioxidant enzymes (SOD, GST) play an important role in defending the cells against free radical-mediated oxidative damage[22], SOD is one of the enzymes on free radical scavenging, inhibition of free radical reaction *in vivo*, it can prevent xanthine dehydrogenase into xanthine oxidase, reduce the production of free radicals, protect liver cells. When oxidative damage or free radicals occurred, the activity of SOD decreased. Therefore, the activities of SOD, GST reflect the degree of oxidative damage. In this study, after treated with different concentrations of GPS, the increasing of MDA caused by TCDD effectively reduced (*P<0.01*) and the activity of SOD also increased significantly (*P<0.01*), 3 different concentrations of GPS can reduce the content of MDA caused by TCDD (*P<0.01*). The activity of SOD increased significantly (*P<0.01*), which showed that GPS can anti the liver injury caused by TCDD. The similar results have been shown in SD rats[23].

TNF-α, IL-1β are the important immunomodulatory cytokines, mainly produced by monocytes- macrophage activation, which have strong anti-infection and anti-cancer effects. It was reported that TNF-α, IL-1β mediated many pathophysiological process in inflammation reaction, played an important role in the pathogenesis of many diseases[24-26]. Mass of TNF-α and IL-1β induces proinflammatory genes, and persistent hepatic injury and inflammation leading to the progressive liver damage, fibrosis, and finally cirrhosis [27, 28]. IgM is immune globulin, which reflects the damage degree of liver disease. In this experiment, after treated with TCDD, the levels of the immune factors TNF-α, IL-1β, IgM increased in different degree (*P<0.01* or *P<0.05*). This indicated that TCDD caused some damage to fish liver. After treated with different concentrations of GPS, GPS in pre and post group at the concentration of 0.2, 0.4 mg mL^{-1} decreased significantly the amount of TNF-α (*P<0.01*); the amounts of IL-1β, IgM decreased significantly (*P<0.01*). This showed that GPS had protective effect on liver injury caused by TCDD.

Western blotting is a well-established, inexpensive and accurate way of measuring protein content.CYP1A is the important subgroup of CYP450, its activity level can directly influence the therapeutic effect of drugs and toxic effect. The expression level of CYP450 have been popularly used to screen and research new drugs in the world[29-33]. It could predict the effectiveness and potential toxicity of drugs *in vitro* and *in vivo*. In this experiment, after treated with TCDD, we found that TCDD significantly increased the expression of CYP1A, in different treatment group, order of dosing also influence the expression of CYP1A. In post treatment group, CYP1A expression decreased gradually with the drug concentration increasing, which indicated that the high concentration of GPS had certain inhibition on CYP1A expression. In the pre-treatment group, the expression of CYP1A was not obvious regularity. In pre and post treatment group,CYP1A expression decreased gradually along with the increase of GPS. From the results, we knew that GPS has good effect on relieving TCDD damage.

A number of evidence support the idea that the regulation of adaptive metabolism requires an AhR partnership with the aryl hydrocarbon receptor nuclear translocator (ARNT)[34]. In this study, the expression of AhR2, ARNT2, CYP1A mRNA increased significantly in TCDD treatment group compared to the normal control. The similar results have been shown in atlantic salmon (salmo salar) [35]. It was reported that TCDD as the ligand of AhR, binding with the AhR of cytoplasm entering the cellular nucleus, and then combined with the specific enhancer sequence, induced the ARNT, CYP1A mRNA expressions[36]. When precision cut liver slices were treated with 3 different concentrations of GPS, pre-treatment, post-treatment and pre-and post-treatment of the PCLS with GPS at all the three concentrations reduced the expressions of AhR2, ARNT2 mRNA induced by TCDD in different degrees .

CONCLUSIONS

In summary, the present findings demonstrate that GPS plays a protective role against liver damage induced by TCDD in Jian carp. The hepatoprotective effects of GPS are closely associated with the elevation of the hepatocyte antioxidative capacity and inhibition of the expression of AhR2, ARNT2, CYP1A.

ACKNOWLEDGEMENTS

This study was supported by National Natural Science Foundation of China (31202002) , Jiangsu Science and Technology Department (BK2012535) and Central Public-Interest Scientific Institution Basal Research Fund (2014A08YQ01).

REFERENCES

[1] Yang, J.,Li, X. D.,Yan, M.,Chen, T.,Lu, S. Y.,Yan, J. H.,Olie, K.,Buekens, A. (2015) De Novo Tests on Medical Waste Incineration Fly Ash: Effect Of Oxygen And Temperature. Fresenius Environmental Bulletin (24),587-595.

[2] Talorete, T. P. N.,Isoda, H.,Maekawa, T. (2001) Alkylphenolic compounds and their effect on the injury rate, survival and acetylcholinesterase activity of the rat neuronal cell line PC12. Cytotechnology (36),163-169.

[3] Natsume, Y.,Satsu, H.,Hamada, M.,Kitamura, K.,Okamoto, N.,Shimizu, M. (2005) In vitro system for assessing dioxinabsorption by intestinal epithelial cells and for preventingthis absorption by food substances. Cytotechnology (47),79-88.

[4] Fang, L.,Liang, X. F.,Chen, W. X.,Li, G. G.,He, S.,Liu, X. X.,Yu, Y.,Shen, D. (2015) Differential Regulation Of Microcystin Detoxification-Related Liver Genes by Lps In Two Chinese Carps Resistant Or Sensitive To Microcystin-Lr. Fresenius Environmental Bulletin (24),997-1003.

[5] Marinkovic, N.,Pasalic, D.,Ferencak, G.,Grskovic, B.,Stavljenic Rukavina, A. (2010) Dioxins and human toxicity. Arhiv za higijenu rada i toksikologiju (61),445-453.

[6] Weisglas-Kuperus, N.,Patandin, S.,Berbers, G. A.,Sas, T. C.,Mulder, P. G.,Sauer, P. J.,Hooijkaas, H. (2000) Immunologic effects of background exposure to polychlorinated biphenyls and dioxins in Dutch preschool children. Environmental health perspectives (108),1203-1207.

[7] Longnecker, M.,Michalek, J. (2000) Serum dioxin level in relation to diabetes mellitus among Air Force veterans with background levels of exposure. Epidemiology (11),44-48.

[8] Bertazzi, P. A.,Zocchetti, C.,Guercilena, S.,Consonni, D.,Tironi, A.,Landi, M. T.,Pesatori, A. C. (1997) Dioxin exposure and cancer risk: a 15-year mortality study after the 'Sevesoaccident'. Epidemiology (8),646-652.

[9] Xu, Y.,Li, T.,Ding, Z.,Wu, W. J. (2010) Influence and mechanism of 2,3,7,8-tetrachlorodibenzo-p-dioxinon the growth of fish and control it by feeding. Feed industry (231),4-8.

[10] Gandolfi, A.,Wijeweera, J.,Brendel, K. (1996) Use of precision-cut liver slices as an in vitro tool for evaluating liver function. Toxicologic pathology (24),58-61.

[11] Lerche-Langrand, C.,Toutain, H. (2000) Precision-cut liver slices: characteristics and use for in vitro pharmaco-toxicology. Toxicology letters (153),221-253.

[12] Olinga, P.,Meijer, D.,Slooff, M.,Groothuis, G. (1998) Liver slices in in vitro pharmacotoxicology with special reference to the use of human liver tissue. Toxicology in vitro (12),77-100.

[13] Turkez, H.,Geyikoglu, F.,Yousef, M. I. (2013) Beneficial effect of astaxanthin on 2,3,7,8-tetrachlorodibenzo-p-dioxin-induced liver injury in rats. Toxicol Ind Health (29),591-599.

[14] Turkez, H.,Geyikoglu, F.,Yousef, M. I. (2012) Modulatory effect of L-glutamine on 2,3,7,8 tetrachlorodibenzo-p-dioxin-induced liver injury in rats. Toxicology And Industrial Health (28),663-672.

[15] Yang, L.,Wang, H.,Luo, F. (2007) Study on Scavenging free Radical Activity with Polysaccharides in Glycyrrhiza Uralcnsis Fisch Journal of Tarim University (19),1-3.

[16] Li, F., Zhao, J.,Chi, X.,Yang, B.,Yan, X.,Liu, H. (2009) Effect of Glycyrrhiza Polysaccharide on Immunomodulation in Mice. Chinese Journal of Information on Traditional Chinese Medicine (16),35-36.

[17] Fent, K. (2001) Fish cell lines as versatile tools in ecotoxicology: assessment of cytotoxicity, cytochrome P4501A induction potential and estrogenic activity of chemicals and environmental samples. Toxicology in vitro (15),477-488.

[18] Elferink, M. G.,Olinga, P.,Draaisma, A. L.,Merema, M. T.,Bauerschmidt, S.,Polman, J.,Schoonen, W. G.,Groothuis, G. M. (2008) Microarray analysis in rat liver slices correctly predicts in vivo hepatotoxicity. Toxicology and applied pharmacology (229),300-309.

[19] Visen, P. K.,Saraswat, B.,Dhawan, B. N. (1998) Curative effect of picroliv on primary cultured rat hepatocytes against different hepatotoxins: an in vitro study. Journal of pharmacological and toxicological methods (40),173-179.

[20] Cao, L. P.,Jia, R.,Du, J. L.,Ding, W. D.,Yin, G. J. (2012) Effect of Glycyrrhiza glabra Extract hydroperoxide (t-BHP)-induced Hepatotoxicity in Hepatocytes of Jian Carp(Cyprirnus carpio var. jian). Journal of Agricultural Biotechnology (20),1192-1200.

[21] Hu, Y. Y.,Liu, C. H.,Wang, R. P.,Liu, C.,Liu, P.,Zhu, D. Y. (2000) Protective actions of salvianolic acid A on hepatocyte injured by peroxidation in vitro. World journal of gastroenterology : WJG (6),402-404.

[22] Ozden, S.,Catalgol, B.,Gezginci-Oktayoglu, S.,Arda-Pirincci, P.,Bolkent, S.,Alpertunga, B. (2009) Methiocarb-induced oxidative damage following subacute exposure and the protective effects of vitamin E and taurine in rats. Food and chemical toxicology : an international journal published for the British Industrial Biological Research Association (47),1676-1684.

[23] Tang, N.,Liu, Y.,Ren, D. (2003) Experimental study on the effects of TCDD on SOD,GST,MDA in livers of SD rats. Chinese journal of industrial medicine (16),335-337.

[24] Gilbert, F. B.,Cunha, P.,Jensen, K.,Glass, E. J.,Foucras, G.,Robert-Granie, C.,Rupp, R.,Rainard, P. (2013) Differential response of bovine mammary epithelial cells to Staphylococcus aureus or Escherichia coli agonists of the innate immune system. Veterinary research (44),40.

[25] Gómez, C.,Buijs, R.,Sitges, M. (2014) The anti-seizure drugs vinpocetine and carbamazepine, but not valproic acid, reduce inflammatory IL-1β and TNF-α expression in rat hippocampus. Journal of neurochemistry (130),770-779.

[26] Song, X.,Zhang, W.,Wang, T.,Jiang, H.,Zhang, Z.,Fu, Y.,Yang, Z.,Cao, Y.,Zhang, N. (2014) Geniposide plays an anti-inflammatory role via regulating TLR4 and downstream signaling pathways in lipopolysaccharide-induced mastitis in mice. Inflammation (37),1588-1598.

[27] Akarasereenont, P.,Bakhle, Y. S.,Thiemermann, C.,Vane, J. R. (1995) Cytokine-mediated induction of cyclo-oxygenase-2 by activation of tyrosine kinase in bovine endothelial cells stimulated by bacterial lipopolysaccharide. British journal of pharmacology (115),401-408.

[28] Domitrović, R.,Jakovac, H.,Blagojević, G. (2011) Hepatoprotective activity of berberine is mediated by inhibition of TNF-α,COX-2, and iNOS expression in CCl4-intoxicated mice. Toxicology, (280),33-43.

[29] Ma, Y.,Sachdeva, K.,Liu, J.,Ford, M.,Yang, D.,Khan, I. A.,Chichester, C. O.,Yan, B. (2004) Desmethoxyyangonin and dihydromethysticin are two major pharmacological kavalactones with marked activity on the induction of CYP3A23. Drug metabolism and disposition: the biological fate of chemicals (32),1317-1324.

[30] Ma, Y.,Sachdeva, K.,Liu, J.,Song, X.,Li, Y.,Yang, D.,Deng, R.,Chichester, C.,Yan, B. (2005) Clofibrate and perfluorodecanoate both upregulate the expression of the pregnane X receptor but oppositely affect its ligand-dependent induction on cytochrome P4503A. Biochemical pharmacology (69),1363-1371.

[31] Cabrera, M. A. S.,Dip, R. M.,Furlan, M. O.,Rodrigues, S. L. (2009) Use Of Drugs That Act on the Cytochrome P450 System In the Elderly. Clinics (64),273-278.

[32] Sinz, M.,Wallace, G.,Sahi, J. (2008) Current industrial practices in assessing CYP450 enzyme induction: preclinical and clinical. The AAPS journal (10),391-400.

[33] Yu, Q.,Zuo, N.,Jia, H.,Li, J.,Wang, J.,Li, S. (2009) The effect of Selenium on main subtypes of hepatic microsomal cytochrome P450s in chickens with exposure of Fluoride. Acta Veterinaria Et Zootechnica Sinica (40),922-927.

[34] Whitlock, J. P., Jr.,Okino, S. T.,Dong, L.,Ko, H. P.,Clarke-Katzenberg, R.,Ma, Q.,Li, H. (1996) Cytochromes P450 5: induction of cytochrome P4501A1: a model for analyzing mammalian gene transcription. FASEB journal : official publication of the Federation of American Societies for Experimental Biology (10),809-818.

[35] Hansson, M. C.,Hahn, M. E. (2008) Functional properties of the four Atlantic salmon (Salmo salar) aryl hydrocarbon receptor type 2 (AHR2) isoforms. Aquatic toxicology (86),121-130.

[36] Baker, T. R.,Peterson, R. E.,Heideman, W. (2014) Using Zebrafish as a Model System for Studying the Transgenerational Effects of Dioxin. Toxicological sciences : an official journal of the Society of Toxicology (138),403-411.

Received: **24.08.2015**
Accepted: **17.12.2015**

CORRESPONDING AUTHOR

Dr. Guojun Yin
International Joint Research Laboratory for Fish Immunopharmacology, Freshwater Fisheries Research Center, Chinese Academy of Fishery Sciences, Wuxi 214081, China Tel.: +86 510 85551442; Fax: +86 510 85551442

E-mail: yingj@ffrc.cn

© by PSP Volume 25 – No. 7/2016, pages 2331-2342 Fresenius Environmental Bulletin

DIFFERENTIATIONS IN NUTRIENTS OF RECONSTRUCTED SOILS ON OPEN-CAST MINE DUMP OF LOESS AREA

Yingui Cao[1, 2], Wei Zhou[1, 2], Zhongke Bai[1, 2], Jinman Wang[1, 2], Xiaoran Zhang[1]

1. School of Land Science and Technology, China University of Geosciences, Beijing 100083, China;
2. Key Lab of Land Consolidation, Ministry of Land and Resources of the PRC, Beijing 100035, China

ABSTRACT

This study is to analyze the nutrient differentiations in the reconstructed soils in the open-cast mine dump at micro-topography level. Soils were sampled in dump at half shady, shady, half sunny and sunny slopes. The results are summarized as follows. Firstly, the soil nutrient status was improved, and the variability of nutrients was noticeable, with medium levels of variability. Secondly, the means of the soil nutrients at the slopes was slightly higher than that at the platforms. Thirdly, the means of the soil nutrients tended to decrease with an increase in altitude, although obvious differences in nutrients at different altitudes were not observed. Fourthly, the means of soil nutrients exhibited an increasing, decreasing, and increasing trend with slope increasing. Additionally, the mean of the soil total nitrogen was significantly different between the low and medium slopes, and a similar significant difference occurred between the medium steep and high steep slopes. Fifthly, the means soil nutrients at the shady slope was lower than that at half shady slope, and the means of the soil organic matter, the soil total nitrogen and the soil available phosphorus at the sunny slope were lower than that at the half sunny slope. The mean of the soil available phosphorus at the half shady slope was significantly different from that at the shady, sunny and half sunny slopes, whereas the mean of the soil available potassium was significantly different between the half shady and half sunny slopes.

KEYWORDS:
land reclamation; soil reconstruction; soil nutrients; micro-topography; open-cast mine

INTRODUCTION

Open-cast mining has a strong impact on the environment and constitutes degraded ecosystems resulting from mineral extraction for over long periods of time, and the intensity depending on the morphology of the deposit and on the nature of the minerals (Cerqueira et al. 2012; Peňa et al. 2015). Mining operations resulted in significant losses of soil nutrient, microbial biomass C and microbial quotients (Banning et al. 2008). Mine soils are unfavorable environments for plants due to the poor substrate structure, lack of nutrients (Borden and Black 2005; Varennes et al. 2011).

Soil reconstruction can restore or rebuild land that is destroyed in industrial areas and mine areas, and the goal of soil reconstruction is reconstructing suitable soil profiles, soil nutrient conditions and stable geomorphological landscapes to restore soil productivity and improve soil environmental quality over a relatively short period of time. Appropriate mining and reconstruction techniques are often required that employ engineering, physical, chemical, biological and ecological measures (Stephens et al. 2003; Hu et al. 2005). The process of soil reconstruction involves replacing the overburden, grading it to the original contour, and spreading the topsoil to about 30 cm depth. These new altered soils are called reconstructed mine soils, which are relatively young and developing from a mixture of fragmented rocks and soil (Sencindiver and Ammons 2000). Topsoil is an essential component for land reclamation in mine areas (Gilbert 2000; Ghose 2001). Currently, academics agree that it is hard to reconstruct topsoil and modern land reclamation technology research should focus on soil reconstruction factors (Bradshaw 1997; Hu and Chong 1999; Bian and Zhang 2000; Bai et al. 2001; Cao et al. 2014; Dikinya 2015). Therefore, soil reconstruction is the focus and core task in land reclamation (Topp et al. 2010; Cao et al. 2013;

Wang et al. 2015).

However, without viable soil parent materials, it is impossible or difficult to achieve satisfactory growth of crops and vegetation (Šourková et al. 2005; Banning et al. 2008; Shrestha and Lal 2011; Kijjanapanich et al. 2014). After final placement, the surface mine spoils are often graded to a smooth condition prior to application of herbaceous seeds (Fields-Johnson et al. 2012). Soil quality indicators should be useful to evaluate the changes brought about by assisted phytostabilization of mine soils. Parameters related with biological and biochemical status of soils have been proposed as sensitive indicators of soil ecological stress during a restoration process (Tejada et al. 2006; De et al. 2011; Bartuška et al. 2015). The reconstruction of soil nutrient is an important embodiment of the land reclamation effect (Forján et al. 2014; Kelly et al. 2014). Generally, soil nutrients include soil organic matter, soil total and available nitrogen, phosphorus, and potassium. Soil formation and organic carbon accumulation in post-mining landscapes depend on the growth of vegetation cover and the mineralization of plant debris, which are obviously limited by the contents of nitrogen and phosphorus of soils (Šourková et al. 2005).

Soil organic matter is a soil quality control indicator that affects soil nutrient, and it was incorporated into the Controlling Standards on Land Reclamation Quality promulgated by the Ministry of Land and Resources, China in 2013. Soil organic matter plays a key role in early soil forming processes and reestablishment of ecosystem functions on reclaimed post mining sites. The quantity and quality of soil organic have strong influences on other essential soil characteristic such as aggregation and water holding, nutrient accumulation and the soil's biochemical and microbial properties (Chodak et al. 2009; Wick et al. 2013; Pietrzykowski and Daniels 2014). Recovery of soil organic matter is critical to the success of rehabilitation schemes following major ecosystem disturbance (Banning et al. 2008). There is typically a substantial decrease in soil organic matter content when topsoil is removed, stockpiled and then spread on rehabilitated land (Williamson and Johnson 1990). Soil organic matter then slowly increase as above-ground vegetation develops on the dump site (Akala and Lal 2001; Bendfeld et al. 2001; Graham and Haynes 2004).

Mining and reclamation activities also cause drastic loss of the antecedent soil nitrogen in mined (Ganjegunte et al. 2009). Nitrogen accumulation is controlled by organic carbon input and N_2 fixation (Anderson et al. 2008; Fu et al. 2010). Shrestha and Lal (2011) observed that soil total nitrogen concentrations for 0-15 cm depth ranged from 1.10 to 2.96 g/kg in the undisturbed site compared with

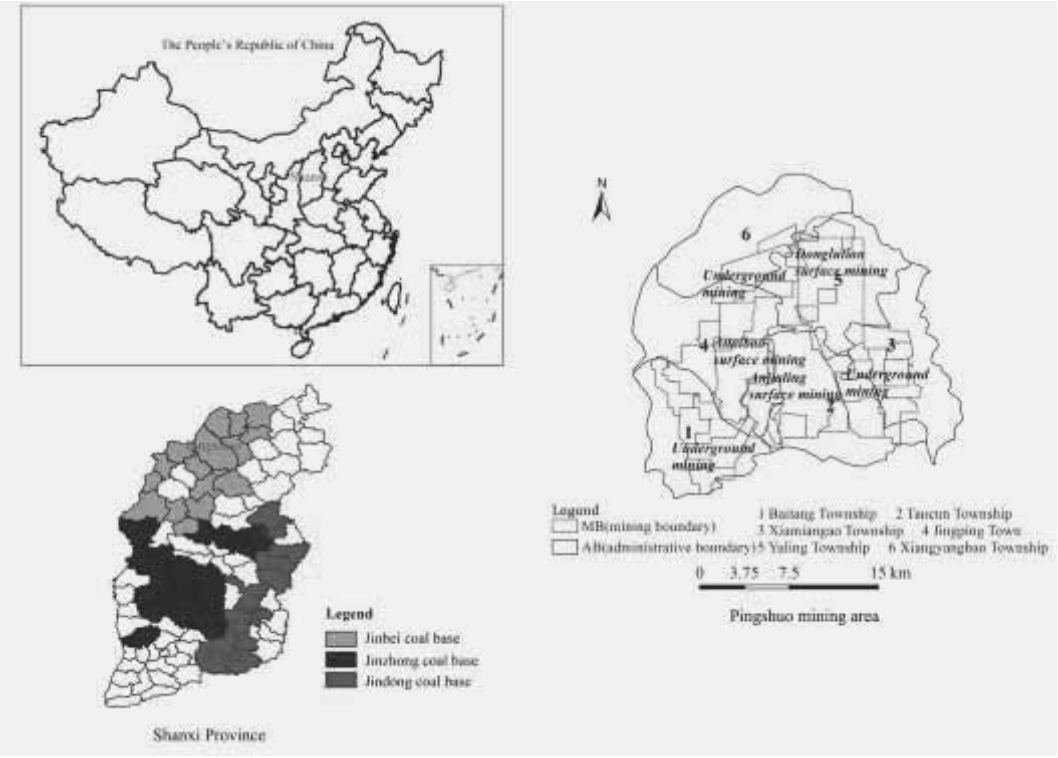

FIGURE 1
Location of the study area.

0.54 to 1.10 g/kg in the reclaimed mine sites, indicating a large loss of nitrogen by mining and reclamation activities. Land use will impact the nitrogen accumulation (Shrestha and Lal 2007; Keskin and Makineci 2009).

Soil phosphorus is determined by soil organic matter, pH of soil substrate and weathering process (Anderson et al. 2008; Fu et al. 2010). Frouz et al. (2011) indicated that soil organic matter was significantly positively correlated with soil available phosphorus and soil available potassium. Soil available phosphorus was negatively correlated with pH and positively correlated with soil available potassium.

Soil nutrients in the reconstructed soils of an open-cast mine are highly variable (Bai et al. 2001), and as the land is reclaimed, the soil nutrients increase, although they remain highly variable (Fan et al. 2010; Cao et al. 2013). Researches on reconstructed soil nutrient mainly focused on soil organic matter accumulation with little attention to other nutrients. The assessment of reconstructed soil nutrient includes not only the soil organic matter, but the total and available nitrogen, phosphorus, and potassium. Meanwhile, the nutrients display distinct spatial heterogeneity due to the surface micro-topography of dump sites with little attention. This study was primarily based on the characteristics of reconstructed soil nutrients in an opencast mine dump site and spatial distribution and variability of soil organic matter, total nitrogen, and available phosphorus and potassium of surface soils in different micro-topography. The goal was to provide a reference for optimizing land reclamation technology at the micro-topography and improve the quality of reconstructed soil in mine areas by examining the causes for the differences in the spatial distribution and variability.

TABLE 1
Quadrat location, site type and primary vegetation type.

Quadrat number	Coordinates		Site type	Vegetation type
	Longitude	Latitude		
S_1	112°19′46″	39° 27′38″	platform	acacia × elm
S_2	112°20′05″	39° 27′28″	platform	acacia × elm
S_3	112°19′45″	39° 27′45″	platform	acacia × elm
S_4	112°19′46″	39° 27′42″	slope	acacia
S_5	112°19′48″	39° 27′47″	slope	acacia
S_6	112°19′50″	39° 27′48″	platform	acacia × elm
S_7	112°19′51″	39° 27′53″	slope	acacia × elm
S_8	112°19′51″	39° 27′56″	platform	acacia × elm
S_9	112°20′10″	39° 27′22″	slope	acacia
S_{11}	112°20′11″	39° 27′20″	slope	acacia
S_{12}	112°20′11″	39° 27′21″	platform	acacia × elm
S_{13}	112°20′13″	39° 27′17″	slope	acacia × elm
S_{14}	112°20′12″	39° 27′18″	platform	apricot × Chinese pine
S_{15}	112°20′11″	39° 27′14″	slope	acacia × elm
S_{16}	112°20′11″	39° 27′16″	platform	acacia
S_{17}	112°19′45″	39° 27′37″	slope	acacia × elm
S_{18}	112°19′38″	39° 27′37″	platform	acacia × elm
S_{19}	112°19′35″	39° 27′35″	slope	caragana
S_{20}	112°19′34″	39° 27′34″	platform	aspen × Chinese pine × elm
S_{21}	112°19′28″	39° 27′36″	slope	acacia × elm
S_{22}	112°19′27″	39° 27′35″	platform	acacia × elm
S_{23}	112°20′17″	39° 27′40″	slope	acacia × Chinese pine × elm
S_{24}	112°20′01″	39° 27′42″	platform	acacia × elm
S_{25}	112°20′14″	39° 27′34″	slope	acacia × elm
S_{26}	112°20′20″	39° 27′36″	platform	acacia × elm
S_{27}	112°19′52″	39° 27′37″	slope	acacia × Chinese pine × elm

FIGURE 2
Distribution of quadrats in the south dump of the Antaibao open-cast mine.

Study area. The study area is located in Pinglu District of Shuozhou City, Shanxi Province, China (Figure 1) and belongs to a typical ecologically fragile area at Loess Plateau. The area was used as an open dump in Antaibao open-cast mine of China Coal Group from 1985-1989. The study area is located in the northern of Ningwu coalfield, and the base of Ningwu coalfield is a set of ancient metamorphic rocks. The total thickness of sedimentary is 2600-3500m. The newest strata in the center of Ningwu coalfield is the Mesozoic Jurassic, and the surrounding stratum from inside are the Mesozoic Triassic, the Paleozoic Permian, the Carboniferous, the Ordovician, the Cambrian, the Archean Wutai Group. The dip angle of stratum is above 30°, some stratum is up to 70°-80°and even upside down. There are lots of reverse faults distributing in the study area (Tang and Liu 1996). The landform type is the loess hilly, and the zonal soils are chestnut soil and loessal soil. The soils are low soil organic matter content, poor soil structure, and weak resistance to water erosion and wind erosion (Bai et al. 1998).

From the types of reclamation in the dump, engineering reclamation with towed scraper was adopted in the beginning, and ecological reclamation with ecological succession was adopted in the later (Bai et al. 1999; Wu and Xue 2003). The dump was 1360-1465 m high with slope of 20°-40° and volume of 1.16 x 10^8 m^3 at the end of dumping (Ma et al. 2006) and composed of soil-rock mixture which made up of 46.98% rocks with size equal or greater than 50 mm, 15.48% gravel with size of 50-5 mm and 37.54% gravel or sand soil with size less than 5 mm (Bai et al. 1997). The ground surface was mainly covered by loess, laterite and red-loess. Beginning from 1990, the dump was reclaimed with vegetation configuration mode of grass-shrub-arbor.

Sampling and testing. Sampling. A total of 27 sampling quadrats along the 4 aspects were designed based on the position, altitude, slope. Sampling was conducted in Summer from July 9th 2014 to July 12th 2014. There were sunny and the average temperature was 26 °C. Due to inaccessibility of one sampling quadrat, a total of 26 quadrats were sampled at a slope-plat alternate way. Each quadrats was 10 m × 10 m at the platform and has guarantee 10 m × 10 m vertical projection area at slope with 10 m width and variable length based on the slope. Each quadrat was labeled with nail stake at the corner and located with center's coordinates using GPS. Table 1 shows each quadrat location, site and main vegetation types and Figure 2 shows the distribution of each quadrat in the dump. Samples were collected within each quadrat using five-point sampling method. In detail, after removal of the foliage at the surface, mixed samples were randomly collected 5 times from the 0-10 cm soil layer using auger drill. All samples were serially numbered and stored for further analysis.

Testing. The Chinese Academy of Agricultural Sciences performed the tests on the samples. The soil organic matter was determined with an oil bath $K_2Cr_2O_7$ volumetric method, total nitrogen was determined with the semi-micro Kjeldahl method, available phosphorus was performed with an adapted Olsen method, and available potassium was determined with a 1.0 mol L^{-1} NH_4OAc extraction and flame photometry (Bao

2000).

RESULTS AND ANALYSIS

Basic statistical characteristics of the nutrient status of reconstructed soils. The basic characteristics of the nutrient status of reconstructed soils are shown in Table 2. The soil organic matter was 46.75 g/kg on average and ranged from 4.63 to 183.83 g/kg; the soil total nitrogen was 1.18 g/kg on average and ranged from 0.28 to 3.00 g/kg; the soil available phosphorus was 4.30 mg/kg on average and ranged from 2.42 to 7.46 mg/kg; and the soil available potassium was 158.04 mg/kg on average and ranged from 56.00 to 274.00 mg/kg. The spatial variability of the nutrients in the reconstructed soils is expressed using the coefficient of variation, and a value of less than 0.1 indicates low variability, equal to or greater than 0.1 and equal to or less than 1.0 indicates moderate variability, and greater than 1.0 indicates high variability (Zheng et al. 2004; Lian et al. 2006). In this study, the coefficients of variation indicated that the soil organic matter, soil total nitrogen, and soil available phosphorus and soil potassium were moderately variable, and the soil organic matter was the most variable. The coefficients of variation for the soil available phosphorus and potassium were relatively low and had moderate to low variability, whereas the coefficients of variation for the soil organic matter and the soil total nitrogen had moderate to high variability. The Kolmogorov-Smirnov (K-S) test indicated that the values were normally distributed and satisfied the statistical requirements.

Differences in the nutrient status of reconstructed soils between slopes and platforms. The nutrient status of the reconstructed soils from the slopes and platforms is shown in Table 3, which indicates that the means of the soil organic matter, the soil total nitrogen and the soil available phosphorus at the slopes are slightly higher than those at the platforms, whereas the mean of the soil available potassium at the slopes is slightly lower than that at the platforms. Additionally, the standard deviations of soil organic matter and total nitrogen at the slopes are slightly higher than those at the platforms, whereas for the soil available phosphorus and potassium, the standard deviations show an opposite trend.

The differences in the reconstructed soil nutrients from the slopes and platforms are evaluated with an analysis of variance (ANOVA), and the significant differences are not observed. Therefore, the nutrients of reconstructed soils at elevation level, slope level and aspect level can be analyzed without considering the differences at slope and platform.

TABLE 2
Basic statistical characteristics of the reconstructed soil nutrients.

Index	Average	Mean	Maximum	Minimum	Range	Standard deviation	Coefficient of variation (%)	K-S test
Soil organic matter (g/kg)	46.75	36.48	183.83	4.63	179.20	38.79	82.97	0.86
Total nitrogen (g/kg)	1.18	1.07	3.00	0.28	2.72	0.67	56.78	0.80
Available phosphorus (mg/kg)	4.30	4.01	7.46	2.42	5.04	1.40	32.56	0.64
Available potassium (mg/kg)	158.04	155.0	274.00	56.00	218.00	56.43	35.71	0.49

The data are calculated based on 26 quadrats.

TABLE 3
Differences in reconstructed soil nutrient status at slopes and platforms.

Site type	Soil organic matter (g/kg)	Total nitrogen (g/kg)	Available phosphorus (mg/kg)	Available potassium (mg/kg)
Slope (l_1)	56.23 ± 46.72	1.42 ± 0.75	4.52 ± 1.37	150.46 ± 52.03
Platform (l_2)	37.28 ± 27.52	0.94 ± 0.50	4.07 ± 1.45	165.62 ± 61.66

N = number of quadrats; $Nl_1 = 13$ and $Nl_2 = 13$

TABLE 4
Differences in reconstructed soil nutrient status at different altitudes.

Altitude	Soil organic matter (g/kg)	Total nitrogen (g/kg)	Available phosphorus (mg/kg)	Available potassium (mg/kg)
Low altitude (h_1)	51.65 ± 26.02	1.45 ± 0.61	4.77 ± 1.85	185.50 ± 62.35
Medium altitude (h_2)	48.52 ± 57.90	1.22 ± 0.83	4.34 ± 1.65	148.38 ± 59.25
High altitude (h_3)	43.13 ± 30.80	1.02 ± 0.59	4.03 ± 1.00	150.75 ± 51.95

N = number of quadrats; $Nh_1 = 6$, $Nh_2 = 8$, and $Nh_3 = 12$. Different letters indicate significant differences at $P < 0.05$.

Differences in nutrient status at different altitudes. To analyze the differences in nutrient status with altitude in the dump, the soil nutrient status was assumed to be same between the slope level and aspect level. The quadrats were divided into three groups based on altitude, the quadrats with altitude equal or greater than 1320 m, but less than or equal to 1360 m were assigned in low altitude group, with altitude greater than 1360 m, but less than or equal to 1400 m were assigned in medium altitude group, and with altitude greater than 1400 m, but less than or equal to 1440 m were in high altitude group. The differences in nutrient status of reconstructed soils according to altitude are shown in Table 4, which shows that with altitude increasing, the means of the soil organic matter, the soil total nitrogen, and the soil available phosphorus and potassium tended to decreasing.

The ANOVA for the nutrients of reconstructed soils at different altitudes show that the soil organic matter, the soil total nitrogen, and the soil available phosphorus and potassium are not significant difference at different altitudes.

Differences in nutrient status at different slopes. To study the differences in the nutrient status of the reconstructed soils at different slopes, we assumed that the nutrient status of reconstructed soils had no significant difference with different altitudes and aspects and assigned the slopes into 4 categories: 1) slow slope of less than or equal to 6°, 2) medium slope of greater than 20° but less than or equal to 25°, 3) medium steep slope of greater than 30° but less than or equal to 35° and high steep slope of more than 35° but less than or equal to 40°. The nutrients of the reconstructed soils for the 4 slopes are shown in Table 5.

The means of the soil organic matter, the soil total nitrogen, and the soil available phosphorus and potassium show an increasing, decreasing and increasing trend with increasing of slope. Additionally, the means of the soil organic matter, the soil total nitrogen, and the soil available phosphorus are higher at the low slope than these at the high steep slope, although the mean of the soil available potassium shows the opposite trend.

An ANOVA of the nutrients from the different slopes show that there is no significant difference in the soil organic matter and the soil available phosphorus at the different slopes. The total nitrogen is not significantly difference between low and medium steep slopes and between medium and high steep slopes. However, significant differences are found between the low slope, medium steep slope and medium steep slope, high steep slope. The soil available potassium at the low slope is not significant difference with the medium slope, the medium steep slope and the high steep slope, but it is significant difference among the medium, medium steep and high steep slopes.

TABLE 5
Differences in reconstructed soil nutrient status at different slopes.

Slope	Soil organic matter (g/kg)	Total nitrogen (g/kg)	Available phosphorus (mg/kg)	Available potassium (mg/kg)
Low slope (s_1)	37.28 ± 27.52	0.94 ± 0.50a	4.07 ± 1.45	165.62 ± 61.66ab
Medium slope (s_2)	58.91 ± 36.01	1.71 ± 0.78b	5.39 ± 0.12	210.00 ± 55.46b
Medium steep slope (s_3)	31.85 ± 14.69	0.96 ± 0.38a	3.66 ± 1.05	127.00 ± 23.08a
High steep slope (s_4)	79.00 ± 65.48	1.70 ± 0.89b	4.86 ± 1.71	138.20 ± 50.15a

N = number of quadrats; $Ns_1 = 13$, $Ns_2 = 3$, $Ns_3 = 5$, and $Ns_4 = 5$. Different letters indicate significant difference at $P < 0.05$.

TABLE 6
Differences in reconstructed soil nutrient status at different aspects.

Slope direction	Soil organic matter (g/kg)	Total nitrogen (g/kg)	Available phosphorus (mg/kg)	Available potassium (mg/kg)
Shady slope (a_1)	43.67 ± 25.33	1.04 ± 0.47	2.92 ± 0.30a	165.00 ± 51.87ab
Half shady slope (a_2)	49.18 ± 28.80	1.50 ± 0.62	5.27 ± 0.26b	194.80 ± 50.22b
Sunny slope (a_3)	41.04 ± 25.70	1.07 ± 0.54	4.53 ± 1.54b	156.50 ± 54.16ab
Half sunny slope (a_4)	55.96 ± 70.65	1.23 ± 1.05	4.77 ± 1.56b	121.33 ± 59.41a

N = number of quadrats; $Na_1 = 7$, $Na_2 = 5$, $Na_3 = 8$, and $Na_4 = 6$. Different letters indicate significant difference at $P < 0.05$.

Differences in nutrient status at different aspects. To explore the differences in nutrient status of the reconstructed soils at different aspects in the dump, we assumed that the nutrients were not significant difference at different altitudes and slopes. The quadrats were divided into 4 different groups with different aspect. Group 1 contains 7 quadrats: S_1, S_3, S_4, S_5, S_6, S_7 and S_8 which are at a shady slope. Group 2 contains 5 quadrats, S_{23}, S_{24}, S_{25}, S_{26} and S_{27} which are at half shady slope. Group 3 contains 8 quadrats, S_2, S_9, S_{11}, S_{12}, S_{13}, S_{14}, S_{15} and S_{16}, which are at sunny slope. Group 4 contains 6 quadrats, S_{17}, S_{18}, S_{19}, S_{20}, S_{21} and S_{22}, which are at half sunny slope. The differences in nutrients of the reconstructed soils according to the aspects are shown in Table 6.

The means of the soil organic matter, the soil total nitrogen, and the soil available phosphorus and the soil potassium at the shady slope are lower than those at the half shady slope, and those at the sunny slope are lower than those at the half sunny slope except for the soil available potassium, which shows an opposite trend.

An ANOVA of the nutrients at different aspects indicate that the soil organic matter and the soil total nitrogen are not significant difference at the shady slope, half shady slope, sunny slope and half sunny slope. Significant differences are observed for the soil available phosphorus at the shady slope, half shady slope sunny slope and half sunny slope, but no significant difference is observed among the half shady slope, sunny slope and half sunny slope. The soil available potassium is not significant difference at the half shady slope, the shady slope and the sunny slope. The soil available potassium is significant difference between the half shady slope and the half sunny slope, whereas it is not significant difference among the half sunny slope, shady slope and sunny slope.

DISCUSSIONS AND CONCLUSIONS

Discussions. In the study area, the means of the soil nutrients at low altitudes was higher than that at high altitudes, and exhibiting soil nutrient decreasing with altitude increasing. This result was consistent with the results of Qiu et al. (2004) and Liu et al. (2005) for a small watershed at the Loess Plateau because soil erosion from rainfall at high altitudes caused the deposition of soil nutrients at low altitudes and the eroded water was enriched with soil nutrients. The differences in means of the soil nutrients at different altitudes in the study area were not significant, which was inconsistent with the results of Qiu et al. (2004) for the undamaged landscape. This result is relevant because of alternations of slope-platform site types in the dump, which produces an artificial topography (Molotilov and Norri 2007). Slopes and platforms are found at different elevations, and soil nutrients are washed onto the platforms at each altitude level and retained. The soil organic matter, the soil total nitrogen and the soil available potassium tended to decreasing with increasing altitude up to 1,400 m, which was opposite to the observations at altitudes of more than 1,400 m. Thus, the division at 1,400 m might provide a dividing line between high and medium altitudes and a boundary of microclimate in the study area. Guo et al. (2012) found that an altitude of 1,000 m was the dividing line between regional climates in mountainous areas of North China. As the altitude increased and temperature decreased, the air humidity and surface soil moisture increased, which resulted in slower decomposition and a greater accumulation of soil organic matter (Tripathi et al. 2012; Liu et al. 2014).

The soil organic matter, the soil total nitrogen, and the soil available phosphorus and potassium showed a *Z*-shaped changes with slope elevation, and the transitions of nutrient values occurred between the medium and medium steep slopes. The soil nutrients between the low and medium slopes showed an increasing trend with the slope increasing, which was similar to the trend of nutrients between the medium steep and high steep slopes. Lian et al. (2008) found that the soil nutrients of small watersheds on the Loess Plateau had a tendency to increasing with the slope

increasing in the range of 3-8° and 8-15°, although the differences were not significant, which was consistent with the results of this study. However, a decreasing trend in soil nutrients was observed between the medium and medium steep slopes. Additionally, the means of the soil total nitrogen and the soil available phosphorus at the medium slopes were significant differences compared with that of the medium steep slopes. Wang et al. (2013) and Gou et al. (2015) showed that the soil organic matter, the total nitrogen, and the available phosphorus and potassium in the surface soils of the reclaimed waste dump had a significant negative correlation with slope. Higher slopes are commonly considered to have poor soil and water conservation, which would affect plant growth and reduce biomass and result in decreased surface soil nutrients (Jongman et al. 1995; Bai et al. 1998; Ghosh et al. 2014). The mean of the soil organic matter at the high steep slope was 52.79 g/kg except for S_{21}, which had a value of 183.83 g/kg. Thus, the means of the soil organic matter, the soil of total nitrogen and the soil available phosphorus at low slope were similar to those at medium steep slope, and the difference was not significant. Additionally, the means of the soil organic matter, the soil total nitrogen and the soil available phosphorus at medium slope soil were similar to those of the high steep slope, and the difference was also not significant. The soils in high-steep slope were closer to these in medium slope, the difference was not significant. The means of the soil available potassium existed large difference between the low slope and the medium steep slope, but the difference was not significant. The means of the soil available potassium existed large difference between the medium slope and the high steep slope, but the difference was significant. The quadrats with low slope were primarily distributed at the platform and at high altitude, and this study showed that the surface soil nutrients of platform were low, including the soil organic matter. The quadrats with high steep slope were primarily at low and medium altitudes, which further confirmed that at high altitude, the soil organic matter of the surface soil was low. At the same altitude, the soil organic matter had a tendency to decreasing with slope increasing. For example, the mean of the soil organic matter in quadrat S_{23} at medium slope was 99.63 g/kg, the mean of the soil organic matter in quadrat S_7 at medium steep slope was 37.80 g/kg, and the mean of the soil organic matter in quadrat S_{25} at high steep slope was 36.91 g/kg.

The means of the soil organic matter, the soil total nitrogen, and the soil available phosphorus and potassium at shady slope were lower than that of half shady slope. Gong et al. (2007) and Peng et al. (2010) observed that vegetation growth was affected by aspect because of changes in rain and wind and aspect indirectly influenced the distribution of soil nutrients. Gao et al. (2013) suggested that the half shady slope accepted intense and chronic solar radiation, and full photosynthesis promoted the growth of plants and nutrient accumulation in the litters, which increased the amount of the soil organic matter for microbial decomposition and subsequent release of nitrogen by soil mineralization, which increased the soil total nitrogen (Wang et al. 2003; Qiu et al. 2004). The mean of the soil available potassium at half shady slope was higher than that on shady slope, and the difference was significant. This result was primarily caused by increased vegetation growth and large amounts of organic phosphorus compounds in the litters, which produced phosphates by hydrolysis (Peng et al. 2010). Additionally, the litters decomposed by rhizosphere microorganisms produce an increased amount of phenolic acids, which effectively promoted the decomposition of potassium minerals (Zheng and Chang, 2006). Therefore, high means of the soil available potassium was observed at the half shady slope. The means of the soil organic matter, the soil total nitrogen and the soil available phosphorus at sunny slope were lower than that of half sunny slope, but the differences were not significant. This result was primarily because the sunny slope was dry and had more vegetation growth than the half sunny slope, which promoted the rapid decomposition of the soil organic matter. The increasing demand for nutrients for the growth of vegetation slightly reduced the nutrients of the surface soils (Zhao et al. 2000). The mean of the soil available potassium at sunny slope was higher than that of half sunny slope, which was primarily because the mean of the soil gravel content at sunny slope was 44.83%, a significantly higher than the 23.56% at half sunny slope (Cao et al. 2015). With the higher soil gravel content, more decomposable potassium-bearing minerals were available (Frouz et al. 2011), and the mean of the soil available potassium at sunny slope was higher.

CONCLUSIONS

(1) After 20 years reclamation, the nutrient status of reconstructed soils was significantly improved, but medium variability was observed in each nutrient indicator, and the soil organic matter showed the highest variability. The means of soil nutrients except the soil available potassium at slopes were slightly higher than those at platforms, although the differences were not significant.

(2) The means of soil nutrients showed a decreasing tendency with altitude increasing, but the differences were not significant. The mean soil nutrients showed an increasing, decreasing, and increasing trend with increasing of slope, and the means of soil organic matter, the soil total nitrogen

and the soil available phosphorus at low slope were lower than those at high steep slope, although the soil available potassium showed the opposite pattern. The mean of soil total nitrogen was significant difference between low slope and medium slope, which was similar to the result between medium steep slope and high steep slope. The mean of the soil available potassium at medium slope was significant difference from that of medium steep slope and high steep slope.

(3) The means of soil nutrients at shady slope were lower than those of half shady slope. The means of the soil organic matter, the soil total nitrogen and the soil available phosphorus at sunny slope were lower than those of half sunny slope, although the soil available potassium showed the opposite trend. The mean of the soil available phosphorus was significant difference among shady slope and half shady slope, sunny slope and half sunny slope. The mean of the soil available potassium was significant difference between half shady slope and half sunny slope.

ACKNOWLEDGEMENTS

The study was supported by the National Natural Science Foundation of China (41571508), the Basic Scientific Research Foundation for Outstanding Teachers (2-9-2015-173), and the Key Special Projects of Shanxi Science and Technology (20121101007). Thank Master student Yuanqing Lu, Zhili Yu, Hongdan Wang, Qian Qin, Wenwen Gao for their hard work for sampling.

REFERENCES

[1] Akala, VA, Lal, R (2001) Soil organic carbon pools and sequestration rates in reclaimed mine soils in Ohio. J Environ Qual 30: pp. 2098-2104

[2] Anderson, JD, Ingram LJ, Stahl, PD (2008) Influence of reclamation management practices on microbial biomass carbon and soil organic carbon accumulation in semiarid mined lands of Wyoming. Appl Soil Ecol 40: pp. 387-397

[3] Bai, ZK, Hu, ZH, Wang, ZG (1998) Artificial accelerated erosion and classification of the dump in surface mine. J Soil Eros Soil Water Conser 4: pp. 34-40

[4] Bai, ZK, Li, JC, Wang, WY, Ding, XQ, Chai, SJ, Chen, JJ, Lu, CE, Zhao, JK (2001) Ecological rehabilitation of degraded mined land of Antaibao open-cast mine in Pingshuo, Shanxi, China. Chin Land Sci 14: pp. 1-4

[5] Bai, ZK, Wang, ZZ, Zhao, JK, Tong, ZA, Chen, JJ (1997) Characteristics of soil erosion and its control in Antaibao Open-pit mine. J Chin Coal Soc 22: pp. 542-547

[6] Bai, ZK, Zhao, JK, Li, JC, Wang, WY, Lu, CE, Ding, XQ, Chai, SJ, Chen, JJ (1999) Ecosystem damage in a large opencast coal mine: A case study on Pingshuo surface coal mine, China. Acta Ecol Sin 19: pp. 870-875

[7] Banning, NC, Grant , CD, Jones, DL, Murphy, DV (2008) Changes in physical and chemical properties of soil after surface mining and reclamation. Soil Biol Biochem 40: pp. 2021-2031

[8] Bao, SD (2000) Analyses of Soil Agriculture Chemistry. Beijing: Chinese Agriculture Publish

[9] Bartuška, M, Pawlett, M, Frouz, J (2015) Particulate organic carbon at reclaimed and unreclaimed post-mining soils and its microbial community composition. Catena 131: pp. 92-98

[10] Bendfeld, ES, Burger, JA, Daniels, WL (2001) Quality of amended mine soils after sixteen years. Soil Sci Soc Am J 65: pp. 1736-1744

[11] Bian, ZF, Zhang, GL (2000) Modified index of reclaimed soil productivity. Acta Ped Sin 37: pp. 124-130

[12] Borden, RK, Black, R, (2005) Volunteer revegetation of waste rock surfaces at the Bingham Canyon Mine, Utah. J Environ Qual 34: pp. 2234-2242.

[13] Bradshaw, A (1997) Restoration of mined lands: Using natural processes. Ecol Eng 8: pp. 255-269

[14] Cao, YG, Bai, ZK, Zhang, GJ, Zhou, W, Wang, JM, Yu, QF, Du, ZZ (2013) Soil quality of surface reclaimed farmland in large open-cast mining area of Shanxi province. J Agro-Environ Sci 23: pp. 2422-2428

[15] Cao, YG, Bai, ZK, Zhao, ZQ, Zhang, GJ, Zhou, W, Wang, JM, Jing, M, Song, XJ (2014) Development of soil physicochemical properties of reclaimed croplands in a large open-cast mining area on the Loess Plateau. J Food Agric Environ 12: pp. 1045-1053

[16] Cao, YG, Wang, JM, Bai, ZK, Zhou, W, Zhao, ZQ, Ding, X, Li, YN (2015) Differentiation and mechanisms on physical properties of reconstructed soils on open-cast mine dump of Loess Area. Environ Earth Sci 73: pp. 4849-4862

[17] Cerqueira, B, Vega, FA, Silva, LFO, Andrade,

L (2012) Effects of vegetation on chemical and mineralogical characteristics of soils developed on a decantation bank from a copper mine. Sci Total Environ 421-422: pp. 220-229

[18] Chodak, M, Pietrzykowski, M, Niklinska, M (2009) Development of microbial properties in a chronosequence of sandy mine soils. Appl Soil Ecol 41: pp. 259-268

[19] De, CM, Cordovil, S, Varennes, AD, Pinto, R, Fernandes, RC (2011) Changes in mineral nitrogen, soil organic matter fractions and microbial community level physiological profiles after application of digested pig slurry and compost from municipal organic wastes to burned soils. Soil Biol Biochem 43: pp. 845-852

[20] Dikinya, O (2015) Heavy metals and radionuclide status and characterisation of pre-mined soils in Serule, North East Botswana. Environ Earth Sci 73: pp. 5405-5413

[21] Fan, WH, Li, HF, Bai, ZK, Qiao, JY, Xu, JW (2010) Effect of gangue spontaneous combustion on reclaimed soil quality of large-scaled opencast mine in loess area. Trans Chin Soc Agr Eng 26: pp. 319-324

[22] Fields-Johnson, CW, Zipper, CE, Burger, JA, Evans, DM (2012) Forest restoration on steep slopes after coal surface mining in Appalachian USA: Soil grading and seeding effects. For Ecol Manag 270: pp. 126-134

[23] Forján, R, Asensio, V, Rodríguez-Vila, A, Covelo, EF (2014) Effect of amendments made of waste materials in the physical and chemical recovery of mine soil. J Geochem Expl 147: pp. 91-97

[24] Frouza, J, Kalčík, J, Velichová, V (2011) Factors causing spatial heterogeneity in soil properties, plant cover, and soil fauna in a non-reclaimed post-mining site. Ecol Eng 37: pp. 1910-1913

[25] Fu, Y, Lin CC, Ma, JJ, Zhu, TC (2010) Effects of plant types on physico-chemical properties of reclaimed mining soil in Inner Mongolia, China. Chin Geogr Sci 20: pp. 309-317

[26] Ganjegunte, GK, Wick, AF, Stahl, PD, Vance, GF (2009) Accumulation and composition of total organic carbon in reclaimed coal mine lands. Land Degr Dev 20: pp. 156-175

[27] Gao, HY, Ai, YW, Wang, KX, Chen, CQ, Pan, DD, Li, CR, Li, W (2013) Effects of slope position and aspect on humus component and organic matter of the synthetic soil on the rock slope. J Soil and Water Conserv 27: pp. 244-248

[28] Ghose, MK (2001) Management of topsoil for geo-environmental reclamation of coal mining areas. Environ Geol 40: pp. 1404-1410

[29] Ghosh, BN, Sharma, NK, Alam, NM, Singh, RJ, Juyal, GP (2014) Elevation, slope aspect and integrated nutrient management effects on crop productivity and soil quality in North-west Himalayas, India. J Mount Sci 11: pp. 1208-1217

[30] Gilbert, M (2000) Minesite rehabilitation. Trop Grassl 34: pp. 147-154

[31] Gong, J, Chen, LD, Fu, BJ, Wei, W (2007) Integrated effects of slope aspect and land use on soil nutrients in a small catchment in a hilly loess area, China. Intern J Sustain Dev World Ecol 14: pp. 307-316

[32] Gou, Y, Chen, H, Wu, W, Liu, HB (2015) Effects of slope position, aspect and cropping system on soil nutrient variability in hilly areas. Soil Res 53: pp. 338-348

[33] Graham, MH, Haynes, RJ (2004) Organic matter status and the size, activity and metabolic diversity of the soil microflora as indicators of the success of rehabilitation of mined sand dunes. Biol Fertil Soils 39: pp. 429-437

[34] Guo, YL, Liu, YZ, Wang, LH (2012) Soil fertility and desalination trends in table lands with different land use at different altitudes in north China. J Soil Water Conserv 26: pp. 131-134

[35] Hu, ZQ, Chong, SK (1999) Study on the effect of deep tillage on reclaimed soil physical properties improving. Chin J Soil Sci 12: pp. 248-250

[36] Hu, ZQ, Wei, ZY, Qin, P (2005) Concept of and methods for soil reconstruction in mined land reclamation. Soils 37: pp. 8-12

[37] Jongman, RHG, Terbraak, CJF, Vantongeren, OFR (1995) Data Analysis in Community and Landscape Ecology. Cambridge: Cambridge University Press

[38] Kelly, CN, Peltz, CD, Stanton, M, Rutherford, DW, Rostad, CE (2014) Biochar application to hardrock mine tailings: Soil quality, microbial activity, and toxic element sorption. Appl Geochem 43: pp. 35-48

[39] Keskin, T, Makineci, E (2009) Some soil properties on coal mine spoils reclaimed with black locust (Robinia pceudoacacia L.) and umbrella pine (Pinus pinea L.) in Agacli-Istanbul. Environ Monit Assess 159: pp.

407-414

[40] Kijjanapanich, P, Annachhatre, AP, Esposito, G, Lens, PNL (2014) Use of organic substrates as electron donors for biological sulfate reduction in gypsiferous mine soils from Nakhon Si Thammarat (Thailand). Chemosphere 101: pp. 1-7

[41] Lian, G, Guo, XD, Fu, BJ, Hu, CX (2006) Spatial variability of bulk density and soil water in a small catchment of the loess plateau. Acta Ecol Sin 26: pp. 647-654

[42] Lian, G, Guo, XD, Fu, BJ, Hu, CX (2008) Spatial variability and prediction of soil nutrients on a county scale on the loess plateau. Acta Ped Sin 45: pp. 577-584

[43] Liu, SL, Guo, XD, Lian, G, Fu, BJ, Wang, J (2005) Multi-scale analysis of spatial variation of soil characteristics in Loess Plateau. J Soil and Water Conserv 19: pp. 105-108

[44] Liu, YH, Wei, XT, Zhong, MY, Wu, RX, Pan, D, Shao, XQ (2014) Analysis on the soil physicochemical properties of alpine meadow at different altitudes in Gannan. Grassl and Turf 34: pp. 1-7

[45] Ma, R, Han, WB, Bai, ZK (2006) Research of ravaged indexes of water and soil loss of dumping site of large opencast coal mine in loess area. J Henan Agr Univ 20: pp. 50-53

[46] Molotilov, SG, Norri, VK (2007) Formation of high overburden dumps in open-casts. J Min Sci 43: pp. 516-521

[47] Peña, A, Mingorance, MD, Guzmán-Carrizosa, I, Fernández-Espinosa, AJ (2015) Improving the mining soil quality for a vegetation cover after addition of sewage sludges: Inorganic ions and low-molecular-weight organic acids in the soil solution. J Envir Manag 150: pp. 216-225

[48] Peng, WX, Song, TQ, Zeng, FP, Wang, KL, Fu, W, Liu, L, Du, H, Lu, SY, Yin, QC (2010) The coupling relation ships between vegetation soil and topography factors in karst mixed evergreen and deciduous broadleaf forest. Acta Ecol Sin 30: pp. 3472-3481

[49] Pietrzykowski, M, Daniels, WL (2014) Estimation of carbon sequestration by pine (Pinus sylvestris L.) ecosystems developed on reforested post-mining sites in Poland on differing mine soil substrates. Ecol Eng 73: pp. 209-218

[50] Qiu, Y, Fu, BJ, Wang, J, Chen, LD (2004) Spatiotemporal variation and influencing factors of soil nutrients of small watershed in Loess Plateau. Progr in Nat Sci 14: pp. 294-299

[51] Sencindiver, JC, Ammons, JT (2000) Minesoil genesis and classification. Ch. 23. In: Barnhisel, R.I., Darmody, R.G., Daniels, W.L. (Eds.), Reclamation of Drastically Disturbed Lands: Agronomy Series #41. American Society of Agronomy, Madison, Wisconsin, USA

[52] Shrestha, RK, Lal, R (2007) Soil carbon and nitrogen in 28-year-old land uses in reclaimed coal mine soils of Ohio. J Environ Qual 36: pp. 1775-1783.

[53] Shrestha, RK, Lal, R (2011) Changes in physical and chemical properties of soil after surface mining and reclamation. Geoderma 161: pp. 168-176

[54] Šourková, M, Frouz, J, Šantrůčková, H (2005). Accumulation of carbon, nitrogen and phosphorus during soil formation on alder spoil heaps after brown-coal mining, near Sokolov (Czech Republic). Geoderma 124: pp. 203-214.

[55] Stephens, PR, Hewitt, AE, Sparling, GP, Gibb, RG, Shepherd, TG (2003) Assessing sustainability of land management using a risk identification model. Pedosphere 13: pp. 41-48

[56] Tang, MZ, Liu, XL (1996) Geology and sedimentary environmental analysis of bauxite deposits in Ningwu, Shanxi. Geol Min Res N Chin 11: pp. 580-585

[57] Tejada, M, Hernandez, MT, Garcia, C (2006) Application of two organic amendments on soil restoration: Effects on the soil biological properties. J Environ Qual 35: pp. 1010-1017

[58] Topp, W, Thelen, K, Kappes, H (2010) Soil dumping techniques and afforestation drive ground-dwelling beetle assemblages in a 25-year-old open-cast mining reclamation area. Ecol Eng 36: pp. 751-756

[59] Tripathi, N, Singh, RS, Chaulya, SK (2012) Dump stability and soil fertility of a coal mine spoil in Indian dry tropical environment: A Long-Term Study. Envir Manag 50: pp. 695-706

[60] Varennes, A, Qu, G, Cordovil, C, Gonçalves, P (2011) Soil quality indicators response to application of hydrophilic polymers to a soil from a sulfide mine. J Haz Mater 192: pp. 1836-1841

[61] Wang SY, Shi Y, Niu JJ, Fan, LY (2013) Influence of vegetation restoration models on soil nutrient of coal gangue pile. Acta Geogr Sin 68: pp. 372-379

[62] Wang, J, Fu, BJ, Qiu, Y, Chen, LD, Yu, L (2003)

Spatial distribution patterns of soil nutrients in a small catchment of the Loess Plateau: Kriging method. Geogr Res 22: pp. 373-379

[63] Wang, JM, Zhang, M, Bai, ZK, Guo, LL (2015) Multi-fractal characteristics of the particle distribution of reconstructed soils and the relationship between soil properties and multi-fractal parameters in an opencast coal-mine dump in a loess area. Environ Earth Sci 73: pp. 4749-4762

[64] Wick, AF, Daniels, WL, Orndorff, ZW, Alley, MM (2013) Organic matter accumulation post-mineral sands mining. Soil Use Manag. 29: pp. 354-364

[65] Williamson, JC, Johnson, DB (1990) Mineralization of organic matter in top soils subjected to stockpiling and restoration at opencast coal sites. Plant Soil 128: pp. 241-247

[66] Wu, Q, Xue, D (2003) Division on types of land reclamation method in mining area. N Geol 36: pp. 247-252

[67] Zhao, Z, Li, P, Wang, NJ (2000) Distribution patterns of root systems of main planting tree species in Weibei Loess Plateau. Chin J Appl Ecol 11: pp. 37-39

[68] Zheng, JY, Shao, MA, Zhang, CX (2004) Spatial variation of surface soil bulk density and saturated hydraulic conductivity on slope in loess region. Res Soil Water Conserv 18: pp. 53-56

[69] Zheng, SA, Chang, QR (2006) The influence of different plantations on the soil fertility on Loess Plateau. J Northwest A & F Univ 34: pp. 119-123

Received: **17.12.2015**
Accepted: **01.09.2015**

CORRESPONDING AUTHOR

Wei Zhou
School of Land Science and Technology, China University of Geosciences, Beijing 100083, China.

E-mail: zhouw@cugb.edu.cn

© by PSP Volume 25 – No. 7/2016, pages 2343-2355 Fresenius Environmental Bulletin

GREEN SYNTHESIS OF IRON NANOPARTICLES USING *Garcinia mangostana* L. PERICARP EXTRACT AND THEIR APPLICATION FOR DEGRADATION OF ANTHRAQUINONE DYE

Jing-Feng Gao, Hong-Yu Li, Kai-Ling Pan, Xiao-Yan Fan, Chun-Ying Si

College of Environmental and Energy Engineering, Beijing University of Technology, Beijing 100124, China

ABSTRACT

Iron nanoparticles were first green synthesized using polyphenols extracted from *Garcinia mangostana* L. pericarp (GM-Fe NPs) and used as a catalyst to decolorize Reactive Brilliant Blue KN-R (RBB, anthraquinone dye) in the Fenton-like oxidation system. Polyphenols were used as reducing and capping agents in the synthesis of GM-Fe NPs, which was demonstrated by scanning electron microscope (SEM), X-ray energy-dispersive spectrometer (EDS), X-ray diffraction (XRD), Fourier transform infrared spectroscopy (FTIR) of GM-Fe NPs and the variations of total polyphenols during synthesis. The XRD patterns suggested that the synthesized GM-Fe NPs were mainly amorphous in nature. The effects of extract to $FeCl_3$ ratio, dosage of GM-Fe NPs and initial dye concentration on the RBB decolorization were also investigated. The optimal ratio of extract to $FeCl_3$ for the synthesis was 5 : 1. The decolorization efficiency of RBB increased with the increasing GM-Fe NPs dosage. With the initial RBB concentration ranging from 250 to 750 mg/L, the decolorization efficiency can reach more than 97.83 % after 180 min. The combined first-order kinetic model can well explain the RBB degradation. UV-vis spectra showed that color groups in the visible region had been degraded and no new peaks appeared. The green synthesized GM-Fe NPs could be employed as a low-cost, efficient and alternative catalyst in Fenton-like oxidation system for RBB removal.

KEYWORDS:

Garcinia mangostana L. pericarp, green synthesis, iron nanoparticles, Reactive Brilliant Blue KN-R, fenton-like system

INTRODUCTION

Green synthesis of iron nanoparticles (Fe NPs) from plant extracts has got much attention because of its low cost, environmental friendly procedure and simple reaction conditions. Due to its large specific surface area and high surface reactivity, Fe NPs could be used as catalyst in Fenton-like system to degrade various environmental contaminants [1, 2], such as biocide 4-chloro-3-methyl phenol [3], monochlorobenzene [2] and azo dye Orange II [4] from aqueous solution. Meanwhile, Moon et al. suggested that the process of Fenton-like system with Fe NPs as catalyst was far better than the process using ordinary iron particles as catalyst [5]. Therefore, the green synthesis of Fe NPs became the focus of research.

Generally, Fe NPs can be synthesized through diverse chemical and physical methods, such as vacuum sputtering [6], thermal cracking [7] and reactions of ferrous ions or ferric ions with sodium borohydride [8]. As known to all, without the present of dispersant agents, nanoparticles agglomerate rapidly to form larger aggregates in water because they are sensitive to ionic strength and composition [9]. In the present of dispersant agents, the nanoparticles could be coated with the charged dispersant molecules, which provide the strong and long-range electrostatic repulsions to keep steric stabilization [9, 10] and decrease the aggregation of nanoparticles. For this reason, dispersant or surfactant agents are needed in the chemical synthesis of Fe NPs to prevent agglomeration [1]. Therefore, the chemical synthesis of Fe NPs always required strict conditions, high cost or potentially toxic reagents, which limited their applications. Compared to chemical synthesis, green synthesis is of obvious advantage and own more extensive application prospects.

In the process of green synthesis of Fe NPs, the polyphenols from plant extract were occupied as capping and reducing agents. Polyphenols are biodegradable, nontoxic and water soluble at room temperature, and they can reduce iron ions to synthesize Fe NPs. Besides, polyphenols can provide electrostatic repulsion to minimize agglomeration of Fe NPs [2]. Recently, the polyphenols extracted from green tea [2, 4, 11-13], eucalyptus leaf [14] and Terminalia chebula [1] have been used to green synthesize Fe NPs. Especially, green tea was most widely applied due to its abundant polyphenols content. However, whether other plant extract rich in polyphenols is available for green synthesis of Fe NPs is still limited. Hence, it should pay more attention to explore the polyphenol-rich natural materials in further studies.

As a typical anthraquinone dye, Reactive Brilliant Blue KN-R (RBB) is widely used for dyeing cellulosics and cotton fabric [15]. Also, RBB is a representative of the highest volume commercial reactive dye, which contains the 2-sulfatoethyl sulfone moiety. For the majority of vinyl sulfone reactive dyes, the fixation degree ranges between 75 and 80% on cotton, indicating that 20–25% of the dyes enter the waste effluent [15]. Because anthraquinone dyes were light, thermal stable and non-biodegradable, and their degradation products were toxic and cancerigenic [16], the treatment of anthraquinone dye wastewater was needed urgently. However, few researches have reported the degradation of anthraquinone dye using green synthesized Fe NPs in Fenton-like system.

In this study, the pericarp of Garcinia mangostana L. (GM) was firstly used to synthesize Fe NPs, named as GM-Fe Nano Particles (GM-Fe NPs). As agricultural and forestry waste, the GM pericarp have been confirmed to contain abundant polyphenols [17]. The extract from GM pericarp can be used to green synthesis of GM-Fe NPs and can protect GM-Fe NPs from oxidation and agglomeration. The GM-Fe NPs were characterized by scanning electron microscope (SEM), X-ray energy-dispersive spectrometer (EDS), X-ray diffraction (XRD) and Fourier transform infrared spectroscopy (FTIR). Then, it was used as a catalyst in Fenton-like system to treat RBB. Stability of total polyphenols in GM extracts, effects of ratio of extract to $FeCl_3$ on synthesis of GM-Fe NPs, effects of GM-Fe NPs dosage and initial dye concentration on RBB removal were studied. First-order, second-order and combined first-order kinetics models were applied to describe the decolorization process. In addition, UV-vis spectra and FTIR spectra were used to realize dyes degradation and functional groups during RBB decolorization process.

MATERIALS AND METHODS

Dyes and chemicals. GM was obtained from a local market in Beijing, China. RBB (C.I. Reactive Blue 19, molecular formula = $C_{22}H_{16}N_2Na_2O_{11}S_2$, λ_{max} = 601 nm) was purchased from Tianjin Shengda Chemical Factory (China). Its molecular structure was displayed in Fig. 1.

Following chemicals were also used in the experiments without further purification: $FeCl_3{\cdot}6H_2O$, Na_2CO_3, and 30 % H_2O_2 solution, which were purchased from Sinopharm Chemical Reagent Beijing Co. Ltd. (China). Folin-Ciocalteu's phenol reagent and gallic acid were purchased from Shanghai Labaide Biotechnology Co. Ltd. (China). All the reagents used were analytical grade.

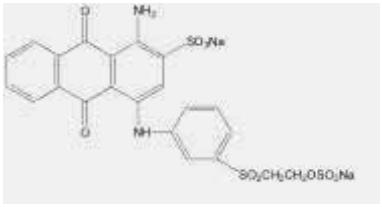

FIGURE 1
Chemical structure of RBB dye

Synthesis of GM-Fe NPs. The pericarps of GM were washed with deionized water and tumble-dry at 105 °C for 1 h. The dry GM pericarps were ground in a homogenizer, and sieved to the desired mesh size (0.3–0.6 mm). The extract of GM pericarps was prepared by boiling GM pericarps (60.0 g/L) at 90 °C for 30 min. After cooling down to room temperature, the extract was vacuum filtered with a filter paper (pore size 15–20 μm, diameter 7 cm). As shown in Table 1, different volume of extract was added to similar $FeCl_3$ solution (0.10 M) to synthesis GM-Fe NPs at room temperature. To ensure the ferric irons was reduced by polyphenols, the total polyphenols content was measured according to the method described by the International Organization for Standardization (ISO) 14502-1 [18].

TABLE 1
Systhesis of GM-Fe NPs at different volume ratio of extract to $FeCl_3$

Number of samples	Volume ratio of extract to $FeCl_3$
S1	5 : 1
S2	2 : 1
S3	1 : 1
S4	0.5 :1
S5	0.2 :1

Characterization of GM-Fe NPs. SEM and EDS. SEM (Hitachi S-4300, Japan) was used to observe the morphology of GM-Fe NPs. The GM-Fe NPs were washed with acetone twice, and dried in vacuum freeze-drying machine (Labconco Freezone 1 L, USA). Subsequently, the dried particles were fixed on the conductive adhesive film and coated with gold. Then, the morphology of GM-Fe NPs was qualitatively analyzed. The chemical composition of GM-Fe NPs was also analyzed by EDS.

XRD. XRD, D8 Advance diffractometer (Bruker, Germany), was applied to measure the crystallinity of GM-Fe NPs in the scanning range between 10° and 80° using Cu Kα (λ=1.54A) radiation.

FTIR. The original GM-Fe NPs powder and the GM-Fe NPs powder after decolorization were characterized using a Bruker Vertex 70 FTIR spectrometer (Bruker, Germany). The sample and KBr were mixed with a ratio of 1:100 and flattened under high pressure, and then were immediately measured in the range of 400 – 4000 cm^{-1} with a resolution of 4 cm^{-1}.

Dye degradation experiments. Batch experiments were carried out in 150 ml beakers by adding 45 ml RBB solution, 5 ml H_2O_2 solution (10 %) and GM-Fe NPs solution. The beakers were shaken at 150 rpm at 25 °C in a water bath shaker (GFL 1086, Germany). In all the experiments, two replicates were applied, and the average values were taken for use.

Under the insurance of same quantity of GM-Fe NPs, the effect of "different ratio of extract to $FeCl_3$" on decolorization was investigated. The GM-Fe NPs solution originated from S1 to S5 (Table 1) were mixed with 45 ml 250 mg/L RBB solutions and 5 ml 10 % H_2O_2 solutions. Based on decolorization efficiency, diameter and dispersion of GM-Fe NPs, the solution S1 was applied to produce GM-Fe NPs using for the next experiments.

To investigate the influence of GM-Fe NPs dosage on decolorization, different dosages of GM-Fe NPs solution (1 ml, 2 ml, 4 ml and 5 ml) were add to 45 ml of 250 mg/L RBB solutions and 5 ml of 10 % H_2O_2 solutions. To assess the effect of initial RBB concentration, the initial concentrations of 45 ml RBB solution varied from 250, 375, 500 to 750 mg/L, GM-Fe NPs solution was fixed at 5 ml and 10 % H_2O_2 solutions was set as 5 ml.

In order to investigate the dye degradation and intermediate transformation, the UV–vis spectra analysis was carried out. In the presence of GM-Fe NPs (1 ml) and 10 % H_2O_2 solutions (2 ml), the variances of UV-vis spectra of 50 mg/L RBB dye (45ml) were measured from 380 to 800 nm with a fixed slit width of 3 nm by UV-vis spectrophotometer (UV-2802PC, Unico, Shanghai, China).

RESULTS AND DISCUSSION

Characterization of GM-Fe NPs. SEM. Eq. (1) depicted the basic principle of $FeCl_3$ reduced to GM-Fe NPs by polyphenols. After adding the extract, the color of the solution immediately turned to black, indicating the reduction of ferric irons. The morphologies of GM-Fe NPs of sample S1–S5 were characterized by SEM and shown in Fig. 2a–e. Fig. 2a–c clearly showed that the GM-Fe NPs were spherical and scattered evenly. Mean diameter of the sample S1–S4 was 85±21 nm (number=100d), 103±24 nm (number=100), 108±28 nm (number=100) and 123±29 nm (number=80), respectively. For sample S4, the strong adhesion between nano particles was

observed, which resulted in only 80 particles could be selected to measure; for sample S5, the adhesion was too serous to measure. Previous studies confirmed that GM pericarp contained large amounts of polyphenols [17]. With the decrease of GM polyphenols added, the size of GM-Fe NPs increased, which was in agreement with Nadagouda et al.'s study [13]. It was found that the average size of GM-Fe NPs (S1–S3) was smaller than ZVI synthesized using PVP as preagglomeration stabilizers [19]. Meanwhile, the dispersion of GM-Fe NPs was different, and particles shown in the Fig. 2a had the best dispersion; with the decrease of polyphenols content, the dispersion of GM-Fe NPs decreased (Fig. 2b–e). Here, polyphenols played the roles of capping and reducing agents in the synthesis of GM-Fe NPs [11], which can effectively prevent particle aggregation and control the size and dispersion of GM-Fe NPs.

$$\text{Polyphenols} + Fe^{3+} \rightarrow Fe^{0} + \text{Quinone} \quad (1)$$

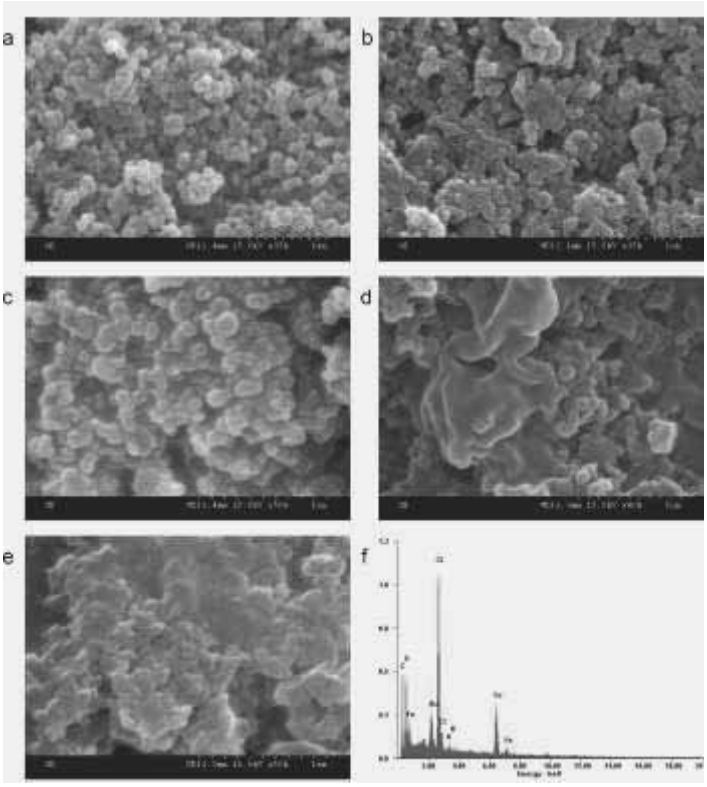

FIGURE 2
SEM images of GM-Fe NPs at different volume ratio of extract to $FeCl_3$ (a) 5:1; (b) 2:1; (c) 1:1; (d) 0.5:1; (e) 0.2:1; (f) EDS spectrum

EDS. The EDS spectrum of GM-Fe NPs (sample S1) exhibited intense peaks of C, O, Fe, Cl, Au and K (Fig. 2f). The K element was a key nutrient for plant growth. The existence of Au was detected because of sputter coating with Au in the sample pretreatment of SEM. The content of C, O, Fe and Cl in the GM-Fe NPs was 27.49 wt%, 25.22 wt%, 21.22 wt% and 16.77wt%, respectively. Fe and Cl were derived from $FeCl_3$ used in the synthesis of GM-Fe NPs. The C and O were the basic elements of polyphenols and other carbon-containing organic matters in the extract of GM pericarps. It was suggested that the polyphenols could wrap on the surface of GM-Fe NPs and play a protective role in the generation of GM-Fe NPs. In Shahwan et al.'s report [4], the content of Fe was 27.8 wt% in the synthesis of Fe NPs by green tea extracts, which was higher than that in this experiment. The reason might be that tea extracts had nearly the highest polyphenols content in the leaves of plant [20]. However, the content of Fe synthesized by the extract of eucalyptus leaf was 16.17 wt% [14], which was lower than this study.

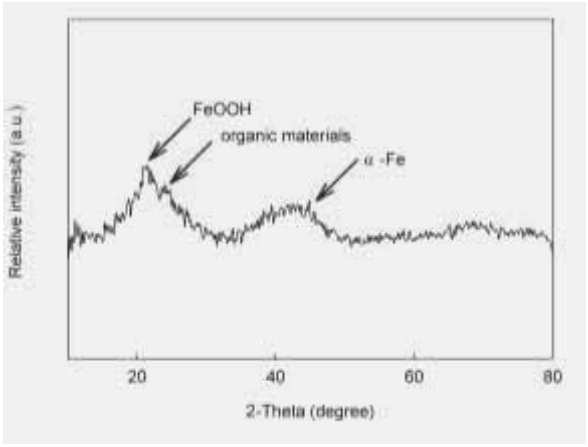

FIGURE 3
XRD patterns of GM-Fe NPs

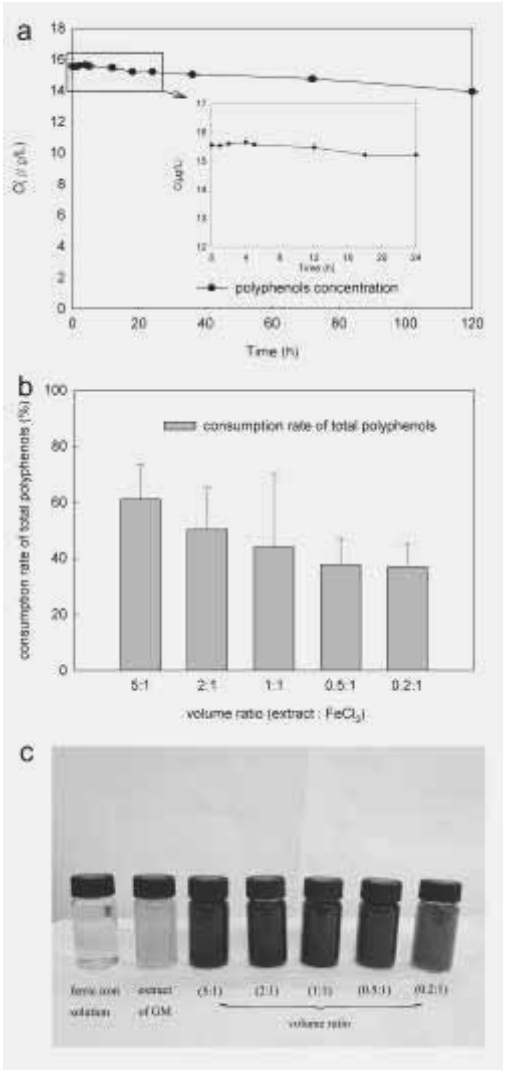

FIGURE 4
Variations of total polyphenols (a) in GM extracts with time ; (b) at different ratio of extract to FeCl3; (c): color change of the solutions

XRD. The XRD image of GM-Fe NPs was shown in Fig. 3. Obvious diffraction peaks were deficient except the peak at $2\theta = 23.76^{o}$ which belonged to iron oxohydroxide (FeOOH) [2]. The shoulder peak at $2\theta = 25^{o}$ corresponded to organic materials absorbed from *Garcinia mangostana* L. pericarp as a capping or stabilizing agent [1, 14]. A less obvious characteristic peak at $2\theta = 44.7^{o}$ could be identified as Fe^{0} (α-Fe) [2]. The patterns suggested that the synthesized GM-Fe NPs were mainly amorphous in nature. A similar pattern was observed for iron NPs synthesized using *Terminalia chebula* aqueous extract [1] or *Eucalyptus* leaf extract [14]

Variations of total polyphenols. The stability of total polyphenols in GM extracts was shown in Fig. 4a. The stability tests were performed in triplicate, and the average values were used. In 24 hours, the concentration of total polyphenols in the extracts only decreased from 15.55 μg/L to 15.20 μg/L, indicating a stable state. From 24 h to 72 h, the concentration decreased to 14.75 μg/L, and then to 13.93 μg/L at 120 h. To maintain total polyphenols in a stable condition, the GM extracts within 24 hours were used to synthesize the GM-Fe NPs.

Fig. 4b and c proved that the total polyphenols in GM extracts reacted with ferric irons in the mixed solution. The total polyphenols consumption rate of sample S1–S5 was 61.13 %, 50.27 %, 43.98 %, 37.64 % and 36.98 %, respectively (Fig. 4b), and the color turned from dark to nigger-brown (Fig. 4c). The total polyphenols consumption rate decreased with the decreasing content of total polyphenols in the reaction system. Polyphenols served as reducing and capping agents for the synthesis of GM-Fe NPs. Under a higher concentration of total polyphenols, less aggregation of GM-Fe NPs was found, which resulted in their higher specific surface area and smaller particle size (Fig. 2a–c) [13]. Moreover, the higher consumption rate of total polyphenols under higher concentration of total polyphenols was also observed. The GM-Fe NPs aggregated easily under low initial concentration of total polyphenols resulting in less specific surface area, larger size of GM-Fe NPs (Fig. 2d and e), lower consumption rate of total polyphenols and lower reduction rate of ferric irons (Fig. 4b). The darkest S1 was the optimal choice, for the higher polyphenols content was in favor of improving the synthesis of GM-Fe NPs (Fig. 4c).

Effects of extract to $FeCl_3$ ratio on decolorization. The ratio of extract to $FeCl_3$ (from S1 to S5) was an important factor affecting the properties of GM-Fe NPs, and further influencing the decolorization characteristic of GM-Fe NPs. So, the optimal ratio should be investigated through the decolorization of RBB in a Fenton-like system. Fig. 5 showed the degradation process of RBB by different ratio of extract to $FeCl_3$ (S1 to S5). Decolorization efficiency of RBB increased with the increasing of polyphenols content. The degradation rate of sample S1 was far greater than the others. And the decolorization efficiency of the sample S1 to S5 can reach 90.58 %, 86.96 %, 86.67 %, 87.65 %, 88.35 % and 83.60 % at 3 h, respectively. The results suggested that sample S1 was a better choice than others.

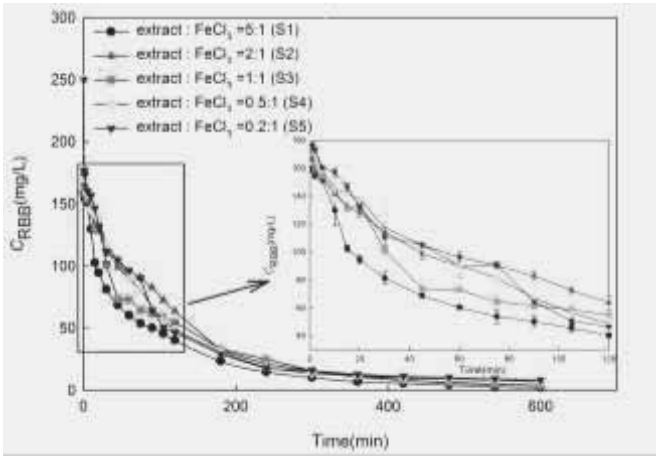

FIGURE 5
The degradation process of RBB by different ratio of extract to $FeCl_3$ in Fenton-like system

Effects of GM-Fe NPs dosage on decolorization. Fig. 6 showed the effect of GM-Fe NPs dosage on the decolorization of RBB. The initial RBB concentration was set as 250 mg/L. Decolorization efficiency of 88.98 %, 90.58 %, 96.85 % and 98.2 % was achieved at 180 min at different GM-Fe NPs dosages of 1 ml, 2 ml, 4 ml and 5 ml, respectively. It was found that the decolorization efficiency of RBB increased with the increasing GM-Fe NPs dosage. In the hybrid system, the increased dosage of GM-Fe NPs could increase total surface area and availability of GM-Fe NPs to RBB dye. It might be the main reason for the decolorization efficiency of RBB increased with increasing GM-Fe NPs dosage. Therefore, 5 ml of GM-Fe NPs dosage, the relatively good choice, was selected for the subsequent experiment.

Effects of initial dye concentrations. Decolorization efficiency was achieved at 93.65 %, 93.41 %, 94.94 % and 90.57 % at 60 min with the RBB concentration of 250 mg/L, 375 mg/L, 500 mg/L and 750 mg/L, respectively (Fig. 7a). The decolorization efficiency varied slightly with different initial RBB concentration and similar degradation profiles were observed. After 180 min, the decolorization efficiency was all more than 97.83 %, indicating that GM-Fe NPs had good capacity on RBB removal in Fenton-like system.

Under 750 mg/L RBB concentration, Fenton-like system of GM-Fe NPs plus H_2O_2 and Fenton system of ferric irons plus H_2O_2 achieved decolorization efficiency of 90.57 % and 79.41 % at 60 min, respectively (Fig. 7a). After 180 min, the decolorizeation efficiency of Fenton system was achieved at more than 90 %, which was lower than that of Fenton-like system (97.83%). In the presence of H_2O_2, the GM-Fe NPs, which were prepared from ferric irons and GM extracts, had a better effect on RBB decolorization than that of ferric irons.

Kinetic analysis. The equation of nth-order reaction kinetic model was shown as Eq. (2) [21].

$$dC/dt = -kC^n \quad (2)$$

where C was the concentration of RBB dye, n was the order of the reaction, t was the reaction time, k was the reaction rate constant (min^{-1}).

According to Eq. (2), the RBB decolorization in a Fenton-like system by GM-Fe NPs under different initial dye concentration can be represented through the first-order, second-order and combined first-order reaction (Eqs. (3), (4) and (5)).

$$C = C_0\exp(-kt) \quad (3)$$

$$C = C_0/(1+kC_0t) \quad (4)$$

$$C = C_1\exp(-k_1t) + C_2\exp(-k_2t) \quad (5)$$

Where C_0 was the concentration of RBB dye at time t = 0, C_1, C_2 represented the initial RBB concentrations of two independent first-order reactions and k_1 and k_2 denoted the empirical rate constant (min^{-1}), respectively. The parameters of the three kinetic models are presented in Table 2. The regression coefficients of the first-order and second-order kinetic models were less than 0.9554

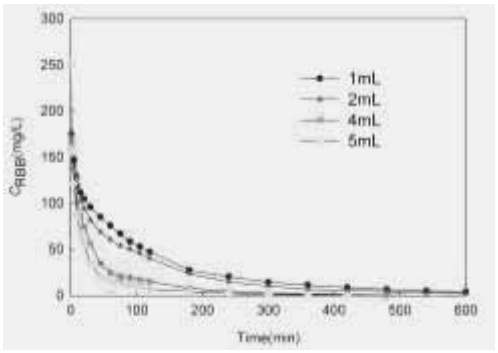

FIGURE 6
The effect of GM-Fe NPs dosage on the decolorization of RBB

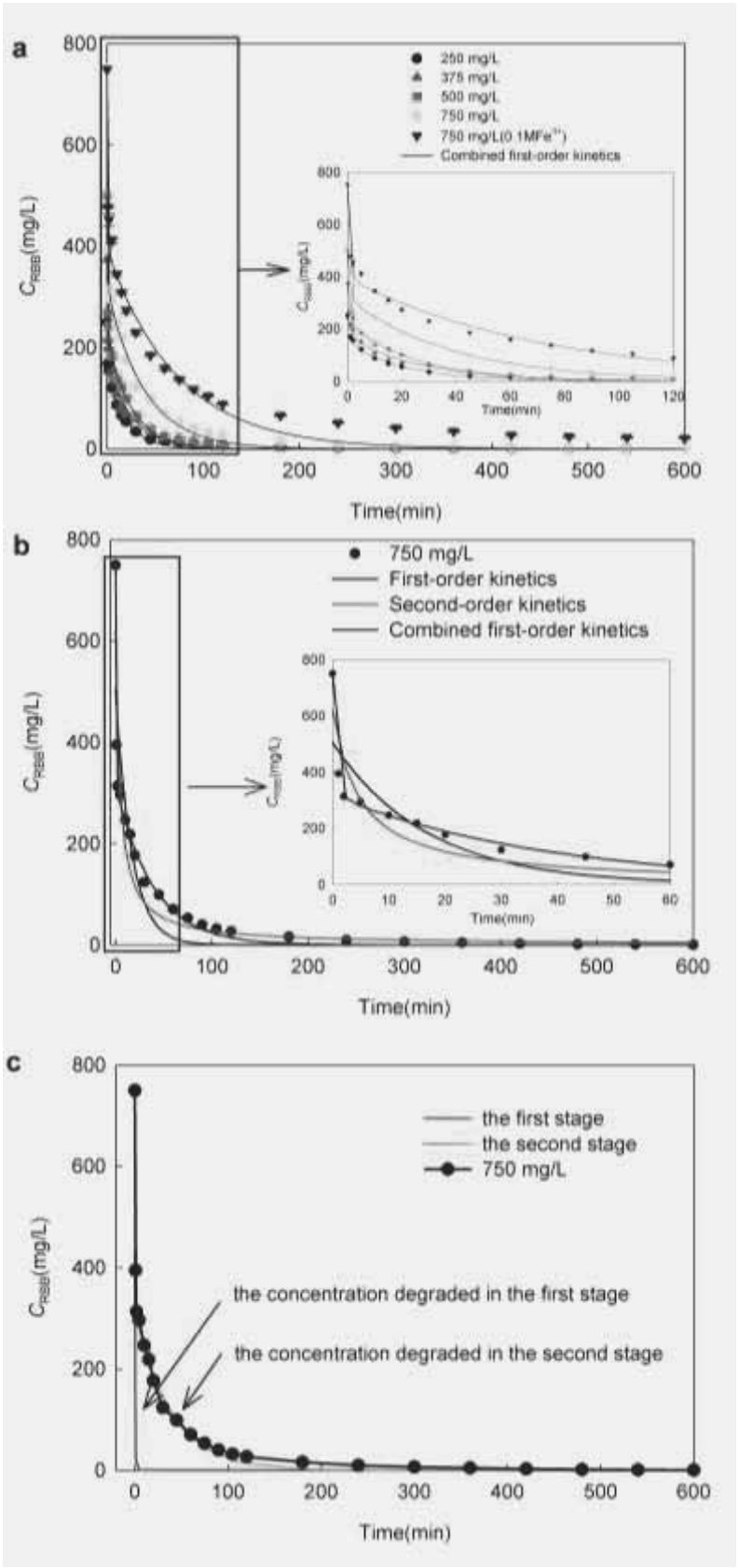

FIGURE 7
Effect of initial dye concentration on RBB removal

TABLE 2
Kinetic parameters for Fenton-like oxidation of RBB

C_0	First-order		Second-order		Combined first-order		
(mg/L)	k(min^{-1})	R^2	k(L/(mg·min)$^{-1}$)	R^2	k_1(min^{-1})	k_2(min^{-1})	R^2
250	0.0794	0.9554	0.1994	0.9863	1.1211	0.0484	0.9938
375	0.0940	0.9094	0.2747	0.9689	1.1431	0.0375	0.9915
500	0.0920	0.8915	0.3198	0.9566	1.5362	0.0404	0.9969
750	0.0597	0.8472	0.2141	0.9140	1.6474	0.0258	0.9975

and 0.9863, respectively. Compared with first-order and second-order kinetic model, the combined first-order rate model fitted best with the decolorization data by the high regression coefficients of more than 0.9915. Also, using initial RBB concentration of 750 mg/L as the example, Fig. 7b showed a visual comparison of the three kinetic models.

Many researchers had found that the Fenton-like system for dye degradation was described by pseudo-first-order or pseudo-second-order kinetic model [22, 23], which were different from the findings of this study. However, Wang et al. [21] and Malik et al. [24] had reported similar results with this study. The degradation process of Fenton-like system can be divided into two stages. The first stage can be represented by the following equations [24, 25]:

$Fe^0 + H_2O \rightleftharpoons Fe^{2+} + H_2 + OH^-$ (6)

$Fe^0 + O_2 + 2H_2O \rightleftharpoons Fe^{2+} + 4OH^-$ (7)

$H_2O_2 + Fe^{2+} \rightleftharpoons \cdot OH + OH^- + Fe^{3+}$ (8)

Hydroxyl radicals may react with ferrous ions generating ferric irons or react with organics as follows [26]:

$OH + Fe^{2+} \rightarrow OH^- + Fe^{3+}$ (9)

$OH + Organics \rightarrow Products$ (10)

Ferric irons produced in the first phase can be used in the second stage as follows [26]:

$H_2O_2 + Fe^{3+} \rightleftharpoons H^+ + FeOOH^{2+}$ (11)

$FeOOH^{2+} \rightleftharpoons HO_2\cdot + Fe^{2+}$ (12)

$HO_2\cdot + Fe^{2+} \rightleftharpoons HO_2^- + Fe^{3+}$ (13)

$HO_2\cdot + Fe^{2+} \rightleftharpoons O_2 + Fe^{3+} + H^+$ (14)

The reaction rate of Eq. (8) is much faster than that in Eq. (11) and (12) [24]·[27]. It means that ferrous ions are consumed quickly, but reproduced slowly. When large amount of ferrous ions are present, large amount of hydroxyl radicals are produced, consequently, the oxidation rate of organic compounds is fast [24]. Hydroxyl radicals react rapidly and non-selectively with most organic compounds by H-abstraction and addition to C-C unsaturated bonds. Compared to hydroxyl radicals, hydroperoxyl radical ($HO_2\cdot$) is much less reactive [27]. Therefore, in the presence of a large number of ferrous ions, the first stage reaction carried out quickly, and the second stage reaction was very slow. Accordingly, k_1 was greater than k_2 in the combined first-order rate model. Here, the degradation of RBB with initial concentration of 750 mg/L was chosen as an example (Fig. 7c). As shown in Fig. 7c, time t was substituted into the two stage of the combination equation, respectively. C_1 of the first stage (red line) dropped to zero in 10 min, and C_2 of the second stage (green line) slowly decreased to zero in 200 min. Meanwhile, with the increase of RBB concentration, C_1 of the first stage reaction increased from 40.07 % at 250 mg/L to 57.61 % at 750 mg/L. k_1 also increased from 1.1211 min^{-1} to 1.6474 min^{-1}, while k_2 showed a decreasing trend. With the increasing dye concentration, more H_2O_2 was decomposed into hydroxyl radicals and reacted with the increasing dye, and less H_2O_2 participated in the reaction with ferric irons (the second stage reaction), leading to the decrease of the second stage reaction rate.

Decolorization of anthraquinone dyes by different methods was compared with this study. Reactive Blue 4 of 100 mg/L was reduced by 55.9 g/L ZVI with the pseudo first-order rate constant of 0.029 h^{-1} [28]. 0.3 mM Fe^{2+} and 3 mM H_2O_2 were occupied to degrade 100 mg/L anthraquinone dye Reactive Blue 19 with the kinetic constant of 0.04 min^{-1}. The kinetic constants above were lower than k_1 and k_2 in this study. A mixed methanogenic culture was occupied to degrade 300 mg/L RBB, 95 % of the RBB was degraded in 14 days [29]. *Dichomitus squalens* immobilized on pine wood was applied to degrade 50 mg/L Remazol Brilliant Blue, 94 % of the dye was degraded in one day [30]. 55.7 % of 100 mg/L Reactive Blue 2 was

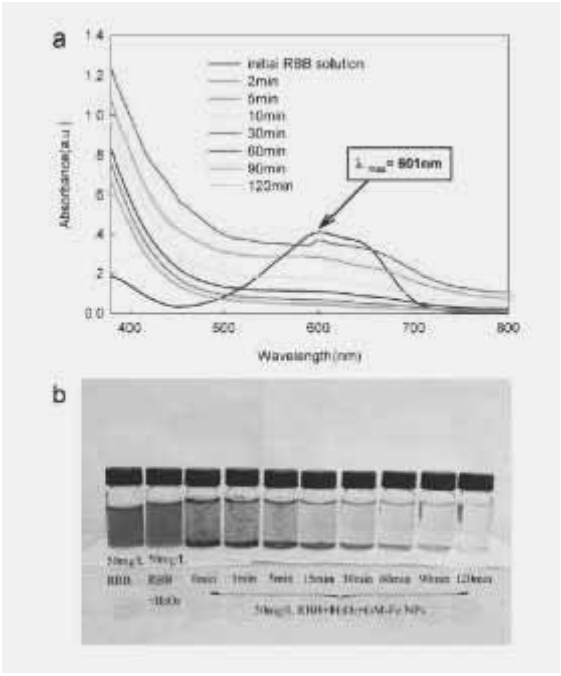

FIGURE 8
Variations of dye concentration with time (a) UV spectra; (b) color change of the solution

decolorized in 60 min by using dried activated sludge as an adsorbent [31]. In two days, 84 % of the 300 mg/L Reactive Blue 4 was biodegraded [32]. Compared with the decolorization methods mentioned above, the application of GM-Fe NPs as Fenton-like system for RBB decolorization was featured with eco-friendly, low cost and rapid decolorization speed, which exhibits a good application prospect for decolorizing anthraquinone dyes.

UV-vis spectra analysis. The changes of UV-vis spectra of 50 mg/L RBB dye degradation by GM-Fe NPs Fenton-like system were shown in Fig. 8a. As shown in Fig. 8a, the characteristic peak attributed to the anthraquinone ring of RBB dye at 601 nm decreased from 0.411 to 0.038 after 120 min degradation. At the same time, the color turned from blue to light yellow (Fig. 8b). According to Eq. (6) to Eq. (14), the light yellow was the color of ferric irons. These results indicated that color groups in the visible region had been degraded, and no new peaks appeared.

FTIR spectra analysis. Fig. 9 depicted the FTIR spectra of the original GM-Fe NPs powder and the GM-Fe NPs powder after decolorization. The FTIR spectrum of original GM-Fe NPs displayed a number of absorption peaks. The band at 1057 cm^{-1} was due to C-N stretching vibration of aliphatic amines [14, 33]; the band around 1437 cm^{-1} was responsible for germinal methyl [33]; the absorption band at 1518 cm^{-1} was ascribed to symmetric stretching vibrations of -COO- functional group [34]; the band at 1616 cm^{-1} was corresponded to aromatic ring or C=C stretching vibration [35], and the band around 3368 cm^{-1} was due to O-H stretching vibration in hydroxyl groups [1, 14]. The result was in agreement with the FTIR spectra of GM pericarp [35]. After the degradation of RBB dye, FTIR spectra of GM-Fe NPs changed obviously, most of the bands disappeared and two new bands at 1734 and 3447 cm^{-1} appeared, which denoted C=O group and O-H stretching vibration in hydroxyl groups, respectively. The FTIR results indicated that during the degradation of RBB, GM-Fe NPs reacted with RBB; also, the extract of GM coated on GM-Fe NPs, using as capping agent [14], were damaged during Fenton-like reaction (Eq. (6) to (14)).

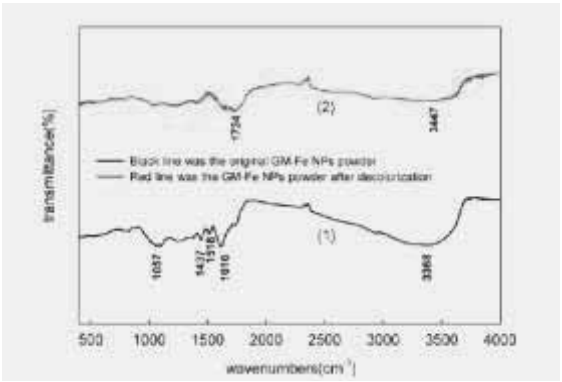

FIGURE 9
FTIR spectra of (1) original GM-Fe NPs powder; (2) GM-Fe NPs powder after decolorization

CONCLUSIONS

GM-Fe NPs were first green synthesized in one step by using the extract of GM pericarp under mild conditions. The polyphenols in the extract of GM pericarp played the roles of reducing and capping agents, which was confirmed by SEM, EDS, XRD and FTIR spectra of GM-Fe NPs and variations of total polyphenols during the synthesis of GM-Fe NPs. The GM-Fe NPs were mainly amorphous in nature. The optimal ratio of extract to $FeCl_3$ for the synthesis of GM-Fe NPs was 5 : 1, and the mean particle size of GM-Fe NPs was about 85 nm.. The GM-Fe NPs were occupied as a

catalyst in the Fenton-like oxidation system to degrade RBB dye. With the increasing GM-Fe NPs dosage, the decolorization efficiency of RBB increased from 88.98 to 98.2%. Under the use of 5mL GM-Fe NPs, the decolorization efficiency can reach more than 90% at 60 min and more than 97.83 % after 180 min when the initial RBB concentration ranged between 250 mg/L to 750 mg/L. The combined first-order kinetic model can well explain the RBB degradation process. UV-vis spectra indicated that color groups of RBB in the visible region had been degraded, and no new peaks appeared. In this study, the green synthesis of GM-Fe NPs could realize the effective use of the agriculture waste GM and had the potential for the RBB removal from wastewater.

ACKNOWLEDGEMENTS

We would like to thank the NSFC (51078007, 51378027) and Beijing Talent Foundation of BJUT (2013-JH-L06) for the financial supports of this study.

REFERENCES

[1] Kumar, K.M., Mandal, B.K., Kumar, K.S., Reddy, P.S. and Sreedhar, B. (2013) Biobased green method to synthesise palladium and iron nanoparticles using Terminalia chebula aqueous extract. Spectrochim. Acta. A., 102, 128-133.

[2] Kuang, Y., Wang, Q.P., Chen, Z.L., Megharaj, M. and Naidu, R. (2013) Heterogeneous Fenton-like oxidation of monochlorobenzene using green synthesis of iron nanoparticles. J. Colloid Interf. Sci., 410, 67-73.

[3] Xu, L. and Wang, J. (2011) A heterogeneous Fenton-like system with nanoparticulate zero-valent iron for removal of 4-chloro-3-methyl phenol. J. Hazard. Mater., 186, 256-264.

[4] Shahwan, T., Abu Sirriah, S., Nairat, M., Boyaci, E., Eroglu, A.E. and Scott, T.B. et al. (2011) Green synthesis of iron nanoparticles and their application as a Fenton-like catalyst for the degradation of aqueous cationic and anionic dyes. Chem. Eng. J., 172, 258-266.

[5] Moon, B., Park, Y. and Park, K. (2011) Fenton oxidation of Orange II by pre-reduction using nanoscale zero-valent iron. Desalination, 268, 249-252.

[6] Kuhn, L.T., Bojesen, A., Timmermann, L., Nielsen, M.M. and Morup, S. (2002) Structural and magnetic properties of core–shell iron–iron oxide nanoparticles. J. Phys.-Condens. Mat., 14, 13551-13567.

[7] Karlsson, M.N.A., Deppert, K., Wacaser, B.A., Karlsson, L.S. and Malm, J.O. (2005) Size-controlled nanoparticles by thermal cracking of iron pentacarbonyl. Appl. Phys. A., 80, 1579-1583.

[8] Wang, C. and Zhang, W. (1997) Synthesizing nanoscale iron particles for rapid and complete dechlorination of TCE and PCBs. Environ. Sci. Technol., 31, 2154-2156.

[9] Saleh, N., Kim, H., Phenrat, T., Matyjaszewski, K., Tilton, R.D. and Lowry, G.V. (2008) Ionic Strength and composition affect the mobility of surface-modified Fe. Environ. Sci. Technol., 42, 3349-3355.

[10] Tiraferri, A., Chen, K.L., Sethi, R. and Elimelech, M. (2008) Reduced aggregation and sedimentation of zero-valent iron nanoparticles in the presence of guar gum. J. Colloid Inter. Sci., 324, 71-79.

[11] Hoag, G.E., Collins, J.B., Holcomb, J.L., Hoag, J.R., Nadagouda, M.N. and Varma, R.S. (2009) Degradation of bromothymol blue by 'greener' nano-scale zero-valent iron synthesized using tea polyphenols. J. Mater. Chem., 19, 8671-8677.

[12] Smuleac, V., Varma, R., Sikdar, S. and Bhattacharyya, D. (2011) Green synthesis of Fe and Fe/Pd bimetallic nanoparticles in membranes for reductive degradation of chlorinated organics. J. Membrane Sci., 379, 131-137.

[13] Nadagouda, M.N., Castle, A.B., Murdock, R.C., Hussain, S.M. and Varma, R.S. (2010) In vitro biocompatibility of nanoscale zerovalent iron particles (NZVI) synthesized using tea polyphenols. Green Chem., 12, 114-122.

[14] Wang, T., Jin, X., Chen, Z., Megharaj, M. and Naidu, R. (2014) Green synthesis of Fe nanoparticles using eucalyptus leaf extracts for treatment of eutrophic wastewater. Sci. Total Environ., 466, 210-213.

[15] Gao, J., Si, C. and He, Y. (2015) Application of soybean residue (okara) as a low-cost adsorbent for reactive dye removal from

aqueous solution. Desalin. Water Treat., 53, 2266-2277.

[16] Gao, J., Zhang, Q., Su, K. and Wang, J. (2010) Competitive biosorption of Yellow 2G and Reactive Brilliant Red K-2G onto inactive aerobic granules: simultaneous determination of two dyes by first-order derivative spectrophotometry and isotherm studies. Bioresource Technol., 101, 5793-5801.

[17] Yu, L., Zhao, M., Yang, B., Zhao, Q. and Jiang, Y. (2007) Phenolics from hull of Garcinia mangostana fruit and their antioxidant activities. Food Chem., 104, 176-181.

[18] ISO. (2005) Determination of substances characteristic of green and black tea. Part 1: Content of total polyphenols in tea. Colorimetric method using Folin-Ciocalteu reagent. International Organization for Standardization, ISO, 14502-1:2005(E).

[19] He, Y., Gao, J., Feng, F., Liu, C., Peng, Y. and Wang, S. (2012) The comparative study on the rapid decolorization of azo, anthraquinone and triphenylmethane dyes by zero-valent iron. Chem. Eng. J., 179, 8-18.

[20] Machado, S., Pinto, S.L., Grosso, J.P., Nouws, H., Albergaria, J.T. and Delerue-Matos, C. (2013) Green production of zero-valent iron nanoparticles using tree leaf extracts. Sci. Total Environ., 445, 1-8.

[21] Wang, S. (2008) A comparative study of Fenton and Fenton-like reaction kinetics in decolourisation of wastewater. Dyes Pigments, 76, 714-720.

[22] Haji, S., Khalaf, M., Shukrallah, M., Abdullah, J. and Ahmed, S. (2015) A kinetic comparative study of azo dye decolorization by catalytic wet peroxide oxidation using Fe-Y zeolite/H_2O_2 and photooxidation using UV/H_2O_2. React. Kinet. Mech. Cat., 114, 795-815.

[23] Rache, M.L., Garcia, A.R., Zea, H.R., Silva, A.M.T., Madeira, L.M. and Ramirez, J.H. (2014) Azo-dye orange II degradation by the heterogeneous Fenton-like process using a zeolite Y-Fe catalyst-Kinetics with a model based on the Fermi's equation. Appl. Catal. B-Environ., 146, 192-200.

[24] Malik, P.K. and Saha, S.K. (2003) Oxidation of direct dyes with hydrogen peroxide using ferrous ion as catalyst. Sep. Purif. Technol., 31, 241-250.

[25] Zhou, T., Li, Y., Ji, J., Wong, F. and Lu, X. (2008) Oxidation of 4-chlorophenol in a heterogeneous zero valent iron/H_2O_2 Fenton-like system: kinetic, pathway and effect factors. Sep. Purif. Technol., 62, 551-558.

[26] Walling, C. (1975) Fenton's reagent revisited. Accounts Chem. Res., 8, 125-131.

[27] Pignatello, J.J. (1992) Dark and Photoassisted Fe^{3+}-catalyzed degradation of chlorophenoxy herbicides by hydrogen peroxide. Environ. Sci. Technol., 5, 944-951.

[28] Epolito, W.J., Yang, H., Bottomley, L.A. and Pavlostathis, S.G. (2008) Kinetics of zero-valent iron reductive transformation of the anthraquinone dye Reactive Blue 4. J. Hazard. Mater., 160, 594-600.

[29] Lee, Y.H. and Pavlostathis, S.G. (2004) Decolorization and toxicity of reactive anthraquinone textile dyes under methanogenic conditions. Water Res., 38, 1838-1852.

[30] Susla, M., Novotny, C. and Svobodova, K. (2007) The implication of Dichomitus squalens laccase isoenzymes in dye decolorization by immobilized fungal cultures. Bioresource Technol., 98, 2109-2115.

[31] Aksu, Z. (2001) Biosorption of reactive dyes by dried activated sludge: equilibrium and kinetic modelling. Biochem. Eng. J., 7, 79-84.

[32] Lee, Y.H., Matthews, R.D. and Pavlostathis, S.G. (2006) Biological decolorization of reactive anthraquinone and phthalocyanine dyes under various oxidation-reduction conditions. Water Environ. Res., 78, 156-169.

[33] Das, R.K., Borthakur, B.B. and Bora, U. (2010) Green synthesis of gold nanoparticles using ethanolic leaf extract of Centella asiatica. Mater. Lett., 64, 1445-1447.

[34] Bao, P.H.D., Ba, D.N., Hoang, D.N. and Phuong, T.N. (2013) Synthesis of magnetic composite nanoparticles enveloped in copolymers specified for scale inhibition application. Adv. Nat. Sci.-Nanosci. Nanotechnol., 4, 45016-45017.

[35] Chen, Y., Huang, B., Huang, M. and Cai, B. (2011) On the preparation and characterization of activated carbon from mangosteen shell. J. Taiwan Inst. Chem. E., 42, 837-842.

Received: **17.08.2015**
Accepted: **21.12.2015**

CORRESPONDING AUTHOR

Dr. Jing-Feng Gao
College of Environmental and Energy Engineering
Beijing University of Technology
Beijing 100124, CHINA

e-mail: gao.jingfeng@bjut.edu.cn
gao158@gmail.com

© by PSP Volume 25 – No. 7/2016, pages 2356-2363 Fresenius Environmental Bulletin

DETERMINATION OF PHENOLIC COMPOUNDS FROM TURKISH KERMES OAK (*Quercus coccifera* L.) ROOTS BY HIGH PERFORMANCE LIQUID CHROMATOGRAPHY; ITS ANTIMICROBIAL ACTIVITIES

Eyyüp Karaogul[1*], Ekrem Kirecci[2], M. Hakkı Alma[1]

[1]Department of Forest Industry Engineering, Kahramanmaraş Sütçü İmam University, Kahramanmaraş, Turkey
[2]Department of Medical Microbiology, Faculty of Medicine, Kahramanmaraş Sütçü İmam University, Kahramanmaraş, Turkey

ABSTRACT

The aim of the study was to identify the extractable phenolic compounds in the roots of Turkish Kermes Oak (*Quercus coccifera* L.), and its antimicrobial activities. The roots were extracted by using conventional hot water extraction method as a function of time. Phenolic compounds were determined by using high performance liquid chromatography (HPLC). And, antimicrobial activity tests were carried out using disc diffusion method with six different bacteria and one fungus (yeast) species. The extraction yields were 22.19%, 22.76%, 23.16% and 22.82% for 30, 60, 90 and 120 min, respectively. It was also found that about 30-38% of the total compounds in the oak roots were determined by HPLC for all the extractions. Ten active compounds (e.g., caffeic acid, (-) gallocatechin, fumaric acid, gallic acid, catechin, protocatechuic acid ethyl ester, syringic acid, t-3-hydroxycinnamic acid, 4-hydroxybenzoic acid and ellagic acid) were found in the oak root extract. The concentration of main compounds in the oak roots were fumaric acid (about 12-22 mg/kg), (-) gallocatechin (about 1-12 mg/kg), ellagic acid (about 3-5 mg/kg) and gallic acid (about 1-2 mg/kg) for all the extraction times. Furthermore, some of the Gram-positive and Gram-negative bacterial species and the fungus strain were inhibited.

KEYWORDS:
Turkish kermes oak roots, phenolic compounds, main compounds, extraction times, HPLC, antimicrobial activity.

INTRODUCTION

There is an in increasing concern in the measurement and use of plant antibacterial and antifungal activities for ethno botanic research as well as scientific research and industrial purposes. Roots of plants and their other products from secondary metabolism have been using in folk medicine, food flavoring, fragrance and pharmaceutical industries [1].

Ever green oaks dominate most forest habitats in the Mediterranean region [2]. Kermes oak (*Quercus coccifera* L.) species are particularly important in the maki vegetation. Although its distributions and habitats are overlapping, ecological differences among them exist. *Q. coccifera* is more thermophilous than other oaks species and appears to have contrasting environmental requirements. Kermes oak is more frequent in arid and disturbance-prone environments, predominantly on limestone substrates [3].

Tannins are complex polyphenolics found widely in the plant kingdom [4]. Tannins are detected in leaves, twigs, flower, fruits, tree bark and tree roots. They are water soluble polyphenols that are commonly available in higher herbaceous and woody plants [5]. Gallic acid is an important gallotannin belonging to the hydrolysable class, while catechin belongs to the non-hydrolysable class [6-7].

The interest in natural tannins in the plants relies on the wide variety of relevant properties, namely, antioxidant, anti-inflammatory, radical scavenger and antimicrobial properties [8-10]. Especially, the interest in natural phenolic compounds for nutraceutical and cosmetic applications has considerably increased in recent years because of the above-mentioned properties and adverse effects resulted from synthetic counterparts [11].

According to ethno botanic researches from people in the Kaledibi village from Cemendag region of Kahramanmaras, Turkey, it was reported that *Q. coccifera* have been used in the healing skin burn and stomach wound. Due to the healing properties just mentioned, the oak root extracts were applied every day on skin burning for 1-2 weeks. Ito et al. (2002) have reported the presence of several phenolic acids

as tannins, namely, ellagic acid in the extracts of wood and leaves and (-) gallocatechin in the extracts of bark from *Q. coccifera*. However, the information available on the phenolic fraction known as tannins of wood, leaves and bark from *Q. coccifera* is scarce despite the fact that this group of components can also be easily extracted from those residues [12].

Judaki et al. (2014) have studied antimicrobial activity of tree fruit of *Q. coccifera*. The results of this study showed positive antimicrobial effect against two microorganisms [13]

Gunes et al. (2014) have also reported that the fruit extract of *Q. coccifera* had strong antimicrobial efficay on *S. albus, M. luteus and S.aureus* [14].

Q. coccifera root extracts locally have a great importance owing to folkloric information and no study has been done on the chemical composition of roots from *Q. coccifera* and its biological activities so far. Therefore, we aimed to study the phenolic fraction and microbial activities of roots of *Quercus coccifera*.

MATERIAL AND METHODS

Roots of *Q. coccifera* L. (RQC) were collected from geographical location with the altitude of 1411 m in Ahir hill, latitude of 37º 37' 15,11'' and longitude of 37º 03' 54,2'' in Kahramanmaraş province located in the Mediterranean region of Turkey. *Q.coccifera* L. was diagnosed by Lecturer Tolga OK from Department of Forestry Engineering, Kahramanmaraş Sütçu İmam University (KSU), Kahramanmaraş, Turkey. Voucher specimen number was 44, and voucher specimen was deposited in Herbarium of Forestry Faculty in Kahramanmaraş Sütçu İmam University (KASOF). Reference chemicals, such as gallic acid, ellagic acid, caffeic acid, fumaric acid, catechin, protocatechuic acid ethyl ester, syringic acid, t-3 hydroxycinnamic acid, 4-hydroxy benzoic acid and (-) gallocatechin were supplied by Sigma Chemicals Co. Methanol, phosphoric acid and acetonitrile, which are elluents in high performance liquid chromatograph (HPLC) grade and purchased form Merck Co. Deionized water used throughout the experiments was generated by a Millipore water purification system and filtered with a 0.22 µm membrane in Central Laboratory of KSU.

Preparation of extracts. The roots of the Kermes oak were dried and pulverized by willey mill and sieved granulometric fraction for 40-60 mesh. The RQC powders were used for extraction and HPLC analysis. About 2 g of RQC powder was mixed with boiling water of 200 ml. The samples were extracted by using conventional hot water extraction method for 30, 60, 90 and 120 min, respectively. Half ml of each extract was removed and centrifuged at 5000 rpm for 10 min. The supernatant was collected and stored at 4 ºC. Finally, extraction yields (EY) were calculated as follows:

$$EY\ (\%) = \frac{Wo - W1}{Wo} x100$$

where, Wo is the initial oven-dry weight of a sample before soaking in water (g) and W_1 is the oven-dry weight of the sample after extraction (g).

Preparation of standard solution. Standard stock solutions of gallic acid (200 mg/kg), ellagic acid (100 mg/kg), caffeic acid (250 mg/kg), fumaric acid (300 mg/kg), catechin (200 mg/kg), protocatechuic acid ethyl ester (330 mg/kg), syringic acid (120 mg/kg), t-3 hydroxycinnamic acid (150 mg/kg), 4-hydroxybenzoic acid (400 mg/kg) and (-) gallocatechin (100 mg/kg) were prepared in methanol and stored away from light at 4 ºC. Different concentrations of working solutions were prepared by appropriate dilution of the stock solution.

HPLC analysis. Liquid chromatography of the oak roots extracts was carried out on a Shimadzu HPLC system with LC-20AD pumping system and a SPD-20A UV detector. Wavelengths used to detect the phenolic compounds were 278 nm. The column used was a ODS Hypersil C-18 (250 x 4.6 mm x 5 µm). The elution was performed with 0.1% of phosphoric acid (A) and acetonitrile (B). The gradient profile was as follows: 0 min, 8% B; 35 min, 22% B; 45 min 8% B and then held for 5 min to initial conditions. The flow rate was 0.8 ml/min. The chromatographic column was washed with the initial conditions to stabilize for 10 minute. The concentrations of each compound were reported as mg/kg on the basis of total weight of oven-dry oak roots and percent amount on the basis of total compounds determined by HPLC.

For good separation; an appropriate chromatographic column, mobile phase and detection wavelength are critically important. So, various mobile phases consisting of phosphoric acid-acetonitrile, acetic acid-methanol, methanol-acetonitrile and methanol-water were investigated under different gradient conditions. The detection wavelength was chosen according to the maximum adsorption wavelengths for all the reference compounds between 200-400 nm wavelengths. The desired components form the RQC were identified by comparing both the retention times and UV spectra with those of the authentic standard. After several tests, suitable column and the phosphoric acid-acetonitrile mobile phase mentioned above were

TABLE 1
Regression equation, retention time, correlation coefficient of reference compounds on HPLC.

No	Reference Compound	Retention Time (min)	Regression equation[a]	Correlation coefficient (r^2)
1.	Caffeic acid	16.10	$y = 1.29.10^{-5}x$	0.9978
2.	(-) Gallocatechin	7.70	$y = 4.48.10^{-5}x$	0.9930
3.	Fumaric acid	5.13	$y = 6.16.10^{-4}x$	0.9986
4.	Gallic acid	5.41	$y = 6.81.10^{-6}x$	0.9993
5.	Catechin	12.44	$y = 5.28.10^{-5}x$	0.9920
6.	Protocatechuic acid ethyl ester	37.44	$y = 2.49.10^{-5}x$	0.9957
7.	Syringic acid	17.06	$y = 1.84.10^{-5}x$	0.9834
8.	t-3-hydroxycinnamic acid	30.53	$y = 5.17.10^{-6}x$	0.9812
9.	4-hydroxybenzoic acid	13.73	$y = 1.24.10^{-5}x$	0.9865
10.	Ellagic acid	26,61	$y = 9.88.10^{-6}x$	0.9850

[a]x: peak area of components, y: concentration of components

found suitable condition for simultaneous separation and determination. Perfect agreement between standard and sample spectra was found in all the analyzed samples.

All the calibration curves were plotted based on linear regression analysis of the integrated peak areas (x) versus concentrations (y, mg/ kg) of the 10 marker constituents in the reference solution at four different concentrations. Regression equation, retention time and correlation coefficient of 10 marker constituents in HPLC were listed in Table 1.

Furthermore, in this study for analysing condensed tannins (e.g., catechin, gallocatechin etc.) and hydrolysable tannins (e.g., gallic acid, ellagic acid etc.) presents in RQC samples, under the same chromatographic conditions was developed. Various mobile phase systems were investigated when the method was established. The results showed that the solvent system consisting of A-phosphoric acid and B-acetonitrile was found to be the best one for influence on the chromatographic separation

Preparation of test microorganisms. Gram-positive bacteria (*Staphylococcus aureus*-ATCC 25923*, Staphylococcus epidermidis*-Clinical isolate), Gram-negative bacteria [*Escherichia coli*-Clinical isolate*, Acinetobacter baumannii***-**Clinical isolate (Nosocomial Pathogen), *Pseudomonas aeruginosa*-Clinical isolate (Nosocomial Pathogen), *Klebsiella pneumonia*-Clinical isolate] and fungi (yeast) (*Candida albicans*-ATCC 90028) were employed for determination of antibacterial and antifungal activity. The microorganisms that can be pathogenic for humans were used in this study. The strains of bacteria and fungi were obtained from the stock cultures (clinical isolates and standard strains) of Microbiology Laboratory, in the Department of Medical Microbiology, Faculty of Medicine, Kahramanmaras Sutcu Imam University, Kahramanmaras, Turkey. These bacteria were maintained on Blood agar base (Oxoid CM55, Basingstoke, Hampshire, UK). The fungus was maintained on Sabouraud-dextrose agar (Oxoid CM41, Basingstoke, Hampshire, UK), which is often used with antifungal for the isolation of the pathogenic fungi. These isolates (bacteria and yeast) were identified using conventional biochemical tests [15] and confirmed by API test system (BioMèrieux, France).

Antimicrobial susceptibility testing. For the purpose of antimicrobial activities, seven microorganisms were used. Agar cultures of the test microorganisms were prepared as described by Gulcin et al. (2008). Three to five similar colonies were selected and transferred with loop into 5 ml of Tryptone soya broth (Oxoid CM129, Basingstoke, Hampshire, UK). Tryptone soya broth is a highly nutritious versatile medium, which is recommended for general laboratory use and used for the cultivation of aerobes and facultative anaerobes, including some fungi. The broth cultures were incubated for 24 h at 37°C. For screening, sterile, 6-mm diameter filter paper disc were impregnated with 20 and 40 µl of the water extracts. *Q. coccifera* extract dissolved in sterile water for the assay by magnetic stirrer. Then the paper discs placed onto Mueller Hinton agar (Oxoid CM337, Basingstoke, Hampshire, UK). The inoculum

for each organism was prepared from broth cultures. The concentration of cultures was to 10^8 colony forming units (1×10^8 cfu/ml). The results were recorded by measuring the zones of growth inhibition surrounding the disc. Clear inhibition zones around the discs indicate the presence of antimicrobial activity: amoxicillin-clavulanic acid (20/10 µg/disc), gentamicin (10 µg/disc), ampicillin-sulbactam (10/10 µg/disc), ciprofloxacin (5 µg/disc, BD BBL™ Sensi-Disc™) and antifungal Fluconazole (25 µg/disc) were used as reference standards, which recommended by the Clinical and Laboratory Standards (CLSI). In vitro antimicrobial susceptibility testing of isolates were carried out using the disc diffusion method according to the CLSI on Mueller-Hinton agar (Merck, Germany) plates [16].

RESULTS

Extraction yields in conventional extraction method. The extraction yields of the oak roots studied are shown in Table 2. It was evident from table 2 that the extraction yields obtained were found to be closed to each other depending on the time.

TABLE 2
Extraction yields of *Quercus coccifera* roots as a function of time.

Time (min)	Extraction Yield (%)
30	22.19
60	22.76
90	23.16
120	22.82

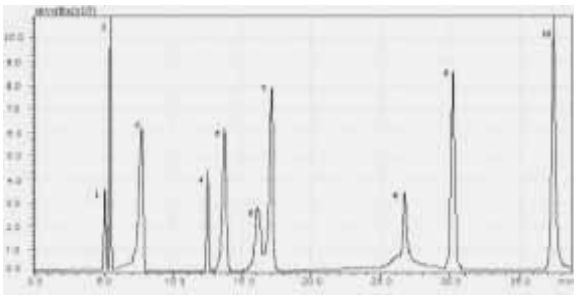

FIGURE 1
Typical chromatograms of the standard mixture. (1) fumaric acid, (2) gallic acid, (3) (-) gallocatechin, (4) catechin, (5) t-3-hydroxycinnamic acid, (6) caffeic acid, (7) syringic acid, (8) ellagic acid, (9) t-3 hydroxycinnamic acid, (10) protocatechuic acid ethyl ester.

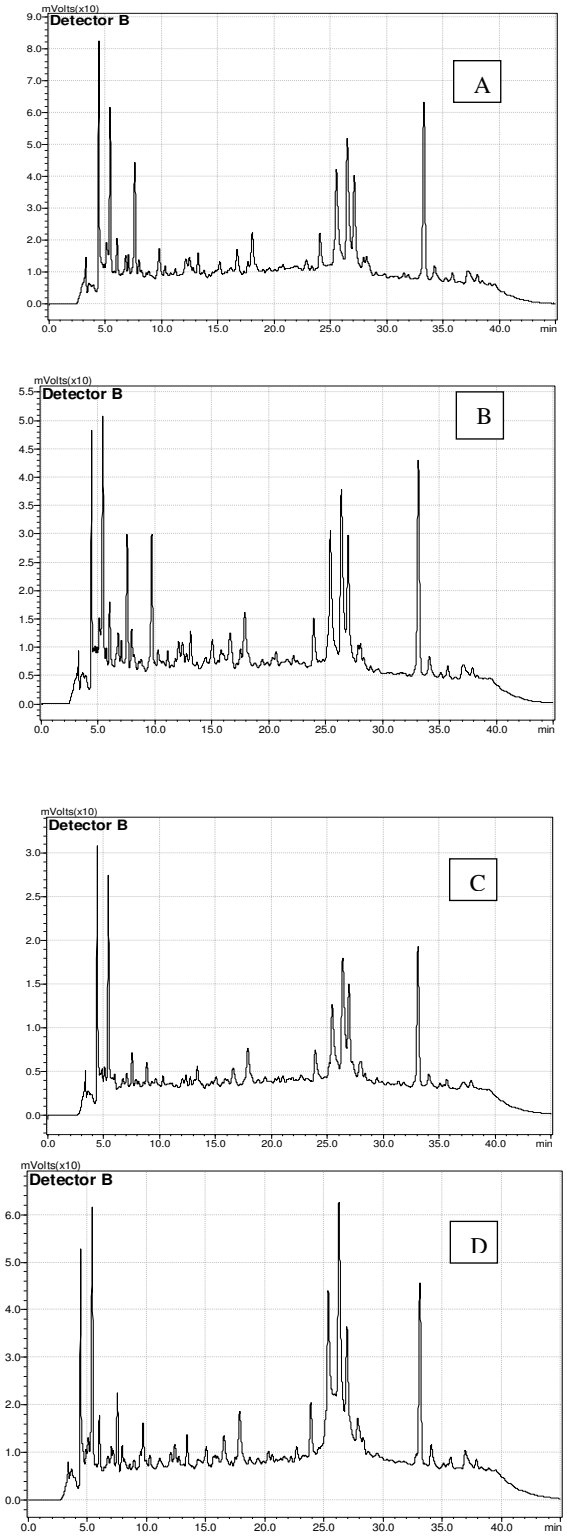

FIGURE 2
Typical chromatograms of the RQC for (A) 30, (B) 60, (C) 90 and (D) 120 min extraction time respectively in conventional extraction method.

TABLE 3
Chemical compound and their concentrations (mg/kg and percent) determined by HPLC study.

No	Chemical Compounds	Extraction time (min)							
		30		60		90		120	
		mg/kg	%*	mg/kg	%	mg/ kg	%	mg/ kg	%
1.	Caffeic acid	0.07	0.24	0.03	2.87	0.04	2.45	0.94	1.37
2.	Ellagic acid	4.35	8.82	3.57	19.42	3.21	8.45	5.23	19.26
3.	Fumaric acid	22.84	1.85	20.14	0.85	14.13	0.93	12.12	0.6
4.	Gallic acid	2.32	11.75	1.74	6.86	1.84	11.24	2.23	7.79
5.	Catechin	1.56	1.29	1.67	0.76	0.93	1.04	1.1	1.12
6.	Protocatechuic acid ethyl ester	1.96	0.88	1.03	1.44	0.28	1.03	2.38	1.588
7.	Siringic acid	0.69	-	0.12	0.12	0.07	-	0.13	-
8.	t-3-hydroxy cinnamic acid	-	-	-	-	0.03	-	0.02	-
9.	4-Hydroxy benzoic acid	0.09	0.51	0.1	0.2	0.14	3.03	0.6	1.15
10.	(-) Gallocatechin	12.28	7.99	9.56	5.04	1.47	2.33	5.65	2.59
	Total		**33.33**		**37.56**		**30.35**		**35.37**

*The percentage of compounds determined by HPLC.

HPLC analysis. The established method was applied to analyze the solution of reference compounds and RQC samples. Typical chromatograms of the pure standards and *Q. coccifera* roots in HPLC are shown in Figures 1 and 2.

The HPLC identification of tannin compounds was carried out by comparing peak retention times with reference compounds run under the same experimental conditions for all the samples. The HPLC evaluations of the RQC extracts as concentration (mg/kg) and percent amount as functions of extraction time periods were given in Table 3.

No study has been done on the chemical composition of the roots from *Q. coccifera* so far. However, Ito et al. (2002) have notified the entity of several phenolic acids, namely, ellagic acid in extracts of wood and leaves and (-) gallocatechin in the extracts of bark from *Q. coccifera*. Yet, the information available on the phenolic fractions, known as tannins, of wood, leaves and bark are still scarce.

It was clear from Table 3 that total amount of phenolic compounds determined were 33.33%, 37.56%, 30.35% and 35.37% for extraction time of 30, 60, 90 and 120 mim, respectively.

The highest concentration (12.12-22.84 mg/kg) was found to be for fumaric acid, followed by (-) gallocatechin (2.33-12.28 mg/kg), ellagic acid (3.21-5.23 mg/kg) and gallic acid (1.74-2.32 mg/kg) for the whole extraction times. Besides, smaller amounts of catechin, protocatechuic acid ethyl ester, syringic acid, t-3 hydroxycinnamic acid and 4-hydroxy benzoic acid were also determined for all the extraction time periods studied. On the other hand, in view of percent amount the highest percentage was for ellagic acid (8.32-19.45%), followed gallic acid (6.86-11.75%), and (-) gallocatechin (2.33-7.99%) for all the extraction times, consecutively.

Although the extraction yields did not considerably differ by varying extraction times, the concentration (mg/kg) and percent amount values were affected by extraction time for all the compounds studied. In the meantime, major component values also varied with concentration (mg/kg) and percent amount in all the extraction time studied here.

As also indicated in Table 3, when the extraction time of the RQC increased from 30 min to 90 min, the main phenolic compounds generally decreased. This phenomenon may be explained by the degradation effect of temperature applied for long time.

However, with the exception of fumaric acid, the concentrations of the other compounds clearly increased with increasing extraction time from 90 min to 120 min, indicating the efficient penetration of water into the plant cell in prolonged time period.

Antimicrobial activity. In antimicrobial activities, six different bacteria and one fungus (yeast) species were used to screen the possible antibacterial

TABLE 4
Antibacterial and antifungal activities of *Quercus coccifera* against the bacteria strains based on disc diffusion assay.

	Inhibition zone for Extracts (mm)[a]		Inhibition zone for antibacterial reference (mm)[a]								Inhibition zone for fungal reference (mm)[a,b]
	Q20[c] µl	Q40[d] µl	AMC		AMP		CN		CIP		FCA
			S	R	S	R	S	R	S	R	
Staphylococcus aureus	ND	11	-	15	-	15	-	12	32	-	-
Staphylococcus epidermidis	ND	12	20	-	-	18	15	-	35	-	-
Escherichia coli	ND	12	-	ND	-	ND	22	-	-	ND	-
Klebsiella pneumonia	ND	8	-	ND	-	ND	21	-	35	-	-
Pseudomonas aeruginosa	ND	ND	-	ND	-	ND	-	ND	-	ND	-
Acinetobacter baumannii	ND	ND	-	ND	-	ND	-	ND	-	ND	-
Candida albicans (yeast)	ND	8	-	-	-	-	-	-	-	-	ND

[a]Antimicrobial results are average of triplicate easurements, [b]AMC: Amoxicillin-clavulanic acid (20/10 µg/disc: AMP: Ampicillin-sulbactam (10/10 µg/disc), CN: Gentamicin (10 µg/disc), CIP: Ciprofloxacin (5 µg/disc), FLU: Fluconazole (25 µg/disc), [c]Q20 µl and [d]Q40 µl: Water extract concentration of *Quercus coccifera,* ND: Not detected activity at this concentration (resistant), S: Sensitivity, R: Resistant.

and antifungal activities of the distilled water extract of the RQC.

Table 4 depicted the antibacterial and antifungal activities of *Q. coccifera* against the bacteria strains by using disc diffusion assay. As can be seen from this table, some of the Gram-positive and Gram-negative bacterial species, and the fungus strains were inhibited by the RQC extract with a concentration of 10,000 ppm in the amount of 20 and 40 µl. The antibacterial activity of the RQC extract with the amount of 20 µl was not detected against *S. aureus, E. coli, S. epidermidis, A. baumannii*, and *P. aeruginosa.* However, the RQC extracts of 40 µl showed strong antibacterial activity against *S. aureus, S. epidermidis* and *E. coli* (see Table 4).

Judaki et al. (2014) have detected that the entity at its highest concentration the aqueous extract of *O. coccifera* had an inhibition zone of 27.2 and 23.7 mm on *S. aureus* and *P. aeruginosa*, consecutively. The MIC and MBC values for tree fruit extract from *Q. coccifera* were 10 and 12.5 µg/ml for *S. aureus* and 10 and 17.5 µg/ml for *P. aeruginosa*, consecutively [13]. The results of this study revealed that there were the strong antimicrobial effects of *Q. coccifera* fruit aqueous extract on *S. aureus* and *P. aeruginosa* [13].

Additionally, it was reported by Gunes et al (2014) that *S. albus, M. luteus and S. aureus* bacteria were inhibited by the fruit extract of *Q. coccifera* resulting in an inhibition zone of 13-15 mm [14].

Yet, the information available on the antimicrobial of wood, leaves and bark are still scarce Nevertheless, no study has been done on the antimicrobial activity of the roots from *Q. coccifera* so far.

DISCUSSION AND CONCLUSIONS

The RQC was extracted by using conventional extraction method and analyzed by employing HPLC. The results indicated that the extraction yields were 22.19%, 22.76%, 23.16% and 22.82% for 30, 60, 90 and 120 min, respectively. Moreover, major component identified in all the extraction time periods were found to be fumaric acid, (-) gallocatechin, ellagic acid and gallic acid for hot water conventional

extraction applied. The highest concentration (22.84 mg/kg) was for fumaric acid, while the lowest concentration (0.02 mg/kg) was for t-3-hydroxy cinnamic acid. On the other hand, major components were gallic acid, ellagic acid and (-) gallocatechin based on the percentage amount of total components in the extract.

Though the extraction yields determined for various time periods were closed to each other, differences in phenolic compounds amongst extraction times were observed. On the other hand, the findings demonstrated that the main phenolic compounds decreased with increasing extraction time due to the degradation effect of temperature exposed for longer time.

Furthermore, the microbial study demonstrated that some of the Gram-positive and Gram-negative bacterial species and the fungus strain were inhibited by RQC with amounts of 20 and 40 µl. Nevertheless, the antimicrobial activities of standard antibiotics, namely, Amoxicillin-clavulanic acid and ampicillin-sulbactam, studied herein were not detected against *S. aureus, S. epidermidis, E. coli, K. pneumonia, P. aeruginosa,* and *A. baumannii.* However, the RQC extracts with the amount of 40 µl gave strong antibacterial activity against *S. aureus, S. epidermidis* and *E. coli*. It was also important to notice that the antimicrobial activities of the 20 µl RQC extract were not found against all the microorganisms studied here.

ACKNOWLEDGEMENTS

We would like to extend our kind thanks to Scientific Research Project Division affiliated to Kahramanmaras Sutcu Imam University, Turkey, for its financial supporting to this study completed under project number of BAP 2011/4-31 YLS.

REFERENCES

[1] Alma, M. H., Karaogul, E., Ertaş, M., Altuntaş, E., Karaman, Ş. and Dıraz, E. (2012). Chemical Composition of Seed Oil From Turkish Prunus Mahaleb L., Analytical Chemistry Letters, ACL 2(3), 182-185.

[2] Takhtajan, A., (1986). Floristic Regions of the World. University of California Press, Berkeley, 522.

[3] Martinez-Ferri, E., Manrique, E., Valladares, F., Balaguer, L., (2004). Winter photoinhibition in the field involves different processes in four co-occurring Mediterranean tree species. Tree Physiol. 24, 981-990.

[4] Hagerman, A. E. and Butler L. G., (1978). Protein precipitation method for the quantitative determination of tannin. J. Agric. Food Chem. 26(4), 809-812

[5] Scalbert, A (1991). Antimicrobial properties of tannins. Phytochemistry 30, 3875-83.

[6] Santos-Buelga, C., Scalbert, A. (2000). Proantocyanidins and tannin-like compounds-nature, occurrence dietary intake and effects on nutrition and health. Journal of the Science of Food and Agriculture, 80, 1094-1117.

[7] Miranda, C. M., Wyk, C. W., Bijl, P., Basson, N. J. (1996). The effect of areca nut on salivary and selected oral microorganisms. International Dental Journal 46, 350-6.

[8] Balasundram, N., Sundram, K., Samman, S., (2006). Phenolic compounds in plants and agri-industrial by-products: antioxidant activity, occurrence, and potential uses. Food Chem. 99, 191–203.

[9] Noferi, M., Masson, E., Merlin, A., Pizzi, A., Deglise, X., (1997). Antioxidant character-istics of hydrolysable and polyflavonoid tannins: an ESR kinetics study. J. Appl. Polym. Sci. 63, 475-482.

[10] Proestos, C., Boziaris, I.S., Nychas, G.-J.E., Komaitis, M., (2006). Analysis of flavonoids and phenolic acids in Greek aromatic plants: investigation of their antioxidant capacity and antimicrobial activity. Food Chem. 95, 664-671.

[11] Ito, N., Hirose, M., Fukushima, S., Tsuda, H., Shirai, T., Tatematsu, M., (1986). Studies on antioxidants: their carcinogenic and modifying effects on chemical carcino-genesis. Food Chem. Toxicol. 24, 1071-1082.

[12] Ito, H., Yamaguchi, K., Kim, T.H., Khennouf, S., Gharzouli, K., Yoshida, T. (2002): Dimeric and Trimeric Hydrolyzable Tannins from Quercus coccifera and Quercus suber, J. Nat. Prod., 65, 339-345,

[13] Judaki A., Panahi J., Havasian M. R., Tajbakhsh P., Roozegar M. A. (2014). Bioinformation, 10 (11): 689-692.

[14] Gunes H., Okyay M., Celebi F. Tul B., (2014). Journal of Applied Biological Sciences, 8(2), 16-21.

[15] Gulcin İ., Tel A. Z., Kirecci E., (2008). Antioxidant, Antimicrobial, Antifungal, and Antiradical Activities of Cyclotrichium Niveum (BOISS.) Manden and Scheng, International Journal of Food Properties, 11: 450–471

[16] CLSI. (2012). Clinical Laboratory Standards Institute. Performance standards for antimicrobial susceptibility testing, Wayne (PA): The Institute, M100–S22.

Received: **15.08.2015**
Accepted: **18.12.2015**

CORRESPONDING AUTHOR

Eyyup Karaogul
Kahramanmaras Sutcu Imam University
Faculty of Forest
Department of Forest Industry Engineering
Onikisubat/Kahramanmaras 46100 TURKEY

e-mail : e.karaogul@ksu.edu.tr
: e.karaogul@hotmail.com

© by PSP Volume 25 – No. 7/2016, pages 2364-2373 Fresenius Environmental Bulletin

ANALYSIS OF SPIROMESIFEN AND SPIROMESIFEN-ENOL IN CABBAGE AND TOMATO BY LIQUID CHROMATOGRAPHY MASS SPECTROMETRY (LC-MS/MS)

Lekha Siddamallaiah.[1, 2], Soudamini Mohapatra [1*], Gourishankar Manikrao [1], Radhika Buddidathi.[1] and Debi Sharma[1]

[1]Pesticide Residue Laboratory, Indian Institute of Horticultural Research, Bangalore, India
[2]Center For Post Graduate Studies, Jain University, #18/3, 9th Main, 3rd Block, Jayanagar, Bangalore 560011

ABSTRACT

Spiromesifen is a novel insecticidal/acaricidal compound derived from spirocyclic tetronic acids which gives prolonged control of insect pests of cabbage and tomato. Spiromesifen exhibits low acute toxicity, but short-term and long-term exposure can cause adverse effect on human and animal health. The QuEChERS method in conjunction with LC-MS/MS was validated for analysis of spiromesifen and its metabolite, spiromesifen-enol in cabbage and tomato. The mass spectrometer was operated in the positive multiple reaction monitoring (MRM) mode for spiromesifen and negative MRM mode for spiromesifen-enol. The recoveries were in the range of 72.16-105.27% with relative standard deviation (RSD) <20% and measurement uncertainty (MU) within 4.8-10.7%. The limit of detection (LOD), limit of quantification (LOQ) for both analytes was 0.0015 µg mL^{-1} and 0.005 mg $kg^{-1,}$ respectively. The method was linear in the range of 0.005-0.1 mg kg^{-1}. The method developed is a suitable tool to analyze spiromesifen (sum of spiromesifen and spiromesifen-enol, expressed as spiromesifen) below the EU MRL of 0.02 mg kg^{-1} in cabbage and 1.0 mg kg^{-1} in tomato. The method was used to analyze both compounds in real samples of cabbage and tomato.

KEYWORDS:
Liquid chromatography-mass spectrometry (LC-MS/MS), Method validation, QuEChERS, Spiromesifen, Spiromesifen-enol

INTRODUCTION

Spiromesifen {3-mesityl-2-oxo-1-oxaspiro [4.4] non-3-en-4-yl 3, 3-dimethylbutyrate} is a miticide/insecticide that belongs to the class spirocyclic phenyl substituted tetronic acid. It is an excellent and innovative compound for controlling whiteflies (*Bemisia and Trialeuroides spp.*) and mites (*Tetrancychus and Panonychus spp.*). When used according to the recommendation it provides outstanding control of whiteflies and mites resistant to other insecticides and miticides [1]. Spiromesifen is a lipid biosynthesis inhibitor, acts by inhibiting lipid metabolism enzyme acetyl Co-A carboxylase and cause significant decrease in the fat lipids. It has no cross resistance to the more commonly used neonicotinoids [2]. The major metabolite of spiromesifen is spiromesifen-enol, which is formed by hydrolysis of the parent compound. The residue definition for enforcement purposes is the sum of spiromesifen and spiromesifen-enol, expressed as spiromesifen [3].

Cabbage and tomato are the two important vegetable crops consumed throughout the world. The annual world production of cabbage was 68 million metric tons for the year 2011 (Food and Agricultural Organization of the United Nations). Cabbage is a good source of vitamin C, fiber and beta-carotene, and also acts as an anti-carcinogenic agent [4]. It is most commonly affected by aphids [5]. Tomato is consumed in many ways, fresh as well as processed. It contains carotene and lycopene, the most beneficial natural antioxidants. It is reported to prevent prostate cancer, decreased risk of breast cancer, head and neck cancer [6]. The most common tomato pests are psyllid and whiteflies. Spiromesifen could give effective control of aphids and psyllid of cabbage and whiteflies of tomato [7-10].

The available information on the residue analysis of spiromesifen in various substrates involved multiple steps and using large volume of organic solvents. The analysis was carried out using gas chromatograph-mass spectrometer (GC-MS) where only the parent compound was detected [11-13]. Since the major metabolite spiromesifen-enol, is included in the residue definition of spiromesifen, it is essential to analyze both the compounds at a level which is the legal limit or maximum residue limit (MRL). In our laboratory we have analyzed spiromesifen-enol by HPLC and GC-MS, where the parent compound could be detected at 0.01 µg mL^{-1}, but the metabolite could not be detected even at 1µg mL^{-1}. QuEChERS is a widely accepted method for the analysis of pesticide residues in various

matrices. It requires low volume of solvent compared to other methods [14]. It is a very flexible

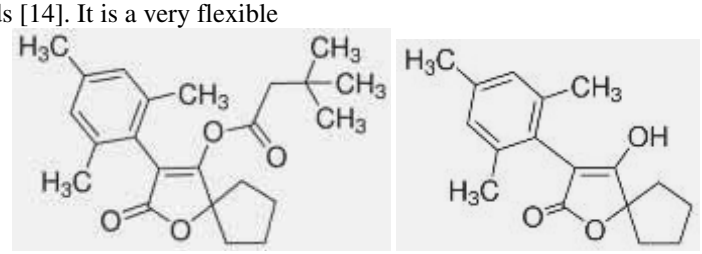

FIGURE 1
Chemical structure of (a) spiromesifen, (b) spiromesifen-enol.

method that can be modified depending on the analyte, matrix and analytical instrument [15]. The above study has been carried out to validate the analytical method (QuEChERS) for analysis of spiromesifen and spiromesifen-enol in cabbage and tomato by LC-MS/MS at below their MRLs. The validation was carried by studying the various method validation parameters to provide evidence that the method is fit for the intended use [16].

MATERIALS AND METHODS

Chemicals and reagents. Spiromesifen (99% purity) and spiromesifen-enol (99.5% purity) were procured from Sigma Aldrich, India (Figure 1). LC-MS/MS grade acetonitrile, acetic acid, methanol, ammonium formate and formic acid were procured from Sigma Aldrich, India. Magnesium sulphate, sodium sulphate and sodium acetate used were of analytical grade and procured from Rankem Fine Chemicals Limited, India. Magnesium sulphate was activated in a muffle furnace at 500º C for 5 hours and kept in desiccator before use. Primary secondary amine (PSA) of particle size 40 µm was procured from Agilent technologies, India. PTFE membrane filter of pore size 0.2 µm was procured from Phenomenex, India. The deionized water for the mobile phase was obtained from a Millipore water purification system (ELIX, Merck Millipore, India Pvt. Ltd) and filtered using Millipore GV filter paper of pore size 0.22 µm.

Preparation of standard solutions. Stock solutions of spiromesifen and spiromesifen-enol were prepared by dissolving 10 mg of spiromesifen and spiromesifen-enol in 10 mL LC-MS/MS grade acetonitrile. Working standards were prepared by further dilutions of the stock solution. Calibration standards were prepared in pure solvent as well as with matrix blank of cabbage and tomato at the concentration levels of 0.0015, 0.0025, 0.005, 0.01, 0.025, 0.05, 0.1µg mL^{-1}. Matrix match standards are prepared by concentrating 1 mL of the blank samples of cabbage and tomato using low volume concentrator (Turbo vap® LV concentrator, caliper life sciences, USA) and adding the required aliquot of the standard. The stock and working standards are stored at -20ºC.

Sample preparation and spiking. Cabbage and tomato were grown at the Experimental farm of Indian Institute of Horticultural Research (IIHR), Bangalore, India, without application of pesticides. About 2 kg of the sample was collected and cut into small pieces. The samples were homogenized thoroughly in a high volume robot coupe homogenizer (Blixer ® 6 V.V, France). A subsample of (200 g) was taken and further homogenized with a silent crusher M (Heidolph Instruments, Germany). The homogenized samples (15 g) were weighed in 50 mL polypropylene centrifuge tubes. The samples were spiked with spiromesifen and spiromesifen-enol at 0.0025, 0.005, 0.01, 0.025, 0.05 and 0.1 mg kg^{-1}. The extraction and purification of the spiked cabbage and tomato samples was carried out by the QuEChERS method [14]. The spiked samples (15 g) were treated with 15 mL of 1% acetic acid in acetonitrile (LC-MS/MS grade) and shaken for 1 min. Anhydrous magnesium sulfate (6 g) and sodium acetate (1.5 g) were added to the tubes and shaken for 2 min. The tubes were centrifuged at 4100 rpm for 10 min using a Restek centrifuge (Q-Sep 3000, Bellefonte, PA 16823, USA). The upper acetonitrile extract (3 mL) was transferred to a 15 mL centrifuge tube to which 150 mg primary secondary amine (PSA) sorbent and 450 mg anhydrous magnesium sulfate were added. The tubes were shaken for 1 min and centrifuged again. The supernatant acetonitrile phase was filtered through PTFE membrane filter (0.2 µm pore size) and analyzed by LC-MS/MS. The real samples collected from markets around Bangalore city (India) were prepared and analyzed in the same manner as described above for the spiked samples.

LC-MS/MS analysis. Analysis of cabbage and tomato was performed using LC-MS/MS system containing 1290 infinity LC (Agilent technologies, Palo Alto, CA, USA) coupled with 6460 triple Quad mass spectrometer. The separation of the anlaytes was performed using a Zorbax Eclipse Plus C18 column (2 X 100 mm id, 1.8 µm

particle size). The column was maintained at a constant temperature of 40º C±0.8º C. The mobile phase was composed of (A) water with 0.1% ammonium formate (5 mM) and 0.01% formic acid, v v^{-1} and (B) methanol with 0.1% ammonium formate (5 mM) and 0.01% formic acid, v v^{-1}. A flow rate of 0.4 mL min^{-1} was maintained. A gradient programme started with 85% A and 15% B phase (0-1 min). A linear gradient was then established in order to reach a 50% A and 50% B composition at 6 min, 5% A and 95% B at 12 min; return to the initial conditions at 18 min. The samples were transferred to 1.5 mL vials and 2 µL was injected using an auto-sampler. For determination of spiromesifen residues the electrospray ionization (ESI) probe was operated in the positive mode and for spiromesifen-enol residues in the negative mode by multiple reactions monitoring (MRM). The instrument parameters were optimised and two most abundant MS/MS (precursor–product) ion transitions were monitored; one for quantification and another for confirmation (quantifier and qualifier). For confirmation, the ion ratio calculated as percent ratio of peak areas of the qualifier and quantifier MRMs for spiromesifen (21.3%) and spiromesifen-enol (12.3 and 15.6%) were used (Table 1). An additional ion transition was monitored for confirmation of spiromesifen-enol.

TABLE 1
Mass spectrometry parameters in the multiple reaction monitoring (MRM) for the determination of spiromesifen and spiromesifen-enol.

Compound	Retention time (min)	Precursor ion	Product ion	Dwell time (Sec)	Fragmentor	Collision Energy (CE)	Cell Accelerator voltage	Polarity	Ion ratio %
Spiromesifen	13.3	371	272.9	6	55	3	7	Positive	
Spiromesifen-enol		371	255.0	6	55	20	7	Positive	21.3
		271	209.0	6	150	16	7	Negative	
	7.1	271	206.7	6	150	20	7	Negative	12.3
		271	158.7	6	150	31	7	Negative	15.6

Validation of the analytical method. The analytical method used for the analysis of spiromesifen and spiromesifen-enol in cabbage and tomato was validated by taking into consideration the various method validation parameters such as: accuracy, precision, limit of detection (LOD), limit of quantification (LOQ), linearity, range, selectivity and measurement uncertainty.

Accuracy and precision. Accuracy is the closeness of agreement between the value, which is accepted as a conventional, true value or as an accepted reference value. Precision is the measure of degree of repeatability of an analytical method under normal operating conditions and expressed as the percent relative standard deviation (RSD). The two most common precision measures are repeatability and reproducibility. The accuracy and precision of the analytical method was studied by spiking the cabbage and tomato samples at six concentration levels such as, 0.0025, 0.005, 0.01, 0.025, 0.05 and 0.1 mg kg^{-1} and each spiking was carried out with six replicates. The intraday and inter-day precision was determined by analyzing six spiked samples in a single day and over 6 six days.

Limit of detection (LOD) and Limit of quantification (LOQ). The LOD of the method was determined by LC-MS/MS analysis of spiromesifen and spiromesifen-enol at seven levels in the concentration range of 0.0015-0.1 µg mL^{-1}. The lowest concentration at which the analytes could be detected corresponding to a signal: noise ratio of 3:1 was considered the LOD. The LOQ was determined as the lowest concentration of the analyte in a sample that could be reliably determined in a complex matrix at a signal: noise ratio of 10:1.

Linearity and range. Linearity is the ability of the method to elicit the test results that are directly proportional to analyte concentration within a given range. Range is the interval between lower and upper levels of analyte that have demonstrated to be determined with the stated precision and accuracy. The range of the analytical method was determined by analyzing spiromesifen and spiromesifen-enol at six different levels in the concentration range of 0.0025-0.1 µg mL^{-1}. Calibration curve was drawn by analyzing matrix matched standards at seven different concentrations in the range of 0.0015-0.1 µg mL^{-1} and it was used for quantification of spiromesifen and spiromesifen-enol residues in cabbage and tomato (Figure 2).

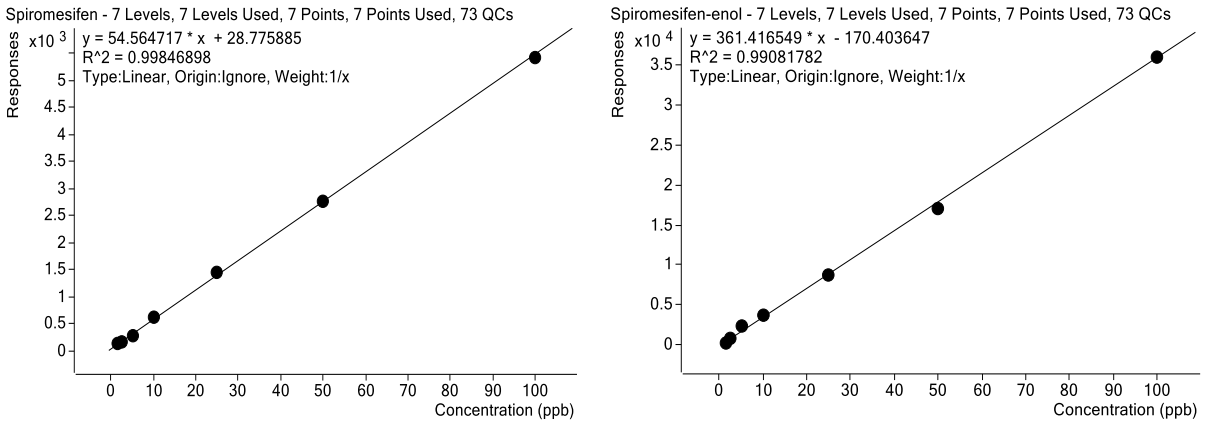

FIGURE 2
Calibration curve of (a) spiromesifen, (b) spiromesifen-enol.

Selectivity. Selectivity is the measure, which assess the reliability of measurement to identify a compound in a complex matrix without interference from other components in the matrix. To study the selectivity of the method, blank and spiked samples were analyzed in a low to high concentration ranges in all the matrices.

Measurement uncertainty. Measurement uncertainty is the quantitative parameter that describes the range of the experimental results within which the true values can be expected to lie. The factors that are contributing towards the uncertainty of the sample are listed as type-A and type-B uncertainties. Type-A uncertainty was evaluated by determining the relative standard deviation of repeated observations i.e., recovery. The type B uncertainties was contributed by sample volume measure, temperature, purity of reference standard, mass of reference standard, volume of standard solution prepared, dilution of stock solution, mass of sample etc. Relative uncertainty of each component was calculated. All individual uncertainties were computed and the combined uncertainty was estimated using the formula given below. The expanded uncertainty was determined at a confidence level of 95% by using the coverage factor K=2.

Where R U_{comb} is the relative combined uncertainty

R U_{rec} is the relative uncertainty from repeated observations (recovery)

$RU_{vol\ sample\ and\ temp}$ is the relative uncertainty from sample volume and temperature

R $U_{conc\ of\ ref\ std}$ is the relative uncertainty from concentration of reference standard

R $U_{vol\ of\ ref\ std}$ is the relative uncertainty from volume of reference standard

R $U_{m\ of\ ref\ std}$ is relative uncertainty from mass of reference standard

R $U_{m\ of\ sample}$ is the relative uncertainty from mass of sample

RESULTS

Accuracy and precision. The accuracy of the analytical method was evaluated by spiking blank cabbage and tomato samples with spiromesifen and spiromesifen-enol at six different concentration levels in the range of 0.0025-0.1 mg kg^{-1}. Each concentration was analyzed in six replicates. The recoveries of the spiromesifen and spiromesifen-enol in cabbage and tomato are presented in the Table 2. The recoveries at the spiking range of 0.005-0.1 mg kg^{-1} were found to be in the acceptable range of 70-120%, whereas at 0.0025 mg kg^{-1} it was <70% [16]. Spiromesifen recoveries of cabbage was in the range of 77- 90.23% and spiromesifen-enol, 72.16-87%. The recoveries of tomato were in the range of 96-105.27% for spiromesifen and 74.50-85.45% for spiromesifen-enol. Precision of the analytical method was determined by calculating the repeatability of the spiked sample analysis (intraday and inter-day) at five levels (with six replicates each) and it was expressed as RSD%. The intraday RSD% of spiromesifen and spiromesifen-enol analysis in

$$\text{R Ucomb} = \sqrt{\left(\text{R Urec}\right)^2 + \left(\text{R Uvol sample and temp}\right)^2 + \left(\text{R Uconc ref std}\right)^2 + \left(\text{R Uvol ref std}\right)^2 + \left(\text{R Um ref std}\right)^2 + (\text{R Um sample})^2}$$

cabbage and tomato are given in the Table 2. The RSD values of spiromesifen in cabbage were in the range of 5.8-8.7% and spiromesifen-enol, 5.3-8.6%. The RSD values of spiromesifen in tomato were 3.6-8.7% and spiromesifen-enol, 5.7-9%. The inter-day precision (obtained by analyzing six replicates over six days) values were always <20%. The precision of the analytical method (RSD%) were within the acceptable range of ≤20% [16].

Limit of detection (LOD) & Limit of quantification (LOQ). The LOD of the method was determined by injecting the spiromesifen and spiromesifen-enol standards from lower to higher concentration of 0.0015-0.1µg mL^{-1}. The LOD of the spiromesifen and spiromesifen-enol was 0.0015 µg mL^{-1}, the concentration at which the peak could be identified at a signal to noise ratio of 3: 1. The LOQ of the method was 0.005 mg $kg^{-1,}$ which is the lowest spiking level at which satisfactory recovery could be obtained at the signal: noise ratio of >10. The LOQ of both compounds were below the EU regulatory requirement for cabbage (0.02 mg kg^{-1}) and tomato (1 mg kg^{-1}). As spiromesifen-enol is included in the residue definition of spiromesifen it is necessary to analyze this metabolite at a sufficiently low level. The earlier study carried out on analysis of spiromesifen in tomato, the reported LOQ was 0.05 mg kg^{-1}, whereas for apple, chilli and eggplant it was 0.01 mg kg^{-1} [11-13, 17]. In all these studies the residue level of only spiromesifen was reported. In the current study analysis of spiromesifen and spiromesifen-enol could be carried out in cabbage and tomato at below the MRL levels.

Linearity. The linearity of the method was evaluated by analyzing spiromesifen and spiromesifen-enol at seven concentrations in the range 0.0015 - 0.1µg mL^{-1}. A seven point calibration curve was drawn analyzing matrix match standards of cabbage and tomato. The calibration curve was linear in the range of 0.0015 - 0.1 µg mL^{-1} with the correlation coefficient always >0.99 for both analytes.

Selectivity. The selectivity of the method is the ability to determine the analytes in the presence of other matrix components. Identification of the spiromesifen and spiromesifen-enol was carried out by comparing the retention time and ion ratio. The precursor and product ion for spiromesifen, spiromesifen-enol and the ion ratio are presented in Table 1. The total ion chromatogram (TIC) of blank; matrix matched and spiked sample of cabbage and tomato with spiromesifen and spiromesifen-enol are presented in Figures 3 and 4. The extracted ion chromatogram of spiromesifen and spiromesifen-enol is presented in Figure 5.

TABLE 2
Recovery (%) and RSD (%) of spiromesifen and spiromesifen-enol from cabbage and tomato at different spiked levels.

Spiked level (mg kg^{-1})	Cabbage				Tomato			
	Spiromesifen		Spiromesifen-enol		Spiromesifen		Spiromesifen-enol	
	Recovery± SD[a]	RSD %	Recovery± SD[a]	RSD %	Recovery± SD[a]	RSD %	Recovery± SD[a]	RSD %
0.005	77.00±6.7	8.7	72.16 ± 6.2	8.6	96.00 ± 8.4	8.7	74.50 ± 6.7	9.0
0.010	80.30±6.2	7.7	76.64 ± 6.0	7.9	100. 90 ± 7.8	7.7	78.30 ± 6.3	8.1
0.025	83.57±5.5	6.6	79.74 ± 5.8	7.2	102.24 ± 5.7	5.6	82.60 ± 5.3	6.4
0.050	84.78±5.4	6.4	83.28 ± 5.5	6.6	104.16 ± 4.6	4.4	83.60 ± 5.2	6.2
0.100	90.23±5.2	5.8	87.08 ± 4.6	5.3	105.27 ± 3.7	3.6	85.45 ± 4.8	5.7

[a]Average of 6 replicate analyses ± SD

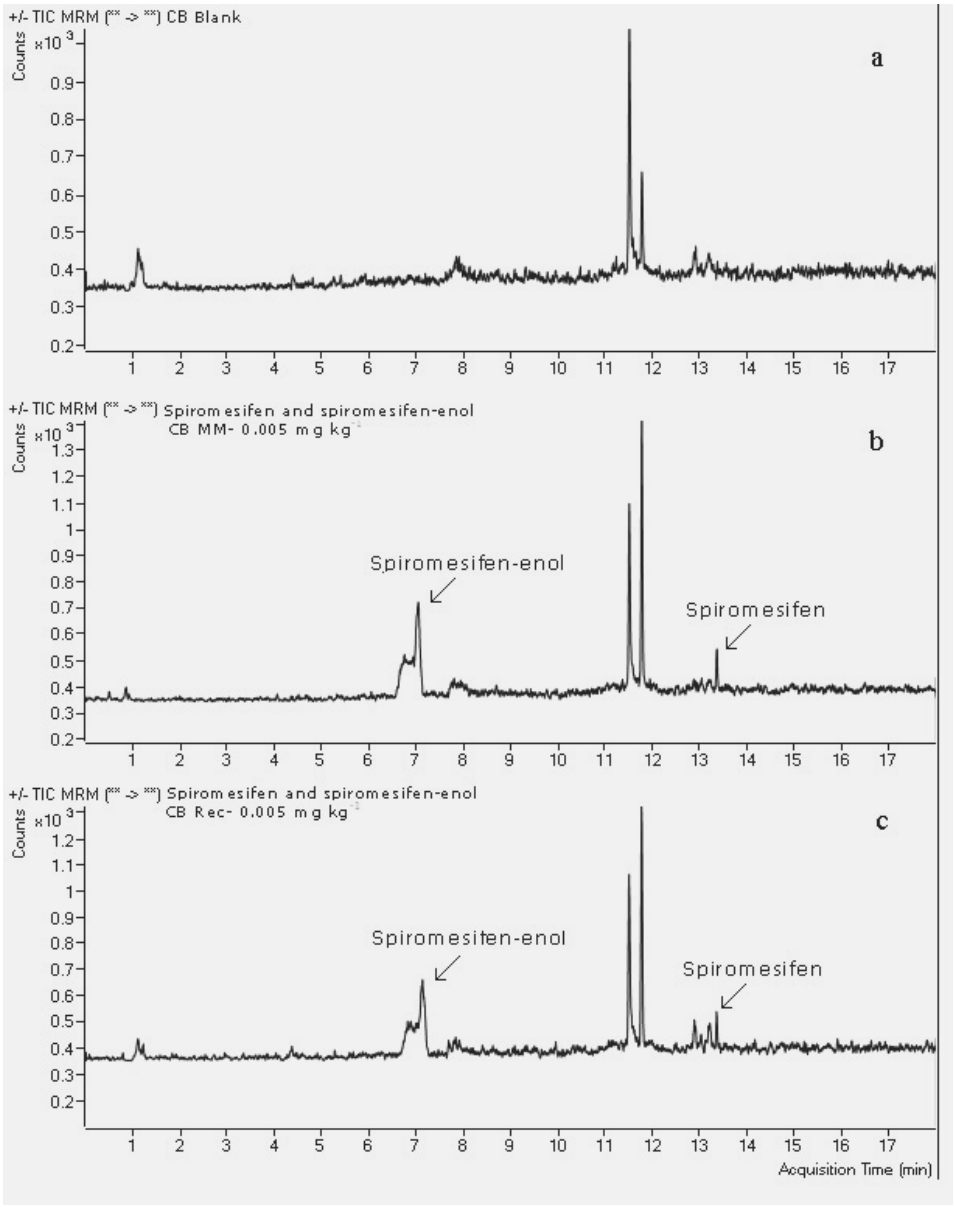

FIGURE 3
TIC of (a) blank cabbage, (b) cabbage matrix matched standard of spiromesifen and spiromesifen-enol at 0.005 mg kg^{-1}, (c) cabbage sample spiked with spiromesifen and spiromesifen-enol at 0.005 mg kg^{-1}.

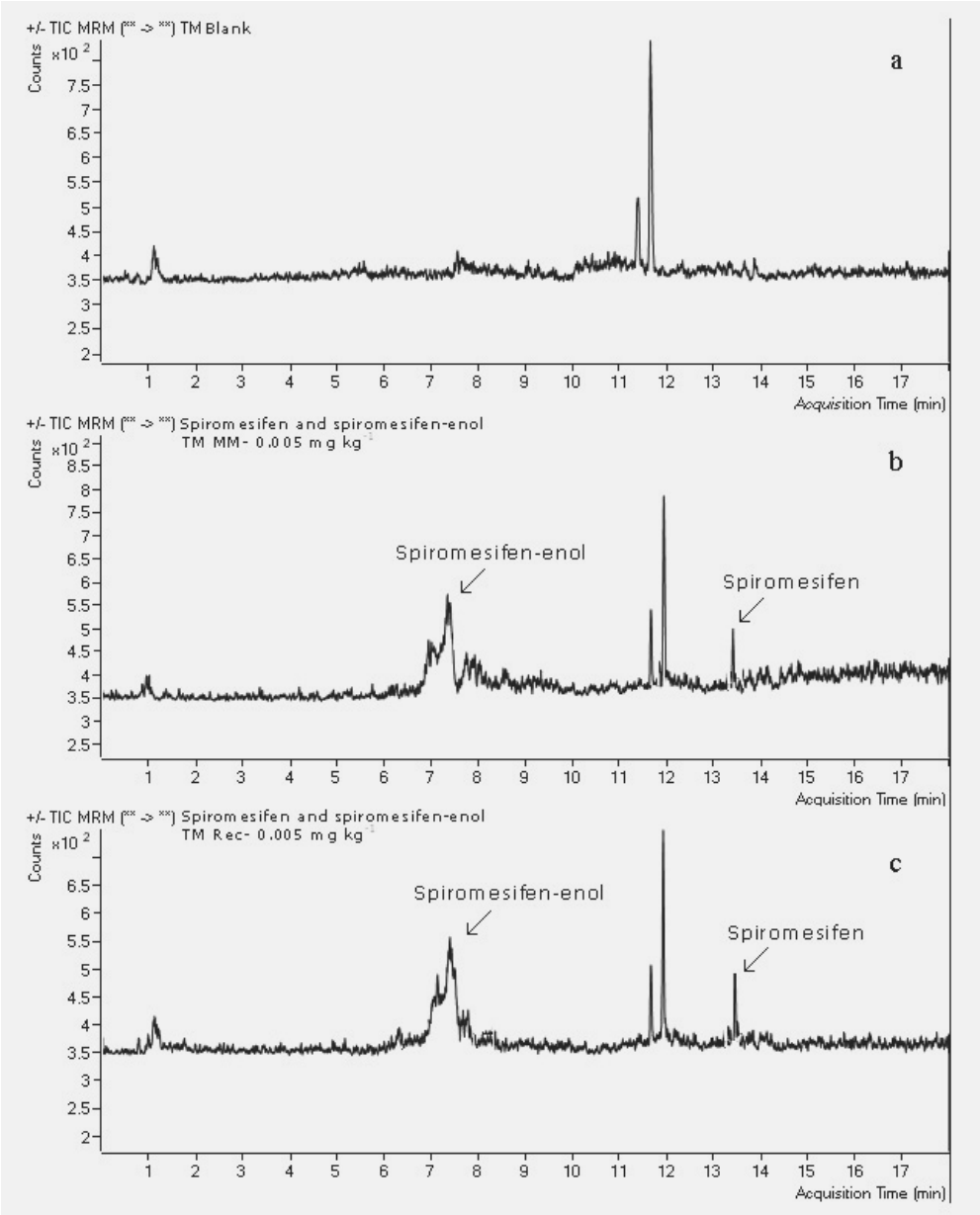

FIGURE 4
TIC of (a) blank tomato, (b) tomato matrix matched standard of spiromesifen and spiromesifen-enol at 0.005 mg kg^{-1}, (c) tomato sample spiked with spiromesifen and spiromesifen-enol at 0.005 mg kg^{-1}.

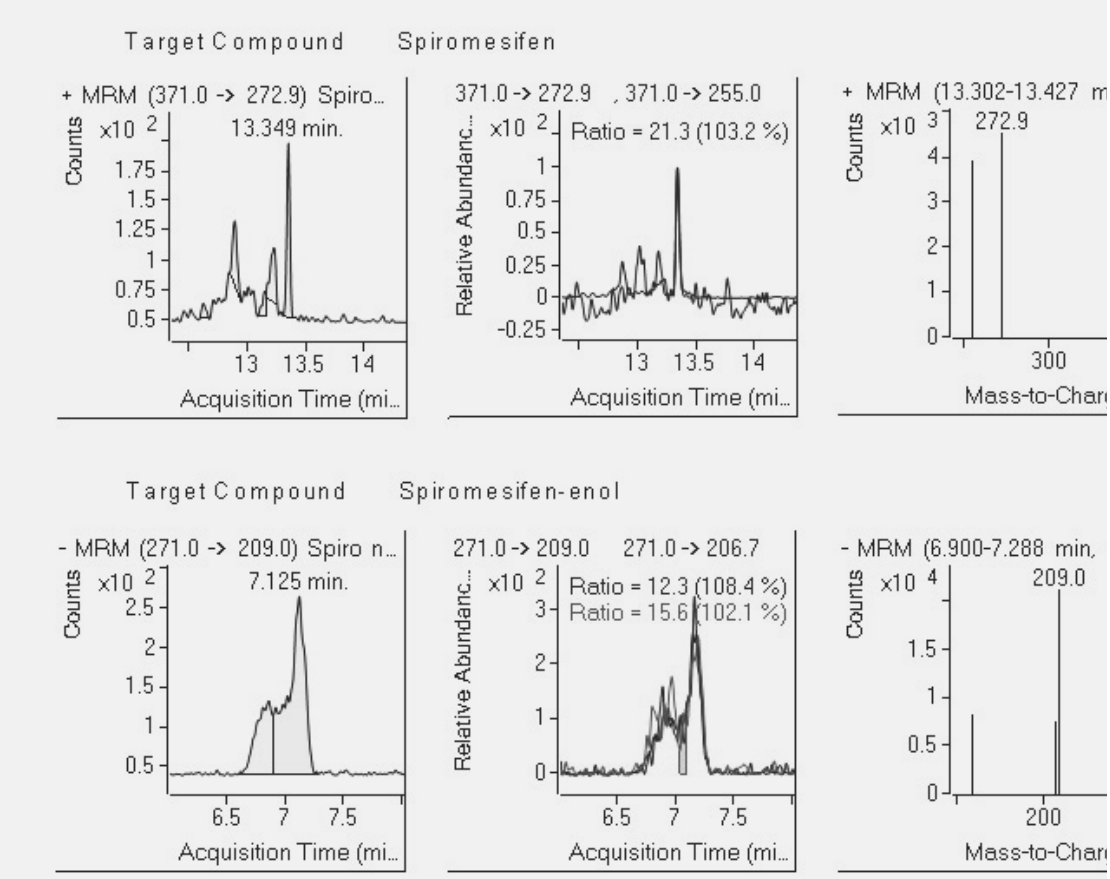

FIGURE 5
Extracted ion chromatograms of (a) spiromesifen MRM transitions (ESI positive ion mode), (b) spiromesifen-enol MRM transitions (ESI negative ion mode).

$$\text{ME (\%)} = \frac{\text{Peak area of matrix standard} - \text{Peak area of solvent standard}}{\text{Peak area of solvent standard}} \times 100$$

Matrix effect. The sample matrix can have a considerable effect on the analysis of pesticides and the quality of the results obtained**.** Matrix effect is caused by other components of the sample except the specific compound to be quantified [18]. The response of the analytes is affected by the co-extractives that are present in the sample matrix [19]. To compensate matrix effect on the quantification of the analytes, matrix matched standards were used for computing the recovery percent. The matrix effect could be determined by analyzing solvent and matrix match standards of spiromesifen and spiromesifen-enol by LC-MS/MS. The percent matrix effect expressed as ME% was calculated by using the equation above.

Matrix effect led to signal suppression of spiromesifen in cabbage (upto 37%) and tomato (upto 54%). For spiromesifen-enol matrix effect led to signal enhancement of nearly 18% in cabbage, whereas in tomato signal suppression was observed upto 41%.

Measurement uncertainty. The combined uncertainties were computed by combining type A and type B uncertainty values. The coverage factor K=2 was used to obtain the uncertainties at 95% confidence level. The uncertainty values associated with analysis of spiromesifen and spiromesifen-enol in cabbage and tomato are presented in the Table 3. The uncertainties of spiromesifen analysis in cabbage were in the range of 7.2-10.4% and spiromesifen-enol, 6.7-10.2%. The uncertainties of spiromesifen in tomato were in the range of 4.8-10.3% and spiromesifen-enol, 7.0-10.7%. The uncertainties obtained were high at the low spiking concentration level and decreased when the spiking concentration increased.

TABLE 3
Uncertainty of measurement in the analysis.

Spiked level (mg kg^{-1})	Uncertainty (%)			
	Cabbage		Tomato	
	Spiromesifen	Spiromesifen- enol	Spiromesifen	Spiromesifen-enol
0.005	10.4	10.2	10.3	10.7
0.010	9.3	9.5	9.3	9.7
0.025	8.0	8.7	6.9	7.9
0.050	7.8	8.0	5.6	7.6
0.100	7.2	6.7	4.8	7.0

Method application. The method validated for analysis of spiromesifen and spiromesifen-enol in cabbage and tomato was used for the analysis of these two compounds in the real samples. Cabbage and tomato samples (20 each) were collected from the retail markets of Bangalore city. The residues of spiromesifen and spiromesifen-enol were not detected in any of the samples.

DISCUSSION AND CONCLUSIONS

A method for the simultaneous quantification and confirmation of spiromesifen and spiromesifen-enol using LC-MS/MS with electrospray ionization was developed and validated. The analytical method gave satisfactory results for both compounds in cabbage and tomato and found to be fit for the purpose. The LOD and LOQ of the analytical method for the analysis of spiromesifen and spiromesifen-enol were 0.0015 µg mL^{-1} and 0.005 mg kg^{-1}. Linearity was good with the relative coefficients >0.99 for both analytes. The average recoveries of spiromesifen and spiromesifen-enol in cabbage and tomato were found to be well within the prescribed analytical limits [16]. The suitability of the method developed and validated with the complete instrumental analysis was applied for the routine analysis of cabbage and tomato samples. The combination of the QuEChERS method and LC-MS/MS provided efficient sample preparation and analysis of the samples by two ion transitions that allowed the quantification and confirmation of the analytes simultaneously, thereby enabling the rapid monitoring of the real samples.

ACKNOWLEDGEMENTS

The authors thank Director, IIHR, Bangalore, India and Coordinator, AINPPR, New Delhi for providing facilities to carry out this study.

REFERENCES

[1] Ilias, A., Roditakis, E., Gripou, M., Nauen, R., Vontas, J., Tsagkarakou, A. (2012). Efficacy of ketoenols on insecticide resistant field populations of two spotted spider mite Tetranchymus urticae and sweet potato whitefly Bemisia tabaci from Greece. Crop Protection, 42, 305-311.

[2] Prabhaker, N., Toscano, N.C. (2008). Spiromesifen: A new pest management tool for whitefly management: Fourth International Bemisia Workshop International whitefly Genomics Workshop, ed. by Stansly PA and Mckenzie CL. Journal of Insect Science, USA, 8, 39-40.

[3] Anonymous. (2012). Reasoned opinion on the modification of the existing MRL for spiromesifen in tea. EFSA Journal, 10, pp 3050.

[4] Gullet, N.P., Ruhul Amin, A.R., Bayraktar, S., Pezzuto, J.M., Shin, D.M., Khuri, F.R., Aggarwal, B.B., Surh, Y.J., Kucuk, O. (2010). "Cancer prevention with natural compounds". Seminars in Oncology, 37, 258-281.

[5] Kumari, B. (2008). Effects of household processing on reduction of pesticide residues in vegetables. ARPN Journal of Agricultural and Biological Sciences, 3, 46-51.

[6] Freedman, N.D., Park, Y., Subar, A.F., Hollenbeck, A.R., Leitzmann, M.F., Schatzkin, A., Abnet, C.C. (2008). Fruit and vegetable intake and head and neck cancer risk in a larger United states prospective cohort study. International Journal of Cancer, 122, 2330-2336.

[7] Nauen, R., Reckmann, U., Thomzik, J., Thielert, W. (2008). Biological profile of spirotetramat (Movento®)- a new two-way systemic (ambimobile) insecticide against sucking pest species. Bayer Crop Science Journal, 61, 245-277.

[8] Page-Weir, N.E.M., Jamieson, L.E., Chhagan, A., Connolly, P.G., Curtis, C. (2011). Efficacy of insecticides against the tomato/potato psyllid (Bactericera cockerelli). New Zealand Plant Protection, 64, 276-281.
[9] Modesto, J.C., Fenille, R.C. (2004). Chemical control of whitefly (Bemisia argentifolii Hemiptera: Aleyrodidade) on the chrysanthemum (Dendranthema morifolium). Arquivos do Instituto Biologico (Sao Paulo), 71, 499-502.
[10] Modesto, J.C., Fenille, R.C. (2005). Effect of chemical control of whitefly (Bemisia tabaci biotipo B) on the poinsettia (Euphorbia pulcherrima). Cultura Agronomica, 14, 41-49.
[11] Sharma, K.K., Dubey, J.K., Kumar, A., Gupta, P., Kalpana., Singh, B., Sharma, I.D., Nath, A. (2005). Persistence and safety evaluation of spiromesifen on apple (Malus domestica L) in India. Pesticide Research Journal, 17, 77-81.
[12] Sharma, K.K., Rao, C.S., Dubey, J.K., Patyal, S.K., Parihar, N.S., Battu, R.S., Sharma, V., Gupta, P., Kumar, A., Kalpana., Jaya, M., Singh, B., Sharma, I.D., Nath, A., Gour, T.B. (2007). Persistence and dissipation kinetics of spiromesifen in chilli and cotton. Environmental Monitoring Assessment, 132, 25-31.
[13] Sharma, K.K., Mukherjee, I., Singh, B., Mandal, K., Sahoo, S.K., Banerjee, H., Banerjee, T., Roy, S., Shah, P.G., Patel, H.K., Patel, A.R., Beevi, N., George, T., Mathew, T.B., Singh, G., Noniwal, R., Devi sunita. (2014). Persistence and risk assessment of spiromesifen on tomato in India: a multilocational study. Environmental Monitoring Assessment, 186, 8453-8461.
[14] Anastassiades, M., Lehotay, S.J., Stajnbaher, D., Schenck, F.J. (2003). Fast easy multiresidue method employing acetonitrile/partioning and "Dispersive Solid-Phase Extraction" for determination of pesticide residues in produce. Journal of AOAC International, 86, 412-431.
[15] Lehotay, S.J., Koesukwiwat, U., van der Kamp, H., Mol, H.G.J., Leepipatpiboon, N. (2011). Qualitative aspects in the analysis of pesticide residues in fruits and vegetables using fast, low-pressure gas chromatography – time-of-flight mass spectrometry. Journal of Agricultural Food Chemistry, 59, 7544-7556.
[16] SANCO (2013). Guidance document on analytical quality control and validation procedures for pesticide residues analysis in food and feed. 1-46. Available from ec.europa.eu/food/plant/pesticides/documents/docs/qualcontrol_en.pdf (accessed on 18 December 2014)
[17] Sharma, K.K., Dubey, J.K., Mukherjee, I., Parihar, N.S., Battu, R.S., Singh, B., Kumar, A., Gupta, P., Kalpana, B., Singh, B., Sharma, I.D., Nath, A. (2006). Residual behavior and risk assessment of spiromesifen (Oberon 240 SC) on eggplant (Solanum melonongena L) in India: a multilocational study. Bulletin of Environmental Contamination and Toxicology, 76, 760-765.
[18] Smeraglia, J., Baldrey, S.F., Watson, D. (2002). Matrix effect and selectivity issues in LC-MS-MS. Chromatographia Supplement, 55, 95-99.
[19] Santilio, A., Girolimetti, S., Barbini, D.A. (2014). Estimation of the validation parameters for a fast analysis of herbicide residues by LC-MS/MS. Food Additives and Contaminants, 31, 845-851.

Received: **08.09.2015**
Accepted: **27.12.2015**

CORRESPONDING AUTHOR

Soudamini Mohapatra
Pesticide Residue Laboratory,
Indian Institute of Horticultural Research, Bangalore, India.

e-mail: soudamini_mohapatra@rediffmail.com

© by PSP Volume 25 – No. 7/2016, pages 2374-2382 Fresenius Environmental Bulletin

EVALUATION OF GENETIC DIVERSITY AMONG *MELIA AZEDARACH* L. (MELIACEAE) WITH RAPD MARKERS

Nadir Ali Rind[1*, 2], Ozlem Aksoy[2], Muhammad Umar Dahot[1], Salih Dikilitas[2], Muhammad Rafiq[1], Burcak Tütünoglu[2]

[1]Institute of Biotechnology and Genetic Engineering, University of Sindh, Jamshoro, Pakistan
[2]Department of Biology, Faculty of Science and Literature, University of Kocaeli, Turkey

ABSTRACT

Melia azedarach L. (Chinaberry) is fleshy fruited small to medium sized tree native to China and North Western India. It grows in Pakistan and Turkey in various areas facing great environmental changes to maintain its survival. The species is valued for its high quality wood, medicinal, ornamental and shade purposes. The present work was aimed to estimate the genetic variation among the populations of *Melia azedarach* that were collected from five different locations in Turkey and three different locations in Pakistan. 14 RAPD primers producing polymorphic and monomorphic bands were analyzed. Genetic distances were calculated for all the species studied by RAPD-PCR. The lowest genetic similarity and the highest genetic polymorphic values were determined. It was observed that there is a clear split among populations from different areas in Turkey and Pakistan. These differences may be due to eco-geographical association with genetic variation and should be conserved to retain the genetic diversity of the species. Appropriate conservation strategies were suggested in conclusion.

KEYWORDS:
Melia azedarach L., genetic diversity, conservation, RAPD-PCR, medicinal plant, environmental effect.

INTRODUCTION

M. azedarach, belongs to *Meliaceae* family commonly known as chinaberry, locally called tespih ağacı or zamzalak (Turkey exotic) and bakine (Pakistan native), is a highly valuable tree and is recognized as a multipurpose medicinal plant[1, 2, 3]. Deciduous tree height up to 15 m (50 ft) tall, twigs stout with purplish bark, dotted with buff-colored lenticels. Mature wood is used for furniture and agricultural implements, boxes, poles, and tool handles because of its resistance to termites, while immature wood and twigs are used as fuel wood. The species has been identified as a potential alternate pulpwood species [4]. It is reported by [5] in Flora of Turkey and East Aegean Islands, *M. azedarach* is a small tree with bipinnate leaves, ovate leaflets, fragrant flowers 10-20 mm in diameter. Its populations are restricted in small areas in Pakistan and in certain cities in Turkey naturally growing in Izmir, Adana, Hatay and also in Kocaeli [6]. *M. azedarach* adopt well in soils with sandy clay, good drainage, and deep soils with pH alkaline. It grows almost on hills up to the high elevation (700-1400 meters above sea level) rainfall 600 to 2000 mm/year [7, 8, 9, 10].

Since many years in the result of socio-economic changes, adverse environment, as well as mismanagement has generated lot of interest in the tropics for the conservation of plant genetic diversity studies [11]. Most species of perennial plants such as trees, under the ever changing environments, rely on the available genetic diversity for stability and survival. To understand the species population study of genetic structure needs much importance for their conservation, planning and sustainable management [12]. Nowadays scientific research has been focused significantly in the applications of molecular biology methods to conserve and use of molecular genetic resources of plants. Molecular techniques have been applied to understand the specific gene action, generate genetic maps and development of gene transfer techniques. These techniques have important roles in the field of phylogeny and the evolution of species. It has been applied to increase the understanding of genetic variation within and between the species, and molecular markers have been divided in to two groups' biochemical and DNA markers [13, 14]. Molecular markers are probes or specific primers which detect genomic locus, due to its presence distinguish the chromosomal trait as well as used to check the differences in the sequences of nucleic acid at particular location in the whole genome [15, 16].

Genetic polymorphism is due to change in nucleotide base which alters the primer binding with in amplified region this leads the different loci products either present or absent [17]. RAPD (Random Amplified Polymorphic DNA) reported as first PCR based molecular markers to be applied in genetic variation analysis; it is one of the most

extremely used molecular techniques having simplicity, low cost and high speed. Thus RAPD markers have been used in many crops providing appropriate and rapid assessment of genetic diversity among different genotypes [17, 18, 19]. RAPD technique is usually applied to detect the viability of DNA among species and also among closely related individuals with in species, as well as used to detect the presence of variation in nucleotides arrangement with in DNA [20]. The genetic diversity maintenance is considered as an important tool for long-term survival and important response of populations to change in the environment [21]. Some reports are available about genetic variation of *M. azedarach* in community forests of West Java [22], and about plant recovery of cryopreserved apical meristem tips of *M. azedarach* using encapsulation/dehydration and assessment of their genetic stability [23]. [24] Studied with *Melia volkensii* populations and evaluated significant genetic differences with the use of RAPD markers to assess genetic diversity, appropriate conservation and management strategies. In present study the RAPD-PCR was used to characterize the genetic similarity and diversity among the populations of *M. azedarach* collected from different locations in Turkey and Pakistan to provide baseline information for establishment of conservation strategies for this species.

MATERIALS AND METHODS

Collection of the plant material. Leaf samples of *M. azedarach* were collected from the mature trees on random bases from five different locations in Turkey and three different locations in Pakistan. Among the natural distribution ranges in both countries Turkey (Adana, Istanbul, Kocaeli, Izmir, and Edirne) and Pakistan (Karachi, Hyderabad, and Khairpur Mirs). Samples were washed with distilled water and evaporated extra surface water at room temperature then stored at -20^{0}C. The sites where these populations are located differ from each other in the terms of vegetation structure, soil and climate [25]. The map in fig 1. shows the *M. azedarach* collection points used for RAPD-PCR applications fig 2. shows the whole plant, leaves, stem and fruits.

A: Adana, B: Izmir, C: Kocaeli, D: Istanbul, E: Edirne, F: Karachi,
G: Hyderabad, H: Khairpur Mirs. ▲: Turkey locations ■: Pakistan locations ★: Capitals of the countries

FIGURE 1
The locations of *M. azedarach* samples collected from Turkey and Pakistan.

FIGURE 2
***Melia azedarach* A. flowers, fruits and leaves, B. whole plant.**

DNA extraction, RAPD-PCR amplification. Leaf samples of *M. azedarach* were taken from -20^{0}C, ground in liquid nitrogen and total genomic DNA was extracted with protocol and reagents followed by Sigma-Aldrich GenEluteTM Plant genomic DNA Mini-prep Kit. Total amount of DNA was quantified through Qubit® 2.0 Fluorometer. Protocol fluorometer used 199 µL Qubit buffer plus 1µL Qubit reagent to prepare reaction buffer then for standard 190 µL of reaction buffer 10 µL of standard from kit followed by 199 µL of reaction buffer and 1µL of DNA sample quantified against standard. Nineteen primers table.1 (Thermo Scientific) were used for RAPD analysis; fourteen primers that produced clear and reproducible fragments were selected for further PCR reactions. The PCR reaction was performed with an initial denaturation steps one cycle of 15 min at 94°C, followed by 44 cycles of 94°C for 1 minute denaturation, 36°C for 1 minute annealing and 72°C for 2 minute extension followed by a final extension period of 5 minutes at 72°C. PCR was allowed to ensure full extension of all amplied products [24]. The amplifications were carried out in triplicate. PCR products and a 100-bp DNA ladder (Gene-On) were resolved electrophoretically in 1 % agarose gels containing 0.5µl ethidium bromide, and run at 100V for about 1 hr. RAPD banding patterns were visualized using UVP gel documentation system.

TABLE 1
Total number of RAPD markers applied for PCR amplification process.

S No.	RAPD marker	Primer base pairs sequence 5'-3'	S No.	RAPD marker	Primer base pairs sequence 5'-3'
01	OPAD-01	5'-CAAAGGGCGG-3'	11	OPC-14	5'-TGCGTGCTTG-3'
02	OPU-07	5'-CCTGCTCATC-3'	12	OPC-13	5'-AAGCCTCGTC-3'
03	OPU-05	5'-TTGGCGGCCT-3'	13	OPC-08	5'-TGGACCGGTG-3'
04	OPU-03	5'-CTATGCCGAC-3'	14	OPC-06	5'-GAACGGACTC-3'
05	OPN-05	5'-ACTGAACGCC-3'	15	OPC-05	5'-GATGACCGCC-3'
06	OPN-02	5'-ACCAGGGGCA-3'	16	OPC-12	5'-TGTCATCCCC-3'
07	OPF-14	5'-GGTGCGCACT-3'	17	OPA-02	5'-TGCCGAGCTG-3'
08	OPF-05	5'-CCCGATCAGA-3'	18	OPC-19	5'-GTTGCCAGCC-3'
09	OPC-18	5'-TGAGTGGGTG-3'	19	OPC-09	5'-CTCACCGTCC-3'
10	OPC-15	5'-GACGGATCAG-3'			

Statistical Analysis. Polymorphism was observed in RAPD profiles included disappearance of a normal band and appearance of a new band comparing all samples with RAPD profiles. Amplified bands were scored as 1 (presence) or 0 (absence). Only strong bands were scored for

analysis. The size and images of each amplification product were captured using the Vision Works LS Version 6.8 automatically estimated using a high resolution scan and digitalized images evaluated directly for RAPD analysis. The data was scored from the RAPD profiles through PAST version 3.08, were subjected to UPGMA cluster analysis to establish the relationship among the eight accessions selected from the different areas [32]. Genetic similarity coefficient among the different localities of *M. azedarach* was estimated through coefficient matrix [41]. The polymorphism percentage was estimated by dividing the number of polymorphic bands over the total number of amplified bands.

RESULTS AND DISCUSSIONS

This study focused towards genetic diversity and similarity among *M. azedarach* species of Turkey and Pakistan collected from eight different locations with the use of 14 RAPD primers with reproducible PCR bands. With the use of all primers 58.95% polymorphism was noted. The average number of total amplified polymorphic bands is found to be 20 were observed among all primers n=8 samples. Highest number of polymorphic bands was 7 with the use of OPN-05 in Adana samples. Highest 67.5% polymorphism was observed in Izmir samples. Among the primers highest 100% polymorphism was noted with the use of OPC-08, OPC-18 and OPN-02 primers. All monomorphic bands were observed with the use of OPAD-01 and OPF-14 markers. The amplification products among 14 primers are shown in table-2 represented as total scoring bands and % polymorphic bands. Mean±CI (mean±Confidence Interval) 55.74±4.65 % percentage of polymorphic bands was observed.

Genetic similarity was calculated according to coefficient matrix method [41]. Similarity represented highest and lowest divergence values 0.756 and 0.388 respectively. Highest difference was observed between Adana and Karachi, second most genetic divergence coefficient was observed between Adana and Hyderabad as shown in Table 3. Highest similarity value was observed between Edirne and Kocaeli, second highest similarity coefficient was noted between Khairpur Mirs and Hyderabad. According to results genetic similarity ranged from 0.358 to 0.756, their net similarities with the mean value noted 0.644±0.210 (Table-3).

TABLE 2
Total number of amplified fragments, number and percentage of polymorphic bands in *M. azedarach* populations. PB: Polymorphic bands, %PB Percentage of polymorphic bands, Mean±CI: Mean ±Confidence interval.

S No.	RAPD marker	Annealing Temperature °C	Total score	P/B	% PB
01	OPAD-01	36°C	8	0	00
02	OPU-07	36°C	27	19	70.37
03	OPU-05	36°C	31	23	74.19
04	OPU-03	36°C	25	17	68
05	OPN-05	36°C	46	22	47.82
06	OPN-02	36°C	10	10	100
07	OPF-14	36°C	8	0	00
08	OPF-05	36°C	35	12	34.28
09	OPC-18	36°C	16	16	100
10	OPC-15	36°C	12	4	33.33
11	OPC-14	36°C '	16	8	50
12	OPC-13	36°C	13	5	38.46
13	OPC-08	36°C	21	21	100
14	OPC-06	36°C	17	11	64
Total			285	168	58.95%
Average		Mean± CI	16.55±2.6	12±2.8	55.74±4.65%

TABLE 3
Jaccard's similarity matrix of *M. azedarach* DNA samples, D Areas: Different Areas, ADA: Adana, IST: Istanbul, KOC: Kocaeli, IZM: Izmir, EDI: Edirne, KAR: Karachi, HYD: Hyderabad, KHA: Khairpur Mirs.

D. Areas	ADA	IST	KOC	IZM	EDI	KAR	HYD	KHA
ADA	1.0000	0.6041	0.5106	0.5294	0.4893	0.3584	0.3888	0.4600
IST	0.6041	1.0000	0.5319	0.6122	0.5106	0.4313	0.4339	0.5416
KOC	0.5106	0.5319	1.0000	0.5208	0.7567	0.4565	0.4583	0.5454
IZM	0.5294	0.6122	0.5208	1.0000	0.6363	0.6087	0.5714	0.6304
EDI	0.4893	0.5106	0.7567	0.6363	1.0000	0.5714	0.5000	0.5952
KAR	0.3584	0.4313	0.4565	0.6087	0.5714	1 .0000	0.6136	0.5681
HYD	0.3888	0.4339	0.4583	0.5714	0.5000	0.6136	1 .0000	0.7561
KHA	0.4600	0.5416	0.5454	0.6304	0.5952	0.5681	0.7561	1 .0000

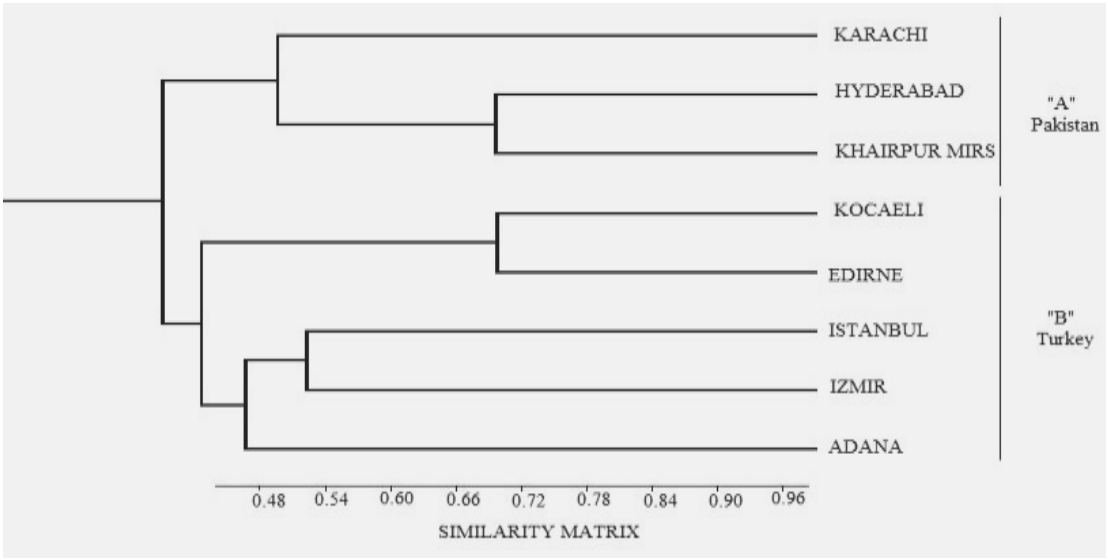

FIGURE 3
Dendrogram based on Jaccard's pair-group method genetic similarities for 8 different populations of *M. azedarach* based on 14 RAPD markers.

According to UPGMA dendogram two main clusters were produced mentioned as: "A" Pakistan and "B" Turkey. Based on cluster "A" Khairpur and Hyderabad samples having DNA75% similar to each other, the second similarity matrix cluster "A" Khairpur and Karachi 56% have genetic material resemble to each other similarly Hyderabad and Karachi 61% similar to each other as shown in figure 3. On the other hand Cluster "B" Turkey samples highest genetic similarity was observed 75.6% between Edirne and Kocaeli samples, Adana and Istanbul 60% resemble to each. It was evaluated that highest divergence in the genetic material was noted 75% between Karachi (Pak) and Adana (Turk) *M. azedarach* L plant species.

In genetic variability studies dendrogram cluster analysis is an important consideration. RAPD data is used to construct dendrogram

revealed DNA markers based on genetic identification among the living organisms. In our study samples from Pakistan and Turkey has been investigated with the use of RAPD markers showed more than half percentage of polymorphism. *M. azedarach* DNA samples belongs to Turkey having great genetic diversity with the samples from different locations in Pakistan. The UPGMA dendogram based on the similarity matrix associated in to two major branches of clusters associations of Turkey and Pakistan. Among these samples, Adana and Karachi DNA samples have highest genetic diversity. Genetic diversity of samples shows higher possibility allowing them more easily to adapt under gradual environmental variations.

Plant species in different areas facing environmental challenges to maintain their survival influenced by genetic variability it contains in its DNA. Many factors can affect genetic diversity of plants like genetic drift; breeding system, distribution range and the way of seed disperse [33]. According to present results genome of the *M. azedarach* having great genetic diversity due to environmental conditions belongs to eight different areas in both countries. The major goal of maintenance of genetic diversity is the conservation programs, as the long-time survival of species in the changing environment [34]. For the assessment of genetic variability and study of phylogenic relationships within and among the plant populations RAPD can be considered as an essential tool. Many reports are available concerned with the determination of genetic variability with the use of RAPD markers [21, 23]. Populations prefer to adopt their local climates and change their genome according to the change in climatic conditions. As indicated in previous reports that different climatic factor effects on DNA and leads to produce different type of living organisms [35, 36].

Our study have been supported by Yulianti, et al., [22], they applied RAPD markers to study the genetic variation of *M. azedarach* (Mindi) community forest in West Java and reported 19% polymorphism. Pandiyan et al., [37] reported 42.39% polymorphism with the use of RAPD markers to study the genetic diversity analysis among Green gram genotypes. Genetic divergence among the samples of *M. azedarach* may be explained as a result of effects due to hydrophobic connection or climatic differentiation factors. Kamran, et al., [38] reported 60.8% genetic polymorphism with the use of RAPD primers to study the genetic diversity of *Jatropha curcas* L plants. These results justify that genetic polymorphism produced due to environmental factors and genetic parameters [39].

This is the first molecular study splitting *M. azedarach* plant species facing two different climatic conditions in Turkey and Pakistan. However Yulianti, et al., [22] have worked using RAPD markers and found genetic variations among *M. azedarach* in forests of West Java Indonesia and having limited study in forest. Runo, et al., [24] studied *Melia volkensii* genetic structure collected from eastern and costal populations of Kenya. They reported genetic differences due to eco-geographical effects on genome and suggested some conservation strategies of these populations. Dhillon et al., [40] have also worked on assessment of genetic diversity in *Azadirachta indica A.* Juss based on DNA fingerprinting in India and reported 68.4% polymorphism with the use of RAPD markers. However present study has been extended among the populations of *M. azedarach* and it is also a comparative study in their genome that belongs to eight different locations of both countries. It has been evaluated that genetic diversity found among the plant species may be due to ecogeographical differences and variable climatic conditions between both countries.

The plant species were collected from Kocaeli and Edirne were resemble to each other, having highest genetic similarity may be due to their similar geographical conditions. Karachi and Adana having highest divergence in genome may be because of different environmental conditions and adaptation against the climatic factors. It is reported that genotoxic effects of environmental chemical pollutants, causes genetic damage that can exist longer period [26]. Physical and chemical mutagenic factors due to different geographical localities cause irreversible DNA damages. UV, ionization radiations, high soil salinity and other chemical mutagens effects on the genome [27, 28, 29]. For the conservation of plant genetic resources two strategies like in situ and ex situ should be applied. In situ implimentation is particularily difficult due to anthropogenic influence [30]. Ex situ conservation can be applied following various methods like seed storage, *in vitro* propagation, DNA storage, pollan storage, botanical gardens [31]. *M. azedarach* populations should be conserved separately because the mixing of populations may give rise to outbreeding depression, loss of adaptation or breakup of co-adapted gene complexes, which should be avoided during *M. azedarach* conservation. The results obtained from this study were the first to describe population genetic parameters for this species, and will provide valuable baseline information for the future population studies and management actions. Investigations are still not sufficient, it needs future applications to apply the other markers like SSR and RAPD and area of the collection of plant samples will be increased that will show great combination and more beneficial achievements. Different conservation strategies should be applied

to conserve the genome of the naturally growing *M. azedarach* populations.

CONCLUSIONS

Study of the genetic diversity of *M. azedarach* populations of both countries with the use of RAPD markers were presented in two different clusters of UPGMA dendrogram which indicates high genetic diversity. On the bases of study out comes environment has great effects on genome and it leads to genetic diversity. Among the studied populations Adana and Karachi locations showed highest genetic diversity, having DNA samples belong to two different climates of their respective countries (Table 3.). When compared with the other populations, and being medicinal plant we suggested that this populations should be primarily conserved. The conservation of *M. azedarach* in gene banks and botanical gardens is recommended for ex situ and in situ conservation. *M. azedarach* grows better in sandy clay, good drainage, and deep soils with acidic pH between 5.5-6.5, full sun and average water conditions and also the area should considered to be compatible with the ecological needs of the plant.

ACKNOWLEDGEMENTS

This study was approved TUBITAK-2216 research project and funded by TUBITAK (Türkiye Bilimsel ve Teknik Araştırma Kurumu). Authors are highly thankful to Head Department of Biology Professor Dr. Fazıl ÖZEN Faculty of Arts and Sciences, Kocaeli University, Turkey for their generous support and encouragement.

REFERENCES

[1] Tomar, O.S., Minhas, PS, Sharma, V.K., Singh, YP, Gupta, RK. (2003) Performance of 31 tree species and soil conditions in a plantation established with saline irrigation. Forest Ecol Manag 177, 333-346.

[2] Skellon, J.H., Thorburn, S., Spence, J., Chatterjee S.N. (1962) The fatty acids of neem oil and their reduction products. J Sci Food Agr. 13, 636-643.

[3] Orwa, C., Mutua, A., Kindt, R., Jamnadass, R., Anthony, S. (2009) Agroforest tree database: a tree reference and selection guide version 4.0. World Agroforestry Centre, Kenya.

[4] Chauhan, R.S., Kaul, M.K., Kumar, A., Nautiyal, M.C. (2008) Pollination behaviour of *Nardostachys jatamansi*: an endangered medicinal and aromatic herb. Sci Hortic 117, 78-81

[5] Davis, Ph. D. Science. (1966) Flora of Turkey and the East Aegean Islands 11, 521.

[6] Damarli Bitkiler. (2012) Turkiye Bitkileri Listesi page 622.

[7] Martawijaya, A., Iding, K., Mandang, Y.I., Soewanda, A.P., Kosasih, K. (1989) Atlas of Indonesian woods. Vol. 2. Forestry Research and Development Agency. Bogor. [Indonesia].

[8] Soerianegara, I., Lemmens, J. (1995) Plant Resources of South-East Asia No. 2. Auxiliary plants. PROSEA. Bogor.

[9] Ahmed, S., Idris, S. (1997) *Melia azedarach* L. In: Hanum, F., van der Maesen, L.J.G. (eds) Plant resource of south-east asia No. 11. Auxiliary plants. F Hanum and L.J.G. van der Maesen. Prosea, Bogor 187-190.

[10] Wulandini, R., Widyani, N. (2004) *Melia azedarach* Linn. Brief information seed. No. 30. Directorate of Forest Tree Seed and Indonesian Forest Seed Project. Ministry of Forestry. Jakarta. [Indonesia]

[11] Young, A., Merriam, H.G. (1992) The effect of forest fragmentation on genetic variation in an *Acer saccharium*. (March sugar maple) population. Paper to: International symposium on population genetics and gene conservation of forest trees. Carcaus Maubuuisson, France. 24-28

[12] Sun, M., Wong, K.C., Lee, J.S.Y. (1998) Reproduction biology and population genetic structure of *Kandelia candel* (Rhizophoraceae) a viviparous mangrove species. Am J Bot 85, 1631-1637.

[13] Linda, M., Arshiya, N., Pagnotta, M.A. (2009) Assessing plant genetic diversity by molecular tools. Diversity 1, 19-35

[14] Kumar, L.S. (1999) DNA markers in plant improvement: An overview. Biotechnol Adv 17, 143–182.

[15] Barcaccia, G., Pallottini, L., Arzenton, F., Parrini, P. (2000) Comparing linkage maps of flint maize (*Zea mays* var. indurata) Italian landrace based on an F1 and BC1 populations. Conve Soci Ital di Genetica Agraria 120-121.

[16] Bardak, A. (2007) Genetic diversity of diploid and tetraploid cottons determined by SSR markers and its relationship with fiber quality traits, MSc, Kahramanmaraş Sütçü İmam University Institute of Natural and Applied Sciences.

[17] Rafalski, J.A., Tingey, S.V. (1993) RFLP map of soybean (*Glycine max*) 2N = 40. In: Genetic Maps. Cold Spring Harbor Laboratory, Cold Spring Harbor, New York, pp. 149-156.

[18] Welsh, J., McClelland, M. (1990) Fingerprinting genomes using PCR with

arbitrary primers. Nucleic Acids Res 18, 7213-7218.
[19] Ragot, M., Hoisington, D.A. (1993) Molecular markers for plant breeding: comparisons of RFLP and RAPD genotyping costs. Theor Appl Genet 86, 975– 984.
[20] Song, B.K., Clyde, M.M., Wickneswari, R., Normah MN (2000) Genetic relatedness among *Lansium domesticum* accessions using RAPD markers. Ann Bot 86, 299-307.
[21] Hueneke, F.L. (1991) Ecological implication of genetic variation in plant populations. Genetics and Conservation of Rare Plants. Oxford University Press, New York, pp. 31-44.
[22] Yulianti Iskander, Z.S., Nurheni, W., Igk Tapa, D., Dida, S. (2011) Genetic variation of *Melia azedarach* in community forests of West Java assessed by RAPD. J of Biological Diversity 12 (2), 64-69.
[23] Adriana, S., Mirta, F., Ricardo, M., Sofia, O., Luis, M. (2004) Plant recovery of cryopreserved apical meristem tips of *Melia azedarach* L. using encapsulation/dehydration and assessment of their genetic stability. Euphytica J. 135, 29-38.
[24] Runo, M.S., Muluvi, G.M., Odee, D.W. (2004) Analysis of genetic sructure in *Melia volkensii* (Gurke.) populations using random amplified polymorphic DNA. Afr J Bio. 3 (8), 421-425.
[25] Pratt, D.J., Gwynne, M.G. (1977) Rangeland management and Ecology in East Africa. Hodder and Stoughton, London p 310.
[26] Toma´s, G., Zdenka, P., Ji˘rina, S., Irena, Z., Anita, M. (2008) DNA damage in potato plants induced by cadmium, ethyl methanesulphonate and rays. Env Exp Bot 62,113–119.
[27] Roy, S., Roy Choudhury, S., Das K.P. (2013) The interplay of DNA polymerase λ in diverse DNA damage repair pathways in higher plant genome in response to environmental and genotoxic stress factors. Plan Sig. Be. 8 (1), 113-115.
[28] Waterworth, W.M., Drury, G.E., Bray, C.M., West, C.E. (2011) Repairing breaks in the plant genome: the importance of keeping it together. New Phytol 192, 805-822.
[29] Tuteja, N., Singh, M.B., Misra, M.K., Bhalla, P.L., Tuteja, R. (2001) "Molecular mechanisms of DNA damage and repair: progress in plants," Crit Rev Biochem Mol, 36(4), 337-397.
[30] Zawko, G., Krauss, S.L., Dixon, K.W., Sivasithamparam, K. (2001) Conservation genetics of the rare and endangered *Leucopogon obtectus* (Ericaceae). Mol Ecol 10(10), 2389-2396.
[31] Nybom, H. (2004) "Comparison of different nuclear DNA markers for estimating intraspecific genetic diversity in plants" Mole Eco 13(5), 1143-1155.
[32] Hammer Harper DAT., Ryan, PD. PAST. (2001) Paleontological statistics software package for education and data analysis. Palae Electro 4(1),1-9.
[33] Sasikala, T.P., Kamakshamma, J. (2015) Genetic diversity assessed through RAPD markers in *Terminalia pallida* Brandis. J. Pharm. Sci. and Res. Vol. 7(2), 58-62.
[34] Barrett, S.C.H., Kohn, J.R., Falk, D.A., Holsinger, K.E. (1991) Genetic and evolutionary consequences of small population size in plants: implications for conservation, Genetics and conservation of rare plants, Oxford University press: 3-30.
[35] Huang, Z.H., Liu, N.F., Zhou, T.L., Ju, B. (2005) Effects of environmental factors on population genetic structure in chukar partridge (*Alectoris chukar*). J Arid Environ 62, 427-434.
[36] Jin, Y.T., Liu, N.F. (2008) Ecological genetics of *Phrynocephalus vlanqalii* on the north Tibetan (Qinghai) Plateau: Correlation between envrionmental factors and population genetic variability. Biochem. Genet 26, 598-604.
[37] Pandiyan, M., Senthil, N., Sivakumar, P., Muthiah, A.R., Ramamoorthi, N. (2010) Genetic diversity analysis among green gram genotypes using RAPD markers. Elec J Pl Breed 1(4), 466-473.
[38] Subramanyam, K., Dowlathabad, M.R., Devanna, N., Aravinda, A., Pandurangadu, V. (2010) Evalution og Genetic Diversity among *Jatropha curacas* L. by RAPD analysis. Indian J Biota 9, 283-288.
[39] Kamran, A., Altaf, A., Anis, C., Mohd, M., Sayeed, A., Mohd, A., Mallick, N. (2014) Genetic diversity analysis of *Zingiber officinale* Roscoe by RAPD collected from subcontinent of India. Saud Jour of Boils Sci. 21, 159-165.
[40] Dhillon, R.S., Mohapatra, T., Singh, S., Boors, K.S., Sing, K. (2007) Assessment of genetic diversity in *Azadirachta indica* based on DNA fingerprinting Indian, J of Biotechnology 6, 519-524.
[41] Jaccard, P. (1908) Nouvelles recherches sur la distribution florale. Bull Soc Vaud Sci Nat. 44, 223-270.

Received: **30.09.2015**
Accepted: **11.01.2016**

CORRESPONDING AUTHOR

Nadir Ali Rind
Institute of Biotechnology and
Genetic Engineering (IBGE),
University of Sindh,
Jamshoro, 76080, Pakistan

e-mail: nadir_rind27@yahoo.com

© by PSP Volume 25 – No. 7/2016, pages 2383-2392 Fresenius Environmental Bulletin

SYNERGY EFFECT OF ^{60}CO Γ-RAY AND H_2O_2 ON DEODORIZATION AND DECOLORIZATION OF WASTE COOKING OIL

Yu-Lin Xiang, Yu-Rong Jiao[1], Bin Shi[1], Tian-Yu Liu[2]

1. College of Chemistry and Chemical Engineering, Yulin University, Yulin 719000 Shaanxi Province, China
2. School of Chemical Engineering & Technology, Tianjin University, TianJin, 300072, China

ABSTRACT

Waste cooking oil was effectively deodorized and decolorized by ^{60}Co γ-ray in the presence of H_2O_2. The existence of a synergetic effect on the deodorization and the decolorization was illustrated through UV/VIS spectrophotometry, FT-IR and sensory analyses, and the saponification performance of waste cooking oil was measured. Results showed that odor and color of waste cooking oil through a combined treatment of ^{60}Co γ-ray/H_2O_2 were remarkably improved. Saponification analysis indicated that the color and performance of waste cooking oil met the requirements of soap production. The quality evaluation of the product suggested that the smell of the soap was light, the decontamination ability was fine and the skin felt well after cleaning. Additionally, according to a preliminary cost estimate, the combined process of ^{60}Co γ-ray/H_2O_2 was more profitable and more feasible than the alone process using either ^{60}Co γ-ray or H_2O_2.

KEYWORDS:
Waste cooking oil; deodorization; decolorization; ^{60}Co γ-ray/H_2O_2

INTRODUCTION

The enormous production of waste cooking oil (WCO) from restaurants and homes is a serious environmental problem around the world [1, 2]. These years, reutilization of the WCO as a resource has attracted worldwide attention. In some countries, the WCO has been used as environmental-friendly material in oleochemical industries, soap manufacture, and even animal husbandry [3]. The use of the WCO as a material not only reduces the production cost but also assists in the disposal[4]. However, the WCO has some shortcomings such as color depth and odor, which have hampered application of the WCO.

There are many decolorization or deodorization methods, such as adsorption[5], electrochemical oxidation [6], TiO_2 photocatalytic oxidation[7], UV/H_2O_2 [8], coagulation [9], reverse osmosis [10], enzymatic decolorization [11] and so forth. These methods are efficient to deodorize or decolorize, but having some problems such as high-cost, low-yield, and destruction of some compositions [12, 13].

Gamma radiation is an effective technology for contaminant destruction, harmful residues in the system are fewer after irradiation, and processing time is short[14, 15]. The technology can efficiently degrade many bio-refractory materials, such as polyvinyl alcohol[16], cellulose[17] and polysaccharides[18]. Hydrogen peroxide, on the other hand, is widespreadly applied due to its strong oxidizing properties, environmentally friendly behavior, lower investment costs. These properties can be still enhanced in conjunction with the UV radiation[19] or gamma radiation[20]. Combining hydrogen peroxide and gamma radiation has been applied successfully in some environmental pollutant treatments [20-22]. However, the combining process has not been studied for deodorization and decolorization of the WCO.

It is, therefore, the purpose of this study to investigate the mechanism of deodorizing and decolorizing of the WCO with hydrogen peroxide and gamma radiation. Finally, cost analysis, sensory evaluation, FT-IR and saponification analysis for the WCO were also discussed.

MATERIALS AND METHODS

Materials. Hydrogen peroxide (H_2O_2), Hydrochloric acid (HCl), potassium hydroxide (KOH), sodium hydroxide (NaOH), acetic acid (CH_3COOH) and sucrose （$C_{12}H_{22}O_{11}$） were of analytical reagent grade.

The WCO was obtained from a restaurant in Yulin, China. Because of the production background

of the employed WCO, it can't be directly applied, and a series of pre-treatment processes were needed. Firstly, the WCO was filtrated in order to remove all suspended solid particles and food debris. Then, the WCO was heated at 75 ℃ and was washed with de-ionized water at 75 ℃ (10 % of the WCO volume). After that, the WCO mixture was centrifuged at 1000 rpm during 20 min to separate water-soluble salt impurities. Finally, the treated WCO was kept in a glass vessel and held under vacuum at 75 ℃ for 40 min in order to eliminate water.

Experimental procedure. In order to study the synergy effect of ^{60}Co γ-ray and H_2O_2 on deodorization and decolorization of the WCO, a sequence of experiments were carried out, which ran as follows: ^{60}Co γ-ray /H_2O_2, ^{60}Co γ-ray alone and H2O2 alone. Above all, 50 ml of the treated WCO was placed in a 100 ml flask, and kept electric-heated thermostatic water bath (setting temperature: 30 to 70 ℃) for 15 min. The experiment was initiated by adding the preset amount of H_2O_2 (0 to 0.9% by volume), then the mixture was exposed to gamma radiation doses of 0 to 9 kGy in a cobalt-60 irradiator and dose rate was 70 Gy/min, during the radiation procedure, the mixture was turned 360° ceaselessly. Finally, the treated WCO were stored in a clean, dry, air-tight container, in a cool dark place at room temperature for 140 days. Sensory analyses was carried out on the treated samples, immediately after experiment, and at orderly intervals of 2 weeks.

Decolorization measurement. The color was measured by a UV/Vis spectrophotometer at a wave-length corresponding to the maximum absorbance of the WCO (λ_{max}=485 nm). The decolorization efficiency, D (%), was calculated by Equation(1):

$$D = \frac{A_0 - A_t}{A_0} \times 100\% \qquad (1)$$

Where D is decoloration efficiency, %; A_0 and A_t is absorbance value before and after decoloration, respectively.

Sensory analysis. Sensory evaluation of the treated WCO was determined using 15 trained staff members[23]. The odor was depicted before and after treatment. Firstly, the numbered sample in capped test tube was handed over to each staff in isolated booths. Each evaluator scored for odor of the sample using a five point scoring method where: 5=like extremely; 4=like moderately; 3=neither like nor dislike; 2=dislike moderately; 1=dislike extremely. Scores above 3 showed the treated WCO was acceptable. The sensory evaluation was conducted at orderly intervals of 2 weeks.

Response surface methodology. The RSM was used to optimize the experiment process. Radiation dose (X_1), H_2O_2 addition (X_2) and temperature (X_3) were considered to be the WCO property variables. Table1 presents the ranges and the levels of the factors in RSM.

According to statistics theory, the three-factor, three-level Central Composite Design (CCD) experimental design consisted of 20 experimental runs. The experimental design is shown in Table 2.

The experimental results were fitted according to Eq. 2 as a quadratic polynomial regression equation.

$$Y = \beta_0 + \sum_{i=1}^{k} \beta_i X_i + \sum_{i=1}^{k} \beta_{ii} X_i^2 + \sum_{i=1}^{k} \sum_{j=1}^{k} \beta_{ij} X_i X_j + \varepsilon \qquad (2)$$

Where Y is the predicted response, β_0 is the intercept term, β_i is the linear effect, βii is the square effect, and β_{ij} is the interaction effect; X_i and X_j are the variables, i and j are the index numbers for the pattern, and ε is the error.

TABLE 1
Variables and levels.

factors	symbol	coded levels				
		-1.68	-1	0	1	1.68
radiation dose(kGy)	X_1	1	3	5	7	9
H_2O_2(%)	X_2	0.1	0.2	0.3	0.4	0.5
temperature(℃)	X_3	30	40	50	60	70

TABLE 2
Results of CCD experimental design.

run	factors			response values	
	X_1(coded)	X_2(coded)	X_3(coded)	decolorization efficiency(%)	sensory scores
1	5(0)	0.3(0)	50(0)	81.36	4.13
2	5(0)	0.3(0)	70(1.68)	75.66	3.03
3	5(0)	0.3(0)	50(0)	88.25	4.88
4	7(1)	0.4(1)	40(-1)	51.2	1.49
5	7(1)	0.2(-1)	60(1)	92.23	2.08
6	5(0)	0.1(-1.68)	50(0)	91.24	2.33
7	5(0)	0.3(0)	30(-1.68)	44.10	2.52
8	3(-1)	0.4(1)	60(1)	59.43	2.65
9	5(0)	0.3(0)	50(0)	83.37	4.5
10	3(-1)	0.2(-1)	60(1)	48.39	2.67
11	3(-1)	0.4(1)	40(-1)	27.4	1.52
12	7(1)	0.4(1)	60(1)	96.21	1.52
13	3(-1)	0.2(-1)	40(-1)	56.3	1.6
14	5(0)	0.3(0)	50(0)	89.41	4.63
15	5(0)	0.5(1.68)	50(0)	81.09	3.18
16	9(1.68)	0.3(0)	50(0)	73.59	1.42
17	5(0)	0.3(0)	50(0)	85.77	4.3
18	7(1)	0.2(-1)	40(-1)	84.71	1.15
19	1(-1.68)	0.3(0)	50(0)	21.87	2.66
20	5(0)	0.3(0)	50(0)	86.91	4.93

Saponification. The WCO (2.0 g) was filtered at 40 ℃, and the mass ratio of KOH to WCO was 1:2. Firstly, 20 ml of distilled water and 20 ml 1 N KOH were added gradually at 90 ℃. After the mixture was stirred for 4 h, the addition of KOH became a quarter of the total. After 1 h, the WCO was emulsified. Then, one half amount of KOH was added, the rest of KOH was added after 2 hours. In the process, the mixture was constantly stirred, water evaporated was replenished constantly and pH kept at 9.5±0.5. When the sample changed from emulsified shape to solid, saponification was completed. A blank was executed under the same conditions.

FT-IR spectroscopy. FT-IR spectra of the WCO before and after treatment were recorded using a Fourier Transform Spectrometer (IR Prestige-21). It is used to investigate the component changes of treated and untreated WCO. The wavenumber range of the spectrometer is 4600 to 500 cm^{-1} using 100 scans at 4 cm^{-1} resolution.

Statistical analysis. The design-expert (version 8.0.6) software was used to design the response surface. In order to minimize the systematic error, Each sample measurement was replicated 3 times. The differences were less than 5%, and the results were subjected to the ANOVA analysis using the Origin8.0.

RESULTS AND DISCUSSION

Color and sensory evaluation. In order to investigate whether a synergy effect of ^{60}Co γ-ray and H_2O_2 is operative in the deodorization and decolorization of the WCO, the experiments were operated (^{60}Co γ-ray/H_2O_2, radiation alone and H_2O_2 alone). The volume of the pretreated WCO was 50 ml, the pretreated temperature was 35 ℃. H_2O_2 addition was 0.25, 0 and 0.25 ml for ^{60}Co γ-ray/H_2O_2, H_2O_2 alone and radiation alone process, respectively. Radiation doses was 5, 0 and 5 kGy for ^{60}Co γ-ray/H_2O_2, H_2O_2 alone and radiation alone process, respectively. The sensory evaluation score (S) and the decolorization efficiency (D) of the WCO in storage periods are illustrated in Fig. 1.

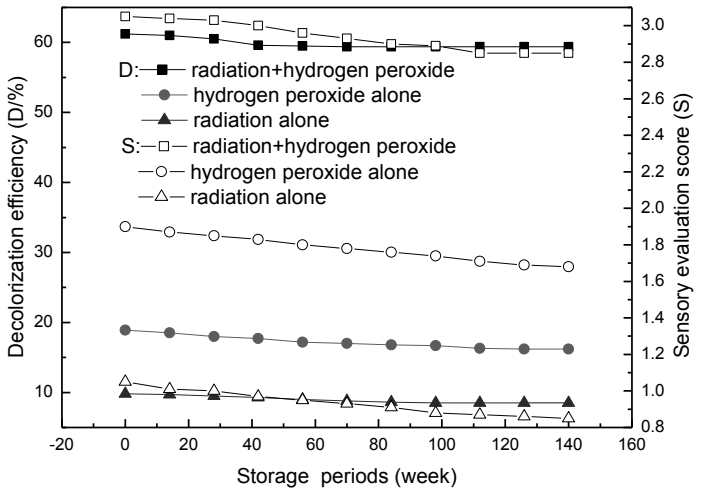

FIGURE 1
Sensory evaluation score and decolorization efficiency of the WCO in storage periods.

When the WCO was exposed to gamma ray radiation without H_2O_2, the decolorization efficiency was 9.8%. Under H_2O_2 oxidation, the decolorization efficiency was 18.9%. It is attractive to notice that in the combined system (^{60}Co γ-ray/H_2O_2), the decolorization efficiency rose to 61.2%. The working together of H_2O_2 and radiation to produce an effect higher than the sum of their individual effects. Therefore, the synergy effect of ^{60}Co γ-ray and H_2O_2 is operative in the decolorization of the WCO. The explanation could be, that gamma radiation can split H_2O_2 or H_2O into ions and free radicals. The radiolysis processes can be described as following equation[24]:

$$H_2O_2 \xrightarrow{\gamma-rays} 2\cdot OH$$

$$H_2O \xrightarrow{\gamma-rays} \cdot OH, \cdot H, H_3O^+, e_{aq}^-, H_2O$$

Simultaneously, hydrated electron will also act rapidly with H_2O_2 to produce OH radical.

$$H_2O_2 + e_{aq}^- \rightarrow \cdot OH + HO^-$$

OH radical is very sensitive to the colored materials, and the colored materials will be ruptured quickly when exposed to small quantity of the radicals[25]. Consequently, the increase in the decolorization efficiency would be ascribed to an increase in the radicals in the combined system.

As storage time went by and the decolorization efficiency of all samples showed a downward trend during storage. Lin (2009) reported that oil color became darker, it may have been because inactivation of the radicals occured and the reverse started with the storage time lasting[26]. However, the decolorization efficiency of the sample under the combined system was always highest.

The sensory evaluation score of non-processed WCO was regarded as 0. Under individual H_2O_2 oxidation, the score was 1.9; Under individual radiation process, the score was 1.05; Under the working together of H_2O_2 and radiation, the score rose to 3.05, which is highest of all. The score of all samples decreased with the storage time lasting. But the score of the sample under the combined system was always highest of all. Thus, the odor of the WCO can also be improved under the combined ^{60}Co γ-ray and H_2O_2 treatment. It may have been because the degradation of odor materials might occur in the combined ^{60}Co γ-ray and H_2O_2 treatment, as follows[27]:

$$H_2O \xrightarrow{\gamma-rays} \cdot OH, \cdot H, H_3O^+, e_{aq}^-, H_2O$$

$$\cdot H + H_2O_2 \rightarrow \cdot HO + H_2O$$

$$H_2O_2 + e_{aq}^- \rightarrow \cdot OH + HO^-$$

$$H_2O_2 \xrightarrow{\gamma-rays} 2\cdot OH$$

$$M + \cdot OH \rightarrow \cdot M + H_2O$$

$$M + \cdot H \rightarrow \cdot M + H_2$$

$$\cdot M \rightarrow M_1 + M_2$$

Consequently, some odor materials (M) were broken down into the other materials (M_1, M_2) without terrible smell. The smell of the WCO was improved. With the storage time lasting, the reverse were taking over gradually, and odor materials were produced again, the smell of the WCO became terrible.

Response surface test.

Regression model. The relations of three effect factors (radiation dose, H_2O_2 addition, and temperature) to decolorization and to deodorization were investigated by multiple regression analysis. According to the CCD experimental design, the results are shown in Table 2. The second order polynomial equations were gained to explain the experiment process. Eq. 3 and Eq. 4 represent the decolorization efficiency and the sensory evaluation score as a function of the coded units, respectively.

$$D = 85.81 + 16.10X_1 - 4.72X_2 + 9.50X_3 - 1.46X_1X_2 + 3.55X_1X_3 + 9.68X_2X_3 - 13.23X_1^2 + 0.36X_2^2 - 8.93X_3^2 \quad (3)$$

$$S = 4.83 - 0.31X_1 + 0.081X_2 + 0.29X_3 - 0.015X_1X_2 - 0.15X_1X_3 - 0.10X_2X_3 - 1.01X_1^2 - 0.84X_2^2 - 0.84X_3^2 \quad (4)$$

Where D and S are the predicted values for the decolorization efficiency and the sensory evaluation score, respectively. X_1, X_2 and X_3 are model terms that represent radiation dose, H_2O_2 addition, and temperature, respectively. It can be seen that the selected variables show significant effect on decolorization and deodorization of the WCO within the ranges tested.

An analysis of variance (ANOVA) was carried out to gain sum of P values, F values, squares(SS), degrees of freedom (df) and mean squares (MS) by fitting the quadratic polynomial equation with the data of Table 2, and the results are showed in Table 3 and Table 4.

For decolorization efficiency, the Model F-value of 123.92 implies that the model is significant. There is only a 0.01% chance that a "Model F-Value" this large could occur due to noise. Values of "Prob>F" less than 0.0500 indicate model terms are significant. In this case X_1, X_2, X_3, X_1X_3, X_2X_3, X_1^2, X_3^2 are significant model terms. That values are greater than 0.1000 indicate the model terms are not significant. The "Lack of Fit F-value" of 0.84 implies the Lack of Fit is not significant relative to the pure error. Non-significant lack of fit is good. The "Pred R-Squared" of 0.9622 is in reasonable agreement with the "Adj R-Squared" of 0.9831. "Adeq Precision" measures the signal to noise ratio. A ratio greater than 4 is desirable. Adeq ratio of 36.716 indicates an adequate signal. Thus, decolorization efficiency model can be used to navigate the design space.

For sensory evaluation, the Model F-value of 15.06 implies the model is significant. There is only a 0.01% chance that a "Model F-Value" that large could occur due to noise. Values of "Prob> F" less than 0.0500 indicate model terms are significant. In this case X_1, X_3, X_1^2, X_2^2, X_3^2 are significant model terms. The Lack of Fit is not significant relative to the pure error. Adeq Precision of 10.345 indicates an adequate signal. So sensory evaluation model can be used to navigate the design space.

Response surfaces and contour plots. Response surfaces and contour plots are universally applied to ascertain the optimum values and facilitate a better understanding of the interactions between variables. The interactions between the variables and responses are shown in Fig. 2.

Figure 2a presents the effects of radiation dose (X_1) and temperature (X_3) on the decolorization efficiency while H_2O_2 addition (X_2) was fixed at middle level. As we can see from the figure, the contour plot showed imperfectly elliptical. This demonstrates that there was less interaction between radiation dose and temperature. Furthermore, when the temperature was about 62 ℃, the decolorization efficiency reached the maximum for a given radiation dose, while the temperature both lower and higher than 62℃ could lead to the decline of the decolorization efficiency. The trend was similar to the previous study[28]. A possible explanation may be that, for a lower temperature (below 62℃), an increase of the temperature reduced the WCO viscosity and augments the capacity of molecular diffusion, thus led to an quick performance in the decolorization reaction [29], whereas excess the value (above 62℃) would aggravate the lipid oxidation, compromise the decolorization efficiency .

The effect of varying H_2O_2 addition (X_2) and temperature (X_3) on the decolorization efficiency is showed in Figure 2b. As seen here, with a fixed middle level of radiation dose, the decolorization efficiency exhibited a monotonic decline with the H_2O_2 addition increasing. The decline in decolorization efficiency as the H_2O_2 addition increases could be explained that too much H_2O_2 addition bring about alternative oxidations, and new color substance was formed. thus leading to a decline of the decolorization efficiency[30]. In addition, the temperature played a more significant role in the response than the H_2O_2 addition from the contour plot. Consequently, increasing temperature was favorable for improving the color of the WCO.

TABLE 3
Variance analysis for the established regression model of the decolorization efficiency.

Source	Sum of squares	df	Mean square	*F* value	Prob>F
Model	9389.46	9	1043.27	123.92	< 0.0001
X_1	3537.96	1	3537.96	420.24	< 0.0001
X_2	304.25	1	304.25	36.14	0.0001
X_3	1232.29	1	1232.29	146.37	< 0.0001
X_1X_2	17.02	1	17.02	2.02	0.1855
X_1X_3	100.89	1	100.89	11.98	0.0061
X_2X_3	749.43	1	749.43	89.02	< 0.0001
X_1^2	2521.08	1	2521.08	299.45	< 0.0001
X_2^2	1.89	1	1.89	0.22	0.6456
X_3^2	1149.41	1	1149.41	136.53	< 0.0001
Residual	84.19	10	4.07		
Lack of fit	38.32	5	7.66	0.84	0.5759
Pure error	45.87	5	0.19		
Cor total	9473.65	19			
R^2=0.9911 R^2_{Adj}=0.9831 CV=4.09%					

TABLE 4
Variance analysis for the established regression model of the sensory evaluation score.

Source	Sum of squares	df	Mean square	*F* value	Prob>F
Model	29.04	9	3.23	15.06	0.0001
X_1	1.34	1	1.34	6.27	0.0312
X_2	0.090	1	0.090	0.42	0.5312
X_3	1.18	1	1.18	5.52	0.0407
X_1X_2	1.800E-003	1	1.800E-003	8.399E-003	0.9288
X_1X_3	0.19	1	0.19	0.90	0.3660
X_2X_3	0.088	1	0.088	0.41	0.5356
X_1^2	14.72	1	14.72	68.69	< 0.0001
X_2^2	8.28	1	8.28	38.63	< 0.0001
X_3^2	8.12	1	8.12	37.91	0.0001
Residual	2.14	10	0.21		
Lack of fit	1.64	5	0.33	3.28	0.1089
Pure error	0.50	5	0.10		
Cor total	31.18	19			
R^2=0.9313 R^2_{Adj}=0.8694 CV=16.19%					

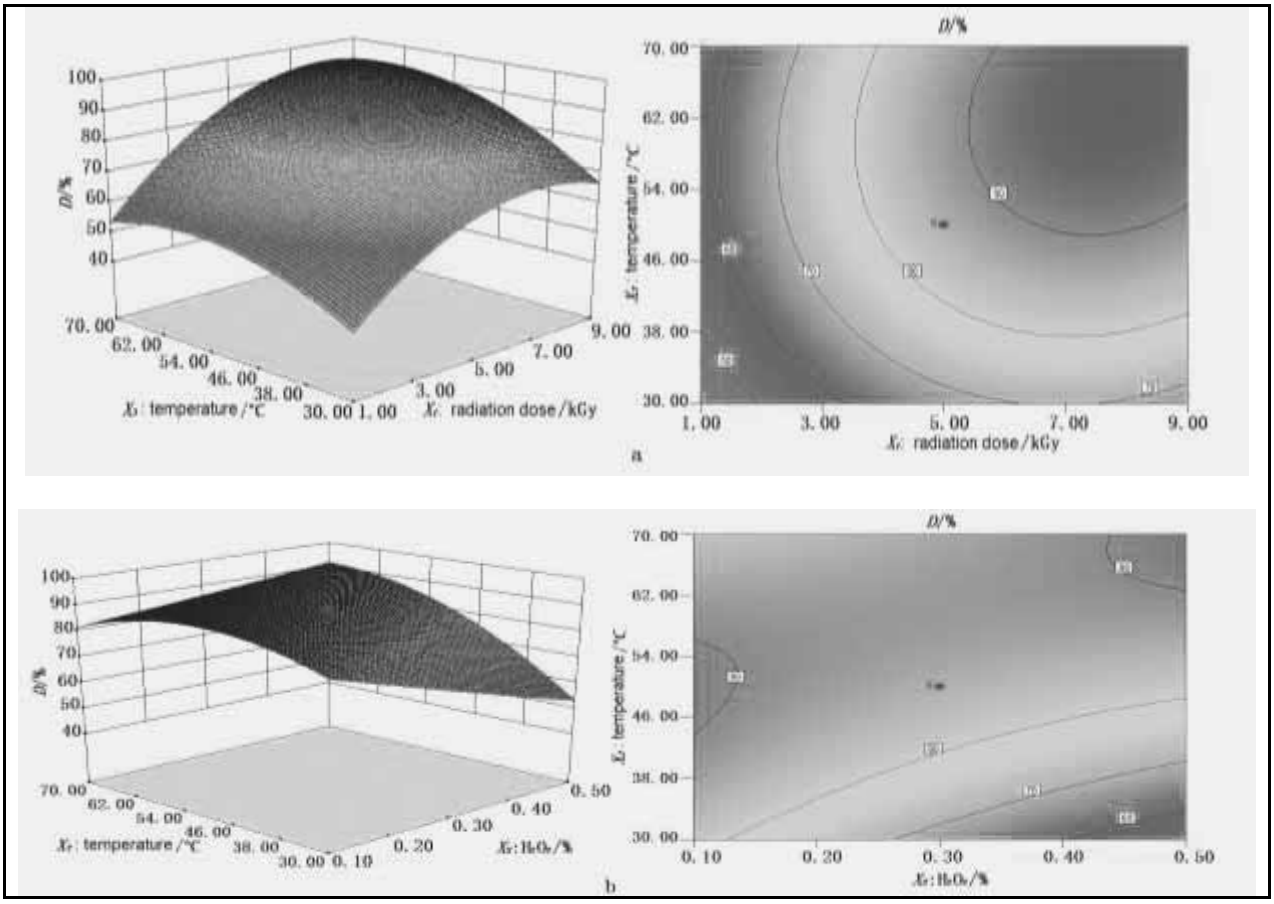

FIGURE 2
Response surface curves and contour plots showing the effects of interactions of the factors on decolorization efficiency: (a) radiation dose and temperature, (b) H2O2 and temperature.

TABLE 5
Verification of the Model.

run	radiation dose(kGy)	H_2O_2(%)	temperature (℃)	predicted value		experimental value	
				D(%)	*S*	*D*(%)	*S*
1	5.55	0.29	56	90.05	4.53	90.2	4.42
2	5.6	0.30	56.5	90.24	4.52	89.9	4.58
3	5.65	0.30	57	90.51	4.5	89.5	4.55
The standard deviations＜5%							

Optimization of WCO properties and model verification. In this study, the optimal condition was obtained by using RSM. Optimal condition for the response at a radiation dose 5.58kGy was determined to be a H_2O_2 addition of 0.29% (v/v), and temperature 56.33 ℃. Under this optimal condition, the decolorization efficiency and sensory evaluation score were expected to be 90.21% and 4.52, respectively. To confirm the availability of the optimization process and the adequacy of the model, three sets of experiments were performed near the optimum conditions. Each set experiment was repeated three times. the decolorization efficiency and sensory evaluation score were obtained by using the optimal conditions, as shown in Table 5. The data from table 5 shows that the predicted and experimental values match well. The good agreement testifies the validity of the models for simulating the

decolorization and sensory evaluation process of the WCO with ^{60}Co γ-ray/H_2O_2 method.

Feasibility analysis.

Saponification value. The saponification value (SV) of the WCO was 190 mg/g. The SV above 185 mg/g showed that the WCO sufficed for the manufacture of soap[31]. The SV of the processed WCO (under the optimal condition: radiation dose 5.6kGy, H_2O_2 addition 0.29% (v/v) and temperature 56.5 ℃) was 195 mg/g, that was higher than the unprocessed WCO. It was probably due to the fact that hydroxyl radicals disintegrated the macromolecules into micromolecules, and the fat molecules might interacted with each other [32]. However, the smaller molecular weight was, the larger saponification value was. Figure 3 presents that the soaps were made from the processed WCO. The quality evaluation of the products showed that the soaps had the fine decontamination ability, foam were moderate, the smell was light, and the skin felt well after cleaning.

FIGURE 3
The soaps from the processed waste cooking oil.

Spectral analysis. Fig. 4 presents the FT-IR spectra of the WCO under different conditions, the blue line represents the unprocessed WCO, and the red line represents the treated WCO with ^{60}Co γ-ray/H_2O_2 under optimal condition. The region of 1500 cm^{-1} to 2000 cm^{-1} represents the double bond stretching region. As seen here, The band trend is much similar, but the band intensity of the treated WCO is weaker than the unprocessed WCO. This observation shows that the amounts of the double bond substance became less in the treated WCO. The most color organic compound have the structure of double bond, the color is eliminated after the double bond rupture[33]. It has been reported that the aldehydes and ketones in the WCO have sour odor [34]. The C=O double bond might rupture in the treated WCO, sour odor is removed. Therefore, the color and odor of the treated WCO was improved.

Cost estimate. Because the treatment effect the individual radiation process was not ideal, a comparison of the treatment costs of the WCO by the ^{60}Co γ-ray /H_2O_2 and the individual H_2O_2 process was studied. Considering acceptable saponification performance and sensory quality, the highest decoloration efficiency was 65% for the studied WCO, which was obtained by the individual H_2O_2 process at room temperature, so the value was chose as the specified decoloration efficiency. The costs were made up of H_2O_2 chemical and gamma ray energy consumption. The unit expenditure of gamma ray and H_2O_2 (30%, AR) are 0.001319 dollars/ml, and 0.0001905 dollar/ml[21], respectively. As shown in Table 6, the cost of the individual H_2O_2 process was 0.0002638 dollars/ml, which was higher than the cost of the ^{60}Coγ-ray/H_2O_2, 0.0001945 dollars/ml. Therefore, the ^{60}Co γ-ray/H_2O_2 process was feasible for decoloration of the WCO.

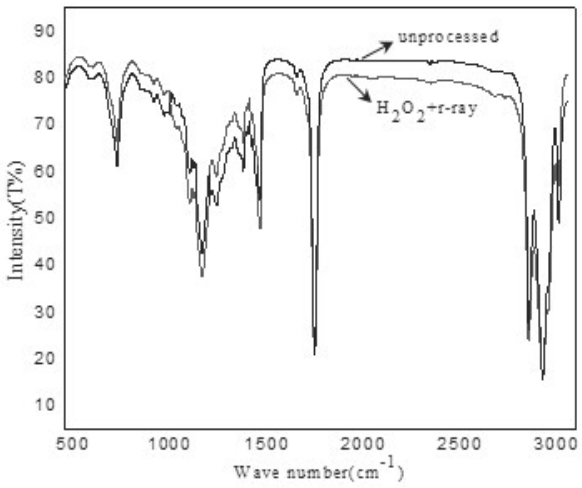

FIGURE 4
Infrared spectrum of the waste cooking oil.

TABLE 6
Cost estimate.

Process	H_2O_2 (mL/mL)	Irradiation (dollars/mL)	Total Costs (dollars/mL)
^{60}Co γ-ray / H_2O_2	0.003	0.0001905	0.0001945
H_2O_2	0.2	0	0.0002638

CONCLUSION

Synergy effect of ^{60}Co γ-ray and H_2O_2 on deodorization and decolorization of waste cooking oil was visible. Taking the decolorization efficiency and sensory evaluation score into consideration, the optimal condition was determined on the basis of RSM tests, as follows: radiation dose 5.58kGy, H_2O_2 addition 0.29%(v/v), and temperature 56.33 ℃. Under the optimal condition, the decolorization efficiency and sensory evaluation score increased to 90.21% and 4.52, respectively. The experimental results agreed very well with the predicted values from the models, with R^2 value of 0.9911 (for decolorization) and 0.9313(for sensory evaluation). Under the ^{60}Co γ-ray/H_2O_2 treatment, odor and color of the WCO were improved. FT-IR analysis demonstrated the amounts of the double bond substance became less in the treated WCO, and it is possible that there is a definite relation between the decolorization and the amounts of the double bond substance. In addition, the cost of ^{60}Co γ-ray/H_2O_2 method was more acceptable than the individual H_2O_2 process. The soaps from the processed WCO had the fine decontamination ability, and the skin felt well after applying.

ACKNOWLEDGEMENT

The authors are grateful for the funding and support provided by the following projects: the Scientific Research Starting Foundation for high-level professionals in Yulin University of China (No. 12GK04), the Natural Sciences Special Foundation of Shaanxi Provincial Education Department in China (2013JK0880).

REFERENCES

[1] Kalam, M.A., Masjuki, H.H., Jayed, M.H., Liaquat, A.M. (2011) Emission and performance characteristics of an indirect ignition diesel engine fuel led with waste cooking oil. Energy. 36(1), 397-402.

[2] Felizardo, P., Neiva CorreiaM, J., Raposo, I. (2006) Production of biodiesel from waste frying oils. Waste Manage. 26(5), 487-494.

[3] Thamsiriroj, T., Murphy, J.D. (2010) How much of the target for biofuels can be met by biodiesel generated from residues in Ireland? Fuel. 89(11), 3579-89.

[4] Canakci, M., Gerpen, J.V., (2001) Biodiesel production from oils and fats with high free fatty acids. Trans ASAE. 44, 1429-36.

[5] David J. Sessa, Debra E. Palmquist, (2009) Decolorization/deodorization of zein via activated carbons and molecular sieves. Industrial Crops and Products. 30, 162-164.

[6] Riera-Torres, M., Gutiérrez, M. C. (2010) Colour removal of three reactive dyes by UV light exposure after electrochemical treatment. Chemical Engineering Journal. 156, 114-120.

[7] Chen, S.F., Liu, Y.Z. (2007) Study on the photocatalytic degradation of glyphosate by TiO_2 photocatalyst. Chemosphere. 67, 1010-1017.

[8] Aleboyeh, A., Aleboyeh, H., Moussa, Y. (2003) "Critical" effect of hydrogen peroxide in photochemical oxidative decolorization of dyes: acid orange 8, acid blue 74 and methyl orange. Dyes Pigments. 57, 67-75.

[9] Gengec, E., Kobya, M., Demirbas, E., Akyol, A., Oktor, K. (2012) Optimization of baker's yeast wastewater using response surface methodology by electrocoagulation. Desalination. 286, 200-209.

[10] Fargues, C., Sagne, C., Szymczyk, A., Fievet, P., Lameloise, M. L. (2013) Adsorption of small organic solutes from beet distillery condensates on reverse-osmosis membranes: consequences on the process performances. Journal of Membrane Science. 446, 132-144.

[11] Kurade, M.B., Waghmode, T.R., Kagalkar, A.N., Govindwar, S.P. (2012) Decolorization of textile industry effluent containing disperse dye Scarlet RR by a newly developed bacterial-yeast consortium BL-GG. Chemical Engineering Journal. 184, 33-41.

[12] MengWen, C., ChiaChun, C., JiaMing, C. (2010) Dye decomposition kinetics by UV/H_2O_2: Initial rate analysis by effective kinetic modelling methodology. Chemical Engineering Science. 65, 135-140.

[13] Doshi, V.A., Vuthaluru, H.B., Bastow, T. (2005) Investigations into the control of odour and viscosity of biomass oil derived from pyrolysis of sewage sludge. Fuel Processing Technology. J. 8, 885-897.
[14] Getoff, N. (2002) Factors influencing the efficiency of radiation-induced degradation of water pollutants. Radiat. Phys. Chem. 65, 437-446.
[15] Glowacki, J. (2005) A review of osteoinductive testing methods and sterilization processes for demineralized bone. Cell Tissue Bank. 6, 3-12.
[16] Zhang, S.J., Yu, H.Q. (2004) Radiation-induced degradation of polyvinyl alcohol in aqueous solutions. Water Res. 38, 309-316 .
[17] Chung, B.Y., Lee, J.T., Bai, H.-W., Kim, U.-J., Bae, H.-J., Wi, S.G., Cho, J.-Y. (2012) Enhanced enzymatic hydrolysis of poplar bark by combined use of gamma ray and dilute acid for bioethanol production. Radiat. Phys. Chem. 81, 1003-1007.
[18] Jo, B.W., Choi,S.K. (2014) Degradation of fucoidans from Sargassum fulvellum and their biological activities. Carbohydr. Polym. 111, 822-829.
[19] Galindo, C., Jacqes, P., Kalt, A. (2000) Photodegradation of the aminoazobenzene acid orange 52 by three advanced oxidation processes: UV/H_2O_2, UV/TiO_2 and VIS/TiO_2: comparative mechanistic and kinetic investigations. J Photochem Photobiol. 130, 35-47.
[20] Shaoqing, Y., Jun, H., Jianlong, W. (2010) Gamma radiation -induced degradation of p-nitrophenol (PNP) in the presence of hydrogen peroxide (H_2O_2) in aqueous solution. Journal of Hazardous Materials. 177. 1061-1067.
[21] Shi Peixin. (2004) Principle and Technology of Food Irradiation Processing. Chinese Agricultural Science and Technology Press, Beijing. 78-81.
[22] Xiang Yulin, Zhang Weijiang, Zheng Hao. (2010) Synergetic decolorization and deodorization of sludge protein foaming solution by ^{60}Co γ -ray irradiation/H_2O_2 oxidation. Process Safety and Environmental Protection. 88, 285-291.
[23] Gill, C. O., Jeremiah, L. E. (1991) The storage life of non-muscle of fats packaged under vacuum or carbon dioxide. Food Microbiology. 8, 339-353.
[24] Woods RT, Pikaev AK. (1994) Applied radiation chemistry: radiation processing. New York: Wiley. 341-342 .
[25] Wang Feng, Ha Yiming, Zhou Hongjie. (2005) Effect of irradiation on the nutrient composition of food. Food & Machinery. 21(5). 45-48.
[26] Lin Tse-Li , Lin Chun-I. (2009) Performances of peanut hull ashes in bleaching water-degummed and alkali-refined soy oil. Journal of the Taiwan Institute of Chemical Engineers. 40, 168-173.
[27] Xiang Yulin. (2011) Study on Improving Performances of Sludge Protein Foaming Solution by ^{60}Co-ray/H_2O_2 and Chemistry Methods. Tianjin University. 56-62.
[28] JI Xiang, ZHANG Shao-min, CAI Lu. (2012) Optimization of decoloring process for waste oils. Journal of Inner Mongolia University of Science and Technology. 185-188.
[29] Sabah E. (2007) Decolorization of vegetable oils: Chlorophyll-a adsorption by acid-activated sepiolite. Journal of Colloid and Interface Science. 310, 1-7.
[30] LIANG Fang-hui, YIN Ping-he, ZHAO Ling, WANG Yao. (2006) Decoloration of swill oil. China Oils and Fats. 31(2), 15-17.
[31] Deng Qi. (2004) Studies on Bleach Technology and Saponification Technology of Waste Edible Oil from Catering Trade. Jinan University. 55-56.
[32] Denniston, K.J., Topping, J.J., Cariet, R.L. (2004) In: General Organic and Biochemistry, fourth ed. McGraw Hill Companies, New York. pp. 432-433.
[33] Lu Yujie. (2011) Study on low temperature hydrogen peroxide bleaching system of cotton fabric. Dong Hua University.49-50.
[34] XU Hong-yong, CHENG Lian, WANG Dong-feng, ZENG Shi-qiao, YIN Zhao-ping, XU Yu-cheng. (2012) Identification of Recycled Cooking Oil by FT-IR. Modern Food Science and Technology. 28(6), 707-708,719.

Received: **30.09.2015**
Accepted: **19.01.2016**

CORRESPONDING AUTHOR

Yu-lin Xiang
College of Chemistry and Chemical Engineering,
Yulin University,
Yulin 719000 Shaanxi Province, CHINA

e-mail: yulinx@126.com

© by PSP Volume 25 – No. 7/2016, pages 2393-2403 Fresenius Environmental Bulletin

INVESTIGATION OF THE PARTICULATE MATTERS ON THE LEAVES OF *PLATANUS* SP. IN DENIZLI, TURKEY USING FESEM-EDS

Pinar Ili[1*], Nazan Keskin[2], Fikret Sari[3]

[1]Pamukkale University, Denizli Health Services Vocational High School, Department of Medical Services and Techniques, Denizli, Turkey.
[2]Pamukkale University, Faculty of Medicine, Department of Histology and Embryology, Denizli, Turkey.
[3]Pamukkale University, Faculty of Science and Arts, Department of Biology, Denizli, Turkey.

ABSTRACT

Particulate matters (PM) are released from plants, workshops, power generation, residential heating and motor vehicle emissions etc. and cause heavy-metal pollution in urban ecosystems. PM accumulate on the leaves of higher plants growing along roadsides. Plant leaves can be used as bioindicators for the heavy-metal pollutants in urban environments. The possible sources of the PM can be identified using determination of their morphology, size and chemical composition. *Platanus* sp. is widely cultivated near the roadsides of Denizli, Turkey. In this study, we aimed to investigate the possible sources of the PM on the leaf of *Platanus* sp. using Field Emission Scanning Electron Microscope-Energy Dispersive Spectroscopy (FESEM-EDS) during 2013-2014. Leaves were collected from urbanized areas and a control region. The size distribution and the chemical composition of the PM showed some similarities and distinct differences in the study areas. These data suggested that investigated areas were mainly affected from anthropogenic activities and crustal sources depending on their locations. In conclusion, the results of this study are significant in helping understand the possible origins using chemical composition and size of the PM using FESEM-EDS. Also, roadside plants can be used as important bioindicators for the assessment of PM in the urban environment.

KEYWORDS:
Platanus sp., particulate matter, FESEM-EDS, air pollution

INTRODUCTION

Urbanization and industrialization can lead to heavy-metal pollution in urban ecosystems. Roadsides in urban and industrial areas are mainly affected by particular matters (PM) released from plants, workshops, power generation, residential heating and motor vehicle emissions etc. Hazardous chemicals may cause adverse effects on human health and the environment and are released into the environment by a number of natural and/or anthropogenic activities [1]. Hence, analysis of heavy-metal pollutants in urban environments has been of growing interest with the goal to identify the extent and content of PM.

Plants can be used as useful bioindicators for the assessment of environmental pollution in soil and atmosphere of urban areas [2-5]. They have a great ecological importance and so on, have attracted attention of environmental investigations. In this respect, several studies were carried out using plants such as mosses and lichens [6-9] and higher plants [10-19] as bioaccumulators or bioindicators in environmental investigations.

Plants are generally known to be in need of several major elements such as Phosphorus (P), Calcium (Ca), Magnesium (Mg) for their normal growth process. On the other hand, excessive amounts of these elements in soil may have toxic effects on the plants [20]. These elements are deposited in different parts of plants such as on leaf surfaces as PM. They can be originated from both soil and atmospheric pollution. The identification of the morphology and chemical composition of the PM on the leaves of plants may indicate the nature of contaminant present in the surrounding area and possible sources as well [21,22].

In general, *Platanus* sp., also known as planes or plane trees, is a large deciduous tree growing 20-50 m, with a trunk up to 3 m or more in circumference. *Platanus* sp. is also widely cultivated trees near the roadsides of the city, Denizli. The city of Denizli, in the southwest corner of the Aegean Region of Turkey, is a fast growing and industrializing city with about 963464 inhabitants within the extent of the municipal area. The major industries in the city are textile, leather, machinery, manufacturing and metal working industries. In this study, we purposed to find out elemental compositions and sizes of PM on the leaf surfaces of *Platanus* sp. collected in years 2013 and 2014 along the roadsides of different locations with

varying degrees of high traffic and urbanization density. The controls were collected from Mount Honaz (the highest mountain in the Aegean Region) which was considered unpolluted area of Denizli city. Then, all samples were analyzed using Field Emission Scanning Electron Microscope-Energy Dispersive Spectroscopy (FESEM-EDS) techniques.

MATERIALS AND METHODS

Leaf samples of *Platanus* sp., including controls from Mount Honaz, were collected in September 2013 and June 2014 from five different regions of Denizli (Table 1). All of the leaf samples were taken from trees at a height of at least 2.2 m above the ground. The shade and air dried unwashed samples were dried in an oven at 60°C for 4 hours [23].

Portions of dried leaf samples were mounted on Aluminum (Al) stubs and coated with Carbon (C) before the analysis. The micrographs of the leaf samples were recorded using FESEM (Zeiss, Supra 40VP) with accelerating voltage of 10 keV, at High Vacuum (HV) mode and Secondary Electron Detector (SE2). The quantification elemental analysis to identify the weight percentage of major and minor elements present in the samples was done using EDS.

PM (particles 0.005<PM<100 µm in diameter) are classified according to its size: Ultrafine or PM0.1 (particles<0.1 µm in diameter); fine or PM2.5 (particles≤2.5 µm in diameter); coarse or PM10 (particles≤10 µm in diameters); total suspended particles (TSP) (particles<40 µm) [24,25]. Investigation of element composition, size distribution and source apportionment can be useful to better understand and manage the effects of aerosols on health and air quality [26]. For this purpose, the calculation of the diameter of the particles on the leaf surfaces was performed with specific software on the micrographs of the leaf samples.

RESULTS

FESEM analysis of the morphology and size of the particles deposited on unwashed *Platanus* sp. leaf surfaces was performed, and it was observed that these particles were in irregular forms on the samples collected in both years. They were found in both single and clustered particles on the leaf surfaces. However, there were not a lot of PM on the leaf surfaces of control when compared to the samples collected from polluted areas (Figure 1).

Chemical species concentrations of PM. The FESEM-EDS analysis was made from samples collected from different regions in both years. FESEM micrograph illustrated the accumulation of the different sized (diameters ranging from approximately 1 to 45 µm) particles on the leaf surfaces collected along the roadsides of urbanized area. In addition, EDS analyses showed that there were distinct differences and also some similarities in the elemental composition of the particles. The representative FESEM images and the EDS spectrums of one of the investigated areas are presented in Figure 2.

TABLE 1
Description of locations of leaves sampled in Denizli, Turkey.

Region no.	Region name	Distance from the city center	Remarks
1	Kayalar	About 4 km west of the highway entering the city	Has heavy vehicular traffic emissions and industrial activities
2	Ucgen	In center	Has heavy vehicular traffic emissions and other anthropogenic activities
3	Ulus	About 2 km	Has heavy vehicular traffic emissions and other anthropogenic activities
4	Campus	About 3 km	Has vehicular traffic emissions, construction of new buildings and other anthropogenic activities
5	Honaz	About 20 km east of downtown Denizli	Near the organized industrial zone and has other anthropogenic activities
Control	Honaz Mountain	About 17 km southeast of Denizli city	Unpolluted area

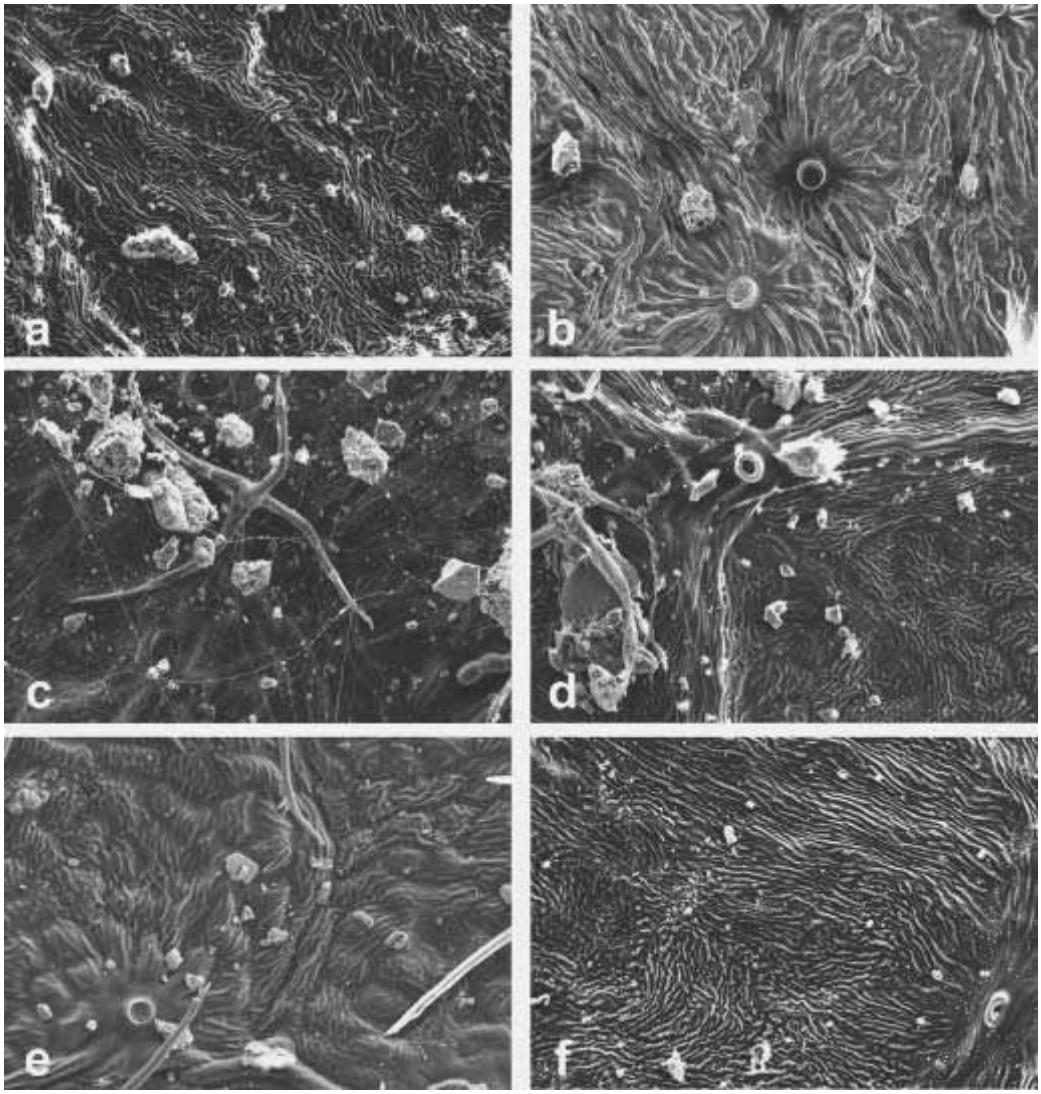

FIGURE 1
FESEM micrographs of particles deposited on the surfaces of *Platanus* sp. leaves, in Kayalar (a), Ucgen (b), Ulus (c), Honaz (d), and Campus (e) in 2013 and Control (f) in 2014 at 1000X magnification. Note that there is no much more PM in control compared with the other regions.

The weight percentages of the elements in the particles of the samples obtained from EDS analysis were exhibited some differences in terms of sample collection time and/or regions in both years (Table 2; Figure 3). According to the analyses;

1) In Kayalar; C and Ca contents decreased, while Silicon (Si), Al, Iron (Fe), Mg, Sodium (Na), Potassium (K) and Sulfate (S) contents increased in 2014. Oxygen (O) contents were almost the same in both years.

2) In Ucgen; Si, Al, Ca, Mg, K, Ca and S contents decreased, but C, Fe and Na contents increased in 2014. The O content was almost the same for both years.

3) In Ulus; O and C contents decreased, whereas Si, Al, Fe, Mg, Na, K and S contents increased in 2014.

4) In Honaz; O, Al, Mg, Na, K and Ca contents decreased however C, Si, Fe and S contents increased in 2014.

5) In Campus; C and Na contents decreased, but O, Al, Fe, Mg, K, Ca and S contents increased in 2014. Si contents of particles were almost the same in both years.

6) In Mount Honaz (control); Na, Flour (F), S, Chlorine (Cl), Copper (Cu), Nitrogen (N), P, Chromium (Cr), Arsenic (As) and Tungsten, also known as Wolfram (W), detected on the contaminated leaves were not detected. Interestingly, the alkaline earth element Mg is higher in the control than in all other samples.

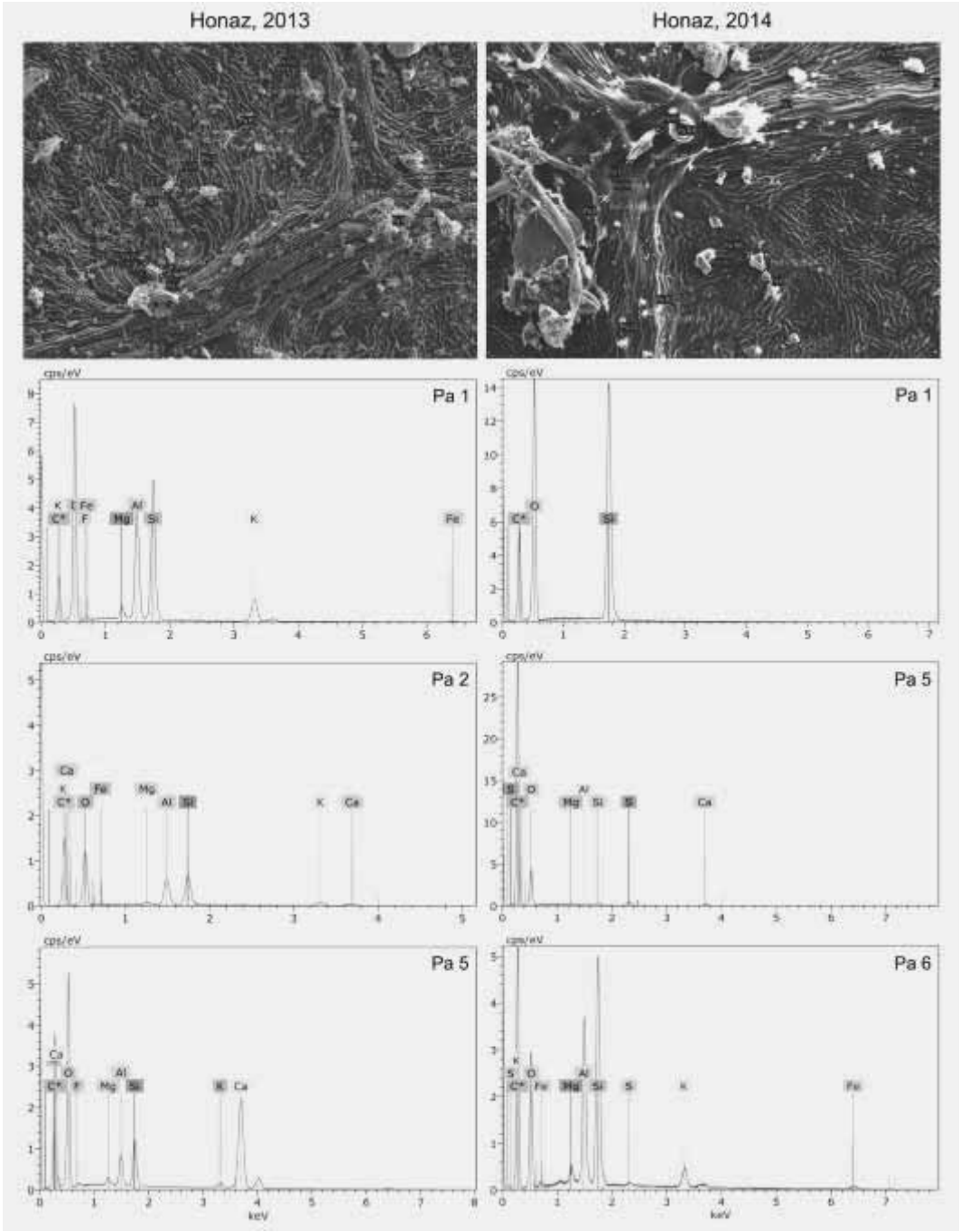

FIGURE 2
FESEM micrographs showing diameters of some deposited particles at 1000X magnification and the representative EDS spectrums of three particles (ranging from 1.965-25.72 µm) selected from the leaf surfaces of the collected samples from Honaz in 2013 and 2014.

The C contents of the particles represented remarkable changes as increasing and decreasing values in all regions in the years. A remarkable increase in Ucgen and Honaz and a remarkable decrease in Kayalar, Ulus and Campus were observed. In Ucgen, the small amounts of Cu and As were found in 2013, and the small amounts of N and P were found in 2014. The Cl was detected on the samples of Kayalar, W was detected on the samples of Ulus, and F was detected in Honaz in 2013. The heavy metal Cr was present only in the samples of Kayalar in 2014.

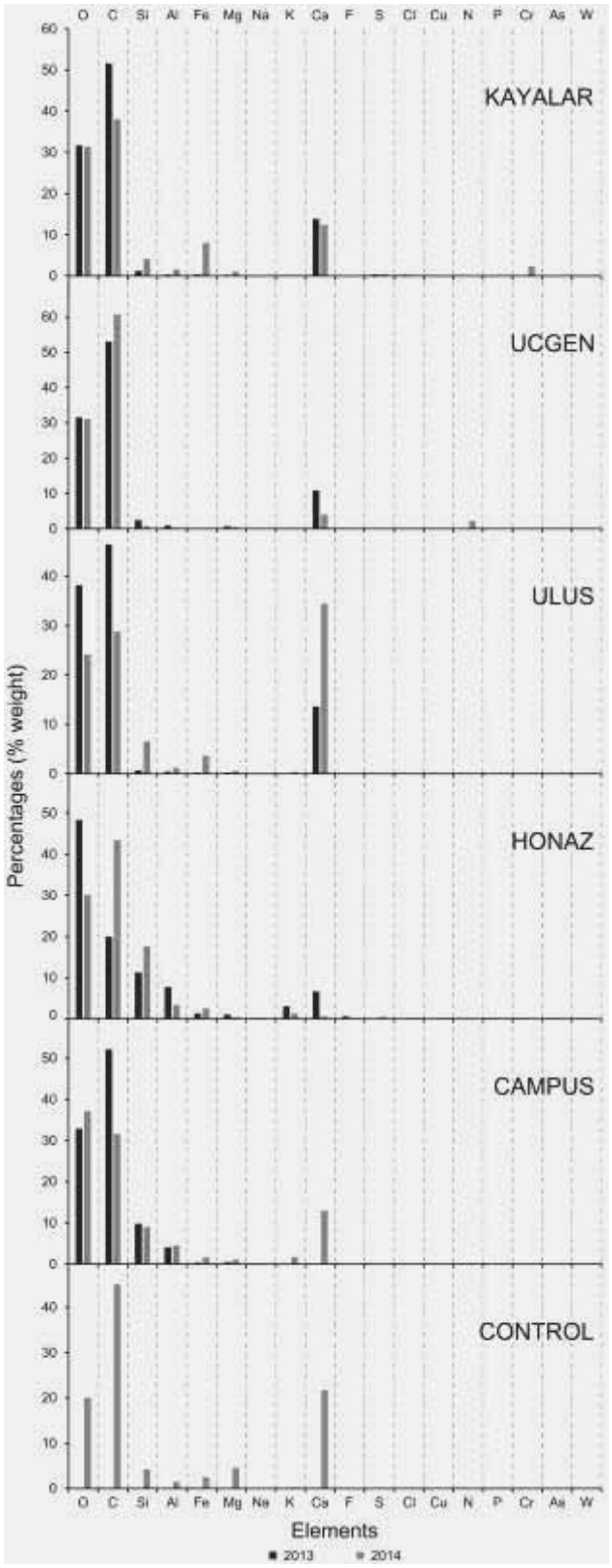

FIGURE 3
Comparative percentages (% weight) of the elements on the leaves collected from study regions in 2013 and 2014. Note that some of the elements analyzed exhibited decrease and increase in percentages, some are completely absent in some regions of the study area.

TABLE 2

FESEM-EDS analytical data (average wt. %) on particles constituting on leaves of *Platanus* sp. collected in September, 2013 and June, 2014 from the study area with controls.

Elements	Years	Kayalar	Ucgen	Ulus	Honaz	Campus	Control
O	2013	31.730	31.527	38.190	48.287	32.880	
	2014	31.380	31.190	24.143	30.123	37.153	20.073
C	2013	51.630	53.033	46.463	19.960	52.133	
	2014	38.073	60.743	28.790	43.417	31.627	45.087
Si	2013	1.237	2.460	0.730	11.267	9.823	
	2014	4.107	0.747	6.527	17.620	9.013	4.247
Al	2013	0.330	0.903	0.470	7.703	4.093	
	2014	1.593	0.260	1.257	3.400	4.547	1.510
Fe	2013	0.370	0	0.227	1.317	0.387	
	2014	8.077	0.027	3.677	2.537	1.623	2.520
Mg	2013	0.227	0.710	0.250	0.987	0.477	
	2014	1.110	0.473	0.577	0.417	1.097	4.597
Na	2013	0	0.050	0	0.187	0.203	
	2014	0.083	0.153	0.103	0	0.150	0
K	2013	0	0.213	0	3.017	0	
	2014	0.273	0	0.390	1.380	1.750	0.237
Ca	2013	13.827	10.883	13.623	6.650	0	
	2014	12.487	4.083	34.460	0.600	13.013	21.723
F	2013	0	0	0	0.627	0	
	2014	0	0	0	0	0	0
S	2013	0.353	0.113	0	0	0	
	2014	0.460	0.050	0.067	0.513	0.023	0
Cl	2013	0.293	0	0	0	0	
	2014	0	0	0	0	0	0
Cu	2013	0	0.003	0	0	0	
	2014	0	0	0	0	0	0
N	2013	0	0	0	0	0	
	2014	0	2.240	0	0	0	0
P	2013	0	0	0	0	0	
	2014	0	0.033	0	0	0	0
Cr	2013	0	0	0	0	0	
	2014	2.360	0	0	0	0	0
As	2013	0	0.103	0	0	0	
	2014	0	0	0	0	0	0
W	2013	0	0	0.043	0	0	
	2014	0	0	0	0	0	0

Size distributions. Figure 4 represents the average concentrations of the chemical elements in the PM of different diameter deposited on the leaves in all regions. One group of elements (such as C and S) was present in high percentages in the PM2.5 particles. Some of metals had higher percentages in the PM10 particles. These were K, Cu, N and W. The high percentages obtained for O, Si, Al, Fe, Mg, Na, Ca, F, Cl, P, Cr and As in the TSP (Figure 4). It was remarkable that the average trace metal concentrations were highest at industrial and traffic hotspots by even one order of magnitude in the cases of Cr, As, W and Cu.

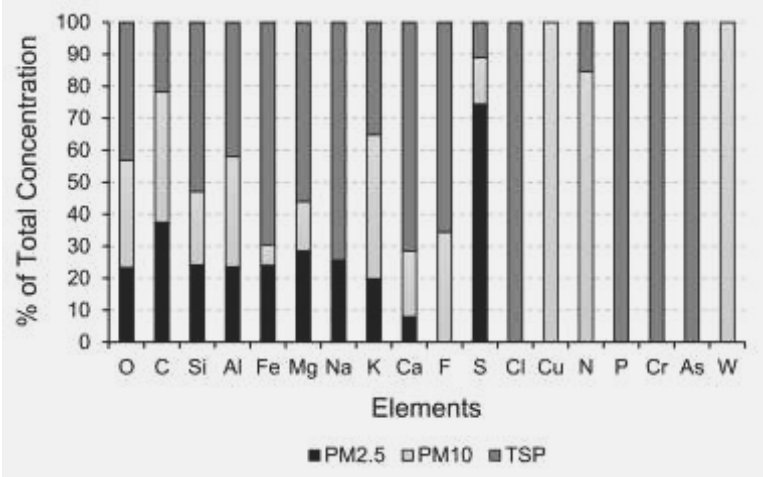

FIGURE 4
The average concentration distribution of the individual elements according to size fraction from all regions in both years.

DISCUSSION

Tree leaves can be used to perform FESEM-EDS analysis for air pollution monitoring [22]. In this study, the analyses were carried out in order to examine the shape, size and elemental composition of the particles on the leaf surfaces of *Platanus* sp. which were collected from urbanized regions of Denizli using FESEM-EDS.

In the previous studies, it has been shown that TSP is rich in Fe [27,28], Al, Mg [28,29], Si, P, Cr [29] and Ca [28]. It has been suggested that Mg, Al, Si, P and Cr could be originated from soil or road dust [29] and Ca, Mg and Al could be related with dust resuspension [28]. Besides, Tomašević et al. [30] reported that soil dust mainly contained Si, Al, Fe, Mg, N, S, Ca, K and Cl. In this study, we found Si, Al, Fe, Mg, Na, Ca, F, Cl, P, As, Cr, K, C, S and N in TSP. According to the data of previous studies, we can suggest that Si, Al, Fe, Mg, Ca, P and Cr containing TSP found on the leaf surfaces of *Platanus* sp. may be originated from soil or road dust.

P is emitted from different sources (such as emissions from dust and sea-salt transport, volcanic eruptions, biogenic sources and combustion of fossil fuels, biofuels and biomass) [31]. As can be released from natural sources (such as wind-blown soil and volcanoes) as well as being released from anthropogenic sources (such as nonferrous metal mining and smelting, pesticide application, coal combustion, wood combustion and waste incineration) (http://www.atsdr.cdc.gov/toxprofiles/tp2-c6.pdf). F can be found in air, water, plants and animals, and are also naturally-occurring component of rocks and soil, and it can be released from anthropogenic factors (such as combustion of fluorine-containing materials, coal-fired power plants) and natural sources (such as volcanic emissions and the resuspension of soil by wind) (http://www.atsdr.cdc.gov/toxprofiles/tp11-c6.pdf) [32]. Cl can be originated from incineration of organohalide polymer wastes [33]. In the present study, P containing TSP in 2014 and As containing TSP in 2013 in Ucgen (has heavy vehicular traffic emissions and other anthropogenic activities) may be related with coal combustion, soil dust or pesticide application. TSP, which contains F and Cl, were detected only in Honaz and in Kayalar in 2013, respectively. Because these areas are close to the organized industrial (Honaz) and the municipal waste incineration zone (Kayalar), and have another anthropogenic activities, presumably, F and Cl contents in TSP can be originated from soil dust or anthropogenic factors and from incineration of organohalide polymer wastes, respectively.

Karanasiou et al. [34] found Al, Fe, Cu and Cr in PM10, which were originated from soil dust or mechanical abrasion processes. Lough et al. [35] reported that PM10 contained crustal elements such as Si, Fe, Ca, Na, Mg, Al and K, and tailpipe emissions and brake and tire wear related elements such as Cu, Zn, Sb, Ba, Pb and S. Ca, Mg, Fe and Al were found as most abundant elements in TSP and PM10, and Ca, Mg and Al were estimated to be originated from resuspension of dust [28]. Zhang et al. [36] also reported that C-dominant particles (average diameters of 8.43 μm) were formed from unburned coal. In the present study, K, Cu, N, W, C, Al, Ca, S, Si, Fe, Mg and F were detected in PM10. It has been suggested that PM10 can be formed from soil dust, mechanical abrasion processes, tailpipe emissions, brake and tire wear, dust resuspension and unburned coal in the urbanized areas in Denizli. These results showed similarities with the data which inform that PM10

usually contain crustal materials and fugitive dust from roads and industry [37].

In the atmosphere, three forms of N are of special importance. These are; a: NO_X (oxidized N; as an unnecessary waste product of combustion processes, such as traffic and industries), b: NH_3 (reduced N; from agricultural practices) and c: N_2O (from soils nitrification and de-nitrification processes) [38]. In this study, N was found highly in PM10 in 2014, in Ucgen. This may be released from traffic, industries and soils nitrification and de-nitrification processes.

W is one of the rare elements. It can be released to the atmosphere either naturally as wind-blown dusts or from anthropogenic processes such as ore processing, hard-metal fabrication, tungsten carbide production and use, and municipal waste combustion (http://www.atsdr.cdc.gov/toxprofiles/tp186-c6.pdf). In this study, W was detected on the leaf samples as an accumulated PM in Ulus in 2013, and it indicates the possibility of soil contamination originated from natural sources.

It has been shown that PM2.5 can be rich in Fe [34,39,40], Al [34,40] and Na [40]. Together with these elements, Ca, K, Mg and Ti were considered as crustal origin elements [41]. Also, the origin of Al and Fe was estimated as soil dust or mechanical abrasion processes [34]. Additionally, mineral, organic and elemental C were described as most important components present in the PM2.5, and the main source of these particles was suggested as heavy fuel combustion, traditional brick production-agricultural burning, crustal, road traffic and secondary organic aerosols [42]. Besides, C rich particles were described as soot by Tomašević et al. [30]. In the present study, C, S, Si, Fe, Mg, Al, Na, K and Ca in PM2.5 on the leaf surfaces of *Platanus* sp. were observed. Fe, Al, Si, Mg, S, Na, K and Ca containing PM2.5 may be related with soil dust or mechanical abrasion processes, and C rich PM2.5 can be related with crustal sources, road traffic and secondary organic aerosols or suggested as soot emitted from heavy fuel combustion.

Besides, S formed by sulfur dioxide emissions from power plants and industrial facilities (http://www.epa.gov). Tomašević et al. [30] and Lough et al. [35] reported that there was K in soil dust. Ca can be emitted from cement, iron and steel plants, and coal combustion in domestic and industrial boilers [43]. It has been also demonstrated that the geological dust contains high Ca [44]. In this study, S, K and Ca were detected in study areas having heavy vehicular traffic emissions, industrial activities, construction of new buildings and other anthropogenic activities. In the light of previous studies, the origins of S, K and Ca can be speculated to be coal combustion, power plants and industrial facilities; soil dust; industrial activities and coal combustion in domestic boilers, respectively.

In addition to all, it should be noted that the dust deposition on leaves may have physical and chemical phytotoxic effects on plants [45]. Coating with dust of the leaves may cause abrasion and radiative heating and reduce the photosynthetically active photon flux. Also, while other materials may be taken up across the cuticle, leaf surface injury may occur in the presence of acidic and alkaline materials [46]. For instance, opening and closing of stomata hindered by the presence of nutrition elements (Ca, Fe, Mg, K and Mn) on foliage surface [47]. Even though P is known as an essential element for plant growth, internal precipitation of P by Al inhibits plant growth [48]. Additionally, it has been shown that airborne pollutants may influence leaf elemental composition of *Quercus ilex* L. leaves [49]. The effects of F on vegetation have been also known for many years. It has been reported that F from the air can be adsorbed to the surface of leaves and accumulated internally, and it can be translocated both outward to the surface and upward to the tips [50]. Some plants accumulating high levels of F in their leaves exhibit acute necrosis, chlorosis or both [51]. Cr has toxic effects on plant growth and development (such as alterations in the germination process and in the growth of roots, stems and leaves), deleterious effects on photosynthesis, water relations and mineral nutrition, and causes metabolic alterations by a direct effect on enzymes or other metabolites or by generating reactive oxygen species (oxidative stress) [52].

It has been also reported that combustion emissions cause over half of the fine particle (PM2.5) air pollution and most of the primary particulate organic matter [53]. The chemical and structural characterization of airborne PM is of great importance in the evaluation of possible risk to human health and the identification of pollution sources [54]. Personal exposures to airborne particles between various combustion emissions and other sources [including vehicles (e.g., diesel and gasoline vehicles), heating and power sources (e.g., including coal, oil, and biomass), indoor sources (e.g., cooking, heating, and tobacco smoke), secondary organic aerosols and pollutants derived from long-range transport] may cause oxidative and DNA damage that can lead to reproductive and cardiovascular effects [53]. It has been reported that in general, <PM10 size fractions have the highest toxicity, contain higher concentrations of extractable organic matter, and possess a relatively high radical-generating capacity [55]. Exposure to ambient metals like Nickel (Ni), Vanadium (V), and Zinc (Zn) and Elemental Carbon (EC) from heating oil and/or traffic at levels characteristic of urban environments may be associated with respiratory symptoms (such as

wheeze and cough) among very young children [56]. Larger PM (larger than 10 µm) can irritate the eyes, nose and throat, but do not usually reach the lungs, while the particles less than 10 µm can be inhaled deep into the lungs (http://www.cwru.edu/med/epidbio/mphp439/partmatter_cordis.pdf; http://www.ehib.org/page.jsp?page_key=90). Short- and long-term exposures to air pollution affecting a number of different systems and organs, such as minor upper respiratory irritation, chronic respiratory and heart disease, lung cancer, acute respiratory infections in children and chronic bronchitis in adults, aggravating pre-existing heart and lung disease, or asthmatic attacks, caused premature mortality and reduced life expectancy [1].

The results of this study are significant in helping understand the possible origins using chemical composition and size of the PM which are known to have the deleterious effects on the health of human and plant in Denizli, Turkey and in improving our understanding of the true picture of particle sources and composition in different regions.

CONCLUSIONS

In summary, FESEM-EDS analysis of some PM on the leaves of *Platanus* sp. in various regions of Denizli in 2013-2014 showed that;

1) Particle size differences (approximately from 1 to 45 µm) mainly depend on its origin.

2) Particularly, study areas (Kayalar, Ucgen, Ulus, Campus and Honaz) were influenced by anthropogenic activities, such as vehicular emission and local industrial activities or crustal matters.

3) FESEM-EDS is a useful technique for the determination of the size and the chemical compositions of the PM.

4) Roadside plants could be used as important bioindicators for the assessment of PM in the urban environment.

ACKNOWLEDGEMENTS

The works of analysis were conducted at Pamukkale University Electron Microscope Unit (PAUEMB), Kinikli-Denizli, Turkey. A part of the manuscript was presented at the "2nd International Conference on Environmental Science and Technology (ICOEST'2014)", Side, Antalya, Turkey, 2014.

REFERENCES

[1] Kampa, M. and Castanas, E. (2008) Human health effects of air pollution. Environ. Pollut., 151(2), 362–367.

[2] Gautam, P., Blaha, U. and Appel, E. (2005) Magnetic susceptibility of dust-loaded leaves as a proxy of traffic-related heavy metal pollution in Kathmandu City, Nepal. Atmos. Environ., 39(12), 2201–2211.

[3] Madejón, P., Marañón, T., Murillo, J.M. and Robinson, B. (2004) White poplar (*Populus alba*) as a biomonitor of trace elements in contaminated riparian forests. Environ. Pollut., 132(1), 145–155.

[4] Mingorance, M.D. and Oliva, S.R. (2006) Heavy metals content in *N. oleander* leaves as urban pollution assessment. Environ. Monit. Assess., 119(1-3), 57–68.

[5] Rossini, O.S. and Mingorance, M.D. (2006) Assessment of airborne heavy metal pollution by aboveground plant parts. Chemosphere, 65(2), 177–182.

[6] Giordano, S., Adamo, P., Sorbo, S. and Vingiani, S. (2005) Atmospheric trace metal pollution in the Naples urban area based on results from moss and lichen bags. Environ. Pollut., 136(3), 431–442.

[7] Jalkanen, L., Mäkinen, A., Häsänen, E. and Juhanoja, J. (2000) The effect of large anthropogenic particulate emissions on atmospheric aerosols, deposition and bioindicators in the Eastern Gulf of Finland Region. Sci. Total Environ., 262(1-2), 123–136.

[8] Riget, F., Asmund, G. and Aastrup, P. (2000) The use of lichen (*Cetraria nivalis*) and moss (*Rhacomitrium lanuginosum*) as monitors for atmospheric deposition in greenland. Sci. Total Environ., 245(1-3), 137–148.

[9] Szarek-Łukaszewska, G., Grodzińska, K. and Braniewski, S. (2002) Heavy metal concentration in the moss *Pleurozium schreberi* in the Niepołomice Forest, Poland: Changes during 20 years. Environ. Monit. Assess., 79(3), 231–237.

[10] Akgüç, N., Özyiğit, İ.İ. and Yarcı, C. (2008) *Pyracantha coccinea* Roem. (Rosaceae) as a biomonitor for Cd, Pb and Zn in Mugla Province (Turkey). Pak. J. Bot., 40(4), 1767–1776.

[11] Aksoy, A., Sahin, U. and Duman, F. (2000) *Robinia pseudo-acacia* L. as a posssible biomonitor of heavy metal pollution in Kayseri. Turk. J. Bot., 24, 279–284.

[12] Aksoy, A. and Demirezen, D. (2006) *Fraxinus excelsior* as a biomonitor of heavy metal pollution. Pol. J. Environ. Stud., 15(1), 27–33.

[13] Aksoy, A. and Öztürk, M.A. (1997) *Nerium oleander* L. as a biomonitor of lead and other

heavy metal pollution in Mediterranean Environments. Sci. Total Environ., 205(2-3), 145–150.
[14] Aksoy, A. and Sahin, U. (1999) *Elaeagnus angustifolia* L. as a biomonitor of heavy metal pollution. Turk. J. Bot., 23, 83–87.
[15] Celik, A., Kartal, A.A., Akdoğan, A. and Kaska, Y. (2005) Determining the heavy metal pollution in Denizli (Turkey) by using *Robinio pseudo-acacia* L. Environ. Int., 31(1), 105–112.
[16] Dongarrà, G., Sabatino, G., Triscari, M. and Varrica, D. (2003) The effects of anthropogenic particulate emissions on roadway dust and *Nerium oleander* leaves in Messina (Sicily, Italy). J. Environ. Monitor., 5(5), 766–773.
[17] Hodson, M.J. and Sangster, A.G. (1998) Mineral deposition in the needles of white spruce [*Picea glauca* (Moench.) Voss]. Ann. Bot., 82(3), 375–385.
[18] Keskin, N. and Ili, P. (2012) Investigation of particular matters on the leaves of *Pinus nigra* Arn. subsp. *pallasiana* (Lamb.) Holmboe in Denizli (Turkey). Pak. J. Bot., 44(4), 1369–1374.
[19] Yılmaz, R., Sakcalı, S., Yarcı, C., Aksoy, A. and Ozturk, M. (2006) Use of *Aesculus hippocastanum* L. as a biomonitor of heavy metal pollution. Pak. J. Bot., 38(5), 1519–1527.
[20] Agrios, G.N. (2005) Plant Pathology (fifth edition). Elsevier Academic Press, California.
[21] Campos-Ramos, A., Aragón-Piña, A., Galindo-Estrada, I., Querol, X. and Alastuey, A. (2009) Characterization of atmospheric aerosols by SEM in a rural area in the western part of México and its relation with different pollution sources. Atmos. Environ., 43(39), 6159–6167.
[22] Ram, S.S., Majumdar, S., Chaudhuri, P., Chanda, S., Santra, S.C., Maiti, P.K., Sudarshan, M. and Chakraborty, A. (2012) SEMEDS: An important tool for air pollution bio-monitoring. Micron 43(2-3), 490–493.
[23] Ramamurthy, N. and Kannan, S. (2009) SEM-EDS analysis of soil and plant (*Calotropis gigantea* Linn) collected from an industrial village, Cuddalore DT, Tamil Nadu, India. Rom. J. Biophys., 19(3), 219–226.
[24] Particulate Air Pollution (2015) http://www.carexcanada.ca/en/particulate_air_pollution/#sources.
[25] Shen, G., 2014. Emission Factors of Carbonaceous Particulate Matter and Polycyclic Aromatic Hydrocarbons from Residential Solid Fuel Combustions. Springer Theses, DOI: 10.1007/978-3-642-39762-2_2, Springer-Verlag Berlin Heidelberg.
[26] Hu, X., Ding, Z., Zhang, Y., Sun, Y., Wu, J., Chen, Y. and Lian, H. (2013) Size distribution and source apportionment of airborne metallic elements in Nanjing, China. Aerosol Air Qual. Res., 13(6), 1796–1806.
[27] Allen, A.G., Nemitz, E., Shi, J.P., Harrison, R.M. and Greenwood, J.C. (2001) Size distributions of trace metals in atmospheric aerosols in the United Kingdom. Atmos. Environ., 35(27), 4581–4591.
[28] Loyola, J., Arbilla, G., Quiterio, S.L., Escaleira, V. and Bellido, A.V. (2009) Concentration of airbone trace metals in a bus station with a high heavy-duty diesel fraction. J. Brazil. Chem. Soc., 20(7), 1343–1350.
[29] Petaloti, C., Triantafyllou, A., Kouimtzis, T. and Samara, C. (2006) Trace elements in atmospheric particulate matter over a coal burning power production area of Western Macedonia, Greece. Chemosphere, 65(11), 2233–2243.
[30] Tomašević, M., Vukmirović, Z., Rajšić, S., Tasić, M. and Stevanović, B. (2005) Characterization of trace metal particles deposited on some deciduous tree leaves in an urban area. Chemosphere, 61(6), 753–760.
[31] Wang, R., Balkanski, Y., Boucher, O., Ciais, P., Peñuelas, J. and Tao, S. (2015) Significant contribution of combustion-related emissions to the atmospheric phosphorus budget. Nat. Geosci., 8, 48–54.
[32] Ando, M., Tadano, M., Asanuma, S., Tamura, K., Matsushima, S., Watanabe, T., Kondo, T., Sakurai, S., Ji, R., Liang, C. and Cao, S. (1998) Health effects of indoor fluoride pollution from coal burning in China. Environ. Health Persp., 106(5), 239–244.
[33] Manahan, S.E. (2000) Environmental Chemistry (seventh edition). CRC Press LLC, Boca Raton.
[34] Karanasiou, A.A., Sitaras, I.E., Siskos, P.A. and Eleftheriadis, K. (2007) Size distribution and sources of trace metals and N-alkanes in the Athens urban aerosol during summer. Atmos. Environ., 41(11), 2368–2381.
[35] Lough, G.C., Schauer, J.J., Park, J.S., Shafer, M.M., DeMinter, J.T. and Weinstein, J.P. (2005) Emissions of metals associated with motor vehicle roadways. Environ. Sci. Technol., 39(3), 826–836.
[36] Zhang, X.L., Wu, G.J., Yao, T.D., Zhang, C.L. and Yue, Y.H. (2011) Characterization of individual fly ash particles in surface snow at Urumqi Glacier No. 1, Eastern Tianshan. Chin. Sci. Bull., 56(32), 3464–3473.
[37] Amann, M., Derwent, R., Forsberg, B., Hurley, F., Krzyzanowski, M., Kuna-Dibbert, B., Larssen, S., de Leeuw, F., Liu, S.J., Schneider, J., Schwarze, P.E., Simpson, D., Stedman, J., Straehl, P., Tarrasón, L. and van

Bree, L. (2006) Health risks of particulate matter from long-range transboundary air pollution. WHO Regional Office for Europe, Denmark.
[38] Erisman, J.W., Brydges, T., Bull, K., Cowling, E., Grennfelt, P., Nordberg, L., Satake, K., Schneider, T., Smeulders, S., Van der Hoek, K.W., Wisniewski, J.R. and Wisniewski, J. (1998) Summary statement. In: Nitrogen, the Confer-N-s, Proceedings of the First International Nitrogen Conference. Van der Hoek, et al., editors. Elsevier, Oxford, 3–12.
[39] Sagnotti, L., Taddeucci, J., Winkler, A. and Cavallo, A. (2009) Compositional, morphological, and hysteresis characterization of magnetic airborne particulate matter in Rome, Italy. Geochem. Geophy. Geosy., 10(8), DOI: 10.1029/2009GC002563.
[40] Yongjie, Y., Yuesi, W., Tianxue, W., Wei, L., Ya'nan, Z., Liang, L., 2009. Elemental composition of PM2.5 and PM10 at Mount Gongga in China. Atmos. Res., 93(4), 801–810.
[41] Caggiano, R., Macchiato, M., Ragosta, M., Sabia, S., Scardaccione, G.A. and Trippetta, S. (2008) Trace elements in daily collected PM1 samples and source identification. AAAS08-Advanced Atmospheric Aerosol Symposium, Napoli, 169-176.
[42] Murillo, J.H., Ramos, A.C., García, F.A., Jiménez, S.B., Cárdenas, B. and Mizohata, A. (2012) Chemical composition of PM2.5 particles in Salamanca, Guanajuato Mexico: source apportionment with receptor models. Atmos. Res., 107, 31–41.
[43] Lee, D.S. and Pacyna, J.M. (1999) An industrial emissions inventory of calcium for Europe. Atmos. Environ., 33(11), 1687–1697.
[44] Chow, J.C, Watson, J.G., Kuhns, H., Etyemezian, V., Lowenthal, D.H., Crow, D., Kohl, S.D., Engelbrecht, J.P. and Green, M.C. (2004) Source profiles for industrial, mobile, and area sources in the big bend regional aerosol visibility and observational study. Chemosphere, 54(2), 185–208.
[45] Farmer, A.M. (1993) The effects of dust on vegetation—a review. Environ. Pollut., 79(1), 63–75.
[46] Grantz, D.A., Garner, J.H.B. and Johnson, D.W. (2003) Ecological effects of particulate matter. Environ. Int., 29(2-3), 213–239.
[47] Maňkovská, B., Oszlányi, J. and Barančok, P. (2008) Effects of air pollution on key tree species of the Carpathian Mountains. Ekologia Bratislava, 27(3), 248–268.
[48] Wright, K.E. (1943) Internal precipitation of phosphorus in relation to aluminium toxicity. Plant Physiol., 18(4), 708–712.
[49] Alfani, A., Maisto, G., Iovieno, P., Rutigliano, F.A. and Bartoli, G. (1996) Leaf contamination by atmospheric pollutants as assessed by elemental analysis of leaf tissue, leaf surface deposit and soil. J. Plant Physiol., 148(1-2), 243–248.
[50] Jacobson, J.S., Weinstein, L.H., Mccune, D.C. and Hitchcock, A.E. (1966) The accumulation of fluorine by plants. J. Air Pollut. Control Assoc., 16(8), 412–417.
[51] Haidouti, C., Chronopoulou, A. and Chronopoulos, J. (1993) Effects of fluoride emissions from industry on the fluoride concentration of soils and vegetation. Biochem. Syst. Ecol., 21(2), 195–208.
[52] Shanker, A.K, Cervantes, C., Loza-Tavera, H. and Avudainayagam, S. (2005) Chromium toxicity in plants. Environ. Int., 31(5), 739–753.
[53] Lewtas, J. (2007) Air pollution combustion emissions: characterization of causative agents and mechanisms associated with cancer, reproductive, and cardiovascular effects. Mutat. Res., 636(1-3), 95–133.
[54] Ochsenkühn-Petropoulou, M., Lyberopoulou, T., Argyropoulou, R., Tsopelas, F. and Ochsenkühn, K.M. (2009) Chemical and structural characterization of airborne particulate matter in an industrial and an urban area in Greece. Fresenius Environ. Bull., 18(11A), 2210–2218.
[55] de Kok, T.M., Driece, H.A., Hogervorst, J.G. and Briedé, J.J. (2006) Toxicological assessment of ambient and traffic-related particulate matter: a review of recent studies. Mutat. Res., 613(2-3), 103–122.
[56] Patel, M.M, Hoepner, L., Garfinkel, R., Chillrud, S., Reyes, A., Quinn, J.W., Perera, F. and Miller, R.L. (2009) Ambient metals, elemental carbon, and wheeze and cough in New York City children through 24 months of age. Am. J. Respir. Crit. Care Med., 180(11), 1107–1113.

Received: **02.10.2015**
Accepted: **10.03.2016**

CORRESPONDING AUTHOR

Pinar Ili
Department of Medical Services and Techniques
Denizli Health Services Vocational High School
Pamukkale University
Kınıklı Campus
20070 Denizli - TURKEY

e-mail: pili@pau.edu.tr

© by PSP Volume 25 – No. 7/ 2016, pages 2404-2410 Fresenius Environmental Bulletin

CONTAMINATION AND ACCUMULATION OF HEAVY METALS IN BRINJAL (*SOLANUM MELONGENA* L.) GROWN IN A LONG-TERM WASTEWATER-IRRIGATED AGRICULTURAL LAND OF SARGODHA, PAKISTAN

Kafeel Ahmad[1], Zafar Iqbal Khan[1], Asma Ashfaq[1], Nudrat Aisha Akram[2], Muhammad Ashraf[3,4], Sumaira Yasmeen[1], Vincenzo Tufarelli[5], Vito Laudadio[5], Mariano Fracchiolla[6], Eugenio Cazzato[6]

[1]Department of Botany, University of Sargodha, Pakistan
[2]Department of Botany, GC University Faisalabad, Pakistan
[3]Pakistan Science Foundation, Islamabad, Pakistan
[4]Department of Botany & Microbiology, King Saud University, Riyadh, Saudi Arabia
[5]Department of DETO, University of Bari 'Aldo Moro', Valenzano, Italy
[6]Department of Agro-Environmental and Territorial Sciences, University of Bari 'Aldo Moro', Bari, Italy

ABSTRACT

In this study, we investigated metal and metalloid (Pb, Mn, Ni, Co, Cu, Cd, Zn, Se, Mo, Fe, As and Cr) concentrations in brinjal (*Solanum melongena* L.) as well as at two different cultivated sites in the vicinity of Sargodha. At both study sites (I and II), mean concentrations of As and Cd in soil and Mn, Ni, Cu (23.9, 28.9), Zn (61.2, 74.7), Mo (16.1, 18.3), and Cd (0.82, 1.11) in *S. melongena* were above the permissible limits as given by USEPA and WHO, respectively. The results revealed significant correlations between soil and vegetables for metals viz. Mn, Co, Ni, Zn, Cd and Pb. The trend of bioconcentration factor (BCF) at both sites was: 0.05-295.6 with higher BCF was observed for Cr (229.4, 295.6). High pollution load index at site-II indicated that this vegetable may cause toxic effects in humans due to high metal accumulation in the consumable parts of the vegetable. It is concluded that more effective controls should be taken to reduce pollution in this study area.

KEYWORDS:
Wastewater, Permissible limits, Vegetable, Soil, Pakistan

INTRODUCTION

With the passage of time, the consumption of wastewater in the agricultural production has gained an importance world-over as an economic substitute. Wastewater is frequently available and it is rich with essential nutrients. Wastewater also fulfills the requirements of water for crop plants. At the eve of 19th century, wastewater cultivated area in Pakistan was approximately 73,000 ha which is now progressively increasing day by day. However, there are several reports which depict that wastewater of most regions/places contain a large amount of a variety of heavy metals [1-3].

Different crops including major vegetable crops cultivated in most of peri-urban areas in many developing countries, including Pakistan, are irrigated with sewage wastewater [4]. Thus, it is naive to expect that such vegetables accumulate heavy metals through wastewater irrigation to a varying extent. Of many summer vegetables, brinjal (*Solanum melongena*) is a very popular vegetable because it is used for the preparation of a variety of dishes [5]. However, in view of a report brinjal production declined considerably during 2013 due to irrigation with wastewater [6].

Accumulation of heavy metals in vegetables gradually becomes perilous for the living organisms that consume them. Because many essential processes could be disrupted by outsized concentrations of toxic metals like Pb, Cd and Mo. Growth and reproduction of vegetables are also affected by Zn, Pb, Co and Cr [7]. Thus, the present study was conducted to determine the bioconcentration of Cr, Mn, Fe, Co, Ni, Cu, Zn, As, Se, Mo, Cd and Pb in cultivated soil and *S. melongena.* Therefore, the objectives of this research were to analyze the transfer of heavy metals and metalloids from soil to the edible portion of *S. melongena* and to determine pollution level of metals so as to avoid metal hazards and toxicity.

MATERIALS AND METHODS

Sample collection and preparation. The present study was conducted on two different sites (Phularwan and Purana Chaba) of Sargodha to evaluate the level of heavy metal toxicity. Site-I (Phularwan) situated at 50 km radius was under canal water irrigation and site-II (Purana Chaba) located at 67 km from Sargodha District was irrigated with wastewater. Ten samples of canal and wastewater irrigated soil and *S. melongena* were collected randomly from each site. The collected vegetables were washed with dH2O to remove contaminants. The samples were air dried and placed in an oven (65 ^{0}C) for 72 h. Soil samples were analyzed for pH, EC and organic matter. Each of soil and vegetable samples (each 2.0 g) was wet digested with H2SO4, HNO3 and HCl (1: 2: 1) until the solution became transparent. After cooling, the digested sample was filtered and the filtrate was finally maintained to 0.05 L with distilled H2O [8].

Analysis of metal and metalloid concentrations. The Cr, Mn, Fe, Co, Ni, Cu, Zn, Mo, Cd and Pb concentrations in the filtrate of digested soil and vegetable samples were estimated using an AAS (Model 2380, Perkin Elmer). Selenium (Se) and As contents in the samples were analyzed by a GFAA (graphite furnace atomic absorption). Standard stock solutions of 1000 ppm for all the metals were obtained from the Biological Laboratory (University of Sargodha).

Statistical analysis. The average concentrations of metals and metalloids in the vegetable and soil samples were evaluated by the SPSS: Statistical Program for Social Sciences. ANOVA (one-way) was applied to the data for metals and metalloids in soil and vegetables. Relationships between the soil and vegetable metals were also determined. In order to determine relationships between heavy metals of soil and vegetables the Pearson's correlation was applied. The significance differences between mean data were determined at 0.001, 0.01, and 0.05 probability levels [9].

Bioconcentration factor. The bioconcentration factor was calculated according to Khan et al. [10] who defined it as the relative tendency of a metal to be accumulated by a particular species of plant. Bioconcentration factor = Metal concentration in edible part/ Metal concentration in soil

Pollution load index. Pollution load index was applied to investigate the metal contents following Liu et al. [11]. PLI = Metal concentration in investigated soil/ Reference value of the metal in soil.

RESULTS

Analysis of variance of the data showed a significant effect of the two sites on concentrations of metals and metalloids like Fe, Co, Ni, Zn, As, Se and Pb in soil, whereas a non-significant effect of the sites was found on soil Cr, Mn, Cu, Mo and Cd concentrations (Table 1).

TABLE 1
Analysis of variance of data for metal concentrations (mg/kg) in soils at two different sites.

Metals and metalloids	Site
Cr	0.002ns
Mn	579.2ns
Fe	66.26**
Co	346.5***
Ni	7.321***
Cu	1.032ns
Zn	26.41**
As	26.97*
Se	1.981***
Mo	3.332ns
Cd	50.79ns
Pb	116.2**

***, **, * = significant at 0.001, 0.01 and 0.05, levels; ns = non-significant.

A non-significant effect of sampling sites on concentrations of Se, Mo and Cd in brinjal plants, whereas a significant effect of the sites was observed on Cr, Mo, Fe, Co, Ni, Cu, Zn, As and Pb concentrations (Table 2).

TABLE 2
Analysis of variance of data for metal concentrations (mg/kg) in *S. melongena* at two different sites.

Metals and metalloids	Site
Cr	482.3***
Mn	64.33**
Fe	202.4***
Co	0.692**
Ni	70.09***
Cu	64.12*
Zn	454.1***
As	56.73***
Se	0.041ns
Mo	12.74ns
Cd	0.225ns
Pb	3.172***

***, **, * = significant at 0.001, 0.01 and 0.05, levels; ns = non-significant.

TABLE 3
Physico-chemical parameters of soil at two different sites.

Physico-chemical parameters	Site-I	Site-II	MS
pH	8.1 ±1.2	7.9±0.3	0.14*
EC (dSm-1)	1.34±1.13	1.55±1.11	0.21ns
Organic matter (%)	0.88±0.2	0.95±0.4	0.032**
Textural class	Clay loam	Clay loam	

MS= mean squares

Physico-chemical parameters of soil. The mean value of pH of soil at site-I was 8.1 and at site-II was 7.9. Electrical conductivity of soil at site-I was 1.34 dSm^{-1} and at site-II was 1.55 dSm^{-1}. Mean value of organic matter at site-I was 0.88 and at site-II was 0.95 (Table 3).

Metals and metalloids in soil. The concentrations of Cr, Mn, Fe, Co, Ni, Cu, Zn, Se, Mo and Pb in soil were within the critical values except for As and Cd. The concentrations (mg/kg) of metals and metalloids in the canal water at site-I ranged from 0.07 to 56.1, those in the wastewater used for irrigation at site-II ranged from 0.09 to 59.3. At site-II, mean concentrations of metals were higher as compared to those at site-I. Levels of metals at site-I were: Cr (0.07), Mn (18.9), Fe (42.9), Co (14.3), Ni (2.15),Cu (4.02), Zn (6.71), As (56.1), Se (2.44), Mo (7.88), Cd (10.9) and Pb (39.2), respectively, however at site-II were: Cr (0.09), Mn (34.8), Fe (48.4), Co (26.2), Ni (4.23),Cu (4.66), Zn (9.96), As (59.3), Se (3.33), Mo (9.04), Cd (15.4) and Pb (46.1) mg/kg, respectively. Of the heavy metals, mean concentrations were maximum for As (56.1, 59.3 mg/kg) and minimum for Cr (0.07, 0.09 mg/kg) at both sites.

Metals and metalloids in vegetable. Mean concentration of metals and metalloids like Mn, Ni, Cu, Zn, Mo and Cd at site-I and Mn,Ni, Cu, Zn, As, Mo, Cd and Pb at site-II were above the permissible limits (WHO 1996). Theconcentrations (mg kg-1) of metals and metalloids at site-I were in the range 0.64-74.4, while at site-II they ranged from 0.83 to 79.5. The concentrations (mg kg-1) for different metals and metalloids at site-I were: Cr (15.4), Mn (74.4), Fe (50.1), Co (0.64), Ni (8.83), Cu (23.9), Zn(61.2), As (4.06), Se (0.72), Mo (16.1), Cd (0.82) and Pb (8.14), respectively, while at site-IIwere Cr (29.3), Mn (79.5), Fe (78.4), Co (1.16), Ni (14.3), Cu (28.9), Zn (74.7), As (8.82), Se(0.83), Mo (18.3), Cd (1.11) and Pb (19.4), respectively (Table 5).

TABLE 4
Metal and metalloid concentrations (mg kg^{-1}) in soil samples obtained from two sites in Sargodha District.

Metals and metalloids	Sampling sites		Permissible maximum limit
	Site-I	Site-I	
Cr	0.07±0.01	0.09±0.04	400
Mn	18.9±1.26	34.8±1.27	80
Fe	42.9±0.64	48.4±1.42	21000
Co	14.3±0.83	26.2±0.85	65
Ni	2.15±0.09	4.23±0.19	50
Cu	4.02±0.19	4.66±0.33	50
Zn	6.71±0.52	9.96±0.41	200
As	56.1±0.39	59.3±1.54	40
Se	2.44±0.09	3.33±1.11	3
Mo	7.88±0.66	9.04±0.25	40
Cd	10.9±0.54	15.4±0.29	3
Pb	39.2±1.33	46.1±0.81	300

Permissible maximum limit (USEPA, 1997)

TABLE 5
Metal and metalloid concentrations (mg kg-1) in the edible part *S. melongena* obtained from two sites in Sargodha, District.

Metals and metalloids	Sampling sites		Permissible maximum limit (mg/kg)
	Site-I	Site-II	
Cr	15.4±0.29	29.3±0.09	50
Mn	74.4±0.69	79.5±1.62	30
Fe	50.1±1.78	78.4±2.65	1000
Co	0.64±0.05	1.16±0.09	1
Ni	8.83±0.76	14.3±0.52	2
Cu	23.9±0.52	28.9±1.75	20
Zn	61.2±0.66	74.7±0.77	50
As	4.06±0.19	8.82±0.22	7
Se	0.72±0.67	0.83±0.47	-
Mo	16.1±0.83	18.3±1.29	5
Cd	0.82±0.32	1.11±0.56	0.5
Pb	8.14±0.91	19.4±1.66	10

Permissible maximum limit of WHO Standards [17]

TABLE 6
Bioconcentration factor for vegetable/soil system.

Site	Bioconcentration factor											
	Cr	Mn	Fe	Co	Ni	Cu	Zn	As	Se	Mo	Cd	Pb
Site-I	229.4	3.92	1.16	0.05	3.51	5.95	9.13	0.07	0.29	2.04	0.08	0.21
Site-II	295.6	2.33	1.63	0.05	3.34	6.21	7.49	0.15	0.25	2.03	0.07	0.42

Bioconcentration factor. A maximum bioconcentration factor for Cr (229.4-295.6) and minimum for Co (0.05) was recorded at both sites. BCF at site-I was: Cr (220.4), Mn (3.92), Fe (1.16), Co (0.05), Ni (3.51), Cu (5.95), Zn (9.13), As (0.07), Se (0.29), Mo (2.04), Cd (0.08) and Pb (0.21), while at site-II was: Cr (295.6), Mn (2.33), Fe (1.63), Co (0.05), Ni (3.34), Cu (6.21), Zn (7.49), As (0.15), Se(0.25), Mo (2.03), Cd (0.07) and Pb (0.42) (Table 6).

Correlation between the metal concentrations in soil and the vegetable. Correlation between the metal concentrations in soil and the vegetable was positive and significant for Mn (r = 0.789**), Fe (r= 0.811**), Co (r= 0.819**), Ni (r= 0.937**), Zn (r=0.877**), Cd (r= 0.863**) and Pb (r= 0.716*), however, positive and non-significant correlation was observed for Cr (r= 0.556ns), Cu (r=0.196ns), As (r= 0.615ns), Se (r= 0.332ns) and Mo (r= 0.324ns) between the soil and the vegetable (Table 7).

TABLE 7
Correlation between metal concentrations in soil and *S. melongena.*

Correlation	
Metals and metalloids	Soil-vegetable
Cr	0.556^{ns}
Mn	0.789^{**}
Fe	0.811^{**}
Co	0.819^{**}
Ni	0.937^{**}
Cu	0.196^{ns}
Zn	0.877^{**}
As	0.615^{ns}
Se	0.332^{ns}
Mo	0.324^{ns}
Cd	0.863^{**}
Pb	0.716^{*}

**, Correlation is significant at the 0.01 *, Correlation is significant at the 0.05; ns. No-significant

TABLE 8
Pollution load index for metals and metalloids in soil.

Pollution Load Index												
Metals and metalloids	Cr	Mn	Fe	Co	Ni	Cu	Zn	As	Se	Mo	Cd	Pb
Soil	1.48	1.8	1.12	1.82	1.68	1.16	1.49	1.06	1.36	1.15	1.41	1.18

Pollution load index. In the present investigation high pollution load index was observed for soil Co (1.82). In soil, the pollution load index was in the order: Co (1.82) > Mn (1.8) > Ni (1.68) > Zn (1.49) > Cr (1.48) > Cd (1.41) > Se (1.36) > Pb (1.18) > Cu (1.16) > Mo (1.15) > Fe (1.12) > As (1.06) as shown in Table 8.

DISCUSSION

High mean value of pH was found at site-I irrigated with canal water and those of EC and organic matter was at site-II irrigated with wastewater. It has been reported that irrigation with wastewater increases soil electrical conductivity and organic matter, declines soil pH, and could bring about the buildup of metals in the irrigated soils [12]. The values of As at both sites were slightly higher than the critical concentration (40 mg/kg) of this metal as stated by Alloway [13]. High levels of As and Cd in soil could have been due to the industrial uses of heavy metals released from pesticides and fertilizers used therein. Cao et al. [14] reported high concentrations (mg/kg) of heavy metals like Cr (99.5), Cu (35.9), Zn (108.2), Cd (0.156) and low for Pb (32.8) as compared to those found in the present investigation. Critical values (mg/kg) of metals in soil reported by EMSC [15] such as Cr (97.8) and Pb (26.2) were higher and for Cd (0.13) lower than the mean concentrations of Cr, Cd and Pb observed in the current study. The lower soil Pb concentration in the test area may have been due to the town traffic which is reasonably lower as compared to the relatively larger towns of the country. The contents of soil Se in both sites were found to be high in the present study, which can be ascribed to nature of soil of the region being calcareous because such soils usually possess high amount of selenium [16].

Heavy metal concentrations in the vegetables were different at both sites, which may be attributed to differential absorption capacity of the vegetable for different heavy metals [17], although high levels of metals and metalloids were found at both sites. Manganese contents in the vegetable at both sites were not in the safe limit permitted for food according to WHO which recommended 2-9 mg/kg of Mn per day for an adult [18]. The Co values found during the current study were lower than those observed by Tsafe et al. [19]. Based on the results of the current investigation there seems to be no warranted need of Co supplementation. Lower levels of heavy metals like Cu (4 mg kg-1), Zn (50 mg kg-1), Cd (0.27 mg kg-1), and Pb (5.5 mg kg-1) have been reported in different vegetables grown in contaminated areas from Baia Mare, Zlatna and Copsa Mica [20]. Sharma et al. [21] have found much lower level of Ni in the area irrigated with sewage water as compared to that reported in the present investigation. This difference may be due to samples collection in different seasons as reported by Sharma et al. [21] as they did sampling during two specific periods in the year i.e. summer (April-May) and winter (December- January) and whereas in the current study sampling was conducted only during December to January.

The BCF depends on the bioavailability of metals. High bioconcentration factor for Cr suggests that Cr accumulated in the vegetable tissues through some sources other than air. Low BCF for Co suggests low bioavailability of Co. This study indicated that the atmosphere was the main source of uptake of Se, Cu, Cd and Pb in vegetables. For example, Ding and Pan [22] reported that 50% of Pb content in vegetables was derived from the atmosphere. The BCF for Cd (5.65) and Pb (4.23) reported by Atayese et al. [23] was higher as compared to that recorded in the present investigation. Cadmium and lead toxicity symptoms are reported to become severe after a long time of continuous consumption. The uptake of Fe at both sites was comparatively low in the vegetable which is still not clear [24].

Statistically significant correlations between concentrations of metals in soils and vegetable were observed. In the present investigation, positive and significant correlations between the soil and the vegetable with respect to Mn, Co, Ni, Zn, Cd and Pb suggest an efficient transport of metals from the soil to the vegetable. According to Kloke et al. [25], correlation of zinc and copper between soil and vegetables was high but that of cobalt and nickel was also significant. Significant correlations of metals like Cr, Fe, Cu, As, Se and Mo indicated that they may

have originated from common wastewater application. The correlation of As with Fe and Cr showed their common source from tannery industries, while a strong association of Cd, Zn, and Cu showed common sources, and these metals have been derived from anthropogenic sources, especially the municipal sewage system or paint industry [26].

It is a measure of the degree of overall contamination at the sampling sites in vegetables and soils. In the present study, soil was highly contaminated with Co. The distribution of metal concentration in the study area showed that this area has been affected by anthropogenic activity particularly by wastewater, which might have led to a high accumulation of some heavy metals (Co, Cr and Ni). The accumulation of these metals in the soil affected normal levels of metals in *Solanum melongena* used for the study. This is possibly due to the bioavailable metals content in soil exerts a significant impact on soil quality and its eventual uptake by plants and humans [27-31].

CONCLUSIONS

It is concluded that Mn, Ni, Cu, Zn, Mo and Cd contamination in all samples of *Solanum melongena* has a potential to cause severe health hazards, because the levels of these heavy metals were above the permissible limits in the vegetable for human consumption. It is truly essential to note heavy metal accumulation in soil because they significantly affect agricultural production as well as human health through contaminated food consumption. Thus, an urgent attention is needed for regular monitoring of these toxic metals and metalloids.

ACKNOWLEDGEMENTS

The Higher Education Commission, Pakistan is acknowledged for providing the financial support through a research project # 2484/13 to the first and second authors.

REFERENCES

[1] Strauss, M. and Blumenthal, U.J. (1990) Human waste use in agriculture and aquiculture: utilization practices and health perspectives. International Reference Centre for Waste Disposal, p. 48.

[2] Singh, K.P., Mohon, D., Sinha, S. and Dalwani, R. (2004) Impact assessment of treated/untreated wastewater toxicants discharge by sewage treatment plants on health, agricultural, and environmental quality in wastewater disposal area. Chemosphere 55, 227-255.

[3] Kalavrouziotis, I. K., Carter, J., Varnavas, S. P., Mehra, A. and Drakatos, P. A. (2006). Towards an understanding of metal contamination in food crops and soils related to road traffic. Fresenius Environmental Bulletin 15, 170-175.

[4] Marques, A. P., Rangel, A. O., Castro and P. M. 2007. Effect of arsenic, lead and zinc on seed germination and plant growth in black nightshade (*Solanum nigrum* L.) vs. clover (*Trifolium incarnatum* L.). Fresenius Environmental Bulletin 16, 896-903.

[5] Agoreyo, B.O., Obansa, E.S. and Obanor, E.O. (2012) Comparative nutritional and phytochemical analyses of two varieties of Solanum melongena. Sci. World J. 7, 1-8.

[6] Aslam, D.M. and Amin, S. (2013) Fruits, vegetables and condiments statistics of Pakistan 2011-2012. Government of Pakistan Ministry of National Food Security and Research, Islamabad.

[7] Barakat, M.A. (2011) New trends in removing heavy metals from industrial wastewater. Arab. J. Chem. 4, 361–377.

[8] Vukadinovic, V. and Bertic, B. (1988) Book on Agrochemistry and Plant Nutrition. University J.J. Strossmayer in Osijek, Faculty of Agriculture. Osijek. Croatia, p. 56.

[9] Steel R.G.D. and Torrie, J.H. (1980) Principles and procedures of statistics. A Biometrical Approach, 2. McGraw-Hill, New York.

[10] Khan, S., Farooq, S., Shahbaz, S., Khan, M.A. and Sadique, M. (2009) Health risk assessment of heavy metals for population via consumption of vegetables, World Appl. Sci. J. 6, 1602-1606.

[11] Liu, W.H., Zhao, J.Z., Ouyang, Z.Y., Soderlund, L. and Liu, G.H. (2005) Impacts of sewageirrigation on heavy metal distribution and contamination in Beijing, China. Environ Int. 31, 805–812.

[12] Paul, S.M., A. Khurana, S. Milkha and B. Aulakh. (2010). Influence of wastewater application and fertilizer use on the quality of irrigation water, soil and food crops: case studies from Northwestern India. World Congress of Soil Science, Soil Solutions for a Changing World Brisbane, Australia. pp.75-78

[13] Alloway, B.J. (1999) Heavy metal in soil. New York. John Wiley and Sons. pp. 20-28.

[14] Cao, H., J. Chen, J. Zhang, H. Zhang, L. Qiao and Y. Men. (2010) Heavy metals in rice and

garden vegetables and their potential health risks to inhabitants in the vicinity of an industrial zone in Jiangsu, China J. Environ. Sci. 22, 1792–1799.
[15] EMSC (Environmental Monitoring Station of China) (1993) Background Value of Soil Elements in China. China Environmental Science Press, Beijing.
[16] Tisdale, S.L., Nelson, W.L., Beaton, J.D. and Havlin, J.L. (1993) Soil Fertility and Fertilizers.3rd edition. Macmillan Publishing Cooprative, New York, USA.
[17] Singh, A., Sharma, R.K., Agrawal, M. and Marshall, F.M. (2010) Risk assessment of heavy metal toxicity through contaminated vegetables from waste water irrigated area of Varanasi, India. Trop. Ecol., 51(2): 375-387.
[18] WHO (World Health Organization) (1994) Quality Directive of Potable Water. 2, p. 197. Geneva.
[19] Tsafe, A.I., Hassan, L.G., Sahabi, D.M., Alhassan, Y. and Bala, B.M. (2012) Evaluation of heavy metals uptake and risk assessment of vegetables grown in Yargalma of Northern Nigeria. J. Basic Appl. Sci. Res. 2, 6708-6714.
[20] Lacatusu R. and Lacatusu, A.R. (2008) Vegetable and fruits quality within heavy metals polluted areas in Romania. Carpath. J. Earth Environ. Sci. 3, 115-129.
[21] Sharma, R.K., Agrawal, M. and Marshall, F. (2007) Heavy metals contamination of soil and vegetables in suburban areas of Varanasi, India. Ecotox. Environ. Safe. 66, 258–266.
[22] Ding, A.F. and Pan, G.X. (2003) Contents of heavy metals in soils and Chinese cabbages from some urban vegetable fields around Nanjing and the human health risks. Ecol. Environ. 12, 409–411.
[23] Atayese, M.O., Eigbadon, A.I., Oluwa, K.A. and Adesodun, J.K. (2008) Heavy metal contamination of amaranthus grown along major highways in Lagos, Nigeria. Afr. Crop Sci. 16, 225 – 235.
[24] Brummer, G.W., Gerth, J. and Herms, U. (1986) Heavy metal species, mobility and availability in soils. Soil Geol. 149, 382–398.
[25] Kloke, A., Sauerbeck, D.R. and Vetter, H. (1994) Changing metal cycles and human health. Nriagu. Journal of Springer-Veriag, Berlin, p. 113.
[26] Rahman, S.H., Khanam, D., Adyel, T.M., Islam, M.S., Ahsan, M.A. and Akbor, M.A. (2012) Assessment of heavy metal contamination of agricultural soil around Dhaka export processing zone (DEPZ), Bangladesh: Implication of seasonal variation and indices. Appl. Sci. 2, 584-601.
[27] Muller, G. (1969) Index of geoaccumulation in sediments of the Rhine. River 2, 108-118.
[28] Guo, X., Sun, D., Zhang, K., Tian, K. and Lu, X. (2012). Relationship between above ground productivity and nutrient cycling in three freshwater wetland types along a water level gradient. Fresenius Environmental Bulletin 21, 1827-1832.
[29] Addo, M.A., Darko, E.O., Gordon, C., Nyarko, B.J.B., Gbadago, J.K., Nyarko, E., Affum, H.A. and Botwe, B.O. (2012) Evaluation of heavy metals contamination of soil and vegetation in the vicinity of a cement factory in the Volta Region, Ghana. Int. J. Sci. Technol. 2, 40-50.
[30] Khan, Z.I., Ahmad, K., Ashraf, M., Shoaib, N., Parveen, R., Bibi, Z., Noorka I.R., Tahir, H.M., Akram, N.A., Ullah, M.F., Yaqoob, R., Tufarelli, V., Fracchiolla, M. and Cazzato, E. (2016) Assessment of toxicological health risk of trace metals in vegetables mostly consumed in Punjab, Pakistan. Environmental Earth Sciences 75(5), 1-5.
[31] Khan, Z.I., Ahmad, K., Ashraf, M., Parveen, R., Bibi,, Z., Mustafa, I., Noorka, I.R., Tahir, H.M., Akram, N.A., Ullah, M.F., Yaqoob, R., Tufarelli, V., Fracchiolla, M. and Cazzato E. (2016) Risk assessment of heavy metal and metalloid toxicity through a contaminated vegetable (*Cucurbita maxima*) from wastewater irrigated area: A case study for a site-specific risk assessment in Jhang, Pakistan. Human and Ecological Risk Assessment: An International Journal 22(1), 86-98.

Received: **07.10.2015**
Accepted: **24.02.2016**

CORRESPONDING AUTHOR

Prof. Vincenzo Tufarelli,
Department DETO, Section of Veterinary Science and Animal Production, University of Bari 'Aldo Moro', Valenzano, Italy

Email: vincenzo.tufarelli@uniba.it

© by PSP Volume 25 – No. 7/ 2016, pages 2411-2418 Fresenius Environmental Bulletin

GROWTH AND NICKEL UPTAKE KINETICS OF ESCHERICHIA COLI DURING CONTINUOUS ACCLIMATION

Laiyan Wu[1], Anping Yang[2*], Yalan Yang[1],Jirong Lan[1], Songbo Wang[1 *]

[1]Key Laboratory of Catalysis and Materials Science of the State Ethnic Affairs commission and Ministry of Education, College of Resources and Environmental Science, South-Central University for Nationalities, Wuhan 430074, P. R. China
[2]Department of Testing and Analysis, Hubei Provincial Environmental Monitoring Center Station, Wuhan 430072, China)

ABSTRACT

Growth and Ni uptake kinetics of different *Escherichia coli* generations acclimated under Ni-rich conditions were investigated in this study. Pre-cultured E. coli (C–H) showed an enhanced adaptability with short lag phase, long log phase, and stationary period after the bacteria were thrice acclimated . The growth and Ni uptake of acclimated E. coli increased two to five times and two to ten times, respectively. An increase in maximum bioaccumulation was observed in the order of generation III, II, and I; among these generations, III was the highest. The specific growth rate and bioaccumulated Ni^{2+} increased to 10 mg/g (generation II) and 17 mg/g (generation III) dry cell weight, which were consistently higher than those of the controls and the former generation. Results suggested that acclimation enhanced the resistance and bioaccumulation capacity of E. coli; by contrast, the living biomass amount at long exponential and stationary phase was responsible for the Ni uptake. Low **nickel concentration** between two generations take positive effect on the resistance of *E. coli* in Ni (II) medium. FTIR analysis revealed that hydroxyl, carboxyl, and amide groups were involved in the Ni sorption. TEM was also performed to investigate the cell microstructure. TEM results demonstrated that that the morphological characteristics of microorganisms were partly affected by Ni. Thick secretions were dispersed on the surface and around the acclimated *E. coli*.

KEYWORDS:
nickel ion; *Escherichia coli;* kinetics; acclimation

INTRODUCTION

Heavy metals are extremely toxic pollutants that cause major environmental problems by contaminating ecosystems. Heavy metals directly affect human beings by damaging the nerves, liver, and bones and by blocking the functional groups of vital enzymes via the food chain[1, 2]. Ni^{2+} is commonly used in our daily activities, industrial materials, such as catalysts in the food industry, paints, and batteries, and industrial processes, such as leather tanning, wood preservation, pulp processing electroplating[3], and metallurgy, Ni^{2+} levels can reach as high as 2.205–2.900 mg/L (rinse waters) in plating plants, 0.19–0.51 mg/L in mine drainages, 0.46–3.40 mg/L in acidic and 0.01–0.18 mg/L in alkaline waters[4], 0–40 mg/L in wastewaters from paint industries, and 0.25–67 mg/L in wastewaters from ink industries [5]. As non-biodegradable and widely used materials, heavy metals, such as Ni (II), spread and accumulate in the environment rapidly and reach toxic levels. The removal of heavy metals is a persisting problem. Conventional technologies[6], such as chemical precipitation, oxidation-reduction processes, filtration, ion exchange, electrochemical treatment, membrane technologies, adsorption, and evaporation, are expensive and inefficient, especially in the removal of high concentrations in large-scale wastewater treatments.

Biological treatments based on growing, resting, or non-living organisms and other biomasses have been extensively investigated because of their excellent performance at low heavy metal concentrations[2, 7]. Therefore, environmentally friendly, highly efficient, cost-effective, and easily accessible sorbents should be developed. For instance, microorganisms or marine organisms are widely used as effective biosorbents in heavy metal removal[8-10]. Living organisms perform high metal bioaccumulation but exhibit resistance to high metal pollutant concentrations[11, 12]. Genetically engineered microorganisms[13, 14] and isolated fungal biomass[15, 16] have been applied to remove and recover Ni^{2+} and Hg^{2+} from aqueous solutions via an express metal transport system involving the products of nixA gene and via metallothionein or glutathione-S-transferase-fusion protein and enzyme [17]. However, the screening of Ni-resistant species is a complex work, and protective mechanisms of excessive metal accumulation are not available, despite this advantage, heavy metal specificity and accumulation ability can be enhanced through genetic engineering. The construction of genetically engineered Escherichia coli depend on technologies and harsh conditions, and its environmental adaptability and availability have yet to be investigated.

This study aimed to 1) obtain Ni-resistant E. coli through continuous generation acclimation under Ni-rich conditions;2)aimed to investigate the kinetics of Ni^{2+} uptake and biomass growth in different generations during acclimation and to evaluate the Ni^{2+} bioaccumulation mechanism by acclimated E. coli. Furthermore, the effects of Ni2+ concentration on the simultaneous growth and bioaccumulation of different generations, properties of functional groups, and morphological changes was also explored in this study.

MATERIALS AND METHODS

Microorganisms, Media, and Growth Conditions. E. coli (CCTCC AB 91097) was kindly supplied by the College of Life Science, Wuhan University, China. All strains were grown in LB medium with different Ni2+concentration. The LB medium was composed of 5 g L-1 sodium chloride, 3 g L-1beef extract, and 10 g L-1 bacteriological peptone with pH of 7.4 adjusted by sodium hydroxide (1 mol L-1). Precultures were performed in 500 mL Erlenmeyer flasks containing 200 mL of the LB medium and incubated on a rotary shaker at 180 rpm at 37 ℃. The E. coli growth was determined by optical density at 600 nm (OD600), which is considered to be the growth yields of living biomass at different time [18]. The dry weight of cells was determined from OD600 using the value of 0.37 g dry weight per liter of OD600 1.0. To each freshly prepared acclimation medium, Ni(II) using nickel nitrate ranged from 20 - 300 mg L-1 were added in LB medium.

Uptake Experiments. During the incubation period, cells were harvested at the different time intervals by centrifuged at 10,000 rpm for 2 min. The supernatant fraction washed by sterile distilled water was analyzed by atomic absorption spectrophotometer (AA6300; Shimadzu, Japan) with an air-acetylene flame. Bioaccumulation was determined as the equation （1）

$$Uptake\% = \frac{(Ci - Ct)}{Ci} \times 100\% \qquad (1)$$

where Ci and Ct was the initial and residual metal ion concentration in the supernatant. (mg Ni(II)/L), All the experiments were carried out at least three times. The values used in calculations were mostly the arithmetics average of the experimental data.

Acclimation of *E.coli* for nickel(II)-resistence. The cultures grown in the LB with nickel(II) ions (generation Ⅰ) were collected, then incubuted in acclimation medium (generation Ⅱ) at optimal culture conditions, subsequencely 1mL of the late exponential growth phase culture harvested from generation Ⅱ were transferred to another acclimation medium to domesticate for the third time as showed in table 1. All the experiments were carried out in triplicates. Generation Ⅱfor *E.coli* C,D , which extract from the generation Ⅰ A(30 $mg \cdot L^{-1}$), B(100 $mg \cdot L^{-1}$) were cultrivated in 20 $mg \cdot L^{-1}$, and these cultures were also used to acclimate generation Ⅱ *E.coli* E, F at a concentration of 150 $mg \cdot L^{-1}$, the precultures without Ni(II) were incubated in concentration of 20 $mg \cdot L^{-1}$ and 150 $mg \cdot L^{-1}$ were prepared as control 1, control 2. The strains of generation Ⅱ *E.coli* D, F showed better growth and higher nickel uptake were futher cultivated in higher concentration of Ni(II) medium of 300 $mg \cdot L^{-1}$ was marked as Generation Ⅲ *E.coli* G,H.

Analytical methods. The *E.coli* acclimated at different Ni(II) concentration were harvested for transmission electron microscope obeservation (FEI Tecnai G20), other samples were washed with distilled water for several times, and then freeze-dried for FTIR (Nicolet NEXUS-470).

RESULTS AND DISCUSSION

Kinetics of simultaneous cell growth and Ni uptake (SG&U) of generations I, II, and III *E. coli* during acclimation. Studies on acclimated Ni-resistant or genetically engineered microorganisms are abundant; as a result, excellent effects are elicited on Ni^{2+} uptake[13, 14]. Simultaneous Ni accumulation and cell propagation at different initial Ni^{2+} concentrations have been occasionally evaluated[19, 20]; however, only a few studies have investigated *E. coli* SG&U in different generations during Ni acclimation. The time-dependent SG&U data under optimal pH and temperature conditions were observed (Fig. 1–3). The growth of *E. coli* was hardly inhibited and the life cycle of this bacterium was extended as Ni^{2+}concentration increased. Ni uptake showed a similar tendency during acclimation; this result indicated that the amount of biomass may play a key role in Ni^{2+} uptake.

An extended lag period of 7 and 16 h, log period of 44 h, and a stationary period of 60 h were observed in generation Ⅰ (Table 2). However, pre-cultured *E. coli* C-H (generation II and III) showed better adaptability and shorter lag phase than their corresponding controls. Figs. 2(a) and 2(b) reveal that the growth of *E. coli* C-F significantly increased after this bacterium was acclimated in Ni^{2+}, and OD600 reached 4.5, which was two to three times greater than that of the controls. By contrast, Ni^{2+} uptake ranged from 8% to 14% which was four times greater than that of the controls (2% to 4%).

The Ni^{2+} uptake of generation II *E. coli* (C,D) cultivated at a low concentration was two to four times greater than that of *E. coli* (E,F) cultivated at a high concentration. The growth of *E. coli* was strongly inhibited, that is, only approximately 0.3 of OD600 was achieved after more than 200 h of incubation; the removal rate of Ni^{2+} decreased to 2.5% at 300 mg/L. However, the growth of *E. coli* GH after this bacterium acclimated in generation II increased up to 10 times, with five times of Ni^{2+} uptake. These results suggested that the acclimation enhanced the growth and Ni^{2+} uptake of these

TABLE 1
Generations and concentrations of Ni(II) ions during acclimation

	Generation Ⅰ	Generation Ⅱ	ΔC	Generation Ⅲ	ΔC
Concentration($mg \cdot L^{-1}$) of Ni (II) ions	30(A)	30-20(C)	−10	30-20-300(G)	280
		100-20(D)	−80		
	100(B)	30-150(E)	120	30-150-300(H)	150
		100-150(F)	50		

microorganisms. Moreover, Ni^{2+} uptake accelerated remarkably after the cells passed the lag phase. The whole Ni^{2+} uptake process ended in the exponential phase or the stationary phase at which cell propagation occurred rapidly. The Ni^{2+} was released, but this process occurred more slowly than the death of biomass in the following life phase. This finding probably marks the death of *E. coli*; as a consequence, Ni^{2+} is released from living biomass. Nevertheless, the non-living biomass also adsorbed this part of Ni^{2+}.

The maximum amount of bioaccumulated Ni^{2+} increased to 10 and 17 mg/g dry cell weight at generations II and III, respectively, and these findings were two to four times greater than those of the original cell. The specific growth rate increased in generation II, and this finding is two to three times greater than that in generation I. Therefore, the uptake contributed to the enhancement of Ni resistance of *E. coli* C-F. The biomass growth from the decrease in OD600 was inhibited by the increase in Ni^{2+} level. However, bioaccumulation increased, and this increase indicated that the cell bioaccumulation capacity was enhanced several times.

Living biomass undergoes sequestration during metal biosorption and bioaccumulation; biosorption is a passive metal uptake process, which is relatively rapid, independent of temperature and metabolic energy, and may involve a reversible binding of heavy metals to the cell wall[21-24]. Conversely, bioaccumulation is an active-energy-driven process on the basis of metabolism, this process occurs through precipitation and transport across cell membranes[25-27]. The exponential growth phase probably involves highly active enzymes in the mechanisms of heavy metal uptake[28-30]. Thus, biomass with a long exponential phase and stationary phase (SRT) showed an efficient Ni accumulation behavior. The uptake ratio increased as the growth of biomass accelerated in the late exponential phase or SRTs. Therefore, expanded SRTs may be recommended in the heavy metal removal by bacteria. In this study, the exponential phases of these acclimated *E. coli* were reduced as a sign of adaptability; by contrast, the SRTs lasted more than 100 h (Table 2).

However, the Ni uptake was reduced as the number of cells decreased. Bioaccumulation is an active biosorption through intracellular accumulation that occurs more slowly than biosorption, which is cell surface accumulation. In this study, the maximum Ni accumulation occurred in the late exponential phase or SRT, and these bacteria may exhibit the optimal bioaccumulation capacity. Ni^{2+} was gradually released into the system with the death of biomass but was further maintained in equilibrium. Two stages of the release of Ni^{2+} were observed. The first stage involved the breakdown of physicochemical interactions between Ni^{2+} and functional groups, and some of the bioaccumulated Ni^{2+} may be further discharged.

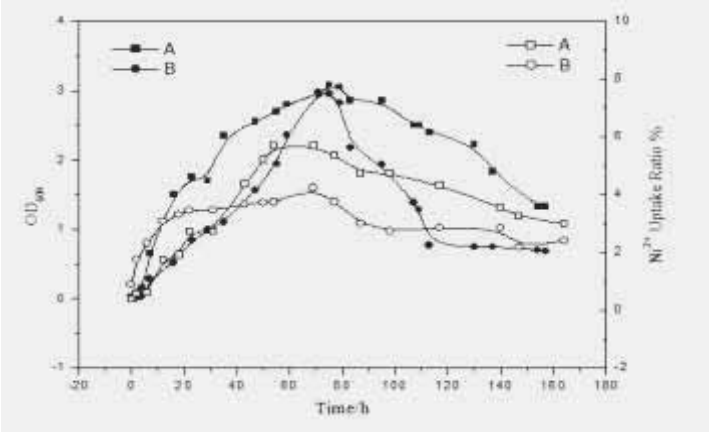

FIGURE 1
Kinetics of generation I cellular growth ■●a) and Ni(II) uptake □○, Concentration of Ni (II): A:30 mg L^{-1}, B: 100 mg L^{-1}.

TABLE 2
Comparison of life cycle and Ni(II) bioaccumulation, specific growth rate (μ) of acclimted generation *E.coli* at different Ni(II) levels.

	Lag phase	Exponential	Stationary	Decline	μ (h^{-1})	q_{max}bioaccumulation
A	0–7	7–47	47–113	113-	0.0688	5.7
B	0–16	16–59	59–123	123-	0.0496	3.8
C	0–4	4–35	35–154	154-	0.0763	9.1
D	0–2	2–23	23–177	177-	0.1340	11.3
Control11	0–6	6–47	47–98	98-	0.058464	7.5
E	0–47	47–75	75–203	203-	0.0746	9.3
F	0–11	11–47	47–180	180-	0.0646	10.0
Control2	0–58	58–75	75–145	145-	0.022509	4.6
G	0–150	150–290	290–366	366-	0.0169	11.5
H	0–150	150–221	221–408	408-	0.0329	16.9
Control3	0–192	192–247	247–320	320-	0.014304	4.1

q_{maxbio}accumulation: The specific Ni2+ bioaccumulation capacity , calculated from q (mg/g dry cell) = V(Ci -Ct)/mt, where Vwas the sample volume (L), mt were the weight (g) of dry cell.
bioaccumulated nickel(II) ion concentration at the end of growth; Uptake: specific nickel(II) uptake defined as the ratio of bioaccumulated concentration of nickel(II) at the end of the growth to the initial nickel(II) ion contration; μ: specific growth rate of exponential phase, calculated as $\mu=\ln(N_2/N_1)/t$

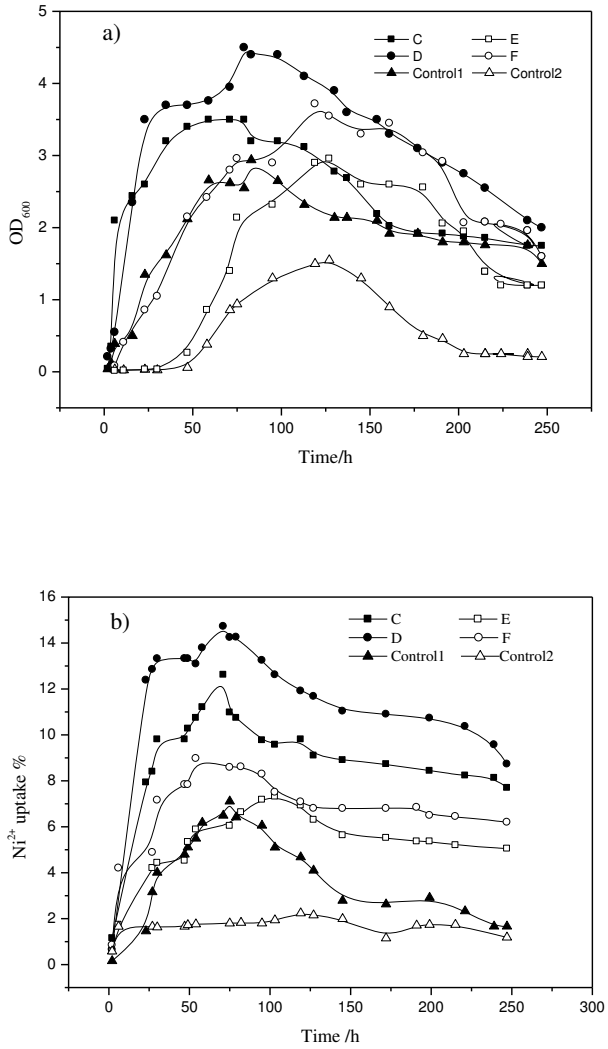

FIGURE 2
Growth a) and nickel uptake b) for generation Ⅱ*E.coli* (C,D,E,F)

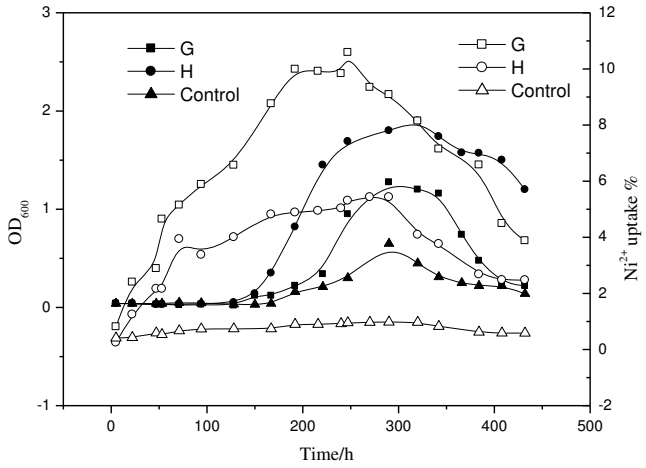

FIGURE 3
Kinetics of generation Ⅲ *E.coli*(G,H) cellular growth (■●▲) and Ni(II) uptake (□○△)

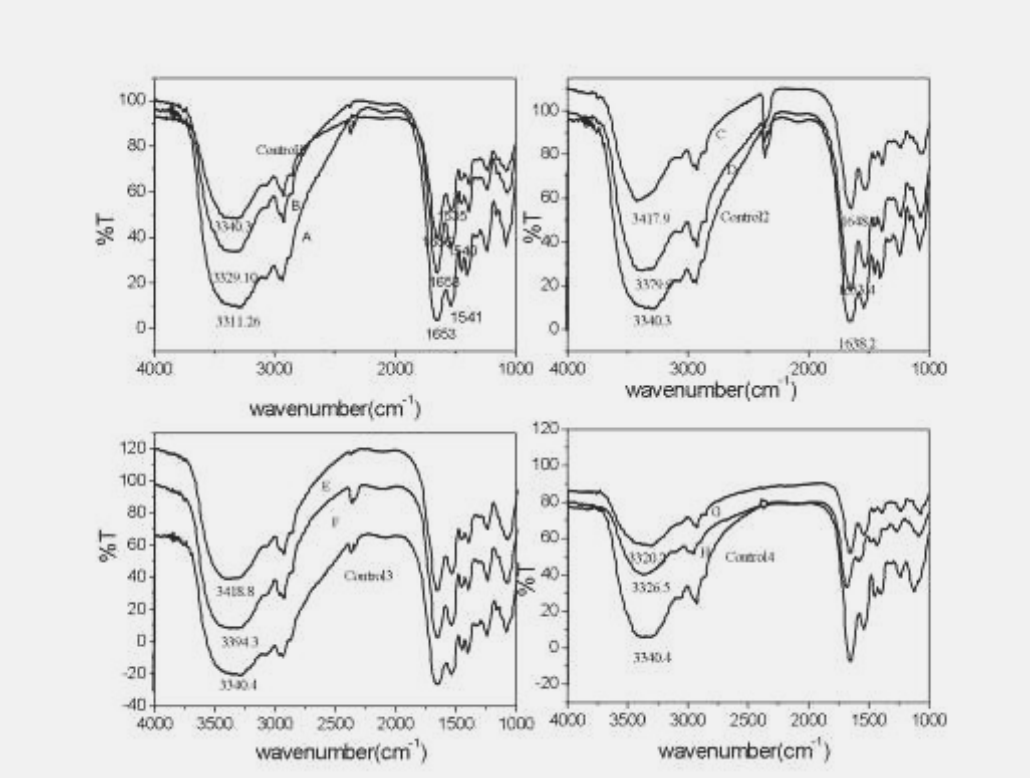

FIGURE 4
FTIR of *E. coli* generations I, II, and III

Ni^{2+} was mostly biosorbed reversibly on the surface of living biomass and may be rapidly released during cell death. Conversely, the bioaccumulated Ni^{2+} may be immobilized through intracellular precipitation, methylation, and other mechanisms, and Ni^{2+} was discharged slowly or finitely; this result is consistent with Ni^{2+} released in the decline phase. Acclimation may have slowed the release of Ni^{2+} because the Ni^{2+} uptake of generation II decreased smoothly in the decline phase. Although high Ni content negatively affected the biomass growth of generation III, the exponential phases of *E. coli* GH achieved high accumulation capacity.These results suggested that acclimation improved the bioaccumulation capacity of *E. coli*. The acclimation of *E. coli* in different concentrations was also investigated. *E. coli* (DF) that acclimatized at a low concentration gradient with ΔC of −80 mg·L^{-1} and 50 mg·L^{-1} had faster and better growth, whereas *E. coli* (H) with ΔC of 150 mg·L^{-1} lasted in a long SRT and Ni uptake was folded to *E. coli* G. Diaz-Ravina[31] noted that metal-resistant *E. coli* showed a concentration-depended effect. These observations may indicate that **ΔC** between two generations influence the resistance of *E. coli* in Ni^{2+} medium.

FTIR characterization of *E. coli* generation I, II, and III. The broad and strong peaks near 3340 cm^{-1} for generation I to III had shifted to approximately −30 cm^{-1} to 100 cm^{-1}, which may be attributed to the interactions among the metal ions, hydroxyl, and amide groups (Fig. 4). The peaks at 1071 and 1232 cm^{-1} assigned to alcoholic C–O and C–N stretching vibrations shifted consistent to the overlapping of O–H and N–H stretching vibrations. The peaks at 1656 and 1535 cm^{-1} were assigned to C=O and N–H stretching vibration[32], indicating that the presence of hydroxyl and amide groups on the biomass were shifted from −10 cm^{-1} to 20 cm^{-1}. The significant shifts of these specific peaks after metal ion adsorption suggested that chemical interactions between the metal ions and the amide groups occurred on the biomass surface. The broad peak at 3381 cm^{-1} shifted to 3397 and 3415 cm^{-1}, indicating that hydroxyl, carboxyl, and amide groups were involved in the Ni sorption. The peak at 1071 cm^{-1} also shifted, demonstrating that hydroxyl groups were involved in the metal ion accumulation. These results indicated that the carboxyl, hydroxyl, and amide groups on the biomass surface were all involved in the accumulation of Ni.

TEM characterization of *E. coli* generations I, II, and III during acclimation. TEM images of *E. coli* generations I, II, and III are shown in Fig. 5. Ni (II) was not observed to affect the morphology of the microorganism, but the cell wall became fragile and some parts of the cell membrane were broken after Ni acclimation. Thick secretion was observed on the surface of the acclimated microorganisms, whereas the crystallized extracellular secretion were found further dispersed around *E. coli*. These compounds may play an important role in the Ni resistance of microorganisms. Many researches indicated that surface functional groups, as well as intra/extracellular secretions, can reduce the toxicity of Ni in microorganisms. Some chelation of peptides, such as phytochelatin, metallothionein, polysaccharide, and acid amides[33, 34] can reduce Ni toxicity by synthesizing metal carbonate crystals [8, 35].

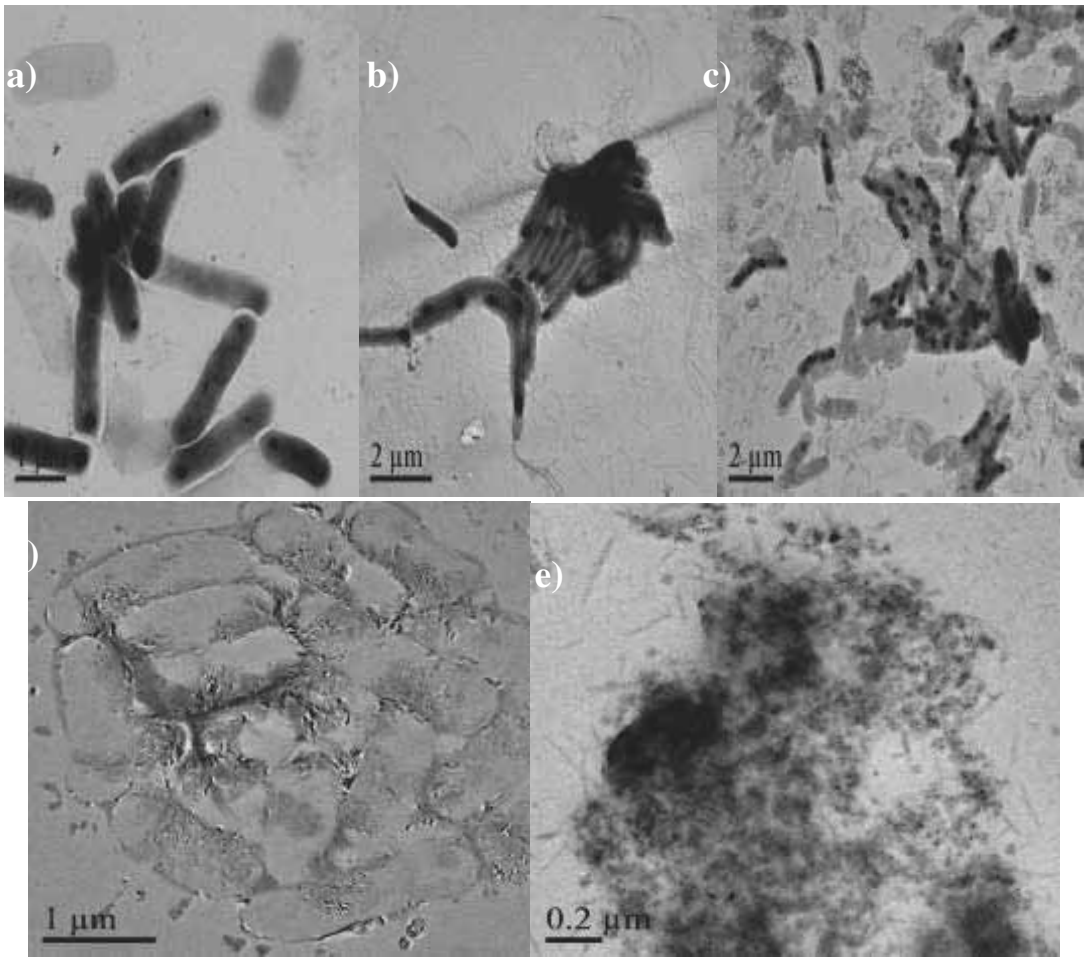

FIGURE 5
TEM images of *E.coli* generations I, II, and III. a) *E. coli* without Ni, b) generation I, c) generation II, d) generation III, and e) secretion of generation Ⅲ

CONCLUSION

In this study, *E. coli* was continuously acclimated three times at different Ni concentrations. During this process, the kinetics of simultaneous cell growth and Ni uptake (SG&U), as well as surface characteristics were investigated. The sharp growth increase (two to ten times) of *E. coli* C-F after acclimation and the extended late exponential or SRTs, where cell propagation occurred rapidly, lead to the acceleration of Ni^{2+} uptake (by four to five times for generation II and III. These results suggested that pre-culturing *E. coli* in Ni showed better adaptability and shorter lag phase compared with untreated controls. Moreover, the acclimation concentration gradient between two generations also affected the resistance of *E. coli*.

The FTIR and TEM analysis showed that the functional groups on the surface, such as hydroxyl, carboxyl, and amide groups, caused Ni acclimation to induce some extracellular secretion and crystal-like materials.

ACKNOWLEDGEMENT

This research was supported by National Natural Science Foundations of China (No.21307164 and 31200361), and funded by "Study Abroad for CSC Sponsored Chinese Citizen" and "Academic Research Abroad from Soutj-Central University for Nationalities Sponsored Outstanding Young Teacher"

REFERENCE

[1] Choudhary S, Sar P. Characterization of a metal resistant Pseudomonas sp.isolated from uranium mine for its potential in heavy metal (Ni2+, Co2+, Cu2+,and Cd2+) sequestration. Bioresour Technol 2009;100:2482-92.
[2] Zakhama S, Dhaouadi H, Henni FM. Nonlinear modelisation of heavy metal removal from aqueous solution using Ulva lactuca algae. Bioresoure Technology. 2011;102:786-96.
[3] Shakya PR. Nickel Adsorption by Wild Type and Nickel Resistant Isolate of Chorella SP. Pakistan Journal of Analytical Environment Chemistry. 2007;8:1-2.

[4] Patterson JW. wasterwater treatment technology: Ann Arbor Science Publishers; 1977.
[5] Donmez G, Aksu Z. The effect of copper (II) ions on the growth and bioaccumulation properties of some yeasts. Process Biochem. 1999;35:135-42.
[6] Kadukova J, Stofko M. Biosorption of heavy metal ions from aqueous solutions. Environmental Research Trends. New York: Nove Science Publishers 2007. p. 133-52.
[7] Vijayaraghavan K, Yun YS. Bacterial biosorbents and biosorption. Biotechnol Adv 2008;26:266-91.
[8] Davis TA, Volesky B, Mucci A. A review of the biochemistry of heavy metal biosorption by brown algae. Water Research. 2003;37:4311-30.
[9] He J, Chen JP. A comprehensive review on biosorption of heavy metals by algal biomass: Materials, performances, chemistry, and modeling simulation tools. Bioresource Technology. 2014;160:67-78.
[10] Bulgariu L, Bulgariu D, Rusu C. Springer Handbook of Marine Biotechnology: Springer Berlin Heidelberg; 2015.
[11] Deng X, Wilson D. Bioaccumulation of mercury from wastewater by genetically engineered Escherichia coli. Applied Microbiology and Biotechnology 2001; 56: 276-9.
[12] Koçberber N, Dönmez G. Chromium(VI) bioaccumulation capacities of adapted mixed cultures isolated from industrial saline wastewaters. Bioresour Technol. 2007;;98:2178-83.
[13] Deng X, Li QB, Lu YH, Sun DH, Huang XR. Bioaccumulation of nickel from aqueous solutions by genetically engineered Escherichia coli. Chenb Water Research 2003; 37 2505-11.
[14] Deng X, Zheng Y, Li Q. Effect of ambient conditions on simultaneous growth and bioaccumulation of mercuric ion by genetically engineered E. coli JM109; . Journal of Hazardous Materials 2006;B13: 6233-238.
[15] Aytar PNAR, Gedikli SERAP, Buruk YELIZ, Çabuk A, Burnak N. Lead and nickel biosorption with a fungal biomass isolated from metal mine drainage: Box-Behnken experimental design. International Journal of Environmental Science and Technology. 2014;11:1631-40.
[16] Nagarajan N, Gunasekaran P, Rajendran P. Genetic characterization, nickel tolerance, biosorption, kinetics, and uptake mechanism of a bacterium isolated from electroplating industrial effluent. Canadian Journal of Microbiology. 2015; 61:297-306.
[17] Rouhollahi F, Zamani A, Karimi K, Etesami N. Enhancement of nickel biosorption on fungal biomass by enzymatic and alkali pretreatments. International Journal of Environmental Science and Technology. 2014; 11:1911-8.
[18] Nourbakhsh M, Sag Y, Ozer D, Aksu Z, Kutsal T, Caglar A. A comparative study of various biosorbents for removal of chromium(VI) ions from industrial wastewaters. Process Biochemistry. 1994; 24:1-5.
[19] Wu L, Yu J, Sun X, Li B. The Effect of Nickel(II) Ions on the Growth and Bioaccumulation Properties of Escherichia coli Environmental Progress & Sustainable Energy 2009;28:234-9.
[20] Preetha B, Viruthagiri T. Bioaccumulation of chromium(VI), copper(II) and nickel(II) ions by growing Rhizopus arrhizus. Biochemical Engineering Journal. 2007;34:131-5.
[21] Neff JM. Bioaccumulation in Marine Organisms. UK: Elsevier, ; 2002.
[22] L. Pane C, Solisio A, Lodi GL, Mariottini A. Converti, Effect of extracts from Spirulina platensis bioaccumulating cadmium and zinc on L929 cells, Ecotoxicol. Environ Safety 2008; 70 121-6.
[23] Mejare M, Bülow L. Metal-binding proteins and peptides in biremediation and phytoremediation of heavy metals. Trends Biotechnology. 2001; 19 67-73.
[24] S. Cangeevaram S, Dhanarani J, Park M, Dexilin K. Thamaraiselvi, Biosorption of chromium and nickel by heavy metal resistant fungal and bacterial isolates, J. . Hazard Mater 2007;146 270-7.
[25] Hussein H, Farag S, Kandil K, Moaward H. Tolerance and uptake of heavy metals by Pseudomonads. Process Biochem 2005;40 955-61.
[26] Muse JO, Carducci CN, Stripeikis JD, Tudino MB, Fernandez FM. A link between lead and cadmium kinetic speciation in seawater and accumulation by the green alga Ulva lactuc. Environ Pollut 2006;141: 126-30.
[27] Anand PJ, Isar S, Saran R, Saxena Kl. Bioaccumulation of copper by Trichoderma viride. Bioresource Techno. 2006; 97 1018-25.
[28] Ito H, Inouhe M, Tohoyama H, Joho M. Effect of copper on acid phosphatase activity in yeast Yarrowia lipolytica. Z Naturforsch. 2007;62 70-6.
[29] Tsekova K, Galabova D. Phosphatase production and activity in copper(II) accumulating Rhizopus delemar. Enzyme Microb Technol. 2003;33 926-31.
[30] Macaskie LE, Empson RM, Cheethman AK, Grey CP, Skarnulis AJ. Uranium bioaccumulation by a Citrobacter sp. as a result of enzymatically mediated growth of polycrystalline HUO2PO4. Science. 1992;257:782-874.
[31] Diaz RM, Baath E. Development of metal tolerance in soil bacterial communities exposed to experimentally increased metal levels. Apply Environmental Microbialogy. 1996;62:2970-7.
[32] Pan H, Ge X P, Liu R X. Characteristic features of Bacillus cereus cell surfaces with biosorption of Pb(II) ions by AFM and FT-IR. Colloids and Surfaces B: Biointerfaces. 2006;52:89–95.
[33] Abboud P, Wilkinson KJ. Role of metalmixtures(Ca,Cu and Pb) onCd bioaccumulation andphytochelatinproductionby Chlamydomonas reinhardtii. EnvironPollut. 2013;179:33-8.
[34] Satofuka H, Fukui T, Atomi HI. Metal-bingding properties of phytochelatin-related petides. J Inorg Biochem. 2001;86:596-602.

[35] Rautaray D, Ahmad A, Sastry M. Biosynthesis of zirconia nanoparticles using the fungus Fusarium oxysporum. Journal of Materials Chemistry. 2004; 14:2303-3305.

Received: **04.10.2015**
Accepted: **17.01.2016**

CORRESPONDING AUTHOR

Songbo Wang,
College of Resources and Environmental Science, South-Central University for Nationalities, Wuhan 430074, P. R. China.

E-mail:wulaiyan@163.com

© by PSP Volume 25 – No. 7/2016, pages 2419-2426 Fresenius Environmental Bulletin

CHROMOSOME AND NUCLEOLUS MORPHOLOGICAL CHARACTERISTICS IN ROOT TIP CELLS OF PLANTS UNDER METAL STRESS

Xiangjun Liu, Qiuyue Shi, Jinhua Zou, Junran Wang, Hangfeng Wu, Jiayue Wang, Wusheng Jiang and Donghua Liu

Tianjin Key Laboratory of Animal and Plant Resistance, College of Life Sciences, Tianjin Normal University, Tianjin 300387, China

ABSTRACT

Mainly based on our previous work, we comprehensively evaluated chromosome and nucleolus morphological characteristics in root tip cells of plants stressed by Al and some heavy metals. Cell division is disturbed and chromosome aberration is induced in the root tips treated by excessive concentration of the metals used. This review also highlights the toxic role of the metals on nucleolus in root tips using silver staining, indirect immunofluorescent microscopy and western immunoblot analysis. After the metal treatment, obviously toxic phenomenon appear that nucleolar particles containing argyrophilic proteins leached out from the nucleus to the cytoplasm. Evidence demonstrates that these proteins are nucleophosmin, nucleolin and fibrillarin. Western immunoblot analysis confirms the findings obtained by indirect immunofluorescence.

KEYWORDS:
Metal ions, cell division, nucleolus, nucleoprotein (NP)

INTRODUCTION

Metals release to environment both from natural and anthropogenic sources accumulate in soil and are absorbed by plants leading to many toxic effects especially in roots [1]. Disturbances in growth and morphogenesis are the visible symptoms of stressor action. Evidence demonstrates that most compounds penetrate into the plant through the root system [2]. It is well known that roots are the primary target of metal phytotoxicity. Besides growth restrictions observable at the macroscopic level, cell and molecular studies will give more detailed information on qualitatively and quantitatively harmful effects at the microscopic level.

Allium cepa, Allium sativum Vicia faba and *Hordeum vulgare* provide a useful genetic system for screening and monitoring environmental pollutants and are most widely used in many laboratories because they are excellent plants for environmental monitoring, with many advantages such as low cost, a large number of roots, short test time, ease of storage and handling, and ease of observing abnormal phenomena of chromosomes, nuclei and nucleoli affected during cell division [3–9].

Metal toxicity in plants is well documented. However, Limited information is available about the comprehensive evaluation of the toxic effects of metal ions such as Al, Cd, Pb, Cr, Cu, Mg, Ni, Zn, Mn and Co on cell division and nucleolus in root tip cells of plants. In this review, we, mainly based on our previous work, comprehensively evaluate the toxic effects of the metal ions on chromosome and nucleolus morphological characteristics in root tips of plants.

EFFECTS ON CHROMOSOME MORPHOLOGY

Plants are sensitive to Al and some heavy metals. Excessive metal ions often disturb cell division and induce chromosome aberration. The standard types of aberrant chromosome behavior referred to in the modified *Allium* test, introduce by Fiskesjö [3], were observed after treatments with the metals.

C-mitosis. C-mitosis as described by Levan [10] is, in varying degrees, found in all the treated roots (Fig. 1a). C-mitosis, at a low concentration, is a most common type of chromosome aberrations. C-mitosis reflects slight or moderate cytological toxicity. Pb and Al are thought to be extremely c-mitotically active [5,11].

Chromosome stickiness. The sticky chromosome arises from improper folding of the chromosome fiber into single chromatids and that chromosomes become attached to each other by subchromatid bridges [12–13]. There are two types of chromosome stickiness in the root tip cells

exposed to the metals: sticky chromosomes at metaphases (Fig. 1b) and sticky chromosomes exhibit c-mitosis (Fig. 1c). Sticky chromosomes reflect highly toxic effects, usually of an irreversible type, and probably lead to cell death, which is a toxic characteristic at high concentration of metal ions.

Chromosome bridges. Chromosome bridges are due either to breaks in chromosomes or chromatids (often resulting in fragments) or to chromosome stickiness (disturbing the normal cell division). Anaphase bridges are observed in the roots exposed to the metal ions studied. Three types of chromosome bridges are observed: anaphase bridges involved one or more chromosomes (Fig. 1d,e), sticky bridges and (Fig. 1f) and anaphase configuration with chromosome bridges exhibiting disintegration (Fig. 1g). Chromosome bridges are somewhat damaged and the damage is reversible or irreversible depending on whether it is a sticky bridge or a result of breaking and rejoining of chromosomes. Chromosome fragments (Fig. 1h) and lagging chromosomes were often found in root tips exposed to the metals.

The evidence indicates that the effect of the tested metal ions on cell division is dependent on the concentration and duration of treatment. The metal ions can, in varying degrees, cause chromosome irregularities, including c-mitosis, chromosome bridges, chromosome stickiness and so on. Chromosome aberration can provide both qualitative and quantitative data on the effects of exposure to a mutagen [14].

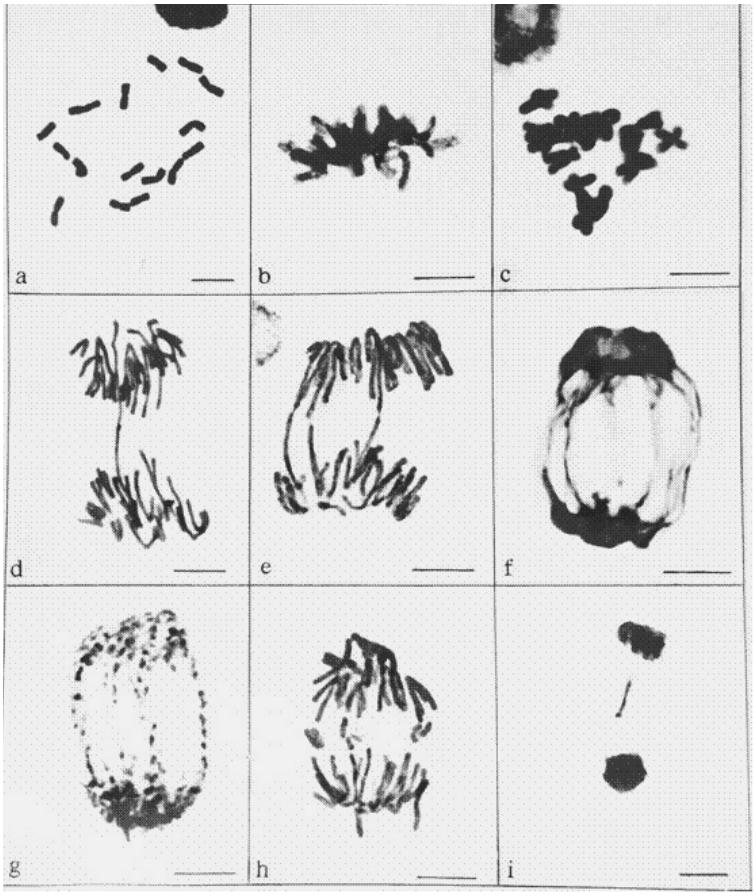

FIGURE 1

Chromosome abnormalities induce by the metal ions in *Allium cepa* root tips. (a) c-metaphase (10^{-3} M Cr^{3+}, 48 h); (b) Chromosome stickiness (10^{-4} M Cr^{3+}, 48 h); (c) Sticky chromosome exhibiting c-mitosis (10^{-2} M Al^{3+}, 72 h); (d–e) Chromosome bridges. (d) 10^{-5} M Ni^{2+}, 48 h. (e) 2×10 M Cr(VI) ($Cr_2O_7^{2-}$), 96 h; (f) Chromosome bridges exhibiting stickiness (10^{-3} M Zn^{2+}, 48 h); (g) Chromosome bridges exhibiting disintegration (10^{-3} M Zn^{2+}, 96 h); (h) Chromosome fragment (10^{-4} M Pb^{2+}, 48 h); (i) Lagging chromosome (10^{-5} M Co^{2+}, 48 h). *Scale bar* = 10 µm. Reprinted from Liu et al. [5], with permission.

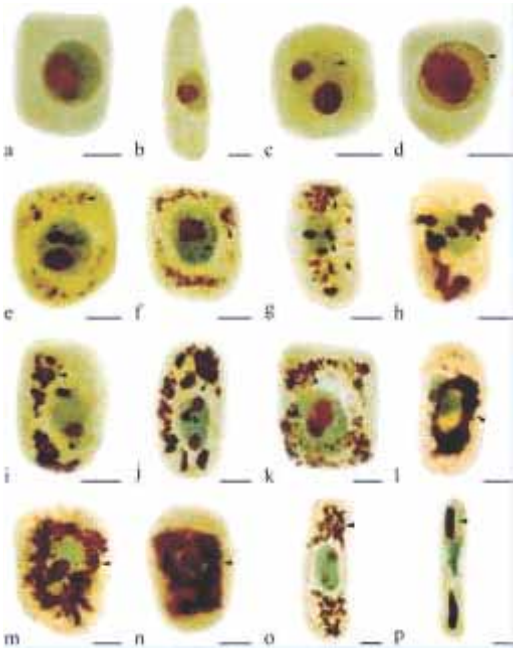

FIGURE 2

Effects of different concentrations of Al on nucleoli in root tip cells of *Allium cepa* var. *agrogarum* L. (a–b) Control cells; (c) Small amounts of silver-stained materials in nucleus (0.5 µM Al, 24 h); (d) Large amounts of silver stained materials in nucleus with increasing Al concentration and prolonging treatment time (5 µM Al, 48 h); (e–f) Silver-stained materials extruded from the nucleus into the cytoplasm (50 µM Al, 24 h); (g–k) Showing the leaching materials located near the nucleus and more and more materials accumulated in the cytoplasm with prolonging the duration of treatment (50 µM Al, 48 h); (l–n) Showing the materials enclosed the nucleus, and accumulated in the cytoplasm and occupied nearly the whole cytoplasm (50 µM Al, 72 h); (o–p) In long cells, the silver-stained materials gathered at the cell ends. (50 µM Al, 72 h) and large rod-like structures formed (50 µM Al, 72 h). *Scale bar*=10 µm. Arrowhead shows silver-stained materials. Reprinted from Qin et al. [26], with permission.

EFFECTS ON NUCLEOLI

Nucleoli are nuclear domains present in almost all eukaryotic cells. They not only specialize in the production of ribosomal subunits but also play roles in many fundamental cellular activities [15]. The nucleolus has long been known as a place for ribosome biogenesis. Because production of ribosome is a major metabolic activity, nucleolus function is tightly coupled to cell growth and proliferation [16]. However, the nucleolus can be disturbed by various stimuli such as UV, ionizing irradiation or actinomycin D, heat shock, genotoxic injury and metal ions [17–23]. Under stress conditions, some NP locations are changed and distributed disorderly in and out of nucleolus, furthermore altering their expressions and functions [18–19].

In 1983, Fiskesjö first proposed 'Al-structure' phenomenon that Al ions could induce nucleolar material extruded from the nuclei into the cytoplasm in root tip cells of *A. cepa* under Al stress using the Feulgen-light green procedure [20]. The phenomenon was not found in *Allium* tests with some ten other metal ions [24].

The nucleolus is known as a nuclear structure and is responsible for ribosome biogenesis and further transcript process [25]. It contains a set of acidic, nonhistone proteins that can bind silver ions and are selectively visualized by silver methods. Changes of argyrophilic proteins in nucleoli can be showed specifically under various stimuli using the silver staining method. In 1991, the 'Al-structure' phenomenon in the root tips of *A. cepa* exposed to Al was confirmed by Liu and Jiang [23] using the silver staining technique for the first time. Fig. 2 reveals in detail nucleolus abnormalities induced by Al in *A. cepa* root tips [26]. Zhang [27] confirmed the phenomenon in the root tips of *H. vulgare* exposed to Al using the silver method. After that, we found that besides Al, some heavy metals such as Cd, Pb, Cu, Ni, Co, Mg and Hg could also affect nucleoli and induce the phenomenon mentioned above in *A. cepa*, *Allium sativum, H. vulgare, Vicia*

faba, *Zea mays* and *Pinus massoniana* [5,9,17–19,28–31], but the amounts of extruded materials were less than in the Al treatment. Evidence from electron microscopy showed that the silver-stained particles in the nucleoli of *Lupinus angustifolius* L. root meristematic cells exposed to Pb were released from the nucleus into the cytoplasm [32]. The nuclear pore complex (NPC) is thought to be the most important channel for nuclear material [33]. The nucleolar material is released from the nucleus into the cytoplasm may be explained by the fact that the proteins are affected after the metal exposure, leading to the NPC to lose selectivity. In this way, the interaction between NPs and rRNA can be disturbed due to inhibition of rRNA synthesis, leading to the relocation of the NPs [34].

Further experiments were designed to examine the nature of the silver-stained particles and what types of NPs were extruded from the nucleolus into the cytoplasm under the metal stress. Using nucleolar mass spectrometry analyses, about 700 nucleolar proteins are identified, and some of them are required for ribosomal biogenesis and others are not related to the event [35]. Nucleophosmin, nucleolin and fibrillarin belong to NPs and participate in rRNA processing, cell activities, and especially take key roles in rDNA transcripts and ribosome assembly [36–37]. Boulon et al. [38] indicated that nucleolus is a center to sense stress and can coordinate the stress response. Nucleolar morphology, composition and function will change if nucleolus is disturbed under metal stress. We confirm, based on our previous work, that Al, Cd, Pb and Cu can induce alterations of the three nucleoproteins in the cellular localization in nucleoli of some plant root tips exposed to stress [9,11,18–19,30,39].

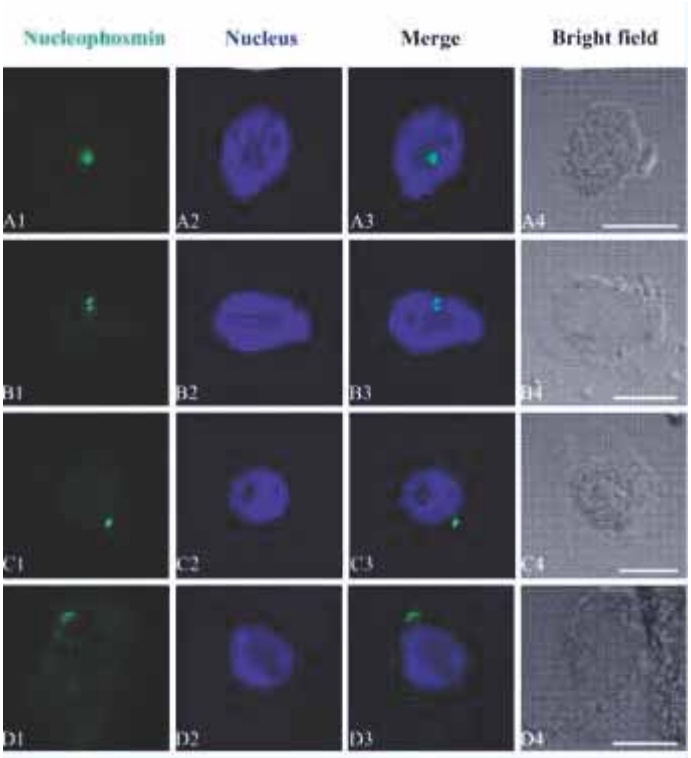

FIGURE 3

Effects of different concentrations of Al on the translocation of nucleophosmin. Simultaneous location of nucleophosmin after the reaction with primary anti- nucleophosmin antibody and secondary antibody conjugated with FITC (green) and DNA after the reaction with DAPI (blue) in the same single optical section obtained with the confocal scanning laser microscopy. (A1,B1,C1,D1) Nucleophosmin detection; (A2,B2,C2,D2) DNA detection; (A3,B3,C3,D3) Merged image of "nucleophosmin detection" and "DNA detection"; (A4,B4,C4,D4) Bright field image of the cells. (A1–A4) Nucleophosmin was localized in nucleolus in control cells; (B1–B4) Showing that nucleophosmin was migrated from nucleolus to nucleoplasm in the cells exposed to10^{-4} M Al for 72 h; (C2–C4,D1–D4) Showing that nucleophosmin was scattered in cytoplasm of the cells exposed to 10^{-2} M Al for 72 h and the intensity of nucleophosmin signals increased in cytoplasm. *Scale bar* =10 µm. Reprinted from Zhang et al. [9], with permission.

The evidence from indirect immunofluorescent microscopy demonstrate that nucleophosmin, fibrillarin and nucleolin are localized in nucleoli in control groups. Nucleophosmin (Fig. 3), nucleolin (Fig. 4) and fibrillarin (Fig. 5) are migrated from the nucleoli to the nucleoplasm or to cytoplasm under Al, Cd, Pb and Cu stress [11,18–19,39], which is consistent with the phenomena obtained from silver staining method. Chen and von Mikecz [40] indicated that $HgCl_2$ dislocates fibrillarin from the nucleolus in human cells. Ni and Zhang [41] observed that nucleophosmin shuttled from the nucleoli to the nucleoplasm, or even, to the cytoplasm in the wheat root-tips exposed to wortmannin (a specificinhibitor of PI3K) by indirect immunofluorescence staining, suggesting that wortmannin can not only damage nucleolar structure, but also inhibit its function. Actinomycin D is reported to causes dislocation of fibrillarin from the nucleolus to the nucleoplasm in tobacco cells [42]. Inhibition of rRNA synthesis can affect the interaction between NPs and rRNA, inducing the relocation of the NPs [34]. Evidence from immunofluorescence microscopy showed that cucurbitacin B could induce translocation of nucleophosmin from the nucleolus to nucleoplasm [43].

Furthermore, data from western blotting reveal that the three major NPs are over expressed under the stress in comparison to control, indicating that the metals have toxic effects on nucleoli, which is good with the results obtained from indirect immunofluorescent microscopy [11,17–19,31]. Nucleophosmin and nucleolin are known to be stained by silver [44–45], and fibrillarin is distinguished from these two NPs by its lack of affinity for silver [46]. Therefore, we suggest that these metals may also have toxic effects on other kinds of NPs besides argyrophilic and acidic nucleolar proteins. However, the mechanism needs to be further studied.

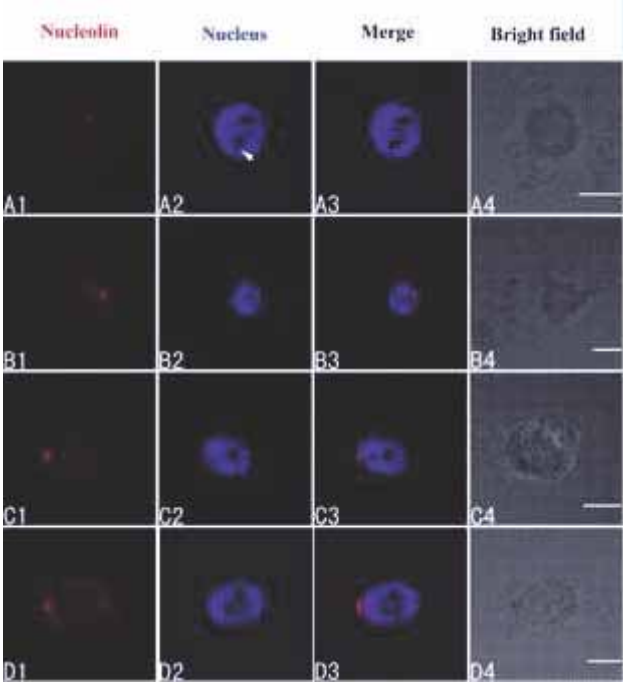

FIGURE 4

Simultaneous detection of nucleolin after incubation with primary anti-nucleolin antibody and secondary antibody conjugated with TRITC (Tetramethylrhodamine isothiocyanate) (red), and of DNA after incubation with DAPI (blue) in the same single optical section using confocal microscopy. (A1,B1,C1,D1) Nucleolin detection; (A2,B2,C2,D2) DNA detection; (A3,B3,C3,D3) Merged image of "nucleolin detection" and "DNA detection"; (A4,B4,C4,D4) bright field image. (A1–A4) Nucleolin in nucleolus of control cells; (B1–B4) The migration of nucleolin from the nucleolus to the nucleoplasm in cells treated with 100 μM Pb for 24 h; (C1–C4,D1–D4) Nucleolin in the cytoplasm of cells treated with 100 μM Pb for 48 h (C1–C4) and 72 h (D1–D4). *Scale bars*=10 μm. Arrowhead shows nucleolus. Reprinted from Jiang et al. [11], with permission.

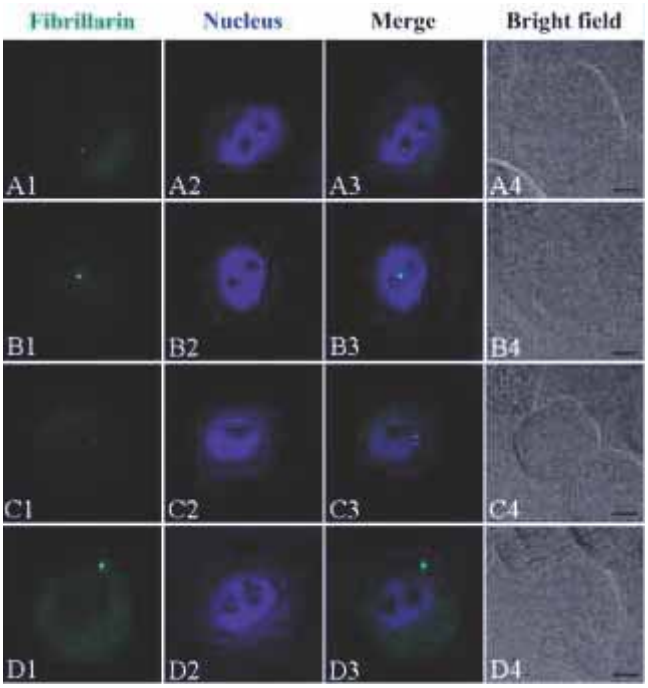

FIGURE 5
Simultaneous detection of fibrillarin after incubation with primary anti-fibrillarin antibody and secondary antibody conjugated with FITC (green), and of DNA after incubation with DAPI (blue) in the same single optical section using confocal microscopy. (A1,B1,C1,D1) Fibrillarin detection; (A2,B2,C2,D2) DNA detection; (A3,B3,C3,D3) Merged image of "fibrillarin detection" and "DNA detection"; (A4,B4,C4,D4) bright field image. (A1–A4) Fibrillarin in the nucleolus of control cells; (B1–B4) Migration of fibrillarin from the nucleolus to the nucleoplasm. (C1–C4) Fibrillarin on the way from nucleoplasm to cytoplasm. (D1–D4) Fibrillarin scattered in the cytoplasm. *Scale bar*=10 µm. Reprinted from Wang et al. [39], with permission.

CONCLUSIONS

Based on the information provided in this article, it is concluded that (1) The effect of the tested metal ions on cell division is dependent on the concentration and duration of treatment. The metals can, in varying degrees, disturb cell division comprising c-mitosis and lagging chromosomes, anaphase bridges, and chromosome stickiness in root tip cells of plants. (2) Metals can induce the extrusion of silver-stained materials containing argyrophilic proteins from the nucleolus into the cytoplasm. (3) Indirect immunofluorescence detects nucleolar material containing nucleophosmin, nucleolin and fibrillarin and their movement into the cytoplasm following metal stress. (4) Western blotting analysis reveal higher expression of the three major nucleoproteins in the treated roots, which is good online with the results obtained by indirect immunofluorescence. (5) The data presented above can be also used as valuable and early markers in cellular changes induced by metals for the evaluation of metal contamination.

ACKNOWLEDGMENTS

This project was supported by the National Natural Science Foundation of China (grant number 30972331). The authors wish to express their appreciation to the reviewers of this paper.

The authors have declared no conflict of interest.

REFERENCES

[1] Glińska, S., Bartczak, M., Oleksiak, S., Wolska, A., Gabara, B., Posmyk, M. and Janas, K. (2007) Effects of anthocyanin-rich extract from red cabbage leaves on meristematic cells of *Allium cepa* L. roots treated with heavy metals. *Ecotox Environ Safe* 68, 343–350.

[2] Kozhevnikova, A.D., Seregin, I.V., Bystrova, E.I., Belyaeva, A.I., Kataeva, M.N. and Ivanov, V.B. (2009) The Effects of Lead, Nickel, and Strontium Nitrates on Cell

Division and Elongation in Maize Roots. *Russ J Plant Physiol* 56, 242–250.

[3] Fiskesjö, G. The *Allium* test as a standard in environmental monitoring. *Hereditas* **1985,** *102,* 99–112.

[4] Jiang, W.S. (1994) Liu D.H. Effects of Cd^{2+} on the nucleolus in root tip cells of *Allium cepa*. J Environ Sci 6, 382–386.

[5] Liu, D.H., Jiang, W.S., Wang, W. and Zhai, L. (1995) Evaluation of metal ion toxicity on root tip cells by the *Allium* test. *Israel J Plant Sci* 43, 125–133.

[6] Liu, D., Jiang, W. and Gao, X. (2003/2004) Effects of cadmium on root growth, cell division and nucleoli in root tips of garlic. *Biol Plantarum* 47, 79–83.

[7] Liman, R., Akyılk D., Eren, Y. and Konuk, M. (2010) Testing of the mutagenicity and genotoxicity of metolcarb by using both Ames/Salmonella and Allium test. *Chemosphere* 80, 1056–1061.

[8] Özkara, A., Akyil, D. and Erdoğmuş, K.M. (2011) Evaluation of germination, root growth and cytological effects of wastewater of sugar factory (Afyonkarahisar) using *Hordeum vulgare* bioassays. *Environ Monit Assess* 183, 517–524.

[9] Zhang, H.H., Jiang, Z., Qin, R., Zhang, H., Zou, J.H., Jiang, W.S. and Liu, D.H. (2014) Accumulation and cellular toxicity of aluminum in seedling of *Pinus massoniana. BMC Plant Biol* 14, 264.

[10] Levan, A. (1938) The effect of colchicine on root mistosis in *Allium*. *Hereditas* 24*,* 471-486.

[11] Jiang, Z., Zhang, H.N., Qin, R., Zou, J.H., Wang, J.R., Shi, Q.Y., Jiang, W.S. and Liu, D.H. (2014) Effects of Lead on the Morphology and Structure of the Nucleolus in the Root Tip Meristematic Cells of *Allium cepa* L. *Int J Mol Sci* 15, 13406–13423.

[12] McGill, M., Pathak, S. and Hsu, T.C. (1974) Effects of ethidium bromide on mitosis and chromosomes: A possible material basis for chromosome stickiness. *Chromosoma* 47, 157–164.

[13] Klásterá, I., Natarajan, A.T. and Ramel, C. (1976) An interpretation of the origin of subchromatid aberrations and chromosome stickiness as a category of chromatid aberrations. *Hereditas* 83, 153–162.

[14] Grant, W.F. (1978) Chromosome aberrations in plants as a monitoring system. *Environ Health Perspect* 27, 37–43.

[15] Stępiński, D. (2014) Functional ultrastructure of the plant nucleolus. *Protoplasma* 251, 1285–1306.

[16] Shaw, P. and Brown, J. (2012) Nucleoli: composition, function, and dynamics. *Plant Physiol* 158, 44–51.

[17] Zhang, S.S., Zhang, H.M., Qin, R., Jiang, W.S. and Liu, D.H. (2009) Cadmium induction of lipid peroxidation and effects on root tip cells and antioxidant enzyme activities in *Vicia faba* L. *Ecotoxicology* 18, 814–823.

[18] Qin, R., Jiang, W.S. and Liu, D.H. (2013) Aluminum can induce alterations in the cellular localization and expressionof three major nucleolar proteins in root tip cells of *Allium cepa* var. *agrogarum* L. *Chemosphere* 90, 827–834.

[19] Qin, R., Jiang, W.S. and Liu, D.H. (2013) Cadmium can induce alterations in the cellular localization and expression of three major nucleolar proteins in root tip cells of *Vicia faba* L. *Plant Soil* 368, 365–373.

[20] Fiskesjö, G. (1983) Nucleolar dissolution induced by aluminium in root cells of Allium. *Physiol Plantlantarum* 59, 508–511.

[21] Fiskesjö, G. (1990) Occurrence and degeneration of 'Al-structures' in root cap cells of *Allium cepa* L. after Al-treatment. *Hereditas* 112, 193–202.

[22] Ivan, K. Petra, O. and Pavla, R. (2005) Expression and translocation of major nucleolar proteins in relation to the transcriptional activity of the nucleolus. *J Appl Biomed* 3, 175–186.

[23] Liu, D.H. and Jiang, W.S. (1991) Effects of Al^{3+} on the nucleolus in root tip cells of *Allium cepa*. *Hereditas* 115, 213–219.

[24] Fiskesjö, G. (1988) The *Allium* test – an alternative in environmental studies: the relative toxicity of metal ions. *Mutat Res* 197*,* 243–260.

[25] Olson, M.O.J. and Dundr, M. (2005) The moving parts of the nucleolus. *Histochem Cell Biol* 123, 203–216.

[26] Qin, R., Jiao, Y.Q., Zhang, S.S., Jiang, W.S. and Liu, D.H. (2010) Effects of aluminum on nucleoli in root tip cells and selected physiological and biochemical characters in *Allium cepa* var. *agrogarum* L. *BMC Plant Biol* 10, 225.

[27] Zhang, Y.X. (1995) Effects of aluminum chloride on the nucleus and nucleolus in root tip cells of *Hordeum vulgare*. *Mut Res* 335*,* 137–142.

[28] Liu, D.H., Jiang, W.S., Meng, Q.M., Zou, J., Gu, J.G. and Zeng, M.A. (2009) Cytogenetical and ultrastructural effects of copper on root meristem cells of *Allium sativum* L. *Biocell* 33, 25–32.

[29] Jiang, W.S. and Liu, D.H. (2000) Effects of Pb^{2+} on Root Growth, Cell Division, and Nucleolus of *Zea mays* L. *Bull Environ Contam Toxicol* 65, 786–793.

[30] Qin, R., Zhang, H.N., Li, S.S., Jiang, W.S. and Liu, D.H. (2014) Three major nucleolar proteins migrate from nucleolus to nucleoplasm and cytoplasm in root tip cells of *Vicia faba* L. exposed to aluminum. *Environ Sci Pollut Res* 21, 10736–10743.

[31] Zhang, H.N., Jiang, Z., Zhang, H.H., Zou, J.H., Jiang, W.S. and Liu, D.H. (2015) Aluminum can induce three nucleolar proteins migrated from nucleolus to cytoplasm in root tips of *Hordeum vulgare* L. *Fresen Environ Bull* 24(4a), 1372–1379.

[32] Balcerzak, Ł. Glińska, S. and Godlewski, M. (2011) The reaction of Lupinus angustifolius L. root meristematic cell nucleoli to lead. *Protoplasma* 248*,* 353–361.

[33] Van der Aa, M.A., Mastrobattista, E., Oosting, R., Hennink, W., Koning, G. and Cormmelin, D. (2006) The nuclear pore complex: the gateway to successful nonviral gene delivery. *Pharm Res* 23, 447–459.

[34] Rubbi, C.P. and Milner, J. (2000) Non-activated p53 co-localizes with sites of transcription within both the nucleoplasm and the nucleolus. *Oncogene* 19*,* 85–96.

[35] Andersen, J.S., Lam, Y.W., Leung, A.K., Ong, S.E., Lyon, C.E., Lamond, A.I. and Mann, M. (2005) Nucleolar proteome dynamics. *Nature* 433*,* 77–83.

[36] Sobol, M., Gonzalez-Camacho, F., Rodríguez-Vilariño, V., Kordyum, E. and Medina F.J. (2006) Subnucleolar location of fibrillarin and NopA64 in *Lepidium sativum* root meristematic cells is changed in altered gravity. *Protoplasma* 228, 209–219.

[37] Gjerset, R.A. (2006) DNA damage, p14ARF, Nucleophosmin (NPM/B23), and cancer. *J Mol Hist* 37, 239–251.

[38] Boulon, S., Westman, B.J., Hutten, S., Boisvert, F.M. and Lamond, A.I. (2010) The nucleolus under stress. *Mol Cell* 40*,* 216-227.

[39] Wang, J.R,, Shi, Q.Y., Zou, J.H., Jiang, Z., Wang, J.Y., Wu, H.F., Jiang, W.S. and Liu, D.H. (2015) Cellular localization of copper and its toxicity on root tips of *Hordeum vulgare*. *FresenEnviron Bull* 24, 2394–2405.

[40] Chen, M. and von Mikecz, A. (2000) Specific inhibition of rRNA transcription and dynamic relocation of fibrillarin induced by mercury. *Exp Cell Res* 259*,* 225–238.

[41] Ni, X.L. and Zhang, F.X. (2014) PI3K is involved in nucleolar structure and function on root-tip meristematic cells of *Triticum aestivum* L. *Acta Histochem* 116*,* 838–843.

[42] Makimoto, Y., Yano, H., Kaneta, T., Sato, Y. and Sato, S. (2006) Molecular cloning and gene expression of a fibrillarin homolog of tobacco BY-2 cells. *Protoplasma* 229*,* 53–62.

[43] Duangmano, S., Sae-lim, P., Suksamrarn, A., Domann, F.E. and Patmasiriwat, P. (2012) Cucurbitacin B inhibits human breast cancer cell proliferation through disruption of microtubule polymerization and nucleophosmin/B23 translocation. *BMC Complem Altern M* 12*,* 185.

[44] Derenzini, M. (2000) The AgNORs. *Micron* 31, 117–120.

[45] Sushil, L.M.D. (2011) AgNOR expression in central nervous system tumours. *J Med Biol Sci* 4, 1–9.

[46] Strauss, P.R. and Wilson, S.H. (1990) The Eukaryotic Nucleus: Molecular Biochemistry and Macromolecular Assemblies; The Telford Press: Caldwell, NJ, USA, pp. 783–811.

Received: **07.10.2015**
Accepted: **06.02.2016**

CORRESPONDING AUTHOR

Donghua Liu
Tianjin Key Laboratory of Animal and Plant Resistance College of Life Sciences Tianjin Normal University Tianjin 300387, CHINA

e-mail: donghua@mail.zlnet.com.cn

by PSP Volume 25 – No 7/ 2016 pages 2427-2435 Fresenius Environmental Bulletin

IDENTIFICATION AND CHARACTERIZATION OF DEOXYNIVALENOL-DEGRADING BACTERIAL STRAIN BACILLUS CIRCULANS C1-5-9

Long Miao[1,2],Chen Xinliang[2], Zhang Yi[2], Li Peng[2], He Jianbin[2*]

[1]College of Life and Engineering, Shenyang Institute of Technology, Fushun 113122, China;
[2]College of Animal Husbandry And Veterinary, Shenyang Agricultural university, Shenyang,110866,China

ABSTRACTS

The aim of this study was mainly to find bacteria to degrade deoxynivalenol (DON) . A bacterial strain, which can effectively use DON as sole carbon and energy source, was isolated from the feces of the hens feeding mould contamination feed by enrichment screening. Based on the analysis of physiological and biochemical characteristics, 16S rDNA gene sequence homology and phylogenetic tree, the isolate strain was identified. Its degradation characteristics and degradation capability of the DON were tested by ELISA method. This bacterial strain was identified as Bacillus circulans and named C1-5-9 . Results showed that this strain could utilize DON as sole carbon source for growth, and could degrade 98.85 % of DON after 72h shaking culture at 180 $r \cdot min^{-1}$, 37℃ and pH 7.0 with adding nitrogen source. Its degradation rate was increased by adding exogenous carbon and nitrogen source into the medium, and the degradation rate improved by adding exogenous nitrogen source was more effectively than by adding carbon source. The crude enzyme extracted from the strain had a degrading activity of DON, and the degrading enzymes were the extracellular enzyme, which had a strong tolerance to pH and good thermal stability. This is the first report of the Bacillus circulans strain able to degrade DON.

KEYWORDS:
deoxynivalenol; biodegradation; bacillus circulans; degrading characteristics

INTRODUCTION

Deoxynivalenol (DON, vomitoxin), the most abundant type B trichothecene, which is produced by the fungus Fusarium graminearumthat contaminates corn, wheat, and barley [1], is characterized by a high stability under different environmental conditions and resistance to high temperature [2]. The consumption of DON-contaminated food and feed can induce acute and chronic toxic effects. The adverse effects of acute exposure are including symptoms of gastrointestinal illness such as nausea, vomiting, diarrhea and hemorrhage[3,4,5,6]. The chronic exposure to this toxin induces anorexia, reduced food intake, weight gain and altered nutritional efficiency[7,8,9]. From the perspective of cell level, it reports that DON increases pro-inflammatory gene expression [10], impairs the cell division, proliferation, differentiation and cell membrane integrity, and induces apoptosis [11].

Various physical and chemical methods have been developed to decrease DON contamination, such as by ozone, ammonia, chlorine, hydrogen peroxide, sodium bisulfite, sodium carbonate, and chlorine dioxide, however, these methods can cause damage to product nutrition, the change of organoleptic qualities, the effect of undesirable health, and high cost for equipment [12,13]. These disadvantages spurred on the recent emphasis on biological methods to degrade mycotoxin. To date, several DON-degrading fungi and bacteria have been isolated from agricultural soil, infested plant material, and animal digestive tracts[14], such as Eubacterium sp. strain BBSH797[15], Agrobacterium-Rhizobium E3-39[16], Marmoricola sp. MIM116[17], Nocardioides sp. WSN05-2[18], Bacillus sp. LS100[19], Aspergillus tubingensis NJA-1[20].

In the present study, a nwe strain, named Bacillus circulans C1-5-9 capable of efficient biodegradation of DON was isolated. The character of the strain and its crude degrading enzymes to degrade DON in liquid medium was also evaluated. This supplying a new strain for bio-degradation of DON.

MATERIALS AND METHODS

Culture medium. The mineral medium MM(L^{-1}): $Na_2HPO_4 \cdot 2H_2O$ 8.5 g, KH_2PO_4 3.0 g, NaCl 0.5 g, NH_4Cl 1.0 g, $MgSO_4 \cdot 7H_2O$ 0.5g, $CaCl_2$ 14.7 mg, $CuSO_4$ 0.4 mg, KI 1.0 mg, $MnSO_4 \cdot H2O$ 4.0 mg, $ZnSO4 \cdot 7H_2O$ 4.0 mg, H_3BO_3 5.0 mg, $H_2MoO_4 \cdot 2H_2O$ 1.6 mg, $FeCl_3 \cdot 6H_2O$ 2.0 mg,

pH7.0~7.2, 121.5 ℃ sterilization for 25 min. Enrichment culture medium (L^{-1}): the need quantity of DON add in the culture solution of the mineral medium of bacteria

DON. DON was purchased from Sigma Aldrich (St. Louis, MO, USA). Stock solutions of DON were prepared in sterile MilliQ water (Millipore, Billerica, MA, USA) at a concentration of 1% (wt/vol), filtered and stocked at −20° C

Samples. Soil samples were collected from the feces of hens,which were fed the mouldy feed for the isolation of microorganisms capable of degrading DON.

Enrichment of bacterial cultures for DON degradation. One gram of the collected samples were added into 50ml of sterile distilled water in conical flask and fully mixed. The 1ml of the mixed suspensions were taken and added into 250ml of the mineral medium containing with 200 μg/mL of DON, and were incubated at 37°C for 7days with shaking. Then, 100 μL of these cultures was added to 250mL of MM containing 100 μg/mL DON, followed by 7 days of incubation with shaking at 37°C. This procedure was repeated three times. And then the 100μL of these cultures were coated and cultured on the MM solid medium containing with 100 μg/mL DON at 37°C until the single colony was grown. The single colonies were picked and inoculated in the MM liquid medium containing with 100 μg/mL DON at 37°C for 7days, and the concentrations of DON in the culture media were monitored by ELISA detection kit of the DON . One culture sample was found to decrease the DON concentration, and the DON degrading bacteria were isolated from this sample.

Calculation of the residue and degradation rate of DON. The 1 mL of the culture medium was taken and centrifugated in 10000 rpm/min for 5min, then the residual amount of DON in the supernatant was measured by the ELISA detection kit of the DON. The same concentration of DON in the MM was as the positive control at the same time, and the culture conditons were same as the experimental group. Each strain was done for three replicates,and the mean values were calculated. The degradation rate of DON was calculated according to the following formula:The degradation rate of DON% = M_0-M_n/M_0 * 100(M_0 was the average value of DON in the control group, and M_n was the average of the average of DON in each strain group.

Identification of the highest degradation rate of the isolated strains. The nucleotides of partial 16S rRNA gene were amplified by colony PCR using 27f and 1492r primers. The amplicons were purified by agarose electrophoresis and recycled by agarose recycling kit (Sangon Biotech,Shanghai, Co.,Ltd.). The recycled 16S rRNA gene was purified and sequenced by Sangon Biotech,Shanghai, Co.,Ltd. The result of the 16S rRNA gene sequence was submitted to GenBank and identified using BLAST (NationalCenter for Biotechnology Information, http://www.ncbi.nlm.nih.gov), and aligned by the clustalX1.83 program. Phylogenetic trees were constructed by MEGA 5.1 program using neighbor-joining.

Degradation characteristics of strain under pure culture conditions. The 250ml flask containing 100mL MM was adding DON and the highest degradation strain suspension. In the final system, the concentration of the DON was 20μg/mL and the OD_{600} of the strain was 0.2.

The effect of initial pH on the degradation. The initial pH of the pure culture was adjusted at 5.0, 6.0, 7.0, 8.0, 9.0, 10.0 by using 0.1 mol·L^{-1} HCl and 0.1 mol·L^{-1} NaOH. The cultures were incubated with the strain shaking at 180 rpm and 37°C and taken 1ml for determination at 30h, 60h, 90h, 120h, 150h and 180h followed by analysis of the DON concentrations remaining in the cultures.

The effect of temperature on the degradation. The cultures were inoculated with the strain shaking at 180rpm and at 10°C, 20°C, 30°C,37°C, 40°C, and taken 1ml for determination at 30h, 60h, 90h, 120h, 150h and 180h followed by analysis of the DON concentrations remaining in the cultures.

The effect of nutrient substrate on the degradation. The 1g of yeast extract, petone, beef extract, glucose, starch was added into the MM liquid culture medium, respectively. These MM liquid cultures were inoculated with the srain shaking at 180rpm under the optimum pH and temperature conditions, and taken 1ml for determination at 30h, 60h, 90h, 120h, 150h and 180h, followed by analysis of the DON concentrations remaining in the cultures.

Extraction of crude degrading enzyme of DON and its character of degradation. The bacterial cells were obtained by centrifugated at 8000g for 10min after the strain was cultured in MM liquid medium containing 100μg/mL DON at shaking for 24h. The bacterial cells were washed with phosphate buffer solution (50mmol/L, pH7.0) for 2 times, and then suspended in the 1ml of the same buffer solution. The cell suspension was broken for 20min by Ultrasonic crusher (working for 5s and stopping for 5s) in at the condition of ice bath, and then centrifugated at 10000g for 10min at 4°C. The supernatant was the crude enzyme liquid. The 1mL of the crude enzyme, 3mL of the

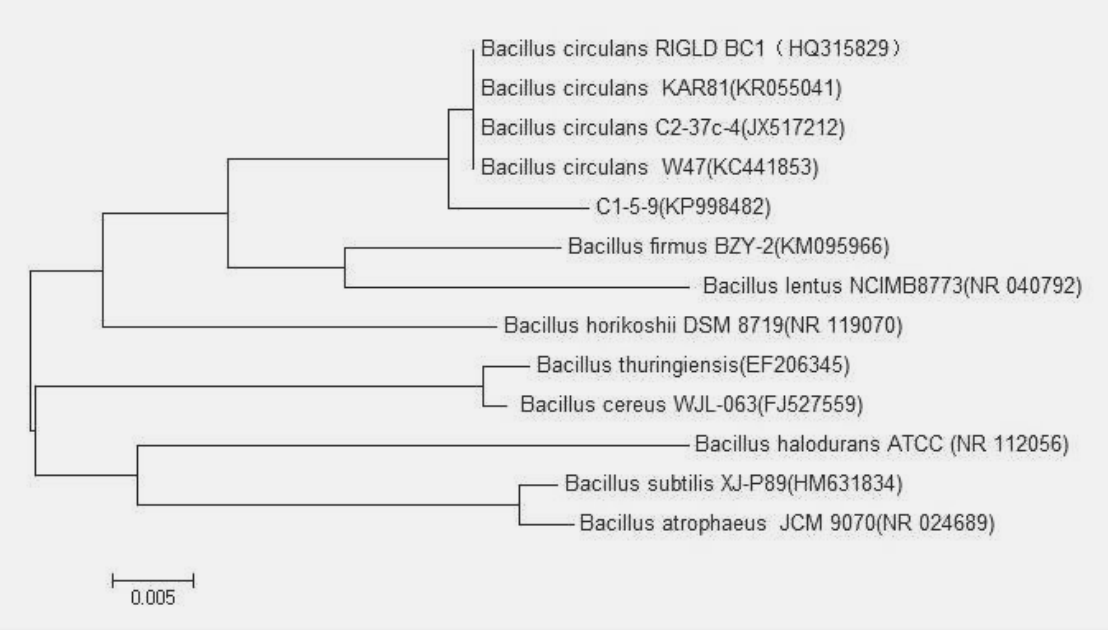

FIGURE 1
Phylogenetic tree based on 16S rRNA gene sequences of the strain C1-5-9(KP998482) and related microorganisms. 0.005 substitutions per nucleotide position.

50mmol/L phosphate buffer solution and the final concentration

20μg/mL of DON were mixed and cultured for 6h under the different conditions of pH(5.0-9.0) and temperature(15-40°C). After termination of the reaction, the remains of DON was detected by DON ELISA kit. The control group was LB culture medium and the supernatant of the cells lysis.

RESULTS AND DISCUSSIONS

Screening and identification of the degrading bacteria. It was showed that 3 strains from the feces had the abiltiy of degrading DON by using enrichement culture methods and DON as the only carbon source. A bacterial strain(named C1-5-9) that had the highest ability of degrading DON was selected. The strain C1-5-9 is a Gram-positive, spore-forming,-shaped bacterium. The sequence of its 16S rDNA was 1450bp, accepted by GenBank and the accession number was KP998482.1, revealed that C1-5-9 is closely related to the Bacillus circulans, which belongs to the genus Bacillus, as illustrated in the phylogenetic tree in Fig. 1. On the basis of these characteristics, C1-5-9 was inferred to be a member of the Bacillus circulans.

Degradation characteristics of strain under pure culture conditions. Effect of the initial pH and different temperature on the degradation ability of the strain C1-5-9

The degradation ability of the strain C1-5-9 in different initial pH was shown in Figure 2. And the growth of the strain C1-5-9 and the ability of the strain C1-5-9 under the different initial pH conditions were shown in Figure 3. From the Figure 2 and 3, It was showed that the initial pH has great influence on the growth of the strain and degradation of DON. The strain could grow in pH at 6.0-9.0, and it grew well in pH at 7.0-8.0. However, the strain could not grow well and the degradation rate were low when the the pH at 5.0 and 10.0.

The degradation ability of the strain C1-5-9 at different temperatures was shown in Figure 4. The results showed that it was increased gradually with the increase of temperature in the range of 10°C~37°C. The degradation ability was the best when the temperature was in the range of 30°C-37°C, and the degradation rate were reached to 97% and 99% at 30°C and 37°C for incubating for 140h respectively . It showed that the degradation rate of DON was little difference when the temperature were at 30°C and 37°C. It maybe because that it was no difference that the strain grew at 30°C and 37°C. However, the degradation rate was lower when the temperature was at 10°C , 20°C and 40°C than that were at 30°C and 37°C. The degradation rate was very low at first when the temperature were in the range of 10°C-20°C, but it was increased in the later period of degradation. It may be that the degradation ability of the strains was restored after a period of adaptation.

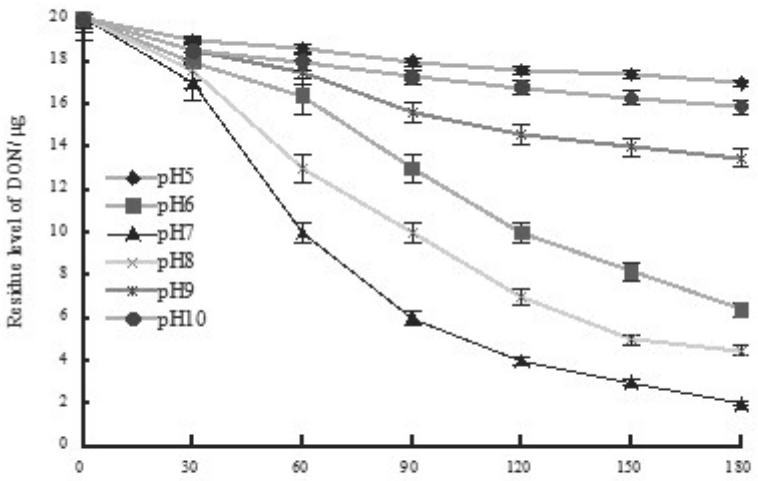

FIGURE 2
Effect of different initial pH on degradation of DON.

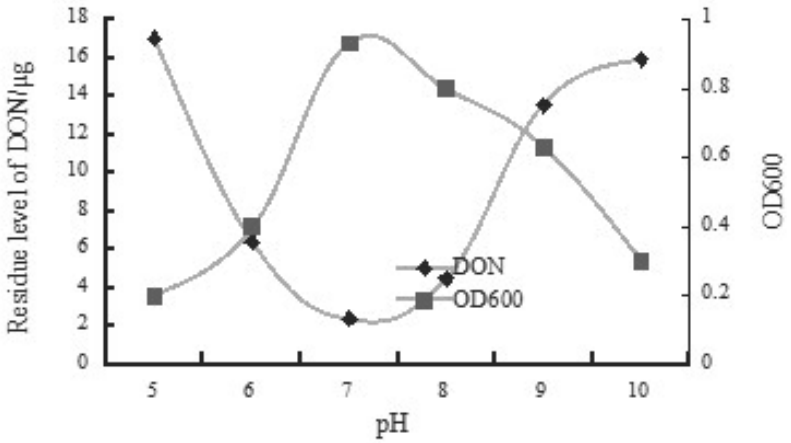

FIGURE 3
Degradation of DON and growth of the strain Bacillus circulans C1-5-9 at diffetent initial pH.

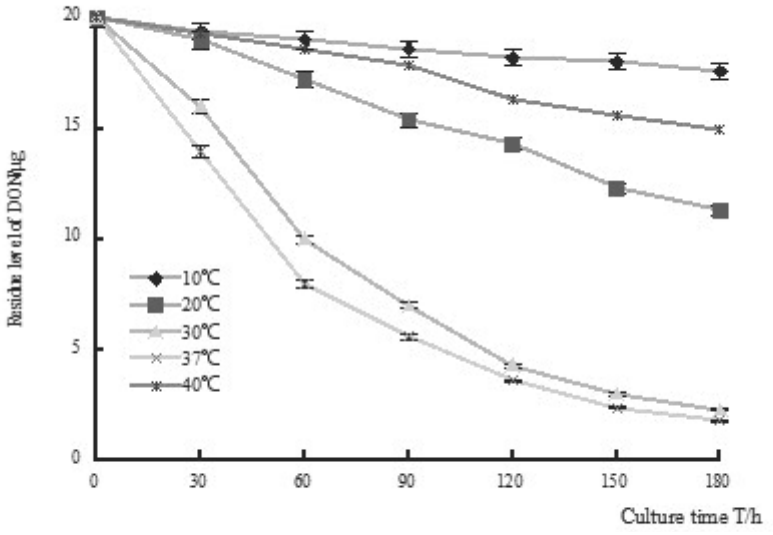

FIGURE 4
Effect of different culture temperature on degradation of DON.

The effect of nutrient substrate on the degradation. The effect of the strain on the degradation of DON could be significantly improved by the addition of exogenous nutrients in the MM liquid. The growth of the strain and the degradation rate of DON were all increased with the additon of exogenous nutrients, and the degradation rate reached to 98.85% at 180h with adding peptone. The degradation rate effected by adding the organic nitrogen source was better than by adding organic carbon source. The strain can use the exogenous nutrient and DON at the same time.

Growth and degradation characteristics of strain Bacillus circulans C1-5-9 at the optimal conditions. The growth and degradation of the strain was studied at the optimal temperature 37°C, pH7.0 and the MM medium containing 500mg/L of peptone, which conditions were determined as above. The strain entered the exponential phase at 12h, and the degradation rate of DON increased with the increase of the number of the bacterial cells. The residue of the DON only 0.22 μg/ml at 72h as it was shown in Figure 6. This result showed that at the optimal conditions, It improved the dagradation rate and shortened the time of degradation.

Determination of the crude enzyme degradation. The effects of the temperature and pH on the enzymatic degradation of the crude enzyme extracted from the strain was shown in Figure 7 and Figure 8. It showed that the high degradation activity of the crude enzyme were at the temperature 25°C~40°C, and the optimum degradation temperature of the strain was 37°C. It could be speculated that the degradation enzyme of the crude enzyme had good thermal stability. The crude enzyme had the highest degradation rate of DON at pH 7, and the degradation rate at pH 6.0~9.0 was more than 80%. It showed that the degradation enzyme was not sensitive to pH and had a strong tolerance to pH.

The crude enzyme had the activity of degrading DON, which showed that the key enzymes of degrading DON were contained in the crude enzyme. In MM culture medium without DON, the strain C1-5-9 was not able to grow, and the activity of degrading DON was not detected in the cell extracts of the strain. The srtain could be grow well in LB medium, but the activity of the crude enzyme was very low(Data not shown). It was speculated that the degradation of the enzyme is inducible enzyme.

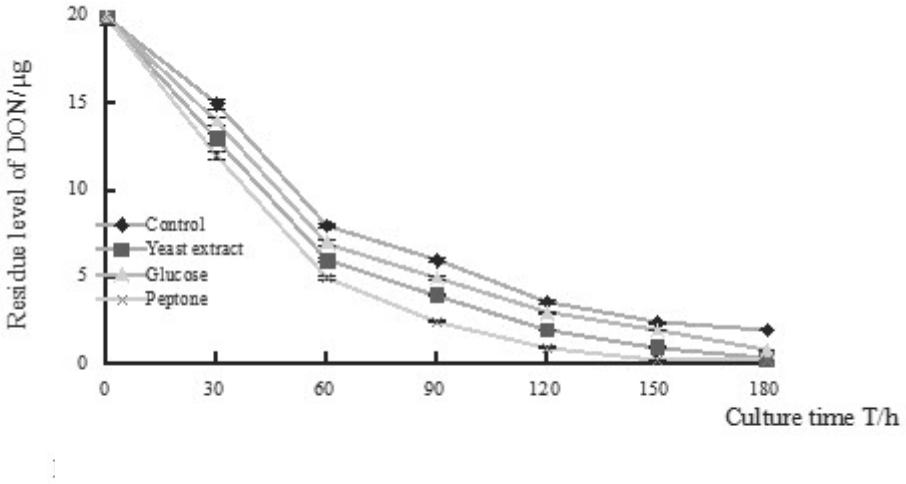

FIGURE 5
Effect of different nutrient substrate on degradation of DON.

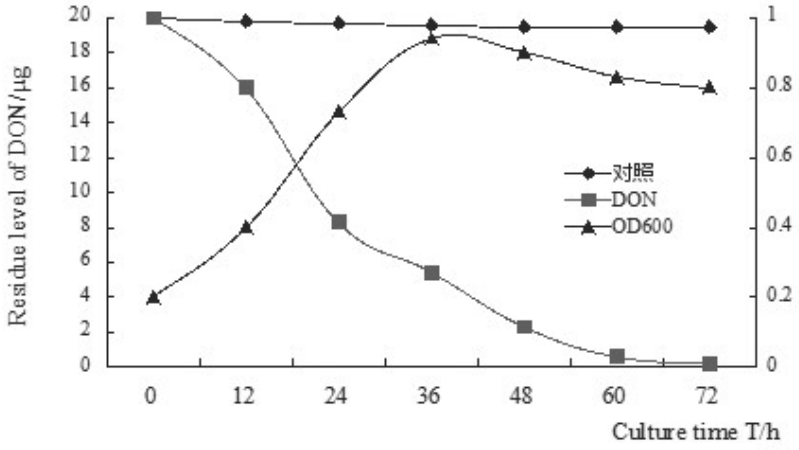

FIGURE 6
Degradation of DON and the growth of Bacillus circulans C1-5-9 at the optimal conditions.

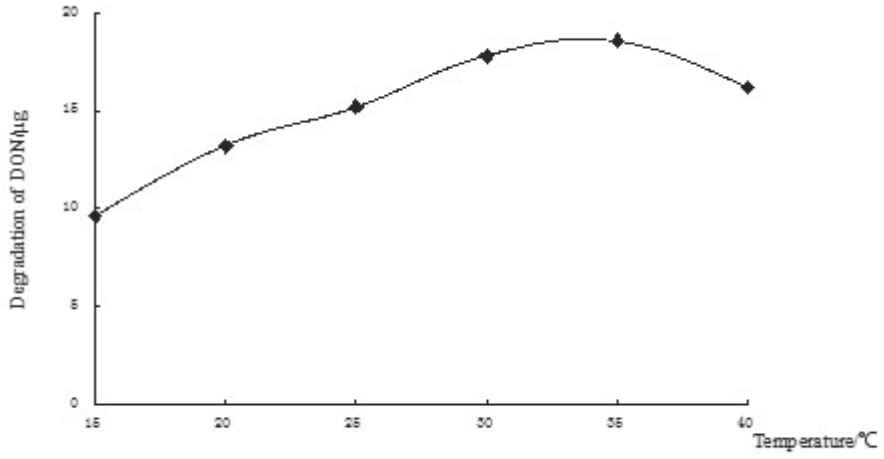

FIGURE 7
Effect of different temperature on crude enzymatic degradation of DON.

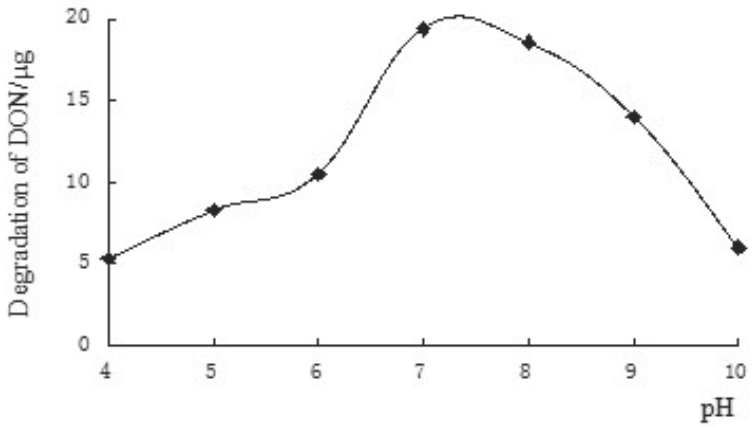

FIGURE 8
Effect of pH on crude enzymatic degradation of DON.

CONCLUSION

In conclusion, our work has successfully isolated a higher degrading DON bacteria from the feces of the hens, which were named as Bacillus circulans C1-5-9. It is a new bacterial resource for degrading DON, and the degradation rate of the strain for DON(20 μg/ml) was 98.85 % when incubated for 72 h at 37°C and pH7.0 with nitrogen source such as peptone in a rotary shaker (180 rpm). And the catabolic enzymes of the strain were the extracellular enzyme, and had a strong tolerance to pH and good thermal stability.

ACKNOWLEDGMENTS

This work was supported by the National Natural Science Foundation of China (Beijing, China, Grant Nos. 31201961, 31302152); China Postdoctoral Science Foundation (2014M551125); The general research project of the Education Department of Liaoning Province(L2014561).

REFERENCES

[1] Pestka, J.J. (2010) Deoxynivalenol: Mechanisms of action, human exposure, and toxicological relevance. Arch Toxicol 84:663–679.

[2] Wolf-Hall, C.E., Hanna, M.A., Bullerman, L.B. (1999) Stability of deoxynivalenol in heat-treated foods. Journal of food protection, 62(8), 962–964.

[3] Amuzie, C.J., Pestka, J.J. (2010) Suppression of insulin-like growth factor acid-labile subunit expression-a novel mechanism for deoxynivalenol-induced growth retardation. Toxicol. Sci 113, 412–421.

[4] Voss, K.A. (2010) A new perspective on deoxynivalenol and growth suppression. Toxicol. Sci113, 281–283.

[5] Bryden, W.L. (2007) Mycotoxins in the food chain: human health implications. Asia Pacific journal of clinical nutrition16 Suppl 1, 95–101.

[6] Oswald, I.P., Marin, D.E., Bouhet, S., Pinton, P., Taranu, I., Accensi, F. (2005) Immunotoxicological risk of mycotoxins for domestic animals. Food addit and contam 22(4), 354–60.

[7] Flannery, B.M., Wu, W., Pestka, J.J. (2011) Characterization of deoxynivalenol-induced anorexia using mouse bioassay.Food and chemical toxicology: an international journal published for the British Industrial Biological Research Association 49(8), 1863–1869.

[8] Abysique, A., Tardivel, C., Troadec, J.D., Félix, B. (2015) The Food Contaminant Mycotoxin Deoxynivalenol Inhibits the Swallowing Reflex in Anaesthetized Rats. PLoS One20; 10(7), e0133355.

[9] Alizadeh, A., Braber, S., Akbari, P., Garssen, J., Fink-Gremmels, J. (2015) Deoxynivalenol Impairs Weight Gain and Affects Markers of Gut Health after Low-Dose, Short-Term Exposure of Growing Pigs.Toxins (Basel). 7(6), 2071-95.

[10] Pestka, J.J. (2008) Mechanisms of deoxynivalenol-induced gene expression and apoptosis. Food Addit Contam 25, 1128–1140.

[11] Zhou. H.R., Harkema, J.R., Hotchkiss, J.A., Yan, D., Roth, R.A., Pestka, J.J. (2000) Lipopolysaccharide and the trichothecene vomitoxin (deoxynivalenol) synergistically induce apoptosis in murine lymphoid organs. Toxicol Sci 53, 253–263.

[12] Galvano, F., Piva, A., Ritieni, A., Galvano, G. (2001) Dietary strategies to counteract the effects of mycotoxins: a review. J Food Protect 64, 120 – 131.

[13] Karlovsky, P. (2011) Biological detoxification of the mycotoxin deoxynivalenol and its use in genetically engineered crops and feed additives.Appl Microbiol Biotechnol 91(3), 491-504.

[14] McCormick, S.P. (2013) Microbial Detoxification of Mycotoxins.J Chem Ecol 39, 907 – 918.

[15] Fuchs, E., Binder, E.M., Heidler, D., Krska, R. (2002) Structural characterization of metabolites after the microbial degradation of type A trichothecenes by the bacterial strain BBSH 797. Food Addit Contam19, 379 – 386.

[16] Shima, J., Takase, S., Takahashi, Y., Iwai, Y., Fujimoto, H., Yamazaki, M., Ochi, K. (1997) Novel detoxification of the trichothecene mycotoxin deoxynivalenol by a soil bacterium isolated by enrichment culture.Appl Environ Microbiol 63(10), 3825-3830.

[17] Ito M, Sato I, Koitabashi M, Yoshida S, Imai M, Tsushima S (2012) A novel actinomycete derived from wheat heads degrades deoxynivalenol in the grain of wheat and barley affected by Fusarium head blight. Appl Microbiol Biotechnol96(4):1059-70.

[18] Toshima, H., Koitabashi, M., Ito, M., Karlovsky, P., Tsushima, S. (2011) Nocardioides sp. strain WSN05-2, isolated from a wheat field, degrades deoxynivalenol, producing the novel intermediate 3-epi-deoxynivalenol. Appl Microbiol Biotechnol.9(2), 419-27.

[19] Li, X.Z., Zhu, C., De Lange, C.F., Zhou, T., He, J., Yu, H., Gong, J., Young, J.C. (2011) Efficacy of detoxification of deoxynivalenol-contaminated corn by Bacillus sp. LS100 in reducing the adverse effects of the mycotoxin on swine growth performance. Food Addit Contam Part A Chem Anal Control Expo Risk Assess.28(7), 894-901.

[20] He, C., Fan, Y., Liu, G., Zhang, H. (2008) Isolation and identification of a strain of Aspergillus tubingensis with deoxynivalenol biotransformation capability. International Journal of Molecular Sciences 9(12), 2366-2375.

[21] Kuroda, K., Waki, M., Yasuda, T., Fukumoto, Y., Tanaka, A., Nakasaki, K. (2015) Utilization of Bacillus sp. strain TAT105 as a biological additive to reduce ammonia emissions during composting of swine feces.Biosci Biotechnol Biochem 79(10), 1702-11.

[22] Kandasamy, S., Dananjeyan, B1., Krishnamurthy, K1., Benckiser, G. (2015) Aerobic cyanide degradation by bacterial isolates from cassava factory wastewater.Braz J Microbiol46(3), 659-66.

[23] Rana, S., Jindal, V., Mandal, K., Kaur, G., Gupta, V.K. (2015) Thiamethoxam degradation by Pseudomonas and Bacillus strains isolated from agricultural soils.Environ Monit Assess 187(5), 300.

[24] Liu, J., Huang, W., Han, H., She, C., Zhong, G. (2015) Characterization of cell-free extracts from fenpropathrin-degrading strain Bacillus cereus ZH-3 and its potential for bioremediation of pyrethroid-contaminated soils. Sci Total Environ 523, 50-58.

[25] Bott, G., Lingens, F. (1991) Microbial metabolism of quinoline and related compounds. IX. Degradation of 6-hydroxyquinoline and quinoline by Pseudomonas diminuta 31/1 Fa1 and Bacillus circulans 31/2 A1.Biol Chem Hoppe Seyler 72(6), 381-3.

[26] Wu, S.J., Zhang, H.X., Hu, Z.H., Chen, J.M. (2009) Gene cloning and overexpression of dichloromethane dehalogenase from Bacillus circulans WZ-12.Huan Jing Ke Xue 30(8), 2479-84.

[27] Anand, A.A., Vennison, S.J., Sankar, S.G., Prabhu, D.I., Vasan, P.T., Raghuraman, T., Geoffrey, C.J., Vendan, S.E. (2010) Isolation and characterization of bacteria from the gut of Bombyx mori that degrade cellulose, xylan, pectin and starch and their impact on digestion.J Insect Sci 10, 107.

Received: **08.10.2015**
Accepted: **25.12.2015**

CORRESPONDING AUTHOR

He Jianbin
College of Animal Husbandry And Veterinary, Shenyang Agricultural University,
Shenyang,110866 - CHINA

e-mail: hejianbin69@163.com

© by PSP Volume 25 – No. 7/2016, pages 2436-2443 Fresenius Environmental Bulletin

CORRECT COMBUSTION BLACK LOCUST (*ROBINIA PSEUDOACACIA* L.) WOOD IN BOILER A LOW-TEMPERATURE LOW POWER

Artur Kraszkiewicz, Artur Przywara

Department of Machinery Exploitation and Management of Production Processes, Faculty of Production Engineering, University of Life Sciences in Lublin, Poland

ABSTRACT

The aim of the study was assessment and analyze the burning process of black locust wood in a low-temperature water boiler with upper grate combustion. Tests were carried out by varying of supply primary and secondary air in the context of reduction emission of CO, NO and SO_2, and to achieve the smallest chimney energy loss. The result of the research is that ecologically acceptable black locust wood burning in the boiler low-temperature hot water boiler with upper grate combustion, can occur at ensuring that in each phase combustion air supply in excess of not more than $\lambda = 2$. With these assumptions a black locust wood burning causes minimal emissions of CO, NO and SO_2 into the atmosphere thereby obtained a high pyrotechnic efficiency ranged about 80%. Improvement of combustion of wood in these heating devices is seen in the feeding of primary and secondary air in conjunction with the control of the excess in relation to the phases of the combustion process. The analysis should be subjected to the initial and final phase of the combustion process of wood logs in relation to the construction solutions of boilers.

KEYWORDS:
Black locust, biomass combustion, emissions

INTRODUCTION

Black locust is gaining popularity as an energy crop species, due to the biological characteristics of the species allowing the rapid growth and obtain the significant increase wood logs based on crops of arable land where nutrients condition is low [1; 2]. Equally black locust wood has desired technical parameters such as moisture after cutting, heat of combustion and the density [3; 4; 5]. Hence, this species is grown for energy purposes on large surfaces, mainly native habitat conditions in North America [6] as well as introduced species in other countries, for example in Hungary, Germany and China [7].

Single-family residential construction usually utilises individual heat sources. The approximate number of hard-coal-fired and wood logs devices adapted to be fired (central-heating boilers, ceramic stoves, metal and kitchen stoves) amounts to over 17 million units. Unfortunately, despite their high quality parameters, these carbons are fired in obsolete stoves and boilers, or in boilers for coke firing, which, among other things, results in high emissions into the air. This group of traditional low-power boilers and stoves is characterised by manual, periodic fuel feeding, the lack of strict quality requirements for fuels, and by low-energy efficiency (65-75%) and high emissions, except for boilers with primary- and secondary-air division and boilers with a primary degassing chamber [8; 9; 10].

The combustion process of wood fuels and other types of fuel should be characterised by complete fuel burn-up and low emissions of combustion products. Contemporary heating equipment utilising solid biofuels, fired with wood logs or wood pellets, are today highly-efficient machines for heat generation. There are many solutions for plant biomass combustion or co-firing plants that facilitate the efficient utilisation of energy contained therein. The selection of an appropriate combustion technology is conditional on system power, physical and chemical parameters of fuel, and the size and shape of fuel [11; 12]. Another important thing is that the combustion of biomass fuels takes place at a flame temperature of up to 850°C – during combustion – and below 400°C during granulate incandescence [13; 14; 15]. Modern heating devices for solid biofuels, fed with wood logs or pellet today are high-performance machines that produce heat. On the other hand, it is often the case that biomass fuels are fired using the same heating equipment as for coal firing, mainly due to the substantial costs of upgrading the system. This results not only in the reduced efficiency of such combustion, but, more importantly, with varied emissions of such substances as carbon oxide (CO), nitrous oxides (NO_x) and sulphur dioxide (SO_2). There is no monitoring of these emissions. Literature also seems to be lacking information on the volume of such emissions for

the phases of the combustion process and kind of the form of biofuels used [16; 17].

The aim of the study was assessment and analyze the burning process of black locust wood in a low-temperature water boiler with upper grate combustion. Tests were carried out by varying of supply primary and secondary air in the context of reduction emission of CO, NO and SO_2, and to achieve the smallest chimney energy loss.

MATERIALS AND METHODS

The research used as fuel logs wood of black locust. Dimensions wood billets were measured using a calliper. Defined also its basic technical characteristics, using the following methods to the mark in working condition:

- moisture – the gravimetric method in line with the PN-EN 14774-1:2010 standard [18];
- density – the ksylometric method;
- heat of combustion – in line with the PN-EN 14918:2010 standard [19];
- ash content – in line with the PN-EN 14775:2010 standard [20].

Test stand are: bottom-combustion upper boiler with a fixed grate with a nominal power of 10 kW, fed periodically (Fig. 1). Furthermore, it was equipped with an airflow ventilator, secondary air fan as well as and a service liquid circulation pump. These devices were controlled using an ST-28 microprocessor controller. Water flow rate in the boiler amounted to 85 $dm^3 \cdot h^{-1}$. The boiler was connected to the chimney made of a steel pipe with a diameter of 0.1 m and a length of 3 m. Combustion gases were collected from the chimney at a distance of 1 m from the smoke conduit. A measuring probe was connected to the Madur Eljack Electronics PGD-100 gas conditioner, from which gasses were directed to an exhaust-gas analyser Photon Madur Eljack Electronics. The gas measurements from NDIR sensors were for CO, NO_x, SO_2, whereas electrochemical sensors measured O_2. The temperature of the exhaust gas and air supplied to the boiler was measured by means of sensors NiCr-Ni (K), and PT-500.

The measurement and temperature of exhaust-gas contents was conducted continuously, i.e. from initiation (ignition) to burning out. The results were recorded in the analyser database every 2 seconds. Air fuel ratio (λ) was calculated using the formula:

$$\lambda = 20{,}95/(20{,}95\text{-}O_2)$$

where:

O_2 – oxygen content by volume in dry gas [%].

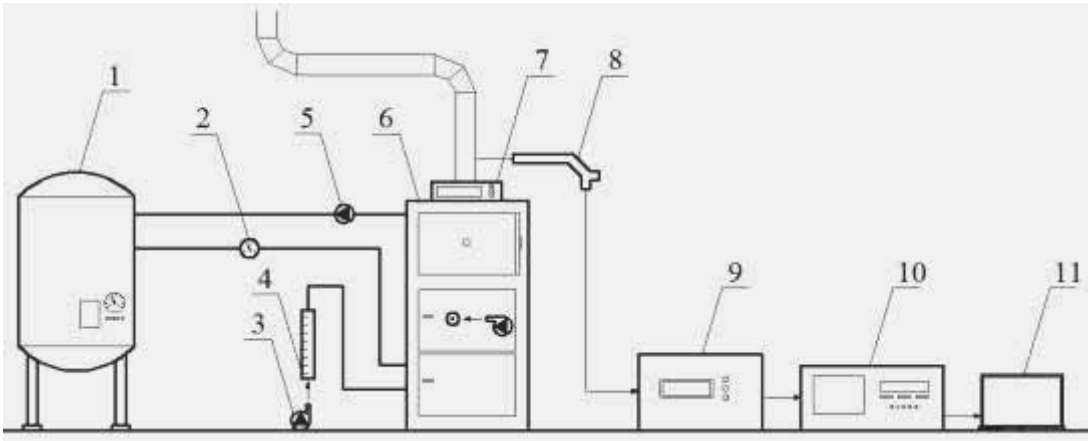

Source: own study

FIGURE 1

Diagram of measuring system: 1- heat exchanger, 2- water flow rate meter, 3- air fan, 4-flow meter, 5- pump operating fluid, 6- boiler, 7- microprocessor-based controller boiler, 8- secondary air fun, 9- probe with heated hoses, 10-dryer flue gas, 11-gas analyzer, 12- personal computer.

TABLE 1
Characteristic of variables during tests.

No.	Signature	Primary air	Flow rate of primary air [m·s^{-1}]	Secondary air	Flow rate of secondary air [m·s^{-1}]
1	PA1	+	0,36	-	0
2	PA2	+	0,98	-	0
3	PA3	+	1,23	-	0
4	PA4	+	1,43	-	0
5	PA5	+	2,6	-	0
6	PA1SA	+	0,36	+	0,98
7	PA2SA	+	0,98	+	0,98
8	PA3SA	+	1,23	+	0,98
9	PA4SA	+	1,43	+	0,98
10	PA5SA	+	2,6	+	0,98

+/- appear/lack

Calculated also exhaust gas losses (q_A) and a pyrotechnic efficiency (ETA) based on the data collected from completed combustion processes. The loss of exhaust gas is defined as the difference between the exhaust gas temperature and the temperature of the mixture burnt in relation to fuel properties and the amount of oxygen in the exhaust gas. To calculate this magnitude used the following formula [13]:

$$q_A = (t_A - t_L) \cdot (\frac{A_2}{20,95 - O_2} + B) \ [\%]$$

where:
q_A – loss of exhaust gas [%];
t_A – air temperature [ºC];
t_L – temperature of combusted mixture [°C];
O_2 – oxygen content by volume in dry gas [%];
A_2 – characteristic coefficient for fuel - biomass – 0,650;
B – characteristic coefficient for fuel - biomass – 0,008.

However, the difference between a loss of gases and a whole represented exhaust pyrotechnic performance ETA. During researches burned fuel samples a weight of 2 kg, by modifying the primary and secondary air. Therefore, performed ten different tests in three reps. The variables used in the study are shown in Table 1.

The obtained concentration results of CO, NO_x and SO_2 in exhaust gases was juxtaposed to a dry exhaust-gas jet volume containing 10% of oxygen and to normal conditions (mg·m^{-3}) at 0°C and 1013 mbar, in line with the guidelines of the PN-EN 303-5:2002 standard [21]. The data group included three stages in the combustion process, which were subject to statistical analysis using the STATISTICA 10.0 software by means of the two-way analysis of variance and Tukey's test. The materiality level in all analyses was defined at α = 0.05.

RESULTS

The average values of the physical properties of the black locust wood logs in question are presented in Table 2.

TABLE 2
Physical properties of black locust wood.

Fuel parameters in the working state- mean values	Unit	Black locust wood logs
Length	mm	300
Width	mm	30
Moisture	%	10
Heat of combustion	MJ·kg^{-1}	18,38
Ash	%	0,36

The respective stages of the combustion process of individual raw materials can be identified by observing the oxygen content in combustion gas. The first stage commenced with the ignition of the fuel and lasted until the lowest stable oxygen content in combustion gas had been reached. Next, the second stage began, in which the oxygen content in exhaust gas remained stable. The third stage, including the afterburning of fuel, commenced as the oxygen content in combustion gas started to grow, and lasted till the end of the oxidation reaction. Phases of the combustion process are important for the analysis of the results, which in the literature omit the initial phase and final portion of fuel combustion process.

Figure 1 shows the mean values of CO emission indicators converted to normal conditions 10% of the oxygen in the exhaust and combined with the corresponding mean values of indicators of excess air in the three analyzed phases of combustion.

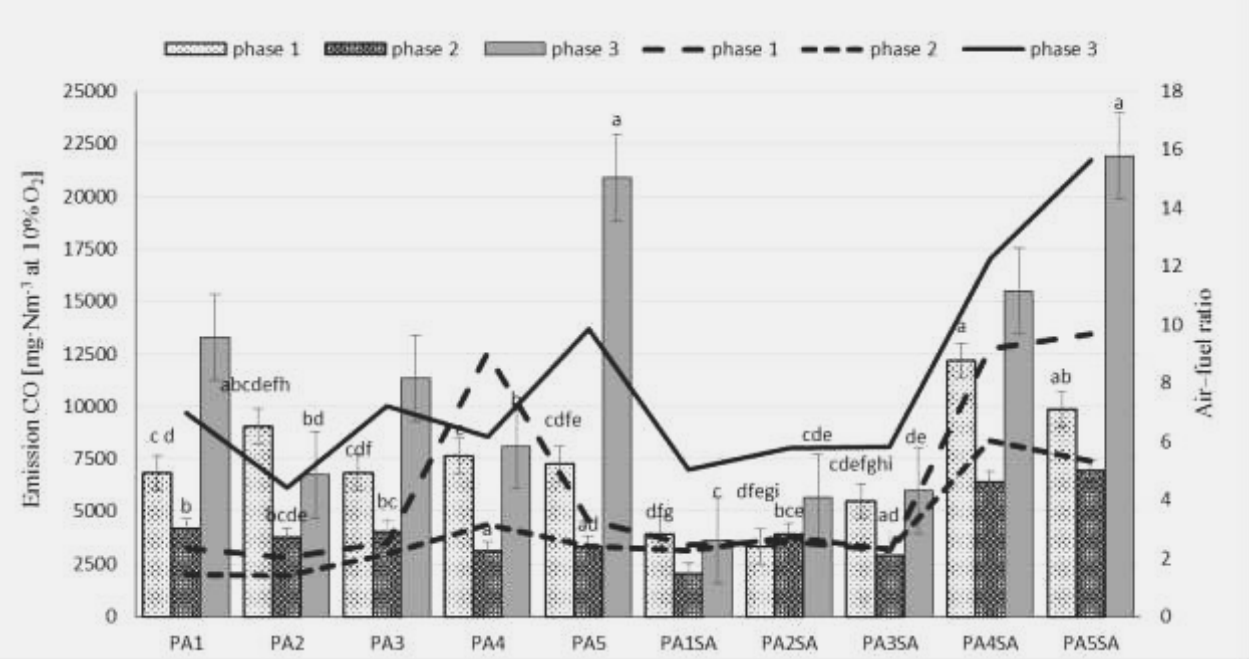

FIGURE 1
Effect of feeding air way to the mean of CO emission factors at the combustion process of black locust wood with detailing its phases (a-a, b-b etc. homogeneous groups).

The mean values of CO emission indicators in the combustion process of black locust wood with detailing its phases depending on the air delivery were varied. The smallest value (slightly more than 2500 mg·Nm^{-3} at 10% O_2) were observed during the combustion tests with the three lowest primary air flow velocities and the lowest rate of secondary air - PA1SA; PA2SA and PA3SA. The values of phases 1 and 3 in relation to phase 2 were approximately twice as large (Figure 1). In these tests, the excess air indicator typically maintained at a level less than 2, only in phase 3 the excess air was greater and the indicator was about 6. However, in tests using only primary air (PA1, PA2, PA3, PA4 and PA5) was observed that with increasing velocity of air blowing into the boiler increased emission of carbon monoxide (CO). In phase 1 and 3 it was 2-3 times higher than in the identical setting of the primary air but using the secondary air. The excess air ranged from 2 to 6 depending on the phase (Figure 1). It was also observed that the greatest emissions, significantly exceeding the standard for biomass fuels (stored in the PN-EN 303-5:2002) occurred in phase 3. Reduction of CO emissions also not obtained using the higher velocity of the secondary air - PA4SA tests and PA5SA - and even given a counterproductive. The excess air in the tests in phases 1-3 were approximately 6, 10 and 14 (Figure 1).

Statistical analysis showed significant differences between the mean values of CO emission indicators in particular phases of tests and Tukey's test carried out pointed to the CO emission indicators in phases 1-3, respectively 9, 5 and 4 homogeneous groups (Figure 1). Effect of feeding air way to the mean values of NO emission indicators at the combustion process of black locust wood with detailing its phases is shown in Figure 2.

The mean values of NO emission indicators in combustion process of black locust wood with detailing its phases depending on the method of feeding of air were less differentiated than for CO emission indicators. The smallest values at the level of 200-250 mg·Nm^{-3} at 10% O_2 were observed during the test burn with the primary air velocity of 0.98 m·s^{-1} and the lowest secondary air velocity - test PA2SA (Figure 2). During the tests, PA1-PA4, PA1SA and PA3SA, the emissions were higher by approximately 50 mg·Nm^{-3} at 10% O_2. In this tests, the emissions of NO in relation to the sequentially occurring phases of the combustion process generally characterized by a decreasing trend. Whereas the excess air indicator generally maintained at about 2 only in phase 3 was higher and was about 6. However, in tests PA5, PA4SA and PA5SA, in which the excess air was higher, emission of NO was almost two times higher than for others (Figure 2).

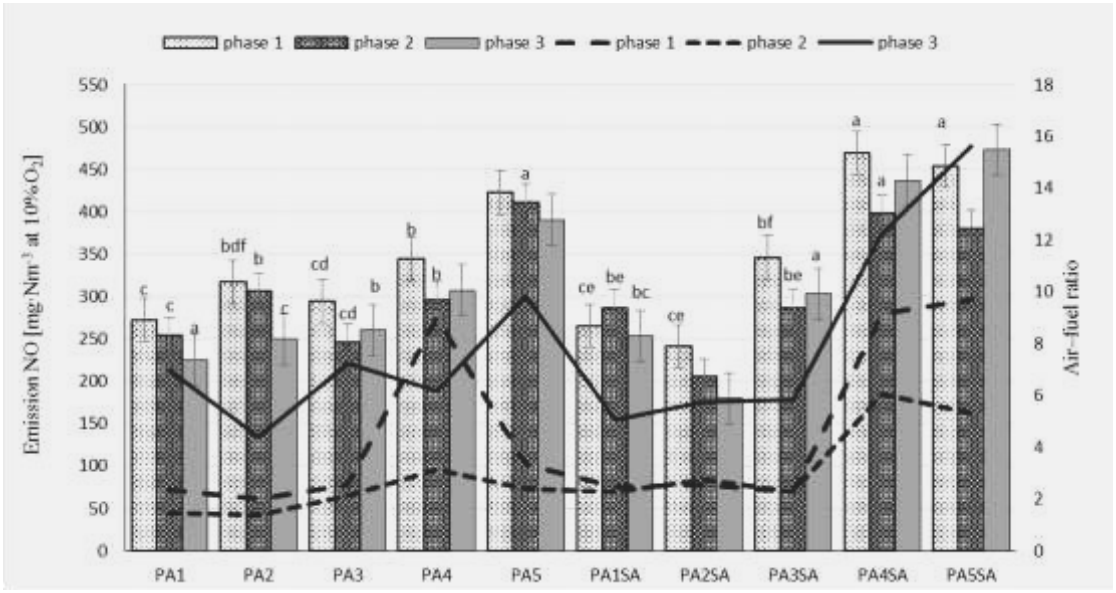

FIGURE 2
Effect of feeding air way to the mean emission factors of NO at the combustion process of black locust wood with detailing its phases (a-a, b-b etc. homogeneous groups).

Statistical analysis showed significant differences between the mean values of NO emission indicators in particular phases of tests and Tukey's test carried out pointed to NO emission indicators in phases 1-3 respectively 6, 5 and 3 homogeneous groups (Figure 2). The mean values of emission of SO_2 by combustion process of black locust wood with detailing its phases depending on the method of feeding air way were varied with similar variability as the values of CO emission indicators.

The lowest values were observed during the combustion test with three lowest velocities primary air and secondary air lowest velocity - the tests PA1SA; PA2SA and PA3SA. The values of the phases 1 and 3 in relation to phase 2 were about 100% higher, only PA2SA test remained at the same level of about 50 mg·Nm^{-3} at

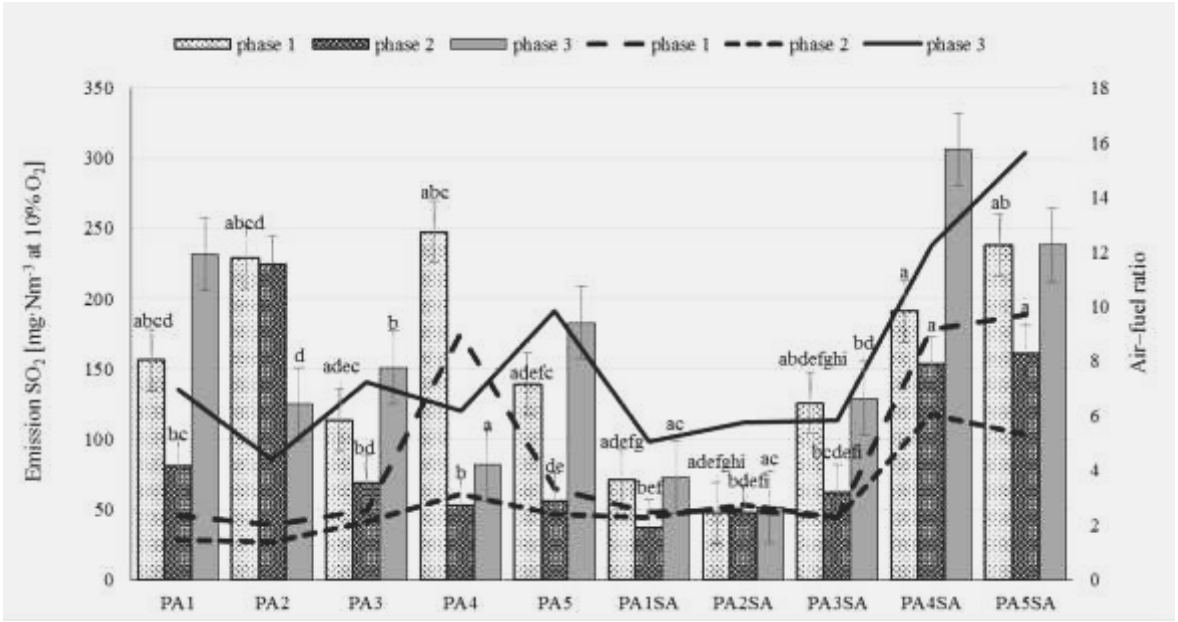

FIGURE 3
Effect of feeding air way to the mean emission factors of SO2 at the combustion process of black locust wood with detailing its phases (a-a, b-b etc. homogeneous groups).

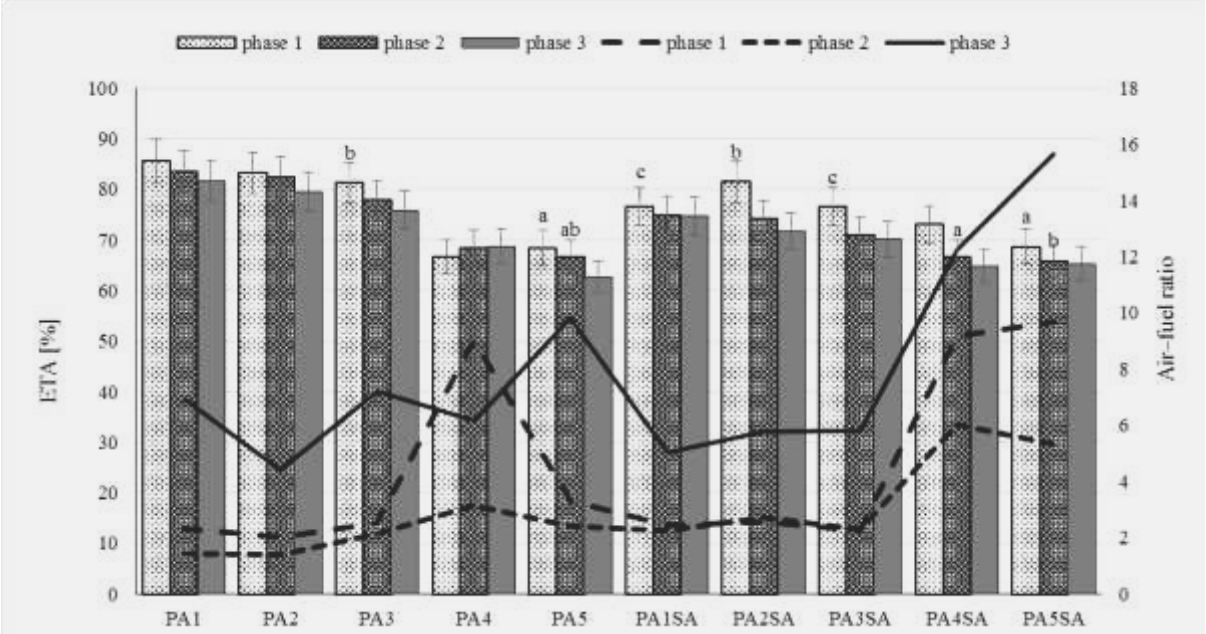

FIGURE 4
Effect of feeding air way to the pyrotechnic performance (ETA) at the combustion process of black locust wood with detailing its phases.

10% O_2 (Figure 3). However, in the tests using only primary air (PA1, PA2, PA3, PA4 and PA5) significant differences analyzed values were observed. The second phase of the combustion process in these trials characterized by the lowest SO_2 emissions over 50 mg·Nm^{-3} at 10% O_2, while the other two issues were higher and sometimes even five times. Especially for SO_2 emission factors observed that the greatest emissions, much higher than in the other tests occurred using the largest velocity of primary and secondary air - PA4SA and PA5SA (Figure 3).

Statistical analysis showed significant differences between the mean values of SO_2 emission factors during the particular phases of tests and Tukey's test carried out pointed to emission factors in phases 1-3 respectively 9, 9 and 4 homogeneous groups (Figure 3).Figure 4 shows the effect of feeding air way on pyrotechnic performance (ETA) in the combustion process of black locust wood with detailing its phases.

In the test conditions the highest of pyrotechnic efficiency for PA1 and PA2 for which the mean values exceed 80% were observed. Slightly lower values in the range of 70-80% were observed for the PA1SA and PA2SA, where also primary and secondary air had been fed. The lowest pyrotechnic efficiency during the ongoing studies (below 70%) reached the variants with the greatest air velocities – PA4, PA5, PA4SA and PA5SA (Figure 4).

Statistical analysis showed significant differences between the mean values pyrotechnical efficiency during the particular phases of tests and Tukey's test carried out pointed to emission indicators in phases 1-3 respectively 3, 2 and 0 homogeneous groups (Figure 4).

DISCUSSION

Analysis of the results classified in different phases of combustion and for black locust wood logs is difficult because the available literature data concerning emissions of CO, NO and SO_2 include general values for wood without distinguishing by species and the mean values for the whole combustion process. Often they are emissions from different structurally heating devices and laboratory positions. Black locust wood is generally regarded as a valuable fuel material and tillage of this tree stands for energy purposes occupies major parts of the world. Therefore, analysis is necessary for combustion process taking into account chemical and physical properties of this biofuel.

A characteristic feature of solid biofuels is high content of volatile particles and associated with this, varied in terms the phases of combustion. Drying, burning of polycyclic hydrocarbons and other simpler forms, and finally burning only the coal, creates a problem in that each of these phase needs a completely different aeration conditions. Drying in principle does not need oxygen, while the combustion of hydrocarbons need a suitable amount of air, that will cover the demand for oxygen in the

reaction of oxidation in low excess. This affects the emissions of carbon monoxide, which for maintain the lowest value requires proper air ratio for fuel [10; 13]. The technique of the upper combustion, combustion countercurrent, of the traditional domestic installations (furnaces, boilers) using in a spread, individual heating systems, characterized not only by high emissions but also low energy efficiency [8].

The burning of biomass in such devices without heating the air distribution division on primary and secondary leads to a reduction of efficiency process and significant value of CO emissions. However, NO and SO_2 emissions depend mainly on the content of nitrogen and sulfur in biomass [22]. Moreover, staged combustion of biomass fuels is also a method to reduce the thermal emission of NO and SO_2 [23].

By Kordylewski [24] and Juszczak [25] during combustion of wood from the furnaces a carbon monoxide is emitted, typically in the range of 100÷1000 $mg \cdot m^{-3}$. In adverse conditions combustion its participation in the exhaust gas can reach up to a few percent. While a typical NO emissions in the combustion of wood is in the range from 170 to 920 $mg \cdot m^{-3}$, and due to the limited sulfur content in the wood there is no emission of SO_2.

However, in studies Temmerman et al. [26] were analyzed burning wood for the emission of CO, NO and SO_2 at 13% O_2 content in the flue gas amount to 189.98; 144.09 and 14.06 $mg \cdot Nm^{-3}$. In studies Nosek et al. [27] were analyzed burning wood for the emission of CO and NO_x content in the flue gas amount to 5000-7000; 8-110 $mg \cdot m^{-3}$.

In the course of studies was found, that black locust wood burning in respect of different air delivery systems and division on particular phases of this process, the most effective nullify the emissions of CO, NO and SO_2 led feeding air in two phases as primary and secondary so as to maintain the excess to 2 - tests PA1SA, PA2SA, PA3SA. The emission factors analyzed for these biofuels in second phase of the combustion process were comparable with data given from literature [24; 26]. For the other used to test fuels, emissions of CO, NO and SO_2 were much higher, particularly when fed velocities primary and secondary air above 1,5 and 2 $m \cdot s^{-1}$. Equally pyrotechnic efficiency of the combustion processes for the variants, where the velocity of primary and secondary air was the lowest ranged from 70 to just over 80% - PA1, PA2, PA1SA and PA2SA. In other cases the efficiency was about 70%.

In this study was observed a significant emissions of CO, NO and SO_2 into the atmosphere. Especially differential values were noted in the pending phases of black locust wood combustion for CO emissions. The study indicated direction to minimize these emissions through the selection of air distribution. It should be noted that using the electronic controller of the combustion process is required to develop accurate algorithms that control the air flow to the boiler.

CONCLUSIONS

1. Ecologically acceptable black locust wood burning in the boiler low-temperature hot water boiler with upper grate combustion, can occur at ensuring that in each phase combustion air supply in excess of not more than $\lambda = 2$. With these assumptions a black locust wood burning causes minimal emissions of CO, NO and SO_2 into the atmosphere thereby obtained a high pyrotechnic efficiency ranged about 80%.

2. Improvement of combustion of wood in these heating devices is seen in the feeding of primary and secondary air in conjunction with the control of the excess in relation to the phases of the combustion process.

3. The analysis should be subjected to the initial and final phase of the combustion process of wood logs in relation to the construction solutions of boilers. Expedient would be to extend studies to other species and forms of biomass plant and their impact on the course of the combustion process low-power devices.

REFERENCES

[1] Rédei K, Osvath-Bujtas Z, Veperdi I, 2003. Black Locust (Robinia pseudoacacia L.) Improvement in Hungary: a Review. Acta Silvatica & Lignaria Hungarica, 4: 127-132.

[2] Kraszkiewicz A. 2008. Timber production estimates in erosion prone sandy slopes tree stands of black locust. Pamiętnik Puławski, 148: 39-48. (in Polish)

[3] Kraszkiewicz A. 2008. Heat of combustion and calorific value assessment of chosen sortiments of black locust for certain thickness classes. MOTROL, 10: 67-72. (in Polish)

[4] Kraszkiewicz A. Szpryngiel M. 2008. Moisture content of robinia (False Acacia) wood in the aspect of its use for energy production purposes. Inżynieria Rolnicza, 9 (107): 159-164. (in Polish)

[5] Kraszkiewicz A. 2009. Analysis of selected chemical properties of black locust (Robinia pseudoacacia L.) wood and bark. Inżynieria Rolnicza, 8 (117): 69-75. (in Polish)

[6] Huntley J.C. 1990. Robinia pseudoacacia L. black locust. Silvics of North America, Vol. 2: 755-761.

[7] Zhang J. 2014. Planting Black Locust (Robinia pseudoacacia) Forest as a Biomass Energy Resource. Coastal Saline Soil Rehabilitation

and Utilization Based on Forestry Approaches in China: 157-164.
[8] Kubica K. 2010. Efficient and environmentally friendly source of heat - low emission limitation. Katowice: Guide. (in Polish)
[9] Niu W., Liu X., Huang G., Chen L., and Han L. 2013. Physicochemical Composition and Energy Property Changes of Wheat Straw Cultivars with Advancing Growth Days at Maturity. Energy Fuels, 27 (10): 5940–5947.
[10] Hansen M., Jein A., Hayes S. and Bateman P. 2009. English Handbook for Wood Pellet Combustion - Pellet Atlas. München, Germany.
[11] Głodek E. 2010. Combustion and biomass co-firing. Instytut Ceramiki i Materiałów Budowlanych w Opolu. (in Polish)
[12] Obernberger I., Brunner T. and Barnthaler G. 2006. Chemical properties of solid biofuels - significance and impact. Biomass and Bioenergy, 30(11): 973-982.
[13] Rybak W. 2006. Combustion and co-combustion of solid biofuels. Wrocław: Wyd. Politechniki Wrocławskiej. (in Polish)
[14] Nussbaumer T. 2002. Combustion and co-combustion of biomass. In: Proceedings of the 12th European biomass conference, vol. 1: 7-31.
[15] Olsson M. and Kjällstrand J. 2002. Emissions from burning of softwood pellets. In: Proceedings of the First World Conference on Pellets. Stockholm, Sweden: 111-114.
[16] Petrocelli D. and Lezzi A. M. 2014. CO and NO emissions from pellet stoves: an experimental study. J. Phys.: Conf. Ser. 501, 012036 (http://iopscience.iop.org/1742-6596/501/1/012036)
[17] Žandeckis A., Kirsanovs V., Dzikēvičs M. and Blumberga D. 2013. Experimental study on the optimisation of staged air supply in the retort pellet burner. Agronomy Research 11 (2): 381–390.
[18] PN-EN 14774-1:2010 Solid biofuels – Methods for themdetermination of moisture content – Oven dry method – Part 1: Total moisture – Reference method
[19] PN-EN 14775:2010 Solid biofuels – Methods for the determination of ash content
[20] PN-EN 14918:2010 Solid Biofuels – Method for the determination of calorific value
[21] PN-EN 303-5:2002 Boilers – Part 5: Heating boilers for solid fuels with manual and automatic fuel charge with nominal power up to 300 kW – Terminology, requirements, testing and marking (in Polish)
[22] Demirbas A. 2007. Hazardous Emissions from Combustion of Biomass. Energy sources, Part A: Recovery, Utilization, and Environmental Effects, Volume 30, Issue 2: 170-178.
[23] Hinckley J. and Doshi K. 2010. Emission Controls for small Wood-Fired Boilers. United States Forest Service.
[24] Kordylewski W. 2008. Combustion and fuel. Wrocław: Oficyna Wydawnicza Politechniki Wrocławskiej. (in Polish)
[25] Juszczak M. 2002. Ecological burning waste wood. Industrial research limit of carbon monoxide and nitrogen oxide. Poznań: Wyd. Pol. Poznańskiej.
[26] Temmerman M., Mignon Ch. and Pieret N. 2011. Influence of increasing shares of miscanthus on physical and mechanical properties of pellets produced in an industrial softwood pellets plant. In: Farm machinery and process management in sustainable agriculture. Lublin, Poland: 151-166.
[27] Nosek R., Holubčík M. and Papučík Š. 2014. Emission Controls Using Different Temperatures of Combustion Air. The Scientific World Journal Volume 2014 (2014), Article ID 487549, 6 pages

Received: **08.10.2015**
Accepted: **28.01.2016**

CORRESPONDING AUTHOR

Ph.D. Artur Kraszkiewicz
Department of Machinery Exploitation and Management of Production Processes, University of Life Sciences in Lublin, Głęboka Street 28, 20-612 Lublin, Poland

e-mail: artur.kraszkiewicz@up.lublin.pl

© by PSP Volume 25 – No. 7/2016, pages 2444-2453 Fresenius Environmental Bulletin

RUNOFF POLLUTANT CHARACTERISTICS AND FIRST FLUSH ANALYSIS IN DIFFERENT URBAN FUNCTIONAL AREAS: A CASE STUDY IN CHINA

Ping Xu*, Junchao He, Yajun Zhang, Jianqiang Zhang, Kunpeng Sun

Key Laboratory of Urban Stormwater System and Water Environment, Ministry of Education, Beijing University of Civil Engineering and Architecture, Beijing, China

ABSTRACT

From 2013 to 2014, three different urban functional areas, commercial and industrial area C_1, residential area C_2 and landscape area C_3, in Guang-Ming New District of Shenzhen, China, were selected as the study area. Runoff quantity and concentrations of six pollutants of 32 rainfall runoff events were monitored. Event Mean Concentrations (EMCs), Mass First Flush (MFF_n), first flush strength and probabilities of the six pollutants were analyzed. Correlation between EMCs and rainfall characteristics and first flush control volume for three different catchments were discussed. Results showed that the mean EMCs for SS, COD and TP in catchment C_1 were 2.4, 3.4 and 2.5 times than that in catchment C_2, 3.2; 3.1 and 1.3 times than that in catchment C_3. The catchment C_2 was recorded the highest mean EMC for TN. About 70~80% of rainfall events can exhibit first flush phenomenon, but no strong flush (30/80) in the study area. Based on the probability of first flush from high to low, the sequence of three catchments was $C_1 > C_2 > C_3$. The catchment C_2 recorded the highest first flush strength and then was followed by the catchment C_1 and C_3. The sequence of pollutants based on first flush strength from high to low was SS > COD > TP > TN. In order to control runoff pollutants, 7 mm for catchment C_1 and C_2, 8 mm for catchment C_3 were suggested as first flush control volume.

KEYWORDS:
Urban road runoff; EMC; MFF_n; First flush strength; First flush control volume.

INTRODUCTION

With the construction of residential and commercial areas, factory areas, traffic roads and et al, an increase in impervious underlying surfaces led to more runoff and faster mobilization and transport of pollutant in urbanized and industrialized areas [1,2]. Pollutants accumulated significantly in runoff can seriously threaten urban water environment quality, especially in the first part of a storm runoff event [3,4]. However, runoff characteristics of various pollutants are great randomness, variability and complexity [5,6]. Therefore, it is of great significance to determine runoff pollutants characteristics with scientific basis. Many researches showed runoff characteristics and first flush differed with land use, surface sediments, human activities and et al. besides rainfall characteristics (rainfall depth, duration, mean intensity, max intensity and antecedent dry days)[7-9]. Qianqian Zhang et al found the road with a high slope would lead to higher runoff velocity and stronger flushing [10]. Monitoring results by Sea-Won Kim et al also showed that runoff characteristics of non-point pollutants in different land uses were distinctly different and sit-specific [11]. However, some results indicated that land use variation did not affect first flush strength for pollutants yet [12]. It would be helpful to design more effective stormwater control measures by understanding patterns in pollutant export with respect to the runoff hydrograph. In order to assess the effects of different urban functional areas on runoff pollutant characteristics and first flush, a monitoring activity and field measurements of runoff quantity and concentrations of six pollutants were carried out during 32 rainfall events from 2013 to 2014 in Guang-Ming New District of Shenzhen, China. Three different urban functional catchments, commercial and industrial area C_1, residential area C_2 and landscape area C_3 were selected as the study area. Event Mean Concentrations (EMCs), Mass First Flush (MFF_n), first flush strength and probabilities of the six pollutants were analyzed. Correlation between EMCs and rainfall characteristics and first flush control volume for three different catchments were discussed.

MATERIALS AND METHODS

Study area description. The study area was located in Guang-Ming New District, a being urbanized and industrializing district of Shenzhen

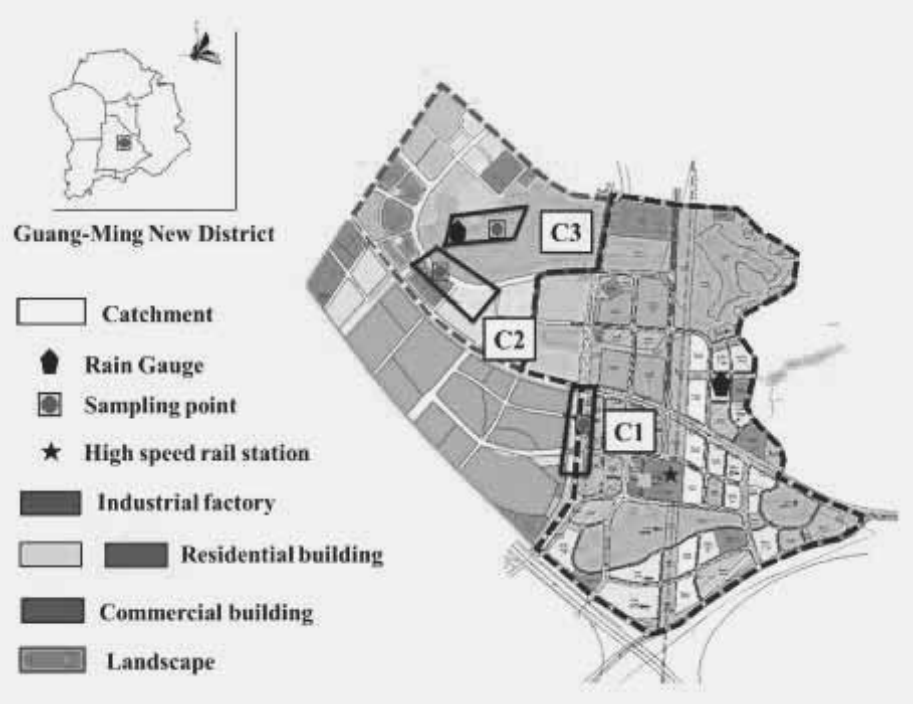

FIGURE 1
Map of study area and locations of study catchments.

in south China. It has a mild, subtropical maritime monsoon climate. The average annual temperature is 22℃ and average annual relative humidity is 79%. The perennial prevailing wind direction is northeast and southeast. The average annual precipitation is 1615 mm, 86% of which falls from April to September. Typhoon usually accompanied by heavy storms is most likely to occur from June to August. The average frequency is 4.8 times per year.

Runoff samples were collected from three different urban functional catchments: commercial and industrial area C_1, residential area C_2, landscape area C_3 (Figure 1).

Catchment C_1 is made up of impermeable asphalt motorway, impermeable asphalt pavement and permeable green belt. The total impermeable and permeable areas occupy 89% and 11% respectively. C_1 is encircled by electronic factories and commercial buildings. Moreover, a high speed rail station is nearby the catchment. Catchment C_2 contains 76% impermeable asphalt motorway, 13% permeable brick pavement and 11% permeable green belt. It is surrounded by residential buildings, construction building sites and a park. Catchment C_3 lies in the park and is made up of 66% impermeable asphalt pavement and 34% permeable grassy area on a slope. Basic characteristics of three catchments are summarized in Table 1.

All study areas belong to public urban areas in Shenzhen. The field studies did not involve endangered or protected species. No specific permission was required.

TABLE 1
Basic characteristics of three catchments.

Characteristics	C_1	C_2	C_3
Total area(hm^2)	0.767	0.694	0.65
Impervious area (%)	89	76	66
Road slope (‰)	9	30	10
Drainage system	Separate	Separate	Separate
Average traffics (vehicles/h)	410	145	-

TABLE 2
Analysis methods of runoff pollutants.

Item	Analysis method	Standard
SS	Weight method	GB 11901-89
COD	Rapid digestion and spectrophotometric method	HB/T 399-2007
NH_4-N	Nessler's reagent spectrophotometry method	HJ 535-2009
NO_3-N	Phenol disulfonic acid spectrophotometric method	HJ/T 346-2007
TN	UV spectrophotometry method	HJ 636-2012
TP	Persulfate digestion spectrophotometric method	GB 11893-89

Sampling and analyses. Rainfall amounts and durations were automatically recorded by rain gauge (JDZ-1, China). To measure the runoff flow rate of the road, automated flow meters (Hach9000, USA) were installed at the inlet of the drainage network in the gully. Samples were collected manually by researchers with rich sampling experience in the rainfall events. Once runoff flow was observed, sampling was conducted at 5-min intervals in the first 30 min, then at 10-min intervals during 30 to 60 min and at 30-min intervals afterwards. The samples were stored in 500ml polyethylene bottles at the sites. They were placed in containers with ice bags and transported to the laboratory for chemical analyses. Concentrations of six pollutants - suspended solids (SS), chemical oxygen demand (COD), ammonia nitrogen (NH_4-N), nitrate nitrogen (NO_3-N), total nitrogen (TN) and total phosphorus (TP) - were analyzed according to China standard methods. The analysis methods are summarized in Table 2.

Event mean concentration (EMC). Taking into account high variability of pollutant concentrations throughout a given rainfall runoff event, a single index known as EMC was used to compare the pollution between rainfall events [11]. The EMC represents a flow-weighted average concentration computed as the total pollutant mass divided by the total runoff volume for an event duration, as shown in Eq. (1) [13].

$$EMC = \frac{M}{V} = \frac{\int_0^t c(t)q(t)dt}{\int_0^t q(t)dt} \quad (1)$$

Where, M is the total pollutant mass over entire event duration, mg; V is the total runoff volume over entire event duration, L; c(t) is the pollutant concentration as function of time, mg·L^{-1}; q(t) is runoff flow rate as function of time, L·min^{-1}; t represents time over entire runoff duration, min.

Mass First Flush (MFFn). MFF_n is a ratio of cumulative mass to the cumulative flow volume [14-16]. It is defined as follows:

$$MFF_n = \frac{\frac{\int_0^t c(t)q(t)dt}{M}}{\frac{\int_0^t q(t)dt}{V}} \quad (2)$$

Where, n is the percentage of cumulative runoff volume, rang from 0 to 100%; M is the total pollutant mass over entire event duration, mg; V is the total runoff volume over entire event duration, L; c(t) is the pollutant concentration as function of time, mg·L^{-1}; q(t) is runoff flow rate as function of time, L·min^{-1}; t is the time from runoff occurrence to when the n% cumulative runoff is observed, min.

MFF_n is used as an index for first flush intensity. First flush phenomenon occurs if MFF_n >1.0 [14].

First flush strength. The first flush strength is quantified by relating the cumulative pollutant mass to cumulative runoff volume using a power function as follows [9]:

$$m(t) = \left[v(t)\right]^b \quad (3)$$

Where, m(t) is normalized dimensionless cumulative mass; v(t) is normalized dimensionless cumulative runoff volume; b is the first flush coefficient. Eq. (3) is log transformed to yield a linear regression as shown in Eq. (4).

$$Inm(t) = bInv(t) \quad (4)$$

The first flush strengths for various constituents are categorized as 4 zones: zone 1 ($0 < b \leq 0.185$) strong flush; zone 2 ($0.185 < b \leq 0.862$) moderate flush; zone 3 ($0.862 < b \leq 1.0$) weak flush; zone 4 ($1.0 < b \leq +\infty$) no first flush [17].

TABLE 3
Rainfall characteristics of sampled events.

Catchment	Variable	R_d （mm）	R_{dur}（min）	I (mm/min)	I_{max}（mm/min）	ADD（h）
C_1 (n=10)	Min/max	1.8/42.9	26/255	0.02/0.78	0.3/2.8	5/232
	Median/mean	12.2/14.2	127/113.6	0.15/0.2	1.0/1.05	29/60.3
	SD/C.V	11.3/0.8	63.8/0.6	0.25/1.2	0.8/0.77	69.3/1.1
C_2 (n=7)	Min/max	5.1/17.0	35/130	0.04/0.26	0.3/2.8	23/144
	Median/mean	11.4/12.0	56/72.9	0.23/0.18	1.5/1.37	96/81.4
	SD/C.V	3.7/0.3	31.8/0.44	0.08/0.44	0.77/0.56	39.8/0.48
C_3 (n=15)	Min/max	7.1/20.0	38/114	0.13/0.39	0.3/2.8	16/176
	Median/mean	14.8/14.2	80/68.3	0.23/0.24	1.0/1.3	72/78.8
	SD/C.V	3.6/0.3	29.3/0.4	0.1/0.4	0.6/0.5	56.1/0.7

Statistical analysis. Pearson product-moment correlation coefficient was used to analyze the correlation of EMC and rainfall characteristics. Kolmogorov-Smirnov test was used to examine the validity of normal distribution. Pearson correlation and Kolmogorov-Smirnov test were performed in SPSS 19.0 (SPSS Inc., USA).

RESULTS

Rainfall characteristics. A total of 32 rainfall events were sampled at three catchments, 10 events at catchment C_1, 7 events at catchment C_2, and 15 events at catchment C_3, from May 2013 to September 2014. The rainfall variables, namely rainfall depth (R_d), rainfall duration (R_{dur}), average rainfall intensity (I), max rainfall intensity (I_{max}) and antecedent dry days (ADD) are given in Table 3.

The rainfall depths range from 1.8 to 42.9mm, R_{dur} from 26 to 255min, I_{max} from 0.3 to 2.8mm/min, ADD from 5 to 232h. It shows that 32 rainfall events cover the common types of rainfall, with a fully representative, which can provide reliable guarantee for the results.

Event mean concentrations (EMCs). The calculated EMCs of different pollutants from three catchments are presented in Table 4.

The catchment C_1 recorded the highest means EMCs for SS, COD and TP. That was greatly associated with heavy traffic (410 vehicles/h). The sources of high concentrations of SS, COD and TP were mainly from the debris of vehicle tire and asphalt road. Opher and Friedlerb showed that the abrasion and weathering of vehicle tire and asphalt material in urban road could bring mass street sediments, which often contained hydrocarbon and phosphate matters [7]. Moreover, the asphalt road is a source of organic contamination [18,19]. At the same time, atmospheric deposition was another source of pollutants in industrial and commercial area [10,20]. The sediments and organic contamination could be washed out and lead to SS, COD and TP increasing in runoff. For catchment C_2, there was the highest means EMC for TN. By comparison the concentrations of NH_4-N and NO_3-N in three catchments, it could be concluded that the high concentration of organic nitrogen was the main reason, which was most likely associated with the wash-off of food waste and sullage for construction living activity in catchment C_2. Compared with catchment C_1 and C_2, higher coefficients of variation of pollutants could be observed in catchment C_3. High concentrations of pollutants could be caused by strong flush for the grassy area on a slope. Furthermore, compared with the corresponding values in grade V surface water standard of China (GB3838-2002), the mean EMCs for SS, COD and TP in catchments C_1 were 11.8, 4.1 and 1.5 times higher. The mean EMCs for TN in catchments C_2 were 2.9 times higher. The mean EMCs for SS, COD, TN and TP in catchments C_3 were also higher.

To sum up, in Guang-Ming New District, the higher traffic volume mainly contributed to SS, COD and TP in urban road. It also suggests that regular cleaning maintenance of surface cleaning is very important. Moreover, TN was greatly influenced by human activities.

TABLE 4
EMCs of different pollutants in different catchments.

Catchment	EMC (mg·L^{-1})						
	Variable	SS	COD	NH_4-N	NO_3-N	TN	TP
C_1	Min/max	34.9/530.4	22.9/358.3	0.07/0.88	0.29/1.93	0.79/3.28	0.14/0.98
	Median/mean	361.9/352.6	162.7/162.6	0.53/0.48	1.07/1.07	1.86/2.03	0.65/0.58
	SD/C.V	170.7/0.48	110.9/0.68	0.28/0.59	0.51/0.48	0.75/0.37	0.30/0.52
C_2	Min/max	45.1/248.9	12.3/82.9	0.12/1.20	0.73/2.19	0.93/13.84	0.05/0.55
	Median/mean	143.7/147.4	46.3/48.4	0.66/0.68	1.73/1.48	5.52/5.82	0.20/0.23
	SD/C.V	65.8/0.45	22.3/0.46	0.36/0.53	0.50/0.34	4.28/0.74	0.18/0.81
C_3	Min/max	13.7/371.9	9.6/243.7	0.11/2.0	0.26/3.26	1.0/12.6	0.05/0.95
	Median/mean	66.1/110.8	26.5/52.6	0.64/0.81	0.81/0.95	1.94/3.47	0.46/0.43
	SD/C.V	101.7/0.92	64.2/1.22	0.55/0.68	0.74/0.78	3.24/0.93	0.31/0.71
Water quality standard		≤30	≤40	≤2.0	-	≤2.0	≤0.4

Suspended solids standard is the second category of urban wastewater discharge standards of China (GB18918-2002); other pollutants standards are the grade V surface water standard of China (GB3838-2002)

Mass First Flush (MFF_n). To quantitatively assess the first flush effect, the box plots of MFF_n for various pollutants in three catchments were presented in Figure 2.

According to figure 2, MFF_n ratios for SS, COD, NH_4-N, NO_3-N, TN and TP were almost more than 1.0 in catchment C_1. Moreover, MFF_n ratios for above pollutants showed obvious decreases as runoff progress. Similar phenomena could be observed in MFF_n ratios for SS, COD and TP in catchment C_2, and MFF_n ratios for COD, NH_4-N and TN in catchment C_3. Ming et al. showed that a decreasing trend in MFF_n as runoff progress suggests dilution of pollutant concentration over

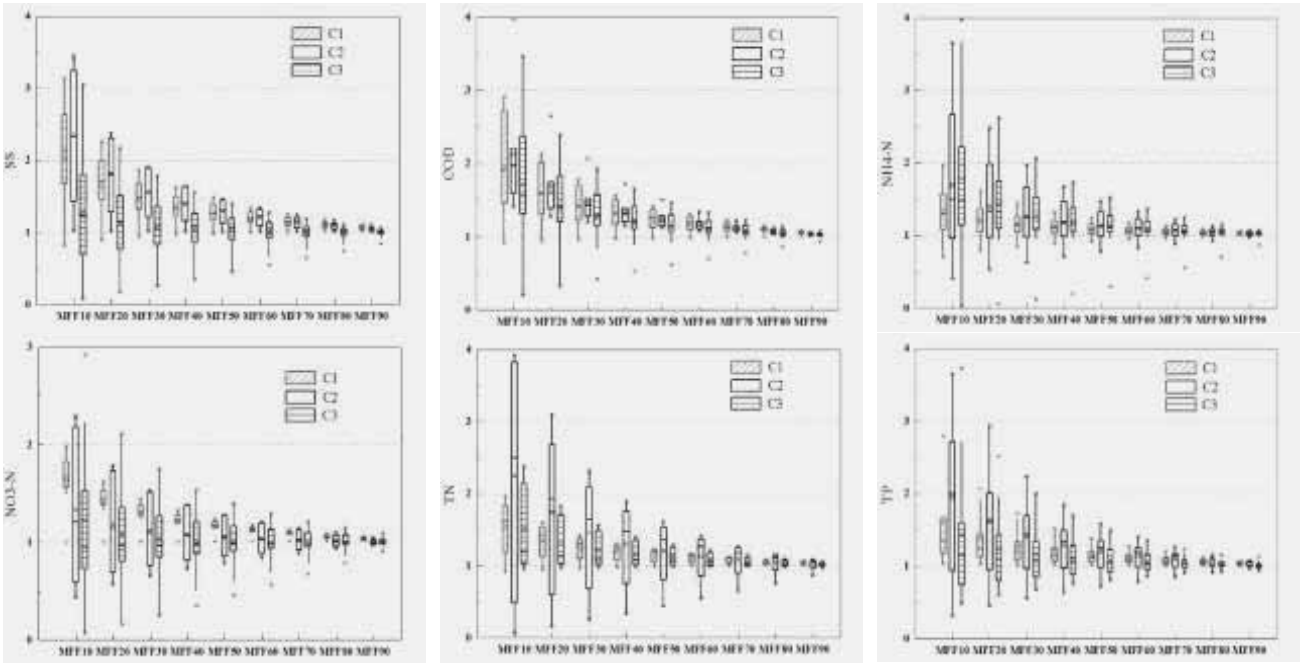

FIGURE 2
Box plots of MFF_n of various pollutants

TABLE 5
Mean MFF_{30} of various pollutants in three catchments.

Ranking	C_1		C_2		C_3	
	Variable	MFF_{30}	Variable	MFF_{30}	Variable	MFF_{30}
1	SS	1.44	SS	1.55	NH_4-N	1.29
2	COD	1.42	COD	1.46	COD	1.28
3	NO_3-N	1.38	TN	1.45	TN	1.22
4	TP	1.28	TP	1.41	TP	1.16
5	TN	1.25	NH_4-N	1.26	SS	1.06
6	NH_4-N	1.12	NO_3-N	1.12	NO_3-N	1.03

time, which is also explained that first flush effect of these pollutants was strong [9].

The pollution loads transported by the first 30% of runoff volume as an important benchmark was used to evaluate the magnitude of first flush by most researchers [21]. The MFF_{30} ratios for various pollutants in three catchments were ranked by their mean values as shown in Table 5.

According to table 5, the highest loadings of SS, COD, TN and TP were observed in the first 30% of the runoff volume in catchment C_2. The mean MFF_{30} were 1.55 for SS, 1.46 for COD, 1.45 for TN, 1.41 for TP respectively. These correspond to removals of 46.5% for SS, 43.8% for COD, 43.5% for TN and 42.3% for TP in the first 30% runoff volume. For catchment C_1, removal rates corresponding to mean MFF_{30} were 43.2% for SS, 42.6% for COD, 41.4% for NO_3-N, 38.4% for TP, 37.5% for TN. The mean MFF_{30} for pollutants in catchment C_3 were the lowest among three catchments. The highest removal rate was 38.7% for NH_4-N in the first 30% of the runoff volume. Ming et al reported means MFF_{30} of 46 % for SS, 45 % for COD, 52 % for NH_4-N and 44 % for TP in tropical urban catchments in Johor, Malaysia [9]. Ma et al found means MFF_{30} of 44 % for SS, 39 % for COD, 32 % for TN and 43 % for TP in Dongguan City, China [22]. The results showed that besides rainfall intensity, rainfall amount and runoff depth, pollutants wash-off mechanism were also influenced by characteristics of the catchments.

First flush strength and probability. The first flush coefficients, b values of various pollutants, are shown in Table 6.

According to Table 6, no rain event have met the criterion of 30/80 proposed by Bertrand et al. [17], which indicates that no strong flush in 32 rainfall runoff events at all catchments. Except SS and NO_3-N in catchment C_3, moderate and weak flush phenomenon was observed for other pollutants. Based on b values, the degree of first flush strengths in all catchments was $C_2 > C_1 > C_3$. For catchments C_1 and C_2, degree of first flush strengths for various pollutants was SS > COD > TP > TN.

Comprehensive probability of various pollutants in all catchments is shown in Figure 3.

There were 70~80% of rainfall runoff events occurred first flush phenomenon in the study area. Most of them belonged to moderate flush. Moreover, the order of first flush probability in all catchments was $C_1 > C_2 > C_3$, which indicates that first flush occurred easily in the residential catchments, commercial and industrial catchments rather than in the park. That was most likely related to the size of impervious rate. The pollutants that the probability of first flush was 100% included TP in catchment C_1, SS and COD in catchment C_2. The biggest probability for first flush in catchment C_3 was 86% for TN. Therefore, for catchment C_1 and C_2, some technologies should be designed for initial pollutant control.

TABLE 6
First flush coefficient (b values) of various pollutants.

Ranking	C_1		C_2		C_3	
	Variable	b values	Variable	b values	Variable	b values
1	SS	0.74±0.20	SS	0.67±0.18	TN	0.85±0.15
2	COD	0.75±0.17	COD	0.70±0.14	COD	0.85±0.31
3	NO_3-N	0.79±0.08	TP	0.78±0.35	NH_4-N	0.90±0.54
4	TP	0.82±0.14	TN	0.86±0.61	TP	0.91±0.23
5	TN	0.84±0.11	NH_4-N	0.87±0.29	SS	1.04±0.42
6	NH_4-N	0.93±0.16	NO_3-N	0.95±0.26	NO_3-N	1.09±0.47

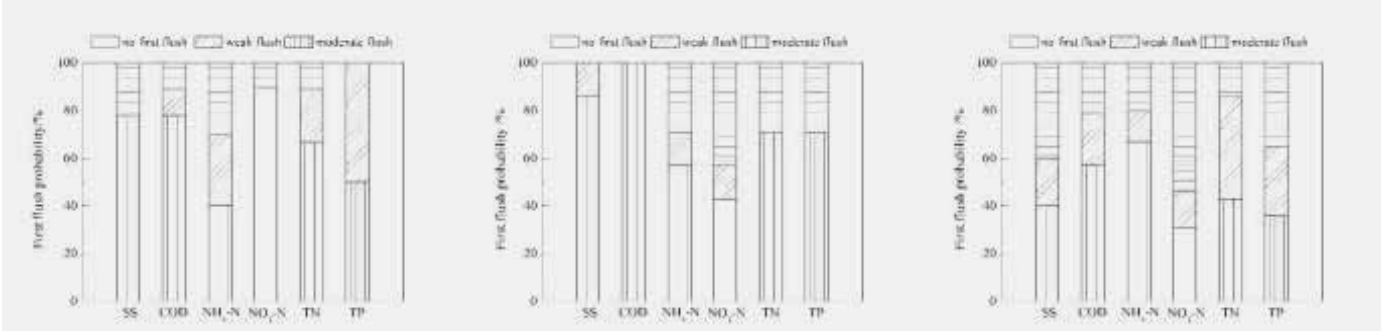

C_1 C_2 C_3

FIGURE 3
First flush probability of various pollutants.

DISCUSSION AND CONCLUSIONS

Correlation of EMCs and rainfall characteristics. Table 7, 8, 9 showed the Pearson coefficients between EMCs and rainfall parameters with different catchments.

SS and COD, SS and max intensity (I_{max}), COD and I_{max} in catchment C_1 and C_2 showed the high correlation of 0.75 ($p<0.05$), 0.68 ($p<0.05$), 0.58 and 0.92 ($p<0.01$), 0.76 ($p<0.05$), 0.88 ($p<0.05$), implying that SS and COD always attach to each other for granular pollutants, which can be washed away in a stream. I_{max} has large impact on the discharge of particulate pollutants, and the rainfall intensity is stronger, the wash-off of SS and COD is easier. Moreover, for catchment C_1 and C_2, rainfall depth (R_d) and SS, R_d and COD also showed the high correlation, implying that R_d has some impact on the discharge of particulate pollutants in the roads. SS and TP showed a high pollutant correlation with 0.66 ($p < 0.05$) in catchment C_1. The reason for this correlation between SS and TP was due to that phosphorus has a bonding capacity with granular pollutants during a rain storm [23]. However, duration (R_{dur}), mean intensity (I), and antecedent dry days (ADD) seemed to be less correlated with the discharge characteristics of runoff pollutants.

TABLE 7
Pearson coefficients between EMCs and rainfall parameters for catchment C_1.

Variable	SS	COD	NH_4-N	NO_3-N	TN	TP	R_d	R_{dur}	I	I_{max}	ADD
SS	1.00	0.75*	0.27	0.32	0.37	0.66*	0.50	0.09	-0.21	0.68*	0.43
COD		1.00	-0.04	0.26	0.45	0.45	0.62*	0.26	-0.06	0.58	0.45
NH_4-N			1.00	0.03	0.16	-0.26	0.02	-0.11	-0.08	0.07	0.12
NO_3-N				1.00	0.58	0.15	-0.01	-0.05	0.45	0.09	0.01
TN					1.00	0.58	0.56	-0.06	0.64	0.15	0.66
TP						1.00	0.05	0.51	0.02	-0.37	0.46

Correlation is significant at the 0.05 level (two-tailed); ** Correlation is significant at the 0.01 level (two-tailed)

TABLE 8
Pearson coefficients between EMCs and rainfall parameters for catchment C2.

Variable	SS	COD	NH_4-N	NO_3-N	TN	TP	R_d	R_{dur}	I	I_{max}	ADD
SS	1.00	0.92**	0.57	-0.12	0.08	0.55	0.66*	-0.22	0.52	0.76*	-0.40
COD		1.00	0.26	-0.34	-0.25	0.48	0.72*	-0.26	0.44	0.88*	-0.32
NH_4-N			1.00	0.50	0.81*	0.23	-0.14	0.20	-0.09	-0.08	-0.27
NO_3-N				1.00	0.42	0.23	-0.41	0.81*	-0.71	-0.32	0.47
TN					1.00	0.49	-0.54	0.13	-0.26	-0.65	-0.37
TP						1.00	0.09	-0.15	0.09	-0.28	-0.31

* Correlation is significant at the 0.05 level (two-tailed); ** Correlation is significant at the 0.01 level (two-tailed)

TABLE 9
Pearson coefficients between EMCs and rainfall parameters for catchment C3.

Variable	SS	COD	NH_4-N	NO_3-N	TN	TP	R_d	R_{dur}	I	I_{max}	ADD
SS	1.00	0.21	0.48	-0.09	-0.06	0.25	0.37	0.32	-0.17	0.03	-0.22
COD		1.00	0.69**	0.13	0.51	-0.46	-0.33	-0.02	-0.04	0.62*	0.03
NH_4-N			1.00	0.54*	0.72**	-0.12	-0.11	0.22	0.36	0.29	-0.24
NO_3-N				1.00	0.83**	-0.19	-0.22	0.03	-0.21	-0.18	-0.34
TN					1.00	-0.48	-0.32	0.02	-0.28	0.15	-0.14
TP						1.00	-0.05	0.31	-0.47	-0.53	-0.46

* Correlation is significant at the 0.05 level (two-tailed); ** Correlation is significant at the 0.01 level (two-tailed)

For catchment C_3, COD and NH_4-N, NH_4-N and NO_3-N, NH_4-N and TN, NO_3-N and TN showed the correlation of 0.69 ($p<0.01$), 0.54 ($p<0.05$), 0.72 ($p<0.01$), 0.83 ($p<0.01$), implying that between COD and different forms nitrogen has great influence on each other in dissolving pipe flow. I_{max} had large impact on the discharge of COD, 0.62 ($p<0.05$), but other rainfall parameters seemed to be less correlated with the runoff pollutants.

To sum up, I_{max} and R_d are the main factors affecting the discharge characteristics of runoff pollutants in the catchment C_1 and C_2; I_{max} is the main factors in the catchment C_3. Moreover, SS could be used as indicator of runoff pollutants control for catchments in residential or commercial and industrial district; COD could be adopted as indicator of runoff pollutants control for the catchments in a park.

First flush control volume. First flush control volume is crucial for designing urban runoff quality control structures. BMP in US showed that the required runoff depth for transporting 50% of the total pollutant loading is particularly critical benchmark for urban runoff pollutants control [24], and first flush volume is always applied in the control structures. Therefore, the runoff depth for transporting 50% of the total pollutant loading was selected as the first flush control volume. According to the results above, SS for catchment C_1 and C_2, COD for catchment C_3 were used as indicator of runoff pollutants control. The proportions of abandon runoff volume for transporting 50% of the total pollutant loading were 36% for catchment C_1, 34% for catchment C_2 and 41% for catchment C_3. Based on designed rainfall depths 28mm and the annual runoff control ratio of 70% in the study area, the first flush control runoff depths are 7.1mm for catchment C_1, 6.7mm for catchment C_2 and 8.0mm for catchment C_2, respectively. Among the 32 rainfall events sampled in the study area, runoffs of 7 out of 10 events were more than 7.1mm in catchment C_1, that of 5 out of 7 events were more than 6.7mm in catchment C_2, that of 12 out of 15 events were more than 8.0mm in catchment C_3.

The runoff pollutants characteristics in three different urban functional catchments were researched in this study. The important results are shown as follows:

According to mean EMCs of SS, COD and TP from high to low, the sequence of three catchments was $C_1>C_2>C_3$. The mean EMCs for SS, COD and TP in catchment C_1 were 2.4, 3.4 and 2.5 times than that in catchment C_2, 3.2; 3.1 and 1.3 times than that in catchment C_3. That was most likely associated with the high traffic volume. The catchment C_2 was recorded the highest mean EMC for TN. Food waste from residents and sullage for construction living activity may be one important reason for this phenomena. Most runoff pollutants in three catchments were higher than the corresponding values in grade V surface water standard of China (GB3838-2002).

About 70~80% of rainfall runoff events occurred first flush phenomenon. Most of them belonged to moderate flush. Based on the probability of first flush from high to low, the sequence of three catchments was $C_1>C_2>C_3$.

The catchment C_2 was recorded the highest first flush strength, then was followed by the catchment C_1 and C_3. The sequence of pollutants based on first flush strength from high to low was SS > COD > TP > TN. For catchment C_2, removal rates corresponding to mean MFF_{30} were 46.5% for SS, 43.8% for COD, 43.5% for TN and 42.3% for TP.

I_{max} and R_d were the main factors affecting runoff pollutants characteristics in the catchments C_1 and C_2; I_{max} was the main factors in the catchment C_3. For catchments C_1 and C_2, SS could be used as main indicator to control runoff pollutants. For catchments C_3, COD could be selected as indicator to control runoff pollutants.

In order to control runoff pollutants, 7 mm for catchments C_1 and C_2, 8 mm for catchment C_3, were suggested as first flush control volume.

ACKNOWLEDGEMENTS

The study was funded by Major Science and Technology Program for Water Pollution Control and Treatment (2010ZX07320-003, 2010ZX07320-002), Research Foundation of KLUSSWE-ME&BUCEA (PXM2014 014210 000057).

The authors have declared no conflict of interest.

REFERENCES

[1] Qin H.P., Li Z.X., Fu G.T. (2013) The effects of low impact development on urban flooding under different rainfall characteristics. Journal of Environmental Management, 129: 577-585.

[2] XiaoJun Zuo, Rajendra Prasad Singh Chouhan, DaFang Fu, et al. (2011) Particle size distribution variation during highway runoff settling. Fresenius Environmental Bulletin, 20(4A): 1020-1026

[3] Sansalone J.J., Cristina C.M. (2004) First flush concepts for suspended and dissolved solids in small impervious watersheds. Journal of Environmental Engineering, 130(11): 1301-1314.

[4] Jae-Woon Jung, Ha-Na Park, Kwang-Sik Yoon, et.al. (2013) Event Mean Concentrations (EMCs) and First Flush Characteristics of Runoff from a Public Park in Korea. Journal of the Korean Society for Applied Biological Chemistry, 56:597-604.

[5] Krein, A & Schorer, M. (2000) Road runoff pollution by polycyclic aromatic hydrocarbons and its contribution to river sediments. Water Research, 34(16): 4110-4115.

[6] Gnecco I, Berretta C, Lanza LG, et.al. (2005) Stormwater pollution in the urban environment of Genoa, Italy. Atmospheric Research, 77(1-4): 60-73.

[7] Opher, T. & Friedler, E. (2010) Factors affecting highway runoff quality. Urban Water Journal, 7(3): 155-172.

[8] Li Chunlin, Liu Miao, Hu Yuanman, et al. (2014) Characterization and first flush analysis in road and roof runoff in Shenyang, China. Water Science & Technology, 70(3): 397-406.

[9] Ming Fai Chow, Zulkifli Yusop. (2014) Sizing first flush pollutant loading of stormwater runoff in tropical urban catchments. Environmental Earth Sciences, 72: 4047-4058.

[10] Zhang Q.Q., Wang X.K., Hou P.Q., et al..(2013) The temporal changes in road stormwater runoff quality and the implications to first flush control in Chongqing, China. Environmental Monitoring and Assessment, 185:9763-9775.

[11] Sea-Won Kim, Joon-Seok Park, Daeik Kim, et al. (2014) Runoff characteristics of non-point pollutants caused by different land uses and a spatial overlay analysis with spatial distribution of industrial cluster: a case study of the Lake Sihwa watershed. Environmental Earth Sciences, 71:483-496

[12] J.M. Hathaway, R.S.Tucker, J.M. Spooner, et al.. (2012) A traditional analysis of the first flush effect for nutrients in stormwater runoff from two small urban catchments. Water, Air, & Soil Pollution, 223:5903-5915

[13] Sansalone J. & Buchberger S.. (1997) Partitioning and first flush of metals in urban roadway storm water. Journal of Environmental Engineering, 123(2): 134-143.

[14] Zhen-Bang., Hong-Gang Ni., Hui Zeng, et al. (2011) Function formula for first flush analysis in mixed watersheds: A comparison of power and polynomial methods. Journal of Hydrology, 402, 3: 333-339

[15] Han Y.H., Lau S.L., Kayhannian M, et al.. (2006) Correlation analysis among highway stormwater pollutants and characteristics. Water Science & Technology, 53: 235-243.

[16] Barco J., Papiri S., and Stenstorm M.K.. (2008) First flush in a combined sewer system. Chemosphere, 71:827-833.

[17] Bertrand-Krajewski J.L., Chebbo G., Saget A. (1998) Distribution of pollutant mass vs volume in stormwater discharges and the first flush phenomenon. Water Research, 32:2341-2356.

[18] Drapper, D. Tomlinson, R. & Williams P. (2000) Pollutant concentrations in road runoff: Southeast Queensland case study. Journal of Environmental Engineering, 126(4): 313-320.

[19] Huang, DJ, Ao P, Ho C, et.al.. (2007) Multivariate analysis for stormwater quality characteristics identification from different urban surface types in Macau. Bulletin of Environmental Contamination and Toxicology, 79 (6): 650-654.

[20] Wu J.S., Allan C.J., Saunders WL, et.al.. (1998) Characterization and pollutant loading estimation for high-way runoff. Journal of Environmental Engineering, 124(7): 584-592.

[21] Li L.Q., Yin C.Q., He Q.C., et.al. (2007) First flush of storm runoff pollution from an urban catchment in China. Journal of Environmental Sciences, 19: 295-299.

[22] Ma Y., Ma Y.W., Wan J. Q., et al. (2011) Characterization of rainfall runoff pollution transportation in different underlying surface of Dongguan City. China Environmental Science, 31(12): 1983-1990. (In Chinese)

[23] Wang L., Liang T., Zhang Q..(2013) Laboratory experiments of phosphorus loss with surface runoff during simulated runoff.

Environmental Earth Sciences, 70(6): 2839-2846.
[24] Lee E.J., M.C. Maniquiz, J.B. Gorme, et al. (2010) Determination of cost-effective first flush criteria for BMP sizing. Desalination and Water Treatment, 19:157-163.

Received: **08.10.2015**
Accepted: **03.02.2016**

CORRESPONDING AUTHOR

Ping Xu
No. 1 Zhanlan Road,
Xicheng District,
Beijing, China.

e-mail: xuping@bucea.edu.cn

© by PSP Volume 25 – No. 7/2016, pages 2454-2460 Fresenius Environmental Bulletin

ANALYSING THE EFFECT OF ELEMENTS UPON SOME ENDEMIC PLANTS SPREADING OVER DIFFERENT HABITATS

Etem Osma, Ali Kandemir

Erzincan University, Faculty of Science and Arts, Department of Biology, Erzincan, Turkey

ABSTRACT

Herein this study, the endemic plants showing different distribution, found in small populations in different habitats (such as serpentine, gypsum-bearing, calcareous etc.) and the concentration of the elements in the soil they grow were determined. It was investigated whether the soil content of elements of some endemic plant species unique to Erzincan have effects upon the spreading in limited habitats. Root and leaves of 7 endemic plants, *Psephellus aucherianus, Ferulago glareosa, Silene dumanii, Silene nerimaniae, Tanacetum alyssifolium, Verbascum alyssifolium, Psephellus erzincani* and soil samples from the area they grow up were collected. Elemental analysis in plants and soils were conducted in the laboratory with ICP-OES device after the preliminary treatment. Elements of the habitats and features of collected soil samples were revealed. In the study, the correlation between element concentration in the roots of collected plants and element concentration in the soil they grew was determined.

KEYWORDS:
Elements, Endemic Plant, Habitat, ICP-OES

INTRODUCTION

Turkey is one of the most important countries of the world with its fairly rich plant diversity [1]. The 3.649 out of 11.707 plant species growing in the country are endemic [2]. Topography variety, soil structure, climatic conditions, the presence of high mountains, geological history of our country and its transitional feature between the two continents are the most important indicators of plant diversity [3]. Erzincan is one of the most important areas of Turkey in terms of its plant diversity. It is known that the number of endemic plants spreading over Erzincan has been gradually increasing through the studies that have been carried out recently, and has reached up to 437 as of now. Forty-eight of these plant species are indigenous to Erzincan. The species indigenous to Erzincan generally maintain their survival in habitats comprised of gypsum, serpentine, and calcareous bedrock [5-6]. Endemic plants are the ones spreading over a narrow area or region. It is necessary to understand why these species are endemic [7].

Only the species growing in gypsum-bearing environments are defined as "certain gypsum plants [8]. *Verbascum alyssifolium, Psephellus erzincani* and *Tanacetum alyssifolium* are included among the certain gypsum plants [9]. The soils including gypsum and serpentine have a content that limits the survival of plants. Adaptation mechanisms of plants into these soils cannot be understood adequately [10, 11]. *Silene dumanii* and *Silene nerimaniae* are serpentinized species indigenous to Erzincan [9]. One of the information that should be obtained in order to start for the protection studies of a species population is to reveal the ecology of the species. Calcareous soils are rich in terms of plants species, and create pastures. These areas are more under the different conditions caused by people and animals. The endemic plants especially in these regions are in danger of extinction [12, 13].

Although the gypsum-bearing areas in Turkey are fairly smaller rather than the other countries, these areas are important endemic centres. Even though gypsum-bearing areas form through ebb, the endemics encountered in these areas are generally seen in arid and semi-arid regions, as well. Not performing agricultural and stockbreeding activities in these areas creates a natural protection area for the endemic taxa. The gypsum-bearing areas in our country occupy a wide area between Sivas and Erzincan [14, 15].

Herein this study we carried out the experiment in order to determine the element content of was to determine the element content of different areas (such as serpentine, gypsum-bearing- calcareous, etc.) and to specify whether elements had effect upon the spreading of plants in limited areas.

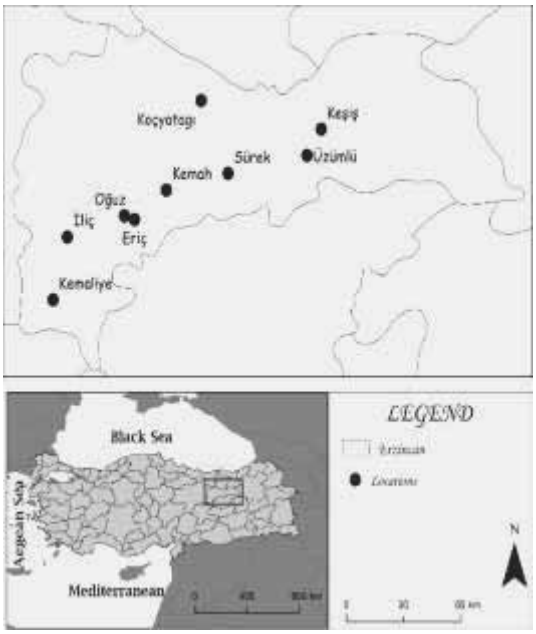

FIGURE 1
Study area.

MATERIALS AND METHODS

The province of Erzincan is located between 39 45' 12' southern latitudes and 40 46'30' eastern longitudes on the world map. The land forms of the province split by the Karasu tributary of River Fırat are Mountain Munzur on south border, Mountain Keşiş on north border, and two lowlands and defiles extending along Karasu Valley between these mountains. Erzincan has a continental climate, and its climate is more moderate than the other provinces in Eastern Anatolia (Figure 1.). The province with 10.7°C annual average of temperature has 344 mm annual precipitation average per square meter [15].

In total, 7 different endemic plants were studied, including *Psephellus aucherianus* (DC) Wagenitz, *Ferulago glareosa* Kandemir & Hedge, *Silene dumanii* Kandemir, Genç & Genç, *Silene nerimaniae* Genç, Kandemir & Genç, *Tanacetum alyssifolium* (Bornm.) Grierson, *Verbascum alyssifolium* Boiss., *Psephellus erzincani* Wagenitz & Kandemir (Table 1). Samples were taken by hand using vinyl gloves, and carefully packed into polyethylene bags [16]. Only the edible parts of each plant were analysed. In addition, soil samples were collected from the sampling sites. Samples were divided into two sub-samples; the ones in the first sub-group were thoroughly washed several times with tap water, and subsequently by distilled water in order to remove dust particles in a standardized procedure; the rest of the plants were untreated, and then dried in oven at 80ºC for 24 h. At each site, the soils were sampled from the top 10 cm by means of a stainless steel trowel to avoid contamination. To ensure consistent distribution of metals in the soil samples, all materials were grounded in a micro-hammer cutter and filtered via a 1.5-mm sieve [17, 18].

Dried and milled samples were powdered, and kept in clean polyethylene bottles. In addition, the soil samples were collected with a stainless steel crab. These samples were dehydrated in open air and passed through a 2-mm sieve. After homogenization, the soil samples were stored in clear paper bags before analysis. The samples (0.5 g dry weight) were digested with 10 ml pure HNO_3 (65%) using a CEM MARS 5 (CEM Corporation Mathews, NC, USA) microwave digestion system. The digestion conditions were as follows; the maximum power was 1200 W, the power was at 100%, the ramp was set for 20 min, the pressure was 180 psi, the temperature was 210ºC, and the hold time was 10 min. After digestion, solutions were evaporated to near dryness in a beaker. The volume of each sample was adjusted to 10 mL using 0.1 M HNO_3. The determination of the elements in all samples was carried out by using a Varian Inductively Coupled Plasma–Optical Emission Spectrometry (ICP–OES) [17, 19]. In statistical analysis, p-values as $\leq$ 0.05 were regarded as significant; the average value of samples was at 95% confidence interval. In addition, the correlation between the soils and plant samples was also examined [18].

TABLE 1
Endemic plants and habitats.

Endemic Plants	Family	Habitat		Localities	
Psephellus aucherianus	*Compositae*	Calcareous	İliç	Eriç	
Ferulago glareosa	*Apiaceae*	Kolluviyal	Kemah	Sürek	
Silene dumanii	*Caryophylaceae*	Serpentine	Kesiş	Üzümlü	
Silene nerimaniae	*Caryophylaceae*	Serpentine	Koçyatağı	Kemaliye	Eriç
Tanacetum alyssifolium	*Compositae*	Gypsum	Kemaliye	Oğuz	
Verbascum alyssifolium	*Scruphulariceae*	Gypsum	İliç		
Psephellus erzincani	*Compositae*	Gypsum	İliç	Oğuz	

TABLE 2
Metal concentration (µg/g dw) of plants grown in serpentine area.

	Silene nerimaniae									*Silene dumanii*			
	Soil			Root			Leaf			Soil		Root	
Element	I	II	III	I	II	III	I	II	III	I	II	I	II
Cd	0.5	0.6	0.4	0.3	0.1	0.2	0.2	0.4	0.2	0.2	0.5	0.1	0.2
Pb	6.4	6.6	6.2	1.8	0.9	0.1	2.2	1.8	1.9	24.1	8.3	2.1	2.2
Na	64.2	106.8	66.0	65.1	47.0	83.3	98.9	74.9	94.5	180.9	88.0	35.9	53.3
Mg	82,169.9	84,323.9	71,719.9	13,452.9	6,539.2	6,575.6	27,200.4	25,609.7	19,656.8	56,475.9	73,391	3,636.9	12,913.8
K	524.4	475.0	529.5	39,138.0	5,1437.1	29,871.0	29,489.6	4,7134.8	30,951.5	3,640.4	1,330.7	38,883.6	27,390.4
Ca	4,236.5	2,145.6	8,208.0	8,066.8	16,576.4	7,017.2	10,704.5	10,492.7	9,452.1	5,683.0	4,014.2	14,098.5	11,741.4
P	35	42.2	33.3	464	983.9	469.2	767.3	1,090.4	1,075.3	349.7	110.6	998.5	807.4
Fe	38,450.0	42,660.6	35,069.6	6,674	3,422.4	2,058.1	12,509.9	10,515.2	9,142.4	41,207.3	44,551.3	1,671.5	7,591.1
Cu	4.3	0.7	5.8	1.5	14.4	0.6	1.1	2.9	14.8	13.4	6.7	36.5	9.5
B	35	11.7	9.8	11.6	12.8	10.4	17.5	12.8	14.9	20.5	16.2	17.4	19.5
Mn	1,531.2	754.5	536.0	232.0	43.5	6.1	381.7	148.9	113.6	697.6	712.1	34.4	135.2
Zn	24.6	20.5	15.2	11.0	17.4	6.9	15.6	16.7	32.5	51.0	24.1	30.6	19.9
Ni	1,318.0	1,751.8	1,145	160.6	61	52.7	332.8	310.5	261.5	982.9	1,647.9	22.2	246.1
Cr	475.2	371.6	314.8	60.1	20.1	11.0	114.9	69.9	62.7	340.5	312.8	6.8	33.0
S	226.8	652.2	1,251.1	1,297.4	6,355.7	1,011.4	1,186.3	1,458.5	1,397.6	1,175.0	1,712.3	1,581.6	1,081.8
Co	89.7	77.6	57.1	13.8	3.7	2.8	19.2	9.5	9.6	47.2	71.8	1.7	4.7
Al	2,799.3	2,449.3	3,413.4	1,019.9	1,343.3	347.2	1,666.5	1,020.8	1,089.6	8,599.5	5,111.5	848.8	1,410.6

RESULTS AND DISCUSSION

Important data were obtained in the study we carried out in different habitats (gypsum, serpentine, calcareous and kolluviyal). When element concentrations of the habitats where *S. nerimaniae* has grown spreading in serpentine area were analysed, it was determined that the concentration of elements was parallel to each other. It was also specified that Ni, Co, Fe, Mg and Cr elements in these habitats had very high concentrations. The element concentration of the habitats where *S. dumanii* plant has grown was noticed to be similar to each other; and moreover, there were striking similarities between the habitats where *S. nerimaniae* was collected. The element concentration two plants obtained from the habitats they survive was noticed to be parallel to each other (Table 2.).

Because the soils in serpentine habitats decompose hard, they are generally in a flowing stone shape. Because these soils include too much Mg, it is really hard for the plants to survive. There are also plants providing adaptation into these areas. In serpentine areas, heavy metals such as nickel, cobalt, and chrome are abundant [3]. Serpentine soils are present in several different regions of the world, and include the plants indigenous to those areas. In the studies carried out with these soils; whereas Mg, Fe, Ni, Cr, and Co were at high concentration, the level of Ca was determined to be low. High magnesium content was noticed to inhibit calcium uptake. Accordingly, the number of plant species in these areas is scarce and different [20]. The plants as Ni-hyperaccumulator were determined to be endemic for the serpentine soils [21]. In serpentine soils, organic matter is weak and the water retention value is low. Consequently, serpentine habitats can cause the plants to get stressed depending upon drought [22]. In their studies, some researchers determined that the plants species grow as endemic in soils with high metal concentration, and these have the property of accumulating more heavy metals [23, 25].

Soil and plant samples for the plants of *V. alyssifolium, P. erzincani* and *T. alyssifolium* were collected from gypsum-bearing areas. The element concentrations were noticed to be similar to each other in habitats where these three plants survive. Especially in gypsum-bearing areas, S, Fe, Ca concentrations were determined to be at a high level. Metal uptake of plants' roots and leaves from the soil was specified to be similar to each other (Table 3).

TABLE 3
Metal concentration (µg/g dw) of plants grown in gypsium areas.

	Psephellus erzincani						*Tanacetum alyssifolium*						*Verbascum alyssifolium*		
Element	Soil		Root		Leaf		Soil		Root		Leaf		Soil	Root	Leaf
	I	II	I	II	I	II	I	II	I	II	I	II			
Cd	0	0	0	0	0.02	0	0	0	0.2	0.2	0.1	0.1	0	0.1	0.1
Pb	0.7	4.3	2.8	2.4	0.9	0.7	1.9	2.0	1.4	0.6	2.1	1.0	4.1	3.3	0.5
Na	14.5	70.5	36.6	44.2	34.5	85.36	28.4	55.4	32.7	28.3	28.3	24.3	337.7	579.4	92.9
Mg	650.7	2,300.8	959.4	1,503.8	522.8	1,674.8	1,093.3	1,262.9	855.3	745.4	1,192.6	1,423.3	5,108.2	3,654.1	1,369.2
K	616.9	4,522.1	15,124.8	15,382.1	11,771.1	30,656.8	1,045.9	1,273.2	3,518	5,297.8	25,059.7	26,947.7	5,906.72	13,226.7	9,647.5
Ca	80,021.4	66,927.5	56,497.9	36,381.2	23,609.6	29,250.5	86,049.5	83,479.5	39,029.2	32,664.3	25,614.4	1,8256.6	86,850.2	32,491.6	12,936.1
P	8,601.8	75.7	743.8	227.7	196.7	716.4	13.5	13.5	175.3	228.5	991.8	958.0	55.9	302.8	362.1
Fe	1,819.1	11,463.7	4,355.2	4,298.7	1,714.1	1,626.8	2,736.1	5,769.2	1,871.9	1,748.0	2,327.2	1,587.8	13,697.1	7,587.6	1,546.5
Cu	1	3.1	7.8	11.8	3.2	16	1.4	21.7	10.3	8	21.4	21.1	9.8	45	5.13
B	1.9	4.6	20.4	12.4	12.6	13.4	3.8	1.9	7.4	6.5	16.0	14.4	14.9	33.1	23.5
Mn	34.2	118.8	52.4	23.4	21.1	35.9	42.2	72.3	31.4	43.9	30.2	6.3	200.9	133.3	78.1
Zn	2.3	15.9	15.2	10.6	8.1	11.9	3.2	2.5	8.9	2.4	39	19.2	12.9	35.3	12.5
Ni	4.7	69.8	11.5	20.9	3.3	11.1	4.8	312.2	4.2	5.9	2.7	4.9	90.6	58.9	6
Cr	3.3	41.08	5.12	9.59	3.54	1.95	5.0	560.1	3.4	4.2	3.8	3.3	33.8	17.2	3.5
S	57,641.8	23,621.5	32,403.1	7,746.2	8,674.4	9,849.8	68,226.5	49,758.8	7,710.5	5,825.3	10,709.9	6,341.5	50,142.9	1,355.3	1,554.9
Co	1.04	4.78	1.92	2.03	0.97	2.45	1.5	5.9	1.1	1.0	1.1	0.7	2.4	3.58	0.95
Al	1,734.8	6,493.2	3,721.9	3,644.1	1,676.9	1,444.6	2,374.9	3,019.1	1,670.9	1,461.8	1,998.9	1,428.1	7,386.2	5,150.1	1,469.5

When *F. glareosa* habitat was analysed, the amount of Ca, K, Fe, Al, Na, and Cu elements in the soil was at a high level. Additionally, Mg and Cr were lower rather than the gypsum-bearing areas, and higher rather than the serpentine areas. The plant of *F. glareosa* was noticed to take Mn element more as being different from the other habitats. The plant of *P. auchierianus* has grown in calcareous and serpentine habitats. The soil characteristics of the habitats were closer to each other, and element uptake of the plants was observed to be parallel to each other (Table 2-4.).

TABLE 4
Metal concentration (µg/g dw) of plants grown in calcerous and kolluviyal areas.

	Ferulago glareosa						*Psephellus auchierianus*					
	Soil		Root		Leaf		Soil		Root		Leaf	
Element	I	II	I	II	I	II	I	II	I	II	I	II
Cd	0	0	0.2	0	0	0.1	0.6	0	0.2	0.1	0.1	0.1
Pb	8.3	9.6	0.2	0.2	0	0.1	7.2	18.1	0.4	1.2	0	0.7
Na	265.1	443.2	92.9	106.9	32.5	28.9	132.3	1,021.6	34.3	180.9	28.9	78.5
Mg	12,733.2	15,392.6	1,510.9	1,591.3	1,392.6	1,376.1	85,581.3	4,977.5	3,412.2	1,031.2	1,979.5	1,301
K	12,440.6	14,032.4	28,411.7	23,143.5	32,767.6	28,665.2	776.9	22,785.6	17,022.9	14,089.6	32,788.2	26,338.1
Ca	78,241.3	86,012.5	6,264.4	7,740.4	11,735.6	19,045.1	1,074.1	61,723.1	7,982.3	20,029.1	16,089.7	18,753.8
P	228.8	348.9	412.5	418.9	655.3	783.4	2.8	341.5	554.3	618.9	878.7	472.5
Fe	24,557.3	31,679.8	1,024.1	917.3	415.1	320.8	42,152.6	33,333.9	2,951.7	2,505.5	670.7	1,943.4
Cu	16.1	23.8	17.5	1.9	3.7	3.9	0.2	22.6	2.4	18.8	0.8	10.5
B	23.2	31.6	12.3	15.5	35.8	52.1	10.3	50.1	8.9	19.2	12.4	29.2
Mn	377.9	486.1	457.5	403.3	477.8	271.7	661.4	427.5	38.9	21.1	20.3	29.6
Zn	33.5	45.9	11.9	6.2	4.5	12.1	19.4	60.2	15.5	22.4	6.4	9.7
Ni	217.7	295.9	6.5	3.9	1.8	1.1	1,601.6	53.4	70.1	3.4	28.1	29.9
Cr	120.7	581.1	6.4	3.1	1.8	1	404.2	44.5	12.3	2.8	3	49.6
S	744.9	834.5	995.9	1,088	4,799.9	6,643	180	561.8	1,294	1,602.5	2,329	1,770.6
Co	13.7	17.1	1.4	0.8	0.4	0.5	70.7	6.6	4.5	0.9	5.8	3.7
Al	8,660.5	9,580.6	836.9	752.1	405.1	299.7	2,703.7	9,951.1	1,095.9	2,216.7	325.2	1,330.1

TABLE 5
Relationships between heavy metal concentration in plant samples and soil samples for different station types Correlation coefficient (r); *p<0.05; **p<0.01significant).

Element	*S. nerimania*	*T. alyssifolium*	*P. erzincani*	*F. glareosa*	*S. dumanii*	*V. alyssifolium*	*C.aucherianus*
Cd	0.214	0.770**	ND	-0.480	0.768**	ND	0.817
Pb	0.467*	-0.656**	0.651**	-0.580	-0.105	0.954**	0.715**
Na	-0.449*	-0.640**	0.333	0.652**	-0.427	0.996**	0.608*
Mg	0.324	-0.222	0.914**	0.134	0.977**	-0.070	0.984**
K	-0.384	0.307	0.083	-0.531	0.966**	-0.714*	-0.953**
Ca	-0.472*	-0.705**	0.446	0.828**	0.560*	-0.929**	0.980**
P	0.575**	0.518*	0.495*	0.214	0.939**	0.111	0.986**
Fe	0.449*	-0.525**	0.116	-0.245	0.928**	0.287	0.613**
Cu	-0.359	-0.391	0.606**	-0.508**	0.816**	0.585	0.989**
B	-0.521*	0.169	0.241	-0.659*	-0.773**	0.660	0.983**
Mn	0.702**	-0.378	-0.669**	0.008	0.909**	0.274	0.780**
Zn	0.188	0.363	0.416	-0.675*	0.601**	0.630	0.953**
Ni	-0.181	-0.294	0.970**	-0.619*	0.988**	-0.206	0.991**
Cr	0.747**	0.644**	0.862**	-0.531	0.791**	0.012	0.992**
S	-0.173	0.573*	0.650**	0.767**	0.428	0.518*	0.978**
Co	0.718**	-0.012	0.760**	-0.559	0.818**	0.067	0.988**
Al	0.671**	-0.082	-0.090	-0.257	-0.866**	-0.266	0.975**

When the ecological features of the selected endemic plants we studies were analysed, it was noticed that the habitats they have survived had different element concentrations. The correlation was analysed for each metal between the roots of plants and the soils they survive. When correlation results were evaluated, positive and negative relationships were observed. In some metals, significant relationships were determined between the endemic plants and soil. It was noticed that there was a quite high relationship between *P. aucherianus* and soil. In general, it is possible to say that the relationship between the plants and elements that have high concentration was significant. In serpentine areas, several studies have been carried out especially upon Ni element. The data obtained from the several studies carried out in serpentine areas and our data were compatible with each other. Whereas Mg/Ca rate was very high in serpentine areas we studied, Ca/Mg rate was higher in other habitats (Table 5.).

The data obtained from serpentine areas by [20] and [26] and our data were very similar to each other. [27] analysed some elements in soils and plants growing in serpentine areas. The results they obtained and our results were in parallel with each other. The data obtained by [28] and [29] related to the Ni element in some plants had higher rate than the data we obtained. According to comprasion the analysis of data we obtained with [30] soil contain high level Fe, Mg but Zn , the level of Co, Cr, Ca and Ni is parellel, whereas plants contain high level of Mg, low level of Ni, and Ca level is parallel in both studies. In comparison of our studies with [31], in serpentine soil plants, the level of Ca, Mg, Fe, Ni, Mn, Cr, Co are parallel to our results, whereas Cu, Zn, Pb level is lower then our estimates.

When we compared the data we obtained with the data required to be present in soils and plants as mentioned in the studies carried out up to now, we noticed that whereas Mg, Ni, Co, Fe and Cr elements were at a high amount in soil in serpentine areas, Ni, K and Cr elements were more than the value they should have. When we analysed the gypsum-bearing areas, it was determined that Ca, Fe and S elements were at a high ratio in soil and plants, and whereas K and Ca concentrations were noticed to be higher in plants, Fe was determined to be high in plants and soil in calcareous areas. In studies related to the protection of a scarce and endangered plant, it is necessary to know the ecology of the species, characteristics of the species and the population size, as well. If the data related to an endangered species is known well, efficient methods can be developed to protect the species. For protecting species, it is necessary to answer several questions such as the environment where the species survive, distribution, biotic interactions, morphology, physiology, population, behaviour, inheritance, and interaction with human. The studies that have been carried out rarely provide answers for those.

We know that several factors are efficient in distribution of endemic plants. With the study we carried out, we can say that the element contents of serpentine, gypsum-bearing and calcareous areas have been different from each other. When the

concentrations of elements in plants and soil and the correlation between the soil and plants were analysed, we considered that elements could be efficient in spreading of the endemic plants. Furthermore, we believe that genetic, physiologic and ecologic studies should be carried out in order to have more information related to the adaptation of endemic plants into the habitats they survive.

REFERENCES

[1] Özhatay, N., Byfield, A., Atay, S. (2005) Important Plant Areas in Turkey: 122 Key Botanical Sites. WWF Türkiye Doğal Hayatı Koruma Vakfı, İstanbul.

[2] Güner, A. (2012) Türkiye Bitkiler Listesi. ANG Vakfı. Sayfa XV.

[3] Avcı, M. (2005) Diversity and Endemism in Turkey's Vegetation. İstanbul Üniversitesi, Edebiyat Fakültesi, Coğrafya Dergisi 13, 27-55.

[4] Davis, PH. (ed) (1965-1985) Flora of Turkey and the East Aegean Islands, Edinburg: Edinburg University Press.

[5] Kandemir A, Türkmen Z. (2008) The flora of Üzümlü-Sakaltutan (Erzincan-Gümüşhane) Turk Jof Bot 2, 265-304.

[6] Özhatay, N., Kültür, Ş., Gürdal, M.B. (2011) Check-List of additional taxa to the supplement flora of Turkey V. Turk J of Bot 35, 589-624.

[7] Van Dyke, F. (2010) Conservation Biology, Second. Ed., Springer Science and Business Media 104.

[8] Symon, D.E. (2007) Lists of gypsophilous plants from southern Australia. J Adelaide Bot Gard 21, 45–54.

[9] Kandemir, A., Sevindi, C., Korkmaz, M., Çelikoğlu, Ş. (2015). IUCN threatened categories on endemic taxa which is specific to Erzincan (Turkey). Bağbahçe Bilim Dergisi 2(1), 43-65.

[10] Schecter, S.P., Bruns, T.D. (2008) Serpentine and non-serpentine ecotypes of Collinsia sparsiflora associate with distinct arbuscular mycorrhizal fungal assemblages. Mol Eco 17, 3198–3210.

[11] Palacio, S., Johnson, D., Escuderoc, A., Montserrat-Martíd, G. (2012) Root colonisation by AM fungi differs between gypsum specialist and non-specialist plants: links to the gypsophile behaviour. J of Arid Environ 76, 128-132.

[12] Schnoor, T.M., Olsson, P.A. (2010) Effects of soil disturbance on plant diversity of calcareous grasslands. Agric Ecosyst Environ 139, 714–719.

[13] Lee, M.A., Sally, A. (2013) Power direct and indirect effects of roads and road vehicles on the plant community composition of calcareous grasslands. Environ Poll 176, 106-113.

[14] Akpulat, H.A., Celik, N. (2005) Flora of gypsum areas in Sivas in the eastern part of Cappadocia in Central Anatolia, Turkey. J of Arid Environ 61, 27–46.

[15] Korkmaz, M., Özçelik, H. (2013) Soil-plant relations in the annual Gypsophila (Caryopyhllaceae) taxa of Turkey. Turk J Bot 37, 85-98.

[16] Anonymous (2015) tr.wikipedia.org/wiki/Erzincan

[17] Alam, M.G.M., Snow, E.T., Tanaka, A. (2003) Arsenic and heavy metal contamination of vegetables grown in Samta Village, Bangladesh. Sci Total Environ 308, 83-96.

[18] Demirezen, D., Aksoy, A. (2006) Heavy Metal Levels in Vegetables in Turkey Is Within Safe Limits for Cu, Zn, Ni and Exceeded For Cd and Pb. J of Food Qual 29, 252-265.

[19] Osma, E., Ozyigit, I.I., Demir, G., Yasar, U. (2014) Assesment of Some Heavy Metals in Wild Type and Cultivated Purslane (Portulaca oleracea L.) and Soils in Istanbul, Turkey, Fresenius Environ Bull 23(9); 2181-2189.

[20] Aksoy, A., Öztürk, M. (1996) Phoenix dactylifera L. as a Biomonitor of Heavy Metal Pollution in Turkey. J Trace Microprobe Tech 14(3), 605-614.

[21] Ghaderian, S.M., Mohtadi, A., Rahiminejad, M.R., Baker, A.J.M. (2007) Nickel and other metal uptake and accumulation by species of Alyssum (Brassicaceae) from the ultramafics of Iran. Environ Pollut 145,293-298.

[22] Alves, S., Nabais, C., Goncalves, M.L.S., Margarida, M. (2011) Correia dos Santos Nickel speciation in the xylem sap of the hyperaccumulator Alyssum serpyllifolium ssp. lusitanicum growing on serpentine soils of northeast Portugal. J Plant Physiol 168, 1715-1722.

[23] Yokoo, T., Kobayashi, S., Oginuma, K., Fujikawa, K., Mitsui, Y., Ikeda, H., Setoguchi, H. (2009) Genetic structure among and within populations of the serpentine endemic Heteropappus hispidus ssp. leptocladus (Compositae). Biochem Syst Ecol 37, 275–284.

[24] Blaylock, M.J., Huang, J.W. (2000) Phytoextraction of Metals,In: I.Raskin and B.D.Ensley (Ed.) Phytoremediation of Toxic Metals : Using Plants to Clean Up The Environment, John Wiley and Sons,Inc,Toronto, Canada, p 303.

[25] Dahmani-Muller, H., Oort, F., Gelie, B., Blabene, M. (2000) Strategies of Heavy Metal Uptake by Three Plants Species Growing Near a Metal Smelter. Environ Pollut 109, 231-238

[26] Raskın, I., Ensley (Ed) (2000) Phytoremiadiaitan of toxic metals: using plants

to clean up to enviroment, John Wiley and Sons, N. York, 303 pp.
[27] Rakic, T., Ilijevic, K., Lazarevic, M., Grzetic, I., Stevanovic, V., Stevanovic, B. (2013) The resurrection flowering plant Ramonda nathaliae on serpentine soil– coping with extreme mineral element stress. Flora 208, 618-625.
[28] Wenzel, W.W., Bunkowskia, M., Puschenreitera, M., Horak, O. (2003) Rhizosphere characteristics of indigenously growing nickel hyperaccumulator and excluder plants on serpentine soil. Environ Poll 123, 131–138.
[29] Reeves, R.D., Adıgüzel, N. (2004) Rare plants and nickel accumulators from turkish serpentine soils, with special reference to Centaurea Species. Turk J.of Bot 28, 147-153.
[30] Altınözlü, H., Karagöz, A., Polat, T., Ünver, İ. (2012) Nickel hyperaccumulation by natural plants in Turkish serpentine soils. Turk J Bot 36, 269-280.
[31] Bani, A., Imeri, A., Echevarria, G., Pavlova, D., Reeves, R.D., Morel, J.L., Sulçe, S. (2013) Nickel Hyperaccumulation in The Serpentine Flora of Albania. Fresenius Environ Bull 22(6), 1792-1801.
[32] Tzonev, R., Pavlova, D., Sánchez-Mata, D., de la Fuente, V. (2013) Contribution to the knowledge of Bulgarian serpentine grasslands and their relationships with Balkan serpentine syntaxa. Plant Biosystems 147(4), 955-969.

Received: **14.10.2015**
Accepted: **27.01.2016**

CORRESPONDING AUTHOR

Etem Osma
Erzincan University, Faculty of Science and Arts, Department of Biology, Erzincan, Turkey

Email: eosma@erzincan.edu.tr

© by PSP Volume 25 – No. 7/2016, pages 2461-2465 Fresenius Environmental Bulletin

DETERMINATION OF THE RESISTANCE DEVELOPMENT POTENTIAL TO SPIROMESIFEN AND THE ENZYM ACTIVITIES OF THE B AND Q BIOTYPES OF COTTON WHITEFLY *BEMISIA TABACI* (GENN.) (HEMIPTERA:ALEYRODIDAE)

Utku Yükselbaba[1] and Hüseyin Göcmen[1]

[1] Department of Plant Protection, Faculty of Agriculture, University of Akdeniz, 07070, Antalya, Turkey.

ABSTRACT

In this study we determined the resistance development potential to spiromesifen and changes in esterases (EST), glutathione S-Transferases (GST), cyctochrome P450 Monooxygenases (P450) and acetylcholinesterases (AChE) enzyme activities of the B and Q biotypes of cotton whitefly *Bemisia tabaci* (Genn.). Leaf dip bioassay was used to calculate lethal concentration (LC_{50}) values of the biotypes. Spiromesifen was applied to first nymph stage at different dosages. Selection bioassays were carried out for the assays described above . After 8 selection with spiromesifen, the resistance to spiromesifen resulted in 3.5 fold increase in B biotype, 2 fold in Q biotype. EST activity was increased by 21.5 fold in Q biotype, 1.61 fold in B biotype and the changes in EST activity was statistically significant in Q biotype but not in B biotype. AChE activity was increased by 2.50 fold in B biotype, 2.26 fold in Q biotype and the changes in AChE activity was statistically significant in both B and Q biotypes. P450 activity was increased by 1.08 fold in B biotype, 1.77 fold in Q biotype and the changes in P450 activity was statistically different in Q biotype but not in B biotype. There was negative change in GST activity in both biotypes. After selection with spiromesifen, there was an increase in EST activity which was higher in Q biotype than B biotype. The results showed that EST activity is more significant in resistance mechanism to spiromesifen than AChE and P450 activities.

KEYWORDS:
Bemisia tabaci, biotype, spiromesifen, insecticide resistance, enzyme activity

INTRODUCTION

Cotton whitefly *Bemisia tabaci* (Genn.) is considered a highly cryptic species complex of diverse biotypes with differences in host range, development rate, insecticide resistance and virus-transmission capabilities [1]. Differential susceptibility or resistance to insecticides has been suggested as contributing to or arising from the biological distinctiveness of biotypes [2]. Biotypes "B" and "Q" are the two most widespread and devastating biotypes in Mediterreanean region and Asia [1,2]. The B biotype is defined by high fitness parameters such as high fecundity and fertility while the Q biotype is associated with outbreaks of severe insecticide resistance. The Q biotype has reported to develop resistance to all major insecticide groups [3]

In many agricultural systems worldwide, the extensive use of new insecticides against *B. tabaci* has resulted in high resistance levels to conventional insecticides such as organophosphates, carbamates, pyrethroids, chlorinated hydrocarbons and insect growth regulators [4,5,6,7,]. Therefore new chemical molecules that specifically target this insect pest and exhibit low toxicity to the environment are needed. One of the new insecticide classes that have recently been developed are tetronic acid derivatives. Spiromesifen is an insecticide from this new class of spirocyclic tetronic acids that acts effectively against whiteflies. It acts as an inhibitor of acetyl-CoA-carboxylase, a lipid metabolism enzyme and causes a significant decrease in total lipids [7]

The objectives of this study were to determine the potential of resistance development to spiromesifen and the changes in enzyme activities of B and Q biotypes of *B. tabaci*. This has been the first study on the resistance of B and Q biotypes of *B. tabaci* to insecticide Spiromesifen in Turkey.

.

TABLE 1
Insecticide selection doses.

	Recommended Dose (ai^{-1}) mg/lt	1.Selection Dose (ai^{-1})mg/lt (SD)	2. SD	3. SD	4. SD	5. SD	6. SD	7. SD	8. SD
Spiromesifen	14.4	0.144	0.29	0.29	0.72	0.72	1.44	2.88	2.88

MATERIALS AND METHODS

Biotype determination. Biotypes were identified according to mitochondrial Cytochrome Oxidase I (mtCOI) sequences by Frochlich et al [8] and modified by İkten et al [9]. Biotype B was collected from Antalya-Yurtpınar and Biotype Q from Aydın-Koçarlı regions.

Insecticide Bioassay. Leaf deap bioassays were carried out to determine LC_{50} values of spiromesifen (Oberon SC 240). Insecticide bioassays were conducted as described by Mann et al [10] with some modifications. A minimum of five mixed sex whitefly adults were aspriated into a modified clip cages holding a true cotton leaf. Following a 24 hours oviposition period, adults were removed and the plants were kept under controlled conditions (26 ºC 16:8 h L:D photoperiod) for hatching of eggs and development of the nymphs. When eggs were hatched after 6 days, leaves infested with first instar nymphs were dipped for 10 seconds in 100 ml of the serial dilutions of spiromesifen and de-ionized water containing Triton 100 –X. Three replicates were included per dilution for each test. Mortality of first instars were recorded after eight days. Mortality criteria of first instars was based on the dryness of individuals and whether they separated from the leaf when lifted with a brush. Pupa and surviving next stage nymphs were counted as alive.

Selection procedure were done as decribed above. Each biotype were selected eight times with the doses at Table 1. After each selection, surviving nymphs were maintained in new cages for subsequent selections**Biochemical assays.** Thirty adult females were homogonized at +4ºC in 300µl ice-cold 0.1M sodium phosphate buffer ($NaPHO_4$), Ph7.6, containing 0.1% (w/v) TritonX-100. The homogenates were centrifujed at 10000g at +4ºC for 5 minutes and supernatant used as enzym source. Activities were measured in µQuant™ Microplate Spectrophotometer BİOTEK MQX200.

Esterase Activity. EST activity was determined using 1-naphthyl acetate (α-NA) as substrate according to Stumph and Nauen [11] with slight modifications. Five enzym source (0.5 whitefly equivalents) added to the wells of 96 - well plate, containing, 25 µl of 0.2M $NaPHO_4$ Ph 6.0. The assay was started by adding 200 µl substrate solution consisted 15 mg of fast blue RR salt dissolved in 25 ml $NaPHO_4$ (0.2M Ph 6.0) and 250 µl 100 mM α-NA in acetone to each well, giving a final volume of 250 µl. Wells with buffer and substrate solution served as control for the nonenzymatic reaction. The EST activity was measured continuously at 450nm in a microplate reader for 10 min and the measurement were made in three replicates. The carboxylesterase activity was expressed as nmol naphthol/min/mg protein. A linear naphthol standard curve was obtained by using concentrations between 0.4 and 2.5 nmol 1-naphthol in 250 ml Fast Blue RR salt solution (1% acetone).

Acethylcolinesterase Activity. AChE activity was determined using dithionitrobenzoate (DTNB) acetylthiocholine (ATChI) according to Alon et al. [12] with slight modifications. A 40 µl of enzym from the source described above (4 whitefly equivalents) added to the wells of a microtiter plate containing 40 µl 0.1M $NaPHO_4$ Ph 7.6 and Triton X-100. Buffered solutions of 100 µl 5 mM ATChI and 100 µl 1.5 mM DTNB were added to the wells of a microtiter plate. AChE activity was measured continuously in a microplate reader as described above at 405nm for 20 min. Wells with buffer, DTNB and ATChI solutions served as control for the nonenzymatic reaction. Results given as OD/min/mg protein.

Glutathione S-Transferase Activity. GST activity was determined using 1-chloro-2, 4-dinitrobenzene (CDNB) and reduced glutathione (GSH) as a substrates according to Hemingway [13] with a few modifications. A 200 µl substrate solution (2.5 ml 10 mM GSH containing 125 µl 60 mM CDNB dissolved in 0.1 M pH 6.5 $NaPHO_4$) was added to the wells of 96 - well plate and 10 µl enzym source added to the each well. GST activity was measured continuously in a microplate reader at 340 nm for 5 min. Wells with buffer and substrate solution served as control for the nonenzymatic reaction. Changes in absorbance per minute were converted into nmol CDNB conjugated/min/mg protein using the extinction coefficient of the resulting 2,4-dinitrophenyl-glutathione: $\varepsilon_{340} = 9.6\ mM^{-1}\ cm^{-1}$ [14].

Cytochrome P450 Monooxygenase Activity. P450 activity was determined using P-nitroanisole

(PNOD) as a substrate according to Hansen and Hodgson [15] with slight modification. 100 µl 2 mM PNOD solution (in 0.1M pH 7.4 $NaPHO_4$) and 30 µl enzym source were added to each well of a 96 - well plate. After incubation at 27 ºC for 2 min, the reaction was initiated by addition of 10 µl 9.6 mM NADPH (in 0.1 M pH 7.6 $NaPHO_4$). The optical density was measured at 450 nm for 10 min. Wells with buffer PNOD and NADPH served as control. Results given as OD/min/mg protein.

The amounth of protein in the enzyme source was determined according to Bradford [16] using BSA as standard

Data Analyses. Estimations of Probit parameters of insecticide bioassays datas were calculated by POLO-PC [17]. The parameters included calculations of LC_{50} values and their corresponding 95% confidence limits.

Significance of Enzym activities of biotypes were analyzed by Mann-Whitney U test. Analyses were conducted with the SPSS 17 statistical program [18]

RESULT AND DISCUSSION

Following 8 selection with spiromesifen, changes in LC_{50} values of B and Q biotypes were found to be 3.65 and 2.13 fold respectively. In rearing of biotypes B and Q stock culture populations without insesticide application, they were decrease in resistance of 0.2 and 0.5 fold respectively (Table 2).

The results showed that there was increase in LC_{50} values of both biotypes B and Q after selections but these were below the recommended dosage. This result were contrary to findings of İlias et al. [19] and Kontsedalov et al. [7]. Spiromesifen caused 40% adult mortality and more effective to the first instars. Field resistance development were not observed after using this insecticide for a year in İsrael [7]. Ilias et al. [19] found no increase in resistance after 4 times selection with spiromesifen. Furthermore No development of resistance were detected in Q biotype of *B. tabaci* after three successive treatment with spiromesifen in Spain [20].

The results of the enzyme bioassays indicated that there was an increase in EST, AChE and P450 activities in both B and Q biotypes. GST activity decreased dramatically in both biotypes. In B biotype there was increase in EST, AChE and P450 activity, 1.61, 2.50 and 1.08 folds respectively. There was significant increase in AChE activity but not in EST and P450 activities in B biotype. In Q biotype there was increase in EST, AChE and P450 activity, 21.5, 2.26 and 1.77 folds respectively. There was significant increase in AChE, EST and P450 activities in Q biotype (Table 3). In contrast,

TABLE 2
Probit parameters of spiromesifen bioassays of *Bemisia tabaci* B and Q biotypes.

Population (Biotype)	LC_{50} (ai^{-1}) mg/lt (%95 confidence interval)	Probit fit line			Slope(±SE)	N	RR
		X^2	df	P			
B stock culture	0.4 (0.1- 0.8)	20.06	7	2.8	2.11±0.28	476	1
B biotype selection	1.4 (1.1- 1.8)	250.7	27	9.2	1.89±0.10	3651	3.5
B stock culture (untreated)	0.08 (0.04 – 0.13)	642.7	35	18.3	0.91±0.03	3973	0.2
Q stock culture	0.4 (0.3- 0.54)	11.2	8	1.4	2.47±0.22	712	1
Q biotype selection	0.8 (0.7- 1.0)	488.5	71	6.8	1.38±0.04	7171	2
Q stock ulture (untreated)	0.2 (0.16 – 0.26)	80.5	20	4.0	1.40±0.06	3040	0.5

(RR: Resistance Ratio, N: Number of whitefly used for bioassays)

TABLE 3
Enzym activities of Bemisia tabaci B and Q biotypes in selection assays with Spiromesifen.

		EST (nmol/min/mg protein)	AChE (OD/min/mgprotein)	P450 (OD/min/mg protein)	GST (nmol/min/mgprotein)
Q	Stock culture	4.76 ± 2.23[b*]	9.79 ± 0.44[b**]	2.59 ± 0.07[b**]	2.14 ± 0.13[a**]
	Selection	102.58 ± 22.05[a]	22.19 ± 0.66[a]	4.26 ± 0.14[a]	0.99 ± 0.02[b]
B	Stock culture	88.63 ±31.12[a]	11.77 ±0.52[b]	3.83±0.14[a]	0.94 ±0.05[a]
	Selection	143.59±34.32[a]	29.51 ±1.83[a]	4.15±0.08[a]	0.80 ±0.01[a]

[*] Within a given column followed by the same letter are not significantly different. Each biotype evaluated separately for each enzyme.

there was a higher increase in B biotype than Q in insecticides bioassays. In enzyme bioassays, the increases of EST and P450 were not significant in B biotype as a result of the initial resistance of B biotype (Table 3). EST activity values of B biotype before and after selection support this argument. These results revealed that the main resistance mechanism to spiromesifen were EST activity and AchE and P450 activities had less effect on the resistance mechanism based on the increased ratios of activities in both biotypes especially Q.

In this study, there was an increase in EST activity as shown Table 3, which was more than the increase in LC_{50} values in biotype Q as seen in Table 2. Contrary, in B biotype, the values shown in Table 2, B biotype had higher value of RR than Q biotype. Also, there was higher EST activity in stock culture population because the resistance already existed within the population. After selection bioassays, there was a 1.6 fold increase in EST activity (Table 3). The results showed that spiromesifen had lower effect to adult whitefly as related with the EST activity. Spiromesifen had less effective on adult stage than first instar as expected. EST activity increased as a result of the differences in body size. Similar results were reported in previous studies [21, 22, 7]. In laboratory bioassays, Spiromesifen was found to be highly toxic to nymphs, causing ~100% mortality to first and second instars nymphs, and moderately toxic to old nymphs and slightly toxic to adults [21]. The insecticide reported to have a very specific and strong effect on the egg and nymphal stages while it had moderate effect on adults and late nymphal stages [7]. Spiromesifen was significantly more active against early instars of whiteflies based on lower LC50 values recorded compared to the fourth instars [22].

CONCLUSION

In conclusion, overall results showed that the Q biotype of *B. tabaci* has developed more resistance to spiromesifen than B biotype and EST activity plays a major role in the resistance mechanism.

ACKNOWLEDGEMENTS

This project has been supported by Scientific Projects Coordination Unit of Akdeniz University (Antalya, Turkey). We are deeply grateful to them for their support.

REFERENCES

[1] Yuan, L., Wang, S., Zhou, J., DU, Y., Zhang Y. and Wang, J. (2012) Status of insecticide resistance and associated mutations in Q-biotype of whitefly *Bemisia tabaci*, from eastern China. Crop Protection, 31: 67-71.

[2] Horowitz, A.R., Kontsedalov, S., Khasdan V. and Ishaaya, I. (2005) Biotypes B and Q of *Bemisia tabaci* and their relevance to neonicotinoid and pyriproxyfen resistance. Archives of Insect Biochemistry and Physiology, 58: 216–225.

[3] Kontsedalov, S., Abu-Moch, F., Lebedev, G., Czosnek, H., Horowitz A.R. and Ghanim, M. (2012) *Bemisia tabaci* biotype dynamics and resistance to insecticides in Israel during the years 2008-2010. Journal of Integrative Agriculture, 11(2): 312-320.

[4] Denholm, I., Cahill, M., Byrne F.J. and Devonshire, A.L. (1996) Progress with documenting and combating insecticide resistance in *Bemisia*. In: Gerling, D., Mayer, R.T. (Eds.), *Bemisia*: 1995 Taxonomy,

Biology, Damage, Control and Management. Intercept, pp: 577–603 Andover.

[5] Horowitz, A.R., Mendelson, Z., Weintraub, P.G. and Ishaaya, I. (1998) Comparative toxicity of foliar and systemic applications of acetamiprid and imidacloprid against the cotton whitelfy, *Bemisia tabaci* (Hemiptera: Aleyrodidae). Bulletin of Entomological Research, 88: 437-442.

[6] Elbert, A. and Nauen, R. (2000) Resistance of *Bemisia tabaci* (Homoptera: Aleyrodidae) to insecticides in southern Spain with special reference to neonicotinoids. Pest Management Science, 56: 60–64.

[7] Kontsedalov, S., Gottlieb, Y., Ishaaya, I., Nauen, R., Horowitz A.R. and Ghanim, M. (2009) Toxicity of spiromesifen to the developmental stages of *Bemisia tabaci* biotype B. Pest management science, 65(1): 5-13.

[8] Frohlich, D.R., Torrez-Jerez, I., Bedford, I.D., Markham P.G. and Brown, J.K. (1999) A phylogeographical analysis of the *Bemisia tabaci* species complex based on Mitochondrial DNA markers. Molecular Ecology, 8: 1683–1691.

[9] Yükselbaba, U., İkten, C. and Göçmen, H. (2012) Determination of the biotypes of *Bemisia tabaci* (Genadius) (Hemiptera Aleyrodidae) populations from Antalya Province of Turkey by sequence analysis of Mitochondrial Cytochrome Oxidase I (mtCOI) gene region. *QBOL-EPPO Conference on DNA Barcoding and diagnostic methods for plant pests, 21-25June 2012, Haarlem, Netherlands: 29.*

[10] Mann, R. S., Schuster D. J. and Toapanta, M. (2012) Baseline toxicity of spiromesifen to biotype B of *Bemisia tabaci* in Florida. Florida Entomologist 95(1) : 95-98

[11] Stumpf, N. and Nauen, R. (2002) Biochemical markers linked to abamectin resistance in *Tetranychus urticae* (Acari: Tetranychidae). Pesticide Biochemistry and Physiology, 72: 111–121.

[12] Alon, M., Alon, F., Nauen R. and Morin, S. (2008) Organophosphates' resistance in the B-biotype of *Bemisia tabaci* (Hemiptera: Aleyrodidae) is associated with a point mutation in an ace1-type acetylcholinesterase and overexpression of carboxylesterase. Insect Biochemistry and Molecular Biology, 38: 940-949.

[13] Hemingway (1998). WHO/CDS/CPC/MAL/98.6.

[14] Habig, W.H., Pabst M.J. and Jakoby, W.B. (1974) Glutathione S-transferases, the first step in mercapturic acid formation. The Journal of Biological Chemistry, 249: 71-75.

[15] Hansen, L.G. and Hodgson, E. (1971) Biochemical characteristics of insect microsomes N-and O-demethylation. *Biochemical* Pharmocology, 20: 1569-1578.

[16] Bradford, M.M. (1976) A rapid and sensitive method for quantitation of microgram quantities of protein utilizing the principle of protein-dye-binding. Analytical Biochemistry, 72 : 248-254.

[17] Leora software (2008) Polo-Plus, (Probit analyz programme).

[18] Anonymus (2008) SPSS Statistics for Windows, Release 17.0, SPSS Inc.

[19] Ilias, A., Roditakis, E., Grispou, M., Nauen R. and Vontas, J. (2012) Efficacy of ketoenols on insecticide resistant field populations of two-spotted spider mite *Tetranychus urticae* and sweet potato whitefly *Bemisia tabaci* from Greece. Crop protection 42: 305-311.

[20] Guthrie, F., Devine, G., Denholm, I., and Nauen, R. (2003) Biological evaluation of spiromesifen against *Bemisia tabaci* and an assessment of resistance risks. Proceedings BCPC International Congress–Crop Science and Technology, 10–12 November 2003 2003. 795–800.Glasgow. United Kingdom.

[21] Liu T.-X. (2004) Toxicity and efficacy of spiromesifen, a tetronic acid insecticide, against sweetpotato whitefly (homoptera: aleyrodidae) on melons and collords. Crop Protection, 23: 505-513.

[22] Prabhaker, N., Castle, S.J., Buckelew L. and Toscano, N.C. (2008) Baseline susceptibility of *Bemisia tabaci* B biyotype (Hemiptera: Aleyrodidae) populations from California and Arizona to spiromesifen. Journal of Economic Entomology 101(1): 174-181.

Received: **09.10.2015**
Accepted: **18.02.2016**

CORRESPONDING AUTHOR

Utku Yükselbaba
Department of Plant Protection
Faculty of Agriculture
University of Akdeniz
07070 Antalya – TURKEY

e-mail: uyukselbaba@akdeniz.edu.tr

© by PSP Volume 25 – No. 7/2016, pages 2466-2472 Fresenius Environmental Bulletin

TREATMENT OF SALINE DYE WASTEWATER USING GLOW DISCHARGE PLASMA

LiLi Xu[1], Haolin Li[1, 2], Sadia Rashid[3], Chensi Shen[3,*], Yuezhong Wen[1], Tengbing He[1]

[1]Institute of Environmental Science, Zhejiang University, Hangzhou 310058, China
[2]College of Life Science, Guizhou University, Guiyang 550025, China
[3]College of Environmental Science and Engineering, Donghua University, Shanghai 201620, China

ABSTRACT

Saline organic wastewater is one of the major problems in wastewater treatment industry. This study evaluated the ability of the glow discharge plasma technique to degrade the saline dye in an aqueous solution. Experimental results showed that the electrolyte concentration, initial pH, and initial C. I. Acid Red 73 (AR 73) concentration impact the AR 73 degradation significantly. Decreasing the electrolyte concentration, lowering the solution pH, and reducing appropriate amount of AR 73 to the solution were found to be favorable for AR 73 degradation. In addition, the common coexisting ions had a negligible negative impact on AR 73 degradation during the discharge process. The glow discharge plasma treatment also exhibited high degradation efficiency for other anionic and cationic dyes. In comparison with the photocatalytic degradation, electrocatalytic oxidation, and high density plasma, this process offers simple technology, higher energy efficiency, and easier applicability to salt-containing wastewater. Overall, the results reported herein indicated that glow discharge plasma may become a competitive saline dye wastewater treatment technology.

KEYWORDS:
dye; degradation; glow discharge plasma; saline wastewater

INTRODUCTION

Nowadays, organic compounds as a major group of pollutants in wastewater are of concern worldwide due to their severe problems for the environment and human health. Thus, in the case of unavoidable pollutant emissions, these emerging pollutants must be treated to satisfy the stringent water quality regulations before discharging into aquatic ecosystem. However, most investigations that have reported on the removal of organic pollutant have focused on its removal from fresh wastewater, while few studies have concentrated on the removal of organic pollutant from saline wastewaters, despite the fact that saline effluents containing organic compounds are generated by a number of industries, such as textiles, food-processing, pesticide production, leather and petroleum industry [1, 2]. The high salinity has been proved to strongly inhibit the survival, growth and reproduction of microorganisms, consequently causing the difficulties in aerobic and anaerobic biological degradation for the saline wastewater.

More recently, nonthermal plasma technologies (electrical discharge processing) have offered an innovative approach to the problem of degrading organic pollutants [3-5]. Nonthermal plasma technologies include pulsed corona discharge, dielectric barrier discharge, surface discharge, dc discharge processes, glow discharge [6-14]. Among these methods, glow discharge plasma (GDP) is considered as a promising alternative for the oxidative degradation of aqueous organic pollutants due to stable operation, low discharge voltage and much higher yields of high oxidation potential species such as ·OH and H_2O_2 produced in the liquid-phase than those expected on the basis of Faraday's law[15-19]. In addition, it can be run in water with higher conductivity compared with pulsed corona discharge plasma [20, 21].

In this study, we report the treatment of saline dye wastewater using glow discharge plasma and the effect of various degradation parameters on the degradation of azo dye in water are investigated. As we know, wastewater discharged from dyeing processes can be one of the biggest contributors to textile effluent; this comprises mainly residual dyes and auxiliary chemicals [22]. Among these dyes, azo dyes represent the largest class of dyes [23, 24].

MATERIALS AND METHODS

The DC high-voltage power unit (variable voltage of 0-600 V and current of 0-600 mA) was supplied by Beijing Da Hua Radio Factory. The reactor contained a cylindrical vessel with an inner diameter of 40 mm is the same with our previous report [24]. 50 mL portion of the sample solution

was poured into the reactor for treatment. A DC high voltage of 525V was applied across the electrodes through a DC power source to start the reaction. During the reaction, the solution was gently stirred with a magnetic stirrer, and a 5 mL sample was periodically taken out to determine the AR73 concentration and to analyze its degraded products.

The determination method of dye can use the first step in the determination of absorbance and then converted into a method for determination of the concentration to show up, to make a first 10, 20, 30, 40, 50, 60 mg/L AR73 line, and then respectively 100, 150, 200 mg/L range of sample 5 times dilution to the line.

RESULTS AND DISCUSSION

The effect of electrolyte concentration. In this experiment, the applied voltage was 525 V, the AR 73 degradation was proceeded in sodium sulfate electrolytic solution. The effect of electrolyte concentration was investigated from 1.5 g/L to 5.0 g/L. Figure 1 shows the AR 73 degradation under different electrolyte concentration. The curve can be divided into two sections. In the range of 1.5-3.5 g/L sodium sulfate solution, the degradation rate of AR 73 decreased with increasing initial sodium sulfate concentrations. This is because the interactions of positive and negative ions were enhanced; as a result the migration rate of ions was slowed and then the electrical conductivity decreased. In the range of 3.5-5.0 g/L sodium sulfate solution, the degradation rate of AR 73 became relatively steady due to the serious electrode wear in high electrolyte concentration.

The influence of different pH. The initial pH value is an important factor in wastewater treatment. The influence of initial pH of the solution has been investigated by many researchers. For different substrates, pH value shows different effects. In this study, 50 mL AR 73 solutions at concentration of 50 mg/L with different initial pH values from 4.0 to 9.0 were placed into the reactor during the discharge process. 1.0 mL sample was drawn periodically from the solution for the purpose of analysis of AR 73 concentration. The effect of pH values on the degradation AR 73 is shown in Figure 2. It can be seen that more rapid AR 73 degradation rates were obtained at relatively lower pH values during the first 20 min and then remained steady at all pH values. It may be attributed to following reasons: First is that the oxidative ability of the oxygen-containing radical is quite strong under acidic conditions. Consequently, the degradation rates of AR 73 were increased in acidic medium. The second is probably that in basic conditions the carbon dioxide resulting from the AR 73 degradation dissolved in the solution to produce carbonate ions, which would mostly act as •OH scavenger in basic medium and therefore inhibited AR 73 degradation.

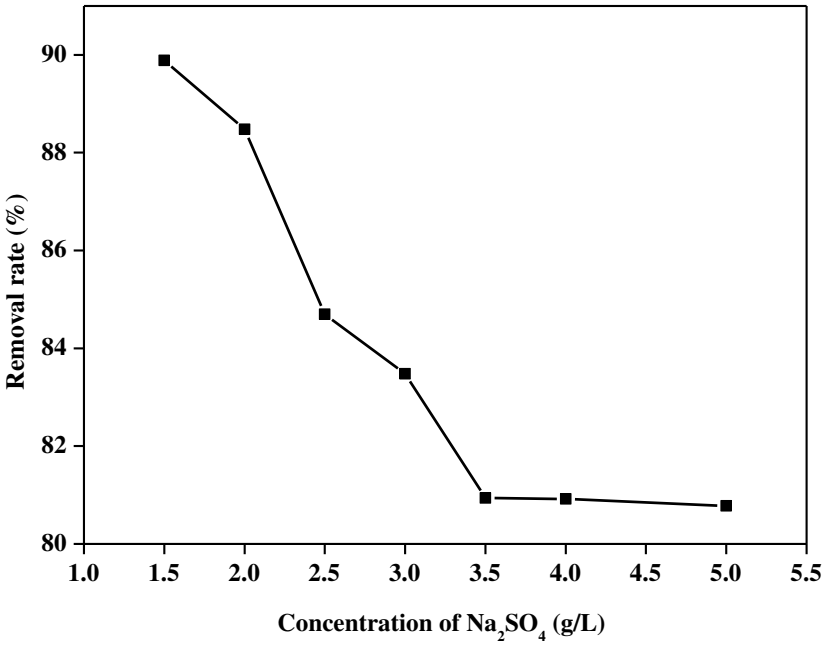

FIGURE 1
Degradation efficiency of AR 73 under different electrolyte concentration (Initial concentration 50 mg/L, 50mL, T=25 ºC, pH 7.0±0.2).

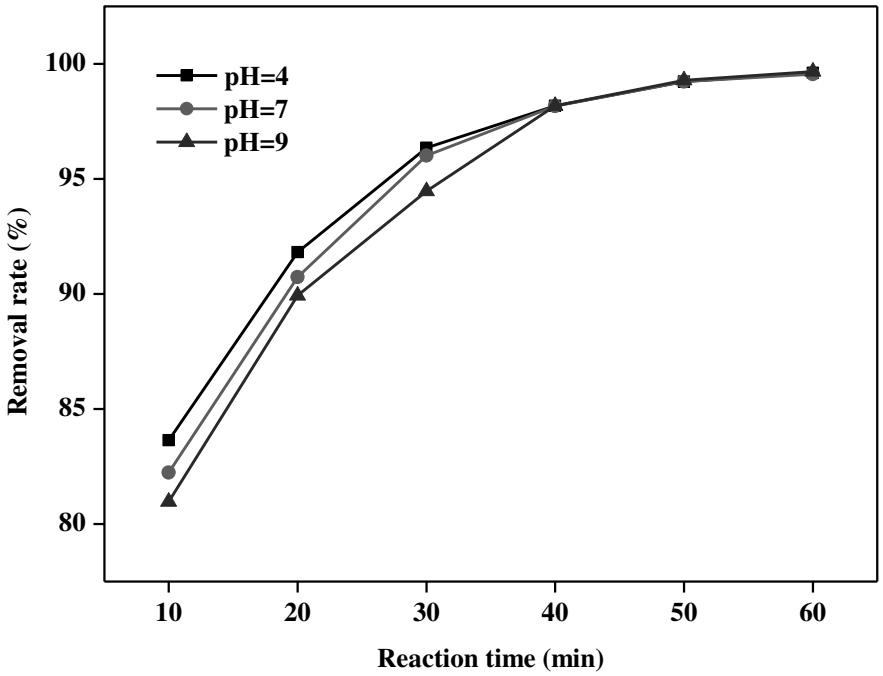

FIGURE 2
Effect of different pH on AR 73 degradation (Initial concentration 50 mg/L, 50 mL, T=25 ºC, Na_2SO_4 2.0 g/L).

Effect of the coexisting ions. In addition, the presence of the common ions that coexist with the dye may influence the discharge treatment. Therefore, the effect of the ionic strength is important in this study of AR 73 degradation during the discharge process. The common cations, such as Na^+, Ca^{2+}, K^+, Mg^{2+}, and NH_4^+, and the common anions, such as NO_3^-, CO_3^{2-}, HCO_3^-, PO_4^{3-}, and $H_2PO_4^-$, were used in the coexisting ions investigation. The influences of the coexisting ions on the AR 73 degradation during the discharge process are shown in Figure 3. It can be seen from Figure 3a that the above common cations exerted no evident change in the AR 73 degradation under the discharge treatment, showing that the presence of the common cations had no significant influence on the dye degradation by glow discharge plasma. However, when glow discharge plasma was performed in phosphate solution, as shown in Figure 3b, the degradation rate of AR 73 (77.4%) was lower in sodium phosphate solution than in blank control solution (88.6%). It might be attributed that phosphate ions acted as radical scavenger and therefore inhibited AR 73 degradation. The degradation rate of AR 73 with other coexisting anions equaled to that in blank control solution. Therefore, there is no negative impact on dye degradation for the discharge process except phosphate ions. This result demonstrates the practicality for the application of the glow discharge plasma on dyestuff wastewater treatment.

The influence of different concentration of dye. Furthermore, the initial concentration of dyes is an important parameter in practical applications. The influence of the initial concentration on the degradation efficiencies of AR 73 by glow discharge plasma was investigated at pH 7.0. The discharge time was 60 min and the degradation efficiency was determined at initial AR 73 concentrations of 50, 100, 150, and 200 mg/L. It is seen from Figure 4 that high initial concentration resulted in lower color removal. For example, when the initial AR 73 concentration is 50 mg/L, over 51% of color can be removed within 10 min of discharge treatment, whereas only about 11% can be removed in the case of 200 mg/L within the same treatment time. However, after 20 min of discharge treatment, high degradation occurred with increasing AR 73 concentrations. The higher concentrations of AR 73 increased the collisions between the AR 73molecules and chemically active species. Therefore, the degradation rate increased with increasing initial concentrations of AR 73 as the discharge process.

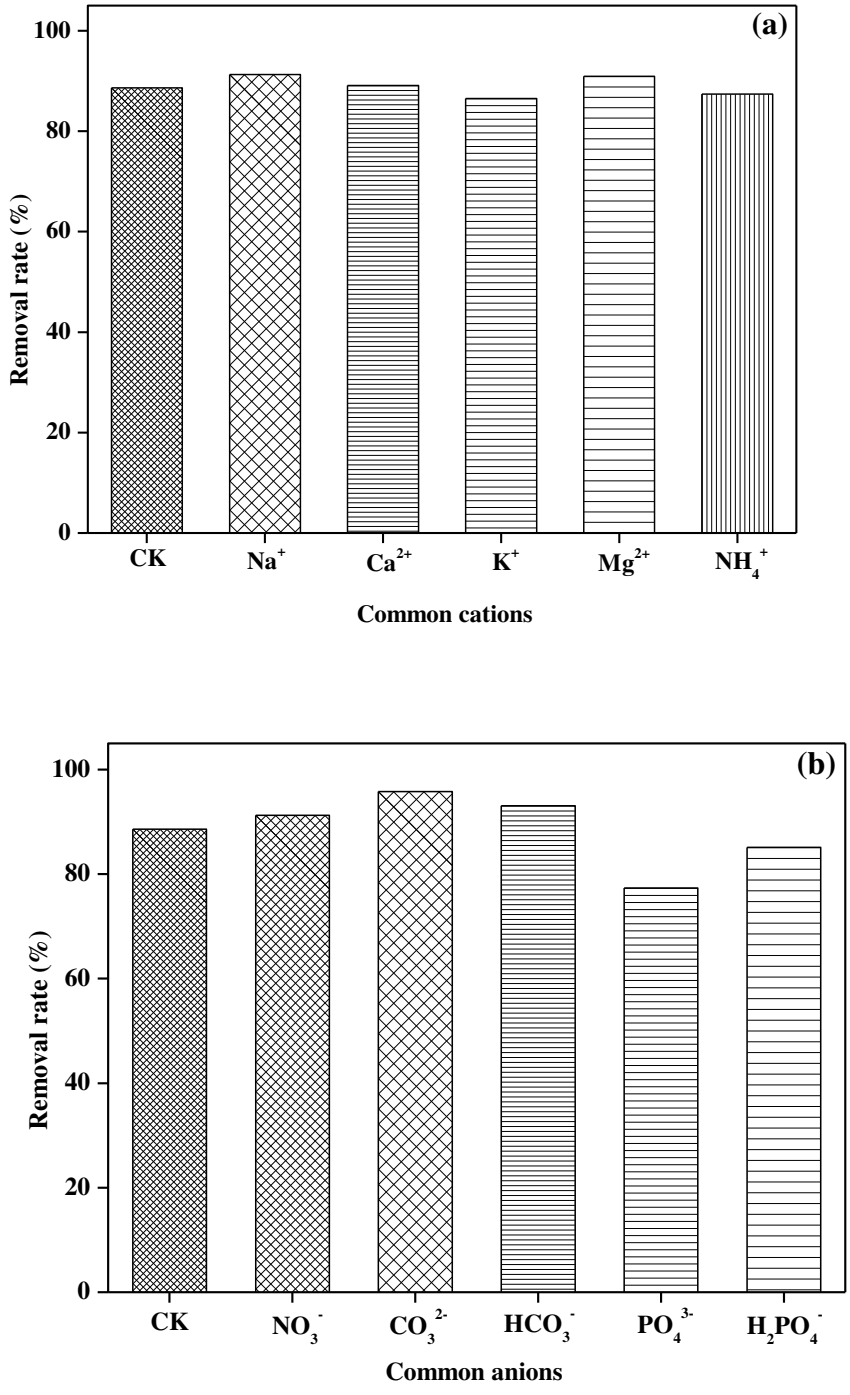

FIGURE 3
Effect of the common cations (a) and common anions (b) on AR 73 degradation (Initial concentration 50 mg/L, 50 mL, T=25 ºC, pH 7.0±0.2, Na_2SO_4 2.0 g/L).

Degradation of other dyes. It is well known that different chemical structures with different functional groups directly impact the degradation behaviors of dyes. The same discharge treatments used for AR 73 were applied to the removal of a variety of other dyes. Anionic dyes, including C. I. Reactive Blue 74 (RB 74), C. I. Reactive Blue 194 (RB 194), C. I. Reactive Red 24 (RR 24), C. I. Acid Blue 25 (AB 25), C. I. Acid Blue 40 (AB 40), C. I. Acid Blue 62 (AB 62), C. I. Acid Blue 113 (AB 113), C. I. Acid Blue 193 (AB 193), as well as a cationic dye, Rhodamine B, were chosen as typical dye pollutants. The degradation rates of the nine dyes after discharge treatment for 30 min are presented in Table S1 (in supporting information).

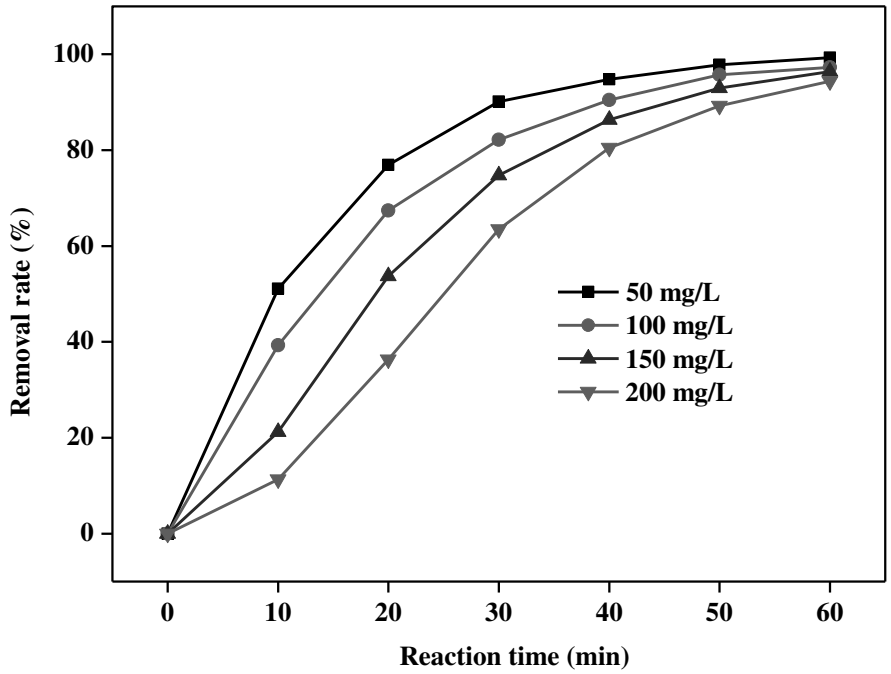

FIGURE 4
Degradation efficiency of AR 73 under different concentration of dye (The volume is 50 mL, T=25 ºC, pH 7.0±0.2, Na_2SO_4 2.0 g/L).

The result suggested that both anionic dyes and cationic dye could be degraded by using glow discharge plasma reactors, demonstrating the viability of glow discharge plasma for dyestuff wastewater treatment. These nine dyes have different chemical structures with different functional groups that influence the reactivity of the molecules in degradation processes. In addition, COD (Chemical Oxygen Demand) and TOC (Total Organic Carbon) are important indicators of water contamination. The COD value of the solution increased after discharge treatment, as well as the control experiment without dye pollutants (the data were not shown). The reason maybe that the H_2O_2 formed during the degradation process would be oxidized by dichromate during the measurement of COD through the reaction, as shown below, and this could affect the COD values. This result was consistent with previous results.

$$3H_2O_2 + Cr_2O_7^{2-} + 8H^+ \rightarrow 3O_2 + 2Cr^{3+} + 7H_2O \quad (1)$$

The TOC value indicates a loss of aromaticity and overall degree of compound degradation. TOC changes during the dye pollutants degradation are shown in Table S2 (in supporting information). It can be seen that the removal rate of TOC (below 25%) was much lower than the dye pollutants degradation rate (over 85%). This indicated that there were some residual intermediate products presented in the final treated samples by glow discharge plasma, demonstrating that complete degradation of dyes is expected to require a longer discharge treatment time.

Energy efficiency of AR 73 degradation. Energy efficiency is an important parameter required for comparing different techniques and for future scaling up of the process to industrial scale applications. In this study, the energy efficiency is defined as the number of moles of AR 73 converted from the solution per Joule of energy supplied to the system (J_{AR73}), which can be calculated using Equation (2) as follows:

$$J_{AR73} = \frac{(1/2)C_0V}{UIt_{1/2}} \quad (2)$$

Which C_0 is the initial AR73 concentration in mol/L, V is the liquid volume in L, U is the applied voltage in V, I is the current in A, $t_{1/2}$ is the reaction time required for decomposing half of the initial AR73 molecules in s, The J_{AR73} under different conditions were shown in Table 1.

TABLE 1
Energy efficiency for AR 73 degradation by glow discharge plasma.

C_0 (mg/L)	Method	$t_{1/2}$ (s)	J_{AR73} (mol/J)	Reference
50	Glow discharge plasma	600	7.94×10^{-8}	This work
100	Glow discharge plasma	810	5.88×10^{-8}	This work
150	Glow discharge plasma	1125	6.35×10^{-8}	This work
200	Glow discharge plasma	1500	6.35×10^{-8}	This work
200	Photocatalytic degradation	6000	0.02×10^{-9}	Orlov *et al.*
20	Electrocatalytic oxidation	4500	0.15×10^{-9}	Wu
50	High-density plasma	135	2.65×10^{-9}	Johnson *et al.*

Previous studies have shown that the energy efficiencies were 0.02×10^{-9}, 0.15×10^{-9}, and 2.65×10^{-9} mol/J for photocatalytic degradation, electrocatalytic oxidation, and high density plasma, respectively. As shown in Table 3 that the energy efficiency J_{AR73} is quite high than in the range from 5.88×10^{-8} to 7.94×10^{-8} mol/J. With further design improvements and reactor optimization, glow discharge plasma may become a competitive wastewater treatment technology.

DISCLOSURE STATEMENT

No potential conflict of interest was reported by the authors.

REFERENCES

[1] Li Jf, Guan YS, Cheng FQ, and Liu Y. (2015) Treatment of high salinity brines by direct contact membrane distillation: Effect of membrane characteristics and salinity. *Chemosphere*. **140,** 143-149.

[2] Li, XC, Gao BY, Yue QY, Ma DF, Rong HY, and Teng PY. (2015) Effect of six kinds of scale inhibitors on calcium carbonate precipitation in high salinity wastewater at high temperatures, J. *Environ Sci.* **29,** 124-130.

[3] Hijosa-Valsero M, Molina R, Montràs A, Müller M, and Bayona J-M. (2014) Decontamination of waterborne chemical pollutants by using atmospheric pressure nonthermal plasma: a review. *Environ Technol Rev*.**3**, 71-91.

[4] Malik M-A, Ghaffar A, and Malik S-A. (2001) Water purification by electrical discharges. *Plasma Sources Sci Technol.* **10,** 82-91.

[5] Wen YZ, Jiang XZ, and Liu WP. (2002) Degradation of 4-chlorophenol by high-voltage pulse corona discharges combined with ozone. *Plasma Chem Plasma Process.* **22,** 175-185.

[6] Johnson D-C., Shamamian, V-A., Callahan, J-H, Denes, F-S., Manolache, S-O. and Dandy, D-S. (2003) Treatment of methyl tert-butyl ether contaminated water using a dense medium plasma reactor: a mechanistic and kinetic investigation. *Environ Sci Technol*. **37**, 4804-4810.

[7] Wen YZ, and Jiang XZ. (2001) Decomposition of CO_2 using pulsed corona discharge combined with catalyst. Plasma Chem Plasma Process. **21,**665-678.

[8] Wen YZ, and Jiang XZ. (2001) Pulsed corona discharge-induced reactions of acetophenone in water. Plasma Chem Plasma Process. **21,** 345-354.

[9] Wen YZ, Shen CS, Ni YY, Tong SP, and Yu F. (2012) Glow discharge plasma in water: A green approach to enhancing ability of chitosan for dye removal. *J Hazard Mater.* **201,**162-169.

[10] Jiang B, Zheng JT, Qiu S, Wu MB, Zhang QH, Yan ZF, and Xue QZ. (2014) Review on electrical discharge plasma technology for wastewater remediation. *Chem Eng J.* **236,** 348-368.

[11] Locke BR, and Thagard SM. (2012) Analysis and review of chemical reactions and transport processes in pulsed electrical discharge plasma formed directly in liquid water. *Plasma Chem Plasma Process.* **32,** 875-917.

[12] Ognier S, Iya-sou D, Fourmond C, and Cavadias S. (2009) Analysis of mechanisms at the plasma–liquid interface in a gas–liquid discharge reactor used for treatment of polluted water. *Plasma Chem Plasma Process.* **29,** 261-273.

[13] Li SP, Jiang YY, Cao XH, Dong YW, Dong M, and Xu J. (2013) Degradation of nitenpyram pesticide in aqueous solution by low-temperature plasma. *Environ Technol.* **34,** 1609–1616.

[14] Huang FM, Chen L, Wang HL, and Yan ZC. (2010) Analysis of the degradation mechanism of methylene blue by atmospheric pressure dielectric barrier discharge plasma. *Chem Eng J*.**162**, 250-256.

[15] Liu YJ, and Jiang XZ. (2005) Phenol degradation by a nonpulsed diaphragm glow

discharge in an aqueous solution. *Environ Sci Technol.* **39,** 8512-8517.

[16] Wang L, Jiang XZ, and Liu YJ. (2008) Degradation of bisphenol A and formation of hydrogen peroxide induced by glow discharge plasma in aqueous solutions. *J Hazard Mater.* **154,** 1106–1114.

[17] Wang L, Jiang X, and Liu Y. (2007) Efficient degradation of nitrobenzene induced by glow discharge plasma in aqueous solution. *Plasma Chem Plasma Process.* **27,** 504-515.

[18] Gao JZ, Ma DP, Guo X, Wang AX, Fu Y, Wu JL, and Yang W. (2008) Degradation of anionic dye eosin by glow discharge electrolysis plasma. *Plasma Sci Technol.* **10,** 422-427.

[19] Tong SP, Ni YY, Shen CS, Wen YZ, and Jiang XZ. (2011) Degradation of methyl tert-butyl ether (MTBE) in water by glow discharge plasma. *Water Sci Technol.* **63,** 2814-2819.

[20] Yin XL, Bian WJ, and Shi JW. (2009) 4-chlorophenol degradation by pulsed high voltage discharge coupling internal electrolysis. *J Hazard Mater.* **166,** 1474-1479.

[21] Wen Y, and Jiang X. (2000) Degradation of acetophenone in water by pulsed corona discharges. *Plasma Chem Plasma Process.* **20,** 343-351.

[22] Xu LL, Li XF, Ma JQ, Wen YZ, and Liu WP. (2014) Nano-MnO_x on activated carbon prepared by hydrothermal process for fast and highly efficient degradation of azo dyes. *Appl Catal A.* **485,** 91-98.

[23] Shen CS, Shen Y, Wen YZ, Wang HY, and Liu WP. (2011) Fast and highly efficient removal of dyes under alkaline conditions using magnetic chitosan-Fe(III) hydrogel. *Water Res.* **45,** 5200-5210.

[24] Shen CS, Wen YZ, Shen ZL, Wu J, and Liu WP. (2011) Facile, green encapsulation of cobalt tetrasulfophthalocyanine monomers in mesoporous silicas for the degradative hydrogen peroxide oxidation of azo dyes. *J Hazard Mater.* **193,** 209-215.

Received: **31.10.2015**
Accepted: **17.02.2016**

CORRESPONDING AUTHOR

Dr. Chensi Shen
College of Environmental Science and Engineering
Donghua University
Shanghai 210620 – P. R. CHINA

e-mail: shencs@dhu.edu.cn

© by PSP Volume 25 – No. 7/2016, pages 2473-2483 Fresenius Environmental Bulletin

WATER REGULATION OF NONVEGETATED BIOSWALES ON URBAN SURFACE RUNOFF AND ITS SIMULATION

Li Jiake[1], Jiang Chunbo[1], Lei Tingting[1], Li Yajiao[2], Li Wenying[1]

1. State Key Laboratory Base of Eco-hydraulic Engineering in Arid Area, Xi'an University of Technology, No.5 South Jinhua Road, Xi'an, Shaanxi 710048, China
2. School of Architecture and Civil Engineering, Xi'an University of Science and Technology, No.58 Yanta Road, Xi'an, Shaanxi,710054,China

ABSTRACT

As a typical low-impact development bioretention technology, bioswale organically combines runoff pollution control and rain utilization through accumulation and hysteresis. This study designed and built multiple bioswales based on investigation and monitoring in Xi'an road runoff water and rainfall curve through simulated rainfall experiment and mathematical statistics analysis to clear the water cut effect of bioswale and its influencing factors. Moreover, the main influencing factors on the water cut effect was simulated with the regression model. Results showed that most test grooves delay time of the overflow flood peak shortened from 15 min to 30 min with an increase in inflow volume. The overflow flood peak reduction rate was between 8.96% and > 95%, and the overflow volume reduction rate was 23.62% to > 95%. The filler for different design objectives was selected and obtained perfectly by comparing artificial fillers. The runoff volume reduction rate had an obvious linear relationship with the main influencing factors of inflow water, interval operation time, and packing types. Two methods of the stepwise regression model were used to simulate water cut effect. Both methods have high precision, but the first method is better than the second method.

KEYWORDS:
Bioswale, road surface runoff, test, influencing factors, cut effect, simulation

INTRODUCTION

Water shortage has become a bottleneck factor of urban economic development in China. It has led to an increased regional total rainfall runoff, decreased peak flow time, reduced groundwater runoff recharge through infiltration, and other problems with urbanization development [1]. Green vegetation interception and soil osmosis can reduce the velocity of rainwater runoff; thus, some countries attach great importance to bioretention technology, which is widely applied in engineering practices, together with water-sensitive urban design and sustainable urban drainage systems, to reduce road rainwater runoff and meet target reduction goals [2,3].

Bioswale is a kind of bioretention facility. Many studies show that urban development negatively affects hydrology and the water quality of surrounding streams and other natural bodies [4]. Previous studies on bioretention system mainly focus on water quality purification effect [5], whereas studies on volume and flood peak control are rare. Davis studied more than 49 storm events of two field-scale bioretention facilities installed at the University of Maryland and demonstrated that bioretention system can effectively reduce the impact of the development on hydrologic regimes in urban areas [6]. The monitored results of 28 field rainfall events of bioretention facilities (i.e., 1% of the catchment area) in Australia's Monash University showed that the average flood peak reduction rate is 80% [7]. Attention has been recently given to rainwater utilization in China. However, the research on bioretention technology is insufficient. Meng et al. [8] studied the performance of infiltration, controlling, emission, and long-term purification effect of biological retention system on road rainwater in the last four years through small and pilot tests. The results showed that the average delay time of the traditional sand packing system is 19.3 min on rainfall runoff produced by the catchment area 10 times of itself with a return period of 0.13a to 3.2a. The lagging time of flood peak is 65.7 min, the flood peak reduction rate is 84.3%, and the largest water retention without seriously impacting plant

growth is 5 h.

According to research, quantitative methods on the ability of flood peak reduction and reduction of the amount of runoff through bioretention facilities in China are still relatively rare. Moreover, the disposal effects of high rainfall intensity and the frequency of bioretention facilities must be combined with regional characteristics for further research. The specific objectives of the study are as follows: (1) to study the situation of bioretention facilities in relation to the delay time and reduction effect of runoff water and peak flow on different influencing factors, such as hydraulic loading, packing types, interval time; (2) to obtain the relationship between bioswales water cut effect and three factors through statistical analysis, thereby providing the basis for the relationship model; and (3) to research the correlation between the bioswale water cut effect and its main influencing factors through regression analysis, thereby establishing the regression equation.

MATERIALS AND METHODS

Experiment device. According to the groundwater level, the distance from the building and the environmental conditions, bioretention facilities can be classified into three types, which are permeable, semi-permeable and non-permeable.

According to surrounding conditions, shape, size, location, and scope of application, bioretention facilities can also be classified into rain garden, retention belt, retention flower bed, and tree pool. They can also be classified based on the designed purpose: to control runoff pollution and to control runoff volume [9,10].

This experiment uses two sets of pilot-scale cells, which are similar with the retention belt. These cells were designed and constructed in the outdoor test field of Xi'an University of Technology. A set of 10 bioswales has a width of 0.5 m (i.e., 1–5 bioswales were permeable, and 6–10 bioswales had an antiseepage property). The following is the specification of each groove: 2 m × 0.50 m × 1.05 m (length × width × depth). Another set of 8 bioswales has a width of 1 m (i.e., W1–W2 and E1–E2 bioswales were permeable, and W3–W4 and E3–E4 bioswales had an antiseepage property) and specification of 2.50 m × 1.0m × 1.05 m (length × width × depth). Each bioswale contains the following layers: aquifer, planting soil, artificial packing layer, and gravel drainage layer from top to bottom. We selected 10 bioswales to study the different factors influencing the effect of water cut based on the purpose of the experiment, number, and settings, as shown in Table 1. The concrete structure design is shown in Fig. 1 and Fig. 2.

TABLE 1
Experiment Device Settings.

Number	4[b]	6	7	8	9	10	W3	W4	E3	E4
Covering layer	5cm	5cm	5cm	5cm	5cm	5cm	5cm	5cm	5cm	5cm
Planting soil	30cm	—	30cm	30cm	30cm	30cm	30cm	30cm	30cm	30cm
Packing layer	FS 1:1[a]	SSH 18:1:1[a]	FS 1:1[a]	BFSS 1:1[a]	BFS	Soil	BFSS 1:1[a]	FS 1:1[a]	Soil	BFS
Gravel layer	15cm	15cm	15cm	15cm	15cm	15cm	15cm	15cm	15cm	15cm
Submerged depth [c]	0	700	0	550	350	150	550	0	150	350
Width(m)	0.5	0.5	0.5	0.5	0.5	0.5	1.0	1.0	1.0	1.0

Note: Planting soil is Xi'an local loess; [a] packing layer blending ratio for volume; [b] antiseepage-treated bioswales are at the bottom except for #4. FS is fly ash + sand, SSH is sand + soil + humus; BFSS is blast furnace slag + Sand; BFS is blast furnace slag. [c] The height between the water outlet and the bottom of bioswales as submerged zone height. This experiment selects the height that has effective purification effect in the prepilot test.

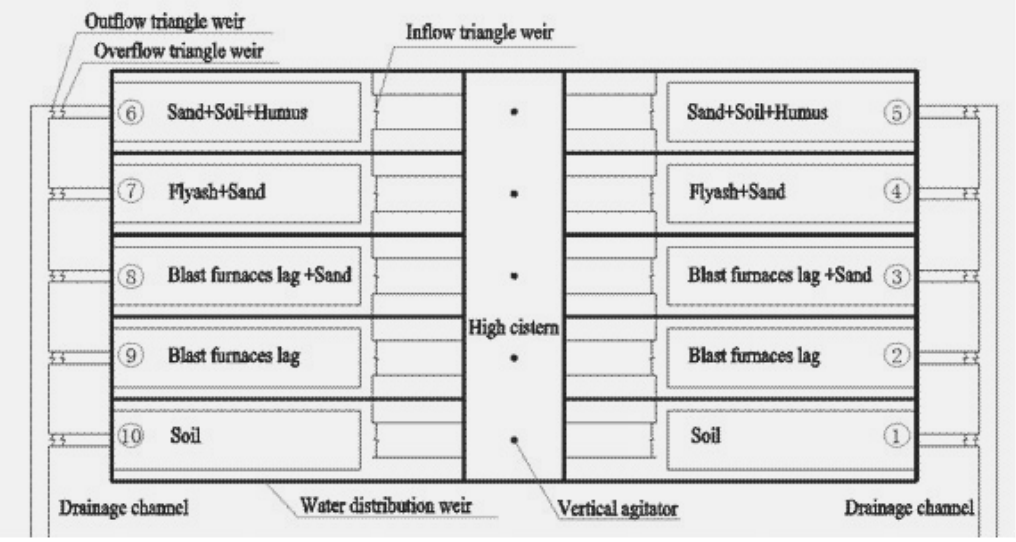

(a) Floor plan of bioswales pilot plant (0.5m width)

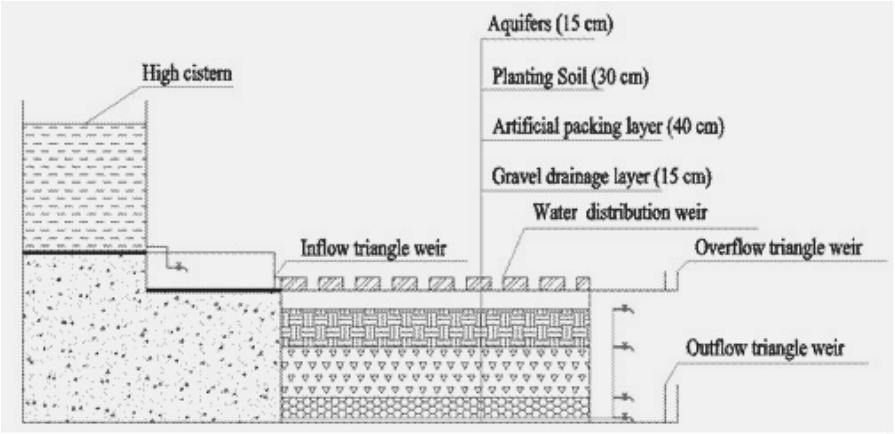

(b) Section of Bioswales Pilot Plant

FIGURE 1

Specific constructions in each bioswale consist of the aquifer, covering layer, planting soil layer, artificial packing layer, rice stone layer, and gravel layer from top to bottom. The screened sizes of BFS, rice stones, and gravels are 0.6–1.5 cm, 0.3–0.6 cm, and 1.5–3 cm, respectively.

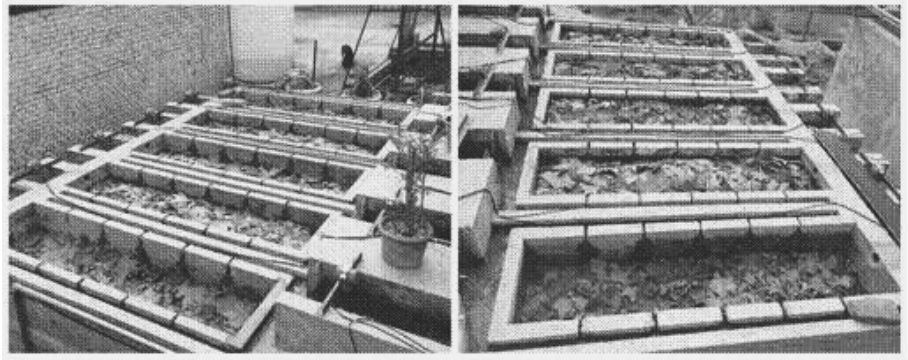

FIGURE 2

Partial pictures of the test on the bioswale pilot plant. 0.5 m-wide bioswales; each bioswale surface is laid on 5 cm fresh platane leaves.

Inflow water and rainfall pattern. The main factors that influence the cut effect of bioswales include the following: inflow water, packing types, and interval operation time. We design three rainfall intensities in this experiment: low, medium, and high, which corresponding to . We also design rainfall with 60 min duration and investigate the runoff volume and peak flow reduction effect on different inflow waters. The chosen interval times are 1 and 3 d to study the runoff volume and peak flow reduction effect at different interval times in the medium inflow volume conditions. The medium inflow volume (i.e., 2-year return period and rainfall volume of 60 min) is chosen as an example in the analysis of different filler types of runoff volume and peak flow reduction effect. The results of the previous minor test are summarized, and the confluence area is calculated with the detention pond area computation equation (1) [11]:

$$A_f = \frac{A_d \cdot H \cdot \varphi \cdot d_f}{60 \times K \cdot T(d_f + h) + h_m \cdot (1 - f_v) \cdot d_f + n \cdot d_f{}^2} \quad , \tag{1}$$

where A_f indicates the area of the bioswale (m^2), A_d indicates the confluence area (m^2), H indicates the design rainfall (m), φ indicates the runoff coefficient, d_f indicates the total layer thickness of planting soil and medias, T indicates single-game rainfall duration, h indicates the aquifer average depth (i.e., half of the maximum depth, h_m), f_V indicates the ratio of the reservoir section on the vegetation and bioswale areas, and n indicates the average porosity of planting soil layer and packing layer.

The rainfall duration (60 min) and return period (0.5a, 2a, 5a) are used in Xi'an rainstorm intensity formula [12]. The rainstorm intensity of different return periods is calculated, corresponding to low, medium, and high, which are the three kinds of water volume. A_d , φ(0.9), and q are used in Equation (2) to calculate the design flow rate Q_1. According to the equation, $V = Q \times T$ obtains the inflow water when T = 60 min, and the outflow water procedure varies because the sizes of two sets are different. A test is conducted to simulate rain from start to end of the complete process, which involves "rises–summit–falling." The Chicago rainfall pattern is selected as the rain type [13].

$$Q_1 = \frac{A_d \times \varphi \times q}{10000} \quad , \tag{2}$$

where q indicates the rainstorm runoff intensity ($L \cdot s^{-1} \cdot ha^{-1}$), P indicates the return period, and t indicates the rainfall duration (min).

Monitoring and Analysis Method. The inflow, outflow, and overflow weirs are installed with level monitoring gauges (XMTJ3246R). Their record frequency is 1 s to determine the water volume after calculation. For single rainfall, the reduction rate of rainfall runoff volume of the bioswale is 100% when the rainfall is less than H(design rainfall). When the rainfall is greater than H, the reduction rate of the rainfall runoff volume is calculated using Equation (3), and the reduction rate of the peak flow is calculated using Equation (4).

$$\eta = \frac{V_{\text{inf } low} - V_{overflow}}{V_{\text{inf } low}} \times 100\% , \tag{3}$$

$$\gamma = \frac{Q_{in\ \max} - Q_{out\ \max}}{Q_{in\ \max}} \times 100\% , \tag{4}$$

where η indicates the runoff volume reduction rate, $V_{overflow}$ indicates the overflow water (m^3), and V_{inflow} indicates the inflow water (m^3). γ indicates the reduction rate of the peak flow, $Q_{in\ max}$ indicates the peak inflow (m^3), and $Q_{out\ max}$ indicates the peak overflow or outflow discharged from the bottom pipes (m^3).

The water cut of bioswales is closely related to the porosity of packing. The packing permeability coefficient is also an important content of the geological survey report in practical engineering design. Thus, the water cut test mainly inspects the composition of influence of the bioswale (media) on water cut, and the media porosity and permeability are estimated through the simple device and small experiment in the laboratory. The estimated results are presented in Table 2.

TABLE 2
Filter porosity and media permeability coefficient.

Medias	Porosity (%)	Medias	Permeability coefficient (m/d)
Gravel	43.5	SSH	1.21
Fly ash	37.3	BFS	1.35
BFS	44.6	FS	0.22
Sand	33.8	BFSS	1.20
Soil	43.3	Soil	0.50

Note: SSH is sand + soil + humus; BFS is blast furnace slag; FS is fly ash + sand, BFSS is blast furnace slag + sand.

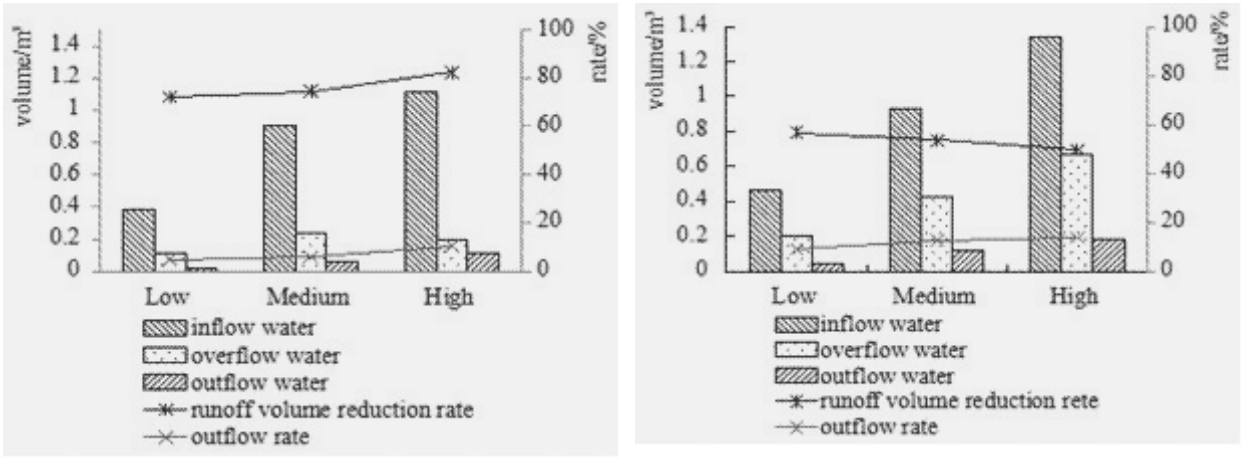

#4 #7

FIGURE 3
Reduction rate of the runoff volume and outflow rate of #4 and #7 bioswale.

RESULTS AND DISCUSSION

Influence of Inflow Water on Runoff Water and Peak Flow. This experiment selects the runoff volume in three return periods (0.5a, 2a, 5a) in combination with the design of the bioswale size to draw the corresponding low, medium, and high three hydraulic loads and to conclude the water cut effect of bioswales on different rainfall intensities, in which 10 bioswales have the same interval running time. The water test in the set height of submerged zone is conducted three times.

At different inflow waters, the following are the reduction rates of the runoff volume of each bioswale: #4 (flyash + sand), 72.19% to 82.38%; #6 (sand + soil + humus [SSH]), 83.79% to 99.99%; #7 (flyash + sand [FS]), 52.85% to 68.19%; #8 (blast furnace slag + sand [BFSS]), 41.27% to 65.14%; #9 (blast furnace slag [BFS]), 27.28% to 65.11%; #10 (soil), 41.92% to 44.29%; #W3 (BFSS), 25.3% to 58.96%; #W4 (FS), 27.51% to 50.55%; #E3 (soil), 28.09% to 56.12%; #E4 (BFS), 23.62% to 40.86%. Pan et al. [14] designed three typical runoff processes—small, medium, and heavy—to monitor the inflow and outflow process of bioretention units. The results showed that the runoff cut rate is between 12.83% and 48.12% by biological stranded pool, the average reduction rate of the flood peak is 70.85%, the flood peak delay time is approximately 26.6 min. The bioswale facilities in the present study have considerably better cutting rate than those in the study of Pan et al., possibly because the latter's device uses a large ratio of sand, thereby increasing permeability. Additionally, the latter's reduction rate of the total runoff volume is presented as the percentage of inflow water and outflow water. This observation indicates that the calculation in this experiment uses the percentage of inflow and overflow water. However, the outflow in most of the test grooves is larger than the overflow. Therefore, the runoff reduction rate varies. In different inflows, the outflow rate of #4 is lower than #7. All the

influencing factors are similar between #4 and #7, except that the bottom of #4 does not perform antiseepage treatment. However, #7 performs seepage controlling. This part of runoff seeping is directed into the ground, and the effect of conserving underground water when runoff water infiltrates the impervious bioswales is achieved (Fig. 3).

Under the condition of different inflow waters, all cells except #4 show that an increase in inflow water results in a decrease in the reduction rate of the overflow flood peak and in an increase in the reduction rate of the outflow flood peak. The delay time of the overflow flood peak shortens with an increase in feed water. All the cell delay times of the overflow flood peak range from 15 min to 30 min. The delay time of the discharge flood peak ranges from 25 min to 30 min. Sharkey's study showed that the outflow rate is 70% at the bottom, and the overflow rates are 11% and 19% through evapotranspiration losses when anaerobic areas are set [15]. In the traditional bioretention facility in which no seepage exists at the bottom, the losses of outflow, overflow, infiltration, and evaporation are 50%, 23%, 8%, and 19%, respectively. Bioretention facilities have more obvious volume reduction effect when anaerobic zone is increased than traditional biological stranded facilities. Based on the effects of algorithm height, the contrast between cut effect and flood peak lag time should be under the same algorithm, which is in a different matrix combination and the same inflow water.

Interval Time Influenced on Runoff Water and Peak Flow. The interval time for giving the packing a "break" or "buffer time" normalizes the packing from the saturation. Thus, the runoff reduction rate may be increased. In a confluence drainage system, the municipal drainage pipe deposition of wastewater pollutants in sunny days is the pollution source in the rainfall process. Therefore, an increase in the interval time between rainfall events increases the accumulated pollutants in a drainage system, thereby increasing rainfall runoff pollution load [16]. The accumulated pollutants also affect drainage capacity. In this study, two interval times are selected: 48 h between test 2 and test 1 and 96 h between test 3 and test 2.(Fig. 4).

Discrete rainfall events are identified if they are separated by a dry period greater than 6 h [17]. In this study, the shortest interval time is 48 h. The results of the field test on the storage and penetration of roofing rainwater through the rain garden show that the rain garden can effectively cut off and infiltrate runoff water when the loess in Xi'an area is chosen as the substrate [18]. This study concludes that most 0.5 m devices for the runoff and flood peak reduction rates decrease with an increase in interval time. For 1 m devices, the runoff reduction rate is shown in Fig. 5, which proves that the infiltration of performance is not restored after a three-day interval time in winter days through the analysis of the test results in three different interval times. The delay time of the overflow flood peak of most grooves is between 17 and 30 min. The delay time of the discharge flood peak is between 25 and 33 min. The retention time of #8 and #9 filter is more than 50 min. The delay time of the flood peak is no longer affected by an increase in interval time, which is probably affected by temperature.

Bioretention facilities are mainly used in processing light rain with high frequency and early occurrence of heavy rain events, which have a low frequency. If the capacity of rainwater reaches the limit, the excess is discharged through the overflow system. According to the experimental results, bioswales have a certain cutting effect on the high-frequency rainfall and flood retention effect.

Influence of Packing Types on Runoff Water and Peak Flow. The type of media in bioretention systems has an important role in influencing the quality of the treated run-off, and the plant soil in the local area varies considerably in terms of physicochemical properties, thereby resulting in variable hydraulic conductivity and effluent run-off quality [19]. This study chooses various artificial media in the test apparatus (Table1) . The permeability coefficient varies in different artificial packing. Thus, the reduction effect test of the runoff and flood peak flow influenced by packing types is conducted. We choose the medium volume as inflow water. Considering the pollutant purification effect in the previous experiment, each bioswale is equipped with different submerged heights (as shown in Table 1). We can choose the algorithm in the practical engineering to achieve effective purification ability by adjusting the outlet height of the perforated pipe. The experimental results are shown in Fig. 5.

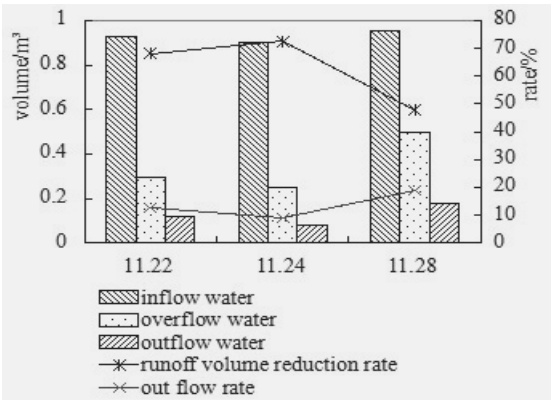

#7

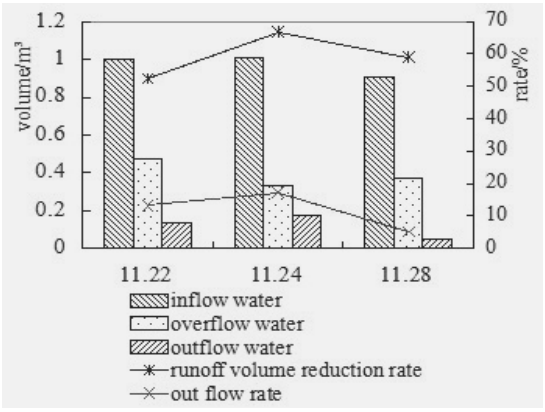

#8

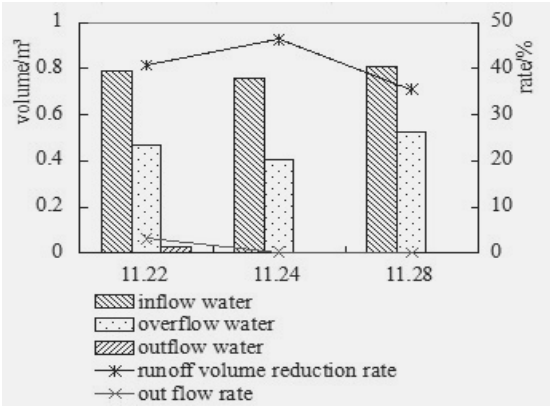

#9

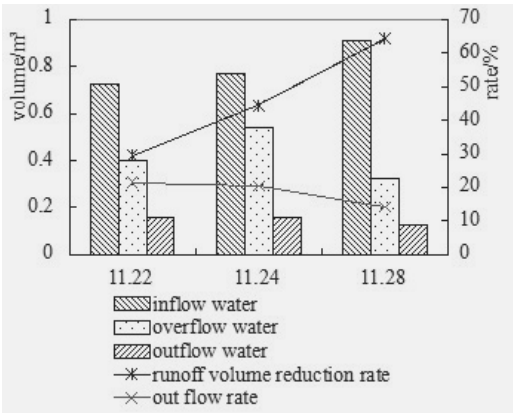

#10

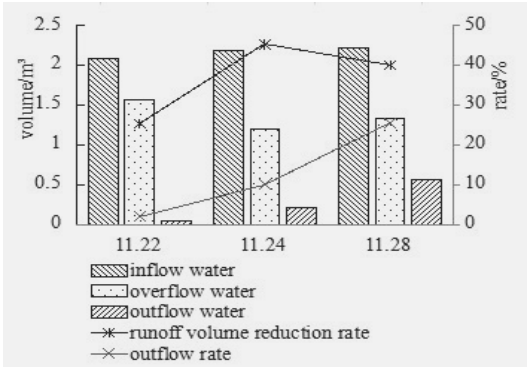

#West 3

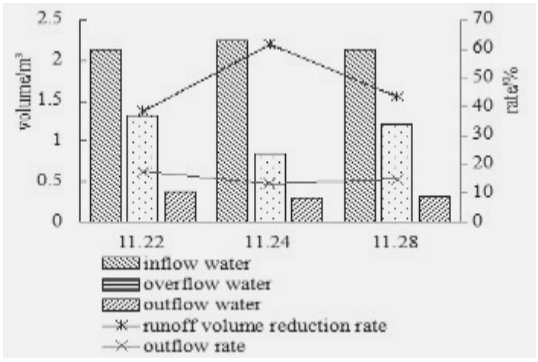

#West 4

FIGURE 4
Reduction rate of the runoff volume and outflow rate of the bioswale parts.

The function of packing types has a key role in bioretention systems. In the set submerged height cases, all bioswales have the same inflow water and different packing types. The order of peak flow cut rate and the cutting effect in different kinds of media are presented in this paper. The runoff volume reduction rate order for the 0.5 m test devices is as follows: SSH > soil > BFSS > FS > BFS. The runoff volume reduction rate order of 1 m test devices is as follows: FS > BFS > BFSS > soil. In engineering applications, if the main purpose of constructing bioswale facilities reduces the runoff volume, selecting media according to the runoff volume reduction rate orders is possible. The sequence of each 0.5 m bioswale outflow is as follows: SSH > FS > Soil > BFSS > BFS. The sequence of each 1 m bioswale outflow is as follows: BFSS > FS > Soil > BFS. The difference of the outflow rate is referred in 0.5 m bioswales if the main purpose for collecting rainwater is recycling. Manual packing can be selected according to the upper orders.

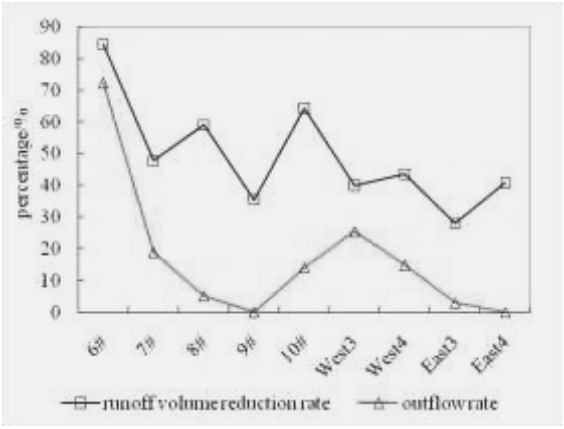

(a) Volume reduction rate

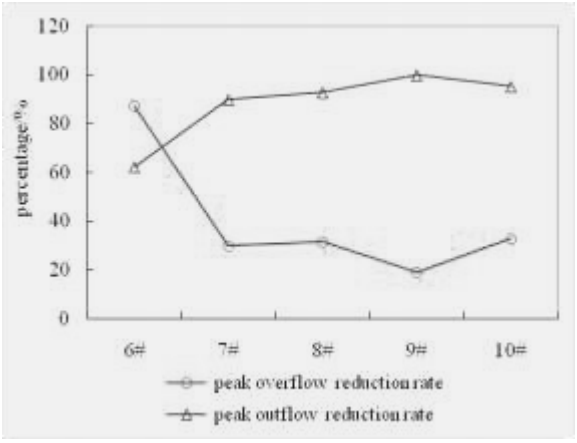

(b) Peak flow reduction rate

FIGURE 5
Volume and peak flow reduction rates of different packing types.

Effect–Factor Relationship Analysis. This study uses the curve analysis function of the SPSS software to establish the relationship between the cutting effect and four influencing factors that influence the bioswale water cut effect. These factors are inflow water, interval rainfall time, kinds of media, and submerged height.

In bioswale systems, the runoff reduction rate is 100% when the rainfall is less than the design runoff water for a single rain event. When the inlet water exceeds the design flow of bioswales, overflow occurs, causing bioswales to lose their ability to continue to delay and store storm water runoff. In addition, after precipitation enters the bioswale devices, saturated soil and layered packing distribute water first. Thus, the produced runoff exceeds the infiltration ability. Moreover, different interval rainfall time lead to different moisture contents in soil and all kinds of packing in the device. The longer the interval running time is, the more conducive it is to empty the device. At the same time, the longer the interval time is, the larger the evaporation capacity of the unit is. In bioswale facilities, different kinds of packing have a great impact on the runoff reduction effect. The size of the porosity has a direct relationship with the permeability of the packing, and permeability differences among all kinds of packing also cause differences in the runoff volume reduction rates. According to the principle of large specific surface area, high porosity belongs to porous inert carriers when choosing packing.

Multiple sets of test grooves are analyzed to determine the relationship between the influencing factors and runoff reduction and to obtain an accurate curve analysis of this relationship. After conducting the model summary and estimating the parameters, a series of models are obtained. The result shows that the relationship between runoff reduction and the main influencing factors of inflow water, interval operation time, and kinds of media indicates that R^2 is higher than 0.6. This observation indicates that the three influencing factors have a linear relationship with the reduction rate of the runoff volume.

Simulation of Reduction Rate by Models. Curve analysis indicates that the reduction rate and influencing factors have linear relationships, which affect the reduction rate of inflow water, interval time, and packing types. Thus, the regression equation between the reduction rate and various factors is solved with the stepwise regression model of linear analysis in the SPSS software. This study adopts two methods of stepwise regression model to simulate the effect of water reduction. The procedure is performed nine times, that is, three times for each condition (i.e., low, medium, and high water volumes). Six field test data are chosen to establish the model, including two tests from different water volumes as the first method. The remaining three field test data are used for the test. We set up the regression model as follows:

$$Y = a_0 + a_1X_1 + a_2X_2 + a_3X_3 + a_4X_4 + a_5X_5, \quad (5)$$

where Y indicates the water reduction rate, X_1 indicates the inflow water, X_2 indicates the interval running time, X_3 indicates the porosity, X_4 indicates the permeability coefficient, and X_5 indicates the

submerged zone height.

Simulation uses the stepwise enter method, whereas other options use the system default settings to obtain the output result of the preceding definition model. From R^2 of the model and the standard error of the estimate indicate that the R^2 value is high, which shows a good fitting degree of the common variable ratio and model and data. According to the regression coefficient of the model, constant, unstandardized regression coefficient values, and standardized regression coefficient are included, and the significance is tested. The regression equation is obtained from the following stepwise regression; (6)

The rest of the data are placed in the regression equation for inspection, and the predictive values are obtained. The measured results are compared with the predicted results, as shown in Fig. 6.

The model results are inspected with the deterministic coefficient (i.e., Ens, Nash–Sutcliffe simulation efficiency coefficient), when the measured values Q_0 equal the simulated values Q_P, Ens = 1. Ens is close to 1, which shows that the model efficiency is high. If Ens is negative, the credibility of the average values simulated by the models is lower than the credibility of the measured average values. The measured and predictive values are placed in the Nash–Sutcliffe coefficient calculation equation in the simulation. The obtained result is Ens = 0.86, and the inspection result is Ens = 0.74. The difference between the values calculated via the stepwise regression method and original data is small. The simulation results can accurately reflect the measured values. The result is analyzed based on the histogram and normal probability, and the result of the simulation results agree with the normal distribution, thereby showing a good credibility of the simulation values. Similarly, in method 2, nine field test data are chosen from each bioswale of #6, #7, #8, and #9, including three games from the small, medium, and large water. The data from #10 are used for the test, and the regression equation is (7)

$$Y = 270.93 - 0.015X_1 + 6.865X_2 - 5.321X_3 + 22.533X_4 - 0.023X_5, \quad (6)$$

$$Y = 285.404 - 0.016X_1 + 2.679X_2 - 5.616X_3 + 20.568X_4 - 0.032X_5. \quad (7)$$

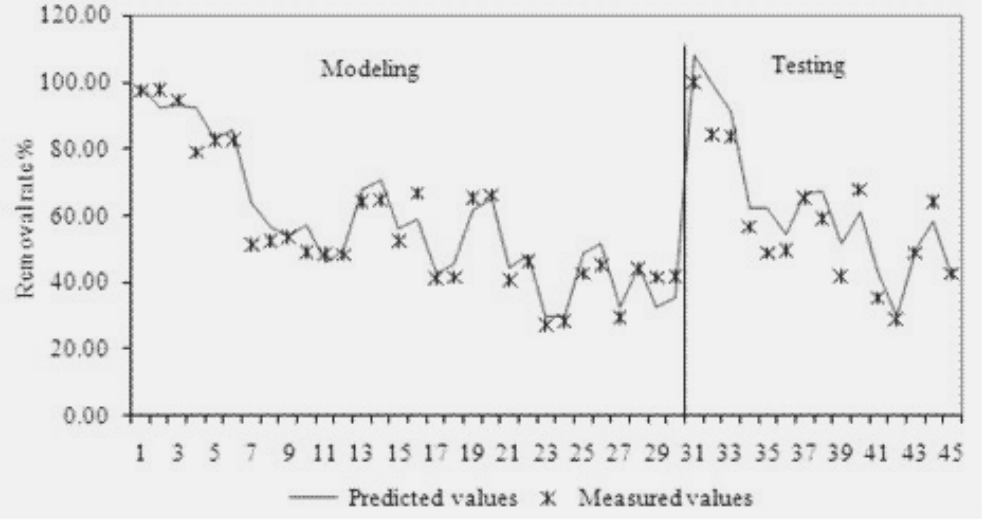

FIGURE 6

Measured and predicted comparison chart. In the simulation, two data from each of the small, medium, and high cases of water quantity are taken. Six field test data are used to establish model, and three residual field test data are taken from 12/19/ 2013 (small quantity), 11/28/2013 (medium quantity), and 12/30/2013 (high quantity) for testing.

The simulated results (Ens) in method 1 are greater than those in method 2 (i.e., the predictive and inspection results are 0.84 and 0.70, respectively) both in the simulation and test. Therefore, the credibility of the regression model calculated by method 1 is high, and the prediction results are accurate.

CONCLUSIONS

This study considered different inlet waters, interval running time, and packing types. Three main factors influence the running effect of bioswales on the runoff volume and reduction rate of the flood peak flow. The test shows that 0.5 m cells without seepage controlling results in a decrease of the runoff reduction rate with an increase in inlet water. The unit runoff reduction rate cannot increase with an increase in interval time, even though the trend of the runoff reduction rate declines. In actual engineering, to reduce the runoff volume, medias can be selected in the following order: SSH > soil > BFSS> FS >BFS. The delay time of the overflow flood peak of all the test grooves is between 15 and 30 min. The longest duration is approximately 20 min. Moreover, the curve analysis function of the SPSS software is used to establish the relationship between the factors and cutting effect. R^2 is higher than 0.6, which indicates that the three influencing factors have a linear relationship with the reduction rate of the runoff volume. In the future studies, we must consider long-term operation to investigate the effects on different seasonal temperatures. The actual rainfall process, including light to heavy rainfall events, to establish the relationship between the parameters of actual facilities and the cutting effect.

ACKNOWLEDGMENTS

This work was supported by the National Natural Science Foundation of China (nos. 51279158 and 51409211) and the Natural Science Foundation of Shaanxi Province (no. 2015JZ013).

REFERENCES

[1] Li, J. K., Liu, Z. C. Huang, N. J., Zhang, J. Y., Li, H. E., Shen, B. (2014) Advance in the Study on Bioretention Technology for Low-impact Development. Arid Zone Research,31(3),431-439.

[2] Baek, S.S., Choi, D.H., Jung, J.W., Yoon, K.S., Cho, K. H. (2015) Evaluation of a hydrology and run-off BMP model in SUSTAIN on a commercial area and a public park in South Korea. Desalination and Water Treatment, 55(2): 347-359.

[3] Singh, G., Kandasamy, J. (2009) Evaluating performance and effectiveness of water sensitive urban design. Desalination and Water Treatment, 11(1-3):144-150.

[4] Barco, J., Hogue, T., Curto, V., and Rademacher, L. (2008) Linking hydrology and stream geochemistry in urban fringe watersheds. Journal of Hydrology, 360(1-4), 31-47.

[5] Demir, V. and Bin-Shafique, S. Effect of the presence of phosphate based fertilizer on metal removal capacity of native bioretention materaials. Fresenius environmental bulletin, 2013, 22(1): 123-127.

[6] Davis, A. P. (2008) Field Performance of Bioretention: Hydrology Impacts. Journal of Hydrologic Engineering ,13(2):90-95.

[7] Hatt B. E., Fletcher T. D., Deletic A.(2009). Hydrologic and pollutant removal performance of stormwater biofiltration systems at the field scale. Journal of Hydrology, 365(3-4):310-321.

[8] Meng, Y. Y., Wang H. X., Zhang, S. H., Chen, J. G.(2013). Experiments on detention, retention and purifying effects of urban road runoff based on bioretention. Journal of Beijing Normal University(Natural Science), 49(2/3):286-291. (in Chinese)

[9] Wang, W. L. (2011). The experimental and application research about rainwater bioretention technology. Beijing:Beijing University of Civil Engineering and Architecture.(in Chinese)

[10] Wan, Q. X. (2010). Preliminary Research of Rain Garden Design. Beijing: Beijing Forestry University.(in Chinese)

[11] Xiang, L. L., Li, J. Q., Kuang, N., Che, W., Li, Y., Liu, X. D. (2008). Discussion on the design methods of rainwater garden. China Water & Wastewater.,34(6):47~51.(in Chinese)

[12] Lu, J. S., Chen, Y., Zheng, Q., Du, R., Wang, S. P., Wang, J. P. (2010). Derivation of rainstorm

intensity formula in Xi'an City. China Water & Wastewater, 26(17):82-84.(in Chinese)
[13] Cen, G. P., Shen J., Fan R.S.,(1998). Research on rainfall pattern of urban design storm. Advance in Water Sciences, 9(1):41-47. (in Chinese)
[14] Pan, G. Y., Xia, J., Zhang, X., Wang, H. P., Liu, E. M. (2012). Research on simulation test of hydrological effect of bioretention units. Water Resources and Power, 2012,30(5):13-15.(in Chinese)
[15] Sharkey L. J. (2006).The Performance of Bioretention Areas in North Carolina: A Study of Water Quality, Water Quantity, and Soil Media. North Carolina State University (BAE-NCSU).
[16] Chebbo G., Ashley R., Gromaire M. C.(2003). The nature and pollutant role of solids at the water-sediment interface in combined sewer networks. Water Science & Technology, 47(4):1-10.
[17] Liu, J.Y., and Davis, A. P. (2014). Phosphorous speciation and treatment using enhanced phosphorous removal bioretention. Environmental Science & Technology,48(1),607-614.
[18] Tang, S. C., Luo, W., Jia, Z. H., Yuan, H. C.(2012). Experimental study on infiltrating stormwater runoff with rain garden in Xi'an,China. Journal of soil and water conservation, 26(6):75-84. (in Chinese)
[19] Guo, H., Lim, F.Y., Zhang, Y., Lee, L.Y., Hu, J.Y., Ong, S.L., Yau,W.K., Ong, G.S. (2015) Soil column studies on the performance evaluation of engineered soil mixes for bioretention systems.Desalination and Water Treatment, 54(13):3661-3667.

Received: **01.09.2015**
Accepted: **14.03.2016**

CORRESPONDING AUTHOR

Li Jiake
State Key Laboratory Base of Eco-hydraulic Engineering in Arid Area
Xi'an University of Technology
No.5 Jinhua South Road, Xi'an, Shaanxi
710048 - CHINA

e-mail: xaut_ljk@163.com

© by PSP Volume 25 – No. 7/2016, pages 2484-2489 Fresenius Environmental Bulletin

ENVIRONMENTAL EFFECTS ON BIOLOGIC ACTIVITIES OF POLLEN SAMPLES OBTAINED FROM DIFFERENT PHYTOGEOGRAPHICAL REGIONS IN TURKEY

Zeliha Selamoglu[1*], Hasan Akgul[2], Hamide Dogan[1]

[1]Department of Biotechnology, Faculty of Arts and Science, Nigde University, 51240 Nigde, Turkey
[2]Department of Biology, Faculty of Arts and Science, Akdeniz University, 07070 Antalya, Turkey

ABSTRACT

Bee pollen is considered a health food with a wide range of therapeutic properties. This study aimed to determine the environmental effects on biologic activities of pollen samples obtained from eleven different environmental sources and geographical origins in Turkey (Artvin, Balikesir, Duzce, Edirne, Kahramanmaras, Mersin, Mugla, Nigde, Ordu, Sivas and Van). Pollen samples were kept at +4ºC until extracted. Total antioxidant status, total oxidant status and oxidative stress indexes in pollen samples extracted with specific methods were defined with *in vitro* analyses and results comparised. These characteristics of pollen were analysed by the most sensitive and reliable measurement kits developed newly. The highest total antioxidant capacity was observed (P<0.01) in pollen samples obtained from Artvin and Balikesir provinces. Total antioxidant capacities of pollen samples collected from different regions demonstrated differences because of different phytogeographic characteristics of regions in Turkey. Antioxidant properties of pollen depended on phenolic compounds that could change according to plant vegetation of pollen obtained from different regions.

KEYWORDS:
Antioxidant, *in vitro* analyses, Oxidant, Pollen, Turkey.

INTRODUCTION

Composition of bee pollen, can vary due to their botanical and geographic origin, contain carbohydrates, amino acids, proteins, lipids, vitamins, minerals, phenolic compounds, flavonoids, concentrations of phytosterols and are also rich in phytochemicals [1-4]. These compounds bear great significance not only for the activities of honeybees but also for consumer health due to their presence in the composition of honey. Pollens are also rich in flavonoid and phenolic compounds [5].

Bee pollen is considered a health food with a wide range of therapeutic properties, among which: antimicrobial, antifungal, antioxidant, anti-radiation, hepatoprotective and anti-inflammatory activities [6]. In addition, it has been determined to trigger beneficial effects in the prevention of prostate problems, arteriosclerosis, gastroenteritis, respiratory diseases, allergy desensitization, improving the cardiovascular and digestive systems, body immunity and delaying aging [7]. These therapeutic and protective effects have been related to the content of polyphenols [6].

Phytochemicals, such as phenolic compounds are considered beneficial for human health since they decrease the risk of degenerative diseases by reducing oxidative stress and inhibiting macromolecular oxidation. They have been shown to possess free radical-scavenging and metalchelating activity in addition to their reported anticarcinogenic properties [2]. Usually it contains vanillic acid, protocatechuic acid, gallic acid, p-coumaric acid, hesperidin, rutin, kaempferol, apigenin, luteolin, quercetin, isorhamnetin caffeic acid and naringenin [3,4]. This composition tends to be species-specific, and has been related to the therapeutic properties (antibiotic, antineoplasic, antidiarrhoeic and antioxidant) of pollen. It is known that the evaluations of the antioxidant activity in chemical or *in vitro* biological systems do not represent real activity [3,4,8,9].

Their antioxidant effects are largely related to their free radical scavenging activity. The composition, which varies with botanical origin, is at the same time responsible for a high level of antioxidant activity [5]. Recent studies have shown that flavonoids obtained from pollen of different geographical or botanical origin contain compounds with various nutritional relevance. The free radical reactions and scavenging capacities to reactive oxygen species of the pollen may be due to factors such as differences in atmospheric or environmental conditions, soil or physiology of plant [10,11]. Although we aimed to determined of total

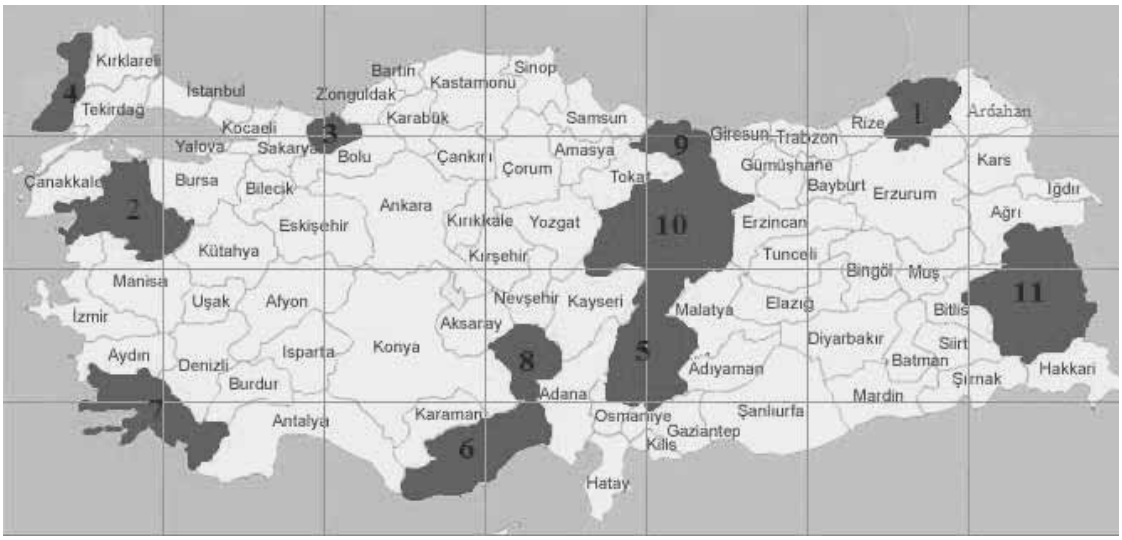

FIGURE 1
Locations of pollen samples collected from Turkey; 1. Artvin, 2. Balikesir, 3. Duzce, 4. Edirne, 5. Karamanmaras, 6. Mersin, 7. Mugla, 8. Nigde, 9. Ordu, 10. Sivas, 11. Van.

antioxidant status, total oxidant status and oxidative stress indexes of pollen samples obtained from different phytogeographical regions and environmental sources with *in vitro* analyses.

MATERIALS AND METHODS

Collection os pollen samples. Pollen samples were collected from eleven different locals (Artvin, Balikesir, Duzce, Edirne, Kahramanmaras, Mersin, Mugla, Nigde, Ordu, Sivas and Van) on seven regions of Turkey (Figure 1). These samples were gathered from beekeepers at different months in 2011, because of flowering and maturation of pollen show differences as depent on condition of ecological, geographical and climatic [12]. The samples were stored at 4^{o} C until analyses.

Preparation of pollen extraction. Pollen samples (5 g) were extracted 25 mL of 70% ethanol and these solutions were mixed until homogeneous. Extracts were homogenized in a sonicator (Selectra Ultrasons) at 15 min (Selectra Ultrasons). Obtained solutions were filtered (Whatman no 4 filter paper) and concentrated at 40^{o}C under reduced pressure in a rotary evaporator (Heildolph Heizbad HB Digit). Prepared extracts were stored until analyses [3,13].

Biochemical analyses. Total antioxdant status (TAS). TAS were evaluated using commercially available kits (Rel assay, Turkey). This method is founded on the whitening of characteristic color of a more stable ABTS (2,2′-Azino-bis (3-ethylbenzothiazoline-6-sulfonic acid)) radical cation by antioxidants. The assay has extreme sensitive data, which are lower than 3%. The results were expressed as mmol Trolox equivalent/L [14].

Total oxidant status (TOS). TOS were measured using commercially available kits (Relassay, Turkey). In the new method, oxidants present in the samples oxidized the ferrous ion-o-dianisidine complex to ferric ion. The oxidation reaction was enhanced by glycerol molecules abundantly present in the reaction medium. The ferric ion produced a colored complex with xylenol orange in an acidic medium. The color intensity, which could be measured spectrophotometrically, was related to the total amounts of oxidant molecules present in the sample. The assay was calibrated with hydrogen peroxide and the results were expressed in terms of micromolar hydrogen peroxide equivalent per liter (μmol H_2O_2 equivalent/L) [15].

Oxidative stress index (OSI). The oxidative stress index (OSI) was determined with the ratio of TOS to TAS. For calculation, the resulting unit of TAS was converted to μmol/L, and the OSI value was calculated according to the following Formula: OSI (arbitrary unit) = TOS (μmol H_2O_2 equivalent/L) / TAC (μmol Trolox equivalent/L) [16-18].

Statistical analysis. All data were analyzed by comparing means with one-way ANOVA method using SPSS software (Chicago, IL, USA; Version 16.0). The mean differences among the provinces

TABLE 1
The TAS, TOS and OSI values of pollen samples obtained from different regions.

Parameters / Locals	n	TAS (mmol Trolox Equiv. /L)	TOS (umol H_2O_2 Equiv./L)	OSI (TOS/TAS)
Artvin	5	3.81±0.030[a]	42.17±0.680[d]	1.11±0.023[d]
Balikesir	5	3.83±0.029[a]	38.94±0.417[e]	1.02±0.011[e]
Duzce	5	3.22±0.025[ef]	13.57±0.178[h]	0.42±0.007[h]
Edirne	5	3.25±0.025[def]	11.84±0.082[i]	0.36±0.003[i]
Kahramanmaras	5	3.19±0.023[f]	13.01±0.186[h]	0.41±0,008[h]
Mersin	5	3.29±0.018[de]	21.85±0.210[g]	0.66±0.006[g]
Mugla	5	3.56±0.031[c]	45.68±0.234[c]	1.28±0.011[c]
Nigde	5	3.04±0.001[g]	21.23±0.255[g]	0.70±0.008[g]
Ordu	5	3.25±0.047[def]	31.17±0.319[f]	0.96±0.019[f]
Sivas	5	3.66±0.029[b]	58.32±0.197[a]	1.59±0.015[a]
Van	5	3.34±0.052[d]	48.92±0.168[b]	1.46±0.026[b]
OVERALL	55	3.40±0.036	31.52±2.110	0.91±0.056

For each parameter, different letters in the same column represent statistically significant mean differences (P<0.01)

were compared with Duncan's multiple comparison test.

RESULTS

Total antioxidative status (TAS) of pollen samples. Total antioxidant capacities of pollen samples were determined using commercial kits. TAS values of analysed pollen samples are showed in table 1. Recent studies antioxidatnt properties of pollens obtained from different phytogeographical by honeybee indicated that pollens collected by bees generally show characteristic antioxidant data depending on to its botanical origin [7,9,19].

TAS values of pollen samples obtained from Artvin, Balikesir, Duzce, Edirne, Kahramanmaras, Mersin, Mugla, Nigde, Ordu, Sivas and Van regions were determined as respectively 3.81±0.030, 3.83±0.029, 3.22±0.025, 3.25±0.025, 3.19±0.023, 3.29±0.018, 3.56±0.031, 3.04±0.001, 3.25±0.047, 3.66±0.029 and 3.34±0.052 mmol Trolox Equiv./L. Compared to TAS data pollen samples collected from eleven different regions; pollen samples obtained from Artvin and Balikesir locals have statiscally significant the highest (P<0.01) TAS levels. Statiscally significant the lowest (P<0.01) TAS values were determined in pollen samples of Duzce, Edirne, Kahramanmaras, Mersin, Nigde and Ordu areas. Compared of TAS levels of pollen samples obtained from Mugla, Sivas and Van regions weren't observed statiscally significant a different (P>0.01).

Total oxidant status (TOS) of pollen samples. The investigation of TOS data of pollen samples obtained from different regions: TOS values of Pollen samples of Artvin, Balikesir, Duzce, Edirne, Kahramanmaras, Mersin, Mugla, Nigde, Ordu, Sivas and Van locals are respectively 42.17±0.680, 38.94±0.417, 13.57±0.178, 11.84±0.082, 13.01±0.186, 21.85±0.210, 45.68±0.234, 21.23±0.255, 31.17±0.319, 58.32±0.197 and 48.92±0.168 µmol H_2O_2 Equiv./L. The investigation of TOS values of pollen samples from eleven different regions: pollen samples of Sivas and Van areas are statiscally significant the highest (P<0.01) TOS data. Pollen samples procure from Duzce, Edirne and Kahramanmaras regions were determined to have statiscally significant the lowest (P<0.01) TOS values. Each other of pollen samples collected from Artvin, Balikesir and Mugla regions weren't observed statistically significant a difference in TOS values (P>0.01). A statiscally significant difference between TOS values of pollen samples from Mersin and Nigde weren't determined (P>0.01). TOS data of pollen sample taken from Ordu region is low according to oxidant status of pollen samples from Artvin, Balikesir and Mugla areas.

Oxidative stress index (OSI) of pollen samples. The OSI data of pollen samples obtained from Artvin, Balikesir, Duzce, Edirne, Kahramanmaras, Mersin, Mugla, Nigde, Ordu, Sivas and Van were determined as respectively 1.11±0.023, 1.02±0.011, 0.42±0.007, 0.36±0.003, 0.41±0.008, 0.66±0.006, 1.28±0.011, 0.70±0.008, 0.96±0.019, 1.59±0.015 and 1.46±0.026. Compared

to OSI data of pollen samples collected from eleven different regions were observed statistically significant the highest (P<0.01) OSI values in pollen samples of Sivas and Van areas and statistically significant the lowest (P<0.01) OSI levels in pollen samples Duzce, Edirne and Kahramanmaras. In OSI data pollen samples obtained from Artvin, Balikesir and Mugla regions weren't statistically significant a difference (P>0.01). OSI data of pollen samples of Artvin, Balikesir and Mugla are statistically significant lower than OSI data pollen samples Sivas and Van regions (P<0.01). OSI value of Ordu region's pollen is statistically significant lower than OSI values of Artvin, Balikesir and Mugla regions's (P<0.01). There weren't a statistically significant different (P>0.01) among pollen samples obtained from Mersin and Nigde. OSI data of pollens of Mersin and Nigde were statistically significant lower than OSI data of pollens of Artvin, Balikesir and Mugla (P<0.01).

DISCUSSION AND CONCLUSION

In the present study, TAS data of eleven pollen samples collected by honeybee from different phytogeographical locals of Turkey were in the range of 3.04±0.001 and 3.83±0.029 mmol Trolox Equivalent/L. In a study carried out by Cheng et al., when the concentration of sample ranged from 25 to 125 lg/mL, the percentage DPPH scavenging activity ranged from 7.68% to 87.94% and SCPE exhibited a dose dependent scavenging of DPPH radical in a measurement concentration range [3]. Carpes et al. determined antioxidant activities of the pollen samples extracted with 60, 70 and 80% of ethanol and did not present statistical significant difference between the extraction conditions [19]. The higher value for antioxidant activity index was 83.30% for the pollen from Alagoas state and 81.15% for Parana state pollen. The highest degree of antioxidant activity was found in the extraction at 60% of ethanol solution for Parana state pollen, which also showed the highest concentration of polyphenol compounds. In our study, we used to ethanol exract for determined to pollen samples's antioxidant capacities. Leja et al. [20] and Marghitas et al. [21] observed that there are differences the antioxidant capacities of pollen samples collected by honeybee from different plant species. These results show parallel with our results that TAS values of pollen samples collected from different locals are different. The monospecific mesquite honeybee pollen samples have reported a significant activity as inhibitors of lipid peroxidation in vivo systems and may contribute to exogenous defense against oxidative stress [8]. Previous studies on pollen samples's antioxidant capacities indicated that the presence of correlation between the organic compounds such as polyphenols and flavonoids and antioxidant activity and the species-specific flavonoid and phenolic acid contents and profiles play a significant role in determining the particular antioxidant capacity of pollen of different botanical origin [6,8,22,23].

TOS values of pollen samples provided from eleven different phytogeographical regions were determined as 11.84±0.082 to 58.32±0.197 µmol H_2O_2 Equiv./L and OSI (TOS/TAS) levels of pollen samples obtained from different locals were established as 0.36±0.003 to 1.59±0.015. OSI data of honeybee pollen samples obtained from Duzce and Kahramanmaras regions were lower than pollen samples's OSI data of other regions. Based on these results we said that antioxidant properties of pollen samples collected from these two locals are better than antioxidant properties of pollens of other locals.

We studied *in vitro* analyses could be use usefully to define the antioxidant properties of pollen samples. Which these analyses were tested with newly developed researching kits be capable of extremely reliable, sensitive, rapid and simple according to other methods.

In this study was determined to antioxidant capacities of pollen samples obtained different eleven locals and environments, they are different ecological and geographical structure, of Turkey. As a result of obtained data was demonstrated that the antioxidant capacities of pollen samples collected from different regions may vary as depending on phytogeographical, climatic and ecological feature of localities.

ACKNOWLEDGEMENTS

We thank to Scientific Research Project Found of Nigde University under the Project number (FEB 2011/24) for financial support of this work.

The authors declare that they have no conflict of interest.

REFERENCES

[1] Eraslan, G., Kanbur, M. and Silici, S. (2009a) Effect of carbaryl on some biochemical changes in rats: The ameliorative effect of bee pollen. Food and Chemical Toxicology, 47, 86–91.

[2] Morais, M., Moreira, L., Feas, X. and Estevinho, L.M. (2011) Honeybee-collected pollen from five Portuguese Natural Parks: Palynological origin,

phenolic content, antioxidant properties and antimicrobial activity. Food and Chemical Toxicology, 49, 1096–1101.

[3] Cheng, N., Ren, N., Gao, H., Lei, X., Zheng, J. and Cao, W. (2013) Antioxidant and hepatoprotective effects of Schisandra chinensis pollen extract on CCl4-induced acute liver damage in mice. Food and Chemical Toxicology, 55, 234–240.

[4] Kandiel, M.M.M., El-Asely, A., Radwan, H.A. and Abbass, A.A. (2014) Modulation of genotoxicity and endocrine disruptive effects of malathion by dietary honeybee pollen and propolis in Nile tilapia (Oreochromis niloticus). Journal of Advertising Research, 5(6), 671-684.

[5] Eraslan, G., Kanbur, M., Silici, S., Liman, B.C., Altınordulu, S. and Sarıca, Z.S. (2009b) Evaluation of protective effect of bee pollen against propoxur toxicity in rat. Ecotoxicology and Environmental Safety, 72, 931–937.

[6] Pascoal, A., Rodrigues, S., Teixeira, A., Feas, X. and Estevinho, L.M. (2014) Biological activities of commercial bee pollens: Antimicrobial, antimutagenic, antioxidant and anti-inflammatory. Food and Chemical Toxicology, 63, 233–239.

[7] Estevinho, L.M., Rodrigues, S., Pereira, A.P. and Feas, X. (2012) Portuguese bee pollen: palynological study nutritional and microbiological evaluation. International Journal of Food Science and Technology, 47, 429–435.

[8] Almaraz-Abarca, N., Campos, M.G., Avila-Reyes, J.A., Naranjo-Jimenez, N., Corral, J.H. and Gonzalez-Valdez, L.S. (2007) Antioxidant activity of polyphenolic extract of monofloral honeybee collected pollen from mesquite (Prosopis juliflora, Leguminosae). Journal of Food Composition and Analysis, 20, 119–124.

[9] LeBlanc, B.W., Davis, O.K., Boue, S., DeLucca, A. and Deeby, T. (2009) Antioxidant activity of Sonoran Desert bee pollen. Food Chemistry, 115, 1299–1305.

[10] Silva, T.M.S., Camara, C.A., Lins, A.C.S., Barbosa-Filhoa, J.M., Silva, E.M.S., Freitas, B.M., and Santos, F.A.R. (2006) Chemical composition and free radical scavenging activity of pollen loads from stingless bee Melipona subnitida Ducke. Journal Of Food Composition And Analysis, 19, 507–511.

[11] Saric, A., Balog, T., Sobocanec, S., Kusic, B., Sverko, V., Rusak, G., Likic,S., Bubalo, D., Pinto, B., Reali, D. and Marotti, T. (2009) Antioxidant effects of flavonoid from Croatian Cystus incanus L. rich bee pollen. Food and Chemical Toxicology, 47, 547–554.

[12] Akyol, E. and Kaftanoglu O. (2001) Colony characteristics and the performance of Caucasian (Apis mellifera caucasica) and Mugla (Apis mellifera anatoliaca) bees and their reciprocal crosses. Journal of Apicultural Research, 40, 3-4.

[13] Qin, F., and Sun, H.X. (2005) Immunosuppressive activity of Pollen Typhae ethanol extract on the immune responses in mice. Journal of Ethnopharmacology, 102, 424–429.

[14] Erel, O. (2004) A novel automated direct measurement method for total antioxidant capacity using a new generation, more stable ABTS radicalcation. Clinical Biochemistry, 37, 277-85.

[15] Erel, O. (2005) A new automated colorimetric method for measuringtotal oxidant status. Clinical Biochemistry, 38, 1103-11.

[16] Harma, M., Harma, M. and Erel, O. (2003) Increased oxidative stress in patients with hydatidiform mole. Swiss Medical Weekly, 133, 563-536.

[17] Kosecik, M., Erel, O., Sevinc, E. and Selek, S. (2005) Increased oxidative stress in children exposed to passive smoking. International Journal of Cardiology, 100, 61–4.

[18] Yumru, M., Savas, H.A., Kalenderoglu, A., Bulut, M., Celik, H. and Erel, O. (2009) Oxidative imbalance in bipolar disorder subtypes: a comparative study. Prog Neuropsychopharmacology Biol Psychiatry Aug 31, 33(6), 1070-4.

[19] Carpes, S.T., Begnini, R., Alencar, S.M. and Masson, M.L. (2007) Study of preparatıons of bee pollen extracts, antioxidantand antibacterial activity. Ciência Agrotecnology Lavras, 31(6), 1818-1825.

[20] Leja, M., Mareczek, A., Wyzgolik, G., Klepacz-Baniak, J. and Czekonska, K. (2007) Antioxidative properties of bee pollen in selected plant species Food Chemistry, 100, 237–240.

[21] Marghitas, L.A., Stanciu, O.G., Dezmirean, D.S., Bobis, O., Popescu, O., Bogdanov, S. And Campos, M.G. (2009) In vitro antioxidant capacity of honeybee-collected pollen of selected floral origin harvested from Romania. Food Chemistry, 115, 878–883.

[22] Campos, M.G., Webby, R.F., Markham, K.R., Mitchell, K.A. and Cunha, A.P.

(2003) Age-induced diminution of free radical scavenging capacity in bee pollens and the contribution of constituent flavonoids. Journal of Agricultural And Food Chemistry, 51, 742–745.

[23] Almaraz-Abarca, N., Campos, M.G., Avila-Reyes, J.A., Naranjo-Jimenez, N., Herrera-Corral, J. and Gonzalez-Valdez, L.S. (2004) Variability of antioxidant activity among honeybee-collected pollen of different botanical origin. Interciencia, 29, 574–578.

Received: **21.10.2015**
Accepted: **18.02.2016**

CORRESPONDING AUTHOR

Zeliha Selamoglu
Department of Biotechnology,
Faculty of Arts and Science
Nigde University
51240 Nigde – TURKEY

e-mail: zselamoglu@nigde.edu.tr

© by PSP Volume 25 – No. 7/2016, pages 2490-2499 Fresenius Environmental Bulletin

INFLUENCE OF HEAT GENERATED FROM GARBAGE COMPOSTING ON SLUDGE ANAEROBIC DIGESTION PERFORMANCE

Qi-wu Jie [1,2], Yi-yong Luo [3], Zheng-song Wu [1,2,*], Qiang He [1,2], Xue-bin Hu [1,2], Yan-ting Li[1,2], Shao-jie Wang [1,2], Kun Zhong [1,2] , Wei Lu [4]

[1]Key Laboratory of Three Gorges Reservoir Region's Eco-Environment, Ministry of Education, Chongqing University, 400045, China
[2]National Centre for International Research of Low-carbon and Green Buildings, Chongqing University, 400045, China
[3]Southwest Municipal Engineering Design & Research Institute of China, 610081,China.
[4]Chengdu Drainage CO.,LTD., Chengdu, 610042, China

ABSTRACT

The influence of heat generated from garbage composting on the performance of sludge anaerobic digestion was studied in a self-designed TIDGTS (the integration of domestic garbage and town sludge) reactor with dosing rates of 20%, 25%, and 30%. Result shows that the heat generated from garbage composting provides sludge digestion with an appropriate mesophilic environment. When the environment temperature is 20–35 °C, the temperature in the garbage chamber and sludge chamber is 30–45 °C and 30–40 °C, respectively, during the entire reaction. The dosing rate of 25% is the optimum proportion for the reactor. Under normal conditions, the soluble chemical oxygen demand is 200–260mg/L, volatile fatty acids are 60–130 mg/L, and organic matter removal rate is 22.87%.The average gas production is 41.80L/d and the chemical oxygen demand of the effluent is 191.8–547.1mg/L, with an average of 363.182mg/L. Sludge anaerobic digestion in TIDGTS follows the Monod dynamic model, and the fitted curve results show that the correlation coefficient is 0.9167,0.9306, and 0.8992 when the dosing rate is 20%,25%, and 30%, respectively. These findings suggest a linear relationship.

KEYWORDS:
Sludge; Anaerobic digestion performance; Compost; Temperature

INTRODUCTION

The production of waste activated sludge has increased over the previous years because of the increasing number of waste water treatment plants and the requirements for more stringent effluent quality regulations [1].Given that sludge is always accompanied by organic pollutants, heavy metals, and pathogens, secondary pollution can occur if it is not treated appropriately with decrement stabilization and other resources [2-4].Anaerobic digestion is effective in odor removal, pathogen reduction, and energy recovery in the form of methane; thus, it is regarded as the main method for maintaining the stability and reclamation level of sludge [5].Heat is required in anaerobic digestion, mainly to raise the temperature for digesting incoming sludge, compensating losses through the sludge digester, and partly for piping between the heat source and the digester [6].Temperature is an important factor that affects anaerobic digestion [7-9]. Therefore, outer heat sources are chosen to maintain the temperature requirement in anaerobic digestion. Braguglia al. compared the performances of ultrasound (mechanical) and ozone (chemical) pretreatment in excess sludge semi-continuous digestion using a water bath heated at 37 °C [10]. To observe the effect of the thickening and digestion of sludge, Du and Liu et al. pumped sludge to incorporate sludge thickening into digestion reaction after heating sludge to 38–40 °C using an electronic heater in a sludge allocated box [11]. After studying the pretreatment mechanisms during the thermophilic–mesophilic temperature phase of primary sludge anaerobic digestion, Ge et al. used temperature-controlled water jackets to maintain temperature during pretreatment stages and submerged electrical heating elements during the primary methanogenic stages [12]. Shao et al. studied enhanced anaerobic digestion and sludge dewatering capability through alkaline pretreatment and its mechanism of placing the digestion reactor in an incubator at (37.0±0.1)°C [13]. Qiao et al. researched up-flow anaerobic sludge blanket reactors and biogas production from supernatant hydrothermally treated sludge in cities by placing samples in an oil bath [14]. A large amount of heat is generated during the process of garbage aerobic composting [15-17]. The authors took advantage of the heat generated through composting to obtain the temperature requirement for anaerobic digestion stages. They designed an integrated reactor for sludge thickening and digestion, and then transferred heat from garbage aerobic composting

TABLE 1
Characteristics of the garbage used in the study.

Parameter	Value	Parameter	Value
Moisture content	0.75–0.8	VS/TS (mg/L)	0.92–0.4

TABLE2
Characteristics of the waste-activated sludge used in the study.

Parameters	Value	Parameters	Value
pH	6.86–8.38	VFA (mg/L)	68.6–188.7
Alkalinity(mg/L)	166.56–947.31	Moisture content	0.96–0.99
SCOD (mg/L)	48.1–130.3	VS/TS (mg/L)	0.29–0.42

to anaerobic digestion, which maintains a stable temperature in the reactor.

MATERIALS AND METHODS

Reactor introduction. Sludge thickening and digestion reaction [18] are combined with composting in a TIDGTS(the integration of domestic garbage and town sludge)reactor [19]. TIDGTS consists of two parts: 1) a 600L garbage aerobic composting reactor, called the garbage composting chamber; and 2) a 110L sludge thickening and digestion chamber, which is surrounded by the garbage composting chamber and provides an area for sludge thickening and digestion. The latter is divided into a 56L external reaction chamber, a 25L inner chamber, a 6L sludge thickening chamber, a 20L settling region, and a 3L gas collection region.

Substrate. The sludge used in this experiment was collected from a mud-storage basin in a sewage treatment plant. The garbage, which was collected from a waste transfer station in a university, was manually sorted kitchen garbage. The characteristics of the sludge and garbage are shown in Tables 1 and 2, respectively.

Experimental principle and process. The heat generated from garbage aerobic composting was used to provide a comfortable and stable temperature to the environment for the thickening and digestion of sludge. The selected garbage was added to the garbage composting chamber from the inlet throat at the top of the chamber. An aeration process was then performed via an aeration pump. Afterward, the garbage leachate was discharged from the bottom of the garbage composting chamber. Furthermore, fresh garbage was added to the chamber every few days to stabilize temperature.

The residual sludge was guided to the allocated box and allowed to flow into the external reaction chamber through the control valve with the help of gravity. It then began to thicken at the bottom of external reaction chamber. Afterward, the condensed sludge entered the inner chamber through the digestion reaction via a hole. Finally, the digested sludge was discharged from the bottom of the reactor. The biogas produced in the sludge digestion process was exhausted outside the reactor after being measured with a scrubbing bottle and a wet-type gas flow meter. Moreover, the top of the external reaction chamber was connected to a measuring tank, which was used to measure supernatant volume. The experiment is illustrated in Figure 1.

Start-up and operation. Seed sludge (50L) was added into the sludge chamber, and 10L fresh sludge was added daily until the amount of sludge reached the set limitation. A small amount of biogas is present in the reactor at that moment. Thus, the bacteria contained in sludge reacted under an anaerobic condition. Fresh sludge (14L) was mixed at the rate of 12.5% and put into the reactor to maintain a low-load treatment environment. Considering solids retention time (SRT), the system simply exhausted water instead of sludge during the early stage of the start-up process. When the solid sludge reached the supernatant, the digested sludge began to be exhausted according to the moisture content of the added and discharged sludge. Consequently, a balanced environment of sludge concentration is maintained. During the aforementioned processes, biogas and digested sludge were carefully observed and continuously tested. The start-up process can be judged as a success when the system satisfies the following standard requirements. 1) Biogas is produced stably. 2) Parameters such as pH, alkalinity, and volatile fatty acids (VFA) remain at a normal level. 3) A considerable reduction in the dosing rate of organic matter in the digested sludge is achieved.

The digested degree of sludge was observed under fresh sludge dosing rates of 20%, 25%, and 30% after the reactor started up and operated stably.

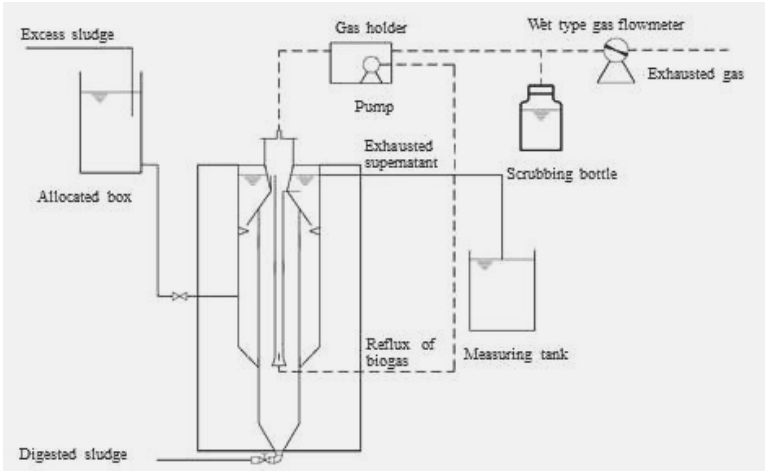

FIGURE 1
Flow diagram of the experiment.

Chemical analysis. Temperature was measured using a temperature control meter (XTA-7000). Moreover, the concentrations of volatile solids (VS) and total solids (TS) were determined through the drying method at the temperature of 103–105 °C and 600 °C, respectively. Meanwhile, pH was measured through ZD-2 auto potential titration. The concentrations of VFA were determined through the distillation method. Chemical oxygen demand (COD) was measured according to Chinese standards (the oxidation method with potassium dichromate). In addition, biogas amount was measured using a wet-type gas flow meter.

Calculation. Calculating VS/TS. The dosing rate of organic matter in dry sludge, namely, VS/TS, can be defined asω(Eq.1):

$$\omega = \frac{m_2 - m_3}{m_2 - m_1} \times 100\% \quad (1)$$

where m_2 is the total mass of the crucible and the sludge sample after a drying process (g), m_3 is the total mass of the crucible and the sludge sample after a firing process (g),and m_1 is the mass of the crucible (g).

Calculating VFA. The concentration of acetic acid is used to represent VFA (Eq.2) as follows:

$$\rho = \frac{c \times V_2 \times M \times 1000}{V_1 \times 0.7} \quad (2)$$

where c is the concentration of NaOH standard solution (mol/L), V_2 is the volume of NaOH standard solution used during the titration process (mL),and M is the molar mass of acetic acid (M=60.05).The correction factor is 0.7, assuming that only 70% VFA can be obtained from the distillate.

Mathematical analysis. The Monod dynamic model is applied. The correlation between effluent concentration and substrate degradation rate can be verified, and a fitted curve equation is calculated as follows:

$$\frac{1}{v} = \left(\frac{K_S}{v_{max}}\right)\frac{1}{S_e} + \frac{1}{v_{max}} \quad (3)$$

where v is the specific degrading rate of the substrate, S_e is the COD concentration of the effluent, and K_s is the saturation of the substrate. Data fitting and modeling parameters were solved using Origin 8.0.

RESULTS

Effect of temperature on the sludge thickening and digestion chamber. The temperature variations of the reactor and the environment are shown in Figure 2.

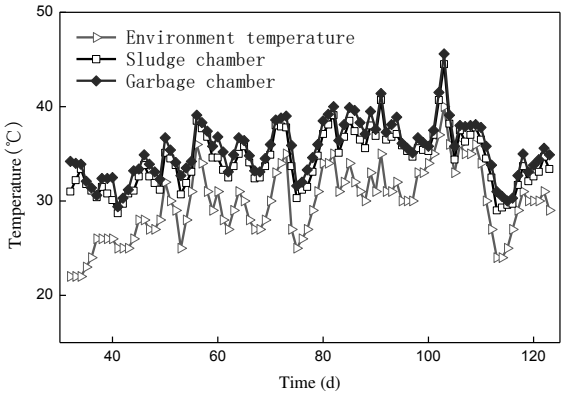

FIGURE 2
Temperature of the tanks and the environment with time

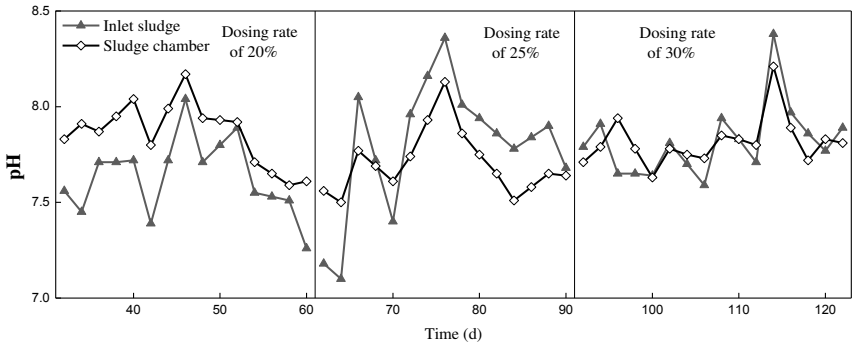

FIGURE 3
pH of the sludge with time.

As shown in Fig. 2, the temperature of the environment varied the most (from 20 °C to 35 °C) during the operating process in the reactor. The temperature in the garbage chamber is higher than that in the outside environment because of the heat produced by garbage composting, whose temperature remained stable at 30–45 °C. The sludge chamber had a similar temperature condition as the garbage chamber. Sludge anaerobic digestion can proceed smoothly at 30–40 °C.

pH variation in the sludge chamber. Appropriate pH is an important indicator of whether the reactor is operating in a stable condition. As shown in Fig. 3, pH varied under different operating conditions.

The figure shows that the pH of the inflowing sludge varied the most. It fluctuated substantially between 7.1–8.38. This phenomenon mainly resulted from the fact that inflowing sludge was collected directly from the mud pool of the sewage plant. However, the time during which the sewage plant exhausted the excess sludge was not fixed and resulted in differences in the properties of the samples. Moreover, although pH fluctuation was observed in the inner chamber, the amplitude of variation was considerably narrower than the inflow under three different operating conditions. Although the pH values of some samples were above 8.0, those of most samples remained at 7.5–8.0. Thus, the reactor is capable of resisting impact load.

Variation of VS/TS. Organic mass content was indicated in VS/TS. The change curve of VS/TS in the inflow and the effluent (Figure 4) shows that organic mass in sludge tends to have a low content at the dosing rate of 20%. Organic mass content (VS/TS) was 0.3–0.5 most of the time, whereas the effluent was 0.24–0.28, which was lower than the inflow. VS/TS increased to 0.32–0.38 under the condition of a 25% sludge proportion and a stable VS/TS value of 0.25–0.27 in effluent. Furthermore, when the dosing rate was 30%, the VS/TS value of the inflow rose to 0.32–0.41, and that of the effluent reached 0.25–0.3. Organic mass removal rate was 18.87%, 22.87%, and 23.41% with the average VS/TS at the dosing rates of 20%, 25%, and 30%, respectively.

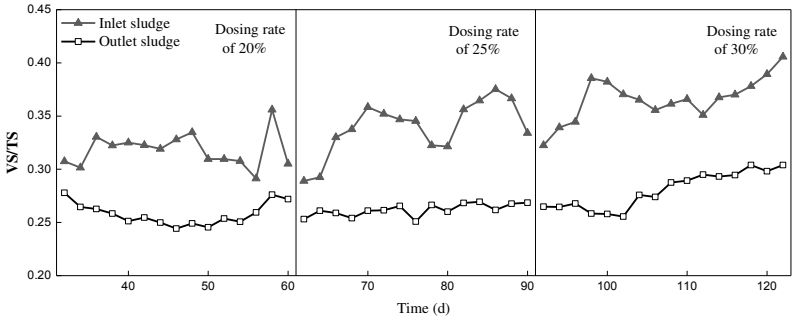

FIGURE 4
VS/TS of sludge with time.

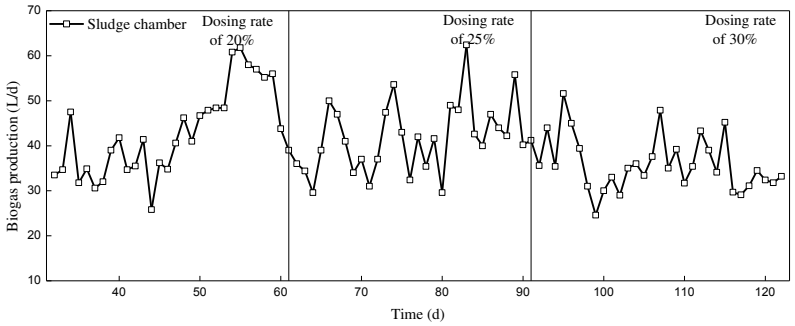

FIGURE 5
Volume of biogas with time.

Gas production. The variation in gas production in the sludge chamber is shown in Figure 5.During the experiment, gas production fluctuated wildly in the sludge chamber because of the fluctuation in temperature. When the dosing rates of sludge were 20%, 25%, and 30%, the average gas production were 42.96L/d (258.8m^{3}CH$_4$/t VS), 41.80L/d (201.9 m^{3}CH$_4$/t VS), and 35.91L/d (144.2 m^{3}CH$_4$/t VS), respectively.

COD of the effluent. The COD curve in the effluent of the supernatant from the sludge chamber is shown in Figure 6.At the dosing rates of 20%, 25%, and 30%, the COD in the supernatant of the sludge chamber were 156.7–207.2, 191.8–507.2, and 223.2–468.6mg/L. The average values were 268.8, 363.182, and 384.4 mg/L, respectively.

Intermediate products. Soluble COD (SCOD) and VFA are important intermediate products that indicate the effect of sludge hydrolysis in the sludge anaerobic digestion process. As a general rule, an increasing SCOD is beneficial to biogas yield during the treatment of sludge [20]. However, VFA yield is a significant indicator of the hydrolysis fermentation degree of organic mass [21].

Variation of SCOD. Figure 7 presents the SCOD variation curve under different dosing rates. The SCOD of inflow were in relatively low stages (less than 110mg/L) when the reactor was operated. It fluctuated between 150–250mg/L at the dosing rate of 20%. However, when the dosing rate was increased to 25%, SCOD reached 270mg/L during the sixth day. It decreased slowly in the following days, but the process was relatively stabilized when the minimum concentration reached 200mg/L. As dosing rate increased to 30%, SCOD fluctuated from 170mg/L to 200mg/L except in some individual points. These results are obviously less than those when the dosing rate is 20% in average probably because hydraulic retention time is shortened as reactor load increases.

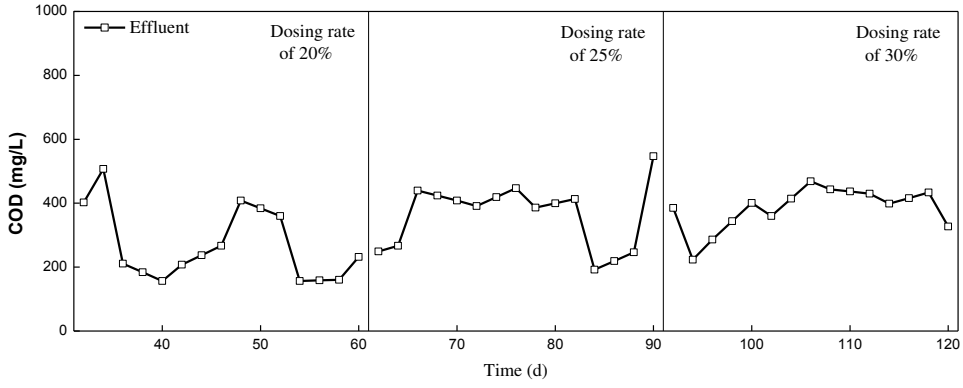

FIGURE 6
COD of the effluent with time.

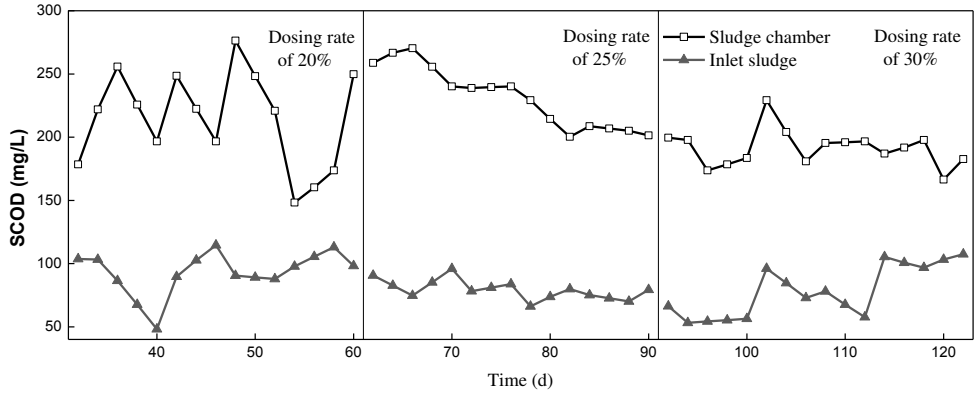

FIGURE 7
SCOD of the sludge with time.

Variation of VFA.
Figure 8 shows the variation of VFA in the inner chamber (the VFA of inflow was 70–200 mg/L). When the dosing rate was 20%, VFA fluctuated from 60 mg/L to 140 mg/L, which is low and stable compared with that of the inflow. When the dosing rate increased to 25%, VFA tended to increase gradually, but its overall level remained low at 60–130mg/L. Given that VFA did not accumulate during that time, the methanogens in the reactor were highly active. The VFA produced during the hydrolysis reaction process were decomposed rapidly by the methanogens. Thus, the process exhibited high gas production. When the dosing rate was 30%, the VFA concentration in the sludge chamber increased significantly until 381mg/L was reached. Although alkalinity decreased as VFA increased, the pH value did not obviously decrease because the pH value of inflow began as mildly alkaline and remained as such in the entire environment [22]. However, given the buffer action of alkalinity, the system consumed part of alkalinity to alleviate acidification. Thus, the pH value tended to be stable. In general, VFA tended to remain at a low stage and did not accumulate in the reactor at 20%and 25% dosing rates. Thus, the methanogens is reaction could be fully conducted compared with at a dosing rate of 30%.

DISCUSSION AND CONCLUSIONS

Discussion of the influence of heat generated from garbage composting on sludge anaerobic digestion performance. Temperature is a major influencing factor in sludge digestion. The aim of this study is to maintain an environment with a suitable temperature for sludge digestion using domestic garbage compost. Experiments showed that heat was better transmitted between the garbage chamber and the sludge chamber. In addition, the heat produced by garbage composting can compensate for the heat required in mesophilic

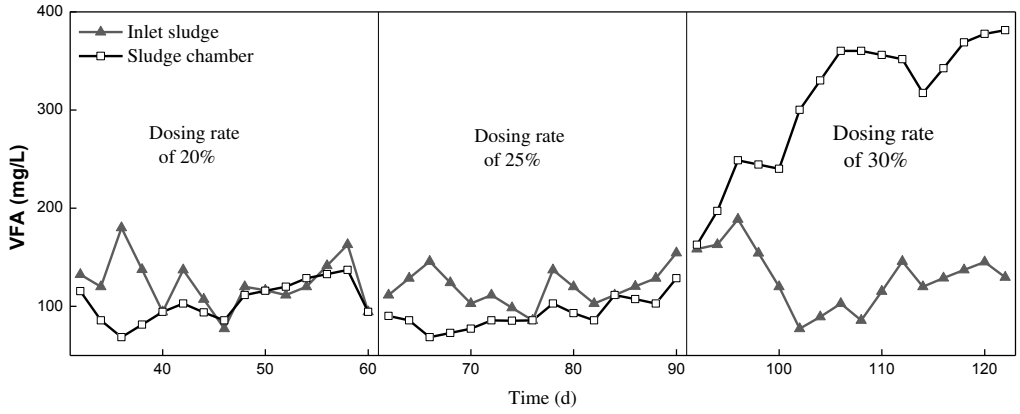

FIGURE 8
VFA of the sludge with time.

sludge digestion. Moreover, the garbage chamber functioned as a temperature buffer to the sludge chamber. It lessened the fluctuation of temperature in the sludge chamber to a certain degree, which benefited sludge digestion.

Under this temperature condition , organic mass removal rate was insufficiently high. However, according to the investigation of Saha et al. the disintegration of a pulp mill was only 9%–23% because the inflow had a low organic mass and sludge had low biodegradability [23]. Therefore, the dosing rates of 20% and 25% exhibited better effect than the 30% dosing rate. The increased volumetric loading contributed to gas loss. Under a high load condition, the products of hydrolytic acidification (e.g., VFA) could not be ingested in a timely manner by methanogens. Then, VFA began to accumulate when the alkalinity of the reactor was low. This event impaired the activity of methanogens, contributed to the inhibition of methanogenesis reaction, and finally led to a loss in gas production. According to Suvi Bayr studied in thermophilic anaerobic digestion of pulp and paper mill primary sludge and the co-digestion of primary and secondary sludge (210−230 m3 CH4/tVS). However, the result is considerably higher than that obtained by Jokela (45 m3CH4/t VS) [24-25].Therefore, dosing rate increased along with the average COD. Moreover, with the increasing high load, solid organic materials were transformed into small soluble molecular substances, which increased the COD in the effluent. Thus, insoluble organic molecules were discharged when they were not hydrolyzed completely, which contributed to the increase in COD as dosing rate increased (Figure 6).

The SCOD in the inner chamber was higher than the inflow under the three conditions in this study. Thus, the reactor can promote hydrolysis. When the dosing rate was 25%, SCOD was higher and stable compared with when the dosing rates were 20%and 30%. This result shows that hydrolysis reaction can occur efficiently and steadily, which may result in a high and stable gas production rate. Compared with the variation in SCOD (Figure 7), SCOD did not decline significantly when the dosing rate was 30% while VFA accumulated significantly. This result could be attributed to the inhibition of the methanogens is reaction or the VFA produced by acid-forming bacteria was not used by the methanogens in time, which also led to low gas production.

Discussion of Monod dynamics model. The method applied in the sludge chamber was anaerobic digestion, which is a complicated biochemical reaction process. Furthermore, organic matrix decomposition and biomass accumulation were conducted concurrently. This experiment, which was based on the Monod dynamic model, was performed to analyze the Kinetics of substrate degradation. The following assumptions were made.

①TIDGTS is operated under a steady state.

②The materials are fully mixed in the reactor. The concentrations of the materials are similar in all parts of the reactor.

③ Under anaerobic condition, organic matter removal follows the law of first order reaction kinetics.

According to the Monod fundamental equation and mass balance equation,

$$\frac{1}{\mathrm{v}} = \left(\frac{K_S}{\mathrm{v}_{\max}}\right)\frac{1}{S_e} + \frac{1}{\mathrm{v}_{\max}}$$

where v is the specific substrate degradation rate (d^{-1}), S_e is the concentration of COD in effluent (mg/L),and K_s is the substrate saturation concentration (mg/L). The fitting and model parameters were solved using Origin 8.0. According to the experimental results, the model was fitted with 1/v as dependent variables and $1/S_e$ as independent variables.

Figures 9, 10, and 11show that the correlation coefficient at dosing rates of 20%, 25%, and 30% were 0.9167, 0.9306, and 0.8992, respectively, which suggest a good linear dependence relation between 1/v and $1/S_e$. The variation of model parameters as K_s and v_{max} was presented in Table 3.The largest specific substrate degradation rate was increased as the dosing rate increased. When the dosing rate increased from 20% to 25%,v_{max} increased by 57.0%. However, it only increased by 17.7% when the dosing rate increased from 25% to 30%, which may be attributed to the enzyme reaction being the main process of organic matter degradation. Thus, while enzyme concentration remained within a certain range, the specific substrate degradation rate increased rapidly as the sludge dosing rate increased but slowly under a high dosing rate. Thus, 25% is a better dosing rate because it can reduce the volume of the reactor chamber while maintaining a high specific substrate degradation rate. The kinetic equation at the dosing rate of 25% is

$$\mathrm{v} = \frac{0.521S}{27042.6 + S}$$

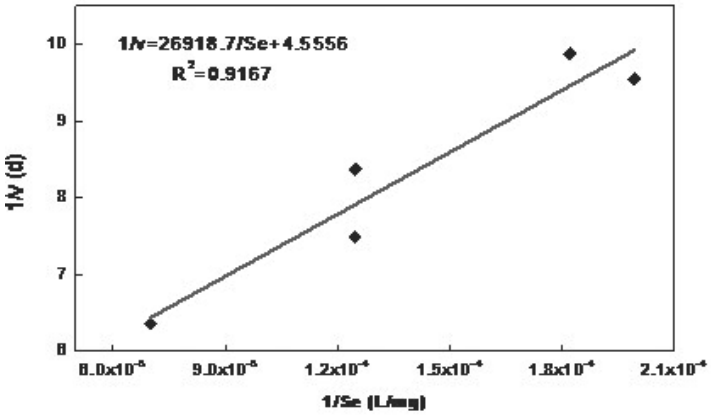

FIGURE 9
Solution of the kinetic parameters at a dosing rate of 20%.

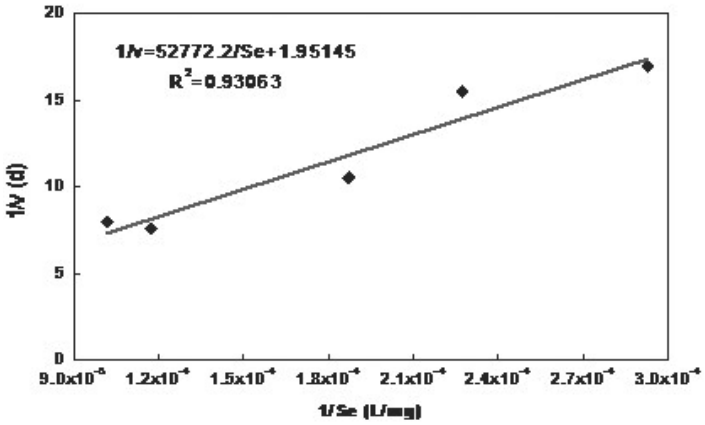

FIGURE 10
Solution of the kinetic parameters at a dosing rate of 25%.

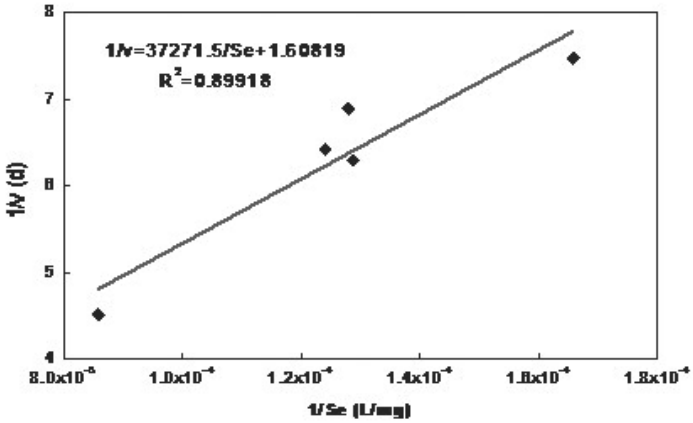

FIGURE 11
Solution of the kinetic parameters at a dosing rate of 30%.

TABLE3
Solution of the kinetic parameters.

Dosing Rate (%) / Parameter values	20	25	30
K_s (mg/L)	5908.9	27042.6	23176.0
v_{max} (d^{-1})	0.220	0.512	0.622

Conclusion. The heat generated from domestic garbage composting provided a good condition for moderate temperature sludge anaerobic digestion.

Sludge dosing rates of 20%, 25%, and 30% were observed to study anaerobic digestion in the reactor. The results show that the SCOD, VFA, and pH value of the chamber tended to remain stable at the dosing rates of 20% and 25%, which indicate good operation. When the dosing rate was increased to 30%, the alkalinity in the sludge chamber decreased as VFA increased sharply, which shows a certain tendency toward acidification. The optimal operating point was the dosing rate of 25%. During normal operation, SCOD and VFA were 200 mg/L and 60–130 mg/L, respectively. Moreover, the removal rate of organic matter was 22.87%. Gas production and the COD of the effluent were 41.80L/d and 363.18mg/L on average, respectively.

Monod dynamic models were built based on the result, and these models presented a significant correlation.

ACKNOWLEDGEMENTS

This work was financed by the Fundamental Research Funds for the Central Universities (106112014CDJZR210008), Major National Water Pollution Control and Management of Science and Technology Projects (2012ZX07307-001), and the 111.Project (No. B13041).

REFERENCES

[1] Carvajal, A., Peña, M. and Pérez-Elvira, S. (2013). Auto hydrolysis pretreatment of secondary sludge for anaerobic digestion. Biochemical Engineering Journal 75, 21-31.

[2] Cinar, S., Onay, T. T. and Erdincler, A. (2004). Co-disposal alternatives of various municipal wastewater treatment-plant sludges with refuse.Advances in Environmental Research, 8, 477–482.

[3] Dolgen, D., Alpaslan, M. N. and Delen N. (2007). Agricultural recycling of treatment-plant sludge: a case study for a vegetable-processing factory.Journal of Environmental Management, 84(3), 274-81.

[4] Wang, F. Y., Rudolph, V. and Zhu, Z. H. (2008). Sewage sludge technologies. Encyclopedia of Ecology, (1), 3227-3242.

[5] Pilli, S., Bhunia, P., Yan, S., LeBlanc, R. J., Tyagi, R. D. and Surampalli, R. Y. (2011). Ultrasonic pretreatment of sludge: a review. Ultrasonics sonochemistry, 18(1), 1-18.

[6] Zupančič, G. D. and Roš, M. (2003). Heat and energy requirements in thermophilic anaerobic sludge digestion. Renewable Energy, 28(14), 2255-2267.

[7] El-Mashad, H. M., Zeeman, G., Loon, W. K. P. V., Bot, G. P. A. and Lettinga, G. (2004). Effect of temperature and temperature fluctuation on thermophilic anaerobic digestion of cattle manure. Bioresource Technology, 95(2), 191–201.

[8] Appels, L., Baeyens, J., Degrève, J. and Dewil, R. (2008). Principles and potential of the anaerobic digestion of waste-activated sludge. Progress in Energy & Combustion Science, 34(6), 755–781.

[9] Müller JA. (2001). Prospects and problems of sludge pre-treatment processes. Water Science & Technology A Journal of the International Association on Water Pollution Research, 44.

[10] Braguglia, C. M., Gagliano, M. C. and Rossetti, S. (2012). High frequency ultrasound pretreatment for sludge anaerobic digestion: effect on floc structure and microbial population. Bioresource technology, 110, 43-49.

[11] Du, J., He, Q., Liu, H. X. and Yang, G. L. (2009). Study on startup experiment of sludge treatment by internal circulation thickening and digestion (ICSTD) reactor. Chinese Journal of Environmental Engineering, 8(3), 1429-1432.

[12] Ge, H., Jensen, P. D. and Batstone, D. J. (2010). Pre-treatment mechanisms during thermophilic–mesophilic temperature phased anaerobic digestion of primary sludge. Water research, 44(1), 123-130.

[13] Shao, L., Wang, X., Xu, H. and He, P. (2012). Enhanced anaerobic digestion and sludge dewaterability by alkaline pretreatment and its mechanism.Journal of Environmental Sciences, 24(10), 1731-1738.

[14] Qiao, W., Peng, C., Wang, W. and Zhang, Z. (2011). Biogas production from supernatant of hydrothermally treated municipal sludge by upflow anaerobic sludge blanket reactor. Bioresource technology, 102(21), 9904-9911.

[15] Gonzales, H. B., Sakashita, H., Nakano, Y., Nishijima, W. and Okada M. (2010). Food waste mineralization and accumulation in

biological solubilization and composting processes. Chemosphere, 79(2), 238–241.
[16] Karnchanawong, S. and Suriyanon, N. (2011). Household organic waste composting using bins with different types of passive aeration. Resources Conservation & Recycling, 55(5), 548–553.
[17] Elango, D., Thinakaran, N., Panneerselvam, P. and Sivanesan, S. (2009). Thermophilic composting of municipal solid waste. Applied Energy, 86(5), 663-668.
[18] Liu, H. (2009). Study on integration of sludge thickening and digestion reactor [J]. Chinese Journal of Environmental Engineering, 3(9), 1663-1666.
[19] Wu, Z., Zhi, Y., He, Q., Tang, S., Ling, J. and Pan, M. (2013). Development of integrated reactors for domestic garbage and town sludge. Journal of Chongqing University, 1, 022.
[20] Grönroos, A., Kyllönen, H., Korpijärvi, K., Pirkonen, P., Paavola, T., Jokela, J. and Rintala, J. (2005). Ultrasound assisted method to increase soluble chemical oxygen demand (SCOD) of sewage sludge for digestion.Ultrasonics Sonochemistry, 12(1), 115-120.
[21] Tan, R., Miyanaga, K., Uy, D. and Tanji, Y. (2012). Effect of heat-alkaline treatment as a pretreatment method on volatile fatty acid production and protein degradation in excess sludge, pure proteins and pure cultures [J].Bioresource Technology, 118,390–398.
[22] Banks, C. J. and Humphreys, P. N. (1998). The anaerobic treatment of a ligno-cellulosic substrate offering little natural pH buffering capacity. Water Science and Technology, 38(4), 29-35.
[23] Saha, M., Eskicioglu, C. and Marin, J. (2011). Microwave, ultrasonic and chemo-mechanical pretreatments for enhancing methane potential of pulp mill wastewater treatment sludge. Bioresource technology, 102(17), 7815-7826.
[24] Suvi Bayr, Jukka Rintala. Thermophilic anaerobic digestion of pulp and paper mill primary sludge and co-digestion of primary and secondary sludge [J].water research 46 (2012) 4713-4720.
[25] Jokela, J., Rintala, J., Oikari, A., Reinikainen, O., Mutka, K. and Nyrönen, T. (1997). Aerobic composting and anaerobic digestion of pulp and paper mill sludges. Water science and technology, 36(11), 181-188.

Received: **23.10.2015**
Accepted: **28.02.2016**

CORRESPONDING AUTHOR

Zheng-song Wu
Key Laboratory of Three Gorges Reservoir Region's Eco-Environment,
Ministry of Education,
Chongqing University, 400045, China

e-mail: zhswu2006@126.com

© by PSP Volume 25 – No. 7/2016, pages 2500-2508 Fresenius Environmental Bulletin

STUDY ON EFFECT OF POLLUTION ON GENOTOXIC DAMAGE IN CIRRHINUS MRIGALA AND CATLA CATLA FROM RIVER CHENAB

Bilal Hussain[*, 1], Tayyaba Sultana[1], Salma Sultana[1], Khalid A. AlGhanim[3], Shahid Mahboob[1, 3]

[1]Department of Zoology, Wildlife and Fisheries, Government College, University, Faisalabad, Pakistan.
[2]Department of Bioinformatics and Biotechnology, Govt. College, University, Faisalabad, Pakistan.
[3] Department of Zoology, College of Science, King Saud University, P. O. Box 2455, Riyadh, Saudi Arabia.
[4]Nuclear Institute for Agriculture and Biology, Faisalabad, Pakistan.

ABSTRACT

Comet and Micronucleus assays have been used to assess DNA damage in *Catla catla* and *Cirrhinus mrigala* procured from polluted sites of river Chenab. Heavy metals Cd, Cu, Mn. Zn, Pb, Cr, Sn and Hg were analyzed from water samples. All physicochemical parameters and heavy metals were observed beyond the permissible limits defined by various international agencies. Comet assay exhibited significant ($p<0.05$) DNA damage in *Catla catla* as 17.54±1.45, 12.05±1.55 and 11.25±1.01% DNA in the tail. Tail moment was 7.37±1.40, 4.70±0.76 and 7.60±0.97, Olive moment was 6.88±0.91, 4.24±0.62 and 5.79±0.59, respectively. Highly significant ($p<0.01$) damage was reported in *Cirrhinus mrigala* as 22.27±1.51%, 17.59±1.8% and 22.82±1.60% DNA in comet tail, tail moment was 13.20±1.60, 8.72±1.42 and 11.54±1.62, olive moment as 9.66±0.91, 7.15±0.80, 9.60±0.72 from selected polluted sites. Significant ($p<0.05$) differences were reported polluted and farmed fish. Micronucleus assay exhibited similar results for single and double micronucleus induction as 24.33±4.25, 2.44±0.66 in *Catla catla* and 45.22±3.80, 8.62±0.85/thousand cells, respectively in *Cirrhinus mrigala*. Nuclear abnormalities were found as 6.14±0.90 and 09.44±1.80/thousand cells, respectively in both species. These findings infer that these novel fish DNA damage assays to detect genotoxicity, could be used as an expedient toxicity screening of aquatic environments.

KEYWORDS:
DNA fragmentation, Biomarker, Indian major carps, genotoxicity

INTRODUCTION

Industrial development, expansion of urban populations and increased coverage of industrial, domestic water supply and sewerage give rise to larger quantities of municipal wastewater. Disposal of toxic sewage wastes with large volume of water could reduce biological oxygen demand to the lethal level by removing entire oxygen from the water body. Few toxic chemicals are released into the different water bodies in developing countries e.g., compounds of Hg, Zn, Pb and Cu etc. causing death of aquatic organisms even at very low concentrations. This can cause metabolic activation giving rise to toxic metabolites in the nervous tissues. Among the various sources of noxious aquatic pollutants are the pesticides, insecticides, and trace metals [1]. These toxic compounds reach water bodies as residues and their effects may persist for years or even more. Rivers and streams receive pollutants from agricultural, sewage and industry drainage systems that are designed to flow into the rivers [2]. Pollution from sewage, industrial effluents and agrochemicals produce various effects depending on the nature of the toxicity of these compounds and quantity of wastes washed down [3].

Aquatic organisms have an extensive role as a bioindicator to examine freshwater ecosystems for pollution. Variations in genome induced by genotoxic contaminants can cause mutations. DNA damaging agents require continuous monitoring and detection [4]. There is an urgency to evolve the molecular basis those can spot the influence of environmental contaminants for various aquatic organisms. [5] mentioned that a "micro-gel electrophoresis technique for detection of DNA damages in a single cell. [6] introduced same technique under alkaline pH >13 conditions for detecting DNA damage in individual cell, comet assay. This assay presents advantages in comparison of other genotoxicity assays, having sensitivity for detecting low levels of DNA damage

and requirement of a small number of cells per sample" [7].

The micronucleus (MN) test is another alternative promising and popular technique. This bioassay is a marker of cytogenetic damage induced by aneugenic or clastogenic compounds. Determination of cytogenetic changes considered as an important technique to monitor pollution threats if any to aquatic organisms [8]. Micronucleus bioassay was introduced for the application in mammals and now it was afterwards modified and applied in fish [9-10]. The objective of this research work was to use the comet assay and micronucleus tecchniques in *Catla catla* and *Cirrhinus mrigala* blood cells and to determine whether these assays are a dependable biomarker of DNA damages of water pollution in fishes from two different feeding niches.

MATERIALS AND METHODS

Fish were collected from the River Chenab in Pakistan, through its 190 km stretch of study area of Trimmu Head. The river Chenab in this stretch is polluted due to the discharge of untreated domestic and industrial waste into the River Chenab through the Chakbandi Drain at latitude 31.570º and longitude 72.534º. "Three sites viz. Wara Thatta Muhammad Shah (R1), Bela Reta (R2) and Bandimahni Beg (R3) were selected along the length of the River Chenab after receiving polluted water from Chakbandi Drain. Two sites Libhan Wala (U1) and Thali (U2) were selected as upstream sites before entering the drain into the River Chenab in Tehsil and District Jhang for comparison of wild fish". Dragnets and gill nets were used to catch the fish from the selected sites (R1, R2 and R3) of the river, as well as upstream of this area. Farmed fish supplied to the consumer having toxicants was designated as "positive control", and toxicant free was designated as controls. The weight of the sampled fish was varied from 500-880 g. Seven fishes were collected from each sampling site. "All the fish specimens were freshened out in running de-chlorinated tap water. Venous blood was collected from the caudal vein of each fish in heparin-coated tubes."

Preparation of fish samples. All the fish specimens were collected and shifted in plastic bags in the research laboratory. Fish samples were prepared by following method described by [11]. The tissue samples were then washed with distilled water and then cut into small pieces with a knife. The muscle sample was oven dried at 65 °C weight and dried samples were powdered with a help of glass mortar, and stored in airtight plastic vials inside desiccators.

Water analysis. "The selected heavy metals analyzed were tin (Sb), chromium (Cr), lead (Pb), zinc (Zn), manganese (Mn), copper (Cu), cadmium (Cd) and mercury (Hg). The concentration of each metal was detected by using heavy metal kits and according to [12] APHA (1998), using a Hitachi polarized Zeeman Atomic Absorption Spectrophotometer AAS, 2000 series. The blanks and calibration standard solution were also analyzed in the same way as for the samples. The instrument calibration standards were set using a diluting standard (1000 ppm) supplied by Merck, Germany. A known 1000 mg/l concentration of all the above mentioned metal solutions was prepared from their salts. All reagents used were of analytical grade. The percent recoveries in all the cases were within the acceptable limits of 70% to 120%, as per regulatory guidelines".

Comet Assay. Immediately after blood sampling, a small amount of blood (40 µL) was diluted with phosphate buffered saline and stored in ice. "The comet assay was performed on erythrocytes following the technique of [6] with slight modifications by [13]. Lysis: 1 h, at 4 °C, in a lysis buffer. DNA unwinding: 30 min, in the dark, in an electrophoresis buffer. Electrophoresis: 20 min, 300 mA, 25 V, and neutralization: three washes for 5 min each in buffer. Slides were fixed with absolute ethanol for 10 min and kept under refrigeration until cytological analyses. Slides were stained with ethidium bromide and analyzed under a fluorescent microscope. The length of DNA migration measured DNA damage, which was visually determined in 250 randomly selected cells as 50 per slide for each fish. DNA damage was by Comet Score V5 and classified into five classes based on the Comet tail length and DNA damage".

Micronucleus assay. "Fresh blood was smeared on the slides, which were then air-dried before being fixed in cold Corney fixative for 5 min. After fixing, the slides were stained in aqueous 10% Giemsa for 30 minutes. Five fishes were analyzed for a total of 25,000 erythrocytes/fish sample. The frequencies of micronuclei in the erythrocytes were detected using a binocular microscope under T1200x magnification. Erythrocytes with intact cellular and nuclear membranes were scored using the same criteria"

TABLE 1
Comparison of means of heavy metals selected chemical quality variables in the River Chenab (Means ± SE).

Sites	Cd mgL^{-1}	Cu mgL^{-1}	Mn mgL^{-1}	Zn mgL^{-1}
R1	0.137 ± 0.013C	0.905 ± 0.215E	01.57 ± 0.160C	00.217 ± 0.037E
R2	0.136 ± 0.015C	0.865 ± 0.214EF	01.55 ± 0.136C	00.209 ± 0.035F
R3	0.132 ± 0.012CD	0.820 ± 0.205F	01.39 ± 0.139D	00.206 ± 0.035F
	Pb mgL^{-1}	Cr mgL^{-1}	Sn mgL^{-1}	Hg mgL^{-1}
R1	1.602 ± 0.155C	0.351 ± 0.053D	0.307 ± 0.039D	0.993 ± 0.033BC
R2	1.350 ± 0.122D	0.291 ± 0.042E	0.275 ± 0.032DE	1.015 ± 0.018BC
R3	1.294 ± 0.123D	0.248 ± 0.033F	0.263 ± 0.032E	0.895 ± 0.014CD
	Phenols mgL^{-1}	Sulfates mgL^{-1}	BOD mgL^{-1}	COD mgL^{-1}
R1	01.65 ± 0.147E	266.81 ± 47.230D	71.66 ± 2.35F	148.45 ± 14.62F
R2	01.45 ± 0.123F	252.38 ± 48.276E	62.76 ± 1.86G	136.05 ± 12.42G
R3	01.35 ± 0.137G	247.05 ± 46.681E	51.89 ± 1.45H	125.09 ± 14.75G
	pH	TDS mgL^{-1}	Salinity mgL^{-1}	Conductivity mS/m
R1	10.32 ± 0.055CD	1595.714 ± 222.64E	1394.44 ± 155.21E	02.31 ± 0.341E
R2	10.14 ± 0.021D	1478.32 ± 222.22F	1252.05 ± 148.20F	02.17 ± 0.272F
R3	10.02 ± 0.046E	1216.47 ± 235.55G	923.55 ± 135.11G	01.72 ± 0.322G

"Means sharing the same letter in a row or in a column are statistically non-significant (P>0.05). R1-3; polluted experimental sites in the river, BOD; Biochemical Oxygen demand, COD; Chemical Oxygen demand".

"as in previous studies [14-15]. Nuclear abnormalities (NAs) in the erythrocytes were scored by following [16-17]".

Statistical analysis. A mean, standard error and analyses of variance (ANOVA) was worked out through SPSS 9 for PC. The means were compared by using Duncan's Multiple Range test. Probability values of $p<0.05$ were considered significant. TriTek Comet Score™ Freeware 1.6.1.13 software for image analysis by Tritek Corporation (2010) was used for DNA damage analysis.

RESULTS AND DISCUSSION

Water quality parameters analyzed showed an acute level of pollution load in the River Chenab (Table 1). The level of Cadmium, Copper, Manganese, Zinc, Lead, Chromium, Tin and mercury in the water samples collected in summer from different sampling sites of River Chenab were ranged as 0.132±0.012- 0.137±0.013, 0.820±0.20-0.905±0.21 ,1.39±0.139-1.57±0.160, 0.206-±0.035, 0.217±0.037, 1.294±0.123-1.602±0.155-,0.248±0.033-0.351±0.053, 0.263±0.032-0.307±0.039, 0.895±0.014-1.015±0.018 mg/L, respectively. Higher values of heavy metals were observed in winter that might be due to no dilution of river water in winter as in winter only

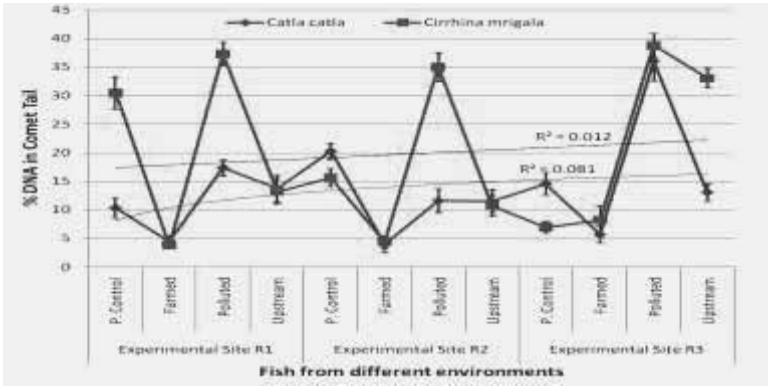

FIGURE 1
DNA damage (%) in *C. catla* and *C. mrigala*, type and site interactions.

TABLE 2
Comet assay for *C. catla* and Species, site and type interactions
Species and site interaction (means ±SE).

Sites	Comet Assay Components				
	Head Diameter (px)	*Tail Length (px)*	*DNA in Tail %*	*Tail Moment*	*Olive moment*
R1	112.61 ± 3.65	26.85 ± 2.75	11.25 ± 1.01	7.37 ± 1.40	6.88 ± 0.91
R2	94.62 ± 2.80	17.55 ± 1.51	12.05 ± 1.55	4.70 ± 0.76	4.24 ± 0.62
R3	83.55 ± 2.65	26.52 ± 2.22	17.54 ± 1.45	7.60 ± 0.97	5.79 ± 0.59
Mean	96.92 ± 3.03A	23.64 ± 1.70B	13.61 ± 1.08B	6.55 ± 1.04B	5.63 ± 0.69B
Species and type interaction (means ±SE)					
Control +ve	98.77 ± 3.55bc	27.22 ± 2.66bc	14.44 ± 1.52cd	7.33 ± 1.32bc	6.75 ± 0.78bc
Farmed	67.62 ± 2.22fg	4.35 ± 0.66e	5.57 ± 0.82e	0.56 ± 0.17d	1.22 ± 0.23d
Polluted	83.22 ± 3.25de	27.68 ± 2.22bc	22.77 ± 1.81b	9.55 ± 1.24bc	6.24 ± 0.66bc
Upstream	137.44 ± 4.21a	34.55 ± 3.25ab	11.90 ± 1.75d	8.76 ± 1.71bc	7.66 ± 1.25bc
Species, site and type interaction (means ±SE)					
R1 . +ve	118.55 ± 566cde	32.52 ± 5.44c-i	11.42 ± 1,75d-j	7.22 ± 2.31d-h	6.12 ± 1.280c-h
R1 . F	77.52 ± 3.92h-l	5.42 ± 1.66lmn	4.88 ± 1.28hij	0.42 ± 0.19h	0.98 ± 0.32gh
R1 . P	103.54 ± 8.52d-h	31.55 ± 5.44c-i	18.51 ± 2.54d-g	11.21 ± 2.55b-h	9.12 ± 1.77b-e
R1 . U	158.62 ± 7.22a	38.12 ± 7.51b-h	14.75 ± 2.49d-j	14.22 ± 3.98a-g	12.62 ± 2.88abc
R2 . +ve	71.82 ± 3.44j-m	24.77 ± 3.60e-l	21.28 ± 3.65cde	10.76 ± 2.50b-h	8.92 ± 1.62b-f
R2 . F	73.35 ± 2.77i-m	3.42 ± 0.868mn	4.22 ± 1.35j	0.62 ± 0.223h	0.97 ± 0.25gh
R2 . P	86.55 ± 4.55f-k	19.32 ± 2.28g-n	12.60 ± 2.19d-j	4.22 ± 0.82gh	4.18 ± 0.81e-h
R2 . U	143.82 ± 7.22abc	19.77 ± 3.21g-n	12.52 ± 4.22d-j	4.28 ± 1.22fgh	3.66 ± 0.52e-h
R3 . +ve	112.92 ± 6.77def	23.66 ± 2.80e-m	15.40 ± 1.75d-j	6.08 ± 1.62d-h	6.80 ± 1.22c-h
R3 . F	58.27 ± 1.71lmn	3.55 ± 0.66mn	6.57 ± 1.51g-j	0.78 ± 0.18h	2.28 ± 0.41gh
R3 . P	59.74 ± 3.55lmn	33.41 ± 2.56c-i	37.11 ± 4.16a	15.62 ± 1.99a-e	7.75 ± 0.64c-g
R3 . U	104.52 ± 4.66d-g	46.82 ± 5.77a-d	14.33 ± 2.44d-j	11.45 ± 2.70b-h	8.25 ± 1.72b-f

"Means sharing similar letter in a row or in a column are statistically non-significant (P>0.05). Small letters represent comparison among interaction means and capital letters are used for overall mean. S1-3; polluted Experimental sites in the River, Fish Types (F; farmed, P; polluted, U; upstream, +ve; positive control)".

drain water flow through the length of the river. Water dilution only happened in summer due to the rains and the water from the glaciers. However, concentrations of these metals were recorded substantially higher than the [18] permissible limits

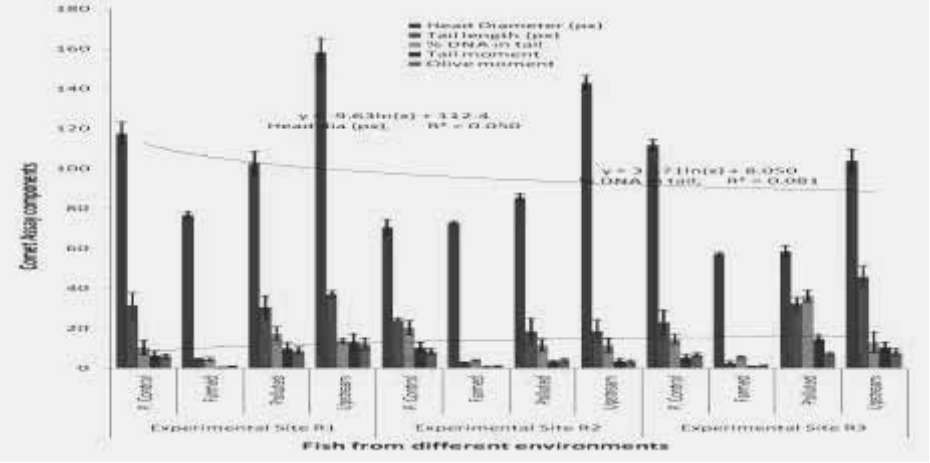

FIGURE 2
Comparative analyses of comet assay of blood from *C. catla* collected from different environments.

(Pb 0.0025, Cd 0.02, Cr 0.011, Zn 0.12 and Cu 0.009) and were more than enough to put adverse effects on the fish health. In this study water quality variables were observed faraway ahead the permissible limits (Table 1) and significant ($p<0.05$). summer due to the rains and the water from the glaciers. However, concentrations of the studied metals were recorded substantially higher than the [18] permissible limits (Pb 0.0025, Cd 0.02, Cr 0.011, Zn 0.12 and Cu 0.009) and were more than enough to put adverse effects on the fish health.

DNA damage in *Cirrhinus mrigala* was higher in polluted sites of the river (Figure 1). In Comet assay head diameter in *Catla catla* exhibited significant differences for sites R1, R2 and R3 and upstream indicating the damage but there was non-significant difference in fish procured from control and upstream.

TABLE 3
Comet assay results for *C. mrigala* and Species, site and type interactions Species and site interaction (means ±SE).

Sites	Comet Assay Components				
	Head Diameter (px)	*Tail Length (px)*	*DNA in Tail %*	*Tail Moment*	*Olive moment*
Site 1	90.88 ± 4.24	32.42 ± 2.66	22.27 ± 1.51	13.20 ± 1.60	09.66 ± 0.91
Site 2	78.32 ± 3.70	23.41 ± 2.70	17.59 ± 1.38	08.72 ± 1.42	07.15 ± 0.80
Site 3	91.87 ± 3.44	31.75 ± 2.27	22.82 ± 1.60	11.54 ± 1.62	09.60 ± 0.72
Mean	87.02 ± 2.791B	29.13 ± 2.104A	20.89 ± 1.05A	11.15 ± 1.14A	08.80 ± 0.52A
Species and type interaction (means ±SE)					
Control $^{+ve}$	109.70 ± 5.224b	36.52 ± 360	17.66 ± 1.53bcd	09.72 ± 1.46bc	07.92 ± 0.87bc
Farmed	52.31 ± 1.07h	02.20 ± 0.38e	05.45 ± 0.93e	00.57 ± 0.20d	01.22 ± 0.31d
Polluted	88.33 ± 3.08cd	41.41 ± 3.14a	37.01 ± 1.43a	19.19 ± 2.03a	13.68 ± 1.00a
Upstream	94.37 ± 4.05cd	33.79 ± 3.06ab	19.00 ± 1.52bc	10.86 ± 1.45b	09.32 ± 0.75b
Species, site and type interaction (means ±SE)					
R1 . +ve	148.62 ± 11.65ab	65.74 ± 6.24a	30.47 ± 2.85abc	23.12 ± 3.52a	16.40 ± 1.95a
R1 . F	51.86 ± 1.65lmn	01.32 ± 0.34n	03.81 ± 0.64j	00.12 ± 0.04h	00.65 ± 0.13h
R1 . P	104.02 ± 4.66def	50.34 ± 5.71abc	37.29 ± 2.51a	23.48 ± 3.90a	16.22 ± 2.04a
R1 . U	55.94 ± 4.35lmn	09.02 ± 1.75j-n	13.20 ± 2.18d-j	01.92 ± 0.39h	02.06 ± 0.38fgh
R2 . +ve	37.42 ± 2.84n	06.36 ± 1.23k-n	15.58 ± 2.55d-j	01.97 ± 0.59h	02.63 ± 0.44e-h
R2 . F	52.76 ± 2.06lmn	01.62 ± 0.44n	04.35 ± 1.08ij	00.28 ± 0.10h	00.79 ± 0.19gh
R2 . P	89.44 ± 6.53f-j	43.42 ± 6.61b-e	34.96 ± 2.53a	19.78 ± 4.26ah	13.83 ± 1.96ab
R2 . U	129.10 ± 7.22bcd	37.78 ± 5.83b-g	10.73 ± 1.80d-j	08.55 ± 2.34c-h	07.12 ± 1.42c-g
R3 . +ve	141.72 ± 4.76abc	35.12 ± 6.27b-h	06.93 ± 0.99f-j	04.06 ± 1.06e-h	04.72 ± 0.87d-h
R3 . F	52.32 ± 1.87lmn	03.66 ± 0.98lmn	08.19 ± 2.48e-j	01.31 ± 0.57h	02.23 ± 0.88fgh
R3 . P	71.54 ± 3.39i-m	30.48 ± 3.13c-i	38.80 ± 2.42a	14.30 ± 1.82a-f	10.99 ± 0.90a-d
R3 . U	98.08 ± 4.84e-i	54.56 ± 5.19ab	33.06 ± 2.66ab	22.12 ± 3.02a	17.22 ± 1.80a

"Means sharing similar letter in a row or in a column are statistically non-significant ($P>0.05$). Small letters represent comparison among interaction means and capital letters are used for overall mean. S1-3; polluted Experimental sites in the River, Fish Types (F; farmed, P; polluted, U; upstream, +ve; positive control"

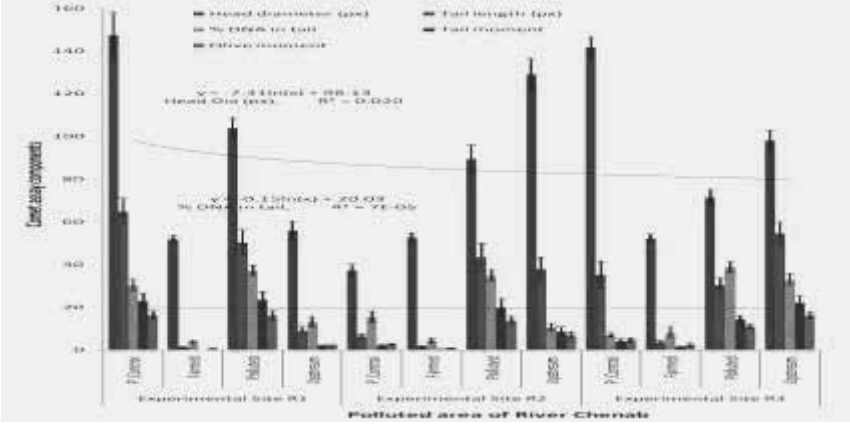

FIGURE 3
Comparative analyses of comet assay of blood from *C. mrigala* collected from different environments.

Significant differences in tail length were observed among *C. catla* collected from farmed, polluted and upstream sites except site R2. We observed significant differences for DNA in tail in fishes from site R1, farmed and polluted. Non-significant difference was observed in *C. catla* procured from commercial farm and upstream (Figure 2). Significant differences were noted for +ve control and all other types from site R2. Fish collected from the sampling site R3 exhibited significant differences for polluted and upstream, but differences remained non-significant among farmed and upstream as 5.57±0.63% and 14.44±1.52% (Table 2). Significant differences for tail moment in *C. catla* was noted only in fish collected from polluted and upstream sites. There was non-significant difference for tail moment in *C. catla* procured from farm and upstream. In case head diameter in *C. mrigala* blood collected from site R1 showed significant ($p<0.05$) differences (Figure 3). Similar results were noted for comet tail in comet assay in *C. mrigala* (Table 3).

Significant differences ($p<0.05$) were recoded for percentage DNA damage in tail of *C. mrigala* collected from fish farm and polluted site also fish procured from polluted and upstream sites. Non-significant differences were recorded in fish collected from control and upstream. Fish collected from fish farm and upstream exhibited non-significant ($p>0.05$) differences in pollution load. Significant differences exhibited in fishes collected from site R2 but differences remained non-significant between farmed

TABLE 4
Correlation matrix for comet assay results of Blood from *C. mrigala*.

	Catla catla					*Cirrhinus* ***mrigala***				
	T. DNA	**Type**	**H. dia**	**T. length**	**T. mome**	**T.DNA.**	**Type**	**H. dia**	**T. length**	**T. mome**
Type	0.141					0.285				
	0.683					0.351				
H. dia	-0.128	0.428				0.279	-0.027			
	0.688	0.171				0.377	0.954			
T. length	0.571*	0.388	0.491			0.742**	0.181	0.840**		
	0.060	0.214	0.116			0.008	0.590	0.002		
T. mome	0.822**	0.328	0.237	0.872**		0.911**	0.270	0.581*	0.927**	
	0.001	0.309	0.471	0.000		0.000	0.410	0.060	0.000	
O. mome	0.575*	0.265	0.490	0.875**	0.908**	0.905**	0.255	0.607*	0.940**	0.996**

	0.052	0.414	0.109	0.000	0.000	0.000	0.431	0.040	0.000	0.000

"Upper values indicated Pearson's correlation coefficient; Lower values indicated level of significance at 5% probability. * = Significant (P<0.05); ** = Highly significant (P<0.01) T.DNA % length, T. moment; Tail moment, O. mome; Olive moment".

and upstream. Significant differences were recorded among the fishes collected from control, polluted and upstream and R3 site. DNA damage was maximum in the fish obtained from site R3, closely followed by R1 and R2. Differences were significant for tail moment in *C. mrigala* procured from polluted and upstream. Non-significant (p>0.05) differences for site R2, +ve control, farmed, polluted and upstream. Significant differences (p<0.05) for olive moment in fishes collected from site R1, fish farm and polluted sites. *C. mrigala* tail length exhibited highly significant correlation to DNA in tail and head diameter (Table 4). *C. mrigala* exhibited significant differences (p<0.05) for site R2 and fish farm and between control and upstream. The differences were significant in control, R3 and polluted site.

Highest frequency for micronucleus induction and nuclear abnormalities were observed in fishes procured from the polluted sites of the river Chenab (Table 5). *C. catla* exhibited lower frequencies of micronucleus induction compared to *C. mrigala* collected from the polluted sites. A considerable *amount* of changes in the frequency of micronucleus induction in *C. mrigala* even from the less polluted site (upstream of Chakbandi drain). Probably it is because of the reason that that *C. mrigala* is bottom feeder and have possibility of maximum exposure and pollution load from sediments. Negligible amount of this type of DNA damage was observed in the fish obtained from a controlled farm.

Various pollutants present in the freshwater ecosystem cause genetic changes leading to somber mutations [19]. This study was undertaken to determine the effect of pollutants on *Catla catla* and *C. mrigala*'s to assess changes in their genetic makeup and to use this DNA fragmentation as a biomarker of water pollution. It may serve as an early

TABLE 5
Analysis of variance and Micronucleus test of *C. catla* and *C. mrigala* blood Species and site interaction (Means ±SE).

Source of variation	Degrees of	F-value for	F-value for MNd	F-value for NAs
Species	2	11.95**	3.81*	4.72*
Type	3	61.76**	15.22**	23.31**
Species × Type	6	3.11*	3.01 *	3.55*

Fish Type	Micronucleus assay (*Catla catla*)		
	Single Micronucleus	*Double Micronucleus*	*Nuclear Abnormalities*
Polluted	24.33 ± 4.25bc	02.92 ± 1.24b	06.14 ± 0.90cd
Upstream	08.22 ± 1.26cd	01.58 ± 0.82b	03.42 ± 0.42d
Control (Farmed)	02.44 ± 0.66d	00.15 ± 0.00b	01.12 ± 0.36d
+ve. Control	44.72 ± 5.42a	09.22 ± 3.52ab	18.52 ± 2.60a
Mean	19.93 ± 4.330B	03.46 ± 1.23B	07.30 ± 1.71B
Fish Type	Micronucleus assay (*Cirrhinus mrigala*)		
	Single Micronucleus	*Double Micronucleus*	*Nuclear Abnormalities*
Polluted	45.22 ± 3.80a	06.72 ± 0.85ab	09.44 ± 1.80a-d
Upstream	21.71 ± 4.45bcd	05.42 ± 1.62b	10.33 ± 1.17a-d
Control (Farmed)	08.62 ± 2.35cd	01.48 ± 0.41b	07.44 ± 1.90bcd
+ve. Control	38.52 ± 3.82ab	08.87 ± 2.55ab	16.33 ± 2.51ab
Mean	28.52 ± 3.74A	05.62 ± 1.16AB	10.88 ± 1.32A

* = "Significant (P<0.05); ** = highly significant (P<0.01), MNs; Micronucleus single, MNd; Micronucleus double, NAs; Nuclear abnormalities. Means sharing similar letter in a row or in a column are statistically non-significant

(P>0.05). Small letters represent comparison among interaction means and capital letters are used for overall mean. Frequency calculated per thousand of cells".

warning and freshwater ecosystem. Our results were in line with those reported by [20] as they already suggested to use such DNA fragmentation in fish as a fish biomarkers caused by water pollution. [20, 22] reported increase in the frequency of micronucleus induction and nuclear abnormalities in erythrocytes of fish collected from contaminated environments.

In this study the increase in the levels of genotoxic damage in C. catla and C. mrigala from polluted sites compared to the fish procured from a maintained fish farm. These findings were corroborating with the findings from comet assay data on *C. catla* and *C. mrigala* reported by [23]. Significant correlation was noted among the MN frequencies, nuclear abnormalities and DNA damage in this study by comet assay. These results were in line with the previous study in which fish exposed to cyclophosphamide, cypermethrin, and textile mill effluent produced [23]. [24] mentioned that gill cells are more sensitive for genotoxic effect compared to kidney and liver in *Oreochromis mossambicus*. The possibility to use kidney, liver or other such tissues for genotoxicity monitoring have various limitations, such as a low mitotic index of cells. That's why, the use of connective tissues such as blood erythrocytes is more advantageous in genotoxic studies [15]. Many authors mentioned that NAs may be caused as a result to exposure to genotoxic chemicals [14]. In this significant DNA damage was observed in *C. mrigala* procured from the polluted sites of the River Chenab and even from the less polluted sites of the river upstream to the entrance of the drain into the river. Water quality parameters were exceeding the permissible limits defined by various international organizations indicating higher intensity of the water pollution in river Chenab. [13] reported higher erythrocyte MN and NAs induction frequencies in *Pholis gunellus* obtained from highly polluted sites compared to the clean areas. The results previously reported by multiple authors were substantiated that the genotoxicity of a bottom feeder fish *C. mrigala is* more *vulnerable* to the toxicants from sediments *to* the surface feeder fish *C. catla*. These findings indicated that DNA damage could be successfully used as a biomarker of water pollution to use it as an early warning for the monitoring of freshwater ecosystems in the country.

CONCLUSION

Water of the River Chenab was found highly polluted by genotoxicants. The study exposed that bottom dwelling species could be used as a bioindicator of particular aquatic environment, hence the DNA fragmentation as a biomarker of pollution as revealed by the *Cirrhinus mrigala* for early warning and monitoring of the freshwater bodies.

ACKNOWLEDGEMENTS

The authors would like to express their sincere appreciation to the Deanship of Scientific Research at King Saud University for its funding of this research through the Research Group Project No. RG-1435-012.

REFERENCES

[1] Mahboob S, Niazi F, Al-Ghanim KA, Sultana S, Al-Misned F, Ahmed Z (2015) Health risks associ ated with pesticide residues in water, sediments and the muscle tissues of Catla catla at Head Balloki on the River Ravi. Environ Monit Assess, 187:81 DOI 10.1007/s10661-015-4285-0

[2] Abo-El-Nasser M, Salah HA, Salah SE (1992) Haematological and histopathological studies of cadmium chloride on the fresh water fish Tilapia nilotica, Proc. 5th Conj, Fac Vet Med Assiut. Univ Nov 8-10, Egypt.

[3] Siliem TA, Menofiya J (1993). Some impacts of chemical changes of the water of Ratama fish ponds. Agri Res 18(2): 1837-1862.

[4] Villela IV, Oliveira IM, Silva J, Henriques JAP (2006) DNA damage and repair in haemolymph cells of golden mussel (Limnoperna fortunei) exposed to environmental contaminants. Mutat Res 605(1-2):78-86.

[5] Ostling O, Johanson KJ (1984) Microelectrophoretic study of radiation-induced DNA damages in individual mammalian cells. Biochem and Biophy Res Corp 123(1): 291-298.

[6] Singh NP, McCoy MT, Tice RR, Schneider RR (1988) A simple technique for quantification of low levels of DNA damage in individual cells. Exp and Cell Res 175(01): 184-191.

[7] Tice RR, Agurell E, Anderson D, Burlinson B, Hartmann A, Kobayashi H, Miyamae Y, Rojas E,

Ryu JC, Sasaki YF (2000) Single Cell Gel/Comet Assay: guidelines for in vitro and in vivo genetic toxicology testing. Environ Mol Mutagen 35(3): 206-221.

[8] Dixon DR, Pruski AM, Dixon LRJ, Jha AN (2002) Marine invertebrate ecogenotoxicology: a methodological overview. Mutagen 17(6): 495-507.

[9] Russo C, Rocco L, Morescalchi MA, Stingo V (2004) Assessment of environmental stress by the micronucleus test and the comet assay on the genome of teleost populations from two natural environments. Ecotox and Environ Saf 57(2): 168–174.

[10] Baršienė J, Rybakovas A, Lang T, Andreikėnaitė L, Michailovas A (2013) Environmental genotoxicity and cytotoxicity levels in fish from the North Sea offshore region and Atlantic coastal waters. Mar Pollu Bull 68(1-2):106-16.

[11] Mahboob S, Al-Balwai HFA, Al-Misned F, Ahmad Z (2014) Investigation on the Genotoxicity of Mercuric Chloride to freshwater Clarias gariepinus. Pak Vet J 34: 100-103.

[12] APHA (1998). Standard Methods for the Examination of Water and Waste water. 20th Ed., American Public. New York. USA.

[13] Cavalcante DGSM, Martinez CBR, Sofia SH (2008) Genotoxic effects of Roundup® on the fish, Prochilodus lineatus. Mutat Res 655(1-2): 41–46.

[14] Bombail W, Aw D, Gordon E, Batty J (2001) Application of comet and micronucleus assays to butterfish (Pholis gunnellus) erythrocytes from the Firth of Forth, Scotland. Chemosphere, 44:383–392.

[15] Serrano-Garcia L, Montero-Montoya R (2001) Micronuclei and chromatin buds are related genotoxic events. Environ Mol Mutagen 38(01): 38–45.

[16] Cavas T, Gozukara SE (2005) Micronucleus Test in Fish Cells: A Bioassay for In Situ Monitoring of Genotoxic Pollution in the Marine Environment. Environ Mol Mutagen 46(01):64-70.

[17] Carrasco K, Tilbury KL, Myers MS (1990) Assessment of the piscine micronucleus test as an in situ biological indicator of chemical contaminant effects. Canad J of Fish and Aqua Sci 47:2123–2136.

[18] USEPA (1999) National recommended water criteria-correction. EPA 822/Z-99-001. USEPA, Washington, DC.

[19] Galindo, B. A., Troilo, G., Cólus, I. M. S., Martinez, C. B. R. and Sofia, S. H., 2010. Genotoxic Effects of Aluminum on the Neotropical Fish Prochilodus lineatus. Water Air and Soil Pollution, 212(1-4), 419–428.

[20] Richards JP, Glegg AG, Cullinane S (2000) Environmental regulation: industry and the marine environment. J Environ Manag 58:119–134.

[21] Van-Der-Oost R, Beyer J, Vermeulen NPE (20030 Fish bioaccumulation and biomarkers in environmental risk assessment: a review. Environ Toxicol and Pharmacol 13(2): 57–149.

[22] Pietripiana D, Modena M, Guidetti P, Falugi C, Vacchi M (2002) Evaluating the genotoxic damage and hepatic tissue alterations in demersal fish species: a case study in the Liguarian Sea (N.W Mediterranean). Mar Pollu Bull 44(3):238–343.

[23] Pavlica M, Štambuk A, Malovi´c L, Mladini´c M, Göran I, Klobuˇ VC (2011) DNA integrity of chub erythrocytes (Squalius cephalus L.) as an indicator of pollution related genotoxicity in the River Sava. Environ Monit and Assess 77(1-4):85-94.

[24] Cavas T, Ergene-Gozukara S (2003) Evaluation of the genotoxic potential of lambda-cyhalothrin using nuclear and nucleolar biomarkers in fish cells. Mutat Res 534(1-2): 93–99.

Received: **22.10.2015**
Accepted: **07.03.2016**

CORRESPONDING AUTHOR

Shahid Mahboob
Department of Zoology, Wildlife and Fisheries, Government College, University, Faisalabad, Pakistan.

E. mail: shahidmahboob60@hotmail.com

© by PSP Volume 25 – No. 7/2016, pages 2509-2513 Fresenius Environmental Bulletin

EFFECT OF FORESTRY AFFORESTATION ON SOME SOIL PROPERTIES: A CASE STUDY FROM TURKEY

Nilufer Yazici*, Aysen Turan

Faculty of Forestry, Suleyman Demirel University TR-32260, Isparta-TURKEY

ABSTRACT

The effect of afforestation on soil properties is among the most important and immeasurable commercial outputs in plantation forestry. This study was carried out to determine the effect of afforestation on soil properties (i.e. organic matter, phosphorous, nitrogen, clay, dust, field capacity, wilting point, electrical conductivity and moisture capacity and pH, sand, lime and volume weight values) based on afforested and unafforested areas sampled from the western part of Turkey via collected soil samples at two depths (0-30 cm and 30-60 cm). Organic matter, phosphorous, nitrogen, clay, dust, field capacity, wilting point and available water capacity were higher in afforested areas, while the opposite was true for pH, sand, lime and volume weight values. Soil depth generally showed differences ($p \leq 0.05$) for the studied soil properties between areas and within areas according to the results of analysis of variance.

KEYWORDS:
Forest soil, organic matter, plantation, soil quality, soil depth

INTRODUCTION

Depending on the conditions of the world, people use the ecosystem in which they live, and are a part of, to excessively change it for their own benefit. As a result, changes in the ecosystem reveal irremediable ecological problems; these problems influence us as individuals and as a society. One of the greatest damages caused by people is erosion; soil which is formed over quite a long time can be transferred in a very short time due to erosion.

The most important measure in preventing erosion is forestation studies. In this sense, various special forestation studies, basically erosion control, arid and semi-arid area forestation and dune forestation, gained speed at the end of the 19th century. The aim in conducting forestation studies in areas which suffer from erosion is to compensate for people's need for wood raw materials, improve water which has become unbalanced, prevent and decrease erosion siltation damage and provide livelihoods for people of the region in the future.

A strong link exists between forestry practices such as afforestation and soil properties. Afforestation plays an important role in conversion of unproductive forests to productive forests and also improving soil properties for present and future productivity of forests. Afforestation also offers a more economical and environmentally sound solution to increase soil quality than the use of chemical nutrients. Also, soil properties have main effects on successful afforestation. It is thus important to examine the effect of afforestation on soil properties. However, while many studies have been conducted on soil properties for different purposes [1-9], examination of the effect of afforestation on soil properties or their interaction is very limited [10-14].

This study was conducted to examine the effect of afforestation on soil properties to discuss and draw conclusions regarding future afforestation and other forestry practices.

MATERIAL AND METHODS

The study was carried out in a natural forest area located at latitude 38° 56' N, longitude 29°33' E, with an average elevation of 1620 m. at 107 ha in the Kutahya district of western Turkey in 2013.

Annual rainfall and the range of temperatures are 561.8 mm and -27.4°C to +36.8°C. The natural forests of the region have *Pinus nigra* Arnold., *Juniperus* spp. Bieb., *Quercus* spp., *Pinus brutia* Ten., *Cedrus libani* A. Rich., *Alnus glutinosa* L., *Castanea sativa* Mill., *Populus* spp. and *Abies* spp.

The study area was divided into two areas (afforested and unafforested) at the same aspect and altitude to minimize the other environmental effects. The afforested area was planted by 2+1-year-old Anatolian black pine (*Pinus nigra* Arnold.) seedlings at spacing 2x1 m in 2000 and then re-planted with broadleaves in 2002-2003. Twenty soil materials were sampled from 10 soil profiles in each area, and one sample of each soil depth (0-30 cm and 30-60 cm) was taken**.** Forty soil samples were analysed after pretreatments such as cleaning from different materials, drying and sieving on the samples for texture (sand, clay and dust), organic

material, pH, lime, nitrogen, phosphorus, electrical conductivity (EC), field capacity, wilting point, volume weight and available water capacity analysis.

Texture (sand, clay and dust) analysis. Soil samples were analyzed by Bouyoucus' hydrometer [15].

pH. pH was measured using a 1/2.5 soil sample and pure water ratio by Beckman H5 Electrode pH meter [16-18].

Organic material. The amount of organic material was determined by Walkey-Black methods using 5 g soil samples [16-17, 19].

Total nitrogen and phosphorus. Total nitrogen and phosphorus were determined by the Sömi-Mikro Kjeldahl' method [16, 19] and Olsen method by "Spectronic-20 D" [16], respectively.

Electrical conductivity/total lime (CaCO3). EC, also called salinity, was determined at 25C° using saturated water by a conductivity bridge apparatus [16, 20], while total lime was determined by the Scheibler Kalsimeter method [21].

Field capacity and wilting point. These were determined by saturated water at 0.33 bar pressure for field capacity and 15 bar pressure and then at Owen at 24 hours [22].

Available water capacity. This was determined by soil moisture equipment using the difference between field capacity and wilting point [23].

Volume weight. This was determined on soil samples taken by the cylinder method at 105˚C during 24 hours [17, 24].

The data were analyzed using the SPSS statistical program [25]. Also, soil depths and areas were compared by analysis of variance (ANOVA) for characteristics.

RESULTS AND DISCUSSION

Soil texture. Averages of clay and dust were higher in the afforested area than in the unafforested area, while the opposite was true for sand (Table 1). Higher clay in the afforestation area was an expected result because of soil maintenance by plantations and soil treatments. Similar results were also reported in early studies [10, 11]. Different soil treatments have been applied in plantations to improve soil properties, as emphasized in earlier studies [26-29].

The surface of soil (0-30 cm) had more clay and dust than deep soil (30-60 cm) in both areas, except for sand (Table 1). These results were consistent with [10, 30]. Results of the ANOVA showed significant ($p<0.05$) differences in both area and depth for sand and clay. However, they were similar for dust according to the ANOVA. Similar results were reported in the *Robinia pseudoacacia* plantation [10].

Organic material. Organic material was higher in both soil depths of the afforested area (5.24% and 3.89%) than in the unafforested area (2.93% and 1.61%). The soil surface had more organic material than the deep soil (30-60 cm). Also, organic materials generally were kept at the surface of the soil, as emphasized in my studies [12, 31].

Significant differences ($p<0.05$) were found for organic material between both areas and depths. This also was reported in early studies [i.e. 11, 32].

Total nitrogen and phosphorus. Averages of total nitrogen and phosphorus are provided for the area and soil depth in Table 2. Significant differences ($p<0.05$) were found for total nitrogen and phosphorus between both area and depth. As expected, the afforested area and soil surface contained higher nitrogen and phosphorus than the unafforested area and deep soil (Table 2). In addition, results of the ANOVA showed significant ($p<0.05$) differences in both area and depth for total nitrogen and phosphorus, as reported by [11]. Similar results were also reported for phosphorus [33] and nitrogen [34] for soil depth.

TABLE 1
Averages of clay, sand and dust (%) for the areas and soil depths.

	Clay %		*Sand%*		*Dust%*	
	afforested	unafforested	afforested	unafforested	afforested	unafforested
0-30 cm	36.44	27.89	53.48	62.66	17.41	16.32
30-60 cm	24.15	19.34	62.93	71.43	15.53	11.83

TABLE 2
Averages of total nitrogen and phosphorus (%) for the areas and soil depths.

	Nitrogen%		*Phosphorus%*	
	afforested	unafforested	afforested	unafforested
0-30 cm	0.25	0.13	3.12	1.66
30-60 cm	0.13	0.09	1.50	0.86

Electrical conductivity and total lime. The averages of EC, a term used to describe a measurement unit of salinity, were 47.35 and 50.21 in the soil surface (0-30 cm) of afforested and unafforested areas, while they were 47.33 and 60.12 in deep soil (30-60 cm) (Table 3). As seen in Table 3, total lime was also higher in the unafforested area and deep soil. However, areas and soil depths showed similar ($0.05<p$) performance for similar salinity and total lime; total lime changed for soil depth [11].

Field capacity, wilting point and available water capacity. Afforestation had positive effects on field capacity, wilting point, and available water capacity (Table 4), as also reported by [3, 10]. The effects were also higher in surface soil than in deep soil (Table 3). Also, the difference in results was also supported by the results of ANOVA ($p<0.05$). However, many factors were associated with field capacity, wilting point and available water capacity [5, 35, 36].

Volume weight. Volume weights were 0.72 g/cm^3 and 0.82 g/cm^3 at the soil surface of afforested and unafforested areas, while they were 0.76 g/cm^3 and 0.92 g/cm^3 at deep soil (30-60 cm). Also, significant differences ($p<0.05$) were found for volume weights between both area and depth, as reported by [3, 37, 38].

CONCLUSIONS

Results of the study showed that afforestation has positive effects in improving soil properties. However, changes in soil properties take long periods of time. Thus, it is necessary to collect more data to draw accurate conclusions. One can argue that afforestation should be used to improve soil properties, especially in unproductive areas, based on the primary results of the study. Many environmental factors, such as aspect, altitude, forest tree species, and plantation density on soil properties, can also contribute and should be investigated for different regions.

ACKNOWLEDGMENTS

This study was a part of an M.Sc. thesis, prepared under the supervision of Dr. Nilufer Yazici. The authors thank Professor Nebi Bilir for his valuable comments, which helped to improve the manuscript; we also thank the Research Department of Suleyman Demirel University for financial support (project no: 3544-YL1-13).

TABLE 3
Averages of electrical conductivity and total lime (%) for the areas and soil depths.

	Electrical conductivity		*Total lime %*	
	afforested	unafforested	afforested	unafforested
0-30 cm	47.35	50.21	1.5	2.2
30-60 cm	47.33	60.12	1.2	1.5

TABLE 4
Averages of field capacity, wilting point and available water capacity (%) for the areas and soil depths.

	Field capacity%		*Wilting point%*		*Available water capacity%*	
	afforested	unafforested	afforested	unafforested	afforested	unafforested
0-30 cm	47.33	37.73	29.20	19.95	18.13	17.78
30-60 cm	34.35	27.48	17.82	16.08	16.53	11.40

REFERENCES

[1] Zhao, M.Y., Zhao, W.W., Qiu, Y., Feng, Q. and Zhong, L.N. (2014) Scale effect analysis of the influence of land-use types and environmental factors on soil nutrients: A case study in loess areas of Northern Shaanxi, China. Fresenius Environmental Bulletin, 23 (3): 787-794.

[2] Ekberli, I. and Kerimova, E. (2005) Changes in some physico-chemical parameters in irrigated clay soils of Shirvan plain Azerbaijan. J. of Fac. of Agric., OMU, 20(3):54-59.

[3] Babur, E. (2012) Investigations on some physical properties of the soils under different land use type in aalyan-atasu dam creek watershed. Graduate School of Natural and Applied Science, Black Sea Technical University, MSc. Thesis, Trabzon, Turkey.

[4] Wei, W., Liding, C., Bojie, F., Zhilin, H., Dongping, W. and Lida, G. (2007) The effect of land uses and rainfall regimes on runoff and soil erosion in the semi-arid Loess Hilly Area, China. Journal of Hydrology, 335: 247– 258.

[5] Gol. C., Unver, I. and Ozhan, S. (2004) The relations between land use types and moisture contents at the surface soil in the Cankiri-Divan region. Forestry Faculty Journal of Suleyman Demirel University, A(2): 17-29.

[6] Nougeira, M.A., Albıno, U.B., Brandao-Junıor, O., Braun, G., Cruz, M.F., Dias, B.A., Duarte, R.T.D., Gioppo, N.M.R., Menna, P., Orlandi, J.M., Raimam, M.P., Rampazo, L.G.L., Santos, M.A., Silva, M.E.Z., Vieira, F.P., Torezan, J.M.D., Hungria, M. and Andrade, G. (2006) Promising indicators for assessment of agro ecosystems alteration among natural, reforested and agricultural land use in southern Brazil. Agriculture, Ecosystems and Environment, 11-22.

[7] Neufeldt, H., Resck, D.V.S. and Ayarza, M.A. (2002) Texture and land-use effects on soil organic matter in Cerrado Oxisols, Central Brazil. Geoderma, 107:151-164.

[8] Fattet, M., Fu, Y., Ghestem, M., Ma, W., Foulonneau, M., Nespoulous, J., Le Bissonnais, Y. and Stokes, A. (2011) Effects of vegetation type on soil resistance to erosion: Relationship between aggregate stability and shear strength. Catena, 87: 60– 69.

[9] Novo, L.A.B. and González, L. (2014) The influence of soil moisture on Brassica juncea grown in copper mine soil amended with technosol, and its impact on phytoremediation. Fresenius Environmental Bulletin, 23 (7): 1560-1563.

[10] Yuksek, T., Ozalp, M., Yuksek F., Erdogan., E., Dehset, F. and Inanli, E. (2010) Effect of erosion afforestation of *Robinia Pseudeoacacia* L. on soil properties in Artvin-Pamukcular Watersheed. Third Blacksea Forestry Congress.

[11] Cavdar, G. (2011) Investigating the effects of afforestation efforts on some soil properties in semi-arid lands: A case study in Polatli (Sarioba). Graduate School of Natural and Applied Science, Black Sea Technical University, MSc. Thesis, Artvin, Turkey.

[12] Atmaca, F. and Tuluhan, Y. (2006) Effects of afforestation on soil properties in Turan Emeksiz coast. Journal of Eastern Mediterranean Forestry Research Institute, 12.

[13] Olmez, Z. (1997) An evaluation of Scotch pine (*Pinus sylvestris* L.) plantation in Ardanuc forest enterprise. Graduate School of Natural and Applied Science, Black Sea Technical University, MSc. Thesis, Trabzon, Turkey.

[14] Tufekcioglu, A., Altun, L., Kalay, H.Z. and Yilmaz, M. (2005) Effects of some soil properties on the growth of hybrid poplar in the Terme-Golardi Region of Turkey. Turkish Journal of Agriculture and Forestry, 29: 221-226.

[15] Bouyocous, G.J. (1951) A recalibration of the hydrometer method for making mechanical analysis of soil. Argon Journal, 43:434-438.

[16] Jackson, M.L. (1962) Soil chemical analysis. Constable and Company Ld., London.

[17] Gulcur, F. (1974) Physical and chemical analysis of soil. Forestry Faculty of Istanbul University press.

[18] Tuzuner, A. (1990) Handbook of soil and water analysis. Ministry of Agriculture and Forestry.

[19] Chapman, H.D. and Pratt, P.F. (1961) Method of analysis for soils, plant and waters. University of California, Division of Agricultural Science.

[20] Richards, L.A. (1954) Diagnosis and improvement of saline and alkaline soils, USDA Handbook.

[21] Kacar, B. (1993) Chemical analysis of plant and soil. Agricultural Faculty of Ankara University.

[22] Klute, A. and Dirksen, C. (1986) Hydraulic conductivity and diffusitivity laboratory methods of soil analysis. Am. Soc. Agron., 687-732.

[23] Schlichting, E. and Blume, E. (1966) Bodenkundliches practikum. Verlag Paul Parey.

[24] Blake, G.R. and Hartge, K.H. (1986) Bulk density. Agronomy Monograph, 363-375.

[25] Ozdamar, K. (1999) Statistical analysis by package programs. Kaan Publishing, Eskisehir.

[26] Yuksek, F., Kucuk, M., Yuksel, E. and Guner, S. (2010) Effect of erosion afforestation on soil properties in Artvin. Third Blacksea Forestry Congress.

[27] Querejeta, J.I., Roldan, A., Albaladejo, J. and Castillo, V. (2000) Soil physical properties and moisture content affected by site preparation in the afforestation of a semiarid rangeland. Soil Science Society America Journal, 64: 2087–2096.

[28] Ramos, M.C., Cots-Folch R. and Martínez-Casasnovas, J.A. (2007) Effects of land terracing on soil properties in the Priorat region in Northeastern Spain: A multivariate analysis. Geoderma, 142: 251–261.

[29] Gonzales, A.P., Vieira, S.R. and Castro, M.T.T. (2000) The effect of cultivation on the spatial variability of selected properties of an umbric horizon. Geoderma, 97: 273-292.

[30] Gurlevik, N., Ozkan, K. and Gulcu, S. (2009) Effects of prescribed burning and mechanical site preparation on soil properties in a Kermes oak field in Isparta region. Forestry Faculty Journal of Suleyman Demirel University, A(1): 24-37.

[31] Babalık, A.A. (2014) The effect of aspect factor in Isparta-Arapdağı Rangeland on the dry forage yield and botanical composition. Res. J. Biotech, Vol. 9 (9), 73-78.

[32] Zengin, N. (2010) Coarse root biomass properties in Scotch pine stands of Alucra, Giresun. Graduate School of Natural and Applied Science, Black Sea Technical University, MSc. Thesis, Artvin, Turkey.

[33] Williams, R.D., Naney, J.W. and Ahuja, L.R. (1984) Soil properties and productivity changes along a slope. Proceedings of the National Symposium on Erosion and Soil Productivity.

[34] Gol, C. (2002) The relationships between land use types and some soil properties in the Cankiri-Eldivan region. Graduate School of Natural and Applied Science, Ankara University, PhD Thesis, Ankara, Turkey.

[35] Wall, A. and Heiskanen, J. (2003) Water retention characteristics and related physical characteristics of soil on afforested agricultural land in Finland. Forest Ecology and Management, 186: 21-37.

[36] Onstad, C.A., Pierce, F.J., Dowdy, R.H. and Larson, W.E. (1984) Erosion and productivity interrelations on a soil landscape. Proceedings of the National Symposium on Erosion and Soil Productivity, 193-200.

[37] Tufekcioglu, A., Yuksek, T. and Kalay, H.Z. (2002) Investigation of *Robinia pseudoacacia* plantations based on biomass and soil properties in Gumushane-Torul district. Symposium of Gumushane.

[38] Williams, A.G., Ternan, J.L., Fitzjohn, C., Alba, S. and Perez-Gonzalez, A. (2003). Soil moisture variability and land use in a temperate-humid environment. Land Degradation and Development, 12: 477-484.

Received: **22.10.2015**
Accepted: **07.01.2016**

CORRESPONDING AUTHOR

Nilufer Yazici
Faculty of Forestry
Suleyman Demirel University
TR-32260, Isparta – TURKEY

e-mail: niluferyazici@sdu.edu.tr

© by PSP Volume 25 – No. 7/2016, pages 2514-2518 Fresenius Environmental Bulletin

PREPARATION, CHARACTERIZATION AND APPLICATION OF H_3PO_4 ACTIVATED MAIZE TASSEL FOR REMEDIATION OF EUTROPHIC PHOSPHORUS

Adebayo M. Shofolahan[1], Nana M. Agyei[1], Jonathan O. Okonkwo[2]

[1]Department of Chemistry, Sefako Makgatho Health Sciences University, P.O. Box 235, Medunsa 0204, South Africa.
[2]Department of Environmental, Water & Earth Sciences, Tshwane University of Technology, Private Bag x680, Pretoria 0001, South Africa.

ABSTRACT

Technologies for phosphate removal from contaminated waters, such as chemical precipitation with lime, are expensive. In this study the feasibility of utilizing low-cost activated maize tassel for the adsorptive removal of phosphate was assessed. Raw maize tassel powder was impregnated with H_3PO_4 and activated at 600°C under an inert atmosphere of N_2 in the ratios 0.5:1, 1:1, 1.5:1, 2:1 and 2.5:1 (w/w H_3PO_4: tassel). The activated products were characterized by BET. Activation resulted in an increase in specific surface area and porosity. CAT 4 (2:1) with S_{BET} 803.8 m^2/g and pore size 2.22 nm was further characterized by SEM and used for adsorption studies. Batch experiments were performed to study the removal of phosphate from simulated samples; the optimal parameters were found to be: contact time of 90 min, pH 7 and adsorbent dosage of 1.5 g per 100 mL solution. The adsorption data were fitted to the Langmuir isotherm model ($R^2 > 0.99$), yielding an estimated adsorption capacity of 15.31 mg PO_4^{3-} (as P) per g adsorbent. The activated product was successfully applied for the remediation of phosphate in selected sewage samples.

KEYWORDS:
Maize tassel, H_3PO_4 activation, eutrophication, phosphate removal.

INTRODUCTION

The increase in agricultural and industrial activities in developing countries has led to the use of phosphorus as an essential resource and material. However, elevated levels of phosphates in surface and underground water from industrial and agricultural activities stimulate the growth of micro and macro organisms in water bodies, leading to eutrophication [1]. Hence, the total phosphate (as P) concentration in effluents from municipal and industrial sources should be reduced to 1.0 mg/L or less in order to meet environmental requirements [2]. Various methods are available for phosphate removal including chemical precipitation, microbiological treatment and adsorption. Chemical precipitation uses lime, alum or ferric chloride as the common precipitants for efficient phosphate removal. However, problems such as the cost of the process and production of large amounts of sludge during the treatment of the wastewater arise [1]. As an alternative option, adsorption technology for removal of phosphate from aqueous solutions using cheap, easily available materials such as red mud [3], modified wheat residue [4] and fly ash [5] have been reported. Adsorption processes have merits; such as low-cost, fast operation and favourable performance, and have drawn considerable attention in recent years.

Maize tassel is the male part of the maize plant which is usually discarded after harvesting. It is a lignocellulosic material possessing several desirable characteristics for an adsorbent; a low cost material, mesoporous with a high adsorption capacity for trace metal ions [6] and organics [7]. In order to enhance phosphate adsorption we attempted to activate maize tassel with phosphoric acid and use it to remove phosphate from simulated aqueous solutions as well as real environmental samples in batch experiments.

MATERIALS AND METHODS

Preparation of raw and activated maize tassel adsorbents. Maize tassel was plucked off the woody parts of the maize plant, thoroughly washed with 0.01 M HCl followed by distilled water to remove dust and other impurities from their surfaces and then air-dried at room temperature. The material was milled using Laboratory Mill 3 100 (Stockholm, Sweden). Varying amounts of H_3PO_4 (85% w/w) from Sigma (Pretoria, South Africa) were added as an activating agent to 20 g portions of raw maize tassel powder to produce

materials with 0.5:, 1:1, 1.5:1, 2:1 and 2.5:1 (w/w H_3PO_4: tassel) impregnation ratios. The impregnated materials were dried at 110 °C for 12 h and then activated at 600 °C under an inert atmosphere of nitrogen at a flow rate of 200 cm^3/min. After cooling, any residual H_3PO_4 was removed by washing with hot deionised water until the pH of the washings increased to *ca* 6. The activated materials were dried at 110 °C for 4 h, cooled and coded as CAT1, CAT2, CAT3, CAT4 and CAT5, respectively.

Characterization of the adsorbents. The prepared adsorbents were characterized to obtain some of their physicochemical properties. The BET surface area (S_{BET}) and pore structural parameters were determined from the adsorption-desorption isotherms of nitrogen at 77 K (-196 °C) using a Micrometrics (TriStar 3000) Surface Area and Porosity Analyzer. The surface morphologies were studied using a JEOL-7500 Field Emission Scanning Electron Microscope (CSIR, Pretoria) at an accelerating voltage of 2 kV.

Adsorption studies. Batch adsorption studies were performed to study the effects of some of the experimental parameters known to influence the efficiency and rate of adsorption from aqueous solution. To study the effect of contact time, 1 g portions of adsorbent were added to 100 mL of 80 mg L^{-1} PO_4^{3-} solution in ten (10) 250 mL flasks. The mixtures were agitated using a thermostatic Labcon platform shaker (Labotech, Johannesburg) at 120 rpm for 60 min at 25 ºC. A flask was removed after 10, 20, 30, 40, 60, 80, 90 and 100 min, the contents were filtered through 0.45 μm membranes and the concentration of phosphate in the filtrates was determined by UV/VIS molecular absorption spectrophotometry using a modified standard yellow (λ= 470 nm) vanadomolybdate-phosphoric acid method [8]. The effect of pH was studied by conducting equilibrium adsorption studies at pH 1.0, 2.0, 4.0, 6.0, 8.0 and 10.0 using the optimized contact time. The effect of adsorbent dosage was studied for 0.25, 0.5, 1.0, 1.5, 2.0 and 2.5 g adsorbent per 100 mL solutions using the optimized contact time and pH.

Application of activated maize tassel. The potential of activated maize tassel for phosphate remediation in real environmental samples was assessed by applying the adsorbent to samples taken from three sewage treatment plants in Pretoria sited at Daarsport (domestic and industrial), Medunsa (domestic and hospital) and Sandspruit (domestic).

RESULTS AND DISCUSSION

BET characterization of the adsorbents. The BET isotherms exhibited a type IV isotherm with a hysteresis loop which indicates the mesoporous nature of the adsorbent. Values for the specific surface area and pore structural properties are given in Table 1.

The values of the pore sizes corroborate the isotherm shape indication of mesoporosity, as they all fall in the range 2 to 50 nm. The specific surface area of activated maize tassel powder (419-806 m^2/g) is greater than those reported for some other low cost adsorbents such as carbon from cassava peel (270 m^2/g) [9]. In a screening experiment (data not shown here) CAT4 was found to be the most effective for phosphate removal and it was selected for use in further studies.

SEM technique was used to elucidate the surface morphology of the raw and activated maize tassel (Figure 1). As it can be seen from Figure 1a, the raw tassel shows a mesh-like structure with long chains and some pores. It can also be seen from the micrograph (Figure 1b) that the external surface of the chemically activated maize tassel carbon is full of cavities.

TABLE 1
BET surface area and pore structural properties of the adsorbents.

Adsorbent	S_{BET} (m^2/g)	Pore volume (cm^3/g)	Pore size (nm)
Raw tassel	2.54	0.006	8.61
Activated tassel			
CAT1 (0.5:1)	418.6	0.214	2.04
CAT2 (1:1)	564.1	0.292	2.07
CAT3 (1.5:1)	699.0	0.372	2.12
CAT4 (2:1)	803.8	0.447	2.22
CAT4 (2.5:1)	806.4	0.413	2.14

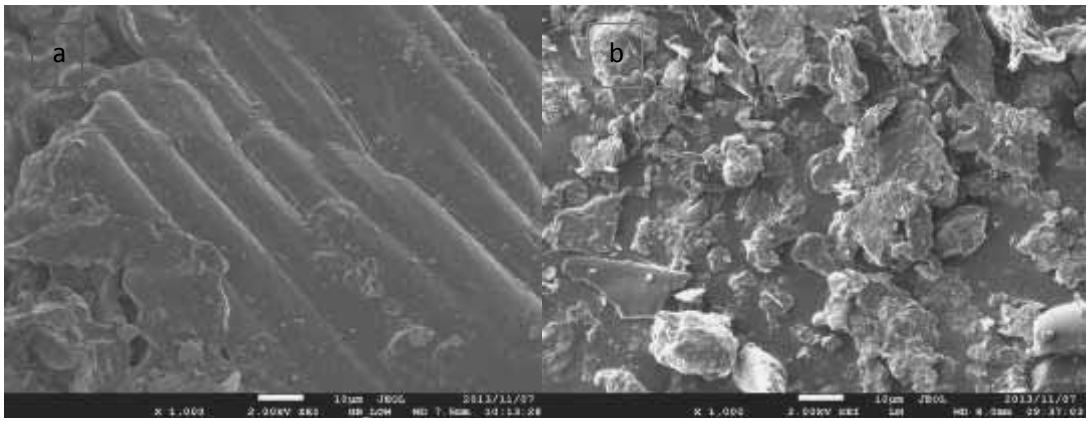

FIGURE 1
SEM images of the raw maize tassel (a) and activated maize tassel (b).

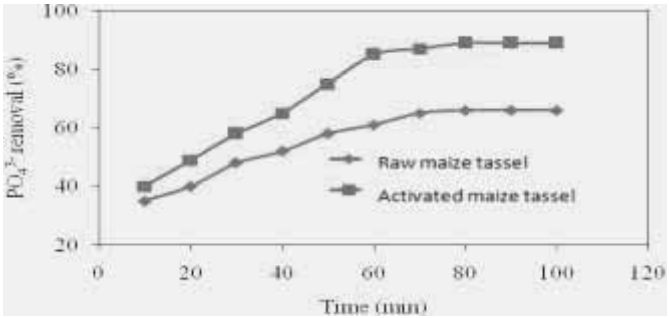

FIGURE 2
Effect of contact time on the efficiency and rate of phosphate removal (Conditions: 100 mL of 80 mg/L PO_4^{3-}; 1.0 g adsorbent; 25°C).

Batch adsorption studies. The variation of percent phosphate removal with time for the adsorbents is illustrated in Figure 2. It can be seen that activated maize tassel removed phosphate at a faster rate and with higher efficiency than raw maize tassel. The uptake of phosphate by activated maize tassel virtually ceased after a contact time of about 70 min, compared to about 90 min for raw maize tassel, with 85% and 66% phosphate removal at equilibrium, respectively. Similar trends using different adsorbents for phosphate removal have been reported [5,10]. A contact time of 90 minutes was used in further experiments to study the effects of pH and adsorbent dosage, yielding optimised parameters of pH 7 and 1.5 g adsorbent per 100 ml solution, respectively.

Adsorption Isotherms. Adsorption equilibrium is established when the amount of solute being adsorbed onto the adsorbent is equal to the amount being desorbed. An equilibrium adsorption isotherm is predicted when the solid phase concentration is plotted against liquid phase concentration graphically. In the present study, two models, namely Langmuir and Freundlich were used to interpret the equilibrium data [11, 12].

A summary of the parameters for both Langmuir and Freundlich isotherm plots are shown in Table 2. Based on the coefficients of determination (R^2) it may be concluded that phosphate adsorption followed the Langmuir rather than Freundlich isotherm for both raw and activated maize tassel. This suggests that the adsorption occurs on a homogeneous surface by monosorption sorption without significant interaction between adsorbed molecules. The Langmuir constant, q_{max} [11] was 15.31 mg/g for activated maize tassel, which was greater than the q_{max} of 10.46 mg/g for raw maize tassel, as expected.

TABLE 2
Langmuir and Freundlich parameters for phosphate adsorption using raw and activated maize tassel.

Isotherm	Parameter	Raw tassel	Activated tassel
Langmuir	Equation [11]	y= 0.6109x-0.0956	y= 1.0788x-0.0653
	R^2	0.9934	0.9976
	q_{max} (mg/g)	10.46	15.31
	b (L/mg)	0.156	0.0605
Freundlich	Equation [12]	y= 0.6003x-0.2069	y= 1.4413x-0.1869
	R^2	0.938	0.9772
	K_F (mg/g)	1.23	1.20
	n	1.67	0.69

Application of the activated maize tassel for phosphate remediation from environmental wastewaters. Based on the promising results obtained in the batch studies of phosphate removal from simulated aqueous solutions by activated maize tassel, the adsorbent capability was evaluated using real wastewater samples at the optimized conditions. Samples from three selected sewage treatment plants in Northern Pretoria, South Africa were used. The results are shown in Table 3**.** The levels of phosphate found in the raw sewage samples (18-43 mg/L) were very high, an indication of the vital importance of treatment before discharge into local water bodies to prevent possible eutrophication. Evidently the microbiological treatment processes used at these plants are quite efficient for nutrients; bringing phosphate levels in the effluent down to below 5 mg/L. Significantly, batch treatment with activated maize tassel produced an even greater reduction to values below 1 mg/L, which meets widely accepted environmental requirements [2].

TABLE 3
PO_4^{3-} remediation in sewage samples.

Sampling site	Analyte	Raw sewage (mg/L)	After MB treatment[b] (mg/L)	After AMT treatment[c] (mg/L)
Medunsa	PO_4^{3-} (as P)	28.0 ± 0.47	4.2 ± 0.21	0.32 ± 0.03
	COD	510 ± 28	*NM*	110 ± 6.8
	BOD	164 ± 12	*NM*	42 ± 1.8
Sandspruit	PO_4^{3-} (as P)	18 ± 1.25	2.9 ± 0.16	0.45 ± 0.044
	COD	239 ± 14	*NM*	86 ± 5.2
	BOD	103 ± 4.3	*NM*	35 ± 2.1
Daarsport	PO_4^{3-} (as P)	43 ± 0.82	3.7 ± 0.15	0.60 ± 0.037
	COD	602 ± 24	*NM*	118 ± 9.2
	BOD	211 ± 14	*NM*	58 ± 4.2

[a]Mean values ± SD (n = 3)
[b]Microbiological treatment by the sewage treatment plants.
[c]Activated maize tassel batch treatment (Conditions: 100 mL sample solution, 1.5 g adsorbent; pH 7; 25°C; 90 min contact time)
NM (Not measured)

Chemical oxygen demand (COD) which is a measure of the amount of decaying matter (usually organics) that consume dissolved oxygen, and biochemical oxygen demand (BOD) which is a measure of the amount of oxygen consumed by the bacteria that bring about the decomposition, are important water quality parameters. Both of these parameters were found to decrease significantly after batch treatment of the sewage samples with chemically activated maize tassel. This is hardly surprising, as the removal of organics such as methylene blue from aqueous medium with activated tassel was recently reported [7].

CONCLUSIONS

In this study chemically activated maize tassel was prepared, characterized and used for the removal of phosphate from aqueous solutions. Activation yields a product with higher specific surface area and total pore volume- characteristics of a good candidate for consideration as an adsorbent. Process parameters for optimal rate and efficiency of phosphate removal were established. The experimental adsorption data was fitted to various kinetic and isotherm models; the best fits were obtained for pseudo-second-order and Langmuir isotherm models. The adsorbent was successfully applied to real environmental samples. The results from this study have shown the potential of activated maize tassel to be used as a low-cost and effective biosorbent for the removal of phosphate from environmental wastewaters.

REFERENCES

[1] Droste, R.L. (1997) Theory and practice of water and wastewater treatment. John Wiley & Sons, Inc., New York.

[2] Eckenfelder, RL. (1980) Principles of Water Quality Management. CBI Publishing Company, Inc, Boston, Massachusetts.

[3] Zhao, Y., Wang, J., Luan, Z., Peng, X., Liang, Z. and Shi, L. (2009) "Removal of phosphate from aqueous solution by red mud using a factorial design." Journal of Hazardous Materials 165.1: 1193-1199.

[4] Wang, Y., Gao, B.Y., Yue, W.W. and Yue, Q.Y. (2007) Adsorption kinetics of nitrate from aqueous solutions onto modified wheat residue. Colloids and Surfaces A: Physicochemical and Engineering Asapects 308.1: 1-5.

[5] Agyei, N.M., Strydom, C.A., and Potgieter, J.H. (2002) The removal of phosphate ions from aqueous solution by fly ash, slag, ordinary Portland cement and related blends. *Cement and Concrete Research* 32: 1889-1897.

[6] Moyo, M., Chikazaza, L., Nyamunda, B.C. and Guyo, U. (2013) Adsorption batch studies on the removal of Pb(II) using maize tassel based activated carbon. Journal of Chemistry, 2013.5: 1–8.

[7] Olorundare, O.F., Msagati, T.A.M., Krause, R.W.M., Okonkwo,J.O. and Mamba,B.B. (2014) Steam activation, characterisation and adsorption studies of activated carbon from maize tassels. Chemistry and Ecology, 30: 473-490.

[8] Arnold, E. (1985) Phosphorus. In: Standard Methods for the Examination of Water and Wastewater, American Public Health Association.

[9] Rajeshwari, S., Sivakumar, S., Senthilkumar, P. and Subburam, V. (2001) Carbon from cassava peel, an agricultural waste, as an adsorbent in the removal of dyes and metal ions from aqueous solution. Bioresource Technology. 80.3: 233-235.

[10] Agyei, N.M. (2009) The mechanism of phosphate removal from aqueous solution by fly ash and slag. Fresenius Environmental Bulletin 18: 1614-1617.

[11] Langmuir, I. (1916) The constitution and fundamental properties of solids and liquids. Part I: Solids, Journal of the American Chemical Society 38: 2221–2295.

[12] Freundlich, H.M.F. (1907) Ueber die adsorption in Loesungen. Journal of Physics and Chemistry 57: 384–470.

Received: **12.10.2015**
Accepted: **24.02.2016**

CORRESPONDING AUTHOR

Nana M. Agyei
Department of Chemistry
Sefako Makgatho Health Sciences University
PO Box 235, Medunsa 0204, SOUTH AFRICA

e-mail: nana.agyei@smu.ac.za

© by PSP Volume 25 – No. 7/2016, pages 2519-2530 Fresenius Environmental Bulletin

ATMOSPHERIC LEVELS OF BTEXS, $PM_{2.5}$, PM_{10} AND HEAVY METALS AT ALGIERS CITY

Kerchich Yacine[a], Moussaoui Yacine[b], Kerbachi Rabah[c]

[a]University Dr. Yahia Fares, Medea, Ain D'heb, 26001, Medea, Algeria.
[b]University of Kasdi Merbah, Faculty of Mathematics and Materiel Sciences, Ouargla, Street of Ghardaia, 30.000, Ouargla, Algeria.
[c]National Polytechnic School, Laboratory of Sciences and Techniques of Environment, BP 132, El-Harrach, Algiers, Algeria.

ABSTRACT

This study presents the levels of air pollution by BTEX, $PM_{2.5}$ and PM_{10} and their content of heavy metals such as: lead (Pb), iron (Fe) and copper (Cu) at the background site in Algiers (Algeria) from April to November 2010. Radiello as a passive sampler was used for BTEX sampling and a high volume samplers (HVS) equipped with a cascade impactor at a four levels was used for particles collecting. The Radiello samplers was analyzed by gas chromatography equipped with flame ionization detector (GC-FID), while the heavy metals associated with $PM_{2.5}$ and PM_{10} particles were analyzed by atomic absorption spectrophotometer (AAS). Until the period sampling, the average concentration of $PM_{2.5}$ and PM_{10} were respectively 49.9 and 77.4 µg m^{-3}. While, the average concentration of benzene, toluene, ethylbenzene, (m+p)-xylene and o-xylene were respectively: 7.7; 29.5; 5.1; 15.5 and 6.1 µg.m^{-3}. All BTEXs and $Pb_{PM2.5}$ were strictly correlated with $PM_{2.5}$, the p-value were 0.034, 0.028, 0.045, 0.034, 0.021 and 0.044 respectively for benzene-$PM_{2.5}$, toluene-$PM_{2.5}$, ethylbenzene-$PM_{2.5}$, (*p*+*m*)-xylene-$PM_{2.5}$, o-xylene-$PM_{2.5}$ and $PM_{2.5}$-$Pb_{PM2.5}$. The ratios of (m+p)-xylenes vs. ethylbenzene was used in the order to identify the staying of the pollutants in the atmosphere. Both concentrations of PM_{10} and benzene exceeded largely the limits set by the European Union Directives (30/1999 and 69/2000). Within heavy metals detected in PM_{10} and $PM_{2.5}$, the lead was the most abundant with average concentration of 0.27 µg m^{-3}.This study shows clearly, the road traffic was the dominated source emission at Algiers City, in addition to this latter, other minor source were not excluded.

KEYWORDS:
PM_{10}, $PM_{2.5}$, benzene, toluene, ethylbenzene, and xylene, Heavy metals, Urban pollution, Algiers.

INTRODUCTION

The monitoring of air pollution by particles with aerodynamic diameter less than 2.5 µm ($PM_{2.5}$) and 10 µm (PM_{10}), and the mono-aromatic hydrocarbons such as benzene, toluene, ethybenzene and xylenes, also called BTEX, in crowded urban areas is a big concern for both scientists and local authorities, according to their harmful impact on the human health and environment [1].

According to their origin, both natural and anthropogenic fine particles found in the atmosphere are complex mixtures containing numerous chemical compounds that act as catalysts for many chemical reactions [2, 3]. In this respect, epidemiological studies have proved the harmful effects of PM_{10} and $PM_{2.5}$ even at low concentrations [4-10]. $PM_{2.5}$ are fine particles and so called alveolar particles, while PM_{10} are the coarse particles. Concerning BTEX, previous studies have shown that xylenes are highly reactive, they contribute to the ozone formation and hence to climate change [11]. BTEX cause various disorders in people exposed [12]. Several countries have recently revised their air quality guidelines and proposed new regulations. The European Union (EU) Air Quality Directives EC/30/1999 and EC/69/2000 established in 2010 the annual average limit of benzene and PM_{10}, set respectively at 5 µg.m^{-3} and 20 µg.m^{-3}. For PM_{10}, a daily value of 50 µg.m^{-3} in a limit of 7 days per year has also been fixed. Regarding $PM_{2.5;}$ the annual limit value has been set at 15 µg.m^{-3} by the American Environmental Protection Agency [13]. Several studies of air pollution caused by fine particles and BTEX in big cities worldwide showed that the principal emission source is the vehicle emissions. However, these pollutants are considered as a relevant tracer for the road traffic [14, 15].

Algiers is a metropolis exceeding 3.5 million inhabitants and hosting one million vehicles (2009) which corresponds to more than one fourth of the total national car fleet. During the last decade, the national traffic growth was essentially related to the use of cars as a mean of commuting. According to

the National Office of Statistics - Algeria (NOS), passengers using motor vehicles exceeded 88% of the total transport stream in 2004. The rate of car diffusion in Algiers, which reaches 35 vehicles for 100 people, is high with regards to developing countries. The automobile fleet is very older, when the average age reaching 11 years, and has a poor maintenance. Despite the fact that the car renewal rate in Algeria increased up to 5 % per year, most of the fleet is not equipped with catalytic converters [16]. As a consequence, air pollution in Algiers seems overall induced by the urban and inter-urban traffic, with vehicles using fuels which are not conform to environmental standards. Northern Algeria experiences today a rapid development in urbanization, which has a heavy impact on ambient pollution. Without any reliable air monitoring network in Algiers, which is necessary to make both population and authorities take precautions in case of air pollution events, only some monitoring data collected by scientists and researchers are available and can give an idea about the air quality in Algiers [17-20]. However, these data are still insufficient.

In this context, the present study is to evaluate the air pollution levels of mono-aromatic organic compounds (BTEX), $PM_{2.5}$ and PM_{10} and their content of heavy metals (Pb, Fe and Cu) in the urban area of Algiers and extend the literature.

MATERIALS AND METHODS

Sampling area and period. The sampling area is located in Bouzareah, Algiers (36° 48' 36" N, 3° 02' 18" E, altitude 350 m above the sea (Figure 1)). The site sampling is very close to the Mediterranean Sea and there the car traffic is high and frequent. Hence, ideal to determine the influence of urban and marine aerosol. Samples have been collected about 50 m away from the main road. The sampling campaign has been done daily until the period between April-November 2010. The meteorological data were obtained from National Office of Meteorology during the sampling period [21].

Sampling methods. PM_{10} and $PM_{2.5}$ sampling. The particulate matter was deposited onto glass fiber filters by using high-volume samplers (Model VFC, Anderson, USA) equipped with size-selective inlet cascade impactors. Particles were separated into two fractions, the former characterized by aerodynamic diameters lying between 2.5 and 10 µm and marked as $PM_{2.5-}$

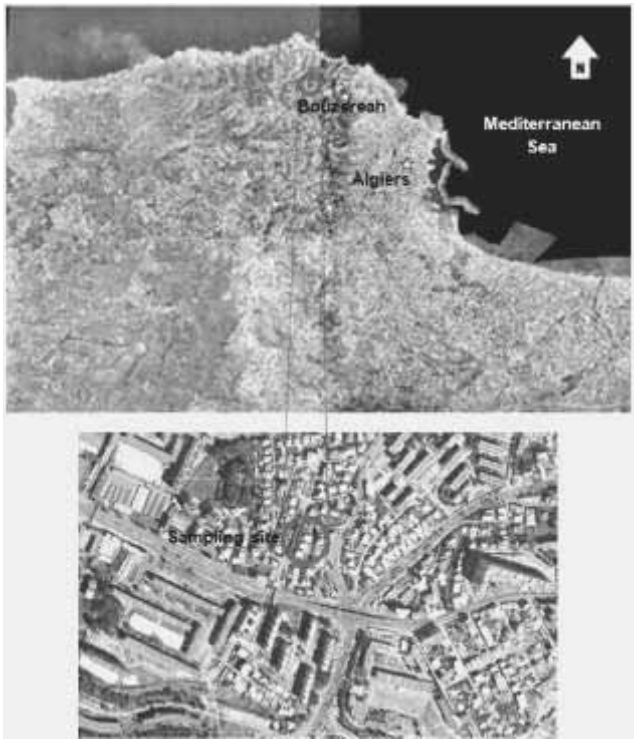

FIGURE 1
Map of the sampling site.

$_{10}$, the latter having an aerodynamic diameter less than 2.5 µm ($PM_{2.5}$). Particulates were collected over 24 h at 1.1 m^3 min^{-1} flow rate, every week day and starting at 8:00 am. Thus each sample corresponds to ~1584 m^3. Both the front fiberglass filter 10 x 12 cm^2 for PM_{10} and 20.3 x 25.4 cm^2 for $PM_{2.5}$ (GFF, Whatman) were previously conditioned in a room of constant relative humidity and temperature and were gravimetrically tarred [22], individually wrapped with aluminium foils and stored on pre-baked glass plates. The filter made on glass microfiber used as substrate collection of particles matter was weighted before (pre-sample) and after (sample) sampling at the same percentage of relative humidity (RH). After use, the loaded filters were wrapped again with aluminium foils, transported to the laboratory, and stored at low temperature (4 °C) until chemical processing, in order to prevent the analyte from any degradation. In total 130 samples were collected over the sampling campaign.

BTEX sampling. Monoaromatic hydrocarbons were collected by Radiello diffusive samplers, patented by Foundation Salvatore Maugeri (FSM). The samplers consisted of stainless steel net cylinder, with 100 mesh grid opening, packed with 530 mg of activated charcoal. The Radiello tubes have been exposed during the period of April-November 2010, each two weeks, a duplicate Radiello tubes exposed, which is enough to rich the concentration of pollutant in the sampling media. Every month, one Radiello tube was used as blank sample, in the total 32 tube have been collected.

Analysis. PM_{10}, $PM_{2.5}$ mass concentration measurements and heavy metals analysis. The particulate matter (PM_{10} and $PM_{2.5}$) mass was gravimetrically determined by weighting filters after drying for 48 hours in a desiccator. The heavy metal concentration (Pb, Fe and Cu) in each sample was determined by atomic absorption spectrometry (Model SOLAAR, Thermo Electron Corpor., Cambridge, UK) according to standard analytical procedures [23].

For total metal determination, particles matter $PM_{2.5}$ and PM_{10} sample collected into microfiber glass filter were digested using 10 mL nitric acid and 10 mL perchloric acid at 210 °C during 1.5 h. After cooling, 0.1 N HCl was added to fill a 100 mL volumetric flask [24] and the total amounts of metals (Pb, Fe, Cu) were measured by atomic absorption spectrometry (AAS). In addition, each sample was analyzed in triplicate. The overall recovery ratios of Pb, Cd and Cu (associated to $PM_{2.5}$ and PM_{10}) were 88–116% for Pb, 108–124% or Fe and 110–124% for Cu.

BTEX analysis. After sampling, the activated charcoal was transferred into a vial and first fortified with 10 µL of 2-fluorotoluene solution supplied by Supelco (internal standard with concentration of 10 µg mL^{-1}). Then, 2 mL of carbon disulfide (CS_2, purchased from Fluka, reference 84713; low in benzene, 99.5%) was added. The sample was slightly shaken during 30 min at room temperature.

Analyses of BTEX were performed on gas chromatography with flame ionization detection (GC-FID) (GC-17A, Shimadzu; Noisiel, France). The chromatographic column was Bentone 34/DNDP SCOT type (0.5 mm x 15 m; Supelco; Bellefonte, PA). The injector and detector temperatures were held at 250 °C. The column was kept at constant temperature of 90 °C for 15 min. Split injection of 5 µL; split ratio 25:1; were injected into column at 1 $mL.min^{-1}$ flow rate of Nitrogen used as carrier gas [20]. The compounds identification was carried out by comparing the features of the eluted sample peaks with those of authentic analyte standards and GC retention time. Each sample was injected twice and the average values have been reported. Blank tubes were analyzed in the same way as the samples and all results were corrected [25-26].

Quality assurance/Control. All analytical procedures were monitored using strict quality assurance and control measures. Laboratory and field blanks consisted of Radiello passive sampler devices were run in each field campaign. Three laboratory blanks and eight field blanks were analyzed in total.

External calibration combined with internal calibration (addition of internal standard 2-fluorotoluene 10 µL) procedure was adopted for BTEX analysis, five points of each compounds of BTEX family were prepared by dilution 10 $\mu g.mL^{-1}$ as mother solution, the calibration points were 10, 15, 20, 40 and 100 $\mu g.mL^{-1}$.

The detection limit (DL) of the method for each BTEX was determined as equal to three times the standard deviation of the signal obtained from three replicate measurements of blanks, divided by the slope of the calibration curve. DLs as low as 0.05 to 1 µg m^{-3} were achieved for the BTEX series.

All analytical results recorded exceeded the corresponding DLs. To evaluate the analyte recoveries, three blanks of passive sampling devices were spiked with the target BTEX from 0.04 to 35 mg L^{-1}. Recoveries ranged from 80 ± 5% to 110 ± 3%.

TABLE 1
Average concentrations of air pollutants recorded in Bouzereah-Algiers.

Pollutants	Number of samples	Monthly average concentration (µg.m^{-3})	Standard deviation	Minimum value (µg.m^{-3})	Maximum value (µg.m^{-3})
Bz.	28	7.73	3.30	3.25	12.03
Tol.	28	28.19	18.67	0.92	58.68
E.Bz.	28	5.54	5.66	2.08	18.02
(m,p)-Xyl.	28	15.99	8.51	2.65	29.93
o-Xyl.	28	6.34	3.53	2.65	12.00
$BTEX_{total}$	28	63.80	38.09	11.65	130.67
PM_{10}	130	77.40	18.00	40.9	105.6
Pb_{PM10}	90	0.273	0.10	0.11	0.670
Fe $_{PM10}$	90	0.258	0.10	0.110	0.60
Cu $_{PM10}$	90	0.250	0.10	0.10	0.790
$PM_{2.5}$	120	49.90	10.92	39.10	66.4
$Pb_{PM2.5}$	90	0.187	0.11	0	0.280
Fe $_{PM2.5}$	90	0.083	0.04	0	0.11
Cu $_{PM2.5}$	90	0.063	0.04	0	0.080

Bz.: Benzene,Tol.: Toluene, E.Bz.: Ethylbenzene, Xyl.: Xylene

RESULTS AND DISCUSSION

Concentration of BTEX, $PM_{2.5}$ and PM_{10}. The average concentrations of BTEX, $PM_{2.5}$, and PM_{10} heavy metal associated to the particles matter (average ± SD) measured in the urban site of Bouzareah, are shown in Table 1.

According to the table 1, the pollutants as benzene, particulate matter (PM_{10} and $PM_{2.5}$) and Pb are the most abundant among those recorded. Their concentrations ranged from 0.92 to 58.68 µg.m^{-3}; from 40.9 to 105.6 µg.m^{-3}; from 39.1 to 66.4 µg.m^{-3}and from 0 to 0.28 µg.m^{-3} for benzene, PM_{10}, $PM_{2.5}$ and Pb respectively. Among BTEX compounds recorded, toluene was the most abundant species, since it account between 12% and 44% of the total BTEX concentration.

However, the contribution of alveolar $PM_{2.5}$ fraction accounts about 64% of the average mass of PM_{10}. This indicates that $PM_{2.5}$ comprises a large fraction in PM_{10} in the study area. This result shows that PM_{10} measured in Bouzareah is highly enriched in alveolar particles and therefore have an adverse health effect. This result was also confirmed in the literature [27].

We can also see that lead has the highest level among analyzed heavy metals. With an average concentration of 0.273 µg.m^{-3}, it contributes about 0.32% of the total mass of particles matter ($PM_{2.5}$ or PM_{10}). Lead induced pollution in this area is lower than the limit value of 0.5 µg.m^{-3} recommended by WHO, but the limit value recommended by EU, which is 0.2 µg.m^{-3}, was slightly exceeded. Iron, which is partially a tracer of natural pollution, does not reach high levels.

This element remains, with copper, below the level of lead. The examination of the mass distribution shows that lead is distributed among various fractions of particles in a completely different way from those of iron and copper. Indeed, Fe and Cu are highly enriched in PM_{10} fractions while Pb is relatively enriched in $PM_{2.5}$. The mass fractions examination shows that the Pb is most abundant in $PM_{2.5}$, it represents 0.37% of $PM_{2.5}$ and 0.32% in PM_{10}. Conversely, Fe which is mainly from the earth's crust, was very abundant in PM_{10} (0.33%) than in $PM_{2.5}$ (0.17%). Therefore the results obtained were very similar than those recorded by Oucher et al., 2012 in urban area [27].

Lead founded at Bouzareah, mainly come from road traffic, which represent a main source emission, there is also two outcomes sources emissions, the farmer is the mineral dust emissions from desert in the warmer seasons [28], the latter is the sea salt emissions in the colder season [29], in addition to these sources, a minor contribution of some anthropogenic activities in this area (Repair car body garage and cement plant).

The results obtained in this study are an agreement with previous studies realized in the Mediterranean region, showing the influence of source emissions (road traffic, anthropogenic and natural emission) on the concentration of heavy metals associated with fine particles. The annual concentrations of lead in the ambient air varied between 0.2 and 0.5 µg.m^{-3} recorded in France, Spain and Italy [30-33].

The average concentration during the period sampling in the conducting study of benzene, $PM_{2.5}$ and PM_{10} are respectively 7.73 µg.m^{-3}, 49.9 µg.m^{-3} and 77.4 µg.m^{-3}. These levels exceed all international standards and represent around 1.5, 3 and 4 times respectively the limit of benzene (5 µg.m^{-3}), $PM_{2.5}$ (15 µg.m^{-3}) and PM_{10} (20 µg.m^{-3}) recommended.

The annual average concentrations of PM_{10} and $PM_{2.5}$ found are within the range of 9-100 µg.m^{-3}, levels measured in other studies conducted between 2008 and 2012 in 1600 cities [34]. For example, according to the some previous studies

conducted in big cities worldwide, the annual average concentration for PM_{10} was 63 $\mu g.m^{-3}$ in Rome (Italy, about 2.5 million inhabitants), 55 $\mu g.m^{-3}$ in Izmir (Turkey, about 3.4 million inhabitants) and 80 $\mu g.m^{-3}$ in Ahmedabad (India, about 3.6 million inhabitants) [34].

The annual average concentration for $PM_{2.5}$ was lower than those recorded at Antananarivo (Madagascar); with 59 $\mu g.m^{-3}$ and Ulaanbaatar (Mongolia) with 63 $\mu g.m^{-3}$ and higher than those founded at Liège (Belgium) with 20.8 $\mu g.m^{-3}$, Aalborg (Denmark) with 16.9 $\mu g.m^{-3}$and similar to those recorded at Kuwait City and Mexicali (Mexico) both with 51 $\mu g.m^{-3}$ [33, 34, 36].

The variation of the BTEX concentration recorded in this study is in good agreement with those recorded in previous studies. This study shows that benzene, toluene, ethylbenzene and total xylenes (m-, p- and o- isomers) measured at urban site in Bouzereah were lower than those measured at Rome (Italy) [37], Guangzhou, Nanhai and Macau (South China) [38] and at Cross Harbor (Hong Kong) [39]. However, they were higher than those measured at Algiers (winter and summer 2006-2007) [40], at Helsinki (Finland) [41], at Yokohama (Japan) [42], at Berlin (Germany) [43] and recorded at London (England) [43].

Regarding to the benzene, similar concentrations were recorded in Algiers in previous studies [20] (see Table 2).

Monthly variation. The monthly variation of BTEX, $PM_{2.5}$ and PM_{10} concentration is illustrated in the Figure 2 and 3. As shown, the concentration profiles over months of BTEX, $PM_{2.5}$ and PM_{10} present the same trend.

BTEX species exhibit remarkable monthly variation concentrations recorded in the study area. The observed trends can by explain by the characteristics of meteorological conditions (Table 3), variations in the source strength, the OH radical availability and insolation that keep the removal process of the VOC species of the atmosphere [44]. Generally, BTEX concentration levels are higher during cold seasons. This fact is related to the photochemical activity and heating sources. According to the Figure 2, BTEX concentration levels recorded during winter are higher than those recorded during summer (July and August), contrary in November, where the situation is reversed. This is probably due to the variation of outcome of atmospheric conditions, rainfall frequency of 63 % recorded in November and dilution of pollutants in this site. These results were confirmed by decreasing particulate matter concentration.

TABLE 2
BTEX levels in ambient air of various cities worldwide ($\mu g\ m^{-3}$).

Cities	Bz.	Tol.	E.Bz.	(m+p)-Xyl.	o-Xyl.
Helsinki [41]	2.1	6.6	1.3	4.1	1.6
Roma [37]	35.5	99.7	17.6	54.1	25.1
Yokohama (Japan) [42]	1.7-3.7	4.7-34.3	0.5-3.8	1.0-2.0	0.1-0.8
Berlin (Germany) [43]	6.9	13.8	2.8	7.5	2.9
London (England) [43]	2.7	7.2	1.4	3.7	1.5
Guangzhou. Nanhai and Macau (South China) Urban and road sites [38]	20-51.5	39.1-85.9	3-24.1	14.2-95.6**	-
Cross Harbor-Tunnel in Hong Kong [39]	30.51	200.82	15.07	45.67 **	-
Algiers (Roadside, background and rural) [20]	1.1-26.8	3.5-63.3	2-12	4.9-46.8	2.2-14.7
Present study	7.73	28.19	5.54	15.99	6.34

** (*o-*,*m-* and *p-*)Xylenes

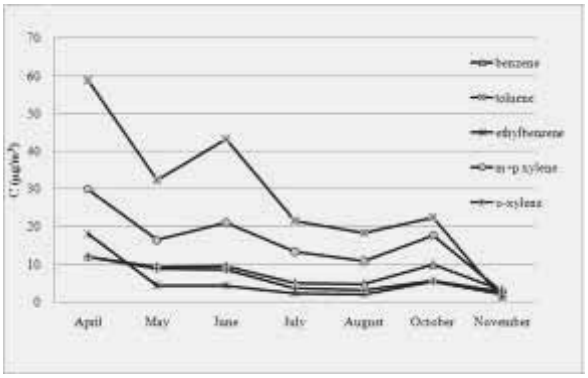

FIGURE 2
Monthly variations of BTEX concentrations.

Regarding to monthly variations of particulates in both size ranges PM_{10} and $PM_{2.5}$ (Figure 3), the highest average of $PM_{2.5}$ and PM_{10} are recorded in April, 52.1 $\mu g.m^{-3}$and 97.6 $\mu g.m^{-3}$ respectively, while those presenting low levels are recorded in May, July and August. Several studies show that levels of fine particles reach their maximum in autumn, winter and spring and decrease during summer [45]. In our case, the highest value coincides with the end of spring period. This trend is probably due to low rainfall (Rainfall frequency recorded during the month of April was 40%, however 70 % of the total precipitations per day were lower to 5 mm) occurring during sampling days and to the decreasing road traffic density during summer (see Table 3).

On the other hand, the results obtained with 95% confidence for a sampling period of 7 months for PM_{10} (mean + confidence limits) are (77.39 ± 10.83 $\mu g.m^{-3}$), $PM_{2.5}$ (30.79 ± 11.08 $\mu g.m^{-3}$), benzene (7.73 ± 2.39 $\mu g.m^{-3}$), toluene (28.19 ± 13.81), ethylene (5.54 ± 4.15), (p + m)-xylene (15.99 ± 6.23 $\mu g.m^{-3}$) and o-xylene (6.34 ± 2.59 $\mu g.m^{-3}$). These results show that the confidence limits values vary widely.

TABLE 3
Meteorological conditions during the sampling period.

Month	T	T_M	T_m	H	PP	%PP	V
April	15.9	19.8	15	68	47.3	40	17.0
May	17.4	22.7	16.6	52.8	00	0	17.5
June	20.9	24.8	19.9	62.3	00	0	8.9
July	26.2	28.1	22.5	67.2	00	0	14.5
August	25.0	28.1	22.4	68.2	40.1	8	10.7
October	17.9	24.4	18.1	55.5	13.5	17	15.3
November	13.8	19.7	14.3	57.1	171.5	63	14.7

T: Average temperature (°C), T_M: Average maximum temperature (°C), T_m: Average minimum temperature (°C), H: Average relative humidity (%), PP: Average precipitation and/or melting snow total (mm), %PP: rainfall frequency, V: Average wind speed ($km.h^{-1}$).

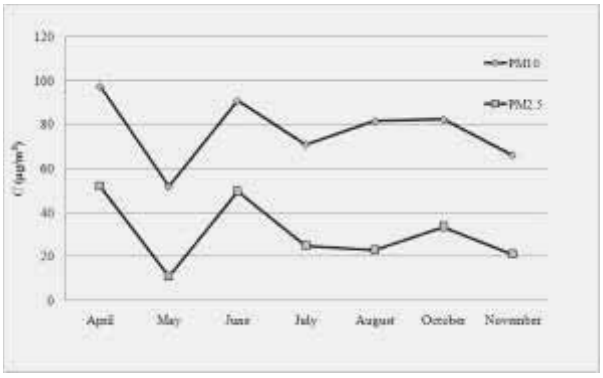

FIGURE 3
Monthly variations of PM10 and PM2.5 concentrations.

Inter-species correlation. Statistical analyses (Table 4) show that the concentrations of most important pollutants, benzene-$PM_{2.5}$ (p-value = 0.034), toluene-$PM_{2.5}$ (p-Value = 0.028), ethylbenzene-$PM_{2.5}$ (p-value = 0.045), (*p*+*m*)-xylene-$PM_{2.5}$ (p-value = 0.034), o-xylene-$PM_{2.5}$ (p-Value = 0.021) and $PM_{2.5}$-$Pb_{PM2.5}$ (p-value = 0.044) recorded during this study have good correlations. Regarding to lead, we can see there is no correlation between Pb and PM_{10} (r^2 = 0.12, $p < 0.05$). However, an acceptable correlation between concentrations of $Pb_{PM2.5}$ and $PM_{2.5}$ is observed. This implies that lead road traffic is associated with particles of $PM_{2.5}$.

PM_{10} might be induced by anthropogenic activities, geological dust, road dust suspension and secondary aerosol formation which is different from vehicle emission [14]. Also PM_{10} were induced by dust storm transportation to the site sampling from other places, which can have an important pollutant sources, hence the weak correlation between BTEX and PM_{10} obtained in the study area. However, an acceptable correlation between concentrations of $Pb_{PM2.5}$ and $PM_{2.5}$ is observed. This implies that lead road traffic is associated with particles of $PM_{2.5}$.

The mean correlation (r^2) between and BTEX-PM_{10} (r^2 = 0.6) is not as good as that found between BTEX-$PM_{2.5}$ (r^2 = 0.8) and PM_{10}-$PM_{2.5}$ (r^2 = 0.85). This fact can be explained by the several sources outcomes of BTEX and PM_{10}.

TABLE 4
Correlation coefficients among the main pollutants recorded in Bouzereah.

*N.S.		PM_{10}	$PM_{2.5}$	Pb_{PM10}	$Pb_{PM2.5}$	Bz.	Tol.	EBz	(m+p)-Xyl.	o-Xyl.
130	**PM_{10}**	1.00	0.85	0.30	0.29	0.63	0.47	0.63	0.48	0.74
120	**$PM_{2.5}$**	-	1	0.12	0.6	0.82	0.87	0.55	0.82	0.93
90	**Pb_{PM10}**	-	-	1	0.18	0.29	0.55	0.88	0.56	0.43
90	**$Pb_{PM2.5}$**	-	-	-	1	0.51	0.38	0.29	0.30	0.68
28	**Bz.**	-	-	-	-	1	0.78	0.55	0.90	0.82
28	**Tol.**	-	-	-	-	-	1	0.72	0.93	0.87
28	**EBz.**	-	-	-	-	-	-	1	0.73	0.65
28	**(m+p) - Xyl.**	-	-	-	-	-	-	-	1	0.80
28	***o*-Xyl.**	-	-	-	-	-	-	-	-	1

* Number of samples.

BTEX and PM_{10} ratios: spatial/monthly pattern Concerning the relative concentration of aromatic compounds, Nelson and Quigley [46] proposed the use of the ratio between (*m* + *p*)-xylene and ethylbenzene (X/E) to evaluate the extent of photochemical reactivity in the atmosphere in order to provide an indication of urban plumes age. Because ethylbenzene has a relatively long lifetime, lower values of X/E indicate a longer age [47]. In our study, an average X/E value of 3.7 for all results (Figure 4) has been estimated. This value is lower than compared to those reported in the literature, which is equal to 4.5 [43] and higher than those founded in Italy and China with average values of 3.1 and 2.97 respectively [14, 37].

This ratio is very useful to determine the staying of pollutants in the atmosphere, high values of this ratio means that air masses have stayed a long time in the atmosphere (old emissions) and low values of this ratio indicate that air masses are recent (fresh emissions). Kuntasal et al., 2005, gives a value of 3.8 for this ratio [48, 49]. Gasoline fresh emissions have shown ratio values between 3.8 and 4.4. In this study, the average ratio calculated, indicates that most air masses correspond to the "fresh emissions". However fresh emissions has as origin a local source, in this case the resulting emissions of road traffic, without exclude the industrial emissions, which represent a minor contribution in site of Bouzareah.

On this basis, the X/E ratio gives an indication about the fact that the pollutants freshly emitted, tend to stagnate in the sampling area or are produced elsewhere and then drift to the sampling area. However, for conclusive results about this point which is beyond the aim of this study, additional data are required.

Regarding to monthly variations of the $PM_{2.5}/PM_{10}$ ratio, the values varied between 20 and 60 %, the highest average ratio was recorded in July and the lowest was recorded in April (Figure 5).

Several previous studies conducted at 24 cities in USA and Canada has shown that the ratio of $PM_{2.5}/PM_{10}$ varied between 30 and 70%, depending on the location of measurement [50].

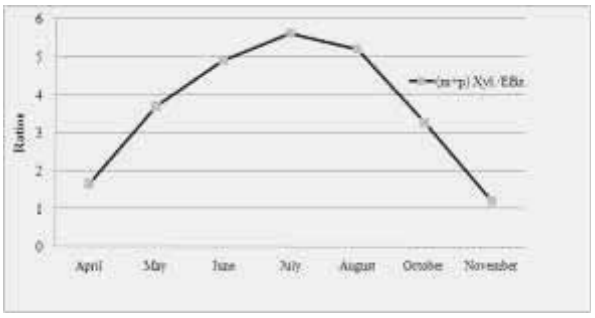

FIGURE 4
Monthly variation of ratios of (m+p)-Xyl./EBz.

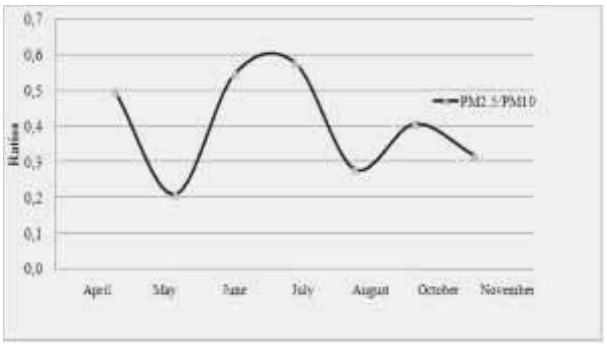

FIGURE 5
Monthly variation of ratios of PM2.5/PM10.

Others ratios found at different sites are presented in Table 5. The ratios found in Bouzareah are similar to those found at United Kingdom [51-52] and Canada [53], but lower to those recorded at Germany [54] and California [55].

Several factors influence $PM_{2.5}/PM_{10}$ ratio, which is increases with the emissions from motor vehicles and high-temperature processes [56]. It also increases as a result of stronger photochemical reactions or fewer resuspended coarse particles from road surfaces [56].

TABLE 5
$PM_{2.5}$ to PM_{10} ratios at different sites

Cities	Average (%)
Germany [54]	68
California [55]	50-66
United Kingdom [51]	60
United Kingdom [52]	55
Canada [53]	40
Present study	58

Other meteorological conditions, such as rain, solar radiation and atmospheric stability, may also affect the ratio [56]. Others studies were shown a $PM_{2.5}/PM_{10}$ ratio is generally higher during the heating period particularly in rural areas [57]. The highest value obtained in July is probably due to the number of Hours sunshine [58] that characterizes this month (10 Hours max.) And moderate winds (3.8 m/s) [21], recorded during this period (Table 3), which favored the slow dispersion of the particles and photochemical reactions.

Ranking of BTEX with respect to ozone formation. Potential and Reactivity with OH. The ozone formation potential (OFP) is the capacity of a VOCs contribution to the process that produces ozone. The amount of ozone produced doesn't only depend on the amount of VOC emitted but also on its reactivity. Carter and co-workers developed methods for ranking photochemical reactivity of VOC inducing ozone formation, one of the most widely used method is the Maximum Incremental Reactivity (MIR) [59]. They proposed to use the MIR scale for regulatory applications because it reflects the reactivity under environmental conditions which are most sensitive to effects of VOC controls [60-61].

TABLE 6
MIR coefficient, BTEX-OH rate constant and ranking of BTEX according to mass concentration, ozone formation potential and reaction with OH leading to formation of oxidants in Bouzereah, Algiers.

BTEX	MIR coeff.	OH·	BTEX ($\mu g.m^{-3}$)	[(a)] O_3 formation potential	[(b)] Reaction with OH
Bz.	0.42	1.23	12.03	5.05	4.64
Tol.	2.70	5.96	58.68	158.45	93.02
EBz.	2.70	7.10	18.02	48.67	29.56
(m, p) Xyl.	8.20	23.60	29.93	245.45	163.14
o-Xyl.	6.50	13.70	12.00	78.00	37.97

[a]BTEX x MIR, [b] BTEX in (ppb) x BTEX-OH· (10^{-12} cm^3/molecule/s) x10^{12}.

Using this scale, the ozone formation potential (OFP) is calculated by multiplying the average concentration registered by the MIR coefficient of each VOC species. These unitless MIR coefficients are intended for use in conditions displaying relatively high NO_x concentrations, which may be used as an important tool in ozone control programs. The reactivity of VOC with OH radical depicts the ability of the hydrocarbon to form higher oxidized products like aldehydes, ketones, acids, organic peroxy radicals, etc.

The ranking of BTEX species according to their mass concentration, to ozone formation potential and reaction with OH is given in Table 6. The rate constants of VOC-OH reactions and MIR coefficients were taken from the literature [60, 62-63]. Based on the MIR scale, xylenes (*m*-/*p*-xylene and *o*-xylene) are the most dominant contributors to ozone formation among BTEX and they represent 60% of the total ozone produced by the total BTEX covered in this study. This result is in a good agreement with the observation in Seoul [64] and Porto Alegre [65]. Toluene is the second largest contributor to ozone formation. Ozone formation potential of benzene is minimum, although it is the most hazardous species among BTEX.

Reaction of BTEX with OH radical, which leads to the formation of higher oxides, follows the pattern (*m*+*p*)-xylene > toluene > *o*-xylene > benzene > ethylbenzene for this urban site in Table 6. This pattern is confirmed by others authors [66].

CONCLUSION

The average concentrations of benzene, PM_{10}, $PM_{2.5}$ and Pb associate to the particles ($PM_{2.5}$ and PM_{10}) measured during the period April-November 2010 in urban area located in Bouzareah (Algiers, Algeria), varied respectively from 3.25 to 12.03 $\mu g.m^{-3}$, 40.9 to 105.6 $\mu g.m^{-3}$, 39.1 to 66.4 $\mu g.m^{-3}$ and 0 to 0.280 $\mu g.m^{-3}$. The levels recorded exceed greatly the annual average set at 5, 20, 15 and 0.2 $\mu g.m^{-3}$ respectively for benzene, PM_{10}, $PM_{2.5}$ and Pb required for urban areas by US-EPA and EU Air Quality. Concentration levels of different pollutants show monthly variations during the sampling period. The results obtained with 95% confidence for the sampling period showing confidence limits percentages vary widely. Road traffic, meteorological conditions of Algiers and pollutants reactivity could be responsible for those seasonal variations. The inter-species ratios of different species indicate the role of vehicular contribution to the high levels of BTEX, PM_{10} and $PM_{2.5}$ in the ambient air of Algiers. The correlation between different species also suggests that there could be only one predominant source, which could most likely be the vehicular emission in the case of BTEX, $PM_{2.5}$ and Pb. This study also enables the identification of the main BTEX ozone precursors. Results obtained in this study indicate that Bouzareah is highly affected by air pollution. It is necessary to adopt policies to improve air quality in Algiers City. These policies should include the implementation of measuring air quality stations to intervene in the situation when the regulated pollutants limit will be exceeded.

REFERENCES

[1] De Vizcaya-Ruíz, A., Sordo-Cedeño, M., and Ostrosky-Wegman, P. (2006). Effect of chemical composition on the induction of DNA damage by urban airborne particulate matter. Environmental and Moleculr Mutagenesis. 47, 199-211.

[2] Feilberg A., and Nielsen, T. (2000). Effect of aerosol chemical composition on the photodegradation of nitro-polycyclic aromatic hydrocarbons. Environment Science Technology. 34, 789-97.

[3] Turpin BJ, Saxena, P., Andrews, E. (2000). Measuring and simulating particulate organics in the atmosphere: problems and prospects. Atmospheric Environment. 34, 2983-3013.

[4] Samet, J.M., Zeger, S.L., Dominici, F., Curriero, F., Coursac, I., Dockery, D.W.,

Schwartz, J., Zanobetti., A. (2000b). The national morbidity, mortality, and air pollution study. Part II: morbidity and mortality from air pollution in the United States. Research Report/Health Effect Institute 94, 5-70.

[5] Peters, A., Dockery, D.W., Muller, J.E., and Mittleman., M.A. (2001). Increased particulate air pollution and the triggering of myocardial infarction. Journal of the American Heart Association 103, 2810-2815.

[6] Pope, C.A., Burnett, R.T., Thun, M.J., Calle, E.E., Krewski, D., Ito, K., and Thurston, G.D. (2002). Lungcancer, cardiopulmonary mortality, and long-term exposure to fine particulate air pollution. Journal of the American Medical Association 287, 1132-1141.

[7] Ozelkan, E., Karaman, M., Mostamandy, S., Uca Avci, Z.D., Toros, H., (2015). Derivation of PM_{10} levels using OBRA on LANDSAT 5 TM images: a case study in Izmir, Turkey. Fresenius Environmental Bulletin. 24 (4), 1585-1596.

[8] Wang, S.M., Yu, H., Song, L., Xie, Y.C., Zhu, Q.H., (2015). Air quality in a mountainous City: A case study in Chongqing, China. Fresenius Environmental Bulletin. 24 (9), 2699-2706.

[9] Vicente, A.B., Sanfeliu, T., Jordan, M.M., Pardo, F., (2013). PM_{10} air quality assessment in an industrialized area of the Mediterranean Basin. Proposal for an air quality plan. Fresenius Environmental Bulletin. 22(3), 870-878.

[10] Dundar, M.S., Altundag, H., Yilmazcan, O., Kaygaldurak, S., (2013). Determination of some heavy metal contents in PM_1 and PM_{10} airborne particulate matters by AAS analysis. Fresenius Environmental Bulletin. 22 (11), 3179-3183.

[11] Finlayson-Pitts, B.J., and Pitts, J.N. (1993). Atmospheric chemistry of tropospheric ozone formation: scientific and regulatory implications. Journal of Air and Waste Management Association. 43,1091-1100.

[12] WHO (World Health Organization). (1996). Updating and revision of the air quality Guidelines for Europe. EUR/ICP/EHAZ9405/MT12. WHO Regional Office for Europe, Copenhagen.

[13] EPA.1997. EPA's Office of Air Quality Planning and Standards (National Ambient Air Quality Standards). Environmental Protection Agency, Washington DC.

[14] Iovino, P., Salvestrini, S., and Capasso, S. (2007). Background atmospheric levels of aldehydes, btex and PM10 pollutants in a medium-sized city of southern Italy. Annali di Chimica, 97, by Società Chimica Italiana.

[15] Sharma, K., Singh, R., Barman, S. C., Mishra, D., Kumar, R., Negi, M.P.S., Mandal, S. K., Kisku, G., Khan, C.A.H., Kidwai, M.M., Bhargava., S.K. (2006). Comparison of Trace Metals Concentration in PM10 of Different Locations of Lucknow City, India. Bulletin of Environmental Contamination and Toxicology. 77, 419-426.

[16] NOS (National Office of Statistics), Algeria. (2010). http://www.ons.dz. accessed on March 20, 2010.

[17] Kerbachi, R., Boughedaoui, M., Bounoua, L., and Keddam, M. 2006. Ambient air pollution by aromatic hydrocarbons in Algiers. Atmospheric Environment. 40:3995– 4003. doi:10.1016/j.atmosenv.2006.02.033

[18] Ladji, R., Yassa, N., Baldicci, C., Cecinato, A., Meklati, B.Y. (2009). Annual variation of particulate organic compounds in PM10 in the urban atmosphere of Algiers. Atmospheric Research. 92, 258-269.

[19] Moussaoui, Y., Balducci, C., Cecinato, A., and Meklati, B.Y. 2010. Chemical composition of extractable organic matter of airborne particles in urban and rural atmospheres of northern Algeria. Fresenius Environmental Bulletin. 19,2497-2508.

[20] Kerchich, Y., Kerbachi., R. (2013). Measurement of BTEX (benzene, toluene, ethybenzene, and xylene) levels at urban and semirural areas of Algiers City using passive air samplers. Journal of the Air & Waste Management Association. 62, pp. 1370-1379.

[21] NOM (National Office of Meteorology), Algiers. (2010). http://www.meteo.dz (accessed on March 10, 2010).

[22] USEPA-Method IO-3.1. (1999). Compendium of Methods for the Determination of Inorganic Compounds in Ambient Air; EPA/625/R-96/010a. Selection, Preparation and Extraction of Filter Material.

[23] USEPA-Method IO-3.2. (1999). Compendium of Methods for the Determination of Inorganic Compounds in Ambient Air; EPA/625/R-96/010a. Determination of Metals in Ambient Particulate Matter Using Atomic. Absorption (AA) Spectroscopy.

[24] Risser, J.A., and. Baker, D.E. (1990). Plant Analysis. In: Westernman, R.L., (Ed.), Soil Testing and Plant Analysis. Part III SSSA. SSA, U.S.A., pp: 390-427.

[25] Fondazione Salvatore Maugeri, Italy. 2008. Instructin manual for Radiello sam-pler. http://www.radiello.com (accessed June 26, 2008).

[26] www.sigma-aldrich.com/supelco.(1995).

[27] Oucher,N., and Kerbachi., R. (2012). Evaluation of Air Pollution by Aerosol Particles Due to Road Traffic: A Case Study

from Algeria. Procedia Engineering. 33, 415-423.

[28] Ladji, R., Yassaa, N., Balducci, C., Cecinato, A. (2010). Organic components of Algerian desert dusts. Chemosphere .81, 925-931.

[29] Moussaoui, Y., Boumechhour, A., Jaffrezo, J.L., and Meklati, B.Y. (2013). The chemical composition of inorganic and carbonaceous materials in PM_{10} from urban and rural Algerian areas. Fresenius Environmental Bulletin. 22, 1357-1366.

[30] López J.M., Callén, M.S., Murillo, R., García, T., Navarro, M.V., de la Cruz, M.T., and Mastral, A.M. 2005. Levels of selected metals in ambient air PM10 in an urban site of Zaragoza (Spain). Environmental Research. 99, 58-67.

[31] Chalbot, M.C., Lianou, M., Vei, I.C., Kotronarou, A., and Kavouras, I. G. (2013). Spatial attribution of sulfate and dust aerosol sources in an urban area using receptor modeling coupled with Lagrangian trajectories. Atmospheric Pollution Research. 4, 346-353.

[32] Mbengue, S., Alleman, L. Y., and Flament. P. (2014). Size-distributed metallic elements in submicronic and ultrafine atmospheric particles from urban and industrial areas in northern France. Atmospheric Research. 135-136, 35-47.

[33] EEA (European Environment Agency). (2014). Air quality in Europe. N°5. Available from: www.eea.europa.eu/.../air-quality-in-europe-2014. 15 August 2015. ISSN 1977-8449.

[34] WHO. (2010). Annual means PM_{10} by city. Available from: www.who.int/gho/phe/.../oap_city_2003_2010.xls, accessed 2 May 2011.

[35] MEF (Ministère de l'environnement et des Forêts). 2007. Rapport sur l'Etat de
l'Environnement de Madagascar, Madagascar.

[36] W. B (The World Bank. Air pollution in Ulaanbaatar). (2009). Discussion Paper. 2009.

EEA (European Environment Agency). 2011. Air Base: public air quality database - Air pollution. Available from: http://www.eea.europa.eu/themes/air/airbase, accessed 2 May 2011.

[37] Brocco, D., Fratarcangeli, R., Lepore, R., Petricca, M., and Ventrone, I. (1997). Determination of aromatic hydrocarbons in urban air of Rome. Atmospheric Environment. 31, 557-566. doi:10.1016/S1352-2310(96)00226-9.

[38] Wang, X.M., Sheng, G.Y., Fu, J.M., C.Y., Chan, Lee, S.C., Chan, L.Y., and Wang, Z.S. (2002). Urban roadside aromatic hydrocarbons in the three cities of the Pearl River Delta, People's Republic of China. Atmospheric Environment. 36, 5141-5148. doi:10.1016/S1352-2310(02)00640-4.

[39] Ho, K.F. Lee, S.C., Guo, H., and Tsai, W.Y. (2004). Seasonal and diurnal variations of volatile organic compounds (VOCs) in the atmosphere of Hong Kong. Science of the Total Environment. 322, 155-166. doi:10.1016/j.scitotenv.2003.10.004.

[40] Kerchich, Y., Kerbachi, R., Khatraoui, H. (2011). Ambient air levels of aromatic organic compounds BTEX in the urban area of Algiers. Asian Journal of Chemistry. 23, 323–330.

[41] Hellén, H., Hakola, H., Laurila, T., Hiltunen, V., and Koskentalo, (2002). T. Aromatic hydrocarbon and methyl tert-butyl ether measurements in ambient air of Helsinki (Finland) using diffusive samplers. Science of the Total Environment. 298, 55-64.

[42] Yamamoto, N., Okayasu, H., Murayama, S., Mori, S., Hunahashi, K., and Suzuki, K. (2000). Measurement of volatile organic compounds in the urban atmosphere of Yokohama, Japan, by an automated gas chromatographic system. Atmospheric Environment. 34, 4441-4446. doi:10.1016/S1352-2310(00)00168-0.

[43] Monod, A., Sive, B.C., Avino, P., Chen, T., Blake, D.R., and Rowland, F.S. (2001). Monoaromatic compounds in ambient air of various cities: A focus on correlations between the xylenes and ethylbenzene. Atmospheric Environment. 35, 135-149. doi:10.1016/S1352-2310(00)00274-0.

[44] Singh, HB., and Zimmerman, PB. (1992). Atmospheric distributions and sources of nonmethane hydrocarbons. In: Nriagu JO, editor. Gaseous Pollutants: Characterization and Cycling. New York, USA: Wiley. pp. 177-225.

[45] Cheng, Y., Ho, K.F., Lee, S.C., and Law, S.W. (2006). Seasonal and diurnal variations of $PM_{1.0}$, $PM_{2.5}$ and Pm_{10} in the roadside environment of hong kong, China Particulogy. Vol. 4, No. 6, 312-315.

[46] Nelson, P.F., and Quigley, S.M. (1983). The m,p-xylenes:ethylbenzene ratio. A technique for estimating hydrocarbon age in ambient atmosphere. Atmospheric Environment. 17, 659-662. doi:10.1016/0004-6981(83)90141-5.

[47] Atkinson, R. (1990). Gas-phase tropospheric chemistry of organic compounds. Atmospheric Environment. 24A:1-41.

[48] Kuntasal, O. O., Karman, D., Wang, D., Tuncel, S., Tuncel, G. (2005). Determination of volatile organic compounds in microenvironments by multibed adsorption and short-path thermal desorption followed by

gas chromatographic-mass spectrometric analysis, Journal of Chromatography A. 1099, 43-54.

[49] Ceron-breton, J. G., Ceron-breton, R. M., Rangel-marron, M., Villarrealsánchez G., and Uresti-gómez, A.Y. (2013). Determination of BTX levels in ambient air of one urban site located at the southwest of Mexico City during spring. Recent Advances in Energy, Environment, Economics and Technological Innovation. pp.19-27. ISBN: 978-960-474-343-8.

[50] Spengler, J. D., Koutrakis, P., Dockery, D.W., Raizenne, M., and Speizer, F.E. (1996). Health effects of acid aerosols on North American children: air pollution exposures. Environmental health perspectives. 104, 492-499.

[51] Dockery, D.W., and Pope, C.A. (1994). Acute respiratory effects of particulate air pollution. Annual Review of Public Health. 15, 107-132.

[52] Janssen, N.A.H., Van Mansom, D.F.M., Van de Jagt, K., Harssema, H., and Hoek, G. (1997). Mass concentration and elemental composition of airborne particulate matter at street and background locations. Atmospheric Environment. 31, 1185-1193.

[53] Cheng, L., Sandhu, H.S., Angle, R.P., and Myrick, R.H. (1998). Characteristics of inhalable particulate matter in Alberta cities. Atmospheric Environment. 22, 3835-3844.

[54] Israel, G.W., Erdmann, A., Shen, J., Frenzel, W., and Ulrich, E.1992. Analyse der Herkunft und Zusammensetzung der Schwebestaubimission. Report of Technical University Berlin. Germany UBA F+E No. 10402597.

[55] Chow, J.C., Watson, J.G., Fujita, E.M., Lu, Z., Lawson, D.R., and Ashbaugh, L.L. (1994). Temporal and spatial variations of $PM_{2.5}$ and PM_{10} aerosol in the Southern California air quality study. Atmospheric Environment. 28, 2061-2080.

[56] Sun, C.H., Lin, Y.C., and Chiu-Wang, S.W. (2003). Relationships among Particle Fractions of Urban and Non-urban Aerosols. Aerosol and Air Quality Research, Vol. 3, No. 1, pp.07-15.

[57] Gomišček, B., Hauck, H., Stopper, S., and Preining, O. (2004). Spatial and temporal variations of PM1, PM2.5, PM10 and particle number concentration during the AUPHEP-project. Atmospheric Environment. 38, 3917-3934.

[58] Zhang, R.J., Cao, J.J., Lee, S.C., Shen, Z.X., and Ho, K.F. (2007). Carbonaceous aerosols in PM_{10} and pollution gases in winter in Beijing. Journal of Environmental Science. 19, 567-571.

[59] Carter, W.P.L. (1997). Maximum Incremental Reactivity Excel Spreadsheet.

[60] Carter, WPL. (1994). Development of ozone reactivity scales for volatile organic compounds. Journal of the Air & Waste Management Association. 44, 881-99.

[61] Weir, B.R., Rosenbaum, A.S., Gardner, L.A., Whitten, G.Z., and Carter., W. (1988). Architectural Coatings in the South Coast Air Basin: Survey, Reactivity, and Toxicit Evaluation, Final Report to the South Coast Management District, SYSAPP-88/137, Systems Applications, Inc., San Rafael, CA (December).

[62] Atkinson, R. (1997). Gas-phase tropospheric chemistry of volatile organic compounds 1. Alkanes and alkenes. Journal of Physical and Chemical Reference Data. 26, 215-90.

[63] Carter, WPL. (1990). A detailed mechanism for the gas-phase atmospheric reaction of organic compounds. Atmospheric Environment. 24A, 481-518.

[64] Na, K., Moon, KC., and Kim. Y.P. (2005). Source contribution to aromatic VOC concentration and ozone formation potential in the atmosphere of Seoul. Atmospheric Environment. 39, 5517-24.

[65] Grosjean, E., Rasmussen, R.A., Grosjean, D. (1998). Ambient levels of gas phase pollution in Porto Alegre, Brazil. Atmospheric Environment. 32, 3371-9. Available from: http://pah.cert.ucr.edu/~carter/rcttab.htm. accessed 15 June 2015.

[66] Raza, R.H., Khillare, P.S., Agarwal, T., Shridhar, V., and Balachandran., S. (2008). Spatial and temporal variation of BTEX in the urban atmosphere of Delhi, India. Science of the total environment 392, 3.0-40.

Received : **28.10.2015**
Accepted : **24.12.2015**

CORRESPONDING AUTHOR

Yacine Kerchich
University Dr. Yahia Fares
Medea, Ain D'heb, 26001, Medea – ALGERIA

e-mail: y_kerchich@hotmail.com

© by PSP Volume 25 – No. 7/ 2016, pages 2531-2538 Fresenius Environmental Bulletin

LEVANT VOLES (MICROTUS GUENTHERI (DANFORD AND ALSTON 1880)) PREFER SOUTHERLY-FACING SLOPES IN AGRICULTURAL SITES AT HATAY, TURKEY

Mustafa Yavuz, Mehmet Rizvan Tunc

Akdeniz University, Faculty of Sciences, Department of Biology, Campus 07058 Antalya-TURKEY

ABSTRACT

In this study, *Microtus guentheri's* preferred habitat type and characteristics (aspect, slope etc.) were studied. 234 (113 ♀♀; 121 ♂♂) individuals were caught as dead and 118 (52 ♀♀; 66 ♂♂) as living, then living individuals were tagged, measured, and released. The samples were taken from the various habitats found within the province of Hatay (Turkey), during June-August 2010. Respectively, among the 234 dead and 118 living voles, 112 (47.86%) and 53 (44.92%) were from agricultural areas, 103 (44.02%) and 56 (47.46%) from roadsides near to agricultural areas, 19 (8.12%) and 9 (7.63%) were caught in grasslands. In the sample of 234 dead and 118 living voles, 158 (67.52%) and 73 (61.86%) were caught in areas with slopes of 31-60°. In those areas with slopes of 0-45°, there were strong positive correlations between the capture frequency in traps and the slope ($r_{snaptrapping}$=0.911; p<0.0001 and $r_{livetrapping}$=0.897; p<0.001). On the other hand, a very strong negative correlations were found between capture frequency and slope for the areas with slopes of 46-90° ($r_{snaptrapping}$= -0.933; p<0.002 and $r_{livetrapping}$= -0.874; p<0.002). Most of the individuals in traps ($n_{snaptrapping}$= 171; 73.08% and $n_{livetrapping}$=84; 71.19%) were captured on south, southeast, and southwest exposures, but did not differ between east and west. Also, the highest mean temperature were found on slopes of 30-60° in the south-facing sites. Moreover, there are significant positive correlations between altitude of sites and frequency of capture in snaptraps and Sherman livetraps ($r_{snaptrapping}$=0.941; n=6; p=0.001, $r_{livetrapping}$=0.903; n=6; p=0.001, respectively). So, while altitude of sites increase, trapping success and population density ($r_{density}$=0.938; n=6; p=0.001) are on the increase.

KEYWORDS:
Microtus guentheri, Hatay, preferences, exposure, slopes

INTRODUCTION

Microtus guentheri is found in particularly high numbers in clover and wheat fields and their neighbouring roadsides. It can be said that, As voles generally prefer to live in colonies in areas with dense vegetation, especially steppe, grassy plains and agricultural or fallow fields, they were seen to have concentrated on the edges of crop fields or fallow fields [1]. As voles prefer to make their burrow systems by the roadside and on sloping agricultural land, the like this areas in our study are at highest risk of invasion by voles.

Rodents of the Family Arvicolidae, and especially members of the genus *Microtus* Schrank (1798) are where agriculturally important. These species cause a great amount of damage to agricultural products. Most rodents are known to be prolific, their populations reaching high numbers within a short time [1,2,3,4,5,6]. They are also known to cause great damage not only to grassland vegetation [7] but also to agricultural crops [8,9,10,11,12]. According to Yiğit et al. [6], there are six species of rodents in Turkey (*Microtus guentheri, M. socialis*, *Spermophilus citellus*, *S. xanthaprymnus*, *Spalax leucodon* and *S. ehrenbergi*) which are "extremely harmful to agriculture". In a parallel study to the above, Özkurt et al. [13] examined the damaging effects of the species *M. guentheri* on agricultural crops, but gave only partial brief information relating to their life history and ecological characteristics. For this reason, particularly in regions where agricultural activity is a major source of income, attention must be given to understanding the ecology of these species and the various ways in which they are helpful or harmful to their environment.

What is the importance, understanding the ecology of these species? As Turkey is an agricultural country, any damage to its agricultural produce has a significant impact on the economy. A large budget is put aside and much time and effort are spent each year to prevent agricultural damage and to keep disturbance to non-targeted species into a minimum [14, 15,16]. Unfortunately there are

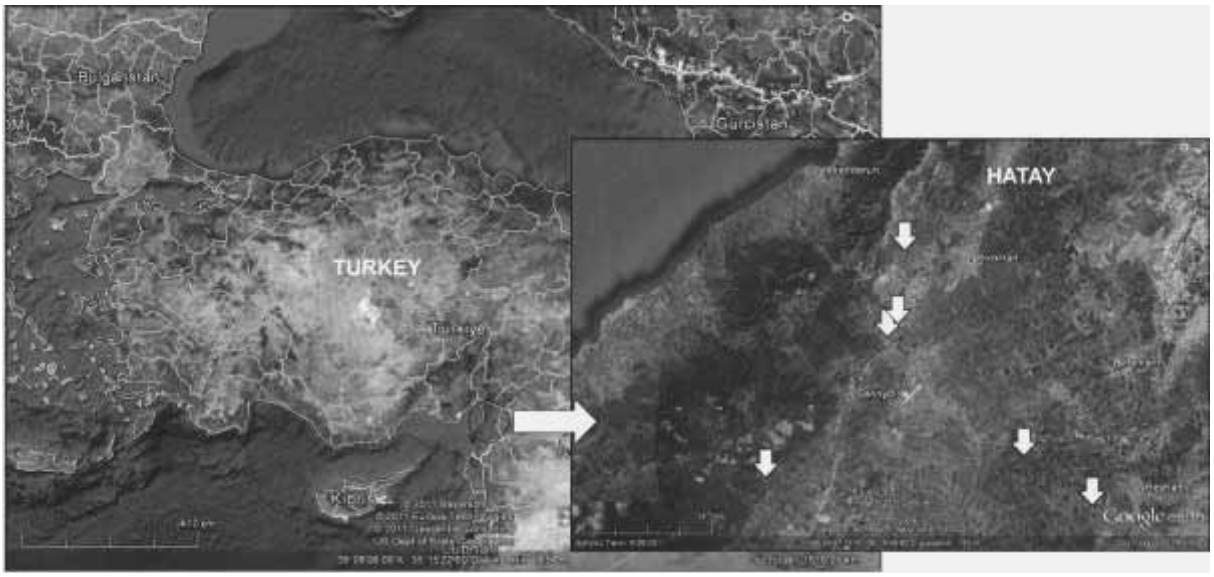

FIGURE 1
Map of southern Turkey showing locations of study sites.

only a limited number of studies on the ecology and habitat preferences of the voles in Turkey [1,6,13,17,18,19,20,21,22].

In this study, *Microtus guentheri*, which is widespread in the Hatay region, which is a town/province in south-eastern Anatolia in Turkey, was investigated. Its preferred habitat type and characteristics (exposure, slope etc.) were studied.

MATERIALS AND METHODS

This research is based on 234 (113 ♀♀; 121 ♂♂) dead and 118 (52 ♀♀; 66 ♂♂) living voles, taken from the various habitats (agricultural land, roadside and grassland) found within the province of Hatay (Turkey), during June-August 2010.

Field studies and observations. Levant voles were caught in various habitats in six trapping areas (Kırıkhan, Serinyol, Derince, Karlısu, Reyhanlı, and Karahüyük) (Fig. 1). In each site where sample was collected the habitat type, the degree of slope, its exposure to the sun, and the diameter of the burrow holes in the nearby surrounding area were recorded.

The samples for calculating trapping efforts and density in habitats were taken, in Antalya and surrounding areas by placing 100 snaptraps and 20 Sherman live traps in each site, independently trap type of each other, specified according to the degree of its slope and its exposure. Fifty snaptraps were set on south-facing slopes and fifty snaptraps set on north-facing slopes at suitable locations two hours before sunset on the day of arrival in the field and checked the following morning one hour before sunrise or at sunrise (snaptrapping). All of the live traps were set in the morning and checked the following morning (livetrapping). Only one trap was placed in 10 m^2, approximately. If any live individuals were caught, the dorsal fur was dyed for calculating population density (see below), and it was noted if these voles were recaptured. The bait used in the traps consisted of roasted peanuts mixed with some chewed bread. Each site was surveyed for a total of five days (per five days x one year), for a total of 500 snaptrap-nights and 100 sherman live trap-nights per site, and 4000 snaptrap-nights and 800 sherman live trap-nights in the study as a whole.

In addition, data were collected on the population density and degree of slope of the site in which the voles were caught. Population density was calculated with Mark-Recapture Population Sampling Method of Lincoln-Peterson.

According to this method, during the first trapping, an initial random sample of individuals was captured in live traps. Live individuals were then marked by the dorsal fur dyeing and released. During the second trapping, a second random sample of the individuals was captured. Some of these animals were marked animals and others were not. Then following mathematical equation was used to determine an estimate the total number of animals in the population for each slope groups [23,24]:

N = MC/R

N = Estimate of total population size
M = Total number of animals captured and marked on the first trapping ("Marked" animals)

C = Total number of animals captured on the second trapping ("Captured" animals)
R = Number of marked animals recaptured on the second trapping ("Recaptured" animals)

In order to investigate the relationship between temperature changes with exposure and population dynamics, the temperature was taken in burrow tunnels located in fields with varying degrees of slope. A pocket thermometer was placed in the gallery entrance or exit holes at a depth of 20-25 cm. Data were collected on the same day between 12 noon and 1 pm (daytime) and between 11 and 12 pm (nighttime). As no burrow systems were found on slopes from 81-90°, the temperatures here were measured by placing a thermometer in the soil at a depth of 25 cm.

Statistical analysis. To determine the habitat preferences of the species captured, the slopes of capture sites were divided into two groups: 0-45° and 46-90°, to ensure normality and homogeneity of data distribution. The relationship between slope and frequency of capture was evaluated using the Pearson correlation and least-square regression. Next, the Student's-t test was performed to investigate whether there was any difference in the average frequency of capture between the two groups living on different degrees of slope.

While investigating preferences for topographic exposure of burrow system, the data were again divided into two main groups: the first South group (all of the Southeast, South, and Southwest data points were grouped) and the second North group (all of the Northeast, North, and Northwest data were grouped). The values for East and West exposures were assumed to be an average for both groups. The Student's t-test was also used to test for differences in frequency of capture between the two exposure groups. To measure the way in which temperature is affected by topographic exposure, burrow systems' temperatures were divided into the same exposure groups (South and North). First we compared the average burrow systems temperature for South and North facing slopes using the Student's-t test. Following this, the variability of day and night temperatures and the difference between them were confirmed using Pearson Correlation. ANOVA was used to test the relative importance of temperature and slope exposure on vole numbers. The use of the sign was acceptable only at low values of $p<0.05$).

RESULTS

Research areas, locations of captures, and number of voles investigated. The samples of *M. guentheri* caught by snaptraps and sherman traps were collected in eight localities (see above) in Hatay. There were total of 234 individuals at snaptrapping, including 113 ♀♀ (48.29%) and 121 ♂♂ (51.71%). Also, there were total of 118 individuals are captured at live traps (52 ♀♀ (44.07%) and 66 ♂♂ (55.93%)).

There were significant positive correlations between altitude of sites and frequency of capture in snaptraps and sherman traps ($r_{snaptrapping}=0.941$; n=6; p=0.001, $r_{livetrapping}=0.903$; n=6; p=0.001, respectively). Furthermore, while altitude of sites increased, trapping success and population density ($r_{density}=0.938$; n=9; p=0.001) also increased.

Preferred habitat type. It was observed that voles' burrow systems are generally made in the unploughed strip at the edge of agricultural fields and on roadsides. For snaptraps, 112 (47.86%) individuals were caught in agricultural areas, 103 (44.02%) in roadsides near to agricultural areas, and 19 (8.12%) were caught in grasslands. For sherman traps, 53 (44.92%) individuals were caught in agricultural areas, 56 (47.46%) from roadsides near to agricultural areas, and 9 (7.63%) were caught in grasslands. *M. guentheri* was not encountered in other habitat types. Moreover, population densities reflect these capture rates 276 (57.62%) individuals were estimated from agricultural areas, 128 (26.72%) from roadsides near to agricultural areas and only 75 (15.66%) were estimated from grasslands.

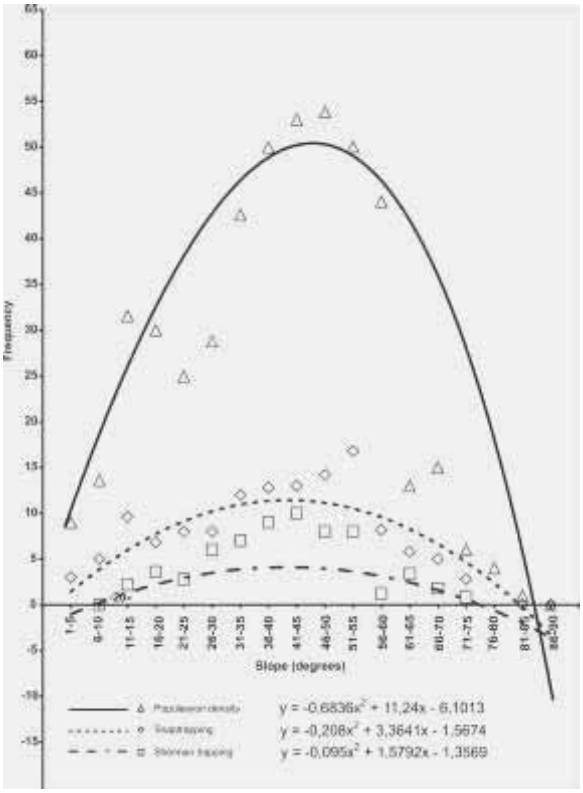

FIGURE 2
Frequency of voles caught and population density as a function of slope.

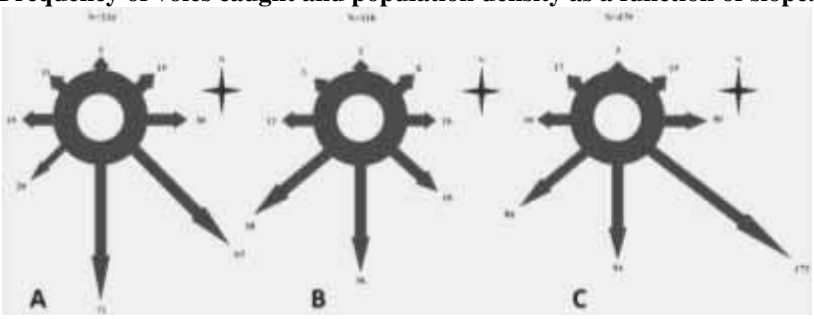

FIGURE 3
A. Capture frequencies in snaptraps according to compass direction of slope exposure; B. Capture frequencies in sherman traps according to compass direction of slope exposure; C. Population densities according to compass direction of slope exposure.

Preferred degree of slope for nesting sites on habitat . The relationships between the degree of slope and frequency of capture in snaptraps, frequency of capture in Sherman traps, and population density are given in Figs 2, 3 and 4. An equal trapping effort of 100 x 5 days snaptraps and 20 x 5 days Sherman traps each was made for steep and shallow slopes. Most individuals in snaptraps and Sherman traps (n = 158, 67.52% and n = 73, 61.86%, respectively) were caught in areas with slopes of 31-60°. Population density was also very high at these areas (see Fig. 2). For slopes of 0-45°, there were strong positive correlations between the slope and frequency of capture in snaptrap ($r_{snaptrapping}$ = 0.911; n = 9; p < 0.0001) and Sherman trap ($r_{livetrapping}$ = 0.897; n = 9; p < 0.001), as well as between slope and population density ($r_{density}$ = 0.965; n = 9; p < 0.001). On the other hand, for areas with slopes of 46-90° there were strong negative correlations between slope and frequency of capture in snaptrap ($r_{snaptrapping}$ = -0.933; n = 9; p < 0.002) and Sherman trap ($r_{livetrapping}$ = -0.874; n = 9; p < 0.002), and between slope and population density ($r_{density}$ = -0.876; n = 9; p <0.001) (Fig. 2). In areas with 0-45° slopes 143 individuals were caught in the snaptraps and 66 individuals Sherman traps, whereas on slopes of 46-90°, 91 individuals were caught in the snaptraps and 52 individuals Sherman traps set. The differences between the two

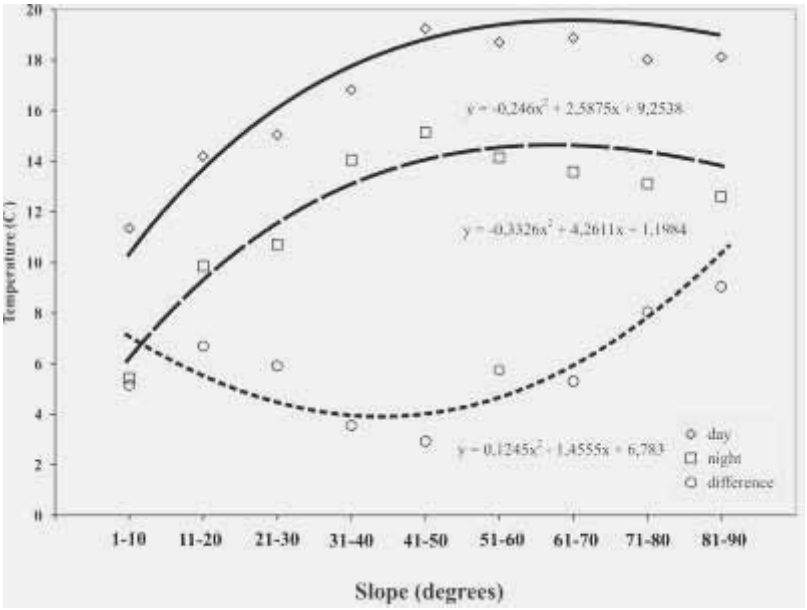

FIGURE 4
Relationship between average temperatures (daytime, nighttime and day-night difference) taken in burrow systems located on south-facing slopes as a function of degree of slope.

slope groups for capture frequency (For 0-45°: $mean_{snaptrapping}$= 10.842 ±1.798, $mean_{livetrapping}$ = 6.361±1.290; and for 46-90°: $mean_{snaptrapping}$ = 8.546±1.322, $mean_{livetrapping}$= 3.563±1.469, respectively) were not statistically significant ($t_{snaptraping}$ = 0.786; df = 16; p>0.355, $t_{livetarpping}$ = 0.914; df = 16; p>0.278).

Preferred habitat exposure. Captures were assigned to eight compass directions according to the site's direction of exposure to the sun (aspect). Trapping indices demonstrate that southerly directions (slopes facing south, southeast, or southwest) were preferred, because 171 (73.08%) of voles captured there in snaptraps and 84 (71.19%) is Sherman traps. Also 355 (74.11%) of population of these species was found in the southern slopes as indicated by density index. The differences of capturing between northern and southern exposures were found to be statistically significant ($t_{snaptraping}$=3.008; df=8; p<0.010, $t_{livetrapping}$ = 2.156; df=8; p<0.021, $t_{density}$=2.33; df=8; p<0.014, respectively). Such difference between east and west exposures ($t_{snaptraping}$=1.005; df=8; p>0.05, $t_{livetrapping}$=1.003; df=8; p>0.05, $t_{density}$=1.563; df=8; p>0.05, respectively) was not found.

Temperature regime in the south-facing areas. Figure 4 presents the data on temperatures measured inside the burrow systems on south-facing slopes. For gentle slopes (0-45°), there was a strong positive correlation between the average day and night burrow temperatures and the slope ($r_{daytime}$=0.973; p<0.004, $r_{nighttime}$=0.985; p<0.0002 respectively; Fig. 4). A strong negative correlation, however, was found between the difference in day and night-time temperatures and the slope ($r_{difference}$= -0.941; p<0.005). On the other hand, for steep slopes (46-90°), negative but comparatively weak correlations between the average day and night-time burrow temperatures and slope ($r_{daytime}$= -0.703; p>0.202, $r_{nighttime}$= -0.785; p<0.051 respectively; Figure 4) were recorded.

Moreover a positive correlation was found between the difference in day and night temperatures and the slope ($r_{difference}$=0.938; p<0.008). Additionally, both day and night-time temperatures were significantly different between the slope categories as was the magnitude of the daily shift in temperature ($F_{daytime}$=53.194; df=8; df=351; p<0.0001, $F_{nighttime}$=98.467; df=8; df=351; p<0.0001, $F_{difference}$=289.381; df=8; df=351; p<0.0001 respectively). This means that the voles on gentle slopes experience an increase in the average temperature of their burrows as the slope increases from 0-45° (at least on sunny days). On the other hand, voles living on steep south-facing slopes (46-90) experience a slight decrease in temperature as the steepness increases. The day and night burrow temperatures were statistically significantly different for both gentle and steep slopes ($t_{daytime}$=9.790; df=199; p<0.0001, $t_{nighttime}$=8.065; df=199; p<0.0001, $t_{difference}$=7.003; df=199; p<0.0001).

Temperature regime in the north-facing areas. Figure 5 presents the data on burrow temperatures on north-facing slopes. On gentle slopes (0-45°), the temperatures were negatively correlated with average day and night burrow temperatures ($r_{daytime}$= -0.723; p<0.0001, $r_{nighttime}$= -0.787; p<0.0001 respectively; Fig. 5). A weak negative correlation was found ($r_{difference}$= -0.150; p<0.010) between the difference in day and night temperatures and the degree of slope (Fig. 5). On the other hand, for steep north-facing slopes (46-90°) (Fig. 5), while a negative and comparatively weaker correlation ($r_{daytime}$= -0.357; p<0.0001) was found between the average daytime burrow temperature and the degree of slope, no relationship could be found between the average night temperature and the degree of slope ($r_{nighttime}$ = -0.065; p>0.364). A negative correlation ($r_{difference}$= -0.401; p<0.0001) was found between the day and night-time temperature difference and the degree of slope (Fig. 5). In addition, both the day and night temperatures were different from each other for the two slope categories ($F_{daytime}$=58.943; df=8; df=351; p<0.0001, $F_{nighttime}$=39.480; df=8; df=351; p<0.0001 respectively). Also, the magnitude of the daily changes in temperatures was different between the slope categories, i.e. greater on the gentle slopes ($F_{difference}$=27.017; df=8; df=351; p<0.0001). On the other hand, the day and night-time and the difference values measured for gentle slopes (0-45°), and the values measured for steep slopes (46-90°), were expressed as; $t_{daytime}$=17.674; df=199;p<0.0001, $t_{nighttime}$=12,003; df=199; p<0.0001, $t_{difference}$=8.957; df=199; p<0.0001 respectively, being greater on the gentle slopes. Finally, comparing north and southfacing slopes, the two exposures differ in average day temperature, average night temperature, and the magnitude of the day/night differences ($t_{daytime}$=51.663; df=359; p<0.0001, $t_{nighttime}$=33.182; df=359; p<0.0001, $t_{difference}$=28.121; df=359; p<0.0001 respectively).

DISCUSSION

During the course of this research in Hatay, it became clear that *M. guentheri* occurs in Kırıkhan, Serinyol, Derince, Kuzeytepe, Karlısu, Reyhanlı, Paşaköy and Karahüyük. During field observations it was revealed that the adults with dyed fur were recaptured often (86.21%). This species was found in particularly high numbers in clover and wheat fields and their neighbouring roadsides. In addition, they were also observed in grasslands containing herbaceous wild plants. It can be said that, as voles generally prefer to live in colonies in areas with dense vegetation, especially steppe, grassy plains and agricultural or fallow fields, they were seen to have concentrated on the edges of crop fields or fallow fields. As voles prefer to make their burrow

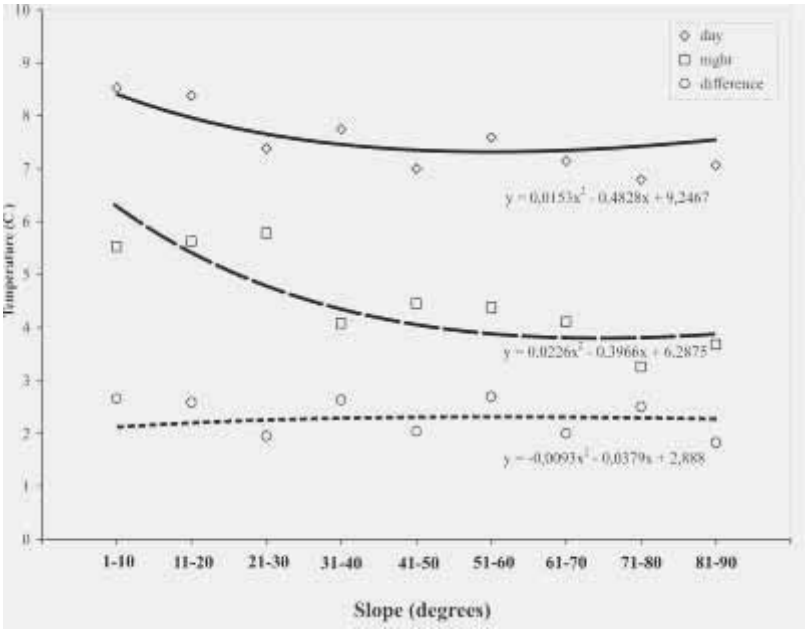

FIGURE 5
Relationship between mean temperatures taken in burrow systems located on north-facing slopes as a function of degree of slope.

systems by the roadside and on sloping agricultural land, the study areas of Serinyol, Reyhanlı and Karahüyük are at highest risk of invasion by voles, also trapping successes are high at these sites than other sites. In these study sites, cereal crop production is usually carried out on sloping land in fields adjacent to roadsides. Many burrows were encountered during field observations in cereal crop production areas. The frequencies of capture and population densities were highest in this type of field. On the other hand, in the study sites of Kırıkhan, Serinyol, Derince, Kuzeytepe, and Karahüyük, relatively little cereal crop production is carried out and the average degree of slope is found to be quite low. As seen, the frequencies of capture and population densities were low in these areas. Results show that, with regard to the species' preferred habitat and degree of slope, fields with an average slope of 31-60°, particularly those used for cereal crops, and that are adjacent to roads are at greater risk.

Sloping fields are exposed to more solar radiation during the daytime [25]. For this reason, they heat more quickly than fields in flatter areas, and reach a higher temperature (especially those facing south). They cool down slowly because of the solar radiation absorbed during the day. Therefore, the differences between the day and night-time temperatures in sloping fields are comparatively lower (see Fig. 4.a). So solar radiation is absorbed by the soil during the day and slowly dissipates overnight, and because the difference in day/night temperatures is smaller on slopes than flat areas, it is logical that slopes should retain more heat and hence have higher mean temperatures than flat surfaces. As seen in this study, for the south facing fields, as the degree of slope increases to 30-71 degrees, the difference between the day and night-time temperature decreases. The fact that the highest temperatures were found on slopes between 30 and 60° is in accordance with the most favoured slope preferences determined in this study. As a result, building burrow systems in areas exposed to the sun is a type of behaviour selected during the process of evolution which gives the homoeothermic species significant advantages. The fact that most of the burrow systems in the areas that were studied were made in fields with southerly exposure supports the idea that this behaviour was adaptive. Furthermore, the burrow systems made on slopes which provide the greatest amount of exposure to the sun between sunrise and sunset also have comparatively low levels of humidity. Few burrow systems were made, and therefore few voles caught, on the slopes with the least exposure to the sun (North, Northeast and Northwest). Finally, our findings on ecological preferences of *M. guentheri*, are smilar to 1, 26 and 27 in references.

ACKNOWLEDGEMENTS

This work was supported as a Research Project (Project No: 2009.01.0105.005) by the Akdeniz University Research Foundation.

REFERENCES

[1] Yavuz, M., Öz, M., Albayrak, İ. 2010. Levant Voles (*Microtus guentheri* (Danford and Alston 1880)) Prefer Southerly-Facing Slopes in Agricultural Sites at Antalya, Turkey. North Western Journal of Zoology, 6 (1): 36-46.

[2] Giusti, G. A. (2004) Assessment and monitoring of California vole (*Microtus californicus*) feeding damage to a coastal redwood (*Sequoia sempervirens*) restoration project. Proceedings: Vertebrate Pest Conference 21: 169-173.

[3] Lidicker, W.Z., JR. (1988) Solving the enigma of Microtine cycles. Journal of Mammalogy, 69:226-235.

[4] Sullivan, K.L., Curtis, P.D. (2002) Voles, Wildlife Damage Management Fact Sheet Series, Cornell Cooperative Extension,Ithaca, N.Y. Cornel University.

[5] Xavier, L., Bretagnolle, V., Yoccoz, N.G. (2006) Vole population cycles in northern and southern Europe: Is there a need for different explanations for single pattern? Journal of Animal Ecology 75 (2): 340-349

[6] Yiğit, N. Çolak, E. Sözen, M. and Özkurt, Ş. (1999) Türkiye Kemiricilerinin (Mammalia: Rodentia) Habitatları ve Tarım Alanları Üzerine Etkileri. *Gazi Üniversitesi Fen Bilimleri Enstitüsü Dergisi*, Ankara 12(4): 885-905

[7] Hagenah, N. Prins H.H.T., Olff, H. (2009) Effects of large herbivores on murid rodents in a South African savana. Journal of Tropical Ecology 25:483–492.

[8] Byers, R. E. (1984) Control and management of vertebrate pests in deciduous orchards of the eastern United States. *Hort. Rev*., 6, 253-285.

[9] Clark, J. (1984) Vole control in field crops. *Proc. Vertebr. Pest Conf*., 11:5-6.

[10] Howe, H. F. (2002) Vole herbivory shapes vegetation in experimental tallgrass prairie restorations (Illinois and Wisconsin). *Ecological Restoration*, 20:278–279

[11] O'Brien, J. M. (1994) Voles. Pages B177-B182 in S. E. Hygnstrom, R. M. Timm, and G. E. Larson, eds. *Prevention and control of wildlife damage*. Univ. Nebraska Coop. Ext. Lincoln.

[12] Sullivan, T.P., Krebs, J.A., Kluge, H.A. (1987) Survey of mammal damage to tree fruit orchards in Okanagan Valley of British Columbia. Northwest Science 61 (1): 23-31.

[13] Özkurt, Ş., Yiğit, N., Çolak, E. and Sözen, M. (1999) *Microtus guentheri* (Danford ve Alston 1880) (Mammalia: Rodentia)'nın İç Anadolu Bölgesindeki Tarım alanları Üzerine Etkisi ve Mücadele Yöntemleri. *Gazi Üniversitesi Fen Bilimleri Enstitüsü Dergisi*, 12(4): 907-919, Ankara.

[14] Corrigan, R. M. (2003) Rats and mice. pp. 11-119. In: Handbook of Pest Control, 9th Ed., Cleveland, GIE Publications.

[15] Mendelssohn, H. and Paz, U. (1977) Mass mortality of Birds of prey caused by Azodrin an organophosphorus insecticide. *Biol. Conserv.*, 11: 163-170.

[16] Timm, R.M., Marsh, R.E. (1997) Vertebrate Pests. Pp. 954-1019. In: Moreland D. (Ed.): Handbook of Pest Control. Mallis 8th edition. Mallis Handbook & Technical Training Company, Cleveland.

[17] Alkan, B. (1966) Türkiye'nin bahçe ve ağaç fareleri (Mammalia: Gliridae) üzerine bazı incelemeler, *Bitki Koruma Bülteni*. 6 (1), 1-10.

[18] Bodenheimer, F. S. (1958) Türkiye'de ziraata ve ağaçlara zararlı olan kemiriciler ve bunlarla savaş hakkında bir etüd (Çeviri: N. Kenter), Bayur matbaası, Ankara. 1-320pp.

[19] Kıral, E. and Benli, O. (1979) Orta Anadolu'nun Kemirici Türleri ve Zarar Yaptığı Kültür Bitkileri. *Bitki Koruma Bülteni*, 19 (4): 191-217.

[20] Osborn, D.J. (1962) Rodents of The Subfamily Microtinae from Turkey. *Mammalia*, 43: 515-529.

[21] Tunçdemir, Ü. (1987) Karadeniz Bölgesi'ndeki zararlı kemirici türlerinin yayılış alanları ve zarar yaptığı bitkilerin tespiti üzerine araştırmalar, *Bitki Koruma Bülteni*, 27(1-2). 65-85.

[22] Kryštufek, B. and Vohralik, V. (2005) *Mammals of Turkey and Cyprus. Rodentia I: Sciuridae, Dipodidae, Gliridae, Arvicolinae*. Koper, 1-292.

[23] Krebs, C.J. (1999) Ecological Methodology, 2nd Ed.. Addison-Welsey Educational Publishers Inc., Menlo Park, CA.

[24] Pollock, K.H., Nichols, J.D., Brownie, C., Hines, J.E. (1990) Statistical inference for capture-recapture experiments. Wildlife Monographs 107: 1-97.

[25] Porter, W.P., J.L. Sabo, Tracy, C.R., Reichman, O.J. and Ramankutty, N. (2002) Physiology on a Landscape Scale: Plant-Animal Interactions, *Integ. and Comp. Biol*., 42: 431–453.

[26] Yavuz, M., Öz, M. and Albayrak, İ. (2008) Antalya ilinde yayılış gösteren tarla farelerinin (Rodentia: *Microtus guentheri*) habitat tercihleri ve yuva anatomisi, Tabiat ve İnsan, Yıl; 42 sayı; 3, 2-7.

[27] Yavuz, M., Öz, M., Albayrak, İ. (2008) Six new Localities of The Levant Vole, *Microtus guentheri* Danford and Alston, 1880 (Mammalia: Rodentia) from Antalya Province, in Turkey. Journal of Aplied Biological Sciences (JABS) 2(3): 21-24.

Received: **26.09.2015**
Accepted: **28.02.2016**

CORRESPONDING AUTHOR

Mustafa YAVUZ,
Akdeniz University, Faculty of Sciences, Department of Biology, Campus 07058 Antalya-TURKEY

Email: myavuz@akdeniz.edu.tr

by PSP Volume 25 – No 7/ 2016 – pages 2539-2553 Fresenius Environmental Bulletin

FACTORS AFFECTING THE STUDENTS' ENVIRONMENTAL AWARENESS, ATTITUDES AND BEHAVIORS IN ONDOKUZ MAYIS UNIVERSITY, TURKEY

Mehmet Bozoglu[1*], Abdulbaki Bilgic[2], Bakiye Kilic Topuz[1] and, Yuksel Ardali[3]

[1]Ondokuz Mayis University, Faculty of Agriculture, Department of Agricultural Economics, 55200 Samsun, Turkey
[2]Ataturk University, Faculty of Agriculture, Department of Agricultural Economics, 25240 Erzurum, Turkey
[3]Ondokuz Mayis University, Faculty of Engineering, Department of Environmental Engineering, 55200 Samsun, Turkey

ABSTRACTS

This study aimed to determine the students' environmental awareness, attitude and behavior levels and factors influencing their environmental awareness, attitude and behavior. A face-to-face survey with 621 candidate graduate students in the Ondokuz Mayis University was used to collect the data. The environmental awareness, attitude and behavior were determined by the students' assessments based on a five-point Likert scale. The ordered probit procedure was used to determine factors affecting the students' environmental awareness, attitudes and behaviors. The study reveals that the candidate graduate students' environmental awareness, attitude and behavior are found to be high. The probit models showed that both environmental attitude and behavior were influenced by the environmental education and information factors, while the socio-demographic factors generally have important impacts on the students' environmental awareness as expected. While the variables of gender had the highest impacts on the students' environmental awareness, both awareness and curiosity levels towards environmental news had the highest influences on the students' environmental attitude and behavior, respectively. To increase the students' environmental literacy levels, the departments should put sufficient compulsory environment courses on their programs, and they should focus on providing their graduates with environmental attitudes and behaviors.

KEYWORDS:
Environment, awareness, attitudes, behavior, ordered probit, Turkey

INTRODUCTION

Natural resources are being consumed at a faster rate than they can be restored [1]. The uncontrolled and uncoordinated usage of environmental sources resulted in environmental problems such as deforestation, loss of biodiversity, pollution, ozone depletion, global climate change and over-consumption of natural resources [2, 3]. Environmental problems are the most vital problems we face today and all are mostly due to the human behavior [4, 5], or they are anthropogenic of origin [6]. Such threats to the environment are generally listed as industrialization, over population, developments in science and technology and increasing needs and globalization [7].

Environmental issues are being eroded with more university education in the long run, since universities educate young generations expected to be the future leaders in many different areas in the society, and who will be the decision-makers and therefore their graduates are expected to deal with sustainability issues in both their' personal and professional lives [8]. Students should acquire an appropriate range of awareness, understanding, and concepts about the environment while they were in school, so that critical judgment can be achieved [9]. Environmental education can help create positive awareness and attitudes about environmental issues, whilst curbing the negative role of human actions on the environment [10, 11]. Therefore, universities are sole responsible for increasing their students' environmental awareness, attitudes and behaviors to create an environmentally sustainable future [12].

Environment is defined as all factors affecting the physical, biological, socio-psychological, socio-economic and cultural life of an individual or society [13]. Environmental awareness is defined as an understanding of natural systems combined with how they interact with human social systems [14], while many consider this as the ultimate driving force that stimulates knowledge [15]. Contrarily, environmental attitude is defined as learned tendencies in the form of consistent behaviors against environment either positive or negative [16], providing a good understanding of the set of beliefs, interests or rules that influence environmentalism or pro-environmental action [17]. On the other hand, behavior is what people do, whether it is environmentally appropriate or inappropriate [18]. Since environmental behavior is considered as the basis of the environmental crisis, social scientists have long been interested in the causation of this behavior [1].

The rise of environmental issues has produced many studies with students on explaining the variation in individual knowledge, awareness, attitudes and behaviors toward the environment. Aklin et al. [19] attempted to identify the main determinants which predict a person's awareness of environmental issues, while many other researches revealed the relation between environmental awareness, concern, knowledge and behavior [20-27]. In parallel, some other researchers have investigated whether schools [1] and infusions of environmental education [28] make a difference in environmental awareness and attitudes among students. Ogunbiyi and Ajiboye [29] examined pre-service teachers' knowledge and attitudes to some environmental education concepts. Grob [30] estimated a structural model for environmental attitudes and behaviors, whilst Bradley et al. [10] and Kaiser et al. [31] overemphasized that attitude is the most important factor affecting individual behavior. While Klöckner [32] and Masud and Kari [33] examined the determinants of individuals' environmentally relevant behaviors, Tanner [34] identified prevalent constraints inhibiting individuals' environmental behaviors. Environmental awareness, attitudes and behaviors may vary with gender, age, education, income, family, residence, country, political tendency, knowledge/awareness of the environment, school and etc. [35-38].

In Turkey, researchers have investigated university students' environmental knowledge, responsibility, risk perceptions, attitude, and behaviors. For example, Beyhun et al. [39] determined the students' environmental risk perception levels and their determinants in one of the country's Medical Schools and stated that stress, damage of ozone layer and motor vehicle accidents were found as high or very high risk factors towards environment. On the other hand, Yilmaz et al. [40] examined the university students' environmental knowledge levels and determined that the environmental education was not sufficient enough so that students generally tended to obtain information about environmental issues from the media. Contrarily, Sadik and Sadik [41] investigated environmental knowledge and attitudes of those who are teacher candidates at Cukurova University and found that they had a moderate environmental knowledge level and positive environmental attitude, but with a low level of the environmental behavior. In parallel, a study conducted among science teacher candidates in thirteen universities in the country to obtain their environmental attitudes found very high level of environmental attitudes of candidates [42]. Similar results were also echoed in other studies [43-49]. However, to our knowledge there was no specific study to investigate awareness, attitudes and behavior levels of the candidate graduates towards environmental issues and how their determinants affect perceptions of these issues. Therefore, this study was to identify this relationship and levels of awareness, attitudes and behavior among the students of the Ondokuz Mayis University in Turkey who would soon graduate.

Universities have the responsibility to prepare their graduates for preserving the environment. Every department is related with the environment and their graduates' professional activities can somehow effect the environment. Therefore, every department should prepare responsible graduates for a more livable environment. The emerging interest of universities to participate in the increase in the consciousness of environmental values makes it necessary to explore the candidate graduates' environmental awareness, attitude and behavior. However, it is very important to explore if the time students spend at the university actually improves their environmental awareness, attitude and behavior. Determining environmental awareness, attitude and behavior of the candidate graduates is also crucial in establishing the sustainability of a community.

Based on the logical approach described in the previous section, it is an important task to analyze the levels of awareness, attitudes and behavior attributed to environmental issues by university students, since it can present significant results to draw appropriate decisions about the effective educational programs for students who are currently enrolled and future generations on environmental issues. The aim of this study was to determine the environmental awareness, attitude and behavior levels of the students and understand how socio-demographic, economic, and environmental-related factors influence their environmental awareness, attitude and behavior. The research results can contribute to the program curricula and shed light on penetrative protection of the environment those policy makers of local in particular and central government in general seek for.

MATERIALS AND METHODS

Ondokuz Mayis University is a state university and has totally 52,301 undergraduate and graduate students at 5 graduate institutions, 16 faculties, 2 colleges, 1 conservatory and 12 vocational schools [50]. The population of this study includes all candidate students for graduation at the undergraduate programs of the departments, which are somehow related with environment, under the body of the faculties of Ondokuz Mayis University. Totally 621 students participated in the study, and the number of participant students from the departments were as follows: Agricultural Economics (26), Agricultural Construction and Irrigation (20), Horticulture (27), Plant Protection

(31), Field Crops (24), Agricultural Biotechnology (32), Agricultural Machinery (20), Soil Science and Plant Nutrition (30) and Animal Science (18) all from the College of Agriculture, and Environmental Engineering (43), Food Engineering (55) and Industrial Engineering (42) from the College of Engineering, while Biology (37), Chemistry (33) and Geography (89) from the College of Science and Education, and lastly Science Teacher (72) and Biology Teacher (22) from the College of Education.

This study used a survey technique to collect the data. The technique aims to reveal a past or current phenomenon [51] or determine participants' views or characteristics such as interest, skill and/or attitude [52]. The survey consisted of totally 64 questions and four parts: The first part contained 12 items to measure socio-demographic and economic characteristics of the students such as age, gender, family size, education of mother and father, residence, monthly income of family, information sources on environment, frequency of following environmental news, research and developments, the most important institution about environment, membership to environmental organizations, and whether the student has taken courses about the environment. The second part included 26 items to measure the students' environmental awareness. The third part contained 11 items to measure the students' environmental attitude, and the last part included 15 items to measure the students' environmental behaviors. The Likert scale measurement was used for every statement of environmental awareness, attitude and behavior on a 5 point scale. Each alternative item is assigned from 5 (strongly agree) to 1 (strongly disagree) for favorable items. In case of unfavorable items (2, 5, 7, 9, 10, 11, 13, 16, 18, 20, 21, 23, 36, 37 and 40) in Table 3, the scoring is reversed from 1 (strongly agree) to 5 (strongly disagree). The students were asked to indicate whether they agree or disagree with each item, as well as the magnitude of their agreement or disagreement. The students were then categorized in three groups according to their average response score for the questions. The student who scored less than 2.5 was classified under the low environmental awareness, attitude and behavior group, 2.5 to 3.5 was classified under the moderate environmental awareness, attitude and behavior group, and more than 3.5 was classified under the high environmental awareness, attitude and behavior group.

The students' environmental awareness, attitude and behavior scores were given in Table 1 based on their statements. To calculate and interpret the mean values of the level of agreement for each item of awareness, attitude and behavior, an interpretative scale was developed as follows: If the mean value was less than 2.5, it meant the participant strongly disagreed or disagreed. If the mean value was from 2.5 to 3.5, it was neutral, and if the mean value was higher than 3.5, it meant that the participant agreed or strongly agreed. Based on this scale, of 26 environmental awareness statements, while 21 statements were agree or strongly agree, 3 awareness statements were neutral and 2 awareness statements were disagree or strongly disagree. The three items of environmental awareness with the highest means were "Creating environmentally conscious individuals is compulsory for future generations to live in a healthy and safe environment (mean=4.41)", "Using insecticides and herbicides for agriculture is not harmful for the environment (mean=4.29)" and "Environmental activities help raise awareness of environmental issues (mean=4.25)". The three items of environmental awareness with the lowest means were "The malnutrition in underdeveloped countries is a consequence of environmental problems (mean=3.11)", "The university is not sensitive enough towards environmental problems (mean=2.37)" and "Environmental education is not enough in Turkey (mean=1.89)".

Of 11 environmental attitude statements, while 10 statements were agree or strongly agree, only 1 statement was neutral. The three items of environmental attitude with the highest means were "People who spit on or litter the ground should be interfered (mean=4.43)", "We should try to protect Earth's plants and animals, even though it is expensive (mean=4.38)" and "Courses of environment must be practical (mean=4.37)". The three items of environmental attitude with the lowest means were "I think I am very sensitive about environmental issues (mean=3.65)", "I prefer the option of highway construction to the protection of plant species (mean=3.61)" and "For my country, I prefer technological development to noise pollution (mean=3.32)".

TABLE 1
Average awareness, attitude and behavior scores.

	Statements	Level			
		Low	Moderate	High	General
Awareness	1.Creating environmentally conscious individuals is compulsory for future generations to live in a healthy and safe environment***	1.33	3.77	4.60	4.41
	2.Using insecticides and herbicides for agriculture is not harmful for the environment***	1.33	3.38	4.55	4.29
	3.Environmental activities help raise awareness of environmental issues***	1.50	3.73	4.42	4.25
	4.Environmental protection is a constitutional obligation**	2.00	3.63	4.37	4.21
	5.Field activities related to the environment are a waste of time, within class activities are important***	1.83	3.53	4.39	4.20
	6.If universities carry out more activities on environment, it will help better understand environmental issues***	1.50	3.57	4.38	4.19
	7.Protecting the environment is a duty of the state, not people**	2.17	3.65	4.24	4.10
	8.Human mistreat the environment **	2.00	3.45	4.23	4.05
	9.Environmental education activities are useful only for children***	1.17	3.57	4.19	4.04
	10.A squatter is not an environmental problem**	2.00	3.28	4.23	4.02
	11.I believe that environmental problems are exaggerated.	2.67	3.38	4.19	4.02
	12.Rapid population growth is a serious environmental problem**	2.00	3.32	4.15	3.97
	13.Air, water and soil are inexhaustible resources***	1.17	3.20	4.19	3.96
	14.Necessity of using water filters at homes is an indicator of water pollution***	1.50	3.52	4.08	3.94
	15.Being sensitive to the environmental problems is not an obstacle for the development of a country***	1.83	3.38	4.09	3.93
	16.The idea of environmental protection was invented by western people to prevent the development of developing countries	2.67	3.45	4.03	3.90
	17.I increasingly need more information about the effects of our activities on the environment***	1.83	3.42	4.00	3.86
	18.There is no desertification problem in Turkey***	1.83	3.28	3.96	3.80
	19.Immigration affects negatively environmental problems	2.50	3.17	3.95	3.79
	20.Delivering environmental education does not help solving environmental problems**	1.83	3.09	3.89	3.71
	21.No international institution or organization should intervene on using the natural resources.	2.33	3.02	3.81	3.64
	22.There have not been enough protest meetings for protecting the environment in Turkey.	2.50	2.97	3.55	3.42
	23.The increase of natural gas usage in Turkey did not contribute to the solution of the air pollution problem.	2.67	3.05	3.44	3.36
	24.The malnutrition in underdeveloped countries is a consequence of environmental problems.	2.67	2.65	3.23	3.11
	25.The university is not sensitive enough towards environmental problems***	4.00	2.52	2.32	2.37
	26.Environmental education is not enough in Turkey***	4.67	2.16	1.80	1.89
Attitude	27.People who spit on or litter the ground should be interfered.**	2.50	3.89	4.58	4.43
	28.We should try to protect Earth's plants and animals, even though it is expensive.**	2.50	4.00	4.50	4.38
	29.Courses of environment must be practical.**	2.33	3.92	4.51	4.37
	30.People who pollute the environment should be fined.**	2.50	3.91	4.50	4.36
	31.Newspapers, magazines and televisions should make more programs about environmental issues.**	2.67	3.95	4.48	4.36
	32.I love to visit recreation areas outside of the city.**	2.33	3.99	4.47	4.36
	33.Courses about environment should be compulsory.	2.83	3.36	4.23	4.05
	34.Regardless of their position, any country engaging in nuclear testing should be protested.	2.67	3.45	3.77	3.70
	35.I think I am very sensitive about environmental issues.**	2.50	3.39	3.73	3.65
	36.I prefer the option of highway construction to the protection of plant species.	2.83	3.13	3.74	3.61
	37.For my country, I prefer technological development to noise pollution.	2.50	3.08	3.38	3.32
Behavior	38.I take care of using both sides of papers when I write something.**	2.67	3.91	4.32	4.22
	39.I usually economically use resources such as water and electricity.	2.17	3.77	4.13	4.04
	40.When I am outside of the room, I do not turn the lights off, because I think it does not consume energy very much.	3.83	3.62	3.97	3.90
	41.I like participating in the environmental protection activities, because it is the best way to understand the environment.**	2.50	3.37	3.94	3.82
	42.I often talk about environmental issues with people around me.*	2.33	3.29	3.82	3.71
	43.I often watch television programs about environmental issues.	2.67	3.22	3.72	3.61
	44.I usually use public transports such as the tram in order to avoid air pollution.*	2.50	3.34	3.57	3.52
	45.I usually read publications on the environmental issues.	3.00	3.17	3.59	3.50
	46.I take care of buying recycling packaged products in my daily life.	3.00	3.08	3.57	3.46
	47.I take care of collecting household waste separately in my daily life.	3.00	2.89	3.38	3.28
	48.I take care of consuming products which do not contain harmful substances to the ozone layer.	3.33	2.99	3.35	3.28
	49.I choose courses about environment as elective courses at the university.	3.33	2.66	3.36	3.23
	50.I vote politicians who are concerned about environmental protection.	2.50	2.97	3.29	3.22
	51.When I get a chance, I plant seedling.	2.83	3.03	3.14	3.11
	52.I join actively in activities of environmental issues.	3.33	2.78	2.85	2.84

***, **, * denote that there are statistical differences among the groups at 1%, 5% and 10% significance levels, respectively.

Of 15 environmental behavior statements, 8 statements were agree or strongly agree, 7 statements were neutral. The three items of environmental behavior with the highest means were "I take care of using both sides of papers when I write something (mean=4.22)", "I usually economically use resources such as water and electricity (mean=4.04)" and "When I am outside of the room, I do not turn the lights off, because I think it does not consume energy very much (mean=3.90)". The three items of environmental behavior with the lowest means were "I vote politicians who are concerned about environmental protection (mean=3.22)", "When I get a chance, I plant seedling (mean=3.11)" and "I join actively in activities of environmental issues (mean=2.84)".

The questionnaire was pre-tested and modified to improve its reliability. The questionnaires were conducted with students at the beginning of classes by lecturers in May 2015. The students answered the survey questions in about 15 minutes. SPSS 17.0 and Limdep 10 software programs were used for data analysis.

Descriptive statistics were used to identify variables reflecting socio-demographic and economic characteristics and environmental awareness, attitude and behaviors of the students. To compare the socio-demographic and economic, and environmental variables in which students were identified low, moderate and high for subsequent awareness, attitude and behavior groups, ANOVA and Kruskal Wallis tests were used for parametric and non-parametric variables, respectively. The ordered probit model was used to determine the environmental awareness, attitude and behaviors of the students by means of socio-demographic, economic and environmental variables.

Definitions of variables were presented in Table 2. The dependent variable had three response categories for which students have stated their understanding levels of environmental awareness, attitude and behavior. Since the dependent variable takes discrete values and these values are inherent ordinal ranking, the ordered model fits the data best [53-56].

TABLE 2
Definitions of the model variables.

Variable name	Variable definition
GENDER	Female=0, Male=1
AGE	Age (year old)
HOUSHSIZE	Household size (people)
MOTHEDUC	Mother education (year)
FATHEDUC	Father education (year)
RESIDENCE	If student lives in rural residences =1, other = 0
FAMINCOM	Household monthly income (₺, Turkish Lira)
ENVCOUR	If the student takes two or more courses about environment =1, other = 0
INFSMEDIA	If the main information source of environmental awareness is the media =1, others=0
INFSUNIV	If the main information source of environmental awareness is university =1, others=0
INFSINST	If the main information source of environmental awareness is the state institutions =1, others=0
FENVNEWS	If student follows usually or always environmental news =1, other = 0
MEMENVO	If student is a member of voluntary environmental organizations=1, other=0
ENVAWARL	Level of environmental awareness (<2.5=low awareness level, 2.5-3.5= moderate awareness level and, 3.5 > high awareness level)
ENVATTL	Level of environmental attitude (<2.5=low sense level, 2.5-3.5= moderate sense level and, 3.5 > high sense level)
ENVBEHL	Level of environmental behavior (<2.5=low behavior level, 2.5-3.5= moderate behavior level and, 3.5 > high behavior level)

The ordered model, for which the dependent variable was coded 0 as low, 1 as moderate, and 2 as high each for awareness, attitude or behavior, is expressed as

$$y_i^* = \boldsymbol{\beta}'\mathbf{x}_i + \varepsilon_i, \quad \varepsilon_i \sim F(\varepsilon_i \mid \theta), \; E(\varepsilon_i \mid \mathbf{x}_i) = 0, \; and \; Var(\varepsilon_i \mid \mathbf{x}_i) = 1 \tag{1}$$

where y^* is the unobserved "latent" dependent variable, $\boldsymbol{\beta}$ is a vector of coefficients to be estimated, ***x*** *is* a vector of explanatory variables, ε a vector of error terms (e.g., we assume normal distribution as $\varepsilon \sim N[0,1]$) and F stands for any distribution that a researcher might consider.

The above observation mechanism results from a complete censoring of the latent limited dependent variable as follows:

$$\begin{aligned} y_i &= 0 \quad if \; y_i \le \mu_0, \\ y_i &= 1 \quad if \; \mu_0 < y_i \le \mu_1, \\ y_i &= 2 \quad if \; \mu_1 < y_i \le \mu_2, \end{aligned} \tag{2}$$

where y is the observed counterpart to y^*, while μ_j represents the threshold values or the cutoff points. The cutoff points vary with the individual respondents. We expect students with similar socio-demographic and economic characteristics, and environmental awareness, attitude or behavior to have similar cutoff points, resulting with the cutoff points being normally distributed [57, 58].

If we assume that the ε is normally distributed across observations, then the probability of choosing a specific ranking by a respondent can be expressed as [54, 57, 59].

$$\Pr ob[y_i = j] = \Pr ob[y_i^* \; is \; in \; the \; jth \; range] = \Phi(\mu_j - \boldsymbol{\beta}'\mathbf{x}_i) - \Phi(\mu_{j-1} - \boldsymbol{\beta}'\mathbf{x}_i) \tag{3}$$
$$j = 0, 1, 2.$$

where Φ is the normal cumulative density function (cdf), μ_j and μ_{j+1} represent the upper and lower threshold values for category j, respectively. Note that $\mu_{-1} = -\infty$ and $\mu_0 = 0$.These probabilities are specifically as follows:

$$\begin{aligned} \Pr ob[y_i = 0] &= \Phi(-\boldsymbol{\beta}'\mathbf{x}_i) \\ \Pr ob[y_i = 1] &= \Phi(\mu_1 - \boldsymbol{\beta}'\mathbf{x}_i) - \Phi(-\boldsymbol{\beta}'\mathbf{x}_i) \\ \Pr ob[y_i = 2] &= \Phi(\mu_2 - \boldsymbol{\beta}'\mathbf{x}_i) - \Phi(\mu_1 - \boldsymbol{\beta}'\mathbf{x}_i) \end{aligned} \tag{4}$$

The log likelihood function is:

$$\begin{aligned} \log L &= \sum_{i=1}^{N} \sum_{j=0}^{2} y_{ij} \log\left(\Phi(\mu_j - \boldsymbol{\beta}'\mathbf{x}_i) - \Phi(\mu_{j-1} - \boldsymbol{\beta}'\mathbf{x}_i)\right) \\ &= \sum\nolimits_{y_i=0} \log\left(\Phi(-\boldsymbol{\beta}'\mathbf{x}_i)\right) + \sum\nolimits_{y_i=1} \log\left(\Phi(\mu_1 - \boldsymbol{\beta}'\mathbf{x}_i) - \Phi(-\boldsymbol{\beta}'\mathbf{x}_i)\right) + \\ &\quad \sum\nolimits_{y_i=2} \log\left(\Phi(\mu_2 - \boldsymbol{\beta}'\mathbf{x}_i) - \Phi(\mu_1 - \boldsymbol{\beta}'\mathbf{x}_i)\right) \end{aligned} \tag{5}$$

Marginal effects were calculated to determine a unitary effect of each exogenous variable on each of the three categories of the dependent variable. The marginal effect of a continuous variable for the ordered probit model for three categories can be calculated as [57, 60].

$$\frac{\partial \Pr ob(y_i = 0)}{\partial x_k} = -\phi\left(\hat{\boldsymbol{\beta}}'\mathbf{x}_i\right)\hat{\beta}_k,$$
$$\frac{\partial \Pr ob(y_i = 1)}{\partial x_k} = \left[\phi\left(-\hat{\boldsymbol{\beta}}'\mathbf{x}_i\right) - \phi\left(\hat{\mu}_1 - \hat{\boldsymbol{\beta}}'\mathbf{x}_i\right)\right]\hat{\beta}_k, \quad (6)$$
$$\frac{\partial \Pr ob(y_i = 2)}{\partial x_k} = \left[\phi\left(\hat{\mu}_1 - \hat{\boldsymbol{\beta}}'\mathbf{x}_i\right)\right]\hat{\beta}_k$$

where ϕ is the normal probability density function. Marginal effects for a dummy variable, on the other hand, can be calculated as the difference between Φ of the corresponding probability with and without the presence of the variable in question. For example,

$$\frac{\partial \Pr ob(y_i = 0)}{\partial x_m} = \Phi\left(-\hat{\boldsymbol{\beta}}'\mathbf{x}_i\Big|_{x_m=1}\right) - \Phi\left(-\hat{\boldsymbol{\beta}}'\mathbf{x}_i\Big|_{x_m=0}\right) \quad (7)$$

The standard errors of these marginal effects can be obtained by utilizing the delta method.

RESULTS AND DISCUSSIONS

Descriptive statistics of the variables used in the models were presented in Table 3. Regarding socio-demographic and economic variables, while 57% of the students were male, 43% of the students were female. There were statistical gender differences among the groups in terms of awareness and behavior ($p<0.00$ and $p<0.05$). The average age of the students was 23 years old, and there were statistical differences among the groups in terms of age ($p<0.10$). The average household size was 5.04, and there were not statistical differences among the groups in terms of household size. While the average education duration of mothers and fathers were about 7 and 9, respectively, there were statistical differences among the groups in terms of the mother education duration ($p<0.01$). While 16.1% of the students were from the rural residences, 83.9% of the students were from the urban residences. There were statistical differences among the environmental awareness groups in terms of residence ($p<0.05$). The average family monthly income was ₺ 2.5 thousand, and there was no statistical difference among the groups in terms of income.

Regarding environmental variables, 64.7% of the students took two or more courses about environment and there were statistical differences among the environmental attitude and behavior groups in terms of the number of courses taken ($p<0.05$ and $p<0.10$). While 81% of the students use the media as a main information source about environmental issues, 22.5% and 18.4% of the students use university and other institutions as a main information source, respectively. There were a statistical difference among the environmental attitude and behavior groups in terms of the variable of university information source ($p<0.05$ and $p<0.01$, respectively). Fifty eight percent of the students follow usually or always environmental news, and there were statistical differences among the environmental awareness, attitude and behavior groups in terms of the following frequency of environmental news ($p<0.01$). Only 10.5% of the students were members of an environmental organization, and there were statistical differences among the environmental awareness and behavior groups in terms of membership ($p<0.05$ and $p<0.01$). The average environmental awareness score was 3.80, and this meant that the students had a high level of environmental awareness. There were statistical differences among the environmental attitude and behavior groups in terms of environmental awareness ($p<0.01$). The average environmental attitude score was 4.05, indicating that the students had a high level of environmental attitude. There were statistical differences among the environmental behavior groups in terms of environmental attitude ($p<0.01$). The average environmental behavior score was 3.52, and this indicates that the students had a high level of environmental behavior. There were statistical differences among the groups in terms of environmental awareness, attitude and behavior. Our results echoed with previous findings. For example, Ozsoy [42] indicated that pre-service science teachers had a high level of environmental attitudes, whilst Altinoz [61] concluded that the science education candidate teachers' environmental attitudes were found to be at a high level and contrarily their environmental knowledge and behavior occurred at low levels. However,

TABLE 3
Descriptive statistics of the variables used in the environmental awareness, attitude and behavior models.

Variables	General (N=621)	Environmental awareness level			Environmental attitude level			Environmental behavior level		
		Low (n=6)	Moderate (n=122)	High (n=493)	Low (n=16)	Moderate (n=166)	High (n=539)	Low (n=27)	Moderate (n=252)	High (n=342)
GENDER	0.433	0.833***	0.549	0.400	0.438	0.500	0.425	0.444**	0.500	0.383
	(0.496)	(0.408)	(0.500)	(0.490)	(0.512)	(0.504)	(0.495)	(0.506)	(0.501)	(0.487)
AGE	23.068	22.167*	22.598	23.195	23.688*	22.485	23.193	23.259*	22.683	23.336
	(2.815)	(0.753)	(1.689)	(3.033)	(3.995)	(1.491)	(2.799)	(2.105)	(2.352)	(3.133)
HOUSHSIZE	5.040	4.667	4.779	5.110	5.250	5.106	5.026	5.407	4.929	5.094
	(1.776)	(1.033)	(1.561)	(1.828)	(1.844)	(1.781)	(1.776)	(2.325)	(1.603)	(1.847)
MOTHEDUC	6.628	3.167***	7.975	6.337	6.438	7.478	6.529	5.852	6.743	6.604
	(3.761)	(2.137)	(4.204)	(3.571)	(3.705)	(4.178)	(3.703)	(3.890)	(3.832)	(3.702)
FATHEDUC	8.940	7.167	9.298	8.873	8.500	9.035	8.942	8.222	9.030	8.931
	(3.911)	(5.193)	(3.848)	(3.910)	(3.983)	(4.199)	(3.879)	(3.588)	(4.034)	(3.848)
RESIDANCE	0.161	0.333**	0.082	0.178	0.188	0.212	0.154	0.222	0.143	0.170
	(0.368)	(0.516)	(0.275)	(0.383)	(0.403)	(0.412)	(0.361)	(0.424)	(0.351)	(0.3769)
FAMINCOM	2467.021	1750.000	2331.230	2509.351	2368.750	2356.515	2483.469	2218.148	2513.135	2452.690
	(2064.585)	(1036.822)	(1131.474)	(2243.444)	(1285.156)	(1254.041)	(2161.963)	(1015.480)	(1984.762)	(2182.917)
ENVCOUR	0.647	0.667	0.574	0.665	0.750**	0.455	0.668	0.630**	0.587	0.693
	(0.478)	(0.516)	(0.497)	(0.472)	(0.447)	(0.502)	(0.471)	(0.492)	(0.493)	(0.462)
INFSMEDIA	0.810	0.667	0.803	0.813	0.750	0.803	0.813	0.815	0.845	0.784
	(0.393)	(0.516)	(0.399)	(0.390)	(0.447)	(0.401)	(0.391)	(0.396)	(0.362)	(0.412)
INFSUNIV	0.225	0.167	0.172	0.239	0.188**	0.106	0.241	0.185***	0.167	0.272
	(0.418)	(0.408)	(0.379)	(0.427)	0.403	0.310	0.428	(0.396)	(0.373)	(0.446)
INFSINST	0.184	0.167	0.164	0.189	0.063	0.212	0.184	0.185	0.151	0.208
	(0.387)	(0.408)	(0.372)	(0.392)	0.250	0.412	0.388	(0.396)	(0.359)	(0.406)
FENVNEWS	0.580	0.667***	0.418	0.619	0.500***	0.258	0.622	0.296***	0.349	0.772
	(0.494)	(0.516)	(0.495)	(0.486)	0.516	0.441	0.485	(0.465)	(0.478)	(0.420)
MEMENVO	0.105	0.000**	0.041	0.122	0.125	0.030	0.114	0.037***	0.060	0.144
	(0.307)	(0.000)	(0.199)	(0.328)	0.342	0.173	0.318	(0.192)	(0.238)	(0.351)
ENVAWARL	3.797	2.135	3.274	3.934	3.124***	3.446	3.849	3.459***	3.682	3.890
	(0.401)	(0.180)	(0.232)	(0.262)	0.738	0.421	0.343	(0.661)	(0.411)	(0.327)
ENVATTL	4.053	2.561	3.644	4.172	2.801	2.985	3.602	3.064***	3.875	4.262
	(0.580)	(1.156)	(0.624)	(0.481)	(0.742)	(0.426)	(0.511)	(0.874)	(0.534)	(0.445)
ENVBEHL	3.516	2.867***	3.206	3.601	2.801***	2.985	3.602	2.193***	3.119	3.913
	(0.556)	(0.481)	(0.586)	(0.517)	(0.742)	(0.426)	(0.511)	(0.274)	(0.264)	(0.304)

Note: The numbers in parentheses indicate standard deviations. ***, **, * denote that there are statistical differences among the groups at 1%, 5% and 10% significance levels, respectively

Erkal et al [45] found the university students' environmental attitudes as above the medium level, while Karatekin [62] determined social science candidate teachers' environmental knowledge, behavior and literacy levels as intermediate. Timur [63] found that the environmental knowledge and behavior levels of science education candidate teachers as intermediate, and their level of environmental attitude were high.

Estimates of the ordered probit for the probabilities of the environmental awareness, attitude and behavior of the students were presented in Table 4. The chi-square value for the environmental awareness (69.83 with 12 degrees of freedom) was statistically significant at the 0.01 level of probability. The estimated threshold value was positive and statistically significant (μ=1.655) at the same level of probability. This indicated that there was a natural ordering among the three response categories of environmental awareness of the students. Thirteen independent variables were included in the ordered probit model, and the estimated coefficients of these variables were tested using *t*-test statistics. Of the 13 independent variables, 7 socio-demographic and economic characteristics and, 6 environmental education characteristics were statistically significant at the 0.10 level of probability or better. The statistically significant socio-demographic and economic variables were gender, age, mother education, father education, residence and family income. Fernandez-Manzanal et al. [17] underlined also that socio-demographic development had an important role in the formation and growth of environmental awareness. However, Fransson and Garling [21] found that residential area had influences on environmental concern. The significant environmental variables were environmental courses taken, information source of media and usually or always following environmental news. This is because as the students are more likely from rural areas and generally follow environmental news from media. Some studies [40, 64, 65] stated that university students in Turkey had usually got their environmental knowledge from the mass media. However, Sadik and Sadik [41] determined that the internet and television as the most important factors in raising the university students' environmental awareness. However, the variables of household size, university and other institutions as main information sources and membership to environmental clubs or organizations had no statistical influence on the environmental awareness.

The results indicate that the environmental awareness increases as the student's age, father education, family income and number of environmental courses taken boost. Timur et al. [49] found that pre-service teachers' taking environment classes significantly increased their environment awareness levels which did not statistically differ their behaviors towards environment. On the other hand, the likelihood of the environmental awareness of the student would be higher with younger and less educated mother. Of the socioeconomic variables, the marginal effect for gender indicated that if the student was male, his likelihood of having a high environmental awareness decreased by 16.8% points. However, the likelihood of having a moderate and low environmental awareness increased by 1.84 and 0.11% points, respectively. This is because women tended to display a higher level of commitment and responsibility than men in social aspects and collective actions [17], and they were more environmental sensitive [22, 41, 66]. Previous studies [17, 44, 67-70] echoed with our findings. The marginal effect for age indicated that if the student had a higher age, his likelihood of having a high environmental awareness increased by 1.95% points. However, the likelihood of having a moderate and low environmental awareness decreased by 1.84 and 0.11% points, respectively. If the mother had a longer education duration, his likelihood of having a high environmental awareness decreased by 1.8% points. However, the likelihood of having a moderate and low environmental awareness increased by 1.7% and 0.0015% points, respectively. If the father had a longer education duration, his likelihood of having a high environmental awareness increased by 1.0% points. However, the likelihood of having a moderate and low environmental awareness decreased by 1.0 and 0.1% points, respectively. If the student was from rural areas, his likelihood of having a high environmental awareness increased by 11.0% points. However, the likelihood of having a moderate and low environmental awareness decreased by 10.5 and 0.5% points, respectively. If the student took more than two courses about environment, his likelihood of having a moderate environmental awareness increased by 5.8% points. However, the likelihood of having a low environmental awareness decreased by 5.5 percent.

If the information source of the student was the media, his likelihood of having a high environmental awareness increased by 9.29% points. However, the likelihood of having a moderate and low environmental awareness decreased by 8.7 and 0.6% points, respectively. If the student usually or always followed environmental news, his likelihood of having a high environmental awareness increased by 10.4% points. However, the likelihood of having a moderate and low environmental awareness decreased by 9.8 and 0.6% points, respectively.

The chi-square value for the environmental attitudes (61.26 with 13 degrees of freedom) was statistically significant at the 0.01 level of probability. The estimated threshold value was positive and statistically significant (μ=0.947) at the same level of probability. This indicated that there was a natural ordering among the three response categories of the environmental attitudes of students.

TABLE 4

Ordered Probit estimates for the probability of students' environmental awareness, attitude and behavior.

	Environmental awareness				Environmental attitude				Environmental behavior			
		Marginal effect				Marginal effect				Marginal effect		
	Coeff.	Y=0	Y=1	Y=2	Coeff.	Y=0	Y=1	Y=2	Coeff.	Y=0	Y=1	Y=2
GENDER	-0.626***	0.010**	0.156***	-0.167***	0.107	-0.003	-0.015	0.019	-0.237**	0.007*	0.086**	-0.093**
AGE	0.075***	-0.001**	0.018***	0.019***	-0.068***	0.002***	0.010***	-0.012***	-0.025	0.000	0.009	-0.010
HOUSHSIZE	0.040	-0.000	-0.009	0.010	-0.033	0.001	0.004	-0.006	-0.030	0.000	0.011	-0.011
MOTHEDUC	-0.069***	0.000**	0.017***	-0.018***	-0.012	0.000	0.001	-0.002	-0.002	0.000	0.001	-0.001
FATHEDUC	0.038*	-0.000	-0.009*	0.010*	0.058***	-0.002**	-0.008***	0.010**	-0.001	0.000	0.000	-0.000
RESIDANCE	0.505***	-0.004**	0.105***	0.110***	0.026	-0.000	-0.003	0.004	0.149	-0.004	-0.054	0.058
FAMINCOM	0.000**	0.000	0.000**	0.000*	0.000	0.000	0.000	0.000	0.000	0.000	0.000	0.000
ENVCOUR	0.220*	-0.055*	0.058*	0.000	-0.011	0.001	-0.002	0.000	0.113	-0.003	-0.041	0.044
INFSMEDIA	0.328**	-0.006	-0.086*	0.092*	0.209	-0.008	-0.032	0.041	-0.306**	0.007**	0.110**	-0.118**
INFSUNIV	0.200	-0.002	-0.046	0.049	0.307	-0.009*	-0.041*	0.050*	0.150	-0.004	-0.054	0.058
INFSINST	0.188	-0.002	-0.043	0.045	0.013	-0.000	-0.001	0.002	-0.053	0.001	0.019	-0.021
FENVNEWS	0.392***	-0.006*	0.098***	0.104***	0.437***	-0.017**	-0.066***	0.083***	1.002***	-0.04***	-0.340***	0.383***
MEMENVO	-0.001	0.000	0.000	-0.000	-0.001	0.000	0.000	-0.000	0.001	0.000	-0.000	0.000
ENVAWARL					0.799***	-0.028***	-0.117***	0.146***	-0.155	0.056	-0.061	0.000
ENVATTL									0.802**	-0.02***	-0.291***	0.316***
Mu :	1.65509***				0.94684***				2.11599***			
Log-Likelihood :	-305.25056				-252.19175				-405.23229			
Chi squared :	(12) 69.82779				(13) 61.25905				(14) 221.43063			
McFadden R^2 :	0.1026383				0.1082999				0.2145864			
N :	621				621				621			

***, **, * denote significance levels at 1%, 5% and, 10%, respectively.

Fourteen independent variables were included in the ordered probit model and the estimated coefficients of these variables were tested using *t*-test statistics. The statistically significant socio-demographic variables were age and father education. The significant environmental variables were environmental awareness and following environmental news. However, the variables of household size, university and other institutions as a main information sources and membership to environmental clubs or organization had no statistical influence on the environmental attitude. The results verified the likelihood for environmental attitudes increases with a decrease in age of the student. Kağıtçıbaşı [71] stated that environmental attitude started at a very early age, and if there was no important experience or circumstances, it did not change easily. However, Masud and Kari [33] concluded that age had a positive influence on environmental attitudes. Ercan and Bilen [70] determined that education levels of both mother and father did not play a role on their environmental attitudes, whilst Ozsevgec and Artun [72] underlined that educated parents with sufficient knowledge about the environment would transfer these information and experiences to their children, and they could develop positive environmental attitudes. As a student had a higher environmental awareness score and usually or always followed environmental news, it was likely that his environmental attitudes would be higher. Masud and Kari [33] found also that environmental awareness had a great influence on communities' perception and attitudes. Fernandez-Manzanal et al. [17] underlined also that it was essential to increase the awareness of the actions that made environmental problems worse and to define the behavior that helped prevent and mitigate these problems. The marginal effect for age indicated that if the student had an older age, the likelihood of having high environmental attitudes decreased by 1.25% points. However, the likelihood of having a moderate and low environmental awareness increased by 1.01 and 0.25% points, respectively. If the student's father had a longer education duration, the likelihood of having high environmental attitudes increased by 1.08% points. However, the likelihood of having moderate and low environmental attitudes decreased by 0.87 and 0.21% points, respectively. If the student had a higher environmental awareness, the likelihood of having high environmental attitudes increased by 14.6% points. However, the likelihood of having moderate and low environmental attitudes decreased by 11.77 and 2.87% points, respectively. If the student usually or always followed environmental news, his likelihood of having a high environmental attitude increased by 8.38% points. However, the likelihood of having a moderate and low environmental attitude decreased 6.64 and 1.74 percentage points, respectively.

The chi-square value for the environmental behavior (221.43 with 14 degrees of freedom) was statistically significant at the 0.01 level of probability. The estimated threshold value was positive and statistically significant (μ=2.116) at the same level of probability. This indicated that there was a natural ordering among the three response categories of students' environmental awareness. Fifteen independent variables were included in the ordered probit model, and the estimated coefficients of these variables were tested using *t*-test statistics. The statistically significant socio-demographic variable was only gender. The significant environmental variables were the environmental attitude, information source of media and usually or always following environmental news. However, the variables of household size, university and other institutions as a main information sources, membership to environmental clubs or organizations and taking environmental courses had no statistical influence on the students' environmental behavior. The results verified that if the student was male and used the media as the information source, so the likelihood of the student to behave environmental friendly would be less. Some previous studies [33, 73] contradicted with this phenomenon by indicating that men were more concerned about environmental issues, whilst some studies concluded that the students' levels of environment knowledge and behavior did not significantly differ on gender [62, 63, 74]. On the other hand, as the student had a higher environmental attitude and usually or always followed environmental news, the likelihood for the student to behave environmental friendly would be higher. Altinoz [61] concluded that taking environment classes increased the science and technology pre-service teachers' environmental knowledge and behavior. Karatekin [62] found that while taking environment courses at the university significantly differed the students' environmental behaviors. Timur et al. [48] concluded also that the level of environmental literacy of teacher candidates, who took courses on environment, was higher than the candidate teachers who did not. Monroe et al. [75] underlined also that behavior, in general, was supported by knowledge and attitude, but there was no direct cause-and-effect progression from knowledge to attitude and/or behavior. The marginal effect for gender indicated that if the student was male, his likelihood of having a high environmental behavior decreased by 9.36% points. However, the likelihood of a having moderate and low environmental behavior increased by 8.60 and 0.76% points, respectively. However, if the main information source of student was the media, the likelihood of having a high environmental behavior decreased by 11.84% points. However, the

likelihood of having a moderate and low environmental behavior increased by 11.07 and 0.77% points, respectively. If the student's attitudes were more environmental friendly, the likelihood of having a high environmental level increased by 31.64% points. However, the likelihood of having moderate and low environmental levels decreased by 29.19 and 2.46% points, respectively. If the student usually or always followed environmental news, his likelihood of behaving more environmental friendly increased by 38.31% points. However, the likelihood of having moderate and low environmental levels decreased by 34.07 and 4.23% points, respectively.

CONCLUSIONS

In this study, the average levels of environmental awareness, attitudes and behaviors of students were found to be high. Control variables as socio-demographic and economic factors generally had important impacts on the students' environmental awareness. Our findings verified also that the students' environmental attitude and behavior were generally affected by explanatory variables of environmental education or information. Gender had very high impacts on the environmental awareness and behaviors of the students in question. Thus, female students were more interested in environmental issues and their likelihood of high environmental awareness and behaviors were higher by 16.8% and 9.4% than male students, respectively. Age had an important impact on both the students' environmental awareness and attitudes, whereas, age had no impact on the students' environmental behavior. As students aged, their environmental awareness increased. However, as the students' age increased, their environmental attitudes decreased. The students form the rural residences had higher positive environmental awareness than the urban residence students. This might be that the rural residence students were more practically involved with environment, so that they are obliged to protect their surrounding resources. While high level of mother education had negative influence on the students' environmental awareness, high level of father education had positive influence on the students' environmental awareness and attitude.

As the curiosity levels of the students towards environmental news increased, their environmental awareness, attitude and behavior levels increased as well. While the mass media as a main information source had an important positive influence on the students' environmental awareness, it had a negative influence on their environmental behaviors. While the students who took two or more environment courses had significantly higher environmental awareness, this had no influence on their environmental attitudes and behaviors. Since the students had taken about 3.4 environment courses, this number might not be enough to show their environmental attitude or behavior in their graduation time. Whereas, some departments don't have any course or enough courses related to environment in their curricula of education programs, they may have a direct or indirect impact on environment by their activities. The students' environmental awareness had the biggest positive influence on their environmental attitudes. Thus, if the students had higher environmental awareness, their attitudes would be more environmentally-conscious. However, this study concluded that the students who had higher environmental awareness would not behave more environmentally-conscious. The students' environmental attitudes had very high positive influence on their environmental behaviors. Thus, if the students had higher environmental attitudes, they would behave more environmentally-conscious. However, our study concluded that environmental awareness of the students was not sufficient for them to put this awareness into practice in their daily life.

This study provided a clear picture about the environmental awareness, attitude and behavior levels of candidate graduates from undergraduate programs and the determinants on their environmental sensitivities. Therefore, this study would help decision makers to improve the curricula of undergraduate programs and to formulate better strategies for conserving environment. Considering the results of the current study, the following suggestions could be put forward:

To increase the graduates' environmental awareness, the departments should put sufficient environment courses as compulsory on their programs. To increase the students' environmental awareness's and attitudes, the departments should focus especially on male students in the classes by encouraging them to participate in environmental conservation activities such as nature and environmental trips. However, it should be benefited actively from the leadership of female students on environmental education and conservation activities. The departments should try to improve the younger students' environmental awareness by interference with older age students. The departments should enable the students to share their environmental knowledge and experiences in their classes and environmental activities. Since mass media was the main information source of the students, the departments should use mass media intensively to facilitate the transmission of environmental information and promote more positive environmental attitudes. However, mass media should give accurate information to the society on time. Providing accurate information by mass media could influence the student's behaviors

positively. The department should prepare the graduates as responsible people to preserve the environment by bringing them environment-related knowledge, awareness, skills and values. In order to increase the students' environmental awareness, attitudes and behaviors, the departments should focus on increasing the students' curiosity levels towards the environmental news, and nature executions or tours should be organized. To increase the students' environmental attitudes, the departments should focus on providing the students with environmental awareness. To increase an environmentally responsible behavior, the departments should focus on providing environmental attitudes to their students.

Environmental institutions or organizations should focus on especially the families in urban areas to increase their environmental awareness by means of lifelong environmental education programs. Since the students are influenced by non-formal environments to a great extent, the environmental awareness and attitudes of the parents should be raised by informing them about the difficulties of environmental problems which they are not even aware of. The environmental literacy levels of parents should be taken into account as an explanatory variable into the models to explain the students' environmental awareness, attitudes and behaviors in the future researches. This study is limited to Ondokuz Mayis University. The research subject should be also conducted in other departments and universities to compare the levels of environmental literacy.

ACKNOWLEDGEMENTS

The authors thank all students participating in the surveys and the lecturers for their help in applying the surveys in Ondokuz Mayis University. The authors are grateful to the editor and anonymous referees for their very useful comments and suggestions. The authors gratefully acknowledge the help of Birol Kurt and Emine Bol Yazici (International Relations Office of Ondokuz Mayis University) in the English editing of this article.

REFERENCES

[1] Coertjens, L., Boeve-De Pauw, J., De Maeyer, S. and Van Petegem, P. (2010) Do schools make a differences in their students' environmental attitudes and awareness? Evidance from Pisa 2006. International Jopurnal of Science and Mathematics Education 8, 497-522.

[2] Décamps, H. (2000) Demanding more of Landscape Research (and research). Landscape and Urban Planning 47, 105-109.

[3] Thapa, B. (2001) Environmental concern: A comperative analysis between students in recreation and park management and other departments. Environmental Education Research 7, 39-53.

[4] Watson, K. and Halse, C. M. (2005) Environmental attitudes of pre-service teachers: a conceptual and methodological dilemma in cross-culturel data collection. Asia Pasific Education Review 6 (1), 59-71.

[5] Negev, M., Garb, Y., Biller, R., Sagy, G. and Tal, A. (2010) Environmental problems, causes, and solutions: an open question. The Journal of Environmental Education 4 (2), 101-115.

[6] Stern, P. C. (1992) Psychological dimension of global environmental change. Annual Review of Psychology 43, 269–302.

[7] Davis, J. (1998) Young children, environmental education, and the future. Early Childhood Education Journal 26 (2), 117-123.

[8] Corcoran, P. B. and Wals, A. E. J. (2004) Higher education and the challenge of sustainability, problematics, promise and practice. Dordrecht, The Netherlands: Kluwer.

[9] Palmer, J. (1998) Environmental Education in the 21st Century: Theory, Practice, Progress and Promise. New York: Routledge.

[10] Bradley, J. C., Waliczek, T. M. and Zajicek, J. M. (1999) Relationship between environmental knowledge and environmental attitude of high school students. The Journal of Environmental Education 30 (3), 17–21.

[11] Salequzzman, M. D. and Stocker, L. (2001) The context and prospects for environmental education and environmental career in Bangladesh. Int J Sustain High Educ 2(2), 104–121.

[12] Corcoran, P. B., Walker, K. E. and Wals, E. J. (2004) A critique of case-studies and case stories: A sustainability in higher education. Environ. Education Res. 10, 7-21.

[13] Ozmen, D., Cetinkaya, A. and Nehir, S. (2005) Üniversite öğrencilerinin çevre sorunlarına yönelik tutumları. TSK Koruyucu Hekimlik Bülteni 4(6), 330-344.

[14] Mancl, K. M., Carr, K. and Morrone, M. (2003) Profile of Ohio adults with low environmental literacy. The Ohio Journal of Science 103(3), 38-41.

[15] Madsen, P. (1996) What can universities and professional schools do to save the environment? In J. B. Callicott and F. J. da Rocha (Eds.), Earth Summit Ethics: toward a reconstructive postmodern philosophy of environmental education. NY: Albany State University of New York Press, 71-91 pp.

[16] Perlstring, L. (1997) Measuring environmental attitudes: the new environmental paradigm. Retrieved from www.docstoc.com/docs/20845968/Environmental-Attitude.
[17] Fernández-Manzanal, R., Rodríguez-Barreiro, L. and Carrasquer, J. (2007) Evaluation of environmental attitudes: analyisi and results of a scale applied to university students. Inc.Sci Ed 91, 988-1009.
[18] Hernandez, O. and Monroe, M. (2000) Thinking about behavior. In B. Day and M. Monroe (Eds.), Environmental education and communication for a sustainable world. Handbook for international practitioners (pp. 17-22), Academy for Educational Development, Washington, DC.
[19] Aklin, M., Bayer, P., Harish, S. P. and Urpelainen, J. (2013) Understanding environmental policy preferences: New evidence from Brazil. Ecological Economics 94, 28-36.
[20] Dillon, P. J. and Gayford, C. G. (1997) A psychometric approach to investigating the environmental beliefs, intentions and behaviours of preservice teachers. Environmental Education Research 3, 283-297.
[21] Fransson, N. and Gärling, T. (1999) Environmental concern: Conceptual definitions, measurement methods, and research findings. Journal of Environmental Physhology 19, 369-382.
[22] Tikka, P. M., Kuitunen, M.T. and Tynys, S. M. (2000) Effects of educational background on students' attitudes, activity levels, and knowledge concerning the environment. The Journal of Environmental Education 31(3), 12–19.
[23] Jensen, B. (2002) Knowledge, action and pro-environmental behaviour. Environmental Education Research 8(3), 325–334.
[24] Bamberg, S. (2003) How does environmental concern influence specific environmentally related behaviours? A new answer to an old question. Journal of Environmental Psychology 23, 21-32.
[25] Wong, K. K. (2003) The enwironmental awareness of university students in Beijing, China. J. Contemporary China 12, 519-536.
[26] Hsu, S. J. (2004) The effects of an environmental education program on responsible environmental behavior and associated environmental literacy variables in Taiwanese college students. The Journal of Environmental Education 35(2), 37-48.
[27] McMillan, E. E., Wright, T. and Beazley, K. (2004) Impact of university-level environmental studies class on students' values. The Journal of Environmental Educatin 35(3), 19–28.
[28] Hassan, A. and Ismail, M. Z. (2011) The infusion of environmental education in chemistry teaching and students' awareness and attitudes towards environment in Malaysia. Prodecia-Social and Behavioral Sciences 15, 3404-3409.
[29] Ogunbiyi, J. O. and Ajiboye, J. O. (2009) Pre-service teachers' knowledge of and attitudes to some environmental education concepts using value education strategies. Anthropologist 11(4), 293-301.
[30] Grob, A. (1995) A structural model of environmental attitudes and behaviour. Journal of Environmental Physhology 15, 209-220.
[31] Kaiser, F. G., Wölfing, S. and Fuhrer, U. (1999) Environmental attitude and ecological behaviour. Journal of Environmental Physhology 19, 1-19.
[32] Klöckner, C. A. (2013) A comprehensive model of the pyschology of environmental behaviour-a meta analysis. Global Environmental Change 23, 1028-1038.
[33] Masud, M. M. and Kari, F. B. (2015) Community attitudes towards environmental conservation behaviour. Marine Policy 52, 138-144.
[34] Tanner, C. (1999) Constrains on environmental behaviour. Journal of Environmental Phychology 19, 145-157.
[35] Klaczynski, P. A. and Reese, H. W. (1990) Educational trajectory and action orientation: Grade and track differences. Journal of Youth and Adolescence 20(4), 441–462.
[36] Schahn, J. and Holzer, E. (1990) Studies of environmental concern. The role of gender, knowledge and background variables. Environment and Behavior 22, 767–786.
[37] Zelezny, L. (2000) Elaborating on gender differences in environmentalism. Journal of Social Issues 5(3), 443-458.
[38] De La Vega, E. L. (2004) Awareness, Knowledge and Attitude About Envıronmental Education: Responses from Environmental Specialists, High School Instructors, Students, and Parents. PhD Thesis, The College of Education, the University of Central Florida, Orlando, 97 p.
[39] Beyhun, N. E., Vaizoğlu, S. A., Mete, A., Okur, S., Ongun, M., Orçan, S. and Güler, Ç. (2007). Environmental risk perception of last grade students in Hacettepe University Medical Faculty within 2005-2006 education period. TSK Koruyucu Hekimlik Bülteni 6(5), 345-350.
[40] Yilmaz, A., Morgil, I., Aktuğ, P. and Göbekli, I. (2002) Knowledge of the secondary school and university students on the environment, environmental concepts and problems and

suggestions. Hacettepe Üniversitesi Eğitim Fakültesi Dergisi 22, 156-162.
[41] Sadik, F. and Sadik, S. (2014) A study on environmental knowledge and attitudes of teacher canditates. Procedia-Social and Behavioral Sciences 116, 2379-2385.
[42] Ozsoy, S. (2012) A survey of Turkish pre-service science teachers' attitudes towards the environment. Journal of Educational Reserach 12(46), 121-140.
[43] Önder, S. (2006) A servey of awareness and behavior in regard to environmental issues among Selçuk University Students in Konya, Turkey. Journal of Applied Sciences 6(2), 347-352.
[44] Aydin, F. and Çepni, O. (2010) University students' attitudes towards environmental problems: a case study from Turkey. International Journal of the Physical Sciences 5(17), 2715-2720.
[45] Erkal, S., Kilic, I. and Sahin, H. (2012) Comparison of environmental attitudes of university students determined via new environmental paradigm scale according to the students' personal characteristics. Journal of Educational Reserach 12(49), 21-39.
[46] Gürbüz, H. and Çakmak, M. (2012) An investigation of biology education department students' attitude towards environment. Dicle Üniversitesi Ziya Gökalp Eğitim Fakültesi Dergisi 19, 162-173.
[47] Kolomuç, A. and Açışlı, S. (2013) A comparison of the attitudes of prospective science teachers and prospective social teachers towards the environment. International Journal of Social Science 6(7), 687-696.
[48] Timur, S., Timur, B. and Yilmaz, S. (2013) Determining primary school candidate teachers' levels of environmental literacy. Anthropologist 16(1-2), 57-67.
[49] Timur, S., Timur, B. and Karakas, A. (2014) Investigating pre-service teachers' knowledge and behaviors toward environment. Anthropologist 17(1), 25-35.
[50] OMU. (2015). From <http://oid.omu.edu.tr/istatistikler/mevcutsay.html.> (Retrieved July 15, 20015)
[51] Karasar, N. (2010) Bilimsel Araştırma Yöntemi. Nobel Yayın Dağıtım, Ankara.
[52] Buyukozturk, S., Kilic, C., Akgun, O. E., Karadeniz, S. and Demirel, F. (2009). Bilimsel Araştırma Yöntemleri, Pegem A Yayincilik, Ankara.
[53] McLean-Meyinsse, P. E. (1997). Factors influencing early adoption of new food products in Louisiana and Southeast Texas. J. Food Distrib. Res. 28(3), 1–10.
[54] Abdel-Aty, M. A. (2001) Using ordered probit modeling to study the effect of ATIS on transit ridership. Transp. Res. Part C 9, 265-267.
[55] Boz, I. and Akbay, C. (2005) Factors influencing the adoption of maize in Kahramanmaras province of Turkey. Agricultural Economics 33, 431-440.
[56] Tsui, H. C. (2014) What affects happiness: Absolute income, relative income or extected income? Journal of Policy Modelling 36, 994-1007.
[57] Chen, K., Ali, M., Veeman, M,, Unterschultz, J. and Le, T. (2002) Relative importance rankings for pork attributes by Asian origin consumers in California: Applying an ordered probit model to a choice-based sample. J. Agric. Appl. Econ. 34(1), 67–79.
[58] Maddala, G. S. (1983) Limited-Dependent and Qualitative Variables in Econometrics. Cambridge University Press, Cambridge.
[59] Greene, H. W. (1993) Econometric Analysis. Fifth Edition, Prentice Hall, New Jersey.
[60] Liao, T. F. (1994) Interpreting Probability Models: Logit, Probit, and Other Generalized Linear Models. Sage, Thousand Oaks, CA.
[61] Altinoz, N. (2010) Fen bilgisi Öğretmen Adaylarının Çevre Okuryazarlık Düzeyleri. Master Thesis (Unpublished), Sakarya University, Sakarya.
[62] Karatekin, K. (2011) Sosyal Bilgiler Öğretmen Adaylarının Çevre Okuryazarlık Düzeylerinin Belirlenmesi. PhD Thesis (Unpublished), Gazi University, Ankara.
[63] Timur, S. (2011) Fen Bilgisi Öğretmen Adaylarının Çevre Okuryazalık Düzeylerinin Belirlenmesi. PhD Thesis (Unpublished), Gazi University, Ankara.
[64] Ibis, S. (2009) Biology Teacher Candidates' Views on Global and National Environmental Issues. MA Thesis (Unpublished), Institution of Education Sciences, Gazi University, Ankara.
[65] Daştan, T. (2007) Evaluation of Environmental Problems in Turkey against the Biology Teachers' Perspectives. Master Thesis (Unpublished), Institution of Education Sciences of Gazi University, Ankara.
[66] Mohai, P. (1991) Men, women and the environment. An examination of the gender gap in environmental concern and activism, Society and Natural Resources 5, 1–19.
[67] Davidson, D. and Freudenberg, W. (1996) Gender and environmental risk concerns: A review of available research. Environment and Behavior 28, 302–339.
[68] Yilmaz, O., Boone, W. J. and Andersen, H. O. (2004) Views of elementary and middle school Turkish students toward environmental

issues. International Journal of Science Education 26(12), 1527-1546.
[69] Alp, E., Ertepinar, H., Tekkaya, C. and Yilmaz, A. (2006) A statistical analysis of children's environmental knowledge and attitudes in Turkey. International Research in Geographical and Environmental Education 15(3), 210–223.
[70] Ercan, O and Bilen, K. (2014) A research on electronic waste awareness and environmental attitudes of primary school students. Anthropologist 17(1), 13-23.
[71] Kağıtçıbaşı, Ç. (1988) İnsan ve insanlar: Sosyal Psikolojiye Giriş. Evrim Basım Yayım Dağıtım, İstanbul.
[72] Ozsevgec, T. and Artun, H. (2012) Ilkogretim ogrencilerinin cevreye yonelik tutumlarina etki eden faktorlerin degerlendirilmesi. X. Ulusal Fen ve Matematik Egitimi Kongresi 27-30 Haziran, Nigde Universitesi, Nigde.
[73] Shen, J. and Saijo, T. (2008) Re-examining the relations between socio-demographic characteristics and individual environmental concern: evidence from Shang-hai data. J Environ Psychol 28(1), 42–50.
[74] Budak, D. B., Budak, F., Zaimoğlu, S., Kekeç, S. and Sucu, M. Y. (2005) Behaviour and attitudes of students towards environmental issues at faculty of agriculture Turkey. Journal of Applied Sciences 5, 1224-1227.
[75] Monroe, M., Day, B. and Grieser, M. (2000). GreenCOM weaves four strands. In B Day and M Monroe (Eds.), Environmental education and communication for a sustainable world. Handbook for international practitioners. Washington, DC: Academy for Educational Development, pp. 3-6.

Received: **04.10.2015**
Accepted: **17.12.2015**

CORRESPONDING AUTHOR

Mehmet Bozoglu
Ondokuz Mayis University,
Faculty of Agriculture,
Department of Agricultural Economics,
55200 Samsun, Turkey

e-mail: mehmetbo@omu.edu.tr

© by PSP Volume 25 – No. 7/2016, pages 2554-2562 Fresenius Environmental Bulletin

KINETICS OF THE OZONE OXIDATION OF WEAK ACID BRILLIANT GREEN IN AQUEOUS SOLUTION

Yongjun Shen,1,2 Qihui Xu,1 Yuwei Pan,1,3 Jiandong Ding1 and Yi Wang1

[1] School of Chemistry and Chemical Engineering, Nantong University, Nantong 226019, China

[2] Jiangsu Eastern Coast and Yangtse River Area Development Institute, Nantong 226019, China

[3] Key Laboratory of Pollution Process and Environmental Criteria, Ministry of Education, Tianjin Key Laboratory of Urban Ecology Environmental Remediation and Pollution Control, College of Environmental Science and Engineering, Nankai University, Tianjin 300071 China

ABSTRACT

An ozone system was used to study the degradation of weak acid brilliant green and the kinetic model of degradation was established in this paper. The effects of oxygen flow rate, temperature, initial concentration of the weak acid brilliant green and pH were investigated through a series of batch tests. To be specific, in this study, the kinetics of ozonation of weak acid brilliant green were investigated under different experimental conditions in an ozone reactor (50-150 mg/L dye, 293-333 K, ozone flux in 16-60 L/h, pH in 1-13 range). A relatively suitable degradation temperature of dye was chosen at 293 K. The degradation rate increased with the increase of pH. It can be observed that with the increase of the initial concentration of weak acid brilliant green, the degradation rate decreased. Enhancing oxygen flow rate also enhanced the removal of dye. The kinetic model of weak acid brilliant green was established and the rate constants and the kinetic system of the reaction between ozone and dye were obtained by fitting the experimental data to a kinetics model based on a first order reaction. The ozonation processes and the impacts of ozone on dying wastewater degradation were clearly identified.

KEYWORDS:

Ozonation, dyes wastewater, weak acid brilliant green, kinetics model

INTRODUCTION

In terms of its considerable economic contribution, there has been a rapid development of dye production and consumption, and enormous volume of dye-containing wastewater has been generated.[1] The printing and dyeing wastewater is known to be degraded very slowly by microorganisms.[2] This has become an important issue that seriously threats the environment and human health.[3]

At present, several treatment technologies such as adsorption[4], flocculation[5], electrochemical oxidation processes[6] are used to remove the organic matters from dye wastewater.[7] However, these conventional treatments still can not solve some problem. For example, these above treatments need more time to degrade printing and dyeing wastewater or the degradation can not meet the requirements of the out-water. Therefore, several advanced oxidation process (AOPs) have been proposed for the complete destruction of organic dyes in aqueous water.[8] In AOPs, ozone, in particular, has been recognized as an efficient oxidant for treatment of some industrial wastewater.[9] Ozone-based AOPs involving the generation of radical intermediates, particularly the hydroxyl radicals (·OH) which are highly reactive with most organic compounds,[10-12] can be widely used in dye industrial areas. Since ozone was very effective in removing color from textile wastewater, numerous published studies have emerged over the last decades.[13] However, when applied, most of studies completed on the treatment of wastewater were restricted to the exposition of experimental data with no inclusion of the kinetics governing the process. The purpose of the paper was to study dynamic models of ozonation based on the weak acid brilliant green as the object.

In this paper, the main work of study was to investigate the decomposition of weak acid brilliant green by ozone oxidation process. More specifically, it was to investigate the effects of the main parameter influence on the degradation amount

such as (pH, temperature, oxygen flow rate, initial concentration). Dynamic model was established and verified according to the above experimental datum and detailed analyses.

EXPERIMENTAL

Experiment procedure. The molecular formula of weak acid brilliant green is $C_{20}H_{13}N_2NaO_5S$. Fig. 1 showed the molecular structure of weak acid brilliant green and its UV/Vis spectrum. The ozone reactor and the technical processes can be seen in Fig. 2 (1.oxygen bottle; 2.glass rotameter; 3.ozone generator; 4.venturi jet; 5.thermommeter; 6.thermal couple; 7.resistance wire; 8.rotor; 9.thermostatic water bath; 10.reactor; 11.circulating pump; 12.attemperator; 13.KI absorption bottle). In the course of the experimental run, the pure oxygen in oxygen bottle was measured by glass rotameter and then entered the ozone generator for reaction. Furthermore, it was necessary to ensure the total flow rate remain unchanged. Part of the gas mixture was released to the outdoor after the production rate of ozone getting stable and the other part of the gas mixture evenly added into the reaction solution by Venturi water injector. Afterwards, the ozone contacted with the solution for reaction. The reaction temperature was indicated by thermocouple in the reaction process. In addition, the thermostatic water bath was used to control the reaction temperature, so as to meet the temperature condition of experimental operation. At the end of the reaction, the residual ozone in the off-gas was released into the KI absorption bottle, and was absorbed by the KI solution with mass fraction of 2%. The distilled water was used to clean a beaker, and to configurate weak acid brilliant green whose concentration was 100 mg/L (analytical pure, Shanghai Jiaying Co., Ltd.). NaOH or H_2SO_4 was used to adjust suitable pH to a certain value. The absorbance of the reaction solution was determined by ultra-violet and visible spectrophotometer (752N).

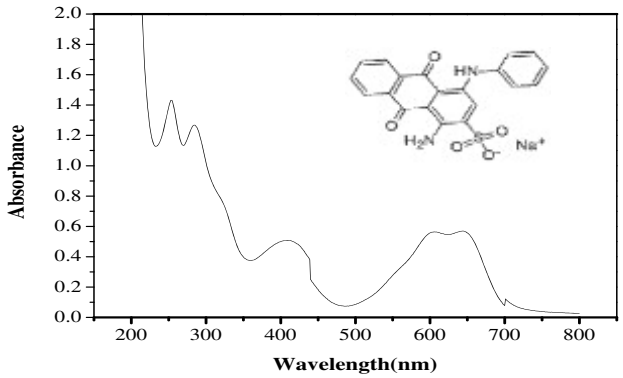

FIGURE 1
Molecular structure and UV/Vis spectrum of weak acid brilliant green.

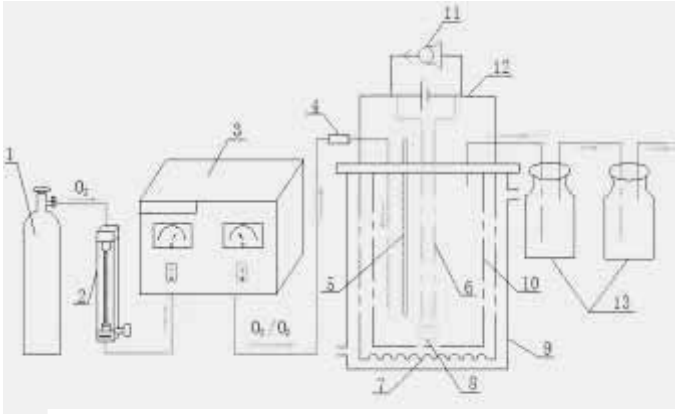

FIGURE 2
Schematic diagram of experimental set-up.

RESULTS AND DISCUSSION

The analysis of the ozone degradation of weak acid brilliant green. The effect of initial pH on weak acid brilliant green degradation. Fig. 3(a) showed that under the condition of weak acid brilliant green initial concentration of 100 mg/L, the ozone flux of 32 L/h and temperature of 293 K, the effects of ozone degradation were respectively investigated with the pH varied from 1 to 13.

It can be found from Fig. 3 that in the range of pH from 1 to 13, the degradation rate was strongly pH dependent. The degradation rate increased with the increase of pH. It was also not difficult to see that it had higher degradation rate at alkaline condition. Under the acid condition, the dominance of the degradation reaction of the weak acid brilliant green was direct oxidation of ozone molecules.[14] At this time the generation of hydroxyl radicals (·OH) was suppressed. In alkaline conditions, the ·OH oxidation played a leading role. At OH^- catalytic ozone, decomposition triggered a chain reaction to obtain the ·OH which was more lively than ozone molecules. And they can quickly and indiscriminately reacted with weak acid brilliant green, so as to speed up the weak acid brilliant green removal rate.[15] Under alkaline conditions, OH^- can help produce hydroxyl radicals. The above discussions also indirectly demonstrated that hydroxyl radical was indeed present. [16]

By processing the data and fitting the figure, the reaction was determined for the first order reaction. And the changing of k_{obs} with pH could be shown in the following data. What can be seen from Fig. 3(b) and Fig. 3(c) that k_{obs} increased together with pH but they were two linear upward trend lines. When pH < 6.21, k_{obs} rose faster; when the pH > 6.21, k_{obs} went up slowly. Under the condition of low pH, the reaction was mainly related to molecular O_3 degradation. When pH was elevated, OH^- had a catalytic effect on ozone decomposition. It had generated a lot of strong oxidizing ·OH to promote the degradation of the weak acid brilliant green. When the pH was greater than a certain value, the increasing rate of the k_{obs} was leveling off, for the ·OH from ozone decomposition was sufficient.[17]

The influence of initial concentration of weak acid brilliant green degradation. Fig. 4(a) showed that under the condition that pH of 6.21, the ozone flux of 32 L/h and temperature of 293 K, the effects of ozone degradation were respectively studied with the initial concentration of the weak acid brilliant green solution for 50, 75, 100, 125 and 150 mg/L.

It can be seen from Fig. 4(a) that with the increase of initial concentration, the degradation rate decreased. After putting into ozone, the instantaneously generated ·OH was changeless. From the principle of chemical equilibrium, the larger the concentration of reactant was, the more beneficial it was for chemical reactions to move forward, which was helpful to increasing degradation and the efficiency of ozone.[18] However, as the high initial concentration of reaction solution leaded to the high content of the intermediate product and made the productions of hydroxyl free radicals be limited so that promoted the reverse reaction.[19] Finally, it leaded to the decrease of the calculated degradation rate.

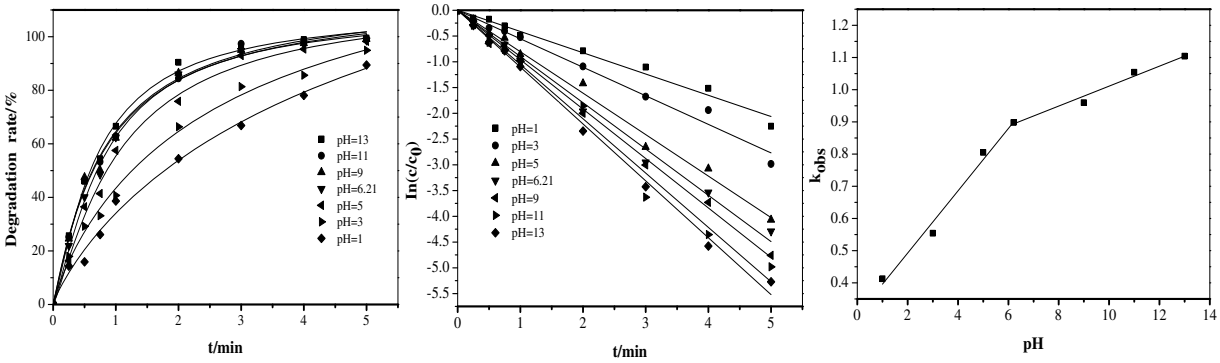

(a) (b) (c)

FIGURE 3

(a)The effect of initial pH on degradation rate, (b)The pseudo-first-order kinetics fitting curve in different initial pH, (c)The diversification of k_{obs} in different pH.

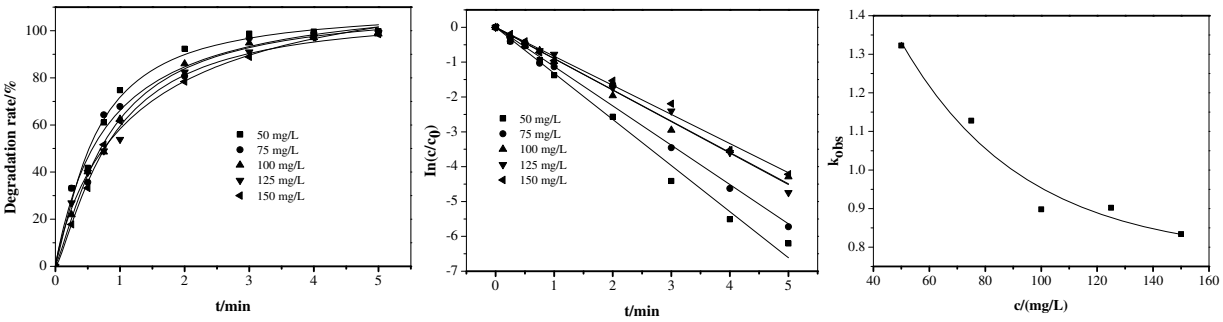

(a) (b) (c)

FIGURE 4

(a)The effect of initial concentration on degradation rate, (b)The pseudo-first-order kinetics fitting curve in different initial concentration, (c)The diversification of k_{obs} in different concentration.

By processing the data and fitting the figure, the reaction was determined for the first order reaction. And the changing of k_{obs} with initial concentration could be shown in the following figures. From Fig. 4(b) and Fig. 4(c), it could be seen that k_{obs} decreased from 1.32 to 0.83 when the initial concentration of the weak acid brilliant green increased from 50 mg/L to 150 mg/L, and the change of k_{obs} with concentration was very obvious. This was because that there were the intermediate products in the reaction process, which participated in the competition reaction. The higher the initial concentration was, the larger the amount of the intermediate products was, and the more obvious the inhibitory effect on the reaction was.

The influence of ozone flux of weak acid brilliant green degradation. The initial concentration of weak acid brilliant green was set at 100 mg/L, the pH value was controlled at 6.21 and the temperature was on 293 K, then the effects of ozone degradation were respectively investigated under the conditions of the ozone flux in 16 L/h, 24 L/h, 32 L/h, 40 L/h, 50 L/h and 60 L/h.

Fig. 5(a) showed that the weak acid brilliant green degradation rate increased with the increase of ozone flux, but when the flow rate was over the optimal value of ozone, the degradation rate decreased instead. It was mainly because that with the increase of ozone flux, dosing quantity increased which also made the flow rate per unit area increase accordingly.[20] The amount of ozone and ·OH increased in the reaction system. In consequence, it would be beneficial to the degradation of weak acid brilliant green.[21] However, with the increase of the flow rate, liquid phase the main body of ozone generation accumulated, and the concentration increased. When the ozone concentration exceeded a certain value, the ozone in the liquid phase tended to saturate, and achieved the stable concentration of ozone.[22] As a result, ozone utilization rate reduced and the growth of the degradation rate of weak acid brilliant green became small too.

By processing the data and fitting the figure, the reaction was determined for the first order reaction. The changing of k_{obs} with flow rate could be shown in the following Fig. 5(a) and Fig. 5(c) showed that k_{obs} increased gradually with the increase of ozone flux. Nevertheless, the increase was not linear. When the flow rate of ozone exceeded a certain value, the increase trend of k_{obs} gradually flattened out. This was because that the greater the ozone flow rate was, the more the hydroxyl free radicals in the reaction system were. At the same time, the degradation of weak acid brilliant green was promoted. When the ozone flux reached a certain value, however, the amount of ·OH in the liquid phase tended to saturate, and its effect on the degradation of weak acid brilliant green was less, so the increase of k_{obs} was slow.

The influence of temperature on the weak acid brilliant green degradation. Under the conditions that the initial concentration of weak acid brilliant green was set at 100 mg/L, the pH value was adjusted to 6.21 and ozone flow was controlled to 32 L/h. The effects of ozone degradation were respectively examined under the condition of the water bath temperature of 293 K, 303 K, 313 K, 323 K and 333 K.

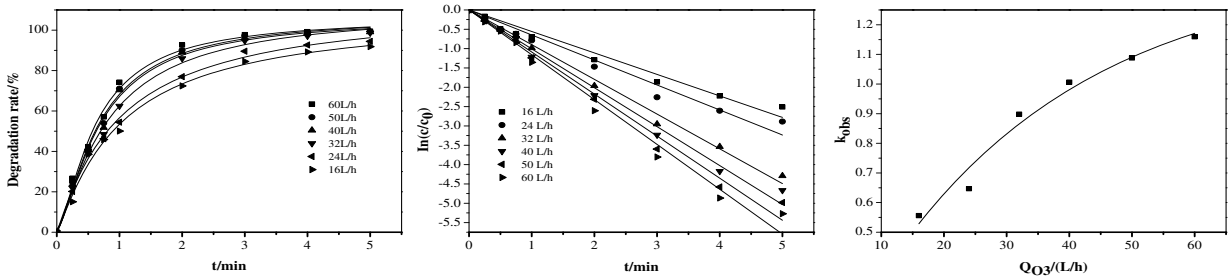

(a) (b) (c)

FIGURE 5

(a)The effect of ozone dosage on degradation rate, (b)The pseudo-first-order kinetics fitting curve in different initial ozone dosage, (c)The diversification of k_{obs} in different initial ozone dosage.

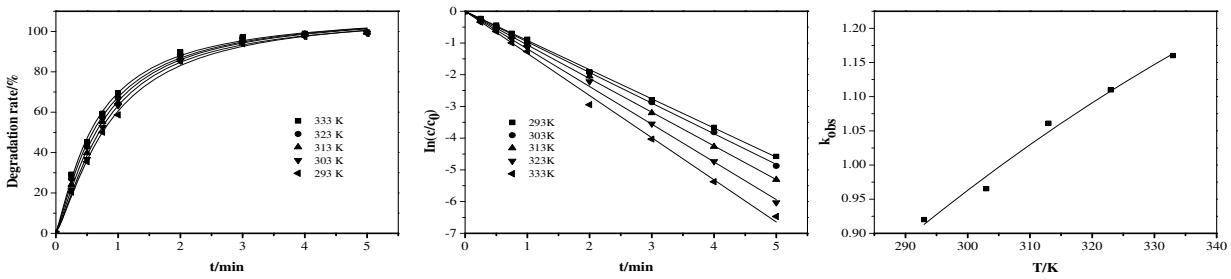

(a) (b) (c)

FIGURE 6

(a)The effect of temperature on degradation rate, (b)The pseudo-first-order kinetics fitting curve in different initial temperature, (c)The diversification of k_{obs} in different initial temperature

Fig. 6(a) showed that in the experiment where the temperature was above 293 K, as the temperature rose, degradation rate also rose. This reason was that according to the principle of chemical balance, with the increase of reaction temperature, the activation energy reduced, the generation rate of hydroxyl radicals improved, the degradation reaction rate of weak acid brilliant green speeded up, and the degradation rate increased.[23]

By processing the data and fitting the figure, the reaction was determined for the first order reaction. And the changing of k_{obs} with the temperature could be shown in the following figures. Fig. 6(b) and Fig. 6(c) showed that the higher the temperature was, the greater the k_{obs} was. When temperature increased from 293 K to 333 K, k_{obs} increased from 0.92014 to 1.16. But the growth was not linear. As the temperature continued to rise, the increase of k_{obs} became slowly until the temperature increased to a certain value. It shows that in the early stage of the range, with the rise of the temperature, activation energy basically remained unchanged. When the degradation rate accelerated, the increasing amplitude of the k_{obs} got faster.

Ozone degradation kinetics analysis of weak acid brilliant green. It has been said that the mechanisms of ozone reactions may follow two possible degradation pathways which simultaneously exist during ozone reaction processes: molecular ozone attack (direct reaction) and the free radical mechanism (indirect reaction). The following reaction kinetic Eq. 1 was obtained:

$$-\frac{dc_i}{dt} = k_{o_3} c_i + k_{OH} c_i c_{\bullet OH} \quad (1)$$

The Eq. 8 could be explained that degradation rate of dye follows first order kinetic with respect to both ozone and dye. (c_i: the concentration of weak acid brilliant green, O_3: ozone in the solution, ·OH: hydroxyl free radical in the solution.) k_{O3} was the reaction rate constant between ozone molecule and weak acid brilliant green, and $k_{\cdot OH}$ was the reaction rate constant between hydroxyl radicals and weak

acid brilliant green.[24]

Under simplified conditions, weak acid brilliant green degradation can be thought of as conforming to the fitting of first order reaction,[25] namely:

$$\frac{dc}{dt} = k_{obs}c \quad (2)$$

The logarithm was taken on both sides, and the Eq. 3 can be got:

$$\ln(c/c_0) = k_{obs}t \quad (3)$$

The dynamics model of ozone degradation of weak acid brilliant green. The whole reaction of ozone degradation may proceed through two pathways, including direct reaction by molecular O_3 and indirect reaction by ·OH both direct oxidation of ozone. Therefore, there must be a certain relationship between the apparent rate constant k_{obs} and affecting factors including ozone flux Q, temperature T, pH value and the initial concentration of the weak acid brilliant green c_0. The following empirical model could be used to fit:[26-28]

$$k_{obs} = A(-E/RT)Q_{O_3}^{\alpha}c_0^{\beta}\left[OH^-\right]^{\gamma} \quad (4)$$

The logarithm removed on both sides, and the Eq. 5 can be got:

$$Ink_{obs} = InA - E/RT + \alpha InQ_{O_3} + \beta Inc_o + \gamma In[OH^-] \quad (5)$$

For linear fitting the data of different experimental conditions, the results can be seen in Table 1.

TABLE 1
kobs of the weak acid brilliant green under different conditions for the ozonation.

pH	c_0/(mg/L)	Q_{O3}/(L/h)	T /K	k_{obs}/min^{-1}
1	100	32	293	0.412
3	100	32	293	0.553
6.21	100	32	293	0.898
9	100	32	293	0.959
13	100	32	293	1.104
6.21	50	32	293	1.323
6.21	125	32	293	0.902
6.21	100	16	293	0.555
6.21	100	40	293	1.007
6.21	100	60	293	1.159
6.21	100	32	303	1.061

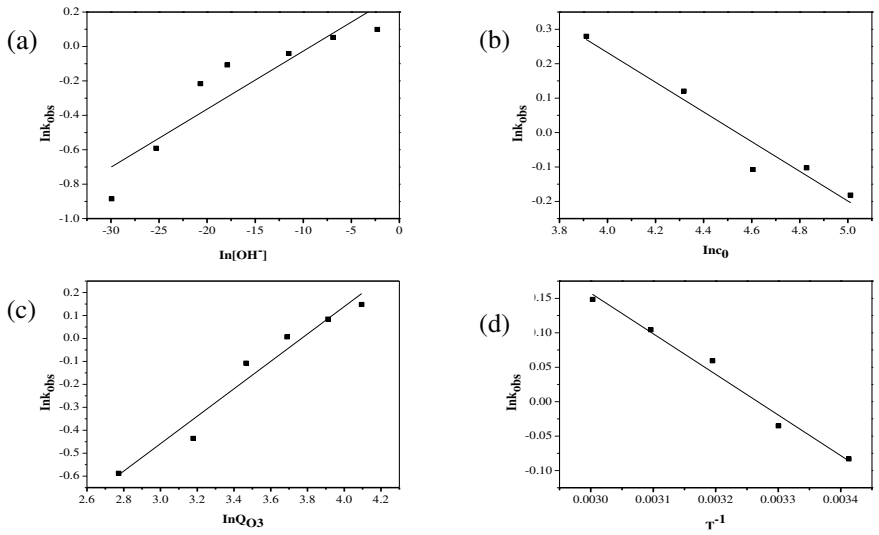

FIGURE 7
(a)The fitting curve of Ink_{obs}- In[OH^-], (b) The fitting curve of Ink_{obs}-Inc_0
(c)The fitting curve of Ink_{obs}-In Q_{O3} , (d)The fitting curve of Ink_{obs}-InT^{-1}.

$$Ink_{obs} = InA + 0.0337In[OH^-] - 0.431Inc_o + 0.598InQ_{O_3} - 589.49/T \quad (6)$$

$$k_{obs} = A\exp(-4901/RT)Q_{O_3}{}^{0.598}c_0{}^{-0.431}\left[OH^-\right]^{0.0337} \quad (7)$$

$$k_{obs} = 10.95\exp(-4901/RT)Q_{O_3}{}^{0.598}c_0{}^{-0.431}\left[OH^-\right]^{0.0337} \quad (8)$$

$$c = c_0\exp(-k_{obs}t) \quad (9)$$

$$c = c_0\exp\left\{-10.95\exp(-4901/RT)Q_{O_3}{}^{0.598}c_0{}^{-0.431}\left[OH^-\right]^{0.0337}t\right\} \quad (10)$$

From the regression results of Fig. 7(a), the straight slope γ=0.0337 can be got. From regression of Fig. 7(b), straight slope β=-0.431 was got. From regression of Fig. 7(c), the straight slope α=0.598 was got. From the regression results of Fig. 7(d), the slope of a straight line was calculated to be -E/R=589.49, and E=589.49×8.314=4901 J·mol^{-1}.

Therefore, the experience model was as follows Eq. 6 and Eq. 7.

Bringing the data in Table 1 to the above empirical model, the mean value of A was got to be 10.95. Bringing A into this empirical model, then the empirical model was as follows Eq. 8 and Eq. 9.

The kinetics model of ozone degradation for weak acid brilliant green was as follows Eq. 10.

In order to study the dynamic model of ozone degradation of weak acid brilliant green, other experimental points were used in different periods to conduct model calculation, and compare the error between the actual concentration and the model values in different reaction time. The results were shown in Table 2. Table 2 showed that the model error was within 20%, and the model was relatively stable, and pH had the greater impact on the stability of model.

CONCLUSIONS

Through the above analysis, pH, ozone dosing quantity, temperature and the initial concentration of weak acid brilliant green had significant influence on the degradation efficiency. When pH was in the range of 1-13, ozone flux was within 16-60 L/h, temperature was within 293-333 K and initial concentration was within 50-150 mg/L, the ozone oxidation of weak acid brilliant green conformed to the rule of pseudo first order kinetics degradation.

The establishment of indirect oxidation kinetics model showed that when pH was 6.21, ozone flux was 24 L/h, temperature was 293 K and initial concentration was 100 mg/L; when the weak acid brilliant green was degraded after 5 min, the measured degradation was 94.43% while the model degradation was 94.70%. It achieved quite stable effect with the model error was only 0.29%. Meanwhile, the model value k_{obs} was 10.28 while the measured value k_{obs} was 10.25. In addition, the max error was also within 20%. Hence, the model was relatively stable, and had a good prediction on the ozone oxidation process of weak acid brilliant green.

TABLE 2
Ozone degradation parameters of the weak acid brilliant green and its comparison of stability analysis model.

pH	c_0/(mg/L)	Q_0/(L/h)	T/K	t/min	Model /(mg/L)	Value/(mg/L)	error/ %
5	100	32	293	1	44.05	50.25	14.07
11	100	32	293	2	7.33	8.59	17.19
6.21	75	32	293	3	3.52	2.87	18.47
6.21	150	32	293	2	33.04	32.43	1.85
6.21	100	24	293	3	10.28	10.25	0.29
6.21	100	50	293	2	9.52	9.94	4.41
6.21	100	32	293	1	41.97	41.38	1.41
6.21	100	32	313	2	13.75	12.98	6.25

ACKNOWLEDGEMENTS

The authors acknowledge the financial support of the National Natural Science Foundation of China (No.21246010), Jiangsu Eastern Coast and Yangtse River Area Development Institute (Z201402) and Prospective research project of industry and university cooperation in Jiangsu Province (BY2015047-03)

REFERENCES

[1] Rau, J.; Knackmuss, H.J.; Stolz, A. (2002) Effects of different quinoid redoxmediators on the anaerobic reduction of azo dyes by bacteria. Environ Sci Technol. 36, 1497-1504.

[2] Baig, S.; Coulomb, I.; Courant, P.; Liechti, P. (1999) Treatment of landfill leachates: Lapeyrouse and Satrod case studies. Ozone Sci Eng. 21, 1-22.

[3] Biard, P.F.; Couvert, A.; Renner, C.; Levasseur, J.P. (2011) Intensification of volatile organic compounds mass transfer in a compact scrubber using the O_3/H_2O_2 advanced oxidation process: kinetic study and hydroxyl radical tracking. Chemosphere 85, 1122-1129.

[4] Wang, S.B.; Li, H.T.; Xie, S.J. (2006) Physical and chemical regeneration of zeolitic adsorbents for dye removal in wastewater treatment. Chemosphere 65, 82-87.

[5] Azhdarpoor, A.; Nikmanesh, R.; Khademi, F. (2014) A study of reactive Red 198 adsorption on iron filings from aqueous solutions. Environ Technol. 35, 2956-2960.

[6] Li, C.C. (1995) Indirect oxidation effect in electrochemical oxidation treatment of landfill leachet. Water Res. 29, 193-197.

[7] Talarposhti, A.M.; Donnelly, T.; Anderson, G.K. (1994) Colour removal from a simulated dye wastewater using a two-phase anaerobic packed bed reactor. Water Res. 35, 425-432

[8] Chelme-Ayala, P.; Gamal El-Din, M.; Smith, D.W. (2010) Kinetics and mechanism of the degradation of two pesticides in aqueous solutions by ozonation. Chemosphere 78, 557-562.

[9] Sanches, S.; Barreto, M.; Pereira, V.J. (2010) Direct water treatment of priority pesticides using low pressure UV photolysis and advanced oxidation. Water Res. 44, 1809-1818.

[10] Staehelin, J.; Hoign´e, J. (1985) Decomposition of ozone in water in the presence of organic solutes acting as promoters and inhibitors of radical chain reactions. Environ Sci Technol. 19, 1206-1213.

[11] Shu, H.Y.; Chang, M.C. (2005) Decolorization effects of six azo dyes byO_3, UV/O_3 and UV/H_2O_2 processes. Dyes Pigments. 65, 25-31.

[12] Song, S.; Xu, X.; Xu, L.; He, Z.; Ying, H.; Chen, J. (2008) Mineralization of CI Reactive Yellow 145 in aqueous solution by ultraviolet-enhanced ozonation. Ind Eng Chem Res. 47, 1386-1391.

[13] Chen, K.C.; Wang, Y.H. (2012) Control of disinfection by-product formation using ozone-based advanced oxidation processes. Environ Technol. 33, 487-495.

[14] Staehelin, J.; Hoigne, J. (1982) Decomposition of ozone in water: Rate of initiation by hydrogen peroxide. Environ Sci Technol. 16, 678.

[15] Forster, R.J.; Pellegrin, Y.; Keyes, T.E. (2007) pH effects on the rate of heterogeneous electron transfer across a fluorine doped tin oxide/monolayer interface. Electrochem Commun. 9, 1899-1906.

[16] Kusvuran, E.; Gulnaz, O.; Samil, A.; Erbil, M. (2010) Detection of double bond-ozone stoichiometry by an iodimetric method during ozonation processes. J Hazard Mater. 175, 410-416.

[17] Pi, Y.; Schumacher, J.; Jekel, M. (2005) Decomposition of aqueous ozone in the presence of aromatic organic solutes. Water Res. 39, 83-88.

[18] Lopez-Lopez, A.; Pic, J.S.; Debellefontaine, H. (2007) Ozonation of azo dye in a semi-batch reactor: a determination of the molecular and radical contributions. Chemosphere 66, 2120-2126.

[19] Park, A.Y.; Cho, S.H.; Chung K.D.; Kim, D.S. (2004) Degradation of 4-chlorophenol and humic acid using ozone as the oxidant and the influence of transition metal ionic additives. J Kor Soc Waste Mgmt. 21, 634-645.

[20] Koch, M. (2002) Ozonation of hydrolyzed azo dye reactive yellow 84(CI). Chemosphere 46, 109-113.

[21] Adams, C.D.; Gorg, S. (2002) Effect of pH and gas-phase ozone concentration on the decolorization of common textile dyes. J Environ Eng. 128, 293-298.

[22] He, Z.; Song, S.; Xia, M.; Qiu, J.; Ying, H.; Lu, B.; Jiang, Y.; Chen, J. (2007) Mineralization of C.I. Reactive Yellow 84 in aqueous solution by sonolytic ozonation. Chemosphere 69, 191-199.

[23] Sotelo, J.L.; Beltr´an, F.J.; Benitez, F.J.; Beltr´an-Heredia J. (1989) Henry's law constant for the ozone–water system. Water Res. 23, 1239-1246.
[24] Lucas, M.S.; Dias, A.A.; Sepia, A.; Amaral, C.; Peres, J.A. (2007) Degradation of a textile reactive azo dye by a combined chemical-biological process: Fenton's reagent yeast. Water Res. 41, 1103-1109.
[25] Zhao, W.R.; Shi, H.X.; Wang, D.H. (2004) Ozonation of Cationic Red X-GRL in aqueous solution: degradation and mechanism. Chemosphere 57, 1189-1199.
[26] Rinker, E.B.; Ashour, S.S.; Johnson, M.C.; Kott, G.J.; Rinker, R.G.; Sandall O.C. (1999) Kinetics of the aqueous phase reaction between ozone and 2,4,6-trichlorophenol. AIChE J. 45, 1802-1807.
[27] Sanchez-Polo, M.; Rivera-Utrilla, J. (2006) Ozonation of naphthalenetrisulphonic acid in the presence of activated carbons prepared from petroleum coke. App Catal B Environ. 67, 113-120.
[28] Bader, H.; Hoigné, J. (1985) Determination of ozone in water by the indigo method. Water Res. 15, 449-456.

Received: **27.10.2015**
Accepted: **26.02.2016**

CORRESPONDING AUTHOR

Yongjun Shen
School of Chemistry and Chemical Engineering
Nantong University
No. 9, Seyuan Road, Nantong
226019, CHINA

e-mail: zjuenv@163.com

© by PSP Volume 25 – No. 7/2016, pages 2563-2566 Fresenius Environmental Bulletin

MEASURE OF ENVIRONMENTAL STRESS BIOMARKERS IN THE SHRIMP *PALAEMON ADSPERSUS* FROM THE MELLAH LAGOON (ALGERIA): SPATIAL AND TEMPORAL VARIATIONS

Hamida Benradia, Hinda Berghiche and Noureddine Soltani

Laboratory of Applied Animal Biology, Department of Biology, Faculty of Science
Badji Mokhtar University 23000 Annaba, Algeria

ABSTRACT

The objective of this study was to investigate the impact of anthropogenic activities on the water quality of the Mellah lagoon using the shrimp *Palaemon adspersus* (Crustacea, Decapoda) as a bioindicator. The activities of glutathion S-transferase (GST) and acetylcholinesterase (AChE), biomarkers of oxidative stress and neurotoxicity, respectively, were measured in shrimps collected from each site. The samples were collected for two consecutive years (i.e. 2013 and 2014) and two seasons, summer and autumn, were considered in each year. Three sampling sites were chosen: the first one corresponds to the channel of the Mellah lagoon (site 1) is considered as reference site, the second one located in the output of El Mellah River (site 2) is characterized by their proximity to urban activities, and the last one situated in the output of R'kibet River (site 3) is exposed to agricultural and domestic activities. GST and AChE activities were found to vary between sites and by season and year. The results showed a significant induction in GST and also a significant inhibition in AChE activities in individuals from the sites 2 and 3 compared to those of the site 1. Indeed, marked responses are observed in the summer compared to autumn. Also, induction of GST and inhibition of the activity of AChE were higher in 2014 compared to 2013. The differences recorded between the sites studied in the Mellah lagoon are related to their level of pollution, while the seasonally and annually variations were due to the water supply by the Rivers during rainy periods.

KEYWORDS:
Pollution, Biomonitoring, Lagoon El Mellah, Crustacea, *Palaemon adspersus*, Glutathione S-transferase, Acetylcholinesterase.

INTRODUCTION

Urbanization, industrialization and agricultural intensification have caused an increase and diversification of discharges which caused in long-term a high risk of degradation of ecosystems. Coastal lagoons are receiving increasing attention worldwide in recognition of their multiple uses and services [1, 2], but also because of their exposure to anthropogenic disturbances and stress [3, 4]. Today aquatic ecosystems were exposed to pollution such as radioactive wastes, organic matter, heavy metals, polychlorinated biphenyls (PCBs), pesticides, polycyclic aromatic hydrocarbons (HAPs) or drugs and nanoparticles [5-8]. These compounds exert their negative impacts on environment even on very low concentrations and often have great spatial and temporal variability which complicates the assessment of quantity released and their impacts on ecosystems [9]. However, both complementary approaches were used as pollution indicators: biomarkers and bioindicators [10-12]. In recent years, ecotoxicological researches on biomarkers have made considerable progress, to synthesize biological responses of organisms to pollutants for diagnosing the degree of contamination and the state of the environments health [9].

The Mellah lagoon belongs to the complex of wetlands National Park of El Kala (PNEK) (North-eastern Algeria), with Oubeira and Tonga lakes. Created in 1983, this park is classed as Biosphere Reserve in 1990 and Category II (National Park) as classified by the International Union for Conservation of Nature. Various studies were performed in ecosystem [13,14,2] exposed to agricultural and domestic pollutants provides by the R'kibet and El Mellah Rivers, causing contamination of aquatic organisms such as fish, mollusks and crustaceans [15, 16]. In this context, the current study, in continuation with previous works especially made on bivalve molluscs from this lagoon [17, 18]. Moreover some crustacean species from the Annaba gulf have been the subject of research on physiological [19-21] and toxicological aspects [22-25]. This study aims to

FIGURE 1
Location of the sampling sites in the Mellah lagoon (Northeast Algeria). Site 1: constriction zone of the channel with Mediterranean, site 2: output of El Mellah River in South of the lagoon, site 3: the output of R'kibet River to West of the lagoon [14].

evaluate the response of two biomarkers, glutathione S-Tansferase (GST) a biomarker of oxidative stress and acetylcholinesterase (AChE) a biomarker of neurotoxicity, measured in *Palaemon adspersus* (Ranthke, 1837) (Crustacea, Decapoda). The activity of both biomarkers was determined during the summer and autumn seasons during two consecutive years 2013 and 2014.

MATERIALS AND METHODS

Study sites and sampling. The Mellah lagoon is located in the extreme northeast of the Algerian coast, between Rosa Cap and Roux Cap (36 ° 53' 565 N - 8 ° 19' 560 E). It is extended from North to South on 4 Km and from East to West on 2 Km covering an area of 865 hectares. The salinity varied from 15.9 to 37.1 psu and the temperature from 11.4 to 30.5 °C [14]. The lagoon communicates with the Mediterranean by a channel with 870 meters long and 15 meters wide [26] and received gentle waters from three rivers: El Mellah and Bouaroug to the South and R'kibet in the West (Fig. 1). Three sites were chosen for collecting the shrimps. The site 1 is considered as reference site, the second one located in the output of El Mellah River (site 2) is characterized by their proximity to urban activities, and the last one situated in the output of R'kibet River (site 3) is exposed to agricultural and domestic activities.

Sampling of shrimps. *P. adspersus* (Rathke, 1837) is a common shrimp distributed in Norwegian coast and South of the Baltic Sea to the Mediterranean Sea. This species is clear with no lines or bands, excepting presence of dark chromatophores on the half ventral rostrum. Shrimps length: 25 mm, weight: 850 mg were fished by the seine net (mesh: 4 mm; length: 1.80 m) at three sites in the Lagoon during two seasons (summer and autumn) of two consecutive years 2013-2014.

Determination of glutathion S-transferase activity. Shrimps were collected and the flesh fragments and the shrimp heads were used for quantification of GST and AChE activities, respectively. GST activities were determined with the soluble fraction as enzyme source. GST activities toward 1-chloro-2, 4-dinitrobenzene (CDNB) were measured [27] as previously described [20]. Flesh fragments were homogenized in sodium; phosphate buffer (0.1 M, pH 6) and centrifuged (14000 g, 30 min). 200 µl of the resulting supernatant was added to 1.2 ml of reaction mixture containing 1 Mm CDNB and 5 Mm reduced glutathione (GST) in the homogenization buffer. Changes in absorbance were recorded at 340 nm.

TABLE 1
Annual rainfall (mm) and number of rainy days during the experimental study.

Years	Rainfall	Number of rainfall days
2013	938	63
2014	649	39

Determination of cholinesterasic activity. The AChE activity was determined [28] as previously described [29] using acetylthiocholine as a substrate. Heads were homogenized in the following solution containing 38.03 mg ethylene glycol tetraacetic (EGTA), 1ml Triton X-100, 5.845 g NaCl and 80 ml Tris buffer (10Mm, pH 7). After centrifugation (9000g, 5 min), the AChE activity was measured in aliquots (100µl) of resulting supernatants added to 100 µl of 5-5' dithiobis -(2-nitrobenzoic acid) (DNTB) in Tris buffer (0.01 M, pH 8) and 1 ml Tris (0.1 M, pH 8). After 5 min, 100 µl acetylthiocholine was added. Measurements were conducted at a wavelength of 412 nm with a run time of 20 minutes. In parallel, total protein content was quantified according to Bradford [30] using bovine serum albumin as a standard. Enzyme activities were expressed as µM/min/mg proteins.

Rainfall data. The annual rainfall data (mm) and number of rainy days from two consecutive years 2013 and 2014 were kindly provided by the Agricultural Service of El-Tarf, Algeria (Table 1).

Data analysis. Results were represented as mean ± standard deviation (SD). The statistical analyses were performed using prism version 6.01 for Windows (GraphPad software, La Jolla California, USA, www Graphpad.com). The homogeneity of variances was checked by Bartlett's and Brown-Forsythe tests. Data from enzyme activities (GST, AChE) were tested using three-way analysis of variance (ANOVA) followed by a post-hoc HSD Tukey test.

RESULTS

Seasonal and annual variations of glutathione S-transferase activities. The GST activity was performed on flesh adults of *P. adspersus* fished in the different sites. Data were summarized in table 1. Results obtained during the summer of 2014 showed a higher significant increase ($p < 0.001$) in the GST activities in *P. adspersus* from the sites 2 (75.17 ± 8.06 µM/ min/mg) and 3 (85.97 ± 25.69 µM/ min/mg) as compared to individuals the site 1 (46.05 ± 3.1 µM/min/mg). In addition, the values of the GST activity in individuals from the site 1 and 3 were higher in summer in comparison to values obtained in autumn. The induction of GST is also higher in 2014 compared to 2013 (Table 2). The three-way ANOVA (sites, seasons and years) showed a significant difference ($F_{2, 41}= 44.96$; $p\leq 0.001$) between the three sites: 1, 2 and 3 between the two seasons: summer and autumn ($F_{1, 41} = 31.25$; $p \leq 0.001$) and the years: 2013 and 2014 ($F_{1, 41} = 318.04$; $p\leq 0.001$) (Table 3).

TABLE 2
Glutathione S-transferase (GST) activity (µM/min / mg protein) in the flesh of *P. adspersus* in three sites from Mellah lagoon in the summer and autumn of 2013 and 2014 (m ± SD, n = 4-7).

Years	Seasons	Site 1	Site 2	Site 3
2013	**Summer**	10.89 ± 1.90 a A	14.19 ± 1.49 ab A	21.24 ± 1.52 b A
	Autumn	6.86 ± 0.48 a A	13.46 ± 2.23 ab A	24.25 ± 2.25 b A
2014	**Summer**	46.05 ± 3.10 a A	75.17 ± 8.06 b A	85.97 ± 25.69 b A
	Autumn	21.16 ± 0.08 a B	61.42 ± 1.02 b A	51.74 ± 4.65 b B

For the same season and year, means followed by the same small letter are not significantly different ($p> 0.05$) while for the same site and season, means followed by the same capital letter are not significantly different ($p> 0.05$).

TABLE 3
Glutathione S-transferase (GST) activities (µM/min/ mg protein) in the flesh of *P. adspersus* in three sites from Mellah lagoon in the summer and autumn of 2013 and 2014 three-way ANOVA.

Sources of variation	FD	SS	MS	F_{obs}	P
Sites	2	6634.9	3317.4	44.96	0.000***
Seasons	1	2305.9	2305.9	31.25	0,000***
Years	1	23468.8	23468.8	318.04	0.000***
Sites/Seasons	2	265.3	132.6	1.80	0.179 ns
Seasons/Years	1	2110.9	2110.9	28.61	0.000***
Sites/Years	2	2302.7	1151.4	15.60	0.000
Interactions Sites/Seasons/Years	2	485.3	242,6	3.29	0.047*
Residual Error	41	3025.4	73.8		
Total	52				

DF: Degrees of freedom; SS: Sum of squares; MS: Mean squares

TABLE 4
Acetylcholinesterase (AChE) activity (µM / min / mg protein) in the head of *P. adspersus* in three sites from Mellah lagoon in the summer and autumn of 2013 and 2014 (m ± SD, n = 4-7).

Years	Seasons	Site 1	Site 2	Site 3
2013	**Summer**	62.03 ± 10,04 a A	51.32 ± 2.09 ab A	45.5 ± 3.25 b A
	Autumn	107.45 ± 13,96 a B	77.77 ± 4.82 b B	66.22 ± 3.54 b B
2014	**Summer**	44.18 ± 6.66 a A	26.38 ± 2.21 b A	14.23 ± 1.08 c A
	Autumn	55.50 ± 2.78 a B	24.44 ± 3.92 b A	15.37 ± 2.85 c A

For the same season and year, means followed by the same small letter are not significantly different (p> 0.05) while for the same site and season, means followed by the same capital letter are not significantly different (p> 0.05)

TABLE 5
Acetylcholinesterase activities (µM / min / mg protein) in the head of *P. adspersus* in three sites from Mellah lagoon in summer and autumn of 2013 and 2014 three-way ANOVA (sites, seasons and years).

DF: Degrees of freedom; SS: Sum of squares; MS: Mean squares

Sources of variation	DF	SS	MS	F_{obs}	P
Sites	2	9766.2	4883.1	101.01	0.000 ***
Seasons	1	2347.1	23471	48.55	0.000 ***
Years	1	19200.3	19200.3	397.17	0.000 ***
Sites/Seasons	2	95.0	47.5	0.98	0.383 ns
Seasons/years	1	3973.7	3973.7	82.20	0.000 ***
Sites/Years	2	89.9	44.9	0.93	0.403 ns
Interactions Sites/Seasons/years	2	861.8	430.9	8.91	0.000***
Residual Error	42	2030.4	48.3	-	-
Total	53			-	-

Seasonal and annual variations of acetylcholinesterase activities. The AChE activity was evaluated in heads of adult *P. adspersus* collected in three sites of Mellah lagoon. As shown in table 4, data obtained in summer 2013 indicated a maximum AChE activity was about 62.03 ± 10.04 µM / min / mg in shrimp collected in the site 1. This activity was inhibited significantly ($p < 0.05$) at the site 2 (51.32 ± 2. 09 µM / min / mg) and the site 3 (45.50 ± 3.25 µM / min / mg) compared to the first one. As for the summer of 2014 showed a significant inhibition ($p < 0.001$) of the AChE activity with the respective values of 26.38 ± 2.21 and 14.23 ± 1 08 µM / min / mg in the sites 2 and 3 compared to the site 1 which was about 44.18 ± 6.66 µM / min / mg. The three-way ANOVA (sites, seasons and years) showed a ($F_{2, 42} = 101.01$; $p \leq 0.001$) between the three sites 1, 2 and 3 between the two seasons, summer and autumn ($F_{1, 42} = 48.55$; $p \leq 0.001$) and the years considered ($F_{1, 42} = 397.17$; $p \leq 0.001$) (Table 5).

DISCUSSION AND CONCLUSIONS

Lagoon environments are sensitive ecosystems due to their situation of interface between continental and marine environments and their proximity to anthropogenic activities. During environmental stress caused by presence of the pollutants, the biochemical responses are immediate in exposed organisms [31]. GST is involved in various operations of transport and biosynthesis intracellular [32]. This is one of the most solicited enzymes during a detoxification process of organisms subjected to pollution [33]. GST and AChE activity were found to vary between sites and by season. Indeed, the results obtained in this study showed an induction of GST in individuals collected from the both polluted sites 2 and 3, compared to reference site 1. This increase in GST activity suggests that the detoxification process against pro oxidation forces, which are mediated by this enzyme, is induced. In addition, the highest levels of GST activity were registered during the summer and also during the year 2013 in comparison to 2014. The climate of the study areas is Mediterranean, with an average annual temperature of 18 °C and an annual rainfall ranging from 650 to 1,000 mm with peak rainfall in winter and deficits occurring typically during summer [34]. Thus, the effect of seasons may be due to autumn rains which promote dilution of pollutants following water supply by the Rivers, while the year effect can be explained by a rainfall higher in 2013 in comparison to 2014. Similarly, in the mollusc *Cerastoderma glaucum*, a maximum of GST activity was recorded in summer and the highest values were obtained from sites 2 and 3 by comparison to the site 1 [16]. Moreover, an induction in the GST activity was observed in several crustacean species such as *Palaemonetes argentinus* a exposed to fenitrothion [35], *Macrobrachium borelli* treated with organophosphorus insecticides [36] and also *Palaemon serratus* exposed to benzo a pyrene (BaP) [37]. Previous studies on the biomonitoring of health status of the Annaba gulf reported a highest GST activities in *Donax trunculus* (Mollusca, Bivalvia) from Sidi Salem as compared to El-Battah [17, 38-40].

Several works were focused on measurement of the enzymes activity involved in the degradation of some neurotransmitters such as AChE [41, 42]. Measurements of AChE activity provided information about exposure to contaminants such as pesticides [43,44] and other contaminants as heavy metals [45] or oils [46]. In the current study, the AChE activity in *P. adspersus* was inhibited in the individuals collected from sites 2 and 3 compared to the site 1. In addition, inhibition is higher in summer compared to the autumn and also in 2013 than 2014. This result suggests a contamination by neurotoxic pollutants such as heavy metals and/or pesticides. Indeed, a contamination of sites 2 and 3 by several heavy metals (iron, nickel and chromium) [47] support the inhibition of AChE activity observed in the clam *Ruditapes decussates* [48] and also our finding using *P. adspersus*. Similarly, an inhibition of AChE activity due to different effluents to the clam *R. decussatus* from the lagoon of Bizerte in Tunisia was also demonstrated [44]. Many studies revealed an inhibition of AChE activity in *P. argentinus* a freshwater shrimp exposed to fenitrothion organophosphoree [35] and in the bivalve *Modiolus babatus* exposed to thermal stress [49] and *Scrobicularia plana* subjected to stress by metal nanoparticles [50]. There is also an inhibition of AChE activity in crabs *Carcinus maenas*, exposed to the fluoranthene [51] and in shrimp *M. borelli* contaminated with organophosphates [36]. Also, inhibition of AChE activity is due to neurotoxic insecticides and metal heavy was observed in the mussel *Dreissenna polymorpha* collected from different contaminated sites from French coast [52] and among the clam *Ruditapes phillipinarium* collected from different contaminated sites from Venice (Italy) [53].

Induction of GST and inhibition of AChE activities were higher in both sites 2 and 3 compared to the site 1 and it was higher in summer and during 2014 compared to 2013. Then, it can be concluded that site 2 and 3 were more polluted to site 1 as supported by heavy metal analysis. The most contaminated sites were located near the sources of the domestic and agricultural pollutants. In addition, season and annual effects were due to the water supply by de River during rainy that dilute the concentration of pollutants. Based on the

biomaker responses, the shrimp *P. adspersus* is more suitable for the assessment of the health status of the Mellah lagoon than the mollusc *C. glaucum* [16].

ACKNOWLEDGEMENTS

This research was supported by the National Fund for Scientific Research of Algeria (Laboratory of Applied Animal Biology to Pr. N. Soltani) and the Ministry of Higher Education and Scientific Research of Algeria (CNEPRU project, code: F 011201440046 to Dr. H. Berghiche).

REFERENCES

[1] Basset, A., Elliott, M., West, R.J., and Wilson, J.G. (2013). Estuarine and lagoon biodiversity and their natural goods and services. Estuar. Coast. Shelf Sci. 132: 1-4.

[2] Magni P., Draredja B., Melouah K., and Como S.. (2015). Patterns of seasonal variation in lagoonal macrozoobenthic assemblages (Mellah lagoon, Algeria). Marine Environmental Research. 109 :168-176.

[3] Boudouresque, C.F., Bernard, G., Pergent, G., Shili, A. and Verlaque, M., 2009. Regression of Mediterranean seagrasses caused by natural processes and anthropogenic disturbances and stress: a critical review. Bot. Mar. 52, 395-418.

[4] Depledge, M.H. and Galloway, T.S. (2005). Healthy animals, healthy ecosystems. Frontiers in *Ecology and the Environment.* 3(5): 251-258.

[5] Galloway, T.S. and Depledge, M.H. (2001). Immunotoxicity in invertebrates: measurement and ecotoxicological relevance. Ecotoxicology. 10: 5-23.

[6] Trabelsi, S. and Dris M.R. (2005). Polycyclic aromatic hydrocarbons in superficial coastal sediments from Bizerte Lagoon, Tunisia. Mar Pollut Bull. 50: 344-9.

[7] Beldi, H., Gimbert, F., Maas, S., Scheifler, R. and Soltani, N. (2006). Seasonal variations of Cd, Cu, Pb and Zn in the edible mollusk *Donax trunculus* (Mollusca, Bivalvia) from the gulf of Annaba, Algeria. African Journal of Agricultural Research. 1(3): 85-90.

[8] Buffet, P.E., Tankoua, O.F., Pan, J.F., Berhanu, D., Herrenknecht, C., Poirier, L., Amiard-Triquet, C., Amiard, J.C., Bérard, J.B., Risso, C., Guibbolini, M., Roméo, M., Reip, P., Valsami-Jones, E. and Mouneyrac, C. (2011). Behavioral and biochemical responses of two marine invertebrates *Scrobicularia plana* and *Hediste diversicolor* to copper oxide nanoparticles. Chemosphere 84: 166–174.

[9] Carriera, S., Costa, P.M., Martins, M., Lobo, J., Costa, M.H. and Caeiro, S. (2013). Ecotoxicological heterogeneity in transitional costal habitats assessed throught the integration of biomarkers and sediment contamination profiles: a case study using a commercial clam. *Arch.* Environ Contam Toxicol. 64: 97-109.

[10] Viarengo, A., Lowe, D., Bolognesi, C., Fobbri, E. and Koehler, A. (2007). The use of biomarkers in biomonitoring: a 2-tier approach assessing the level of pollutants introduced stress syndrome in sentinel organisms. Comp. Biochem. Physiol. 146 C: 281-300.

[11] Lagadic L, Caquet T, Amiard J.C. and Ramade F. Use of biomarkers for environmental quality assessment, first ed. CRC Press, USA.2000.

[12] Chambost-Manciet, Y. (2002). Ampleur et effets biologiques de la contamination métallique (Cd, Cu, Fe, PB et Zn) des sédiments en Mer du Nord. Utilisation de l'étoile de mer *Asterias rubens (L.)* comme bioindicateur et biomarqueur. Mémoire. Université Libre de Bruxelles.

[13] Chaoui, L., Kara, M.H., Faure, E. and Quignard, J.P. (2006). L'ichtyofaune de la lagune du Mellah: diversité, production et analyse des captures commerciales. *Cybium* 30(2): 123-132.

[14] Draredja, B., Melouah, K., Beldi, H. and Benmarce, S. (2012). Diversité De La Macrofaune Benthique De La Lagune Mellah (Parc National D'El-Kala, Algérie Nord-Est). Bull. Soc. Zool. Fr, 137(1-4): 73-86.

[15] Melouah, K., Draredja, B. and Beldi H. (2014). Dynamique de la Coque *Cerastoderma Glaucum* (Mollusca, Bivalvia) Dans La Lagune Mellah (Algérie Nord-Est). *Revue Synthèse, Univ. Annaba. Rev. Sci. Technol*., Synthèse. 28: 34-45.

[16] Mebarki, R., Khebbeb, M.E.H. and Soltani, N. (2015). Biomonitoring of El Mellah Lagoon (Northeast, Algeria): Seasonal Variation of Biomarkers in *Cerastoderma glaucum* (Mollusc, Bivalvia). JEZS . 3(4): 408-413.

[17] Abbes, A., Chouahda, S., and Soltani, N. (2003). Activité comparée de deux biomarqueurs du stress environnemental dans divers tissus chez deux espèces de bivalves pêchées dans la région d'Annaba. Bull. Inst. 8 : 123-126.

[18] Bouzeraa., N, Abbes, A. and Soltani, N. (2004). Analyse des protéines chez trois espèces de bivalves vivants dans des milieux différents, la lagune d'El Mellah et le golfe

d'Annaba. Bull. INSTM, Salammbo 9: 97-100.

[19] Soltani, N. and Bezzazel, N. (2002). Profil des ecdystéroïdes hémolymphatiques et corrélations avec la sécrétion cuticulaire au cours d'un cycle de mue chez la crevette, *Penaeus kerathurus*. Journal de Recherche Océanographique. 27(3-4), 226-231.

[20] Soltani N, Amira A, Sifi K. & Beldi H. (2012). Environmental monitoring of the Annaba gulf (Algeria): measurement of biomarkers in *Donax trunculus* and metallic pollution. Bull. Soc. zool. Fr. 137(1-4): 47-56.

[21] Derbal, F. and Soltani, N. (2008).Cycle cuticulaire et variations de la protéinémie et de la lipémie chez la crevette royale *Penaeus kerathurus* (Forskal, 1775) des côtes Est algériennes. Science & Technologie 28: 80-86.

[22] Morsli, M.S. and Soltani, N. (2003). Effets d'un insecticide inhibiteur de la synthèse de la chitine, le diflubenzuron sur la cuticule de la crevette *Penaeus kerathurus.* J. Rech. Oceanogr. 28 (1/2): 85-88.

[23] Soltani, N., Lechekhab, H. and Smagghe, G. (2009). Impact of insect growth regulator diflubenzuron on biochemical composition of cuticle of shrimp *Penaeus kerathurus*. Comm. Appl. Biol. Sci. Ghent University, 74/1: 137-141

[24] Morsli, M. S., Merad, I., Khebbeb, M.E.H. and Soltani, N. (2015). Potential hazards of a chitin synthesis inhibitor diflubenzuron in the shrimp *Penaeus kerathurus*: biochemical composition of the hemolymph and muscle during the molt cycle. Advances in Environmental Biology. 9(3): 518-525.

[25] Gheid, S., Nadji, S. and Khebbeb M.E.H. (2011). Taux des lipides et des protéines et composition en acides gras du tissu comestible des crustacés et des mollusques pêchés en Algérie : effet du halofenozide (RH-0345) sur la composition en acides gras de *Penaeus kerathurus* (Crustacé, Décapode). Synthèse. 22: 41-47.

[26] ONDPA. (2005). Étude portant sur la connaissance des biomasses des lacs de la wilaya d'El-Tarf et établissement des règles de gestion halieutiques spécifique. Expertises et rapport pour le compte du ministère de pêche et ressources halieutiques 2005.Tome 1 et 2. 420 p.

[27] Habig, W.H., Pabst, M.J. and Jacobi, W.B. (1974). The first enzymatic step in mercapturic acid formation. J. Biol. Chem. 249: 7130-7139.

[28] Ellman, G.L., Courtney, K.D., Abdres, V. and Featherstone, R.M. (1961). A new and rapid colorimetric determination of acetylcholinesterase activity. *Biochem. Pharmacol. Physiol*. 38: 84-90.

[29] Zaidi, N. and Soltani, N. (2013). Laboratory evaluation of environmental risk assessment of pesticides for mosquito control: toxicity of dimilin on a larvivorous fish, *Gambusia affinis.* Advances in Environmental Biology. 7(4): 605-613.

[30] Bradford, M.M. (1976). A radid and sensitive method for the quantification of microgram quantities of protein utilising the principe of protein-dye binding. *Anal. Biochem.* 72: 254-278.

[31] David, E., Tanguy, A., Riso, R., Quiniou, L., Laroche, L. and Morago, D. (2012). Responses of Pacific oyster *Crassostrea gigas* populations to abiotic stress environmentally contrasted estuaries along the Atlantic coast of France. Aquatic toxicology. 109: 70-79.

[32] Sheehan, D., Meade, G., Foley, V.M. and Dowd, C.A. (2001). Structure, function and evolution of glutathione transferases :implications for classification of non-mammalian members of anancient enzyme super family .Biochem J. (360):1-16.

[33] Quiniou, F., Damiens, G., Gnassia-Barelli, M., Geffard, A., Mouneyrac, C., Budzinski, H. and Romeo, M. (2007). Marine water quality assessment using transplanted oyster larvae. Environ. International. 33: 27-33.

[34] Debieche, T.H. (2002). Evolution de la qualité des eaux (salinité, azote et métaux lourds) sous l'effet de la pollution saline, agricole et industrielle - Application à la basse plaine de la Seybouse (Nord-Est Algérien). Thèse d'Etat, Faculté des Sciences et Techniques, Université de Franche-Comté.

[35] Lavarías, S & García, C.F. (2015). Acute toxicity of organophosphate fenitrothion on biomarkers in prawn *Palaemonetes argentinus* (Crustacea: Palaemonidae). Environ Monit Assess. 187: 65.

[36] Lavarías, S., García, C, Crespo, R., Pedrini, N. and Heras H. (2013). Study of biochemical biomarkers in freshwater prawn *Macrobrachium borellii* (Crustacea: Palaemonidae) exposed to organophosphate fenitrothion. Ecotoxicol. Environ. Saf .96: 10-16.

[37] Silva, C., Oliveira, C., Gravato, C. and Almeida, J.R. (2013). Behaviour and biomarkers as tools to assess the acute toxicity of benzo (a)pyrene in the common prawn *Palaemon serrates.* Marine Environmental Research. 90: 39- 46.

[38] Sifi, K., Amira, A. and Soltani N. (2007). Mesure de deux biomarqueurs du stress oxydatif chez un mollusque bivalve (*Donax trunculus*) : corrélation avec la reproduction au niveau du golfe d'Annaba. 9éme journées

tunisiennes des sciences de la mer Tabarka (Tunisie) 15-18 décembre.
[39] Amira, A., Sifi, K. and Soltani N. (2011). Mesure of environmental stress biomarkers in Donax trunculus (Mollusca, Bivavia) from the golf of Annaba (Algeria). European Journal of Experimental Biology. 1(2):7-16.
[40] Bensouda, L. and Soltani-Mazouni, N. (2014). Measure of Oxidative Stress and Neurotoxicity Biomarkers in Donax trunculus from the Gulf of Annaba (Algeria): Case of the Year 2012. Annual Research & Review in Biology 2014 .4 (12): 1902-1914.
[41] Sarkar, A., Holkar, P.K.R. and Patil, S.S. (2010). Application of Acteylcholineesterase Activity in Marine Organisms as a Biomarker of Costal Pollution. National Conference on Emerging Trends in Engineering, Technology and Management, MS2K. 10: 383-386.
[42] Barra, R., Notarianni, V. and Gentili, G. (2001). Biochemical biomarker responses and chlorinate compounds in the fish *Leuciscus cephalus* along a contaminant gradient in a polluted river. Bulletin of Enviro.n Contam. and Toxicol .66: 582-590.
[43] Oliveira, M.M., Silva, L., Filho, M.V., Fernandes, F.C. and Cunha Bastos, J. (2007). Brain Acetylcholinesterase as a Marine Pesticide Biomarker using Brazilian Fishes. Marine Environmental Research. 63: 303-309.
[44] Kamel, N., Jebali, J., M Benkhedher, S., Chouba ,L. and Boussetta, H. (2012). Biochemical response and metals levels in *Ruditapes decussatus* after exposure to treated municipal effeluants. Ecotoxicol. Environ. Saf. 82: 40-46.
[45] Amiard-Triquet, C,. Altamann, S., Amiard, J.C., Ballan-Dufrancais, C., Baumard, P., Budzinski, H,. Crouzet, C., Guarrigue, J.P., His, E, Jeantet, A.Y., Menarsia, R., Mora P., Mouneyrac, C., Narbonne, J.F. and Pavillon, J.F. (1998). Fate and effects of micropolluants in the Girond estuary, France: a multidisciplinary approach. Hydrobiologia. 373/374: 259 - 279.
[46] Tim-Tim, A.L.S,. Morgado, S., Moreira, R., Rangel, A.J.A. Nogueira, A.M. Soares L. and Guilhermino, L. (2009). Cholinesterase and Glutathione S-transferase Activities of Three Mollusk Species from the NW Portuguese Coast in Relation to the Prestige Oil Spill. Chemosphere 77: 1465-1472.
[47] Bendjama, A., Morakchi, K., Meradi, H., Boukari, A., Chouchane, T., Belaabed, B.E. and Djabri, L. (2011).Caracterisation des materiaux biologiques issus d'un ecosysteme naturel« pnek » situe au nord-est de l'algerie. J.Soc.Alger.Chim. 21(1), 45-58.
[48] Abbes, A., Soltani, N. and Djebar, A.B. (2006). Utilisation de l'acétylcholinestérase chez la palourde *Ruditapes decussatus* dans la surveillance d'un système lagunaire El Mellah Algérie. 2ème Colloque Euro-méditerranéen de Biologie Environnementale, Marseille (France), 7-9 décembre 2006, (2) : 22.
[49] Dimitriadis, V.K, Gougoula, C., Anestis, A., Pörtner, H.O. and Michaelidis, B. (2012). Monitoring the biochemical and cellular reponses of marine bivalves during thermal stress by using biolarkers, Marine Environemental Research. 73: 70-77.
[50] Fossi- Tankoua O., Buffet, P.E., Amiard, J.C, Berthet, B., Mouneyrac, C. and Amiard-Triquet, C. (2013). Integrated assessment to festuarine sediment quality based on a multi-biomarker approch in the bivalve Scobiculariaplana. Ecotoxicol. Environ. Saf . 88: 117-125.
[51] Rodrigues, A.P, Lehtonen, K.K., Guilhermino, M. and Guimarães, L. (2013). Exposure of *Carcinus maenas* to waterborne fluoranthene: Accumulation and multibiomarker responses Science of the Total Environment. 443: 454–463.
[52] Palais, F., Dedourge-Geffard, O., Beaudon, A., Pain-Devin, S., Trapp, J., Geffard, O. Noury, P., Gourlay-France, C., Uher, E., Mouneyrac, C., Biagianti-Risbourg, S. and Geffard, A. (2012). One-year monitoring of core biomarker and digestive enzyme responses in transplanted zebra mussels (*Dreissena polymorpha*). Ecotoxicology. 21: 888-905.
[53] Matozzo V, Binelli, A, Parolini M, Previato M, Masiero L, Finos L. and Brassan, H.N. (2012). Inventaire du patrimoine naturel. Muséum d'Histoire Naturelle de France. http:/inpn.mnhn.fr/isb/servlet/ISB Servlet.

Received: **28.10.2015**
Accepted: **23.01.2016**25.07.16

CORRESPONDING AUTHOR

Hinda Berghiche
Ecotoxicology Group
Laboratory of Applied Animal Biology,
Department of Biology, Faculty of Sciences
Badji Mokhtar University, 23000 Annaba, Algeria

e-mail: hindabentoubal@hotmail.ca

by PSP Volume 25 – No 7/ 2016, pages 2567-2574 Fresenius Environmental Bulletin

SIMULTANEOUS REMOVAL OF PB, CD, HG AND AS FROM SMELTING FLUE GAS BY SODIUM SULFIDE SOLUTION

Ma Yixing, Wang Xueqian*, Shi Yong, Xiong Jianlin, Wang Fei, Xu Ke, Ning Ping, Wang Langlang

Faculty of Environmental Science and Engineering, Kunming University of Science and Technology, Kunming 650500, China

ABSTRACTS

Tubular resistance furnace was used as heavy metal generation system to simulate smelter flue gas of heavy metals by heating heavy metal oxides. Sodium sulfide solution was employed to remove lead (Pb), cadmium (Cd), mercury (Hg) and arsenic (As) from the flue gas. The experiment was conducted to investigate the effects of Na_2S concentration, temperature and pH of Na_2S solution as well as the presence of SO_2 on removal efficiency. The results show that the better concentration of sodium sulfide solutions are 0.4 mol/L, 0.4 mol/L, 1.0 mol/L and 0.4 mol/L for Pb, Cd, Hg and As respectively, the better temperatures are 40 ºC, 50 ºC, 40 ºC and 40 ºC respectively, and the better pH is 12. The removal efficiency of Pb, Cd, Hg and As could reach 94.2%, 94.6%, 99.9%, and 93.5% respectively under the optimum conditions. In addition, the presence of SO_2 in smelter flue gas could reduce the removal efficiency of heavy metals. The reasons may be that SO_2 will consume S^{2-} in the solution and change pH, which will result in reduction of the removal efficiency. Physical precipitation is the main process for removing Pb, while for Cd and As chemical precipitation is main, as to Hg, both Physical and chemical precipitation contribute to removing.

KEYWORDS:
Sodium Sulfide; Smelting Flue Gas; Heavy Metal; Precipitation

INTRODUCTION

The major heavy metal pollution species in lead and zinc metallurgy industry are Pb, Cd, Hg and As, which can pollute water, air and soil [1, 2]. Pb, Cd, Hg and As are known to be toxic metals that can accumulate in the human body [3-7].

Lead smoke and dust are the main lead pollution in atmosphere, which mainly come from mining, soldering, petrol burning and lead manufacturing process [8, 9]. For high volatility of lead at high temperature, smelting process generally results serious lead volatilization and environmental contamination. Cadmium pollution mainly comes from lead and zinc metallurgy, coal and trash burning [10]. Cadmium can accumulate in organism and environment for long years [11]. Mercury mainly presents as two states in flue gas: gaseous mercury (Hg^{2+}, Hg^0) and solid particles attached objects [12, 13]. When the temperature is higher than 800 ºC, the mercury compounds easily decomposes into gaseous mercury which has high volatility and low solubility in water. Gaseous mercury is very difficult to control [14, 15]. Gaseous mercury Hg^{2+} and solid particles attached objects are the main status of Hg in smelter flue gas. Arsenic, entering into the environment by the flue gas, is mainly in the form of solid oxide and arsenate particles. The particles suspend in the air and settle to the ground and water, resulting in environment contamination [16, 17].

At present, research focus on mercury and less on lead, cadmium and arsenic. The heavy metals in flue gas are mainly removed by adsorption [18-21], catalytic oxidation [22-25] and chemical method [26, 27]. Sulfuration method [28-31] is one of the chemical precipitation methods, which is widely used in domestic, mainly focus on the removal of heavy metals from waste water while removal from the gas is rare. Sulfuration method is effective for removing Pb, Cd, Hg and As from smelting flue gas simultaneously, as a simple and easy way. The major affecting factors concerning the removal process are the main objectives of this study.

MATERIALS AND METHODS

Equipments and reagents. The equipments required in the experiment are Z-2010 polarized Zeeman atomic spectrophotometer (Tian Mei Technology Co. Ltd.); F-732 cold vapor atomic absorption mercury analyzer (Shanghai Huaguang Instrument Factory); limited tubular atmosphere furnace (Shanghai Yi Feng Electric Furnace Co. Ltd.); corundum tube (Shanghai Yifeng electric furnace Co. Ltd.); air pump (Sensen Group Co. Ltd.); mass flowmeter (Dongguan Dexin.

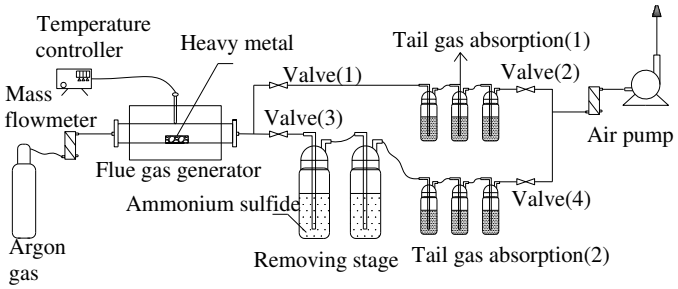

FIGURE 1
Schematic of the experimental apparatus.

Electronics Group Co., Ltd.,); PHS-3C pH meter (Shanghai Lei Yun Experiment Instrument Manufacturer Co. Ltd.).

The chemicals used in the experimental are sodium sulfide (Na_2S), red lead oxide (Pb_3O_4), cadmium oxide (CdO), mercuric oxide (HgO), arsenic trisulfide (As_2O_3), all of which are of analytical grade and purchased in Shanghai Sinopharm Group Co. LTD.

Experimental apparatus. A schematic flow diagram of the experiment is shown in Fig.1. The simulation smelter flue gas of heavy metals is produced from the tubular flow type and then carried by argon to the absorption bottles which are filled with sodium sulfide solution. The simulation flue gas in experiment consists of single heavy metal and each of them is produced by calcining metal compounds which are red lead oxide (Pb_3O_4), cadmium oxide (CdO), mercuric oxide (HgO) and arsenic trisulfide (As_2O_3) respectively. After absorption by sodium sulfide solution, the off gas flow through HNO_3/H_2O_2 mixture (volume 1:1), HNO_3/H_2O_2 mixture (volume 1:1) and acidic $KMnO_4$ solution successively to analyze the content of heavy metals in the mixture. As shown in Fig.1, when valve 1 and valve 2 are open, valve 3 and valve 4 are close for 15 min, the off gas will be absorbed by absorption device (1) to detect the concentration of heavy metals in the simulated flue gas without removing, which denoted as C_0; when open valve 3 and valve 4 are open, valve 1 and valve 2 are for 15 min the off gas will be absorbed by absorption device (2), the concentration of heavy metals in the simulated flue gas after absorbing by sodium sulfide solution can be gain, denoted as C_n

Experiment methods. Smelting flue simulation experiment is made as follows: the initial concentration of simulate smelter flue gas can be controlled by adjusting heating temperature of furnace and gas flow rate. According to a large number of exploratory experiments[32], we get that a better operating temperature of Pb, Cd, Hg and As are 900 ºC, 1000 ºC 450 ºC and 700 ºC respectively, and the flow are 200 ml/L, 200 ml/L, 150 ml/L and 200 ml/L. Under these conditions, the concentration of Pb, Cd, Hg and As in the simulation flue gas can be ranged 10 ~ 15 mg/m^3, 2 ~ 7 mg/m^3, 10 ~ 30 mg/m^3 and 1 ~ 5 mg/m^{3}respectively, which consisting with smelter actual condition. The conditions were employed to generate simulate smelter flue gas.

To study the influence of Na_2S solution concentration on heavy metal absorption, 50 ml Na_2S solution with different concentration (0-0.1 mol/L) were used to absorb Pb, Cd, Hg and As contained in smelting flue gas respectively and then gained a better concentration of Na_2S solution.

The influence of pH on heavy metals absorption was studied, 50 ml better concentration Na_2S solution(based on above experiment) with different pH, which was controlled by adding 1% NaOH or 1% HCl solution, were used to absorb Pb, Cd, Hg and As contained in smelting flue gas respectively.

SO_2 was introduced into Na_2S solution with the better concentration (based on the over work) to study the influence of SO_2 on heavy metal absorption. With the SO_2 addition, the pH of Na_2S solution will decrease. And Na_2S solution with different pH in the process of SO_2 addition were used to absorb Pb, Cd, Hg and As contained in smelting flue gas.

Calculation formula of heavy metals concentrations in flue gas (mg/m^3) is shown with Equation (1).

$$C = \frac{C_L \times V_L}{1000Q \times t} \quad \text{.....(1)}$$

where: C is concentrations of heavy metal in flue gas, mg/m^3; C_L is concentrations of heavy metal in absorption solution, mg/L; V_L is the volume of absorption solution, mL; Q is gas volumetric flow rate, mL/min; t is absorption time, min.

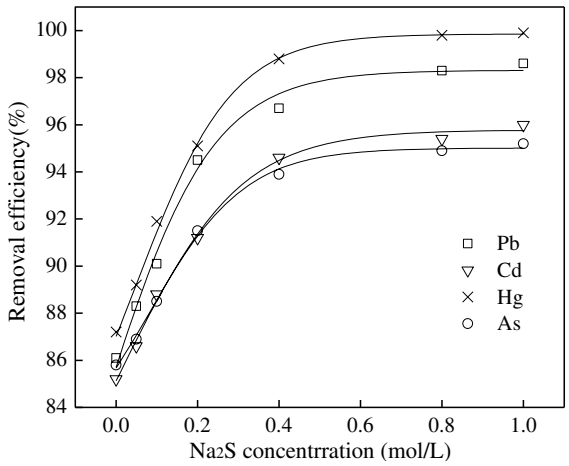

FIGURE 2
The influence of sodium sulfide concentration on removal efficiency of Pb , Cd, Hg and As from flue gas.

The efficiency calculation formula is shown with Equation (2).

$$\eta = (1 - \frac{C_n}{C_0}) \times 100\% \quad \text{..... ..... (2)}$$

where: C_n is concentrations of heavy metal in flue gas after absorption, mg/m^3; C_0 is concentrations of heavy metal in flue gas before absorption, mg/m^3.

The concentration of Pb, Cd, Hg and As in the tail gas absorption solution were detected by flame atomic absorption spectrophotometry (HJ538-2009), flame atomic absorption spectrophotometry (HJ/T 64.1 2001) and cold atomic absorption spectrophotometry (HJ542-2009) respectively.

The phase and crystalline orientation of precipitations were determined by XRD (X-ray diffraction) analysis. In this paper XRD were obtained with a D/MAX-2200 X-ray diffraction at 20~60 kV and 2~50 mA by using Ni-filtered Cu Kα radiation (λ=0.15406 nm) at a rate of 2 (°)/min from 2θ=10° to 90°. The powdered samples of precipitations were analyzed with treatments of washing, drying and grinding. The identification of crystalline phases was made by matching the JCPDS files.

RESULTS AND DISCUSSIONS

Effect of sodium sulfide concentration. Effects of sodium sulfide concentration on the removing of Pb, Cd, Hg and As contained in the flue gas were studied, as shown in Fig. 2Fig. 2 indicates the removal efficiency of Pb, Cd, Hg and As increase with the concentration of Na_2S solution increased, and the outlet concentration of the heavy metals are decreased. When the concentration of Na_2S solution changes from 0 mol/L to 0.4 mol/L, the removal efficiencies of heavy metals increase relatively quickly and reach high rates. Among this, the removal efficiency of Pb increases from 86.1% to 96.7%, Cd increases from 85.2% to 94.6%, Hg increases from 87.3% to 98.8% and As increases from 85.8% to 93.9%.

The concentration of sodium sulfide increase to 0.4 mol/L, the concentrations of Pb, Cd, Hg and As in the outlet flue gas are up to 0.61 mg/m^3, 0.45 mg/m^3, 0.055 mg/m^3 and 0.47 mg/m^{3}respectively. When the concentration is above 0.4mol/L, the removal efficiencies are till increase, but the increase rate become low. In order to reduce the concentration of Hg to meet the emission standard in China (0.015 mg/m^3) the removal efficiency has yet to be improved by increasing the concentration of sodium sulfide. When the concentration of Na_2S solution reach to 1.0 mol/L, the removal efficiency can improve to 99.9%, thus the concentration of Hg in outlet flu gas was just 0.009 mg/L. In spite the fact that the higher is the sodium sulfide concentration the better is the removal effect of heavy metals we can get. Taking the industrial cost into consideration, a better concentration of Na_2S solution to remove Pb, Cd, Hg and As in flue gas are 0.4 mol/L, 0.4 mol/L, 1.0 mol/L and 0.4 mol/L respectively.

Effect of temperature. The effect of temperature on the absorption of Pb, Cd, Hg and As with Na_2S solutions at the better concentrations (4 mol/L, 0.4 mol/L, 1.0 mol/L and 0.4 mol/L respectively) were studied, the results are shown in Fig.3.

As shown in Fig.3, the removal efficiencies of all the heavy metals increase first and then decrease as the temperature increases from 20 ºC to 70 ºC.

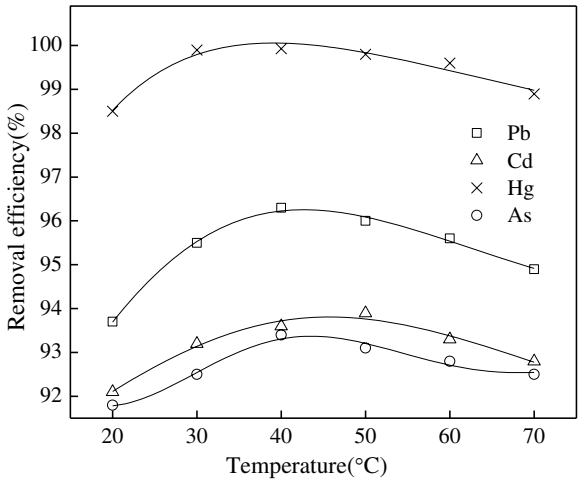

FIGURE 3
The influence of react temperature on removal efficiency of Pb, Cd, Hg and As from flue gas.

Pb, Hg and As gain the highest removal efficiency when temperature is up to 40 °C, which are 96%, 99.9% and 93.4% respectively. As to Cd, the highest removal efficiency is 93.9% at 50 °C. For higher temperatures, the removal efficiency of the three heavy metals will decrease. It might be because with the increase of temperature, the ions in solution became more reactive, reacted with heavy metals more easily, and accelerated the reaction rate with them. When temperature was too high, precipitation dissolving rate increased and inhibited the reaction. Fig.3 shows that when the temperature above 50 °C, the removal efficiencies begin to decrease. Although the rise of temperature can promote the dissolution of metals and improve the ions reactivity, against gas-liquid phase reaction. Therefore, too high temperature of solution will reduce removal efficiencies of heavy metals. By this way it can maintain a higher removal rate. A better temperature of sodium sulfide absorption liquid for the removal of Pb, Cd, Hg and As are 40 °C, 50 °C, 40 °C and 40 °C respectively.

Effect of Ph. The pH value of an aqueous system is one of the most important parameters affecting the absorption behavior, as it influences the surface properties of ionization/dissociation of the molecule.[24] In the solution contained S^{2-}, a part of S^{2-} combined with H^+ and formed HS^- and H_2S. H^+ combined with S^{2-} and formed HS^- and H_2S, which would decrease the use efficiency of S^{2-}. The processes were showed in equations (3) and (4) [33]. Therefore, pH value of $(NH_4)_2S$ solution plays an important role in removal of heavy metals by sodium sulfide solution.

$$K_1 = \frac{[HS^-][H^+]}{H_2S} \qquad pK_1 = 6.99 \quad \text{..... (3)}$$

$$K_2 = \frac{[S^{2-}][H^+]}{HS^-} \qquad pK_2 = 17.4 \quad \text{..... (4)}$$

Based on the better concentration of sodium sulfide and the better reaction temperature in the experiment, effects of pH on removal of Pb, Cd, Hg and As in flue gas were studied. The results are showed in Fig.4. As shown in figure 4 that as pH rises from 2 to 12, the removal efficiencies of heavy metals through a decrease and then increase process. The removal efficiencies of Pb, Cd, Hg and As were in the range of 86.8%~94.2%, 89.5%~94.6%, 96.33%~99.9% and 89.3%~93.5%, with the lowest

efficiency appearing at pH is 7.

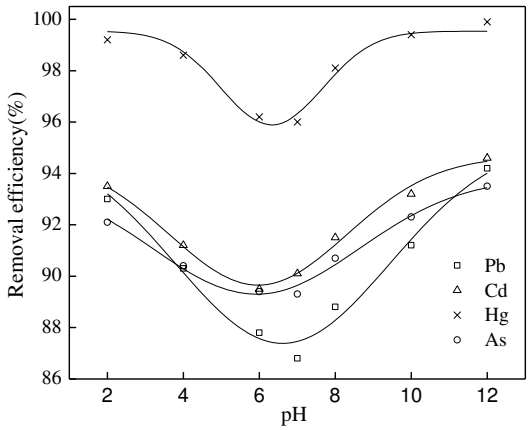

FIGURE 4
The influence of pH on removal efficiency of Pb, Cd, Hg and As from flue gas.

In the experiment, there was some precipitation formed after removal process of Pb, Cd and Hg in alkaline solution, while there was none in acid solution. However, there was precipitation appeared after removal process of As in weak alkaline solution and acid solution. The Pb, Cd and Hg in the off gas will be broken down into ions after absorbed under the strong acid condition, and then react with sulfur ions state ion and to form sulfide precipitation. On account of the strong acidity sulfide precipitation will dissolve quickly, thus most of the heavy metals exist in the state of ions and no precipitation can be observed. In the alkaline solution, the Pb, Cd and Hg in off gas reacted with sulfur ions and formed sulfide precipitation which can't be dissolved. When the pH of solution is around 7, the advantage of strong acid and alkali to remove metals was not obvious, so the removal efficiency was low. It can be seen that the removal efficiency of heavy metals is high under strong acid and strong alkali conditions. For As, there was precipitate appeared in weak alkaline solution and acid solution because As is different with Pb, Cd and Hg. As is easy to combine with water or hydrogen ion and generate arsenic acid (H_3AsO_3) that is Hydroxide arsenic ($As(OH)_3$). H_3AsO_3 is weak acid, the dissociation of it will form arsenic ion, and the equation is showed in equations (5). Arsenic ions react with Na_2S and generate arsenic sulfide no matter in acid or alkaline solution (equation (6)). But As_2S_3 will dissolve when pH is over 8 and change to AsO_3^{3-} and AsS_3^{3-} (equation (7)), which match the potential-pH diagrams of As-S-H_2O [34]. Another, arsenic sulfide solubility is lower under acid condition, so more precipitation appeared in acid solution.

$$H_3AsO_3 \leftrightarrow As(OH)_3 \leftrightarrow As^{3+} + 3OH^- \cdots\cdots\cdots\cdots (5)$$

$$As^{3+} + S^{2-} \leftrightarrow As_2S_3\downarrow \cdots\cdots\cdots\cdots (6)$$

$$As_2S_3 + 6OH^- \leftrightarrow AsS_3^{3-} + AsO_3^{3-} + 3H_2O \cdots\cdots\cdots\cdots (7)$$

Effect of SO_2 content. Most of the lead and zinc ores in nature contain sulfide and the content is as high as 27% ~ 32% [35]. Smelting flue contains a large amount of SO_2 which can affect the removal of the heavy metals. Effects of SO_2 on outlet concentration and removal efficiencies of Pb, Cd and Hg in flue gas were studied. Solution pH will continue to fall with the bubbling of SO_2, so pH was applied to assess the mass of SO_2. The results were similar to the effect of pH in section 2.3.

According to the experiment, it can be gained that SO_2 affect heavy metals removal efficiency by influencing solution pH and the concentration of S^{2-}. For SO_2 addition, the pH of solution declined from 12 to 2, and the removal efficiency of heavy metals increased after a decline. The reactions are easy to take place between sodium sulphide and SO_2, which will consume S^{2-} in the solution, thus inhibiting the S^{2-} react with heavy metals and leading to the decline of removal efficiency of heavy metals. With continuous ventilation of SO_2, SO_2 dissolved in water and generated sulfurous acid, which turned the alkaline solution into acid gradually. The reactions were showed in equation (8).

$$6SO_2 + 4S^{2-} + 3H_2O \rightarrow 3S_2O_3^{2-} + 2HSO_3^- + 2H_2S \cdots\cdots\cdots\cdots (8)$$

With the acidity of solution getting stronger, heavy metals in the flue gas decomposed directly into ions and trapped in the solution. When pH = 7, due to SO_2, the removal rates of heavy metals reduced to a minimum: the removal efficiency of Pb reduced from 94.2% to 88.8%, Cd reduced from 94.6% to 90.2%, Hg reduced from 99.9% to 96.4%,

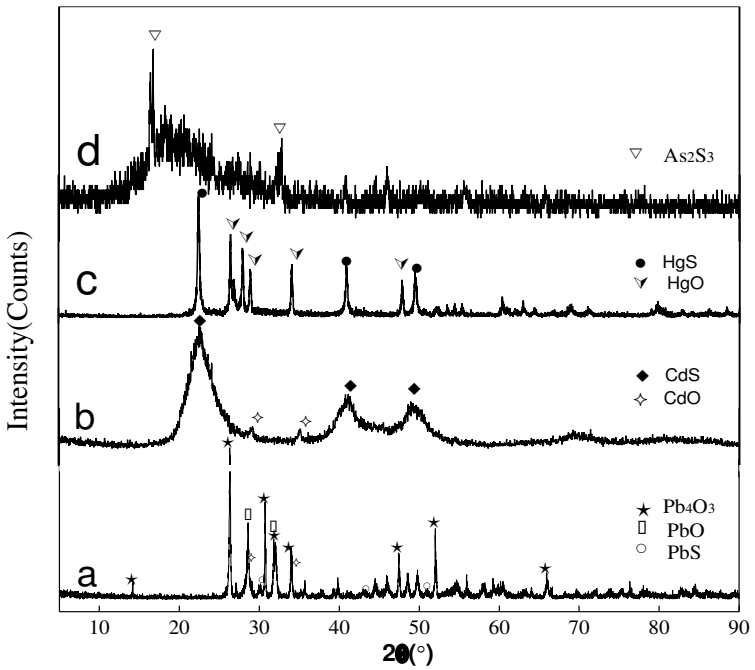

FIGURE 5
The XRD analysis of precipitation (a: Pb, b: Cd, c: Hg, d: As).

and As do from 93.5% to 88.5%. Correspondingly, the exit concentration of the heavy metals were 0.77 mg/m^3、0.78 mg/m^3、0.44 mg/m^3 and 0.55 mg/m^3 respectively. As a result of the work above that SO_2 has a certain inhibitory effect on removal efficiency of the heavy metals in flue gas.

XRD analysis of precipitations. In order to make the process clear that how Na_2S solution removed heavy metals, the precipitations were investigated by XRD analysis. The results of Pd, Cd, Hg and As are showed in a, b, c and d of Fig.5.

It can be seen from Fig.5 a that Pb mainly exists in the form of Pb_4O_3 in the precipitation after the absorption of flue gas, associated with some PbO, as well as few PbS. Pb_4O_3 is the raw material of simulate flue gas. PbO may be converted from Pb_4O_3 in the heating process. These two matters are the major position in the precipitation, PbS can be observed but very few. These indicated that the removal of Pb in the flue gas by Na_2S solution mainly involved in the physical absorption and few of them formed precipitation with Na_2S. CdS is the main composition of precipitation as shown in Fig.5 b. In Fig.5 b, the weak diffraction peaks of CdS are very strong and few weak diffraction peaks of CdO are appeared, which proved that chemical precipitation was absolutely superior to physical precipitation for Cd. From Fig.5 c, both diffraction peaks of HgS and HgO are clearly with HgS has a slight advantage. This indicates that in the precipitation process, both chemical precipitation and physical precipitation were important for removing Hg. It can be observed that As_2S_3 is the main position of the As precipitation after absorption, which indicate chemical precipitation is superior for As**.**

According to the XRD analysis, during the process of the removal of heavy metals by Na_2S solution physical precipitation is the main process for removing Pb; while for Cd and As, chemical precipitation is preponderant; for Hg, both physical and chemical precipitation contribute to removing. It can be inferred that the reactions of chemical precipitation between heavy metals and sodium sulfide solutions are as follows equation (9) - (12):

$PbO+Na_2S+H_2O=PbS\downarrow+2NaOH$ ·····(9)

$CdO+Na_2S+H_2O=CdS\downarrow+2NaOH$·····(10)

$HgO+Na_2S+H_2O=HgS\downarrow+2NaOH$·····(11)

$As_2O_3+Na_2S+H_2O=As_2S_3\downarrow+2NaOH$····· (12)

CONCLUSION

Take removal efficiency and economic benefits into consideration, the better concentration of sodium sulfide solutions are 0.4 mol/L, 0.4 mol/L, 1.0 mol/L and 0.4 mol/L for the removal of Pb, Cd, Hg and As, the better temperatures are 40 ^oC, 50 ^oC, 40 ^oC and 40 ^oC respectively, and the

better pH is 12. Under the better conditions, the removal efficiency of Pb, Cd, Hg and As can reach 94.2%, 94.6%, 99.9% and 93.5% respectively with the outlet concentrations of Pb, Cd Hg and As were 0.65 mg/m^3, 0.45 mg/m^3, 0.01 mg/m^3 and 0.48 mg/m^3.

The presence of SO_2 of in smelter flue gas can reduce the removal efficiency of heavy metals. The reasons may be that SO_2 will consume S^{2-} in the solution, and change pH, which will result in the reduction of the removal efficiency.

During the process of the removal of heavy metals by Na_2S solution, physical precipitation is the main process for removing Pb; while for Cd and As, chemical precipitation is main; as to Hg, both physical and chemical precipitation contribute to removing.

ACKNOWLEDGMENTS

This work was supported by the National Natural Science Foundation of China (No. 51268021, U1137603), 863 National High-tech Development Plan Foundation (No. 2012AA062504)

REFERENCES

[1] Lin, X. J. (2001). Present situation and control methods of heavy metals pollution from lead smelting industry. Nonferrous Metal Engineering, 1, 23 – 27.

[2] Lin, S.Y. (1992). Environmental engineering for Nonferrous metallurgy. Central South Industry University Press, Changsha, 34-39.

[3] Sultanbayeva, G. Sh., Holze R., Chernyakova R. M., & Jussipbekov U. Zh (2013) Removal of Fe^{2+}, Cu^{2+}, Al^{3+} and Pb^{2+}ions from phosphoric acid by sorption on carbonate-modified natural zeolite and its mixture with bentonite. Microporous Mesoporous Mater. 170, 173–180.

[4] Ferramola, M. L., Diaz, M. F. F. P., Honore, S. M., Sanchez, S. S., Anton, R. I., Anzulovich, A. C., & Gimenez, M. S. (2012) Cadmium-induced oxidative stress and histological damage in the myocardium. Effects of a soy-based diet. Toxicol. Appl. Pharmacol. 265, 380-389.

[5] Wang, Y. J., Robison T., & Wiatrowski, H. (2013) The impact of ionic mercury on antioxidant defenses in two mercury-sensitive anaerobic bacteria. BioMetals, 26, 1023 – 1031.

[6] Phoebe, Z. R., & Heather, J. S. (2015) Inorganic nano-adsorbents for the removal of heavy metals and arsenic: a review. RSC Advances, 5, 29885–2990.

[7] Lee, T. (2012) Removal of Heavy Metals in Storm Water Runoff Using Porous Vermiculite Expanded by Microwave Preparation. Water Air Soil Pollut, 223, 3399–3408

[8] Wu, Z. B. (2002) Engineering for air pollution control. Science Press, Beijing, 54-55.

[9] Huang, P. (2009) Current situation of pollution and research on lead smoke and lead dust in the atmosphere. Science and Technology Innovation Herald, 3,109-110.

[10] Taylor, M. P., Mould, S. A., & Kristensen, L. J. (2014) Environmental arsenic, cadmium and lead dust emissions from metal mine operations: Implications for environmental management, monitoring and human health. Environmental Research, 135, 296-303.

[11] Lee, Y. K., Park E. Y., Kim S., Son J. Y., Kim T. H., Kang W. G., Jeong T. C., Kim K. B., Kwack S. J., Lee J., Kim S., Lee B. M., & Kim H. S. (2014) Evaluation of Cadmium-Induced Nephrotoxicity Using Urinary Metabolomic Profiles in Sprague-Dawley Male Rats. Journal of Toxicology and Environmental Health, Part A, 77, 1384-1398

[12] Wang, J., Xu, W., Wang, X H., Wang, W.,H. (2011) Measurement of Mercury in Flue Gas Based on an Aluminum Matrix Sorbent. TSWJ, 11, 2469-2479.

[13] Brachert, L., Kochenburger, T., & Schaber, K. (2013) Facing the Sulfuric Acid Aerosol Problem in Flue Gas Cleaning: Pilot Plant Experiments and Simulation. Aerosol Sci. Technol, 47, 1083-1091.

[14] Cui, X., Ma, L. P., & Deng, C. L. (2011) Research progress of removing mercury from coal-fired flue gas. Chem. Ind. Eng. Prog, 30, 1607-1613.

[15] Monterrozo, R. A., Fan, M. H., ASCE, M., & Argyle, M. D. (2012) Adsorption of Mercury with Modified Thief Carbons. J. Environ. Eng. 138, 386-391.

[16] Gulay, B., Unzile, Y., & Emrecan, E., (2014) Arsenic removal from aqueous solution using pyrite. J CLEAN PROD, 84, 526 – 532.

[17] Zhao, S. J., Ma, Y. P., & Qu, Z. (2014) The performance of Ag doped V_2O_5-TiO_2 catalyst on the catalytic oxidation of gaseous elementalmercury. CATALYSIS SCIENCE & TECHNOLOGY, 4, 4036-4044.

[18] Wendt, J. O. L., & Lee, S. J. (2010) High-temperature sorbents for Hg, Cd, Pb and other

trace metals: Mechanisms and applications. Fuel, 89, 894-903.
[19] Becker, E. M., Rampazzo, R. T., Dessuy, M. B., Vale, M. R., Silva, M. M., Welz, B., & Katskov, D. A. (2011) Direct determination of arsenic in petroleum derivatives by graphite furnace atomic absorption spectrometry: a comparison between filter and platform atomizers. Spectrochim. Acta Part B, 66, 345-351.
[20] Yang, X. F., & Shen, Z. G. (2013) Silica nanoparticles capture atmospheric lead: Implications in the treatment of environmental heavy metal pollution. Chemosphere, 90, 653-656.
[21] Sharma, A., & Lee, B. K. (2014) Cd(II) removal and recovery enhancement by using acrylamide–titanium nanocomposite as an adsorbent, Appl. Surf. Sci., 313, 624–632.
[22] Fang, P., Cen, C. P., & Wang, X. M. (2013) Simultaneous removal of SO_2, NO and Hg0 by wet scrubbing using urea $KMnO_4$ solution. Fuel Process. Technol. 106, 645-653.
[23] Uffalussy, K. J., Miller, J, B., Howard, B. H., Stanko, D. C, Yin, C., & Granite, E.,J. (2014) Arsenic Adsorption on Copper-Palladium Alloy Films. Ind. Eng. Chem. Res. 53, 7821–7827.
[24] Tan, Z. Q., Sun, L.,S., Xiang, J., Zeng, H. C., Liu, Z. H., Hu, S., & Qiu, J. R. (2012) Gas-phase elemental mercury removal by novel carbon-based sorbents. Carbon, 50, 362-371.
[25] Wang, X. Q., Wang P., Ning P., Ma Y. X., Wang F., Guo X. L. , & Lan Y. (2015) Adsorption of gaseous elemental mercury with activated carbon impregnated with ferric chloride. RSC Adv., 5, 24899-24907.
[26] Li, H. G. (1990) Rare metals metallurgy. Metallurgical Industry Press, Beijing, 55-56.
[27] Cheng, G. G., Zhang, G., & Bai, B. F. (2014) Removal of Hg0 from flue gas using Fe-based ionic liquid. Chemical Engineering Journal. 252, 159–165.
[28] Bjorge, D., & Joel, H. (2009) Removal of heavy metals occurring in the washing water of flue gas purification . Chem. Eng. J. 150, 196-203.
[29] Tan, H. Q., He, W. J., & Han, H. D. (2013) Cadmium removal in water emergency treatment of conventional process enhanced by chemical precipitation. Chinese Journal of Environmental Engineering, 7, 848-852.
[30] Xie, H., Zhao, Z. W., Cao, C. F. (2012) Behavior of arsenic in process of removing molybdenum y sulfide method. Journal of Central South University (Science and Technology), 43,435-439.
[31] Pekka, S. & Willis, F. (2000) Precipitation of lead sulfide for surface chemical studies. Colloids and Surfaces A: Physicochemical and Engineering Aspects, 172, 17 - 31.
[32] Shi, Y., Wang, X. Q., Guo X. L. , Ma Y. X., Wang L. L, & Ning P.(2014) Removal of heavy metals from smelting flue gas by ammonium sulfide. The Chinese Journal of Nonferrous Metals, 24, 2900-2905.
[33] Lewis, A. E. (2010) Review of metal sulphide precipitation. Hydrometallurgy. 104, 222–234
[34] Jin, Z. N, Jiang, K. X., Wei, X. J., & Wang, H. B. (1999) Potential-pH diagrams of As-S-H_2O system at High Temperature. Ming and Metallurgy, 8, 47-48.
[35] Wei, X., Li, & C. X. (2013) Zinc extractive metallurgy. Metallurgy Industry Press, Beijing, 6-7.

Received: **29.10.2015**
Accepted: **26.02.2016**

CORRESPONDING AUTHOR

Wang Xueqian
Faculty of Environmental Science
and Engineering,
Kunming University of Science and Technology,
Kunming 650500, China

e-mail: mayixing99@163.com

© by PSP Volume 25 – No. 7/2016, pages 2575-2584 Fresenius Environmental Bulletin

BIOSORPTION OF THALLIUM(I) BY LIVE AND DEAD CELLS OF *BACILLUS* STRAIN ISOLATED FROM WASTEWATER

Long Jianyou[1], Xia Jianrong[1]*, Luo Dinggui[1], Chen Yongheng[2] *

[1]School of Environmental Science and Engineering, Guangzhou University, Guangzhou,510006 China
[2] Innovation Center and Key Laboratory of Waters Safety & Protection in the Pearl River Delta, Ministry of Education, Guangzhou University, Guangzhou, 510006,China

ABSTRACT

The bisorption characteristics of Thallium using live and dead cells of *Bacillus* strain as biosorbents have been investigated in the present research. Optimum condition for biosorption were determined to be: pH adjusted to 6.0, agitated at 150 r/min and at a dose of 1 g/L. For initial Thallium concentration of 0.5-20 mg/L, The adsorption isotherms fitted well with both the Langmuir and Freundlich isotherm models with high values of correlation coefficient (R^2>0.92). Experimental maximum biosorption capacity turned out to be 12.38mg/g for living material and 19.84mg/g for dead sorbents, respectively. The nature of the biosorbents and metal ion interactins were evaluated by Fourier transform infrared(FT-IR) spectroscopy. FT-IR analysis of live and dead biomass revealed the presence of amine, carboxyl, hydroxyl, and carbonyl groups, which are likely responsible for the biosorption of Thallium. And FT-IR analysis indicated that more functional groups were involved in the biosorption process of dead adsorbents, compared with those linked to live biomass, taken together, it can be concluded the dead cell of Bacillus were better and cheaper biosorbents than live ones, which can be a suitable biosorbent for the removal of Thallium ions from aqueous solution.

KEYWORDS:
Bacillus, biosorption Thallium, live, dead

INTRODUCTION

The presence of heavy metals in the environment poses a problem due to their harmful affects on human health. Thallium is considered a non-essential and highly toxic element, which is produced as a by-product in the combustion of coal, cement plants using pyrite,smelting if non-ferrous metals, refining of iron, cadmium and zinc[1-2] A lack of detailed knowledge of distribution and dispersion of TI, from both natural process and human activities has led to an adverse impact on the local ecosystem and human health. Since the discovery of high-temperature superconducting compounds in the system TI-Ca-Ba-Cu-O, thallium has attracted greater attention as a potential pollution source on a large scale in the future[3]. The maximum contaminant levels of thallium in drinking water and wastewater(effuent) set by the United States Environmental Protection Agency (USEPA) are 2 and 140µg/l, respectively[4].

In literatures, metal removal treatment systems using micro-organisms is a cheap and practical alternative to conventional processes, conventional physicochemical methods such as electrochemical treatment, ion-exchange, precipitation, reverse osmosis, evaporation and oxidation/reduction for heavy metal removal from wastewater are expensive, not eco-friendly and inefficient for metal removal from diluted solutions containing from 1 to 100mg/L of dissolve metal[5-6]. In the past few years, more and more biological material have been employed as inexpensive biosorbents in the removal of heavy metals[7]. Some of these alternative adsorbent materials are sea algae[8], yeast biomass[9], maple sawdust[10],brown marine macroalgae[11], coal fly ash[12], etc., including living and non-living microorganisms, in the removal and possibly recovery of toxic or precious metals from industrial wastes, has gained important credibility during recent years[13], such as, The biosorption of thallium from wastewater by *Aspergillus niger* biomass was reported by A.L. John Peter et al. In another study, Saima Q.Memon et al. studied the biosorption of thallium by sawdust. In recent research ,dead microbial strains were also widely used in the biosorption of metal ions, especially in a series of research of Selatnia et al[14-15] and Li[16]. Hower, little work has been done to compare the biosorption of thallium using live and dead cells of bacterial strain[17].

In this study, Bacillus isolated from industial metal mine and exhibited high resistance to a variety of heavy metals. Thallium was used as the target metal pollutant in this work, which is frequently found in the industrial effluents and wastes in China.

The objective of the present work is to investigate the biosorption potenial of live and dead cells of bacterial strain in the removal of thallium from aqueous solution. The influence of different parameters on thallium biosorption, such as pH, agitation speed, biosorbent dose, intial metal concentration and contact time were performed. Different equilibrium and kinetic models were applied to describe the biosorption process of live and dead biomass. while the Fourier transform infrared(FT-IR)analysis were also used in this study to look at potential binding sites and possible functional groups of live and dead biomass.

MATERIALS AND METHODS

Bacterial preparation as a biosorbent. The bacterial strains were cultured in nutrient broth, which contained (per liter of deionized water):peptone 10g/L,yeast extract 5g/L,NaCl 5g/L, and 150 r/min agitation was employed for shake-flask culuring at 25 ℃. Then live cells were harvested by centriguation(14,000 r/min,5min)at the end of the exponential phase, while dead cells were first subjected to autoclaving at 121 ℃ for 30min as suggested by Tamer[18] and A. Selatnia et al[19]. After rinsing with ddH_2O three times, live and dead cells of Bacillus were prepared as biosorbents for Thallium biosorption.

Metal solution for biosorption. A 1000mg/L stock thallium solution used for this study was of analytical grade, and it was supplied by analytical center of Guangzhou.

Effect of pH, agitation speed and biosorbent dose on biosorption. The impact of solution pH ,agitation speed and biosorbent dose on thallium biosorption was investigated using the different biosorbents and conducted at different pH values (ranging from 2.0 to 7.0) containing 20ml of metal solution. The pH adjustment was done with the addition of either 0.1 M HCl or NaOH[20] , agiation speeds from 60-180 r/min and different biomass densities(0.5-2.5g/L)were tested in parallel.

Effect of contact time on biosorption experiments. The bacterial biosorbent(1g/L)was suspended in 20ml of thallium solutions in 100 ml flasks. The cell/metal suspensions were shaken(150r/min) at 25 ℃. The pH of the solution was initially adjusted to 6.0, to avoid precipitaion of thallium in the form of thallium hydroxides[21]. Samples were taken from the solutions at desired time intervals from 0 to 540min and were subsequently centrifuged at 14,000r/min for 5min. the Thallim concentration in the resulting supernatant was determined using FAAS.

FT-IR analysis. Samples were analyzed using Fourier transform Infrared(FT-IR) spectroscopy to give a qualitative and preliminary characterization of the main functional chemical groups present on the bacterial biomass, which are responsible for thallium biosorption. A raw sample and biomass loaded with thallium were analyzed using the KBr pressed disk technique[22-23].

Adsorption experiments. In this study, the biosorption isotherms of thallium were obtained at a pH of 6.0. The sorption experiments were carried out using 50mg of each biosorbent in conjunction with different concentration of thallium in 50ml of deionized water. The solutions were shaken at 150 r/min for 1h until equilibrium was attained. Then, the sample were centrifuged at 14,000 r/min for 5min and the thallium conecntration in the supernatants was measured by FAAS. Experiments were conducted at room temperature(22±1 ℃). All the adsorption experiments were performed in duplicate.

Data evolution. The specific metal biosorption was calculated using the following equation:

$$q_e(mg/g) = \left[\frac{C_i - C_e}{M}\right] * V \qquad (1)$$

Where q_e is the specific metal biosorption (mg meatl/g biomass) , V is the volume of metal solution(L), C_i and C_e are the initial and equilibrium concentration of metal(mg metal/L),respectively, and M is the dry weight of the biomass[24].

RESULTS

Effect of pH on the biosorption capacity. The pH is one of the most important parameters having a strong influence on the adsorption of metal ions. Many research showed that the affinity of cationic species for the functional groups presents on the cellular surface is strongly depended on the pH of the solution. The effect of pH on the biosorptive capacity of Thallium by Bacillus was evaluated at an initial concentration of 20mg/L, 60min contact time, and 25 ℃. At low pH, there was a high concentration of proton in the solution and this proton competed with metal ions in forming a bond with the active sites(the functional groups) on the surface of the strains. These bonded active sites thereafter became saturated and was inaccessible to other catioin. These results were in good agreement with the findings of previous researchers[25]. On the other hand, an increase in pH meant a lower quantity of protons, which caused a decrease in the competition between proton and heavy-metal ions. Hence, an increase in the sorption capacity(or removal efficiency) could be observed. To ensure no interference from metal

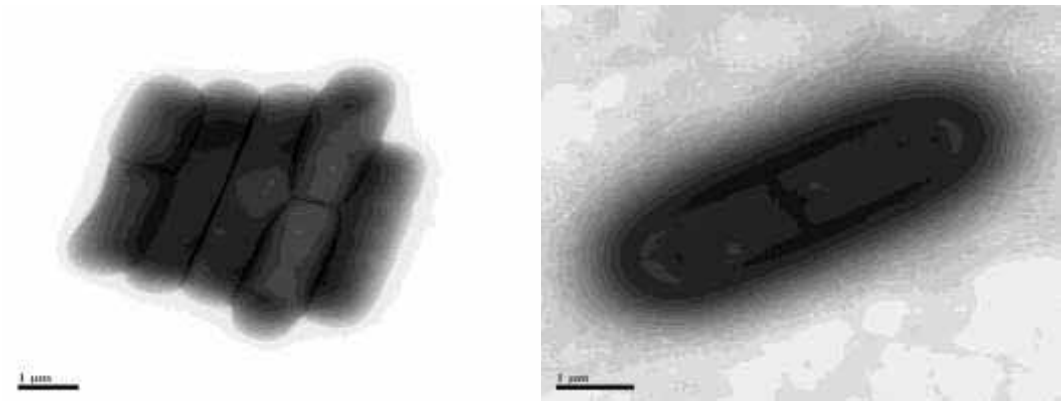

FIGURE 1
Transmission Electron Microscope mocrograph of the crinkly spore surface of strain Bacillus after 24h culture on nutrient agar medium.(JEM-1230).

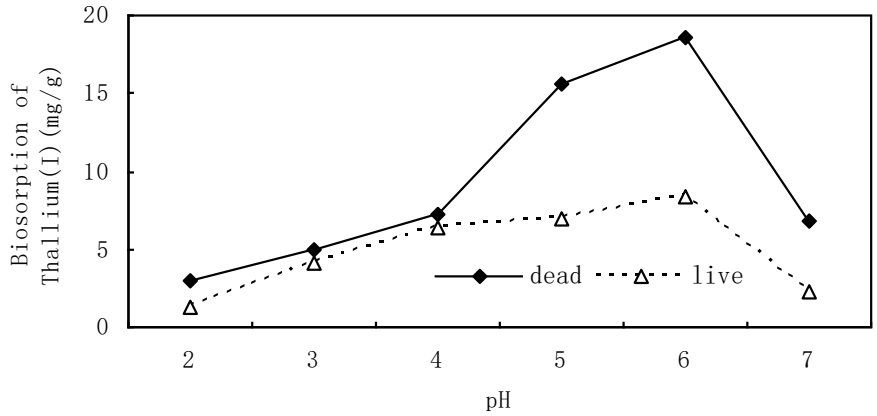

FIGURE 2
Effect of pH on biosorption of Thallium by live and dead cells of Bacillus(Initial Thallium concentration:20mg/l; temperature:25℃; agitation speed 150rpm/min; biosorbent dose:1g/l).

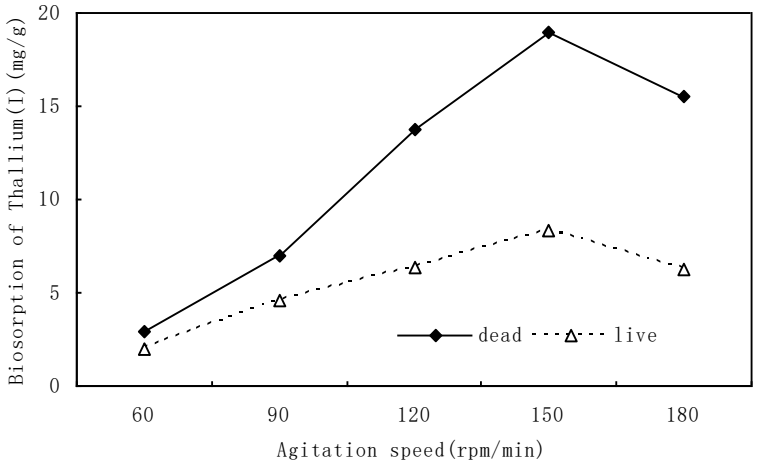

FIGURE 3
Effect of agitation speed on biosorption of Thallium by live and dead cells of Bacillus(Initial Thallium concentration:20mg/l; temperature:25℃; pH:6.0; biosorbent dose:1g/l).

precipitation, subsequent experiments were carried out at pH≤6[26].

Effect of agitation speed on the biosorption capacity. As can be seen in Fig. 3, the effect of agitation speed on Thallium biosorption by live and dead Bacillus had similar trends, where maximum biosorption capability was found at 150 r/min. The monitored biosorption capacity increased to 12.38mg/g for live cells and 19.84mg/g for dead ones as the agitation speed changed from 60 to 180 r/min. It has been reported that in the biosorption system, agitation brought more contant between the metal ions and biosorbent bindings sites, which promoted the transference of Thallium by live and dead biomass was more effective with little high agitation. Showing good agreement with fomer reports of Li [27].

Effect of biosorbent dose. Many researchs have indicated that biosorbent dose was also an important parameter affecting biosorption acpacity as well as removal efficiency. As clearly depicted in Fig. 4 the removal ratio increased gradually as the biosorbent concentration increased from 0.5 to 2.5g/L, simultaneously the biosorption capacity fell inversely. When using live strain, a maximum Thallium biosorption of 12.38mg/g was observed at a dosage of 0.5g/L, while the corresponding removal ration was 47.7%. As shown at the cross point of the two lines for live cells,47.55% of Thallium was removed at a 1.0g/L dosage,where the biosoption capacity was 9.51mg/g, not much lower compared with 8.05mg/g at 1.5g/L or 7.01mg/g at 2.0g/L. As to dead biosorbents, the removal efficiency was only whilst the maximum capacity of 19.08mg/g was attained at the lowest dosage. At the dose of 2.0g/L, 7.84mg/g of biosorption capacity was achieved with 78.35% removal, being better than 6.83mg/g biosorption and 85.65% removal vaules at 2.5g/l dosage, It's obvious that with the increase of biosorbents, more bindings sites were available and thus the removal efficiency went up. However, under specific initial concentration. Redundant biosorbents were not necessary for an efficiency began to reduce with the decrease of metal ions. Hence, it could be stated that 1g/L was the optimum biosorpent dose for further tests, where adequate biosorption capability could be obtained with a high removal ratio.

So far, the optimum conditions for Thaillum biosorption and removal were determined as pH 6.0, agitated at 150 rpm and at a dose of 1g/L, and all the following biosorption experiments were conducted under these conditions.

Effect of initial concentration. As shown in Fig.4, with the increase of initial metal ions, biosorption capacity and removal ratio changed inversely. The Thallium biosorption process of live and dead cells of Bacillus exhibited similar trends over the initial concentration range of 0.5 to 20 mg/L. However, the removal ration of live biosorbents decreased more rapidly compared with that of dead ones. The equilibrium biosorption capability of live biomass was always lower than that of dead strain and the difference seemed to increase with increased initial concentration. The lowest removal ratio was achieved at the highest initial Thallium concentration. Where the equilibrium biosorption capacity for live biomass was 9.79mg/g, while dead cells were able to uptake 14.25mg/g Thallium by each gram of dry cells.

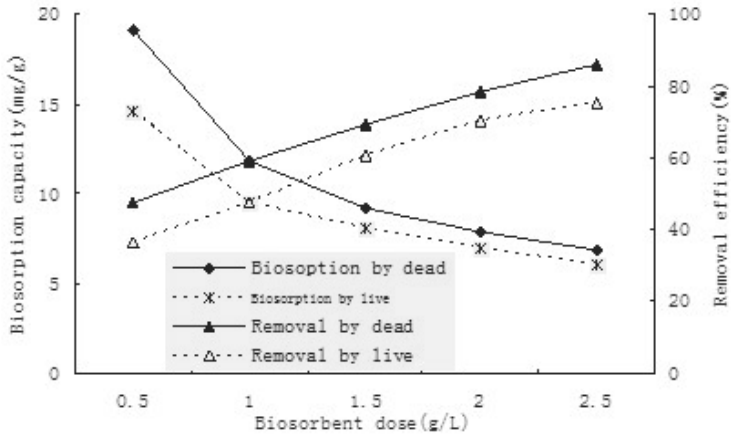

FIGURE 4
Effect of biosorbent dose on biosorption capacity and removal efficiency of Thallium by live and dead cells of Bacillus(Initial Thallium concentration:20mg/l; temperature:25℃; pH:6.0; agitation speed 150rpm/min).

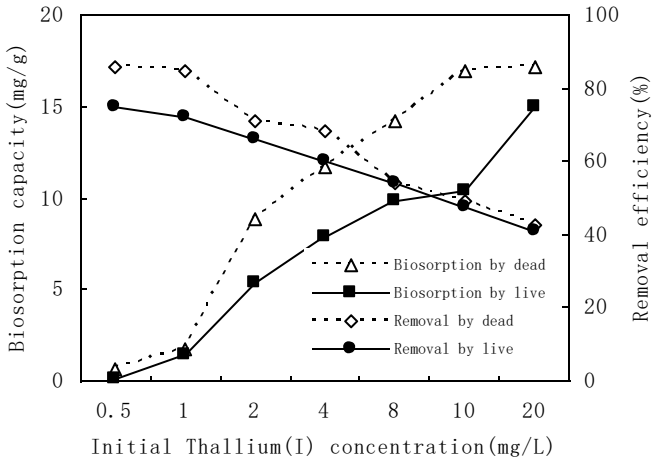

FIGURE 5
Biosorption capacity and removal efficiency of Thallium by live and dead cells of Bacillus over initial concentration ranging from 0.5 to 20mg/l.

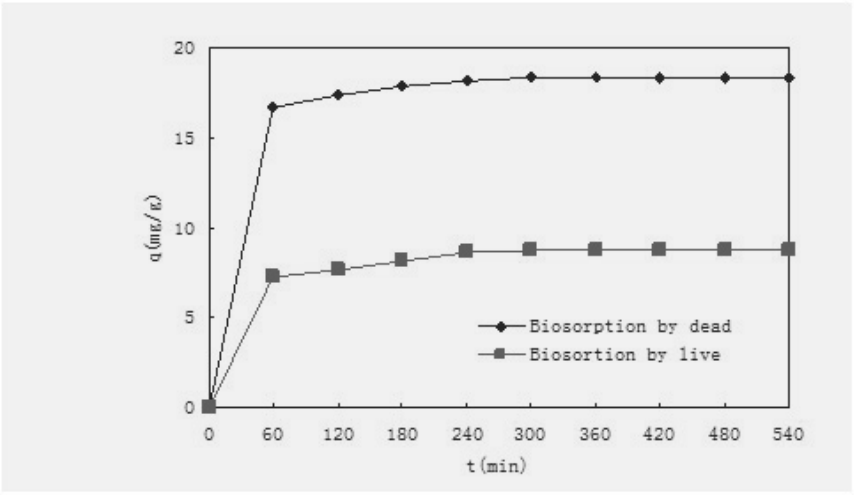

FIGURE 6
Effect of contact time on biosorption of Thallium by live and dead cells of Bacillus at an initial Thallium concentration of 20mg/l.

Effect of contact time. The effect of contact time on biosorption equilibrium by live and dead cells of Thallium at initial concentration of 1g/L were represented in Fig.5, from which the least time required for biosorption equilibrium could be concluded. In the case of dead biomass, the time required for equilibrium was 60min[28], after that the q value was nearly constant,indicate that the first phase of biosorption is always rapid, and it is considered to be a spontaneius process with no energy consumed. When using live cells of Bacillus as biosorbents the contact time necessary to reach equilibrium was different initial metal concentration. When the initial Thallium concentration was 1mg/L, 91% of total biosorption capacity was obtained within 60min, as the capacity began to increase slowly from 60min. it suggested that the intracellular bioaccumuation might also contribute to be uptake of Thallium ions, in addition to the rapid adsorption to the rapid adsorption by the cell surface.

FT-IR analysis. FT-IR analysis was performed to give a qualitative and preliminary analysis of the main functional groups present on the cell wall which may be responsible for Thallium biosorption. Fig.7 represents the FT-IR spectrum for the bacterial biomass controls of lyophilized no added Thallium and the biomass after Thallium biosorptiion. The FT-IR spectra of natural live and dead biomass showed broad and strong bonds at 3378.70cm^{-1} and 3438.58cm^{-1}, respectively, indicating bounded hydroxyl(-OH) or amine(-NH) groups. The peaks at 2951.51 cm^{-1} of live biomass; the peaks at 2943.52 cm^{-1} of dead biomass were attributed to the stretching vibration of (-CH_2) groups. The absorption bonds to observed at 1637.31 cm^{-1} of live biomass, 1645.99 cm^{-1} of dead

biomass are an indication of the presence of C=O, 1398.47 cm^{-1}(live),1372.92 cm^{-1}(dead) are mainly attributed to –NH,-CN stretch and 1245.15 cm^{-1}(live), 1236.37 cm^{-1}(dead) (mainly C-N stretch) could be attributed to the amine I, II and III bonds of protein fractions. The peak at 1245.15 cm^{-1} might also be due to a symmetrical vibration of C=O for live biomass. The moderately strong bonds at 1065.89 cm^{-1} for living material and 1048.3 cm^{-1} for dead biosobent could be assigned to the C-N stretching vibration of an amide bond or C-O stretching of alcohols and carboxylic acids. Praticular absoption bonds for an aromatic structure were also obtained at 579.22 cm^{-1} for live biomass and 570.83 cm^{-1} for dead biomass as reported by LinVien et al[29]. It seemed that the FT-IR spectra of the two biosorbents were nearly the same except for the significants shifts at 3438.58 cm^{-1} and 1372.92 cm^{-1} for dead biomass.

The FT-IR spectrum of the loaded biomass with Thallium, is shown in(Fig.7). A trial to compare between the spectrum of a native biomass with a biosorped one it can reval the following:
The broadening and stretching of the band characterzing the presence of C=O groups was observed at the range of 1630-1650 cm^{-1} and indicates an interaction between Thallium and C=O groups on the surface of the biomass. II) The shifting and broadening of the bands located at 1637.31 cm^{-1} and 1645.99 cm^{-1} [30]were due to the loading effect of metal. These broadenings can be explained by the involvement of H-bonding(Sar et al., 1990).III)The stretching of the 1048.73 cm^{-1} band was attributed to the loading of Thallium as a result of the interaction of Thallium with phosphate groups[31].IV)The bands located in the range 3350-3450 cm^{-1} verify the interaction that took place on both the hydroxyl and amine groups-the bands became more intense and broader after the biosorption reaction had taken place indicationg the formation of more OH^- groups by Thallium complexation. V) Also the bands at 1637, 1645 cm^{-1} became broader after biosorption had taken place on carboxyl. The transmittance of the peaks in the loaded biomass is substantially lower than those in the raw sample of the bacterial biomass[32]. This indicates that bond stretching occurs to a lesser degree due to the prenence of Thallium, and the following peak transmittance is reduced. The change in the transmittance of the amino, hydroxyl, and phosphate groups in the FT-IR spectrum for metal-loaded biomass of Bacillus indicated that these groups are possibly involved in Thalliumbiosorption. These results are in agreement with Norton et al., who stated that the biosorption of Thallium to the biosolids of activated sludge caused a decrease in the absorbance compared to the raw sample.

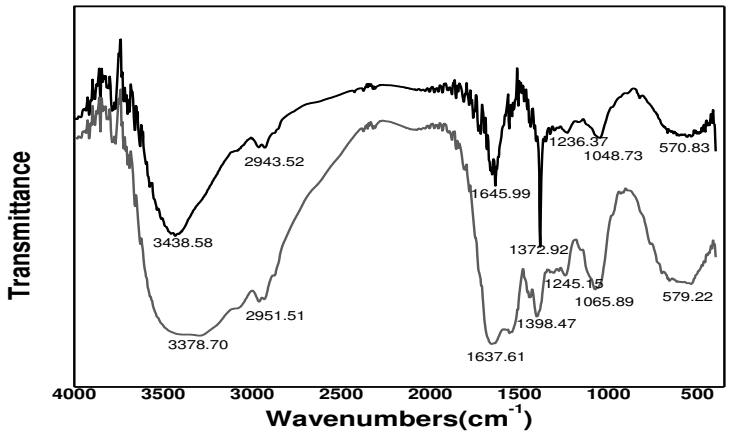

FIGURE 7
FT-IR spectrum of live and dead biosorbents loaded with and without Thallium.

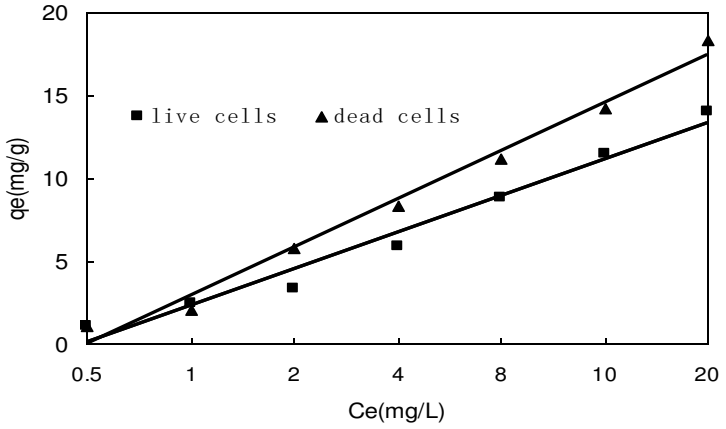

FIGURE 8
The linear form of Langmuir biosorption of Thallium by live and dead cells of Bacillus.

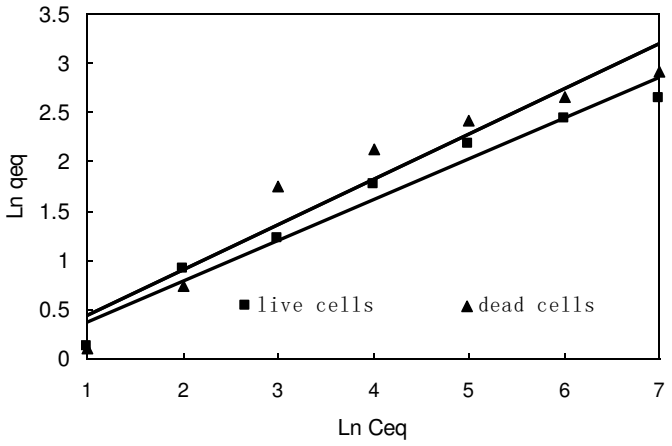

FIGURE 9
The linear form of Freundlich biosorption of Thallium by live and dead cells of Bacillus.

The above observations indicate the involvement of these functional groups in the biosorption process. These result are in good agreement with those obtained by other authors(Komy)et al.,2006; who come to the conclusion that the main functional groups responsible for biosorption of heavy metals are carboxylic, hydroxyl,and amine groups.

Biosorption isotherm. The biosorption isotherm curve represents the equilibrium distribution of metal ions between the aqeous and solid phases. The equilibrium distribution is important in determing the maximum biosorption capacity. Several isotherm models are available to describe this equilibrium distribution. The two most common types for describing biosorption are the Langmuir and Freundlich models[33-34]. The Langmuir isotherm model was chosen to estimate the maximum adsorption capacity corresponding to complete monolayer coverage on the biomass surface. The Freundlich model was chosen to estimate the adsorption intensity of the biosorbent towards the biomass. The mathematical formula of Langmuir equation can be expressed as[35]:

$$q_{eq} = \frac{q_{max} b C_e}{1 + b C_e} \quad (2)$$

The linear Langmuir isotherm is represented by the following equation:

$$C_{eq} / q_{eq} = 1/q_{max}\, b + C_{eq}/q_{max} \quad (3)$$

Where, q_{max} is the Langmuir costant(mg/g) reflecting the biomass adsorption capacity of the metal ion per unit weight of biomass to form a complete monolayer on surface bound at high C_{eq}. The value Langmuir constant, b(L/mg), represents a

TABLE 1
The Langmuir and Freundlich biosorption isotherm constants for Thallium by live and dead Bacillus biosorbents.

strain	Langmuir model			Freunclich		
	q_{max}(mg/g)	b(l/g)	R^2	K_f	n	R^2
live	12.38±0.007	0.1401	0.9739	2.717	0.9321	0.9655
dead	19.84±0.01	0.0667	0.9867	8.722	0.9671	0.9242

ratio of adsorption rate constant to desorption rate constant, which also gives an indication of the affinity of the metal for binding sites on the biosorbent. The maximum adsorption capacity q_{max}, and b can be determined from the linear form of Langmuir equation E_q(3) by plotting C_{eq}/q_{eq} verus C_{eq}.

The Thallium biosorption performance by live and dead cells of Bacillus biomass was achieved by measurements at initial concentration of 0.5-20mg/L, 60min contact time,and pH 6.0 as shown in Fig.4. The figure indicate the relationship between the amount of Thallium adsorbed(mg/g) by live and dead cells versus the concenration of Thallium ion remaining in solutin(C_{eq}). A good fit by the Langmuir model indicates that the biosorption fo Thallium could be characterized by a monolayer formation of the metal on the surface fo the biomass and belongs to a single type pheomenon with no interactions between sorbed metal. The data were found to fit the Langmuir model reasonably well as shown in Fig.5. Linear transfomation of the data using the Langmuir parameters are summarized in Table 1. The maximum biosorption capacity(q_{max})of live and dead cells are 12.38 and 19.84mg/g, respectively. The results indicated that the biosorption of Thallium by dead cells was higher than live cells. The b value of live and dead cells are 0.1401 and 0.0667 l/mg, respectively.

The Freundlich isotherm equation is originally empirical in nature, but it was later interpreted to be used in the case of sorption on heterogeneous surface or surfaces supporting sites to different affinities. The general form of the Freundlich isotherm equation is written as follows[36]:

$$q = K_f C_e^{1/n} \quad (4)$$

The linear form of this model is given in eq.(5)

$$\ln q = 1/n \ln C_e + \ln K_f \quad (5)$$

Where, K_f and n are the adsorption capacity and the intensity of adsorption, respectively. Freundlich parameters can be determined from the linear form of the eq.(5) by plotting the In q verus In C_e, the slope is the value of 1/n and the intercept si equal to In K_f. The linear form of the Freundlich equation for the biosorption of Thallium by live and dead cells of Bacillus is shown in Fig.6. The value of Freucdlich parameters are summarized in Table 1. From Tabel 1, the magnitude of K_f and n show a higher uptake of Thallium using dead cells compared live cells. The highest K_f and n values were 8.722 and 0.9671 for dead cells and 2.717 and 0.9321 for live cells, respectively. Table 1 also indicates that n is greater than unity, indicating tha Thallium ions are favorably adsorbed by live and dead cells of Bacillus.

From Table 1, very high regression correlation coeffcients(>0.92) were found at all Thallium biosorption studied. The high correlation coefficients show that both the Freundlich and Langmuir models describe the biosorption equilibrium of Thallium by the live and dead cells of Bacillus in the studied concentration range.

Generally, these data indicate that the biosorption capacity increased with increased with increasing initial Thallium concentration. This biosorption characteristic indicates that the surface saturation is dependent on the initial metal ion concentration. At low concentration, adsoption sites took up the available metal more quickly. However, at higher concentration, metals need to diffuse into the biomass surface by intraparticular diffusion and greatly hydrolyzed ions will diffuse at a lower rate[37].

DISCUSSION AND CONCLUSIONS

The biosorption of Thallium by live and dead cells of Bacillus strain has been investigated at optimum conditions determined in advance. Batch biosorption experiments with regard to initial metal concentrations, contact time, competitive biosorption and FT-IR analysis were performed in this research. When live and dead cells of Bacillus were employed as biosorbents, the experimental maximum biosorption capacity turned out to be 19.84mg/g and 12.38mg/g, respectively. At various initial Thallium concentrations, batch biosorption data of live and dead cells was fitted with well with the Langmuir and Freundlich adsorption isotherms equations in the studied metal concentration.

Taking into consideration of present findings, dead cells of Bacillus proved to be more efficient and low-cost biosorbents than live ones, which can be utilized as an alternative for the treatment of wastewater.

ACKNOWLEDGEMENTS

This research was financially supported by projects from the National Science Foundation of China(41573119, 41376156, 41372248); Public welfare scientific fund of Environmental Protection Department (201509051);Science and technology plan of Guangzhou(201510010204); National Natural Science Foundation of Guangdong province(S2013010016540) and the Project of the Education Bureau of Guangzhou City (2012A033).

REFERENCES

[1] John Peter, A.L., Viraraghavan, T. (2008) Removal of thallium from aqueous solutions by modified *Aspergillus niger* biomass,Bioresource Technology. 99, 618-625.

[2] Zitko, V. (1975) Toxicity and pollution potential of Thallium, The Science of the Total Environment. 4, 82-92.

[3] Xiao, T., Guha, J., Boyle, D. (2004) Environmental concerns related to high thallium levals in soils and thallium uptake by plants in southwest Guizhou, China, The Science of the Total Environment. 318, 223-244.

[4] Borgmann, U., Chearn, V., Norwood W.P., Lechner J. (1998) Toxicity and bioaccumulation of thallium in Hyalella azteca, with comparison to other metals and prediction of environmental impact, Environ Pollut. 99, 5-14.

[5] Green-Ruiz, C., Tirado, V.R., Gil, B.G. (2008) Cadmium and zinc removal from aqueous solutions by Bacillus jeotgali:Ph,salinity and temperature effects, Bioresource. Technol. 99, 3864-3870.

[6] Andreazza, R., Pieniz, S., Wolf, L., Lee, M.-K., Camargo, F.A.O., Okeke, B.C. (2010) Characterization of copper bioreduction and biosorption by a highly copper resistant bacterium isolated from copper-contaminated vineyard soil, Science of the Total Environment. 408, 1501-1507.

[7] Yuan, H., Zhang, J., Lu, Z. (2009) Studies on biosorption equilibrium and kinetics of Cd^{2+} by Streptomyces sp.K33 and HL-12, Journal of Hazardous Materials.164, 423-431.

[8] E.R.Maria, J.W. Ceri, H.E.G. Philip, (2001) Study of the mechanism of cadmium biosorption by dealginated seaweed waste, Environ. Sci. Tchnol.35, 3025-3030.

[9] G. Yekta, U.Sibel, G. Ulgar, (2005) Biosorption of cadmium and lead ions by ethanol treated bakers yeast biomass, Bioresour, Technol.96, 103-109.

[10] O.Gulnaz, S.Saygideger, E, Kusvuran (2005) Study of Cu biosorption by dried activated sludge:effect of physico-chemical environment and kinetics study, J.Hazard. Mater. B 120, 193-200.

[11] P.Lodeiro, B. Cordero, J.L. Barriada, R. Herrero, V.M.E. Sastre (2005) Biosorption fo cadmium by biomass of brown marine macroalgae, Bioresour. Technol. 96 1796-1803.

[12] W. Jianmin, T. Xinjun, W. Hao, B. Heng (2004) Characterizing the metal adsorption capacity of a class F coal fly ash, Environ. Sci. Technol. 38, 6710-6715.

[13] Jinho Joo, Sedky H.A. Hassan, SangEun Oh (2010) Comparative study of biosorption of Zn^{2+} by Pseudomonas aeruginosa and Bacillus cereus, International Biodeterioration & Biodegradation .64, 734-741.

[14] A. Selatnia, M.Z. Bakhti, A. Madani, L. Kertous, Y. Mansouri (2004) Biosorption of Cd^{2+} from aqueous solution by a NaOH-treated bacterial dead Streptomyces rimosusbiomass, Hydrometallurgy. 75, 11-24.

[15] A. Selatnia, A. Boukazoula, N. Kechid, M.Z. Bakhti, A. Chergui, Y. Kerchich (2004) Biosorption of lead(II) from aqueous solution by a bacterial dead Streptomyces rimosus A. biomass, Biochem. Eng. J. 19, 127-135.

[16] Y. Nacera, B. Aicha (2006) Equilibrium and kinetic modelling of methylene blue biosorption by pretreated dead Streptomyces rimosus: effect of temperature, Chem. Eng. J. 119, 121-125.

[17] Rosa Maria Perez Silva, Arelis Abalos Rodriguez (2009) Biosorption of chromium, copper, manganese and Zinc by Pseudomonas aeruginosa AT18 isolated from a site contaminated with petroleum, Bioresource Technology.100, 1533-1538.

[18] Hussein.H., Farag, S., Kandeel, K., Moawad, H. (2005) Tolerance and uptake of heavy metals by Pseudomonads, Process Biochem. 40, 955-961.

[19] Tamer Akar, Sibel Tunali (2006) Biosorption characeteristics of Aspergillus flavus biomass for removal of Pb(II) and Cu(II) ions from an aqueous solution, Bioresource Technology. 97, 1780-1787.

[20] A.Selatnia, A. Boukazoula, N. Kechid, M.Z.Bakhti, A. Chergi, Y. Kerchich (2004) Biosorption of lead(II) from aqueous solution

by a bacterial dead Streptomyces rimosus biomass, Biochemical Engineering Journal. 19, 127-135.
[21] I. Kiran, T. Akar, A.S. Ozcan, A. Ozcan, S.Tunali (2006) Biosorption kenetics and isotherm studies of Acid Red 57 by dried Cephalosporium aphidicola cells from aqueous solutions, Biochem.Eng.J.31, 197-203.
[22] Lester. J.N. (1982) Role of bacterial extracellular polymers in metal uptake in pure bacterial culture and activated sludge, Water Res.16, 1539-1548.
[23] E. Colak, N. Atar, .A. Olgun (2009) Biosorption of acidic dyes from aqueous solution by Paenibacillus macerans:kinetic, thermodymatic and equilibrium studies, Chem. Eng. J.150, 122-130.
[24] M.I.Kefala, A.I.Zouboulis, K.A.Matis (1999) Biosorption of cadmium by Actinomycetes and sepatation by flotation, Environmental Pollution.104, 283-293.
[25] A. Selatnia, A. Madani, M.Z. Bakhti, L. Kertous, Y. Mansouri, R. Yous (2004) Biosorption of Ni^{2+} from aqueous solution by a NaOH-treated bacterial dead Streptomycesrimosus biomass, Miner. Eng. 17, 903-911.
[26] R.M. Gabr, S.H.A. Hassan, A.A.M. Shoreit (2008) Biosorption of lead and nickel by living and non-living cells of Pseudomonas aeruginosa ASU 6a, Int. Biodeterior. Biodegrad. 62, 195-203.
[27] Huifen Li. Yanbing Lin, Wumeng Guan, (2010) Biosorption of Zn(II) by live and dead cells of Streptomyces ciscaucasicus strain CCNWHX72-14, journal of Hazardous Materials.179, 151-159.
[28] A.L. John Peter, T. Viraraghavan (2008) Removal of thallium from aqueous solutions by modified *Aspergillus niger* biomass, Bioresource Technology. 99, 618-625.
[29] D. Lin Vien, N.B. Colthup, W.G. Fateley (l991) The Handbook on Infrared and Raman Characteristics Frequencies of Organic Molecules, Academic Press, San Diego, DC.
[30] Sadin Ozdemir, Ersin Kilinc, Annarita Poli (2009) Biosorption of Cd, Cu, Ni, Mn and Zn from aqueous solutions by thermophilic bacteria, Geobacillus toebii sub.sp. decanicus and Geobacillus thermoleovorans sub.sp. stromboliensis:Equilibrium, kinetic and thermodynamic studies, Chemical Engineering Journal.152, 195-206.
[31] A.C.A. Costa, F.P.Duta (2010) Bioaccumulation of copper, zinc, cadmium,and lead by Bacillus sp., Bacillus cereus, Bacillus sphaericus, and Bacillus subtilis, Braz.J. Microbiol.32, 876-887.
[32] A.L. Zouboulis, M.X. Loukidou, K.A. Matis, (2004) Biosorption of toxic metals from aqueous solutions by bacteria strains isolated from metal-polluted siols,Process Biochem.39, 909-916.
[33] Volesky, B. (2003) Biosorption process simulation tools, Hydrometallurgy. 71, 179-190.
[34] Volesky, B., Holan, Z.R. (1995) Biosorption of heavy metals. Biotechnology progress, 11, 235-250.
[35] I. Langmuir (1918)The adsorption of gases on plane surfaces of glass.mica and platinum, J.Am.Chem. Soc. 40, 1361-1403.
[36] H.M.F. Freundlich (1906) Über die adsorption lösungen, Z. Phys. Chem. 57, 385-470.
[37] Sar, P., Kazy, S.K., Asthana, R.K., Singh, S.P. (1999) Metal adsorption and desorption by lyophilized Pseudomonas aeruginosa. International Biodeterioration and Biodegradation. 44, 101-110.

Received: **04.11.2015**
Accepted: **28.02.2016**

CORRESPONDING AUTHOR

Jianyou Long
Guangzhou University,
School of Environmental Science and Engineering,
510006 Guangzhou, China.

e-mail: longjyou24@sohu.com

© by PSP Volume 25 – No. 7/2016, pages 2585-2593 Fresenius Environmental Bulletin

MARINE ALGAE – ENVIRONMENT PARAMETERS BY CANONICAL CORRESPONDENCE ANALYSIS (MARMARA SEA –TURKEY)

Arzu Morkoyunlu Yuce [1], Tekin Yeken [1], Umit Kebapci [2]

[1]Kocaeli University, Hereke O. I. Uzunyol Vocational Schools,41000 Kocaeli, Turkey
[2]Faculty of Arts and Sciences, Mehmet Akif Ersoy University, Burdur, Turkey

ABSTRACT

Izmit Bay, located in the Marmara Sea, is a highly important region in terms of aquatic ecosystems, marine transportation, shipping and industrial sector. Due to the residential areas and the industrial activities around the bay, this region is affected by both domestic and industrial wastes.

In this study, the environmental relationships between the macro algae species *Ulva rigida* C. Ag., *Enteromorpha* sp., *Gracilaria* sp., *Porphyra* sp., *Gelidium* sp. and *Ceramium* sp. in the littoral zone of Izmit Bay and the heavy metals in the sea water (Al, Fe, Cd, Zn, As, Cr, Mn) were evaluated using the Canonical Correspondence Analysis (CCA). The same method was also used to evaluate the environmental relationships between these macro algae species and the sea water parameters, such as; NH_4-N (mg/L), NO_3-N (mg/L), NO_3^- (mg/L), PO_4-P (mg/L), PO_4^{-3} (mg/L), suspended solids (mg/L), Temperature (^{0}C), Conductivity (µS/cm), Ph and Dissolved oxygen mg l^{-1}).

According to the Canonical Correspondence Analysis (CCA) results, the marine algae species and the heavy metals show that the correlation between the variables on the axis 1 was significant ($p = 0.01$). *Enteromorpha* sp., *Gelidium* sp., and *Gracilaria* sp. The distributions were positively correlated, especially with the heavy metals such as; As, Mn and Zn, whereas, the situation for *Ulva rigida* C. Ag. and *Ceramium* sp. was the opposite. On the other hand, *Enteromorpha* sp. and *Gelidium* sp., both showed positive correlations with the values of PO_4-P and PO_4^{-3}, where *Ulva rigida* C. Ag. and *Ceramium* sp. showed a negative correlation with these parameters.

KEYWORDS:
Canonical correspondence analysis, heavy pollutant, environmental factors.

INTRODUCTION

In our world, where industrialization is rapidly increasing, ecological and biological balances are also changing. Urban and industrial activities, such as; power industry, transport, municipal waste management, waste dumping sites and fertilisers, contribute to the introduction of significant amounts of pollutants in the marine environment which, directly or indirectly affects the coastal ecosystem. Many contaminants entering the marine environment, however, have the ability to move into various solid components of an ecosystem. For example, heavy metals accumulate in sediment and macro-algae or can be connected within the organic matrix [1]. Marine organisms can be used as monitors to give information on the concentrations of heavy metals in the surrounding environment. Marine algae species are usually used to indicate heavy metal levels in both estuarine and coastal waters all over the world. In benthic food webs, marine algae are the key links, and they act as time integrators of pollutants [2]. Pollution by heavy metals, is considered to be a serious problem, due to their toxicity and their ability to accumulate in the biota [3]. Heavy metals, such as lead (Pb), copper (Cu), cadmium (Cd), zinc (Zn), and nickel (Ni), are among the most common pollutants found in both industrial and urban effluents. In low concentrations, some heavy metals (Cu, Ni, and Mn) are essential trace elements for photosynthetic organisms; however, at higher concentrations, it is important to determine the cause of serious toxic effects of these metals [4]. There are several studies that are related to the water quality, heavy metal and the sources of pollution of the Izmit Bay [5 - 10].The Bay, which is an important region in terms of the marine ecosystem, is heavily affected by the pollutants caused by marine transportation and by discharged industrial and domestic wastes. Illegal discharges into the bay, also lead to an increase in the heavy metal load within the sea area [11].

In this study, the environmental relationships between the macro algae species of *Ulva rigida* C. Ag., *Enteromorpha* sp., *Gracilaria* sp.,*Porphyra* sp., *Gelidium* sp. and *Ceramium* sp., showing a contagious distribution in the littoral zone of İzmit Bay and the heavy metals such as; Al, Fe, Cd, Zn, As, Cr and Mn in the sea water were evaluated using the Canonical Correspondence Analysis (CCA). The same method was also used to evaluate

the environmental relationships of these macro algae species with the sea water parameters; that is, NH_4-N (mg/L), NO_3-N (mg/L), NO_3^- (mg/L), PO_4-P (mg/L), PO_4^{-3} (mg/L), suspended solids (mg/L), Temperature (^{0}C), Conductivity (µS/cm), pH and Dissolved oxygen (mg l^{-1}) respectively.

MATERIALS AND METHODS

Izmit Bay, which has a surface area of 261 km^2, is approximately 50 km long, 1.8-9 km wide and a narrow marine space, that is located at the eastern end of the Marmara Sea. The study area is located between the coordinates of 29° 37.16' and 29° 56.70' E and 40° 39.73' and 40° 49.46' N respectively (Figure 1). The eastern section, which is the smallest component of the entire system, is about 15 km in length and relatively shallow, having a maximum depth of about 35 m. The central section of the İzmit Bay, being the largest component of the system, is about 20 km long, and the bottom topography varies considerably, north-southerly in direction; its northern part is relatively shallow, with an average depth of about 60 m and the depth increases to approximately 180 m in the southern section [12].

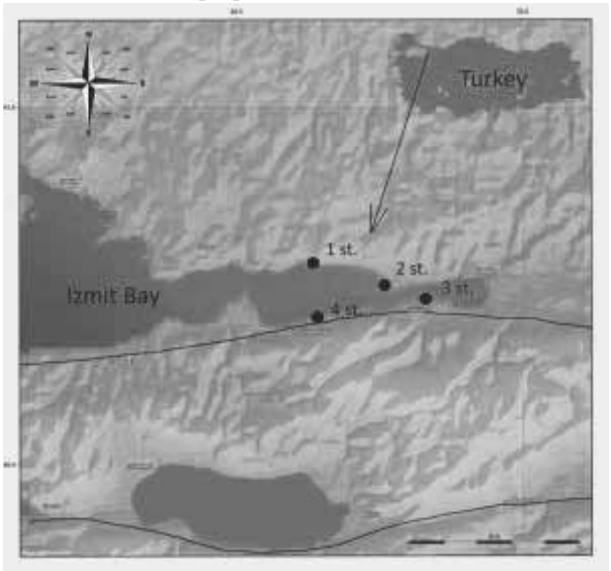

FIGURE 1
The study area in İzmit Bay
(http://www.koeri.boun.edu.tr.sismo.map).

The relationships of the macro algae communities with the concentrations of heavy metal like; Al, Fe, Zn, Cd, As, Cr and Mn and the physicochemical parameters of the sea water were investigated seasonally during the study period, from January 2011 to November 2011 in 4 stations from the coastal region of İzmit Bay (Figure 1). The sampling stations, were chosen in accordance with the objectives of the study, because of the seasonal distribution of the species which were in an orderly manner and the polluting factors which are also at high density. The samples of *Ulva rigida* C. Ag., *Enteromorpha* sp., *Gracilaria* sp., *Porphyra* sp., *Gelidium* sp., *Ceramium* sp. were collected by hand from a depth between 0 and 2.5 m of the Izmit Bay and fixed in a 4% formaldehyde solution. The water samples were collected at the same time with the algal sampling at the research stations, to measure the heavy metal concentrations and physico-chemical parameters.

The concentrations of the heavy metals were measured using an Agilent 7700 series ICP-MS instrument. The temperature of the water, dissolved oxygen, pH, and specific conductivity were measured *in situ* at all sampling stations with portable instruments (with CTD probe, YSI Incorporated). The nutrient concentrations of seawater were measured as milligram per liter (mg/l) by the methods of Solorzano and Mc Greery [13] for ammonia (NH_4-N), Snel and Snel [14] for nitrite (NO_2-N), the Braun Systematik (Methodenblatt N 60) for nitrate (NO_3^-N) and Vanadate-Molybdate-Reagent (Merck Wasseruntersuchung) [15,16] for phosphate (PO_4-P) in the study. For each measurement, analytical grade chemicals were used [17]. Spectrophotometric measurements were carried out by using a Hach DR 2000 spectrophotometer. CCA was used to examine the relationship between the marine algae species, ecological factors, the most important factors in the separation of heavy metals and the distribution of the species [18]. The variables and the algae used in the statistical analysis were abbreviated with relevant codes that are given in Tables 1,2,5 and 6

Canonical Correspondence Analysis (CCA) was used to examine the relationship between the marine algae species and the ecological factors [18]. The variables and the algae used in the statistical analysis, were abbreviated with relevant codes that are given in Tables 1,2,5 and 6.

RESULTS

When the correlation between the marine algae species and the heavy metals were evaluated, *Enteromorpha* sp., *Gelidium* sp., and *Gracilaria* sp. were determined to have a positive correlation, especially with As, Mn and Zn (heavy metals), whereas, *Ulva rigida* C. Ag. and *Ceramium* sp. had negative correlations. Tables 1 and 2.

TABLE 1
Inter-set correlations for 7 factors, that is, heavy pollutants.

Correlations		
Variable and code	Axis 1	Axis 2
Aluminium (Al)	0.483	0.652
Iron (Fe)	-0.181	0.699
Cadmium (Cd)	-0.545	0.818
Arsenic (As)	0.799	0.313
Chromium (Cr)	0.722	0.182
Manganese (Mn)	0.805	0.204
Zinc (Zn)	0.657	0.339

TABLE 2
Inter-set correlations for 6 factors, that is, marine algae species.

Correlations		
Variable and code	Axis 1	Axis 2
Ulva rigida C. Ag. (ulvrig)	-0.875	-0.149
Enteromorpha sp.(entrsp)	0.876	- 0.466
Gracilaria sp.(gracsp)	0.603	0.616
Porphyra sp. (porpsp)	-0.003	0.144
*Gelidium sp.(*gelisp)	0.669	0.394
Ceramium sp.(cerasp)	- 0.739	-0.049

TABLE 3
Monte Carlo test results-eigen values.

Randomized data					
Real data		Monte Carlo test 99 runs			
Axis	Eigenvalue	Mean	Minimum	Maximum	p
1	0.571	0.316	0.124	0.498	0.0101
2	0.172	0.125	0.067	0.202	
3	0.146	0.069	0.024	0.114	

p = proportion of randomized runs with eigen value greater than or equal to the observed eigen value; that is, p = (1 + no. permutations $\geq$ observed)/(1 + no. permutations) p is not reported for axes 2 and 3 because, using a simple randomization test for these axes may bias the p values.

As seen above, the value of the axis 1 indicates the highest change in marine algae distribution. According to the Monte Carlo test (Table 3), the marine algae and the heavy metals show that the correlation between the variables on the axis 1 is significant (p = 0.01).

According to Figure 2, heavy metals, such as; Al, Cd, Mn, Zn and As, all show parallel variations with Ent.sp, Geli.sp and Grac.sp because they are located on the right part of the graph. On the other hand, even though it is not so clear, Fe and Cr tend to be located on the left part of the graph and the species of Cera.sp and ulvrig are also found on the left side of the graph. The distribution of the species indicates insignificant variation in terms of seasons. However, the stations play an important role in deciding the locations of the species in the graph.

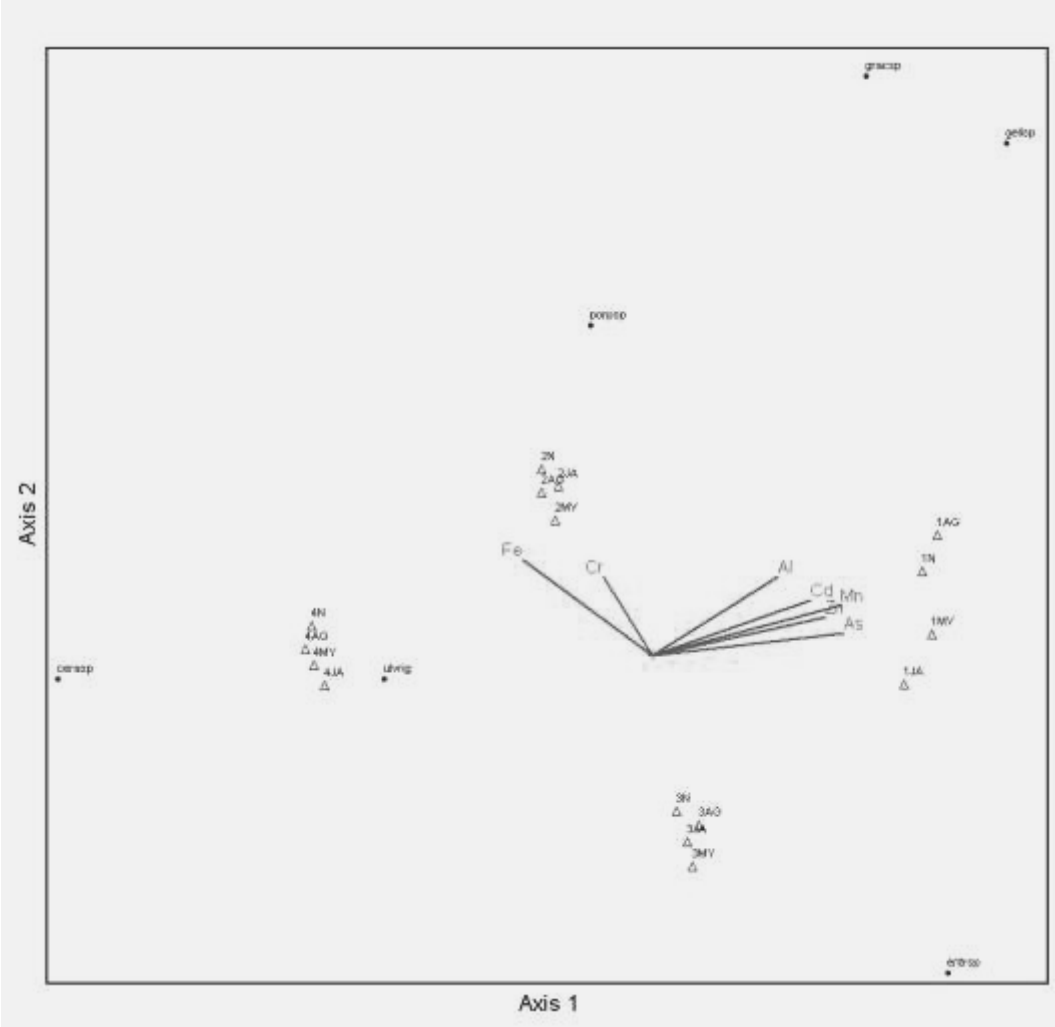

FIGURE 2
The relationships between heavy metals and marine algae.

TABLE 4
Monte Carlo test results: Marine algae - heavy metals correlations.

Randomized data					
Real data		Monte Carlo test 99 runs			
Axis	Spp-Envt Corr.	Mean	Minimum	Maximum	p
1	0.986	0.770	0.599	0.934	0.0101
2	0.968	0.779	0.421	0.965	
3	0.907	0.638	0.342	0.964	

p = the proportion of randomized runs with species-environment correlation is greater than or equal to the observed species-environment correlation; that is, p = (1 + no. permutations ≥ observed)/(1 + no. permutations) p is not reported for axes 2 and 3 because, using a simple randomization test for these axes may result in a biased p values.

In the study, *Ulva rigida* C. Ag., *Enteromorpha* sp., *Gracilaria* sp., *Porphyra* sp., *Gelidium* sp., *Ceramium* sp. and the chemical parameters in the sea water, ((NH_4-N (mg/L), NO_3-N (mg/L), NO_3^- (mg/L), PO_4-P (mg/L), PO_4^{-3} (mg/L), suspended solids (mg/L), Temperature (^{0}C), Conductivity (µS/cm), Ph and Dissolved Oxygen (mg l^{-1})) were evaluated using the Canonical Correspondence Analysis (CCA). The Inter-set correlations for 10 factors, which is the chemical parameters and the Inter-set correlations

TABLE 5
Inter-set correlations for 10 factors, that is, chemical parameters.

Correlations		
Variable and code	Axis 1	Axis 2
NH_4-N (mg/L) - NH4N	- 0.148	-0.446
NO_3-N (mg/L) - NO3N	0.534	0.229
NO_3^- (mg/L) - NO3	0.283	0.930
PO_4-P (mg/L) - PO4P	0.773	- 0.081
PO_4^{-3} (mg/L) - PO43	0.778	- 0.184
Suspended solids (mg/L) sussol	- 0.155	0.065
Temperature (^{0}C) -TEMP	-0.082	0.078
Conductivity (µS/cm) - EC	0.318	- 0.247
pH – pH	-0.267	0.204
Dissolved oxygen (mg l^{-1}) - DO	0.085	- 0.024

TABLE 6
Inter-set corelations for 6 factors i.e. marine algae species.

Correlations		
Variable and code	Axis 1	Axis 2
Ulva rigida C. Ag. (ulvrig)	-0.891	0.157
Enteromorpha sp.(entrsp)	0.855	0.468
Gracilaria sp.(gracsp)	0.571	-0.610
Porphyra sp. (porpsp)	0.050	-0.222
Gelidium sp.(gelisp)	0.702	-0.389
Ceramium sp.(cerasp)	-0.727	0.024

TABLE 7
Monte Carlo test results-eigenvalues.

Randomized data					
Real data		Monte Carlo test 99 runs			
Axis	Eigenvalue	Mean	Minimum	Maximum	p
1	0.566	0.417	0.156	0.553	0.0101
2	0.175	0.164	0.100	0.214	
3	0.152	0.106	0.049	0.163	

p = proportion of randomized runs with eigenvalue greater than or equal to the observed eigenvalue; that is, p = (1 + no. permutations ≥ observed)/(1 + no. permutations) p is not reported for axes 2 and 3 because, using a simple randomization test for these axes may bias the p values.

or 6 factors, the marine algae species are given in Table 5-6.

When the correlation between the marine algae species and the chemical parameters were evaluated for axis 1, *Enteromorpha* sp. (0.855) and Gelidium sp. (0.702) were determined to have a positive correlation with the values of PO_4-P and PO_4^{-3}; whereas, *Ulva rigida* (- 0.891) and *Ceramium* sp. (- 0.727) showed a negative correlation with these parameters as shown in Tables 5 and 6.

Marine algae and chemical parameters showed that axis 1 were significant (p = 0.01). However, the correlations with the other axes were less significant (Table 7).

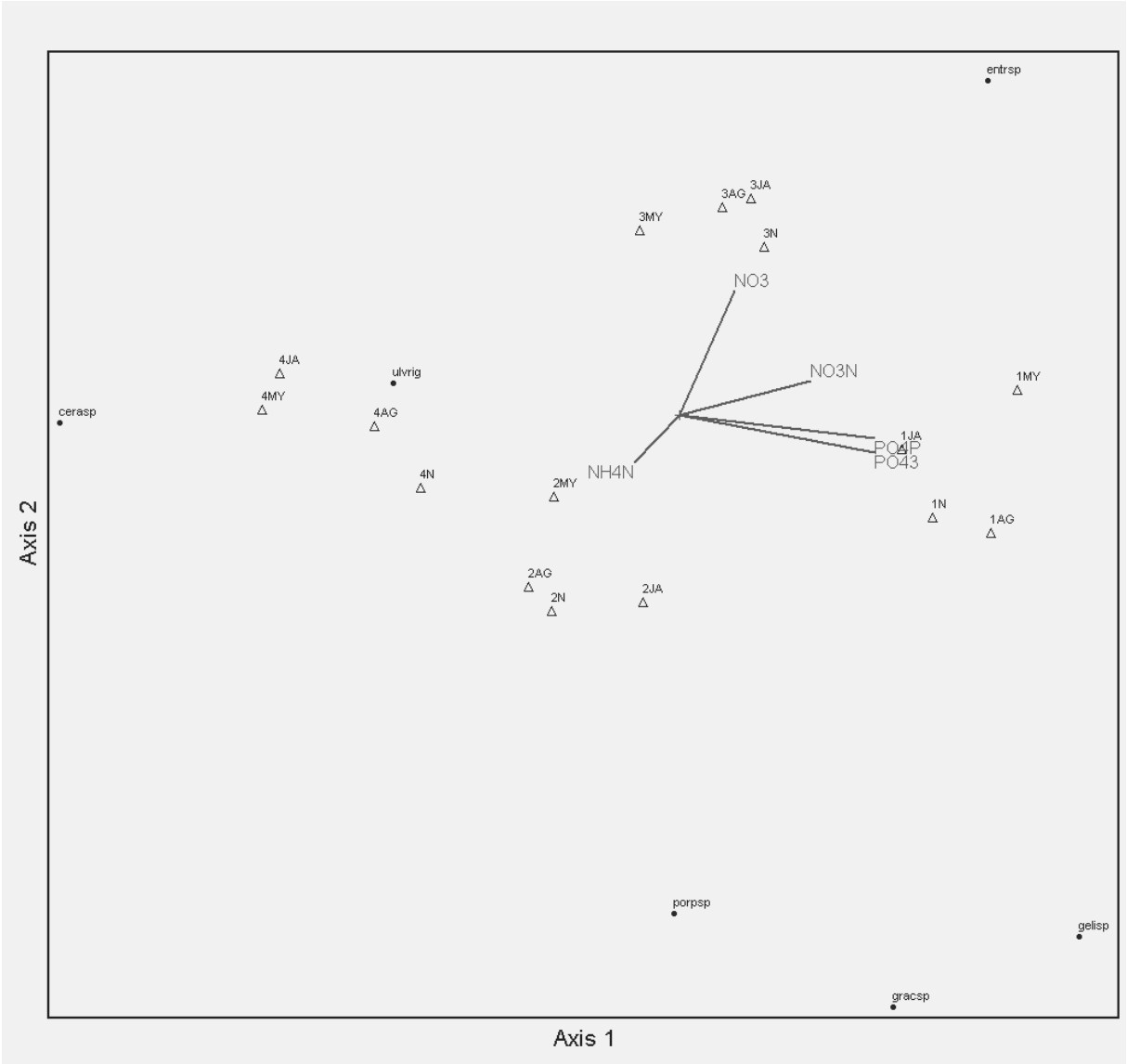

FIGURE 3
The relationships among chemical parameters and marine algae.

NO_3-N, NO_3^-, PO_4-P and PO_4^{-3} showed parallel variations because those chemical parameters are located on the right part of the graph. Ent.sp, Geli.sp and Grac.sp, are also found on the right hand side of the diagram. NH_4-N tends to be located on the left part of the graph and Cera.sp and ulvrig are also found on the left side of the graph. The distribution of the species indicates insignificant variation in terms of the seasons. It was determined that NO_3-N, NO_3^-, PO_4-P and PO_4^{-3} parameters were effective in the distribution of Ent.sp, Geli.sp and Grac.sp in the 1st and 3rd stations, and NH_4-N parameter was effective in the distribution of Cera.sp and ulvrig in the 2nd station. However, the stations play an important role in the locations of the species in the graph which is given in figure 3.

DISCUSSION

Aquatic systems are one of the most important life sources of the ecosystem with their physical, chemical and biological structures. In this study, the relationship between the macro algae in İzmit Bay (*Ulva rigida* C. Ag., *Enteromorpha* sp., *Gracilaria* sp., *Porphyra* sp., *Gelidium* sp. and *Ceramium* sp.) and the environmental parameters were evaluated using Canonical Correspondence Analysis (CCA). In the 4 stations selected in İzmit Bay, water temperature was measured as 16.46±6.11 ºC (maximum 24 ºC, minimum 10 ºC), pH as 7.5± 0.37 (8.1- 7.1), dissolved oxygen as 9.51± 1.43 mg/L (12.7- 7.2), electrical conductivity as 38.18±2.64 µS/cm (41.8 - 30.2), suspended solids as 16.60 mg/L (33.5 – 0.8), PO_4^{-3} as 0.36±0.17 mg/L (1.3 – 0.11), PO_4-P as

TABLE 8
Monte Carlo test results: Marine algae – chemical parameter correlations.

Randomized data					
Real data		Monte Carlo test 99 runs			
Axis	Spp-Envt Corr.	Mean	Minimum	Maximum	p
1	0.982	0.865	0.675	0.978	0.0101
2	0.968	0.893	0.669	0.985	
3	0.903	0.802	0.530	0.979	

p = the proportion of randomized runs with species-environment with correlation greater than or equal to the observed species-environment correlation; that is, p = (1 + no. permutations ≥ observed)/(1 + no. permutations) p is not reported for axes 2 and 3 because, using a simple randomization test for these axes may result to a biased p values.

0.19±0.01 mg/L (0.45-0.11), NO_3^- as 8.16±1.20 mg/L (10.2 - 6.4), NO_3-N as 1.77± 0.05 mg/L (2.1-1.3) and NH_4-N as 0.18±0.02 mg/L (0.5 -0.06). The temperature, the oxygen values and the other physico-chemical parameters of aquatic systems vary depending on the location of the stations, seasons, the polluting factors around them, the amount of the substances in them and wave motions. The values determined in the study show similar results with the previous studies carried out in İzmit Bay [11,12,19].

There were many environmental factors affecting the growth and distribution of marine algae. However, the main impacting factors varied between station areas. According to figure 3, NO_3-N, NO_3^-, PO_4-P and $PO4^{-3}$ showed parallel variations because, those chemical parameters are located on the right of the graph. Ent.sp, Geli.sp and Grac.sp, are also found on the right hand side of the diagram. NH_4-N tends to be located on the left part of the graph, and Cera.sp and ulvrig are found on the left side of the graph. In the study, the values of Nitrate Nitrogen (NO_3-N), Nitrate (NO_3^-), Orthophosphate (PO_4-P) and Phospate (PO_4^{-3}), which are effective in the development of the algae, were determined to be significant in the distribution of the species *Enteromorpha* sp., *Gelidium* sp. and *Gracilaria* sp. It was determined also, that these factors were not very effective in the distribution of the species *Ceramium* sp. and *Ulva rigida,* and were not determinative in the distribution of *Porphyra* sp. as it is a specie that is sensitive to seasonal conditions. The chemical parameters were determined to be effective in the first, second and the third stations. It is considered that the parameters NO_3-N, NO_3^-, PO_4-P and $PO4^{-3}$ determined the distribution of *Enteromorpha* sp., *Gelidium* sp. and *Gracilaria* sp. at stations 1 and 3, whereas, the NH_4-N is effective in the distribution of *Ceramium* sp. and *Ulva rigida* in station 2. Phosphorus may be related to the use of detergents and the discharge of phosphate through the sewage system, particularly in the stations. The composition of macro algal communities, has also been found to reflect changes in environmental conditions.

Heavy metal concentrations were found as Al (<0,001 - 3.79 ppm), Fe (<0,001 - 0.44 ppm), Cd (0.002 - 0.004 ppm), Zn (0.05 - 1.70 ppm), As (<0,001 - 0.03 ppm), Cr (<0,001 - 0.13 ppm), Mn (< 0,001 - 0.18 ppm) in the sea water of İzmit Bay. Due to its complex in marine ecosystems, environmental factors were important in the distribution of marine algae. According to CCA analysis, *Enteromorpha* sp., *Gelidium* sp. and *Gracilaria* sp. were determined to have a positive correlation with the values of Zn, Cd, Mn and As, whereas, *Ulva rigida* and *Ceramium* sp. had a negative correlation. *Entromorpha* sp. and *Gelidium* sp. exhibits remarkable tolerances to a range of most of the environmental factors. However, *Ulva rigida* and *Ceramium* sp. shows a more sensitive distribution of the heavy metals such as; Mn, As, Zn, Cd. In figure 2, Al, Cd, Mn, Zn and As showed parallel variations because, those heavy metals are located on the right part of the graph and *Enteromorpha sp., Gelidium sp*. and *Gracilaria sp.* are also found on the right hand side of the diagram. These species were determined to be more tolerant of the values of Al, Cd, Mn, Zn and As. Fe and Cr tend to be located in the left part of the graph and the species that is, *Ceramium* sp. and *U. rigida* are found on the left side of the graph. The values of Fe and Cr are not thought to be an active factor for *Ceramium* sp. distribution in various environmental conditions and in the distribution of *Ulva rigida*, which is a heavy metal bio-indicator. However, *Porphyra sp.*, which is a sensitive species to environmental factors, being found insignificant in the upper part of the graph, may be due to its low

ecological tolerance. When evaluated in terms of the stations, it was determined that Al, Cd, Mn, Zn and As values at station 1, and Fe and Cr values at Station 2, were higher, compared to the other stations. That is because of the density of the residential areas and heavy industrial plants within the vicinity of Station 1 and Station 2, and its also, a transit area mostly used for maritime transportation. The distribution of the species indicates insignificant variation in terms of the seasons. However, the stations play an important role to decide the locations of the species in the graph. At the same time, physical and chemical characteristics of the seawater are determined largely by the climatic, geomorphological and geochemical conditions prevailing in the drainage basin, and the underlying aquifer. The chemical quality of the aquatic environment varies according to local geology, the climate and the amount of soil cover, and so on[20]. These metals come from the effects of ships gasoline combustion, cathodic protection of the ship's body, metal coating and metal smelter industries (especially Dil Creek), Zn is derived from the domestic and industrial sewage. Fly ash constitutes a major pollutant of the coal burning process and is known to contribute notable quantities of Cd and Zn into the environment [21]. Elevated Cr, and Zn values indicate some anthropogenic pollution by the Dil Creek in the station 1 and station 2. On the other hand, Cd is bound to the ferro- manganese oxides and/or organic matter fraction, suggesting anthropogenic sources [22]. Cr and Zn pigments and their compounds are used in metal plating and probably contributing some quantities of these metals into the coast region. Cd and Zn originate primarily from anthropogenic sources, whereas, the major part of the Al seems to come from natural sources. On the other hand, results showed that *Enteromorpha* sp., *Gelidium* sp. and *Gracilaria* sp. are tolerant to Al, Cd, Mn, Zn and As, while, *Ceramium* sp. and *Ulva rigida* are more tolerant to Fe and Cr. The distribution of the species indicates insignificant variation in terms of seasons. However, the stations play an important role in deciding the locations of the species on the graph. This situation is thought to be as a result of the proximity of the research stations to residential areas, the domestic and industrial pollutants carried by the streams flowing into the sea, marine transportation and fishery activities. In this study, which was carried out seasonally, it was determined that the seasons are not a determinant of the species except *Porphyra* sp. On the other hand, the locations of the stations and their structural properties were determined to be the most effective in the distribution of the other algae species. The difference in the distribution of metals and algae was attributed to the differences in inflow of effluents from industries, anthropogenic wastes, ship unloading and welding activities, which are the probable source of heavy metals in this region.

In conclusion, long-term monitoring studies in the Izmit Bay are necessary for better understanding of the heavy metal and chemical parameters as well as macro algae distributions.

ACKNOWLEDGEMENTS

We would like to thank Dr. Kürşad Özkan and his research team, Dr. Serkan Gülsoy, Dr. Halil Süel, and Dr. M. Güvenç Negiz from the Faculty of Forestry in Süleyman Demirel University, for the full support provided.

REFERENCES

[1] Roberts D.A., Poore, A.G.B., Johnston E.,L. (2006). Ecological consequences of copper contamination in macroalgae: effects on epifauna and associated herbivores. Environmental Toxicology and Chemistry 25 (9), 2470–2479.

[2] Topcuoğlu S., Kılıcı Ö., Belivermiş M., Ergül H.A., Kalaycı G. (2010) Use of marine algae as biological indicator of heavy metal pollution in Turkish marine environment, J.Black Sea/Mediterranean Environment, 16(1):43-52

[3] Nasrabadi, T. (2015) An index approach to metallic pollution in river waters. Int. J. Environ. Res. 9 (1), 385-394.

[4] Santos,W., R., Schmidt, E., C., Felix, M., R., L., Polo, L., K, Kreusch, M., Pereira, D., T.,Costa, G., B., Simioni, C., Chow,F., Ramlov, F., Maraschin, M. and Bouzon, Z. (2014) Bioabsorption of cadmium, copper and lead by the red macroalga *Gelidium floridanum*: Physiological responses and ultrastructure features. Ecotoxicology and Environmental Safety 105, 80–89.

[5] Algan, O., Çağatay, N., Sarıkaya, H.Z., Balkıs, N. and Sarı, E. (1999). Pollution monitoring using marine sediments: A case study on the Istanbul metropolitan area. Tr. J. Eng. Sci. 23: 39-48.

[6] Algan, O., Balkıs, N., Çağatay, N., and Sarı, E. (2004). The sources of metal contents in the shelf sediments from the Marmara Sea, Turkey. Environmental Geology 46: 932-950.

[7] Balkıs, N. and Çağatay, M.N. (2001). Factors controlling metal distribution in the surface sediments of the Erdek Bay, Sea of Marmara. Environ. Int. 27: 1-13.

[8] Bodur, M.N. and Ergin, M. (1994). Geochemical characteristics of the recent sediments from the Sea of Marmara. Chemical Geology 115: 73-101.

[9] Kut, D., Topcuoğlu, S., Esen, N., Küçükcezzar, R. and Güven, K.C. (2000). Trace metals in marine algae and sediment samples from the Bosphorus. Water, Air, Soil Pollut. 118: 27-33.
[10] Güven, K.C., Okuş, E., Topcuoğlu, S., Esen, N., Küçükcezzar, R., Seddigh, E. and Kut, D. (1998). Heavy metal accumulation in algae and sediments of the Black Sea coast of Turkey. Toxicol. Environ. Chem. 67: 435-440.
[11] Morkoç, E. , Okay, O.S., Edinçliler, A. (2008). Land-based sources of pollutants along the Izmit Bay and their effect on the coastal waters. Environmental Geology 56(1), pp 131-138.
[12] Morkoç E., Tuğrul S., Okay, O. S., Legoviç, T. (1994).Eutrophication, limiting nutrient and hydrochemical characteristics of the polluted Bay of İzmit, result of four-years data. International Specialized Conference on Marine Disposal Systems., Nov.,335-344
[13] Solorzano, L., M. J. McGreery (1969) Determination of ammonium inneutral waters by the phenylhypochlorite method. Journal of Limnology and Oceanography, 14: 799-801,
[14] Snel, F.D., C.T. Snel (1957) Colorimetric methods of analysis, Vol II 3rd D. Van Nostrand Company Inc., New Jersey, Toronto, NewYork, London
[15] Mohr, F. R.(1856) Die Bestimmung der Halogenidionen in neutralen Lösungen löslicher Halogenide. In: G. Jander, H. J. Jahr,, H.Knoll (Eds.), Ma analyse, Ed. 221/221a 1969: 224-226. Berlin,.
[16] Krebs, C. J(1989). Ecological methodology, Harper and Raw Publishers, N.Y., 654
[17] Kazancı,N.,Dügel, M(2000). An Evaluation of the Water Quality of Yuvarlakçay Stream,in the Köycegiz-Dalyan Protected Area, SW Turkey, Turk J Zool 24 (2000) 69–80
[18] Ter Braak, C.J.F. and Prentice, I.C. (1988). A theory of gradient analysis. Adv. Ecol. Res., 18: 271-317. DOI: 10.1016/S0065-2504(08)60183-X
[19] Aktan, Y., Aykulu,G.(2005). Colonisation of Epipelic Diatoms on the Littoral Sediments of Izmit Bay: Turk J Bot .,29 83-94
[20] Chapman, D., Water quality assessments - a guide to use of biota,sediments and water in environmental monitoring, published by e&fn spon, an imprint of chapman & hall, © 1992, 1996 unesco/who/unep, printed in great britain at the university press,Cambridge ISBN 0 419 21590 5 (hb) 0 419 21600 6 (pb)
[21] Yasar,D.,Aksu,A.E.,Uslu,O.(2001). Anthropogenic Pollution in ˙Izmit Bay: Heavy Metal Concentrations in Surface Sediments, Turk J Engin Environ Sci 25, 299 – 313.
[22] Aksu, A.,E., Yasar,D., Uslu,O.(1997). Assessment of Marine Pollution in ˙Izmir Bay: Heavy Metal and Organic Compound Concentrations in Surficial Sediments,Tübitak,387-415

Received: **04.11.2015**
Accepted: **28.02.2016**

CORRESPONDING AUTHOR

Arzu Morkoyunlu Yuce
Kocaeli University, Hereke O. I. Uzunyol Vocational Schools,
41000 Kocaeli, Turkey

E-mail: arzu.yuce@kocaeli.edu.tr

© by PSP Volume 25 – No. 7/2016, pages 2594-2604 Fresenius Environmental Bulletin

EFFECTS OF TWO HYDROPONIC PLANTS AND HERBIVOROUS SNAILS ON NUTRIENT VARIATIONS COUPLED WITH ALKALINE PHOSPHATASE ACTIVITIES IN EUTROPHIC WATER

Liangjie Zhang[a], Xin Cao[a], Xingzhang Luo[a], Zheng Zheng[a,*]

[a] Department of Environmental Science and Engineering, Fudan University, 220 Handan Road, Shanghai 200433, P.R. China

ABSTRACT

The impacts of two hydroponic plants (*Cyperus alternifolius* and *Canna generalis*) and the apple snail (*Pomacea canaliculata*) on nutrient change behaviors and kinetics of alkaline phosphatase in eutrophic water were studied in this paper. A mesocosm experiment contained six different treatment systems was conducted from October to November 2014. The total removal rates of *C. alternifolius* and *C. generalis* for total nitrogen (TN), total phosphorous (TP) and chlorophyll a (Chl-a) contents were 74.9%, 79.8%, 85.9% and 70.9%, 79.2%, 83.0%, respectively, and the function of organic P hydrolysis decreased as well, in terms of the lower velocity of reaction (lower V_{max}) in overlying water combined with lower affinity for substrate (higher Km values) in interstitial water and surface sediment. On the contrary, the snails exhibited an activation on alkaline phosphatase in water body (higher V_{max} and lower K_m values), interstitial water (higher V_{max}) and sediment (higher V_{max}), despite the high P concentrations in these mesocosms. No obvious correlation was found between orthophosphate (PO_4^{3-}-P) and alkaline phosphatase activity (APA) in our study, indicated that the "induction-repression" mechanism did not work in hypereutrophic water. Additionally, a remarkable feature is that snails coupled with plants would aggravate eutrophication in water column, due to the grazing of snails on plants as their food source. Our study highlighted to investigate the enzymology mechanism of macrophyte-snail-phytoplankton systems and to give some implications on the restoration of eutrophied water by using floating-bed systems.

KEYWORDS:
Hydroponic plant; Snail; Nutrient; Alkaline phosphatase activity; Eutrophic water

INTRODUCTION

Aquatic plants have been widely used for the treatment of wastewater and restoration of eutrophic water bodies, which are considered to have merits of low cost and aesthetic value [1-3]. Much attention has been paid to the effects of nutrient removal by plants, in relation to constructed wetland systems [4-6]. In those systems, plants are recognized as an indispensable part to regulate biological structures due to their essential chemical and physical properties. Through plant growth, nutrients can be assimilated continuously and eventually removed from water bodies by harvest. Moreover, the plants could provide a sizable surface area for attached microorganisms to thrive, and reduce flow intensity which would encourage particle settling and entrapment of suspended matters [1,5]. However, in terms of in site purification of hypereutrophic water, planted floating-bed technology is more flexible than traditional macrophyte-based constructed wetlands, not only because of occupying no land area, but because the improvement of nutrient uptake rate with rooting in water column directly [7-10].

The utilization of the floating-bed has been also found to be susceptible to ambient environmental factors. The growth of aquatic plants can be suppressed by some freshwater snail species which can graze extensively on macrophyte tissues according to some researches [11,12]. Nevertheless, the relationship existed between herbivorous snails and macrophytes seems to be complicated. Li et al. [13] found that the relationship may be a mutualistic one at low grazing pressure, whereas at high grazing pressure the plant biomass would decline result from overgrazing. But anyway, snails could have important influence on aquatic ecosystem by their metabolism.

Previous studies have mainly focused on either the interactions between snails and aquatic plants or the efficiency of nutrients removal by

macrophytes in waterbody. Few investigations have been carried out to explore the macrophyte-snail-phytoplankon systems from the perspective of enzymology mechanism.

Microbial enzymatic activities are believed to play a key role in the degradation of organic matter in the nutrient cycles of freshwater ecosystems, among which extracellular phosphatases are mostly studied [14]. When soluble inorganic phosphorus is scarce in water column, phytoplankton can produce extracellular phosphatase to hydrolyze organic phosphorus into orthophosphate for the compensation of phosphorus deficiency [15-17]. Thus it is not enough to focus on the nutrient variations without investigating the effects of snails and macrophytes on alkaline phosphatase activity (APA) in aquatic ecosystems. In order to achieve this objective, we conducted a mesocosm experiment of the response of two hydroponic plants and herbivorous snails on nutrient change behaviors coupled with the kinetics of alkaline phosphatase in eutrophic water.

MATERIALS AND METHODS

Material preparation. *C.alternifolius* and *C.generalis* were two of the most common plant species that used in constructed wetland and floating bed systems in many parts of China [5,18]. *C.alternifolius* and *C.generalis* were selected for uniformity in growth state (average root length = 30 ± 1cm) from planted floating-bed in Lake Dianchi (24°40'-25°03'N,102°37'-102°48'E), a typical eutrophic lake located in Southwest China [19], then cleaned with a soft brush and washed with deionized water to get rid of periphyton and acclimated in tap water for four days. When the experiment started, the plants were transplanted into polyethylene foam plates with small holes, through which the roots could completely immerse into water of the mesocosms.

P. canaliculata, as an invasive species, was found to be widely distributed around South China, including Lake Dianchi watershed in Yunnan Province [20]. And Since 1980s, Lake Dianchi has attracted the attention of the whole world for its severe cyanobacterial blooms, the chlorophyll concentration remains at a high level in water column during the bloom [21]. After a long period of eutrophication, macrobenthos can hardly exist except apple snails due to their strong adaptability and competitiveness for food resources [22]. *P.canaliculata* was collected from Lake Dianchi, then rinsed with deionized water and kept without food for one day before being placed into the mesocosms.

Mesocosm structure and experimental design. The mesocosm experiment was performed outdoors by using circular polyethylene plastic tanks (top diameter=45 cm, bottom diameter=30 cm, height=45 cm), consisting of sediments and water column. The sediments were sampled from the north of Lake Dianchi (Fig.1), before being introduced into each tank, the sediments needed to be sieved (mesh size = 1mm) to wipe out macrofauna and then kept at -20℃ for one week to ensure that no animals would be alive [23]. A 10-cm thick layer of homogenized sediments were added to these tanks and the upper part of tanks was subsequently filled with eutrophic lake water carefully that getting from the same sampling site of sediments. All the mesocosms were under a shed of glass roof to receive natural sunlight as well as to avoid the dilution by rainfalls. After equilibration for two weeks, nutrient and Chl-a concentrations in these tanks were:
TN=6.89±0.15mgL^{-1},TP=0.226±0.010mgL^{-1},PO_4^{3-}-P=0.011±0.008mgL^{-1},Chl-a concentration =24.32±0.28ug L^{-1}.

Then the six treatments were set as follows:
1. No plants and snails added (as control systems), hereafter CON;
2. *C. alternifolius* (wet weight=550±10g, per tank) added, hereafter CA;
3. *C. generalis* (wet weight=840±10g, per tank) added, hereafter CG;
4. *P. canaliculata* (wet weight=106.2±0.6g, per tank) added, hereafter PC;
5. *C. alternifolius* (wet weight=550±10g, per tank) + *P. canaliculata* (wet weight=105.5±0.6 g,per tank)added, hereafter AP;
6. *C. generalis* (wet weight=840±10g, per tank) + *P. canaliculata* (wet weight=105.9±1.3 g, per tank) added, hereafter GP.

All treatments were carried out in triplicate. During the period of experiment, dead snails were cleaned out and replaced by living ones with similar size immediately.

Sampling and analysis. Sampling continued approximately six weeks from 1 October to 16 November 2014. Water and surface sediment samples were taken from each tank every week at 8:00-9:00a.m. 100 ml of water was collected at 15cm depth with a siphon pipe for the analysis of water quality parameters and alkaline phosphatase activity (APA). And in order to maintain the water level, appropriate amount of deionized water was added to each tank after sampling every week.

Total nitrogen (TN), total phosphorous (TP) and orthophosphate (PO_4^{3-}-P) were detected with an automatic continuous flow analyzer (San^{++}, Skalar, Netherlands). Chl-a was determined spectrophotometrically after extraction with ethanol

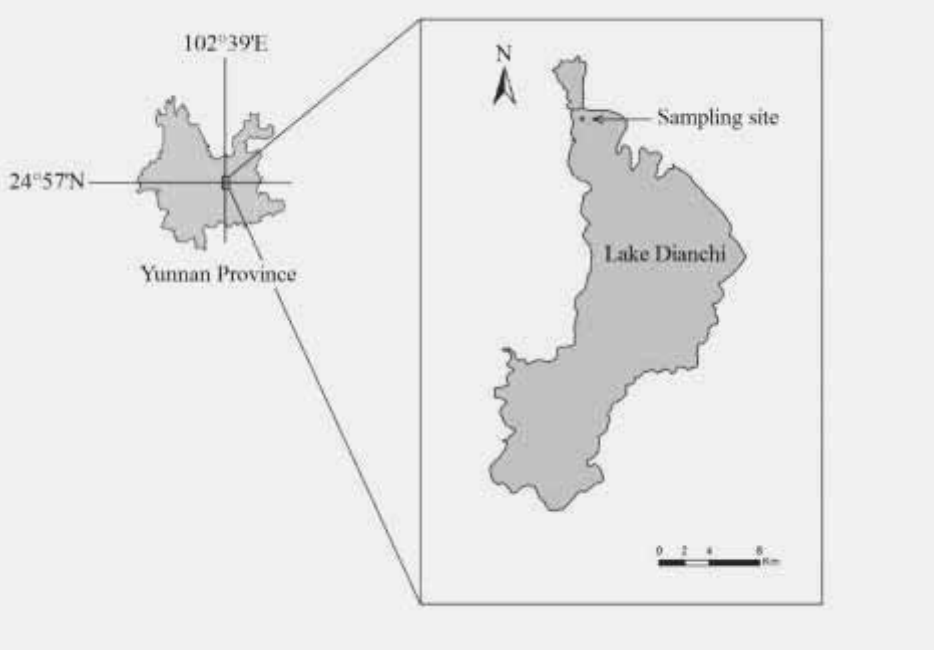

FIGURE 1
Map of sampling site in Lake Dianchi.

which described by Jespersen et al. [24].

APA assays used a modification of the method described by Sayler et al. [25]. The actual procedures were as follows: Sediment samples were slurried by Tris buffer (pH=8.6), then eight concentrations of p-nitro-phenylphosphate (pNPP) substrate were added, which ranged between 0.01 and 3.0mmol l^{-1}. The samples were incubated at 37℃ for 1 h, 1.6 ml of slurry was centrifuged at 3000rpm and 1 ml of the supernatant was mixed with 4 ml of 0.1 M NaOH to stop the reaction. Absorption was measured at 410 nm. pNPP was added to reagent blanks after the reaction had been stopped. APA was converted to absolute units using a standard curve of p-nitrophenol (pNP). Computer programme 'GraphPad Priam 5' was used for the calculation of the kinetics parameters (V_{max} and K_m values) and the values were estimated by fitting Michaelis-Menten equations. All samples were run in triplicate.

APA in unfiltered overlying water and interstitial water (obtained by centrifugation at 3000 rpm for 30 min from the sediment samples) was also determined with a procedure modified from the method described by Berman et al. [26].

Statistical analysis was performed using SPSS 16.0 for windows and the diagrams were drawn by using Origin 8.0.

RESULTS

Effects of different treatments on water column. Variation of nutrient concentrations in overlying water. Fig.2a showed the variations of TN concentrations in the overlying water of different treatment systems. TN concentrations of all systems tended to decrease significantly over time (RM-ANOVAs, time effect, $p<0.05$), from an average initial concentration of 6.89mg L^{-1} to less than 3.0mg L^{-1} by the end of the trial. The total removal rate of TN in a decreasing order is CA, CG, PC, AP, CON and GP (Table 1). In comparison with the CON system, all treatment systems had better performances on the removal of TN except GP system. Among these systems, CA was the best system to removal TN, with total removal rate of 74.9% and it was significantly different from other treatments (RM-ANOVAs, treatment effect, $p<0.05$). TN decreased sharply during the first 4 weeks and then reached a steady state with a final TN concentration less than 1.8 mg L^{-1} in CA system.

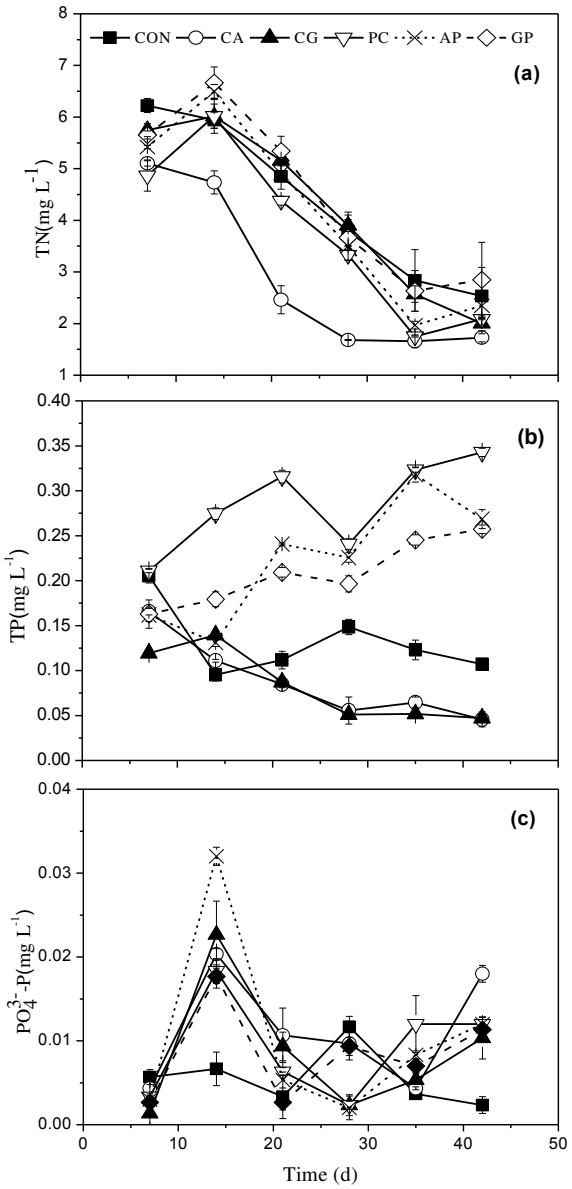

FIGURE 2
Variations of TN(a), TP(b) and PO_4^{3-}-P(c) concentrations in water columns of different treatment systems.

Unlike TN, TP concentrations presented various trends (Fig.2b). TP concentrations of these treatment systems (PC, AP and GP) which added with snails. took on a fluctuant increasing process and were higher than CON system (except the first week). The removal rates of TP concentration in AP, GP and CON systems were 79.8%, 79.2% and 52.7%, respectively (Table 1). Compared with other treatment systems, PC had the largest increase of TP concentration from 0.226 mg L^{-1} to 0.343 mg L^{-1}. However, in CA and CG systems, TP concentration showed a consistent decrease over time and there was no significant difference between them (RM-ANOVAs, treatment effect, $p>0.05$).

PO_4^{3-}-P concentrations in all systems only accounted for few portion of TP throughout the experiment, for example, the proportion of initial

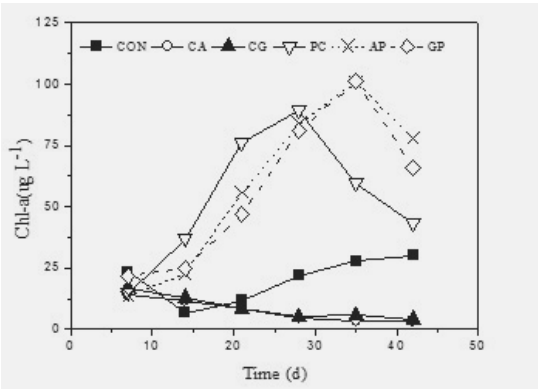

FIGURE 3
Variation of chlorophyll a contents in water columns of different treatment systems

TABLE 1
Nutrient removal rates or variation ranges of different treatment systems.

	CON	CA	CG	PC	AP	GP
TN	63.2%	74.9%	70.9%	69.7%	66.0%	58.7%
TP	52.7%	79.8%	79.2%	-51.7%[a]	-18.8%[a]	-13.8%[a]
PO_4^{3-}-P[b]	0.002~0.012	0.004~0.018	0.000~0.023	0.002~0.018	0.002~0.053	0.003~0.063

[a] the minus indicates an increase of TP concentration,
[b] the unit is mg L^{-1}

PO_4^{3-}-P concentrations of all mesocosms were less than 5% (4.87%) of TP concentrations (Fig.2c). PO_4^{3-}-P concentrations were fluctuating with time in all systems, AP and CA systems were significant different with CON system （ RM-ANOVAs, treatment effect, $p<0.05$）, while other treatment systems had no significant difference with CON system（$p>0.05$）

Variation of Chl-a contents in overlying water. Fig.3 showed the time course of Chl-a concentrations in all systems, Chl-a concentrations were lower in the two plant treatments systems (CA and CG) than in CON system, while in the three snail treatment systems (PC, AP and GP) were higher. The removal rates of Chl-a concentrations in CA and CG systems were 85.9% and 83.0%. Chl-a concentration in PC system was rapidly increasing during the first four weeks and subsequently declined. By contrast, the similar decrease appeared after the fifth week in AP and GP systems.

Effects of different treatments on kinetics of alkaline phosphatase in the mesocosms. Variation of V_{max} and K_m values of alkaline phosphatase in overlying water. Fig.4 reflected the changes of kinetic parameters (V_{max} and K_m) of APA in overlying water, V_{max} values in CA and CG systems were always significantly lower than other treatment systems with a range from 24.77 to 73.10nmol $L^{-1}min^{-1}$. V_{max} values in PC system was gradually increased at the first four weeks and then began to decrease, while a similar pattern was observed in AP and GP systems, the V_{max} values increased at the first five weeks and subsequently declined, which lagged behind PC system. The K_m values in CON system remained fluctuant and were significant higher than in PC system ($p<0.05$), the other treatment systems were lower than CON system except the first week.

Variation of V_{max} and K_m values of alkaline phosphatase in interstitial water. The V_{max} values were less than 75noml $L^{-1}min^{-1}$ in interstitial water after the first week, the PC system had the highest V_{max} values among all the treatment systems. CA and GP' V_{max} values were always higher than CG and AP, respectively. On the contrary, CA' K_m values were lower than CG (except the fourth week) and GP' K_m values were lower than AP (after the second week).

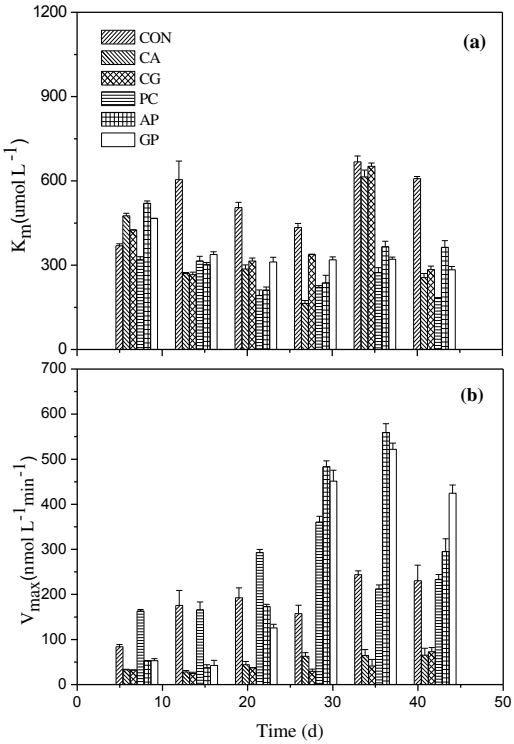

FIGURE 4
Variation in Km (a) and Vmax (b) values of total alkaline phosphatase in different systems in overlying water during study period.

Variation of V_{max} and K_m values of alkaline phosphatase in surface sediments. All treatment systems had little effect on the V_{max} values in surface sediments which fluctuated within a narrow range from 3.356 to 9.837umol $g^{-1}h^{-1}$, the V_{max} values were significant higher in the plant treatment systems (CA and CG) than in CON system, and similarly in the snail added systems (PC, AP and GP) which were higher than in CON system (apart from the first week). In terms of K_m values, CA and CG systems were always higher than surface

sediments of CON system, GP system was higher than AP system in general.

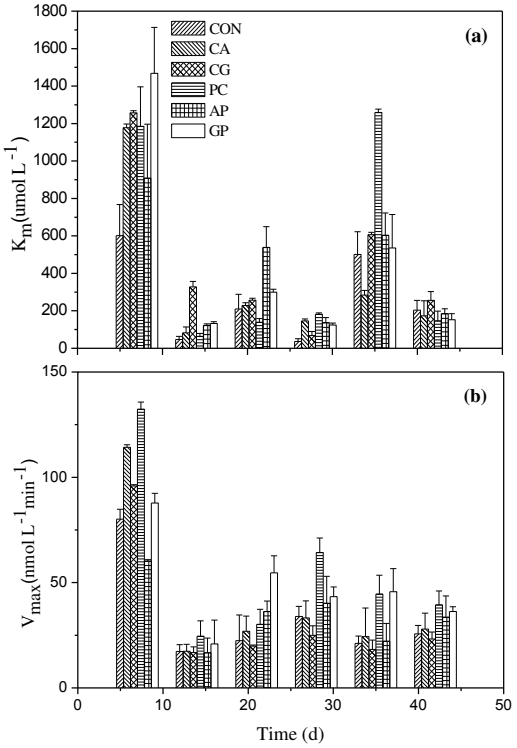

FIGURE 5
Variation in Km (a) and Vmax (b) values of total alkaline phosphatase in different systems in interstitial water during study period.

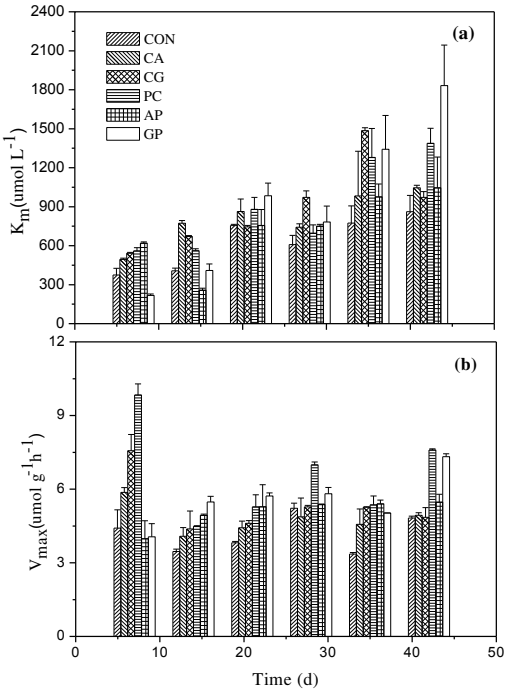

FIGURE 6
Variation in Km (a) and Vmax (b) values of total alkaline phosphatase in different systems in surface sediments during study period.

DISCUSSION

It was observed that *C. alternifolius* and *C. generalis* both had good removal effects of TN, TP and Chl-a during the simulated experiment, while the former plant was slightly better. This result was in accordance with previous study made by Bu et al. [27], who found that using floating beds vegetated with *Canna indica* have better removal performance of COD, TN, TP and Chla than that with *C. alternifolius*, and more than 60% TN and TP were considered to be removed by sedimentation in the floating bed systems. Besides, many macrophytes species such as *M. verticillatum* [28] and *C. globularis var. globularis* [29] were reported to affect algae growth through allelopathic effects. Zhao et al.[30] confirmed that the growth of *C. pyrenoidosa* and *M. aeruginosa* could be strongly depressed by the culture solution of *H. sibthorpioides*, and culture solutions of macropytes were superior to their extract solutions for the control of algal blooms in eutrophic water. The lower level of Chl-a concentrations in CA and CG systems (Fig. 3) suggested that *C. alternifolius* and *C. generalis* might have certain allelopathic effect on algae growth.

Moreover, the obvious lower V_{max} values of APA in overlying water of these two systems could also be partly explained by the inhibition of algal growth, algae were demonstrated as the major producers of alkaline phosphatase in surface water of Łuknajno Lake (Poland) during the phytoplankton blooms, while APA in bacterial size fraction only accounted 9.6% of the total activity [31]. Thus, the rate of enzymatic release of inorganic phosphate decreased with the decreasing of algae biomass, however, the two macrophytes seemed to elevate the substrate affinity of phosphatase in their overlying water (the lower Km values than the control systems), this might differ from the results obtained by Zhou et al. [32] who investigated the impacts of two kinds of submerged macrophytes on phosphatase activity in Lake Donghu, a shallow freshwater lake in China. The APA in filtered and unfiltered water, which sampled from the macrophyte covered zone, were both inactivated with a expression of lower Vmax and higher Km values. One possible explanation is that the DOP in natural waters mainly consisted of a high molecular weight fraction which was against to hydrolysis by alkaline phosphatase [33]. Whereas the organic phosphorus compounds in phytoplankton was more likely to hydrolysed. After decomposition of dead algal cells which could be attributed to plant inhibition in our study, easy-hydrolysable DOP would be released into water bodies, as a result, improved the enzymatic affinity to the substrate [34].On the other hand,

unlike the dynamic real lake investigations, our experiments were conducted under a relative static state, this might also have some effect on the final conclusion.

As to the overlying water, the V_{max} values of CA and CG systems varied over time in interstitial water, and the Km values were higher than the control systems, nevertheless, the V_{max} and Km values in surface sediments were both higher than the control systems. Since the growth of plant roots could smooth water fluctuation and reduce the total suspended substance (TSS) effectively [35], Zhao et al. [36] found that 41% and 54% of TSS can be removed from water column, monitored in integrated floating island systems on June 16 and October 18, respectively.

The particulates, especially organic particulates and decaying algae would accumulate on surface sediment by sedimentation, and the growth of bacteria could be stimulated by decomposition of the organic compounds. Meanwhile, bacteria was regarded as the main producer of alkaline phosphatase in the benthic layer [37]. So the V_{max} values were observed higher in surface sediment of CA and CG systems in our study, the result could also be supported by the observation in Kiel Bight, where an response in enzymatic activity was suddenly emerged through the input of organic matter into the sediments [38]. And in the presence of macrophytes (CA and CG systems), the alkaline phosphatase seemed to be more difficult to utilize the substrate in sediment as well as in interstitial water, in terms of higher Km values. It probably associated with the high molecular-weight humic compounds generated by macrophyte debris, APA could be inactivated by means of humic-enzyme complexation, abiotic mechanism related to iron and humic materials demonstrated to be involved with phosphorus availability under certain conditions [39]. In general, the lower velocity of reaction (lower V_{max} values) in overlying water combined with lower affinity for substrate (higher Km values) in interstitial water and sediment of CA and CG systems, indicated that APA in eutrophic water could be effectively suppressed by *C. alternifolius* and *C. generalis*.

The results of snail treatment system in our experiment suggested that snails could remove TN to some extent, but would increase TP concentrations. Carlsson et al. [40] found that the invasion of *Pomacea* in tropical wetland ecosystems led to elevation of nutrients, however, nitrogen and phosphorous concentrations remained low and even showed a slight temporal decrease when *P. canaliculata* was used to examine the impact on wetland biodiversity and function [41]. Freshwater snails facilitated nutrient cycling and microbial growth through some manners, such as bioturbation and feeding on organic detritus [42,43], dissolved N and P would be excreted into surrounding water through the metabolism of snails. And despite the respiration of snails, the oxygen demand of mollusks was demonstrated less than that of bacteria in eutrophic aquatic systems [44]. Bacterial metabolism along with the respiration of snails consumed so much of the oxygen in water body that resulted in an anoxic state in sediment, causing sediment-bound phosphorus to release and inhibiting diffusion of soluble inorganic nitrogen [45], and the denitrification process was also be enhanced under an anoxic condition These might be regarded as the reasons why TN not increased as TP concentrations in the snail treatment system in our study. The macrophytes could promote aerobic degradation of organic matter and nitrification by transferring oxygen to rhizosphere [1]. Thus, the removal efficiency of TN and the increase range of TP concentration decreased when plants added (AP and GP system).

Chl-a, recognized as an important index of the primary productivity and phytoplankton community, was detected firstly increase and then descend in PC systems. This was not completely consistent with the study conducted by Fang et al. [41], who observed an increase of Chl-a concentration caused by grazing of *P. canaliculata* during an enclosure experiment. Snails and bivalves had the ability to ingest algae, submerged macrophytes and organic detritus via their food chain [46]. Snails seemed not prior to feed on phytoplankton under the condition of sufficient food in the early stage of PC systems, because of its mobility and buoyancy [47]. But snails strengthened their feeding ability on phytoplankton biomass when there was inadequate food in the later stage, led to a decline of Chl-a.

Significant phosphatase activities were recorded in overlying water of PC systems (Fig.4), the V_{max} values in PC systems were higher than in control systems and the Km values were lowest among all the treatment systems. This might because of the growth of microorganism was accelerated by metabolism and bioturbation of snails, taking into account the high phytoplankton biomass (high Chl-a), the APA associated with phytoplankton community seemed to dominate that of bacterial community [48], and the strong positive relationship (R^2=0.84) between Chl-a concentrations (Fig.3) and the V_{max} values of APA (Fig. 4b) in overlying water provided an evidence for the explanation. Similarly, the snails displayed a stronger ability to degrade organic P in interstitial water and sediment in terms of higher V_{max} values as well, although there was no obvious trend of change in Km values. Based on former research, the sediments were found to be the primary site for the hydrolysis of phosphomonoester compounds by

phosphatase, playing an important part in nutrient regeneration processes after the summer algal bloom [49]. The oxygen depletion resulted from respiration of snails followed by anaerobic bacteria proliferation, concomitantly, bacteria, attached to organic matter in sediment, enhanced their APA to release soluble reactive phosphorous into overlying water [50]. Generally speaking, snails would stimulate APA in water body, interstitial water and surface sediment.

A notable feature observed in Chl-a contents (Fig.3) and APA (Fig.4b) in water column was that there appeared a hysteretic effect of variation in AP and GP systems compared to PC system. A possible reason for this phenomenon was that the addition of macrophytes extended the scope of snail food source, so the durations of Chl-a and APA increase lasted longer than the sole snail treatment systems. *P. canaliculata* preferred submerged or floating freshwater macrophytes, and grazing by the snails evoked not only the loss of aquatic plants but an increase in phytoplankton biomass [40,51,52]. We did found the roots of *C. alternifolius* and *C. generalis* were grazed by snails at the end of our experiment, and the *C. generalis* suffered more serious grazing pressure from the snails (Fig.7), furthermore, the higher peak values of Chl-a and APA curves in later stage of AP and GP systems illustrated that the macrophytes lost their important role as inhibitions to algal bloom, when they were treated as food source of snails. More orthophosphate would be released into water column by hydrolysis of the activated phosphatase, and the phosphorous cycle would also be accelerated. Another feature to stress out was that there had no obvious relationship between PO_4^{3-}-P and APA in overlying water in our study, which indicated that the "induction-repression" mechanism was swamped when come to the eutrophic waters [14,17]. ELFA-positive dots or structures indicated that attached bacteria or heterotrophic microorganism played a major role in hydrolysis of organophosphoric compounds by releasing extracellular phosphatases into eutrophic lakes, in order to supplement as an organic carbon source, and this process led to high phosphatase activity [17]. It was indicated that phosphatase activity was not inhibited in eutrophic station.

A notable feature observed in Chl-a contents (Fig.3) and APA (Fig.4b) in water column was that there appeared a hysteretic effect of variation in AP and GP systems compared to PC system. A possible reason for this phenomenon was that the addition of macrophytes extended the scope of snail food source, so the durations of Chl-a and APA increase lasted longer than the sole snail treatment systems. *P. canaliculata* preferred submerged or floating freshwater macrophytes, and grazing by the snails evoked not only the loss of aquatic plants but an increase in phytoplankton biomass [40,51,52]. We did found the roots of *C. alternifolius* and *C. generalis* were grazed by snails at the end of our experiment, and the *C. generalis* suffered more serious grazing pressure from the snails (Fig.7), furthermore, the higher peak values of Chl-a and APA curves in later stage of AP and GP systems illustrated that the macrophytes lost their important role as inhibitions to algal bloom, when they were treated as food source of snails. More orthophosphate would be released into water column by hydrolysis of the activated phosphatase, and the phosphorous cycle would also be accelerated. Another feature to stress out was that there had no obvious relationship between PO_4^{3-}-P and APA in overlying water in our study, which indicated that the "induction-repression" mechanism was swamped when come to the eutrophic waters [14,17]. ELFA-positive dots or structures indicated that attached bacteria or heterotrophic microorganism played a major role in hydrolysis of organophosphoric compounds by releasing extracellular phosphatases into eutrophic lakes, in order to supplement as an organic carbon source, and this process led to high phosphatase activity [17]. It was indicated that phosphatase activity was not inhibited in eutrophic station.

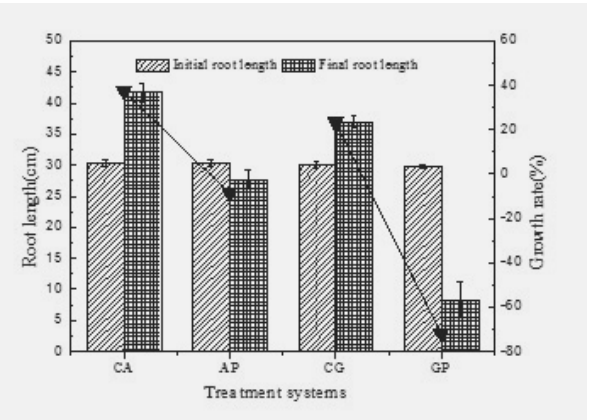

FIGURE 7
Initial and final root lengths of plants and the variation of root growth rate in different treatment systems.

Our study may provide some implications for the restoration of eutrophic water bodies, through our experiment, *C. alternifolius* and *C. generalis* are demonstrated effective on nutrient removal and APA inhabitation, they are appropriate choice for floating bed system construction. Nonetheless, floating bed system should be used with caution when apple snails or other herbivorous snails invade, since their potential grazing on macrophytes can increase the trophic state of water bodies by activating APA. Limited by the scale and

the high density of snails (1486 g m^{-2})used in this trial, further studies are needed to carry out under a larger scale with natural density of snails.

ACKNOWLEDGEMENTS

This work was supported by the grants from the Major Science and Technology Program for Water Pollution Control and Treatment (No. 2012ZX07102-004). We also appreciated the selfless help from the teachers and students in Fudan University.

REFERENCES

[1] Brix H.. (1994) Functions of Macrophytes in Constructed Wetlands. Waterence & Technology., 29, 71-78.

[2] Dai Y., Jia C., Liang W., Hu S. and Wu Z.. (2012) on restoration of a eutrophic waterbody and its optimal coverage. Ecological Engineering., 40, 113–116.

[3] Li J., Yang X., Wang Z., Shan Y. and Zheng Z.. (2014) Comparison of four aquatic plant treatment systems for nutrient removal from eutrophied water. Bioresource Technology., 179, 1–7.

[4] Zimmels Y., Kirzhner F. and Malkovskaja A.. (2008) Application and features of cascade aquatic plants system for sewage treatment. Ecological Engineering., 34, 147–161.

[5] Jiang F.Y., Chen X. and Luo A.C.. (2011) A comparative study on the growth and nitrogen and phosphorus uptake characteristics of 15 wetland species. Chemistry and Ecology., 27, 263-272.

[6] Cao W. and Zhang Y.. (2014) Removal of nitrogen (N) from hypereutrophic waters by ecological floating beds (EFBs) with various substrates. Ecological engineering., 62, 148-152.

[7] Mallison C.T., Stocker R.K. and Cichra C.E.. (2001) Physical and vegetative characteristics of floating islands. Journal of Aquatic Plant Management., 39, 107-111.

[8] Sun L., Liu Y. and Jin H.. (2009) Nitrogen removal from polluted river by enhanced floating bed grown canna. Ecological Engineering., 35, 135–140.

[9] Li X., Song H., Li W., Lu X. and Nishimura O.. (2010) An integrated ecological floating-bed employing plant, freshwater clam and biofilm carrier for purification of eutrophic water. Ecological engineering., 36, 382-390.

[10] Zhu L., Li Z. and Ketola T.. (2011) Biomass accumulations and nutrient uptake of plants cultivated on artificial floating beds in China's rural area. Ecological Engineering., 37, 1460–1466.

[11] Elger A. and Lemoine D.. (2005) Determinants of macrophyte palatability to the pond snail Lymnaea stagnalis. Freshwater Biology., 50, 86–95.

[12] Carlsson N.O.L. and Lacoursière J.O.. (2005) Herbivory on aquatic vascular plants by the introduced golden apple snail (Pomacea canaliculata) in Lao PDR. Biological Invasions., 7, 233-241.

[13] Li K.Y., Liu Z.W. and Gu B.H.. (2009) Density-dependent effects of snail grazing on the growth of a submerged macrophyte, Vallisneria spiralis. Ecological Complexity., 6, 438-442.

[14] Jansson M., Olsson H. and Pettersson K.. (1988) Phosphatases; origin, characteristics and function in lakes. Hydrobiologia., 170, 157-175.

[15] Nedoma J., García J.C., Comerma M., Šimek K. and Armengol J.. (2006) Extracellular phosphatases in a Mediterranean reservoir: seasonal, spatial and kinetic heterogeneity. Freshwater Biology., 51, 1264-1276.

[16] Zhang T., Wang X. and Jin X.. (2007) Variations of alkaline phosphatase activity and P fractions in sediments of a shallow Chinese eutrophic lake (Lake Taihu). Environmental Pollution., 150, 288–294.

[17] Cao X., Song C. and Zhou Y.. (2010) Limitations of using extracellular alkaline phosphatase activities as a general indicator for describing P deficiency of phytoplankton in Chinese shallow lakes. Journal of Applied Phycology., 22, 33-41.

[18] Zhang C.B., Liu W.L., Pan X.C., Guan M., Liu S.Y., Ge Y. and Chang J.. (2014) Comparison of effects of plant and biofilm bacterial community parameters on removal performances of pollutants in floating island systems. Ecological Engineering., 73, 58–63.

[19] Li H., Hou G., Dakui F., Xiao B., Song L. and Liu Y.. (2007) Prediction and elucidation of the population dynamics of Microcystis spp. in Lake Dianchi (China) by means of artificial neural networks. Ecological Informatics., 2, 184–192.

[20] Lv S., Zhang Y., Liu H. X., Hu L., Liu Q., Wei F. R., Guo Y. H., Steinmann P., Hu W., Zhou X. N.. (2013) Phylogenetic evidence for multiple and secondary introductions of invasive snails: Pomacea species in the People's Republic of China. Diversity and Distributions., 19, 147-156.

[21] Hou G., Song L., Liu J., Xiao B. and Liu Y.. (2004) Modeling of cyanobacterial blooms in hypereutrophic Lake Dianchi, China. Journal of Freshwater Ecology., 19, 623-629.
[22] Qiu J.W. and Kwong K.L.. (2009) Effects of macrophytes on feeding and life-history traits of the invasive apple snail Pomacea canaliculata. Freshwater Biology., 54, 1720-1730.
[23] Anschutz P., Ciutat A., Lecroart P., Gérino M. and Boudou A.. (2012) Effects of tubificid worm bioturbation on freshwater sediment biogeochemistry. Aquatic Geochemistry., 18, 475-497.
[24] Jespersen A.M. J. and Christoffersen K.. (1987) Measurements of chlorophyll-a from phytoplankton using ethanol as extraction solvent. Archiv für Hydrobiologie.
[25] Sayler G.S., Puziss M. and Silver M.. (1979) Alkaline phosphatase assay for freshwater sediments: application to perturbed sediment systems. Appl Environ Microbiol., 38, 922-927.
[26] Berman T.. (1970) Alkaline phosphatases and phosphorus availability in Lake Kinneret. Limnology and Oceanography., 15, 663-674.
[27] Bu F. and Xu X.. (2013) Planted floating bed performance in treatment of eutrophic river water. Environmental Monitoring and Assessment., 185, 9651-9662.
[28] Zhu J., Liu B., Jing W., Gao Y and Wu Z.. (2010) Study on the mechanism of allelopathic influence on cyanobacteria and chlorophytes by submerged macrophyte (Myriophyllum spicatum) and its secretion. Aquatic Toxicology (Amsterdam, Netherlands)., 98, 196–203.
[29] Mulderij G., Van Donk E. and Roelofs J.G.M.. (2003) Differential sensitivity of green algae to allelopathic substances from Chara. Hydrobiologia., 491, 261-271.
[30] Zhao J.G., He F.F., Chen Z.H., Li H.J., Hu J.M. and Lin F.P.. (2012) Effect of culture and extract solutions of macrophytes on the growth of three common algae. Journal of Freshwater Ecology., 27, 367-379.
[31] Kalinowska K.. (1997) Eutrophication processes in a shallow, macrophyte dominated lake alkaline-phosphatase activity in Lake Łuknajno (Poland). Hydrobiologia., 342, 395-399.
[32] Zhou Y.Y., Li J.Q. and Fu Y.Q.. (2000) Effects of submerged macrophytes on kinetics of alkaline phosphatase in Lake Donghu. I. Unfiltered water and sediments. Water research., 34, 3737-3742.
[33] Feuillade J., Feuillade M. and Blanc P.. (1990) Alkaline phosphatase activity fluctuations and associated factors in a eutrophic lake dominated by oscillatoria rubescens. Hydrobiologia., 207, 233-240.
[34] Hino S.. (1988) Fluctuation of algal alkaline phosphatase activity and the possible mechanisms of hydrolysis of dissolved organic phosphorus in Lake Barato. Hydrobiologia., 157, 77-84.
[35] Tanner C.C. and Headley T.R.. (2011) Components of floating emergent macrophyte treatment wetlands influencing removal of stormwater pollutants. Ecological Engineering., 37, 474–486.
[36] Zhao F., Xi S., Yang X., Yang W., Li J., Gu B. and He Z.. (2012) Purifying eutrophic river waters with integrated floating island systems. Ecological Engineering., 40, 53–60.
[37] Jamet D. and Devaux J.. (2001) Size-fractionated alkaline phosphatase activity in the hypereutrophic Villerest reservoir (Roanne, France). Water Environ Res., 73, 132-141.
[38] Meyer-Reil L.A.. (1987) Seasonal and spatial distribution of extracellular enzymatic activities and microbial incorporation of dissolved organic substrates in marine sediments. Applied and Environmental Microbiology., 53, 1748-1755.
[39] Jones R.I., Salonen K. and Haan H.D.. (1988) Phosphorus transformations in the epilimnion of humic lakes: abiotic interactions between dissolved humic materials and phosphate. Freshwater Biology., 19, 357–369.
[40] Carlsson N., Brönmark C. and Hansson L.. (2008) Invading Herbivory: The golden apple snail alters ecosystem functioning Asian Wetlands. Ecology., 6, 1575-1580.
[41] Fang L., Wong P.K., Lin L., Lan C. and Qiu J.W.. (2009) Impact of invasive apple snails in Hong Kong on wetland macrophytes, nutrients, phytoplankton and filamentous algae. Freshwater Biology., 55, 1191–1204.
[42] Arango C.P., Riley L.A., Tank J.L. and Hall R.O.. (2009) Herbivory by an invasive snail increases nitrogen fixation in a nitrogen-limited stream, Canadian. Journal of Fisheries and Aquatic Sciences., 66, 1309-1317(1309).
[43] Zheng Z., Lv J., Lu K., Jin C., Zhu J. and Liu X.. (2011) The impact of snail (Bellamya aeruginosa) bioturbation on sediment characteristics and organic carbon fluxes in an eutrophic pond. Clean-Soil, Air, Water., 39, 566–571.
[44] Inoue T. and Yamamuro M.. (2000) Respiration and ingestion rates of the filter-feeding bivalve Musculista senhousia : implications for water-quality control. Journal of Marine Systems., 26, 183–192.

[45] Newell R.I.E.. (2004) Ecosystem influences of natural and cultivated populations of suspension-feeding bivalve molluscs: a review. Journal of Shellfish Research., 23, 51–61.
[46] Connor M.S., Teal J.M. and Valiela I.. (1982) The effect of feeding by mud snails, Ilyanassa obsoleta (Say), on the structure and metabolism of a laboratory benthic algal community. Journal of Experimental Marine Biology and Ecology., 65, 29–45.
[47] Naddafi R., Pettersson K. and Eklöv P.. (2007) The effect of seasonal variation in selective feeding by zebra mussels (Dreissena polymorpha) on phytoplankton community composition. Freshwater Biology., 52, 823-842.
[48] Labry C., Delmas D. and Herbland A.. (2005) Phytoplankton and bacterial alkaline phosphatase activities in relation to phosphate and DOP availability within the Gironde plume waters (Bay of Biscay). Journal of Experimental Marine Biology and Ecology., 318, 213–225.
[49] Degobbis D., Maslowska E.H., Orio A.A., Donazzolo R. and Pavoni B.. (1986) The role of alkaline phosphatase in the sediments of Venice Lagoon on nutrient regeneration, Estuarine. Coastal and Shelf Science., 22, 425–437.
[50] Mhamdi B.A., Azzouzi A., Elloumi J., Ayadi H., Mhamdi M.A. and Aleya L.. (2007) Exchange potentials of phosphorus between sediments and water coupled to alkaline phosphatase activity and environmental factors in an oligo-mesotrophic reservoir. Retour au numéro., 330, 419-428.
[51] Estebenet A.L., (1995) Food and feeding in Pomacea canaliculata (Gastropoda: Ampullariidae). The Veliger., 38, 277-283.
[52] Estebenet A.L., Martin P.R.. (2002) Pomacea canaliculata (Gastropoda: Ampullariidae): life-history traits and their plasticity. Biocell., 26, 83-89.

Received: **13.11.2015**
Accepted: **10.03.2016**

CORRESPONDING AUTHOR

Prof. Zheng Zheng
Department of Environmental Science and Engineering, Fudan University, 220 Handan Road, Shanghai 200433, P.R. China

E-mail: zzhenghj@126.com

© by PSP Volume 25 – No. 7/2016, pages 2605-2612 Fresenius Environmental Bulletin

COMPARISON OF PHYSIOLOGICAL RESPONSES AND NITROGEN AND PHOSPHORUS ABSORPTION IN NYMPHAEA TETRAGONA AND PONTEDERIA CORDATA

Xiao-Ming Lu[1] and Peng-Long Lu[2]

1 Institute for Eco-Environmental Sciences, Wenzhou Vocational College of Science & Technology, Wenzhou 325006, China
2 Advertising Agency, Wenzhou Transportation Group, Wenzhou 325000, China

ABSTRACT

Nymphaea tetragona and *Pontederia cordata* were cultivated in six tanks, to investigate physiological responses in plants and physicochemical characteristics of effluents. Our results indicated that peroxidase activity, and Chla, Chlb, and soluble protein contents all varied significantly between the two species. Peroxidase and catalase activities in *N. tetragona* exceeded *P. cordata* by 0.08 U $(g \cdot min)^{-1}$ and 0.08 mg $(g \cdot min)^{-1}$, while Chla, Chlb, and soluble protein contents of *P. cordata* were higher than *N. tetragona* by 0.19, 0.04, and 24.08 mg g^{-1}. *N. tetragona* roots were longer than *P. cordata*, although culms and leaves were shorter, and tiller numbers, root densities, and biomass were lower than *P. cordata*. Nitrogen and phosphorus contents were higher in *P. cordata* than *N. tetragona*; comparisons of the two species showed differences of 1.88 and 0.30 g kg^{-1} in roots, 3.07 and 0.54 g kg^{-1} in culms, and 4.22 and 0.59 g kg^{-1} in leaves, for nitrogen and phosphorus between *P. cordata* and *N. tetragona*. Removal of total phosphorus and soluble phosphorus was lower for *N. tetragona* than for *P. cordata* by 15.8% and 13.5%, while total nitrogen and NH_4^+-N removal rates were higher by 13.8% and 15.6%.

KEYWORDS

polluted river water; *Nymphaea tetragona*; *Pontederia cordata*; physiological characteristic; phytoremediation

INTRODUCTION

Some reports have demonstrated that macrophytes are effective in treating polluted water, including municipal wastewater [1-2], agricultural non-point source pollution [3-4], and eutrophic water [5]. Macrophytes can take up nitrogen and phosphorus from surface water [6-7], filter suspended particulate organic matter, increase the oxygen concentration in the water, and reduce flow velocity, which increases the water residence time. A study of a waste stabilization pond system showed that the plant uptake of nitrogen is a major mechanism for its removal [7]. Macrophytes promote nitrogen removal in the process of treating wastewater by floating beds, as the efflux of oxygen from plant roots promotes the develop of aerobic nitrifying bacteria [8]. The plant-periphyton complex plays a role as a biofilter in the absorption and retention of cations [9]. Submerged aquatic vegetation can absorb nutrients from both the water column and the sediments, and change the oxygen concentration in the overlying water [10-11]. Other studies have shown that macrophytes can improve the quality of eutrophic river water [12-13].

The physiology of macrophytes has been found to be correlated with water purification. Li *et al.* [14] analyzed the morphological and physiological responses of macrophytes during long-term soaking in wetland wastewater treatment processes. Their results indicated that both the morphology and physiology of the plants were greatly affected. Furthermore, the photosynthesis and transpiration of the plants affect nitrogen removal rates in wetlands [15]. Variations in photosynthesis affect the oxygen release of the roots and the degradation of water pollutants [15]. Zhao *et al.* [16] analyzed the correlation between water quality and the plant physiology and found that changes in the transpiration influenced absorption of most of the dissolved ionic contaminants in the water. Peroxidase (POD) and catalase (CAT) activities in macrophytes have been reported to be correlated with stress tolerance [17-19]. The rate of photosynthesis is an important indicator of the physiological state of the plant, and the output of photosynthetic oxygen is associated with the degree of water purification [8, 20].

Few reports exist on the treatment of polluted river water with *Nymphaea tetragona* and *Pontederia cordata*. Both plants grow best under strong sunlight. Each of them has a widespread distribution and can be commonly found in almost

every province of China. Each of them has ornamental value, as well as a good capacity for removing water pollutants [18, 21], but has not yet been extensively used in ecological restoration projects [16].

Most urban rivers in China have become seriously polluted. Because of this, phytoremediation technology has attracted increasing attention in the field of water pollution treatment. Recently, scientists have compared the purification capacities of some aquatic plant species [22-23]. However, to date, there have been few studies describing both water quality improvement by different plant species and the physiological responses of the plants themselves. The physiological status of the plant is closely correlated with its ability to remove pollutants. Chlorophyll content is associated with the photosynthetic rate, which affects oxygen release by the plant during photosynthesis and also pollutant removal by the plant. Soluble proteins (SP) is vital to the performance of the metabolic activity of photosynthesis. POD (peroxidase) and CAT (catalase) enzymes play an important cooperative role in eliminating and preventing damage caused by active oxygen radicals that are induced by stress [24]. POD is very sensitive to conditions that cause stress, and the variation in its activity is closely correlated with plant resistance to stress [25].

In this study, nine purifying tanks and a reservoir tank were constructed with a planting density of 20 plants (*N. tetragona* and *P. cordata*) per tank used for on-site treatment of severely polluted urban river water. The accumulation of nitrogen (N) and phosphorus (P) in the plants was then determined. The variation in plant physiology and the level of N and P removal was analyzed and compared for the two species. The objective of this study was to compare (1) the efficiencies of the two plant species in their abilities to remove N and P from polluted water, and (2) the physiological responses of the plants. The data from this study will provide valuable guidelines for the use of macrophytes for wastewater treatment and for the ecological restoration of polluted aquatic environments. Our results will also establish a theoretical basis for the application of aquatic plants in the restoration of the heavily polluted urban rivers.

MATERIALS AND METHODS

Device construction and plant cultivation. The Gongye river flows through Taopu town in the Putuo district of Shanghai, China. The river is heavily polluted and the water quality is inferior to the type 5 (ρ (COD) > 40 mg L^{-1}, ρ (NH_4^+-N) > 2.0 mg L^{-1}, ρ (TP) > 0.4 mg L^{-1}), according to the water quality standards of China.

Two aquatic plant species, *Nymphaea tetragona* Georgi (pygmy waterlily) and *Pontederia cordata* L. (pickerelweed), were cultured hydroponically in six tanks (three parallel tanks for each plant species; sk and hk tanks for *N. tetragona* and *P. cordata*, respectively) with the same planting density of 20 plants/tank.

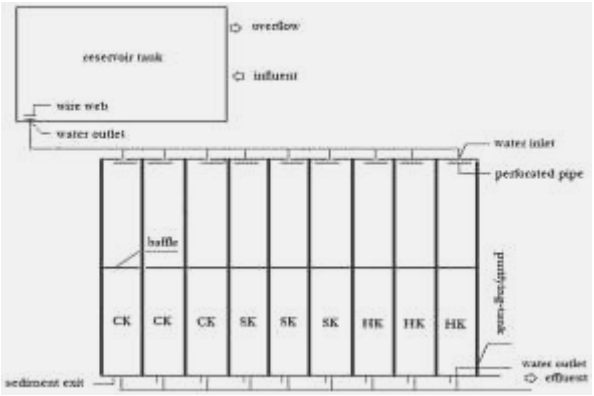

FIGURE 1
The test apparatus that consisted of nine purifying-tanks and one reservoir tank.

A test apparatus that consisted of nine purifying tanks and one ‘‘reservoir’’ tank was used as the experimental system. The device (Figure 1) was composed of one reservoir tank (upper dimensions, length 150 cm, width 100 cm; lower dimensions, length 145 cm, width 95 cm; height, 60 cm) and nine plastic purifying tanks (upper dimensions, length 124 cm, width 62 cm; lower dimensions, length 115 cm, width 55 cm; and height, 76 cm). A tube in the reservoir tank kept a constant water level of 60 cm and ensured that each purifying tank received the same volume of water. An effluent tube in each purifying tank kept a constant water level of 60 cm. A 25SFBX-13D water pump (Boyu Banye Limited, Shanghai) pumped polluted river water through a plastic pipe (diameter 4 cm) into the reservoir tank directly from the polluted river through the fixed effluent tube and into the purifying tanks. A wire mesh with a 0.2-mm pore diameter placed at the water outlet of the reservoir tank prevented suspended matter in the river water from entering the purifying tanks. Each purifying-tank was separated by a baffle through the center and by a space to the tank bottom of about 20 cm to avoid causing water circuit flow. In order to control the effects of the pollutants released from sediment into the water;

each purifying tank had a sediment exit on the bottom to remove the daily accumulation of mud.

The water flow into each tank was continuous with a hydraulic retention time of 8 h. Seedlings of *N. tetragona* and *P. cordata* (height, 10 cm; each seedling had one leaf slice) were collected from Zelong Biology Engineering Limited, Shanghai. No other growth medium was used to cultivate the seedlings directly except the heavily polluted river water. The seedlings were water-cultivated in purifying tanks with the planting density of 20 plants per tank on 26 February 2008, and three additional tanks without plants were established to act as control (CK). The treatment period was from 26 February 2008 to 16 October 2008. There were no human influencing factors and the plants showed natural growth. The test equipment was located in an open field.

Plant sampling and water quality measurements. On July 3, August 3, September 3, 2008, five healthy plants were collected from each tank randomly, and 0.3 g of leaf and root were collected from each of these plants. Simultaneously, water samples were collected from the outlet of each tank for analysis. The water quality was determined using standard method [26] and the average value was obtained for use.

Plant root, culm, and leaf length, biomass, root density and tiller numbers. The plant root density and the number of plant tiller in each tank were measured and then the average value was obtained, respectively. The healthy plants were collected. The lengths of plant root, culm and leaf were measured and the average value was calculated for use.

The biomass (dry weight) of the plant tissues, including the roots and the shoots, were measured in five replicates for each plant and the means were obtained for individual plants.

Leaf chlorophyll contents and N and P contents in the roots, stems, and leaves. The absorption capacity of the plants was indicated by determining nitrogen and phosphorus accumulation in the plant tissues. The N contents in five replicate samples each of roots, culms and leaves were determined by the Dumas combustion method using an automated CN analyzer (LECOCHN-1000, LECO Company, St Joseph, MI, USA). The P contents in five replicates of the corresponding plant tissues were determined by colorimetry (Hitachi U-1100 spectrophotometer) using the vanado-molybdate method after the material was digested in a 3 : 1 (v/v) mixture of concentrated nitric acid of 65–68% (Shanghai Zhenxin No.2 Chemical Plant Co., Ltd.) and perchloric acid of 70–72% (Shanghai Taopu Chemical Factory) [27]. The plant material was dried using GZX-DH30A bake oven (Shanghai Xiheng Shiye Limited, Shanghai, China) at 45 °C.

The method reported by Hegedüs *et al.* [28] was employed to analyze chlorophyll (Chl-a, Chl-b) content. It was modified as follows: 0.05 g plant leaf was soaked in 5 mL of 80 % acetone solution for 24 h and the absorbance of the resulting solution at the wavelengths of 645 and 663nm was measured with a HITACHI U-1100 spectrophotometer (Hitachi, Tokyo, Japan).

Enzyme solution preparation, soluble protein content, and enzyme activity measurements. Fresh roots (0.3 g) and leaves (0.3 g) were prepared and refined in the freezing phosphate solution (pH 7.8), centrifuged at 13,000 r min^{-1} and in 4 °C for 30 min. The supernatant was collected for use.

The soluble protein (SP) content of the root of the plant was measured with Coomassie Brilliant Blue [29]. Standard curve was reported with using bovine serum albumin (BSA) in units of mg g^{-1}. A240 represented the absorbance value at the wavelength of 240 nm. Catalase (CAT) activity in the root was performed by UV-spectrometer analysis [30], where a change of 0.1 A240 units represented one activity unit.

Peroxidase (POD) activity of the roots of the two plant species was analyzed with guaiacol [31]. The variation of the light intensity in per min represented the enzyme activity. A460 represented the absorbance value at the wavelength of 460 nm. A change of 0.1 A460 units represented one activity unit (U), measured in U $(g \cdot min)^{-1}$.

Statistical analyses. The means of each physiological parameter of each plant species (n = 5) and each physiochemical index of three independent water samples were calculated for analysis. Statistical differences in the plant parameters and the water quality indices among various purifying-tanks were assessed by performing Tukey tests.

RESULTS AND DISCUSSION

Comparison of physiological characteristics of *N. tetragona* and *P. cordata*. The roots of *N. tetragona* were longer than those of *P. cordata,* while the culms and leaves were shorter. The number of tillers in *P. cordata* were higher than in *N. tetragona.* The root densities did not vary significantly between the *P. cordata* tank and the *N. tetragona* tank. The POD and CAT activities measured in *N. tetragona* roots were higher than the activities in *P. cordata* roots, while the Chla, Chlb,

and SP contents of *N. tetragona* leaves were less than those of *P. cordata* leaves. The POD activity and the Chla, Chlb, and SP contents varied significantly between *P. cordata* and *N. tetragona*, whereas the CAT activities were not significantly different between the two species.

Comparisons of plant biomass and the N and P contents of the roots, culms, and leaves in *N. tetragona* and *P. cordata*. Plant biomass and the N and P contents of the roots, culms, and leaves of *N. tetragona* were lower than in *P. cordata*. Therefore, the N and P accumulation in *N. tetragona* was less than in *P. cordata.* For the two plant species, the capacity to absorb nutrients through the foliage was different, and plants mainly take up soluble N and P from the water through the foliage [15, 32]. In this study, the aquatic plants in the tanks developed by foliar absorption of soluble N and P from the water, and there was no N and P released from the substrate. Comparing *N. tetragona* and *P. cordata*, we found that for plant parts, the capacity for N and P removal by *P. cordata* was higher than it was for *N. tetragona.* The amounts of N and P absorbed by *N. tetragona* roots were less than in *P. cordata*, which resulted in a decrease in the N and P contents of *N. tetragona* roots. Transport of N and P from the roots to the shoots was then affected, and this led to a reduction in the N and P contents of the shoots. In addition, the *P. cordata* plants were markedly larger than those of *N. tetragona* (Table 1).

Comparison of water quality among the different purifying tanks. The removal rates of chemical oxygen demand (COD), total nitrogen (TN), and NH_4^+-N in the *N. tetragona* tanks were higher than in the *P. cordata* tanks, while the removal rates of TP and soluble P and dissolved oxygen (DO), pH, and water temperature were lower than in the *P. cordata* tanks. The removal of TN and NH_4^+-N mainly depended on degradation and transformation by microorganisms and plant absorption through the foliage, and the former was dominant [15, 32]. For the plants, the absorption of NH_4^+-N by *N. tetragona* was not as effective as it was for *P. cordata* (Table 2). However, the results indicated that the removal rate in the *N. tetragona* tanks was higher than in the *P. cordata* tanks. This was because root length in *N. tetragona* was ~2.6 times that of *P. cordata*, and the difference in root density between the two plants was not significant;

TABLE 1
Comparison of physiological characteristics between *N. tetragona* and *P. cordata* in the different purifying tanks.

Mean	Root cm	Culm cm	Leaf cm	POD U (g·min)$^{-1}$	CAT mg (g·min)$^{-1}$	SP mg g^{-1}	Chla mg g^{-1}	Chlb mg g^{-1}	Tiller amount /tank	Root density /m^2
N. tetragona										
	55.8±4.6a	44.5±3.7a	8.9±0.73a	0.13±0.03a	0.54±0.14a	40.57±7.90a	1.74±0.12a	0.49±0.04a	173±7a	1192± 48a
P. cordata										
	21.5±2.0b	64.0±5.7b	15.2±1.21b	0.05±0.01b	0.45±0.08a	64.65±4.44b	1.93±0.05b	0.53±0.02b	225±10b	1253±61a

Note: all data in the above form are the means ± standard errors of *five* replicates; different letters in the same column mean significant at 5 % level between different purifying-tanks, same as follows.

TABLE 2
Comparison of plant biomass and the N and P contents of roots, culms, and leaves in *N. tetragona* and *P. cordata.*

Mean	N			P							
	Root	Culm	Leaf	Root	Culm	Leaf	Root	Culm	Leaf	Root	Shoot
	Content (g kg^{-1})						Moisture rate (%)			Biomass(DW)(g plant^{-1})	
N. tetragona											
	14.9±1.1a	21.3±1.4a	23.5±1.7a	1.7±0.1a	2.4±0.2a	2.8±0.2a	93.5±2.1a	95.5±2.3a	96.3±2.4a	22.8±0.6a	2.9±0.1a
P. cordata											
	16.8±1.5b	24.3±2.0b	27.7±2.2b	2.0±0.2b	2.9±0.2b	3.4±0.3b	92.3±1.7a	93.2±1.8a	93.7±1.9a	19.7±0.5b	9.0±0.2b

Note: all data in the above form are the means ± standard errors of *five* replicates; different letters in the same column mean significant at 5 % level between *N. tetragona* and *P. cordata*, same as follows. DW= dry weight

therefore, the total root surface area in *N. tetragona* most probably exceeded that in *P. cordata,* which was helpful to the growth of the microorganisms associated with the root surface. In addition, differences in the DO between the *N. tetragona* and *P. cordata* tanks did not vary significantly. Therefore, removal of NH_4^+-N by microorganisms in the *N. tetragona* tanks was more effective than in the *P. cordata* tanks. Additionally, most of the *N. tetragona* culms were immersed in water, which also increased the surface area for the growth of microorganisms, and at the same time, a slightly higher water temperature was also beneficial to the removal of pollutants by microorganisms. The higher levels of P that accumulated in *P. cordata* were evidence of the more effective removal of TP and soluble P in polluted river water in the *P. cordata* tanks as compared to the *N. tetragona* tanks (Table 2). The removal of TP and soluble P was mainly dependent on natural sinks and the foliar absorption by the plants [32]. A lower pH in the *N. tetragona* tank resulted from the higher removal rate of NH_4^+-N. Similarly, the increased growth rate of attached heterotrophic microorganisms on the plant surface in the *N. tetragona* tanks led to the higher removal rate of COD.

The physiological variations between *N. tetragona* and *P. cordata* led to differences in the removal rates of N and P between the two plant species and also the two different types of plant tanks. The Chl content of *P. cord ata* leaves was higher than in *N. tetragona* (Table 1). Under the same levels of illumination, the photosynthetic efficiency of *P. cordata* surpassed that of *N. tetragona*, and the content of photosynthetic metabolites derived from SP increased. Also, the oxygen release increased correspondingly, resulting in the DO concentration in the *P. cordata* tank exceeding that in the *N. tetragona* tank (Table 3). This type of DO increase observed in our study was in agreement with that previously reported by Wang *et al.* [7]. Luo *et al.* [15] also reported that the net photosynthesis rate of reeds was closely correlated with the DO concentration of the water. However, the mechanism behind the variation in pH of the tank water was different from the effects of *Vallisneria spiralis* on the water pH. *V. spiralis* increased the water pH through the photosynthetic absorption of CO_2 in the water [7], while *P. cordata* and *N. tetragona* decreased the pH of the water through foliar absorption of NH_4^+-N. The absorption of N and P by the plants mainly depends on the roots. Thus, the process is correlated with the biological characteristics of the roots and the physicochemical characteristics of the water [33]. In the plant parts, the removal of N and P by *N. tetragona* was weaker than in *P. cordata*. Furthermore, the DO in the *P. cordata* tanks was slightly higher than it was in the *N. tetragona* tanks (Table 3), which was more suitable for the removal of NH_4^+-N by nitrifying bacteria and denitrifying bacteria [34]. However, the morphological characteristics of the roots and culm of *N. tetragona* contributed to the growth of the attached microorganisms, which resulted in higher rates of removal of COD, TN, and NH_4^+-N in the *N. tetragona* tanks. The highly polluted river water caused an increase in superoxide radical levels in the plant, leading to oxidative stress [24]. Li *et al.* [14] also reported that the increase in activity of the resistant enzyme in the plant resulted from the foliar absorption of large amounts of soluble pollutants. Foliar absorption is a key way for plants to remove soluble pollutants such as soluble P, and NH_4^+-N etc. from polluted water Therefore, aquatic plants which are highly tolerant of polluted water are very important for the restoration of polluted urban rivers.

Comparing the two species included in this study (Table 1), the POD activity in the roots of *N. tetragona* was higher than in roots of *P. cordata*, while CAT activities measured in the roots of the

TABLE 3
Comparison of water quality between the different purifying tanks.

Mean	Soluble P removal %	NH_4^+-N removal %	DO mg L^{-1}	pH value	Water temperature °C	COD removal %	TP removal %	TN removal %
N. tetragona tank	36.97±1.8a	43.83±2.2a	0.93±0.1a	7.7±0.1a	31.1±0.1a	54.31±2.7a	48.39±2.4a	39.15±1.9a
P. cordata tank	50.51±2.4b	28.23±1.4b	0.98±0.1a	8.0±0.1a	30.2±0.1a	45.48±2.2b	64.23±3.2b	25.32±1.3b
CK tank	5.62±0.2c	3.75±0.2c	0.12±0.01b	8.2±0.1a	34.5±1.5a	6.36 ±0.3c	6.71±0.3c	3.37±0.1c

Note: all data in the above form are the means ± standard errors of *three* replicates; different letters in the same column mean significant at 5 % level among different purifying-tanks.

two species were not significantly different. The Chl and SP contents in the leaves of *P. cordata* were higher than in *N. tetragona*, and our results indicated that the reproducibility was higher for *P. cordata* than it was for *N. tetragona*. Therefore, *P. cordata* was more tolerant of water pollution and was more suitable for growth in highly polluted river water than was *N. tetragona*. In addition, individuals of *P. cordata* were larger than *N. tetragona*, and plant biomass and the accumulation of N and P were also higher than in *N. tetragona*. Therefore, *P. cordata* has an advantage over *N. tetragona* when used for the restoration of highly polluted urban rivers. However, the morphological characteristics of the roots and culms of *N. tetragona* made them more suitable for the removal of COD, TN, and NH_4^+-N by microorganisms. Furthermore, *N. tetragona* is highly ornamental, and this species should be planted in large floating beds.

CONCLUSIONS

P. cordata was found to be more tolerant of water pollution than was *N. tetragona.* The tiller numbers, amount of biomass, relative N and P accumulation, and the lengths of the culm and leaf of *P. cordata* were also higher than in *N. tetragona*. However, the roots of *P. cordata* were shorter than those of *N. tetragona*. The Chla, Chlb, and SP contents of the leaves of *P. cordata* were higher than in *N. tetragona* by 0.19 mg g^{-1}, 0.04 mg g^{-1}, and 24.08 mg g^{-1}, respectively. However, the activities of POD and CAT in the roots of *P. cordata* were lower than in *N. tetragona* by 0.08 U $(g \cdot min)^{-1}$ and 0.08 mg $(g \cdot min)^{-1}$, respectively. The relative POD activities and the Chla, Chlb, and SP contents were significantly different between the two plant species, while the CAT activities were not. The removal rates of TN and NH_4^+-N in the *N. tetragona* tank were higher than in *P. cordata* by 13.8% and 15.6%, respectively, while the removal rates of TP and soluble P for *N. tetragona* were lower than for *P. cordata* by 15.8% and 13.5%, respectively.

ACKNOWLEDGMENTS

This work was supported by the Science and Technology Innovation Project of Water Pollution Control and Treatment of Wenzhou City (No. S20150001).

REFERENCES

[1] Gérard, M., Jean-Luc, P. and Thierry, L. (2002) Performances of constructed wetlands for municipal wastewater treatment in rural mountainous area. Hydrobiologia, 469, 87-98.

[2] Jing, S. R., Lin, Y. F., Wang, T. W. and Lee, D. Y. (2002) Microcosm wetlands for wastewater treatment with different hydraulic loading rates and macrophytes. J. Environ. Qual., 31, 690-696.

[3] Headley, T. R., Huett, D. O. and Davison, L. (2001) The removal of nutrients from plant nursery irrigation runoff in subsurface horizontal-flow wetlands. Water Sci. Technol., 44, 77-84.

[4] Millhollon, E. P., Rodrigue, P. B., Rabb, J. L., Martin, D. F., Anderson, R. A. and Dans, D. R. (2009) Designing a constructed wetland for the detention of agricultural runoff for water quality improvement. J. Environ. Qual., 38, 2458-2467.

[5] Green, M. B. and Upton, J. (1994) Constructed reed beds: A cost-effective way to polish wastewater effluents for small communities. Water Environ. Res., 66, 188-192.

[6] Tanner, C. C. (2001) Growth and nutrient dynamics of soft-stem bulrush in constructed wetlands treating nutrient-rich wastewaters. Wetl. Ecol. Manag., 9, 49-73.

[7] Wang, C. H., Li, K. Y., Wen, M. Z. and Liu, Z. W. (2007) Effects of Vallisneria asiatica on water environmental factors and its diurnal variation. J. Agro-Environ. Sci., 26, 798-800.

[8] Kowalchuk, G. A., Bodelier, P. L. E., Heilig, G. H. J., Stephen, J. R. and Laanbroek, H. J. (1998) Community analysis of ammonia-oxidising bacteria, in relation to oxygen availability in soils and root-oxygenated sediments, using PCR, DGGE and oligonucleotide probe hybridization. FEMS Microbiol. Ecol., 27, 339-350.

[9] Judith, S. W. and Peddrick, W. (2004) Metal uptake, transport and release by wetland plants: Implications for phytoremediation and restoration. Environ. Int., 30, 685-700.

[10] Caffrey, J. M. and Kemp, W. M. (1991) Seasonal and spatial patterns of oxygen production, respiration and root-rhizome release in Potamogeton perfoliatus L and Zostera marina L. Aquat. Bot., 40, 109-128.

[11] Caffrey, J. M. and Kemp, W. M. (1992) Influence of the submerged plant Potamogeton perfoliatus, on nitrogen cycling in estuarine sediments. Limnol. Oceanogr., 37, 1483-1495.

[12] Gao, J. Q., Xiong, Z. T., Zhang, J. D., Zhang, W. H. and Felicite, O. M. (2009) Phosphorus removal from water of eutrophic Lake Donghu

by five submerged macrophytes. Desalination, 242, 193-204.
[13] Sangeeta, D. and Savita, D. (2009) Water quality improvement through macrophytes – A review. Environ. Monit. Assess., 152, 149-153.
[14] Li, Z. H., Tang, W. H. and Song, Z. W. (2007) Response of the morphological and physiological characteristics of aquatic plants to long-term soaking in the process of constructed wetland wastewater treatment. Acta Scientiae Circumstantiae, 27, 75-79.
[15] Luo, W. G., Wang, S. H., Huang, J., Yan, L. and Huang, J. (2006) Influence of plant photosynthesis and transpiration character on nitrogen removal effect in wetland. China Environ. Sci., 26, 30-33.
[16] Zhao, F., Lu, X. M., Huang, M. S. and Chen, J. J. (2010) Study on the relationship between water quality improvement and Nymphaea tetragona physiological diurnal variation in purification tanks. J. East China Normal Univ. (Nat. Sci.), 56, 50-57.
[17] Zhao, Q., Wu, Z. B., Cheng, S. P. and He, F. (2008) Response of a submersed macrophyte Hydrilla verticillata (L.f) Royle, to sodium dodecylbenzene sulfonate stress. Wuhan Univ. J. Nat. Sci., 13, 221-226.
[18] Lu, X. M. and Huang, M. S. (2010) Nitrogen and phosphorus removal and physiological response in aquatic plants under aeration conditions. Int. J. Environ. Sci. Te., 7, 665-674.
[19] Xiong, H. F., Tan, Q. L. and Hu, C. X. (2010) Structural and metabolic responses of Ceratophyllum demersum to eutrophic conditions. Afr. J. Biotechnol., 9, 5722-5729.
[20] Kirk, G. J. D. and Kronzucker, H. J. (2005) The potential for nitrification and nitrate uptake in the rhizosphere of wetland plants: A modelling study. Ann. Bot., 96, 639-646.
[21] Lu, X. M. and Chen, J. J. (2012) Effects of the diurnal variation of sunlight on water quality and the physiology of Nymphaea tetragona. Toxico. Enviro. Chem., 94, 294-309.
[22] Wang, Q. H., Duan, L. S., Li, R. H. and Wu, J. Y. (2008) Comparison of nutrient uptake from rural domestic sewage of aquatic plants. Acta Agriculturae Boreali-Sinica, 23, 217-222.
[23] Yuan, D. H., Ren, Q. J., Gao, S. X., Zhang, H., Yin, D. Q. and Wang, L. S. (2004) Purification efficiency of several wetland macrophytes on COD and nitrogen removal from domestic sewage. Chinese J. Appl. Ecol., 15, 2337-2341.
[24] Jabs, T. (1999) Reactive oxygen intermediates as mediators of programmed cell death in plants and animals. Biochem. Pharmacol., 57, 231-245.
[25] Li, J. and Zu, Y. G. (2000) Generation of activated oxygen and change of cell defense enzyme activity in leaves of Korean pine seedling under low temperature. Acta Botanica Sinica, 42, 148-152.
[26] SEPA and Editorial Committee of Monitoring and Analytical Methods of Water and Wastewater. (2002) Monitoring and analytical methods of water and wastewater. 4th ed. Beijing: China Environmental Science Press.
[27] Vogel, A. I. and Bassett, J. (1978) Vogel's textbook of quantitative inorganic analysis, including elementary instrumental analysis. 4th ed. London and New York: ELBS Longman Publications.
[28] Hegedüs, A., Erdei, S. and Horváth, G. (2001) Comparative studies of H2O2 detoxifying enzymes in green and greening barley seedlings under cadmium stress. Plant Sci., 160, 1085-1093.
[29] Wessel, D. and Flügge, U. I. (1984) A method for the quantitative recovery of protein in dilute solution in the presence of detergents and lipids. Anal. Biochem., 138, 141-143.
[30] Rao, M. V., Paliyath, G. and Ormrod, D. P. (1996) Ultraviolet-B and ozone-induced biochemical changes in antioxidant enzymes of Arabidopsis thaliana. Plant Physiol., 110, 125-136.
[31] Zhang, Z. L. (1990) Laboratory procedure of plant physiology. Beijing: Higher Educational Press.
[32] Song, K. M. (1999) Phosphorus nutrition of plants: phosphate transport systems and their regulation. Chinese Bulletin of Botany, 16, 251-256.
[33] Fan, G.. L. and Li, W. (2005) Response of nutrient accumulation characteristics and nutrient strategy of Myriophyllum spicatum L. under different eutrophication conditions. Journal of Wuhan Botanical Research, 23, 267-271.
[34] Ouellet-Plamondon, C., Chazarenc, F., Comeau, Y. and Brisson, J. (2006) Artificial aeration to increase pollutant removal efficiency of constructed wetlands in cold climate. Ecol. Eng., 27, 258-264.

Received: **09.11.2015**
Accepted: **14.03.2016**

CORRESPONDING AUTHOR

Xiao-Ming Lu
Institute for Eco-Environmental Sciences, Wenzhou Vocational College of Science & Technology, Wenzhou 325006, China.

E-mail address: 13736961468@163.com (X. Lu).

© by PSP Volume 25 – No. 7/2016, pages 2613-2619 Fresenius Environmental Bulletin

UPTAKE OF IRON AND LEAD FROM AQUEOUS SOLUTION BY SOME GREEN MICROALGAE

A M Farghl Abla, H R Galal Hamedy, A Hassan Eman

Botany Department, Faculty of Science, South Valley University, 83523, Qena, Egypt

ABSTRACT

Morphological changes in the cell wall surface of *Chlorella* are often associated with the metals coordination sphere and microenvironment. In this study, the uptake capacity of green microalgae, *Chlorella vulgaris* and *Chlorella salina* for heavy metals (iron and lead) was evaluated. *C. vulgaris* and *C. salina* were isolated from sewage and marine water (Lake Marriott) respectively. Algal samples were exposed to 200ppm iron (Fe^{2+}) and lead (Pb^{2+}). The scanning electron microscopy techniques (SEM) coupled to energy dispersive X-ray (EDX) was applied to determine if this *Chlorella* is able to uptake of Fe^{2+} and Pb^{2+} which had previously been detected in Lake Marriott and sewage water of El-Salhya Qena, Egypt. *Chlorella* had ability to uptake the essential (Fe^{2+}) and non-essential elements (Pb^{2+}). The percentage of Pb^{2+} and Fe^{2+} uptake was significantly increased in non-living cells more than the living cells of *C. vulgaris* and *C. salina*. The fresh algae have a large affinity between metals uptake. Moreover, the fresh algae uptake the tested metals more than the marine algae.

KEYWORDS:
Biosorption, *Chlorella*, dead biomass, heavy metals, scanning electron microscope, X - ray.

INTRODUCTION

Heavy metals presence in aquatic environment has become a problem because their risks for human health by their accumulation in living tissues throughout the food chain and on the flora and fauna of receiving water bodies [1].

Microorganisms have the ability to bioaccumulation most heavy metals to some degree, though the extent of bioaccumulation varies depending on the bioavailability of the metal, the organism under consideration and concentrations to which they are exposed [2].

Bioaccumulation of heavy metal ions removal may provide an attractive alternative to physico-chemical methods. Biological methods of heavy metals elimination have proven to be beneficial as compared to the chemical and physical ones [3, 4]. Ariff *et al*. [5] recorded the components of microorganism cell wall (lipids, protiens and polysaccharides) offer many functional groups which can be bind metal ions.

Microorganisms directly reduce many highly toxic metals (e.g., Cr, Hg, U) by detoxification pathways. Microbial reduction of some metals to a lower redox state may result in reduced mobility and toxicity [6]. Dead or alive cells absorption mechanisms are different and uptake yields, reception capacity and the amount of metal concentration vary among the organisms [7].

The use of nonliving or chemically pretreated microorganisms (biosorbents) seems to be a preferred option to the use of living cells in industrial applications for the removal of heavy metal ions from wastewater [8]. The use of nonliving biomass may offer some advantages over living cells: there is no need for growth media, not sensitive to toxicity limitations and the biosorbed metal ions can be easily desorbed for reuse [9].

The objective of this study was to determine if *Chlorella* genus (fresh or marine alga) is able to sorption heavy metals ($FeCl_2$ and $PbCl_2$). To achieve this goal we used scanning electron microscopy techniques with combination an energy dispersive X- ray detector and use living and non-living algal biomass to uptake the iron and lead uptake from aqueous solution.

MATERIALS AND METHODS

Microalgal isolate. The marine microalga (*Chlorella salina)* isolated from lake Marriott, Alexandria, while freshwater alga (*Chlorella vulgaris*) isolated from sewage water of El-Salhya sewage station, Qena, Egypt as a toxic pollutant after getting axenic cells culture by using method was described by Christopher and Patterson [10]. Cells were grown in F/2 and Bold's basal liquid medium. Essential (iron) and nonessential (lead) stock solution was added to F/2 and Bold's basal liquid medium to reach a final concentration of 200 ppm. Cultures were incubated at 27°C for 72h in illumination incubator provided by cool white fluorescent lamps set on 14:10 h light : dark photo-period.

Scanning electron microscopy (SEM) and energy dispersive X- ray (EDX) microanalysis for SEM analysis. *Chlorella* cultures were fixed in 2.5% glutaraldehyde for 4 h and washed four times with sterile distilled water. Finally, all samples were mounted on metal stubs and coated with gold. An Inspects' Model scanning electron microscope (FEI, Netherlands, Eind-hoven) was used to view the images and an energy dispersive X-rays INCA system software and X- Act Detector, operated at 20 kV coupled to SEM was used [11].

Study the uptake of iron and lead by living and non-living algal biomass. Fifty ml of *Chlorella* culture was shaking at 100rpm to 7 days to get heavy algal culture. Three replicates for each concentration were used. 60 mg of the pellet culture were suspended in 50 ml of media with various heavy metal concentrations. While the nonliving algal cells obtained by heat killing process by placing the algal cultures on water bath at 50Cº for 2h, then centrifuged to get a palette which then suspension in 50ml of each heavy metals concentration [12]. The samples were make a centrifuge (3000rpm for 15 min) after 3days to get the pellet again this pellet treated with 10ml of mix 9:1 mixture of sulfuric acid: perchloric acid the mixture digests the palette algae till it turned colorless, then cooled and make up to known volume using distilled water to be ready for measuring lead and iron elements. The metal uptakes (M) estimate in unit of µg/mg using the formula:

$$M = C\ V/W$$

C- Spectrophotometer reading of sample concentration estimated in unit's µg/ ml.
V- Volume of sample extraction estimated in unit's ml.
W- Dry weight of the algae estimated in unit's mg.

RESULTS AND DISCUSSION

Scanning electron microscopy (SEM). Scanning Electron Microscopy (SEM) was used to visualize the surface morphology of *Chlorella* species before and after metal binding, allowing for direct observation of any changes appear. The pure sample of *C. vulgaris* (fresh water alga) shows evidence of smooth structures arranged in quite a regular pattern on the surface while these are not present in the essential or nonessential-loaded images (Fig.1a).

After completion of the metal binding obvious morphological changes were seen in the cell wall. The cell wall structure has a varying diameter such as, the morphological changes (shrinking and layer sticking) in the cell wall electron micrographs after Fe (II) adsorption (Fig.1b).

SEM images of the nonessential elements (Pb^{+2}) samples (Fig.1c), reveal honeycomb-like structures which may indicate significant changes in the cell wall surface structure. The surface had a large variation in sizes and the extensive interconnections gave a Flaky" type of appearance after heavy metals adsorption. This could be due to the cell surface of the *C. vulgaris* alga underwent coalescence or rupture or the sputtering process caused by the heavy metals uptake. They tend to collapse and the circle like structure was not clearly seen in Fig.a.

C. salina (marine alga) contains smooth structures similar to those observed for *C. vulgaris*. However, in *C. salina* these cell walls appear to be larger in size and are arranged in quite a regular pattern and smoother than in *C.vulgaris* (Fig.2a). After cation loading in *C. salina* (Pb^{2+}), large visible morphological changes are apparent with the formation of mound-like structures seen in these micrographs.

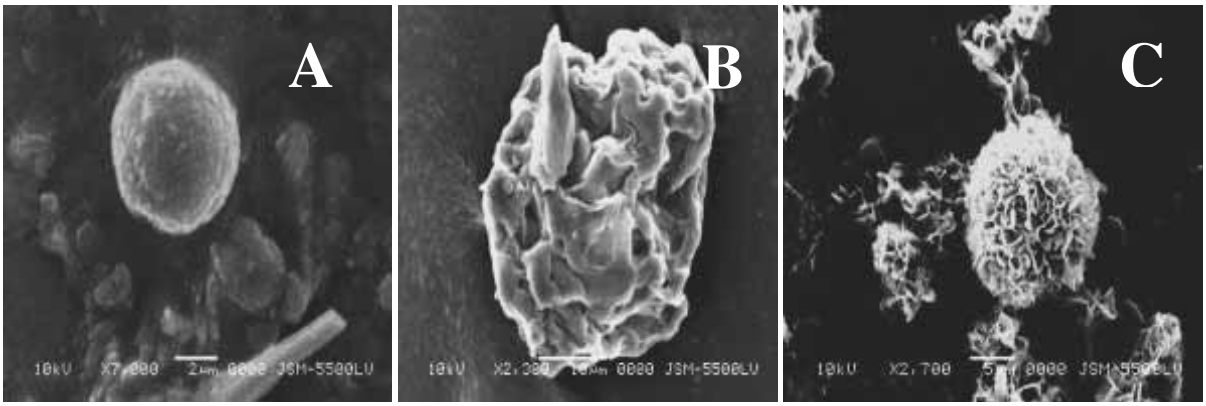

FIGURE 1
SEM micrographs of *C. vulgaris*. A. control, B. after Fe (II) and C. after Pb (II) uptake.

While Fe (II)-loaded algae reveal honeycomb-like structures which may indicate significant changes in the surface structure. These changes may again be related to differences in the ionic radii of the ions resulting in differences in coordination spheres (Figs. 2b and c).

Differences between the structure observed in cation-loaded *C. vulgaris* and cation-loaded *C. salina* indicate that metal binding behavior is different for different species and habitat of the same genus. This is most likely due to surface compositional differences between the algae. The same to the results which found by Suzuki *et al*. [13]

X- ray. In order to characterize the chemical composition and differences between the pure and metal-loaded algae surface were apparent in the *Chlorella* species scanning electron microscopy (SEM) with energy dispersive X-ray spectroscopy (EDX) were used.

The elemental composition of the algal surface was measured by EDX. The EDX spectra of pure and metal-loaded *Chlorella* species are shown in Figures. The peaks presented in each of spectra have been summarized in Table1.

The EDX analyzer can produce a spectrum of the element present in the targeted areas of the sample allowing detectable elements to be quantified or mapped [14].

Some of the peaks from the EDX spectra in the all Figures and Table (1) are not necessarily related to the sample surface, for example Au peaks in EDX spectra originated from the gold sputter coating on the sample while Al peak that sometimes detected comes from the sample holder. Figures of EDX spectra of Fe (II) & Pb (II)–loaded *C. vulgaris* and C. *salina*. Modification: 1000x. from Table (1) it is seen that binding behavior was identical for both green algae.

The control algae had a greater number of peaks than those observed after cation exposure. This is due to alkali and alkaline earth metals (Na^+, k^+, Ca^{++} and Mg^{++}) from fresh and sea water being present in algal cell.

The essential and non essential loaded spectra of the green alga (C*hlorella*) revealed that, the disappearance of alkali and alkaline earth metal peaks. This disappearance indicates the existence of an ion exchange mechanism. As this technique has been used only qualitatively and the scale used for the EDX spectra is arbitrary, unless a peak disappears after metal binding, it is difficult to evaluate changes in peak size or intensity. When algal samples were exposed to metal solution, metal cations may have replaced not only calcium and magnesium peaks but also sodium and potassium peaks was observed in the cation loaded EDX-spectra. Thus, it appears that changes in across linking behavior linked to the metals coordination sphere, resulted in visible morphological changes in the cell wall surface.

Singh *et al*. [15] proposed that replacement of these ions with metal cations altered the nature of the cross-linking due to stronger electrostatic and coordinative bonding between the metal and the negatively charged groups in the cell wall polymers.

Bioaccumulation and biosorption of heavy metals. The results showed that, the percentage of Fe^{2+} uptake was 51.51% and 51.10% in living cells of fresh (*C. vulgaris*) and marine algae (*C. salina*), respectively. While, the percentage of Pb^{2+} uptake was 0.12% and 0.10% in living cells of *C. vulgaris* and *C. salina*, respectively. Furthermore, these percentages were significantly increased to 79.03% and 78.52% for Fe^{2+} and 35.28 % and 2.22% for Pb^{2+} in non-living cells of *C. vulgaris* and *C. salina*, respectively (Fig.7).

It is clear from the results that there was correlation between the natural habitat of the algae and their properties of the heavy metals uptake; also the sorption capacity of fresh water algae was different to those of the marine microalgae

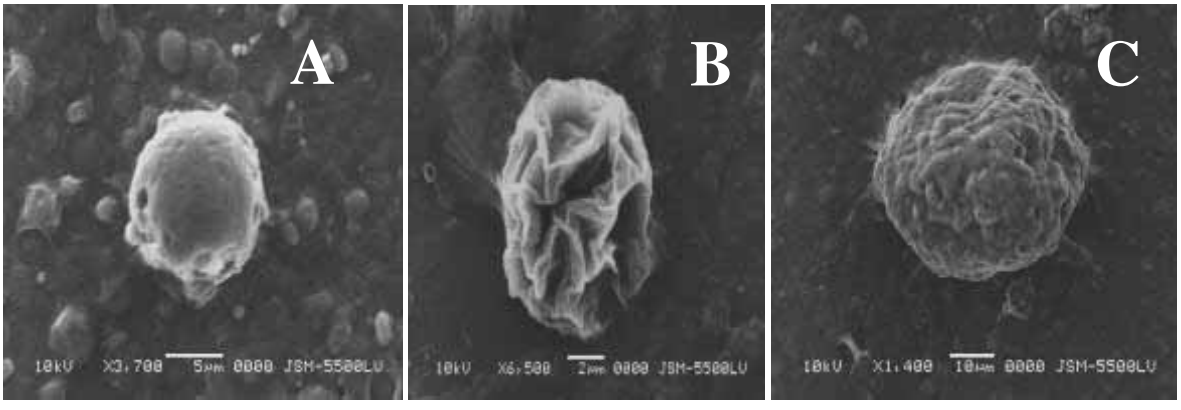

FIGURE 2
SEM micrographs of *C. salina.* A. control, B. after Fe (II) and C. after Pb(II) uptake.

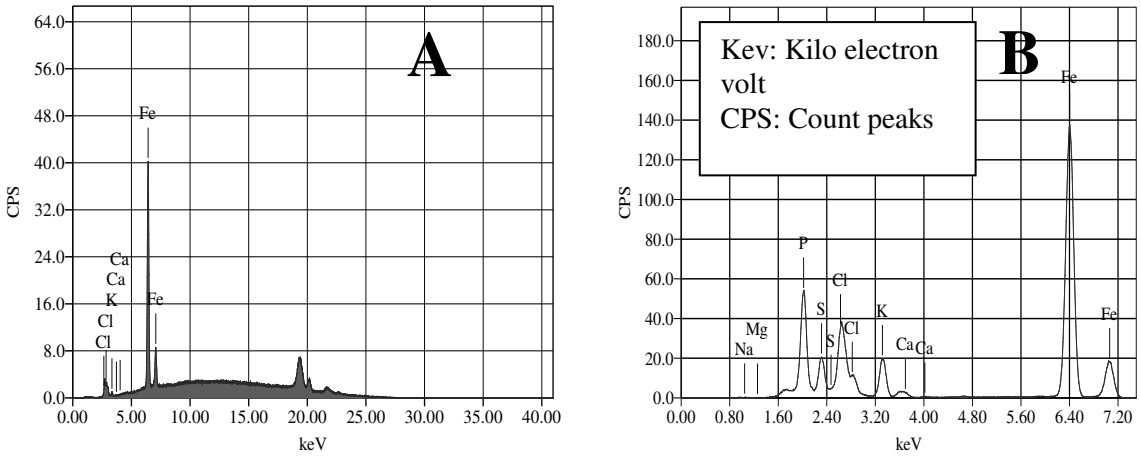

FIGURE 3

X-ray absorption chart of iron uptake by nonliving cells of *C. vulgaris* (A) and *C .salina* cultures (B).

Nevertheless, the preferential sorption of the metals was obvious (Figs.3-6), that is agree with the results of Rabsch and Elbrachter [16], that studied the bioaccumulation of cadmium and zinc in a diatom *Cosinodiscus granii* and found that the heat -killed cells accomplished more metals than did the living cells.

A majority of studies on metal accumulation by algae have been performed with living organisms for environmental, toxicological and pharmaceutical purposes rather than with industrial application in mind. Of late, the attention has shifted to non-living algae and other microorganisms for metal removal and/or recovery [17]. In comparison to live cells, the metal sorption capacity of dead cells may be greater or equivalent [18]. Higher affinity of nonliving cells for metal ions compared with living biomass that might probably due to absence of competing protons produced during metabolism [19].

In conclusion, the initial SEM with EDX constitutes with a set of methodologies have proven to be a useful technique that allow a quick diagnosis of whether a microorganism can uptake a metal or not. *Chlorella* species is a potential algal species for effective removal of heavy metals. Fresh algae had more affinity to uptake the heavy metals from aqueous solution than marine algae. The pretreatment of cells with heat (non-living cell) results in enhanced metal uptake.

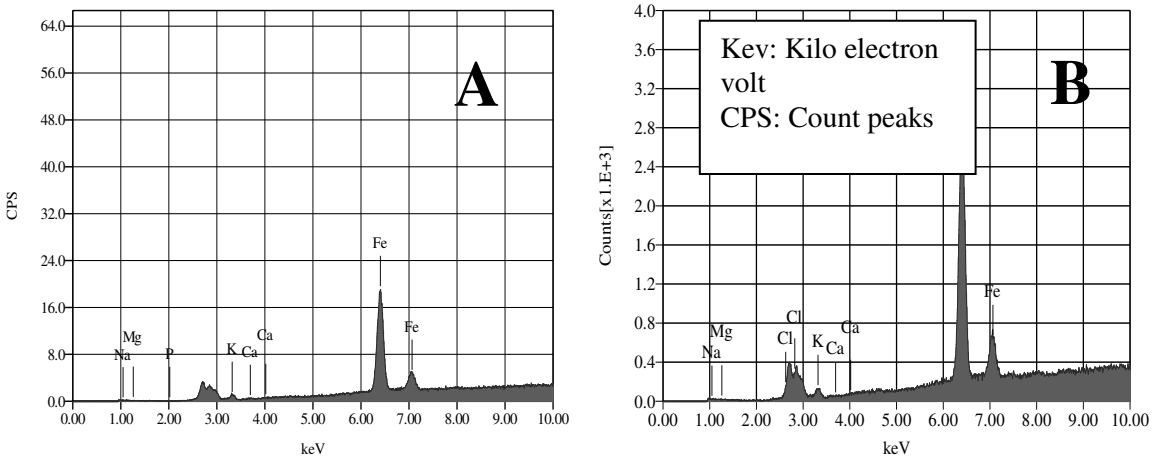

FIGURE 4

X-ray absorption chart of iron uptake by living cells of *C. vulgaris* (A) and *C. salina* cultures (B).

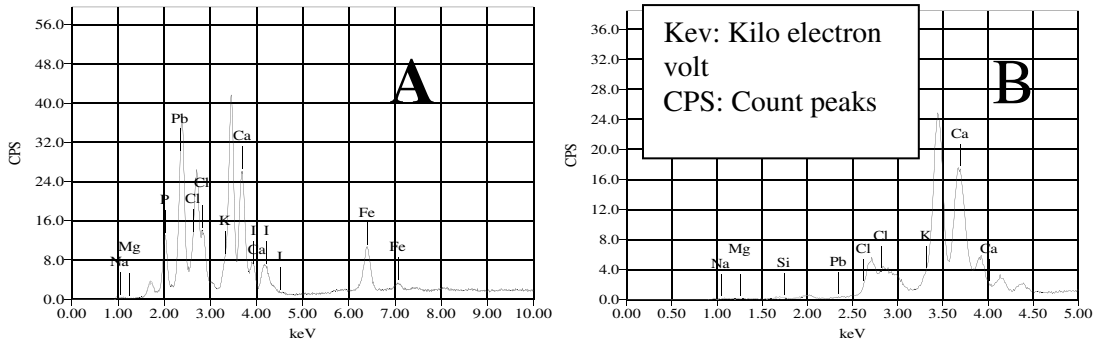

FIGURE 5
X-ray absorption chart of lead uptake by nonliving cells of *C. vulgaris* (A) and *C. salina* cultures (B).

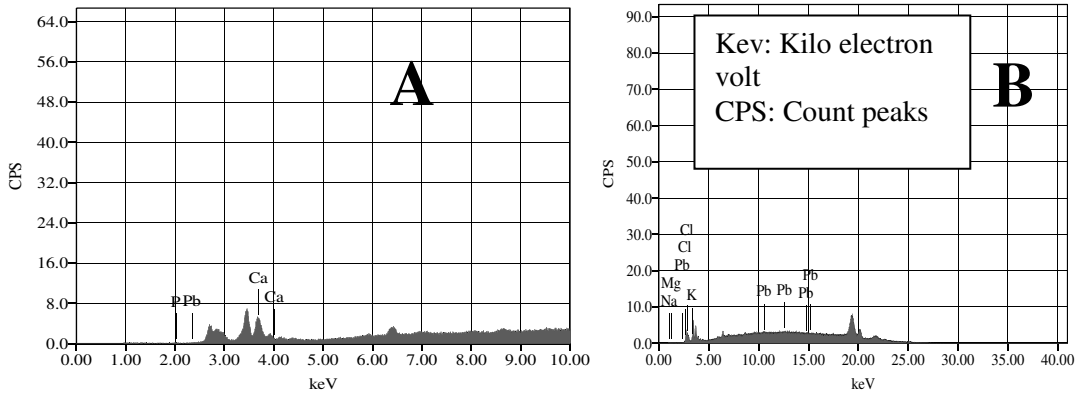

FIGURE 6
X-ray absorption chart of lead uptake by living cells of *C. vulgaris* (A) and *C. salina* cultures (B).

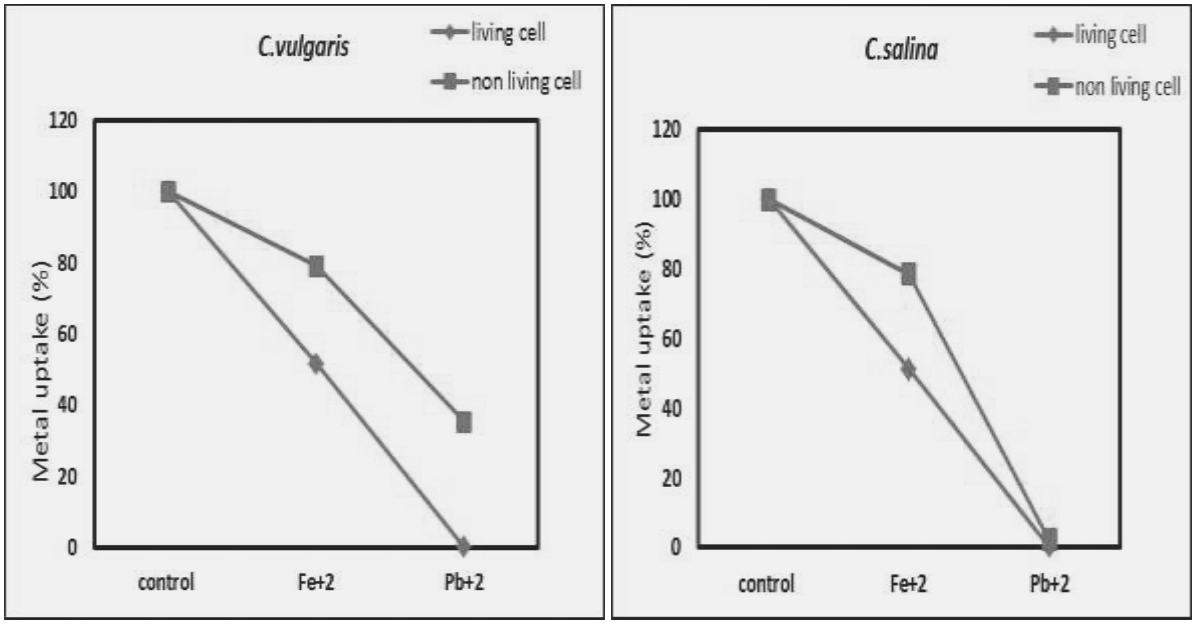

FIGURE 7
Percentage of heavy metals uptake by living and non-living cells of *C. vulgaris* and *C. salina* cultures.

TABLE 1
Iron and lead peaks in the EDX spectra of *C. vulgaris* and *C. salina.*

	C. vulgaris			*C. salina*	
Pure samples	Fe(II) loaded	Pb(II) loaded	Pure samples	Fe(II) loaded	Pb(II) loaded
Sodium	*	*	Sodium	Na(I)	Na(I)
Magnesium	*	*	Magnesium	*	*
Potassium	K(I)	K(I)	Potassium	K(I)	K(I)
Calcium	Ca(II)	*	Calcium	Ca(II)	Ca(II)
Copper	Cu (II)	Cu (II)	Iron	Fe (II)	Fe (II)
Iron	Fe (II)	Fe (II)			
Lead	Pb (II)	Pb (II)	Lead	Pb (II)	Pb (II)

* Band not observed.

REFERENCES

[1] Gupta, N., Khan, D.K. and Santra, S.C. (2008) An assessment of heavy metal contamination in vegetables grown in wastewater-irrigated areas of Titagarh, West Bengal, India. Bulletin of Environmental Contamination and Toxicology, 80, 115–118.

[2] Arunakumara, K.K.I.U. and Xuecheng, Z. (2007) How does lead (Pb^{2+}) at low concentrations affect on *Spirulina (Arthrospira) platensis*. Tropical Agricultural Research and Extension, 10, 47-52.

[3] Fomina, M., Hillier, S., Charnock, J. and Melville, K., Alexander, I. and Gadd, G. (2005) Role of oxalic acid over-excretion in toxic metal mineral transformations by Beauveria caledonica. Applied Environmental Microbiology, 71, 371-381.

[4] Pagnanelli, F., Carolina, C., Beolchini, F. Luisa, G. Vegliò, F. and Toro, L. (2014) Bioactive and passive mechanisms of pollutant removal in bioreduction processes in fixed bed columns: Numerical simulations. Environmental Progress and Sustainable Energy, 33, 70-80.

[5] Ariff, Mel M., Hasan, M.A. and Karim, M.I.A. (1999) The kinetics and mechanism of lead (II) biosorption by powderized *Rhizopus oligosporus*. World Journal of Microbiology and Biotechnology, 15, 291-298.

[6] El-Meleigy, M.A., Abed, N.N. and Sari, I.P. (2011) Fate of cobalt and nickel in *B. firmus* and *B. subtilis.* Natural Science, 9, 175- 189

[7] İlhan, S., Cabuk, A. Filik, C. and Calişkan, F. (2004) Effect of pretreatment on biosorption of heavy metals by fungal biomass. Trakya university journal of Social Science, 5, 11-17.

[8] Tirgar, A., Golbabaei, F. Hamedi, J. and Nourijelyani, K. (2011) Removal of airborne hexavalent chromium using alginate as a biosorbent. International Journal of Envionmental Science and Technology, 8, 237-244.

[9] Arica, M.Y., Tüzün, I. Yalçin, E. Ince, Ö. and Bayramoğlu, G. (2005) Utilisation of native, heat and acid-treated microalgae *Chlamydomonas reinhardtii* preparations for biosorption of Cr (VI) ions. Process Biochemistry, 40, 2351–2358.

[10] Christopher, M.H. and Patterson, D.J. (1983) *Coleps hirtus*, a ciliate illustrating facultative symbiosis between protozoa and algae. Annales de la Station Biologique de Besse-en-Chandesse, 17,278-297.

[11] Dwaish, A.S., Mohammed, D.Y. Jawad, A.M. and AL-kubaicy, A.A. (2011) Determine the uptake of lead in *Chlorella vulgaris* isolated from Tigris River in Baghdad city. International Journal of Scientific and Engineering Research, 2, 1-4.

[12] Inthorn, D., Sidtitoon, N. Silapanuntakul, S. and Incharoensakdi, A. (2002) Sorption of mercury, cadmium and lead by microalgae. ScienceAsia, 28, 253–261.

[13] Suzuki, Y., Kametani, T. and Maruyama, T. (2005) Removal of heavy metals from aqueous solution by nonliving *Ulva* seaweed as biosorbent. Water Research, 39, 1803–1808.

[14] Baruah, S., Hazarika Kalyan, K.r. and Sarma, K.P. (2012) Uptake and localization of Lead in Eichhornia crassipes grown within a hydroponic system. Advances in Applied Science Research, 3, 51-59.

[15] Singh, P., Raghukumar, C. Rajesh, R.P. and Mascarenhas-Pereira, M.B.L. (2013) Heavy metal tolerance in the psychrotolerant *Cryptococcus* sp. isolated from deep-sea sediments of the Central Indian Basin .Yeast, 30, 93-101.

[16] Rabsch, U. and Elbrachter, M. (1980) Cadmium and Zinc uptake, growth and primary production in Coscinodiscus granii culture containing low levels of cells and dissolved organic carbon. Helgoland Marine Research, 3, 79 -88.
[17] Tamilselvan, N., Saurav, K. and Krishnan, K. (2011). Biosorption of selected toxic heavy metals using algal species *Acanthopora spicefera*. Pharmacologyonline, 1, 518-528.
[18] Zoumis, T., Calmano, W. and Forstner, U. (2000) Demobilization of heavy metals from mine waters. Acta Hydrochimica Hydrobiologica, 28, 212-218.
[19] Das, N., Charumathi, D. and Vimala, R. (2007) Effect of pretreatment on Cd^{2+} biosorption by mycelial biomass of Pleurotus florida. African Journal of Biotechnology, 6, 2555–2558.

Received: **09.11.2015**
Accepted: **15.03.2016**

CORRESPONDING AUTHOR

Abla A.M. Farghl
South Valley University
Botany Department
Faculty of Science, 83523, Qena, Egypt

Email: farghla@yahoo.com

© by PSP Volume 25 – No. 7/2016, pages 2620-2627 Fresenius Environmental Bulletin

INSECTICIDAL EFFECTS OF ESSENTIAL OILS OBTAINED FROM SIX PLANTS AGAINST *CALLOSOBRUCHUS MACULATUS* (F.) (COLEOPTERA: BRUCHIDAE), A PEST OF COWPEA (*VIGNA UNGUICULATA*) (L.)

Ayse Usanmaz Bozhüyük[1], Saban Kordali[2], Memis Kesdek[3], Mahmut Alper Altinok[4], Murat Varcin[5] and Mehmet Ramazan Bozhüyük[6]

[1]Department of Plant Protection, Agriculture Faculty, Iğdir University, 76100, Iğdir-Turkey
[2]Department of Plant Protection, Agriculture Faculty, Atatürk University, 25240, Erzurum-Turkey
[3]Department of Environment Protection Technologies, Fethiye Ali Sıtkı Mefharet Koçman Vocational High School, Muğla Sıtkı Koçman University, 48300, Fethiye, Muğla-Turkey
[4]Department of Plant Protection, Seyrani Agriculture Faculty, Erciyes University, Develi, Kayseri-Turkey
[5]Graduate School of Natural and Applied Sciences, Ecological Science, Muğla Sıtkı Koçman University, 48000, Muğla-Turkey
[6]Department of Horticulture, Agriculture Faculty, Atatürk University, 25240, Erzurum-Turkey

ABSTRACT

Callosobruchus maculatus (F.), cowpea seed beetle (Coleoptera: Bruchidae) is one of the most serious pests of cowpea (the black-eyed pea) grains, worldwide. In this study, essential oils of *Artemisia dracunculus* L., *Artemisia santonicum* L., *Artemisia spicigera* C. Koch, *Origanum onites* L., *Satureja thymbra* L. and *Thymus sipyleus* Boiss. were tested for their insecticidal activities against three day-old adults of *C. maculatus* at 25±2 °C, 65±5 % r.h. in dark conditions, at different exposure times (12, 24, 48 and 72 h), and doses (5, 7.5 and 10 µl). It was found that there were the mortalities in all exposure doses and durations. The percentage mortality of adults of *C. maculatus* increased with increasing the concentration of different oils and exposure times. Minimum mortality rate in *C. maculatus* adults (16.6%) was recorded at 12 h with 5 µl essential oil of *O. onites*, while the peak mortality was registered as 100%, at 72 h with 10 µl essential oil of *A. dracunculus*. Additionally, LD_{25}, LD_{50} and LD_{90} values of each essential oil were estimated for *C. maculatus*. Results suggested that the essential oils from the tested plants could be used as potential control agents against *C. maculatus* adults in stored cowpea (the black-eyed pea) protection.

KEYWORDS:
Callosobruchus maculatus, cowpea seed beetle, essential oils, insecticidal effect, mortality percentage.

INTRODUCTION

In recent years, scientists have focused on increasing food production for the need of the rapidly expanding population of the world. Unfortunately, crop loss is still keeping on due to plant diseases, caused by insects, plant pathogen fungi, bacteria and viruses. *Callosobruchus maculatus* (F.), cowpea seed beetle (Coleoptera: Bruchidae), is one of the most important pests of cowpea (the black-eyed pea) grains in the cowpea storages. This pest requires great attention because it is very fairly distributed throughout the tropical and sub-tropical regions of the world. It feeds on cowpea (*Vigna unguiculata* (L.)), also chickpea (*Cicer arietinum* L.), lentil (*Lens culinaris* Medik.), soybean *(Glycine max* Mer.) and haricot beans (*Phaseolus vulgaris* L.). The leguminous plants are a very important source of vegetable protein for millions of people around the world, especially in tropical and subtropical regions. Cowpea seeds have seriously affected by *C. maculatus* and cause maximum damage of 2 to 5 kg seeds with in 45 to 90 days in optimum temperature (30^0±1 ^{0} C) and moisture conditions (75 ± 3 %) [29]. In the past, many residual insecticides such as malathion and pirimiphosmethyl were largely used to control this pest in stored cowpea. However, these chemicals caused hazardous effects such as environmental pollution, toxicity to non-target organisms, pest resistance, pesticide residues, direct toxicity to users and also ozone depletion [1, 16, 41]. However, the natural products are relatively less damaging to environment and mammalian health as compared with synthetic chemicals. Although many studies reported to insecticidal activity of plant essential oils [3, 41, 24, 8, 19, 6, 45, 32], there are

few reports to insecticidal properties of essential oils against *C. maculatus* [40, 33, 20].

Essential oils are genuine plant extracts that contain natural flavours and fragrances grouped as monoterpenes (hydrocarbons and oxygenated derivatives), sesquiterpenes (hydrocarbons and oxygenated derivatives) and aliphatic compounds (alkanes, alkenes, ketones, aldehydes, acids and alcohols) that provide characteristic odours. Many essential oils isolated from various plant species belonging to different genera contain a relatively high amount of monoterpenes. Insecticidal properties of numerous essential oils and some monoterpenes have been extensively studied against various insect species [12, 27, 28, 37, 17, 22, 36, 2, 35, 23].

The genus *Artemisia* is an important genus of the family Asteraceae, which comprises about 1000 genera and over 20,000 species widespread throughout the world. Among them, about 500 species of the genus *Artemisia* are found in Asia, Europe and North America. There are *Artemisia dracunculus* L. and *Artemisia santonicum* L. species of *Artemisia* genus in Turkish flora. The species of *Artemisia* genus are known in Anatolia as ‘‘Acı pelin”, “Ak pelin”, “Yavşan” , “Deniz yavşanı” and “Acı yavşan”. *Artemisia* species is industrially important due to its insecticidal, antifungal, antibacterial, allelopathic and other properties. This genus is very rich in essential oils and bitter substances, including flavon and pinen [46,40].

The genus *Origanum* (oregano) is an important genus within the Lamiaceae family and comprises about 900 species, widespread throughout the world. There are about 20 species of *Origanum* genus in Turkish flora and this genus is very rich in essential oils and bitter substances [11, 5, 14]. The species of *Origanum g*enus are known in Anatolia as ‘‘Yalancı kekik”, ‘‘Kekik”, ‘‘İstanbul kekiği” and ‘‘Keklik otu”. *Origanum* species are traditionally used as a spicy additive for food flauvoring instead of thyme, as sedative, diuretic, degasifier, sweater and antiseptic, and also in the treatment of gastrointestinal diseases and constipation [5]. There are numerous reports on the chemical composition and their various biological activities of *Origanum* species [13, 44, 7, 46, 21, 14].

The genus *Thymus* and *Satureja*, belonging to Lamiacaeae family, are well known as aromatic and medicinal plants and are distributed in northern Anatolia [11, 5]. In Anatolia, *Thymus* L.(thyme) and *Satureja* L.(savory) species are frequently used as herbal tea or additives in commercial spice mixtures of many foods to offer aroma and flavour [5]. The genus *Thymus* L. consists of over 300 evergreen species of herbaceous perennials and subshrubs, native to Southern Europe and Asia [26]. Members of the genus *Thymus* L. are called “kekik” and “sipil kekik” in Turkish and used as herbal tea and condiments. *Satureja* species have been widely used as folk medicines and locally known as “sivri kekik” in Turkey. *Satureja* species are widely grown in Mediterranean region of the world. In Turkey, there are 15 *Satureja* species and five of them are endemic. Among them, the *Satureja thymbra* are consumed as species or herbal teas by the local people [43, 5].

Turkey flora is characterized by the abundance of aromatic plants among its components. The feature differentiating these plants from all others, although they belong to many different families, is the production of chemically related secondary compounds, the low molecular weight and volatile isoprenoids. This remarkable presence of aromatic species is important in determining the candidates with insectidal potential within this ecosystem.

Thus, the aim of the present study was to assess insecticidal effects of the essential oils isolated from six plant species, *Artemisia dracunculus, Artemisia santonicum, Artemisia spicigera*, *Origanum onites, Satureja thymbra* and *Thymus sipyleus* in different localities of Turkey against three day-old adults of *Callosobruchus maculatus*, the cowpea seed beetle.

MATERIALS AND METHODS

Insect material. *Callosobruchus maculatus* adults were collected from private store houses in Bozkurt/Denizli, Turkey and kept on cowpea (the black-eyed pea), (*Vigna unguiculata*) seeds. The cultures were maintained in Deparment of Environment Protection and Technologies, Fethiye Ali Sıtkı Mefharet Koçman Vocational School, Sıtkı Koçman University, Fethiye, Muğla, Turkey. In addition, the cowpea seeds were purchased from a local market and maintained in a freezer at −15°C in order to control any arthropod pests prior to use for bioassay during two days. After, *C. maculatus* adults were reared in 1 L jars containing cowpea seeds. The cultures were maintained in the dark conditions in a growth chamber set at 25±2 °C and 65±5% r.h. without exposure to any insecticide for several generations. Adult insects, three day-old, were used for the fumigant toxicity test. All experimental procedures were carried out under the same environmental conditions as the cultures.

Bioassays. In order to test the toxicity of the oils from six different plants, 20 individuals of *Callosobruchus maculatus* adults (all three-day old) were used. Cowpea seeds were placed in each of Petri dishes (9 cm x 1.5cm). Adults of *C. maculatus* in the Petri dishes were exposed separately to essential oils of *A. dracunculus, A. santonicum, A. spicigera*, *O. onites, S. thymbra* and *T. sipyleus.*

The amounts of essential oils were applied at rates of 5, 7.5 and 10 µl corresponding to 38.46, 50.6 and 76.92 µl/L air oils impregnated into Whatman no. 1 filter paper, which was stuck onto the inner top of the Petri dishes. A filter paper was placed at the bottom of each Petri dish (9cm×1.5cm deep) and 20 adults of *C. maculatus* were placed onto filter paper containing 20 g cowpea (*Vigna unguiculata*) seeds. This prevented direct contact between the oils and *C. maculatus* individuals. The Petri dishes were covered with the lid and transferred to an incubator, and then kept under standard conditions of 25±2 °C, 65±5 r.h. and in the darkness for two days. Mortalities of the adults were then counted at 12, 24, 48 and 72 h. A Petri dish treated with only sterile water was used as control. Each assay was repeated three times for each dose and exposure time combination, and insecticidal activity of the oils was expressed as percent mean mortality of the adults.

Plants And Essential Oils. *Artemisia dracunculus* L., *Artemisia santonicum* L., *Artemisia spicigera* C. Koch, *Origanum onites* L., *Satureja thymbra* L. and *Thymus sipyleus* Boiss. (Lamiaceae) were collected at the flowering stage from different localities of Turkey between June and August of 2013 and 2014. Voucher specimens have been deposited in the herbarium of Ataturk University, Faculty of Agriculture, the Department of Plant Protection, Erzurum, Turkey. Aerial parts of the plants were dried in shade and ground in a grinder. The dried plant samples (500 g) were subjected to hydrodistillation for 4 h using a Clevenger-type apparatus. The oil yields of *A. dracunculus, A. santonicum, A. spicigera, O. onites, S. thymbra* and *T. sipyleus* were 1, 0.21, 0.25, 4.5, 1.17 and 0.98 %(w/w, dry weight basis), respectively. The yield was based on dry materials of plant samples. The essential oils were stored in a freezer at 4 °C for further tests.

Statistical analysis. The differences among the insecticidal activity of tested essential oils were determined according to analysis of variance (ANOVA) test contained in SPSS 17.0 software package. Differences between means were tested through Duncan tests and values with $p<0.01$ were considered significantly different.

TABLE 1
Values followed by different letters in the same column differ significantly at p<0.01 according to Duncan multiple test.
Mean±SE of three replicates, each set up with 20 adults.

Treatment Essential oils	Dose(µl/l)	Mortality(%)			
		Exposure time(h)			
		12	24	48	72
Artemisia dracunculus	5	31.6 ± 1.66 fg	76.6 ± 1.66 fgh	88.3 ± 3.33 efg	95.0 ± 2.88 def
	7.5	35.0 ± 2.88 gh	78.3 ± 1.66 gh	90.0 ± 2.88 fg	96.6 ± 1.66 ef
	10	38.3 ± 1.66 hı	81.6 ± 1.66 h	95.0 ± 0.0 gh	100.0 ± 0.0 f
Artemisia santonicum	5	20.0 ± 2.88 bc	58.3 ± 1.66 d	68.3 ± 1.66 b	90.0 ± 2.88 cd
	7.5	21.6 ± 1.66 bcd	63.3 ± 1.66 d	76.6 ± 3.33 c	95.0 ± 2.88 def
	10	30.0 ± 2.88 efg	73.3 ± 1.66 efg	90.0 ± 2.88 fg	98.3 ± 1.66 ef
Artemisia spicigera	5	26.6 ± 1.66 def	70.0 ± 2.88 e	81.6 ± 1.66 cde	93.3 ± 1.66 cde
	7.5	35.0 ± 2.88 gh	78.3 ± 1.66 gh	86.6 ± 1.66 def	95.5 ± 2.88 def
	10	41.6 ± 1.66 ı	81.6 ± 1.66 h	93.3 ± 1.66 fgh	98.3 ± 1.66 ef
Origanum onites	5	16.6 ± 1.66 b	41.6 ± 1.66 b	68.3 ± 1.66 b	88.3 ± 1.66 bc
	7.5	25.0 ± 2.88 cde	46.6 ± 1.66 bc	65.0 ± 2.88 b	85.0 ± 2.88 b
	10	26.6 ± 1.66 def	51.6 ± 1.66 c	70.0 ± 2.88 b	93.3 ± 1.66 cde
Satureja thymbra	5	25.0 ± 2.88 cde	70.0 ± 2.88 e	81.6 ± 3.33 cde	93.3 ± 1.66 cde
	7.5	26.6 ± 3.33 def	76.6 ± 1.66 fgh	86.6 ± 1.66 def	95.0 ± 2.88 def
	10	30.0 ± 2.88 efg	78.3 ± 1.66 gh	91.6 ± 1.66 fgh	98.3 ± 1.66 ef
Thymus sipyleus	5	21.6 ± 1.66 bcd	71.6 ± 1.66 ef	80.0 ± 2.88 cd	93.3 ± 1.66 cde
	7.5	30.0 ± 2.88 efg	78.3 ± 1.66 gh	93.3 ± 1.66 fgh	98.3 ± 1.66 ef
	10	31.6 ± 3.33 fg	73.3 ± 4.4 efg	88.3 ± 4.40 efg	98.3 ± 1.66 ef
Positive Control (Izoldesis)	10	86.6 ± 1.66 j	91.6 ± 1.66 ı	98.3 ± 1.66 h	100.0 ± 0.0 f
Control (Sterile water)	-	0.0 ± 0.0 a	1.67 ± 1.39 a	3.10 ± 1.43 a	4.44 ± 0.0 a

RESULTS AND DISCUSSION

In the present study, the toxicity effects of essential oils isolated from *A. dracunculus*, *A. santonicum, A. spicigera*, *O. onites*, *S. thymbra* and *T. sipyleus* were tested against adults of *C. maculatus* at the 5, 7.5 and 10 µl doses and at 12, 24, 48 and 72 h exposure times (Table 1; Figure 1, 2, and 3). All essential oils obtained from *A. dracunculus*, *A. santonicum, A. spicigera*, *O. onites*, *S. thymbra* and *T. sipyleus* were displayed toxicity against adults of *C. maculatus* in comparison to control, but the effects of these essential oils varied among each plant species. However, the mortality rates increased with increasing doses and exposure times for essential oils of tested plant species (Table 1; Figure 1, 2 and 3). The highest mortality rate (100%) was observed in the 10 µl dose at an exposure time of 72 h with the essential oil of *A. dracunculus*, while the lowest mortality rate (16.6%) was obtained in the 5 µl at an exposure time of 12 h with the essential oil of *O. onites*. In general, all essential oils caused over 90% mortality rate (except 5 and 7.5 µl doses of *O. onites* oil) after 72 h exposure (Table 1; Figure 1, 2 and 3). The results show that essential oils of *A. dracunculus*, *A. santonicum, A. spicigera*, *O. onites*, *S. thymbra* and *T. sipyleus* have a remarkable insecticidal activity on adults of *C. maculatus*. Statistical analysis results indicated that the effects of the essential oil, doses and exposure times on insect mortality were all statistically very significant ($p < 0.01$) (Table 1).

The lowest mortality rate was fixed as 16.6% in the 5 µl dose after 12 h treatment with essential oil of *O. onites* on the adults of *C. maculatus*, while the highest mortality rate was determined as 41.6% in the 10 µl dose for the essential oil of *A. spicigera* (Table 1; Figure 1, 2 and 3). However, the minimum mortality rate after 24 h treatment with essential oil of *O. onites* was acquired as 41.6% (in the 5 µl), but the maximum mortality rate was observed as 81.6% in the 10 µl doses for the essential oils of *A. dracunculus* and *A. spicigera* (Table 1; Figure 1, 2 and 3). Similarly, the least mortality rate 48 h after the treatments at was counted as 65.0% for *O. onites* essential oil (in the 7.5 µl), whereas the highest mortality rate was observed as 95.0% for essential oil of *A. dracunculus* (in the 10 µl) (Table 1; Figure 1, 2 and 3). In addition to these, the highest mortality rate at 72nd h after the treatment was determined as high as 100%, with the 10 µl dosage of *A. dracunculus* oil. But, the least mortality rate was found as 85.0% for *O. onites* oil (in the 7.5 µl). Besides, the mortality rates after a 72 h exposure were observed between 90% and 100% for all essential oils of all plants (with the exception of *O. Onites,* 85% for the 7.5 µl and 88.3% for the 5 µl) (Table 1; Figure 1, 2 and 3). In comparison with all essential oils of the tested plants, the highest mortality rates were observed with essential oil of *A. dracunculus* in all doses (5, 7.5 and 10 µl) and at all exposure times (12, 24, 48 and 72 h) on the adults of *C. maculatus*, while the essential oil of *O. onites* yielded the lowest mortality rates, among others (Table 1; Figure 1, 2 and 3). According to the test results, it was determined that *A. dracunculus* essential oil had an important insecticidal effect against adults of *C. maculatus.* However, the mortality rates were found to be 100% at the longest exposure period and with the maximum dose in the positive control (Table 1).

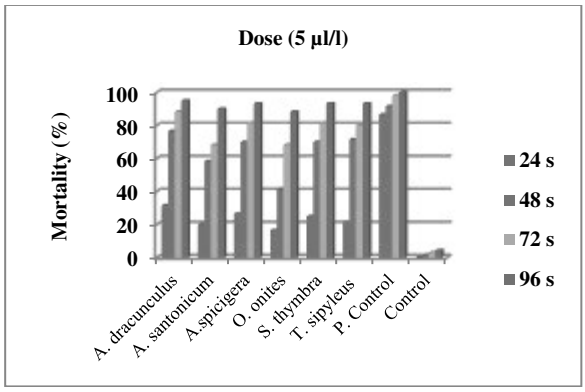

FIGURE 1
Percent mortality of adults of *Callosobruchus maculatus* after treatment with essential oils and treatment times in the 5 µl dose. *Statistically significant (p<0.01).

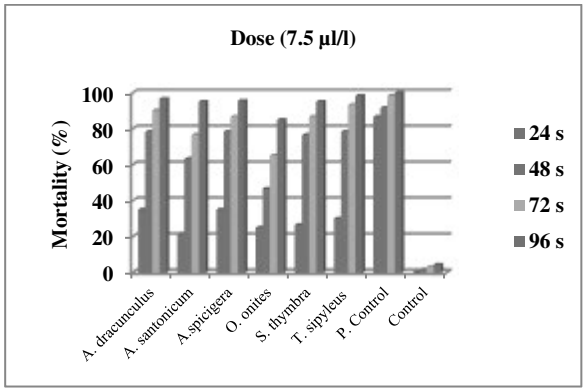

FIGURE 2
Percent mortality of adults of *Callosobruchus maculatus* after treatment with essential oils and treatment times in the 7.5 µl dose. *Statistically significant (p<0.01).

In a former study, it was reported that *A. dracunculus* oil had a toxic effect on adults of *Aphis gossypii* [34]. In another research, it was determined that the essential oil from *A.*

dracunculus had the mortality effects both on first instar larvae and eggs of *Plodia interpunctella* [38]. In the current study, it was determined that *A. dracunculus* oil had an insecticidal effect between 31.6% (in the 5 µl dose**,** after 12 h of exposure) and 100% (in the 10 µl dose, after 72 h of exposure) mortality rates on the adults of *C. maculatus* (Table 1; Figure 1, 2 and 3).

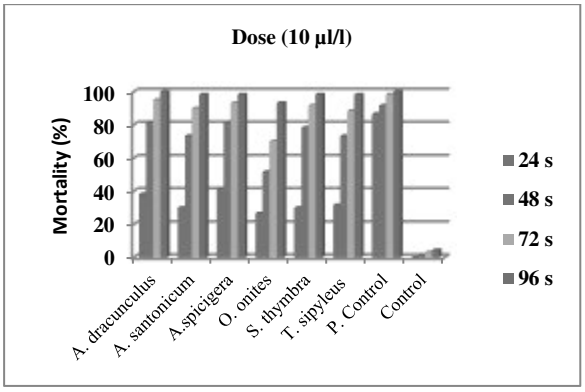

FIGURE 3
Percent mortality of adults of *Callosobruchus maculatus* after treatment with essential oils and treatment times in the 10 µl dose. *Statistically significant (p<0.01).

It had been previously stated that the essential oil recovered from *A. santonicum* had a toxic effect on *Sitophilus granarius* and showed about 80–90% mortality at a dose of 9 µl/l air after 48 h of exposure [23]. Similarly, it was indicated that essential oil of *A. santonicum* had an insecticidal effect on adults of *Sitophilus zeamais* and after 96 h of exposure, in the 20 µl/l air occured up to 100% mortality against this pest [25]. The present study proved that the essential oil of *A. santonium* had a toxic effect in all exposure times and at treatment doses, mortality rates of the adults of *C. maculatus* varied between 20.0% (in the 5 µl dose after 12 h exposure) and 98.3% (in the 10 µl dose after 72 h exposure) (Table 1; Figure 1, 2 and 3).

It was reported that essential oil of *A. spicigera* had a toxic effect against the larvae of *Dendroctonus micans,* the mortality of the larvae of *D. micans* increased significantly after treatment with the essential oil [15]. In another study, it was found that the essential oil of *A. spicigera* had an insecticidal effect on *Sitophilus granarius* [23]. In the current study, it was determined that *A. spicigera* essential oil lead to a minimum of 26.6% (in the 5 µl dose after 12 h of treatment) and a maximum 98.3% mortality (in the 10 µl dose after 72 h of treatment) of adults of *C. maculatus* (Table 1; Figure 1, 2 and 3).

In a previous study, it was stated that the essential oil of *O. onites* had a larvicidal effect on 4th and 5th larval instars of *Thaumetopoea wilkinsoni* (Çetin *et al*., 2006). Another study with *O. onites* showed that essential oil of *O. onites* was highly toxic against the house mosquito, *Culex pipiens* L. (Diptera: Culicidae) [9]. Also, it was determined that *O. onites* essential oil had 80% larval mortality on the larvae of *Culex pipiens* with concentrations between 50-200 ppm [9]. Likewise, *O. onites* oil resulted up to 100% mortality on the larval instars of *Ephestia kuehniella* and *Plodia interpunctella* [4]. In addition, it was found that the essential oils of *O. onites* had a toxic effect on adults of *Sitophilus granarius* [48]. In the present study, the essential oil of *O. onites* lead to the mortality rates between 16.6% (in the 5 µl dose after 12 h) and 93.3% (in the 10 µl dose after 72 h), on the adults of *C. maculatus* (Table 1; Figure: 1, 2 and 3).

In a previous study, the essential oil obtained from *S. thymbra* caused an insecticidal activity on adults of *Ephestia kuehniella*, *Plodia interpunctella* and *Acanthoscelides obtectus* [4]. Similarly, it was stated that *S. thymbra* oil had a toxic effect on the larvae of *Culex pipiens* [31]. In this study, the essential oil of *S. thymbra* lead to minimum 25.0% mortality (in the 5 µl dose after 12 h of treatment) and maximum 98.3% mortality (in the 10 µl dose after 72 h of treatment) (Table 1; Figure 1, 2 and 3). In some earlier studies, the toxicity tests of *T. sipyleus* oil showed that 10 µl of *T. sipyleus* oil resulted with 73% and 72% mortality against *S. granarius* adults and *Ephestia kuehniella* larvae, respectively [47, 48]. In another study, the essential oil of *T. sipyleus* caused between 90% and 100% mortality in the 10 µl dose after 24, 48, 72 and 96 h on the 2nd, 3rd and 4th larval instars of *T. pityocampa* [18]. Similarly, in the present study, it was determined that essential oil of *T. sipyleus* had an important insecticidal effect in the 10 µl dose and at all exposure times (12, 24, 48 and 72 h) between 31.6% and 98.3% with mortality rates on *C. maculatus* adults (Table 1; Figure 1, 2 and 3).

Furthermore, according to LD values (LD_{25}, LD_{50} and LD_{90}), the lowest LD values of *C. maculatus* was recorded for the essential oils of *O. onites* as 0.064 (LD_{25}) and *S. thymbra* 0.218 (LD_{25}), whereas the essential oils of *A. dracunculus* (LD_{25}) and *A. santonicum* (LD_{25}) had the lowest toxicity as 1.016 and 0.979, respectively (Table 2). However, the lowest LD_{50} value was found for the essential oil of *A. santonicum* as 1.722 against *C. maculatus* adults. Similarly, the least toxicity by means of LD_{90} value was obtained with the essential oil of *O. onites*, as 8.029 (Table 2).

TABLE 2
The LD values of essential oils obtained from six plants against adults of *Callosobruchus maculatus*.

Essential oils	LD_{25}	LD_{50}	LD_{90}	X^2	Slope ± SE
Artemisia dracunculus	1.016	1.639	4.064	4.428	3.250 ± 2.031
Artemisia santonicum	0.979	1.722	5.044	5.238	2.748 ± 1.415
Artemisia spicigera	0.383	0.861	4.024	4.902	1.915 ± 1.444
Origanum onites	0.064	0.340	8.029	3.197	0.933 ± 1.033
Satureja thymbra	0.218	0.569	3.512	5.691	1.621 ± 1.459
Thymus sipyleus	0.577	1.108	3.834	5.205	2.378 ± 1.632

In conclusion, the development and wide use of natural or biological insecticides may help to decrease negative effects of synthetic chemicals such as residues in the stored products, insect resistance and environmental pollution. In this respect, natural insecticides appear as easily bio-degradable solutions with relatively low environmental pollution. In the present study, the essential oils isolated particularly from *A. dracunculus*, *A. santonicum, A. spicigera*, *S. thymbra* and *T. sipyleus* were found to be more toxic against *C. maculatus* adults, but *O. onites* oil had a lesser effect. In many cases, their toxicities were also found identical in comparison to the toxicity of current commercial insecticides, widely used as insect reagents to protect the cowpea against adults of *C. maculatus*. Therefore, in the light of the present findings, it can be suggested that these plant essential oils can be used as new and effective insecticidal reagents against adults of *C. maculatus*. However, further studies need to be conducted to evaluate the cost and safety of these reagents, along with the efficiencies under various environmental conditions.

ACKNOWLEDGEMENTS

The authors thank to Mrs. Yeşim Kulapa (9 Eylül University, İzmir, Turkey) for her valuable grammatical improvements on drafts of this manuscript, also to the editors for their critical reviews.

REFERENCES

[1] Arthur, F. H. (1996). Grain protectants: current status and prospects for the future. Journal of Stored ProductResearch, 32, 293-302.

[2] Aslan, İ. Özbek, H. Kordali, Ş. Çalmaşur, Ö. Çakır, A. (2004). Toxicity of essential oil vapours obtained from *Pistacia* spp. to the granary weevil, *Sitophilus granarius* (L.) (Coleoptera: Curculionidae). Journal of Plant Disease and Protection, 111, 400–407.

[3] Aslan, İ. Çalmaşur, Ö. Şahin, F. Çağlar, Ö. (2005). Toxicity of essential oils isolated from three *Artemisia* species and some of their major components to granary weevil, *Sitophilus garanarius* (L.) (Coleoptera: Curculinonidae). Journal of Plant Disease and Protection, 112, 257–267.

[4] Ayvaz, A. Sağdıç, O. Karabörklü, S. Öztürk, İ.(2010). Insecticidal activity of the essential oils from different plants against three stored product insects. Journal of Insect Science, 10, 21, 1-13.

[5] Baytop, T. (1999). Therapy with Medicinal Plants in Turkey: Today and in Future. İstanbul University Press, İstanbul, pp. 166–167.

[6] Benzi, V. S. Murray, A. P. Ferrero, A. A.(2009). Insecticidal and insect-repellent activities of essential oils from Verbenaceae and Anacardiaceae against *Rhizopertha dominica*. Natural Product Communications, 4, 1287-1290.

[7] Bouchra, C. Achouri, M. Hassani, L. M. I. Hmamouchi, M. (2003). Chemicalcomposition and antifungal activity of essential oils of seven Moroccan Labiatae against *Botrytis cinerea* Pers: Fr. J. Ethnopharmacol, 89, 165–169.

[8] Çağlar, Ö. Çalmaşur, Ö. Aslan, İ. Kaya, O. (2007). Insecticidal effect of essential oil of *Origanum acutidens* against several stored product pest. Fresenius Environmental Bulletin, 16, 1395–1400.

[9] Çetin, H. Yanıkoğlu, A. (2006a). A study of the larvicidal activity of *Origanum* (Labiatae) species from southwest Turkey. Journal of Vect. Ecol., 31, 118-122.

[10] Çetin, H. Erler F. Yanıkoğlu A. (2006b). Toxicity of essential oils extracted from *Origanum onites* L. and *Citrus aurentium* L. against the pine processionary moth, *Thaumetopoea wilkinsoni* Tarns., Folia biologica, (Krakow), 54, 153-157.

[11] Davis, P. H. (1982). Flora of Turkey and the East Aegean Islands. vol. 7. Edinburgh University Press, Edinburgh, pp. 297–313.

[12] Don-Pedro, K. N., (1996). Investigation of single and joint fumigant insecticidal action of

citruspeel oil components. Pestic. Science, 46, 79–84.
[13] Daouk, R. K. Dagher, S. M. Sattout, E. J. (1995). Antifungal activity of the essential oil of *Origanum syriacum* L. J. Food Protect., 58, 1147–1149.
[14] Esen, G. Azaz, A. D. Kürkçüoğlu, M. Baser, K. H. C. Tinnaz, A. (2007). Essential oil andantimicrobial activity of wild and cultivated *Origanum vulgare* L. subsp. *Hirtum* (Link) letswaart from the Marmara region, Turkey. Flavour Fragr. J., 22, 371–376.
[15] Göktürk, T. Kordalı, Ş. Çalmaşur, Ö. Tozlu, G. (2011). Insecticidal effects of essential plant oils against larvae of Great Spruce Bark Beetle, *Demdroctonus micans* (Kuelann) (Coleoptera: Curculionidae: Scolytinae). Fresenius Environmental Bulletion, 20, 2365-2370.
[16] Isman, M. B. (2006). Botanical insecticides, deterrents, and repellents in modern agriculture and an increasingly regulated world. Annual Review of Entomology, 51, 45-66.
[17] Isman, M. B. Wan, A. J. Passreiter, C. M. (2001). Insectical activity of essential oils to the tobacco cutworm, *Spodoptera litura*. Fitoterapia,72, 65–68.
[18] Kesdek, M. Bayrak, N. Kordalı, Ş. Usanmaz, A. Contuk, G. Ercişli, S. (2013). Larvicidal effects of some essential oils against larvae of the pine processionary moth, *Thaumetopoea pityocampa* (Denis & Schiffermüller) (Lepidoptera: Thaumetopoeidae). Egyptian Journal of Biological Pest Control, 23, 2, 201-207.
[19] Khalfi, O. Sahraoui, N. Bentahar, F. Boutekedjiret, C. (2008). Chemical compositionand insecticidal properties of *Origanum glandulosum* (Desf.) essential oil from Algeria. Journal of the Science of Food and Agriculture, 88, 1562–1566.
[20] Khani A. Asghari, J. (2012). Insecticide activity of essential oils of *Mentha longifolia*, *Pulicaria gnaphalodes* and *Achillea wilhelmsii* against two stored product pests, the flour beetle, *Tribolium castaneum,* and the cowpea weevil, *Callosobruchus maculatus.* Jour. of Insect Sci.,12, 73,1-10.
[21] Kızıl, S. Uyar, F. (2006). Antimicrobial activities of some thyme (*Thymu*s, *Satureja*, *Origanum* and *Thymbra*) species against important plant pathogens. Asian J. Chem., 18, 1455–1461.
[22] Kim, D. H. Ahn, Y. J. (2001). Contact and fumigant activities of constituents of *Foeniculum vulgare* fruit against three Coleopteran stored-product insects. Pest Manag. Sci., 57, 301–306.
[23] Kordali, Ş. Aslan, İ. Çalmaşur, Ö. Çakır, A. (2006). Toxicity of essential oils isolated from three *Artemisia* species and some of their major components to granary weevil, *Sitophilus granarius* (L.) (Coleoptera: Curculinonidae). Indust. Crops Prod., 23, 2, 162–170.
[24] Kordali, Ş. Çakır, A. Özer, H. Çakmakcı, R. Kesdek, M. Mete, E. (2008). Antifungal, phytotoxic and insecticidal properties of essential oil isolated from Turkish *Origanum acutidens* and its three components, carvacrol, thymol and p-cymene. Bioresource Technology, 99, 8788–8795.
[25] Kordali, Ş. Emsen, B. Yıldırım, E. (2013). Fumigant toxicity of essential oils from fifteen plant species against *Sitophilus zeamais* Motschulsky (Coleoptera: Curculionidae). Egyptian Journal of Biological Pest Control, 23, 2, 241-246.
[26] Konemann, B. (1999). The Illustrated A–Z of over 10,000 Garden Plants and How to Cultivate Them Gordon. Cheers Publication, Hong Kong, p. 885.
[27] Lee, S. Tsao, R. Peterson, C. Coast, J. R. (1997). Insecticidal activityof monoterpenoids to western corn rootworm (Coleoptera:Chrysomelidae), two spotted spider mite (Acari: Tetranychidae), and house fly (Diptera: Muscidae). J. Econ. Entomol., 90, 883–892.
[28] Lee, S. Peterson, C. J. Coats, J. R.(2003). Fumigation toxicity of monoterpenoids to several stored product insects. J. Stored Prod. Res., 39, 77–85.
[29] Mahfuz, I. M, Khalequzzaman. (2007). Contact and fumigant toxicity of essential oils against *Callosobruchus maculatus*. University Journal Zoology, Rajshahi Univ., 26, 63-66.
[30] Mahmoudvand, M. Abbasipour, H. Hosseinpour, M. H. Rastegar, F. Basij, M. (2011). Using some Plant essential oils as natural fumigants against adults of *Callosobruchus maculatus* (F.) (Coleoptera: Bruchidae). Munis Entomology & Zoology, 6,150-154.
[31] Michaelakis, A. Theotokatos, S. A. Koliopoulos, G. Chorianopoulos, N. G. (2007). Essential oils of *Satureja* species: Insecticidal effect on *Culex pipiens* larvae (Diptera: Culicidae). Molecules, 12, 2567-2578.
[32] Mollaei, N. Izadi, H. Dashti, H. Azizi, M. Ranjbar-Karimi, R. (2011). Bioactivity of essential oil from *Satureja hortensis* (Laminaceae) against three stored-product insect species. African Journal of Biotechnology, 10, 34, 6620-6627.
[33] Mollah, J. U. Islam, W. (2007). Toxicity of *Thevetia peruviana* (Pers) Schum. extract to adults of *Callosobruchus maculatus* F. (Colleoptera: Bruchidae). Journal of Agricultural and Rural Development, 5, 105-109.

[34] Mousavi, M. Valizadegan, O. (2014). Insecticidal effects of *Artemisia dracunculus* L. (Asteraceae) essential oil on adult of *Aphis gossypii* Glover (Hemiptera: Aphididae) under laboratory conditions. Archives of Phytopathology and Plant Protection, 47, 14, 1737-1745.

[35] Papachristos, D. P. Karamanoli, K. I. Stamopoulos, D. C. Menkissoglu-Spiroudi, U. (2004). The relationship between the chemical composition of three essential oils and their insecticidal activity against *Acanthoscelides obtectus* (Say). Pest Manag. Sci., 60, 514–520.

[36] Park, I. K. Lee, S. G. Choi, D. H. Park, J. D. Ahn, Y. J. (2003). Insecticidal activities of constituents identified in the essential oil from leaves of *Chamaecyparis obtuse* against *Callosobruchus chinensis* (L.) and *Sitophilus oryzae* (L.). J. Stored Prod. Res., 39, 375–384.

[37] Prates, H. T. Santos, J. P. Waquil, J. M. Fabris, J. D. Oliveira, A. B. Foster, J. E. (1998). Insecticidal activity of monoterpenes against *Rhyzopertha dominica* (F.) and *Tribolium castaneum* (Herbst). J. Stored Prod. Res., 34, 243–249.

[38] Rafiei-Karahroodi, Z. Moharramipour, S. Farazmand, H. et al., (2011). J. Insectıcıdal effect of six native medicinal plants essential oil on ındıan meal moth, Plodia Interpunctella Hübner (lep.: pyralıdae),'' Mun. Ent. Zool, Vol. 6, No. 1, January.

[39] Rauf Tak, I. Dawood, M. Ganai, B. A. Chishti, M. Z. Ahmad, F. Dar, J. S. (2014). Phytochemical studies on the extract and essential oils of *Artemisia dracunculus* L. (Tarragon). African Journal of Plant Science, 8, 1, 72-75.

[40] Regnault-Roger, C. Hamraoui, A. (1995). Fumigant toxic activity and reproductive inhibition induced by monoterpenes on *Acanthoscelides obtectus* (Say) (Coleoptera), a bruchid of kidney bean (*Phaseolus vulgaris* L.). Journal of Stored Products Research, 31, 291-299.

[41] Sampson, B. J. Tabanca, N. Kirimer, N. Demirci, B. Başer, K. H. C. Khan, I. A. Spiers, J. M. Wedge, D. E. (2005). Insecticidal activity of 23 essential oils and their major compounds against adult *Lipaphis pseudobrassicae* (Dav.) (Aphididae:Homoptera). Pest Man. Sc., 61, 1122–1128.

[42] Santos, J. C. Faroni, L. R. D. A. Simões, R. O. Pimentel, M. A. G. Sousa, A. H. (2009). Toxicity of pyrethroids andorganophosphorus insecticides to Brazilian populations of *Sitophilus zeamais* (Coleoptera: Curculionidae). Bioscience Journal, 25, 75-81.

[43] Satıl, F. Dirmenci, T. Tümen, G. Turan, Y. (2008). Commercial and ethnic uses of Satureja (Sivri kekik) species in Turkey. Ekoloji, 67, 1-7.

[44] Sokovic, M. Tzakou, O. Pitarakoli, D. Couladis, M. (2002). Antifungal activities ofselected aromatic plants growing wild in Greece. Nahrung/Food, 46, 5, 317–320.

[45] Taghizadeh, A. Moharramipour, S. Meshkatalsadat, M. H. (2010). Insecticidal properties of *Thymus persicus* essential oil against *Tribolium castaneum* and *Sitophilus oryzae*. Journal of Pest Science, 83, 3-8.

[46] Ved, D. K. Goraya, G. S. (2008). Demand and supply of medicinal plants in India. Bishan Singh Mahendra Pal Singh, Dehradun & FRLTH, Bangalore, India.

[47] Yıldırım, E. Kesdek, M. Aslan, İ. Çalmaşur, Ö. Şahin, F. (2005). The effects of essential oils from eight plant species on two pests of stored product insects. Fresen. Environ. Bull., 14, 23–27.

[48] Yıldırım, E. Kordali, S. Yazıcı, G. (2011). Insecticidal effects of essential oils of eleven plant species from Lamiaceae on *Sitophilus granarius* (L.) (Coleoptera: Curculionidae). Romanian Biotech. Lett., 16, 6702-6709.

Received: **16.11.2015**
Accepted: **12.03.2016**

CORRESPONDING AUTHOR

Ayse Usanmaz Bozhüyük
Igdir University Faculty of Agriculture Department of Plant Protection 76000, Igdir, TURKEY

e-mail: ayseusanmaz@hotmail.com

© by PSP Volume 25 – No. 7/2016, pages 2628-2638 Fresenius Environmental Bulletin

BASED ON 3S TECHNOLOGY LANDSLIDE ENVIRONMENTAL IMPACT FACTORS EVALUATION AND MONITORING RESEARCH IN ARID REGION

Yifeng Cheng [1,2] , Zhihui Liu [1,*]

1. College of Resources and Environmental Science, Key Laboratory of Oasis Ecology of Ministry of Education，Xinjiang University, Urumqi 830046, China;

2. Xinjiang surveying and mapping archives museum (Xinjiang basic geographic information center)，Urumqi 830002,China

ABSTRACT

This study has used 3S technology to interpret landslide disasters in Xinyuan County in Xinjiang, which is in the arid region of northwest China. Field verifications were performed to explore the spatial distribution of landslide hazards. Data-driven theory, a weighted evidence-based model for landslide environmental impact evaluation, susceptibility zoning, and hazard zoning were investigated. An online landslide monitoring system with perception, network, and application layers using Internet of Things technology and based on rain gauges, GPS devices, crack meters, inclinometers, and other sensors will gather information transmitted through the network layer to the application layer of the landslide monitoring system, which will process high-accuracy deformation information and perform early warning analysis. The results showed that 514 landslide hazard points were identified in the study area. Elevation, slope, aspect, lithology, geological faults, and water were shown to be the main environmental factors influencing landslides. In the study area, those areas that were highly susceptible to landslides occupied an area of 674 km^2, moderately susceptible areas 1820 km^2, less susceptible areas 3479 km^2, and non-susceptible areas 1616 km^2. The landslide high-risk area covered 742.51km^2, the moderate-risk area 1816.21km^2, and the low-risk area 5030.46 km^2. A landslide monitoring system that periodically monitors landslide points can be used to obtain accurate information on changes in landslide risk for warning and analysis.

KEYWORDS:
Arid region of Xinjiang; 3S technology; landslide; environmental factor; things; landslide monitoring

INTRODUCTION

According to the National Geological Disasters 2009–2014 briefing statistics in China, the number of landslide disasters occurring in China each year accounted for more than 70% of the total number of geological disasters in the country for that year. Because of the enormous destructive force of landslides and the hazard they pose to the ecological environment, residential and business properties, and human lives, they have attracted the attention of researchers worldwide. Since the 1950s, classifications of form, movement mechanics, sedimentology, and other research studies have been carried out on landslide disasters in China [1]. Elsewhere in the world, landslides have been the object of 100 years of research [2–18].In 1984, Varnes proposed the most widely accepted classification and established the zoning principles that were used in the landslide risk zoning study of the United Nations [19]. In 1998, based on the principles of Varnes, Chuan Tang proposed a technical framework for landslide hazard assessment [20]. On this basis, the principal component superposition method, the gray system evaluation method, fuzzy logic, and multi-factor comprehensive evaluation of knowledge-driven research methods have been widely used to study landslide hazards. Application of these methods depends heavily on experts and researchers with the professional experience to carry out the study based on evaluation of the actual area, subjectivity, and uncertainty. Data-driven methods, including a large amount of evidence and a landslide hazard distribution data history, have been used to determine the statistical environmental impact of different categories of hazard patterns and of large and small factors on landslide disasters. Landslide distribution data for different evaluation periods have been used to make predictive test results more realistic and accurate.

An arid region in Xinyuan County, Xinjiang (western China) was chosen as the study area. The area is characterized by crustal faults, soft geological formations, and many fractured mountains, which constitute a hidden high potential for unstable slopes under heavy rainfall

and similar conditions, and are likely to cause landslides and other geological disasters. Using multi-temporal, multi-scale remote-sensing data and making full use of 3S technology, the weights of the evidence-based model were calculated to evaluate landslide impact factors in the study area and to explore the distribution of the main environmental impact factors. Quantitatively, landslide-prone zoning and dangerous landscape categories were evaluated, using the perception, network, and application layers with the Internet of Things technology to provide early warning and monitoring of landslides online. 3S technology was used to provide a scientific validation environment for landslide impact factor assessment and early warning in arid areas.

MATERIAL AND METHODS

Study area. Xinyuan County is located in northwestern China at longitude 82°28'–84°56'E, latitude 43°03'–43°40'N (Figure 1) and occupies an area of 7589 km2 at an altitude of 747–4229 m. The region has a typical continental semi-arid climate, with annual average temperature of 6.1–9.3°C and annual precipitation of 270–880 mm. The main mountain ranges are the Andier Mountains to the northeast, the Nalati Mountains to the south, and Mount Aburele to the north. Soils are distributed in vertical bands, with significant amounts of sierozem, chernozem, and millet calcium soil. The main rivers are the Kunas, Qiapu, Jiergalang, and Turks Rivers.

FIGURE 1
Research area sampling station.

Remote-sensing interpretation and field verification. DOM data with a resolution of 0.5 meters in 2012 WorldView-2 and Quickbird images were used. DEM data and TM images were downloaded from the Chinese Academy of Sciences Data Cloud, with a resolution of 30 meters for the ASTER GDEM data and 30 meters for the 2011 TM images. The ENVI4.6 and ArcGIS10.0 software packages were used for correction of image geometric precision, mosaicking and cutting, atmospheric correction, image enhancement, and other preliminary and three-dimensional modeling activities. By visual interpretation of remote-sensing images combined with field verification, the spatial distribution of landslide hazards in the study area was determined.

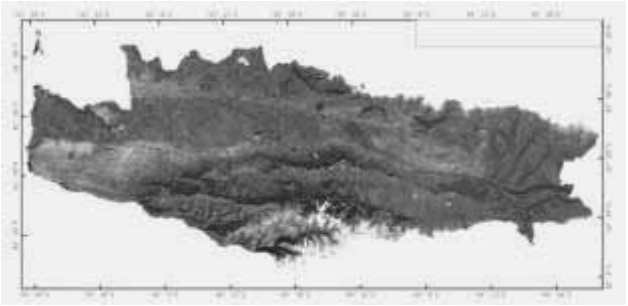

FIGURE 2
Research area landslide hazard distribution.

Analysis of spatial distribution. Using the ArcGIS10.0 software, elevation, slope, and aspect data were extracted from DEM data and road and water data from a 1:100000 topographic map of the study area. NDVI data were extracted from TM images, a study of geological faults and the lithology distribution process was completed, and by superimposing landslide point information data, a complete spatial statistical analysis of the environmental impact of landslides in the study area was carried out.

Evaluation model for environmental impact factors of landslides. A weighted evidence-based model based on Bayesian conditional probabilities was constructed, which could determine the level of evidence of mineralization with an accuracy close to that of mathematical methods using its weight values and could then calculate the probability of mineral development in a particular spatial location, with the objective of defining several levels of forecast targets. The weighted evidence-based approach is based on the number of the smallest pre-analysis units in the study area, the binary evidence maps, landslide disaster events, and posterior probabilities. Each of the environmental impact factors is considered as evidence influencing the landslide hazard zoning factor, and the contribution of each factor to the initial landslide hazard partition is determined by the weighting factor values. In the calculations, each landslide hazard zone is assumed to occupy a small area or a set of individual units, enabling the probability point position to be defined as the probability per unit area, which can be calculated as follows:

$$P\{D\} = N\{D\} / N\{T\} \quad (1)$$

After the probability = probability × evidence before factor factor (2)

$$\log it = \log_e [P / (1 - P)] \quad (3)$$

TABLE 1
The significance level relations of Studentized C and C.

Studentized(C)	0.253	0.542	0.842	1.282	1.645	1.96	2.326	2.576
C value of the significance level	60%	70%	80%	90%	95%	97.50%	99%	99.50%

$$W^+ = \log_e \frac{P\{B/D\}}{P\{B/\overline{D}\}} \quad (4)$$

$$W^- = \log_e \frac{P\{\overline{B}/D\}}{P\{\overline{B}/\overline{D}\}} \quad (5)$$

$$C = W^+ - W^- \quad (6)$$

$$StudentizedC = C/\sigma \quad (7)$$

where P represents the probability of an event; the prior probability P{D} represents the probability of missing evidence given that an event has occurred; B represents the number of units of a factor in the region under consideration; the complement of B represents the number of unit areas in which B does not exist; affects every layer of evidence that a landslide disaster has occurred before the probability represented by the weight and the number obtained by adding the number of posterior probabilities; and W^+, W^- represent respectively evidence of the existence region weighting factor for the region under consideration and evidence for the absence of the factor in the region. The posterior probabilities then undergo a logarithmic mathematical transformation to produce the landslide hazard zoning map. The correlation coefficient C is the correlation between the index and the evidence factor training points. The Studentized C represents the degree of certainty of the correlation coefficient C. σ is the standard deviation of C, which when the Studentized C is greater than 1.5, indicates a significant value of C (Table 1) [21].

Each grid cell was 30 × 30 m in size. With each click representing a landslide as a sequential verification point, 51 verification points were randomly chosen, with the remaining points used as training data. ArcGIS SDM was used to calculate the weights for evidence-based analysis. Elevation, slope, aspect, lithology, geological faults, water, and road data were converted into a continuous 8-bit unsigned integer GRID format. The Spatial Data Modeller Tools software was used to conduct landslide environmental impact analysis and to study the area weighting of the landslide susceptibility and hazard zoning classifications.

Construction landslide online monitoring platform based on Internet of Things technology. A representative study area was selected as Jialangpute, Batebahesayi, and a wild fruit forest improvement field, including three landslide disaster points (Figure 2). Using rain gauges, inclinometers, crack meters and other sensors, ground subsidence, cracking, and displacement data were transmitted via GPRS data in real time to an online landslide monitoring and warning system monitoring center, where the overall surveillance of real-time landslide security status is carried out, while landslide disaster-prone points in the study area are periodically monitored.

RESULTS

Landslide Distribution. Visual interpretation of landslide hazards in the study area revealed a total of 653 landslide occurrences in the field (Figure 3a), and handheld GPS instruments were used to verify a total of 514 points representing landslide disasters (Figure 3b).

The largest number of landslides occurred in the range of 1100–2600 m, representing 96.69% of the total. In the ranges from 800 to 1100 m, 2600 to 2900 m, and 3200 to 3500 m, only isolated points of the landslide distribution were found. (Figure 4a).

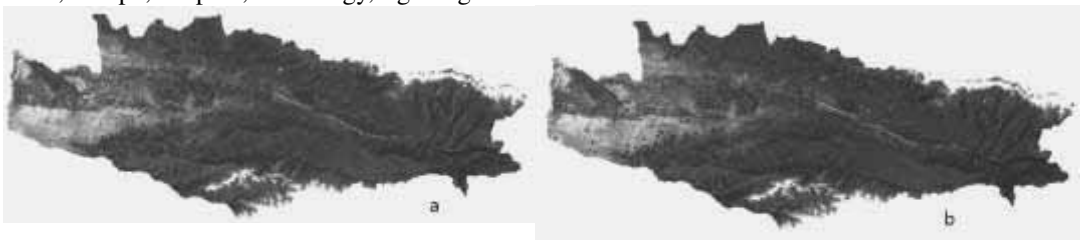

FIGURE 3
Research area landslide hazard interpretation map
(a:Remote sensing interpretation map, b: landslide hazard distribution).

As for slope distribution, landslide points within the range of 0°–40° accounted for 97.86% of the total. (Figure 4b). With regard to spatial orientation, in the ranges of 337.5°–22.5°, 22.5°–67.5°, 67.5°–112.5°, 112.5°–157.5°, 157.5°–202.5°, 202.5°–247.5°, 247.5°–292.5°, 292.5°337.5°aspect, landslide points ranged from 53 to 75, accounting for 10.7% to 14% of the total(Figure 4c).

Landslide hazard was found mainly in quartzite, basaltic andesite, sandstone layered rocks of the hard group, alluvial, gravel, sand, loam and loess granite hard crystalline rock group, with the three lithology distributions accounting for 97.67% of the landslides in the study area. Areas where quartzite, basaltic andesite, and hard sandstone layered clastic group are widespread accounted for 50.19% of the landslides in the study area. (Figure 4d).

In areas with geological faults, in zones within 5000 m of a fault, 487 landslides were identified, accounting for 94.74% of the total. Areas within 500 m of a fault had 131 points representing landslide disasters, accounting for 25.48%. Areas at distances from 500 to 2500 m had 267 points, accounting for 51.94%. (Figure 4e).

In zones within 5000 m of a river, 468 landslides were identified, accounting for 91.05% of the total. Areas within 200 m of a river had 49 points. The zones from 200 to 400 m, 400 to 600 m, and 600 to 800 m accounted for about 7% of the total number of landslides. Areas at distances of 1000 to 2000 m from a river had129 landslides. Areas at distances of 2000 to 3000 m had 86 landslides. Areas at distances of 3000 to 4000 m had 59 landslides(Figure 4f).

In zones within 100 m of a road, 15 landslides occurred.Within 100 to 200 m of a road, 19 landslides occurred. Within 200 to 300 m of a road, there were 14 landslides. Within 300 to 400 m of a road, there were 16 landslides. The zone from 400 to 500 m of a road experienced 12 landslides. Within 500 to 1000 m of a road, there were 63 landslidesl. Within 1500 to 2000 m of a road, there were 71 landslides. Within 2000 m of a road, there were 210 landslides. It follows that the

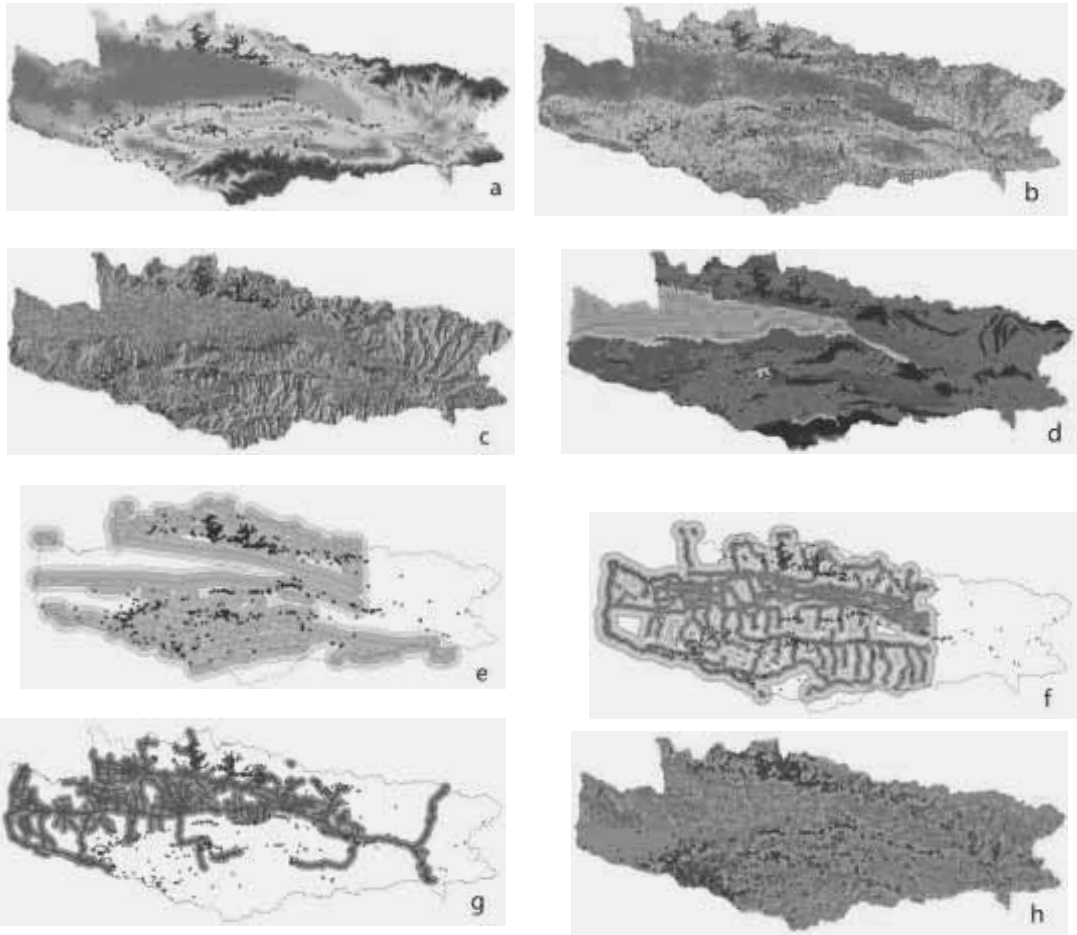

FIGURE 4
The distribution of landslide hazard and environment impact factors
(a: elevation, b: Slope, c: Aspect, d: Lithology, e: Geological faults, f: river, g: road, h:NDVI).

effect of distance from roads on landslide disasters is not dominant in the study area (Figure 4g).
Areas with NDVI values between -1 and 0.5 had 68 landslide disasters. Areas with NDVI values between 0.5 and 0.6 had 99 landslides. Areas with NDVI values between 0.6 and 0.7 had 169 landslides. Areas with NDVI values between 0.7 and 0.8 had 176 landslides. It is apparent that the distribution of landslide hazards becomes denser with increasing NDVI, but that this effect is not dominant in the study area (Figure 4h).

Establishment and evaluation of the environmental impact assessment model.

Environmental impact factor weight calculation. As shown in Tables 2–7, Student's C values were greater than 1.5, indicating a high significance level, under the following conditions: elevation 1100–2000; slope 15°–30° or 35°–45°; rock groups including quartzite, basaltic andesite, sandstone hard layered rocks, alluvial, gravel, sand, loam loess, granite hard crystalline rock group, sandy mudstone, siltstone, and sandstone conglomerate hard-soft white rocks; presence of a fault within 500 m. With respect to river buffer distance, the Student's C values were less than 1.5, indicating low significance.

TABLE 2
The weight calculation result of elevation and landslide.

Elevation class（m）	Number	Area（km^2）	Statistics Unit	W^+	W^-	Studentized C
0-800	0	127.6082	2552.1645	0	0	0
800-1100	2	1645.5759	32911.5178	-2.3092	0.2233	-7.9202
1100-1400	**124**	**972.8251**	**19456.5014**	**0.6105**	**-0.1316**	**6.7582**
1400-1700	**233**	**758.5374**	**15170.7473**	**1.5425**	**-0.5162**	**21.9921**
1700-2000	**109**	**1038.0787**	**20761.5739**	**0.4383**	**-0.091**	**4.6424**
2000-2300	20	931.3412	18626.8247	-1.1516	0.0916	-5.1678
2300-2600	11	734.2844	14685.6881	-1.5019	0.0802	-4.9468
2600-2900	2	538.5175	10770.3506	-2.8018	0.0695	-4.0514
2900-3200	0	420.2304	8404.6079	0	0	0
3200-3500	3	288.9546	5779.0912	-2.179	0.0346	-3.1232
3500-3800	0	117.1717	2343.4344	0	0	0
3800-4229	0	16.2975	325.9498	0	0	0

TABLE 3
The weight calculation result of Slope and landslide.

Slope Class（°）	Number	Area（km^2）	Statistics Unit	W^+	W^-	Studentized C
0-10	76	2649.5771	2649.5771	-0.9491	0.2992	-9.1766
10-15	57	1052.2877	1052.2877	-0.1448	0.0217	-1.1362
15-20	**87**	**928.4295**	**928.4295**	**0.3725**	**-0.0629**	**3.3949**
20-25	**87**	**841.7365**	**841.7365**	**0.494**	**-0.0794**	**4.4729**
25-30	**76**	**736.7767**	**736.7767**	**0.4799**	**-0.0657**	**4.0127**
30-35	46	595.6823	595.6823	0.1549	-0.0142	1.0082
35-40	**49**	**418.7120**	**418.7120**	**0.458**	**-0.0332**	**2.7999**
40-45	**25**	**233.8370**	**233.8370**	**0.5182**	**-0.0209**	**2.396**
45-90	9	132.3838	132.3838	-0.1516	0.0025	-0.3939

TABLE 4
The weight calculation result of Aspect and landslide.

Aspect Class（°）	direction	Area（km^2）	Statistics Unit	W^+	W^-	Studentized C
-1	flat	3.7747	3.7747	0	0	0
0-22.5	North	508.1556	508.1556	0.2184	-0.0174	1.3401
22.5-67.5	northeast	928.1066	928.1066	0.0439	-0.0063	0.3484
67.5-112.5	east	892.5137	892.5137	0.0299	-0.0041	0.231
112.5-157.5	southeast	781.3925	781.3925	0.0721	-0.0086	0.5254
157.5-202.5	south	913.7553	913.7553	0.1478	-0.0218	1.2153
202.5-247.5	southwest	984.5478	984.5478	-0.1327	0.0185	-1.0073
247.5-292.5	Western	1092.7572	1092.7572	-0.0107	0.0018	-0.0908
292.5-337.5	northwest	1009.0307	1009.0307	-0.2201	0.0303	-1.6285
337.5-360	North	475.3884	475.3884	-0.116	0.0073	-0.5937

TABLE 5
The weight calculation result of Lithology and landslide.

Lithology	Area (km²)	Statistics Unit	W+	W-	Studentized C
Quartzite, basaltic andesite, sandstone hard layered clastic group	**3622.9905**	**3622.9905**	**0.1739**	**-0.186**	**3.7251**
Alluvial, gravel, sand, loam loess	**1259.5131**	**1259.5131**	**0.1572**	**-0.034**	**1.5654**
Granite hard crystalline rock group	**961.2135**	**961.2135**	**0.2201**	**-0.0357**	**1.9216**
Sandy mudstone, siltstone, sandstone conglomerate hard - soft white rocks group	**31.4388**	**31.4388**	**2.2514**	**-0.0235**	**6.1433**
Gravelly silty loam soil monolayer structure	425.6379	425.6379	-0.1757	0.0096	-0.8258
Alluvial, gravel, sand, gravelly loam soil multilayer structure	1288.4166	1288.4166	-2.3417	0.1806	-7.046

TABLE 6
The weight calculation result of Geological faults and landslide.

Fault buffer distance (m)	Number	Area(km²)	Statistics Unit	W+	W-	Studentized C
0-500	**131**	**1262.4291**	**1262.4291**	**0.3953**	**-0.1137**	**4.5225**
500-1000	87	1054.7325	1054.7325	0.1535	-0.0308	1.4287
1000-1500	66	872.3214	872.3214	0.0254	-0.0038	0.2001
1500-2000	62	735.3189	735.3189	0.1322	-0.0173	0.9908
2000-2500	52	623.2023	623.2023	0.1377	-0.015	0.9435
2500-3000	31	542.7621	542.7621	-0.2442	0.0191	-1.3121
3000-4000	39	889.5672	889.5672	-0.4422	0.0543	-2.8582
4000-5000	19	765.2052	765.2052	-1.1172	0.0867	-4.8072

TABLE 7
The weight calculation result of river and landslide.

River buffer distan (m)	Number	Area (km²)	Statistics Unit	W+	W-	Studentized C
0-200	49	594.7659	594.7659	0.1304	-0.0141	0.8735
200-400	37	581.1642	581.1642	-0.1852	0.0168	-1.0672
400-600	36	544.9806	544.9806	-0.0525	0.0047	-0.3096
600-800	40	503.7741	503.7741	-0.0004	0	-0.0021
800-1000	32	461.5695	461.5695	0.1571	-0.0131	0.9271
1000-1500	75	997.5942	997.5942	-0.0915	0.016	-0.7471
1500-2000	54	814.8366	814.8366	-0.1136	0.0156	-0.8166
2000-3000	86	1194.3648	1194.3648	0.05	-0.0117	0.484
3000-4000	59	746.9838	746.9838	0.1055	-0.0146	0.794

Reclassification. As shown in Tables 8–13, after reclassification, the Student's C values were greater than 1.5, indicating high significance, under the following conditions: elevation 1100–2000 m; slope 15°–30° or 35°–45°; orientation 0°–22.5° or 157.5°–202.5°; lithology of quartzite, basaltic andesite, sandstone hard layered rocks group, alluvial, gravel, sand, loam loess, granite hard crystalline rock group, sandy mudstone, siltstone, or sandstone conglomerate hard-soft white rocks group; geological fault buffer distance less than 500 m; and river buffer distance less than 200 m, 800–1000 m, or 2000–4000 m. The landslide weighting factor classification table is shown in Figure 5.

TABLE 8
The weight calculation result of reclass elevation and landslide.

Elevation class（m）	Area（km^2）	Statistics Unit	W^+	W^-	Studentized C
0-800、2900-3200、3500-4229	681.6528	6816.528	0	0	0
800-1100、2000-2900、3200-3500	4138.2837	41382.837	-1.7987	0.6991	-15.4201
1100-2000	**2769.5439**	**27695.439**	**0.9222**	**-1.9513**	**17.7382**

TABLE 9
The weight calculation result of reclass Slope and landslide.

Slope Class（°）	Area（km^2）	Statistics Unit	W^+	W^-	Studentized C
0-15、45-90	3833.4132	38334.132	-0.5155	0.3458	-8.4907
30-35	**595.62**	**5956.2**	**0.4537**	**-0.0499**	**3.5447**
15-30、35-45	**3160.4472**	**31604.472**	**0.3242**	**-0.3176**	**6.8064**

TABLE 10
The weight calculation result of reclass Aspect and landslide.

Aspect Class（°）	Area（km^2）	Statistics Unit	W^+	W^-	Studentized C
202.5-360、-1	3610.0746	36100.746	-0.1173	0.0958	-2.2579
22.5-157.5	2602.5003	26025.003	0.0688	-0.0378	1.1026
0-22.5、157.5-202.5	**1376.9055**	**13769.055**	**0.1449**	**-0.0351**	**1.5706**

TABLE 11
The weight calculation result of reclass Lithology and landslide.

Lithology	Area（km^2）	Statistics Unit	W^+	W^-	Studentized C
Quartzite, basaltic andesite, sandstone hard layered clastic group	**3622.9905**	**36229.905**	**0.1635**	**-0.1766**	**3.6198**
Alluvial, gravel, sand, loam loess	**1259.5131**	**12595.131**	**0.1479**	**-0.0322**	**1.5216**
Granite hard crystalline rock group	**961.2135**	**9612.135**	**0.2066**	**-0.0338**	**1.8679**
Sandy mudstone, siltstone, sandstone conglomerate hard - soft white rocks group	**31.4388**	**314.388**	**1.8664**	**-0.0222**	**6.3354**
Gravelly silty loam soil layer structure, the alluvial, gravel, sand, gravelly loam soil multilayer structure	1714.0545	17140.545	-1.253	0.1903	-7.6369

TABLE 12
The weight calculation result of reclass Geological faults and landslide.

Fault buffer distance（m）	Area（km^2）	Statistics Unit	W^+	W^-	Studentized C
0-500	**1262.4291**	**12624.291**	**0.3672**	**-0.1074**	**4.3875**
500-1000	1054.7325	10547.325	0.1438	-0.0291	1.3861
1000-2500	2230.8426	22308.426	0.0875	-0.0462	1.3386
2500-5000	2197.5345	21975.345	-0.5446	0.1854	-5.9736

TABLE 13
The weight calculation result of reclass river and landslide.

River Buffer distance（m）	Area（km^2）	Statistics Unit	W^+	W^-	Studentized C
0-200、800-1000、2000-4000	**2997.684**	**29976.84**	**0.091**	**-0.0864**	**1.8158**
200-800、1000-2000	3442.3497	34423.497	-0.0864	0.091	-1.8158

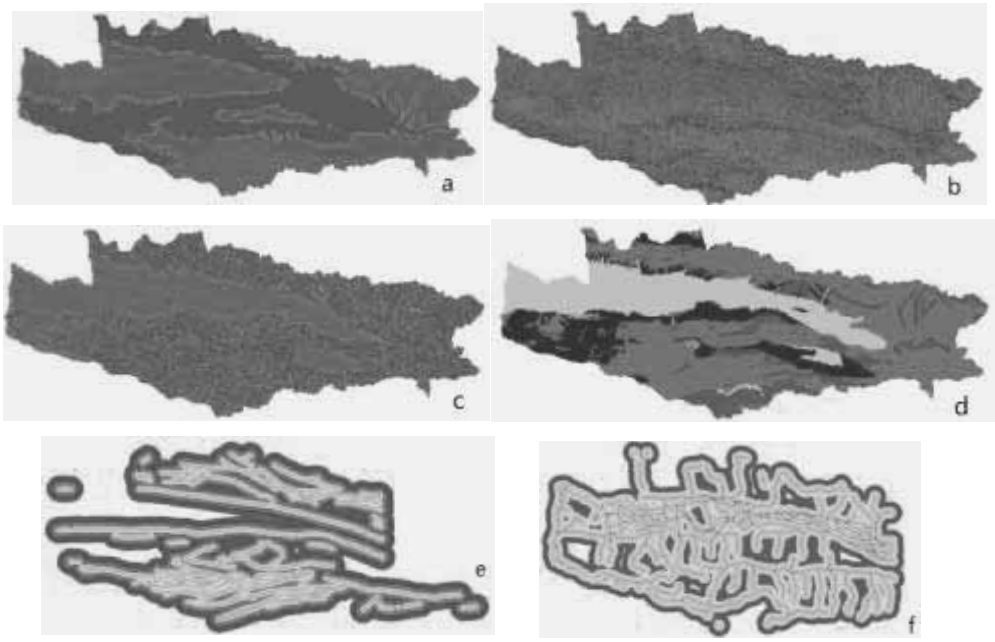

FIGURE 5
The distribution of landslide hazard and environment impact factors in Weight of evidence (a: elevation, b: Slope, c: Aspect, d: Lithology, e: Geological faults, f: road).

Landslide susceptibility and hazard zoning.

Landslide susceptibility zoning. Research area landslide susceptibility zoning as shown in Figure 6.

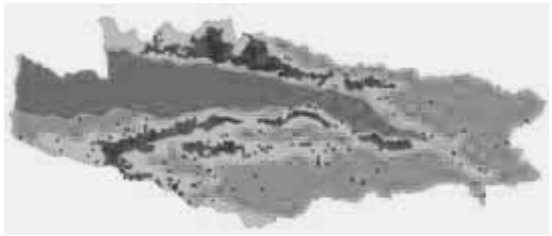

FIGURE 6
Research area landslide susceptibility zoning.

(1) High-susceptibility areas include the northern portion of the Kunas Valley, the hilly areas around the Awulale Mountains, the south side of Yishijilike Hill, the mountain sides of the Nalati watershed, and along the Qiapu River to the south. These areas total 674 km^2, accounting for 8.88% of the study area. The area includes 336 landslide disaster zone distribution points.

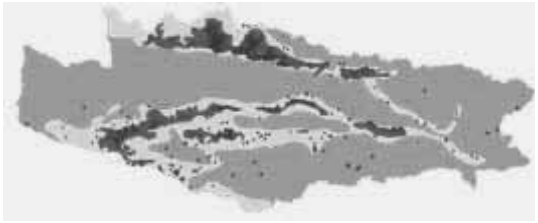

FIGURE 7
Research area landslide hazard zoning.

(2) Moderately susceptible areas in Xinyuan County include the northern part of the Awulale Mountains, around the Tiemulike-Lejiakebu Lake, along the Tuergengsayi River, and the Kansu Valley upstream and downstream around the high-susceptibility areas. Susceptible areas also in Xinyuan County include the southern portion of Yishijilike Hill and the sides of the Nalati Mountain watershed, the upstream part of the southern Qiapu River, around the high-susceptibility Taledesayi and Atibiekesayi areas, and the valley north of the Jiergalang River

TABLE 14
Research area landslide susceptibility zoning statistics.

Classification	Zoning area（km^2）	proportion of the study area	Number Landslide
High-prone areas	674	8.88%	336
prone areas	1820	23.98%	153
Low-prone areas	3479	45.84%	23
Easy-prone areas	1616	21.29%	0

TABLE 15
Research area landslide hazard zoning statistics.

Classification	Zoning area （km^2）	proportion of the study area	Number Landslide
high-risk area	742.51	9.78%	341
middle-risk area	1816.21	23.93%	151
Low-risk area	5030.46	66.28%	23

along the mountain pass. These areas cover 1820 km^2 and account for 23.98% of the study area. They include 153 landslide disaster zone distribution points.

(3) Low-susceptibility areas are distributed in a large area around Xinyuan County High School in the southern forested mountainous and hilly areas above and in the northern Shandong section of the Awulale high mountains. These areas cover 3479 km^2 and account for 45.84% of the study area. They include 23 landslide disaster zone distribution points.

(4) Non-susceptible areas are located in the Kunas Valley plain area, which covers 1616 km^2 and accounts for 21.29% of the study area. No landslide hazards exist in this region.

Landslide hazard zoning. The study area for landslide hazard zoning is shown in Figure 7 and can be categorized as follows:

(1) ***High-risk area***. This area includes the Kunas Valley in Xinyuan County on both sides of the mountains, on both sides of the southern Talede Mountain watershed, along the southern Qiapu River, east of Alemale, the northern valley north of Zeketai town and Awulale on the south side of the mountain. These areas cover 742.51 km^2, account for 9.78% of the study area, and have experienced 341 landslide disasters.

(2) ***Moderate-risk area***. This area is located in southern Xinyuan County, including the Kunas Valley, Talede Mountain, Taledesayi, Atibiekesayi, Taledesayi upstream, the area north of the upstream part of the Jiergalang River, Bayintale, and The northern part of the Kunas Valley (Awulale, Moution, Tiemulike, Tuergengsayi upstream, Kansuggou downstream, and Lasitai at the end of the pass). This area covers 1816.21 km^2, accounts for 23.93% of the study area, and has experienced 151 landslide disasters.

(3) ***Low-risk area***. This area is located in the Nanshan Forest in Xinyuan County, which consists of high mountains and hilly areas, the bed and sides of the Kunas River floodplain, the low mountains and hilly areas to the north of Kansu Awulale Mountain, and the Kunas Valley. These areas cover 5030.46 km^2, account for 66.28% of the study area, and have experienced 23 landslide disasters.

Online Landslide Monitoring System with the Internet of Things. Perception layer. This layer includes various sensors, including a selection tipping bucket rain gauge, a GPS static water level meter, a fixed inclinometer, a surface-type crack meter, and sensors monitoring rainfall, settlement, inclination, and cracking. The alarm values are set to five consecutive days' average daily rate of displacement in the horizontal direction and accumulated in the same direction as the displacement, and twice the vertical displacement in the horizontal direction, as shown in Table 16.

Network layer. This is an external network using GPRS transmission. The perception layer collects data on rainfall, settlement, and displacement of each sensor in a quantity and bandwidth sufficient to meet the needs of GPRS data transmission. This layer contains a heterogeneous network among individual sensors. Rain gauges, inclinometers, and crack meters do not generate data in the absence of rainfall, and the amount of data generated when rain falls is

TABLE 16
Sensor alarm value table.

Grade	Rainfall rate	Settlement Monitoring	Tilt monitoring	Crack monitoring
One alarm value	l 4.0mm/min、60mm/hour、200mm/day	daily rate more than 3mm, total displacement more than 15mm	daily rate more than 2mm, total displacement more than 15mm	daily rate more than 60mm, total displacement more than 300mm
Two alarm value	2.0mm/min、30mm/hour、100mm/day	daily rate more than 3mm, total displacement more than 9mm	daily rate more than 1.5mm, total displacement more than 9mm	daily rate more than 50mm, total displacement more than 250mm
Three alarm value	1.0mm/min、15mm/hour、50mm/day	daily rate more than 3mm, total displacement more than 6mm	daily rate more than 1mm, total displacement more than 6mm	daily rate more than 40mm, total displacement more than 200mm

relatively small. To connect to the network through GPRS data communication and the high-power wireless bridge, a power supply and solar-powered batteries are used.

Application layer. The application layer includes three functional modules: GNSS Monitor, BService, and WebService. This layer analyzes landslide rainfall, internal strain, GPS real-time settlement, and other data, performing collection, transmission, calculation, analysis, and real-time security status updates for overall landslide monitoring. The visual display on the monitor changes over time, and the current state of information and data provides a simple, clear, intuitive, and effective information reference. If heavy rainfall occurs and the soil moisture content exceeds the warning value or the landslide internal deformation anomaly threshold, or if landslide subsidence displacement or displacement rate of change exceeds the warning value, the system can generate timely audible alarms, flashing alarm system animations, large-screen alert prompts, and SMS / e-mail classifications of early warning information that are published to relevant managers and responsible leaders.

CONCLUSION

(1) The environmental factors impacting landslides in the study area are mainly elevation, slope, aspect, lithology, geological faults, water, roads, and vegetation cover. Landslide hazards are most prominent at elevations of 1100 to 2600 m, slopes less than 40°, lithologies of quartzite, basaltic andesite, sandstone layered rocks hard group, alluvial, gravel, sand, loam, and loess granite hard crystalline rock group, and within 5000 m of geological faults and water. The effects of orientation and roads in landslide hazards in the study area proved not to play a dominant role.

(2) A weighted evidence-based, data-driven model of elevation, slope, aspect, lithology, stratigraphic faults, water, roads, vegetation cover, and other hazards in the study area was constructed and used for analysis. The results showed that the Student's C values were greater than 1.5, indicating high significance, in the following situations: elevation 1100–2000 m, slope of 15°–30° or 35°–45°, orientation of 0°–22.5° or 157.5°–202.5°, lithology of quartzite, basaltic andesite, sandstone layered hard clastic rock group, alluvial, gravel, sand, loam loess, granite hard crystalline rock group, sandy mudstone, siltstone, or sandstone conglomerate hard-soft white clastic group, distance from a geological fault less than 500 m, and distance from a body of water of 200 m or less, 800–1000 m, or 2000–4000 m. The influence of roads and vegetation on landslide disasters proved not to play a dominant role.

(3) The research area included 674 km^2 of high-susceptibility areas, 1820 km^2 of moderate-susceptibility areas, 3479 km^2 of low-susceptibility areas, and 1616 km^2 of non-susceptible areas. The landslide study area included 742.51 km^2 of high-risk areas, 1816.21 km^2 of moderate-risk areas, and 5030.46 km^2 of low-risk areas.

(4) Construction of a landslide monitoring system using rainfall data and Internet of Things technology included perception, network, and application layers. Based on these three elements, data are collected from rain gauges, GPS devices, crack meters, inclinometers and other sensors. The sensing layer architecture collects settlement and displacement data via GPRS network layer data communications and a high-power wireless bridge that transfers data across the network to the application layer and the landslide monitoring system. The system then generates high-precision single-epoch deformation information via high-precision GNSS and transfers the deformation information to the real-time early

warning system database for analysis. The results show that the landslide hazard landslide monitoring system can periodically monitor a set of data points, can obtain accurate change information for impact analysis, and can provide appropriate support for development of appropriate disaster prevention and emergency response countermeasures.

REFERENCES

[1] Shucheng Zhang. Mudslides Review [J]. Advances in Mechanics,1989,19(3):365-375.

[2] Crowley J k,Hubbard B E,Mars J C.Analysis of potential debris flow source areas on Mount Shasta,California,by using airborne and satellite remote sensing data[J].Remote Sensing of Environment,2003,87:345-358.

[3] Dennis M,Thad A,Jacek S.Surficial patterns of debris flow deposition on alluvial fans in Death Valley,CA using airborne laser swath mapping data[J].Geomorphology,2006,74:152-163.

[4] Cavalli M,Marchi L.Characterisation of the surface morphology of an alpine alluvial fan using airborne LiDAR [J].Natural Hazards and Earth System Sciences,2008,8:323-333.

[5] Conway S,Decaulne A,Balme M.A new approach to estimating hazard posed by debrisflows in the Westfjords of Iceland[J].Geomorphology,2010,114:556-572.

[6] Blahut J,Horton P,Sterlacchini S.Debris flow hazard modeling on medium scale:Valtellina di Tirano,Italy[J].Natural Hazards and Earth System Sciences,2010,10:2379-2390.

[7] Lopez Saez,Corona C,Stoffel M.Debris-flow activity in abandoned channels of the Manival torrent reconstructed with LiDAR and tree-ring data[J].Natural Hazards and Earth System Sciences,2011,11:1247-1257.

[8] Hong jiang L , Hengxing L,Yi L.Characteristics of spatial distribution of debris flow and the effect of their sediment yield in main downstream of Jinsha River,China[J].Environment Earth Science,2011,64:1653-1666.

[9] Bremer M,Sass O.Combining airborne and terrestrial laser scanning for quantifying erosion and deposition by a debris flow event[J].Geomorphology,2012,138:49-60.

[10] Qin bo Hu,Hai ming Li. Remote Sensing Technology in Nanning-Kunming railway section mudslides survey River Basin [J]. Aerial railway,1994,(3):27-30.

[11] Jiahong Liu,Guangqian Wang. Evaluate the extent of ground-based remote sensing image mudslides activities [J]. Geographic Sciences,2003,23(4):454-459.

[12] Liqiang Tong,Hongfeng Nie,Jiancun Li. Himalayas large debris flow remote sensing survey research and development characteristics [J]. Remote Sensing of Land and Resources,2013,25(4):104-112.

[13] Tang Chuan,Zhang Jun,Shiyun Wan. Based on high-resolution remote sensing of urban debris flow damage assessment [J]. Geographic Sciences,2006,26(3):358-368.

[14] Deng Hui, Precision satellite remote sensing technology in geological disaster survey and evaluation [D]; Chengdu University of Technology,2007.

[15] Gaofeng Wang, YAJIANG Tibet based on remote sensing technology (Millington - Jiacha segment) of debris flow characteristics of the source [D]; Chengdu University of Technology,2011.

[16] Xiaobing Yang. Based on Multispectral Image and DEM debris flow fans Recognition [D]; Lanzhou University,2013.

[17] Chang Ming,Tang Chuan,Zhilin Jiang. Sensing longchi town of Dujiangyan City earthquake zone of dynamic evolution of debris flow provenance [J]. Mountain Science,2014,32(1):89 -97.

[18] Lingjing Li,Yao Xing,Yongshuang Zhang. Earthquake Mian River Basin geological hazards extraction and distribution of research [J]. Journal of Engineering Geology,2014,22(1):46-55.

[19] Varnes,DJ.Landslide hazard zonation:A review of principle and pracirce.UNESCO.Paris,1984.

[20] Tang Chuan,JORGGRUNERT. Evaluation principles and methods of study based on landslide hazard [J]. Geographical Sciences,1998,S1):149-57.

[21] Shiqi Xu ,Tongyang Zao,Zhixin Zhu,Liu Xin,Chen Chuan.ArcGISEvidence right model in copper mineralization Prediction——In Bogda - Harlik metallogenic belt Case [J]. Geology and Prospecting.2013,49(5):981-989.

Received: **16.11.2015**
Accepted: **14.03.2016**

CORRESPONDING AUTHOR

Zhihui LIU
College of Resources and Environmental Science, Key Laboratory of Oasis Ecology of Ministry of Education , Xinjiang University, Urumqi 830046, China

Email83896995@qq.com

© by PSP Volume 25 – No. 7/2016, pages 2639-2645 Fresenius Environmental Bulletin

THE EFFECTS OF COTTONSEED OIL AS ALTERNATIVE TO FISH OIL ON OXIDATIVE STRESS BIOMARKERS AND SOME HEMATOLOGICAL PARAMETERS IN EUROPEAN SEA BASS (*Dicentrarchus labrax* L.)

[a]Aysel Sahan, [a]Orhan Tufan Eroldogan, [b]Ergül Belge Kurutas, [a]Hatice Asuman Yilmaz, [a]Ibrahim Demirkale

[a]Cukurova University, Fisheries Faculty, 01330, Balcalı-Sarıçam Adana- TURKEY
[b]Sütçü İmam University, Faculty of Medicine, 4606, Kahramanmaraş- TURKEY

ABSTRACT

In this study, the effects of using cottonseed oil (CSO) which is one of the vegetable oil sources considered as an alternative to fish oil (FO) in European sea bass, at different ratios on oxidative stress biomarkers and hematological parameters, were investigated. Each group in this study was contained 20 samples with 3 repetitions, making a total of 300 sea bass (35 g). The groups were designed as control (FO) (100%), CSO40 (40%), CSO60 (60%), CSO80 (80%), CSO100 (100%) for a 120 day period.

At the end of the feeding trial, the activities of antioxidant defence enzymes (ADE) which will indicate the oxidative stress, catalase (CAT), superoxide dismutase (SOD), glutathione (GSH) and the levels of malondialdehyte (MDA) were determined. SOD, GSH and CAT levels in CSO100 group increased significantly. On the other hand, hepatosomatic index (HSI) and visceral fat index (VFI) rose with increasing dietary CSO. The haematological parameters, erythrocyte and leukocyte numbers, lymphocyte and neutrophil cell percentages, were higher than the other groups with increasing substitution levels of CSO.

There were no negative effects on the health of fish as hematological and antioxidant enzymes in fish that were fed CSO40 and CSO60. However, it was reported that, the increase in hepatosomatic index and visceral adiposity in CSO80 and CSO100 groups lead to an increase in oxidative stress indicators antioxidant enzymes and hematological parameters, with a similar increase, operated for defending the body.

KEYWORDS:
Dicentrarchus labrax, Cottonseed oil, Fish oil, Vegetable oil, Hematological parameters, Oxidative stress, Antioxidant enzymes.

INTRODUCTION

Balanced feed rations play an important role for the implementation of most of the physiological functions for fish. To generate an economical and balanced ration for feed, finding alternative sources of fish oil that can meet the same need of fish fatty acids without causing metabolic disruption and health disorder will decrease the expenses of the market sector and will benefit the economy. In aquaculture, the energy requirement of fish is fulfilled by using certain amounts of soy, canola, cottonseed, sunflower seed and palm oil, which is supported by various researchers. CSO which is the subject of this study, is a vegetable oil source rich in n-6 PUFA (Polyunsaturated fatty acid). Replacement of fish oil with various vegetable oils containing n-6 PUFA at 40-100% do not cause any problems for growth performance, feed conversion, health problems and stress in fish [1,2,3]. It is emphasized that usage of certain amount of plant oils support the fish immune system against diseases and plays important role for maintaining their health [4,5,6]. In these interactions, the differences in fish species, ingredients of feed rations, lipid balance, dietary specialization, digestive systems and environmental factors are directly related [2,7]. In biological systems aerobic organisms are exposed to various natural or synthetic pollutants during metabolic activities and oxygen radicals. These activities severely damage organism and cause oxidative stress. The biological system minimizes the harm of the oxygen radicals by ADE; SOD, CAT, GSH and MDA [8]. The goal of this study is to investigate the effects of CSO, which was preferred considering the fish health and welfare, on stress indicator liver ADE and hematological parameters. This study is the first of its kind that investigates the usage of CSO as an alternative to fish oil as an indicator of fish health by using antioxidant and hematological data.

TABLE 1
Formulation and contents of diet groups (g/kg).

Contents	Diet Groups (g kg air-dry basis^{-1})				
	FO	**CSO40**	**CSO60**	**CSO80**	**CSO100**
Fish oil	120	72	48	24	0
Cotton seed oil	0	48	72	96	120
Fish meal	425	425	425	425	425
Corn gluten	221	221	221	221	221
Wheat gluten	90	90	90	90	90
Carboxy Methyl Cellulose	42	42	42	42	42
Di Calcium Phosphate	27	27	27	27	27
Min/Vit. Premix	30	30	30	30	30
L-Lysine	20	20	20	20	20
DL-Methionin	25	25	25	25	25

MATERIALS AND METHODS

Experimental Diets. The experimental diets were cold-pelleted and formulated to contain 48% crude protein, 22% lipid and 25.7 MJ kg^{-1} gross energy. The diet was contained different levels of cotton seed oil (40%, 60%, 80% or 100%) and except CSO replaced either 0% (fish oil 100%) of the supplemental dietary lipid content (100 g/kg diet) with the remainder originating from FO (Table 1).

Fish maintenance and Experimental Planned. European sea bass (*Dicentrarchus labrax*) were obtained from a commercial company in Turkey. 300 fishes with an average of 35.2±0.71 g for 5 trials with 3 repetitions were stocked in 15 fiberglass tanks, each with a volume of 400 L (n=20). Water temperature and oxygen levels in fiberglass tanks were measured daily by oxygen meter (Oxyguard). Fish were fed two times a day (at 0900 h and 1900 h) by hand according to apparent satiation. The fishes, following a feeding period, were anaesthetized for 4-5 minutes using 20 ml/L quinaldine sulphate (Sigma Chemical Co., Germany) in bathing method application, weight measurements were carried out and were taken to examination for antioxidant and hematological analyses.

Physiological Indexes. For the visceral fat index (VFI) and hepatosomatic index (HSI) determinations, 10 fishes from each group were taken and the fats surrounding their internal organs were removed from their body. For ADE determinations only livers were removed from the body of the fishes. The VFI and HSI were calculated by the formulas;

VFI (%) = 100× (visceral fat weight (g wet weight) / total body weight (g, wet weight).

HSI = 100× (liver weight (g) / body weight) [9].

Preparation of Liver Homogenates and Antioxidant Enzyme Analysis. For liver antioxidant enzyme analyses, liver tissue samples were homogenized with a Heidolph 50110 R2R0 homogenizer (Schwabach, Germany). Biochemical assays were performed on the supernatant preparation in a Sorvall (Minneapolis, MN, USA) RC-2B centrifugation of the homogenate at 14,000 rpm for 30 min at +4˚C [10]. SOD, CAT, GSH and MDA analyses were performed using the prepared homogenates.

SOD, CAT and MDA were measured by spectrophotometric methods. SOD (U/mg protein) activity was measured according to the method described by Fridovich [11]. CAT (U/mg protein) and GSH (micromol/mg protein) activity were measured by the method of Beutler [12]. MDA (nmole/mg protein) level in the tissue samples was measured with the TBA [13].

Hematological Assay. Blood samples for hematological analysis were taken according to Blaxhall and Daisley [14]. Health assessment was performed by measuring several haematological variables including: erythrocyte (RBC) numbers, hematocrit (Hct), hemoglobin (Hb), leukocyte (WBC) number and leukocyte types (lymphocyte, monocyte and neutrophil**).** The leukocyte types were identified from blood smears and erythrocyte indices were calculated as:

MCV (Mean Corpuscular Volume) (μ^3) = (Hct) (%) ÷ RBC (10^6/mm^3) × 10

MCH (Mean Corpuscular Hemoglobin) (pg) = Hb (g/100 mL) ÷ RBC (10^6/mm^3) × 10

MCHC (Mean Corpuscular Haemoglobin Concentration) = Hb (g/100 mL) ÷ (Hct) (%) × 100 [15].

Total RBC and WBC numbers were determined in thoma chamber according to Blaxhall and Daisley [14]. Examinations were conducted with Olympus BX51 light microscope at 4000x magnification. Results were given as x10^6/mm^3 for RBC and x10^3/mm^3 for WBC numbers. The Hb was determined according to standardized procedure of the cyanomethemoglobin method and given as g/dl [14]. Microhematocrit technique was benefited to determine Hct levels and given as percentage. Blood smears were dried in air and stained with May Grünwald – Giemsa mixture for determined of leukocyte cell types. The results were given as percentage [15].

Statistical Analysis. Comparisons of hematological parameters and antioxidant enzyme results were conducted using One-way-Anova. Duncan multiple comparison test of the one-way ANOVA was used to compare the mean differences. The differences were considered to be significant at $p \leq 0.05$

RESULTS AND DISCUSSIONS

Compositions, formulations and ratios of various feeds are given in Table 1. On the other hand, dissolved oxygen, pH and temperature values measured in the tanks were 7.0 mg/L, 6.9-7.8 and 23.2± 0.9°C. At the end of 120 days feeding period, it was determined that the fish reached to 68.9±1.22 g weights and mortality cases were observed in experimental groups during this period.

In the recent years, vegetable and animal origin raw material sources are the standard used in fish feeds in order to reduce cost and to ensure continuous healthy development instead of using fish meal and fish oil [16]. In the investigation of feeding activity and lipid content of feed in terms of animal health and product quality, HSI (hepatosomatic index) and VFI (visceral fat index) are the important parameters that were used in this assessment. It was reported that, in the comparison between the CSO100 group and other experimental groups, the values for liver physiological index and VFI which indicate the fat accumulation in the body increased significantly, whereas the changes in CSO40 was not significant ($p<0.05$) (Table 2). HSI and VFI are the best indicators for morphological changes caused by the growth of the liver depending on the quality and ratio of lipid and also the fat ratio in the body [17].

Vegetable oil such as CSO that is rich in18:2n-6, the β-oxidation amount is very low and this leads retention of lipids in body tissues. In general, for marine fish, the liver is the primary storage tissue of dietary fatty acids. In the previous studies, hepatocyte vacuolation, lipid infiltration, hepatic lipid modifications (steatosis) and also histological and/or morphological changes were reported in liver tissues in different fish species, which were fed with n-6 PUFA rich vegetable oils [18,19]. In our study, although there were no significant differences in the hepatosomatic index between the group fed with low levels of CSO and FO (control) group, there were significant increases in high levels of CSO and these results confirm those of the previous studies (Table 2).

TABLE 2
HSI (Hepatosomatic Index), VFI (Visceral Fat Index), CAT (Catalase), SOD (Superoxide Dismutase), GSH (Reduced Glutathione) activitiy and MDA (Malondialdehyde) levels of Sea bass.

		Experimental Diets (g kg air-dry basis^{-1})[1]				
		FO	**CSO 40**	**CSO 60**	**CSO 80**	**CSO 100**
%	HSI	1.2±0.06[a]	1.3±0.13[b]	1.7±0.34[b]	1.5±0.36[b]	2.0±0.62[c]
	VFI	2.0±0.52[a]	2.7±0.44[a]	3.3±0.17[b]	3.2±0.29[b]	3.4±0.38[b]
	Antioxidant Parameters					
U/mg protein	CAT	0.081±0.0[a]	0.065±0.01[a]	0.071±0.02[a]	0.382±0.01[b]	0.408±0.01[b]
	SOD	4.140±0.90[a]	3.826±1.03[a]	4.367±0.70[a]	4.505±0.67[a]	5.362±0.68[b]
micromol/mg protein	GSH	0.007±0.00[b]	0.001±0.00[a]	0.003±0.00[a]	0.003±0.00[a]	0.042±0.04[c]
nmole/mg protein	MDA	2.716±0.58[a]	2.640±0.65[a]	2.453±0.45[a]	3.758±0.60[b]	4.108±0.52[b]

Oxidative defence system or ADE (Antioxidant Defence Enzymes) forms as a result of free radicals and various factors (metabolic functions, malnutrition, stress). This negative factors cause oxidative stress in the cells and resulting from imbalance of antioxidants. Superoxide dismutase (SOD), Catalase (CAT) and Reduced Glutathione (GSH) are some of the important enzymatic and non-enzymatic antioxidants. These enzymes are important in terms of reducing the harmful effects of free radicals on living things [20].

According to the obtained oxidative stress results in our study, the antioxidant enzymes, CAT, SOD and non-enzymatic GSH and MDA levels increased in CSO80 and CSO100 groups ($p<0.05$) (Table 2). There were no significant changes in CSO40 and CSO60 groups regarding these paremeters. Feed rich in n-6 PUFA have contents that can cause significant changes, which pioneer the production of radical oxygen species in lipid classes and also in lipid peroxidation. Varghase and Oommen (2000), in their study, as a result of feeding with different vegetable oil mixtures, found that lipid peroxidation and antioxidant enzyme (SOD, GPx) levels increased in all experimental groups and therefore there were significant dysfunctions in cellular metabolism [20]. In our study, the group with high levels of CSO, both HSI and VFI results indicated the lipid accumulation in liver and the body. The increases observed in liver antioxidant enzymes, CAT, SOD and GSH, associated with lipid accumulation, was evaluated as an indicator for body defence meachanism. MDA is one of the products and indicators of lipid peroxidation caused by free radicals and also indicates the level of peroxidation. Lipid peroxidation occurs in cell membranes when SOD, CAT or GSH enzymes are activated or become insufficient. In several studies, there are differences observed in GSH, MDA and some antioxidant enzyme activities level for the fish exposed to different nutritional conditions or xenobiotics [21]. Sitja-Bobadilla et al., 2005, determined the effects of vegetable sources used as an alternative to fish meal on the non-specific defense and oxidative stress in sea bream [22]. The researchers determined that the vegetable sources used as 100% caused steatosis (fat degeneration of liver) in the liver and an increase in antioxidant enzyme values, also reported that the immunological results verify these results [21]. In our study, in high levels of CSO, the increases in MDA levels were interpreted as an indicator of antioxidant enzyme activities for body defense, according to the fat accumulation in the internal organs and the HSI results for liver tissue. In terms of fish feeding, certain amounts of plant oils added to the feed rations as an energy resource, play an important role in metabolic processes, cell membrane structure activity and show resistance against probable stress factors [19]. In our study, the hematological effects of CSO added in different ratios were justified with health indicator parameters. RBC counts, which is an important parameter, similar to the ADE results, significantly

TABLE 3
RBC (Erythrocyte), Hct (Hematocrit), Hb (Hemoglobin) and MCV, MCH, MCHC (RBC indices) of sea bass.

Hematological Parameters	**Experimental Diets (g kg air-dry basis^{-1})[1]**				
	FO	**CSO40**	**CSO60**	**CSO80**	**CSO100**
RBC ($x10^6/mm^3$)	1.94±458.16^b	1.50±255.17^a	1.61±362.5^a	2.57±382.83^c	2.01±457.44^b
Hct (%)	27.11±0.76^b	27.88±3.32^b	27.20±0.84^b	24.64±1.17^a	25.94±2.48^a
Hb (g/dl)	6.32±0.51	6.43±0.86	6.27±0.89	6.40±0.69	6.08±0.74
MCV (μm^3)	148.23±44.09^b	198,59±40,65^c	137.47±48.11^b	97.16±14.40^a	176.90±43.98^c
MCH (pg/cell)	34.63±10.81^a	47,45±16,29^b	39,91±5,97^b	25.29±4.71^a	31.55±7.45^a
MCHC (g/dl)	23.34± 2.03	23.46± 4.53	23.01± 2.87	26.00± 3.02	23.62± 3.53

Values are means±SD. Data in the same line with different superscript are significantly different ($p<0.05$).

TABLE 4
WBC (Leukocyte) counts, Lymphocyte, Monocyte and Neutrophil percentages of Sea bass.

Leukocyte Leukocyte Types	Experimental Diets (g kg air-dry basis^{-1})[1]				
	FO	CSO40	CSO60	CSO80	CSO100
($x10^3/mm^3$) WBC	7500.0±2563.41[a]	6012.5±1090.78[a]	9687.5±1831.03[b]	10125.0±2100.17[b]	10112.5±1980.21[b]
(%)					
Lymphocyte	79.5±5.09[b]	81.5±8.66[b]	82.0±6.59[b]	83.75±2.25[b]	68,3±7,48[a]
Monocyte	10.1± 3.31	12.8± 4.12	12.0± 4.62	11.7± 3.73	12.0± 1.85
Neutrophil	8.2±2.25[b]	8.2±2.71[b]	13.7±3.45[c]	18.7±5.33[d]	6.62±1.92[a]

Values are means±SD. Data in the same line with different superscript are significantly different ($p < 0.05$).

increased in CSO80 and CSO100 groups. Hct, MCV and MCH counts were the lowest among the results for the same group of fish ($p<0.05$) (Table 3). There were no significant differences for Hb and MCHC counts for all experiment groups ($p>0.05$). The differences between WBC results were compatible the changes in ADE and RBC counts (Table 3). The erythrocyte count in organisms broadly associated with the amount of oxygen level in tissues. When the oxygen level decreases, erythropoietic organs and tissues spring into action to balance the condition. In the present study, the increase in HSI and VFI levels might reflect the oxygen consumption induced by caused oxidative stress as an indicator of the fat accumulation in the body compartments. Therefore, this deposition triggers oxygen consumption in the tissues induced by oxidative stress. The increase in RBC values were interpreted as a reaction, to overcome the oxidative stress occurred as a result of the exposition of the body to the high levels of fatty acids especially PUFAs.

In one study, negative and positive correlations investigated between hematological parameters and the highest positive correlation was for Hb-Hct, RBC-MCV and MCHC-RBC in healthy fish. A negative correlation was found between MCH-WBC and MCH-MCHC [23]. In our study, positive and negative relationships regarding erythrocyte indexes determined hematological parameters in healthy sea bass were compatible with those of the previous studies.

Due to the types of plant oils and levels, the presence of pathogens in the environment, fish species, pathogen resistance, feed rations, behaviours, interactions with other fish, feeding time and environmental conditions cause stress in fish, thus resulting in a change in immune system and blood values (6). Studies conducted with alternative plant fish resources indicate that oil resources affect some immunological and hematological parameters and health variation for marine fish [2, 5, 6, 7]. Lymphocytes are of the hematological paremeters that form the basis of the immune defence system of animals and antibody producing cells. Fluctuations in lymphocyte and neuthrophil levels also increase in response to stress [24]. According to the results of the study, hematological parameters as lymphocyte and neutrophil cells in the non-specific cellular system showed sudden significant increase in CSO80. On the other hand, WBC counts increased significantly in CSO80 and CSO100 groups. Monocyte cell amounts showed no significant differences for all experiment groups ($p>0.05$) (Table 4).

Sitja-Bobadilla et al., 2005, evaluated the oxidative stress effects of vegetable oil sources with immunological and antioxidant enzymes. The researchers emphasized that feed with high PUFA content caused damage in fish tissue, and the increase in leukocyte cells and antioxidant system were the stress indicators of the body [22]. The researchers also observed that different ratios of vegetable oils, due to oxidative stress, caused similar responses in antioxidant enzymes and hematological parameters. These responses verify the results of our study.

In growth studies conducted using vegetable oils, it was reported that low levels of vegetable oils caused no significant differences in terms of growth compared to fish oil and no negative effects were observed on health [3, 8]. In our study, the high levels of CSO caused some problems in fish regarding oxidative stress and hematological parameters. Using 80% and 100% CSO as an alternative to fish oil, due to hepato somatic and visceral steatosis, caused oxidative stress and therefore an increase in stress indicator antioxidant parameters (CAT, SOD, GSH and MDA). The increase in enzymes in order to overcome the stress that caused an increase in defense activities similar to that in hematological parameters.

It was concluded that vegetable oil source cottonseed was an economic feed additive, which can easily be supplied. Using 40-60% doses caused no health problems in fish and lipid balance, overdosing, fish size and nutritional needs were important factors to consider.

REFERENCES

[1] Montero, D., Robaına, L., Caballero, M.J., Gınes, R. and Izquıerdo, M.S. (2005) Growth, feed utilization and flesh quality of European sea bass (*Dicentrarchus labrax*) fed diets containing vegetable oil: A time course study on the effect of a re-feeding period with a %100 fish oil diet. Aquaculture. 248: 121-134.

[2] Yue, Y.R. and Zhou, Q.C. (2008) Effect of replacing soybean meal with cottonseed meal on growth, feed utilization, and hematological indexes for juvenile hybrid tilapia, *Oreochromis niloticus* x *O. aureus*. Aquaculture. 284: 185–189.

[3] Eroldoğan, T.O., Turchini, G.M., Yılmaz, H.A., Taşbozan, O., Engin, K., Ölçülü, A., Özşahinoğlu, I. and Mumoğullarında, P. (2012) Potential of Cottonseed Oil as Fish Oil Replacer in European Sea Bass Feed Formulation. Turkish Journal of Fisheries and Aquatic Sciences. 12: 787-797.

[4] Montero, D., Grasso, V., Izquierdo, M.S., Ganga, R., Real, F., Tort, L., Caballero, M.J. and Acosta, F. (2008) Total substitution of fish oil by vegetable oils in gilthead sea bream (*Sparus aurata*) diets: Effects on hepatic Mx expression and some immune parameters. Fish & Shellfish Immunology. 24: 147-155.

[5] Montero, D., Mathlouthi, F., Tort, L., Afonso, J.M., Torrecillas, S., Fernández-Vaquero, A., Negrin, D. and Izquierdo, M.S. (2010) Replacement of dietary fish oil by vegetable oils affects humoral immunity and expression of pro-inflammatory cytokines genes in gilthead sea bream *Sparus aurata*. Fish & Shellfish Immunology. 29: 1073-1081.

[6] Turchini, G.M. and Tocher, D.R. (2010) Fish oil replacement and alternative lipid sources in aquaculture feeds. CRC Press, Boca Raton, FL.

[7] Mourente, G., Good, J.E., Thompson, K.D. and Bell, J.G. (2007) Effects of partial substitution of dietary fish oil with blends of vegetable oils, on blood leukocyte fatty acid compositions, immune function and histology in European sea bass (*Dicentrarchus labrax* L). Br J Nutr. 98: 770-9.

[8] Bayır, A., Sirkecioğlu, A.N., Bayır, M., Arslan, M., Güneş, M., Haliloğlu, H., Aras, N.M., and Arslan, H. (2011) Effects of dietary lipid source on growth, survival, and fatty acid composition of brown trout juveniles, *Salmo trutta*. Isr. J. Aquacult. Bamidgeh. 2: 622-630.

[9] Sloof, W., Van Kreijl, C.F. and Baars, A.J. (1983) Relative liver weights and xenobiotic-metabolizing enzymes of fish from polluted surface waters in the Netherlands. Aquatic Toxicology. 4: 15-29.

[10] Gül, Ş., Belge Kurutaş, E., Yıldız, E., Şahan, A. and Doran, F. (2004) Pollution correlated modifications of liver antioxidant systems and histopathology of fish (Cyprinidae) living in Seyhan Dam Lake, Turkey. Environment International. 30: 605-609.

[11] Fridovich, I. (1974) Superoxide dismutase. Advances in Enzymology. 41: 35-97.

[12] Beutler, E. (1975) Red Cell Metabolism. A manual of biochemical methods. Grune and Stratton Inc., New York.

[13] Uchiyama, M. and Mihars, M. (1978) Determination of malondialdehyde precursor in tissues by thiobarbituric acid. Ann. Biochem. 86: 271-278.

[14] Blaxhall, P.C. and Daisley, K.W. (1973) Routine haematological methods for use with fish blood. J. of Fish Biology. 5: 771-882.

[15] Schreck, C.B. and Moyle, P.B. (1994) Methods for Fish Biology. American Fisheries Society. Exon Company. Maryland. 273-322.

[16] Hardy, R.W. (2006) Worldwide Fish Meal Production Outlook and the Use of Alternative Protein Meals for Aquaculture. 15-17 Novambre. Mexcio. ISBN 970-694-333-5.

[17] Çetinkaya, O. (1995) Fish Feeding, Yüzüncü Yıl Üniversity, Agriculture Faculty Press 137, Van

[18] Leaver, M.J., Villeneuve, L.A.N., Obach, A., Jensen, L., Bron, J.E., Tocher, D.R. and Taggart, J.B. (2008) Functional genomics reveals increases in cholesterol biosynthetic genes and highly unsaturated fatty acid biosynthesis after dietary substitution of fish oil with vegetable oils in Atlantic salmon (*Salmo salar*). Bmc Genomics, 9-299.

[19] Tocher, D. R. (2010) Fish Oil Replacement and alternative Lipid Sources in Aquaculture Feeds. Chapter 14.

[20] Varghese, S. and Oommen, V.O. (2000) Long-term feeding of dietary oils alters lipid metabolism, lipid peroxidation and antioxidant enzyme activities in a teleost (*Anabas testudineus* Bloch). Lipids. 35: 757-762.

[21] Pascual, P., Pedrajas, J.R., Toribio, F., Lo´pez-Barea, J. and Peinado, J. (2003) Effect of food deprivation on oxidative stress biomarkers in fish (*Sparus aurata*) Chemico-Biological Interactions. 145: 191-199.

[22] Sitja-Bobadilla, A., Pena-Lıopis, S., Gomez-Requeni, P., Medale, F., Kaushik, S. and Perez-Sanchez, J. (2005) Effect of fish meal

replacement by plant protein sources on non-specific defence mechanisms and oxidative stress in gilthead sea bream (*Sparus aurata*). Aquaculture. 249: 387-400.

[23] Pradhan, S. C., Patra A. K.and Pal, A. (2014) Hematological and plasma chemistry of Indian major carp, *Labeo rohita* (Hamilton, 1822). J. Appl. Ichthyol. 30: 48–54.

[24] Jahanbakhshi, A., Imanpoor, M.R., Taghizadeh, V. and Shabani, A. (2013) Hematological and serum biochemical indices changes induced by replacing fish meal with plant protein (sesame oil cake and corn gluten) in the Great sturgeon (*Huso huso*) Comp Clin Pathol. 22: 1087-1092.

Received: **17.11.2015**
Accepted: **14.03.2016**

CORRESPONDING AUTHOR

Aysel SAHAN
Cukurova University, Fisheries Faculty, 01330, Balcalı-Sarıçam Adana- TURKEY

E-Mail: ayaz@cu.edu.tr

© by PSP Volume 25 – No. 7/2016, pages 2646-2653 Fresenius Environmental Bulletin

ENHANCEMENT OF CONTINUOUS REMOVAL OF SO_2 ON SURFACE- MODIFIED ACTIVATED CARBON FIBERS BY NITROGEN-CONTAINING FUNCTIONAL GROUPS

Weizhu Wang[1,4], Yan Cheng[2,*], Mengdan Gong[1], Wubo Fan[1], Jiaxiu Guo[1,3], Huaqiang Yin[1,3], Yongjun Liu [1,3,*]

[1] College of Architecture and Environment, Sichuan University, Chengdu 610065, China
[2]College of Geosciences and Environmental Engineering, Southwest Jiaotong University, Chengdu 610031, China
[3]National Engineering Technology Research Center for Flue Gas Desulfurization, Chengdu 610065, China
[4]Chengdu Chuangjing Environmental Engineering Co. Ltd, Chengdu 610041, China

ABSTRACT

The surface-modified activated carbon fibers (ACFs) with rich nitrogen-containing functional groups were prepared by heat-treatment of urea-loaded ACFs. Their nitrogen content, the surface property and the porosity were examined by element analysis, XPS, TGA and low temperature N_2 adsorption, and their SO_2 removal performances were comparatively tested with the pristine ACF and the ACF merely heat-treated without urea-loading (ACF-H). The results revealed that the total nitrogen content of the surface-modified ACFs was much higher than that of the pristine ACFs. In particular, the content of pyridine nitrogen was found to be increased about 4.4 times. The specific surface area and the pore volume of the surface-modified sample were larger than those of the pristine ACF but smaller than those of the ACF-H. However, the surface-modified ACF exhibited a much improved SO_2 removal activity. Its breakthrough SO_2 capacity and SO_2 removal efficiency at the stable stage of the desulfurization process increased 3.0 and 1.64 times, respectively, as compared with the ACF-H. The nitrogen-containing groups, particularly for the pyridinic nitrogen, rather than the developed pore structure should account for the excellent desulfurization activity of the surface-modified ACFs.

KEYWORDS:

Activated carbon fibers; Nitrogen-containing groups; SO_2; Flue gas desulfurization; Urea

INTRODUCTION

Due to technical and economic reasons, severe environmental problems caused by sulfur dioxide pollution are not expected to be satisfactorily solved in the near future in the world , especially in developing countries [1, 2]. Although some commercial flue gas desulfurization technologies were successfully applied worldwide, some of them even produce secondary pollutants. For example, the popular Ca-based SO_2 removal technologies produce low quality gypsum, which is difficult to be used or disposed. Sustainable development calls for breakthroughs in flue gas desulfurization technologies that are economically attractive and sulfur-recoverable.

Desulfurization using carbon-based materials (activated carbon, activated coke and activated carbon fibers) is an alternative, which can recover sulfur as SO_2 or diluted liquid H_2SO_4. The MET-Mitsui-BF process using coal-derived activated coke is a good example and has been practiced on industrial scales for more than two decades [3]. To make this process more efficient, researches on the preparation and modification of activated coke have been carried out to improve the desulfurization ability of activated coke [4, 5].

Compared with activated carbon or activated coke, ACF is considered to be more effective for gas adsorption due to its high specific surface area and narrow pore distribution (<2 nm). In addition, the openings of the nanopores are located on the external surface of the carbon material. Gas molecules could easily access to the adsorption sites in the nanopores without passing through macropores and mesopores, leading to a rapid adsorption and desorption.

Researches on desulfurization using ACFs were carried out early in 1994 [6, 7]. The SO_2 removal performance of ACFs is quite different

with activated carbon or activated coke. After a period of 100% SO_2 removal, the desulfurization efficiency decreases quickly and then reaches a stable period again. The SO2-removal rate of pristine ACF at the second plateau is too low to be utilized. If the SO_2 removal rate at the second plateau can be effectively improved, the desulfurization process using ACFs would proceed continuously like catalysis. However, this appears to have received little or no attention [7]. Therefore, the effort toward this aim is meaningful to the practical application of this technology.

The desulfurization activity of ACFs depends on both the porous structure (including specific surface area, pore volume, and pore size distribution) and the surface functional groups. An effective method to improve the SO_2 removal activity of ACFs is to increase the N-containing surface groups. Research on the N-containing surface modification of carbon materials for various applications has been an active topic. Usually three methods can be used to introduce N-containing groups onto the surface of ACFs: (a) carbonization and activation of N-containing precursor [8], (b) heat treatment of ACFs under NH_3 atmosphere [9, 10], and (c) heat treatment of ACFs impregnated with N-containing compounds [11, 12].

Although previous studies showed the effectiveness of N-modification of ACFs for various purposes, the nature of the nitrogen-containing groups responsible for the improvement of the catalytic activity towards SO_2 oxidation has not been deeply understood. Usually, different nitrogen-containing groups, such as pyridinic- and pyrolic-nitrogen were simultaneously found using the above mentioned preparation methods. However, which kind of nitrogen group contributes most to the enhanced catalytic activity is not yet clear [13, 14]. Additionally, some of the methods mentioned in the literature modified not only the surface chemistry but also the porous texture with the incorporation of nitrogen to carbon surfaces [15], which complexes the determination of the influence from the N-species on the catalytic activity.

In the present study, the nitrogen-containing activated carbon fibers were prepared by a heat-treatment of urea-impregnated ACFs. The SO_2 removal activity was comparatively tested with the pristine ACFs. The SO_2 removal rate at the second plateau of ACFs with surface-modification was dramatically enhanced. The surface chemistry and the porous structure of ACFs were determined by the XPS and low-temperature N_2 adsorption, respectively. The pyridinic nitrogen was clearly found to be mainly responsible for the enhancement of catalytic activity.

EXPERIMENTAL SECTION

Sample preparation. All samples used in this study were derived from commercial viscose-based activated carbon fibers. Pristine ACFs (designated as ACF) was oxidized with 30% HNO_3 solution for 4 h at 60 °C. The samples were filtrated and washed with distilled water until the pH of the filtrate became neutral. The washed ACF was then dried in air at 110 °C for 12 h. Subsequently, 10 g oxidized ACFs were impregnated in 140 ml urea solution with the concentration of 1.2, 2.4 and 3.6 mol/L for 24 h. The samples were dried at the temperature of 60 °C for 12 h, then 110°C for 12 h. Finally, the urea-impregnated ACFs were heat-treated at 750 °C for 1h under a high-purity nitrogen (99.99%) atmosphere. The temperature was raised from room temperature to 750 °C at a ramp rate of 5 K/min. The obtained samples were designated as ACF-N1.2, ACF-N2.4, and ACF-N3.6, where 1.2, 2.4, and 3.6 represents the urea concentration of the impregnation solution.

For comparison, the oxidized ACFs without impregnating urea, designated as ACF-H, were also prepared by the same heat treatment mentioned above.

Sample characterization. The content of carbon, nitrogen, and hydrogen of the samples was determined using an ERBA 1106 (CARLO, Italy) elemental analyzer. The oxygen content was estimated as the difference between 100% and the combined contents of C, N and H.

The XPS measurements were performed on XSAM800 (KRATOS, UK) using monochromated Al Ka (energy 1486.16 eV) excitation source, working at 12kV×12mA. The pressure of the analysis chamber was maintained at 5×10^{-7}Pa. The C, O and N envelopes were curve fitted using Handbook of X-ray photelectron spectroscopy (Chastain J, 1992).

Thermogravimetric measurements were carried out on a XDT Q600 Thermal Analyzer. The temperature was increased from room temperature to 1000 °C with a ramp rate of 5°C /min under a N_2 flow of 100 ml/min.

Nitrogen adsorption-desorption isotherms of the samples were measured using an ASAP 2020 (Micromeritics Instruments Co.) instrument at –196 °C. Prior to each measurement, samples were pretreated at 200 °C under vacuum for 4 h. The specific surface area (S_{BET}) was calculated from the Brunauer-Emmett-Teller (BET) equation. The total pore volume (V_{total}) was approximated from the adsorption amount at P/P_0=0.95. The microporous volume (Vmicro) was calculated from the Dubinin-Radushkevitch (D-R) equation and the

mesoporous volume (Vmeso) was obtained from the difference between V_{total} and V_{micro}.

SO_2 removal activity. Tests on the SO_2-removal activity of the samples were carried out in a fix-bed tubular glass reactor with a diameter of 28 mm. 5g sample was cut into wafer shape with a diameter of 28 mm and packed into the reactor. The simulated flue gas consisted of 3000 ppm SO_2, 5% O_2 , 10% H_2O, and the balance N_2. The total flow rate, the gas space velocity (SV), and the reaction temperature was kept at 900 mL/min, 600 h^{-1} and 80 ℃ , respectively. To determine the outlet SO_2 concentration, the continuous gas flow passed through a H_2O_2 solution (3%) after the reactor, and the formed H_2SO_4 was titrated with NaOH solution (0.1 mol/L), using bromcresol green and methyl red as an indicator [16]. The breakthrough SO_2 removal capacity was calculated through the cumulative amount of the removed SO_2 per unit mass of the sample, when the outlet SO_2 concentration reached 75ppm (200 mg/m^3).

RESULTS AND DISCUSSION

Elemental composition. The elemental composition of all samples obtained by the elemental analysis is presented in Table 1. The surface-modified samples display a very different composition compared to the pristine ACF. Modification of activated carbon fibers by heat treatment with urea (ACF-N1.2, ACF-N2.4, ACF-N3.6) produced nitrogen-rich carbons, which have much higher nitrogen content. The pristine ACF contains 1.25 wt% of nitrogen, which was probably derived from its precursor. With the increase of the urea concentration, the nitrogen content of the surface-modified ACF increased and the ACF-N3.6 displayed the highest content of 5.30 wt%. The nitrogen content of ACF-H also increased to 4.21 wt%. The increase in the nitrogen content of the modified samples should be attributed to the decomposition of the oxygen-containing groups on the surface of ACFs [17].

The oxygen content of all the heat-treated samples (ACF-N1.2, ACF-N2.4, ACF-N3.6, and ACF-H) is significantly lower than that of the pristine ACF. ACF-N2.4 contains the lowest oxygen content (15.49 wt%) and the lowest O/C ratio (0.20). The urea paralysis process produces nitrogen-containing active substances, such as NH_2^+, NH^{2+}, et al [18-19]. On the other hand, the thermal decomposition of oxygen-containing groups on the oxidized ACFs through heat-treatment may produce active sites, where the nitrogen-containing groups can be easily introduced. The ACF-N2.4 contains the lowest oxygen content and relatively high nitrogen content, indicating effective formation of nitrogen-containing groups on the surface of ACF. This would contribute to the improvement of SO_2-removal activity, as will be discussed later.

XPS spectra. Figure 1 shows the XPS spectra of ACF and ACF-N2.4, together with the bonding configurations of the N-containing functional groups on carbon materials. The asymmetric C 1s spectra of the ACF and ACF-N2.4 (Fig. 1(a)) can be fitted primarily as four peaks centered at 284.5, 285.7, 287.1 and 289.1eV, respectively. In detail, the peak at 284.5eV, corresponding to the energy of the sp^2 C=C bond in the C1s spectrum of pyrolytic graphite, proves the graphitic carbon. The peak at 285.7 eV could be assigned to C–O–C or –C–OH bonds. Two other peaks appeared at 287.1 and 289.7 eV could be assigned to –COOH bonds and CO_2, respectively

TABLE 1
Elemental analysis of the pristine ACF and the modified ACFs.

Sample	Elemental analysis (wt%)					
	N	C	H	O*	N/C	O/C
ACF	1.25	68.77	0.90	29.08	0.02	0.42
ACF-N1.2	3.89	70.83	0.90	24.39	0.05	0.34
ACF-N2.4	4.28	79.42	0.82	15.49	0.05	0.20
ACF-N3.6	5.30	72.11	1.54	21.06	0.07	0.29
ACF-H	4.21	68.98	0.70	26.12	0.06	0.38

[20, 21]

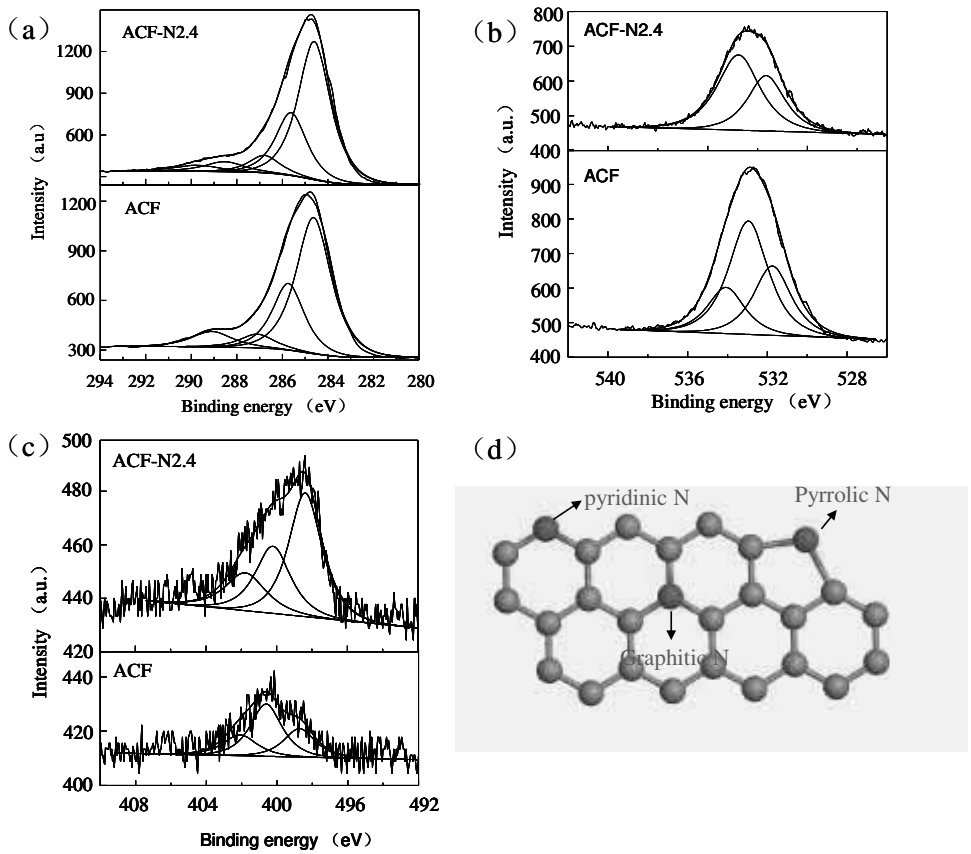

FIGURE 1
XPS spectra:(a) N 1s; (b) O 1s; (c) C 1s and (d) Bonding configurations for N-containing functional groups in carbon materials.

The XPS N1s spectra of ACF and ACF-N2.4 are presented in Fig.1(c). The nitrogen contents of ACF and ACF-N2.4 calculated from the area of the peak are 1.51 wt% and 3.58 wt%, respectively, in agree with the element analysis results. Nitrogen atoms can be incorporated into the graphene sheets to form pyridinic, pyrolic, and graphitic nitrogen, their C-N bonding configurations are illustrated in Fig.1(d) [22]. The XPS N1s peak of ACF and ACF-N2.4 were fitted by three components with the binding energy of 398.5±0.2, 400.5±0.2 and 402 ± 0.2 ev, which are assigned to pyridinic nitrogen(N-6), pyrrolic nitrogen(N-5), and quaternary nitrogen or protonated pyridinic nitrogen (N-Q), respectively [23-25].

Owing to a lone electron pair in the plane of N-6 ring, sulfur dioxide may react more easily with pyridinic nitrogen to form sulphuric acid than pyrrolic nitrogen does [26]. It is interesting to note that the content of pyridinic nitrogen of ACF-N2.4 is much higher than that of ACF. The relative intensity of pyridinic nitrogen of ACF-N2.4 and ACF is 51.39% and 27.54%, respectively. Furthermore, if calculated by the product of the relative intensity and the total nitrogen content, the content of pyridinic nitrogen of ACF-N2.4 is 1.84 wt%, about 4.4 times that of ACF (0.42 wt%). On the other hand, the content of pyrrolic nitrogen of ACF-N2.4 is 1.06 wt%, not significantly different from that of ACF (0.77 wt%). These results indicate that the proposed nitrogen modification process by heat-treatment of the urea-impregnated ACF largely produced pyridinic nitrogen rather than pyrrolic nitrogen.

Thermal analysis. The weight loss curves of ACF, ACF-N2.4, and the pure urea are shown in Figure. 2. The TGA curves of ACF and ACF-N2.4 show three stages of weight losses. The weigh losses at the first stage (below 100°C) for ACF and ACF-N2.4 are of 25.5 % and 13.3%, respectively, owing to the release of water. At the second stage (100 to 800°C), the weigh losses are caused by the decomposition of oxygen-containing groups, including carboxyl groups, phenolic hydroxyl, ether, carbonyl, and quinone into CO and CO_2 [27]. At this stage, the weight losses of ACF and ACF-N2.4 are 14% and 3.4%, respectively. At the last stage (above 800°C), carbon matrix begins to graphitize and the porous structure is gradually destroyed [28]. At both the first and second stages, the weight loss of ACF-N2.4 is much smaller than that of ACF.

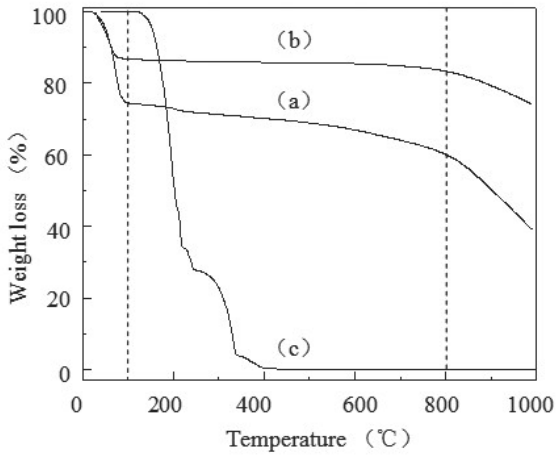

FIGURE 2
TGA profiles of (a) ACF, (b) ACF-N2.4, and (c) pure urea

$$(NH_2)_2CO(s) \rightarrow NH^+_4NCO^- \rightarrow NH_3(g) + HNCO(g) \quad (1)$$
$$NH_3(g) + HNCO(g) \rightarrow H_2O(g) + H_2NC{\equiv}N(g) \quad (2)$$
$$HNCO(g) + H_2O(g) \rightarrow CO_2(g) + NH_3(g) \quad (3)$$

Urea begins to decompose at its melting point of 132 °C. According to the TGA profile, the thermolysis of urea also contains three stages (125-250°C, 250-350°C, and 350-430°C), showing a weight loss of 65%, 31%, and 4%, respectively. When the temperature increased to about 430°C, urea decomposed completely. The thermolysis of urea produces ammonia (NH_3), isocyanic acid (HNCO), cyanamide ($H_2NC{\equiv}N$), carbon dioxide and water, according to the following reactions[29-31]. The nitrogen-containing groups on ACF-N2.4 are probably formed by the reaction of ammonia, isocyanic acid and/or cyanamide and the carbon surface.

N_2 adsorption-desorption isotherms at 77 K. The nitrogen adsorption-desorption isotherms of ACF, ACF-H, and ACF-N2.4 are shown in Fig. 3. These samples exhibit the type I isotherm, which is typical of a sharp rise at the low-pressure range and a plateau at the high-pressure range, according to the IUPAC classification [32], indicating the microporous nature of the ACFs [33]. Table 2 summarizes the specific surface area (S_{BET}), the total pore volume (V_{total}), the microporous volume (V_{micro}), and the mesoporous volume (V_{meso}) of the pristine and the treated ACF samples. The S_{BET}, V_{total} and V_{micro} values of ACF-H（1600 m^2/g, 0.73 ml/g，and 0.65 ml/g, respectively) are obviously higher than that of ACF (1196 m^2/g, 0.57 ml/g, and 0.51 ml/g, respectively). This result indicated that the pre-oxidation with HNO_3 followed by a heat-treatment promotes the development of the microporous structure of ACF. In the case of ACF-N2.4, its corresponding structural parameters (1571 m^2/g, 0.70 ml/g, and 0.63 ml/g, respectively) are slightly smaller than those of ACF-H but larger than those of ACF, suggesting that the urea treatment shows little adverse effect on the pore structure. The less developed pore structure of ACF-N2.4 is possibly due to the blocking effect of nitrogen atoms [34-35].

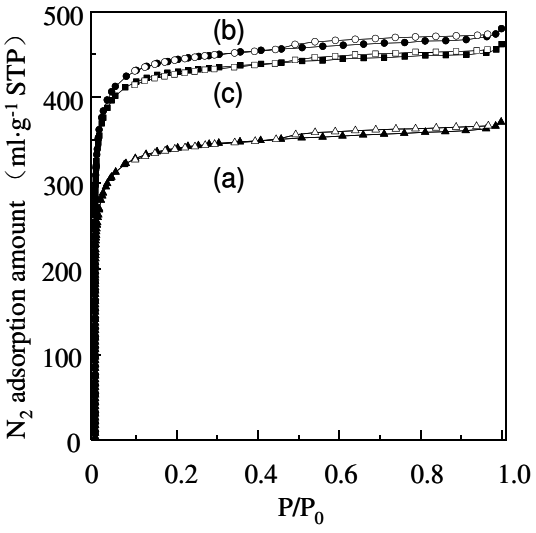

FIGURE 3
N_2 adsorption-desorption isotherms of (a) ACF, (b) ACF-H, and (c) ACF-N2.4. The solid and open symbols represent the adsorption and desorption branches, respectively.

TABLE 2
Structural parameters of ACF, ACF-H, and ACF-N2.4.

Sample	S_{BET} (m^2/g)	V_{Total} (ml/g)	Vmicro (ml/g)	Vmeso (ml/g)
ACF	1196	0.57	0.51	0.06
ACF-H	1600	0.73	0.65	0.08
ACF-N2.4	1571	0.70	0.63	0.07

Evaluation of the SO_2-removal activity. The time courses about the SO_2 removal rate of the samples are shown in Fig. 4. The SO_2 removal performances of all the five samples show similar patterns. The curves show a plateau with 100% SO_2 removal at the beginning of the desulfurization process. After a quick decrease, there is another plateau with lower SO_2 removal rate.

Compared with ACF, ACF-H shows a dramatic enhancement in the desulfurization activity. For ACF, a 100% SO_2-removal ability lasts only 0.1h. However, in the case of ACF-H, the time for maintaining 100% SO_2 removal prolonged to 1h. The SO_2-removal breakthrough capacity of ACF-H is 75.8mg/g, which is much higher than that of ACF (15.5mg/g). Meanwhile, the SO_2 removal rate in the second plateau increased from 21.2% to 35.7%.

The desulfurization activity of ACF was further improved by heat-treatment with urea, as demonstrated by ACF-N1.2, ACF-N2.4 and ACF-N3.6. These samples all show a prolonged time of maintaining 100% SO_2-removal and a dramatically increased removal rate at the second plateau, compared with ACF and ACF-H. Particularly for ACF-N2.4, the 100% SO_2-removal lasts 2.6 h. Its SO_2-removal breakthrough capacity reaches to 230.7 mg/g, which is 15 and 3 times of ACF and ACF-H, respectively. Furthermore, the SO_2 removal rate of ACF-N2.4 at the second plateau increases to 58.4%, which is 2.8 and 1.6 times that of ACF and ACF-H, respectively.

It is worthy to note that both the SO_2-removal breakthrough capacity and the SO_2-removal rate at the second plateau are very important. A dramatic increase in the SO_2-removal rate at the second plateau like exhibited by ACF-N2.4 is very desirable for practical applications. The catalytic oxidation removal of SO_2 using ACF experience the following processes: (1) SO_2 is adsorbed on the internal surface of ACF; (2) SO_2 is oxidized by O_2 into SO_3, and SO_3 further reacts with H_2O into H_2SO_4, which condenses within the pores of ACF; (3) H_2SO_4 releases from the pores by the wash of excess H_2O, the active sites of the SO_2 adsorption and catalytic oxidation ability are recovered [7]. Thus, a new cycle of SO_2 adsorption starts again. The recovery of the active sites makes the operation of a continuous SO_2 removal possible. With the easy release of the by-product H_2SO_4 from the pores, the active sites of ACFs can be effectively recovered. Therefore, the desulfurization process could be changed from interval operations by using adsorbents like activated coke to a continuous one by using ACFs as a catalyst, as mentioned before.

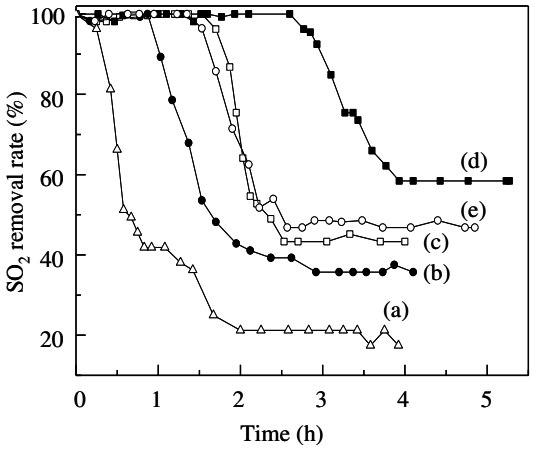

FIGURE 4
Time courses of SO_2 removal performance of (a) ACF; (b) ACF-H, (c) ACF-N1.2, (d) ACF-N2.4, and (e) ACF-N3.6.

In addition, although ACF-N2.4 exhibited a slightly poor porous structure in comparison with ACF-H, it showed a dramatically improved desulfurization activity. The result suggests that the nitrogen-containing groups (particularly for the pyridinic nitrogen) rather than the developed pore structure primarily contributes to the improved desulfurization activity.

CONCLUSIONS

The surface modification of ACF with rich nitrogen-containing functional groups was achieved by the heat-treatment of urea–loaded ACF at 750°C under inert atmosphere. Nitrogen-containing groups were successfully introduced onto the surface of ACF, as demonstrated by element analysis and XPS. Pyridinic nitrogen was the main nitrogen-containing group on ACF-N2.4 under the conditions of this research. Compared with ACF and ACF-H, the SO_2 breakthrough capacity and the desulfurization efficiency of ACF-N2.4 are dramatically enhanced. The observed enhancement in the desulfurization activity should be attributed to the nitrogen-containing groups rather than the physical pore structure. From a practical perspective, it is meaningful to improve as high as possible the SO_2-removal efficiency of ACFs at the second plateau, as this would make the desulfurization process to proceed continuously like catalysis. The observation of a great increase in the desulfurization efficiency at the second plateau suggests a possible route to this aim through surface modification of ACF.

ACKNOWLEDGEMENTS

This work was partly supported by the Sichuan Provincial Science and Technology Agency Public Research Projects (NO. 2012GZX0028), Chengdu, China.

REFERENCES

[1] Q.Y Liu, Z.Y Liu. (2013) Carbon supported vanadia for multi-pollutants removal from flue gas. Fuel, 108, 149-158.

[2] Y. Liu, T.M. Bisson, H. Yang, Z. Xu. (2010) Recent developments in novel sorbents for flue gas clean up. Fuel Process. Technol., 91, 1175-1197.

[3] D.G. Olson, K. Tsuji, I. Shiraishi. (2000) The reduction of Gas Phase Air Toxics from Combustion and Incineration Sources using the MET-Mitsui-BF Activated Coke Process. Fuel Process. Technol., 65-66, 393-405.

[4] P. Davini. (2002) Influence of surface properties and iron addition on the SO_2 adsorption capacity of activated carbons. Carbon, 40, 729-734.

[5] Y. F. Qu, J.X. Guo, Y.H. Chu, M.C. Sun, H.Q. Yin. (2013) The influence of Mn species on the SO_2 removal of Mn-based activated carbon catalysts. Appl. Surf. Sci., 282, 425-431.

[6] S. Kisamori, I. Mochida, H. Fujitsu. (1994) Roles of Surface Oxygen Groups on Poly(acrylonitrile)-Based Active Carbon Fibers in SO_2 Adsorption. Langmuir, 10, 1241-1245.

[7] S. Kisamori, K. Kuroda, S. Kawano, I. Mochida, Y. Matsumura, M. Yoshikawa. (1994) Oxidative Removal of SO_2 and Recovery of H_2SO_4 over Poly(acrylonitrile)-Based Active Carbon Fiber. Energy & Fuels, 8, 1337-1340.

[8] N. Yusof, A.F. Ismail. (2012) Post spinning and pyrolysis processes of polyacrylonitrile (PAN)-based carbon fiber and activated carbon fiber: A review, J. Anal. Appl. Pyrolysis, 93, 1-13.

[9] C.L. Mangun, J.A. DeBarr, J. Economy. (2001) Adsorption of sulfur dioxide on ammonia-treated activated carbon fibers. Carbon 39, 1689-1696.

[10] J.P. Boudou, M. Chehimi, E. Broniek, T. Siemieniewska, J. Bimer. (2003) Adsorption of H_2S or SO_2 on an activated carbon cloth modified by ammonia treatment. Carbon 41, 1997-2007.

[11] E. Raymundo-Pinero, D. Cazorla-Amoros, A. Linares-Solano. (2003) The role of different nitrogen functional groups on the removal of SO_2 from flue gases by N-doped activated carbon powders and fibres. Carbon 41, 1925-1932.

[12] A. Peñas-Sanjuán, R. López-Garzón, M. Domingo-García, F.J. López-Garzón, M. Melguizo, M. Pérez-Mendoza. (2012) An efficient procedure to bond nanostructured nitrogen functionalities to carbon surfaces. Carbon 50, 3977-3986.

[13] M.A. Montes-Morán, D. Suárez, J.A. Menendez, E. Fuente. (2004) On the nature of basic sites on carbon surfaces: an overview. Carbon 42(7), 1219-1225.

[14] L. Xu, J. Guo, F. Jin, H. Zeng. (2006) Removal of SO_2 from O_2-containing flue gas by activated carbon fiber (ACF) impregnated with NH_3. Chemosphere 62, 823-826.

[15] V. Gaur, A. Sharma, N. Verma. (2006) Preparation and characterization of ACF for the adsorption of BTX and SO_2. Chem. Eng. Process.: Process Intensification 45, 1-13.

[16] P. Davini. (2003) Flue gas desulphurization by activated carbon fibers obtained from polyacrylonitrile by-product. Carbon 41, 277-284.

[17] B. Zheng, J. Wang, F.B. Wang, X.H. Xia. (2013) Synthesis of nitrogen doped graphene with high electrocatalytic activity toward oxygen reduction reaction. Electrochem. Commun. 28, 24-26.

[18] Q. Zhu, S. L. Money, A. E. Russell, K. M. Thomas. (1997) Determination of the Fate of

Nitrogen Functionality in Carbonaceous Materials during Pyrolysis and Combustion Using X-ray Absorption Near Edge Structure Spectroscopy. Langmuir. 13, 2149-2157.

[19] J.X. Wang, W.C. Xie, Chin. (1989) An Appraisal of The Surface Chemistry and The Catalytic Oxidative Activity of The Nitrogen-modifed Activated Carbon by XPS . J. of Catal. 10, 357-364.

[20] T.I.T. Okpalugo, P. Papakonstantinou, H. Murphy, J. McLaughlin, N.M.D. Brown. (2005) High resolution XPS characterization of chemical functionalised MWCNTs and SWCNTs. Carbon, 43, 153-161.

[21] C. Pevida, P. Jacquemard, J.P. Joly. (2008) Hysicochemical properties of debris ejected from C/C brakes with different structural orders. Carbon, 46, 994-1002.

[22] M. Seredych, J.H. Denisa, Q.L. Gao, T.J. Bandosz. (2008) Surface functional groups of carbons and the effects of their chemical character, density and accessibility to IONS on electrochemical performance. Carbon, 46, 1475-1488.

[23] R. Pietrzak. (2009) XPS study and physico-chemical properties of nitrogen-enriched microporous activated carbon from high volatile bituminous coal. Fuel, 88, 1871-1877.

[24] H. Darmstadt, C. Roy. (2003) Surface spectroscopic study of basic sites on carbon blacks. Carbon, 41, 2662-2665.

[25] K.X. Li, L. Liu, C.X. Lu, W.M. Qiao, Z.Y. Liu, L. Liu. I. Mochida. (2001) Catalytic removal of SO_2 over ammonia-activated carbon fibers. Carbon, 39, 1803-1808.

[26] J.R. Pels, F. Kapteijn, J.A. Moulijn, Q. Zhu, K.M. Thomas. (1995) Evolution of nitrogen functionalities in carbonaceous materials during pyrolysis. Carbon, 33, 1641-1653.

[27] N. Li, X.L. Ma, Q.F. Zha, K. Kim, Y.S. Chen, C.S. Song. (2011) Maximizing the number of oxygen-containing functional groups on activated carbon by using ammonium persulfate and improving the temperature-programmed desorption characterization of carbon surface chemistry. Carbon, 49, 5002-5013.

[28] B. Zheng, J. Wang, F. B. Wang, X. H. Xia. (2013) Synthesis of nitrogen doped graphene with high electrocatalytic activity toward oxygen reduction reaction. Electrochem. Commun., 28, 24-26.

[29] A. Lundström, B. Andersson, L. Olsson. (2009) Urea thermolysis studied under flow reactor conditions using DSC and FT-IR. Chem. Eng. J., 150, 544-550.

[30] O. Kröcher, M. Elsener. (2009) Materials for thermohydrolysis of urea in a fluidized bed. Chem. Eng. J., 152, 167-176.

[31] H.L. Fang, H.F.M. DaCosta. (2003) Urea thermolysis and NOx reduction with and without SCR catalysts. Appl. Catal. B: Environmental, 46(1) 17-34.

[32] Q.S. Liu, T. Zheng, P. Wang, J.P. Jiang, N. Li. (2010) Adsorption isotherm, kinetic and mechanism studies of some substituted phenols on activated carbon fibers. Chem. Eng. J., 157, 348-356.

[33] L. Ren, J. Zhang, Y. Li, C. Zhang. (2011) Preparation and evaluation of cattail fiber-based activated carbon for 2,4-dichlorophenol and 2,4,6-trichlorophenol removal. Chem. Eng. J., 168, 553-561.

[34] Y.J. Kim, Y. Abe, T. Yanagiura, K.C. Park, M. Shimizu, T. Iwazaki, S. Nakagawa, M. Endo, M.S. Dresselhaus. (2007) Easy preparation of nitrogen-enriched carbon materials from peptides of silk fibroins and their use to produce a high volumetric energy density in supercapacitors. Carbon, 45, 2116-2125.

[35] E. Atanes, A. Nieto-Márquez, A. Cambra, M.C. Ruiz-Pérez, F. Fernández-Martínez. (2012) Adsorption of SO_2 onto waste cork powder-derived activated carbons. Chem. Eng. J., 211, 60-67.

Received: **17.11.2015**
Accepted: **24.03.2016**

CORRESPONDING AUTHOR

Yongjun Liu
College of Architecture and Environment, Sichuan University, Chengdu 610065, China

e-mail: liuyj@scu.edu.cn

© by PSP Volume 25 – No. 7/2016, pages 2654-2661 Fresenius Environmental Bulletin

DAMP WATER STEAM INFLUENCE ON WEEDS AND FOLIAR FUNGAL DISEASES IN SUGAR BEET CROP

Zita Brazienė[1], Regina Vasinauskienė[2, 3]

[1]Lithuanian Research Centre for Agriculture and Forestry Rumokai Research Station, Klausučiai, Lithuania
[2]Aleksandras Stulginskis University Institute of Forest Biology and Silviculture, Faculty of Forest Science and Ecology, Akademija, Lithuania
[3]University of Applied Sciences, Technololody and Landscaping Faculty, Kaunas, Lithuania

ABSTRACT

Field experiments on the influence of damp water steam as a thermal control for weeds and foliar fungal diseases of sugar beet crop were carried out in the Rumokai experimental station of Lithuanian Research Center for Agriculture and Forestry in 2012-2013. The investigation followed the scheme: 1) sugar beets were sprayed with herbicides Betanal Expert 1,0 l ha^{-1} + Goltix 1,0 l ha^{-1}, Betanal Expert 1,25 l ha^{-1}, Betanal Expert 1,25 l ha^{-1} + Nortron 0,3 l ha^{-1} for three times during vegetation; 2) weed control was carried out for 2 times during sugar beets vegetation using damp water steam; 3) weed control was carried out for 3 times during sugar beets vegetation using damp water steam, the remaining weeds among the plants were removed manually; 4) weed control was carried out for three times during sugar beet vegetation applying damp water steam.

The best result was obtained combining damp water steam application for three times and manual weed removal during sugar beets vegetation. This method was the most effective in reducing air-dry mass of weeds as well. In the case when water steam was applied for 2 times the amount of weeds and air-dry mass was almost the same as using chemical weed control, thus, seeking to reduce environmental pollution, herbicides in sugar beet crop protection can be replaced by damp water steam using protection means such as covers or soil beds in order to prevent the crop from the steam.

Dump water steam reduced the development of fungal diseases in sugar beet crop. After the treatment of sugar beet crop with wet water steam for 3 times the severity of Cercospora and Ramularia leaf spots as well as powdery mildew in the end of September were 58.8 – 78.9 % , 51.7 – 52.0 % and 70.8 – 77.6 % less than in the chemically treated plots.

KEYWORDS:
damp water steam, sugar beets, weeds, foliar fungal diseases

INTRODUCTION

Traditional agriculture using intense technologies and constantly increasing production by all means makes a negative impact not only to the nature but for humanity as well. The intense usage of chemical preparations caused the ecological problems [1, 2, 3], therefore the alternative agriculture ways are very relevant at this point. Ecological agriculture is an alternative that aids to solve not only ecological but economical, social as well as cultural problems.

The main problem in ecological farming is the battle against weeds [4, 5]. The weeds affects the amount and quality of yield. The significance of ecological weeds removal is growing together with the increase of ecologically clean products demand. Mechanical weed control is now widely used along ecological farms [6, 7, 8]. Thermal weed control is the other method used quite widely. Not only weeds are affected applying thermal method, but the pests, pathogen microorganisms and plant disease causing agents as well. Various thermal control ways are used in different countries ecological farms including gas burning [9], hot foam [10], hot water [11], damp water steam [12, 13].

Sugar beets are one of the most sensitive plants choked by weeds, because their early stage growth is slow and they can't compete with copiously germinating weeds. The weeds can reduce sugar beets yield by 26-100 % [14, 15]. In order to have clean crop, the sugar beet breeders uses chemical control several times during the plant vegetation. Thus not only the damage to the environment is caused but the resistance to herbicides is increased as well. The usage of alternative weed control could reduce these problems.

Other important problem in sugar beets crop is foliar fungal diseases. The average loss of sugar beets yield caused by foliar fungal diseases comprises 30 %, while under favorable conditions may reach 50 % and more [16]. The greatest damage to sugar beets crop in Lithuania is caused by Cercospora leaf spots (*Cercospora beticola* Sacc.) and Ramularia leaf spots (*Ramularia beticola* Fautrey & F. Lamb.) [17]. Powdery

mildew (*Erysiphe betae* Vanha Weltzien) is spread when the difference between day and night temperatures is big and copious dew is formed on the leaves. Powdery mildew spreads very fast under favorable conditions, thus the fungicides must be used after noticing first symptoms [18].

The aim of the work was to determine the influence of damp water steam as a thermal control to weeds and foliar fungal diseases in sugar beets crop.

MATERIALS AND METHODS

Field experiments were carried out in the Rumokai experimental station of Lithuanian Research Center for Agriculture and Forestry in 2012-2013. The experiments were carnied out on a *Haplic–Epihypogleyic Luvisol* – Idg8–p, granulometric composition was clay loam.

The chosen sugar beets sort was "Ernestina" and preceding crop was winter wheat. Sugar beets were sowed in the second half of April. The crops were sowed using seeding-machine "Monopolis Acord". The density was 6-7 encrusted seed lines per linear meter, the space between rows being 45 cm width. Sugar beets were grown according to technology recommended by the Lithuanian Institute of Agriculture [19]. The trial was arranged in 4 repetitions, were the sugar beets arrangement was systemic. The whole field area was 12 m x 2.7 m = 32.4 m^2 (6 lines, 12 m long), the estimation area was 18 m^2.

The investigation scheme was as follows:

First variant. The sugar beets were chemically treated with herbicides Betanal Expert (active ingredients: phenmedipham 91 g l^{-1}, desmedipham 71 g l^{-1}, ethofumesate 112 g l^{-1}; dosage 1,00 lha^{-1}) + Goltix (active ingredient metamitron 700 g l^{-1}, dosage 1,00 l ha^{-1}); Betanal Expert (dosage 1,25 l ha^{-1}); Betanal Expert (dosage 1,25 l ha^{-1}) + Nortron (active ingredient ethofumesate 500 g l^{-1}; dosage 0,3 l ha^{-1}) for 3 times during vegetation.

Second variant. The weed control for the first time was carried out by treatment with damp water steam in 5-6 days after sowing, when weeds are in the cotyledons stage. The treatment with damp water steam was continuous, the seeds of sugar beet were not germinated yet. The second treatment with damp water steam was carried out when weeds germinated repeatedly. This weed control was arranged covering the sugar beets for protection.

Third variant. Weed control was carried out using damp water steam for 3 times during vegetation period. Thermal weed control was carried out in profiled crop. The first time treatment was continuous, because the sugar beets were not germinated yet. The second ant the third time treatment was carried out in the space between rows, the weeds among sugar beets seedlings were removed manually.

Forth variant. The weeds were controlled thermally by treating with damp water steam for 3 times during the vegetation. The first time treatment was continuous in the profiled crop. The second and the third time treatment was carried out in the space between rows with sugar beets being unprotected from damp water steam influence. The remaining weeds among plants were not removed manually.

The weeds were counted before every spread and after 3 days in four 0.25 m^2 areas of each field. The quantity and air-dried mass of weeds was evaluated in all variations in the first decade of July.

Foliar diseases were diagnosed 2 times: in the first decade of August and in the third decade of September (before harvesting). While estimating the visual evaluation of affected leaves area in percents was carried out.

The intensity of foliar diseases were calculated using equation [20]:

$$R = \frac{\Sigma (a\ b)}{N};$$

were Σ (a b) is the sum of product of foliar disease affect in percent (a) and affected leaves quantity in corresponding percentage group; N is the whole number of inspected leaves.

The data were statistically estimated using software ANOVA [21].

Meteorological conditions. The average day temperature in April was +7.9°C, it is close to standard climate normal (SCN) (Table 1). Nevertheless the temperature distribution was very uneven: the first decade was cold (+2.0°C), the second was close to SCN, the significant thaw set only in 27th-30th of April; the average temperature was +18.7°C. The precipitation exceeded SCN for 2 times in the first two decades (57 mm of rainfall occurred). Because of cool weather and copious precipitation the drying of soil was poor, the sowing of sugar beets was late for 1 week in comparison with the year before. Unusually warm weather after the sowing was favorable for the sugar beets germination.

The weather of May was very changeable, the average day temperature reached +18-21°C and dropped to +8-9 °C for several times. Besides, the period of late frosts was long, the 44.4 mm of rainfall occurred, while SCN was 51.0 mm. The first decade of June was significantly cooler (+12.8°C) in comparison with SCN (+15.2°C).

TABLE 1
Average daily air temperature and amount of precipitation during sugar beet growing Kybartai Weather Station.

Month	Decade	Temperature ºC			Amount of precipitation mm		
		2012	2013	Normal (1961-1990)	2012	2013	Normal (1961-1990)
April	I	2,0	-0,4	4,8	20,6	35,8	13,0
	II	7,8	8,5	5,8	30,1	7,4	14,0
	III	13,8	9,1	7,9	3,6	4,4	17
	per month	7,9	5,7	6,2	54,3	47,6	44,0
May	I	12,6	14,4	10,9	10,7	1,2	16,0
	II	12,3	16,7	12,8	22,9	11,0	17,0
	III	15,8	15,1	13,4	10,8	45,3	18,0
	per month	13,6	15,4	12,4	44,4	57,5	51,0
June	I	12,8	18,1	15,2	22,0	76,0	16,0
	II	16,3	17,2	15,4	26,8	3,3	19,0
	III	15,7	18,0	16,4	49,0	17,9	25,0
	per month	14,9	17,8	15,4	97,8	97,2	60,0
July	I	21,1	18,5	16,4	61,3	15,6	22,0
	II	16,6	17,6	16,9	45,4	40,6	25,0
	III	20,3	19,0	17,3	11,7	5,5	29,0
	per month	19,3	18,4	16,9	118,4	61,7	76,0
August	I	18,5	21,0	17,6	27,3	32,8	25,0
	II	16,0	18,1	16,5	5,7	11,8	26,0
	III	15,8	15,1	15,3	13,2	8,6	28,0
	per month	16,8	18,1	16,5	46,2	53,2	79,0
September	I	14,1	13,6	14,4	12,3	17,9	20,0
	II	13,5	16,9	12,3	16,5	88,5	23,0
	III	12,2	8,5	10,6	30,3	23,2	20,0
	per month	13,3	12,0	12,4	59,1	129,4	63,0

The cold nights slowed down the growth of the plants significantly. The second decade of June was warmer and the temperature was closer to SCN. The precipitation of 97.8 mm occurred in June (SCN is 60.0 mm) and the distribution of it was very uneven; in the 11th of June 18.8 mm rainfall occurred while in the 22nd of June the precipitation reached as much as 29.5 mm. In the month of July warm and wet weather promoted foliar diseases expansion. The temperature in August was close to SCN, the precipitation was 46.2 mm, but due to high humidity and gloomy days (the sun was shining only 30.12 h in the second decade of July) the plants didn't experienced the lack of humidity. The weather of September was favorable for raising sugar beets; the average day temperature was close to SCN, without significant fluctuations, the quantity of precipitation was close to SCN.

The average day temperature of April in 2013 was +5.7 °C, close to SCN. The distribution of temperature was not even: the 1st decade was cold (-0.4 °C), the 2nd and 3rd decades were warmer, average day temperatures were 8.5 and 9.1 °C, respectively. The precipitation of the month was close to SCN, although all precipitation (35.8 mm) occurred in the 1st decade. The drying of soil was poor because of the cool weather and the sowing of summer plants was started 2-3 days later than the year before. Because of enough precipitation and warm weather in May the germination and development of plants was promoted. Copious rain occurred in the 1st decade of June (37.2 mm of precipitation occurred in the 2nd of June) and the plants in lower areas soaked. Warm and sunny days of July and August were favorable for root-crop growth and sugar accumulation. The average temperature of September was close to SCN, nevertheless the big amount of precipitation (88.5 mm in the 2nd decade of September) was hospitable for foliar diseases spread.

RESULTS AND DISCUSSION

Annual weeds were prevalent in the crop of sugar beets in the period of the investigation: Chenopodium album L., Persicaria lapathifolia L., Stellaria media (L.) Vill., Galium aparine L., Lamium purpureum L., it was plenty of Echinochloa crus-galli (L.) Beauv. as well. Perennial weeds found in experimental fields were Elytrigia repens L., Cirsium oleraceum L., Sonchus arvensis L.

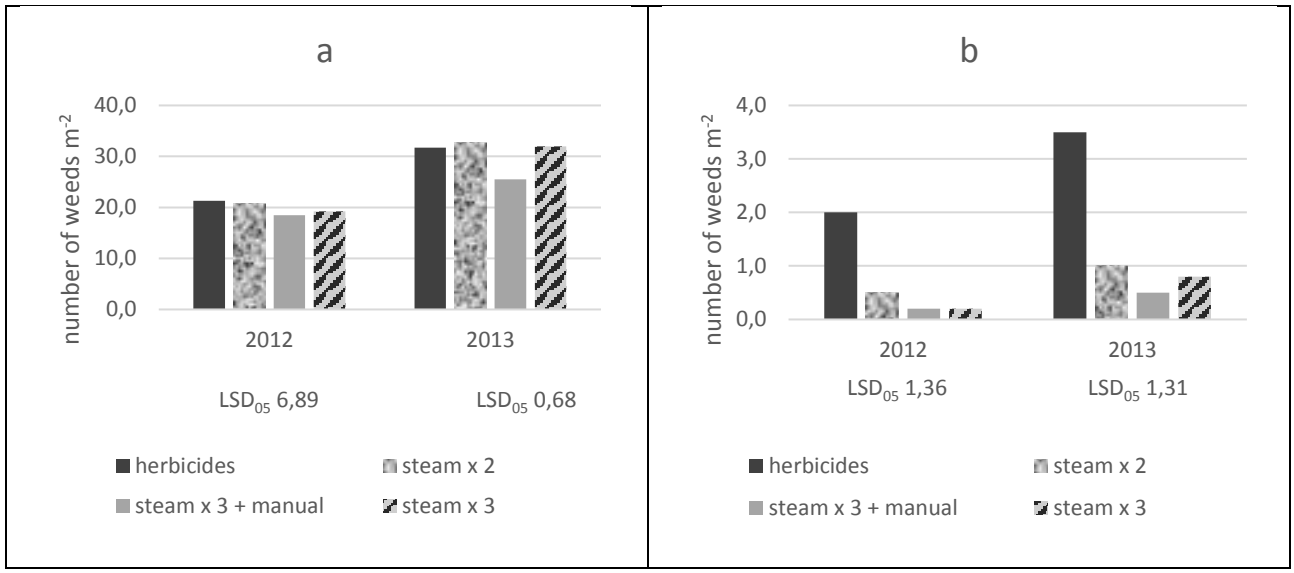

FIGURE 1
Weed grown before (a) and after (b) first weed control.

The amount of weeds in all the variants was similar before the first chemical treatment with pesticides and damp water steam (Fig. 1a). Chenopodium album, Persicaria lapathifolia and Galium aparine constituted the major part of weeds. The sugar beets were not germinated yet at the time, thus the crop was treated continuously. In 3 days after the treatment, the amount of weeds decreased by 97.0-98.7 % in the fields were damp water steam was used (Fig. 1b), while in the fields were herbicides were used, the amount of weeds was reduced by 89.0-90.6 %.

As it was noticed during the second weed control, the germination of weeds was more intense in comparison with the first germination (Fig. 2a). The second weed control was carried out in the 10th -11th of May. The weather was warm enough, the average temperature of the 1st decade of May in 2012 was 12.6 C and in the 2013 it was 14.4 C; the precipitation was low, but the soil was humid enough. The amount of weeds was reliably less before the second weed control in the fields where the chemical weed control was used, because the germinating weeds were still influenced by pre-emergence herbicide (Goltix), used in the first chemical control. In 3 days after the second weed control, the amount of weeds decreased to 1.0-3.5 un. m^{-2} (Fig. 2b).

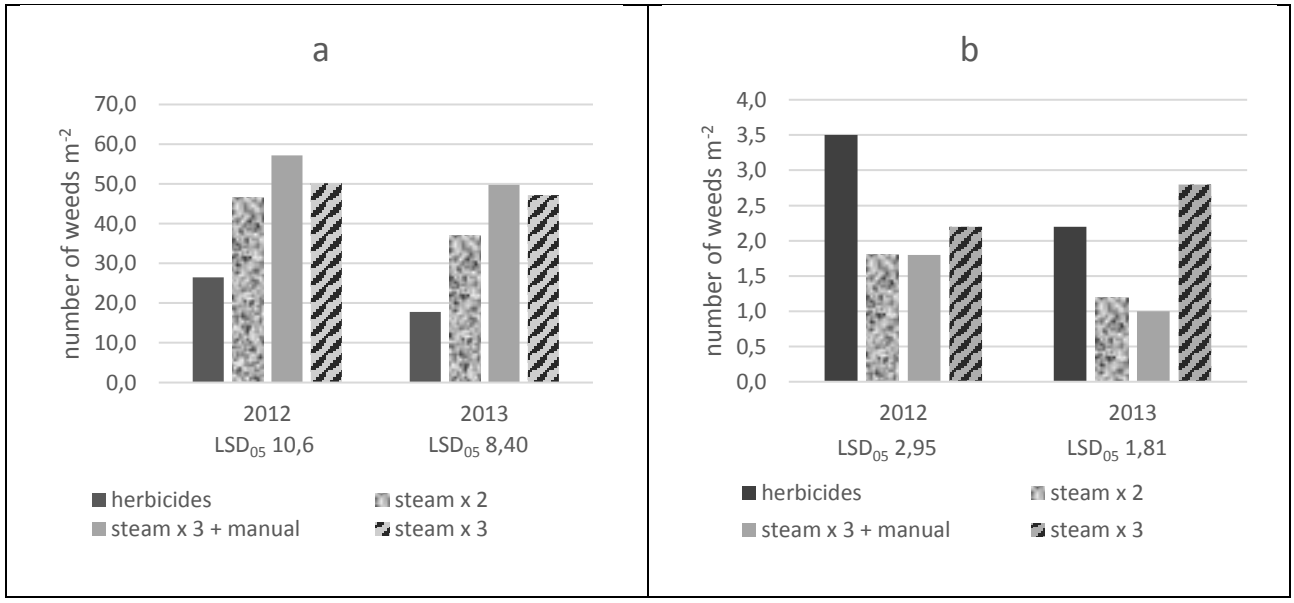

FIGURE 2
Weed grown before (a) and after (b) second weed control.

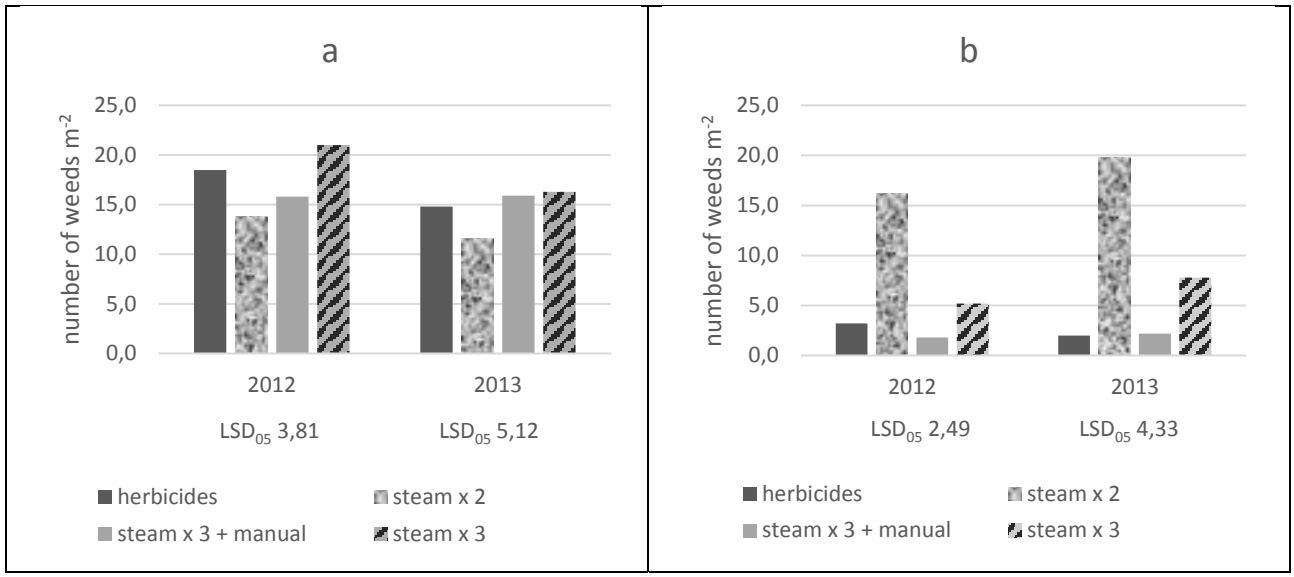

FIGURE 3
Weed grown before (a) and after (b) third weed control.

The germination of weeds was similar in all the fields before the third weed control (Fig. 3a). As the pre-emergence herbicide Goltix was not applied during the second weed control, the amount of weeds in this field did not varied from the other fields. The third weed control was especially effective in the fields, where the herbicides were used as well as in the forth variation, where spread with damp water steam was combined with manual weeds removal (Fig. 3b).

In order to finally evaluate the effect of applied means, we counted the weeds and measured their air-dry mass in one month after the last weed control. The smallest amount of weeds had the fields, where the damp water steam was combined with manual weeds removal (Fig. 4a), there were no significant differences among other variations. The biggest air-dry weed mas was in the fields were damp water steam was applied for 3 times and the remained weeds among the plants were not removed manually (Fig. 4b).

The influence of wet water steam on foliar fungal diseases. It was noticed the decrease of foliar fungal diseases when the weeds in sugar beets were controlled applying damp water steam. In order to correctly evaluate the influence of damp water steam, we carried out the estimation of fungal diseases in the beginning of August and in the end

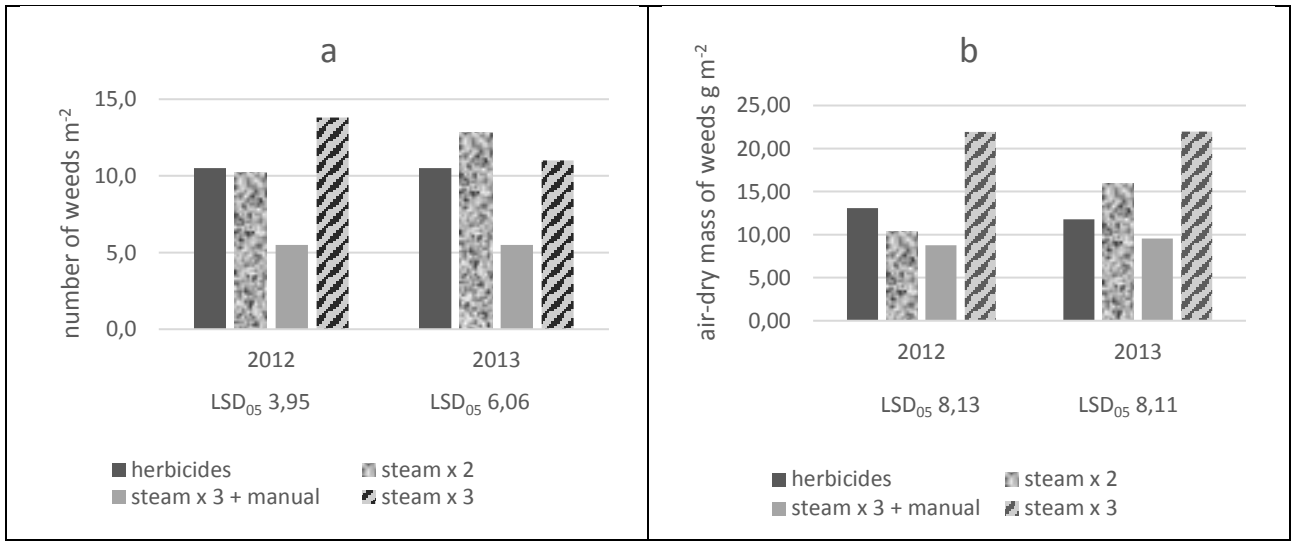

FIGURE 4
Weed grown (a) and air-dry mass of weeds (b) in one month after the last weed control.

TABLE 2
Severity of sugar beet fungal diseases , %.

Variants	I count (08 10)		II count (09 23)	
	2012	2013	2012	2013
	Cercospora leaf spot			
1.Sprayed with herbicides (control)	2,03	1,24	8,80	10,15
2. Sprayed with damp water steam x 2	1,18	0,61	7,46	8,14
3. Sprayed with damp water steam x 3	0,42	0,38	1,86	4,18
LSD_{05}	0,428	0,448	1,265	1,412
	Ramularia leaf spot			
1. Sprayed with herbicides (control)	1,94	1,38	2,01	3,56
2. Sprayed with damp water steam x 2	1,45	1,36	1,04	2,21
3. Sprayed with damp water steam x 3	1,24	1,18	0,97	1,06
LSD_{05}	0,681	0,726	0,629	0,464
	Powdery mildew			
1. Sprayed with herbicides (control)	0,15	0,18	2,14	2,26
2. Sprayed with damp water steam x 2	0	0	1,15	1,24
3. Sprayed with damp water steam x 3	0	0,01	0,48	0,66
LSD_{05}	0,026	0,021	0,523	0,548

of September, before the yielding. We generalized and presented the data from the variations 3 and 4 as from the one common field, because the methodology of applying damp water steam was the same and the manual removal of weeds didn't influence the spread of foliar diseases. Such foliar diseases like cercospora, ramularia and powdery mildew were outspread during the period of investigation. Phomosis and rust diseases appeared only in several places in 2013, thus these cases are not included in the paper. Cercospora severity in the sugar beets crop was low as it was found during the first diseases estimation in the beginning of August; it varied from 1.24 to 2.03 % in the fields, where chemical weed control was used (further named control fields) (Table 2). Cercospora severity in the damp water steam treated fields was 41.9-50.8 % (after spreading for 2 times) and 69.4-79.3 % (after spreading for 3 times) less than in the control fields.

During the second foliar disesases estimation it was found that cercospora was more intence in the 2013. Treatment with damp water steam for 2 times during the first part of sugar beets vegetation reduced the severity by 15.2-19.8 %. Cercospora severity decreased 58.8-78.9 % in the fields, which were treated with damp water steam for 3 times.

Ramularia severity in the sugar beets crop was similar during both foliar diseases estimations. The severity of ramularia in the beginning of August reduced 1.4-36.1 % in the fields treated with damp water steam in comparison with control fields and it depended on the treatment times as well as on the investigation year. Nevertheless, the statistically reliable difference was only in 2012 and only in the fields treated with damp water steam for 3 times. The severity of ramularia in the fields treated with damp water steam was reliably less in comparison with control fields in the end of September.

Outspread of powdery mildew in the investigated fields was late. In the first estimation of diseases only some lesions were found. In the second diseases estimation the severity of powdery mildew in control fields was 2.14-2.26 %. The spreading of sugar beets with damp water steam in the beginning of vegetation caused the reliable decrease of powdery mildew.

CONCLUSIONS

1. The most effective weed control was in the case when damp water steam was applied for 3 times during the vegetation of sugar beets combined with the manual weeds removal as it was noticed during the estimation, carried out in 30 days after the last damp water steam treatment. This method was the most effective in reduction of air-dry weed mass as well.

2. The amount and the air-dry mass of weeds was almost the same in the cases when damp water steam was applied for 2 times (using protective covers fot the 2nd time) and chemical control was applied.

3. In order to reduce the environmental pollution, the use of herbicides in the sugar beets crop can be replaced with damp water steam using protection means (covers or soil beds) in order not to damage the crop.

4. Damp water steam, used during the first half of sugar beets vegetation reduced development of foliar fungal diseases in the crop. After the treatment with the damp water steam for 3 times the severity of cercospora in the end of September was 58.8 – 78.9 %, the severity of ramularia 51.7 – 52.0 % and the severity powdery mildew was 70.8 – 77.6 % smaller than in the fields treated with herbicides.

REFERENCES

[1] Stravinskienė, V. (2009) Aplinkos bioindikacija. Kaunas, 332.

[2] Urbienė, S. (2010) Maisto toksikologijos pagrindai. Akademija, 372.

[3] Lazauskas P., Pilipavičius V. ir kt. (2008) Ekologinis žemės ūkis/ IDP Solutions, Klaipėda, 377.

[4] Edesi, L., Jarvan M., Adamson, A., Lauringson E., Kuht J. (2012) Weed species diversity and community composition in conventional and organic farming: a five-year experiment.

[5] Žemdirbystė / Agriculture, vol. 99 No. 4, p. 339-346

[6] Riemens, M. M., Groeneveld, R. M. W., Lotz, L.A., Kropff, M.J. (2007) Effects of three management strategies on the seedbank, emergence and the need for hand weeding in an organic arable cropping system. Weed Research, vol. 47, No. 5, 442-451

[7] Jodaugienė, D., Raudonius, S., Špokienė, N. (2008) Piktžolių ekologija. Akademija, 108.

[8] Van der Weide, R., Bleeker, P., Achten, V., Lotz, L., Fogelberg, F. Melander, B. (2008) Innovationin mechanical weed control in crop rows. Weed research, 48, 215-224.

[9] Fontanelli, M., Raffaelli, M., Ginanni, M., Lulli L., Frasconi, C., Sorelli, F., Peruzzi, A. (2009) Non-chemical weed control on open-field fresh market tomato in the Serchio Valley (Central Italy). Proceedings of 8th EWRS Workshop and Physical and Cultural Weed Control, Zaragoza, Spain, 41-48.

[10] Tei, F., Stagnari, F., Granier, A. (2003) Preliminary results on physical weed control in spinach. European Weed Research Society. 5th EWRS Workshop on Physical and Cultural Weed Control Pisa, Italy, 164-171

[11] Collins, R.M., Bertram, A., Roche, J.A., Scott, M.E. (2003) Preliminary studies in the comparison of hot water and hot foam for weed control. European Weed Research Society. 5th EWRS Workshop on Physical and Cultural Weed Control Pisa, Italy, 207-215

[12] Hanson, D., Ascard, J. (2002) Influence of developmental stage and time of assessment on hot water weed control. Weed Research, 42, 307-316.

[13] Sirvydas, A., Kerpauskas, P., Nadzeikienė, J., Stepanas, A., Tereščiuk, V.S. (2006) Temperature measurements in research of thermal weed extermination. Proceedings of the international conference „Development of agricultural technologies and technical means in ecological and energetic aspects.“ Lithuania, Raudondvaris, 11, 321-331.

[14] Virbickaite, R., Sirvydas, A.P., Kerpauskas, P., Vasinauskienė, R. (2006) The comparison of thermal and mechanical ways of weed control. Agronomy research, 4 (Special issue), 451-455.

[15] May, M.J. (2003) Economic consequences for UK farmers of growing GM herbicide tolerant sugar beet. Annals of Applied Biology, 142, 41-48.

[16] Dewar, A.M., May, M.J., Waiwod, I.P., Haylock, L.A., Champion, G.T., Garner, B.H., Sands, R.J., Qi, A., Pidgeon, J.O. (2003) A novel approach to the use of genetically modified herbicide tolerant crops for environmental benefit. Proceeding of the Royal Society: Biological Sciences, 270, 335-340.

[17] Wolf, P.F.J., Verreet, J. (2002). An integrated pest management system in Germany for the control of fungal leaf diseases in sugar beet: The IPM sugar beet models. Plant Disease, 86 (4), 336-344

[18] Gaurilčikienė, I., Deveikytė, I., Petraitienė, E. (2006). Epidemic progress of Cercospora beticola Sacc. in Beta vulgaris L. under different conditions and cultivar resistance. Biologija, 4, pp. 54-59.

[19] Dabkevičius, Z., Brazauskienė, I. (2007). Augalų patologija. Akademija, Kėdainių r.: Lietuvos žemdirbystės institutas

[20] Deveikytė I., Petkevičienė B., Kaunas J. (2009). Cukriniai runkeliai: agrobiologija, tyrimai, technologijos: monografija. Lietuvos žemdirbystės institutas

[21] Šurkus J., Gaurilčikienė, I. (2002). Žemės ūkio augalų kenkėjai, ligos ir jų apskaita. Lietuvos žemdirbystės institutas

[22] Tarakanovas P., Raudonius S. 2003. Agronominių tyrimų duomenų statistinė analizė, taikant kompiuterines programas ANOVA, STAT, SPLIT-PLOT iš paketo SELEKCIJA ir IRRISTAT. Lithuanian University of Agriculture (in Lithuanian

Received: **16.11.2015**
Accepted: **16.03.2016**

CORRESPONDING AUTHOR

Dr. Zita Brazienė
Lithuanian Research Centre for Agriculture and Forestry
Rumokai Research Station,
Klausučiai,
LT-70462 Vilkaviškis distr.
Lithuania

E-mail zitamo421@gmail.com

© by PSP Volume 25 – No. 7/2016, pages 2662-2667 Fresenius Environmental Bulletin

BENTHIC DIATOM ASSEMBLAGES FROM MADEN STREAM (ELAZIG-TURKEY): AN EXAMINATION OF COMMUNITY RELATIONSHIPS AND HABITAT PREFERENCES

Vesile Yildirim, A. Kadri Cetin

Biology Department, Science Faculty, Firat University, 23119 Elazığ, Turkey

ABSTRACT

In this stuady, community structure of benthic diatoms in Maden Stream was studied over 1- one year period. A total of 77 taxa were identified in benthic habitats. The aim of this stuady is to describe to epipelic, epilithic, epiphytic diatom communities in Maden Stream and the diversity of species, similarity of benthic diatoms in different habitats of stream. It is clear that certain diatom taxa have microhabitat preferences. *Cretoneis arcus, Frustulia vulgaris, Meridion circulare, Navicula bacillum, N. cari, N. gracilis, N. menisculus, N. tuscula, N. reinhardtti Nitzschia hungarica, Surirella robusta* were recorded in epilithic habitats. *Didymosphenia geminata* was recorded only in epipelic habitats The abundance of diatom taxa recorded varied substantially among the habitat types. The genera *Cymbella*, *Navicula*, *Nitzschia* and *Gomphonema* comprised the most of species and were numerically bigger in most communities. Frequency, diversity and similarity of diatoms varied among habitats.

KEYWORDS:
Benthic diatoms, habitat, streams, substratum, epilithic, epipelic, epiphytic

INTRODUCTION

Benthic diatoms are important members of water ecosystem and they are often dominate as primary producer. Water ecosystems are endangered worldwide by the increasing pollution and eutrophication. Benthic diatoms are not only affected by these processes but they are also excellent bioindicators of them. Their short generation time, attached lifestyle and widespread occurence qualifies them as preferred organisms of the modern bioindicators in systems. In streams and rivers, benthic diatoms are distributed widely on streambed substrata such as surfaces of rocks, stones and plants [1]. Species composition of benthic algal communites sampled at the same site but from different substrates (e.g., rock surface, upper layer of sediment, or water plants) which often differs substantially because some species are better adapted to one microhabitat than to others [2]. Some researchers found distinct communities of diatoms on different substrates in water bodies, indicating species habitat preferences. In a study of sandy streams, it was found that diatom species composition varied more from year to year among micro habitat and stream [3, 4]. In the ecological literature, studies on benthic algae phytoplankton is more than work. Many studies related to environmental variation on diatom community composition but is focused on a few specific stream habitat preferences. By determining the microhabitat and substrate preferences of these benthic diatom taxa, the potantial exist for interferring the past changes in available habitats from fossils diatom asseblages collected from sediment cores and ultimately to reconstruct past environmental and climatic changes responsible for these shifts in habitat availability [5].

The present study was carried out to determine the epipelic, epilithic and epiphytic diatom communities in Maden Stream and characterize the abundances, similarities and diversities on different substrates.

MATERIAL AND METHODS

Site Description. The Maden Stream is located in eastern Turkey (39,39^0-37$^{'}$-32$^{''}$E, 38^0-26$^{'}$-32$^{''}$ N) at an altitude of 1054.The region is surrounded by high mountains. The stream flows through a nutrient-poor sedimentary rock catchment for approximately 46 km and enters the Dicle River. The in stream vegetation is predominantly of *Ranunculus* sp. And *Thypha* sp. , and streambed substrate consist of stones and gravels. The stream is rarely shaded by riparian vegetation.

Epilithic, Epipelic and Epiphytic diatoms were sampled on monthly basis in four stations between January 2008 and December 2008. Epilithic diatoms were collected into plastic containers

monthly as pooling upper-surface by scraping from several rocks. Epiphytic diatoms from dominant macrophytes were taken together with parts of stems or leaves. Epipelic diatoms were collected from the most superficial layer (5-10 mm) of sediment using a 3 cm in diameter core.

In order to prepare permanent diatom slides, organic material of subsamplaes was digested with nitric/sulphuric acid. Neutralized samples were dried on coverslips, whic were mounted on slides with balsam. Two hundered frustules per samples were identified and counted at 1000 X magnification in order to obtain the estimated frequencies of different species of epiphytic, epilithic and epipelic diatoms. Species were identified according to Krammer and Lange-Bertalot [6-9].

Diatom diversity (*H'*) was estimated using the Shannon-Wiener index [10]. Similarity between habitats was calculated with the Sorensen similarity index. All calculations and statistical analyses coduct with SPSS (version 10. 0) software.

RESULT AND DISCUSSION

A total 77 taxa were identified in **t**he stream. The number of diatom taxa recorded varied substantialy among the habitat types. The diatom community in each habitat was generally domined by seven taxa. *Cymbella*, *Navicula*, *Nitzschia* and *Gomphonema* comprised the most of the species and were numerically dominant in most communites. Frequency, diversity and similarity of diatoms varied among habitate. Overall, many diatom taxa appeared to be present on more than one substrate; however, some species showed a strong affinity to only one habitat type. *Fragilaria ulna* was the most common diatom collected from all three habitats (Table 1). This is similar to finding of Cetin [11]. Some diatom species were more abundant in one habitat than another. This is similar to the findings of Stevenson and Hashim [12] and Lim et al. [13]. *Achnanthes lanceolata*, *Cymbella helvetica*, *Diatoma vulgaris, Gomphonema parvulum, Navicula cryptocephala*, *Nitzschia palea* and *Surirella linearis* were the most abundant in the epipelic samples while *Achnanthes minutissima*, *Cymbella affinis*, *C.ventricosa C.minuta, Diatoma tenuis, Gomphonema olivaceum, Navicula pupula, Nitzscia amphibia, N. thermalis, Surirella angustata* were the most numerous taxa in the epilithic samples. *Cocconeis placentula, Cymbella cistula, Gomphonema truncatum, Navicula radiosa, Nitzschia hantzschiana, N. linearis, Rhopalodia gibba* were recorded as the most abundant in the epiphyton. *Cocconeis placentula* were also found in high abundance one plant substrates in other periphytic diatom studies [13]. Species which were significantly confined to plant surfaces were more or less similar to typical epilithic species (e.g. *Achnanthes lanceolata)*, except *Cocconeis placentula*, which is generally assumed on grow preferntially on plants [6-9]. Not suprisingly, many of the diatom species were found on more than one substrate, suggesting that some species take the advantage of more than one habitat type. In addition, a few species showed a strong affinity to only one habitat type. For instance some benthic diatom taxa showed specific distribution in the stream. *Didymosphenia geminata* was recorded only in the epipelic samples. *Ceratoneis arcus, Frustulia vulgaris, Meridion circulare, Navicula gracilis, N. menisculus, N. cari, N.tuscula, N. bacillum, Nitzschia hungarica, Meridion circulare, Surirella robusta* only in the epilthic samples. It is possible that these species are sensitive species with a narrow ecological tolerance. It is known that rare species are important even critical, in community ecology and bioassesment for detecting primary or secondary environmental gradients or impacts.

Cymatopleura eliptica, Cymbella amphicephala, C. gracilis, Diatoma moliformis, Neidium dubium were present on both rock and sediment but not on macrophyte substrates. Epiphytic and epipelic assemblages had fewer number of species compared to epilithic assemblages. Epilithic diatom communites should be more stable than epiphytic and epipelic communites because of inherent stability of stony substrate. The fast growing macrophytes can rather be unstable substrata for algal colonization and growth [14].

Although abundances of benthic diatoms varied in most habitats, the greatest differences in composition were actually in sampling dates rather than habitat within stream. In general, diatoms species composition in the stream was similar to the composition in other aquatic ecosystems [15-18].

Epipelic, epilithic and epiphytic diatoms in the Maden stream were charecterized by high species diversity. The diversities (H') were varied from 2.26 to 3.07 (Fig. 1) . In the sampling period, a total of 54 epipelic diatom taxa was found. Species diversity for epipelic diatoms were varied from 2.26 to 2.98. In the epiphytic assemblage, 60 species were found. Species diversity for epiphytic diatoms were varied from 2.26 to 2.96. In the epilithic diatom community of Maden Stream, the diversity index values varied from 2.61 to 3.01 with the highest diversity in May. Relatively higher diversity values were recorded in epilithic assemblage during the sampling period. Species diversity and abundance of diatoms recorded in the stream exceeded the highest values reported for aquatic habitats in other regions in late spring and early summer [17, 19, 20]. According to Leand [21], temperature strongly infulance phytobentos

TABLE 1
Relative abundance (%) of diatoms occuring in epipelic, epilithic, and epiphytic samples.

Taxa	Relative Abundance(%)		
	Epipelic	Epilithic	Epiphytic
Cyclotella meneghiniana Kützing	2.76	1.39	1.60
Achnanthes minutissima Kützing	2.26	11.89	2.98
A. lanceolata (Brebisson) Grunow	4.46	4.47	3.49
Melosira varians Agardh	3.47	1.93	2.95
Amphora ovalis (Kützing) Kützing	0.14	0.21	0.11
Cocconeis placentula Ehrenberg	3.40	1.24	6.45
Cymatopleura elliptica (Brebisson) W. Smith	0.71	0.58	-
C. solea (Brebisson) W. Smith	2.33	0.16	1.69
Cymbella affinis Kützing	2.08	2.56	3.30
C. amphicephala Naegeli	0.63	0.08	-
C. aspera (Ehrenberg) Cleve	0.39	0.33	0.35
C. caespitosa Kützing	0.71	0.20	0.30
C. lanceolata (Ehrenberg) Kirchner	0.57	0.59	0.42
C. prostrata (Berkely) Cleve	0.31	1,43	1.10
C.helvetica Kützing	4.62	2.86	4.55
C. cistula (Ehrenberg) Kirchner	2.49	1.62	5.65
C. angustata (W. Smith) Cleve	0.71	0.22	0.31
C. ventricosa (C. Agardh)	1.38	3.98	1.02
C.gracilis (Ehrenberg) Kützing	0.47	0.31	-
C.minuta Hilse ex Robh	2.41	2.63	0.70
C.cuspidata Kützing	0.23	0.44	0.50
Cretoneis arcus (Ehrenberg) Kützing	-	0.06	-
Diatoma tenuis Agardh	1.63	3.18	3.00
D. vulgaris Bory	4.46	1.70	2.90
D.moliformis Kützing	1.17	0.98	-
Didymosphenia geminata (Lyngbya)M.Schimidt	0.63	-	-
Diploneis ovalis (Hilse) Cleve	0.96	0.19	0.78
Epithemia adnata (Kützing) Brebisson	0.29	0.13	0.84
E.turgida Ehrenberg		0.18	0.33
Frustulia vulgaris (Thwaiter)		0.04	-
Fragilaria ulna (Nitzsch) Lange-Bertalot	6.62	5.86	6.78
F.arcus (Ehrenberg) Cleve	1.15	1.67	2.93
Gomphonema acuminatum Ehrenberg	0.96	0.57	0.54
G.angustatum Agardh	0.39	1.36	1.17
G.constrictum Ehrenberg	1.66	0.81	1.23
G. truncatum Ehrenberg	0.25	0.05	5.21
G. parvulum (Kützing) Grun	4.04	6.77.	3.34
G. olivaceum (Hornemann) Brebisson	2.02	1.20	0.47
Gyrosigma acuminatum (Kützing) Rabenhorst	1.91	0.31	0.25
Hantzschia amphioxys (Ehrenberg Grunow.	0.80	0.11	0.34
Meridion circulare (Greville) Agardh	-	0.30	-
Navicula cryptocephala Kützing	5.67	1.95	2.85
N.cari Ehrenberg	-	0.02	-
N. cuspidata Kützing	0.18	0.03	0.64

N. gracilis Ehrenberg	-	0.12	-
N. pupula Kützing	1.20	3.58	0.98
N. radiosa Kützing	0.68	0.91	2.81
N. lanceolata (Agardh) Ehrenberg	-	0.23	0.31
N. rhyncocephala Kützing	0.19	0.42	0.73
N. viridula (Kützing) Ehrenberg	-	0.31	0.44
N. tripunctata (O. F. Müller) Bory	0.63	0.79	2.46
N. menisculus Schuman	-	0.09	-
N.tuscula (Ehrenberg) Grunow	-	0.05	-
N.trivialis Lange-Bertalot	2.68	2.06	1.60
N.praeterita Hustedt	-	1.38	1.09
N.salinarum Grunow	-	0.77	1.70
N.reinhardtii Grunow		0.32	-
N.bacillum Ehrenberg	-	0.01	-
Neidium dubium (Ehrenberg) Cleve	1.07	0.02	-
N. iridis (Ehrenberg) Cleve	-	0.01	1.61
Nitzschia amphibia Grunow	1.94	2.48	1.95
N. angustata Grunow	0.97	0.17	0.90
N. hantzschiana Rabenhorst	-	0.05	0.89
N. linearis (Agardh) W. Smith	2.39	1.90	4.11
N. palea (Kütz.) W. Smith	5.50	2.71	4.19
N. sigmoidea (Ehr.) W. Smith	2.55	2.70	2.81
N. gracilis Hantzsch	1.91	1.68	0.36
N. hungarica Grunow	-	0.12	-
N. thermalis Kützing	2.85	6.54	2.36
Pinnularia viridis (Nitzsch.) Ehrenberg		0.03	0.26
Rhopalodia gibba (Ehrenberg) O. Müller	0.10	0.47	1.11
Stauroneis anceps Ehrenberg	-	0.01	0.86
Surirella angustata Kützing		1.68	0.38
S. ovata Kützing	-	0.15	0.24
S. linearis W. smith	0.81	0.23	0.24
S. ovalis Brebisson		0.63	0.27
S. robusta Ehrenberg		0,02	-

communities. Temperature can influence diatoms directly by affeting metabolic processes and cell division and indirectly via changes in physical, chemical and biological properties of river and streams [22]. Patova and Charls [23] reported that mean annual air temperature affected significantly the diatom distribution patterns in rivers significantly. The present study also concluded that high water temperatures supports richness of species in benthic diatoms, while low temperature inhibits their growth and richness of species.

The degree of similarity in all benthic diatom assembleges was high among the habitats (Table 2). Sorensen's similarity coefficient calculated as the highest (0.95) between epipelic and epilithic diatoms in May. In January and February, similarity for all the sampled substrate was between 0.61 and 0.69. Similarity between epipelic and epilithic diatom communities was calculated as 0.35 in December, which was the lowest similarity observedin the stream during the sampling periods. In December, similarity between epilithic and epiphytic diatoms was greater than the similarity between epipelic and epiphytic or similarity between epipelic and epilithic. Species significantly confined to plant surfaces were more or less similar to thypical epilithic species (e.g. *Achnanthes lanceolata*), except *Cocconeis placentula*, which is generally assumed to grow preferentially on plants [6-9]. Eloranta [24] reported that the most significant species confined to the Stone surfaces were *Achnanthes minutissima* and *Gomphonema parvulum*. However, *Cocconesis plasentula* was clearly confined to plants surfaces. Thes findings are similar to those of Eloranta et al. [24]. In our

TABLE 2
Similarities of epipelic, epilithic, and epiphytic diatom communities in Maden Stream.

	Epipelic-Epilithic	Epipelic-Epiphytic	Epilithic-Epiphytic
January	0.61	0.66	0.69
February	0.67	0.62	0.61
March	0.70	0.75	0.87
April	0.79	0.91	0.82
May	0.95	0.85	0.89
June	0.80	0.75	0.87
July	0.68	0.70	0.66
August	0.60	0.72	0.63
September	0.77	0.84	0.82
October	0.71	0.79	0.85
November	0.51	0.63	0.89
December	0.35	0.46	0.73

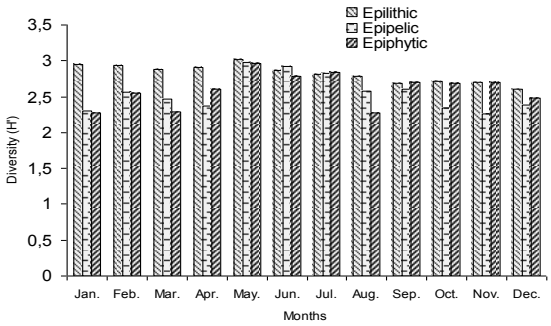

FIGURE 1
Diversities (H') of epipelic, epilithic and epiphytic diatom communities.

study, *Cocconeis placentula* was more abundant in other habitats compared to aquatic macrophyts. The variation in algal dynamics in habitats may ocur as a result of algal adaptation to direct abiotic or biotic pressures orienting from physicochemical differences on habitats in streams [12]. However, we found no correlation between diversity of species *(H)* and selected physicochemical features (temperature, dissolved oxygen, pH and calcium and magnesium consentrations). As in terrestrial ecosystems patchiness in plant distribution may be a function of soil type or drainage patterns, so in benthic communities unevenness may not be random and accidental [25].

Many evironmental factors are probably important for explaning these inconsistencies. Diatoms and other microalgae interact with environmental variations at many scalas. Some environmental conditions may constrain variation in community structure during the community development. Many factors may enhance or limit the differences in benthic algal community dynamics among habitats in streams and there by regulate structure and function of community. The variation in algal abundances and species composition in different habitats in stream may explain invertebrate patchiness by providing food and refugia from predators. In conclusion, we have not fount clear patterns among diatom assemblages in three habitats. Some taxa were observed in all the habitats, while others were uncommon.

REFERENCES

[1] Bere T., (2010) Benthic diatom community struture and habitat preferences along an urban pollution gradient in the Monjolinho River, Sao Carlos, Brasiliensia, 22, 1, 80-92.

[2] Patova G. M. and Charles D. F. (2005) Cohice of substrate in algae-based water quality assesment. J. N. Am. Benthol. Soc. 24 (2) : 415-427.

[3] Winter, J. G. And Duthie H. C. (2000) Stream epilithic, epipelic and epiphytic diatoms: habitat fidelity and use in biomonitoring. Aquatic Ecol. 34: 345-353.

[4] Soinen, J. and Heino J. (2005) Relationship between local population persistence, local abundance and regional occupancy of species: distribution patterns of diatoms in boreal stream. J. Biogeogr. 32: 1971-1978.

[5] Darlene S.S., Kwan C., Douglas M.S.V. (2001) Periphytic diatom assemblages from Bathurst Island, Nunavut, Canadian High Artic: An examination of community relationships and habitat preferences. Journal of Phycology 37: 379-392.

[6] Kramer, K. and Lange-Bertalot H. (1986) Bacillariophyceae. 1. Teil: Naviculaceae. Süsswasserflora von Mitteleuropa. Band 2/1. Gustav Fischer Verlag, Stuttgart, New York. 876 pp.
[7] Kramer, K. and Lange- Bertalot H. (1988) Bacillariophyceae. 2. Teil: Bacillariophyceae, Epithmiaceae, Surirellaceae. Süssvasserflora von Mitteleuropa. Band 2/2. Gustav Fischer Verlag, Stuttgart New York. 596 pp.
[8] Kramer, K. and Lange-Bertalot H. (1991) a. Bacillariophyceae. 3. Teil: Bacillariophyceae, Centrales, Fragilariaceae, Eunotiaceae. Süssvasserflora von Mitteleuropa. Band 2/3.Gustav Fischer Verlag, Stutgart New York.576 pp.
[9] Kramer, K. and Lange-Bertalot H. (1991) b.Bacillariophyceae. 4. Teil: Achnanthaceae. Süssvasserflora von Mitteleuropa. Bad 2/4. Gustav Fischer Verlag, Stuttgart New York. 437 pp.
[10] Shannon, C.E. and Weaver W. (1949) The matematical theory of communication. Univ. of Illinois Press, Urbana 177 pp.
[11] Cetin, A. K. 2008. Epilithic, epipelic and Epiphytic Diatoms in the Göksu Stream: Community relationships and Habitat Preferences. Fershwater ecology, 23, 1, 141-149
[12] Stevenson, R. J. and Hashim S. (1989) Variation in diatom community structure among habitats in sandy streams. J. Phycol. 25: 678-686.
[13] Lim, D. S.S. , Kwan C. and Douglas M. S. V. (2001) Periphytic diatom assamblages from Bahurst Island and habitat preferences. J. Phycol. 37: 379-392.
[14] Burkholder, J. M. and Wetzel R. G. (1989) Microbial colonization on natural and artifical macrophyts in phosphorus-limited, hardwater lake. J. Phycol. 25: 55-65.
[15] Cetin, A. K., Sen ,B. and Yildirim V. (2002) Seasonal variations of epipelic diatoms in gölbaşı Lake with relation to physical-chemical variables. Fresen. Environ. Bull. 11: 306-311.
[16] Cetin, A. K. and Yildirim V. (2003) Epilithic and Epiphytic diatoms of Sürgü Reservoir (Malatya, Turkey). Int. J. Algae 5: 37-45.
[17] Sen, B., and Cetin A. K. (1988) Seasonal Dynamics of benthic diatoms in reservoirs in South- east Turkey. 505-511. Finland. In: Simola, H. (ed.), Proceedings of the 10th International Diatom Symposium, Finnland. Koeltz Scientific Books, Koenigstein.
[18] Yildirim, V., and Cetin A. K. (2006) Epilithic and piphytic diatoms of Gölbaşı Lake (Adiyaman, Turkey). J. Freshwater Ecol. 2: 353-354.
[19] Mosisch, T. D. , Bunn S. E., Davies P. M. and Marshall C. J. (1999) Effects of shade and nutrient manipulation on periphyton growth in subtropical stream. Aquatic Botany 64: 167-177.
[20] Round, F. E. (1984) The ecology of algae. Cambridge University Press. 653 pp.
[21] Leand, H. V. (1995) Distrubution of phytobenthos in the Yakima River basin, Washington, in relation to geology, land use and other environmental factors. Can. J. Fish. Aquat. Sci. 52: 1108-1129.
[22] Bothwell, M. L. (1988) Growth rate responses of lotic periphytic diatoms to experimental phosphorus enrichment: The influence of temperature and light. Can. J. Fish. Aquat. Sci. 45, 261-270.
[23] Patova, G. M. and Charles D. F. (2002) Benthic diatoms in USA rivers: distribution along spatial and environmental gradients. J. Biogeography 29: 167-187.
[24] Soininen, J. Eloranta and P. (2004) Seasonal persistence and stability of diatom communities in rivers: are there habitat specific differences. Eur. J. Phycol. 39: 153-160.
[25] Cox, E.J. (1988) Has the role of the substratum been underestimated for algal distribution patterns in freshwater ecosystem. Biofouling Vol. 1, pp.49-63.

Received: **20.10.2015**
Accepted: **24.03.2016**

CORRESPONDING AUTHOR

Vesile Yildirim
Fırat University Department of Biology, 23119 Elazığ, TURKEY

E-mail: vyildirim@firat.edu.tr

© by PSP Volume 25 – No. 7/2016, pages 2668-2675 Fresenius Environmental Bulletin

A NEWLY FOUND CADMIUM HYPERACCUMULATOR — *CENTELLA ASIATICA* LINN.

Kehui Liu[1, 3], Zhenming Zhou[1, 2], Fangming Yu[1, 2], Menglin Chen[1, 2], Chaoshu Chen[1, 2] Jing Zhu[1, 2], Yongrong Jiang[1, 3]

[1]Key Laboratory of Karst Ecology and Environment Change of Guangxi Department of Education, Guilin 541004, China;
[2]College of Resource and Environment, Guangxi Normal University, Guilin 541004, China;
[3]College of Life and Environmental Science, Guilin University of Electronic Technology, Guilin 541004, China

ABSTRACT

Phytoremediation is a novel biological remediation technique, and searching for new hyperaccumulators is one of the key points during its application. In the present work, both field investigation (Siding lead-zinc Mines, southern China) and laboratory experiment (incubation with five concentration gradient 0 (CK), 0.5, 1, 2.5 and 5 mg L^{-1} Cd) were carried out to testify whether *Centella asiatica* L. is a potential cadmium (Cd) hyperaccumulator. Field results showed that *C. asiatica*. could grow normally even as the soil concentration of Cd was as high as 124 to 1010 mg kg^{-1}. In general, Cd concentrations accumulated in leaves, petioles, and stems were over 100 mg kg^{-1}. The ratio of Cd concentration in petioles to that in roots (P/R: the ratio of Cd concentrations in petiole to those in roots) ranged from 0.83 to 1.84, indicating its good translocate ability to aboveground parts. The laboratory experiment further confirmed its capable characteristic for hyperaccumulation and hypertolerance of Cd, i.e., no negative effects on plant growth, high Cd accumulation in tissues, high antioxdative enzyme activities and the appropriate TF values (P/R > 1). All these results suggested that *C. asiatica* was a new Cd-hyperaccumulator.

KEYWORDS:
Cadmium; *Centella asiatica* L.; Phytoremediation

INTRODUCTION

Cadmium (Cd) is not essential to organism, and its persistence in soil has brought a major global concern as the associating health risks. Because Cd can be biomagnified in the food chains, and become increasingly dangerous to humans and wildlife [1]. Therefore, seeking remedial methods and techniques for Cd contaminated soil and water is extremely urgent and necessary. Phytoremediation is a novel biological remediation technique and has become a hotspot of pollution remediation for its potentially cost-effective, simple engineering operation and environmentally-friendly characters [2-3]. While searching for proper hyperaccumulators that accumulate high levels of heavy metals is a prerequisite for the technique.

So far, more than 450 species that hyperaccumulate heavy metal have been identified in the plant kingdom, while few of them were reported to be Cd hyperaccumulators [4-7]. Meanwhile, the species that can be utilized for Cd phytoremediation usually have some limitations in practice, i.e. small biomass, slow growth, poor resistance or lack of seeds and competitiveness with local plants [8]. Therefore, finding more and new hyperaccumulators for the remediation of Cd contaminated soil and water is necessary.

Centella asiatica Linn (Fig. 1) is one kind of perennial herbs with the characteristics of prostrate stems, stoloniferous, rooted at nodes, and widely distributed in tropics and subtropics area. It tends to grow in swamps, paddy fields or riversides in southern China [9]. Except of its wide geographic distribution, it also possesses characteristics of easy cultivability and high competitiveness. Accidentally, we found this kind of species could grow well in one Lead-zinc mining area in Guangxi, south China, during our vegetation investigation. We wondered whether it has high accumulation or tolerance to Cd. However, little information was available on the accumulation potential and tolerance of Cd for *C. asiatica*. Therefore we conducted hydroponics experiment under controlled conditions to elucidate its hyperaccumulation of Cd. The activities of antioxidative enzymes (SOD, APX, CAT and POD) and chlorophyll (CHL) contents were determined as well to understand the involving mechanisms.

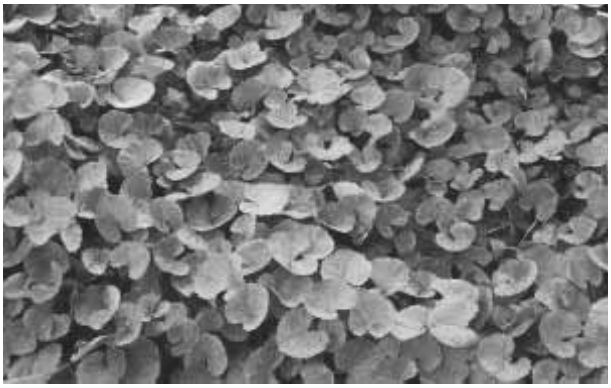

FIGURE 1
***Centella asiatica* Linn.**

MATERIAL AND METHODS

Field survey and sampling. Field surveys were conducted in swamps and ditches of the Siding lead-zinc Mine, which is located in Rongan County, Guangxi Province, southern China (109°31E, 25°01N). The climate in this area is sub-tropical monsoon, with an annual average temperature of 16.4℃ and an average rainfall of 1985 mm. The Siding lead-zinc Mine has vast deposits of lead-zinc mineral resources, covers an area of 13.64 sq km. The mining activities began in 1960 and stopped in 1998 [10], resulting in heavy-metal contamination of soil and water in this area. To investigate plants species kinds and their phytoaccumulations in this mining area, we carried out a preliminary field survey in April 2013 and were surprised to discover that *C. asiatica,* which is a common member of the woodland flora, contained high levels of Cd in shoots. A detailed study on C. *asiatica* was conducted in August 2013. Nine individual plants, named S1 – S9, were collected randomly within the sampling area. The corresponding rhizospheric soil (0-30 cm depth) was gathered concurrently. Soil samples were air-dried and sieved through a 2 mm sieve.

Hydroponic culture. Seedlings of *C. asiatica* were collected from swamps and ditches of the Siding lead-zinc Mine, and pre-cultured in Hoagland nutrient solution for 4 weeks. Then healthy and uniform seedlings were transplanted into the prepared plastic pots, continued to culture in solutions with 5 different Cd concentrations: 0 (CK), 0.5, 1, 2.5 and 5 mg L^{-1} Cd, added as $CdCl_2 \cdot 2H_2O$. Each treatment was triplicated . The solutions were aerated 24h a day, adjusted daily to pH 5.8 with 0.1 mol l^{-1} HCl or 0.1 mol l^{-1} KOH, and renewed every three days to restore volume to their original levels. The experiment was conducted in controlled environmental conditions with a 16-h light period at intensity of 350 μmol m^{-2} s^{-1}, and the day/night temperature of 25 °C/20 °C.

Plants were harvested at 18 d after Cd treatment. After being rinsed with tap water, roots of intact plants were immerged in EDTA-Na solution for 15 min to remove the metal ions adsorbed on the surface. Then the whole plants were washed with tap water and rinsed with deionized water, followed by drying with filter paper. The fresh weight (fw), root length and plant height were determined afterwards. The whole plants were then separated into roots, stems and leaves. The subsamples of different fractions for the determination of Mn concentration were firstly dried at 105 ℃ for 30 min, and then at 70 ℃ to constant weight. The subsamples of different fractions for the measurements of biochemical parameters were frozen immediately in liquid nitrogen and stored in refrigerator at -80 ℃.

Chlorophyll content, enzyme activity and lipid peroxidation, measurements. Chlorophyll content, enzyme activity and Malondialdehyde (MDA) contents were extracted and measured in the same way as our previous study [10].

Determination of Cd accumulation. Cd concentrations in plants and soils were prepared and measured in the same way as our previous study [10].

Calculation. Data were processed with Microsoft Excel 2007 and SPSS13.0 software. All the values expressed were means±standard deviation (S.D.) of three replicates. Data were statistically analyzed by the one-way ANOVA, taking $p < 0.05$ as significant according to the LSD test.

RESULTS

The growth of *C. asiatica* and its accumulation of Cd at field condition. The results of the field investigation showed that only a few species of plants were found in the swamps and ditches in the Siding lead-zinc Mine, i.e. *C. asiatica* and *Miscanthus floridulus*. *C. asiatica* could prostrate and creep about one meter with no macroscopic symptom therein, even though soil Cd concentration in this area was as high as 124 to 1010 mg kg^{-1} (Table 1).

Cd concentrations in soils and in different tissues of *C. asiatica* were listed in Table 1. In general, petioles contained the highest Cd concentrations, ranged from 85.3 mg kg^{-1} to 567 mg kg^{-1} with the average value of 258 mg kg^{-1}, which

TABLE 1
Cd bioaccumulation and transportation of *C. asiatica* growing on the Siding lead-zinc mine.

Sample No.	Cd in plant tissues (mg kg^{-1} DW)				Cd in Soil (mg kg^{-1})	L/R[a]	P/R[b]	S/R[c]	L/S[d]	P/S[e]	S/S[f]
	Leaf	Petiole	Stem	Root							
S1	330.7±16.1	517.0±12.3	361.9±18.2	281.7±14.6	1010.9±31.1	1.17	1.84	1.29	0.33	0.51	0.36
S2	327.9±15.4	567.0±17.1	390.4±7.6	551.6±18.8	338.8±19.9	0.59	1.03	0.71	0.97	1.67	1.15
S3	187.2±14.8	338.1±10.4	203.3±16.2	283.5±16.7	124.3±6.7	0.66	1.19	0.72	1.51	2.72	1.64
S4	164.0±7.6	254.3±10.5	155.3±8.8	253.9±11.9	757.6±37.2	0.65	1.00	0.61	0.21	0.33	0.21
S5	137.8±13.2	171.2±7.5	76.2±5.5	103.1±5.8	233.3±18.5	1.34	1.66	0.74	0.59	0.73	0.33
S6	87.9±7.6	118.8±8.9	111.9±5.6	143.5±8.0	132.3±8.8	0.61	0.83	0.78	0.66	0.89	0.85
S7	135.5±10.2	85.3±3.5	73.4±4.9	71.5±4.4	496.1±71.4	1.90	1.19	1.03	0.27	0.17	0.15
S8	88.2±5.6	165.6±6.9	182.2±11.5	100.1±6.3	397.8±20.2	0.88	1.65	1.82	0.22	0.41	0.45
S9	94.9±5.9	113.6±4.8	108.7±5.1	87.2±5.2	300.1±15.5	1.09	1.30	1.25	0.32	0.38	0.36

Note: Values are means ± S.D. (n = 3). [a, b, c] are the ratio of Cd concentrations in leaves, petioles and stems to those in roots and [d, e, f] are the ratio of Cd concentrations in leaves, petioles and stems to those in soils, respectively.

TABLE 2
Effects of Cd on growth of *C. asiatica*

Cd concentration (mg L^{-1})	Root length (cm plant^{-1})	Plant height (cm plant^{-1})	Fresh weight (g plant^{-1} FW)
0	7.88±0.64a	11.90±2.41b	0.74±0.15c
0.5	9.23±0.64a	21.03±4.33a	1.44±0.35a
1.0	8.83±1.10a	15.20±3.07b	1.29±0.09ab
2.5	8.80±0.56a	13.30±1.67b	1.24±0.39ab
5.0	4.45±0.31b	12.50±3.28b	0.85±0.20bc

Values are means ± S.D. (n = 3). One-way ANOVA (1 factor: type of issue) were performed for each parameter and different letters within the same column meant there was significantly different at $p < 0.05$ based on LSD. (the same below)

were constantly much higher than those in leaves, stems and roots. Cd concentrations in leaves (except S6, S8 and S9), petioles (except S7), and stems (except S5 and S7) were all over 100 mg kg^{-1}, which was the critical concentration for a Cd hyperaccumulator.

The ratio of Cd concentrations in petioles to those in roots (P/R) ranged from 0.83 to 1.84, indicating its good transport capacity to aboveground parts. Because of the high level of Cd concentrations (124 - 1010 mg kg^{-1}) in the corresponding mine soils, the values of L/S, P/S and Stem/S were very low. (L/S, P/S and Stem/S represented the concentration ratios in leaves, petioles, and stems to that in soil, respectively).

The growth of *C. asiatica* and its accumulation of Cd under controlled conditions. Plant growth. The growth response of *C. asiatica* to different Cd supply levels were shown in Table 2. During the whole experiment period, there were no visible toxic symptoms such as necrosis, whitish-brown chlorosis, deformation of young leaves, and growth retardation under any Cd exposure (0-5 mg L^{-1}). Cd supply could promote the increase of plant height and biomass accumulation, especially at low Cd concentration (0.5 mg L^{-1}). The plant height increased by 5.04% - 74.72% under Cd treatments, and the corresponding values were 14.86% - 94.59% in biomass. Root length showed no significant ($p > 0.05$) inhibition below 5 mg L^{-1} Cd treatment. Significant ($p < 0.05$) reduction of root length occurred at 5 mg L^{-1} Cd treatment, which indicated that roots were more sensitive to Cd pollution. Meanwhile, many new roots tillered from the base of the old roots, which may implicate that Cd stimulated the root differentiation.

TABLE 3
Effects of Cd on the contents of chlorophyll and MDA in leaves of *C. asiatica*.

Cd concentration(mg L^{-1})	CHLa	CHL b	CHL (a+b)	CHL(a/b)	MDA
0	0.74±0.10b	0.14±0.01b	0.88±0.11c	5.21±0.45c	3.18±0.15b
0.5	0.99±0.04a	0.17±0.01a	1.16±0.05a	5.82±0.17c	3.36±0.26b
1.0	0.93±0.04a	0.12±0.01c	1.05±0.03b	7.73±0.96b	3.18±0.19b
2.5	0.77±0.02b	0.08±0.01d	0.85±0.01c	9.49±1.30a	3.24±0.30b
5.0	0.79±0.03b	0.15±0.01ab	0.94±0.02c	5.21±0.71c	3.77±0.17a

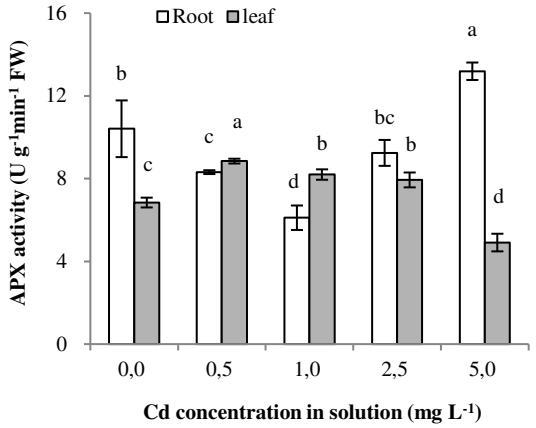

FIGURE 2
Effects of Cd on the enzyme activities in leaves and roots of *C. asiatica*

Chlorophyll and MDA changes in leaves. The changes of chlorophyll and MDA contents under Cd exposure in leaves of *C. asiatica* were shown in table 3. Cd treatments could promote Chl a contents by 6.76% - 33.78% as Cd concentrations in solution ranged from 0.5 mg L^{-1} to 5.0 mg L^{-1}. However, Chl b contents significantly ($p < 0.05$) inhibited at 1.0 and 1.5 mg L^{-1} Cd, and significantly ($p < 0.05$) increased at 2.5 mg L^{-1} Cd, indicating that Chl b were more affected by Cd pollution than Chl a as compared with control. The changes of Chl (a+b) had the same tend as that of Chl a. The ratio of Chl a/Chl b increased first, and then decreased with the increasing Cd supply in solution and peaked at 2.5 mg L^{-1} Cd level, which increased by 82.1% as compared with control. The contents of MDA kept stable at Cd level ≤ 2.5 mg L^{-1}, while significantly increased ($p < 0.05$) at 5.0 mg L^{-1} Cd exposure.

Antioxidative enzymes activities changes in leaves and roots. Effects of Cd on the enzyme activities in leaves and roots of *C. asiatica* were shown in Fig.2. SOD activities were similar at Cd level ≤ 2.5 mg L^{-1}, while increased significantly ($p < 0.05$) at 5.0 mg L^{-1} Cd exposure both in leaves Values are means ± S.D. (n = 3). One-way ANOVA (1 factor: type of issue) were performed for each parameter and different letters within the same tissues meant there was significantly different at $p < 0.05$ based on LSD.and roots. The similar trend was found in POD in leaves. The CAT activities were decreased with the increasing supply of Cd both in roots and leaves. While the changes of APX activities in leaves and roots were more complex: in root, it decreased first, reached its nadir at 1.0 mg L^{-1} Cd; and then increased with the increasing Cd concentration. Compared to the roots, the changes of APX in leaves had adverse trend and peaked at 0.5 mg L^{-1} Cd.

Cd accumulation in plants. Cd accumulations in leaves, petioles, stem and roots of *C. asiatica* increased significantly ($p < 0.05$) with increasing Cd supply in the solution (Table 4). In

TABLE 4
Concentrations of Cd in *C. asiatica* under Cd treatments.

Cd concentration	Leaf	Petiole	Stem	Root	L/R	P/R	S/R
0	1.97±0.06 e	1.64±0.04 e	0.53±0.02 e	1.88±0.25 e	1.04	0.87	0.27
0.5	51.72±0.61 d	85.98±3.67 d	51.01±1.65 d	84.54±2.64 d	0.61	1.02	0.60
1.0	112.34±6.22 c	204.23±11.90 c	187.51±5.90 c	194.94±8.39 c	0.58	1.05	0.96
2.5	167.66±6.96 b	337.52±11.16 b	240.68±5.32 b	316.3±18.40 b	0.53	1.07	0.76
5.0	282.27±7.95 a	604.96±30.05 a	378.28±23.06 a	567.6±33.71 a	0.50	1.07	0.67

general, the contents of Cd were found the highest in petioles, and then followed by that in roots, stems and leaves. The average Cd concentrations in leaves, petioles, stem and roots was 112.34, 204.23, 187.51 and 194.94 mg kg^{-1}, respectively, as *C. asiatica* was treated in solutions with 1 mg L^{-1} Cd, which were all exceeded 100 mg kg^{-1}, the critical value for being a Cd-hyperaccmulator. The absolute Cd accumulations in leaves, petioles, stems and roots were reached its peak at 5 mg L^{-1} Cd treatment. The ratio of P/R exceeded 1 under all Cd treatments, the ratios of L/R (Cd concentration in leaves to that in roots) and S/R (Cd concentration in stems to that in roots) were 0.50 - 0.61 and 0.60-0.96, respectively, both belew 1.

DISCUSSION

Cd hyperaccumlation potential *of C. asiatica*. Cd hyperaccumulators are defined according to the following criteria: (1) the concentrations of Cd in the shoots (stems or leaves) should not be lower than 100 mg kg^{-1} dry weight; and (2) the TF, which is the ratio of the Cd concentration in shoots to that in roots, should be higher than 1 [11]. In the present study, based on the field survey, *C. asiatica* could grow healthily with no observed necrosis and whitish-brown chlorosis. Moreover, the seedlings of *C. asiatica* could grow normally with no visible harm effect even as Cd concentration in soil was as high as 1010 mg kg^{-1}, which demonstrated that *C. asiatica* had high tolerance to Cd stress. The results of hydroponic culture experiment also showed that under high Cd stress (up to 2.5 mg Cd L^{-1} in solution), the plant biomass (FW) were stimulated instead of being inhibited, distinguishing *C. asiatica* from a normal plant as a hyperaccumulator.

Different tissues of *C. asiatica* contained different Cd concentrations, with the highest contents in petioles. And the values of TF were exceeded 1 (except S6), which indicated its strong transport capacity of Cd from roots to shoots. The results from hydroponic culture experiment showed, the concentration of Cd in the leaves, petioles and stems of *C. asiatica* were close to or more than 100 mg kg^{-1}; the concentrations of Cd in plants were significantly ($p < 0.05$) increased with the increasing level of Cd stress, and the values were peaked at 5 mg L^{-1}, the values were 282.27, 604.96, 378.28, and 567.7 mg kg^{-1} in leaf, petiole, stem and root, respectively. The TF values (P/R) were higher than 1.0 for all Cd treatments in *C. asiatica*, indicating that this species has good ability to transfer Cd from underground part to aboveground part. So, both field experiment and controlled experiment explicated that *C. asiatica* had high tolerance to Cd and high capacity to accumulate Cd.

Compared other Cd-hyperaccumulating plants, the TF values were higher than *Solanum photeinocarpum* [5], *Arthrocnemum macrostachyum* [12], and some natural vegetation [13]; but lower than *Solanum nigrum L.* (2.1) [14]), *Sedum alfredii Hance* (>1.5) [15] and *Bidens pilosa* L. [4] (1.3 – 7.4 at the flowering stages and 1.9 – 14.4 in the mature stage).

Plant growth and the mechanisms for the tolerance of *C. asiatica* towards Cd stress. Biomass changes were often concerned as it could immediate explanation whether a plant affected by heavy metal stress. The insignificant decrease in aboveground biomass of a hyperaccumulator growing in a heavy metal polluted environment is one of characteristics for a hyperaccumulator distinguished from a normal plant [16]. No reduction in plant growth or shoot and root dry biomass of *Solanum nigrum* L and *Sedum alfredii* H. were noted as the plants exposure to high Cd concentration (as Cd concentrations in soil were as high as 25mg kg^{-1} [17] and 200 mol L^{-1}[18], respectively) The results by hydroponics experiment also illustrated that *C. asiatica* collected from the swamps and ditches of the Siding lead-zinc Mine, could also grow well in Cd contaminated solution (0.5-5 mg L^{-1}). Cd supplying promoted the plant height increasing and biomass accumulation. And high Cd concentration (5 mg L^{-1}) could significant ($p < 0.05$) decrease the root length but promote new roots differentiation. It might be

one survival strategy for *C. asiatica* under high Cd stress. Its mechanism needs to further study. Meanwhile, the TF were also more than 1, these characteristics were consistent with the general properties of a typical Cd accumulating plant.

Cd is not essential to plant growth, and too high Cd concentration in plants usually causes various phytotoxic symptoms, including leaf chlorosis, root putrescence, growth inhibition, etc. As a hyperaccumulator, not only can enrich heavy metals in tissues, but also have strong detoxification mechanism [19]. Results analyzed from plant growth, contents of chlorophyll and MDA in the present study explicated that Cd had no negative effects on *C. asiatica* even at 5 mg kg^{-1} Cd solutions. The same phenomenon has been found as studying the enhancement of Cd to plant growth of *Lonicera japonica* Thunb [19]. Cd was also known to induce the burst of active oxygen species (AOS) in plant tissues, leading to oxidative stress [4]. The function of SOD in antioxidative defense is to eliminate active oxygen species (AOS), which generates H_2O_2, while the resulting H_2O_2 can be removed by CAT, APX, and POD enzymes. Increased activities of these enzymes commonly have been reported in plants exposed to metals [20]. In the present study, SOD, POD and CAT activities showed significant increase under Cd treatments both in leaves and roots, which efficiently removed the produced H_2O_2 and protected the physiological function of the plants. This is probably the protection mechanism of *C. asiatica* towards the damage caused by Cd. The phenomenon is quite similar to the results of some other metal-accumulators, e.g., *Thlaspi caerulescens, Brassica juncea* [21] and *Solanum nigrum* L. [22]. The efficiency of the protection mechanism can be well revealed by the accumulation of MDA, a breakdown product of lipid peroxidation [23-16]. It is the most widely accepted indicator of oxidative damage Cd has been reported to enhance lipid peroxidation in many plant species, e.g., *Triticum aestivum* [24], *Oryza sativa* [25] and *Allium. Sativum* [26]. The MDA concentration in *C. asiatica* did not show any significant increase as Cd concentration in solution was up to 2.5 mg L^{-1}, indicating an undetectable Cd damage on the plasma membrane of plant cells, which were consistent with the previous report [4].

CONCLUSION

Both the field investigation and the lab hydroponics experiment showed that *C. asiatica* had good tolerance to Cd stress, i.e., with normally growth, no visual Cd toxicity symptoms and strong internal detoxification mechanisms inside plant cells. The results suggested that *C. asiatica* was a Cd-hyperaccumulator since the concentration of Cd in aboveground tissues could be more than 100 mg kg^{-1}, the threshold criterion for a Cd-hyperaccumulator. Meanwhile, TF values were all greater than 1.0.. Besides, *C. asiatica* is a widely distributed perennial herb characterized by prostrate stems, stolonisation, rooted at node and growing in both hygrophytic and terrestrial environments. So, there is a great potential for using *C. asiatica* in the remediation of Cd-contaminated water and soil, especially in mine slopes recovery.

ACKNOWLEDGEMENT

This project was supported by the National Natural Science Foundation of China (No. 41161057, No. 51306811), Guangxi science and technology development project of major projects (No. Guikezhong 1298002-6, No. Guikezhuan 14122008-2), National Natural Science Foundation of Guangxi (No. 2014GXNSFAA118303) and Key Laboratory of Karst Ecology and Environment Change (Guangxi Normal University） Guangxi Department of Education, China (No. YRHJ15Z026, No. YRHJ15K002).

REFERENCES

[1]. Zhou, Q.X., Kong, F.X., Zhu, L. (2004) Ecotoxicology, Science Press, Beijing, China. (in Chinese)

[2]. Pulford, I.D., Watson, C. (2003) Phytoremediation of heavy metalcontaminated land by trees: a review. ENVIRON INT, 29, 529-540.

[3]. Smith, R.D. and Salt, D.E. (1997) Phytoremediation of metals: using plants to remove pollutants from the environment, CURR OPIN BIOTECH, 8, 221-226.

[4]. Sun, Y.B., Zhou, Q.X., Wang, L., Liu, W.T. (2009) Cadmium tolerance and accumulation characteristics of *Bidens pilosa* L. as a potential Cd-hyperaccumulator, J HAZARD MATER, 161:808-814.

[5]. Zhang, X.F., Xia, H.P., Li, Z.A., Zhang, P., Cao, B. (2011) Identification of a new potential Cd-hyperaccumulator *Solanum photeinocarpum* by soil seed bank-metal concentration gradient method. J HAZARD MATER, 189, 414–419

[6]. Liu, Z.L. He, X.Y., Chen, W., Yuan, F.H., Yan, K., Tao, D.L. (2009) Accumulation and tolerance characteristics of cadmium in a potential hyperaccumulator—*Lonicera*

japonica Thunb. J HAZARD MATER, 169:170-175.

[7]. Liu, H., Yuan, M., Tan, S.Y., Yang, X.P., Lan, Z., Jiang, Q.Y., Ye, Z.H. (2015) Enhancement of arbuscular mycorrhizal fungus (Glomus versiforme) on the growth and Cd uptake by Cd-hyperaccumulator *Solanum nigrum*. APPL SOIL ECOL, 89, 44 - 49.

[8]. Xiao, X., Luo, S.L., Zeng, G.M., Wei, W.Z., Wan, Y., Chen, L., Guo, H.J., Cao, Z., Yang, L.X., Chen, J.L., Xi, Q. (2010) Biosorption of cadmium by endophytic fungus (EF) Microsphaeropsis sp. LSE10 isolated from cadmium hyperaccumulator *Solanum nigrum* L., BIORESOURCE TECHNOL, 101, 1668-1674.

[9]. Deletes Florae Reipublicae Popularis Sinica Agendae Academiae Sinicae Edita, (1979) Flora Reipublicae Popularis Sinicae, Science Press, Beijing, China. (in Chinese)

[10]. Yu, F.M., Liu, K.H., Li, M.S., Zhou, Z.M., Deng, H., Chen, B. (2013) Effects of cadmium on enzymatic and non-enzymatic antioxidative defences of rice *(Oryza saliva* L.). INT J PHYTOREMEDIAT, 15, 513-521.

[11]. Baker, A.J.M. and Brooks, R.R. (1989) Terrestrial higher plants which hyperaccumulate metallic elements: a review of their distribution, ecology and phytochemistry. BIORECOVERY, 1, 81-126.

[12]. Redondo-Gómez, S., Mateos-Naranjo, E., Andrades-Moreno, L. (2010) Accumulation and tolerance characteristics of cadmium in a halophytic Cd-hyperaccumulator, *Arthrocnemum macrostachyum*. J HAZARD MATER, 184, 299–307.

[13]. Perez-Sirvent, C., Martinez-Sanchez, M.J., Bech, J., Garcia-Lorenzo, M.L., Bech, J. (2008) Uptake of Cd and Pb by natural vegetation in soils polluted by mining activities. FRESEN ENVIRON BULL, 17, 1666-1671.

[14]. Baker, A.J.M., Brooks, R.R., Kersten, W.J. (1985) Accumulation of nickel by Psychotria species from the Pacific Basin, TAXON, 34, 89–95.

[15]. Baker, A.J.M., McGrath,S.P., Reeves, R.D., Smith, J.A.C. (2000) Metal hyperaccumulator plants: a review of the ecology and physiology of a biological resource for phytoremediation of metal polluted soils, in: N. Terry, G. Baňuelos (Eds.), Phytoremediation of Contaminated Soils and Waters, CRC Press LLC, Boca Raton, FL, USA.

[16]. Wei, S.H. and Zhou, Q.X. (2004) Identification of weed species with hyperaccumulative characteristics of heavy metals, PROG NAT SCI, 14, 1259–1265.

[17]. Sun, Y.B., Zhou, Q.X., Diao, C.Y. (2008) Effects of cadmium and arsenic on growth and metal accumulation of Cd-hyperaccumulator *Solanum nigrum* L., BIORESOURCE TECHNOL, 99, 1103–1110.

[18]. Yang, X.E., Long X.X., Ye, H.B. Calvet, D.V. Stoffella, P.J. (2004) Cadmium tolerance and hyperaccumulation in a new Zn-hyperaccumulating plant species (*Sedum alfrdii* Hance), PLANT SOIL, 259, 181–189

[19]. Li, I.Z., He, X.Y., Wei, C., Yuan, F.H., Kun, Y., Tao, D.I. (2009) Accumulation and tolerance characteristics of cadmium in a potential hyperaccumulator—*Lonicera japonica*Thunb, J HAZARD MATER, 169, 170-175.

[20]. Cao, X.D., Ma, L.Q., Tu, C. (2004) Antioxidative responses to arsenic in the arsenic-hyperaccumulator Chinese brake fern (*Pteris vittata* L.), ENVIRON POLLUT, 128, 317-325.

[21]. Wang, Z., Zhang, Y.X., Huang, Z.B., Huang, L. (2008) Antioxidative response of metal accumulator and non-accumulator plants under cadmium stress, PLANT SOIL, 310, 137-149.

[22]. Sun, R.L., Zhou, Q.X., Sun, F.H., Jin, C.X. (2007) Antioxidative defense and pro-line/phytochelatin accumulation in a newly discovered Cd-hyperaccumulator, *Solanum nigrum* L.. ENVIRON EXP BOT, 60, 468-476.

[23]. Smirnoff, N. (1993) Tansley review No. 52 the role of active oxygen in the response of plants to water deficit and desiccation, NEW PHYTOL, 125, 27-58.

[24]. Wang, M.E., and Zhou, Q.X. (2006) Joint stress of chlorimuron-ethyl and cadmium on wheat *Triticum aestivum* at biochemical levels, ENVIRON POLLT, 144, 572-580.

[25]. Yi, Th., Y.T., Kao, C.H. (2004) Cadmium toxicity is reduced by nitric oxide in rice leaves. PLANT GROWTH REGUL, 42, 227-238.

[26]. Zhang, J., Cui, S., Li, J., Kirkham, M.B. (1995) Protoplasmic factors, antioxidant responses, and chilling resistance in maize. PLANT PHYSIOL BIOCH, 33, 67-75.

Received: 24.11.2015
Accepted: 19.03.2016

CORRESPONDING AUTHOR

Fangming Yu
NO.15 Yucai Road, Guilin, Guangxi Province, China. *C*ollege of Resource and Environment, Guangxi Normal University, Guilin 541004, China;

E-mail: fmyu1215@163.com

© by PSP Volume 25 – No. 7/2016, pages 2676-2681 Fresenius Environmental Bulletin

SPATIAL ANALYSIS WITH GIS MAPPING OF FUNGICIDE CONSUMPTION IN AGRICULTURAL AREAS

Oktay Erdogan[1*], M. Cüneyt Bagdatlı[1], Ahmet Zeybek[2]

[1] The University of Nevşehir Hacı Bektaş Veli, Engineering-Architecture Faculty, Department of Biosystem Engineering, 50300, Nevşehir, Turkey
[2] Muğla Sıtkı Koçman University, Science Faculty, Biology Department, 48000, Muğla, Turkey

ABSTRACT

The development in agriculture has gradually increased the use of fungicides in Turkey. Fungicides negatively affect the life conditions of living organisms in water, air and soil environments. It's important to be aware of the right amounts of chemicals to be used in certain periods. The aim of this study is to spatially determine the amounts of fungicide consumption using Geographical Information System (GIS) mapping, and also to determine the level of distribution in Nevşehir province and districts during the 2010-2014 period. The data obtained from the Turkish Statistical Institute and Nevşehir Directorate of Provincial Food Agriculture and Livestock has been evaluated by the help of Inverse Distance Weighting (IDW) method in the GIS. While the highest amount of fungicide consumption was observed to be 250.0 tons in 2010, the lowest amount of fungicide consumption was determined to be 179.78 tons in 2013. When examining the spatial distribution of fungicide consumption, the highest consumption intensity was observed in the North (Kozaklı district) and Northwest (Hacıbektaş district) of Nevşehir province, and the lowest consumption intensity is determined to be in the Southern (Central district) and South-western (Acıgöl district) agricultural areas through the whole period. According to the spatial distribution, the highest concentration intensity has been observed in Kozaklı and Hacıbektaş agricultural areas in all years.

KEYWORDS:
Fungicide consumptions, spatial analysis, GIS mapping, environment, agriculture

INTRODUCTION

The world's land area is limited and it is not possible to meet this need by opening up new areas for agricultural production. As well as the cultural methods, controlling against disease, pest and weeds should also be performed to ensure high yield efficiency in agricultural production. Loss of product due to plant diseases, pests and weeds is about 35 % in the world [1]. Lack of control can make this loss double folded [2]. Nowadays, pesticides are considered to be indispensable for more production from existing fields in all over the world [3]. The size of the pesticide market in the world is approximately $ 45 billion, while the market in Turkey is estimated to be approximately $ 600 million [4]. The pesticide market is composed of 41.5 % herbicides, plant growth regulators and growth inhibitors, 27.1 % insecticides, 21.5 % fungicides and 9.9 % other chemicals [5]. While 80 % share of the world pesticide market is in developed countries, the share of Turkey is 0.6 % [6]. Latin American countries are ranked top in terms of pesticides consumption, and these countries are followed by Japan, China, Malaysia and New Zealand [7]. The highest number of pesticide consumption in the EU is in the Netherlands and France, the countries with the least amount of consumption are Belgium and Finland. Examining the distribution of the chemicals used on products; we see that 24 % of the total chemicals have been used on fruit and vegetables, 15 % on cereals, 12 % on rice, 11 % on corn, 10 % on cotton, 8 % on soybean, 4 % on sugar beet, 2 % on rapeseed and 14 % on other products [8].

Pesticide consumption is estimated to be 1.3 kg/ha in Turkey [9]. Compared to above mentioned countries, pesticide use per unit area in Turkey is 7 to 28 times lower. However, unlike many developed countries between regions and provinces in Turkey of pesticide use shows a heterogeneous structure [10]. According to data from 2013 year, pesticide consumption is 39.439 tons in Turkey [11]. In the Aegean and Mediterranean Regions the total pesticide consumption accounts for about 50 % of Turkey's whole consumption, while the use of pesticide in the East and Southeast Anatolia Regions of Turkey is only about 10 % [6, 12, 13]. According to the data of 2013, the world consumption of fungicides is estimated to be 645.000 tons [5]. Also in Turkey, fungicide consumption is 16.248 tons, and 206 tons have been consumed in the province of Nevşehir [11, 14]. Considering the studies performed on pesticide and fungicide consumption in Turkey; a study has

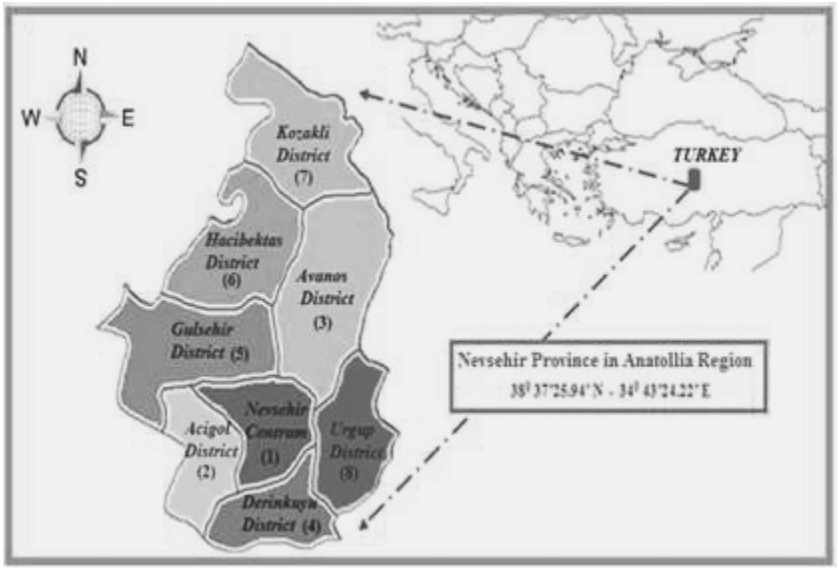

FIGURE 1
Study area, Nevşehir.

annually compared the average annual amount of pesticides consumed in Şanlıurfa province during the 2001-2006 period. The study has concluded a substantially increasing average annual consumption of pesticides [15]. Consumption of pesticides was reported to be 12.199 tons in 2002 in Turkey, with an approximate 50 % growth in 2006, amounting to 18.258 tons, and an increase of 24.22 % in 2007, amounting to 22.681 tons [16]. While many studies have been performed on the spatial mapping of the agricultural areas and products with GIS, there has been no study of the pesticides and particularly fungicide consumption in the spatial mapping and GIS in Turkey. In this study, the distribution of fungicide consumption amounts in the province of Nevşehir and her districts for agricultural purposes during the 2010-2014 period has been aimed to be mapped spatially by GIS. The study is the first of its kind in Turkey in this respect.

MATERIALS AND METHODS

Study area. The Province of Nevşehir has been chosen as our study area. It is located in Turkey's Central Anatolian Region with a 5.392 km^2 land area and geographic coordinates of 38°37′N and 25°94′N latitude and 34°43′E and 24°22′E longitude. The study area consists of Avanos, Gülşehir, Kozaklı, Ürgüp, Hacıbektaş, Acıgöl, Derinkuyu and Central districts of Nevşehir (Fig. 1). Total agricultural area of Nevşehir province (333.160 ha) is about 8.9 % of the total agricultural area in Central Anatolian Region (2.965.124 ha). 68.4 % of these agricultural areas in Nevşehir are used for production of cereals and other crops, 5.4 % for vegetables, 6.6 % for fruit and spicy crops and 19.6 % for fallow production. In the province of Nevşehir potato production accounts to 52 % of Turkey's whole potato production, pumpkin accounts to 32.3% bean production accounts to 10 % of whole production in Turkey [11].

Data use. In this study, data for total consumption of fungicides for the 2010-2014 period have been acquired from the records of the Turkish Statistical Institute [11] and Nevşehir Directorate of Provincial Food Agriculture and Livestock [14].

Method. For Nevşehir's fungicide consumption, Arc GIS 10.3 (Arc Map) software has been used to make spatial evaluations. Inverse GIS, for mapping the spatial environment of fungicide consumption, and Inverse Distance Weighting (IDW) interpolation analysis techniques have been employed. This is the distance across the nearby data points that are based on the technical basis to have more weight. The land area has been established by considering the weighted average of sample points. IDW technique was used in the evaluation of the spatial total fungicide consumption. For determining the total fungicide consumption spatially in the province of Nevşehir, Arc GIS 10.3 software has been used. IDW Interpolation analysis technique is used to spatially map the fungicide consumption in GIS. Equation 1 is used for determining the surface distribution [17].

$$P_i = \frac{\sum_{j=1}^{G} P_j / D_{ij}^n}{\sum_{j=1}^{G} 1 / D_{ij}^n} \quad (1)$$

Where; Pi is the property of location; i: Pj is the property at sampled location; j: Dij is the distance from i to j; G: number of sampled locations; n: inverse distance weighting power.

RESULTS AND DISCUSSION

The total amount of fungicide consumption for the years 2010 to 2014 in Nevşehir province and districts [14] has been provided (Table 1). According to distribution of total fungicide consumption per districts, the highest amount of consumption was observed in Kozaklı (41.40 tons; 35.90 tons; 32.0 tons; 31.20 tons; 34.30 tons respectively), while the lowest consumption level was in the Centrum of Nevşehir (18.50 tons; 15.50 tons; 12.09 tons; 11.38 tons; 13.0 tons respectively) between 2010 and 2014. While fungicide consumption has reached its highest level in 2010, this rate has dropped to its lowest levels during 2012 and 2013, but this amount has increased in 2014 back to the level of 2011 (Table 1).

Changes in fungicide consumption per year are shown in Fig. 2. Examining the distribution of fungicide consumption per year, the highest amount of fungicide consumption was in 2010 by 250 tons, and this amount was decreased by up to 179.78 tons, indicating a downward trend until 2013. However, the amount of fungicide consumption in 2014 was 206.003 tons, and the amount of fungicide consumption in 2011 (210.50 tons) indicated similar levels (Fig. 2).

Accounting for all of the districts, the spatial maps of the total amount of the fungicide consumption in GIS between 2010 and 2014 have been given in Fig. 3. According to the results of all spatial maps, the total amount of the fungicide consumption, particularly in the northern and north-

TABLE 1
Total consumption of fungicides from 2010 to 2014.

		Total consumptions of fungicides (tons)				
Rank	**Districts**	**2010**	**2011**	**2012**	**2013**	**2014**
1	Nevşehir Centrum	18.50	15.50	12.09	11.38	13.00
2	Acıgöl	20.50	16.50	13.00	12.10	14.60
3	Avanos	36.00	31.70	27.10	26.90	31.30
4	Derinkuyu	31.00	22.10	21.00	20.20	23.40
5	Gülşehir	34.00	30.50	27.00	27.40	31.50
6	Hacıbektaş	39.00	33.00	30.00	29.90	31.20
7	Kozaklı	41.40	35.90	32.00	31.20	34.30
8	Ürgüp	29.60	25.30	21.10	20.70	26.70

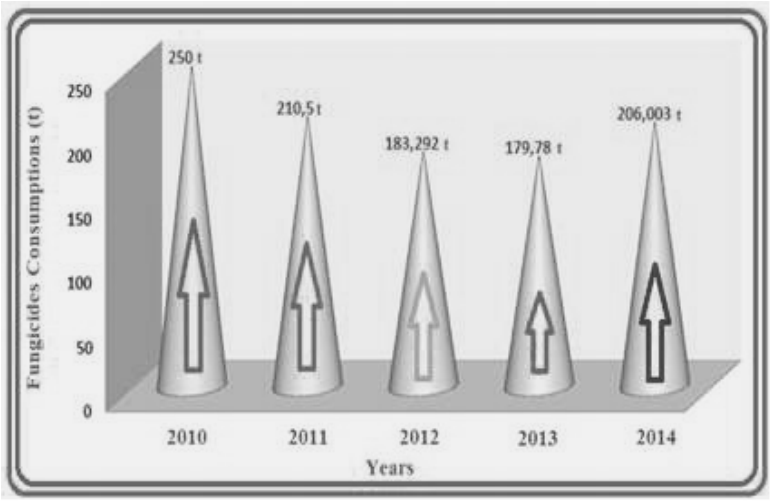

FIGURE 2
Total consumption of fungicide per year in Nevşehir.

western parts of Nevşehir in 2010, Hacıbektaş and Kozaklı districts indicate more intensity when compared to other agricultural areas. These consumption levels have been shown to decrease towards the agricultural areas in the districts located in the southern and south-western parts of Nevşehir. While the amount of total fungicide consumption varies between 37.96 tons - 41.40 tons, in south-western farmlands this amount varies between 18.50 tons - 27.26 tons. In agricultural areas of the Central district of Nevşehir this amount has ranged between 30.92 tons to 31.81 tons. When compared to the other areas in the northern parts of Nevşehir, the total amount of fungicide consumption was higher in Kozaklı district in 2011. The level of use in the northwest district of Hacıbektaş and northwards showed an upward trend when compared to 2010 consumption rates. Again compared to 2010 figures, the consumption rates in the southern and south-western agricultural lands displayed lower rates than those lands in the north, and this reduction intensified towards the district centrums, where the lowest figures have been observed in the Central and Acıgöl districts. The highest amount of consumption has been observed in Kozaklı, by 33.34 tons - 35.87 tons. The least amount of consumption varies between 15.61 tons-18.13 tons and has been observed at Acıgöl and Central districts. Surpassing the other agricultural areas, the 2012 consumption amounts was at the highest levels by 29.50 tons - 32.00 tons in Hacıbektaş and Kozaklı, located north and northwest. The lowest level of consumption, on the other hand, was observed in Acıgöl and Central located in southern and south-western parts of the province, and the figures ranged between 12.09 tons - 14.66 tons. 2013 consumption levels displayed similarities with those of 2010, where the highest consumption was observed in Kozaklı district, located in the north, surpassing the other agricultural areas, and an increase has been observed in the intensity levels of consumption in Hacıbektaş district, particularly surpassing the figures of 2010 and 2012. The maximum amount of consumption was in Kozaklı and Hacıbektaş districts, ranging between 28.50 tons -31.70 tons, while the lowest amount of consumption was in Central Nevşehir and Acıgöl, found to be between 11.38 tons - 13.94 tons, the highest consumption intensity in 2014 year was seen similar to the northern area figures of 2011. Contrary to this, the highest density of consumption in 2010, 2012 and 2013 years were seen in northern and north-western areas. It was determined that the intensity of the lowest consumption significantly in the southwest and in agricultural areas located in the Centrum and Acıgöl. The highest consumption intensity in agricultural areas in the northern district located in Kozaklı 31.61 - 34.30 tons realized that the lowest intensity between 13.00 tons - 15.77 tons been seen in agricultural areas in the Centrum and Acıgöl (Fig. 3).

Fungicide consumption in Central Nevşehir and districts was at the highest level (250.0 tons) in 2010. This amount decreased by 2013, and after 2011, the level dropped to 179.8 tons. In 2014, it has been determined that it reached 206.003 tons, again showing an upward trend in consumption.

Looking at the studies conducted on the use of pesticides in Turkey, a study on determining the pesticides widely used for agricultural production in the province of Isparta and districts, has reported excess use of insecticides and also that, despite in lower amounts compared to insecticides, fungicides and acaricides are also among the preferred groups in the region [18]. It has also been reported that use of pesticides is on the increase, and particularly in the Mediterranean and Aegean Regions, pesticide use is far above the average figures of Turkey, pesticide consumption would increase even further due to developments in crop production and new areas transforming to irrigated farming, and the study concluded that despite the fact that pesticide consumption is generally low in Turkey, the widely consumed pesticides do pose significant risks in terms of environmental and human health [19]. Regarding the use of chemicals in apple production in the province of Antalya, Kızılay and Akçaöz [20] have reported 77.5 % consisted of insecticides, 20.9 % fungicides and 1.6 % acaricides. The amount of pesticides (1.28 kg/ha) used in Konya in 2010 was determined to be similar to the average in Turkey [21].

CONCLUSIONS

Polyculture farming is the preferred method in the province of Nevşehir and their districts, where fungicides are being used against the factors of disease in plants throughout agricultural activities. Fungicide consumption has been observed to be higher in Kozaklı district, located in the north of Nevşehir, when compared to the southern parts of the province. Among the reasons for fungicide consumption to be higher in Kozaklı district compared to other areas, we can point to the intensive existence of greenhouse farming activities. It is a known fact that air-borne diseases are observed in higher levels under greenhouse conditions than field conditions. In this sense, more fungicides are being used in greenhouse farming than field farming. Senseless as well as maximum dosage of fungicide application cause increased amounts of consumption in greenhouse farming.

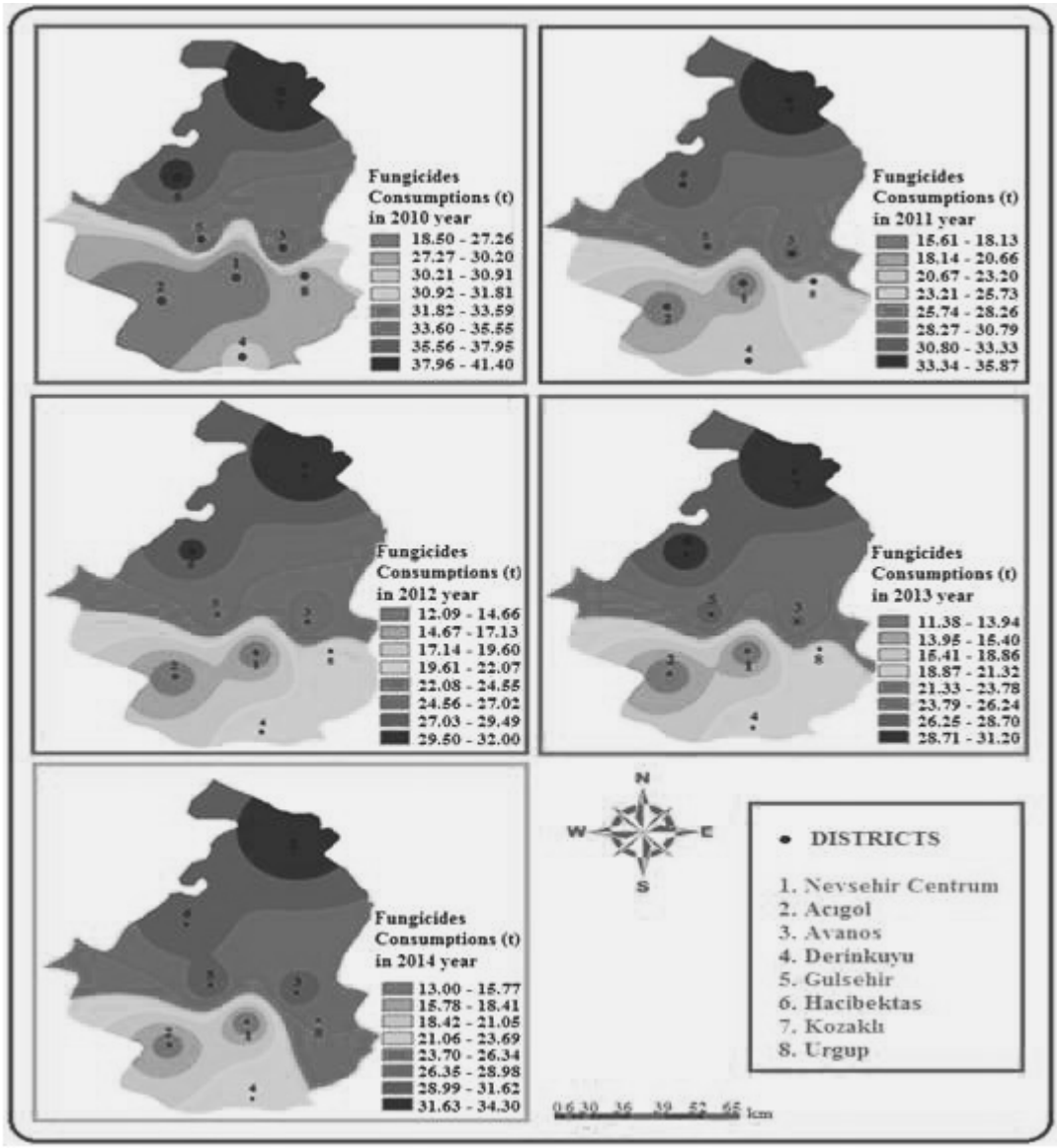

FIGURE 3
Spatial GIS mapping of total consumptions of fungicides between 2010 and 2014 years.

In conclusion, the study on spatially evaluating the total fungicide consumption amounts per year in the province and districts of Nevşehir in GIS environment, recommends more effective training for producers in order to reduce the effective use and consumption of fungicides in agricultural production. The Integrated Pest Management (IPM), encompassing biological, cultural, physical, mechanical and chemical control methods against disease factors should be taken into account and activities related to it's implementation in this regard should be increased.

REFERENCES

[1] Cramer, H.H. (1967). Pflanzenschutz und Welterente, Pflanzenschutz Nachrichten Bayer. Aus der Abteilung Beratung Pflanzenschutz der Farbenfabriken, Bayer A.G., Leverkusen.

[2] Ünal, G. and Gürkan, M.O. (2001). Insecticide: Chemical forms, Toxicology and Ecotoxicology. Ethemoğlu Press, pp. 97-98, Ankara, Turkey.

[3] İnan, H. and Boyraz, N. (2002). Evaluation in General of Agrochemical Usage of Konya Farmer. Selçuk Journal of Agriculture and Food Science, 30, 88-101.

[4] Pesticide Industry (2015). Market Re-search Reports, Statistics and Analysis. Online located at: http://www.reportlinker.com
[5] Chakravarty, S. (2015). World Agrochemical and Pesticide Market to Grow 8.7% annually from 2014 to 2018. Online located at: http://www.marketresearchreports.com
[6] Durmuşoğlu, E., Tiryaki, O. and Canhilal, R. (2010). Pesticide use in Turkey Ruins and durability problems. In:7th Turkey Agricultural Engineering Technical Congress,Ankara, pp. 589-607. (in Turkish)
[7] Blumer, B. (2015). We've Covered the World in Pesticides. Is That a Problem?. Online located at: http://www.washingtpost.com
[8] Dağ, S.S., Aykaç, V.T., Gündüz, A., Kantarcı, M. and Şişman, N. (2000). Agricultural Chemicals Industry and the Future in Turkey. In: 5th Turkey Agricultural Engineering Technical Congress, Ankara, pp. 935-958. (in Turkish)
[9] Burçak, A.A. (2015). Reports of Pesticides, Instrument and Toxicology Research Working Group. Online located at: http://www.tuik.gov.tr
[10] Delen, N., Güngör, N., Durmuşoğlu, E., Turgut, C., Güncan, A. and Burçak, A. (2005). Pesticide use and recycling decrease in susceptibility organism problems in Turkey. In: 6th Turkey Agricultural Engineering Technical Congress, Ankara, pp. 629-348. (in Turkish)
[11] TSI (Turkish Statistical Institute) (2015). Agricultural structure and production. Government Statistic Institute of Prime Minister Publ.Online located at: http://www.tuik.gov.tr (in Turkish)
[12] Turabi, M.S. (2004). Agricultural chemical, license and registration system in the Republic of Turkey. In: Pesticides and Organic Agriculture Conference, Lefkoşa.
[13] Turabi, M.S. (2007). Licensing of plant protection products. In: Pesticides Congress and Exhibition, Ankara, pp. 50-61. (in Turkish)
[14] Ministry of Food Agricultural and Livestock (2015). Reports of Nevşehir Directorate of Provincial Food Agriculture and Livestock. http://Nevşehir.tarim.gov.tr (in Turkish)
[15] Atasoy, A.D. and Rastgeldi, C. (2006). Pesticide Using in Şanlıurfa. In: Proceedings of 5th GAP Engineering Congress, Şanlıurfa, pp. 1462-1467.
[16] Delen, N. (2008). Fungicide. Nobel Press, İzmir, pp. 316, (in Turkish)
[17] Lam, N.S. (1983). Spatial interpolation methods: A review. The American Cartographer, 10, 129-149.
[18] Öğüt, S. and Küçüköner, E. (2008). Important Pesticides used in Isparta and the surrounding agricultural production. In: 10th Turkey Food Congress, Erzurum, pp. 1095-1098. (in Turkish)
[19] Altıkat, A., Turan, T., Ekmekyapar Torun, F. and Bingül, Z. (2009). Use of Pesticides in Turkey and its Effects on Environment. Atatürk University Journal of the Faculty of Agriculture, 40 (2), 87-92.
[20] Kızılay, H. and Akçaöz, H. (2009). Examination of Economic Loss for Pesticide and Fertilizer Application in Apple Production: A Case Study of Antalya Province. TABAD Research Journal of Agricultural Science, 2 (1), 113-119.
[21] Yeşil, S. and Ögür, E. (2011). Evaluation of Plant Protection in Konya and the Turkey Scale Use of Pesticides and Pesticide Possible Drawbacks of Use. In: 1th Konya City Symposium, Konya, pp. 439-449. (in Turkish)

Received: **23.11.2015**
Accepted: **03.04.2016**

CORRESPONDING AUTHOR

Oktay Erdogan
Nevşehir Hacı Bektaş Veli University
Department of Biosystem Engineering
50300 Nevşehir
TURKEY

E-mail: oktaye@gmail.com

© by PSP Volume 25 – No. 7/2016, pages 2682-2686 Fresenius Environmental Bulletin

DETERMINATION OF SOME TRACE ELEMENT LEVELS IN DIFFERENT SEASONS IN MUSCLE, LIVER AND BRAIN TISSUES OF *CLARIAS GARIEPINUS* (BURCHELL, 1822)

Taylan Aktas[1], Alpaslan Dayangac[2], Harun Ciftci[3], Mahmut Yilmaz[2]

[1]Department of Laboratorian and Veterinary Health, Çiçekdağı Vocational School, Ahi Evran University, Kirsehir, Turkey
[2]Department of Biology, Faculty of Art and Science, Ahi Evran University, Kirsehir, Turkey
[3]Department of Basic Medical Sciences, Medical Faculty, Ahi Evran University, Kirsehir, Turkey

ABSTRACT

African sharp-tooth catfish known as *Clarias gariepinus* in international literature is the most common fish species in among freshwater fishes. We investigated levels of Al, Cu, Zn, Fe, Mn and Cr elements in muscle, liver and brain of *C. gariepinus* in different seasons. The fishes used in experiment was obtained in Ceyhan river basin where is situated the south of Turkey. This study was divided as winter group (n=4, female fish) and summer group (n=4, female fish). The organs used in experiment that include muscle, liver and brain tissues were incised. These organs were extracted and were analyzed by AAS (Flame Atomic Absorption Spectrometer) for determination of elements. The accumulation of Al element in summer is lower than winter in muscle tissue, but it is higher in the brain ($p<0.05$). The accumulation of Mn element in summer is higher than winter in brain tissue ($p<0.05$). The accumulation of Fe element in summer is lower than winter in only muscle tissue ($p<0.05$). However, the accumulation of Cr element wasn't evaluated statistically due to below the detection limit. According to obtained results from evidences, accumulation of determined trace elements in various tissues were determined statistically differentness as seasonal. As a result, we suggest that trace element levels may be changed in *C. gariepinus* tissues because of the change of its habitat conditions.

KEYWORDS:
Clarias gariepinus, trace element, muscle, liver, brain, seasonal variation.

INTRODUCTION

C. gariepinus known as African sharp – tooth catfish [1] is the most common fish species in among freshwater fishes [2]. *C. gariepinus* has faster growing ratio, an omnivorous nutrition habit and a resistance against environmental stress in high level in the recent years [3, 4]. African catfishes usually feed with insect larva and various invertebrates [5]. Moreover this species feeds with dead birds, rotten fruits and plant's seed [6]. Copper (Cu) that our studied one of the elements is found as +1 and +2 valency in biological systems and plays a role in the events of the oxidoreduction [7]. Cu is an element that is found very common in nature and is needed in trace amount for organisms [8]. It functions in osteogenesis, development of heart, myelination of spinal cord and tissue pigmentation [9]. Zinc (Zn) is biotic and significant element for humans, animals and plants. It is an essential element for growing, skin coherence and function, ovum maturing, immune system power, wound healing and carbohydrate, lipid (fatty), protein, nucleic acid synthesis [10]. In addition to, this element usually is found trace levels in aquatic environment and concentration of zinc increasing with originating from anthropogenic factor of industrial, mining and agricultural activities [11]. Iron (Fe) element is required for heme protein production in oxygen transport [12]. Fe is bioaccumulation of high level element in *C. gariepinus* species [13]. Aluminum (Al) causes to acute ion regulation, respiratory disorders and accumulation Al^{+3} in freshwater fishes [14]. Manganese (Mn) is found as +2 and +3 valency that has function as component of both enzyme and metalo enzyme [7]. These enzymes have a significant role in detoxification of unchained superoxide radicals in organisms [15]. Chrome (Cr) element has some form that is found as natural in rocks, animals, plants, soil, volcanic dust and gases. Most common of these element forms are Cr^{0}, Cr^{+3}, Cr^{+6} [16]. Behavior of chrome in alive organisms depends to oxidation level, chemical features in oxidation level and physical structure in its environment [17]. Cr level in air and water usually is low. Because of this, nutrients like fruits, plants, meat and ferment creates a significant kind of chrome which took by humans [16].

TABLE 1
Al, Cu, Zn, Fe, Mn and Cr quantities were quantified different in muscle, liver and brain tissues of African sharp-tooth catfish in winter (µg/g) (n=4).

		ELEMENTS					
TISSUES	VALUES	Al	Cu	Zn	Fe	Mn	Cr
Muscle	Min.	6,40	BDL	3,80	7,05	BDL	BDL
	Max.	12,00	0,07	14,20	10,89	0,72	BDL
	Mean	8,9000	0,0175	8,1500	8,6375	0,1975	-----
	SE	1,18181	0,01750	2,22467	0,81053	0,17495	-----
Liver	Min.	5,00	6,72	20,20	61,80	1,35	BDL
	Max.	7,40	68,44	125,80	1401,80	5,00	BDL
	Mean	6,4500	27,2875	50,0500	530,0800	2,7275	-----
	SE	0,58523	14,04735	25,45864	307,43143	0,85511	-----
Brain	Min.	8,95	BDL	1,76	3,78	BDL	BDL
	Max.	18,20	BDL	12,11	14,99	BDL	BDL
	Mean	12,1825	-----	4,9200	8,0300	BDL	-----
	SE	2,14873	-----	2,42243	2,49113	BDL	-----

*BDL: Below Detection Limit, SE: Standard Error.

MATERIALS AND METHODS

In this study, African sharp-tooth catfish (*Clarias gariepinus*) has been obtained four numbers in both winter and summer from drainage canals in Ceyhan-Adana/Turkey river basin.

Preparation of Fish Sample to Trace Element Determination

Muscle, liver and brain tissues of *C. gariepinus* was incised with the help of a sterile scalpel. Afterward, incised samples were left to dry in 45 degree incubator for 4 – 5 days. Seared samples were weighed in assay balance and weights of these samples were standardized to 0.5 gram. Then, weighed samples were placed to Teflon® (polytetrafluoroethylene) tubes conjunction with 1 ml concentrated perchloric acid (Sigma-Aldrich, Germany) and 5 ml concentrated nitric acid (Sigma-Aldrich, Germany). Next, this acid mixture was waited one hour in order to interpenetrate to samples. Thereafter, Teflon® tubes had been placed to microwave solubilization device and had been interacted with 450 watt microwave in 15 minutes four periods. After these processes, solutions are filtered and 1 ml filtered solution is incased cylindrical graduates. Then, 9 ml distilled water is added on 1 ml filtered solution. After, prepared solutions are analyzed in flame AAS (Flame Atomic Absorption Spectrometer) [18].

Statistical Analysis

IBM SPSS 21 program was used in statistical calculation. One – Way Anova Test was made to experiment results. On the other hand, Kruskal – Wallis Test was made for determine to relation between metal accumulations and seasons. Then, "t" test was applied for determine to difference degree of heavy metal values among studied organs [19].

RESULTS

Research Findings. Al, Cu, Zn, Fe, Mn, and Cr quantities were showed respectively in muscle, liver and brain tissues of *C. gariepinus* species in tables. According to "Table 1", most accumulation was in brain, and least accumulation is in liver in Al element. On the other hand, most accumulation in Cu element is in liver, but least accumulation is muscle tissue. Most Fe accumulation is in liver, but least accumulation is in muscle tissue and brain. However, Cr can't be determined due to it was below determine limit in any tissues.

According to "Table 2", most Al accumulation is in brain, but least accumulation in muscle tissue. On the other hand, most Cu accumulation is in liver, but least accumulation muscle and brain tissues. Least Zn accumulation is in brain. Least Fe accumulation is in muscle tissue and brain. Most Mn accumulation is in brain, but least accumulation is in muscle tissue. However, Cr element can't be determined due to it was below determine limit in any tissues.

According to "Table 3", the accumulation of Al element in summer is lower than winter in muscle tissue, but it is higher in brain and these quantities are significant statistically ($p<0.05$). Moreover the accumulation of Mn element in summer is higher than winter in brain that this quantity is significant statistically ($p<0.05$). The accumulation of Fe element in summer is lower than winter in only muscle tissue and this quantity is significant statistically ($p<0.05$). However, the accumulation of Cr element can't be determined.

TABLE 2
Al, Cu, Zn, Fe, Mn and Cr quantities were quantified different in muscle, liver and brain tissues of African sharp-tooth catfish in summer (µg/g) (n=4).

		ELEMENTS					
TISSUES	VALUES	Al	Cu	Zn	Fe	Mn	Cr
Muscle	Min.	4,98	BDL	2,97	2,45	BDL	BDL
	Max.	5,20	BDL	3,20	2,62	BDL	BDL
	Mean	5,0750	-----	3,0875	2,5300	-----	-----
	SE	0,05188	-----	0,05963	0,03629	-----	-----
Liver	Min.	5,93	5,10	15,30	54,12	0,86	BDL
	Max.	6,32	5,23	15,80	56,80	1,13	BDL
	Mean	6,1125	5,1650	15,5675	55,6150	0,9850	-----
	SE	0,08976	0,03227	0,10274	0,57454	0,05545	-----
Brain	Min.	19,97	BDL	2,15	3,38	2,56	BDL
	Max.	20,34	BDL	2,34	3,67	2,70	BDL
	Mean	20,1950	-----	2,2275	3,4900	2,6350	-----
	SE	0,08026	-----	0,04029	0,06646	0,02901	-----

*BDL: Below Detection Limit, SE: Standard Error.

TABLE 3
Trace element quantity of muscle tissue, liver and brain (µg/g) in winter and summer so comparing of these seasonal quantity ($p < 0.05$).

		ELEMENTS					
	TISSUES	Al	Cu	Zn	Fe	Mn	Cr
WINTER (mean)	Muscle	8,9000	0,0175	81,5000	8,6375	0,1975	BDL
	Liver	6,4500	27,2875	50,0500	530,0800	2,7275	BDL
	Brain	12,1825	BDL	4,9200	8,0300	BDL	BDL
SUMMER (mean)	Muscle	5,0750	BDL	3,0875	2,5300	BDL	BDL
	Liver	6,1125	5,1650	15,5675	55,6150	0,9850	BDL
	Brain	20,1950	BDL	2,2275	3,4900	2,6350	BDL
p value	Muscle	0,018*	0,356	0,063	0,000*	0,302	-----
	Liver	0,589	0,166	0,224	0,174	0,088	-----
	Brain	0,010*	-----	0,309	0,118	0,000*	-----

(*) This symbol signs statistical significant difference of each parameter in tissues, BDL: Below Detection Limit.

DISCUSSION AND CONCLUSIONS

Heavy metals in low concentration get high concentrations with anthropogenic factor effects in natural aquatic environment and this condition causes to habitat changes, collective deaths or changes in biotic events [20]. Biological factors like chemical features, organic compounds, growth rate, diet and habitat selecting affect to accumulation of heavy metal in fishes [21, 22]. Heavy metal accumulation and toxic effects of these elements correlate with biotic and abiotic factors of environment were shown in previous studies [23, 24].

In this study, Al element accumulation of fishes in winter was obtained least in liver. On the other hand, Al accumulation levels among tissues in winter were sorted as "liver < muscle < brain", but were sorted as "muscle < liver < brain" in summer. Moreover according to relation between accumulation of Al element and seasons, muscle showed statistically significant decreasing ($p<0.05$), but brain showed statistically significant increasing ($p<0.05$).

Accumulation of Cu element on below detection limit in brain was accepted least in winter and accumulation of Cu element on below detection limit in muscle and brain were accepted least in summer. On the other hand, Cu accumulation levels among tissues in winter were sorted as "brain < muscle < liver", but were sorted as "muscle ≈ brain < liver" in summer. Moreover according to relation between accumulation of Cu element and seasons, decreasing in muscle and liver were not obtained as statistically significant ($p>0.05$), and Cu element accumulation of brain on below detection limit wasn't calculated statistically. In Asi River, Cu element values of muscle tissue in previous studies were lower than values of this study. These variations in results can be originated from terrestrial environments features, industrial, domestic and agricultural activities in environments of research areas. As a result, low Cu element level in this study shown less pollution in this area water than last time. [16, 25-27]. The accumulation of Zn element in brain was determined least in both winter and summer. In addition, Zn accumulation levels among tissues in winter were sorted as "brain < muscle < liver", but were sorted as "brain < muscle < liver" in summer. On the other hand,

according to relation between accumulation of Zn element and seasons, decreasing in any tissues were not obtained statistically significant ($p>0.05$). The accumulation of Fe element in winter was determined least in brain, but in summer was determined in muscle tissue. In addition, Fe accumulation levels among tissues in winter were sorted as "brain < muscle < liver", but were sorted as "muscle< brain < liver" in summer. Moreover according to relation between accumulation of Fe element and seasons, only muscle tissue showed statistically significant decreasing ($p<0.05$), but increasing or decreasing in other tissues showed statistically insignificant ($p>0.05$). Accumulation of Mn element on below detection limit in brain was accepted least in winter and accumulation of Mn element on below detection limit in muscle tissue was accepted in summer. In addition, Mn accumulation levels among tissues in winter were sorted as "brain < muscle < liver", but were sorted as "muscle < liver < brain" in summer. According to relation between accumulation of Mn element and seasons, decreasing in accumulation levels of Mn element in muscle and liver showed statistically insignificant ($p>0.05$). Accumulation of Cr element levels on below detection limit can't be evaluated statistically. In among seasons, the accumulation of element was usually least in summer and most in winter. In among tissues, it was usually least in muscle tissue and most in liver tissue. On the other hand, in last studies, the accumulation of heavy metal in fish tissues was determined least in muscle tissue and most in liver tissue [25, 28, 29].

In this study, most accumulation of element was determined in liver tissue. Moreover according to study of Karadede et al. (1997), the accumulation of Cu, Fe and Zn elements in *Mastacembelus simack* in Atatürk Dam Lake was most in liver tissue [30].

According to study of Mendil and Uluozlu (2007), Fe element was most accumulated element in *Silurus glanis, Capoeta tinca, Leuciscus cephalus, Carassius gibelio* and *Cyprinus carpio* were obtained from Belpinari, Atakoy, Bedirkale, Akin, Boztepe and Avara lakes [31].

In this study, liver showed higher accumulation than muscle tissue in elements were obtained without Cr in both summer and winter. According to study of Dogan (2004) in Hatay, the concentration of heavy metals in *Carasobarbus luteus* were variable in skin, liver and muscle tissue, but metal accumulation in liver was more than the accumulation in muscle tissue [25].

As a result, the accumulation values of Al, Cu, Zn, Fe, Mn and Cr elements in this study are less than acceptable limit values in literature. Therefore, significant accumulation can't be observed in tissues of African sharp - tooth catfish. According to us, trace element accumulation level in same tissues which show statistically difference in different seasons can be originated from dietary value of water which is habitat of fishes and changes in habitat conditions.

ACKNOWLEDGEMENTS

The authors thank Department of Biology and Chemistry in Ahi Evran University for providing necessary facility related with laboratories and AAS device.

REFERENCES

[1] Mitchell, A.J. and Hobbs, M.S. (2007) The acute toxicity of praziquantel to grass carp and golden shiners. North American Journal of Aquaculture, 69:203–206.

[2] Nguyen, L.T.H. and Janssen, C.R. (2002) Embryo-larval toxicity tests with the African catfish (*Clarias gariepinus*). Comparative Sensitivity of Endpoints, 42:256-262.

[3] Ahmad, M.H. (2008) Response of African catfish, *Clarias gariepinus*, to different dietary protein and lipid levels in practical diets. Journal of the World Aquaculture Society, 39:541-548.

[4] Sarker, M.Z.I., Selamat, J., Habib, A.S.M.A., Ferdosh, S., Akanda, M.J.H. and Jaffri, J.M. (2012) Optimization of supercritical CO_2 extraction of fish oil from viscera of African catfish (*Clarias gariepinus*). International Journal of Molecular Sciences, 13:11312-11322.

[5] Yalcin, S., Solak, K. and Akyurt, I. (2001) Certain reproductive characteristic of the Catfish (*Clarias gariepinus* (Burchell, 1822)) living in the river Asi, Turkey. Turkish Journal of Zoology, 25:453-460.

[6] Ergene, S., Portakal, E. and Karahan, A. (1999) Karyological analysis and body proportion of Catfish (*Clariidae*, *Clarias lazera*, Valenciennes, 1840) in the Goksu delta, Turkey. Turkish Journal of Zoology, 23:423–426.

[7] Ozden, Y. (2008) The investigation of bioaccumulation of sediment - bound heavy metals in Enne and Porsuk dam lake to different tissues of *Cyprinus carpio*. MSc Thesis, Institute of Science, Kutahya, Dumlupinar University.

[8] Duffus, J.H. (1980) Environmental toxicology. Edward Arnold (publishers) Ltd., London, Great Britain, pp. 164.

[9] Cousins, R.J. (1985) Absorbtion, transport and hepatic metabolism of copper and zinc: Special reference to metallothionein and ceruloplasmin. Physiological Reviews, 65:238–309.

[10] Turkoglu, M. (2008) Determination of some heavy metal levels in water, sediment and pearl mullet (*Chalcalburnus tarichi* Pallas, 1811) samples from lake Van, Turkey. MSc Thesis, Institute of Science, Department of Fisheries, Van, Yüzüncü Yıl University.
[11] Cicik, B. (2003) The effects of copper – zinc interaction on the accumulation of metals in liver, gill and muscle tissues of common carp (*Cyprinus carpio* L.). International Journal of Environment, 12:32–36.
[12] Lanzkowsky, P. (2000) Iron-deficiency anemia, Manual of Pediatric Hematology and Oncology 3rd edition. USA, Academic Press, pp. 33-47.
[13] Adham, K.G., Hassan, L.F., Taha, N. and Amin, T.H. (1999) Impact of hazardous exposure to metals in the Nile and Delta Lakes on the Catfish *Clarias lazera*. Environmental Monitoring and Assessment, 54:107–124.
[14] Poleo, A.B.S. (1995) Aluminium polymerization – a mechanism of acute toxivity of aqueous aluminium to fish. Aquatic Toxicology, 31:347–356.
[15] Jerome, R., Silvia, P. and Michael, A. (2013) Chapter 6, manganese homeostasis and transport. Metal Ions in Life Sciences, Springer, pp. 34-36.
[16] Caliskan, E. (2005) Research of heavy metal levels in water, sediment and African catfish (*Clarias gariepinus* Burchell, 1822) of the Orontes river. MSc Thesis, Institue of Science, Department of Fisheries, Hatay, Mustafa Kemal University.
[17] Mertz, W. (1987) Trace elements in human and animal nutition – 15th edition. Academic Press, pp. 465-488.
[18] Narin, I., Soylak, M., Elci, L. and Dogan, M. (2000) Determination of trace metal ions by AAS in natural water samples after preconcentration of pyrocatechol violet complexes on an activated carbon column. Talanta, 52:1041-1046.
[19] Duzgunes, O. (1983) Statistical principles and methods in scientific research. Ege University Press, pp. 21.
[20] Heath, A.G. (1995) Water pollution and fish physiology. CRC Press, New York, USA, pp. 359.
[21] Sprenger, M.D., McIntosch, A.W. and Hoenig, S. (1988) Concentrations of trace elements in yellow Perch (*Perca flavescens*) from six acidic lakes. Water Air Soil Pollution, 37:375-388.
[22] Iivonen, P., Piepponen, S. and Verta, M. (1992) Factors affecting trace - metal bioaccumulation in Finnish headwater lakes. Environmental Pollution, 78:87-95.
[23] Nussey, G., Van Vuren, J.H.J. and Du Preez, H.H. (2000) Bioaccumulation of chromium, mangnese, nickel and lead in the tissues of the Moggel, *Labeo umbratus* (Cyprinidae), from Witbank dam, Mpumalanga. Water S. A., 26:269-284.
[24] Adhikari, S., Ghosh, L. and Ayyappan, S. (2006) Combined effects of water pH and alkalinity on the accumulation of lead, cadmium and chromium to *Labeo rohita* (Hamilton). International Journal of Environmental Science and Technology, 3:289-296.
[25] Dogan, M. (2004) Heavy metal levels of fish and water samples obtained from water resource in Hatay region. MSc Thesis, Institue of Science, Hatay-Turkey, Mustafa Kemal University.
[26] Nguyen, H.L., Leermakers, M., Osan, J., Torok, S. and Baeyens, W. (2005) Heavy metals in lake Balaton: Water column, suspended matter, sediment and biota. Science of the Total Environment, 340:213–230.
[27] Singh, K.P., Mohan, D., Singh, V.K. and Malik, A. (2005) Studies on distribution and fractionation of heavy metals in Gomti river sediments—a tributary of the Ganges, India. Journal of Hydrology,1–14.
[28] Maracovecchio, J.E. (2004) The use of *Micropogonias furnieri* and *Mugil liza* as bioindicators of heavy metals pollution in La Plata river estuary. Science of the Total Environment, 323:219-226.
[29] Karadede, H., Oymak, S.A. and Unlu, E. (2004) Heavy metals in Mullet, *Liza abu*, and Catfish, *Silurus triostegus*, from the Atatürk dam lake (Euphrates), Turkey. Environment International, 30:183–188.
[30] Karadede, H., Cengiz, E.I. and Unlu, E. (1997) Investigation of heavy Metal Accumulation in *Mastacembelus simack* (Walbaum, 1792) from the Atatürk Dam Lake. IX. National Aquaculture Symposium, Isparta, Turkey, 1:399–407.
[31] Mendil, D. and Uluozlu, O.D. (2007) Determination of trace metal levels in sediment and five fish species from lakes Tokat, Turkey. Food Chemistry, 101:739-745.

Received: **23.11.2015**
Accepted: **29.03.2016**

CORRESPONDING AUTHOR

Taylan AKTAS
Department of Laboratorian and Veterinary Health, Çiçekdağı Vocational School, Ahi Evran University, Kirsehir, Turkey

e-mail: taylanaktas@gmail.com

© by PSP Volume 25 – No. 7/2016, pages 2687-2692 Fresenius Environmental Bulletin

FISH PROCESSING INDUSTRY WASTEWATER TREATMENT BY SEQUENCING BATCH REACTOR

Oktay Ozkan[a] , Merve Oguz[a*], Ibrahim Uyanik[a]

[a]Erciyes University, Faculty of Engineering, Department of Environmental Engineering, Melikgazi, 38039, Kayseri, TURKEY

ABSTRACT

There has been a rapid increase of fish industries across the world in recent years. The conditions in the fish industries are often nasty with the continual generation of liquid wastes.

Sequencing batch reactor (SBR) is a widely used activated sludge modification, working on the basis of filling, reacting, decanting, and settling occurred within the same reactor. In this study, fish processing wastewater was treated in a 5 liter cylindrical SBR. The effects of different sludge retention times (SRT) on the removal efficiencies on chemical oxygen demand (COD), total nitrogen (TN) and total phosphorus (TP) were examined. The SBR was fed with an organic loading rate of 0.5 mg COD/mg Mixed Liquor Volatile Suspended Solids (MLVSS) at 10, 15 and 20 days of SRT. Daily two cycles consisting of fill, anaerobic/anoxic/aerobic, settle and decant steps were performed. Increasing removal efficiencies were observed with increasing SRTs. The highest system efficiency was obtained at 20 days of SRT with COD, TN, TP removal efficiencies of 73%, 88%, and 89% respectively. The results suggested that fish processing wastewater could be significantly treated using SBR systems although it was not decreased to discharge standards.

KEYWORDS:
Sequencing batch reactor, fish processing wastewater treatment, sludge retention time

INTRODUCTION

Global commercial fish markets and fish farming has grown rapidly over a last few decades [1, 2]. Water is consumed significantly in fish processing industry that, 11 m^3 of wastewater is produced per ton of fish processed [3]. Water consumption in a fish processing industry and high strength wastewater from such an industry are of great concern worldwide.

The common processes in fish processing industries are filleting, freezing, drying, fermenting, canning and smoking [4, 5]. The wastewater quantity and quality of fish processing industries vary with materials used, the fish-processing technique and the final product [6]. Wastewater coming from a fish factory is generally high strength and mainly originates from cleaning operations and washing of raw materials, so it may contain; soluble, colloidal and particulate form of organic contaminants, proteins, lipids and salinity depending on factory and fish types [7-10]. It is difficult to characterize the extent of the problem, but it will be an inevitable consequence of water sources, so of fish, depletion of oxygen, if this wastewater discharged into receiving bodies of water [11-12].

Among the different types of treatment options for these wastewaters, biological processes are the most appropriate ones since the biodegradable organic loading is high, the reagent costs are high and the soluble COD removal is poor in physico–chemical treatment processes [5,7]. Anaerobic treatment in ponds, activated sludge plants, and batch reactors are commonly employed options for fish processing industry wastewater treatment [4]. Aerobic processes such as activated sludge, rotating biological contactor, trickling filter and lagoons are also suitable for organics removal [4]. Most frequently, the biological treatment of fish-processing wastewaters is focused to anaerobic operations [4, 7, 10, 13-14].

SBR has the advantage of being much more flexible than conventional activated sludge processes in terms of matching reaction times to the concentration and degree of treatment required for a particular wastewater. However, the system is not resistible to shock loadings, and monitoring and operating expertise is needed. Since, in Turkey, “Water Pollution Control Regulation” standards [14] in this sector was stringent, it has to be treated through a good management. The aim of the present study was to evaluate the treatment efficiency of an SBR system and investigate the

TABLE 1
Characterization of fish processing wastewater.

MONTH	WEEK	pH	COD (mg/L)	BOD (mg/L)	TN (mg/L)	TP (mg/L)	TSS (mg/L)
March 2010	1	7.8	3702	2775	251	36	604
	2	7.7	3702	2775	251	36	604
	3	7.8	2735	2250	197	27	487
	4	7.9	2696	2125	258	31	407
April 2010	1	8	3788	2502	425	59	432
	2	7.9	3788	2502	425	59	432
	3	7.9	2610	2045	501	128	517
	4	8	2510	2155	207	23	467
May 2010	1	7.7	2395	2095	417	35	353
	2	7.7	2420	2035	568	32	390
	3	7.8	2700	2095	246	28	604
	4	8	3005	2235	196	23	702
June 2010	1	7.9	2911	2155	199	22	661
	2	7.8	2500	2050	216	26	667
	3	7.9	2311	1975	214	22	652
	4	7.9	2550	2100	222	19	572
July 2010	1	8	2865	2120	185	23	605
	2	7.7	2550	2040	192	20	705
	3	7.8	2450	2050	164	19	664
	4	7.8	2602	2105	215	19	669
Average		7.8	2840	2209	278	34	560
Std. D.		0.08	496.1	237.9	118.7	24.9	113.7

effects of the sludge retention time (SRT) on the fishery wastewater treatment.

MATERIAL AND METHODS

Fish Processing Wastewater. The fish processing wastewater was collected from a fishprocessing factory located at the north of Kayseri, Turkey. The characterization of the wastewater used in the present work is given in Table 1. The SBR was inoculated with the sludge obtained from Kayseri Wastewater Treatment Plant (KWTP).

Reactor design and operation. A bench-scale SBR reactor made of Plexiglas with 20 cm height and 15 cm diameter was used in this study. The volume of the reactor was 5 L with an active volume of 3 L. The schematic diagram of the reactor is shown in Figure 1. Real fish processing wastewater was used in this study. The startup period of SBR took 4 days for acclimation of the bacteria. The inoculum was taken from the return sludge of biological wastewater treatment plant of Kayseri, Turkey. The mixed liquor was kept in suspension via a magnetic stirrer at 1200 rpm during anoxic and aerobic phases. The aeration within the SBR was provided in the aeration period only by an aquarium pump (manufacturer: Champion, CX-0078) through a diffuser at a rate of 2500 cm^3/min. Feeding and decanting applications were done from the bottom and sludge level, respectively, by dosage pumps at a flow rate of 3 L/h. The control of the phases was achieved by an automatic time set-up device.

The SBR was operated at room temperature, changed between 20 and 25°C during the experiments. Dissolved Oxygen (DO) and pH were continuously monitored with a multi-parameter measurement device (Hach-Lange HQ40D). Operation was done at adjusted conditions for DO and pH; minimum 2 mg/L of DO during aerobic phase and 7 pH at all phases with 0.02 N sulfuric acid or 0.02 N NaOH solution. During the operation of the SBR, there were 2 cycles per day; each cycle was operated with 5 phases consisting of fill/draw, react, settle and decant. The phases can be discriminated depending on DO concentration in the reactor as anaerobic, aerobic, and anoxic periods. During the fill period DO concentration was less than 2 mg/L of oxygen, providing anaerobic conditions. And after aeration, it was anoxic period. The study consisted of 3 sets of trials, individually inoculated, each have the same operational conditions except for the SRT. The SRTs in Set 1, 2, and 3 were maintained as 20, 15,

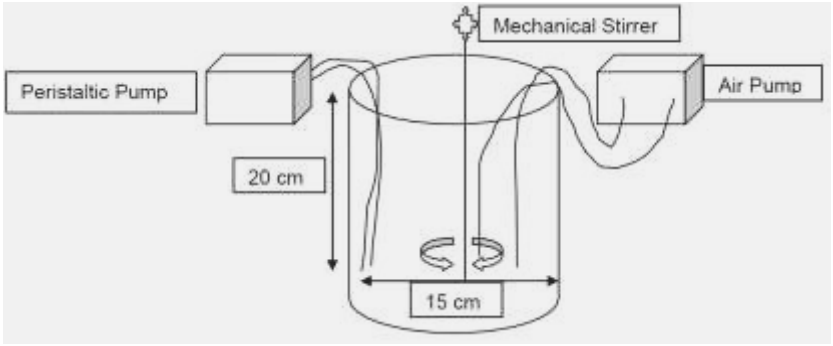

FIGURE 1
Schematic diagram of SBR.

and 10 days, respectively. The first period of the cycle was anaerobic which took 4 hours. Aerobic period was 6 hours. It was half an hour to take place anoxic period, and finally settling and decanting periods were half an hour and one hour, respectively. Food to microorganisms ratio (F/M) was 0.5 mg COD/mg MLVSS. A constant amount of sludge was withdrawn from the reactor to maintain the constant SRT toward the end of the aerobic phase. Influent and effluent samples were analyzed for chemical oxygen demand (COD), total nitrogen (TN), total phosphorus (TP), total suspended solid (TSS), volatile suspended solid (VSS).

Analytical Methods. COD of the samples was analyzed by closed reflux titrimetric method. TN and TP analyses were performed in accordance with the Standard Methods for the Examination of Water and Wastewater by using the standard analyze kit (Hach Lange) (APHA) [15]. TSS was also determined by standard methods (2540 D). To determine the biomass concentration, standard VSS measurement (2540 E) was applied [15]**.** BOD measurements were analyzed using respirometric method of standard methods [115].

RESULTS AND DISCUSSION

Characterization of Fish Processing Wastewater. Table 1 summarizes the characteristics of fish processing wastewater. The pH was in the range of 7.7-8.0, in agreement with the literature. Fish processing wastewater presented a solid content in the range of 353– 705 mg TSS/L, lower than the values reported by Riaño et al. [9] and Chowdhury et al. [4], who observed TS concentrations of 764-1460 mg/L and 2000–3000 mg/L, respectively. The difference can be explained by such factors as differences in the composition of raw fish, unit processes and cleaning operations. COD concentrations were between 2311 and 3788 mg/L, while BOD concentrations were in the range of 1975-2775 mg/L. The wastewater from fish processing operations has high BOD and COD [4]. N and P concentrations showed the following levels: 164-568 mg TN/L, and 19-128 mg TP/L, respectively. The high nitrogen levels are likely due to the high protein content (15–20% of wet weight) of fish and marine invertebrates [4]. Sometimes high nitrogen concentration is observed due to high blood and slime content in wastewater streams.

Chemical Oxygen Demand (COD), Total Nitrogen (TN) and Total Phosphorus (TP) Removal. COD, TN and TP removal efficiencies for the fish processing wastewater during SBR treatment at three different SRTs at the same hydraulic retention time (HRT) were studied. Aeration rate, food to microorganism ratio (F/M), temperature and SRT are important parameters for the activated sludge system performance [4]. We evaluated the treatment efficiency of fish processing industry wastewater changing one of these parameters, SRT. The removal efficiencies were plotted for COD, TN, and TP in FIGURE 2 (A-C).

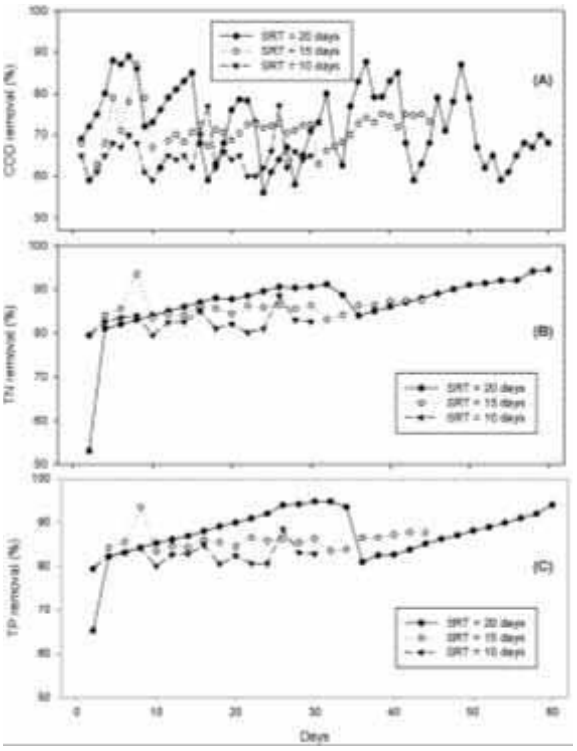

FIGURE 2
Removal efficiencies of COD, TN, and TP at different SRT's

For 10 days of SRT, COD concentration of the influent fish processing wastewater was 2409.5 ± 218 mg/L, with 846 ± 135.1 mg/L for the effluent, which corresponds to a COD removal efficiency of 65 ± 4.4% (Figure 2A). The influent and effluent TN concentrations were 191 ± 45 mg/L and 33 ± 3.1 mg/L, respectively, corresponding to a removal efficiency of 83 ± 2.3% (FIGURE 2-B). The values of 20 ± 3.1 mg/L and 3 ± 0.4 mg/L were recorded for influent and effluent concentrations of TP, respectively, with a removal efficiency of 83 ± 2.1% (Figure 2-C). It can be concluded from the results that the removal mechanism of the nitrogen and phosphorus are biological, since we used inoculum for biological growth, removal efficiencies proved that hypothesis.

The influent and effluent COD concentrations were 2579.4 ± 381.6 mg/L and 747.9 ± 183.5 mg/L, respectively, for 15 days of SRT. The COD removal efficiency was 71 ± 5% as shown in Figure 2-A. TN concentrations were 215 ± 60.1 mg/L in the influent and 30 ± 1.8 mg/L in the effluent, providing a removal efficiency of 85 ± 2.5% (FIGURE 2-B). The concentrations of TP were 24 ± 7.2 mg/L in the influent and 3 ± 0.5 mg/L in the effluent, with a removal efficiency of 86 ± 2.6% (Figure2-C).

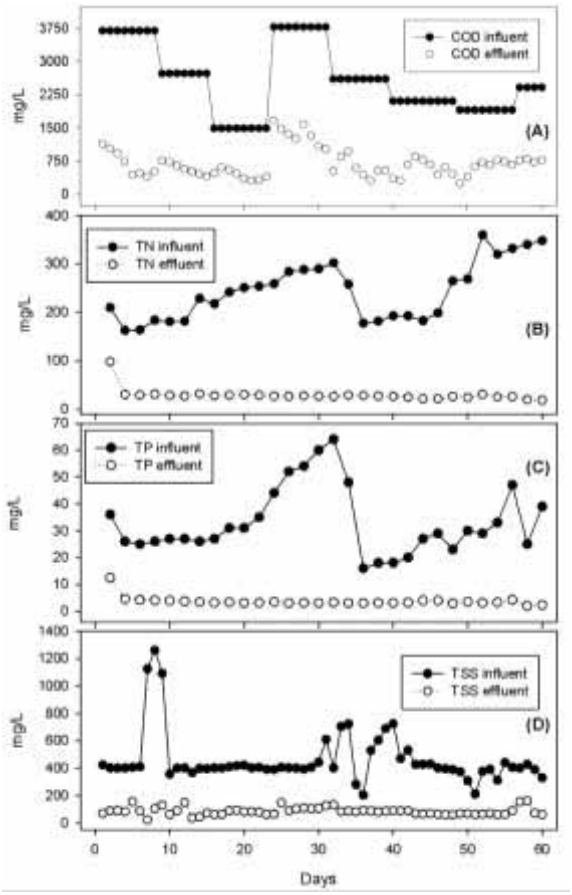

FIGURE 3
Influent and effluent concentrations of COD, TN, TP, and TSS at 20 days of SRT

Average COD removal efficiency for 20 days of SRT was 73 ± 9% (Figure 2-A). Influent and effluent COD concentrations were 1496–3788 mg/L and 321–1667 mg/L, respectively (Figure 3-A).

FIGURE 3Figure 3-B indicates that the TN concentration was between 163–673 mg/L in the influent and 19–98.5 mg/L in the effluent, yielding removal efficiencies of 80–97% (89 ± 5% on average) as plotted in FIGURE 2-B. Initial and final TP concentrations were 16–78 mg/L and 2.0–12.5 mg/L, respectively as shown in

Figure3-C, with removal efficiencies of 81–96% (88 ± 4.5% on average) (FIGURE 2-C). TSS concentrations were also examined at 20 days of SRT and it was 460.4±190.7 mg/L in influent and 86.0±28.4 mg/L at the effluent. Although the removal rates were high for COD, TN, and TP parameters at 20 days of SRT, TSS removal rate was optimum at 15 days of SRT.

Although N and P are normally present in the fish processing wastewater, their concentration is minimal in most cases [11]. That is because of higher removal efficiencies were observed for nitrogen and phosphorus than the COD. This finding showed that carbon is the restrictive element in this balance.

In this study, optimum sludge retention times for COD, TN and TP removal from fish processing wastewater were determined. Removal efficiency fluctuations were observed when weekly new wastewater was fed to the reactor. It was thought that this behavior was due to microorganism acclimation to the new wastewater whose characteristics changed weekly. The highest removal efficiencies for COD, TN and TP were observed in SRT of 20 days, which gave removal efficiencies of 73 %, 89 %, and 88 %, respectively. When the SRT was 15 days, the reactor also gave close results. These results suggested that fish processing wastewater could be effectively treated using SBR reactors with this high SRT of 20 days. In terms of wastewater treatment, several anaerobic and aerobic processes were studied by a number of authors. Riaño et al. [9] studied COD and nutrient removal from a fish processing wastewater using photobioreactors inoculated with microalgae at 23 and 31ºC. During that study, approximately 70% of COD and phosphate removals were achieved regardless of temperature, which is lower than the removal efficiencies obtained by the present work. In another study, Manetti et. al. [3] investigated the potentiality of reuse of fish processing wastewater by association between biological and chemical treatment. They reached high removal efficiencies 89%, 99% and 98% for COD, PO_4^{-3} and NH_4^+, respectively. Higher removal rates may be resulted by the coagulation-flocculation step after the biological treatment. According to Palenzuela-Rollon et al. [5] the application of UASB system is a promising treatment option for fish processing wastewater. They determined the performance of UASB reactor for the treatment of mixed sardine and tuna canning effluent at varying lipid levels. They stated that at low lipid level (203-261 mg/L, 9% of total COD), approximately 78% COD removal can be achieved. Alexandre et al. [7] also received similar COD removal efficiency, 79.9%, using UASB reactor treating fishery wastewater.

Previous studies showed that biological treatment is the best option for such a wastewater. However, activated sludge extended aeration process need higher oxygen requirement compared to other treatment methods. More than 80% COD removal can be achieved with anaerobic fixed filter (AF) and anaerobic fluidized bed (AFB) reactor. A UASB reactor has also advantage which provides 80–95% COD removal. In a study using a multistage Rotating Biological Contactor (RBC) reactor may be suitable for treatment of fish processing wastewater providing 97.4 % COD removal with an Organic Loading Rate (OLR) of 18.44 g/m^2 [12].

In an activated sludge process, the incoming stream is diluted in a completely mixed system and thus, it is more stable to perturbations, i.e., the reactor is more resistant to shock loads of BOD_5 and toxic compounds. In fishery-wastewaters the perturbations are peaks of concentrations of the organic load or flow peaks. The activated sludge process with biological denitrification is a popular technology satisfying stringent standards. The activated sludge technology is dominating over the bio-film process in the practical treatment of fish processing wastewater [4].

The literature review showed that SBR has never used for the treatment of fish processing wastewater before. The removal efficiencies obtained by the current study were close to the ones obtained by the other studies [4] which indicate that the SBR treatment is suitable for the fishery wastewater treatment. Benefits of SBR are easiness in operation and simultaneous removal of carbon, nitrogen and phosphorus.

CONCLUSION

This study indicates that the SBR is a proper process to treat fish processing industry wastewater with high C, P, N content and blood ingredient. The study was performed to determine the effect of different SRTs on the treatment efficiency of fish processing wastewater using the SBR. The study showed that simultaneous carbon, phosphate, and nitrogen removal was possible with the system studied here. During the treatment with three different SRTs, an increasing trend line on removal efficiencies of COD, TN, and TP were observed in terms of increasing SRT. In general, the system could achieve removal efficiencies of 56–89%, 80–97% and 81–96% respectively, for COD, TN, and TP. The COD, TN, and TP removal efficiencies for 20 days of SRT were highest except the TSS with the removal efficiencies of 73%, 89%, 85%, and 88%, respectively. This study suggested that the SBR process with 20 days of SRT could be efficiently applied to treat fish processing wastewater. However, an extensive study must be conducted to improve the management of this wastewater.

REFERENCES

[1] Aloui F, Khoufi S, Loukil S & Sayadi S, Performances of an activated sludge process for the treatment of fish processing saline wastewater, Desalination 246 (2009) 389–396.

[2] Naylor R. L., Goldburg R. J., Primavera J. H., Kautsky N., Beveridge M. C. M., Clay J. Folke C., Lubchenco J. , Mooney H., and

Troell M., Effect of aquaculture on world fish supplies, Nature 405 (2000) 1017-1024.
[3] Manetti A G da Silva, Hornes M O, Mitterer M L, Queiroz M I, Fish processing wastewater treatment by combined biological and chemical processes aiming at water reuse, Desalination and Water Treatment 29 (2011) 196–202.
[4] Chowdhury P, Viraraghavan T, Srinivasan A, Biological treatment processes for fish processing wastewater – A review, Bioresource Technology, 101 (2010) 439–449.
[5] Palenzuela-Rollon A. Anaerobic Digestion of Fish Processing Wastewater with Special Emphasis on Hydrolysis of Suspended Solids, Taylor and Francis, London, 1999.
[6] Alexandre V M F, Valente A M, Cammarota M C, Freire D M G, Performance of anaerobic bioreactor treating fish-processing plant wastewater pre-hydrolyzed with a solid enzyme pool, Renewable Energy, 36 (2011) 3439-3444.
[7] Shengquan Y, Hui W, Chaohua Z, Xiaoming Q, Study of the hydrolytic acidification-SBR process in aquatic products processing wastewater treatment, Desalination, 222 (2008) 318–322.
[8] Riaño B, Molinuevo B, García-González M C, Treatment of fish processing wastewater with microalgae-containing microbiota, Bioresource Technology, 102 (2011), 10829–10833.
[9] Latif M A, Ghufran R, Wahid Z A, Ahmad A, Integrated application of upflow anaerobic sludge blanket reactor for the treatment of wastewaters, Water Research 45 (2011), 4683-4699.
[10] Gonzalez J F, Wastewater Treatment in the Fishery Industry, FAO Fisheries Technical Paper (FAO), No. 355/FAO, Rome (Italy), Fisheries Dept, 1996.
[11] Najafpour G.D., Zinatizadeh A.A.L., and Lee L.K., Performance of a three-stage aerobic RBC reactor in food canning wastewater treatment, Biochemical. Engineering Journal, 30 (2006) 297-302.
[12] Balslev-Olesen P, Lynggaard-Jensen A, Nickelsen C, Pilot-scale experiments on anaerobic treatment of wastewater from a fish processing plant, Water Science and Technology 22 (1990), 463–474.
[13] Punal A, Lema J M, Anaerobic treatment of wastewater from a fish-canning factory in a full-scale upflow anaerobic sludge blanket (UASB) reactor, Water Science and Technology 40 (1999) 57–62.
[14] Water Pollution Control Regulations. Turkish Official Newspaper 25687, 12 December 2004.
[15] Standard Methods for the Examination of Water and Wastewater, 20th Edn., APHA, AWWA, WEF 2540 B.

Received: **26.11.2015**
Accepted: **22.03.2016**

CORRESPONDING AUTHOR

Merve Oguz
Erciyes University, Faculty of Engineering,
Department of Environmental Engineering,
Melikgazi, 38039, Kayseri, TURKEY

Email: merveoguz@erciyes.edu.tr

© by PSP Volume 25 – No. 7/2016, pages 2693-2699 Fresenius Environmental Bulletin

COMPARISON BETWEEN EFFECTS OF THREE TREATMENTS FOR DIFFERENT PERIODS OF TIME ON METHOMYL PESTICIDE IN TOMATO JUICE

Tawfiq Mustafa Al- Antary[1*], Maher Mahmoud Al-Dabbas[2], Asma Mohammad Shaderma[3]

[1]Prof of Pesticides and Economic Entomology, Faculty of Agriculture, Department of Plant Protection, The University of Jordan, Amman, 11942, Jordan.
[2]Assoc. Prof of Food Chemistry, Faculty of Agriculture, Department of Nutrition and Food Technology, The University of Jordan, Amman 11942, Jordan
[3]Ministry of Agriculture, Amman, Jordan

ABSTRACT

This study was conducted to monitor the effect of ozonation at 0.4 ppm, UV-radiation at 254 nm and cooking at 100 ºC on methomyl residues of spiked tomato juice. Ozonation of spiked tomato juice with methomy at 0.4 ppm was found to be the most effective treatment. Complete degradation of spiked methomyl at any of the studied concentrations level was achieved after 30 min of ozone treatment, while the reduction percentages of methomyl after UV-radiation treatment for 30 min was 19.59%. On the other hand, cooking at 100 ºC for 30 min led to reduction percentage of 72.63%. However, the reduction percentages of the studied methomyl were significantly increased with increasing time of exposure and were greatly affected by ozonation treatment. Methomyl was completely degraded after 15 min of treatment at spiked concentration level of 0.1 ppm, while reduction percentages achieved by UV-radiation and cooking at 100 ºC treatments at the same concentration after 15 min were 9.23% and 63.2%, respectively.

KEYWORDS:
Methomyl, Pesticide residues, Ozonation, UV- Radiation, Tomato juice.

INTRODUCTION

Tomato is one of the most common agricultural products in Jordan. It is the main component for several dishes in the Jordanian people diet. Around 129535.9 donums planted with tomatoes in open fields and plastic houses by the year of 2011 to produce 777820.4 tonnes of tomatoes for local use and exportation [1,10, 11,23]. In addition, Jordan produced 2310 tons of tomato processed products like; tomato paste, tomato soup, tomato juice, and ketchup. The total produced and consumed amount in local market is 6181 tons/year and the per capita consumption of processed tomato products is about 1 kg/year [2,10,23]. Agricultural activities are closely associated with intensive use of pesticides to control plant pests and to increase the yield of cultivated areas. Tomatoes have been treated intensively with pesticides to control pests especially *Tuta absoluta* and white fly. However, many of these pesticides are used in large quantities. Carbamate members (Methomyl one of these) was found to be an effective group of pesticides to control plant pests by contact or systemically. This group does not persist for a long time in the environment in comparison with organo-chlorinated pesticides [3,12].

Food and Agricultural Organization (FAO) database showed that in 2007 around 129.13, 1234, 549, 1 and 426 tons of carbamate pesticides were used in Germany, France, Japan, Bahrain and Saudi Arabia, respectively [4]. Carbamate pesticides are classified by the Environmental Protection Agency (EPA) from moderate to highly toxic for humans. They affect the nervous system, which lead to acute toxicity, because they inhabit acetylcholinesterase enzyme (AChE), which regulates acetylcholine (ACh) neurotransmitter [6,25]. The excess ACh accumulation causes different signs and symptoms; convulsions, paralysis, coma, nausea, vomiting, diarrhea, salivation, sweating, blurred vision, hypertension, twitching, skeletal muscle [6]. On the other hand, some carbamate pesticides have a very high decomposition temperature up to 162 ºC and 192 ºC for oxamyl and methomyl from the carbamates, respectively, [7, 8, 26].

In the recent years, the word attention has focused on the removal of pesticide residues by different treatments like; cooking, ozonation, UV-radiation, washing and peeling. It is noticed that these treatments are of great benefits to have safe and healthy food. The objectives of this study is to examine the effect of ozonation at 0.4 ppm, UV-

radiation at 254 nm and cooking at 100 ºC on recovered amounts from spiked tomato juice with methomyl insecticide at different concentration levels for different periods of time.

MATERIALS AND METHODS

This study was conducted at Pesticides Residues Department in the Directorate of Plant Wealth-Ministry of Agriculture, Jordan.

Chemicals and reagents. Anhydrous magnesium sulphate ($MgSO_4$, assay 99%) (Sigma-Aldrich, USA), ashed at 500ºC for 5 hours was carried out before usage to eliminate phthalates and remained water, acetonitrile (CH_3CN, HPLC-grade, assay of 99.8%) (LAB-SCAN analytical sciences, Ireland), Acetic acid (CH_3COOH, assay 99%) (J. T. Baker, USA), Acetone (C_3H_6O, GC-grade, assay 99.8%) (LabChem, USA), Sodium chloride (NaCl, assay 99.9%) (AVONCHEM, UK), Primary Secondary Amine (PSA) sorbent, with 40 – 60 µm particle size (Agela Technologies, USA), Methomyl pesticide ($C_5H_{10}N_2O_2S$, assay 99.5%) was purchased from (Sigma-Aldrich, USA), Ditalimifos ($C_{12}H_{14}NO_4PS$, assay 97.5%) was purchased from (Sigma-Aldrich, USA) and was used as internal standard.

Analytical method. sample preparation and extraction. The method for extraction of pesticide residues in food called QuEChERS (Quick, Easy, Cheap, Effective, Rugged, and Safe) based on the extraction by acetonitrile and partitioning with anhydrous magnesium sulphate was used for extraction of methomyl residues from tomato juice [9,5].

Tomato juice. Homogenized tomato juice samples were extracted follows: Ten grams from each of homogenised subsample was transferred into 50 ml Teflon centrifuge tube. Acetonitrile with 1% acetic acid solution was prepared on v/v basis (25 ml acetic acid in 2.5 L acetonitrile), solution A. Ten ml of solution A was added to the sample and was shaken by the Vortex mixer (Heidolph, Germany) for 1 min at low speed. Four grams of anhydrous $MgSO_4$ and 1 g of NaCl were added to the sample, and then vortexed again for 1 min. Ditalimifos of 0.5 ppm concentration was added as an internal standard. Finally, sample was vortexed for 30 s and centrifuged (Hettich, USA) at 3000 rpm for 5 min. By this step the sample extract ready for clean-up.

Samples clean-up. The same procedures for clean-up were followed for tomato juice, 1 ml of the upper acetonitrile layer was transferred into 10 ml centrifuge tube containing 25 mg PSA as sortbent and 150 mg anhydrous $MgSO_4$, then it was vortexed for 30 s, as a final step the centrifuge tube was centrifuged at 3000 rpm for 5 min. The extract was transferred into 2 ml GC vial.

Since acetonitrile is not compatible with NPD detector, it was replaced completely with acetone after flushing with nitrogen gas, and then the volume was adjusted to 2 ml with acetone. After that samples were analysed with GC-NPD (Agilent 6890N, USA) to determine the residues of methomyl.

Gas chromatography conditions for determination of methomyl. The chromatographic system consisted of a gas chromatography equipped with nitrogen phosphorous detector, splitless injector and the capillary column HP-5 model No.19091J-413 (Agilent, USA). with composition of 5% Phenyl and 95% methy lpolysiloxane, dimensions are 30 m length, 0.32 mm nominal diameter, and 0.52 µm nominal film thickness. The carrier gas was helium. The operating conditions were: injection volume of 1 µl. The temperature program was: injector temperature 250oC, and detector temperature 300 oC [28]. The oven temperature program was modified to get the best response for methomyl as follows: initial temperature 60 oC for 1 min; 5 oC min-1 to 90 oC for 1 min; 20 oC min-1 to 150 oC for 1 min; 6 oC min-1 to 270 oC for 1 min [28]. For data acquisition ChemStation software was used.

Determination of detection Limits (DL). Three independent blank tomato juices samples that previously shown not to contain any residues, were separately extracted in the same day to get the amount corresponding to the desired pesticide retention time using GC-NPD. The mean values ($\overline{X}$) for the amounts of the six replicates and their standard deviation (SD) were calculated separately for each pesticide [28].

The DL for methomyl was calculated according to the following equation [28]:

$$DL = \overline{X} + (3xSD)$$

After determination of DL for each pesticide, a blank sample was spiked with this concentration and determined by GC-NPD.

Blank test. This test was performed to make sure that the solvent and apparatus are free from any residues of methomyl. Ten ml of acetonitrile was placed in 50 ml Teflon centrifuge tube, and then the procedures for extraction and GC-NPD analysis were followed as described previously.

Recovery test. Blank tomato juice samples that are previously analysed and proven to be free from any carbamate residues were used to perform this test.Ten grams of homogenised blank tomato juice samples were placed in 50 ml Teflon centrifuge tube and spiked separately to obtain 0.1, 0.5, 1, 5, and 10 ppm from methomyl. The extraction and clean-up procedures were preceded as previously described.

This test was repeated three times for methomyl at the spiked amounts of 0.1, 0.5, 1, 5 and 10 ppm to assess the efficiency of QuEChERS method for extraction of methomyl.The recovery percentage of each pesticide was calculated according to the following equation:

Recovery percentage (%) = (ppm pesticide detected/ ppm pesticide added) x 100

Effect of tomato juice ozonation, UV-radiation and heat treatment on stability of methomyl. To investigate the declining pattern in methomyl pesticides residues in tomato juice, the samples were treated as follows:

Ozonation at 0.4 ppm. Five tomato juice samples (1 L each) (free from methomyl residues) were spiked with five different concentrations 0.1, 0.5, 1, 5 and 10 ppm for methomyl. Each sample was treated with 0.4 ppm ozone (Ozone generator, model ZA-BF-L, ZAET Fruit and Vegetable Washer, China) for 3, 5, 10, 15 and 30 minutes using the Fruits and Vegetables Washer. The effect of ozone treatment on methomyl was evaluated by analysing tomato juice samples before and after the treatment. The spiked tomato juice samples were held inside the cleaning chamber during ozone treatment. Samples were taken separately after 3, 5, 10, 15, and 30 minutes for each pesticide determination. Each sample was extracted by QuEChERS method and analysed using GC-NPD to determine the recovered amounts of methomyl in order to evaluate the efficiency of ozonation on the reduction percentages of methomyl with time.

UV-radiation at 254 nm. Five tomato juice samples (0.5 L each) (free from methomyl residues) were spiked with five concentrations 0.1, 0.5, 1, 5 and 10 ppm of methomyl. Each sample was treated with UV- radiation model SC1 (Sterilight Ultraviolet Disinfection System, Canada) at 254 nm for 3, 5, 10, 15 and 30 minutes. The effect of UV-radiation treatment on methomyl was evaluated by analysing tomato juice samples before and after the treatment. The spiked tomato juice samples were held between the outer stainless steel jacket and the inner quartz tube during UV-radiation treatment. Samples were taken separately after 3, 5, 10, 15, and 30 minutes for determination of each pesticide. Each sample was extracted by QuEChERS method and analysed using GC-NPD to determine the recovered amount of methomyl in order to evaluate the efficiency of this treatment in degradation of these pesticides with time.

Cooking at 100 ºC. Five tomato juice samples (1 L each) (free from methomyl residues) were spiked with five concentrations 0.1, 0.5, 1, 5 and 10 ppm of methomyl. Each sample was heated up to 100ºC using ordinary kitchen gas (Universal, Jordan). After 100ºC was reached five samples were taken after 3, 5, 10, 15, and 30 minutes. Each sample was extracted by QuEChERS method and analysed using GC-NPD to determine the amounts of methomyl left after heat treatment at 100 ºC for several minutes on reduction of this pesticide.

Control samples. Five tomato juice samples of the collected samples from the local market which shown not to contain any residues were used as control samples for ozonation at 0.4 ppm ozone concentration, UV-radiation at 254 nm and heat treatment at 100 ºC after spiking with different concentration levels from methomyl pesticide.Control samples were spiked with 0.1, 0.5, 1, 5 and 10 ppm of methomyl and kept under room conditions for 30 min to investigate the effect of natural light exposure and room temperature on methomyl reduction percentages, samples were taken after 3, 5, 10, 15 and 30 min for the determination of this pesticide.

Extraction and GC-NPD analysis. The same procedures were followed for extraction and GC-NPD analysis as described earlier for determination of methomyl recovered amounts from spiked tomato juice samples after ozonation, UV-radiation and cooking at100ºC .

Statistical analysis. The design of the experiment was Complete Randomised Design (CRD) with three replicates. Mean values and standard error were calculated and analyzed. The obtained data were subjected to statistical analysis using MSTAT-C programme version 1.4, were Least Significant Difference test (LSD) was used at 0.01 probability level.

RESULTS AND DISCUSSION

Blank test. All the blank tests did not show any residues of methomyl. These blank tests indicated that there were no contaminations due to reagents and/or equipment.

Control sample. The results of the analyzed control tomato juice samples showed that the maximum and minimum reduction percentages of methomyl at studied concentrations levels of 0.1, 0.5, 1, 5 and 10 ppm for different periods of time 3, 5, 10, 15 and 30 min were ranged from 0.098 to 0.984 ppm for methomyl.These values were very small in comparison with corresponding reduction percentages after treatments with ozone, UV-radiation and cooking.

Detection limits (DL) and retention time. The results for the analysis of three blank juice samples in duplicate showed that the minimum detection limits were 0.0032 ppm for methomyl, and the retention time was 3.749 min.

Detection limits (DL) and retention time of methomyl pesticide, using GC-NPD. The present study showed that the detection limits for methomyl was 0.0032 ppm using QuEChERS method for extraction and GC-NPD for determination. Delgado (Delgado *et al.* , 2001) found that the detection limits of methomyl were 0.006 ppm, using same method of extraction and determination of this carbamate pesticide from powdered potatoes. In addition, similar results were reported by [13,27,28], who showed that carbamates were directly and selectively detected using gas chromatography equipped with NPD detector with detection limits ranging from 0.003 to 0.06 ppm.

TABLE 1
Recovery percentages of methomyl residues from tomato juice samples spiked with different concentration levels.

Pesticide	Spiked amount	Recovery %*± SE
	0.1	96.7 ± 0.9
	0.5	97.2 ± 1.2
Methomyl	1.0	96.4 ± 1.0
	5.0	96.9 ± 1.6
	10.0	98.2 ± 0.4

* Values are means of three replicates.

Recovery test. As shown in Table 1, the mean recoveries percentages from blank tomato juice samples of methomyl were ranged from 96.4% to 98.2% for methomyl. Methomyl recoveries were found in the range of 96.4% to 98.2% for methomyl. Using GC-NPD and QuEChERS method for extraction. In agreement with these results, FAO [14,15] found that the recoveries for methomyl were > 90% for different commodities. Moreover, Glauner [16] achieved 98.9 % recovery for methomyl from tomato fruits samples in a study performed to validate QuEChERS method for extraction of 313 compounds in different commodities.

Effect of tomato juice by ozonation. Methomyl reduction percentages achieved by ozonation at 0.4 ppm treatment for all the spiked concentration levels of 0.1, 0.5, 1.0, 5.0 and 10 ppm in all the stages of the treatment after 3, 5, 10, 15 and 30 min were greater than that achieved by UV-radiation and heat treatment (Table 2). After 30 min of treatment, ozonation increased methomyl reduction percentages to 100%, UV-radiation did not increase methomyl reduction percentages more than 20% and heat treatment above 100 ^{o}C increased methomyl reduction percentages more than 60 % as shown in Table 2. His statistical analysis (Table 2) showed that there were significant differences ($P \leq 0.01$) between methomyl reduction percentages after ozonation, UV-radiation and heat treatment, for all the spiked concentration levels at 3, 5, 10, 15 and 30min. Methomyl recovered amount decreased significantly with time after ozonation treatment at 0.4 ppm to reach a concentrations that are below the EU-MRL after 30 min of treatment [12]. Methomyl reduction percentages were increased with increasing ozonation exposure time. More than 90% reduction percentages were achieved after 15, 10 and 5 min for methomyl. The ability of ozonation in reduction of these pesticides amount is related to the ability of ozone to generate hydroxyl radicals in aqueous solution, which are highly effective to decompose methomyl, so as the time of exposure increased hydroxyl radicals continued to be generated throughout the treatment, and more residues degraded. The present results agreed with the results obtained by several authors [17, 18, 19]. The authors concluded that ozonation treatment could be considered as an efficient treatment to remove high concentrations of pesticide residues if ozone generated continuously for a sufficient time of treatment.

Effect of tomato juice UV-radiation at 254 nm. It can be noticed from the results obtained from spiked tomato juices treated with UV radiation at 254 nm that this method was not an efficient in removing methomyl, since the maximum reduction percentages achieved by this treatment were 19.59% after 30 minutes of treatment. This was small reduction percentage in comparison with the corresponding reduction percentages achieved by ozonation and heat treatments. Furthermore, the recovered amounts remained higher than the maximum residues limits

TABLE 2
Comparison between effects of ozonation, UV-radiation and cooking at 100 C for different periods of time on methomyl pesticide reduction percentages using GC-NPD.

Treatment	Spiked amounts (ppm)				
	0.1	**0.5**	**1**	**5**	**10**
			3 min		
Ozonation at 0.4 ppm	63.265[a**]±1.50	58.836[a]±1.11	55.657[a]±1.57	47.847[a]±1.33	42.402[a]±1.88
UV-radiation at 254 nm	1.031[c]±0.02	0.402[c]±0.52	0.847[c]±0.22	0.461[c]±0.42	0.465[c]±0.16
Heat treatment above 100 C	38.947[b]±0.83	38.205[b]±0.96	37.578[b]±0.36	34.209[b]±0.97	31.703[b]±0.94
5 min					
Ozonation at 0.4 ppm	65.306[a]±1.02	60.291[a]±1.81	57.492[a]±1.93	49.989[a]±1.20	44.668[a]±1.17
UV-radiation at 254 nm	3.093[c]±1.17	1.004[c]±0.31	1.164[c]±0.40	0.902[c]±0.23	0.890[c]±0.28
Heat treatment above 100 C	40.000[b]±0.65	40.084[b]±0.91	38.095[b]±0.36	35.967[b]±0.85	32.997[b]±0.51
10 min					
Ozonation at 0.4 ppm	84.694[a]±1.84	79.418[a]±0.28	65.240[a]±0.96	63.627[a]±0.12	57.311[a]±0.25
UV-radiation at 254 nm	6.186[c]±0.95	3.012[c]±0.20	2.328[c]±1.01	2.166[c]±0.29	2.086[c]±0.21
Heat treatment above 100 C	51.579[b]±0.28	52.401[b]±0.12	50.000[b]±0.38	48.198[b]±0.68	45.297[b]±0.82
15 min					
Ozonation at 0.4 ppm	100[a]±0.00	91.476[a]±0.97	87.768[a]±0.32	84.730[a]±0.94	71.575[a]±0.75
UV-radiation at 254 nm	9.278[c]±1.46	9.036[c]±0.61	4.656[c]±0.68	4.030[c]±0.31	3.934[c]±0.62
Heat treatment above 100 C	63.158[b]±0.20	62.839[b]±0.70	58.282[b]±0.68	55.793[b]±0.78	52.706[b]±0.64
30 min					
Ozonation at 0.4 ppm	100[a]±0.00	100[a]±0.00	100[a]±0.00	98.770[a]±0.11	92.125[a]±0.90
UV-radiation at 254 nm	19.588[c]±1.31	17.470[c]±0.77	15.450[c]±1.05	12.252[c]±0.81	10.235[c]±0.75
Heat treatment above 100 C	72.632[b]±0.38	71.608[b]±0.29	68.530[b]±0.29	65.092[b]±0.33	61.836[b]±0.28

* Values are means of three replicates ± SE.
**Means of reduction percentages within the same column for each time sharing the same letters in superscript are not significantly different using LSD test at 0.01 probability level.

even after 30 min of treatment. An explanation to these results might relay on the fact that photodegradation is based on the absorption of light by the molecules, to be promoted to their excited singlet state. This process was slow and need sufficient exposure time of UV-radiation to cause hemolytic cleavage of C–N bond to form radical pairs [20].The present results are also in agreement with results obtained by [21] results. Who noticed that methomyl reduction percentages in aqueous solution after 1 and 6 hours were 39.0% and 92.6%, respectively.

Effect of heat treatment on tomato juice. Heat treatment of spiked tomato juice above 100 °C was an effective treatment to reduce methomyl amounts in tomato juice significantly, since the increased reduction percentages of methomyl was more than 50% for all of the spiked concentration levels after 15 min of treatment. Methomyl recovered amounts of spiked tomato juice at concentration of 5 and 10 ppm were not reduced below the European Union committee MRL of 0.2 ppm [12] after 30 min of heat treatment, which means that high concentration levels need more exposure time than low concentration levels to be reduced below the maximum residue limit. According to the present results, it was clear that the exposure time is an important factor in heat treatment for the reduction of methomyl, residues contents.

The reduction in methomyl recovered amounts could be explained according to the processes that normally occur during cooking, which involve; volatilization, hydrolysis, and thermal breakdown of this compound [22]. The results of this study concur with the results described in the paper of Soliman [24] concerning the persistence of methomyl on okra, after washing and heat treatment. Methomyl percentage of loss after washing with running water for 1 min followed by heat treatment for 5 min was 81.5%.

CONCLUSIONS

The study of the effect of ozonation at 0.4 ppm, UV-radiation at 254 nm and heat treatment above 100

ºC on spiked tomato juice results showed that Ozonation was the most effective treatment to reduce methomyl, spiked amounts significantly below the maximum residue limits, and it is time dependent. Heat treatment was found to be less efficient treatment than ozonation in reducing methomyl, spiked amounts, but more efficient than UV-radiation. UV-radiation was the least efficient treatment to reduce the spiked amounts of methomyl in tomato juice. Exposure time to the ozonation, UV-radiation and heat treatment was an important factor to reduce the spiked amount below the maximum residue limits.

ACKNOWLEDGMENTS

This work was performed with the support of The University of Jordan particularly Research Deanship , and Ministry of Agriculture of Jordan to whom we thank.

REFERENCES

[1] Abou- Arab, M. (1999). Behavior of Pesticides in Tomatoes during Commercial and Home Preparation. Food Chemistry, 65, 509-514.

[2] Akta, W., Sengupta, D. and Chowdhury, A. (2008). Degradation Dynamics and Persistence of Quinolphos and Methomyl in/on Okra (*Ablemoschus esculentus*) Fruits and Cropped Soil. Bulletin of Environment Contamination and Toxicology, 80,74-77.

[3] Aldrige, W. (1971). The Nature of the Reaction of Organophosphrous Compounds and

[4] Carbamates with Esterases. Bulletin of World Health Organization, 44, 25-30.

[5] Anastassiades, M., Lehotay, S., Stajnbaher, D. and Schench, F. (2003). Fast and Easy Multi-residue Method Employing Acetonitrile Extraction/Partitioning and Dispersive Solid-Phase Extraction for Determination of Pesticide Residues in Produce. Journal of AOAC International**,** 86(2), 412-431.

[6] Berger, T., Wilson, W. and Deye, J. (1993). Analysis of Carbamate Pesticides by Packed Column Supercritical fluid. Journal of Chromatography Science, 32(5), 179-184.

[7] Bonnechere, A., Hanot, V., Jolie, R., Hendrickx, M., Bragard, C., Bedoret, T. and Loco, J. (2012). Effect of Household and Industrial Processing on Levels of Five Pesticide Residues and Two Degradation Products in Spinach. Food Control, 25, 397-406.

[8] Corley, J. (2003). Handbook of Residue Analytical Methods for Agrochemicals, USA: John Wiley and Sons Ltd.

[9] Delgado, M., Barosso, S., Tostado, G. and Diez, L. (2001). Stability Studies of Carbamate Pesticides and Analysis by Gas Chromatography with Flame Ionization and Nitrogenphosphorus Detection. Journal of Chromatography A, 921, 287-296.

[10] Department of Statistics (2010). Annual Book, Amman, Jordan.

[11] Department of Statistics (2011). Annual Book, Amman, Jordan.

[12] European Commission (EC) (2005). EU-Pesticides Database, Commission Regulation (EC) No 396/2005

[13] Food and Agriculture Organization (FAO) (2002). FAO Specifications and Evaluations for Plant Protection Products; Methomyl. Retrieved from http:// www.Fao.org/ag

[14] Food and Agriculture Organization (FAO) (2007). Food and Agriculture Organization Statistics. Retrieved from http:// www.Faostat.org

[15] Food and Agriculture Organization (FAO) (2008). FAO Specifications and Evaluations for Plant Protection Products; Oxamyl. Retrieved from http:// www.Fao.org/ag

[16] Glauner, T. (2012). New Tools for Unmatched Sensitivity and Unequivocal Confirmation of Pesticides in Food. Agilent Technologies Publications, USA.

[17] Herweh, J. and Hoyle, C. (1980). Photodegradation of Some Alkyl n-arylcarbamates. Journal of Organic Chemistry, 45(11), 2195-2201.

[18] Lau, T., Chu, W. and Graham, N. (2007). Degradation of the Endocrine Disruptor Carbofuran by UV, O3 and O3/UV. Journal of International Association on Water Pollution Researches, 55(12), 275-280.

[19] Lehotay, S., Dekok, A., Hiemetra, M. and Van-Bodegraven, P. (2005). Validation of a Fast Easy Method for Determination of Residues from 229 Pesticides in Fruits and Vegetables Using Gas and Liquid Chromatography and Mass Spectrometric Detection. Journal of AOAC International, 88(2), 595-614.

[20] Lkeura, H., Kobayashi, F. and Tamaki, M., 2011. Removal of Residual Pesticides in Vegetables Using Ozone Microbubbles. Journal of Hazardous Materials, 186(1), 956-959.

[21] Marrs, T. and Ballantyne, B. (2004). Pesticide Toxicology and International Regulation, (1st ed), London: John Wiley and Sons Ltd.

[22] Mico, M., Chourdaki, S., Bacardit, J. and Sans, C. (2010). Comparison between Ozonation and Photo-Fenton Processes for Pesticide Methomyl Removal in Advanced Greenhouses. Journal of International Ozone Association, 32(4), 259-264.
[23] Ministry of Agriculture (2011). Annual Report, Amman, Jordan.
[24] Muir, D. and Sverko, E. (2006). Analytical Methods for PCBs and Organochlorine Pesticides in Environmental Monitoring and Surveillance. Analytical and Bioanalytical Chemistry, 386(4), 769-789.
[25] Soliman, M. (2012). Effects of UV-Light, Temperature and Storage on the Stability and Biological Effectiveness of some Insecticides. Journal of Plant Protection Research, 52(2), 275-280.
[26] Worthing, C. and Hance, R. (1991). The Pesticide Manual, (9thed.), England: British Crop Protection Council.
[27] Al-Antary, T.M., Al-Dabbas, M. and Shaderma, A. (2015). Evaluation Of Three Treatments on Carbosulfan Removal in Tomato Juice. Fressinius Environmental Bulletin, 24 (3), 733-739.
[28] Alawi, M., Al-Antary, T.M., Estityah, H., Al-Aqqad, S. and Al-Oqlah, K. (2013). Comparative Study for Chlorinated Pesticides in Mother Milk From Jordan in Four Studies Between 1993 and 2003. Fressinius Environmental Bulletin, 22 (1a) 279-285.

Received: **27.11.2015**
Accepted: **22.03.2016**

CORRESPONDING AUTHOR

Tawfiq Mustafa Al- Antary
Prof of Pesticides and Economic Entomology, Faculty of Agriculture, Department of Plant Protection, The University of Jordan, Amman, 11942, Jordan.

Email: tawfiqalantary@yahoo.com

© by PSP Volume 25 – No. 7/2016, pages 2700-2706 Fresenius Environmental Bulletin

CADMIUM UPTAKE AND LOCALIZATION IN ROOTS OF *SALIX MATSUDANA* KOIDZ

Hangfeng Wu, Jiayue Wang, Yangjie Ou, Binbin Li, Wusheng Jiang, Donghua Liu, Jinhua Zou*

Tianjin Key Laboratory of Animal and Plant Resistance, College of Life Sciences, Tianjin Normal University, Tianjin 300387, People's Republic of China

ABSTRACT

Cadmium uptake and localization in roots of *Salix matsudana* exposed to 50 μM Cd for 1, 3, 6, 12 and 24 h were investigated by means of fluorescence labeling and energy-dispersive X-ray analyses (EDXA) in order to promote our understanding of Cd-responsive mechanisms in woody plants. The results indicated that the main route of Cd entry at 1 h was initially through the elongation zone, and later extended to the meristem. After 24 h exposure most Cd were accumulated in the meristem. EDXA analysis revealed that Cd ions were localized in cell walls. The evidence of Cd toxic effects on roots of *S. matsudana* can provide valuable information on understanding better to the mechanisms of Cd accumulation and localization in phytoremediation investigations in woody plants.

KEYWORDS:
EDXA; *Salix matsudana* Koidz; Cd-localization; fluorescence labeling; energy-dispersive X-ray analyses (EDXA)

INTRODUCTION

Cadmium (Cd) tends to accumulate to high and toxic concentration due to modern agriculture, industry and anthropogenic activities [1–3]. There are nearly 5000000 acres of arable land contaminated by heavy metals in China, which has obviously upward trend [4]. It was reported that the concentration of Cd in soil near smelters in China was extremely high, up to 11.2-197.3 mg/kg [5]. Cd can easily be absorbed, transformed, and accumulated in plants tissues where root is the primary site of accumulation [6]. Cd in higher plants is taken up through roots where a major fraction of its deposits and only a small fraction is distributed to other plant tissues [6–7]. Cd toxicity in many nontolerant plants is reported to be associated with the disturbance of mitosis [8–9], toxicity of nucleoli [10–12] and inhibition of plant growth [13–14]. After Cd has been absorbed by roots, it can be deposited in various tissues. Knowledge about its deposition and distribution in tissue compartments can be gained through energy-dispersive X-ray analyses (EDXA) [15–16]. Plant roots are well known as the organs sensitive to environmental stresses [17].

Salix matsudana Koidz is characterized by easy propagation and cultivation, large biomass, fast-growing, deep root system, high transpiration rate and tolerance to hypoxic conditions, making it potentially suitable for phytoremediation [18–21]. Recent study showed that 50 μM Cd neither affected the phenotype nor the growth of *S. matsudana* [22].

Cd toxic effects on Cd accumulation and localization root tissues of *S. matsudana* exposed to 50 μM Cd for different treatment times (1 to 24 h) were carried out by means of fluorescence labelling and EDXA. The data obtained can provide valuable information to understand better the mechanisms of Cd accumulation and localization in phytoremediation investigations in woody plants.

MATERIALS AND METHODS

Plant material and growth conditions. Woody cuttings (25 cm long) from one year-old shoots of *S. matsudana* were collected and fully rinsed with distilled water before starting the experiments. After dipping in distilled water at room temperature, ten-day-old healthy plants were transferred to half-strength Hoagland nutrient solution and grown for a week. Then they were spiked with 50 μM Cd for 1, 3, 6, 12 and 24 h. Cadmium was provided as cadmium chloride ($CdCl_2$). The nutrient solution consisted of 5 mM Ca $(NO_3)_2$, 5 mM KNO_3, 1 mM KH_2PO_4, 1 mM $MgSO_4$, 50 μM H_3BO_3, 10 μM FeEDTA, 4.5 μM $MnCl_2$, 3.8 μM $ZnSO_4$, 0.3 μM $CuSO_4$, and 0.1 μM $(NH_4)6Mo_7O_{24}$, adjusted to pH 5.5. Control seedlings were grown in the nutrient solution alone. The solutions were continuously aerated with an aquarium air pump every day.

Fluorescence labeling of Cd. *S. matsudana* intact roots treated with or without 50 μM Cd for 1, 3, 6, 12 and 24 h were stained using the Cd-specific probe Leadmium™ Green AM solution (Molecular Probes, Life Technologies, California,

USA) in order to investigate the distribution of Cd. After the Cd treatment, the root tips were incubated for 10 min in 20 mM disodium ethylene diamine tetra-acetic acid (Na_2-EDTA) at room temperature, and then thoroughly washed with deionized water. A stock solution of the Cd specific probe was made by adding 50 µL of dimethyl sulfoxide (DMSO) to one vial of the dye. This stock solution was then diluted with 1:10 of 0.85% NaCl [23]. Root tips were immersed in diluted stock solution at 40 °C for 90 min in the dark, and then were washed with 0.85 % NaCl three times. The fluorescence from labeled Cd in root tips was visualized under a Nikon ECLIPSE 90i confocal laser scanning microscope with excitation and emission wavelengths at 488 and 515 nm, respectively. Intact cells exhibit green fluorescence due to Cd specific probe Leadmium™ Green AM.

Sample preparation for scanning electron microscope. Elemental distribution in and composition of experimental plants was determined from samples of freeze-dried root materials. The samples of 1 cm length were cut from the root tips (as young root tissue including the meristem) and more basal parts of root tips exposed to 50 µM Cd for 24 h, and rapidly frozen in liquid nitrogen for 90 min, and then put frozen samples into lyophilizer (Lyophilizer LGJ-10C, Sihuan, Beijing) immediately for 2 days. Cross-sections of the roots (about 1 mm) were coated by gold using the sputter/coater (EMITECH K550X, Quorum Group, England). The energy dispersive X-ray microanalytical studies were carried out using a scanning electron microscope (FEI Nova NANOSEM 230, Oregon, USA) provided with energy dispersive X-ray spectrum analysis (EDXA) (Genesis Apollo 10, EDAX, USA). The spectra were collected by 30 keV and X-ray detector equipped with a super ultra-thin window. The collection time was 120 s. The Cd composition in the roots was displayed as wt% (weight percent in relation to total elements).

Statistical analysis. Data from this investigation were analyzed with Sigma Plot 13.0 using means ± standard error (SE). For equality of averages the *t*-test was applied. Results were considered statistically significant at $P < 0.05$.

RESULTS

Cd distribution in different zones. The investigation on Cd absorption and distribution in the root tips of *S. matsudana* exposed to 50 µM Cd for 1, 3, 6, 12 and 24 h was carried out using the Cd specific probe Leadmium™ Green AM dye. The fluorescent dye was loaded into the roots, showing different fluorescence intensity in the root tips exposed to 50 µM Cd for different treatment times (Fig. 1). Fluorescence spectra were analyzed from line scanning of meristem and elongation zone in the root tips in longitudinal sections. There was no green fluorescence (Cd) in control root tips (Fig. 1A1–A2). A little green fluorescence was found in the elongation zone of the root tips exposed to Cd for 1 h (Fig. 1B1–B2), indicating that Cd ions first entered in this area. A weak green fluorescence was observed and mainly distributed in the elongation zone of the root tips exposed to Cd for 3 h (Fig. 1C1–C2). Then, the fluorescence labeling of Cd gradually extended down to the meristem zone. With prolonged treatment period (6 – 24 h), the labeling of the meristematic cells obviously increased (Fig. 1D1–D2; E1–E2; F1–F2). The most intense fluorescence in meristematic cells was noted after 24 h of incubation (Fig. 1F1–F2). Thus Cd ions were mostly localized in meristematic cells and uptake and accumulation of Cd increased with prolonged treatment time. The fluorescence density was analyzed by ImageJ software, confirming the observations mentioned above. The data showed that the root tips of *S. matsudana* under Cd stress could absorb Cd ions and that the amount of Cd increased ($P < 0.05$) with prolonged exposure (Fig. 2), suggesting that meristem and elongation zone in the roots of *S. matsudana* under Cd stress was the main accumulation site for Cd.

Subcellular localization of Cd. The data from EDXA reveal the subcellular localization of Cd in transverse sections of the meristem zone in *S. matsudan* exposed to 50 µM Cd for 24 h. Protoderm, ground meristem and procambium can be distinguished in very close proximity to the apical meristem (Fig. 5A). The Cd content of cell walls in the three zones of the roots exposed to Cd for 24 h was different, i.e., ground meristem (3.13 Wt%) > procambium (1.44 Wt%) > protoderm (0.92 Wt%) (Fig. 3B–D).

DISCUSSION AND CONCLUSIONS

Plant roots are sensitive to environmental stress. Plant tolerance to heavy metal stress can be estimated based on their root and/or shoot growth inhibition by the metal present in a nutrient solution [24]. Root apical meristems play a key role in the immediate reaction to stress factors by activating signal cascades to the other plant organs. To identify for Cd uptake in living roots, the Leadmium™ Green AM dye as a specific indicator has been successfully used to detect Cd in plant roots [16, 23, 25–26]. It has higher affinity for Cd than internal proteins [27] and is not sensitive to other divalent ions except for lead. The root meristem has been known as one of the most sensitive sites to Cd toxicity. In the present

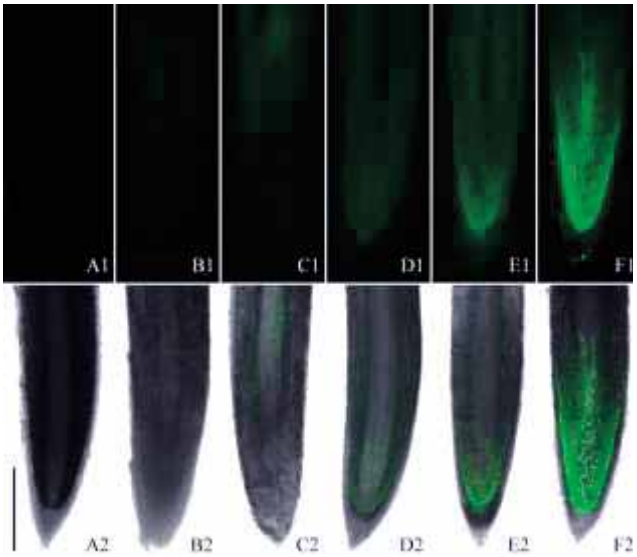

FIGURE 1

Micrographs of roots from *S. matsudana* exposed to Cd using Leadmium™ Green AM dye at longitudinal section. A1–F1. Showing Cd detection images of the roots which were pre-treated with 50 µM Cd for 0 (A), 1 (B), 3 (C), 6 (D), 12 (E) and 24 (F), respectively. A2–F2. Showing fluorescence labeling merged with bright field. All images were taken quadruple magnification, and green fluorescence represented the binding of the dye to Cd. Scale bars = 1000 µm.

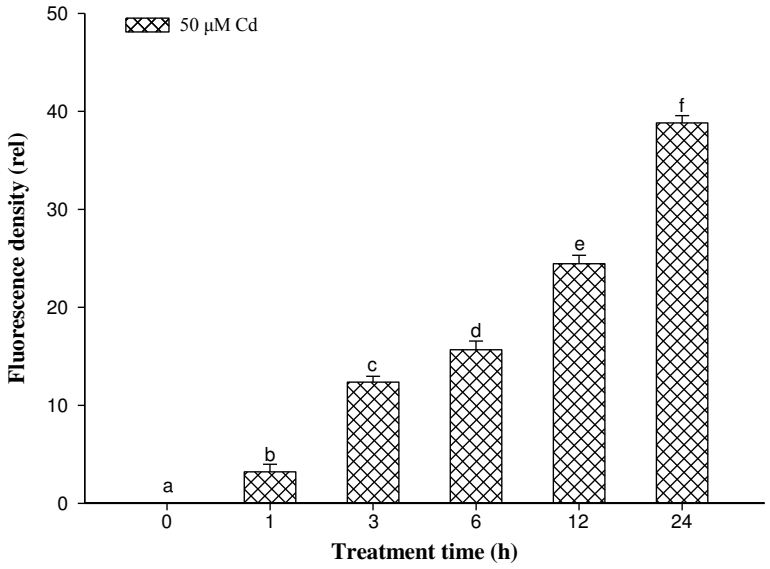

FIGURE 2

Leadamium™ Green AM dye fluorescence density from longitudinal section in *S. matsudana* the roots exposed to 50 µM Cd for 1, 3, 6, 12 and 24 h. Values with different letters differ significantly from each other (n = 5, $P < 0.05$). Data are means ± SE.

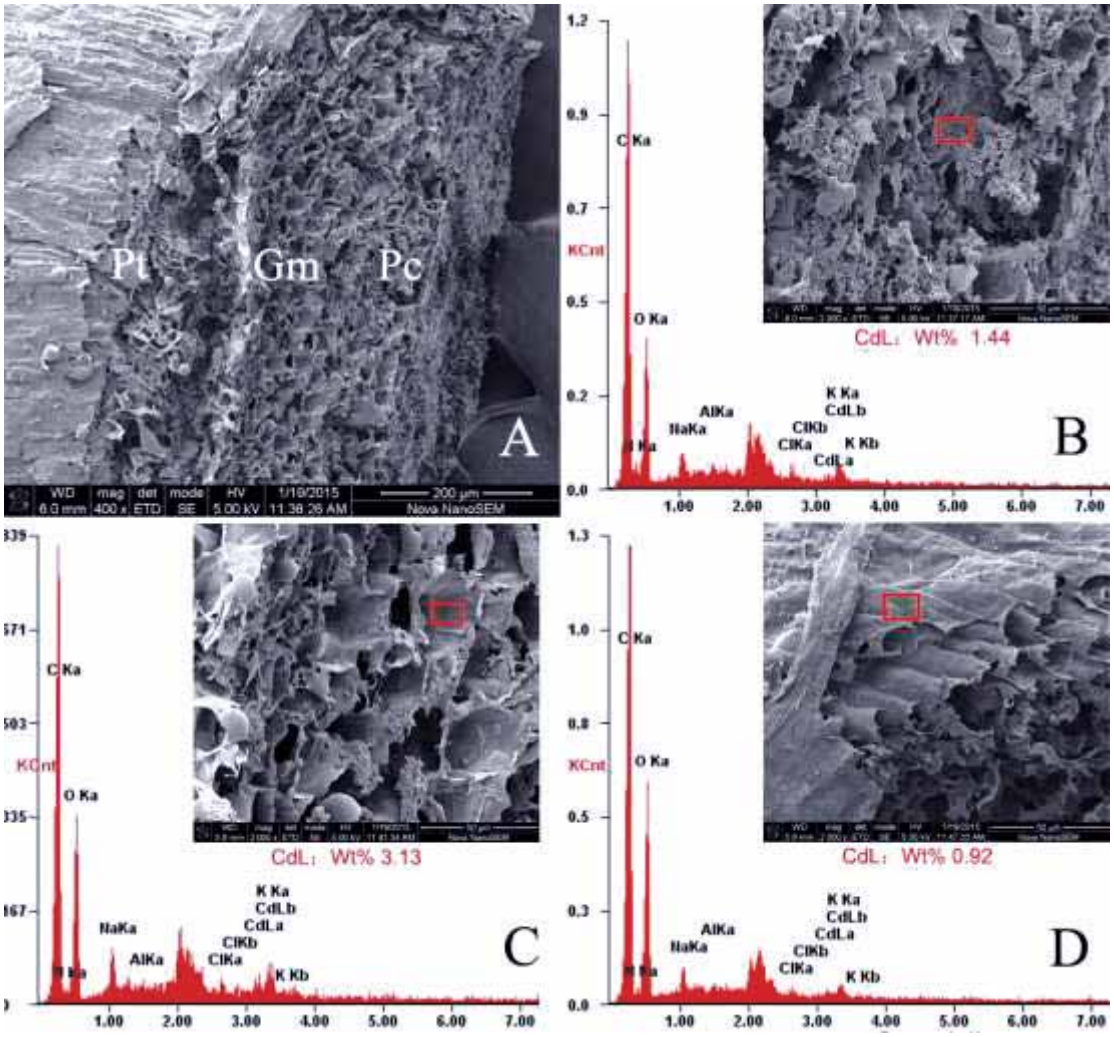

FIGURE 3
EDXA spectra taken from the site of the SEM micrographs, showing Cd localization in cell wall in meristem zone of *S matsudana* root tip cells exposed to 50 µM Cd for 24 h. A. Transverse section of meristem zone (Scale bar = 200 µm). B. Procambium (Scale bar = 50 µm). C. Ground meristem (Scale bar = 50 µm). D. Protoderm (Scale bar = 50 µm). Gm=ground meristem; Pc=procambium; Pt=protoderm. Red box site of the analysis; x-axis-energy [keV].

investigation, uptake and accumulation site of Cd in different plant root zones of *S. matsudana* under Cd stress varied depending on the treatment time. The main route of Cd entry at 1 h was found to be through elongation zone, but it extends down to meristem zone. The high level of Cd appeared in meristem zone after 24 h expose when compared with elongation, suggesting that the meristem zone in the roots of *S. matsudana* is a primary target of Cd toxicity. The results here support our previous observation that Cd was absorbed within hours in the root cells of *Allium sativum* exposed to Cd [28].

Heavy metal binding to the cell wall, chelation by organic molecules at a subcellular level plays an important role in detoxification of heavy metals in plant tissues [29]. Cell wall with negative charge is the first barrier protecting the protoplast from Cd toxicity and has significant capacity for Cd binding and retention [30]. Neumann et al. [31] indicated that the cell wall played a role in metal tolerance when the cell wall volume was high compared to the cytosol and vacuole. Cytochemical evidence also confirms that cysteine-rich proteins, commonly referred to as phytochelatins, were localized in electron dense granules in root cell walls of *A. cepa* [32], which seemed to contribute substantially to Cd detoxification. In the present investigation more Cd ion were observed in meristem zone in roots according to the observation from Leadmium™ Green AM dye. The fluorescence probe can only identify the free Cd ions in tissues, which can not reveal the subcellular localization of Cd. However, data from EDXA in this work indicated that Cd exists in cell wall in the three zones of meristem region, protoderm, ground meristem and procambium, of *S. matsudan* root tips exposed to 50 µM Cd for 24 h, confirming the presence of Cd ions in cell walls. Similarly, we also observed Cd ions in

the cell wall of root tip cells *A. cepa* under Cd stress using EDXA [15]. Thus, cell walls can prevent Cd from entering into the cell interior, and resulting in the reduction of Cd concentration in soluble fractions. Cell fractionation studies suggest that Cd-sensitive plants have lower Cd concentrations in cell walls and higher vacuolar Cd concentrations than Cd-tolerant plants [33]. The tissue fractionation of Cd in *S. matsudana* roots was analyzed in the previous work, indicting that most of the Cd was present in the cell wall containing fraction, while middle and minor parts of this element associated with the soluble and cell organelle fraction (unpublished), which indirectly confirm the observation that Cd exists in cell wall in the three zones of meristem region, protoderm, ground meristem and procambium, of *S. matsudan* root tips. From what is indicated, we suggest that Cd integrated with pectates and proteins in cell wall may be responsible for the adaptation of *S. matsudana* to Cd stress, which is in line with the observations by Fu et al. [34] and Weng et al. [35].

Root tips of plants are the sensitive organ to environmental stresses. Excessive Cd has often caused poisoning and environmental contamination. The findings of the present study confirm that Cd ions can be mainly absorbed in meristem zone in the root tips of *S. matsudana* under Cd stress. Root apical meristems play a key role in the immediate reaction to stress factors by activating signal cascades to the other plant organs. There is a clear correlation between Cd content and cell damage in root tips of *S. matsudana*. EDXA analysis revealed that Cd ions were localized in cell walls, revealing that the characteristics of *S. matsudana* to Cd toxicity. The evidence of Cd toxic effects on roots of *S. matsudana* can provide valuable information on understanding better to the mechanisms of Cd accumulation and localization in phytoremediation investigations in woody plants.

ACKNOWLEDGEMENTS

This project was supported by the National Natural Science Foundation of China. The authors wish to express their appreciation to the reviewers for this paper.

The authors declare no conflict of interests.

REFERENCES

[1] Gallego, S.M., Pena, L.B., Barcia, R.A., Azpilicueta, C.E., Iannonea, M.F., Rosales, E.P., Zawoznik, M.S., Groppa, M.D. and Benavides, M.P. (2012) Unravelling cadmium toxicity and tolerance in plants: Insight into regulatory mechanisms. *Environ Experi Bot* 83, 33– 46.

[2] Tomar, P.C., Lakra, N. and Mishra, S.N. (2013) Effect of cadaverine on *Brassica juncea* (L.) under multiple stress. *Indian J Exp Biol* 51, 758– 763.

[3] Choppala, G., Saifullah Bolan, N., Bibi, S., Iqbal, M., Rengel, Z., Kunhikrishnan, A., Ashwath, N. and Sik Ok, Y. (2014) Cellular mechanisms in higher plants governing tolerance to cadmium toxicity. *Crit Rev Plant Sci* 33, 374– 391.

[4] Gao, F. (2014) The mystery of heavy metal pollution in farmland. *China Land* (2), 14– 15.

[5] Cui, S., Zhou, Q. and Chao, L .(2007) Potential hyperaccumulation of Pb, Zn,Cu and Cd in endurant plants distributed in an old smeltery, northeast China. *Environ Geol* 51, 1043–1048.

[6] Gu, J.G., Qi, L.W., Jiang, W.S. and Liu, D.H. (2007) Cadmium accumulation and its effects on growth and gas exchange in four *Populus* cultivars. *Acta Biol Cracov Bot* 49, 7– 14.

[7] Li, Y., Zhang, S.S., Jiang, W.S. and Liu, D.H. (2013) Cadmium accumulation, activities of antioxidant enzymes, and malondialdehyde (MDA) content in *Pistia stratiotes* L. *Environ Sci Pollut Res* 20, 1117– 1123.

[8] Xu, P., Liu, D. and Jiang, W. (2009) Cadmium effects on the organization of microtubular cytoskeleton in interphase and mitotic cells of *Allium sativum. Biol Plantarum* 53, 387– 390.

[9] Shi, H.P., Feng, Y., Wang, Y.L. and Tsang, P.K.E. (2014) Effect of cadmium on cytogenetic toxicity in hairy roots of *Wedelia trilobata* L. and their alleviation by exogenous $CaCl_2$. *Environ Sci Pollut Res* 21, 1436–1443.

[10] Zhang, S.S., Zhang, H.M., Qin, R., Jiang, W.S. and Liu, D.H. (2009) Cadmium induction of lipid peroxidation and effects on root tip cells and antioxidant enzyme activities in *Vicia faba* L. *Ecotoxicology* 18, 814– 823.

[11] Zou, J.H., Yue, J.Y., Zhang, Z.G.., Jiang, W.S. and Liu, DH. (2012) Effects of cadmium stress on root tip cells and some physiological indexes in *Allium cepa* var. *agrogarum* L. *Acta Biol Cracov Bot* 54: 129–141.

[12] Qin, R., Jiang, W.S. and Liu, DH. (2013) Cadmium can induce alterations in the cellular localization and expression of three major nucleolar proteins in root tip cells of *Vicia faba* L. *Plant Soil* 368, 365–373.

[13] Ge, W., Jiao, Y.Q., Sun, B.L., Qin, R., Jiang, W.S. and Liu, DH. (2012) Cadmium-mediated oxidative stress and ultrastructural changes in root cells of poplar cultivars. *S Afr J Bot* 83, 98–108.

[14] Jiao, Y.Q., Ge, W., Qin, R., Sun, B.L., Jiang, W.S. and Liu, D.H. (2012) Influence of cadmium stress on growth, ultrastructure and

antioxidative enzymes in *Populus* 2025. *Fresen Environ Bull* 21, 1375–1384.
[15] Liu, D.H., Kottke, I. and Adam, D. (2007) Localization of cadmium in the root cells of *Allium cepa* by energy dispersive X-ray analysis. *Biol Plant* 51, 363–366.
[16] Shi, Q.Y., Wang, J.R, Zou, J.H., Jiang, Z., Wang, J.Y., Wu, H.F., Jiang, W.S. and Liu, D.H. (2015) Cadmium uptake and accumulation and its toxic effects on leaves in *Hordeum vulgare. Fresen Environ Bull,* 24, 4504–4511.
[17] Jiang, Z., Qin, R., Zhang, H.H., Zou, J.H., Shi, Q.Y., Wang, J.R., Jiang, W.S. and Liu, H. (2014) Determination of Pb genotoxic effects in *Allium cepa* root cells by fluorescent probe, microtubular immunofluorescence and comet assay. *Plant Soil* 383, 357–372.
[18] Dos Santos Utmazian, M.N., Wieshammer, G., Vega, R., Wenzel, W.W. (2007) Hydroponic screening for metal resistance and accumulation of cadmium and zinc in twenty clones of willows and poplars. *Environ Pollut* 148, 155–165.
[19] Dimitriou, I. and Aronsson, P. (2010) Landfill leachate treatment with willows and poplars efficiency and plant response. *Waste Manage* 30, 2137–2145.
[20] Ling, T., Jun, R. and Fangke, Y. (2011) Effect of cadmium supply levels to cadmium accumulation by *Salix*. *Int J Environ Sci Tech* 8, 493–500.
[21] Rao, G.D., Sui, J.K., Zeng, Y.F., He, G.Y., Duan, A.G.. and Zhang, J.G.. (2014) De Novo Transcriptome and Small RNA Analysis of Two Chinese Willow Cultivars Reveals Stress Response Genes in *Salix matsudana*. *PLOS ONE* 9(10), 1–12.
[22] Yang, J.L., Li, K., Zheng W., Zhang, H.Z., Cao, X.D., Lan, Y.X., Yang, C.P. and Li, C.H. (2015) Characterization of early transcriptional responses to cadmium in the root and leaf of Cd-resistant *Salix matsudana* Koidz. *BMC Genomics* 16, 705.
[23] Zhao, F.Y., Hu, F., Zhang, S.Y., Wang, K., Zhang, C.R. and Liu T (2013) MAPKs regulate root growth by influencing auxin signaling and cell cycle-related gene expression in cadmium-stressed rice. *Environ Sci Pollut Res* 20, 5449–2460.
[24] Wang, M. and Zhou, Q. (2005) Single and joint toxicity of chlorimuron-ethyl, cadmium and copper acting on wheat *Triticum aestivum*. *Ecotoxicol Environ Safe* 60, 169–175.
[25] Lu, L.L., Tian, S.K., Yang, X.E., Wang, X.C., Brown, P., Li, T.Q. and He, Z.L. (2008) Enhanced root-to-shoot translocation of cadmium in the hyperaccumulating ecotype of *Sedum alfredii. J Exp Bot* 59, 3203–3213.
[26] Li, L.Z., Liu, X.L., Peijnenburg, W.J.G.M., Zhao, J.M., Chen, X.B., Yu, J.B. and Wu, H.F. (2012) Pathways of cadmium fluxes in the root of the halophyte *Suaeda salsa. Ecotoxicol Environ Saf* 75, 751–757.
[27] Javed, M.T., Lindberg, S. and Greger, M. (2014) Cadmium uptake in *Elodea canadensis* leaves and its interference with extra- and intra-cellular pH. *Plant Biol* 16, 615–621.
[28] Jiang, W.S., Liu, D.H. and Xu, P. (2009) Cd-induced system of defence in the garlic root meristematic cells. *Biol Plantarum* 53, 369–372.
[29] Wang, X., Liu, Y.G., Zeng, G.M., Chai, L.Y., Song, X.C., Min, Z.Y. and Xiao, X. (2008) Subcellular distribution and chemical forms of cadmium in *Bechmeria nivea* (L.). *Guad Environ Exp Bot* 63, 389–395.
[30] Polle, A. and Schützendübel, A. (2004) Heavy metal signalling in plants:linking cellular and organismic responses. In: Hirt H, Shinozaki K (eds.) Plant Responses to Abiotic Stress, Springer-Verlag, Germany, pp. 187–215.
[31] Neumann, D., Zur Nieden, U., Schwieger, W., Leopold, I. and Lichtenberger O (1997) Heavy metal tolerance of *Minuartia erna*. *J Plant Physiol* 151, 101–108.
[32] Liu, D. and Kottke, I. (2004) Subcellular localization of cadmium in the root cells of *Allium cepa* by electron energy loss spectroscopy and cytochemistry. *J Biosci* 29, 329–335.
[33] Uraguchi, S., Kiyono, M., Sakamoto, T., Watanabe, I. and Kuno, K., (2009) Contributions of apoplasmic cadmium accumulation, antioxidative enzymes and induction of phytochelatins in cadmium tolerance of the cadmium-accumulating cultivar of black oat (*Avena strigosa* Schreb). *Planta* 230, 267–276.
[34] Fu, X.P., Dou, C.M., Chen, Y..X, Chen, X.C., Shi, J.Y., Yu, M.G,. and Xu, J. (2011) Subcellular distribution and chemical forms of cadmium in *Phytolacca americana* L. *J Hazard Mater* 186, 103–107.
[35] Weng, B.S., Xie, X.Y., Weiss, D.J., Liu, J.C., Lu, H.L. and Yan, C.L. (2012) *Kandelia obovata* (S., L.) Yong tolerance mechanisms to cadmium: sub-cellular distribution, chemical forms and thiol pools. *Mar Pollut Bull* 64, 2453–2460.

Received: **07.12.2015**
Accepted: **19.04.2016**

CORRESPONDING AUTHOR

Jinhua Zou
Tianjin Key Laboratory of Animal and Plant Resistance
College of Life Sciences
Tianjin Normal University
Tianjin 300387
PR CHINA

e-mail: skyzjh@mail.tjnu.edu.cn

AUTHOR INDEX

SUBJECT INDEX

FEB – GUIDE FOR AUTHORS

General

FEB accepts original papers, review articles, short communications, research abstracts from the entire sphere of environmental-chemistry,-biology,-microbiology,- technology, -biotechnology and-management, furthermore, about residue analysis/ and ecotoxicology of contaminants.

Acceptance or no acceptance of a contribution will be decided, as in the case of other scientific journals, by a board of reviewers. Papers are processed with the understanding that they have not been published before (except in form of an abstract or as a part of a published lecture, review or thesis);that they are not under consideration for publication elsewhere; that their publication has been approved by all co-authors, if any, as well as- tacitly or explicitly- by the responsible authorities at the institute where the work has been carried out and that, if accepted, it will not be published elsewhere in the same form, in either the same or another language, without the consent of the copyright holders.

Language

Papers must be written in English. Spelling may either follow American (Webster) or British (Oxford) usage but must be consistent. Authors who are less familiar with the English language should seek assistance from proficient colleagues in order to produce manuscripts that are grammatically and linguistically correct.

Size of manuscript

Review articles should not exceed 30 typewritten pages. In addition up to 5 figures may be included.

Original papers must not exceed 14 typewritten pages. In addition up to 5 figures may be included.

Short-Communications should be limited to 4 typewritten pages plus not more than 1 illustration.

Short descriptions of the authors, presentation of their groups and their research activities (with photo) should together not exceed I typewritten page. Short research abstracts should report in a few brief sentences (one-fourth to one page) particularly significant findings. Short articles by relative newcomers to the chemical innovation arena highlight the key elements of their Master and PhD-works in about I page.

Book Reviews are normally written in-house, but suggestions for books to review are welcome.

Preparation of manuscript

Dear authors,

FEB is available both as printed journal and as online journal on the web. You can now e-mail your manuscripts with an attached file. Save both time and money. To avoid any problems handling your text please follow the instructions given below:

When preparing your manuscripts have the formula K/SS (Keep It Simple and Stupid) in mind. Most word processing programs such as MS-Word offer a lot of features. Some of them can do serious harm to our layout. So please do not insert hyperlinks and/or automatic cross-references, tables of contents, references, footnotes, etc.

1. Please use the standard format features of your word processor (such as standard.dot for MS Word).
2. Please do not insert automatisms or secret link-ups between your text and your figures or tables. These features will drive our graphic department sometimes mad.
3. Please only use two fonts for text or tables "Times New Roman" and for graphical presentations "Arial".
4. Stylesheets, text, tables and graphics in shade of grey
5. Turn on the automatic language detection in English (American or British)
6. Please - check your files for viruses before you send them to us!!

Manuscripts should send to:parlar@wzw.tum.de
or:parlar@prt-parlar.de

Thank you very much!

STRUCTURE OF THE MANUSCRIPT

Title page: The first page of the manuscript should contain the following items in the sequence given: A concise title of the paper (no abbreviations). The names of all authors with at least one first name spelled out for every author. The names of Universities with Faculty, City and Country of all authors.

Abstracts: The second page of the manuscript should start with an abstract that summarizes briefly the contents of the paper (except short communications). Its length should not exceed 150-200 words. The abstract should be as informative as possible. An extended repetition of the paper's title is not considered to be an abstract.

Keywords: Below the Summary up to 6 key words have to be provided which will assist indexers in cross-indexing your article.

Introduction: This should define the problem and, if possible, the frame of existing knowledge. Please ensure that people not working in that particular field will be able to understand the intention. The word length of the introduction should be 150 to 300 words.

Materials and methods:
Please be as precise as possible to enable other scientists to repeat the work.

Results: Only material pertinent to the subject must be included. Data must not be repeated in figures and tables.

Acknowledgements: Acknowledgements of financial support, advice or other kind of assistance should be given at the end of the text under the heading "Acknowledgements". The names of funding organisations should be written in full.

References: Responsibility for the accuracy of references rests with the authors. References are to be limited in number to those absolutely necessary. References should appear in numerical order in brackets and in order of their citation in the text. They should be grouped at the end of the paper in numerical order of appearance. Abbreviated titles of periodicals are to be used according to Chemical or Biological Abstracts, but names of lesser known journals should be typed in full. References should be styled and punctuated according to the following examples:

ORIGINALPAPERS:
l. Author, N.N. and Author, N.N. (Year) Full title of the article. Journal and Volume, first and last page.
BOOK OR PROCEEDING:
2. Author, N.N. and Author, N.N. (Year) Title of the contribution.
In: Title of the book or proceeding. Volume (Edition of klitor-s, ed-s) Publisher, City, first and last page

DOCTORALTHESIS:
3. Author, N.N. (Year) Title of the thesis, University and
Faculty, City

UNPUBLISHED WORK:
Papers that are unpublished but have been submitted to a journal may be cited with the journal's name followed by "in press". However, this practice is acceptable only if the author has at least received galley proofs of his paper. In all other cases reference must be made to “unpublished work" or "personal communication".

Discussion and Conclusion: This part should interpret the results in reference to the problem outlined in the introduction and of related observations by the author/s or others. Implications for further studies or application may be discussed. A conclusion should be added if results and discussion are combined.

Corresponding author: The name of the corresponding author with complete postal address

Precondition for publishing:
A minimum number of 25 reprints must be ordered and prepaid.
1 - 4 pp.: 200,- EURO + postage/handling
5 - 8 pp.: 250,- EURO + postage/ handling
More than 8pp: 1.50 EURO/page x number of reprints +postage/ handling.
The prices are based upon the number of pages in our journal layout (not on the page numbers of the submitted manuscript).
Postage/ Handling: The current freight rate is Germany 10 €, Europe 18,00 €, International 30 €.
VAT: In certain circumstances (if no VAT registration number exists) we may be obliged to charge 7% VAT on sales to other EU member countries.MESAEP and SECOTOX members get a further discountof 20% (postage/ handling full).